RSC Smart Materials

Edited by Carmen Alvarez-Lorenzo and Angel Concheiro

Smart Materials for Drug Delivery

Volume 1

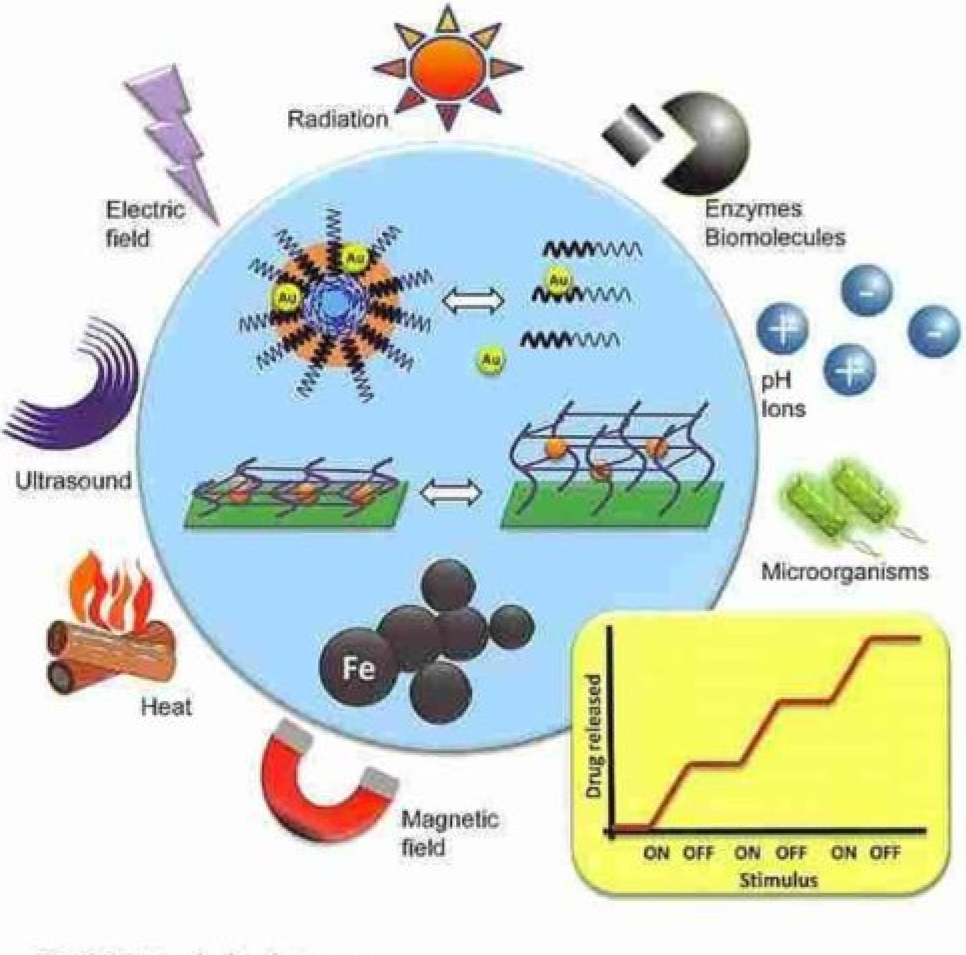
Radiation
Electric field
Enzymes Biomolecules
Au
Au
Au
Au
pH Ions
Ultrasound
Microorganisms
Fe
Heat
Magnetic field
Drug released
ON OFF ON OFF ON OFF
Stimulus

RSC Publishing

Smart Materials for Drug Delivery

Volume 1

Downloaded on 01/09/2013 10:25:44.

Downloaded on 01/09/2013 10:25:44.

RSC Smart Materials

Series Editor:
Hans-Jörg Schneider, *Saarland University, Germany*
Mohsen Shahinpoor, *University of Maine, USA*

Titles in this Series:
1: Janus Particle Synthesis, Self-Assembly and Applications
2: Smart Materials for Drug Delivery: Volume 1

How to obtain future titles on publication:
A standing order plan is available for this series. A standing order will bring delivery of each new volume immediately on publication.

For further information please contact:
Book Sales Department, Royal Society of Chemistry, Thomas Graham House,
Science Park, Milton Road, Cambridge, CB4 0WF, UK
Telephone: +44 (0)1223 420066, Fax: +44 (0)1223 420247
Email: booksales@rsc.org
Visit our website at www.rsc.org/books

Smart Materials for Drug Delivery

Volume 1

Carmen Alvarez-Lorenzo
University of Santiago de Compostela, Spain
Email: carmen.alvarez.lorenzo@usc.es

Angel Concheiro
University of Santiago de Compostela, Spain
Email: angel.concheiro@usc.es

RSC Publishing

Downloaded on 01/09/2013 10:25:44.

Downloaded on 01/09/2013 10:25:44.

RSC Smart Materials No. 2

ISBN: 978-1-84973-877-4
ISSN: 2046-0066

A catalogue record for this book is available from the British Library

© The Royal Society of Chemistry 2013

All rights reserved

Apart from fair dealing for the purposes of research for non-commercial purposes or for private study, criticism or review, as permitted under the Copyright, Designs and Patents Act 1988 and the Copyright and Related Rights Regulations 2003, this publication may not be reproduced, stored or transmitted, in any form or by any means, without the prior permission in writing of The Royal Society of Chemistry or the copyright owner, or in the case of reproduction in accordance with the terms of licences issued by the Copyright Licensing Agency in the UK, or in accordance with the terms of the licences issued by the appropriate Reproduction Rights Organization outside the UK. Enquiries concerning reproduction outside the terms stated here should be sent to The Royal Society of Chemistry at the address printed on this page.

The RSC is not responsible for individual opinions expressed in this work.

Published by The Royal Society of Chemistry,
Thomas Graham House, Science Park, Milton Road,
Cambridge CB4 0WF, UK

Registered Charity Number 207890

For further information see our web site at www.rsc.org

Printed in the United Kingdom by Henry Ling Limited, Dorchester, DT1 1HD, UK

Downloaded on 01/09/2013 10:25:45.

Foreword

In recent years smart materials have found new and promising applications as drug carriers for delivery of new therapeutic agents. At a time when present uses of drug delivery have become rather difficult to launch commercially because of the pressure from generic drug delivery systems, smart materials provide new applications, especially in the treatment of diseases where present formulations have not found good use. Indeed, intelligent biomaterial carriers have attracted significant interest because of the promise to respond to physiological conditions of the body, but also to respond to elevated quantities of analytes responsible for a particular disease.

The present book is a welcome addition to the field of smart polymers and comes to fill a major need in the use of smart materials as carriers for drug delivery. As we read the various chapters it becomes apparent that the editors, Professors Carmen Alvarez-Lorenzo and Angel Concheiro of the University of Santiago de Compostela, have set specific goals for this book and have spent numerous days trying to edit the chapters and balance the book. Their goals are to highlight the design, characterization and investigation of the next generation of "intelligent" or smart polymeric structures and biohybrids that can be used for drug delivery and can "communicate" with their surrounding environment.

The use of smart polymer carriers is a natural approach to the solution of many delivery problems as the discovery and delivery of drugs to cure chronic diseases have been achieved by a combination of intelligent material design and advances in nanotechnology. In particular, there has been considerable work in preparing nanostructured biomaterials for various applications, such as carriers for controlled and targeted drug delivery, micropatterned devices, systems for biological recognition, and others. Since many drugs act as protagonists or antagonists to different chemicals in the body, a delivery system that can respond to the concentrations of certain molecules in the body is

RSC Smart Materials No. 2
Smart Materials for Drug Delivery: Volume 1
Edited by Carmen Alvarez-Lorenzo and Angel Concheiro
© The Royal Society of Chemistry 2013
Published by the Royal Society of Chemistry, www.rsc.org

Downloaded on 01/09/2013 10:25:45.

invaluable. For this purpose, intelligent therapeutics or "smart drug delivery" call for the design of the next generation of responsive devices and materials, both from purely synthetic materials as well as through combination of natural and biological molecules with synthetic materials.

In other advanced pharmaceutical applications, biomimetic materials, especially polymeric networks, capable of biological recognition can be prepared by designing interactions between the building blocks of biocompatible networks and the desired specific ligands and by stabilizing these interactions by a three-dimensional structure. In addition, biomimetic methods are now used to build biohybrid systems or even biomimetic materials (mimicking biological recognition) for drug targeting and tissue engineering devices. Additionally, micro- and nanofabrication techniques have enabled the development of novel biomedical systems, sensors and delivery devices that can improve the therapeutic effect of drugs, such as micro- and nanoscale needles, pumps, valves, and implantable drug delivery devices. These advances are expertly presented in this book.

Why do we observe such an explosion in research in this field now? The development of nanoparticulate systems for biological applications has taken a level of sophistication never before seen in the field of biomedicine. Using intelligent polymers, it is now possible to design new devices for intelligent diagnostics, therapeutics, molecular communication, etc. Such systems can be employed for auto-feedback action, whereby the biomaterial can be designed to rapidly respond to changes in the external biological conditions. This idea may be used to study biological communication and develop novel biological machines. This book presents new molecular techniques which are used to design new biomaterials based on star polymers, symmetric structures of inorganic and organic materials, dendrimers, self-assembled monolayers and biological/synthetic constructs.

In view of the growing need in biological, biomolecular and biomedical engineering for scientists with a broad, but strong, background in materials engineering and biological sciences, this book will promote the investigation and utilization of novel macromolecular structures, biohybrid systems and biopolymers with ability to interact with or recognize external phenomena associated with biological or physiological solutions. The book incorporates educational and research components with emphasis on the synthesis, design, development and analysis of novel structures useful in the biomedical, biochemical, cellular and related fields.

Nanostructured materials have thus created great excitement in research and industrial circles because of numerous and diverse applications in electronic devices, automobile engines, industrial catalysts, and cosmetics. To date, and despite their great promise, applications of nanophase materials in the biomedical field (other than in drug delivery) have been close to nonexistent. Undoubtedly, the capability of synthesizing and processing nanomaterials with tailored structures and enhanced properties provides tremendous opportunities for designing novel biomaterials of exceptional promise for biomedical applications.

Downloaded on 01/09/2013 10:25:45.

Finally, the book addresses some of the novel applications of intelligent materials which can be used in electronic devices. This raises exciting possibilities for combining microelectronics and biotechnology to develop new technologies with unprecedented power and versatility. Thus, in recent years we have seen an explosion in the field of novel microfabricated and nanofabricated devices for drug delivery.

This book covers all the areas addressed above in a most thorough way. Various mechanisms of triggering drug delivery are addressed in a number of chapters. After a careful introduction of the importance of intelligent polymers in drug delivery by the editors Carmen Alvarez-Lorenzo and Angel Concheiro, expert reviews of temperature and pH-sensitive liposomes are presented by David Needham of Duke University and S. P. Vyas and associates of Dr. Harisingh Gour University. The corresponding behavior of temperature and pH-sensitive micelles is addressed by C. Kojima of Osaka Prefecture University. William Pitt and associates of the University of Utah address interesting and important applications of ultrasound-triggered release from micelles.

Polymersomes are a relatively new class of important intelligent polymer structures that can be used in drug delivery. This subject is expertly addressed by Giuseppe Battaglia of the University of Sheffield. Two important aspects of intelligent systems utilize reduction-sensitive nanosystems mostly for intracellular drug delivery, as carefully presented by R. Cheng, F. Meng, C. Deng and Z. Zhong of Soochow University, and enzyme-responsive drug delivery systems, as described by P. F. Caponi and R. V. Ulijn of the University of Strathclyde.

In subsequent chapters, the editors have tried to present important biological applications of all these smart materials. For example, Cameron Alexander and associates from the University of Nottingham address the use of bioresponsive polyplexes and micelleplexes, while the editors give a detailed analysis of our latest knowledge on UV and near-IR triggered release from nanoparticles. Another important triggering mechanism is heating via remote irradiation of gold nanoparticles-based systems, which is addressed by E. K. Lim and associates of Yonsei University. Finally, magnetic-responsive nanoparticles for drug delivery are expertly presented by Ting-Yu Liu of the National Taiwan University and associates.

Recent advances in nanoscale systems based on inorganic materials that are finding applications in drug delivery are presented by Maria Vallet-Regi of the Complutense University (silica nanoparticles) and Gerard Tobias and Emmanuel Flahaut of CMAB-CSIC, Barcelona, Spain and the University Paul Sabatier (smart carbon nanotubes). The use of smart layer-by-layer films is a powerful new method with important applications in drug delivery and is expertly discussed by S. Sukhishvili and S. Pavlukhina of Stevens Institute of Technology.

In the next few chapters, the editors have elected to present new applications of intelligent hydrogels, a subject of major interest to the medical and pharmaceutical fields. Thus, Francesco Puoci and Manuela Curcio of the University

Downloaded on 01/09/2013 10:25:45.

of Calabria discuss temperature- and pH-responsive hydrogels, Jose Carlos Rodriguez-Cabello and associates of the University of Valladolid address elastin-like hydrogels and self-assembled nanostructures, while Mario and Ilaria Casolaro discuss multiple stimuli-responsive hydrogels. The editors Carmen Alvarez-Lorenzo and Angel Concheiro offer an expert presentation of molecularly-imprinted hydrogels and associated techniques. These materials appear to have great promise for a variety of applications. Finally, T. Miyata of Kansai University discusses the latest advances in biomolecule-sensitive hydrogels.

In the development of smart biomaterials, it is often desired to attain spatial control of cells and related biological organisms. Numerous surface micro- and/or nanofabrication techniques have been developed in order to create a material for regulating cell functions for application in tissue engineering, microbiosensors, and other applications requiring a desired pattern of response from the cells. Teruo Okano and H. Takahashi of the Tokyo Women's Medical University present a thorough review of the latest research on intelligent surfaces for cell and tissue delivery. The book ends with another chapter written by the editors Carmen Alvarez-Lorenzo and Angel Concheiro that addresses an important area for current and future applications, that of drug/medical device combination products. Often these combination products are designed with possible stimuli-responsive eluting surfaces and promise to exhibit recognitive characteristics.

I think that all researchers in the field of drug delivery will find this new book a very valuable addition in the field and will use it for many years to come. I know I will.

Nicholas A. Peppas, ScD, NAE, IOM, FBSE
The University of Texas at Austin
Austin, Texas, USA

Downloaded on 01/09/2013 10:25:44.

Preface

Writing a book is an adventure, in words of Winston Churchill. Editing a book is not lesser adventure. It is both a challenging and a rewarding task. We put a foot in this adventure when Prof. Hans-Jörg Schneider encouraged us to think about a book project for the RSC Series on Smart Materials with a focus on Drug Delivery; the second foot was put when the RSC Publications Committee approved our proposal. The design and application of stimuli-responsive materials is a growing field that benefits from contributions of people from diverse backgrounds all around the world. Numerous drug delivery systems with advanced performances based on the features of smart materials have come up in the last years. A wide range of materials with diverse structure, their processing for creating carriers of varied architecture, and the responsiveness to physiological variables, to illness markers or to external stimuli useful for triggering or switching on/off drug release are addressed in the present book. In addition to small synthetic drugs, other classes of therapeutic molecules or even cells are covered. A balance between novelty and clinical possibilities was the criterion followed to choose the contents, which were organized as a function of the carrier architecture and the stimulus that activates the release. Drug-device combination products were also taken into account. An effort has been made to not be lost in the particular details, but to prioritize the general concepts that are behind the design and functioning of intelligent drug delivery systems.

It was truly rewarding when the invited contributors answered very positively to the book project. We are in debt with all of them for their efforts on writing comprehensive as well as educational chapters, covering in detail the state-of-the-art in each assigned topic. Our acknowledgement goes also to Prof. Nicholas Peppas for his always encouraging comments and the kind foreword, and to the people of the RSC editorial office, particularly Mrs. Alice Toby-Brant, for providing an invaluable help with formal and not so formal aspects.

RSC Smart Materials No. 2
Smart Materials for Drug Delivery: Volume 1
Edited by Carmen Alvarez-Lorenzo and Angel Concheiro
© The Royal Society of Chemistry 2013
Published by the Royal Society of Chemistry, www.rsc.org

We finally would like to thank the readers of this book, from who we will be very happy to receive comments and feedback. Working in the interface between stimuli responsiveness and drug delivery is itself a tricky and long adventure, but along the path outstanding advances for therapeutics are already becoming a reality. We hope that this text would serve as a guide for the beginners in the field and as a multidisciplinary meeting point for researchers involved in quite diverse areas.

Carmen Alvarez-Lorenzo
Angel Concheiro
Department of Pharmacy and Pharmaceutical Technology
Faculty of Pharmacy, University of Santiago de Compostela
15782-Santiago de Compostela (Spain)

Downloaded on 01/09/2013 10:25:44.

Downloaded on 01/09/2013 10:25:48.

Contents

Volume 1

Chapter 1 From Drug Dosage Forms to Intelligent Drug-delivery Systems: a Change of Paradigm 1
C. Alvarez-Lorenzo and A. Concheiro

1.1 Evolution of Drug Dosage Forms 1
1.2 Advanced Excipients 4
1.3 Stimuli-responsive Components 9
  1.3.1 Phase Transitions 11
  1.3.2 Memorization of the Conformation. Molecular Imprinting and Recognition 14
1.4 Intelligent Drug-delivery Systems 15
  1.4.1 pH- and/or Ion-responsive DDSs 16
  1.4.2 Enzyme-responsive DDSs 18
  1.4.3 Biochemical-responsive DDSs 19
  1.4.4 Glutathione-responsive DDSs 21
  1.4.5 Temperature-responsive DDSs 21
  1.4.6 Ultrasound-responsive DDSs 23
  1.4.7 Light-responsive DDSs 23
  1.4.8 Magnetic-responsive DDSs 24
  1.4.9 Electric Field-responsive DDSs 24
1.5 Conclusions and Future Aspects 25
Acknowledgements 26
References 26

RSC Smart Materials No. 2
Smart Materials for Drug Delivery: Volume 1
Edited by Carmen Alvarez-Lorenzo and Angel Concheiro
© The Royal Society of Chemistry 2013
Published by the Royal Society of Chemistry, www.rsc.org

Downloaded on 01/09/2013 10:25:48.

Chapter 2 Materials Science and Engineering of the Low Temperature Sensitive Liposome (LTSL): Composition-Structure-Property Relationships That Underlie its Design and Performance **33**
David Needham and Mark W. Dewhirst

2.1 Introduction 33
  2.1.1 Lipids as "Smart Materials" 33
  2.1.2 Micelles, Bilayers and Inverted Micelles 36
2.2 Reverse Engineering the LTSL 36
  2.2.1 Define the Function 37
  2.2.2 LTSL Component Design 39
  2.2.3 Materials Choice and CSP Relationships 40
  2.2.4 Composition-Structure-Properties of Each Component 42
2.3 Production 51
2.4 Performance-in-Service 53
  2.4.1 Performance-in-Service: *in vitro* 53
  2.4.2 Performance-in-Service: *in vivo* (Preclinical) 60
  2.4.3 Performance-in-Service: *in vivo* (Canine and Human Clinical Trials) 64
2.5 Future Prospects 69
  2.5.1 New ThermoDox® Trials and Preclinical Studies 70
  2.5.2 Other Drugs 70
  2.5.3 Other New Thermal-sensitive Formulations (Lipids and Polymers) 71
2.6 Concluding Remarks 72
  2.6.1 The Drug-delivery Problem 72
  2.6.2 A New Paradigm for Local Drug Delivery: Drug Release in the Bloodstream 72
  2.6.3 New Horizons 73
Acknowledgements 74
References 74

Chapter 3 pH-sensitive Liposomes in Drug Delivery **80**
Shivani Rai Paliwal, Rishi Paliwal and Suresh P Vyas

3.1 Introduction 80
3.2 pH-sensitive Liposomes as Smart Drug Carriers 82
3.3 Uptake and Intra-cellular Delivery of Therapeutic Agents from pH-sensitive Liposomes 86
3.4 Therapeutic Applications of pH-sensitive Liposomes 87
  3.4.1 Cancer Chemotherapy 87
  3.4.2 Gene Delivery 89
  3.4.3 Tumor Diagnosis 90

Downloaded on 01/09/2013 10:25:48.

3.5 Conclusion 90
References 91

Chapter 4 Smart Dendrimers 94
Chie Kojima

4.1 Introduction 94
4.2 Temperature-responsive Dendrimers 96
4.2.1 Dendrimers Containing Thermo-sensitive Polymers 97
4.2.2 Dendrimers Containing Thermo-sensitive Moieties 98
4.2.3 Collagen-mimic Dendrimers 99
4.3 Photoresponsive Dendrimers 100
4.3.1 Dendrimers for Photochemical Internalization 100
4.3.2 Dendrimers with Photodegradable Moieties 101
4.4 pH-responsive Dendrimers 102
4.4.1 Dendrimers Containing pH-responsive Moieties 102
4.4.2 Dendrimer Assembly with pH-sensing Moieties 103
4.4.3 Drug-dendrimer Conjugates with pH-responsive Linkages 104
4.5 Redox-responsive Dendritic Polymers 105
4.6 Enzyme-responsive Dendritic Polymers 105
4.7 Theragnostic Dendrimers 108
4.8 Conclusion 109
Acknowledgements 109
References 109

Chapter 5 Temperature- and pH-sensitive Polymeric Micelles for Drug Encapsulation, Release and Targeting 115
Alejandro Sosnik

5.1 (Bio)pharmaceutic Challenges in Therapeutics 115
5.2 Polymeric Micelles 116
5.2.1 Micellar Encapsulation 117
5.2.2 Preparation Methods 118
5.2.3 Physical Stability 119
5.3 Temperature-sensitive Polymeric Micelles 120
5.3.1 Poly(ethylene Oxide)-Poly(propylene Oxide) and Other Polyether Amphiphiles 121
5.3.2 Poly(ethylene Oxide)-Polyester Block Copolymers 127

5.3.3 Poly(*N*-isopropylacrylamide) 128
5.3.4 Substitutes of PEG as Hydrophilic Building Block 132
5.4 pH-responsive Micelles 133
5.5 Translation into Clinics and Perspectives 135
Acknowledgements 137
References 137

Chapter 6 Ultrasound-triggered Release from Micelles 148
William G. Pitt, Ghaleb A. Husseini and Laura N. Kherbeck

6.1 Introduction 148
6.2 Ultrasound 149
6.2.1 Physics of Ultrasound 149
6.3 Micelles 155
6.3.1 Drug Delivery from Micelles 155
6.3.2 Targeting 159
6.3.3 Ultrasound-triggered Release from Micelles 161
6.4 The Future of Ultrasound-triggered Drug Delivery from Micelles 169
References 171

Chapter 7 Smart Polymersomes: Formation, Characterisation and Applications 179
R. T. Pearson, M. Avila-Olias, A. S. Joseph, S. Nyberg and G. Battaglia

7.1 Polymersome Formation 179
7.2 Polymersomes Characterization 185
7.3 Polymersomes as Delivery Vectors 188
7.4 Polymersomes in Medicine and Pharmacy 196
References 202

Chapter 8 Reduction-sensitive Nanosystems for Active Intracellular Drug Delivery 208
Ru Cheng, Fenghua Meng, Chao Deng and Zhiyuan Zhong

8.1 Introduction 208
8.2 Reduction-sensitive Polymeric Micelles 210
8.2.1 Reduction-sensitive Shell-sheddable Micelles 210
8.2.2 Micelles with Reduction-sensitive Core 213
8.2.3 Reduction-sensitive Cross-linked Micelles 214

Downloaded on 01/09/2013 10:25:48.

Downloaded on 01/09/2013 10:25:48.

8.3 Reduction-sensitive Polymersomes 219
8.4 Reduction-sensitive Nanoparticles 221
8.5 Reduction-sensitive Capsules 223
8.6 Reduction-sensitive Nanogels 226
8.7 Conclusions 227
Acknowledgements 227
References 227

Chapter 9 Enzyme-responsive Drug-delivery Systems 232
Pier-Francesco Caponi and Rein V. Ulijn

9.1 Introduction 232
  9.1.1 Exploiting Enzymes in Drug Delivery 234
  9.1.2 Factors to Consider in the Design of ERMs for Drug Delivery 236
9.2 Enzyme-responsive Hydrogels 237
  9.2.1 Chemically Cross-linked Hydrogels 238
9.3 Enzyme-responsive Micelles 244
  9.3.1 Disruptive Enzyme-responsive Micelles 244
  9.3.2 Switchable Micelles 246
9.4 Enzyme-responsive Silica Nanocontainers 248
9.5 Conclusion 251
References 252

Chapter 10 Bioresponsive Polyplexes and Micelleplexes 256
Cameron Alexander and Francisco Fernandez Trillo

10.1 Introduction 256
10.2 pH-responsive Polyplexes 258
10.3 Reducible Polyplexes 261
10.4 Thermo-responsive Polyplexes 269
10.5 Other Stimuli-responsive Polyplexes 273
10.6 Dual Responsive Polyplexes 274
10.7 Conclusions 275
Cell Lines Mentioned in this Chapter 276
References 276

Chapter 11 Advances in Drug-delivery Systems Based on Intrinsically Conducting Polymers 283
Manisha Sharma, Darren Svirskis and Sanjay Garg

11.1 Introduction 283
11.2 Polymerisation 284

Downloaded on 01/09/2013 10:25:48.

11.3 Properties 285
  11.3.1 Conductivity 285
  11.3.2 Stability 285
  11.3.3 Biosensing 286
  11.3.4 Solubility 286
11.4 Characterization 286
  11.4.1 Infrared (IR) and Raman Spectroscopy 286
  11.4.2 Atomic Force Microscopy 287
  11.4.3 Cyclic Voltammetry 287
11.5 Biocompatibility 287
11.6 Mechanisms for Controlled Drug Release 288
  11.6.1 Utilizing Electrostatic Forces in ICPs 288
  11.6.2 Volume Changes in ICPs 289
11.7 Drug-delivery Systems 290
  11.7.1 Reservoir Systems 290
  11.7.2 Actuating Devices 292
  11.7.3 Matrix Type 296
  11.7.4 Miscellaneous Devices 297
11.8 Demonstration of Biological Applications 299
11.9 Conclusions 300
References 300

Chapter 12 UV and Near-IR Triggered Release from Polymeric Micelles and Nanoparticles 304
Manuel Alatorre-Meda, Carmen Alvarez-Lorenzo, Angel Concheiro and Pablo Taboada

12.1 Introduction 304
12.2 UV and Near-IR Light Irradiation 305
  12.2.1 UV-visible Light 305
  12.2.2 Near-IR light 306
12.3 Mechanisms of Light-triggered Release 307
12.4 Light-sensitive Polymeric DDSs 308
  12.4.1 Light-sensitive Polymeric Micelles 308
  12.4.2 Polymeric Vesicles 320
  12.4.3 Polymeric Nano-/microparticles 327
12.5 Conclusion and Outlook 338
Acknowledgements 338
References 339

Subject Index 349

Volume 2

Chapter 13 Remotely Triggered Drug Release from Gold Nanoparticle-based Systems 1
Eun-Kyung Lim, Kwangyeol Lee, Yong-Min Huh and Seungjoo Haam

13.1 Introduction 1
13.2 Gold Nanoparticle-based DDSs 2
13.3 Activatable DDSs Based on Gold Nanoparticles 7
  13.3.1 pH-responsive Au-based DDSs 9
  13.3.2 Glutathione-mediated Au-based DDSs 10
  13.3.3 Photo-active and/or Photodynamic Au-based DDSs 10
  13.3.4 Photothermally Mediated Au-based DDSs 14
  13.3.5 Enzymatically Activated Au-based DDSs 20
13.4 Gold Nanoparticle-based Theranostic Systems 21
13.5 Conclusions and Outlook 23
References 23

Chapter 14 Magnetic-responsive Nanoparticles for Drug Delivery 32
San-Yuan Chen, Shang-Hsiu Hu and Ting-Yu Liu

14.1 Introduction 32
14.2 Hyperthermia Theory of the Magnetic Field 34
14.3 Synthesis and Surface Modification of Magnetic Nanoparticles 37
  14.3.1 Synthesis of Magnetic Nanoparticles 37
  14.3.2 Surface Modification of Magnetic Nanoparticles 38
14.4 Magnetic Nanocarriers for Drug Delivery 40
  14.4.1 Amphiphilic Micelles and Organic Nanoparticles 41
  14.4.2 Temperature-responsive Magnetic Nanocarriers 44
14.5 Nanocarriers with a Magnetic Shell as DDSs 50
  14.5.1 Polymer Drug Carriers with Magnetic Nanoparticle Shells 50
  14.5.2 Mesoporous Silica Capped with Iron-oxide Nanoparticles 51
  14.5.3 Magnetic Single-crystal Shell Drug Nanocarriers 54

Downloaded on 01/09/2013 10:25:48.

14.6 Magnetic-responsive Composite Drug-delivery Membranes 56
14.7 Conclusion 59
References 60

Chapter 15 Smart Drug Delivery from Silica Nanoparticles 63

Montserrat Colilla and María Vallet-Regí

15.1 Introduction 63
15.2 Multi-functionality of Mesoporous Silica Nanoparticles to Design Smart DDSs 66
  15.2.1 Targeting Agents 66
  15.2.2 Polymeric Coatings 68
  15.2.3 Magnetic Nanoparticles 72
  15.2.4 Stimuli-responsive Drug Delivery 75
15.3 Biocompatibility of Mesoporous Silica Nanoparticles 80
15.4 Future Prospects 81
References 82

Chapter 16 Smart Carbon Nanotubes 90

Gerard Tobias and Emmanuel Flahaut

16.1 Introduction 90
  16.1.1 Carbon Nanotubes: Structure and Properties 90
  16.1.2 Carbon Nanotubes in Drug Delivery 91
16.2 Functionalization of Carbon Nanotubes for Biomedical Applications 93
  16.2.1 Covalent Functionalization 93
  16.2.2 Non-covalent Functionalization 95
16.3 External Attachment of Drugs onto Carbon Nanotubes 96
  16.3.1 Delivery of Doxorubicin with Carbon Nanotubes 96
  16.3.2 Delivery of Platinum-based Drugs with Carbon Nanotubes 97
  16.3.3 Delivery of Other Anticancer Drugs by Carbon Nanotubes 98
  16.3.4 Delivery of Other Drugs by Carbon Nanotubes 99

Downloaded on 01/09/2013 10:25:48.

Downloaded on 01/09/2013 10:25:48.

16.4 Encapsulation of Drugs Inside Carbon Nanotubes 100
  16.4.1 Carbon Nanotubes as Nanocontainers 100
  16.4.2 Drug Delivery with Filled Carbon Nanotubes 101
16.5 Toxicity and Environmental Impact of Carbon Nanotubes 104
  16.5.1 Introduction to Toxicity of Carbon Nanotubes 104
  16.5.2 Main Characteristics of Carbon Nanotubes in Terms of Toxicity Investigation 105
  16.5.3 Biological Models 106
  16.5.4 Inhalation 107
  16.5.5 Contamination through the Skin 108
  16.5.6 Translocation 108
  16.5.7 Mechanisms of Protection and Elimination 108
  16.5.8 Genotoxicity 109
  16.5.9 Environmental Impact of Carbon Nanotubes 109
16.6 Conclusions 110
References 110

Chapter 17 Smart Layer-by-Layer Assemblies for Drug Delivery 117
Svetlana Pavlukhina and Svetlana Sukhishvili

17.1 Introduction 117
17.2 LbL Substrates and Templates 117
17.3 LbL Constituents and Architectures 119
17.4 Drug Incorporation Strategies within LbL Assemblies 123
17.5 Drug Release Strategies 124
  17.5.1 Diffusion-controlled Release 124
  17.5.2 Hydrolytic Degradation 125
  17.5.3 pH-triggered Release 129
  17.5.4 Salt-triggered Release 133
  17.5.5 Electrochemical and Redox-activated Release 134
  17.5.6 Temperature-triggered Release 136
  17.5.7 Light-triggered Release 137
  17.5.8 Magnetic Field-triggered Release 139
  17.5.9 Ultrasound-triggered Release 140
  17.5.10 Application of Biological Stimuli 141
17.6 LbL Interfacing Biology 142
Acknowledgements 144
References 144

Downloaded on 01/09/2013 10:25:48.

Chapter 18 pH- and Temperature-responsive Hydrogels in Drug Delivery 153
Francesco Puoci and Manuela Curcio

18.1 Introduction 153
18.2 pH-responsive Hydrogels for Drug Delivery 155
  18.2.1 pH-responsive Microgels 156
  18.2.2 pH-responsive Nanogels 158
18.3 Temperature-responsive Hydrogels for Drug Delivery 161
  18.3.1 LCST Hydrogels 162
  18.3.2 UCST Hydrogels 168
18.4 Dually Responsive Hydrogels for Drug Delivery 170
18.5 Conclusion 173
Acknowledgements 174
Reference 174

Chapter 19 Elastin-like Hydrogels and Self-assembled Nanostructures for Drug Delivery 180
José Carlos Rodríguez-Cabello, Israel González de Torre and Guillermo Pinedo

19.1 Introduction 180
19.2 Elastin-like Recombinamers (ELRs) 181
19.3 ELRs-based Drug-delivery Systems 183
  19.3.1 ELRs-based Hydrogels 184
  19.3.2 ELRs Nanoparticles 190
19.4 Conclusion and Future Perspectives 195
References 196

Chapter 20 Multiple Stimuli-responsive Hydrogels Based on α-Amino Acid Residues for Drug Delivery 199
Mario Casolaro and Ilaria Casolaro

20.1 Introduction 199
20.2 Syntheses 203
20.3 Swelling Properties 204
  20.3.1 Effect of pH and Ions 204
  20.3.2 Effect of the Temperature 209
20.4 Drug Delivery from α-Amino Acid Hydrogels 211
  20.4.1 Loading and Release of Cisplatin 211
  20.4.2 Cytotoxicity of Cisplatin-loaded Hydrogels 214
  20.4.3 Loading and Release of Pilocarpine 217
  20.4.4 Cytotoxicity of Pilocarpine-loaded Hydrogels 220

Downloaded on 01/09/2013 10:25:48.

20.5 Outlook for the Future 221
20.6 Conclusion 224
References 225

Chapter 21 Molecularly Imprinted Hydrogels for Affinity-controlled and Stimuli-responsive Drug Delivery 228
C. Alvarez-Lorenzo, C. González-Chomón and A. Concheiro

21.1 Introduction 228
21.2 Molecular Imprinting Technology 229
21.3 Imprinted Hydrogels 235
  21.3.1 Affinity-controlled Release from Bioinspired Networks 235
  21.3.2 Competitive Displacement Release 240
  21.3.3 Hydrolytically Induced Drug Release 242
21.4 Stimuli-responsive Imprinted Networks 243
  21.4.1 Temperature-sensitive Imprinted Hydrogels 245
  21.4.2 pH-sensitive Imprinted Gels 249
  21.4.3 Light-responsive Imprinted Networks 251
21.5 Conclusions and Future Aspects 254
Acknowledgements 254
References 255

Chapter 22 Biomolecule-sensitive Hydrogels 261
Takashi Miyata

22.1 Introduction 261
22.2 Strategies for Designing Biomolecule-sensitive Hydrogels 262
22.3 Glucose-sensitive Hydrogels 264
  22.3.1 Glucose-sensitive Hydrogels Using Enzymatic Reaction 264
  22.3.2 Glucose-sensitive Hydrogels Using Phenylboronic Acid 266
  22.3.3 Glucose-sensitive Hydrogels Using Lectin 266
22.4 Protein-sensitive Hydrogels 270
  22.4.1 Enzyme-sensitive Hydrogels 270
  22.4.2 Antigen-sensitive Hydrogels 272
22.5 Biomolecule-sensitive Hydrogels Prepared by Molecular Imprinting 276
22.6 Biomolecule-sensitive Hydrogel Particles 279
22.7 Other Biomolecule-sensitive Hydrogels 282
22.8 Conclusion 285
References 285

Downloaded on 01/09/2013 10:25:48.

Chapter 23 Intelligent Surfaces for Cell and Tissue Delivery **290**
Hironobu Takahashi and Teruo Okano

23.1 Introduction 290
23.2 Overview of Polymeric Materials for Cell/Tissue Delivery 291
  23.2.1 Self-regulating Insulin Delivery System as a Substitute for Cell Transplantation 291
  23.2.2 Microencapsulation of Cells with Polymeric Membranes for Cell Delivery 292
  23.2.3 Scaffold-based Cell/Tissue Delivery in Tissue Engineering 293
23.3 The Intelligence of Thermo-responsive Polymers for Cell/Tissue Delivery 294
  23.3.1 Thermo-responsive Poly(*N*-isopropylacrylamide) 294
  23.3.2 Thermo-responsive Encapsulation of Cells for Cell Delivery 294
23.4 Thermo-responsive Surface for Cell Sheet-based Tissue Delivery 295
  23.4.1 Cell Sheet Engineering for Scaffold-free Cell/Tissue Delivery Systems 295
  23.4.2 Thermo-responsive Polymer Grafting on Cell Culture Substrates 295
  23.4.3 Cell Sheet-based Tissue Delivery in Regenerative Medicine 296
  23.4.4 Local Drug Release Technique with Cell Sheet Transplantation 298
  23.4.5 Micro-fabricated Thermo-responsive Surfaces for Delivery of Tissue-mimicking Cell Sheets 301
23.5 Conclusions 307
References 307

Chapter 24 Drug/Medical Device Combination Products with Stimuli-responsive Eluting Surface **313**
C. Alvarez-Lorenzo and A. Concheiro

24.1 Combination Products 313
24.2 Benefits of Combining Medical Devices and Drugs/Biological Products 316
24.3 Materials for Medical Devices 317
24.4 Procedures to Incorporate Drugs 318
  24.4.1 Compounding 318
  24.4.2 Impregnation Using a Swelling Solvent 319

24.4.3 Coating 320
24.4.4 Drug Chemically Bonded to the Surface 320
24.4.5 Polymer Grafting to the Device Surface 321
24.5 Responsive Surfaces for Drug Loading/Controlled Release 325
24.5.1 Polymers Grafted by Means of Chemical Initiators 325
24.5.2 Polymers and Networks Grafted Applying Radiation 329
24.5.3 Surface Modification Applying Plasma Techniques 339
24.6 Conclusions and Future Aspects 341
Acknowledgements 342
References 342

Subject Index **349**

Downloaded on 01/09/2013 10:25:48.

Downloaded on 01/09/2013 10:25:48.

Downloaded on 01/09/2013 10:25:46.

CHAPTER 1

From Drug Dosage Forms to Intelligent Drug-delivery Systems: a Change of Paradigm

C. ALVAREZ-LORENZO* AND A. CONCHEIRO

Departamento de Farmacia y Tecnología Farmacéutica, Facultad de
Farmacia, Universidad de Santiago de Compostela, 15782-Santiago de
Compostela, Spain
*Email: carmen.alvarez.lorenzo@usc.es

1.1 Evolution of Drug Dosage Forms

Drug delivery has experienced unprecedented, outstanding progress in the last decades.[1,2] Dosage forms are almost as old as humanity, since the first human beings tried to find the best way to take and apply the available natural remedies that could ameliorate wounds and diseases. Although rudimentarily, the first civilizations realized that those remedies could not be used in a direct way and they required, for example, previous boiling in water (the seed of the liquid dosage forms) or mixing with components (*e.g.* fats) that enabled prolonged permanence on the application site (the first cataplasms or ointments) or an easier swallow (a solid preparation). Thus, together with the remedy containing the "active pharmaceutical ingredient", other substances named "excipients" (derived from the Latin verb *excipere*, which literally means *to mix*) should be incorporated into the medicines in order to make their administration easier but also to maintain their stability. Preparation of natural remedies with the poorly developed technology available up to the 1800s was a

---

RSC Smart Materials No. 2
Smart Materials for Drug Delivery: Volume 1
Edited by Carmen Alvarez-Lorenzo and Angel Concheiro
© The Royal Society of Chemistry 2013
Published by the Royal Society of Chemistry, www.rsc.org

Downloaded on 01/09/2013 10:25:46.

highly time-consuming task. Mortar, already mentioned in the Holy Scripts, was still in that epoch among the most advanced apparatus for preparing medicines. The industrial revolution was a milestone for the large-scale production of improved dosage forms and for the wide access of the population to medicines.[3] Advances in pharmacology and physiology, the birth of biopharmacy and the evolution development of pharmacokinetics, in the mid-twentieth century, made pharmacists and clinicians realize that the drug release rate from dosage forms is a key feature to achieve therapeutic benefits with minor collateral effects.[4] Although traditional dosage forms were expected to release the drug quite fast, this feature was barely taken into account. In fact, the requirement of a drug dissolution test for solid dosage forms was established for the first time in 1970.[5]

The first generation of controlled release systems (*rate-programmed drug release*) materialized in the 1970s with the aim of prolonging drug release as much as possible, in such a way that this process is the limiting step of the access of the drug to the systemic circulation.[3,5] Therefore, these drug dosage forms should release the drug according to a rate established by design, in a predictable way and disregarding the status of the patient, in order to achieve constant drug levels for a while, minimizing the number of intakes. To face to these demands, novel excipients appeared on the scene, mostly coming from the evolution of polymer science, with the commitment of regulating the release by dissolution, diffusion, erosion or osmotic mechanisms. Maintenance of drug levels in a therapeutically desirable range with lower dose per day improved treatment with short half-life drugs and patient compliance and also decreased the incidence of adverse events.[6] Through searching for controlling not only the time spent in the release but also the site at which the process should occur, a second generation of controlled release systems (*activation-modulated drug release*) appeared. The need to protect labile drugs from harsh environments in the body and to prevent side effects in regions where the drug is not intended to act or to be absorbed, led to devices capable of releasing the drug in specific regions of the body, first at specific sites of the gastrointestinal tract.[7] The release is activated by some physical, chemical or biochemical processes. Examples of excipients suitable for this purpose are polymers with pH-dependent solubility or time-dependent swelling, or that undergo enzymatic degradation at certain regions of the gastrointestinal tract.[8] The methodology and the acceptance criteria for extended-release and delayed-release products appeared in the United States Pharmacopoeia (USP) 21-National Formulary (NF) 16 of 1985,[5] and both first and second generations of controlled release systems are already well implanted in the current therapeutic arsenal.[9] Third-generation controlled release systems (*feedback-regulated drug release*) are envisioned as efficient couriers capable of delivering the drug at the best possible conditions to the target site modulating absorption, distribution and clearance, with the ability to feedback regulated drug release, which fits the physio-/pathological conditions of the body, particularly the progression of the illness.[10–15] The mechanisms behind the three generations of controlled release systems are schematically depicted in Figure 1.1.

Downloaded on 01/09/2013 10:25:46.

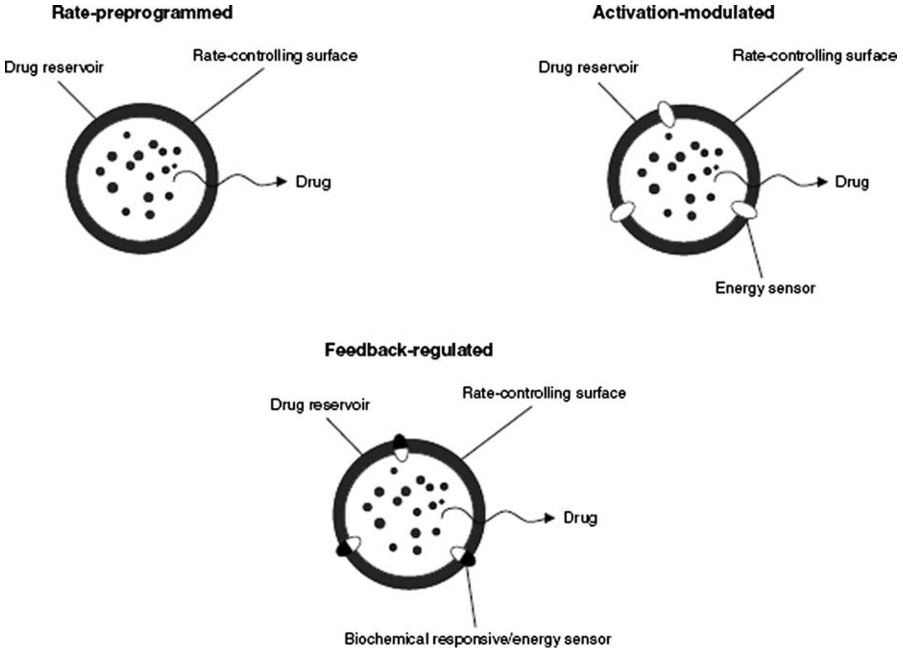
Rate-preprogrammed
Drug reservoir
Rate-controlling surface
Drug
Activation-modulated
Drug reservoir
Rate-controlling surface
Drug
Energy sensor
Feedback-regulated
Drug reservoir
Rate-controlling surface
Drug
Biochemical responsive/energy sensor

Figure 1.1 The three major approaches to control release from drug-delivery systems.
Reproduced from reference 8 with permission from Adis International Ltd.

Compared to the previous generations of controlled delivery systems, the third one involves a change of paradigm regarding the design criteria of drug-delivery systems (DDSs) and demands the availability of "active" excipients instead of the former "passive" ones of rigidly predicted behavior. The purpose is to regulate drug release rate as a function of the intensity/concentration of a triggering agent, such as the concentration of a biochemical substance that may serve as an index of the pathological state. When the triggering agent is above a certain level, release is activated. This induces a decrease in the concentration of the triggering agent and, finally, drug release is stopped. Thus, advanced excipients should now act as sensors and actuators, imitating the recognition role of enzymes, membrane receptors and antibodies in living organisms for regulation of chemical reactions and for maintenance of the homeostatic equilibrium.[16] Nanotechnology is also an important pillar of this third generation of DDSs, since in many cases performance as couriers is only possible if the components are integrated in nano-sized structures able to displace through the different compartments of the body to arrive at the target receptor.[17–20] PEGylation (polyethylene glycol conjugation of drugs or drug carriers), enhanced permeability and retention effect (EPR)-driven passive targeting and ligands-driven active targeting represent three key technologies that stimulate the development of nanocarriers.[1,21] From a therapeutic point of view, a discontinuous release as a function of specific signals is profitable in

Downloaded on 01/09/2013 10:25:46.

many situations, particularly when the drug is: i) very unstable in the biological medium and a premature release before reaching the site of action may lead to degradation (as in the case of peptides and therapeutic proteins); ii) highly toxic and it should accumulate only in the site of action with minimal exposure of the other organs or cells (*e.g.* cancer chemotherapeutics); iii) intended to reach specific cells or cellular structures that are not easily accessible from the general circulation (*e.g.* gene therapy); or iv) intended to be released at the right time mimicking circadian rhythms (*e.g.* hormones and drugs for heart rhythm disorders or asthma).[22–24] Thus, advanced DDSs are not only valuable for problematic new drug candidates and sophisticated biopharmaceuticals, which usually exhibit deficient biopharmaceutic and stability properties,[25,26] but also they may improve and give added value to drugs already in use in order to exploit fully their therapeutic potential.[27,28]

1.2 Advanced Excipients

The evolution from primitive dosage forms to advanced delivery systems is intimately linked to the development of suitable excipients of more and more sophisticated performance.[29,30] Pharmaceutical excipients are defined in the USP 33 as "substances other than the active pharmaceutical ingredient (API) that have been appropriately evaluated for safety and intentionally included in a drug-delivery system". Under such a wide definition, materials of very different chemical composition and functionality are covered. Traditional excipients are substances intended to facilitate the preparation of medicines, *e.g.* making easier some technological steps and providing a sufficient mass to handle each dosage unit, and to ensure stability during storage and fast release of the drug when administered.[30] However, as the physico-chemical features of new drugs become more complex and the therapeutic requirements in terms of site of delivery and release rate are more demanding, novel excipients are required.

The fact that excipients were not considered important for the pharmacological activity of the drug caused them to be largely underestimated until a few decades ago.[30] The modern evolution of excipients runs in parallel with that of biomaterials as a whole (*i.e.* "any material intended to interface with biological systems to evaluate, treat, augment or replace any tissue, organ or function of the body")[31] and hence it is also affected by advances in the joint efforts carried out by people working in different disciplines.[32] In the second half of the twentieth century, the integration of materials science and engineering principles enabled an enormous advance in materials suitable to be in contact with tissues, cells and biological substances for a prolonged time without causing harm. Such a first generation of biomaterials (bioinert materials) was the result of a change of paradigm in the understanding of the materials as entities not to be separately studied as a function of their nature (metals, ceramics, polymers), but to be evaluated regarding the processing–structure–property inter-relationships.[33] The interaction among disciplines initially quite far from each other opened novel ways to face to new challenges regarding functionality of the materials (Figure 1.2). For example,

Downloaded on 01/09/2013 10:25:46.

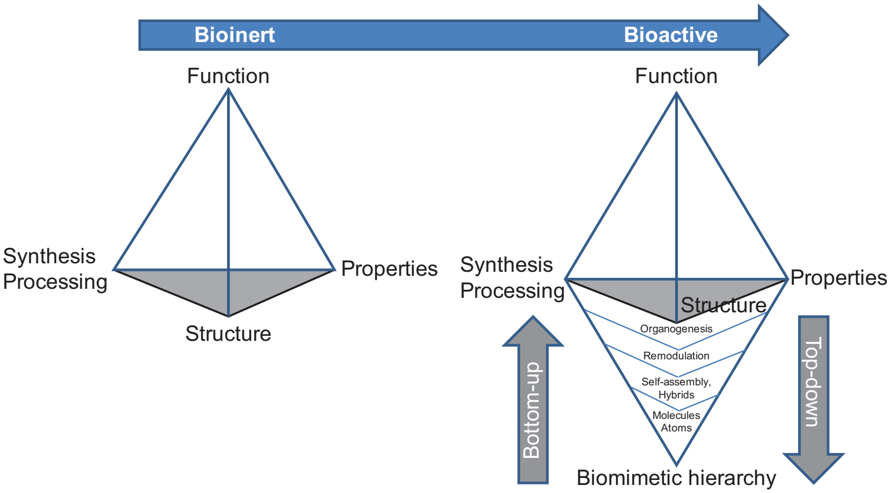

Figure 1.2 Schematic view of how the integration of knowledge from the materials science and engineering fields enabled the design of the first bioinert (not harmful) biomaterials. Later, integration of biology and biomedical sciences improved the performance of the biomaterials, endowing them with the ability to interact effectively with the body's components, to perceive their alterations and to respond in a suitable way. The hierarchical structure of such biomaterials is represented by the increasing length scale from atoms to materials and to supramolecular systems; the hierarchy can be achieved through the assembly of the components to obtain structures of increasing complexity (bottom-up approach) or through the fragmentation of greater structures (top-down approach).
Adapted from reference 33 with kind permission from Springer Science and Business Media.

availability of bioinert materials prompted the development of medical devices suitable to be inserted/implanted in the body for replacing or interfacing with damaged tissues or functions, through a passive interaction with the biological system. The improvements provided by these materials in diagnosis of pathologies, treatment of degenerative and accidental injuries and management of patients at critical conditions have been outstanding. Later on, the joining of biology and biomedical principles encouraged the development of biomaterials that react favorably with the body, making the implant successfully resemble the tissue or function that it is replacing and, for certain applications, enabling the implant to vanish from the body at a rate that fits that of the regeneration of the tissue. The design of this so-called second generation of biomaterials was possible not only due to the notable gain in knowledge about the body's components and their performances, but also because of the new way to look at the biological systems as engineering structures.[34]

The performance of Nature-designed materials is surprisingly outstanding and still hard to mimic if one considers the weakness of the construction elements.[35] The key point is the way the components are combined to create complex structures. Thus, the processing–structure–property paradigm has to

Downloaded on 01/09/2013 10:25:46.

be modified to include the hierarchical structure and the adaptative performance of the natural materials (Figure 1.2). Moreover, this task requires an intense collaboration of people with a background in diverse fields, since no single discipline covers the broad demand of knowledge required for the development of high-performance biomaterials.[33]

Polymers have played a pivotal role in this evolution process.[36] Since Hermann Staundinger set the basis of their structure at the beginning of the twentieth century,[37] there has been an intense breakthrough in the development of polymeric materials destined for a great variety of sanitary applications.[38,39] The confluence of polymer science with biomedical sciences became unavoidable as the design of polymers benefits from knowledge of the conformation and functionality of natural biomacromolecules, with the advantage that the synthetic structures are more stable and can be prepared applying versatile, less-expensive procedures, which can finely control their physico-chemical features and, consequently, their functionality.[2,40,41] The current level of the procedures of synthesis and of the analytical techniques enables the preparation of a well-characterized variety of polymers with a wide range of architectures (multi-block, hyperbranched, cross-linked, hybrid), which can carry out functions that a few years ago were difficult to imagine.[15,42–44] This is not a finished process and, as a consequence, the concept of "biomaterial" is also evolving from homogeneous monoliths towards hybrids and composites, ideally with biomimetic hierarchical and multi-functional structures.[31] Strictly speaking, cells may also be considered as biomaterials, since they have many properties similar to classical materials, for example viscoelasticity, and may be referred to as advanced stimuli-responsive polymeric systems.[45] As recently stated by D.F. Williams, "*the function of a biomaterial must be to direct the course of the medical treatment, be that in diagnosis or therapy, and it must do so by specifically controlling the interactions with biological components of the patient being treated*".[31] In the particular case of excipients, the performance after administration (role as a biomaterial) has to be combined with suitable features during fabrication and storage of the drug dosage forms or delivery systems. Excipients can now be considered as materials able to overcome constraints that prevent the drug from reaching the optimum therapeutic plasma/tissue level.[30] The current trend is to combine excipients that have specific functionality-related characteristics, namely, certain properties to improve the manufacture, the quality and the performance of the drug product.[46] Thus, excipients are categorized regarding functionality into three large groups: those that influence manufacturability, those that influence stability and those that influence drug release and pharmacokinetics.[30] Excipients able to perform at least two of these functions are designed as high-functionality or multi-functional ones.[47] Most of those excipients are polymers and they are expected to fulfill a large list of requirements for being useful not only in oral dosage forms, but also for parenteral drug applications (Figure 1.3).[2]

The third generation of biomaterials is intended to interact proactively with the biological functions, being able to perceive certain signals from the body

Downloaded on 01/09/2013 10:25:46.

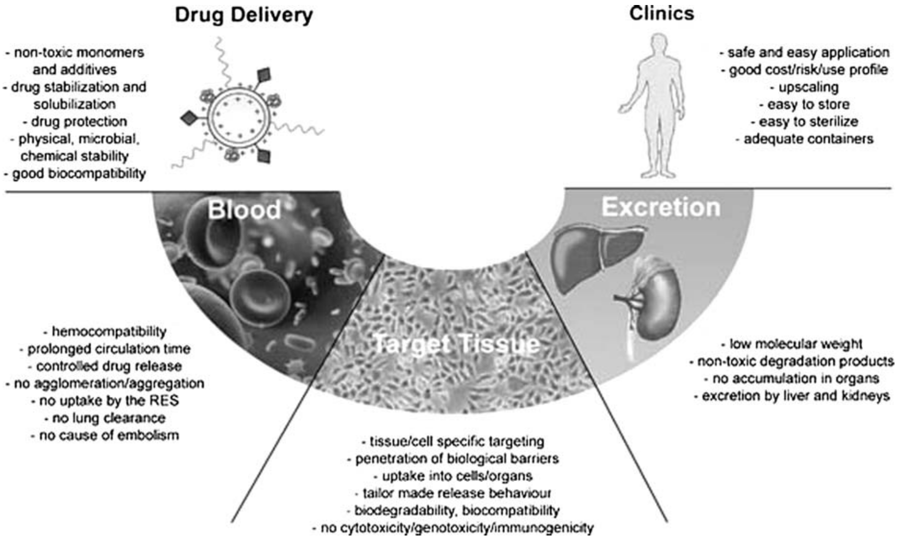
Drug Delivery
- non-toxic monomers and additives
- drug stabilization and solubilization
- drug protection
- physical, microbial, chemical stability
- good biocompatibility
Clinics
- safe and easy application
- good cost/risk/use profile
- upscaling
- easy to store
- easy to sterilize
- adequate containers
Blood
Target Tissue
Excretion
- hemocompatibility
- prolonged circulation time
- controlled drug release
- no agglomeration/aggregation
- no uptake by the RES
- no lung clearance
- no cause of embolism
- low molecular weight
- non-toxic degradation products
- no accumulation in organs
- excretion by liver and kidneys
- tissue/cell specific targeting
- penetration of biological barriers
- uptake into cells/organs
- tailor made release behaviour
- biodegradability, biocompatibility
- no cytotoxicity/genotoxicity/immunogenicity

Figure 1.3 Features to be taken into account when a polymer is intended to be used in a drug-delivery system.
Reproduced from reference 2 with permission of Wiley-VCH Verlag GmbH.

that are processed and transmitted in order to modify the behavior and function of the material (Figure 1.4). This avant-garde generation is also the seed for the development of stimuli-responsive drug carriers that modify their conformation to regulate drug release, and also of theranostic systems that combine diagnosis and drug-delivery capabilities in a single entity. Just as natural materials modulate their conformation and performance as a function of the conditions (stimuli) of the surrounding environment, high-performance components of DDSs should be able to tune the release as a function of the physio-/pathological state of the body, ideally as a function of the illness progression. These evolution issues compelled regulatory agencies to approve "new excipients", defined as "*any inactive ingredients that are intentionally added to therapeutic and diagnostic products, but that: (1) are not intended to exert therapeutic effects at the intended dosage, although they may act to improve product delivery (e.g., enhance absorption or control release of the drug substance); and (2) are not fully qualified by existing safety data with respect to the currently proposed level of exposure, duration of exposure, or route of administration*".[48,49]

Approval of new excipients (mainly of a polymeric nature and, less frequently, lipids and hybrids), although it may take less time than new drugs, requires safety and excretion/elimination assessments,[50,51] and thus additional groups of subjects have to be added in the clinical tests of the drug formulation for receiving the new excipients as placebo.[49] During the time of market exclusivity for the innovator, the new excipient will only be available from a single company, usually at a relatively high price. Furthermore, the use of the

Downloaded on 01/09/2013 10:25:46.

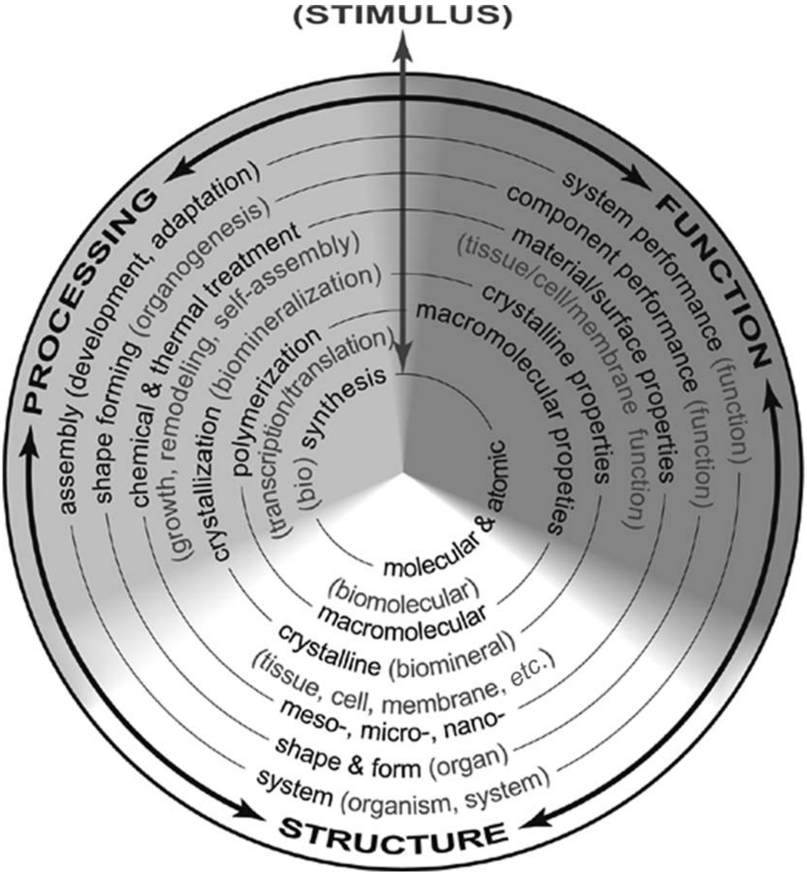
(STIMULUS)
PROCESSING
FUNCTION
STRUCTURE
assembly (development, adaptation)
shape forming (organogenesis)
chemical & thermal treatment
(growth, remodeling, self-assembly)
crystallization (biomineralization)
polymerization
(transcription/translation)
(bio) synthesis
system performance (function)
component performance (function)
material/surface properties
(tissue/cell/membrane function)
crystalline properties
macromolecular propeties
molecular & atomic
(biomolecular)
macromolecular
crystalline (biomineral)
(tissue, cell, membrane, etc.)
meso-, micro-, nano-
shape & form (organ)
system (organism, system)

Figure 1.4 Processing–structure–function relationships in biomaterials showing, in parentheses, the parallelism with biological systems. The adaptive features of biological systems are mimicked in the biomaterials as the ability to respond to stimuli.
Reproduced from reference 33 with kind permission from Springer Science and Business Media.

new excipients may be initially restricted to a certain concentration range and route of administration and may require additional environmental and safety considerations due to the limited information available. Thus, the innovator company has to solidly convince potential customers of the benefits of the new excipient.[49] Compared to the large number of materials for DDSs described in scientific papers, only a minor proportion has been tested in clinical trials, not all of which have proved to be safe.[2] In many cases, the likelihood of an adverse reaction to an excipient depends not only on its concentration, but also on the route, frequency and duration of the administration and on the by-products that may remain after purification.[2] The nanometric size of some advanced DDSs is also a concern, since the properties of a material dramatically change in the nanoscale (particularly the reactivity at the surface), compared to the

Downloaded on 01/09/2013 10:25:46.

micro- and macroscales, and the nanodevices can attain body sites that the conventional carriers have been not reached before.[20] Cytotoxicity, genotoxicity and antigenicity are major issues to be elucidated, and differential aspects of the patients, particularly the age (*e.g.* newborns and infants are not small adults) and the health conditions, should also be taken into account.[52–54] It should also be noticed that unexpected events may appear not in the first administration, but after prolonged use of a certain excipient. For example, an accelerated blood clearance (ABC) phenomenon has been observed for PEGylated nanocarriers; namely, a second dose injected few days later does not behave as "stealth", but rapidly disappears from the bloodstream. Although the origin is still controversial, it seems that PEG activates the immunological response, and the anti-PEG IgMs created are responsible for recognizing the second dose.[55] The lipid dose, the payloads and the way PEG is anchored in PEGylated liposomes seem to play a critical role in the induction of anti-PEG IgM production and, thus, the ABC phenomenon, as addressed in Chapter 3 of this book. Therefore, further studies are required to optimize PEGylated nanocarriers for treating diseases that require repeated administrations.

On the other hand, some excipients can exert certain biological activity by themselves that may have repercussions on the overall pharmacological activity of the system, making the boundaries between excipients and active pharmaceutical ingredients less clear.[41] Some polymers have shown intrinsic therapeutic functionality, particularly as sequestering agents in the gastrointestinal tract.[56,57] In the particular case of the DDSs, some excipients facilitate the cell uptake of the drug, enhancing the membrane permeability not only through physical perturbation of the bilayer, but also by inhibition of efflux pumps through participation in complex cascades inside the cells. One of the more clear examples is that of the poly(ethylene oxide)-poly(propylene oxide) (PEO-PPO) block copolymers that can block P-glycoproteins.[58,59] Polymeric micelles of these copolymers are endowed with a number of unique beneficial features: i) core-shell structure able to host hydrophobic drugs, raising the apparent solubility in aqueous medium; ii) size adequate for systemic administration and for a preferential accumulation (passive targeting) within tumors through the EPR effect; iii) surface suitable for binding of targeting moieties; and iv) unimers that modulate the activity of efflux pumps involved in multi-drug resistance (MDR).[60–62]

1.3 Stimuli-responsive Components

As introduced above, differently from the intrinsically inert components of the traditional drug dosage forms, which dissolve, erode or swell in the physiological environment according to a pre-established pattern, the stimuli-responsive networks, also termed "smart", "intelligent" or "environmentally sensitive" systems, can act as sensors of certain physical or chemical variables of the environment, and behave as actuators undergoing specific changes (as the living systems do).[63,64] In the biomedical field, the responsiveness has to be predictable, reproducible, proportional to the intensity of the signal and, ideally, reversible.[11,65,66]

Downloaded on 01/09/2013 10:25:46.

The DDSs that detect certain changes that take place in the biological medium (for example, in pH, temperature or concentration of some substances), activating or modulating the release rate, are named closed-loop or self-regulated systems. By contrast, the DDSs that switch drug release on/off as a function of specific external stimuli are considered to work in open circuit, and they can provide pulsed drug release when externally activated. Sensitivity to internal (*e.g.* pH, temperature, biomolecules) or external (*e.g.* light, electric or magnetic field) signals of the body is typically achieved by means of semisynthetic or synthetic materials (mostly polymers) that bear functional groups that modify their properties proportionally to the intensity of the signal and that enable transduction into changes in the material features.[63,67,68] The changes can have different levels of complexity; for example, i) a modification of the solubility, the shape or the state of aggregation of single components (*e.g.* assembly/disassembly of micelle unimers or sol-gel transition), ii) a reversible change in conformation of chemically cross-linked networks that lead to phase volume transitions and modifications in affinity towards other chemical groups or molecular entities, or iii) a reversible stretching/shrinking of surface-immobilized chains or networks on inert substrates (Figure 1.5).[2,39,69,70]

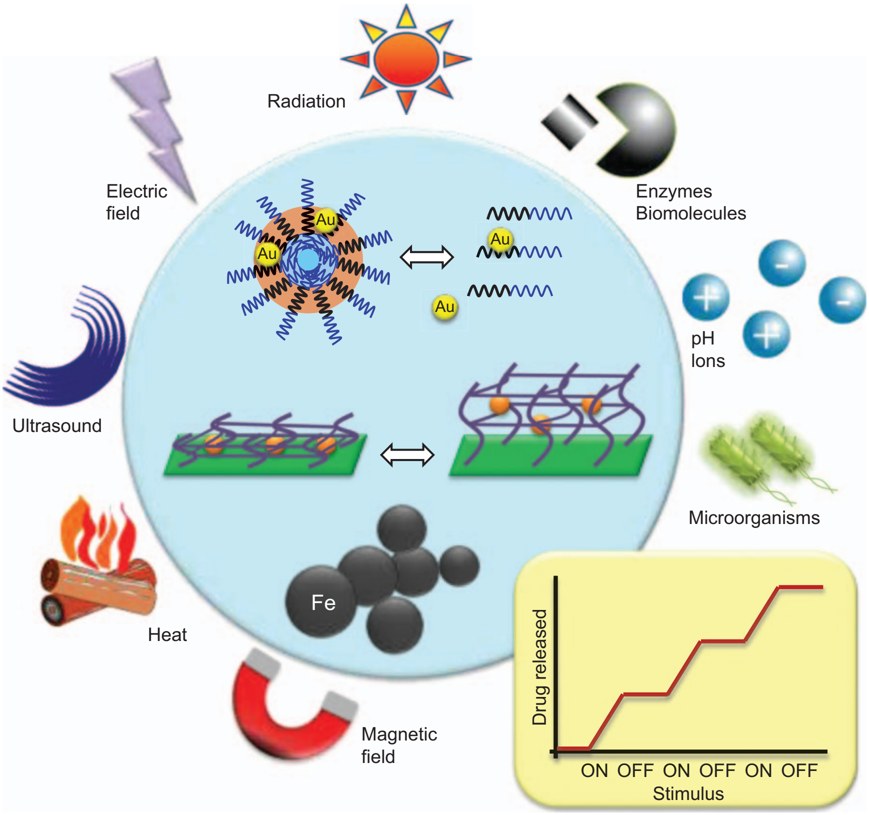

Figure 1.5 Some materials and stimuli suitable for development of stimuli-responsive drug-delivery systems.

Downloaded on 01/09/2013 10:25:46.

1.3.1 Phase Transitions

Polymers are the most widely used components of stimuli-responsive systems since they can be prepared with an unequalled richness of structures that enable many phase transitions to occur, leading to different states of conformation and association. Historically, the elucidation of the transitions began in 1940 when Flory[71] and Huggins[72] paid attention to the phase separations in polymer solutions caused by changes in the polymer–solvent or polymer–polymer interactions. These transitions are of first order except when near the critical point, where they can be of higher order. Later, the study of more complex systems and the evaluation of polypeptides and biological macromolecules attracted the interest of many researchers, who have notably contributed to identify more transitions and to elucidate their thermodynamics and kinetics. Detailed historical reviews on the understanding of the phase transitions can be consulted elsewhere.[73] Up to now ten transitions have been discovered, more than half being exclusive to polymers. The phase transitions are mainly of first order or second order. In the first case, the extensive thermodynamic quantities of volume, energy, entropy or number of moles of the macromolecules show a discontinuity as a function of the intensive quantities of pressure, temperature, chemical potential, *etc*. In the second-order case, no discontinuity is evident, but it appears when the derivatives of the extensive thermodynamic quantities are plotted. Mainly, to be useful as a stimuli-sensitive component for drug delivery, the polymer has to respond to the appearance/disappearance of the stimulus undergoing a first-order phase transition, accompanied by a change in the specific volume of the polymer.[74,75]

The transitions can be classified as a function of the number of macromolecules involved in the process, as follows:[73]

A) Transitions within one molecule, which occur because the sequential connectivity of the monomers along the polymer chain makes the monomers distinguishable from each other, differently from what happens when the monomers are free in a solution that behave similarly. This set of transitions comprises:
   i) *Polymer threading a membrane*, which occurs when a membrane that separates two solutions has holes that enable the passage of single polymer chains. Instead of completely diffuse from one solution to other, the chains remain in the holes attaching/detaching their ends to each side of the membrane. The transition is of first order.
   ii) *Helix to random coil transitions*, typical of single-stranded polypeptides, double-stranded DNA and triple-stranded collagen. A change in temperature or chemical potential alters the intra- and inter-strands hydrogen bonds and triggers diffuse, first-order and second-order transitions in the polypeptides, collagen and DNA, respectively. It should be noted that the first-order transitions of collagen are responsible for their role as the main structural protein in animals, since they confer elasticity. Furthermore, DNA in the cells does not pack alone, but with other molecules to undergo first-order

Downloaded on 01/09/2013 10:25:46.

transitions and to be more packed, since a second-order transition of naked DNA would lead to a random coil conformation with dimensions larger than those of the cells.[36]

iii) *Adsorption of an isolated polymer*, which refers to polymers that interact with surfaces being partially adsorbed forming trains and loops.[76] If one end of the polymer is attached to the surface, the other end remains free, and the monomers do not have attraction for the surface, so the number of contacts with the surface is limited to 1. Above the transition temperature, the number of contacts increases proportionally to the molecular weight of the polymer. In this case, the transition is of second order.

iv) *Equilibrium polymerization/1D crystallization*, as occurs when polymer chains are immersed in a solution of monomers. The chains are far apart from each other and grow (decrease) by means of the addition (deletion) of monomers at one end. The addition of the monomers alters the energy of the polymer and thus, for a certain value, the chain length changes from finite to infinite, experiencing a first-order transition. If the polymer chains interact with each other the scenario is more complicated and second-order transitions may be observed.[77]

v) *Collapse transition*, which refers to the competition between the attractive interactions among monomers that drive the self-collapse of the polymer, and the entropy of the polymer chains (rubber elasticity) that tries to expand the polymer.[78,79] Since each monomer occupies a certain volume in the polymer and the monomers cannot penetrate each other, there is repulsion at short distances. Such repulsion prevails in a good solvent and thus the polymer coils swell.[80] A change in the environmental conditions, such as temperature, pH or solvent composition, can modify the balance between the free energy of the internal (polymer–polymer and polymer–solvent) interactions and the elasticity component. If the attractive interactions between monomers become strong enough, a coil–globule transition occurs at a condition called θ point.[36] This is what occurs when the polymer chains are cross-linked forming a three-dimensional network (hydrogel). In a good solvent, the chains confined between two adjacent cross-linking points tend to behave as polymer coils. If the solvent conditions change towards the θ point, each subchain undergoes a coil-globule transition and, as a result, the network as a whole shrinks. Namely, a volume phase transition occurs, as proved experimentally for first time by T. Tanaka in 1978.[81] Hydrogel collapse can be driven by any one of the four basic types of inter-molecular interactions operational in water solutions and in biological systems, namely, by hydrogen bonds and van der Waals, hydrophobic and Coulomb interactions.[82] The theoretical basis of the critical phenomena in cross-linked networks can be consulted in detail elsewhere.[64,81,83] The enormous number of papers about this transition, compared to the others, is mainly related to the

Downloaded on 01/09/2013 10:25:46.

wide scope of applications that the swelling–collapse phenomenon may have, since the volume phase transition can occur under physiological conditions and notably modifies the flow of fluids through the network and also the diffusion of solutes, such as drugs.[84]

The five transitions described above have in common that they are attributable to the fact that the monomers are connected into flexible long chains and, therefore, small changes in the intensive thermodynamic variables (namely, temperature, pressure, chemical potential) lead to drastic changes in the polymer conformation.

B) Transitions within collections of molecules
  i) *Liquid crystals/plastic crystals*. It has been shown that, above a certain concentration, a dispersion of rigid rods changes from isotropic (random) to nematic (parallel alignment) phase; namely, the rigid rods cannot freely orient. In the isotropic phase, the centre of the mass is liquid and the rods can adopt any orientation. By contrast, in the nematic phase the freedom of the rods to orientate is restricted, although the centre of the mass still has liquid-like freedom (namely, the translational degrees of freedom are maintained). The ordered alignment enables maximum packaging (entropy driven process) and the side groups of the rods to stabilize the nematic phase through favorable interactions between each other. If the system is cooled down, the centre of the mass loses its translational degrees of freedom and a crystal is formed.
  ii) *Glass transitions/sol-gel transitions* are due to a drastic decrease in the configurational entropy. As the temperature of a polymer goes down, the small mobile rods that form each chain and make the polymer flexible (rubber phase) become fewer and larger and therefore more difficult to pack. At a certain temperature, close to the conditions of zero configurational entropy, the rigid rods become stuck in a randomly ordered structure, because each rigid portion cannot accommodate the energetic preferences of all its neighbors simultaneously. This second-order transition leads to the formation of a glass phase. This phenomenon is similar to the situation in which more cross-linking points are introduced among the chains of a polymer dispersed in a solvent and a sol-gel transition is triggered.
  iii) *Crystallization*. Diluted polymer solutions crystallize when the constituent rods align to form ordered, lamellar structures, instead of the disordered ones reported above.[85]
  iv) *Liquid–liquid transitions/polymer blends*. Phase separation phenomena in randomly mixed polymers are dictated by the fact that each polymer prefers to interact with itself and only the entropy favors the mixing. The entropy of mixing is quite large for short polymers, but becomes negligible for large polymers. Thus, in the latter case, the enthalpy component is predominant and triggers the separation of the polymers into nearly pure phases of each one.

Downloaded on 01/09/2013 10:25:46.

v) *Block copolymers/membranes-micelles-vesicles*. Incompatible polymers can be attached together in the form of block copolymers to prevent each of them moving far away. Nevertheless, the tendency to phase separate persists and it leads to microphase separation, namely, a pattern of microdomains, each containing mainly one of the blocks, separated by thin inter-phase regions.[36] Depending on the relative length of each block, the microdomains can take different shapes, forming lamellar, cylindrical or spherical phases. Free-standing membranes, micelles and vesicles can be considered as block copolymer-based phase systems, to which enough solvent has been added to maintain individualized the layers, the cylinders or the spheres.

In addition to the ten classes of transitions described above, it might occur that a material suddenly changes its chemical nature (*e.g.* rupture of certain bonds by hydrolysis or oxidation/reduction) and transforms into another material with different groups. Obviously, thermodynamic transitions can accompany such chemical transformation. Furthermore, it should be taken into account that one transition does not exclude the occurrence of others. Conversely, the transitions are frequently coupled and there are many examples in Nature of such couplings; some of those that refer to natural macromolecules are the cause of detrimental effects on human health (*e.g.* sickle-cell anemia, phi cell body cancers, scleroderma, *etc.*).[73] In fact, it could be stated that organic polymers that can undergo phase transitions are essential for all evolved life-forms, since they are the only material that can fulfill the three main requirements of living systems: i) minimal complexity to form and function, ii) ability to produce different structures in a reproducible way and iii) ability to transmit all information necessary to the forms and functions.

1.3.2 Memorization of the Conformation. Molecular Imprinting and Recognition

The interest in responsive polymers, especially in the biomedical field, can be remarkably increased if the recognition capacity of certain biomacromolecules (*e.g.* receptors, enzymes, antibodies) could be mimicked. Some unique details of the native state of proteins, such as shape and charge distribution, enable them to recognize and interact with specific molecules. Proteins find their desired conformation out of a nearly infinite number. By contrast, as known from recent theoretical developments, a polymer with a randomly made sequence does not fold in just one way.[86–88] Therefore, the ability of a polymer (or polymer hydrogel) always to fold back into the same conformation after being stretched and unfolded, *i.e.* to thermodynamically memorize a conformation, should be related to properly selected or designed non-random sequences. To obtain, under proper conditions, synthetic polymeric systems with sequences able to adopt conformations with useful functions, molecular imprinting

Downloaded on 01/09/2013 10:25:46.

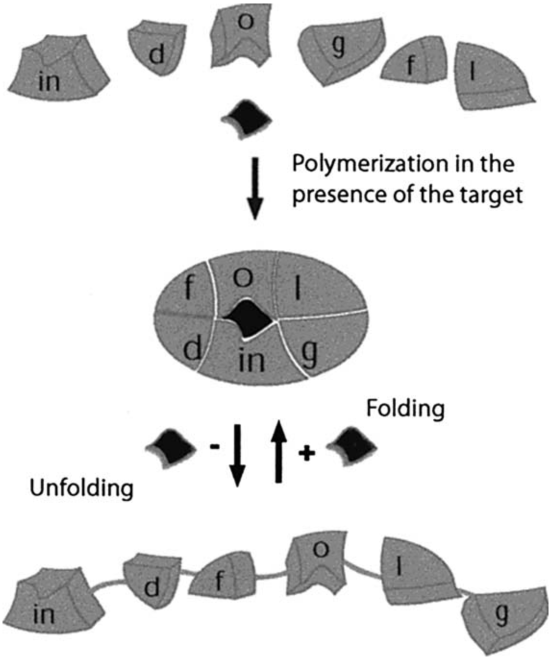

Figure 1.6 Schematic view of the conformational imprinting effect. Reproduced from reference 92. Copyright 2001 American Chemical Society.

technology has been applied.[89–91] Hydrogels can recognize a substance if they are synthesized in the presence of such a substance (which acts as a template) in a conformation that corresponds to the global minimum energy. The "memorization" of this conformation, after the swelling of the network and the washing of the template, will only be possible if the network is able always to fold into the conformation upon synthesis that can carry out its designated function (Figure 1.6).[36,92] This revolutionary idea is the basis of new approaches to design imprinted hydrogels and has been developed at different levels, as explained in Chapters 21 and 22. In the particular case of drug delivery, molecularly imprinted networks enable the control of drug release through a new mechanism: the affinity between the drug and the network.[93–96] Moreover, stimuli-responsive imprinted DDSs can display different affinities for the drug molecules as a function of the nature or intensity of the stimuli, leading to a double regulation of release process by means of stimulus-tunable affinity-controlled release.[97–99]

1.4 Intelligent Drug-delivery Systems

Intelligent DDSs may be defined as a particular type of delivery system that integrates stimuli-responsive excipients able to trigger or switch drug release on

Downloaded on 01/09/2013 10:25:46.

and off when they perceive changes in internal or external factors. The overall purpose is to achieve disease-responsive drug delivery, namely, the drug is intended to be targeted and released only in cells of diseased tissues and/or at a rate that depends on the evolution of the pathological process.[100]

The stimuli that can be *a priori* useful to regulate drug release are quite diverse (Figure 1.5) and they can induce phase transitions in the responsive components without altering their chemical composition (*e.g.* assembly/disassembly, collapse/swelling) but, in some situations, they can alter chemical groups or bonds (*e.g.* through enzymatic or redox reactions) and modify the conformation, solubility or integrity of the delivery system.[67,101,102] In the first case, when only phase transitions are involved, the changes induced by the stimulus are mostly reversible when the stimulus disappears, enabling repeated pulsate release. In the second one, when the chemical groups are also altered, the delivery system is mainly conceived to avoid premature leakage of the drug until the stimulus appears and, if this has enough intensity, the complete discharge of drug may be triggered. The information already available from *in vitro* and, although still incipient, *in vivo* tests demonstrates the suitability of responsive lipids, polymers and polymer/inorganic or metal hybrid structures as components of quite diverse stimuli-responsive delivery systems, like liposomes, micelles, polymersomes, layer-by-layer assemblies, nanoparticles or hydrogels, and also the possibilities of developing drug–medical device combination products.[13,103] The most common internal and external stimuli and the responsive materials used to prepare smart DDSs are summarized in Tables 1.1 and 1.2, with a reference to the chapters in this book in which they are described in detail. In the following paragraphs, a general overview of each stimulus and the mechanisms behind the responsiveness is provided.

1.4.1 pH- and/or Ion-responsive DDSs

The pH gradients existing in the body under healthy and pathological conditions are one of the more explored inner variables as a stimulus to trigger drug release. In fact, the characteristic changes in pH along the gastrointestinal tract have been largely exploited to achieve site-specific oral delivery.[104] Although enteric dosage forms do not fully fit in the category of intelligent DDSs (since, in most cases, it is only a question of site-specific solubility), the basic responsiveness of the polyelectrolytes incorporated in many enteric dosage forms has been transferred to DDSs that can fully exploit such responsiveness under situations in which the pH changes are more tiny and occur inside the tissues or even in the cells. For example, the extra-cellular pH of tumor tissues (6.5–7.0) is slightly lower than that of the blood and healthy tissues (7.4).[105] Inside cells, the differences of pH among the cytosol (7.4), Golgi apparatus (6.4), endosome (5.5–6.0) and lysosome (5.0) are considerable.[106] Inflamed tissues and wounds are also characterized by a decrease in pH to 5.4–7.2, and non-healing wounds can achieve relevant alkaline pH values, up to 8.9.[107] The growth of microorganisms can itself notably alter the pH of the affected tissue, but also can induce the release of body enzymes (*e.g.* metalloenzymes) that cause

Downloaded on 01/09/2013 10:25:46.

Table 1.1 Examples of materials responsive to internal stimuli that can be integrated in intelligent DDSs and some potential applications.[2] The chapters of this book in which they are reviewed are indicated in the last column.

Stimulus	*Mechanism*	*Material*	*Application in DDSs*	*Chapter number*
pH	Change in the protonation degree that modifies solubility, viscosity, swelling	Poly(acrylic acid) (PAA) Poly(methacrylic acid) (PMAA) Poly(diethylaminoethyl methacrylate) (PDEAEMA) Poly(dimethylaminoethyl methacrylate) (PDMAEMA) Poly(hydroxyethyl aspartamide-g-maleic anhydride) Alginate, chitosan	Site-specific oral release Tumor targeting Lysosomotropic agents in gene delivery Infection-induced release	3, 5, 15, 17, 18, 20, 24
Ions/ionic strength	Change in ions nature or concentrations	Poly(acrylic acid) (PAA) Poly(NIPAAm-co-vinylimidazole) Poly(α-amino acid)s	Intra-tumoral delivery Injectable implants	17, 20
Enzymes	Enzymatic conversion that leads to rupture of chains or cross-linking points	Polysaccharides Acrylic networks with azoaromatic bonds Polyesters Peptides as cross-linkers Substrates of metalloproteases Oligonucleotides	Inflamed tissues Tumor targeting Infection (bacteria)-triggered release	9
Biochemicals (glucose, antigens)	Conversion of the biochemical by an enzyme immobilized in the material Induced sol-to-gel transition Competitive binding to antibody coupled polymers	Networks with glucose oxidase Concanavalin-coated polymers Copolymers with coupled antigens and antibodies Molecularly imprinted networks	Feed-back regulated hormone (insulin) release Antigen-triggered release Theragnostic systems	10, 22
Glutathione	Redox conversion	Macromolecules with disulfide bonds	Cytoplasmatic delivery	8
Temperature[a]	Competition between hydrophobic and hydrophilic interactions between components and component-water, that modifies aggregation state or swelling	Poly(*N*-isopropyl acrylamide) (PNIPAAm) Poly(ethylene oxide)-poly(propylene oxide) (PEO-PPO) copolymers Elastin-like polymers	Fever-triggered release Tumor, inflammation targeting Injectable implants External switch drug release on/off Delivery of cells for regeneration of tissue structure or function	2, 4, 5, 17, 18, 20, 23, 24

[a] Changes in temperature can be also triggered through external sources of energy.

Downloaded on 01/09/2013 10:25:46.

further modifications in pH along the healing time. The pH of a wound can even be used as an index of its likelihood to recover completely.[108] Semen has also been shown to induce notable changes in vaginal pH.[109]

As mentioned above, a suitable way to exploit these changes in pH to regulate drug delivery is with the use of lipids and, mostly, polymers that behave as weak acids or bases with pK_as that enable sharp changes in the ionization state at the pH of interest. Carboxylic, sulfonate and primary and tertiary amino groups can modify the degree of ionization due to pH modifications in the physiological range. Nevertheless, it should be noted that the pK_as of repeated chemical groups in a long chain may be notably different from those of the individualized components in solution, and that the copolymerization with hydrophobic monomers (bearing long alkyl groups) shifts the pK_a to higher values.[110–113] The change from neutral to ionized state dramatically alters the conformation and the affinity of the chains for the solvent as well as the interactions among them. The neutralization of the charges makes water become a poor solvent. Thus, the change in the degree of ionization may be translated in the disassembly of weakly bonded components or the swelling/shrinking of covalent networks. For example, networks bearing acid groups swell at alkaline pH but collapse at low pH, while those bearing bases swell in acid medium and shrink when pH rises. Polyampholyte systems containing both types of monomers show the maximum swelling at neutral pH, *i.e.* when both acids and bases are partially ionized.[114] It should also be noted that ionic strength in general, but certain ions in particular (especially di- or multi-valence ones), can notably affect the pH-responsiveness and also the conformation of the polymer chains, altering the affinity for water and the swelling, and even inducing self-associations triggering sol-gel transitions.[115,116] For example, hydrogels carrying moieties of L-valine, L-leucine, L-phenylalanine or L-histidine have been shown to be sensitive to both pH and ions.[117] Therefore, choosing suitable components it is possible to develop systems responsive to almost any situation in the body that involves a change in pH or in the concentration of ions that can form a complex with the ionizable groups.[63,118] Remarkable examples of pH-responsive DDSs are nanogels for tumor-targeting delivery, lysosomotropic micelles and liposomes designed for gene delivery, vaginal gel networks for semen-induced or microorganism-induced release and *in situ* gelling intra-ocular depots.

1.4.2 Enzyme-responsive DDSs

Enzymes in the body are useful both to fix together polymer chains, leading to formation of self-assembled or covalently bonded networks, or to break certain bonds causing disassembly or rupture of the networks.[119] As a consequence, enzymes in healthy bodies may directly act on sensitive drug carriers, notably altering the drug release rate. Furthermore, the disregulation, namely, hypo-/hyperexpression, of the enzymes can lead to the development of a range of disease states and thus such disregulation could be exploited to trigger release in the affected tissues or sites of the body.[120,121]

Downloaded on 01/09/2013 10:25:46.

Thus, an enzyme-responsive DDS requires at least an enzyme-sensitive component that is a substrate of the enzyme, and the drug can be chemically or physically entrapped in the system. To be effective, the DDS has to be able to reach the enzyme and to expose the sensitive groups to it. This is particularly critical when the enzymatic activity is associated to a particular tissue or the enzyme is found at higher concentrations at a certain site. Thus, a detailed knowledge about the extra-cellular barriers or, in the case that the enzyme is located intra-cellularly, about the impediments to enter in the cells is required to attain enzyme-responsive release. The most evaluated enzymes for triggering drug release are hydrolases, which can break covalent bonds that keep together certain components or can modify certain chemical groups altering the balance of electrostatic, hydrophobic, steric or π-π interactions, van der Waals forces or hydrogen bonding.[120,122] For example, proteases can trigger the release of drugs linked to the carrier by a peptide or when the carrier is stabilized by peptide links that are substrates of the enzyme; glycosidases can induce the release from polysaccharide-based carriers; lipases can trigger drug delivery when they hydrolyze the phospholipid building blocks of liposomes; and certain hydrolases can control the assembly or disassembly of inorganic nanoparticles and mostly the degradation of the gatekeepers of the pores in which the drug molecules are hosted.[121] Kinases and phosphatases can be used for reversible rupture of the bonds and, thus, to obtain pulsate drug release.[123] Oxidoreductases have been exploited in a different way, which is commented on in detail in the next section.

So far enzyme-responsive DDSs have been designed in the form of supramolecular assemblies (mainly micelles and liposomes), chemically cross-linked gels and nanocontainers and porous silica nanoparticles with responsive gatekeepers.[120,121,124] They have been shown to be useful for specific release in inflammation sites and tumor cells, and for microorganism-triggered release of antimicrobial agents.[125–128] This latter application, still scarcely explored, is intended to avoid prophylactic and prolonged use of antimicrobials that can lead to toxicity effects in patients and also favor the apparition of resistant variants. For example, the high levels of thrombin-like activity found in wounds infected with *S. aureus* have inspired the development of conjugates of gentamicin with poly(vinyl alcohol) through a thrombin-sensitive peptide linker. The conjugate released gentamicin when it was incubated with thrombin and leucine aminopeptidase together, but not with one enzyme alone. Gentamicin was successfully released upon incubation with *S. aureus* wound fluid, strongly reducing the bacterial number in an animal model of infection.[129]

1.4.3 Biochemical-responsive DDSs

Molecule-responsive systems enable feed-back regulation of the drug delivery rate as a function of the concentration of a specific substance in the body, which may serve as an index of the evolution of a pathological state.[130,131] These systems try to imitate the physiological self-regulating mechanisms by

Downloaded on 01/09/2013 10:25:46.

integrating both biomolecular recognition and responsive behavior in a single structure.[130] These functionalities can be achieved using one of the following two approaches:

i) a specific sensor of the triggering molecule (for example, an enzyme) is attached to a network that also presents ionizable groups; the target biomolecule acts as substrate of the enzyme and it is decomposed in products that alter the pH.[132–134] Some oxidoreductases, particularly glucose oxidase, have been used for this purpose since they can act as sensor in the detection of glucose.[135] Furthermore, oxidoreductases play a central role in oxidative stress, which is related to pathological processes such as Alzheimer's disease and cancer and may open novel applications.[136,137] For example, glucose-responsive nanocarriers have been prepared encapsulating glucose oxidase in PEG-poly(propylene sulfide)-PEG micelles. When glucose permeates in the micelles, glucose oxidase transforms it to gluconolactone and also generates hydrogen peroxide as a side product, which in turn oxidizes the thioethers of poly(propylene sulfide) into sulfoxides and sulfones. This causes the copolymer to become hydrophilic and the micelles to disassembe.[138] Glucose oxidase, catalase and insulin have been trapped together inside poly(2-hydroxyethylmethacrylate-co-*N*,*N*-dimethylaminoethyl methacrylate) hydrogels. Simulating *in vivo* conditions, glucose oxidase converts the glucose in gluconic acid, causing the ionization of the amino groups in the copolymer and thus the swelling of the network and the release of insulin. Catalase was included to provide oxygen to the oxidation reaction. A nice correlation between glucose concentration and release rate of insulin was found.[135] More examples on the potential use of glucose oxidase in the development of glucose-regulated insulin DDSs can be found in the literature.[139,140]

ii) a competitive mechanism, based on links in the network in which a binding agent (lectin, antigen) is involved. In the absence of target biomolecules, the binding agent interacts with a complementary component in the formulation. When the biomolecule appears or reaches a certain concentration, it competes with the complementary component for interacting with the binding agent. This process causes the rupture of the network and triggers the release of the entrapped drugs.[141–145] Lectins are carbohydrate-binding proteins present at the cell's surface that have been explored for preparing DDSs able to interact with glycoproteins and glycolipids. Concanavalin A, a lectin that possesses four binding points, has been shown to be useful in immobilizing glycosylated insulin in particles and membranes. In glucose-free medium, no release happens. By contrast, in the presence of glucose, insulin is easily displaced from the binding to concanavalin A and can be released.[141,145] Instead of lectins, phenylboronic derivatives can also be used to bind saccharides according to a similar mechanism but using totally synthetic platforms, namely, without using proteins.[146] Drug release induced by a competitive

Downloaded on 01/09/2013 10:25:46.

mechanism can also occur by placing antibodies in DDSs that can recognize specific antigens in the body. These DDSs integrate antibodies and antigens that act as cross-linking points. This high specific interaction is broken only when free antigens appear in the medium at a concentration high enough to compete with the antigens that form part of the DDS.[143] As explained in detail in Chapters 21 and 22, totally synthetic molecule-responsive networks can also be obtained by applying the molecular imprinting technology to the synthesis of biochemical-responsive polymers.[98]

1.4.4 Glutathione-responsive DDSs

Glutathione (GSH)-triggered release can be exploited to obtain intra-cellular specific release, namely, in the cytoplasm and/or the nucleus.[147] The intracellular compartments (cytosol, mitochondria and nucleus) contain GSH tripeptide at a concentration 2–10 mM, which is 2 to 3 orders higher than that achieved in the extra-cellular fluids (2–20 μM).[148] Furthermore, tumor tissues may achieve 4-fold greater concentrations of GSH over normal tissues.[149] Block copolymers, polymer networks and cross-linking agents bearing disulfide (-S-S-) bonds are thus suitable to undergo reduction reactions in the presence of GSH, leading to the rupture of the bond to form –SH end groups.[147] As a consequence of the redox process, the nanostructure swells or disassembles and the drug is released. The bond rupture is *a priori* reversible, although this is not a foreseeable situation inside the cells. The therapeutic potential of the glutathione-responsive DDSs has already been demonstrated in animal models, using micelles and polymersomes loaded with anticancer drugs.[150–152]

1.4.5 Temperature-responsive DDSs

Temperature is a widely investigated stimulus for modulation of drug delivery, since it can benefit from pathological states that cause local or systemic increase in temperature (tumors, inflammations, infections, *etc.*) and also from external sources of energy that directly or indirectly may lead to a very precisely localized heating.

Temperature-sensitive polymers used to prepare intelligent systems are usually hydrophilic below their critical temperature of dissolution (LCST). When the temperature is above LCST, the polymer becomes hydrophobic and its conformation changes from expanded (soluble) to globular (insoluble) state.[153] The changes in solubility regulate the assembly into micelles or layer-by-layer structures of temperature-responsive components. If the polymers form part of chemically cross-linked networks, the shrinking of the network causes the squeezing of the drug molecules, usually with a strong initial burst.[154] Polymers with upper critical solution temperature (UCST) may also be useful for preparing self-assembled structures that disassemble in environments of temperature beyond the UCST. Lists of polymers having a critical solubility temperature (CST) can be found elsewhere

Downloaded on 01/09/2013 10:25:46.

and comprise synthetic polymers such as poly-*N*-isopropylacrylamide (PNIPAAm), poly-*N*,*N*-diethylacrylamide, poly(methyl vinyl ether) (PMVE), poly-*N*-vinylcaprolactam (PVCL) and poly(ethylene oxide)-poly(propylene oxide) (PEO-PPO) block copolymers, natural polysaccharides like certain cellulose ethers and elastin-like polypeptides.[155–157] To be useful for drug delivery, the LCST or the UCST should be close to the triggering temperature, namely, a few degrees above/below the normal body temperature. To match that requirement, the temperature responsive polymers can be copolymerized with hydrophobic or hydrophilic monomers in order to tune the critical temperature down and up, respectively.

External modulation of drug release, without interference of physiological temperature changes, can be achieved using temperature-sensitive polymeric micelles and nanogels that contain, among other components, gold nanoparticles. When irradiated with infrared light, gold absorbs the radiation and the temperature in the surrounding environment rises, with the subsequent destabilization/collapse of the micelles or the nanogels.[158] Similarly, alternating magnetic fields can also cause moderate increase in the temperature of the local environment of superparamagnetic particles, as will be explained below.

Table 1.2 Examples of materials responsive to external stimuli that can be integrated in intelligent drug-delivery systems.[2]

Stimulus	*Mechanism*	*Material*	*Application in DDSs*	*Chapter number*
Ultrasound	Temperature increase Cavitation Enhanced cell permeability	Self-assembled polymers or lipids	Tumor therapy	6, 17
UV/Vis light, NIR	Changes in the conformation of chemical groups Heating of gold nanoparticles	Photoresponsive groups like azobenzene, cinnamoyl and spirobenzopyran Gold-nanorods embedded in temperature-responsive materials	Ocular/subcutaneous triggered release Tumor therapy	12, 13, 17
Magnetic field	Movement and heating of superparamagnetic particles under the magnetic field	Particles containing magnetic cores (Fe_3O_4)	Guided targeting Externally triggered drug release Thermo-ablation of tumor cells	14
Electric field	Changes in charge distribution	Polyelectrolytes Intrinsically conducting polymers (ICPs), like polypyrrole (PPy), polyanaline (PANI) and poly(3,4-ethylenedioxy thiophene) (PEDOT)	Local release of growth factors, anti-inflammatory drugs and antiproliferative substances incorporated in electrodes or microchips	11

Downloaded on 01/09/2013 10:25:46.

1.4.6 Ultrasound-responsive DDSs

Ultrasound can be applied to the body using conventional physiotherapeutic equipment. The waves cause local increase in temperature and bubble cavitation, facilitating the penetration of nanostructures into specific regions and the triggering of drug release.[159] Compared to other external stimuli, ultrasound has the advantage of being able to propagate into deep tissues and to be focused directly on the target tissue.[160]

Most tests carried out to activate drug release with ultrasound have been performed with polymeric micelles and more recently with layer-by-layer assemblies, which can be reversibly destabilized due to bubble cavitation. The amount of drug released can be modulated through the control of the frequency, power density, pulse length and inter-pulse intervals.[161] This approach has mainly been tested for treatment of tumors in animal models applying low-frequency ultrasound. When the antitumor formulation is systemically administered, ultrasound should be applied when most micelles have reached the target tissue. This may take several hours for an optimal accumulation of the carrier in the tumor by means of the EPR effect. Application of ultrasound enables a pulsate drug delivery.[162,163] The *in vivo* antitumor effectiveness of this approach is also promoted by the cell membrane perturbation caused by ultrasound (sonoporation), which enhances the intracellular uptake of micelles, drugs and genes.[164,165]

1.4.7 Light-responsive DDSs

The use of light as a triggering agent enables localized drug release in very well-delimited regions of the body, reducing the affection of adjacent tissues to a minimum. There are currently available equipments that can apply innocuous electromagnetic radiation of very specific wavelengths in the range from 2500 to 380 nm to switch drug release on and off. Ultraviolet light or blue light can serve as a triggering agent for topical treatments applied to the eyes, skin or mucous, as is normally used in photodynamic therapy. Radiation of greater wavelengths (infrared) can penetrate deeper in the tissues.[166,167] Near-infrared radiation (NIR) is innocuous and does not cause a significant heating in the area of its application. As light-responsive components, two groups of materials can be distinguished: i) metal particles, mainly gold nanoparticles that absorb the light and transform it in local heating; if the gold particle is incorporated in a temperature-sensitive carrier, the increase in temperature can trigger drug release;[168–170] and ii) organic materials (polymer nanostructures or liposomes) that bear functional groups that change their conformation and, thus, certain features (particularly the hydrophilicity or the position as gatekeeper) when irradiated; this is the case of azobenzene, pyrene, nitrobenzene, cinnamoyl and spirobenzopyran, among others.[171,172] Some light-responsive DDSs are intended for a single use (*i.e.* the light triggers an irreversible structural change that provokes the delivery of the entire dose), while others are able to undergo reversible structural changes when cycles of light/dark are

Downloaded on 01/09/2013 10:25:46.

applied, behaving as multi-switchable carriers that release the drug in a pulsate manner.[171,172]

1.4.8 Magnetic-responsive DDSs

Magnetite (Fe_3O_4) and maghemite (γ-Fe_2O_3) are currently the only non-toxic paramagnetic materials acceptable for biomedical applications.[173] To be administered to the body, superparamagnetic nanoparticles can be coated with or encapsulated into polymeric structures such as micelles and particles or placed inside microporous inorganic carriers, as described in detail in Chapter 14.

Magnetic drug carriers containing temperature-responsive polymers possess three unique features: i) visualization of the drug carrier into the body by means of magnetic resonance imaging; ii) tissue distribution controlled through an external magnetic field, which may be helped if decorated with cell ligands; and iii) triggering of drug release due to a local increase in temperature when an alternating magnetic field is applied.[174,175] The drug is released while the magnetic field is on, leading to site-specific treatment.[176] The increase in temperature can be modulated by the frequency of oscillation and the time of application of the magnetic field; a small increase triggers reversible pulsate drug squeezing as the temperature-responsive network shrinks, while a strong increase may lead to the rupture of the carrier followed by a burst drug release and a simultaneous thermal ablation of the surrounding tissues.[177] It should be noted that cancer cells are destroyed at temperatures close to 43 °C, while normal cells can stand such temperature.[178]

1.4.9 Electric Field-responsive DDSs

Electrical stimuli can be generated using devices suitable for transdermal delivery such as those used for iontophoresis and electroporation, which enables precise control of the intensity, the amount of current, the duration of the pulses and the intervals between successive pulses.[179] DDSs responsive to electric fields can be made using polyelectrolytes with a high density in ionizable groups, as those suitable for pH-responsive delivery, in the form of sheets, microparticles or *in situ* gelling injectable systems for subcutaneous implantation.[179] An electric field can be applied through an electro-conducting patch placed on the skin over the polyelectrolyte network. The potential between the electrodes causes a movement of ions that lead to local changes in pH, which cause the cross-linked polyelectrolytes to shrink or swell, modifying drug-release rate. Alternate shrinking and swelling can easily be achieved by applying pulses of electricity, and this can serve to control the release rate. This approach has been tested for the pulsate delivery of insulin using subcutaneously implanted poly(dimethylaminopropyl acrylamide) microgels[180] and for the transdermal delivery of diclofenac from hydrogels of sodium alginate, carbopol and their blends.[181]

Downloaded on 01/09/2013 10:25:46.

An alternative to the polyelectrolytes is the use of intrinsically conducting polymers (ICP), also called synthetic metals because they possess the electrical, electronic, magnetic and optical properties of a metal.[182] Examples of ICPs suitable for DDSs are polypyrrole (PPy), polyanaline (PANI) and poly(3,4-ethylenedioxythiophene) (PEDOT). The electrical conductivity of the ICPs is due to the uninterrupted and ordered π-conjugated backbone.[183] The ICPs are usually formed on an electrode and can be used in such a way after being loaded with the drug. The electrical signals alter the redox state of the ICP modifying the polymer charge and volume.[184] The drug entrapped in the ICP layer is released when an electrical stimulus is applied, using step potential or cyclic voltammetry. ICP-based DDSs have already been tested for triggering local release of paclitaxel from stents,[185] growth factors from implants,[186] neurotrophins from electrodes implanted in cochlear neurons[187] and drugs and hormones from implanted microchips.[188]

1.5 Conclusions and Future Aspects

The growing number of biocompatible materials that are sensitive to physiological and external stimuli, as well as the versatility of current approaches to integrate them into DDSs, offer unprecedented possibilities for regulating the spatiotemporal release profile of the drugs. Stimuli-responsive DDSs make the delivery of drugs that have serious biopharmaceutical/toxicity constraints possible, and are expected to improve remarkably the therapeutic efficiency of old and new active substances. However, intelligent DDSs may have to face up to safety concerns and *in vivo* management of the responsiveness. The use of macromolecules (*i.e.* enzymes, antibodies or even synthetic polymers) with motifs that can be recognized by the immune system may lead to unexpected reactions in the body after successive administrations and may compromise the performance of the DDS and the health of the patient. Moreover, nano-sized entities produce additional safety concerns, and there is still a paucity of regulations about the assessment of the nanocarriers' fate *in vivo*. Regarding applicability, intelligent DDSs have to fit the switching on/off of the release to the appearance/disappearance of the stimulus in order to avoid delays in the responsiveness.[2] On the other hand, advances in portable trigger devices to activate externally DDSs that can be pre-programmed by nursing staff and/or are easy to use by the patients may improve the cost-effectiveness of the treatments.[16]

Overall, the positive and reliable information on the efficiency of intelligent DDSs coming from *in vitro* and cell culture assays is a valuable support to intensify the translation to animal models and even to clinical studies.[189] Such clinical translation should provide a better understanding of the behavior of the drugs formulated in intelligent DDSs and on how the body responds to the novel materials and therapy protocols. It can be foreseen that the information gathered under *in vivo* conditions serves as feedback for optimizing the features of the responsive materials and the design of more efficient DDSs.

Acknowledgements

Work supported by MICINN (SAF2011-22771), Xunta de Galicia (10CSA203013PR) and FEDER.

Downloaded on 01/09/2013 10:25:46.

References

1. A. S. Hoffman, *J. Control. Release*, 2008, **132**, 153.
2. S. Grund, M. Bauer and D. Fischer, *Adv. Engin. Mater.*, 2011, **13**, B61.
3. L. Krówczynski, *Pharmazie*, 1985, **40**, 346.
4. Y. W. Chien, *Novel Drug Delivery Systems*, 2nd edn. Marcel Dekker, New York, 1992.
5. A. Dokoumetzidis and P. Macheras, *Int. J. Pharm.*, 2006, **321**, 1.
6. R. Langer, *Nature*, 1998, **392**, 5.
7. I. Wilding, *Crit. Rev. Ther. Drug Carrier Syst.*, 2000, **17**, 557.
8. Y. W. Chien and S. Lin, *Clin. Pharmacokinet.*, 2002, **41**, 1267.
9. M. J. Rathbone, J. Hadgraft and M. S. Roberts, *Modified-release Drug Delivery Technology*, Marcel Dekker, New York, 2003.
10. J. Heller and A. S. Hoffman, in *Biomaterials Science*, 2nd edn, ed. B. D. Ratner, Elsevier, San Diego, CA, 2004, p. 628.
11. J. Kost and R. Langer, *Adv. Drug Deliver. Rev.*, 2001, **46**, 125.
12. K. Y. Lee and S. H. Yuk, *Prog. Polym. Sci.*, 2007, **32**, 669.
13. C. Alvarez-Lorenzo, A. M. Puga and A. Concheiro, in *Biomimetic Approaches for Biomaterials Development*, ed. J. F. Mano, Wiley-VCH, New York, 2012, p. 417.
14. J. Kopecek, *Eur. J. Pharm. Sci.*, 2003, **20**, 1.
15. J. Kopecek and J. Yang, *Polym. Int.*, 2007, **56**, 1078.
16. J. Kost, in *Encyclopedia of Controlled Drug Delivery*, vol. 1, ed. E. Mathiowitz, John Wiley & Sons, New York, 1999, p. 445.
17. O. M. Y. Koo, I. Rubinstein and H. Onyuksel, *Nanomedicine NMB*, 2005, **1**, 193.
18. J. D. Byrne, T. Betancourt and L. Brannon-Peppas, *Adv. Drug Deliver. Rev.*, 2008, **60**, 1615.
19. S. Mitragotri, *Pharm. Res.*, 2009, **26**, 232.
20. S. Patel, A. A. Bhirde, J. F. Rusling, X. Chen, J. S. Gutkind and V. Patel, *Pharmaceutics*, 2011, **3**, 34.
21. J. W. Yoo, N. Doshi and S. Mitragotri, *Adv. Drug Deliver. Rev.*, 2011, **63**, 1247.
22. B. B. C. Youan, *J. Control. Release*, 2004, **98**, 337.
23. F. Levi and A. Okyar, *Expert Opin. Drug Deliv.*, 2011, **8**, 1535.
24. N. I. Prasanthi, G. Swathi and S. S. Manikiran, *Int. J. Pharm. Sci. Rev. Res.*, 2011, **6**, Article 014.
25. H. N. Joshi, *Int. J. Pharm.*, 2007, **343**, 1.
26. M. L. Billingsley, *Pharmacology*, 2008, **82**, 239.
27. R. C. Dutta, *Curr. Pharm. Design*, 2007, **13**, 761.

Downloaded on 01/09/2013 10:25:46.

28. S. Kim, J. H. Kim, O. Jeon, I. C. Kwon and K. Park, *Eur. J. Pharm. Biopharm.*, 2009, **71**, 420.
29. J. F. Mano, *Adv. Eng. Mater.*, 2008, **10**, 515.
30. J. Hamman and J. Steenakamp, *Expert Opin. Drug Deliv.*, 2012, **9**, 219.
31. D. F. Williams, *Biomaterials*, 2009, **30**, 5897.
32. M. Vert, *Prog. Polym. Sci.*, 2007, **32**, 755.
33. R. K. Roeder, *JOM-US*, 2010, **62**, 49.
34. D. W. Thompson, *On Growth and Form*, 2nd edn, Cambridge University Press, Cambridge, 1968.
35. M. A. Meyers, P. Y. Chen, A. Y. M. Lin and Y. Seki, *Prog. Mater. Sci.*, 2008, **53**, 1.
36. A. Yu. Grosberg and A. R. Khokhlov, *Giant Molecules: Here, There, and Everywhere...*, Academic Press, San Diego, 1997.
37. H. Ringsdorf, *Angew. Chem. Ind. Ed.*, 2004, **43**, 1064.
38. R. Langer and D. A. Tirrell, *Nature*, 2004, **428**, 487.
39. C. Alvarez-Lorenzo and A. Concheiro, *Mini-Rev. Med. Chem.*, 2008, **8**, 1065.
40. I. Roy and M. N. Gupta, *Chem. Biol.*, 2003, **10**, 1161.
41. R. Duncan, *Nat. Rev. Drug Discov.*, 2003, **2**, 347.
42. L. Y. Qiu and Y. H. Bae, *Pharm. Res.*, 2006, **23**, 1.
43. J. K. Oh, D. I. Lee and J. M. Park, *Prog. Polym. Sci.*, 2009, **34**, 1261.
44. B. Voit and D. Appelhans, *Macromol. Chem. Phys.*, 2010, **211**, 727.
45. K. E. Kasza, A. C. Rowat, J. Liu, T. E. Angelini, C. P. Brangwynne, G. H. Koenderink and D. A. Weitz, *Curr. Opin. Cell Biol.*, 2007, **19**, 101.
46. R. C. Moreton, *Pharm. Technol.*, 2006, **October**, 1.
47. S. M. Sonal, V. K. Jiny, T. P. Aneesh, T. V. Deepa and K. G. Revikumar, *Pharm. Biol. World*, 2008, **August**, 63.
48. FDA Guidance for Industry, Nonclinical studies for the safety evaluation of pharmaceutical excipients, 2005, http://www.fda.gov/ohrms/dockets/98fr/2002d-0389-gdl0002.pdf, accessed May 2012.
49. O. M. Y. Koo and S. A. Varia, *Ther. Deliv.*, 2011, **7**, 949.
50. R. Gaspar and R. Duncan, *Adv. Drug Deliver. Rev.*, 2009, **61**, 1220.
51. N. Bertrand and J. C. Leroux, *J. Control. Release*, 2012, **161**, 152.
52. K. R. Vega-Villa, J. K. Takemoto, J. A. Yañez, C. M. Remsberg, M. L. Forrest and N. M. Davies, *Adv. Drug Deliver. Rev.*, 2008, **60**, 929.
53. A. Elsaesser and C. V. Howard, *Adv. Drug Deliver. Rev.*, 2012, **64**, 129.
54. V. Fabiano, C. Mameli and G. V. Zuccotti, *Pharmacol. Res.*, 2011, **63**, 362.
55. K. Park, *J. Control. Release*, 2010, **142**, 147.
56. K. Dhal, S. C. Polomoscanik, L. Z. Avila, S. R. Holmes-Farley and R. J. Miller, *Adv. Drug Deliver. Rev.*, 2009, **61**, 1121.
57. F. Yañez, I. Chianella, S. A. Piletsky, A. Concheiro and C. Alvarez-Lorenzo, *Anal. Chim. Acta*, 2010, **659**, 178.
58. A. V. Kabanov and V. Yu. Alakhov, *Crit. Rev. Ther. Drug*, 2002, **19**, 1.
59. D. Y. Alakhova, N. Y. Rapoport, E. V. Batrakova, A. A. Timoshin, S. Li, D. Nicholls, V. Y. Alakhov and A. V. Kabanov, *J. Control. Release*, 2010, **142**, 89.

Downloaded on 01/09/2013 10:25:46.

60. J. Jagur-Grodzinski, *Polym. Adv. Technol.*, 2009, **20**, 595.
61. C. Alvarez-Lorenzo, A. Rey-Rico, J. Brea, M. I. Loza, A. Concheiro and A. Sosnik, *Nanomedicine-UK*, 2010, **5**, 1371.
62. C. Alvarez-Lorenzo, A. Sosnik and A. Concheiro, *Curr. Drug Targets*, 2011, **12**, 1112.
63. D. Schmaljohann, *Adv. Drug Del. Rev.*, 2006, **58**, 1655.
64. F. Liu and M. W. Urban, *Prog. Polym. Sci.*, 2010, **35**, 3.
65. S. Sershen and J. West, *Adv. Drug Del. Rev.*, 2002, **54**, 1225.
66. M. Yoshida and J. Lahann, *ACS Nano*, 2008, **2**, 1101.
67. M. Motornov, Y. Roiter, I. Tokarev and S. Minko, *Prog. Polym. Sci.*, 2010, **35**, 174.
68. G. Pasparakis and M. Vamvakaki, *Polym. Chem.*, 2011, **2**, 1234.
69. C. Alexander and K. M. Shakesheff, *Adv. Mater.*, 2006, **18**, 3321.
70. C. Alvarez-Lorenzo, E. Bucio, G. Burillo and A. Concheiro, *Expert Opin. Drug Deliv.*, 2010, **7**, 173.
71. P. J. Flory, *J. Chem. Phys*, 1941, **9**, 660.
72. M. L. Huggins, *J. Chem. Phys*, 1941, **9**, 440.
73. E. A. Di Marzio, *Prog. Polym. Sci.*, 1999, **24**, 329.
74. Y. Hirokawa and T. Tanaka, *J. Chem. Phys.*, 1984, **81**, 6379.
75. I. Y. Galaev, *Russ. Chem. Rev.*, 1995, **84**, 471.
76. W. Feller, *An Introduction to Probability Theory and Its Applications*, Wiley, New York, 1948.
77. S. C. Geer, in *Advances in Chemical Physics*, vol. 90, ed. S. A. Rice and I. Prigogine, Wiley, New York, 1996, p. 261.
78. P. J. Flory, *J. Chem. Phys.*, 1949, **17**, 303.
79. P. J. Flory, *Principles of Polymer Chemistry*, Cornell, New York, 1953.
80. A. Yu., Grosberg and D. V. Kuznetsov, *Macromolecules*, 1992, **25**, 1996.
81. M. Shibayama and T. Tanaka, in *Advances in Polymer Science, Responsive Gels: Volume Transitions I*, ed. K. Dusek, Springer, Berlin, 1993, p. 1.
82. F. Ilmain, T. Tanaka and E. Kokufuta, *Nature*, 1991, **349**, 400.
83. S. Sasaki and H. Maeda, *Phys. Rev. E*, 1996, **54**, 2761.
84. M. A. Cohen Stuart, W. T. S. Huck, J. Genzer, M. Müller, C. Ober, M. Stamm, G. B. Sukhorukov, I. Szleifer, V. V. Tsukruk, M. Urban, F. Winnik, S. Zauscher, I. Luzinov and S. Minko, *Nat. Mat.*, 2010, **9**, 101.
85. J. D. Hoffman and R. Miller, *Polymer*, 1997, **38**, 3151.
86. T. Tanaka and M. Annaka, *J. Intel. Mat. Syst. Struct.*, 1993, **4**, 548.
87. V. S. Pande, A. Yu. Grosberg and T. Tanaka, *Biophys. J.*, 1997, **73**, 3192.
88. C. Alvarez-Lorenzo, J. Chuang, A. Concheiro and A. Yu. Grosberg, in *Smart Polymers: Production, Study and Application in Biotechnology and Biomedicine*, ed. I. Galaev and B. Mattiasson, CRC Press, New York, 2008, p. 211.
89. V. S. Pande, A. Yu. Grosberg and T. Tanaka, *J. Chem. Phys.*, 1994, **101**, 8246.
90. V. S. Pande, A. Yu. Grosberg and T. Tanaka, *P. Natl Acad. Sci.*, 1994, **91**, 12976.

Downloaded on 01/09/2013 10:25:46.

91. G. Wulff, *Angew. Chem. Int. Ed.*, 1995, **34**, 1812.
92. T. Moritani and C. Alvarez-Lorenzo, *Macromolecules*, 2001, **34**, 7796.
93. N. M. Bergmann and N. A. Peppas, *Prog. Polym. Sci.*, 2008, **33**, 271.
94. C. Alvarez-Lorenzo, F. Yañez and A. Concheiro, *J. Drug Deliv. Sci. Tech.*, 2010, **20**, 237.
95. C. J. White and M. E. Byrne, *Expert. Opin. Drug Deliv.*, 2010, **7**, 765.
96. N. X. Wang and H. A. von Recum, *Macromol. Biosci.*, 2011, **11**, 321.
97. C. Alvarez-Lorenzo and A. Concheiro, *J. Chromatogr. B*, 2004, **804**, 231.
98. C. Alvarez-Lorenzo and A.Concheiro, in *Biotechnology Annual Review*, ed. M. R. El-Gewely, Elsevier, Amsterdam, 2006, vol. 12, p. 225.
99. C. Alvarez-Lorenzo, F. Yañez and A. Concheiro, in *Polymeric Biomaterials*, 3rd edn, vol. 2, ed. S. Dumitriu and V. Popa, Taylor & Francis, USA, 2013, p. 85.
100. P. Wanakule and K. Roy, *Curr. Drug Metabol.*, 2012, **13**, 42.
101. S. H. Yuk and Y. H. Bae, *Crit. Rev. Ther. Drug*, 1999, **16**, 385.
102. C. Alexander, *Expert Opin. Drug Deliv.*, 2006, **3**, 573.
103. K. G. Neoh and E. T. Kang, *MRS Bulletin*, 2010, **35**, 673.
104. N. Washington, C. Washington and C. G. Wilson, *Physiological Pharmaceutics: Barriers to Drug Absorption*, 2nd edn, Taylor & Francis, London, 2001.
105. A. S. E. Ojugo, P. M. J. Mesheedy, D. J. O. McIntyre, C. McCoy, M. Stubbs, M. O. Leach, I. R. Judson and J. R. Griffiths, *NMR Biomed.*, 1999, **12**, 495.
106. N. Nishiyama, Y. Bae, K. Miyata, S. Fukushima and K. Kataoka, *Drug Discov. Today Technol.*, 2005, **2**, 21.
107. G. Gethin, *Wounds UK*, 2007, **3**, 52.
108. L. A. Schneider, A. Korber, S. Grabbe and J. Dissemond, *Arch. Dermatol. Res.*, 2007, **298**, 413.
109. K. M. Gupta, S. R. Barnes, R. A. Tangaro, M. C. Roberts, D. H. Owen, D. F. Katz and P. F. Kiser, *J. Pharm. Sci.*, 2007, **96**, 670.
110. Y. Qiu and K. Park, *Adv. Drug Deliver. Rev.*, 2001, **53**, 321.
111. O. E. Philippova, D. Hourdet, R. Audebert and A. R. Khokhlov, *Macromolecules*, 1997, **30**, 8278.
112. R. Siegel and B. A. Firestone, *Macromolecules*, 1988, **21**, 3254.
113. M. Mayo-Pedrosa, N. Cachafeiro-Andrade, C. Alvarez-Lorenzo, R. Martinez-Pacheco and A. Concheiro, *Eur. Polym. J.*, 2008, **44**, 2629.
114. C. Alvarez-Lorenzo, H. Hiratani, K. Tanaka, K. Stancil, A. Yu, Grosberg and T. Tanaka, *Langmuir*, 2001, **17**, 3616.
115. C. Alvarez-Lorenzo and A. Concheiro, *J. Control. Release*, 2002, **80**, 247.
116. P. Mi, L. Y. Chu, X. J. Ju and C. H. Niu, *Macromol. Rapid Commun.*, 2008, **29**, 27.
117. M. Casolaro, I. Casolaro and S. Lamponi, *Eur. J. Pharm. Biopharm.*, 2012, **80**, 553.
118. E. R. Gillies and J. M. Fréchet, *J. Pure Appl. Chem.*, 2004, **76**, 1295.
119. S. R. Van Tomme, G. Storm and W. E. Hennink, *Int. J. Pharm.*, 2008, **355**, 1.

Downloaded on 01/09/2013 10:25:46.

120. R. V. Ulijn, *J. Mater. Chem.*, 2006, **16**, 2217.
121. R. de la Rica, D. Ailia and M. M. Stevens, *Adv. Drug Deliver. Rev.*, 2012, **64**, 967.
122. B. Law and C. H. Tung, *Bioconjugate Chem.*, 2009, **20**, 1683.
123. Z. Yang, G. Liang, L. Wang and B. Xu, *J. Am. Chem. Soc.*, 2006, **128**, 3038.
124. C. Park, H. Kim, S. Kim and C. Kim, *J. Am. Chem. Soc.*, 2009, **131**, 16614.
125. A. A. Aimetti, A. J. Machen and K. S. Anseth, *Biomaterials*, 2009, **30**, 6048.
126. T. L. Andresen, D. H. Thompson and T. Kaasgaard, *Mol. Membr. Biol.*, 2010, **7**, 353.
127. M. J. Webber, C. J. Newcomb, R. Bitton and S. I. Stupp, *Soft Matter*, 2011, **7**, 9665.
128. C. Coll, L. Mondragón, R. Martínez-Máñez, F. Sancenón, M. D. Marcos, J. Soto, P. Amorós and E. Pérez-Payá, *Angew. Chem. Int. Ed.*, 2011, **50**, 2138.
129. M. Tanihara, Y. Suzuki, Y. Nishimura, K. Suzuki, Y. Kakimaru and Y. Fukunisi, *J. Pharm. Sci.*, 1999, **88**, 510.
130. T. Miyata, T. Uragami and K. Nakamae, *Adv. Drug Delivery Rev.*, 2002, **54**, 79.
131. T. Miyata, in *Biomedical Applications of Hydrogels Handbook*, ed. R. M. Ottenbrite, K. Park and T. Okano, Springer, New York, 2010, Part 1, p. 65.
132. X. Cao, S. Lai and L. J. Lee, *Biomed. Microdevices*, 2001, **3**, 109.
133. N. A. Peppas, *J. Drug Del. Sci. Technol.*, 2004, **14**, 247.
134. C. S. Satish and H. G. Shivakumar, *J. Macromol. Sci. A*, 2007, **44**, 379.
135. T. Traitel, Y. Cohen and J. Kost, *Biomaterials*, 2001, **21**, 1679.
136. D. A. Butterfield, S. S. Hardas and M. L. B. Lange, *J. Alzheimers Dis.*, 2010, **20**, 369.
137. J. K. Kundu and Y. J. Surh, *Pharm. Res.*, 2010, **6**, 999.
138. A. Napoli, M. J. Boerakker, N. Tirelli, R. J. M. Nolte, N. A. J. M. Sommerdijk and J. A. Hubbell, *Langmuir*, 2004, **20**, 3487.
139. C. M. Hassan, F. J. Doyle III and N. A. Peppas, *Macromolecules*, 1997, **30**, 6166.
140. W. Zhao, H. Zhang, Q. He, Y. Li, J. Gu, L. Li, H. Li and J. Shi, *Chem. Comm.*, 2011, **47**, 9459.
141. S. Tanna, T. S. Sahota, K. Sawicka and M. J. Taylor, *Biomaterials*, 2006, **27**, 4498.
142. S. Y. Cheng, I. Constantinidis and A. Sambanis, *Biotechnol. Bioeng.*, 2006, **93**, 1079.
143. T. Miyata, N. Asami and T. Uragami, *Nature*, 1999, **399**, 766.
144. Y. Ishihara, H. S. Bazzi, V. Toader, F. Godin and H. F. Sleiman, *Chem. Eur. J.*, 2007, **13**, 4560.
145. K. Makino, E. J. Mack, T. Okano and S. W. Kim, *J. Control. Release*, 1990, **12**, 235.

Downloaded on 01/09/2013 10:25:46.

146. K. Kataoka, H. Miyazaki, M. Bunya, T. Okano and Y. Sakurai, *J. Am. Chem. Soc.*, 1998, **120**, 12694.
147. R. Cheng, F. Feng, F. Meng, C. Deng, J. Feijen and Z. Zhong, *J. Control. Release*, 2011, **152**, 2.
148. F. Q. Schafer and G. R. Buettner, *Free Radic. Biol. Med.*, 2001, **30**, 1191.
149. P. Kuppusamy, H. Li, G. Ilangovan, A. J. Cardounel, J. L. Zweier, K. Yamada, M. C. Krishna and J. B. Mitchell, *Cancer Res.*, 2002, **62**, 307.
150. H. L. Sun, B. N. Guo, X. Q. Li, R. Cheng, F. H. Meng, H. Y. Liu and Z. Y. Zhong, *Biomacromolecules*, 2010, **11**, 848.
151. Y. Li, K. Xiao, J. Luo, W. Xiao, J. S. Lee, A. M. Gonik, J. Kato, T. A. Dong and K. S. Lam, *Biomaterials*, 2011, **32**, 6633.
152. J. Li, M. Huo, J. Wang, J. Zhou, J. M. Mohammad, Y. Zhang, Q. Zhu, A. Y. Waddad and Q. Zhang, *Biomaterials*, 2012, **33**, 2310.
153. T. Tanaka, *Phys. Rev. A*, 1978, **17**, 763.
154. A. Hatefi and B. Amsden, *J. Control. Release*, 2002, **80**, 9.
155. T. Y. Liu, S. H. Hu, D. M. Liu, S. Y. Chen and I. W. Chen, *Nano Today*, 2009, **4**, 52.
156. M. Bikram and J. L. West, *Expert Opin. Drug Del.*, 2008, **5**, 1077.
157. L. Martin, M. Alonso, A. Girotti, F. J. Arias and J. C. Rodriguez-Cabello, *Biomacromolecules*, 2009, **10**, 3015.
158. S. R. Sershen, S. L. Westcott, N. J. Hallas and J. L. West, *J. Biomed. Mater. Res.*, 2000, **5**, 293.
159. T. J. Mason, *Ultrason. Sonochem.*, 2011, **18**, SI 847.
160. H. Zhang, H. Xia, J. Wang and Y. Li, *J. Control. Release*, 2009, **139**, 31.
161. G. A. Husseini, G. D. Myrup, W. G. Pitt, D. A. Christensen and N. Y. Rapoport, *J. Control. Release*, 2000, **69**, 43.
162. N. Rapoport, in *Smart Nanoparticles in Nanomedicine*, ed. R. Arshady and K. Kono, Kentus Books, London, 2006, p. 305.
163. B. J. Staples, W. G. Pitt, B. L. Roeder, G. A. Husseini, D. Rajeev and G. B. Schaalje, *J. Pharm. Sci.*, 2010, **99**, 3122.
164. P. Kamev and N. Rapoport, *Am. J. Phys.*, 2006, **829**, 543.
165. N. Rapoport, in *Nanotechnology for Cancer Therapy*, ed. M. Amighi, CRC Press, Boca Raton, Florida, 2006, p. 417.
166. T. Nagasaki and S. Shinkai, *J. Incl. Phenom. Macro.*, 2007, **58**, 205.
167. R. H. Bisby, C. Mead and C. G. Morgan, *Biochem. Biophys. Res. Commun.*, 2000, **276**, 169.
168. G. B. Braun, A. Pallaoro, G. Wu, D. Missirlis, J. A. Zasadzinski, M. Tirrell and N. O. Reich, *ACS Nano*, 2009, **3**, 2007.
169. J. L. Vivero-Escoto, I. I. Slowing, C. W. Wu and V. S. Y. Lin, *J. Am. Chem. Soc.*, 2009, **131**, 3462.
170. J. Chen, M. Yang, Q. Zhang, E. C. Cho, C. M. Cobley, C. Kim, C. Glaus, L. V. Wang, M. J. Welch and Y. Xia, *Adv. Funct. Mater.*, 2010, **20**, 3684.
171. C. Alvarez-Lorenzo, L. Bromberg and A. Concheiro, *Photochem. Photobiol.*, 2009, **85**, 848.
172. S. Sortino, *J. Mater. Chem.*, 2012, **22**, 301.

Downloaded on 01/09/2013 10:25:46.

173. R. Müller, H. Steinmetz, R. Hiergeist and W. Gawalek, *J. Magn. Magn. Mater.*, 2004, **276**, 272.
174. M. Arruebo, R. Fernández-Pacheco, M. R. Ibarra and J. Santamaría, *Nano Today*, 2007, **2**, 22.
175. C. S. S. R. Kumar and F. Mohammad, *Adv. Drug Deliver. Rev.*, 2011, **63**, 789.
176. C. Alexiou, R. J. Schmidt, R. Jourgons, M. Kremer, G. Wanner, C. Bergemann, E. Huenges, T. Nawroth, W. Arnold and F. P. Parak, *Eur. Biophys. J.*, 2006, **35**, 446.
177. T. Y. Liu, S. H. Hu, D. M. Liu, S. Y. Chen and I. W. Chen., *Nano Today*, 2009, **4**, 52.
178. U. O. Hafeli, *Int. J. Pharm.*, 2004, **277**, 19.
179. S. Murdan, *J. Control. Release*, 2003, **92**, 1.
180. S. Kagatani, T. Shinoda, Y. Konno, M. Fukui, T. Ohmura and Y. Osada, *J. Pharm. Sci.*, 1997, **86**, 1273.
181. S. A. Agnihotri, R. V. Kulkarni, N. N. Mallikarjuna, P. V. Kulkarni and T. M. Aminabhavi, *J. Appl. Polym. Sci.*, 2005, **96**, 301.
182. A. G. MacDiarmid, *Angew. Chem. Int. Ed.*, 2001, **40**, 2581.
183. D. Svirskis, J. Travas-Sejdic, A. Rodgers and S. Garg, *J. Control. Release*, 2010, **146**, 6.
184. D. Svirskis, B. E. Wright, J. Travas-Sejdic, A. Rodgers and S. Garg, *Electroanal.*, 2010, **22**, 439.
185. R. Okner, M. Oron, N. Tal, D. Mandler and A. J. Domb, *Mater. Sci. Eng. C.*, 2007, **27**, 510.
186. Y. Cho, R. Shi, A. Ivanisevic and R. B. Borgens, *Nanotechnology*, 2009, **20**, 275102.
187. R. T. Richardson, A. K. Wise, B. C. Thompson, B. O. Flynn, P. J. Atkinson, N. J. Fretwell, J. B. Fallon, G. G. Wallace, R. K. Shepherd, G. M. Clark and S. J. O'Leary, *Biomaterials*, 2009, **30**, 2614.
188. D. Ge, X. Tian, R. Qi, S. Huang, J. Mu, S. Hong, S. Ye, X. Zhang, D. Li and W. Shi, *Electrochim. Acta*, 2009, **55**, 271.
189. H. Ghandehari, *Adv. Drug Deliver. Rev.*, 2008, **60**, 956.

CHAPTER 2

Materials Science and Engineering of the Low Temperature Sensitive Liposome (LTSL): Composition-Structure-Property Relationships That Underlie its Design and Performance

DAVID NEEDHAM*[a] AND MARK W. DEWHIRST[b]

[a] Department of Mechanical Engineering and Material Science, Duke University, Durham NC 27705, USA, and DNRF Niels Bohr Professor, and HCA Academy Visiting Professor, University Southern Denmark, DK-5230 Odense M, Denmark; [b] Gustavo S. Montana Professor, Director of Tumor Microcirculation Laboratory, Department of Radiation Oncology, Duke University Medical Center, Duke University, Durham, NC 27708, USA
*Email: d.needham@duke.edu

2.1 Introduction

2.1.1 Lipids as "Smart Materials"

As is now commonly known, simply adding water to an otherwise dry lipid sample generates "self-assembled" lamellar structures pretty much immediately.[1] When carried out under the right conditions (*e.g.* above the lipid

---

RSC Smart Materials No. 2
Smart Materials for Drug Delivery: Volume 1
Edited by Carmen Alvarez-Lorenzo and Angel Concheiro
© The Royal Society of Chemistry 2013
Published by the Royal Society of Chemistry, www.rsc.org

solid-liquid phase transition temperature), and then extruded under positive pressure through a 100-nm nanopore filter, a suspension of unilamellar liposomes is produced, with diameters of $\sim 100\,\text{nm}$.[2,3] This simple fabrication process has become the basis for a range of drug-delivery systems based on the biologically ubiquitous and compatible liposome, or small unilamellar vesicle (SUV). Even by the late 1970s a huge number of compounds had been encapsulated in liposomes,[4] and new applications were being sought for this potentially revolutionary drug-delivery system. One of the principal drugs at the time, doxorubicin, was successfully encapsulated into conventional liposomes and tested *in vivo*.[5] As reviewed by Waterhouse *et al.*,[6] the liposome formulations were found to maintain the anticancer activity of free doxorubicin in mice, while at the same time decreasing its associated cardiotoxicity. As a result, two main liposomal formulations of doxorubicin, Doxil® and Myocet™, have been developed and evaluated in clinical trials. Doxil is FDA approved for several clinical indications, and Myocet is approved in Europe and Canada for treatment of metastatic breast cancer in combination with cyclophosphamide.

As listed by Maurer *et al.*,[7] such a self-assembled nanocapsule is made up of just 95,000 molecules of lipid and has an encapsulated volume of 3.8×10^{-19} liters. If a drug is encapsulated at 100 mM, there will be 2.4×10^{4} molecules of drug per nanocapsule. While keeping the drug inside the liposome is a favorable consequence that reduces toxicity[8,9] (and references therein), one major obstacle to a more effective use of liposomes as drug-delivery vehicles is actually to get the drug out, perhaps in response to a local biological or other applied trigger. This is particularly important for treating cancer, especially with the more traditional, highly toxic, chemotherapeutics. Lipids can become "smart materials" when they perform a desired function in response to an environmental change.

Given that we want to use the encapsulating function of lipids as bilayers to achieve some drug-delivery goal, we might immediately start to ask, *"What makes the self-assembly process (that is also critical to encapsulating every cell on the planet) form such ultrathin (5 nm), two-molecule-thick structures?"* and *"How can they be made to have encapsulating and release functions?"* The basis for all materials design and innovation is a deep and detailed understanding of the relationships between a material's *composition*, *structure* and *properties* (CSP; see Chapter 1 in this volume for general concepts), and how these relationships influence *processing* and *performance* of the material in service, in this case in the bloodstream or other tissue-milieu in the body. We will get into much more detail in subsequent sections of this chapter regarding lipids, lipid bilayers and micelles, but to give an initial example of what we mean by CSP relationships, let's look at one of the most common lipids that we have relied on as a prototypical lipid bilayer material, 1-stearoyl-2-oleoyl-*sn*-glycero-3-phosphocholine (SOPC).

As shown in Figure 2.1, SOPC is *compositionally* loaded with carbons and hydrogens with an empirical formula of $C_{44}H_{86}NO_8P$. *Structurally*, it is

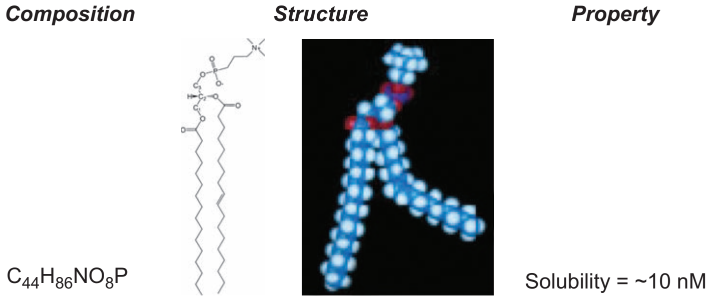

Figure 2.1 Chemical *composition* (empirical formula), molecular *structure* (space filling) and a *property* of solubility for a prototypical lipid bilayer material, 1-stearoyl-2-oleoyl-*sn*-glycero-3-phosphocholine (SOPC).

amphipathic comprising a hybrid structure of a glycerol backbone, a phosphocholine head-group and two hydrocarbon chains. While we will later be concerned with the *properties* of its assembly as bilayers, this molecule also has properties of its own, like its water solubility that is made up of the two amphipathic parts. We see that while the hydrophilic, glycerylphosphorylcholine has a solubility $S = 4.8$ M,[10] the two hydrophobic hydrocarbon tails are so relatively insoluble in water (stearoyloleoylglycerol $S = \sim 5$ nM (ALOGPS predicted value)) that they largely determine the SOPC molecular solubility of only ~ 22 nM (ALOGPS predicted value). Thermodynamically, then, it is this high head-group solubility and extremely low hydrocarbon chain solubility that largely govern the self-assembly of the bilayer in water, *i.e.* an overriding entropic exclusion of the hydrocarbon from water (the so-called hydrophobic effect[11]) and a protection of the assembled hydrocarbon chains by a double interface of the phosphocholine to form a bilayer.[12]

So now we have the basis for a membrane capsule. Beyond this global hydrophobic effect though, there are subtleties that determine additional *composition*-*structure*-*property* relationships that, in turn, underlie and direct our "*Smart Materials Design*". Examples here include the response of the bilayer material to one or more environmental cues, like pH[†],[13] enzymes,[14] or, in our case, temperature.[15,16] This chapter will present and explore the material relationships that went into the discovery, design and performance of the so-called Low Temperature Sensitive Liposome (LTSL). Single Giant Unilamellar Vesicle (GUV) experiments and data that we have carried out and reported over the past 32 years will be presented and described in terms of classical materials science and materials engineering design. These micropipet experiments and analyses are unique to membrane mechanics and were literally instrumental in arriving at the LTSL formulation. This particular LTSL lipid *composition* has combined the benefits of lipid encapsulation (reduced drug toxicity) together with mild hyperthermia (triggered drug release) to provide a clinically attainable way to get a drug like doxorubicin out of the liposome and into all cells of a tumor (neoplastic, stroma, pericytes and endothelia), in unprecedented amounts.[17]

[†] See also Chapter 3. pH-sensitive Liposomes in Drug Delivery, Shivani Rai Paliwal, Rishi Paliwal, and Suresh P Vyas.

2.1.2 Micelles, Bilayers and Inverted Micelles

The best way to start thinking about how to design a "smart" liposome for any application is to understand what makes a particular lipid molecule form a bimolecular leaflet or lipid bilayer, and what makes it form other structures. It would be the transition or transformation to these other *structures* with different *properties* that creates the potential for an environment-sensitive response. Israelachvili *et al*. treated the lipid-packing problem (what it takes to form micelles, bilayers and inverted micelles) in terms of a chain packing parameter.[18] The chain packing parameter is defined relative to the area of the lipid head-group at the lipid-water interface (A), the volume of the entire lipid molecule (V) and its length (l). When $V/Al \sim 1$, lamellar structures are formed, whereas normal micelles and inverted curved structures are obtained for $V/Al < 1$ and $V/Al > 1$, respectively.

With this brief introductory background (see also the references section) let's now look at what these simple rules mean for bilayer *composition-structure-property* relationships for a single lipid bilayer that, in the case of the LTSL, contains a majority of di-chain phosphatidylcholine lipids ($V/Al \sim 1$), and in the same bilayer a minority of a mono-chain phosphatidylcholine ($V/Al < 1$), and a third component, also in low concentration, a distearoyl PEG lipid (also $V/Al < 1$). The goal is to understand in as much detail as possible how this *composition* with bilayer, grain domain and other defect *structures* can have all the *properties* needed for it to load, encapsulate and retain a drug, and trigger the release of the encapsulated drug in response to just a few degrees rise in temperature.

2.2 Reverse Engineering the LTSL

If done as a new product, design is a forward engineering process; if analyzed in hindsight, this is a reverse engineering process. In principle both involve: defining the function of the device; identifying components and analyzing the component design and mechanism; materials choice and their *composition-structure-property* relationships; production; and testing its performance-in-service. Actually, design is never really totally original; there will always be previous materials, designs and components that have some bearing on the particular system under development. In that sense, design, as a process, is continual, on-going and iterative. For this LTSL that already exists, it is interesting and instructive then to look at this process as a "reverse engineering" exercise; so let's reverse engineer the LTSL.

2.2.1 Define the Function

Whether reverse or forward engineering, any materials science and engineering design requires us to create a careful, and as precise as possible, definition of the functions that the design has to achieve. Functionally, what is required for this particular thermal-sensitive "smart drug delivery" system is a lipid-based capsule that can:

a) be loaded with a drug (*e.g.* doxorubicin),
b) retain the drug in processing and upon i.v. administration into the bloodstream,
c) evade the body's defenses (such as opsonization) that would normally take it to the liver and spleen for removal by the reticulo endothelial system, including the macrophage "Kupffer" cells of the liver sinusoids and
d) be triggered to release its drug in the microvasculature of a warmed tumor (by mild hyperthermia).

Functions a), b) and c) have been fairly well established in the liposome literature. However, it was not until they had been fully tested in the clinic[19] (a huge effort) that it was realized that still more effort needed to be put into d) (the triggered release of drug). It was found that, for this advanced pharmaceutical formulation to achieve its full potential in cancer treatment, it is not enough to load and retain drug, and evade the body's defenses.

The design and performance issues centered around the following. It has long been known that tumor vasculature can be hyperpermeable.[20] Especially in animal models, implanted tumors have been characterized to be leaky with enlarged endothelial pores. This leakiness has been deemed critical for allowing liposome-accumulation by the Enhanced Permeability and Retention (EPR) effect.[21,22] As depicted in Figure 2.2A this paradigm relies on the difference in permeability between normal and tumor vasculature. If the tumor vasculature is sufficiently leaky, then, when injected intravenously, liposomes that can retain their drug and have long circulation half-lives should be able to extravasate and accumulate within the tumor tissue; a form of "passive targeting" based on this apparent quirk of rapidly growing tumors.

Thus, in most of the original liposome strategies that were developed in the 40 or so years since liposomes were first explored as drug-delivery systems,[23,24] the thinking was this: because tumor-vascular leakiness had been observed, especially in animal tumor models, all that was needed was a long circulating liposome that was loaded with, and retained, a drug (*i.e.* functions a), b) and c)). Then, it would passively accumulate in the tumor interstitium, thereby delivering drug to any tumor in the body. Because of their small but (in biological terms) relatively large size of 100 nm diameter, the accumulation of liposomes and their encapsulated drug depends exclusively on this EPR

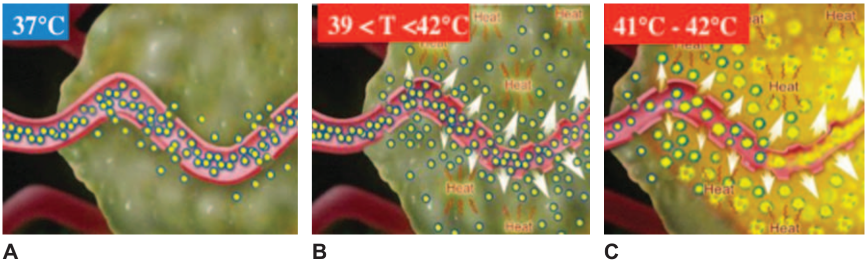

Figure 2.2 The problem and the solution (at least for local tumors). Scheme of the EPR effect that appears to provide only limited access of the relatively large 100 nm diameter liposomes (A); hyperthermia can make the blood vessels more leaky and help with interstitial transport of liposomes and drugs (B); the Thermal Sensitive Liposome does not need to extravasate; it can release its drug in the bloodstream of a warmed tumor and the drug can readily diffuse throughout the neoplasm (C).

effect. However, we and others[25] have demonstrated this apparent passive leakiness in animal tumors models is locally heterogeneous,[26] and can often be minimal, or even absent, across both implanted tumor models[17,27–29] and especially spontaneous tumors (feline patients with soft tissue sarcomas).[30] However, as is shown in Figure 2.2B, hyperthermia can result in a significant increase in liposome accumulation in a tumor. Spontaneous tumors in feline patients were found by SPECT imaging to increase their local permeability to technetium-99m-labeled liposomes.[30] There was a time-averaged range of 2–13-fold increase in liposome accumulation in the tumor under hyperthermic conditions (heated for 1 h at 42 °C) compared with normothermic conditions. Effects of heat on tumor vasculature have actually been well documented. Hyperthermia increases the size to the endothelial junctions, which results in increased vascular permeability.[31,32] In prior studies[33] it was determined that the endothelial pore sizes in heated tumor vessels are between 100 and 400 nm.

More importantly for treating human cancers, *actually in humans*, such poor normothermic leakiness to 100 nm diameter and larger nanoparticle delivery is, as yet, not conclusively proven clinically. Even if they do extravasate, as pointed out by Chen *et al.*,[34] their diameter is larger than or comparable to the inter-fiber distance in the extra-cellular matrix (ECM) and so “stealth” liposomes can remain trapped in the peri-vasculature space for weeks.[25] As a result, even after extravasation from tumor microcirculation, liposomes can accumulate only in perivascular regions and not necessarily release their anticancer drug that quickly, relying perhaps on the dissipation of the liposomal pH gradient and the degradation of lipids by endogenous tumor lipases. The perivascular location may limit drug penetration as well. As drugs slowly leak from these liposomes, they will diffuse along the most dominant concentration gradient. The concentration in blood would be virtually zero, so much of the drug might be reabsorbed into the tumor vasculature and carried away, as opposed to penetrating into the tumor interstitium.

It is this limited access to tumor tissue that prompted our exploring temperature-triggered drug release, where the LTSL would not need to extravasate, but could be made to release its small-molecule drug (*e.g.* doxorubicin) in the warmed microvasculature of the tumor. As is shown in Figure 2.2C, it would now be this small drug that would diffuse into the tumor interstitium, deeply penetrate the whole cancer tissue, cross cell membranes and arrive at its target (the DNA and RNA of all cells in the tumor).[17] Clearly, because of the need for local heating, this strategy would not be applicable to treating patients with widely metastatic disease. Nevertheless, local control of tumors by such minimally invasive, and even non-invasive, methods could represent a major advance in treating solid tumors that are: 1) not amenable to surgical resection or 2) too large for surgery. In the latter case, treatment could downstage (shrink) tumors, thereby permitting later surgical removal. At the very least we might expect debulking of the tumor mass, and a concomitant lessening of disfigurement, pain and suffering by the patient.

In the next section these functions are now evaluated in terms of a component design, developing a mechanism of action. Each component is analyzed in terms of choice of materials available and their CSP relationships that can achieve the functions, given that component design.

2.2.2 LTSL Component Design

The component design of the LTSL concept is shown in Figure 2.3. It comprises basically four components: 1) an encapsulating solid phase membrane, capable of being taken through a solid-liquid phase transition at

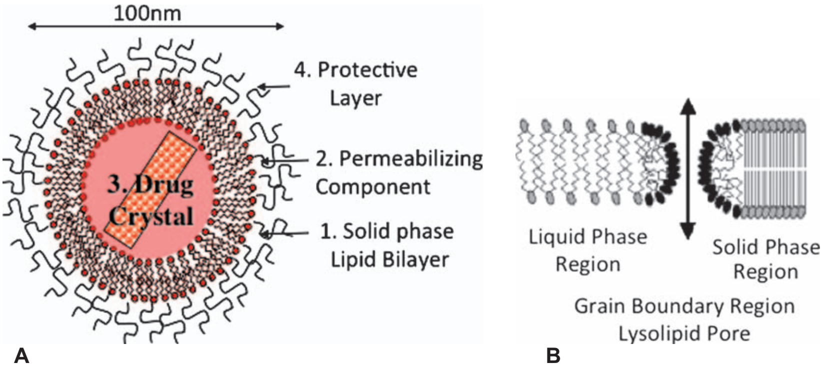

Figure 2.3 Component design of the 100 nm diameter LTSL, comprising: 1) an encapsulating solid phase lipid bilayer; 2) a permeabilizing component; 3) an encapsulated drug; and 4) a protective PEG-layer (A). Mechanistically, could nanopores be created at the grain boundaries? (B).

just above body temperature; 2) a permeabilizing component embedded in the bilayer; 3) an encapsulated drug, in this case doxorubicin, that crystallizes in the liposome interior; and 4) a protective PEG-layer that would avoid opsonization and ensure long circulation half-life. Mechanistically, it was already known that solid phase membranes solidify with nanocrystalline domains with grain boundaries, and that upon melting these grain boundaries seemed to be a site for defects and enhanced permeability to at least ions.[35–37] As will be discussed later in "*Performance*" (Section 2.4), the earlier thermal-sensitive formulations of Yatvin *et al.*[38] only released drug slowly, and so we asked, "*Could this formulation be improved by including a permeabilizing component?*" Given this component design, the reverse engineering task is to evaluate the choice of materials *composition*, review (or obtain *de novo*) *structure* and *property* data for each of them and analyze if and to what extent each material can achieve the functions required.

2.2.3 Materials Choice and CSP Relationships

With the four components of the design identified, we write out a simple materials matrix, as shown in Table 2.1. It is a materials matrix that basically starts the process of evaluating the materials for the design. This is where the design really starts to take shape and very detailed data are required; shown here are just a few of the data (empirical formulae, MWts, solubilities and some of the lipid bilayer properties like transition temperatures, elasticity and strength).

Table 2.1 Materials matrix of composition, structure and properties for each component of the LTSL for doxorubicin delivery.

Components	*Composition*	*Structure*	*Properties*
1. Solid membrane	DPPC $C_{40}H_{80}NO_8P$	Bilayer grains and grain boundaries	MWt: 734.6 g/mol $K_A \sim 2000$ mN/m $T_m = 41.5$ °C
2. Permeabilizing component	MSPC $C_{26}H_{54}NO_7P$	Micellar (aq)	MWt: 523.6 g/mol Water solubility 1 μM Bilayer soluble ~70 mol%
3. Drug	Doxorubicin $C_{27}H_{29}NO_{11}$ (citrate salt)	Crystalline	MWt: 543.5 g/mol p$K_a = 8.3$ Solubility: 20 mM at pH 7.5 and 1.8 mM at pH 4.0
4. Protective layer	DSPE-polyethylene glycol^{2000} $C_{133}H_{267}N_2O_{55}P$	Random helix Mushroom-brush	MWt: 2805.5 g/mol Steric repulsion Water-soluble Bilayer-soluble Chloroform-soluble

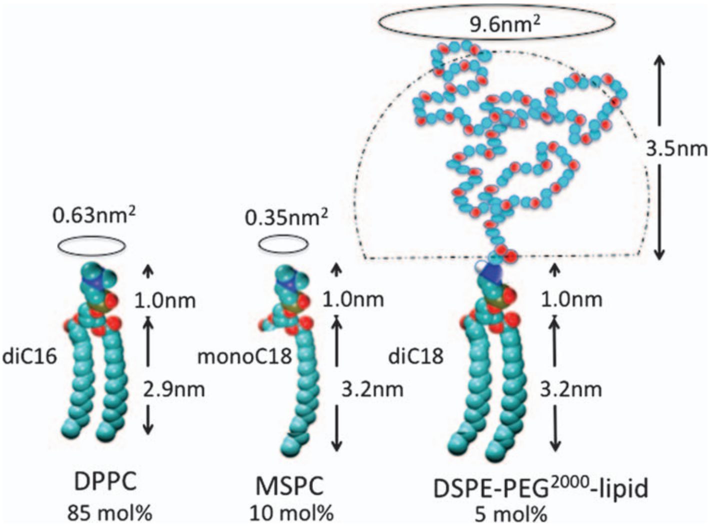

Figure 2.4 The three components of the LTSL lipid membrane: DiPalmitoylPhosphatidylCholine (DPPC); MonoStearoylPhosphatidylCholine (MSPC); DiStearoylPhosphatidylEthanolamine-Poly(ethylene-glycol)^{2000} (DSPE-PEG^{2000}).

The LSTL formulation[‡] (trade name ThermoDox®)[40,41] is composed of a judicial combination of three component lipids, each with a specific function and each affecting specific material properties, including a sharp thermal transition and a rapid onset of membrane permeability to small ions, drugs and small dextran polymers.[42,43] This formulation has been designed to achieve the desired result (functions) of retention of drug and relative stability in the bloodstream yet ultrafast drug release in tumors when triggered by only mild clinically attainable hyperthermia.[44–48]

As shown in Figure 2.4, the three components of the LTSL lipid membrane are:

DiPalmitoylPhosphatidylCholine (DPPC), a diC16 lipid, which acts as the host lipid that forms the bilayer and provides the main acyl chain melting transition at ~41.5 °C;

MonoStearoylPhosphatidylCholine (MSPC), a monoC18PC lipid, which is the permeabilizing component that, when incorporated in the bilayer membrane at several mol%, can induce thermally enhanced permeability to small molecules and ions over and above that given by DPPC alone;[1,46,49,50] and

DiStearoylPhosphatidylEthanolamine-PEG^{2000}, a diC18PE lipid derivatized with a poly(ethylene-glycol) chain of molecular weight 2000 Da

---

[‡] The name Low Temperature Sensitive Liposome (LTSL) is to contrast it with previous liposomes by others: 38. M. B. Yatvin *et al.*, Design of liposomes for enhanced local release of drugs by hyperthermia, *Science*, 1978, **202**, 1290–1293. 39. M. B. Yatvin *et al.*, Selective delivery of liposome-associated cis-dichlorodiammineplatinum(II) by heat and its influence on tumor drug uptake and growth, *Cancer Res*, 1981, **41**, 1602–1607.

(DSPE-PEG^{2000}), which was included for its interfacial stabilizing (stealth) effect.[51] However, as discussed later, it also appears to have a second function, bringing additional steric stability to the lysolipid-induced membrane permeabilization itself, and thus helping to facilitate ultrafast drug release.

Structurally, the dimensions of these lipids can be estimated from measurements of bilayer and hydrocarbon region thickness and area, as determined by simultaneous analysis of small-angle neutron and X-ray scattering data.[52] As liquid phase bilayers, the acyl chain region of DPPC is 2.9 nm long, and MSPC and DSPE are ~3.2 nm. The head-groups are ~1 nm in length. PEG^{2000} is expected to extend a distance of ~3.5 nm from the bilayer interface as determined by X-ray diffraction.[53] Molecular areas are largely determined by the projected areas of the acyl chains, and these change as a function of temperature. In the solid phase the all-*trans* acyl chain confirmations give smaller areas per molecule, while in the liquid phase more gauche kinks are introduced and the areas are slightly larger. Shown are estimates of the areas in the liquid Lα phase: DPPC is 0.63 nm^2;[52] MSPC is expected to be just over half this value having only one acyl chain;[54] and while the phosphatidylethanolamine head-group itself is expected to be smaller in area due to the lack of the three methyl groups (on the PCs), the PEG part of DSPE-PEG projects an area of almost 10 nm^2 at the bilayer interface as "mushrooms".[53]

With regard to their expected self-assembled structures, DPPC has a V/Al ~ 1, and so forms lamellar structures, and provides the bilayer "solvent" in which the other two components are dissolved. With the same phosphocholine head-group, but only one C18 lipid chain, MSPC has a V/Al < 1 and so, when hydrated in water, forms micelles with a critical micelle concentration (cmc) of ~1 μM. Similarly, even though DSPE-PEG^{2000} has two acyl chains and a quite water-soluble phosphatidylethanolanine head-group, its 2000 Da, very water-soluble, polyethylene glycol (CH_2CH_2O) 47-mer polymer confers a larger area per molecule at an interface with water, and therefore also has a V/Al < 1; in water it too forms micelles with a similar ~1 μM cmc. Despite the fact that both of these molecules can actually be classified as detergents and do not form bilayers on their own, when mixed in low concentration with the host bilayer lipid (DPPC), they integrate quite well. Even more, since the acyl chains are similar (di C16, mono C18, di C18) they mix ideally in the solid phase, and do not really broaden the phase transition of the bilayer. The *compositional* key, then, to creating a stable bilayer *structure* is a host bilayer lipid that is a good solvent for any additional components. Namely, keeping the head-group and acyl chain compositions very similar ensures ideal mixing.

2.2.4 Composition-Structure-Properties of Each Component

Each component will now be discussed in the context of the CSP relationships that go into the LTSL design. In choosing the materials we draw on a wealth of literature on liposomes, and try to place the liposomal composition in terms of required material properties.

In order to establish relationships between composition-structure and actual membrane properties, we need a technique that can manipulate individual lipid bilayers, preferably as vesicles that can be viewed in an optical microscope. These lipid vesicles must therefore be tens of microns in size, must represent the membranes of the liposome, and we must be able to apply well-defined stresses and measure accurately any resulting area, bending or shear strain, and be able to control and/or keep track of vesicle volume. Such a technique is micropipet manipulation developed for studying so-called Giant Unilamellar Vesicles (GUVs) by Evans and Needham.[55] Initiated by Rand and Burton,[56] for almost 50 years these micropipet techniques have provided a unique ability to apply well-defined stresses for basic modes of membrane and cellular deformation, and simultaneously to measure the strain, and rates of strain, resulting from these applied stresses.[57] It was then this ability to measure directly these stress and strain parameters that allowed the characterization of the material behavior of individual erythrocytes,[58] leukocytes,[59] and cancer cells[60] in terms of elastic moduli and viscous coefficients as well as inter-surface interactions.[61] Starting in the 1980s the technique was adapted and developed by Evans and Kwok[62,63] and then Evans and Needham[64] to study the simple lipid bilayer membrane as GUVs. In this section, several of these and subsequent experiments that characterized the properties of a series of lipid compositions, leading ultimately to the new concept for rapid permeabilization of the LTSL at its phase transition temperature, are reviewed. It is in these experiments and their results that *Functions* are related directly to *Composition*, *Structure* and *Property*, and hopefully provide the *Performance* necessary for more effective treatments of, in this case, cancer. Thus, many of the lipid bilayer properties (mechanical, thermal, molecular-exchange and their colloidal interactions) that have gone into this LTSL design (and in fact can explain the functions and properties of other liposomes) come largely from our own micropipet experiments on GUV.

2.2.4.1 The Solid Phase Encapsulating Membrane

The encapsulating membrane provides the first two functions: to allow loading of a drug (*e.g.* doxorubicin), and to retain the drug in processing and upon i.v. administration into the bloodstream. The properties that allow or relate to these functions are the Elastic Area Expansivity of the membrane (K_A), its mechanical tensile strength (t_s) and its internal dielectric constant (of ~ 2) that, together with the expansivity, limits the permeability of polar molecules and ions, but can let neutral doxorubicin through. (How this influences drug loading will be discussed in Section 2.2.4.3.)

C*ompositionally*, the encapsulating membrane is composed of DiPalmitoylPhosphatidylCholine (DPPC). Similar to SOPC, it contains a high proportion of carbons and hydrogens, in an empirical formula of $C_{40}H_{80}NO_8P$ (2 CH_2s less than SOPC), which structurally form two C16 acyl chains. Both acyl chains are saturated, meaning they do not contain any C=C double bonds. These saturated chains can exert maximum van der Waals attraction on each other in the solid phase, especially as C–C bond rotation is reduced at low relative temperatures giving a more all-*trans* conformational *structure*.

Structurally, the solid bilayer is made up of crystalline grains with grain boundaries, as shown in Figure 2.5.

The grain structure of the liposome bilayer is evident from the faceted structure shown in Figure 2.5A, a Transmission Electron Microscope (TEM) image of the LTSL itself.[65,66] Also shown in Figure 2.5B are Scanning Electron Microscope (SEM) images of DSPC-PEG-Stearate monolayers on gas microparticles,[67] and in Figure 2.5C is a fluorescent image of a 20-micron diameter gas microparticle monolayer where a fluorescent lipid (BODIPY FL PE) was included in the bilayers and segregated to the grain boundaries because it was not soluble-compatible with the solid grains of DSPC. It is interesting to see that the same micron-sized grains exhibited by the larger solid-lipid monolayers are still preserved as faceted structure even in the 100 nm diameter LTSL liposome, just scaled down with overall domain size.[67]

Property-wise, how strong might we expect this solid bilayer actually to be? And how might we actually measure it? Using the micropipet technique, suction pressures in the milli atmosphere range can be applied to a single vesicle, and the membrane can be made to expand and eventually fail.[55,68] In this experiment, shown in Figure 2.6A, a single GUV is aspirated by a micropipet, and a controlled suction pressure is applied to expand the single bilayer membrane into the pipet. As is also shown in Figure 2.6B, by measuring the length of the membrane projection ΔL in the pipet, along with the external diameter of the vesicle ($2R_v$), and diameter of the pipet ($2R_p$) as a function of suction pressure ΔP, constitutive mechanical relations[57] provide a direct measure of the membrane tension and the resulting area change, *i.e.* membrane tensile stress τ and membrane area change ΔA used to evaluate the stress/strain and the elastic area expansivity modulus K_A.

Experiments like this have been carried out on many lipids and lipid mixtures.[55,67–72] As shown by Needham and Nunn[68] and reviewed by Kim and

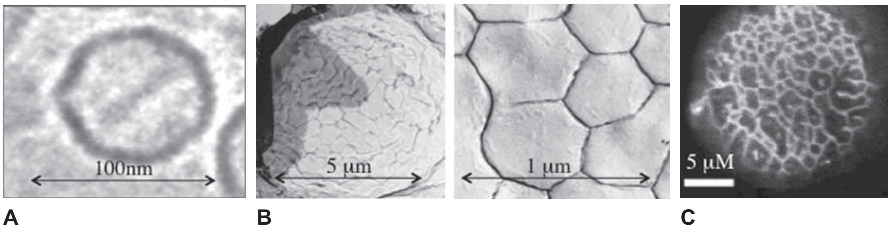

Figure 2.5 *Microstructure*. Transmission Electron Microscope (TEM) image of a single 100 nm diameter LTSL containing doxorubicin (A); Scanning Electron Microscope (SEM) images of an 8 micron diameter gas microparticle stabilized by a monolayer of DSPC : PEG-Stearate 9 : 1, and a higher magnification image of the grains and grain boundaries (B); and larger micro-gas-bubble monolayer (~20 µM), where the lipid monolayer shells incorporate a fluorescent lipid that segregates to the grain boundaries, viewed under epifluorescence (C).

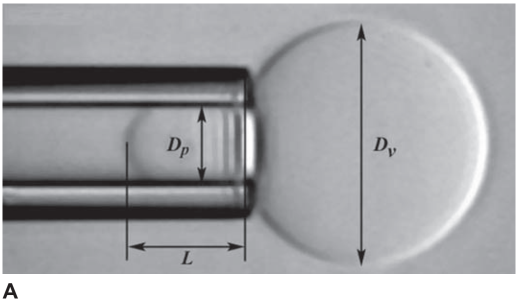

$$\tau = \Delta P R_p / 2(1 - R_p/R_v)$$

$$\Delta A = 2\pi R_p\,(1 - R_p/R_v)\Delta L$$

B

Figure 2.6 Vesicle Area Dilation Experiment. Giant Unilamellar Vesicle (GUV) (25 micron diameter) aspirated into the micropipet (8 micron diameter) ready for the expansion experiment, showing the measureable dimensions, external vesicle diameter D_v, pipet diameter D_p and membrane projection length in the pipet, L_p (the vesicle has a sucrose solution inside and a salt solution outside, creating a refractive index for better visualization) (A); and constitutive equations for determining membrane tension τ from pipet suction pressure ΔP, and radii of vesicle and pipet, and the change in vesicle membrane area ΔA from the radii of pipet and vesicle, and the projection length ΔL (B).

Needham,[69] when taken to the limits of composition, *i.e.* 50 mol% cholesterol in a bilayer composed of a long (diC20) saturated chain phospholipid, membrane elastic moduli can reach several thousand mN/m and tensile strength can be 40 mN/m, which is equivalent to the compressibility and strength of bulk hydrocarbons and polyethylene.

Mechanically, the compressibility and the tensile strength have not been measured for DPPC, but we can show the effect of solidification of a bilayer on its mechanical properties by looking at the lower temperature transition of diC14 (dimyristoylphosphatidylcholine, DMPC) lipid that has been measured.[73] This lipid ($T_m = 24.5\,°C$), its liquid and solid phases, including the area change at its pre- and main-transitions, was studied extensively by Needham *et al.*[73] For this discussion, results showed that while the liquid Lα phase bilayer (at 29 °C, *i.e.* 4.5 °C above its main transition) had an elastic area dilation modulus (K_A) of 145 mN/m, the solid Lβ phase at 8 °C was much stiffer and stronger at 855 mN/m. Between 11 °C and 24.5 °C DMPC has a rippled Pβ' phase pre-transition region; namely, a low-enthalpy transition below the chain-melting transition linked to the formation of periodic ripples. Although ostensibly "solid", in this region the bilayer is still relatively soft ($K_A = 318$ mN/m–228 mN/m measured at temperatures 20 °C and 14.5 °C, respectively). For DPPC, the pre-transition region extends from 41.5 °C down to 35.5 °C.[74] Thus, when extrapolated to DPPC, what these DMPC data show is that the DPPC bilayers as liposomes in the bloodstream at 37 °C are likely to be solid but still relatively soft, and only reach a relatively higher modulus, perhaps 1000 mN/m, at temperatures around, say, room temperature during processing. Since membrane compressibility is directly related to its permeability,[75] the nature of these mechanical states could be very important for determining the ability of the liposome to retain the drug, and indeed the H^+ ions that maintain its cationic nature. In the performance of the design then, we might expect compromised permeability in the bloodstream; later we will see if this is a concern. But, if an inherent leakiness might be the case, then why not make the membrane stronger? In other micromechanical experiments we have shown that the inclusion of cholesterol is the single biggest factor in increasing the elastic modulus of a lipid bilayer.[68] For example, K_A of SOPC and SOPC : Cholesterol 1 : 1 is ~200 mN/m and 1200 mN/m, respectively. For DPPC : Cholesterol 1 : 1 the modulus is 2500 mN/m, and so liposomes made from these membranes would be expected not only to retain drug better, but also remain in the bloodstream longer, because of their high resistance to expansion.[76] As shown in Figure 2.7, when the reticuloendothelial system is functional (*i.e.* not saturated with other lipids), liposomes circulate for longer, the higher their elastic modulus, indicating that less compressible interfaces resist opsonization.[76] In fact, this strategy has been used to great effect for a vincristine liposome formulation. Sphingomyelin : cholesterol 1 : 1 bilayers are very incompressible ($K_A = 1800$ mN/m) and strong ($t_s = 23$ mN/m),[68,69] are extremely impermeable to water,[75] and actually circulate in the bloodstream for extended periods of time, forming the basis for a vincristine liposome that is required to release (leak) small amounts of drug very slowly during its circulation time.[77] However, it has been shown by several techniques (deuterium NMR and Differential Scanning Calorimetry[78] and small-angle X-ray diffraction[79]) that the addition of cholesterol to DPPC bilayers totally abolishes the phase transition beyond 25 mol% cholesterol. Thus, by attempting to strengthen the membrane potentially to improve drug retention we defeat our object of creating a thermally responsive liposome.

Given the inherent encapsulation properties of lipid bilayers, if we are designing for thermal sensitivity and treatments for cancer, then the actual

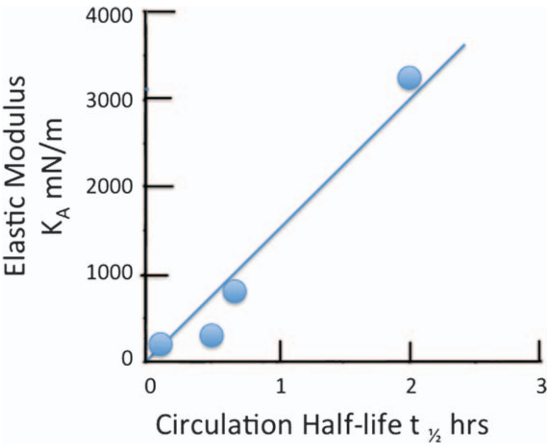

Figure 2.7 Blood circulation half-life as a function of the membrane elastic modulus for conventional liposomes (non-PEGylated); data for unsaturated reticuloendothelial system (RES).

value of the transition temperature has to be the most important property. The choice of DPPC is governed by its transition temperature of 41.5 °C,[74] only a few degrees above body temperature (37 °C). Could other lipids suffice? Not as saturated PCs. The effect of ± 2 CH_2s per chain on the fully hydrated bilayer transition temperature can be seen by comparing T_m of DPPC with that of the diC14 (24.5 °C) and diC18 (55 °C) lipids in the same homologous series, *i.e.* the next one down has a phase transition that is too low, and the next one up is much too high for hyperthermia treatment as the trigger. Mixing the lipids only serves to broaden the transition.[74] Introducing a double bond in one of the acyl chains can lower the transition temperature because it influences chain-chain packing. However, these effects are too large. For example, the DSPC transition (55 °C) is reduced by 50 °C to 5 °C by just introducing one double bond in the 9 position of one of the C18 chains, *i.e.* as SOPC.

With further regard to lipid mixtures and their effect on T_m and drug release, in 1978 Yatvin *et al.*[38] developed the first temperature-sensitive liposome based on the lipid DiPalmitoylPhosphatidylCholine (DPPC). As mentioned earlier, the reason was one of *property*, since it has a transition temperature of 41.5 °C, just above body temperature (37 °C). However, Yatvin *et al.*'s formulation also contained the longer chain lipid DiStearoylPhosphatidylCholine, (DSPC) in a 7 : 1 DPPC : DSPC ratio. The addition of DSPC to the formulation raised the transition temperature of the ideal solid solution bilayer[80] such that the liposome maximally released its encapsulated material in the temperature range of 43–45 °C[39,40,46] Drug release rate was found to be slightly enhanced over non-transitioning bilayers,[46] but was still too slow for therapeutic use. Also the hyperthermic temperatures required were slightly higher than the clinically attainable range.[81] As a consequence, further work and development of this thermal sensitive formulation all but ceased.[81]

In summary, while DPPC seems to be an ideal host lipid with a transition temperature just above body temperature, where the lipid bilayer can become transiently more permeable, its enhanced permeability at the phase transition is not much above a liquid phase lipid at the same temperature.[46] Attempts to increase drug retention by making the bilayer stronger and less compressible, by, say, mixing in cholesterol, only serves to abolish the transition altogether, and including a longer acyl chain lipid like DSPC raises the T_m beyond the attainable mild hyperthermia limit (of ~42 °C) and slightly broadens it, again producing undesirable properties. The answer to this materials choice dilemma was to include a permeabilizing component, *i.e.* a non-bilayer lysolipid.[17]

2.2.4.2 The Permeabilizing Component

The idea for including lysolipid into the DPPC bilayers came from molecular-exchange studies we carried out in the early 1990s. Using three micropipets positioned around the microscope stage (Figure 2.8) one pipet holds the vesicle (right), and two deliver test and bathing solutions (left). The test vesicle is exposed to a solution of lysolipid from the upper flow pipet (Figure 2.8A) creating a change in vesicle membrane area, measured from the change in

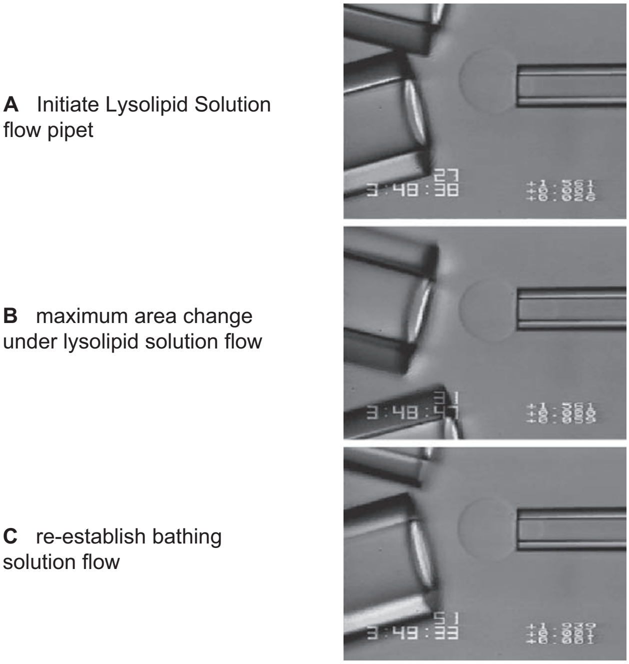

A Initiate Lysolipid Solution flow pipet

B maximum area change under lysolipid solution flow

C re-establish bathing solution flow

Figure 2.8 Molecular Exchange of a bilayer with lysolipid. A) Vesicle exposed to a solution of lysolipid; B) maximum area change under lysolipid flow (1 μM); C) re-establish bathing solution flow and wash out the lysolipid from the membrane.

projection length in the micropipet.[82,83] The maximum area change under lysolipid flow (1 μM) is shown in Figure 2.8B. Under bathing solution flow (Figure 2.8C), the lysolipid is washed out from the membrane and a reduction in projection length is recorded. This experiment showed how a water-soluble lysolipid (*i.e.* monooleoylphosphatidylcholine, MOPC) would partition into a liquid lipid bilayer membrane (SOPC) and expand it. The membrane expansion (at constant holding suction pressure) is readily measured by the micropipet and vesicle geometry.

For MOPC at its cmc of 1 micromolar, the initial maximum area change was ~3% and this occurred in ~200 seconds. Importantly, when the lower flow pipet is repositioned again to deliver the bathing solution (Figure 2.8C) the lysolipid is readily washed out as the surrounding solution is exchanged for a lysolipid-free media. When this change in area is converted to mol% lysolipid, from the known areas per molecule of MOPC (35 Å^2) and SOPC (67 Å^2), this experiment shows that lysolipid saturates the outer monolayer at ~6 mol% MOPC. At higher lysolipid solution concentration, the membrane rapidly takes up the lysolipid and fails at ~16 mol% MOPC largely accumulated in the outer monolayer of the bilayer.[82] Having seen these data, the idea was that if lysolipid could be incorporated in a solid phase bilayer, at, say, 10 mol%, where it might remain trapped because of the higher elastic modulus of the solid phase, then when the bilayer temperature was raised to the transition temperature and lipid started to melt, it might leave or form defects at grain boundaries and so release encapsulated drug. As described in Section 2.4.1, this idea worked, and the drug was indeed released much faster from a DPPC liposome that contained the lysolipid, compared to one composed of DPPC alone.

This is a good example of a *compositional* choice, which included a normally non-bilayer lipid in a bilayer that might form nanopores and so release drug (see Section 2.4.1). That is, lysolipid normally forms highly curved micelles and so could initiate such pore formation at the transition, especially at the grain boundaries. This "smart material" design took years of understanding the mechanical, thermal and exchange properties of lipid bilayer membranes. This information helped to create a new invention,[84,85] prompted by actually seeing, on video, a membrane take up a soluble lysolipid and, more importantly, seeing it leave the bilayer in seconds upon wash out.[82,83]

2.2.4.3 The Drug

With a potentially new thermal-sensitive formulation in the offing, the question was which drug to encapsulate and release? Doxorubicin (also named adriamycin) was one of the first choices of drug to encapsulate in liposomes to be tested against cancer. Doxorubicin intercalates with DNA, stabilizes the topoisomerase II complex after it has broken the DNA chain for replication, preventing the DNA double helix from being resealed, and stopping the process of replication (Figure 2.9).[86]

Doxorubicin forms complexes in pH 7.3 aqueous solution at 37 °C with: DNA-derived bases, nucleosides and nucleotides; amino acids such as tryptophan; proteins such as human serum albumin and hemoglobin; and a broad range of biologically active compounds such as NAD, propantheline, caffeine, chloroquine, imipramine and propranolol.[87] When released into the tumor, it can basically "stick to everything". It therefore has to be delivered not just into the bloodstream, not just to the tumor tissue and not just into the tumor interstitium, but has to cross the membranes of the actual cells of the tumor so that it can exert its action on the DNA in the cell nucleus.

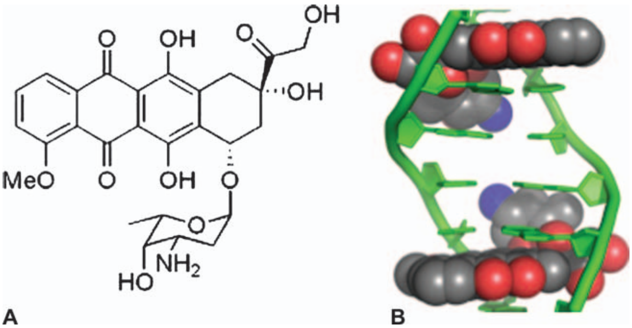

Figure 2.9 Doxorubicin (adriamycin) structure (A) and intercalation into DNA (B).

When administered as free drug, the therapy-limiting toxicity for doxorubicin is cardiomyopathy, which may lead to congestive heart failure and death.[88] It also causes significant gastrointestinal toxicity, with nausea, vomiting and diarrhea (soon after therapy) and stomatitis (within 7 to 10 days of administration). As discussed above, the act of encapsulating it in a liposome reduces this toxicity,[7] but problems still exist in getting the drug out. From a large amount of literature,[§] and experience *in vitro* and *in vivo* with encapsulated doxorubicin, including its FDA approval in commercial formulations, we chose to encapsulate doxorubicin and determine if and to what extent the thermal-sensitive formulation could improve its delivery and efficacy in cancer.

Doxorubicin is a small molecular weight (543.5 g/mol) drug, has a pK_a of 8.3 and so has varying solubility depending on pH (and protonation of the molecule from Dox to $DoxH^+$) (Table 2.1). Cullis *et al.*[89] took advantage of this weak base property and developed a very successful loading method for this and other drugs into liposomes.[89] What they established was that a pH gradient of three units (pH 7.2 outside, pH 4.0 inside) could generate interior concentrations of 1000-fold higher than exterior concentrations, with excellent drug retention properties. From the materials science and engineering perspective, this loading method relied on the solubility of the neutral form of a drug and the low dielectric constant interior of the bilayer, in order to be actively transported to the interior, where it crystallized at lower pH as the citrate salt. In this design, then, drug properties and bilayer properties work together. Moreover, the ionized $DoxH^+$-citrate salt was far less permeable than Dox through the bilayer, and so it was very effectively trapped and prevented from escaping back out of the liposome, hence achieving the functions: (a) load and (b) retain.

2.2.4.4 The Protective Layer

Initially developed in the late 1980s to create the so-called stealth liposomes[51] and incorporated in the LTSL for this very purpose, DSPE-PEG^{2000} was found to have an additional function in the LTSL. As discussed in more detail in Section 2.4.1.4, it appears to be necessary to keep the lysolipid formed pores open. As a molecule though, DSPE-PEG^{2000} is a fairly large molecule (2805.5 g/mol), with most of this molecular mass being in the PEG. PEG itself is extremely hygroscopic, infinitely soluble in water (as a helical structure) and infinitely transferable to chloroform (as a random coil), gaining entropy in the process. Whether realized or not in its initial development, attaching this very water-soluble molecule to a di-chain lipid in order to provide a steric barrier to the hydrated liposome interface meant that, from a processing standpoint, it was possible to dissolve the PEG-lipid in the usual solvents like chloroform and ensure good mixing of lipid components before rehydration to form the liposomes; a very fortuitous use of PEGs solubility properties.

[§] "Liposome" generated 43,029 hits on PubMed, Aug 8th 2012.

As is now well established, the presence of just a few mol% PEG-lipid in a bilayer confers a steric repulsion due to the extension of PEG from the bilayer surface. The structure of the PEG molecule at the interface depends on its surface density, as was well described by several theoretical and experimental studies[53,90,91] Basically, the surface density of the DSPE-PEG^{2000} in a lipid bilayer would need to be ~5 mol% relative to the host lipid in order to form a complete coverage of touching "mushrooms". Higher surface densities would extend the PEG out in a brush conformation and beyond 10–15 mol%, the system starts to form a mixed phase of micelles and bilayers,[53,90] compromising any hope of drug retention.

2.3 Production

Techniques involved in generating liposomal-drug systems in a manner compatible with clinical demands are now very well established.[89] As discussed and reviewed by Cullis *et al.*[89] extrusion procedures rapidly and reproducibly generate liposomes. Also, efficient and stable entrapment of drugs at high drug/lipid ratios are obtained by freeze-thaw protocols, which can allow drug-trapping efficiencies approaching 90%. Active trapping procedures, particularly suitable for doxorubicin and other weak base cations, utilize drug uptake in response to ion gradients, resulting in extremely high drug/lipid ratios and trapping efficiencies approaching 100%. These and other advances have essentially ensured that the manufacture of liposomal drug systems for pharmaceutical applications is now a relatively straightforward process. Doxorubicin can be easily loaded into the LTSL by the pH-gradient method developed by Mayer *et al.*,[92] involving manufacturing the liposomes in a low-pH buffer (*e.g.* sodium citrate, pH = 4.0) and subsequently adjusting the external pH to 7 or higher (Figure 2.10). This can be accomplished directly by the addition of base to the liposome solution (Figure 2.10A).[43] Uptake of the lipophilic (Dox) species is then simply achieved by addition of doxorubicin and a short incubation. As shown in Figure 2.10B,[43] doxorubicin is in equilibrium with H^+ ion at each pH as Dox and $DoxH^+$. At pH 7.2 there is ~6% Dox, which is membrane soluble and so can pass through the membrane into the interior. Once in the interior the low pH shifts this equilibrium to just 0.003% Dox, with the conversion of the majority of doxorubicin to the charged and citrate-complexed (crystallized) form as $DoxH^+$.[93] Hence it is not lipophilic and stays entrapped in the liposome.

For doxorubicin, drug uptake levels as high as 0.29 to 1 (drug to lipid, wt/wt) can be achieved in combination with trapping efficiencies of 98% or higher. Traditionally this is done at ~60 °C. However, adapting these methods of active (pH gradient) loading of doxorubicin for the LTSL, we found that loading could in fact be readily carried out in a matter of minutes below the transition temperature, despite the membrane being in the solid phase of the LTSL lipid mixture at 35 °C (Figure 2.11).[43] The negative controls (NC4 and 7.4) showed that no drug is loaded if there is no pH gradient.

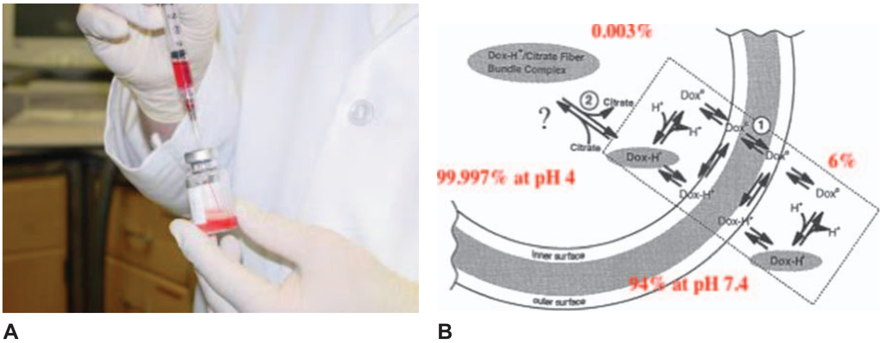
0.003%
Dox-H+/Citrate Fiber Bundle Complex
?
② Citrate
Citrate
Dox-H+
H+
Dox0
H+
Dox0 ①
Dox0
6%
Dox0
H+
H+
Dox-H+
Dox-H+
Dox-H+
99.997% at pH 4
inner surface
outer surface
94% at pH 7.4
A
B

Figure 2.10 Loading LTSL with doxorubicin: addition of doxorubicin to pre-prepared liposomes containing pH 4 citrate buffer inside and suspended in a pH 7.2 buffer (A), and scheme of the acid base equilibria both outside and inside the liposomes during loading (B).

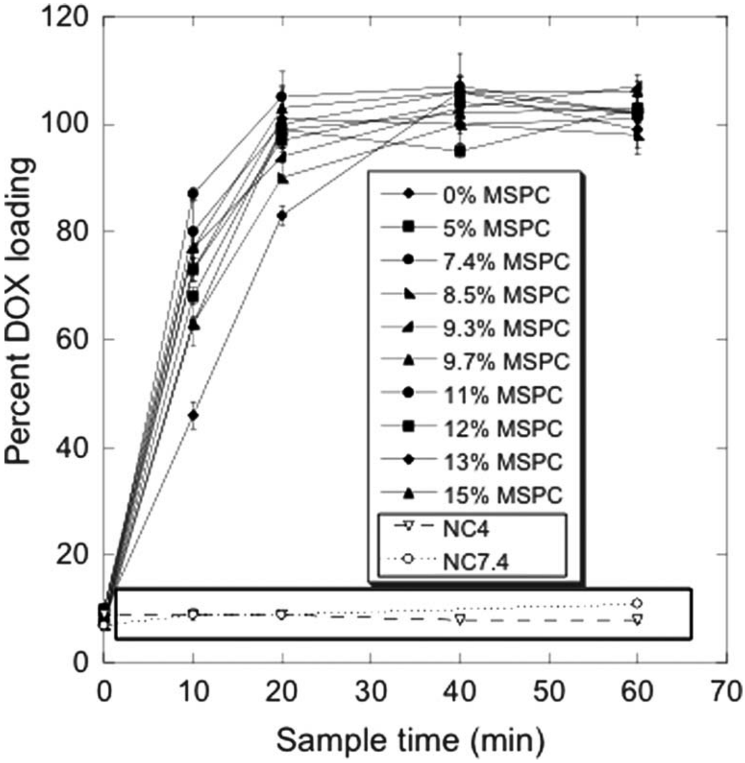

Figure 2.11 Percent Dox loading as a function of membrane MSPC composition at 35 °C at a drug/lipid weight ratio of 0.05 : 1. Negative control NC4 was hydrated and titrated with pH 4.0 citrate buffer. Negative control NC7.4 was hydrated and titrated with pH 7.4 buffer.

2.4 Performance-in-Service

With the doxorubicin successfully loaded into the LTSL formulation, this section summarizes the *in vitro* characterization and the *in vivo* preclinical and clinical trials that have demonstrated the unique ability of this formulation not only to release the drug in the bloodstream of a warmed tumor, but also for the freed drug to penetrate deeply into the tumor and reach its intended molecular target, the DNA of every cancer cell.[17]

2.4.1 Performance-in-Service: *in vitro*

The LTSL has been characterized *in vitro* through a series of experiments including: a) carboxyfluoroscene release; b) dithionite permeability; and c) doxorubicin release as a function of LTSL composition and temperature. Basically, these experiments have shown that the low-temperature, thermally sensitive liposome retains small drug molecules like doxorubicin at 37 °C, and rapidly releases doxorubicin in less than 20 s in response to applied heating equivalent to mild hyperthermia (HT) in the range of 40–42 °C.

Each of these *in vitro* experiments will now be reviewed.

2.4.1.1 Carboxyfluoroscene Release

Initial studies demonstrated the concept of temperature-triggered release from the LTSL by using the common dye CarboxyFluoroscene (CF).[15] When entrapped in a liposome at high concentration (50 mM), its fluorescence is largely quenched. However, it develops intense fluorescence when released from a liposome and diluted into the surrounding media. In an experiment that used the first LTSL formulation (containing 4 mol% MPPC rather than the eventual MSPC, see later), we measured the percent of encapsulated CF released *vs*. time for a series of physiologically important temperatures (37 °C, 38 °C, 39 °C, 39.5 °C and 40 °C). Very little CF was released at body temperature of 37 °C, but as the transition region for the bilayer composition was approached (lower onset temperature 39.5 °C, midpoint 41.3 °C), the rate and amount of CF that was released increased dramatically (Figure 2.12A).

The release was then examined for a series of MPPC compositions from 0 mol%–20 mol% as a function of temperature (at the 5 min. incubation time point) into saline phosphate buffer. The "DPPC alone" composition (containing ~4 mol% DSPE-PEG) became permeable to CF at the lower onset of the transition enthalpy, that is ~1–2 °C lower than the mid point of the bilayer transition temperature (of 41.5 °C) (Figure 2.12B).[15] As expected from earlier studies and theory,[35–37] the rate and amounts released at 5 min. from the DPPC liposome for each temperature are relatively low. The presence of only a few mol% of MPPC contained in the liposome bilayers significantly increased the rate and amount of CF released, and in accordance with its ability to slightly lower the phase transition temperature of the lipid mixture, shifted this release to slightly lower temperatures. Since MPPC caused a slight instability in

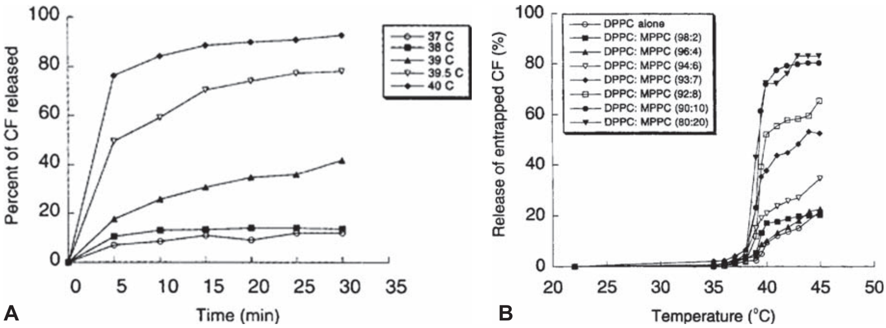

Figure 2.12 Percent of CarboxyFluoroscene (CF) released from LTSL (DPPC : MPPC : DSPE-PEG^{2000}, 86 : 10 : 4) (A), and effect of MPPC concentration in LTSL bilayers on the percent of encapsulated CF released *vs.* temperature measured after 5 min incubation time at each temperature (B). Note DPPC was traded for MPPC and all compositions contained ~4 mol% DSPE-PEG.

processing and the drug was not as well retained as needed, MPPC was replaced for MSPC, a similar lysolipid but with two additional CH$_2$s per acyl chain. This *compositional* change was successful and so the remaining studies and the commercial product contain MSPC, along with the DPPC and DSPE-PEG^{2000}.

2.4.1.2 Dithionite Permeability

Fundamental questions about this release mechanism were still not understood: "Did the approach to the transition, and bilayer melting, really cause the lysolipid to desorb and leave defects as was suggested by the lysolipid-exchange experiments on the GUVs?" or "Did the melting induce the lysolipid to form more permanent pores, as might be expected from the shape hypothesis for its highly curved micelles?"

Additional studies were therefore carried out with a dithionite assay that quenches the fluorescence and absorbance of fluorescent lipids incorporated in the bilayer.[49] If the permeability was due to pores, then a longer lasting exchange might be expected. The dithionite experiments showed that the permeability developed by including lysolipid was long lasting and reversible, giving the first indication of equilibrium structures (possibly pores) in the bilayer.[46] The raw data for this experiment are shown in Figure 2.13. Upon addition of dithionite ion, the NBD lipid absorbance at 465 nm is rapidly quenched for all the outside lipids in the liposome bilayers.[46]

When carried out at 30 °C, where all membranes are relatively impermeable to the dithionite ion, just over half the total signal is quenched, consistent with the difference in curvature between the outside and inside of a 100 nm liposome. Then, as the transition temperature is approached, the membranes become permeable to the ion and the inner monolayer is quenched. The difference in permeability for each membrane is apparent; the presence of 10 mol% MSPC

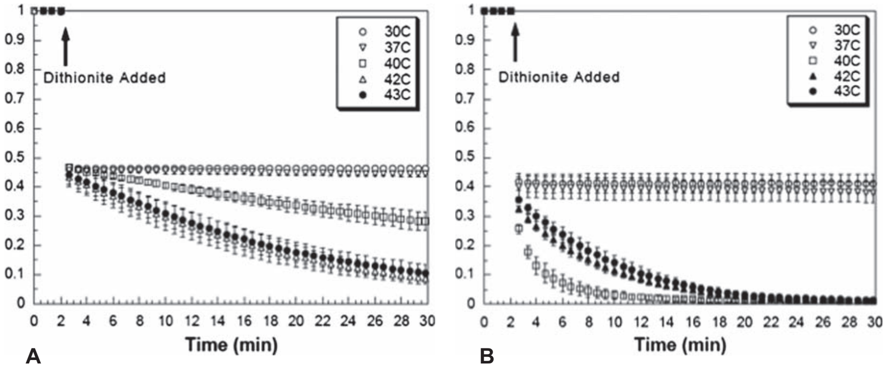

Figure 2.13 Relative absorbance at 465 nm *vs.* time for dithionite permeability through DPPC : DSPE-PEG^{2000} (4%) membranes (A) and DPPC : MSPC (10%) : DSPE-PEG^{2000} (4%) membranes (B) at five different temperatures. Data points and error bars represent the mean and standard deviation, respectively, of three separate experiments.

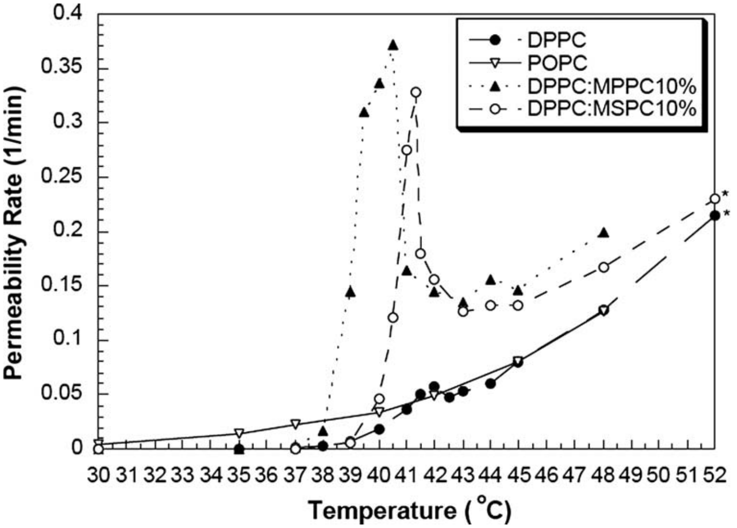

Figure 2.14 Compilation of dithionite ion permeability rate per minute for DPPC, DPPC : MPPC (10%), DPPC : MSPC (10%) and POPC as a function of temperature. Lines connecting the data are presented simply to aid the eye.

(Figure 2.13B) dramatically increases the permeability and even shows an apparent peak at the transition midpoint; namely, the rate of quenching is faster for 42 °C than for 40 °C or 43 °C, which is above T_m. This is more evident in Figure 2.14, which shows a compilation of dithionite ion permeability rates for DPPC, DPPC : MPPC(10%), DPPC : MSPC(10%) and POPC (all containing 4 mol% DSPE-PEG) over the temperature range studied.

Thus, compared to DPPC, the inclusion in the bilayer of a lysolipid at 10 mol% increases the permeability rate at the transition midpoint by 5–6 times. MPPC slightly lowers the bilayer transition temperature and this is reflected in the slightly lower temperature for its maximum permeability to dithionite. The MSPC formulation has a near clinically perfect peak in permeability rate at between 40 °C and 41 °C, *i.e.* at a temperature that is readily achieved by mild hyperthermia. Finally, the "enhanced" permeability rate measured by us and others previously for DPPC is hardly that much above a simple lipid, PalmitoylOleoylPhosphatidylCholine (POPC), which does not have a transition in this range, but is already in its liquid phase. Interestingly, and in accordance with theory,[36] the presence of lysolipid enhances the permeability rate for the bilayer compared to liquid phase DPPC or POPC liposomes, even above the phase transition region. This enhanced permeability effect will be important in its *in vivo* clinical application, where heating is achieved by radio frequency ablation, as discussed in Section 2.4.2.

2.4.1.3 Doxorubicin Release

Finally in this *in vitro* section, it was obviously necessary to test the release of the actual drug, doxorubicin.[43] Figure 2.15A shows just how fast doxorubicin is released from the LTSL when the MSPC bilayer concentration is at ~10 mol% or higher. Over 80% of the drug is released in the first minute and, for the slightly higher MSPC of 12–15 mol%, the drug comes out as fast as it can be measured, with ~90% released in the first 20 s (Figure 2.15B). As explained below, this ultrafast release is essential for the liposome to achieve its function of releasing drug in tumor vasculature so that the freed drug can diffuse into and penetrate the tumor interstitium. Release time is faster than transit time of liposomes through the tumor.

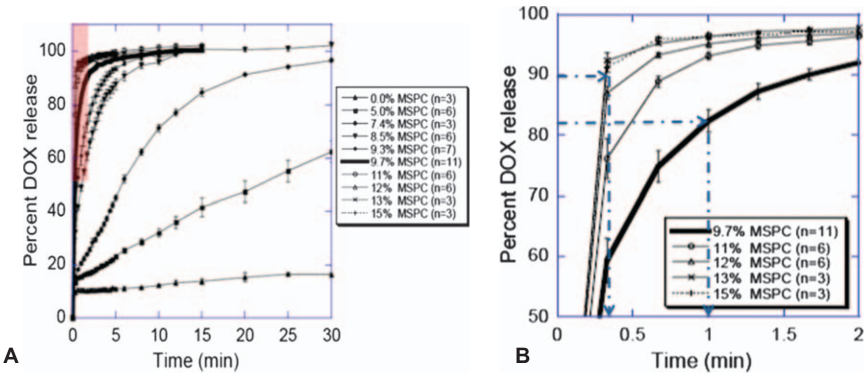

Figure 2.15 Dox release at 41.3 °C from LTSL with increasing membrane fractions of MSPC in the DPPC : MSPC : DSPE-PEG^{2000} liposomes (A). The plot on the right (B) is a zoomed-in view of the red-boxed area in (A), showing the ultrafast release of doxorubicin from the LTSL.

2.4.1.4 Drug Release Mechanism

In understanding the drug release mechanism it is important to realize that each of the components influences the material characteristics of mechanical integrity and strength, interfacial steric stability, thermal melting and membrane grain- and nanostructures. In turn, they are expected to control and allow the manipulation of many of the desired pharmaceutic and clinical-performance criteria of the liposomes, such as the rate of drug loading, circulation half-life, drug retention and the temperature and rate of thermally triggered drug release.

As shown above and in the several publications and reviews that have chronicled its development and testing,[15,16,94–97] compared to DPPC alone, the MSPC-based formulation releases drug within seconds of being heated to its main acyl melting phase transition, because each of these acyl-chain-compatible components are stably (perhaps ideally) mixed in the gel phase of a lipid bilayer and then create what appear to be membrane nanopores at the phase transition, probably at grain boundaries in the melting lipid.[98] It appears that the presence of both MSPC and DSPE-PEG are important to the ultrafast permeability of the LTSL formulation. Both Mills and Wright[43,49] had shown that without lysolipid, even with DSPE-PEG present, doxorubicin permeability was low. In the absence of MSPC, a DPPC : DSPE-PEG^{2000} (increasing DSPE-PEG^{2000} from 2 mol% to 20 mol%) formulation only released <20% doxorubicin at the lipid phase transition, which was probably due to membrane bound doxorubicin (Figure 2.16A). For comparison, the release data for Dox-loaded standard LTSL formulation are also presented in Figure 2.16A (open circles).

Then, in another experiment, where the membrane composition was DPPC : MSPC (90 : 10), *i.e.* with 0% DSPE-PEG^{2000}, significantly slower drug

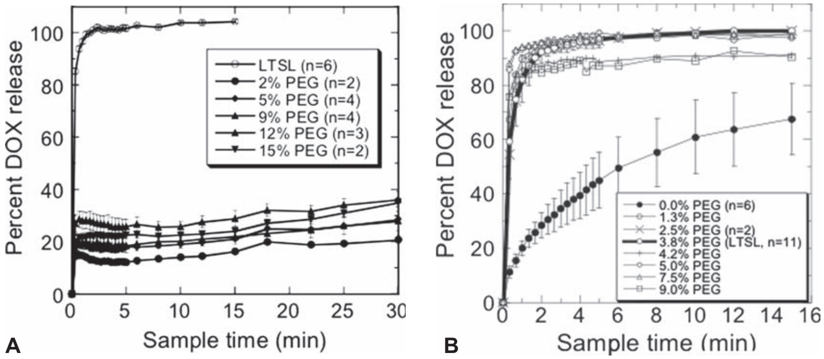

Figure 2.16 The unexpected role of DSPE-PEG^{2000}. Percent Dox released into 20 mM HBS at T_m (41.3 °C) as a function of DSPE-PEG^{2000} in the absence of MSPC (A), and effect of inclusion of DSPE-PEG^{2000} on % Dox release at 41.3 °C from LTSL with increasing membrane mol percents of DSPE-PEG^{2000} in the presence of MSPC (B).

release than the LTSL formulation was observed (Figure 2.16B). It is only with the inclusion of just 1.3 mol% DSPEG-PEG^{2000} that the rate of drug release is increased at the transition temperature.

Even though the DSPE-PEG^{2000} lipid has two acyl chains (Figure 2.3), it has a shape factor similar to MSPC in that the head-group is much larger than the tail-group due to the polyethylene glycol polymer. Thus, DSPE-PEG forms micelles in aqueous solution having a cmc that is actually similar to MSPC of around 1 µl.[99] It could, in principle, support positive curvature in lipid membranes. We therefore hypothesized that the molecular shape of DSPE-PEG^{2000} might make it an important part of lysolipid pore stabilization, and therefore help control, to some extent, the triggered-drug release from LTSL.

Thus, Dox release from DPPC : MSPC liposomes with 0 mol% DSPE-PEG^{2000} was significantly slower than from the LTSL formulation, suggesting that PEG-lipid could be an important factor in stabilizing the postulated permeabilizing pores. Indeed, incorporating only 1.3 mol% of the PEG-lipid increased the release rate and amount to values similar to the LTSL formulation. So here was a situation where a component, DSPE-PEG^{2000}, which was originally included in order to enhance circulation time in the bloodstream, was now providing a second and very important function of enhancing the permeability of the lysolipid-containing bilayers. However, it does not appear to enhance the phase transition permeability of DPPC or form putative nanopores if it is the only included component.

As previously discussed in detail[42] and summarized in Figure 2.17, we therefore propose the following mechanism for drug retention, its possible leakage during the blood-borne transport phase and its ultrafast release at the solid-liquid transition of the LTSL membrane.

Drug Retention and Possible Leakage at 37 °C

Figure 2.17A shows the mixed-lipid bilayer in its solid phase at 37 °C. As modeled by Mouritsen *et al.*[36,100] the chain mismatches between solid, mostly *trans* lipids do not line up exactly with the more liquid-like chains of the grain boundary region. There is a pH gradient across bilayer, and doxorubicin is still in the protonated-unprotonated equilibrium at pH 5.5 (pH is known to rise slightly from its initial value of 4.0 due to Dox loading). Consequently we might expect good retention of the drug and a low doxorubicin permeability through the bilayer matrix itself, and even through the grain boundary defects. However, as discussed earlier, DPPC has a pre-transition around 35 °C, at which point the bilayer, although still solid, enters a slightly less compressible phase (Pβ′). Thus, while the unprotonated form of doxorubicin itself is in low concentration and doxorubicin is actually in crystal form, its retention in the liposome both *in vitro* and *in vivo* could hinge critically on the ability of the bilayer to retain hydrogen ions. Perhaps more significantly, then, any H^+ permeability through defects or solid phase bilayer (blue arrows) would deplete the hydrogen ion concentration inside the liposome, drive the equilibrium towards more unprotonated doxorubicin and the now membrane-soluble

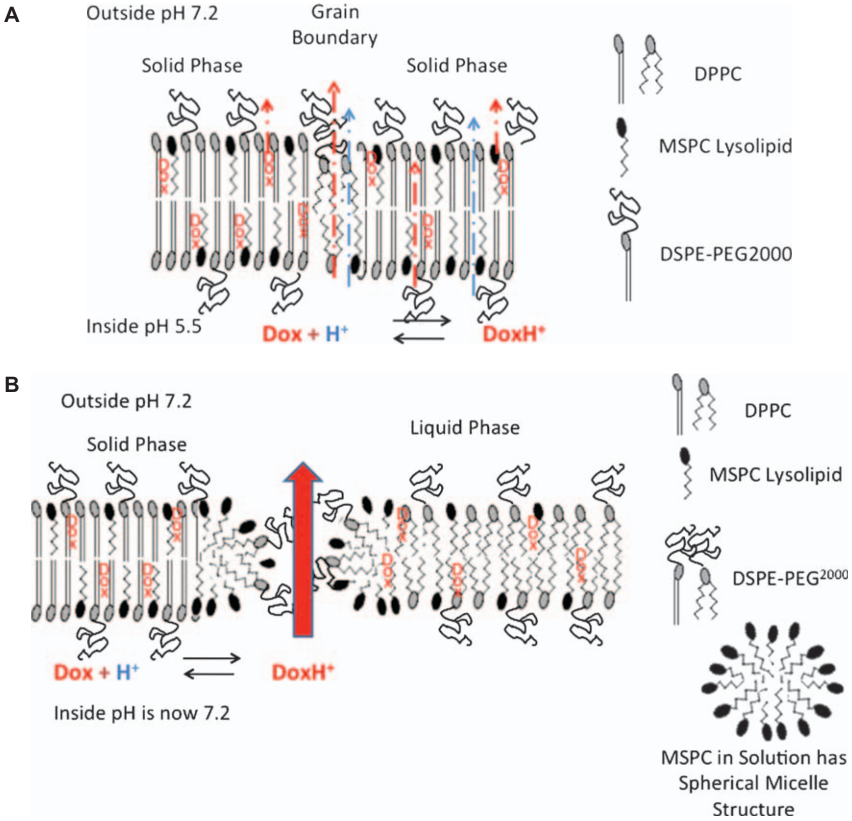
A
Outside pH 7.2
Grain Boundary
Solid Phase
Solid Phase
DPPC
MSPC Lysolipid
DSPE-PEG2000
Dox
Inside pH 5.5
Dox + H⁺
DoxH⁺
B
Outside pH 7.2
Solid Phase
Liquid Phase
DPPC
MSPC Lysolipid
DSPE-PEG2000
Dox + H⁺
DoxH⁺
Inside pH is now 7.2
MSPC in Solution has Spherical Micelle Structure

Figure 2.17 Proposed mechanism for drug retention, leakage and thermally triggered (smart) release. Retention and possible leakage at 37 °C (A) and release at 41 °C (B).

doxorubicin could follow. This is what we think happens in the bloodstream, where doxorubicin has been shown to leak out of the liposome over a period of a few hours. The presence of some bilayer soluble doxorubicin (red "Dox") in the bilayer would also account for the low-level release of doxorubicin in the *in vitro* assays for drug leakage (Figures 2.15 and 2.16).

Rapid Release at 41.5 °C – Role of Nanopores

With MSPC and DSPE-PEG^{2000} in the bilayer, as depicted in Figure 2.17B, the bilayer in the phase transition region acquires enhanced permeability through a purported MSPC pore. As the transition temperature is approached and the grain boundaries begin to melt, lateral lipid transport could well be increased and could allow more lysolipid to assume its preferred curvature (*i.e.* as a convex micelle), relaxing the planar bilayer structure by forming lysolipid-lined nanopores. With a few mol% of DSPE-PEG^{2000} in the bilayer, this MSPC pore is stabilized by PEG-lipid. As a consequence, the hydrogen ion gradient rapidly equalizes, $DoxH^+$ comes out in seconds (large red arrow), as does any remaining embedded Dox in the bilayer. From dextran permeability measurements and other calculations,[43] the size of these nanopores appears to be ~10 nm in diameter, more than large enough to allow the very rapid transport seen for CF, dithionite and doxorubicin.

2.4.2 Performance-in-Service: *in vivo* (Preclinical)

Since 2000 we have tested the LTSL-doxorubicin formulation in growth delay studies using an implanted flank tumor, and in window chamber studies,[101] where the tumor is visualized in bright field, and imaging of doxorubicin and lipid bilayer is accomplished by fluorescence. Doxorubicin is naturally fluorescent, whereas the lipid is visualized by adding a small percentage of fluorescently labeled lipid to the bilayer. Using intravital microscopy it is possible to simultaneously image the location and relative concentration of doxorubicin, the lipid and the microvasculature, in real time as the liposomes are injected i.v., and the tumor is heated. These represent a large body of work that is briefly reviewed in this section. The reader is referred to the papers that are referenced for more information, figures and data.

2.4.2.1 First Preclinical Data

The first preclinical data for this LTSL-doxorubicin[16,45] showed quite amazingly that the LTSL formulation could totally abolish tumor regrowth when administered i.v. to a mouse with a warmed implanted flank tumor (FaDu, a squamous cell carcinoma). When given intravenously, as a bolus injection, combined with local heating (42 °C) of a tumor-bearing leg for just 1 h, Dox LTSL induced greater growth delay compared to saline and free drug controls and other liposomal formulations. All 11 out of 11 tumors were completely regressed out to 60 days. Even though the HT plus LTSL "treatment" was only for 1 hour, the LTSL was much more effective than free drug plus HT, and even Doxil™ plus HT. For LTSLs injected without any HT application, time to tumor progression was 12 days, little better than for normothermic free drug, demonstrating the absolute requirement for the thermal trigger. It was this result that started to point the way to the notion that rapid drug release was a crucial feature of the LTSL, and although Doxil might extravasate in this model, its relatively slow leakage of drug would hamper its potential efficacy. When measured in the same tumor model, tumor drug levels were up to 30 times higher than those achievable with free drug administration, and 3–5 times elevated compared to traditional non-thermal sensitive liposomes that rely on extravasation.[96,102] Moreover, Dox LTSL + HT resulted in half of the doxorubicin being bound to DNA and RNA of tumor cells after only 1 h of treatment, whereas the amount bound after free drug + HT or traditional non-thermally sensitive (Doxil-like) liposomes + HT was not detectable,[45] underlying the fact that in this first hour a Doxil-like liposome did not release any drug.

2.4.2.2 MRI Contrast Data

The timing of liposome injection in relation to application of hyperthermia using manganese as a released contrast agent was tested in a rat fibrosarcoma model.[103] When trapped inside the liposome, the Mn^{++} did not affect the MR signal, because it was sequestered from the surrounding water; when it was released, the MR signal increased profoundly as a result of the interaction of Mn^{++} with the water surrounding the liposome. When Mn-LTSL was injected into an animal with a preheated tumor, release was predominantly in the peripheral tumor vasculature. Overall average tumor drug concentrations were doubled compared with LTSL injection in a tumor that was heated after drug administration; the time to progression (5 × initial tumor volume) was longer (34 days *vs*. 18.5 days, respectively). These results showed that attempts to preload a tumor in the first hour *via* EPR, even with thermally triggered drug-releasing liposomes, were inferior to a vascular release mechanism. One reason is that when LTSL is first injected (as a bolus injection) and then the tumor heated, it takes 15–20 min. to reach thermal steady state with a passive thermal conduction heating method. Over this time the plasma concentration of Dox-LTSL does fall somewhat before the transition temperature in the tumor is reached. This is even more reason to heat first, and inject the LTSL while maintaining the required 42 °C hyperthermic temperature of the tumor.

2.4.2.3 Effect of Drug Release on Tumor Vasculature

If drug was being released into the blood vessels of the tumor, what effects could it be having, perhaps on the vasculature itself? In studies that measured the red blood cell velocity using fluorescent red cells as "tracers",[104] we found that tumor blood flow can actually be shut down by Dox-LTSL + HT in FaDu tumors. The average red blood cells (RBC) velocity was reduced from 0.428 mm/s to 0.003 mm/s and the microvascular density was reduced from 3.93 mm/mm^2 to 0.86 mm/mm^2 at 24 h after just a 1 h treatment. In addition, blood flow stasis and severe hemorrhage occurred immediately after treatment, and there was no blood flow in micro-vessels in five out of six tumors at 6 h and 24 h after the treatment.

To determine if the treatment had the same effects on tumor blood flow in other tumors, Chen *et al.*[34] treated 4T07 tumors with Dox-LTSL plus HT, and concluded that tumor microvascular permeability to drug was more critical than the sensitivity of tumor cells to doxorubicin in determining the anti-vascular efficacy of Dox-LTSL + HT treatment.[34]

2.4.2.4 Other Tumors

Expanding the preclinical testing to a series of other tumors the efficacy of the commercial formulation (ThermoDox®) was re-examined in FaDu and compared in HCT116, PC3, SKOV-3 and 4T07 cancer cell lines.[102] Dox-LTSL + HT resulted in the best antitumor effect in each of the five tumor types. Interestingly, these variations in efficacy were most correlated to *in vitro* cell doubling time.

2.4.2.5 *Triggered, Intravascular Release to Improve Drug Penetration into Tumors*

The most compelling and dramatic evidence for not only release in the bloodstream but also deeper penetration into a tumor than has ever been achieved and measured before, is presented in a new paper by Manzoor *et al.*[17] The traditional goal of nanoparticle-based chemotherapy has been to decrease normal tissue toxicity by improving drug specificity to tumors and, as mentioned earlier, the EPR effect can permit passive accumulation into tumor interstitium in some subcutaneous animal tumors. However, only suboptimal delivery is achieved, especially for 100 nm liposomes, because of heterogeneities of vascular permeability and the density of the interstitial stroma, which limits nanoparticle extravasation and penetration. Further, slow drug release from non-thermally sensitive or environment insensitive liposomes limits bioavailability of the encapsulated drug. We have demonstrated, quite categorically, that the LTSLs release doxorubicin inside the tumor vasculature, but only when the tumor is heated to 42 °C.[17]

As shown in Figure 2.18, real-time confocal imaging of doxorubicin delivery to the FaDu xenograft in window chambers and histologic analysis of flank tumors illustrates that intravascular drug release increases the amount of free drug in the interstitial space. This increases both the time that tumor cells are exposed to maximum drug levels and the drug penetration distance, compared with free drug or traditional PEGylated liposomes (Figure 2.18).

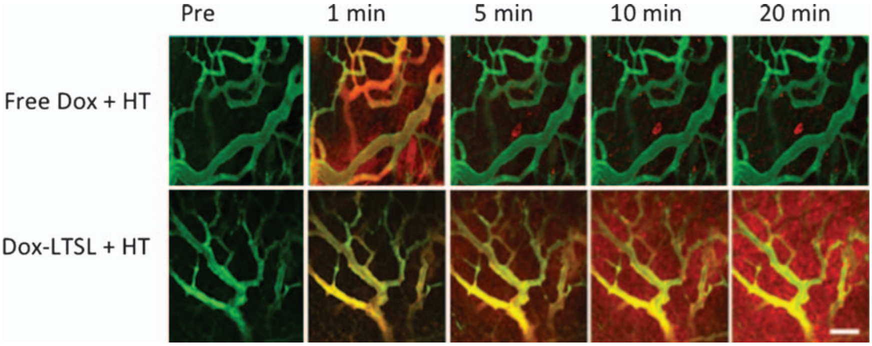

Figure 2.18 Tumor uptake of doxorubicin as a function of time when free doxorubicin (Free Dox + HT) or doxorubicin loaded LTSL (Dox-LTSL + HT) were injected in the warmed tumor (42 °C). Time sequence images of blood vessels (green) and doxorubin (red) for pre-injection, and at time points 1, 5, 10 and 20 min after injection. Scale bar = 100 μm.

Intravenous injection of free Dox, even with applied HT, results in the appearance of drug in interstitial tissue within 1 minute that is quickly reabsorbed into the vasculature within five minutes, with few cells taking up any drug. Heating the tumors with concurrent administration of the Dox-LTSL results in continuous drug delivery to tissue, with uptake of doxorubicin by cells far from vessels that continues to increase though the 20 minutes of observation. Importantly, drug is delivered without liposome extravasation. This proves that the release mechanism occurs by *intravascular* release. Although not shown here, when LTSL is injected without heating the tumor, there is very little if any liposome extravasation and even less doxorubicin in the interstitial tissue than for free drug administration.

The histologic assessment of drug concentration-penetration from vessels in flank FaDu tumors is shown in Figure 2.19.[17] Regarding the actual penetration of drug into the tumor tissue, the Dox-LTSL plus HT regimen achieves much greater concentrations of drug at the endothelial cells and far superior distances from blood vessels into the tumor. Drug levels are expressed as median fluorescence intensity at distances out to 100 µm from the nearest blood vessel for heated tumors. As is clear, Dox-LTSL delivers much more total drug at all distances from vessels compared to Doxil™ and free doxorubicin, including 3.5 times more than free drug at the endothelial cells. Dox-LTSL actually shows maximum delivery at 20 µm (several cell diameters) from blood vessels into the tissue. At the distance at which Dox-LTSL levels start to fall, Doxil™ drug levels are less than half that of Dox-LTSL and have already fallen to approximately one-third of their maximal concentration close to blood vessels. Maximum measureable drug penetration from tumor vasculature *vs.* treatment group shows drug delivered with Dox-LTSL penetrates twice as far as Doxil™ liposomes (78 µm *vs.* 34 µm). These huge improvements in drug bioavailability establish the LTSL plus mild hyperthermia as a new paradigm in drug delivery: rapidly triggered drug release in the tumor bloodstream and deep penetration of drug into the tumor tissue.[17] The average intervascular distance in human

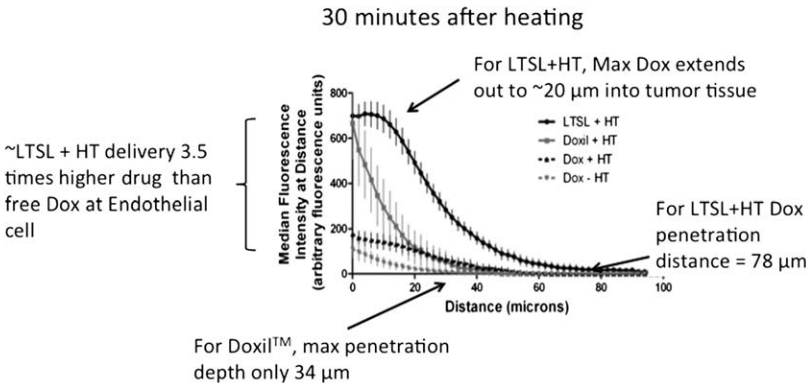

Figure 2.19 Histological assessment of drug concentration-penetration from vessels in flank tumors for Dox-LTSL + HT, Doxil + HT and free Dox ± HT.

esophageal and cervix cancer has been measured and estimated to be in the range of 90–160 μm, respectively.[105] Thus, Dox-LTSL can, on average, deliver doxorubicin to nearly every tumor cell, since the penetration distance is over 70 μm and drug would be delivered from both sides of a tumor core.[105] Of course, these are average values and heterogeneity in delivery is not taken into account. The important point is whether the drug reaches all tumor cells in a concentration adequate to kill them. That is not yet known.

2.4.3 Performance-in-Service: *in vivo* (Canine and Human Clinical Trials)

The big question now is: "*How will Dox-LTSL (or ThermoDox® as it is now commercially called) perform in the clinic?*" Taken in chronological order, here is a brief presentation and discussion of the animal and human trials that have evaluated, or are still evaluating, ThermoDox® with hyperthermia. The commercial doxorubicin-loaded version of the LTSL owes a tremendous amount to the researchers and liposomes that came before it. A more general overview of preclinical and clinical progress for liposomes and temperature-sensitive liposomes including the LTSL is given in recent reviews.[94,96,106]

2.4.3.1 Phase I Studies: Canine

In a Phase I pet canine trial of doxorubicin-containing low temperature sensitive liposomes in spontaneous tumors, of the 20 pet dogs that received 2 doses of Dox-LTSL, 12 had stable disease and 6 had a partial response to treatment.[107] Pharmacokinetic variables were more similar to those of free doxorubicin than the liposomal product. Tumor drug concentrations at a dose of 1.0 mg/kg averaged 9.12 ± 6.17 ng/mg tissue. Taking the density of tissue to be ~1 gm/cm^3, this tissue concentration converts to ~9 mg/L, which is ~17 μM doxorubicin in the tissue sample. For comparison, the IC_{50} of doxorubicin, measured in human neuroblastoma-derived cell lines IMR-32 and UKF-NB-4, was found to be 0.02 μM–3.8 μM,[108] and for human hepatoblastoma HepG2 cells was 1 μM,[109] showing that the Dox-LTSL could deliver doxorubicin to actual canine tumors to concentrations greater than needed for 50% kill measured in cell culture. The conclusion from this work was that "*LTSL-doxorubicin offers a novel approach to improving drug delivery to solid tumors. It was well tolerated and resulted in favorable response profiles in these patients. Additional evaluation in human patients is warranted*".

2.4.3.2 Phase I Studies: Human

The first Phase I human trials were in prostate cancer and hepatocellular carcinoma. The prostate cancer trial[110] was initiated in 2003 in order to determine the maximum tolerated dose of doxorubicin released from

ThermoDox® *via* thermal microwave therapy in patients with adenocarcinoma of the prostate. The trial was terminated in 2009 and data were not released.

The primary liver cancer Phase I trial[111] was initiated in February 2007 and completed accrual by December 2009. It has now advanced to a Phase III (see below). Primary liver cancer is one of the most deadly forms of cancer and ranks as the fifth most common solid tumor cancer. The incidence of primary liver cancer today is approximately 26,000 cases per year in the United States, approximately 40,000 cases per year in Europe and is rapidly growing worldwide at approximately 750,000 cases per year, 55% of which are in China, due to the high prevalence of Hepatitis B and C. The World Health Organization estimates that primary liver cancer may become the number one cancer worldwide, surpassing lung cancer, by 2020. The standard first-line treatment for liver cancer is surgical resection of the tumor; however, 90% of patients are ineligible for surgery. Radio Frequency Ablation (RFA) has increasingly become the standard of care for non-resectable liver tumors, but the treatment cannot adequately ablate larger tumors. There are few non-surgical therapeutic treatment options available, as radiation therapy and chemotherapy are largely ineffective in the treatment of primary liver cancer.

While single-agent doxorubicin has been found to be effective, it has not become a standard treatment for HepatoCellular Carcinoma (HCC) due to its relatively high incidence of severe toxicity, including congestive heart failure and neutropenia. Hence the new initiative to increase the HCC cure rate by combining two approaches: ThermoDox® with Radio Frequency Ablation (RFA). The ThermoDox® Phase I study[111] was a multi-center, open label, single dose, dose escalation study, to evaluate tolerability of ThermoDox® in patients with liver tumors undergoing Radio Frequency Ablation.[113] Patients with unresectable liver cancers underwent RFA with a 30-min. i.v. infusion of ThermoDox® starting 15 min. before RFA. The aims were to determine the maximum tolerated dose (MTD) and dose-limiting toxicity (DLT). Clinically, radio-frequency ablation induces *in situ* thermal coagulation necrosis through the delivery of high-frequency alternating current to the tissues. However, RFA is limited.[114] With currently available devices, the largest focus of necrosis that can be induced with a single application is approximately 4–5 cm in greatest diameter and lesions that size have a high frequency of marginal recurrences. Thus, the diameter of suitable lesions must be less than 3–4 cm. Further, tumors located near large vessels may not be effectively ablated because the heat sink effect of these vessels prevents ablation temperatures from being reached. It is these two scenarios that ThermoDox® is ideal for, because the temperature necessary to cause drug release (41 °C) is over 15 °C lower than the ablation temperature (>55 °C). As shown in Figure 2.20 the placement of an RFA electrode in a liver tumor can produce temperatures in the ablation zone upwards of 60 °C.

It is here that as the ablation temperature drops off (in the range 50 °C–39 °C that, as we saw earlier in its *in vitro* performance (Figure 2.14),[46] ThermoDox® can release its drug at significant rates, and deposit high concentrations of doxorubicin in the heated zone.

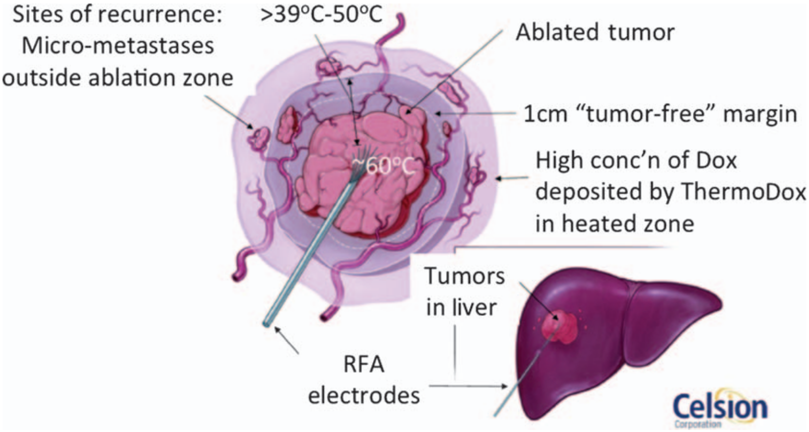
Sites of recurrence: Micro-metastases outside ablation zone
>39°C-50°C
Ablated tumor
1cm "tumor-free" margin
~60°C
High conc'n of Dox deposited by ThermoDox in heated zone
Tumors in liver
RFA electrodes
Celsion Corporation

Figure 2.20 Radio Frequency Ablation of liver tumors.

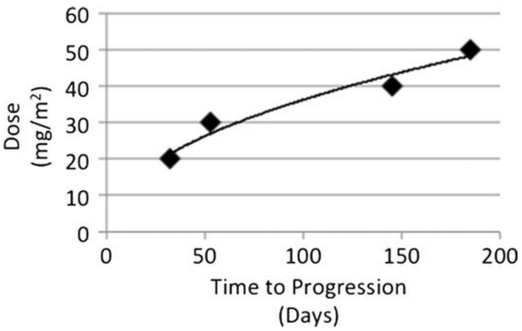

Figure 2.21 Results for Phase I dose escalation study to determine maximally tolerated dose for ThermoDox® in conjunction with Radio Frequency Ablation in the treatment of hepatocellular carcinoma (HCC). Dose response *vs.* time for tumors to progress.

The objective of the Phase I study was to determine the maximum tolerated dose (MTD) of ThermoDox® when used in combination with Radio Frequency Ablation (RFA) in the treatment of primary and metastatic tumors of the liver.[111,112] As reported by Poon *et al.*[113] a total of 24 patients (9 with HCC and 15 with metastatic liver cancer (MLC)) were treated (3, 6, 6, 6, 3 patients at 20, 30, 40, 50 and 60 mg/m^2, respectively). Median tumor size was 3.7 cm (range 1.7–6.5 cm). In total, 28 tumors were treated. Twenty (83%) of the patients had no evidence of local tumor failure after treatment. Despite this only being a Phase I dose escalation toxicity study, as shown in Figure 2.21 there was a dose-response relationship in terms of time to tumor progression (of 32, 53, 135, 185 days, respectively), giving a ~500% increase in progression free survival for the MTD (50 mg/m^2) compared to the lowest starting dose.

Encouragingly, then, there appeared to be a preliminary dose response relationship in terms of time to tumor progression as the study reached its maximally tolerated dose.

2.4.3.3 Phase III Studies: HepatoCellular Carcinoma (HEAT)

Given the efficacy seen in this Phase I trial, clinical testing was moved rapidly to a Phase III, randomized, double-blinded, dummy-controlled study of the efficacy and safety of ThermoDox® in combination with Radio Frequency Ablation (RFA) compared to RFA-alone in the treatment of non-resectable hepatocellular carcinoma.[115] This so-called HEAT study engaged 71 different sites in 11 different countries, and is the largest study ever conducted in intermediate hepatocellular carcinoma. It is looking to treat the usually untreatable large 3 cm–7 cm tumors. It is being conducted under a US Food and Drug Administration (FDA) Special Protocol Assessment, has received FDA Fast Track Designation and has been designated as a Priority Trial for liver cancer by the National Institutes of Health. ThermoDox® has been granted orphan drug designation in both the US and Europe for this indication. The European Medicines Agency (EMA) has confirmed the HEAT study is acceptable as a basis for submission of a marketing authorization application (MAA). In addition to meeting the US FDA and European EMA enrollment objectives, the HEAT study has also enrolled a sufficient number of patients to support registration filings in China, South Korea and Taiwan, three other large and important markets for ThermoDox®.

The arms of the study are:

- Experimental 1: ThermoDox® (50 mg/m^2 in 5% dextrose solution). Start 30 minute infusion about 15 minutes before radio frequency ablation begins.
- Sham Comparator 2: Sham (5% dextrose solution). Start 30 minute infusion about 15 minutes before radio frequency ablation begins.

The Primary Outcome Measures are:

Progression-free survival will be measured from the date of randomization to the first date on which one of the following occurs. (a) Local recurrence, (b) any new distant intrahepatic HCC tumor, (c) any new extrahepatic HCC tumor, (d) death from any cause (time frame: 3 years). A secondary confirmatory endpoint is overall survival.

The Main Inclusion Criteria are:

- Diagnosed hepatocellular carcinoma (HCC).
- No more than 4 HCC lesions with at least one ≥ 3.0 cm and none > 7.0 cm in maximum diameter, based on diagnosis at screening.
- If a subject has a large lesion (5.0–7.0 cm), any other lesions must be < 5.0 cm.

As of May 2012, the HEAT study reached its enrollment objective of 700 patients. The primary endpoint for the study is to measure a 33% improvement in progression-free survival (PFS), with a P value of 0.05. A total of 380 events of progression are required to reach the planned final analysis of the study. 380 PFS events are projected to occur in late 2012. While the data are not at the moment available, there is an interesting comparison that can be made between the dose response seen in the Phase I study and the criteria for this Phase III. As mentioned above, the PFS in the Phase III study is required to show only a 33% improvement compared to RFA alone. This compares very favorably with the increase in PFS in Phase I seen for the dose escalation (from 20 mg/m^2–50 mg/m^2) of almost 500% (the RFA-alone control was not done). While no firm conclusions should be taken from such a limited set of data (and this is indeed the reason a 700-patient multi-center trial is in fact required to obtain useful statistics), it is interesting to compare these two %PFS increase numbers. Also, a second caveat is that in the Phase I trial, median tumor size was 3.7 cm (range 1.7–6.5 cm), which although not the same, is not substantially different, compared to the criteria for the Phase III: "*No more than 4 HCC lesions with at least one* $\geq$*3.0 cm and none* $>$*7.0 cm in maximum diameter*."

2.4.3.4 *Phase I/II Trial Breast Cancer Recurrence at the Chest Wall (RCW) (DIGNITY Study)*

A second human Phase I/II trial, this time in breast cancer,[116] was designed to evaluate the maximum tolerated dose, pharmacokinetics, safety and efficacy of approved hyperthermia and ThermoDox® in patients with breast cancer recurrence at the chest wall (DIGNITY study). The purpose of this study is to evaluate the bioequivalence of ThermoDox® and measure efficacy in recurrent chest wall patients. In the initial Phase I (which was actually started in 2001, but later became non-recruiting[117]), there were several instances of stable disease, partial response and two of complete responses for a dose escalation of 20 mg/m^2–30 mg/m^2. As reported by Vujaskovic,[118] several patients in this trial achieved either partial or complete responses. As shown in Figure 2.22, for one

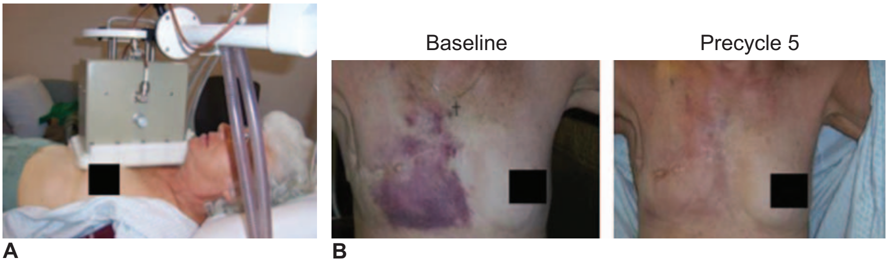

Figure 2.22 Treatment of chest wall recurrence of breast cancer, using a BSD-500 PC System to achieve a temperature goal of 40–42 °C (A) and same patient before treatment and pre-cycle 5 (B).

patient, her widely disseminated chest wall tumor had completely disappeared. This test dose (30 mg/m^2) was only 60% of the expected maximally tolerated dose, and so there were no side effects of the drug. A second patient had a similar complete response at 30 mg/m^2.[118]

The Phase I/II DIGNITY trial studying ThermoDox® for breast cancer[116] has now continued the study in several sites and has demonstrated remarkable clinical benefit in a very late-stage, underserved patient population. As presented at the European Society of Medical Oncology (EMO) conference 2012,[119] the clinical utility of ThermoDox® in this highly treatment-resistant setting points to its potential within a variety of superficial tumors, and could provide medical oncologists with an important tool to combat these often aggressive tumors. According to the lead clinician, the initial experience with hyperthermia and ThermoDox® has been very encouraging and provides initial safety and early efficacy data in several patients showing responses in this highly refractory and debilitating disease. These patients previously received over an average of four prior chemotherapy regimens along with prior radiation therapy. The continuation of the ThermoDox® trial will provide more efficacy data to potentially advance treatment for this patient population.

2.4.3.5 Phase II Colorectal Liver Metastases ABLATE

The third and final on-going human trial is a randomized, double blind, Phase II trial of RFA +/– ThermoDox® for Colorectal Liver Metastases ≥2 cm maximum in diameter.[120] Again, the purpose of this study is to determine the safety and efficacy of ThermoDox®, in combination with RFA in the treatment of recurrent or refractory colorectal liver metastases compared to RFA mono-therapy. The primary outcome of this trial is to evaluate local tumor control defined as complete ablation and where the patient does not experience recurrence within 1 cm of the ablation site.

2.5 Future Prospects

If ThermoDox® and RFA proves to be curative and its synergistic potential is borne out in the Phase III HEAT study, a rational future strategy for HCC lesions >3 cm is to employ RFA plus ThermoDox® as a front-line therapy. Encouraged by the materials science and engineering that went into the design of the LTSL, and the positive results seen in laboratory animal and spontaneous animal cancers, as well as the human clinical trials, additional human clinical trials are being planned or have been started using ThermoDox®. Also, additional drugs are being considered for encapsulation and release by mild hyperthermia. There is also the possibility that infections and abscesses that have elevated local hyperthermia that is intrinsic to the condition may also gain benefit from a local drug release, say of antibiotics or antifungals. This chapter will conclude with just a few remarks about new trials and will briefly discuss other thermal-sensitive liposomes currently in development.

2.5.1 New ThermoDox® Trials and Preclinical Studies

As shown in Table 2.2, a full clinical program is underway for ThermoDox®. In addition to the trials reviewed above, HCC (HEAT), RCW (DIGNITY) and CRLM (ABLATE), new research and preclinical development has started in bone metastases, pancreatic cancer and metastatic liver cancer. The exciting feature here is the adaptation of High Frequency Ultrasound (HIFU) as the source of targeted mild hyperthermia.

In combination with Philips Healthcare, a manufacturer of HIFU systems, Celsion began preclinical studies to assess the benefits of HIFU in combination with ThermoDox® in metastatic bone cancer,[121] that have now (August 2012) just received clearance to initiate a clinical study. This is a joint development program for Celsion's ThermoDox® combined with Philips' Sonalleve MR-HIFU (MR-guided high intensity focused ultrasound) technology for the palliation of painful metastases to the bone caused by lung, prostate, or breast cancers. It is expected that a Phase II study will be initiated in this indication, as well as looking into the treatment of pancreatic cancer with ThermoDox®.

2.5.2 Other Drugs

While ThermoDox® was the first drug to be encapsulated, mainly because of the huge history that we inherited in its liposomal formulations (like Evacet and

Table 2.2 ThermoDox Clinical Programs at Celsion Corporation (August 2012).

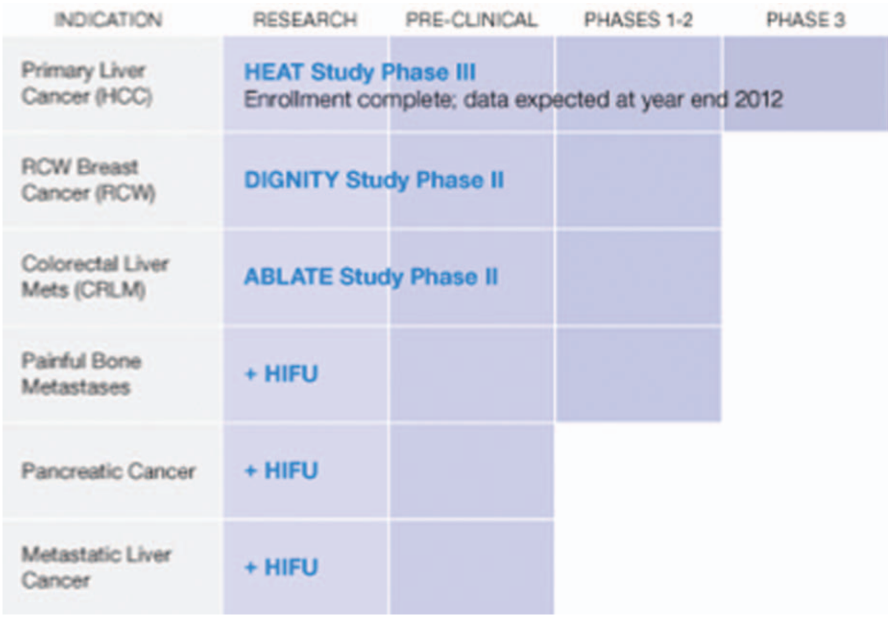

INDICATION	RESEARCH	PRE-CLINICAL	PHASES 1-2	PHASE 3
Primary Liver Cancer (HCC)	**HEAT Study Phase III** Enrollment complete; data expected at year end 2012			
RCW Breast Cancer (RCW)	**DIGNITY Study Phase II**			
Colorectal Liver Mets (CRLM)	**ABLATE Study Phase II**			
Painful Bone Metastases	**+ HIFU**			
Pancreatic Cancer	**+ HIFU**			
Metastatic Liver Cancer	**+ HIFU**			

Doxil), the LTSL is also capable of encapsulating and releasing many other drugs as well as imaging agents that report on heatability, perfusion and small molecule delivery.[97] In published and unpublished work, we and others have already explored the conditions and developed processes for encapsulating *cisplatin*,[122] *carboplatin* and *manganese prophyrins*. It is expected that such membrane impermeable drugs, if well retained, in an LTSL formulation will prove to be an advantage, since drugs like *cisplatin* when encapsulated in the stealth liposomes proved to be less efficacious than free drug. As always, control over the triggered release of the encapsulated drug to increase bioavailability of the drug exclusively at the diseased site has always been one of the biggest challenges.[123] In the Stealth® liposomal formulation (SPI-077) minimal clinical efficacy despite adequate tumor accumulation was observed.[124–126] That is, the steps taken to establish adequate drug loading, circulation half-life, drug retention in the bloodstream and passive tumor accumulation resulted in excessive retention of *cisplatin* in the liposome so that it was not substantially released at the tumor site. Again, the two sides of the same coin compromise each other – good retention in order to reduce toxicity *vs*. not getting the drug out leading to reduced efficacy.

2.5.3 Other New Thermal-sensitive Formulations (Lipids and Polymers)

Modifications and potential improvements to the temperature-sensitive liposome formulation, including different lipid components, are currently ongoing. Others have created and developed their own thermal sensitive liposomes with similar release characteristics and temperatures, but made from different materials. Although the materials data for these formulations are not as complete, and so the absolute details of how they work remain speculative, mechanistically it would seem they have similar bilayer components to create nanopores at purported grain boundaries. Principal among these, Lindner *et al.*[127] designed their temperature-sensitive liposomes composed of the novel lipid 1,2-dipalmitoyl-*sn*-glycero-3-phosphoglyceroglycerol (DPPGOG) and 1,2-dipalmitoyl-*sn*-glycero-3-phosphocholine (DPPC). Hossann *et al.*[128] studied the influence of DPPGOG on *in vitro* stability of the liposome composed of DPPGOG, DSPE-PEG^{2000} and P-lyso-PC. They showed that the release rate of the contents was significantly increased by incorporating DPPGOG or P-lyso-PC in their TSL formulations. Also, Lindner *et al.* formulated liposomes composed of HePC/DPPC/DSPC/DPPGOG and showed that HePC increases the release rate of their TSL in a similar way to lysolipid in the presence of fetal calf serum.[129] Interestingly, DPPGOG facilitates drug release from the liposome under mild hyperthermic conditions (41–42 °C) and leads to a substantially prolonged plasma half-life for the encapsulated drug. Thus, in Lindner's formulations DSPE-PEG^{2000} is not required for long circulation half-life or stabilizing pores; this is apparently achieved by the DPPGOG lipid.

In other studies, temperature-sensitive liposomes have been designed using thermal-sensitive polymers: Hayashi *et al.*[130] studied temperature-sensitive liposomes composed of various phospholipids and coated with poly(*N*-isopropylacrylamide) that show a transition temperature near 32 °C; Kono *et al.*[131] also used polymers composed of dioleoylphosphatidylethanolamine modified with copolymers of *N*-isopropylacrylamide and *N*-acryloylpyrrolidine; and Paasonen *et al.*[132] reported on polymer-coated liposomes with thermal-sensitive poly[*N*-(2-hydroxypropyl) methacrylamide mono/dilactate] (pHPMA mono/dilactate), which has a T_m at 42 °C. Thus, several new studies have introduced the idea of modifications to the bilayer composition or surface of liposomes with temperature-sensitive polymers that retain temperature-triggered release from the liposome. Such modifications may prove useful in the future, but require further, especially clinical, investigation.

2.6 Concluding Remarks

2.6.1 The Drug-delivery Problem

While drug delivery to tumors is traditionally described in terms of total drug per weight or per body surface area, one often dismissed but exceedingly important parameter of chemotherapy is the differential amount of drug delivered to actual tumor cells located close to, as well as further from, blood vessels. Thus, the extent to which a drug present in the bloodstream, either after free drug administration of a bolus or continuous injection, or when delivered *via* a drug-delivery system such as a liposome, can provide a sink of bioavailable drug, penetrate and accumulate in the interstitial tissue and, perhaps more importantly, intra-cellularly, will have a major influence over the efficacious outcome of these treatment modalities. It is in this context that a recent paper[17] compares and contrasts both vascular and tumor concentrations of doxorubicin when administered either as a free drug bolus injection, as traditional "Stealth" (Doxil™) liposomes, or by our relatively new low temperature sensitive liposome formulation (Dox-LTSL) that releases doxorubicin rapidly in the warmed bloodstream upon exposure to only mild hyperthermia (HT).

2.6.2 A New Paradigm for Local Drug Delivery: Drug Release in the Bloodstream

Taken together these studies have prompted the current hypothesis that *the mechanism of enhanced drug delivery and tumor growth delay was due to enhanced drug penetration throughout the whole tumor as a result of rapidly triggered intravascular release of drug from the thermally sensitive liposomes*. If the hypothesis continues to bear out, it represents a new strategy for drug delivery that reduces free drug toxicity by sequestering drug until it reaches the tumor, then releasing drug specifically into the tumor with a localized trigger (mild hyperthermia). While the intravascular release hypothesis has certainly existed since the early work on thermally sensitive liposomes in the late 1970s,[40,133,134] to date, intravascular release has not actually been shown to occur *in vivo*. What the LTSL formulation has demonstrated is that, compared to either free drug administration or the EPR effect required by the more traditional non-thermal sensitive liposomes (Doxil™), intravascular drug release improves drug penetration and levels of accumulation that reach not only more tumor cells, but also stroma, endothelial cells and pericytes.

Thus, our studies so far have introduced and characterized the liposomal system, and have established the fundamental relationships between compositions, structure, property, processing and performance for the main three components.[15,16,46,50] In preclinical studies we have found that this unique formulation offers a more effective way to achieve targeted, local drug release for cancer chemotherapy than more traditional, and even stealth, liposomes.[16,45] It actually offers a new paradigm for drug delivery, *drug release in the bloodstream*, and an antivascular as well as antineoplastic mechanism of tumor kill.[17]

2.6.3 New Horizons

Temperature-sensitive liposomes have progressed significantly since the early work of Yatvin *et al.*,[38] but by no means has the work in this field reached its potential. Only one formulation, LTSL, with only one drug, doxorubicin (as ThermoDox®), has made it to human clinical trials. If these thermal-sensitive liposomes prove to be as effective in humans as in preclinical settings, a push for their use in the treatment of human disease and the encapsulation of a range of existing** and new drugs††, for a series of other indications will likely be made. The beauty of encapsulating already FDA approved drugs is the smoother transition into the clinic. There are many chemotherapeutic drugs currently approved for human use and so with judicial choice, focusing mainly on water-soluble compounds, there are many opportunities for old chemotherapeutics, new molecular-targeted therapies and biological-modifiers, to specific cellular molecular targets waiting to be encapsulated in temperature- and "other"-sensitive liposomes for strategies that bring drugs to local tumors. Since it is commonly said that one drug type cannot treat all cancers, variations in the chemotherapeutic drugs contained in these liposomes are needed. For a temperature-sensitive liposome, two drugs could be encapsulated at antagonistic ratios, and released at the same time in the same place. Also, work is currently being done to broaden the applicability of temperature-sensitive liposomes, especially in the area of encapsulating contrast agents for improved imaging modalities. Such co-encapsulation of a

---

[**] Listed at www.cancer.gov, there are 2,300+ agents that are being used in the treatment of patients with cancer or cancer-related conditions.

[††] According to Dr. Richard Pazdur, head of the FDA's office of oncology products, last year, 10 out of 30 new drugs approved by the FDA were for treatment of cancer. This year over 20 oncology applications are expected to be filed.

drug and an imaging agent has definite clinical potential. Thus, LTSLs and other such thermally triggered-release systems are poised to make a significant impact in the delivery and controlled release of a series of existing and new anticancer compounds in a range of cancers; they just need to be warmed to 41 °C–42 °C.

Acknowledgements

Thanks to all the students, post docs and faculty collaborators who have made this work possible, including, especially, Dr. Zeljko Vujaskovic, and their clinical team; the post docs and graduate students Gopal Anyarambhatla, Garheng Kong, Jeff Mills, Alex Wright, Ana Ponce, Ji-Young Park, Ashley Manzoor, Ben Viglianti; and Michael Tardugno and Nicholas Borys at Celsion. The work was supported by several grants from NIH, including P01-CA42745, RO1-CA87630, RO1-GM40162, as well as 9213-ARG-0608 from the North Carolina Biotechnology Center. Clinical studies have been mainly supported by Celsion Corporation.

References

1. A. D. Bangham, M. M. Standish and J. C. Watkins, *J. Mol. Biol.*, 1965, **13**, 238.
2. M. J. Hope, M. B. Bally, G. Webb and P. R. Cullis, *Biochim. Biophys. Acta*, 1985, **812**, 55.
3. L. D. Mayer, M. J. Hope and P. R. Cullis, *Biochim. Biophys. Acta*, 1986, **858**, 161.
4. G. Gregoriadis, *New Engl. J. Med.*, 1976, **295**, 704.
5. A. Rahman, A. Kessler, N. More, B. Sikic, G. Rowden, P. Woolley and P. S. Schein, *Cancer Res.*, 1980, **40**, 1532.
6. D. N. Waterhouse, P. G. Tardi, L. D. Mayer and M. B. Bally, *Drug Saf.*, 2001, **24**, 903.
7. N. Maurer, D. B. Fenske and P. R. Cullis, *Expert Opin. Biol. Ther.*, 2001, **1**, 923.
8. A. Gabizon, A. Dagan, D. Goren, Y. Barenholz and Z. Fuks, *Cancer Res.*, 1982, **42**, 4734.
9. P. G. Tardi, N. L. Boman and P. R. Cullis, *J. Drug Target.*, 1996, **4**, 129.
10. G. Schumacher and H. Sandermann, *Biochim. Biophys. Acta*, 1976, **448**, 642.
11. C. Tanford, *The Hydrophobic Effect: Formation of Micelles and Biological Membranes*, 2nd edn, Wiley, New York, 1980.
12. J. F. Nagle and S. Tristram-Nagle, *Curr. Opin. Struct. Biol.*, 2000, **10**, 474.
13. R. M. Straubinger, N. Düzgünes and D. Papahadjopoulos, *FEBS Lett.*, 1985, **179**, 148.
14. K. Jørgensen, J. Davidsen and O. G. Mouritsen, *FEBS Lett.*, 2002, **531**, 23.
15. G. R. Anyarambhatla and D. Needham, *J. Liposome Res.*, 1999, **9**, 491.

16. D. Needham, G. Anyarambhatla, G. Kong and M. W. Dewhirst, *Cancer Res.*, 2000, **60**, 1197.
17. A. A. Manzoor, L. H. Lindner, J.-Y. Park, A. J. Simnick, M. R. Dreher, S. Das, G. Hanna, W. Park, G. Koning, T. ten Hagen, D. Needham and M. W. Dewhirst, *Cancer Res.*, 2012, doi: 10.1158/0008-5472.CAN-12-1683.
18. J. Israelachvili, *Intermolecular and Surface Forces*, Academic Press, London, 1992.
19. T. Allen and P. Cullis, *Science*, 2004, **303**, 1818.
20. H. F. Dvorak, J. A. Nagy, J. T. Dvorak and A. M. Dvorak, *Am. J. Pathol.*, 1988, **133**, 95.
21. H. Maeda, *Advan. Enzyme Regul.*, 2001, **41**, 189.
22. H. Maeda and Y. Matsumura, *Crit. Rev. Ther. Drug*, 1989, **6**, 193.
23. G. Gregoriadis, *N. Engl. J. Med.*, 1976, **295**, 704.
24. G. Gregoriadis, *N. Engl. J. Med.*, 1976, **295**, 765.
25. F. Yuan, M. Leunig, S. K. Huang, D. A. Berk, D. Papahadjopoulos and R. K. Jain, *Cancer Res.*, 1994, **54**, 3352.
26. N. Z. Wu, D. Da, T. L. Rudoll, D. Needham, A. R. Whorton and M. W. Dewhirst, *Cancer Res.*, 1993, **53**, 3765.
27. M. H. Gaber, N. Z. Wu, K. Hong, S. K. Huang, M. W. Dewhirst and D. Papahadjopoulos, *Int. J. Radiat. Oncol. Biol. Phys.*, 1996, **36**, 1177.
28. G. Kong, R. D. Braun and M. W. Dewhirst, *Cancer Res.*, 2000, **60**, 4440.
29. G. Kong, R. D. Braun and M. W. Dewhirst, *Cancer Res.*, 2001, **61**, 3027.
30. M. L. Matteucci, G. Anyarambhatla, G. Rosner, C. Azuma, P. E. Fisher, M. W. Dewhirst, D. Needham and D. E. Thrall, *Clin. Cancer Res.*, 2000, **6**, 3748.
31. H. S. Reinhold and B. Endrich, *Int. J. Hyperthermia*, 1986, **2**, 111.
32. C. Song, I. Choi, B. Nah, S. Sahu and J. Osborn, in *Themo-Radiotherapy and Thermo-Chemotherapy*, ed. M. Seegenschmiedt, P. Fessenden and C. Vernon, Springer-Verlag, Berlin, 1995.
33. F. Yuan, M. Dellian, D. Fukumura, M. Leunig, D. A. Berk, V. P. Torchilin and R. K. Jain, *Cancer Res.*, 1995, **55**, 3752.
34. Q. Chen, A. Krol, A. Wright, D. Needham, M. W. Dewhirst and F. Yuan, *Int. J. Hyperthermia*, 2008, **24**, 475.
35. C. W. Haest, J. de Gier, G. A. van Es, A. J. Verkleij and L. L. van Deenen, *Biochim. Biophys. Acta*, 1972, **288**, 43.
36. O. G. Mouritsen and M. J. Zuckermann, *Phys. Rev. Lett.*, 1987, **58**, 389.
37. D. Papahadjopoulos, K. Jacobson, S. Nir and T. Isac, *Biochim. Biophys. Acta*, 1973, **311**, 330.
38. M. B. Yatvin, N. Weinstein, W. H. Dennis and R. Blumenthal, *Science*, 1978, **202**, 1290.
39. M. B. Yatvin, H. Mühlensiepen, W. Porschen, J. N. Weinstein and L. E. Feinendegen, *Cancer Res.*, 1981, **41**, 1602.
40. Celsion, 2010. Available from: http://www.celsion.com.
41. Celsion Corporation, 2012. Available from: http://www.celsion.com.

42. D. Needham, J. Y. Park, A. M. Wright and J. Tong, *Faraday Discuss.*, 2013, DOI: 10.1039/C2FD20111A.
43. A. Wright, in *Mechanical Engineering and Materials Science*, 2006, Duke University, Durham, NC, USA.
44. G. R. Anyarambhatla and D. Needham, *J. Liposome Res.*, 1999, **9**, 491.
45. G. Kong, G. Anyarambhatla, W. P. Petros, R. D. Braun, O. M. Colvin, D. Needham and M. W. Dewhirst, *Cancer Res.*, 2000, **60**, 6950.
46. J. K. Mills and D. Needham, *Biochim. Biophys. Acta*, 2005, **1716**, 77.
47. J. K. Mills and D. Needham, *Methods Enzymol.*, 2004, **387**, 82.
48. D. Needham, G. Anyarambhatla, G. Kong and M. W. Dewhirst, *Cancer Res.*, 2000, **60**, 1197.
49. J. K. Mills, in *Department of Mechanical Engineering and Materials Science*, 2002, Duke University, Durham, NC, USA.
50. J. K. Mills and D. Needham, *Methods Enzymol.*, 2004, **387**, 82.
51. T. M. Allen, C. Hansen, F. Martin, C. Redemann and A. Yau-Young, *Biochim. Biophys. Acta*, 1991, **1066**, 29.
52. N. Kučerka, M. P. Nieh and J. Katsaras, *Biochim. Biophys. Acta*, 2011, **1808**, 2761.
53. A. K. Kenworthy, K. Hristova, D. Needham and T. J. McIntosh, *Biophys. J.*, 1995, **68**, 1921.
54. D. V. Zhelev, *Biophys. J.*, 1996, **71**, 257.
55. E. A. Evans and D. Needham, *J. Phys. Chem.*, 1987, **91**, 4219.
56. R. P. Rand and A. C Burton, *Biophys. J.*, 1964, **4**, 115.
57. E. Evans and R. Skalak, *Mechanics and Thermodynamics of Biomembranes*, CRC, Boca Raton, Florida, 1980.
58. E. Evans and R. M. Hochmuth, *Curr. Top. Membr. Trans.*, 1978, **10**, 1.
59. H. J. Meiselman, M. A. Lichtman and P. L. LaCelle, in *Proceedings of a Symposium Held at the Kroc Foundation, Santa Ynez Valley, California*, May 2–6, 1983, ed. A. R. Liss, Kroc Foundation series, New York, 1984.
60. D. Needham, *Cell Biophys.*, 1991, **18**, 99.
61. E. Evans, in *Physical Basis of Cell-Cell Adhesion*, ed. P. Bongrand, CRC Press, Boca Raton, Florida, 1988.
62. E. Evans and R. Kwok, *Biochem.*, 1982, **21**, 4874.
63. R. Kwok and E. Evans, *Biophys. J.*, 1981, **35**, 637.
64. E. Evans and D. Needham, *J. Phys. Chem.*, 1987, **91**, 4219.
65. L. M. Ickenstein, M. C. Arfvidsson, D. Needham, L. D. Mayer and K. Edwards, *Biochim. Biophys. Acta*, 2003, **1614**, 135.
66. M. Sandström, L. M. Ickenstein, L. D. Mayer and K. Edwards, *J. Control. Release*, 2005, **107**, 131.
67. D. H. Kim, M. J. Costello, P. B. Duncan and D. Needham, *Langmuir*, 2003, **19**, 8455.
68. D. Needham and R. S. Nunn, *Biophys. J.*, 1990, **58**, 997.
69. D. H. Kim, D. Needham, in *Encyclopedia of Surface and Colloid Science*, ed. A. Hubbard, Marcel Dekker, New York, 2001, p. 3057.
70. D. Needham, in *Permeability and Stability of Lipid Bilayers*, ed. E. A. Disalvo and S. A. Simon, CRC Press, Boca Raton, Florida, 1995, p. 49.

71. D. Needham and D. Zhelev, in *Giant Vesicles*, ed. P. L. Luisi and P. Walde, John Wiley & Sons Ltd, Chichester, 2000, p. 103.
72. D. Needham and D. V. Zhelev, in *Vesicles*, ed. M. Rosoff, Marcel Dekker, New York, 1996, p. 373.
73. D. Needham, T. J. McIntosh and E. A. Evans, *Biochem.*, 1988, **27**, 4668.
74. S. Mabrey and J. M. Sturtevant, *P. Natl. Acad. Sci. USA*, 1976, **73**, 3862.
75. M. Bloom, E. Evans and O. G. Mouritsen, *Q. Rev. Biophys.*, 1991, **24**, 293.
76. D. D. Lasic and D. Needham, *Chem. Rev.*, 1995, **95**, 2601.
77. M. S. Webb, T. O. Harasym, D. Masin, M. B. Bally and L. D. Mayer, *Br. J. Cancer*, 1995, **72**, 896.
78. M. R. Vist and J. H. Davis, *Biochem.*, 1990, **29**, 451.
79. S. Karmakar, V. A. Raghunathan and S. Mayor, *J. Phys. Condens. Matter*, 2005, **17**, S1177.
80. D.Marsh, *Handbook of Lipid Bilayers*, CRC Press, Boca Raton, Florida, 1990.
81. G. Kong and M. W. Dewhirst, *Int. J. Hyperthermia*, 1999, **15**, 345.
82. D. Needham, N. Stoicheva and D. V. Zhelev, *Biophys. J.*, 1997, **73**, 2615.
83. D. Needham and D. V. Zhelev, *Ann. Biomed. Engin.*, 1995, **23**, 287.
84. D. Needham, US Patent No. 6,200,598 (filed June 18, 1998), 2001.
85. D. Needham, US Patent No. 6,726,925 (filed December 9, 1999), 2004.
86. C. A. Frederick, L. D. Williams, G. Ughetto, G. A. van der Mare, J. H. van Boom, A. Rich and A. H. J. Wang, *Biochem.*, 1990, **29**, 2538.
87. M. Dalmark and P. Johansen, *Mol. Pharmacol.*, 1982, **22**, 158.
88. E. Saltiel and W. MacGuire, *West J. Med.*, 1983, **139**, 332.
89. P. R. Cullis, L. D. Mayer, M. B. Bally, T. D. Madden and M. J. Hope, *Adv. Drug Deliver. Rev.*, 1989, **3**, 267.
90. K. Hristova and D. Needham, *Liquid Crystals*, 1995, **18**, 423.
91. D. Needham, T. J. McIntosh and D. V. Zhelev, in *Liposomes: Rational Design*, ed. A. Janoff, Marcel Dekker, New York, 1998, p. 13.
92. L. D. Mayer, M. B. Bally and P. R. Cullis, *Biochim. Biophys. Acta*, 1986, **857**, 123.
93. X. Li, D. Cabral-Lilly, A. S. Janoff and W. R. Perkins, *J. Liposome Res.*, 2000, **10**, 15.
94. C. Landon, J. Y. Park, D. Needham and M. W. Dewhirst, *Open Nanomed. J.*, 2011, **3**, 38.
95. D. Needham and A. Ponce, in *Nanotechnology for Cancer Therapy*, ed. M. M. Amiji, CRC Press, Boca Raton, Florida, 2006, p. 677.
96. D. Needham and M. W. Dewhirst, *Adv. Drug Deliver. Rev.*, 2001, **53**, 285.
97. A. M. Ponce, B. L. Viglianti, D. Yu, P. S. Yarmolenko, C. R. Michelich, J. Woo, M. B. Bally and M. W. Dewhirst, *J. Natl Cancer Inst.*, 2007, **99**, 53.
98. J. K. Mills and D. Needham, *Biochim. Biophys. Acta*, 2005, **1716**, 77.
99. L. M. Hays, *Cryobiology*, 2001, **42**, 88.
100. O. G. Mouritsen, K. Jorgensen and T. Honger, in *Permeability and Stability of Lipid Bilayers*, CRC Press, Boca Raton, 1995, p. 137.

101. Q. Huang, S. Shan, R. D. Braun, J. Lanzen, G. Anyrhambatla, G. Kong, M. Borelli, P. Corry, M. W. Dewhirst and C. Y. Li, *Nat. Biotech.*, 1999, **17**, 1033.
102. P. S. Yarmolenko, Y. Zhao, C. Landon, I. Spasojevic, F. Yuan, D. Needham, B. L. Viglianti and M. W. Dewhirst, *Int. J. Hyperthermia*, 2010, **26**, 485.
103. A. M. Ponce, B. L. Viglianti, D. Yu, P. S. Yarmolenko, C. R. Michelich, J. Woo, M. B. Bally and M. W. Dewhirst, *J. Natl Cancer Inst.*, 2007, **99**, 53.
104. Q. Chen, S. Tong, M. W. Dewhirst and F. Yuan, *Mol. Cancer Ther.*, 2004, **3**, 1311.
105. R. Porschen, S. Classen, M. Piontek and F. Borchard, *Cancer Res.*, 1994, **54**, 587.
106. A. Ponce and D. Needham, in *Nanotechnology for Cancer Therapeutics*, ed. M. M. Amiji, CRC Press, Boca Raton, Florida, 2006, p. 667.
107. M. L. Hauck, S. M. LaRue, W. P. Petros, J. M. Poulson, D. Yu, I. Spasojevic, A. F. Pruitt, A. Klein, B. Case, D. E. Thrall, D. Needham and M. W. Dewhirst, *Clin. Cancer Res.*, 2006, **12**, 4004.
108. J. Poljaková, T. Eckschlager, J. Hřebačková, J. Hraběta and M. S. Iborová, *Interdisc. Toxicol.*, 2008, **1**, 186.
109. M. Al-Qubaisi, R. Rozita, S. K. Yeap, A. R. Omar, A. M. Ali and N. B. Alitheen, *Molecules*, 2011, **16**, 2944.
110. Celsion Corporation, *A Dose Escalation, Pharmacokinetics, and Safety Study of Doxorubicin Encapsulated in Temperature Sensitive Liposomes Released Through Microwave Therapy in the Treatment of Prostate Cancer*, NCT00061867, 2003–2009.
111. Celsion Corporation, *A Phase I Dose Escalation Tolerability Study of ThermoDox™ (Thermally Sensitive Liposomal Doxorubicin) in Combination With Radiofrequency Ablation (RFA) of Primary and Metastatic Tumors of the Liver (NCT00441376) Completed*, 2007–2009.
112. R. T. Poon and N. Borys, *Expert Opin. Pharmacother.*, 2009, **10**, 333.
113. B. Wood, R. T. Poon, Z. Neeman, M. Eugeni, J. Locklin, S. Dromi, S. Kachala, R. Prabhakar, W. Hahne and S. K. Libutti, *Phase I study of Thermodox (thermally sensitiveliposomes containing doxorubicin) given prior to radiofrequency ablation for unresectable liver cancers*, in 2007 Gastrointestinal Cancers Symposium, USA.
114. H. Choi, E. M. Loyer, R. A. DuBrow, H. Kaur, C. L. David, S. Huang, S. Curley and C. Charnsangavej, *RadioGraphics*, 2001, **21**, S41.
115. Celsion Corporation, *A Phase III, Randomized, Double-Blinded, Dummy-Controlled Study of the Efficacy and Safety of ThermoDox® (Thermally Sensitive Liposomal Doxorubicin) in Combination With Radiofrequency Ablation (RFA) Compared to RFA-Alone in the Treatment of Non-Resectable Hepatocellular Carcinoma (NCT00617981)*, 2008–2012.
116. Celsion Corporation, *Phase 1/2 Study of ThermoDox With Approved Hyperthermia in Treatment of Breast Cancer Recurrence at the Chest Wall (DIGNITY), NCT00826085*, 2012.

117. Celsion Corporation, *A Randomized Pivotal Clinical Trial in Breast Cancer Patients of Pre-Operative Focal Microwave Thermotherapy Treatment for Early-Stage Breast Disease in Intact Breast, NCT00036998*, 2001.
118. Z.Vujaskovic, in *Society for Thermal Medicine*, Washington, DC, 2007.
119. H. S.Rugo, in *European Society of Medical Oncology*, Vienna, Austria, 2012, p. 363.
120. Celsion Corporation, *Randomized, Double Blind, Phase II Trial of Radiofrequency Ablation +/− Lyso-Thermosensitive Liposomal Doxorubicin (Thermodox) for Colorectal Liver Metastases Greater Than or Equal to 2 cm Maximum Diameter (NCT01464593)*, 2011.
121. Celsion Corporation and Philips Healthcare, *Investigational New Drug/Investigational Device Exemption (IND/IDE) Application for a Phase 2 Study of ThermoDox and MR-HIFU in Bone Cancer*, US FDA, Editor, 2012.
122. J. Woo, G. N. Chiu, G. Karlsson, E. Wasan, L. Ickenstein, K. Edwards and M. B. Bally, *Int. J. Pharm.*, 2008, **349**, 38.
123. A. Kozubek, J. Gubernator, E. Przeworska and M. Stasiuk, *Acta Biochim. Pol.*, 2000, **47**, 639.
124. K. J. Harrington, C. R. Lewanski, A. D. Northcote, J. Whittaker, H. Wellbank, R. G. Vile, A. M. Peters and J. S. Stewart, *Ann. Oncol.*, 2001, **12**, 493.
125. M. S. Newman, G. T. Colbern, P. K. Working, C. Engbers and M. A. Amantea, *Cancer Chemother. Pharmacol.*, 1999, **43**, 1.
126. W. C. Zamboni, A. C. Gervais, M. J. Egorin, J. H. Schellens, E. G. Zuhowski, D. Pluim, E. Joseph, D. R. Hamburger, P. K. Working, G. Colbern, M. E. Tonda, D. M. Potter and J. L. Eiseman, *Cancer Chemother. Pharmacol.*, 2004, **53**, 329.
127. L. H. Lindner, M. E. Eichhorn, H. Eibl, N. Teichert, M. Schmitt-Sody, R. D. Issels and M. Dellian, *Clin. Cancer Res.*, 2004, **10**, 2168.
128. M. Hossann, M. Wiggenhorn, A. Schwerdt, K. Wachholz, N. Teichert, H. Eibl, R. D. Issels and L. H. Lindner, *Biochim. Biophys. Acta*, 2007, **1768**, 2491.
129. L. H. Lindner, M. Hossann, M. Vogeser, N. Teichert, K. Wachholz, H. Eibl, W. Hiddemann and R. D. Issels, *J. Control. Release*, 2008, **125**, 112.
130. H. Hayashi, K. Kono and T. Takagishi, *Bioconjug. Chem.*, 1998, **9**, 382.
131. K. Kono, K. Yoshino and T. Takagishi, *J. Control. Release*, 2002, **80**, 321.
132. L. Paasonen, B. Romberg, G. Storm, M. Yliperttula, A. Urtti and W. E. Hennink, *Bioconjug. Chem.*, 2007, **18**, 2131.
133. J. N. Weinstein, R. L. Magin, M. B. Yatvin and D. S. Zaharko, *Science*, 1979, **204**, 188.
134. M. B. Yatvin, J. N. Weinstein, W. H. Dennis and R. Blumenthal, *Science*, 1978, **202**, 1290.

CHAPTER 3

pH-sensitive Liposomes in Drug Delivery

SHIVANI RAI PALIWAL,*[a,b] RISHI PALIWAL[a] AND
SURESH P VYAS*[a]

[a] Drug Delivery Research Laboratory, Department of Pharmaceutical Sciences, Dr H. S. Gour Vishwavidyalaya (A Central University), Sagar, M.P. India, 470003; [b] Department of Pharmaceutics, SLT Institute of Pharmaceutical Sciences, Guru Ghasidas Vishwavidyalaya (A Central University), Bilaspur, C.G., India, 495009
*Email: srai2k@gmail.com; spvyas54@gmail.com

3.1 Introduction

Liposomes are widely explored carriers for controlled and targeted delivery of drugs, genetic material and diagnostic agents. As explained in Chapter 2, liposomes are spherical structures formed by concentric bilayers of lipids that resemble the natural membranes and enclose aqueous compartments. Surface modified liposomes serve as one of the most suitable carriers capable of bypassing the barriers imposed by the biological environment even up to cellular and subcellular level.[1] They can be designed according to specific therapeutic purposes and clinical/pathological conditions, minimizing exposure of healthy parts of the body to the treatment. Some liposomal products (*e.g.* Doxil® and Ambisome® containing doxorubicin and amphotericin B, respectively) have reached the market and are currently used by clinicians. Several approaches to develop liposomes with targeting and/or release triggering features to improve the therapeutic index of drugs have been tested.

RSC Smart Materials No. 2
Smart Materials for Drug Delivery: Volume 1
Edited by Carmen Alvarez-Lorenzo and Angel Concheiro
© The Royal Society of Chemistry 2013
Published by the Royal Society of Chemistry, www.rsc.org

The composition of liposomal systems can be easily modified to facilitate site-specific release in response to environmental conditions. The pH-sensitive liposomes are specifically designed to control the release of the content in response to acidic pH within the endosomal system without being unstable in plasma.[2] This enables the cytoplasmic delivery of polar materials and even macromolecules, such as antitumor drugs, proteins and DNA.[3,4] Overall, pH-sensitive liposomes combine the protective effects of conventional liposomal systems with specific environment-controlled drug release.

The pH-sensitive liposomes undergo controlled fusion with cellular or endosomal membranes and rapid destabilization in acidic environment such as that of endosomes.[5–8] The pH-sensitive liposomes are generally composed of a neutral cone-shaped lipid dioleoylphosphatidyl-ethanolamine (DOPE) and a weakly acidic amphiphile, such as cholesteryl hemisuccinate (CHEMS).[9] The fusogenic characteristics are due to the polymorphic phase behavior of DOPE, which forms not a bilayer but a hexagonal structure when dispersed in aqueous media. To stabilize DOPE in liposomes, other lipids such as dioleoylphosphatidylcholine (DOPC)[10] or *N*-succinyl-DOPE[11] can be incorporated. These lipids have negatively charged groups, which become neutral in the acidic environment of the endosome, leading to destabilization, fusion with endosomal membrane and content release.[12]

Even being stable in plasma, application of pH-sensitive liposomes is limited by the recognition and sequestration by the phagocytes of the reticulo-endothelial system (RES), which leads to very short circulation half-life. PEGylation of the lipids may help to overcome these inconveniences.[13] On the other hand, the use of lipids with high transition temperatures (distearoylphosphatidylcholine, DSPC; hydrogenated soy PC, HSPC), and the incorporation of cholesterol (Chol) and lipid conjugates such as phosphatidylethanolamine–poly(ethylene glycol) (PE–PEG), may lead to a significant decrease of leakage of the encapsulated drugs during circulation or in the extra-cellular medium. Moreover, they reduce non-specific interactions between liposomes and serum proteins (opsonins), which also helps to prevent liposome clearance by the cells of the RES.

The size of the liposomes can be optimized (<150 nm) to increase the circulation time, make the penetration through fine capillaries easier, cross the fenestration into interstitial space, and be uptaken by cells *via* endocytosis/phagocytosis. These features together with surface PEGylation and use of high transition temperature lipids enable a circulation time long enough for passive accumulation in cancer tissues *via* the enhanced permeability and retention (EPR) effect (Figure 3.1).[14] The availability of the surface for modification with site-directing ligand provides opportunity for active targeting liposomal drug delivery. Compared to other nanocarriers that have not reached the clinical arena yet, the fact that liposomes have been already commercialized since several decades ago is a further motivation for scientists to search for improvements and novel applications of the liposomology. The present chapter highlights the use of pH-sensitive liposomes as smart delivery carriers for drugs and other therapeutic agents.

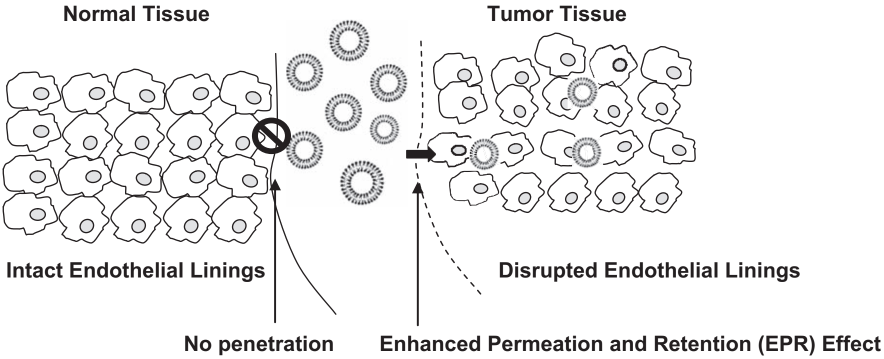
Normal Tissue
Tumor Tissue
Intact Endothelial Linings
Disrupted Endothelial Linings
No penetration
Enhanced Permeation and Retention (EPR) Effect

Figure 3.1 Schematic view of the passive targeting of liposomes to tumor tissues by means of the enhanced permeation and retention (EPR) effect.

3.2 pH-sensitive Liposomes as Smart Drug Carriers

The concept of pH-sensitive drug delivery was introduced in the early 1980s.[15] The altered pH gradients in diseased conditions, such as tumor extra-cellular environments, and in the intra-cellular compartments are exploited for the design of pH-responsive liposomes for specific cancer cell targeting, enhanced cellular internalization and rapid drug release.[16,17] Figure 3.2 depicts the application of pH-sensitive liposomes in cancer therapy: A) the liposome reaches the tumor tissue and destabilizes due to the acidic environment, releasing the drug extra-cellularly, or B) the intact liposome is taken by the cell through endocytosis, the liposome disrupts the endosome before fusion with lysosomes and the drug is released in the cytoplasm. The intra-cellular drug delivery by the pH-sensitive liposomes offers an efficient means of overcoming the multi-drug resistance (MDR) due to the activity of the efflux pumps, one of the major causes of cancer treatment failure. The attachment of receptor specific ligands on such pH-sensitive liposomes potentiates accumulation at tumor cells by active targeting.[18,19] Moreover, multi-functional pH-responsive liposomes have been developed to combine diagnosis and treatment together, namely for theranostics.

The development of strategies to increase the ability of liposomes to mediate intra-cellular delivery of biologically active molecules has been the subject of intensive research activity.[20] The application of such strategies would result in liposomes that could constitute crucial tools to improve the therapeutic efficiency of many drugs. The pH-sensitive liposomes are particularly suitable for delivery of highly hydrophilic molecules or macromolecules to the cytoplasm. The inclusion of lipids with fusogenic properties results in the formation of the so-called “fusogenic” or polymorphic liposomes, since these undergo a phase transition under acidic conditions, in either the absence or the presence of biological membranes.[21]

The pH-sensitive liposomes are able to interact and promote fusion or destabilization of target membranes (either plasma membrane or endosomal

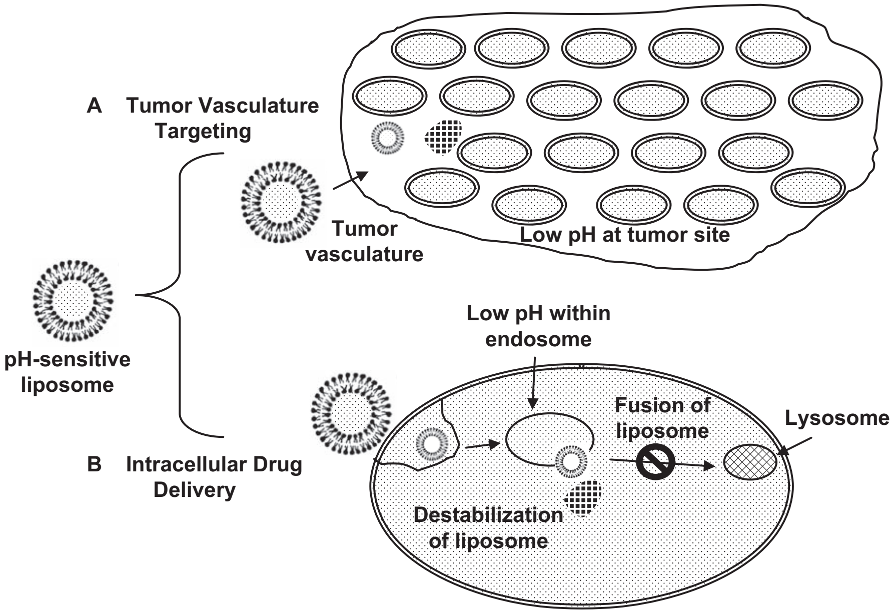
A Tumor Vasculature Targeting
Tumor vasculature
Low pH at tumor site
pH-sensitive liposome
Low pH within endosome
Fusion of liposome
Lysosome
B Intracellular Drug Delivery
Destabilization of liposome

Figure 3.2 Targeted drug delivery using pH-sensitive liposomes: localized release of the anticancer drug in the tumor tissue (A) and mechanism involved in the intra-cellular delivery (B).

membrane) and have been described to release efficiently the encapsulated material into the cytoplasm. The pH-sensitive liposomes are stable at physiological pH (pH 7.4) but undergo destabilization and acquire fusogenic properties under acidic conditions, thus leading to the release of their aqueous contents. The concept of pH-sensitive liposomes emerged from the fact that certain enveloped viruses developed strategies to take advantage of the acidification of the endosomal lumen to infect cells, as well as from the observation that some pathological tissues, *i.e.* tumors, inflamed and infected areas, exhibit an acidic environment as compared to normal tissues. Figure 3.3 represents the biofate of conventional liposomes *versus* pH-sensitive liposomes in a cell.

pH-sensitive liposomes can be grouped in different classes according to the mechanism responsible for triggering the pH-sensitivity. The most commonly recognized concept involves the combination of phosphatidylethanolamine (PE) or its derivatives with compounds containing an acidic group (*e.g.* carboxylic acid group) that act as a stabilizer at neutral pH. More recently, the use of novel pH-sensitive lipids and synthetic fusogenic peptides/proteins, either encapsulated or incorporated in the lipid bilayer, and the association of pH-sensitive polymers with liposomes have been reported. Further, antibodies or ligands for cell surface receptors can be coupled to pH-sensitive or sterically stabilized pH-sensitive liposomes for active targeting. The pH-sensitive liposomes have been used to deliver anticancer drugs, antibiotics, antisense

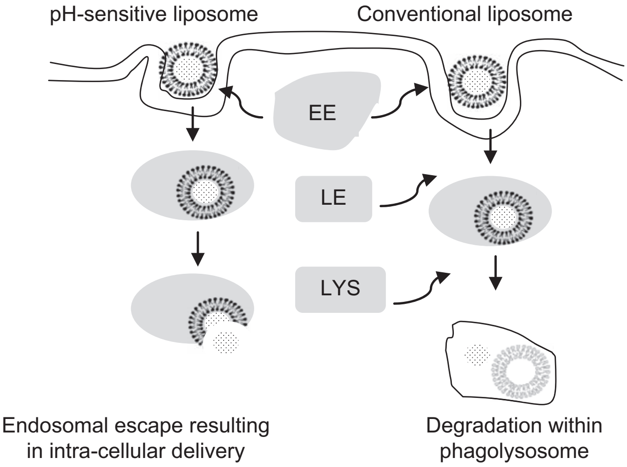
pH-sensitive liposome
Conventional liposome
EE
LE
LYS
Endosomal escape resulting in intra-cellular delivery
Degradation within phagolysosome

Figure 3.3 Biofate of conventional and pH-sensitive liposomes after uptake by a cell. EE: early endosome; LE: late endosome; Lys: lysosome.

oligonucleotides, ribozymes, plasmids, proteins and peptides to cells in culture or *in vivo*.[20–22] Some recent reports are summarized in Table 3.1.

pH-sensitive liposomes offer interesting possibilities for "smart" delivery of antisense oligonucleotides, which are able to inhibit gene expression being, therefore, potentially active for the treatment of viral infections, cancer or inflammatory diseases.[23] However, the poor stability of antisense oligonucleotides in biological medium and their weak intra-cellular penetration make their formulation difficult and it requires the use of "smart" delivery systems, such as anionic pH-sensitive liposomes. These liposome formulations contain a specific phospholipid, phosphatidylethanolamine (PE), which undergoes a transition from lamellar to inverted micellar structures at low pH and allows fusion of liposomal and endosomal membranes. This leads to the destabilization of the endosomes. Therefore, liposomes made of PE are able to release their contents in response to acidic pH within the endosomal system, thus improving the cytoplasmic delivery of oligonucleotides after endocytosis.[23]

It should be noted that the repeated use of stealth liposomes may reduce the accumulation of drug in the tumor site due to the accelerated blood clearance (ABC) phenomenon. The ABC behavior is described as a syndrome of accelerated clearance of polyethylene glycol (PEG)-modified liposomes from the bloodstream when repeatedly injected, accompanied by increased accumulation in the liver and spleen. The reason for this ABC phenomenon is that the first dose of PEGylated liposomes already induces the production of anti-PEG IgM, which can bind to the surface of subsequently injected PEGylated liposomes, leading to substantial complement activation.[24] Chen *et al.*[25] evaluated a novel modified pH-sensitive liposome with a cleavable double smart PEG-lipid derivative (mPEG-Hz-CHEMS) to clarify the mechanism. They observed an intense ABC phenomenon in mice after repeated injection of conventional

Table 3.1 Some recently published reports on pH-sensitive liposomes.

Drug	*Carrier*	*Test*	*Model*	*Concluding remarks*	*Ref.*
Doxorubicin	pH-sensitive immunoliposome	Intra-cellular drug delivery	Cell lines	A multi-functional immunoliposomal nanocarrier containing a pH-sensitive PEG-PE component, TATp, and the cancer cell-specific mAb 2C5 enhances cytotoxicity and carrier internalization by cancer cells. The potential for intra-cellular drug delivery after exposure to lowered pH environment, typical of solid tumors, was highlighted.	30
Doxorubicin	Estrogen-anchored pH-sensitive liposomes	Intra-cellular drug delivery	Mice	The ES-pH-sensitive-SL efficiently suppressed the breast tumor growth in comparison to both ES-SL and free drug. Serum levels of LDH and CPK were assayed for the evaluation of doxorubicin induced cardiotoxicity.	31
Radioactive substance	PEG-folate-coated pH-sensitive liposomes	Antitumor activity and toxicity	Mice	Animals treated with radioactive formulations showed lower increase in tumor volume and significantly higher percentage of necrosis compared with controls.	32
DNA	pH-sensitive liposomes	Transfection	Mice	*In vitro* and *in vivo* transfection studies confirmed that o-carboxymethyl-chitosan-cationic liposome-coated DNA/protamine/DNA complexes (CLDPD) had pH-sensitivity and the outermost layer of CMCS fell off in the tumor tissue, which could not only protect CMCS-CLDPD from serum interaction but also enhance gene transfection.	41
Therapeutic peptide	pH-sensitive stealth liposomes	Nuclear delivery	Cell lines	Stealth pH-sensitive liposomes delivered hydrophilic materials to the cytoplasm. The peptide encapsulated in pH-sensitive stealth liposomes reached the nucleus of tumorigenic and non-tumorigenic breast cancer cells.	46
Cisplatin	pH-sensitive liposomes	Toxicity	Mice	Stealth pH-sensitive-CDDP significantly reduced the renal toxicity.	50

PEG-PE liposomes. By contrast, no ABC phenomenon was observed for mPEG-Hz-CHEMS liposomes, which suggests that the cleavable PEG shell lessens or eliminates the immune response against the liposome.[25]

3.3 Uptake and Intra-cellular Delivery of Therapeutic Agents from pH-sensitive Liposomes

The pH-sensitive liposomes are internalized more efficiently than non-pH-sensitive ones. This has been attributed to the tendency of PE-containing liposomes to form aggregates, due to the poor hydration of its head-group, which can explain their high affinity to adhere to cell membranes. PE presents a minimally hydrated and small head-group, which occupies a lower volume compared to the respective hydrocarbon chains, exhibiting a cone shape (as opposed to the cylinder shape of bilayer stabilizing phospholipids), thus hampering the formation of a lamellar phase. The cone shape of PE molecules favors the establishment of strong intermolecular interactions between the amine and phosphate moieties of the polar head-groups, justifying the strong tendency of these molecules to acquire the inverted hexagonal phase above the phase transition temperature. While at physiological pH stable liposomes are formed, acidification triggers protonation of the carboxylic acid groups of the amphiphiles, reducing their stabilizing effect and thus leading to liposomal destabilization, since under these conditions PE molecules revert into their inverted hexagonal phase. The choice of the amphiphilic stabilizers, as well as its molar percentage with respect to the PE content, are imposed by the desired properties of the liposomes, including the extent of cellular internalization, the fusogenic ability, the pH-sensitivity and the stability in biological fluids. Such properties determine the liposome efficacy to mediate cytoplasmic delivery of the encapsulated molecules. Reviews on pH-sensitive liposome formulation technology can be found elsewhere.[2,21–23,26–28]

The steps involved in the internalization and intra-cellular delivery mediated by ligand (*e.g.* estrogen) anchored pH-sensitive liposomes are depicted in Figure 3.4. After binding to cells, the ligand-anchored liposomes are internalized through the endocytotic pathway. Liposomes are retained in early endosomes, which mature into late endosomes. The potential of pH-sensitive liposomes lies in their ability to undergo destabilization at this stage, thus preventing their degradation at the lysosomal level, and consequently increasing the access of the drug to the cytosolic or nuclear targets. Three mechanisms have been proposed: i) destabilization of pH-sensitive liposomes triggers the destabilization of the endosomal membrane, most likely through pore formation, that leads to cytoplasmic delivery of their contents; ii) upon liposome destabilization, the encapsulated molecules diffuse through the endosomal membrane to the cytoplasm; and iii) fusion between the liposome and the endosomal membranes, leading to cytoplasmic delivery of their contents. The fusogenic properties of PE and its tendency to form an inverted hexagonal phase under certain conditions suggest that hypotheses i) and iii) are

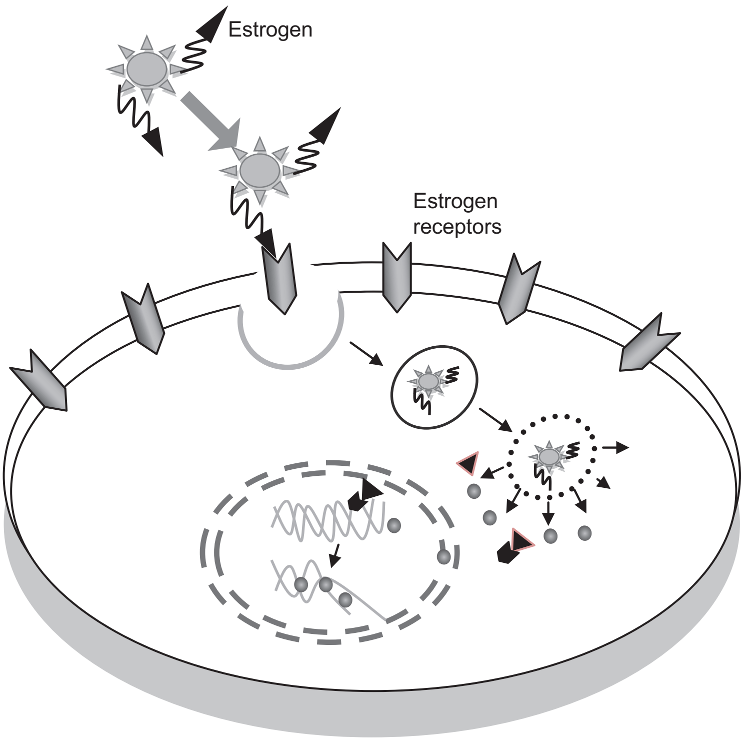

Figure 3.4 Estrogen-anchored pH-sensitive liposomes as nanomodule designed for site-specific delivery of doxorubicin in breast cancer therapy.

the most plausible.[27,28] Independently of the involved mechanisms, the efficacy of cytoplasmic delivery mediated by pH-sensitive liposomes is drastically reduced upon increase of the molecular weight of the encapsulated molecules. Studies performed with high molecular weight proteins (*e.g.* DTA and BSA) indicated that only 0.01–10% of the molecules are released into the cytoplasm, in contrast to nearly 100% release observed with the low molecular weight fluorescent probe calcein.[27,28]

3.4 Therapeutic Applications of pH-sensitive Liposomes

3.4.1 Cancer Chemotherapy

The pH-sensitive liposomes have been tested for numerous applications in drug delivery.[27,29] Engineered liposomes capable of spontaneous accumulation in tumors and ischemic areas *via* EPR effect and further penetration and drug delivery inside tumor or ischemic cells *via* the action of cell-penetrating peptides (CPP) have been reported. These liposomes were simultaneously bearing on their surface CPP (TAT peptide, TATp) moieties and protective PEG chains.

After accumulation in the target site, the PEGylated liposomes lose the PEG coating due to the lowered pH-induced hydrolysis, and penetrate inside cells *via* the now-exposed TATp moieties. These liposomes rendered promising results for chemotherapy in cell cultures as well as in ischemic cardiac tissues using the Langendorff perfused rat heart model and in mice bearing tumors.[30]

Koren *et al.*[31] prepared pH-sensitive PEGylated long-circulating liposomes modified with TATp moieties and cancer-specific monoclonal antibodies (mAb). PE was PEGylated using a degradable pH-sensitive hydrazone bond between PE and long shielding PEG chains (PEG(2k)-Hz-PE). TATp was conjugated to a short PEG_{1000}-PE spacer and mAb to a long PEG chain (PEG_{3400}-PE). At pH 7.4, surface TATp moieties are "hidden" by the long PEG chains. Upon exposure to lower pH, the hydrazone bond is broken, the long PEG chains are removed and the TATp moieties become exposed. Enhanced cellular uptake of the TATp-containing immunoliposomes was observed *in vitro* after pre-treatment at lower pH. The presence of mAb 2C5 on the liposome surface further enhanced the interaction between the carrier and tumor cells but not normal cells. Furthermore, this multi-functional immuno-Doxil® preparation showed increased cellular cytotoxicity of B16-F10, HeLa and MCF-7 cells when pre-incubated at lower pH, indicating TATp exposure and activity. This multi-functional immunoliposomal nanocarrier is claimed for intra-cellular drug delivery after exposure to the lowered pH environment typical of solid tumors.[31] More recently, nanoengineered estrogen receptor (ER) targeted pH-sensitive liposomes for the site-specific intra-cellular delivery of doxorubicin have been developed for breast cancer therapy. Estrone, a bioligand, was anchored on the surface of pH-sensitive liposomes (ES-pH-sensitive-SL) for drug targeting to ERs overexpressed by breast cancer cells. The ES-pH-sensitive-SL showed fusogenic potential at acidic pH (5.5) and *in vitro* cytotoxicity studies (MCF-7 cells) proved this formulation to be more cytotoxic than non-pH-sensitive targeted liposomes. Intra-cellular delivery and nuclear localization of doxorubicin was confirmed by fluorescence microscopy. Further, *in vivo* biodistribution and antitumor activity of the formulations were evaluated on tumor-bearing female Balb/c mice after intravenous administration. The ES-pH-sensitive-SL suppressed the breast tumor growth more efficiently than non-pH-sensitive targeted liposomes and free doxorubicin. The ES-pH-sensitive-SL increased the therapeutic efficacy, being promising nanocarriers for the targeted intra-cellular delivery of anti-cancer agents to breast tumors with reduced systemic side effects.[32]

PEG-coated pH-sensitive and PEG-folate-coated pH-sensitive liposomes containing (159)Gd-DTPA-BMA and radiolabeled through neutron activation technique were developed for *in vivo* tests of antitumoral activity and toxicity on mice bearing solid Ehrlich tumor. The results showed that after 31 days of treatment, animals treated with radioactive formulations had a lower increase in tumor volume and a significantly higher percentage of necrosis. Furthermore, mice treated with radioactive formulations exhibited lower weight gain without significant hematological or biochemical changes, except for toxicity to hepatocytes.[33]

Cisplatin is one of the most active cytotoxic agents and is widely applied *via* intra-peritoneal route in the treatment of peritoneal carcinomatosis. However, cisplatin, a low-molecular-weight compound, is rapidly absorbed by the capillaries in the intra-peritoneal serosa and transferred to the bloodstream, inducing the appearance of systemic side effects, such as nephrotoxicity. Furthermore, the intra-peritoneal cisplatin chemotherapy is limited to patients whose residual tumor nodules are less than 0.5 cm in diameter after surgical debulking. A tissue distribution study in solid Ehrlich tumor-bearing mice revealed that, after administering a 6 mg/kg single intravenous bolus injection of either free radiolabeled cisplatin or stealth pH-sensitive liposomes containing radiolabeled cisplatin, the area under the plasma concentration-time curve (AUC) for stealth pH-sensitive liposomes was 2.1-fold larger than that obtained for free cisplatin.[34] Similar improved biodistribution and targeted delivery of cisplatin to tumor-bearing mice was observed in another study.[35] Long-circulating and pH-sensitive liposomes containing cisplatin successfully avoid severe side effects as well as drug resistance. However, physical (*i.e.* aggregation/fusion) and chemical instability during storage may limit the use of these drug carriers as medicines. Freeze-drying may be a success strategy to improve the stability before use.[36] Immunoliposomes directed by monoclonal antibodies may efficiently target the drug to tumor tissues.[37] Long-circulating pH-sensitive liposomes with epidermal growth factor receptor (EGFR) antibody tested on A549 cells and Balb/c-nu/nu mouse tumor model demonstrated efficient and targeted delivery of gemcitabine for tumors that overexpress the EGFR.[38] Drug targeting is expected to be optimized in the near future as further knowledge about internalization pathways becomes available.[39]

3.4.2 Gene Delivery

The number of biotechnological products such as nucleic acids, proteins and peptides that enter in the therapeutic arsenal is notably increasing. However their *in vivo* efficacy can be severely comprised by the unfavorable physicochemical characteristics. The major obstacle for cell penetration is the large size and hydrophilic nature of the biotechnological molecules, which demand the use of a carrier able to overcome cellular barriers and facilitate cytosolic delivery.[40] Therefore, many different drug-delivery systems including liposomes have been investigated for this purpose. Liposomes are able to provide protection and targeting of the encapsulated macromolecule and may promote cellular internalization.[39–41]

Gene therapy requires the development of multi-functional vectors that could overcome the barrier effects of the membranes of the cell, endosome and nucleus. A pH-sensitive multi-functional gene vector has been developed to attain long circulation without using PEG but showing tumor cellular uptake of the gene carrier.[42] DNA was firstly condensed with protamine into a cationic core that was used as assembly template. Then, additional layers of anionic DNA, cationic liposomes and o-carboxymethyl-chitosan (CMCS) were alternately adsorbed onto the template *via* a layer-by-layer technique, to render CMCS-cationic liposome-coated DNA/protamine/DNA complexes (CLDPD). *In vitro* test with isolated tumor (HepG2) cells and *in vivo* evaluation into tumor-bearing mice confirmed the transfection efficiency. Other reports also confirmed the relevance of the fusogenic properties of the pH-sensitive liposomal membranes for intra-cellular gene transfection.[43–45]

The pH-sensitive stealth liposomes have been reported as suitable vectors for targeting therapeutic peptides to the nucleous.[46] Cellular uptake of peptide-loaded liposomes has been investigated in Hs578t human epithelial cells from breast carcinoma, MDA-MB-231 human breast carcinoma cells and WI-26 human diploid lung fibroblast cells. Two different formulations were tested: long circulating classical liposomes [soybean phosphatidylcholine : CHOL : PEG-750-DSPE (47 : 47 : 6 molar% ratio)] and pH-sensitive stealth liposomes [DOPE : CHEMS : CHOL : PEG750-DSPE (43 : 21 : 30 : 6 molar% ratio)]. The difference between both formulations in terms of peptide delivery from the endosome to the cytoplasm and even to the nucleus was observed as a function of time. Using pH-sensitive stealth liposomes, the peptide was able to reach the nucleus of tumorigenic and non-tumorigenic breast cancer cells.[46] In summary, the available information demonstrates the utility of pH-sensitive liposomes as intra-cellular carrier for bioactives.

3.4.3 Tumor Diagnosis

Liposomes are excellent candidates for the development of theranostic agents and multi-modal imaging probes, since they can release the entrapped imaging probe/radioactive agent/drug in response to a change of physico-chemical variables like pH, redox potential or concentration of specific enzymes that usually occur in the early asymptomatic stage of several diseases such as cancer.[47] The pH-sensitive liposomes trapping ^{99m}Tc have been used for biodistribution studies and scintigraphic imaging in Ehrlich tumor-bearing mice. They accumulate in tumor tissue with high tumor-to-muscle ratio and can be useful for diagnosis of tumors.[48]

Paramagnetic pH-sensitive liposomes have also been developed as imaging tools for visualizing drug-delivery and release processes by means of Magnetic Resonance Imaging (MRI). The proposed formulation allowed the fast and full release of gadoteridol at pH 5.5. The leakage of the imaging reporter from the vesicles was associated with a relaxivity enhancement that allowed its visualization by MRI. It was observed that the release mechanism implies the protonation of the basic sites that leads to vesicle aggregation, thus enabling the expression of the fusogenic property.[49]

3.5 Conclusion

The literature is full of reports on using pH-sensitive liposomes in all areas of drug delivery and more recently also for imaging. The unique characteristics of these “smart” carriers make them an attractive choice for formulation scientists in nanomedicine and nanobiotechnology dealing with tumor and cardiovascular diseases. Particularly, the pH-sensitive liposomes enable efficient intracellular delivery of drugs and genes. Furthermore, most components used for their design have been proved to be safe, which may pave the way for the approval and commercialization of pH-sensitive liposomes.

References

1. S. R. Paliwal, R. Paliwal, G. P. Agrawal and S. P. Vyas, *Nanomedicine UK*, 2011, **6**, 1085.
2. M. S. Hong, S. J. Lim, Y. K. Oh and C. K. Kim, *J. Pharm. Pharmacol.*, 2002, **54**, 51.
3. O. V. Gerasimov, J. A. Boomer, M. M. Qualls and D. H. Thompson, *Adv. Drug. Deliver. Rev.*, 1999, **38**, 317.
4. E. Roux, C. Passirani, S. Scheffold, J. P. Benoit and J. C. Leroux, *J. Control. Release*, 2004, **94**, 447.
5. K. Kono, K. Zenitani and T. Takagishi, *Biochim. Biophys. Acta*, 1994, **1193**, 1.
6. K. Kono, T. Igawa and T. Takagishi, *Biochim. Biophys. Acta*, 1997, **1325**, 143.
7. K. Kono, M. Iwamoto, R. Nishikawa, H. Yanagie and T. Takagishi, *J. Control. Release*, 2000, **68**, 225.
8. K. Hiraka, M. Kanehisa, M. Tamai, S. Asayama, S. Nagaoka, K. Oyaizu, M. Yuasa and H. Kawakami, *Colloid Surface B*, 2008, **67**, 54.
9. M. Z. Lai, W. J. Vail and F. C. Szoka, *Biochemistry-US*, 1985, **24**, 1654.
10. M. S. Webb, J. J. Wheeler, M. B. Bally and L. D. Mayer, *Biochim. Biophys. Acta*, 1995, **1238**, 147.
11. R. Nayar and A. J. Schroit, *Biochemistry-US*, 1985, **24**, 5967.
12. P. Lutwyche, C. Cordeiro, D. J. Wiseman, M. St-Louis, M. Uh, M. J. Hope, M. S. Webb and B. B. Finlay, *Antimicrob. Agents Chemother.*, 1998, **42**, 2511.
13. D. Momekova, S. Rangelov and N. Lambov, *Methods Mol. Biol.*, 2010, **605**, 527.
14. B. Yu, H. C. Tai, W. Xue, J. J. Lee and R. J. Lee, *Mol. Membr. Biol.*, 2010, **27**, 286.
15. M. B. Yatvin, W. Kreutz, B. Horwitz and M. Shinitzky, *Biophys. Struct. Mech.*, 1980, **6**, 233.
16. R. M. Sawant, J. P. Hurley, S. Salmaso, A. Kale, E. Tolcheva, T. S. Levchenko and V. P. Torchilin, *Bioconjug. Chem.*, 2006, **17**, 943.
17. N. Bertrand, P. Simard and J. C. Leroux, *Methods. Mol. Biol.*, 2010, **605**, 545.
18. P. Simard and J. C. Leroux, *Mol. Pharm.*, 2010, **7**, 1098.
19. P. Simard and J. C. Leroux, *Int. J. Pharm.*, 2009, **381**, 86.
20. S. Simoes, J. N. Moreira, C. Fonseca, N. Duzgunes and M. C. de Lima, *Adv. Drug. Deliver. Rev.*, 2004, **56**, 947.
21. S. Simoes, V. Slepushkin, N. Düzgünes and M. C. Pedroso de Lima, *Biochim. Biophys. Acta*, 2001, **1515**, 23.

22. V. A. Slepushkin, S. Simoes, P. Dazin, M. S. Newman, L. S. Guo, M. C. Pedroso de Lima and N. Duzgunes, *J. Biol. Chem.*, 1997, **272**, 2382.
23. E. Fattal, P. Couvreur and C. Dubernet, *Adv. Drug Deliver. Rev.*, 2004, **56**, 931.
24. T. Ishida and H. Kiwada, *Int. J. Pharm.*, 2008, **354**, 56.
25. D. Chen, W. Liu, Y. Shen, H. Mu, Y. Zhang, R. Liang, A. Wang, K. Sun and F. Fu, *Int. J. Nanomed.*, **2011**, 2053.
26. P. Venugopalan, S. Jain, S. Sankar, P. Singh, A. Rawat and S. P. Vyas, *Pharmazie*, 2002, **57**, 659.
27. Z. Vanic, S. Barnert, R. Suss and R. Schubert, *J. Liposome Res.*, 2012, in press.
28. H. Karanth and R. S. Murthy, *J. Pharm. Pharmacol.*, 2007, **59**, 469.
29. D. C. Drummond, M. Zignani and J. Leroux, *Prog. Lipid Res.*, 2000, **39**, 409.
30. A. Kale and V. P. Torchilin, *J. Liposome Res.*, 2007, **17**, 197.
31. E. Koren, A. Apte, A. Jani and V. P. Torchilin, *J. Control. Release*, 2012, **160**, 264.
32. S. R. Paliwal, R. Paliwal, H. C. Pal, A. K. Saxena, P. R. Sharma, P. N. Gupta, G. P. Agrawal and S. P. Vyas, *Mol. Pharm.*, 2012, **9**, 176.
33. D. C. Soares, V. N. Cardoso, A. L. de Barros, C. M. de Souza, G. D. Cassali, M. C. de Oliveira and G. A. Ramaldes, *Eur. J. Pharm. Sci.*, 2012, **45**, 58.
34. A. D. Junior, L. G. Mota, E. A. Nunan, A. J. Wainstein, A. P. Wainstein, A. S. Leal, V. N. Cardoso and M. C. De Oliveira, *Life Sci.*, 2007, **80**, 659.
35. J. G. Araujo, L. G. Mota, E. A. Leite, L. C. Maroni, A. J. Wainstein, L. G. Coelho, P. R. Savassi-Rocha, M. T. Pereira, A. Teixeira de Carvalho, V. N. Cardoso and M. C. de Oliveira, *Exp. Biol. Med.*, 2011, **236**, 808.
36. G. C. dos Santos, E. C. de Oliveira Reis, T. G. Ribeiro Rocha, E. A. Leite, R. G. Lacerda, G. A. Ramaldes and M. C. de Oliveira, *J. Liposome Res.*, 2011, **21**, 60.
37. M. J. Kim, H. J. Lee, I. A. Lee, I. Y. Kim, S. K. Lim, H. A. Cho and J. S. Kim, *Arch. Pharm. Res.*, 2008, **31**, 539.
38. I. Y. Kim, Y. S. Kang, D. S. Lee, H. J. Park, E. K. Choi, Y. K. Oh, H. J. Son and J. S. Kim, *J. Control. Release*, 2009, **140**, 55.
39. L. Di Marzio, C. Marianecci, B. Cinque, M. Nazzarri, A. M. Cimini, L. Cristiano, M. G. Cifone, F. Alhaique and M. Carafa, *BBA-Biomembranes*, 2008, **1778**, 2749.
40. L. Leserman, P. Machy, J. P. Leonetti, P. G. Milhaud, G. Degols and B. Lebleu, *Prog. Clin. Biol. Res.*, 1990, **343**, 95.
41. M. C. Pedroso de Lima, S. Simoes, P. Pires, H. Faneca and N. Duzgunes, *Adv. Drug Deliver. Rev.*, 2001, **47**, 277.
42. P. Li, D. Liu, L. Miao, C. Liu, X. Sun, Y. Liu and N. Zhang, *Int. J. Nanomed.*, 2012, **7**, 925.
43. N. Sakaguchi, C. Kojima, A. Harada, K. Koiwai, N. Emi and K. Kono, *Bioconjug. Chem.*, 2008, **19**, 1588.

44. N. Sakaguchi, C. Kojima, A. Harada, K. Koiwai and K. Kono, *Biomaterials*, 2008, **29**, 4029.
45. N. Sakaguchi, C. Kojima, A. Harada and K. Kono, *Bioconjug. Chem.*, 2008, **19**, 1040.
46. E. Ducat, J. Deprez, A. Gillet, A. Noel, B. Evrard, O. Peulen and G. Piel, *Int. J. Pharm.*, 2011, **420**, 319.
47. L. Andresen, S. S. Jensen and K. Jorgensen, *Prog. Lipid Res.*, 2005, **44**, 68.
48. A. L. de Barros, L. G. Mota, D. C. Soares, M. M. Coelho, M. C. Oliveira and V. N. Cardoso, *Bioorg. Med. Chem. Lett.*, 2011, **21**, 7373.
49. E. Torres, F. Mainini, R. Napolitano, F. Fedeli, R. Cavalli, S. Aime and E. Terreno, *J. Control. Release*, 2011, **154**, 196.
50. E. A. Leite, C. dos Santos Giuberti, A. J. Wainstein, A. P. Wainstein, L. G. Coelho, A. M. Lana, P. R. Savassi-Rocha and M. C. De Oliveira, *Life Sci.*, 2009, **84**, 641.

CHAPTER 4

Smart Dendrimers

CHIE KOJIMA

Nanoscience and Nanotechnology Research Center, Research Organization for the 21st Century, Osaka Prefecture University, Osaka, Japan
Email: c-kojima@21c.osakafu-u.ac.jp

4.1 Introduction

Drug-delivery systems (DDSs) are useful for reducing drug side effects and maximizing drug action. Adequate design of the drug carriers is one critical aspect for successful DDSs. A number of different nanostructures such as liposomes, micelles and polymer particles have been adopted as drug carriers.[1–12] Liposomes and micelles are obtained by self-assembly of their components. In general, large polymers with sizes similar to proteins are more stable than self-assembled nanostructures, but the polymers have a broad molecular weight range and their conformation is barely controllable. Dendrimers are an exception to this rule, since these synthetic macromolecules possess uniform highly branched structures. The differences between common polymers and dendrimers arise from their synthetic pathways: polymers are prepared by polymerization of monomers, while dendrimers are obtained by stepwise synthesis.[13] Figure 4.1 shows the synthetic pathway for a typical and well-studied dendrimer, polyamidoamine (PAMAM) dendrimer, developed by Tomalia *et al.*[14] PAMAM dendrimer is synthesized by repeating Michael addition of the core compound and subsequent amidation. Therefore, the molecular weight is defined and can be controlled by the number of times that the reaction is repeated, namely by the number of *generations*. Even though the monomeric units of most synthetic polymers are tandemly linked, the building units of dendrimers have a branched structure. Therefore, dendrimers have a

RSC Smart Materials No. 2
Smart Materials for Drug Delivery: Volume 1
Edited by Carmen Alvarez-Lorenzo and Angel Concheiro
© The Royal Society of Chemistry 2013
Published by the Royal Society of Chemistry, www.rsc.org

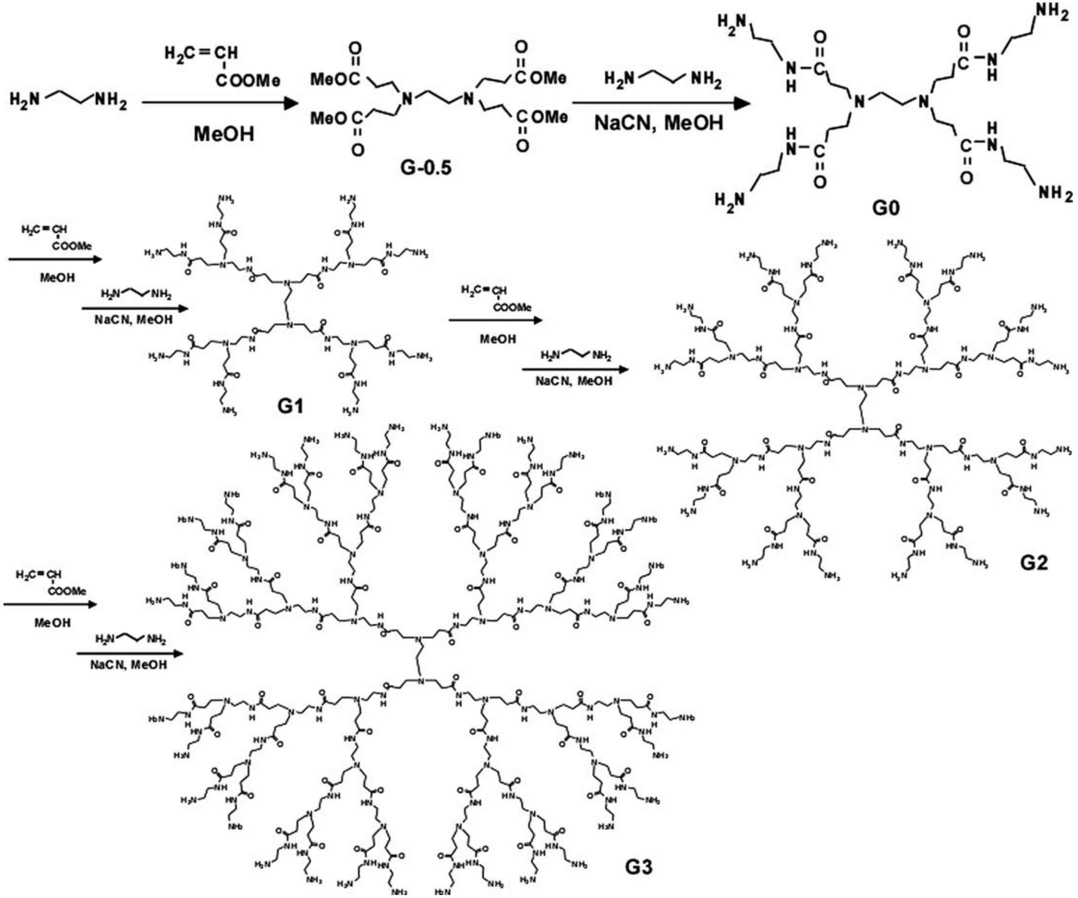
$H_2C=CH$
COOMe
MeOH
G-0.5
H_2N NH_2
NaCN, MeOH
G0
G1
G2
G3

Figure 4.1 Synthetic pathway of a polyamidoamine (PAMAM) dendrimer.

spherical structure and their properties can be controlled by choosing a suitable core, building blocks and/or terminal groups.[13–15]

Dendrimers have been studied as a new type of drug carrier that can be loaded with drug molecules by encapsulation and/or conjugation.[16–25] A number of drug molecules, such as doxorubicin (Dox) or adriamycin (ADR), methotrexate (MTX), 5-fluorouracil (5-FU) and paclitaxel (taxol), can be solubilized and encapsulated by dendrimers *via* hydrophobic interactions, electrostatic interactions and/or hydrogen bonds.[16–25] Some drugs can be conjugated to the terminal group of the dendrimer. Such encapsulation and conjugation properties enable the loading of efficient amounts of drug in the dendritic nanoparticles for DDS applications.[16–25] The controllable and uniform molecular weight, size and chemical composition of dendrimers contribute to the optimization of their properties as drug carriers, and to their chemical and biological reproducibility. Size-controlled nanoparticles can be targeted to tumor tissues taking benefit of the enhanced permeability and retention (EPR) effect, which derives from the permeable blood vessel endothelium and the lack of lymphatics in tumor tissues.[26,27] Therefore, dendritic nanoparticles can accumulate in tissues affected by EPR.[12,16–25] Taken together, dendrimers are suitable as drug carriers because of their drug loading capability, reproducible synthesis and potential to be passively targeted to cancer tissues.

This chapter focuses on the application of dendritic polymers for drug delivery, particularly as components of stimuli-responsive DDSs. There are two categories of stimuli: external and self-regulated internal body stimuli.[17] Temperature and light are already clinically used as external stimuli. Differences in pH and redox-state between various tissues and/or subcellular compartments can occur physiologically or pathologically, and can be used as self-regulated internal body stimuli. To design stimuli-sensitive dendritic polymers, tunable moieties can be incorporated at the terminal groups and/or the core. The dendrimer backbone and the encapsulated molecules can also act as stimuli sensors. In this chapter, various types of stimuli-responsive dendrimers, such as temperature-responsive, photoresponsive, pH-responsive, redox-responsive and enzymatic activity-responsive dendrimers, are described. Since some excellent reviews on dendrimer-based gene delivery have been published,[12,16,22,28] this chapter is focused on drug-delivery systems in *stricto sensu* using stimuli-responsive dendrimers.

4.2 Temperature-responsive Dendrimers

Hyperthermia therapy (thermotherapy) involves the killing of cancer cells by exposure to high temperatures. This therapy is performed using clinically approved radio frequency ablation as a local heating system.[29] Temperature-responsive DDSs can be applied in conjunction with thermotherapy. Temperature-sensitive polymers, of which poly(*N*-isopropylacrylamide) (PNIPAAm) is a representative, exhibit a phase transition at which their solubility drastically decreases. The "cloud point" or lower critical solution temperature (LCST) of PNIPAAm is 32 °C.[1–6] The cloud point is heavily influenced by the balance between the hydrophobicity and hydrophilicity of the polymer and hence it can be tuned by its chemical composition.

4.2.1 Dendrimers Containing Thermo-sensitive Polymers

Temperature-sensitive polymers can be attached to the core or the terminal groups of dendrimers (Figure 4.2A and 4.2B). Kimura *et al.*[30] reported the first temperature-responsive dendrimer, which was prepared by polymerization of NIPAAm from the termini of a polypropyleneimine (PPI) dendrimer with terminal thiol groups (Figure 4.2A). The core of the dendrimer was a cobalt complex, which catalyzed the temperature-dependent oxidation of the thiol compounds.[30] The PNIPAAm-based copolymers, PNIPAAm-b-poly(dimethylaminoethyl methacrylate) and polycaprolactone-b-PNIPAAm, were also conjugated to the dendrimer termini.[31,32] It was reported that the latter dendrimer acted as a temperature-dependent nanocapsule of daidzein, a traditional Chinese medicine. In this dendrimer, polymer layers of polycaprolactone and PNIPAAm acted as drug reservoir and temperature sensor, respectively.[32] For *in vivo* application, modification of polyethylene glycol (PEG) is indispensable. Zhao *et al.*[33] recently reported that both PNIPAAm and PEG-conjugated dendrimers could release indomethacin in a temperature-dependent manner.

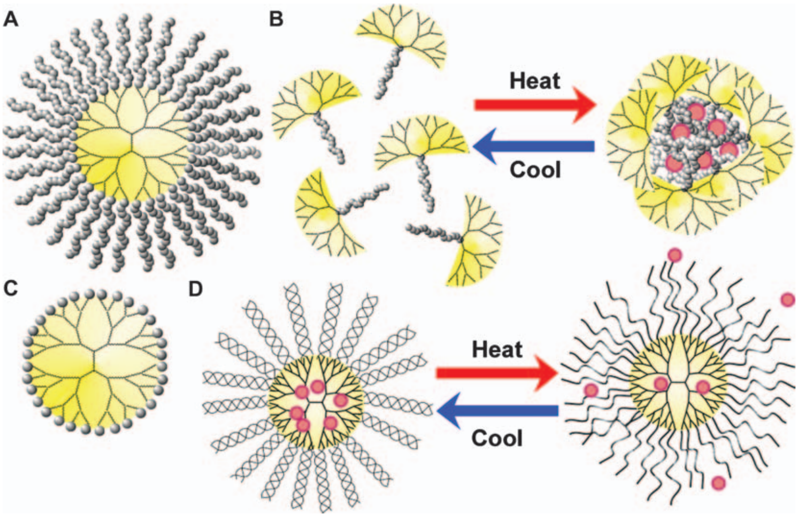

Figure 4.2 Design of temperature-sensitive dendritic polymers. (A) Dendrimer with temperature-sensitive polymers attached at the surface, (B) dendritic polymer assembly with a temperature-sensitive polymer and (C) dendrimer modified with a temperature-sensitive moiety. Grey single balls and linked balls indicate temperature-sensitive moieties and temperature-sensitive polymers, respectively. (D) Temperature dependency of collagen-mimic dendrimer.

Temperature-sensitive polymers can also be attached to the dendrimer core (Figure 4.2B). NIPAAm was polymerized from the core of polyol dendrons, to produce a temperature-dependent dendritic polymer. These polymers underwent self-assembly as a function of temperature.[34,35] Stover *et al.*[36] reported the controlled release of ceramide, a pro-apoptotic drug, using a dendritic polymer composed of poly(L-lactide)-co-NIPAAm and a poly L-lysine dendrimer. The core block polymer associated with ceramide in a temperature-dependent manner. In addition, cellular uptake of the dendritic polymer was sensitive to temperature. The drug action induced by this nanoparticle was of a similar magnitude to that induced by the free drug or the liposomal drug formulation at 37 °C.[36]

4.2.2 Dendrimers Containing Thermo-sensitive Moieties

Incorporation of temperature-sensitive components to dendritic polymers may impart temperature-responsiveness to the dendrimer. Kono's group reported that temperature-sensitive dendrimers could be prepared by modification with only one temperature-sensitive unit at the surface (Figure 4.2C).[37–39] They first reported the temperature-sensitivity of PAMAM and PPI dendrimers after modification with isobutyric acid to provide the isobutylamide (IBAM) group on the dendrimer surface, which is mimetic to the temperature-dependent poly(*N*-vinylisobutyramide).[37] The temperature-sensitivity was largely dependent on the generation number or the molecular weight, different from thermo-sensitive linear polymers. In addition, these dendrimers were also influenced by pH because of their inner tertiary amine.[37] Dendrimers with NIPAAm at the surface were also synthesized as dendritic analogs of PNIPAAm by reacting isopropylamine with succinylated PAMAM dendrimers.[38] Linear PNIPAAm has an endothermal peak near the cloud point, which contributes to dehydration of the polymer. In contrast, temperature-sensitive dendrimers have an extremely small endothermal peak. Therefore, these dendrimers are much different from the linear structured temperature-sensitive polymers.[38] PAMAM dendrimers were also modified with phenylalanine (Phe) instead of NIPAAm and IBAM.[39] This modification also induced thermo-sensitivity under physiological pH. Conversely, leucine and isoleucine were not able to communicate such responsiveness. Tuning of the phase transition temperature to values close to body temperature is crucial for the application of these dendrimers to DDSs. For example, the Phe/dendrimer ratio determines the cloud point.[39] One of the advantages of dendrimers is their ability to encapsulate small molecules. The guest molecule (*e.g.* rose bengal, RB) can also influence the temperature-sensitivity of the dendrimers.[40] We recently synthesized dendritic lipids with IBAM groups. They were assembled into vesicles and tubular micelles in aqueous solution, whose size and morphology were dependent on temperature.[41]

Asthmanikandan *et al.*[42] and Chang and Dai[43] reported oligo(ethylene glycol)-bound dendritic compounds that exhibited temperature-dependent phase transitions. These dendrimers bear hydrophobic and hydrophilic regions and form dendritic micelles, whose morphology changes as a function of temperature. Thayumanavan's group reported that Rhodamine 6G could be encapsulated by these dendritic micelles.[42] Li *et al.*[44] reported the temperature-responsiveness of oligo(ethylene glycol)-containing dendrimers, which is dependent on both the generation number and the terminal structure. The cloud point of the ethoxy-terminated dendrimers was lower than that of the methoxy-terminated ones, due to the greater hydrophobicity of the former. Differently from the decrease in cloud point observed for larger linear polymers, Li's dendrimers of higher molecular weight exhibited a higher cloud point.[44] Therefore, such dendrimers are unique temperature-sensitive polymers. Taken together, oligo(ethylene glycol)-bound dendritic polymers are another class of candidate materials for temperature-sensitive DDSs.

4.2.3 Collagen-mimic Dendrimers

Collagen is the most abundant protein in mammals and is composed of glycine-proline-(hydroxy)proline (Gly-Pro-Pro (Hyp)) repeats, which form a triple helix in a temperature-dependent manner.[45–47] The triple helical structure is formed at low temperature, but it dissociates above the melting point. Thermal denaturation of collagen at high temperature results in the formation of gelatin. The temperature-dependent behavior of collagen is different from that of temperature-sensitive synthetic polymers that have an LCST. In the collagen, the temperature-dependent behavior is induced by alteration of its higher order structure, while in the synthetic polymers it is due to dehydration. Therefore, collagen-related materials provide an alternative temperature-dependent material. Unfortunately, it is difficult for short collagen peptides to form a triple helix, which limits the development of artificial collagen materials. However, a covalent knot of collagen peptides can induce triple helix formation.[45] We reported a collagen model peptide $(\text{Pro-Pro-Gly})_5$-attached dendrimer, in which the peptides knotted at the surface of the dendrimer formed a collagen-like triple helix.[48] Interestingly, unlike in natural collagens, helix formation by this dendrimer was thermally reversible. The collagen-mimic dendrimer could encapsulate a model drug, RB, and release it faster at high temperature. This thermo-sensitivity was based on temperature-dependent helix formation and not on a phase transition. The formation of a collagen-like triple helix at lower temperature may improve the binding properties of RB to the dendrimer owing to enhanced hydrophobic interactions and/or suppressed permeability of RB at the surface (Figure 4.2D).[48] Because the temperature-dependency was insufficient for DDS applications, we also prepared different types of collagen-mimic dendrimers with $(\text{Pro-Hyp-Gly})_n$. Even though the temperature dependency of the release profiles from these dendrimers was much improved, further optimization is still required.[49] It was also reported that the $(\text{Pro-Pro-Gly})_{10}$ and $(\text{Pro-Hyp-Gly})_{10}$ collagen-mimic dendrimers form temperature-dependent hydrogels, which dissolve above 40 °C and below 25 °C, respectively.[50,51] These hydrogels are also useful as smart drug containers.

4.3 Photoresponsive Dendrimers

Photo-irradiation is another possible stimulus that can control drug release and induce cytotoxicity in target cells. Even though both temperature and light are external stimuli, light is easier to be spatiotemporally controlled than temperature. The disadvantage of light is its low depth of penetration. Light within the ultraviolet to visible range can only provide an effect at the surface, while near-infrared light tends to penetrate more deeply into the body. Therefore, the photo-irradiation wavelength is an important factor for DDS applications.

Photodynamic therapy (PDT) is a new clinical treatment for superficial tumors and age-related macular degeneration, which was approved in the 1990s. This technique involves the systemic administration of a photosensitive drug followed by light irradiation to the affected tissue. The photosensitive drug (photosensitizer) generates singlet oxygen following irradiation, and causes oxidative damage to cells. PDT affects only the irradiated areas, because singlet oxygen is short-lived, making this therapy a site-specific and non-invasive treatment.[16,19,20,52,53] Dendrimer nanoparticles encapsulating or conjugating photosensitizers have been reported by several groups.[53–59] Kataoka's group performed a sophisticated study in which they reported that dendritic polymer micelles composed of a photosensitizer-core dendrimer and PEG-block polymers exhibited an efficient PDT effect.[53,54,60] An excellent review on PDT has recently been published by Paszko *et al.*[61]

Photothermal therapy (PTT) is another type of treatment that involves the systemic administration of gold nanomaterials and light irradiation of the affected tissues, similar to PDT with photosensitizers. Gold nanomaterials in the form of nanoparticles, nanoshells and nanorods generate heat under light irradiation, causing damage to the cells.[16,19,62–64] Some biocompatible gold nanoparticles have been studied for PTT.[63,64] We reported that a PEGylated dendrimer encapsulating a gold nanoparticle generated photothermal energy, which could be used for PTT.[65–67] A combination of PDT or PTT and photosensitive drug delivery may be more effective.

4.3.1 Dendrimers for Photochemical Internalization

As described above, photosensitizers generate reactive oxygen species (ROS), such as singlet oxygen, which attack cells. When ROS attack endosomal membranes, drug molecules can escape degradation in endosomes/lysosomes. Therefore, intra-cellular delivery can be controlled by photo-irradiation, a process known as photochemical internalization (PCI).[53,68,69] The groups of Kataoka and Lai have been engaged in the development of dendrimers for PCI. Kataoka's group reported the conjugation of camptothecin (CPT) to PEG-block polymers *via* a disulfide bond. Following light irradiation, photocytotoxicity was enhanced in the presence of polymeric micelles containing phthalocyanine-core dendrimers (dendrimer-phthalocyanine, DPc).[70] Lai's group reported the preparation of Dox- and saporin-conjugated dendrimers *via* cleavable linkages,

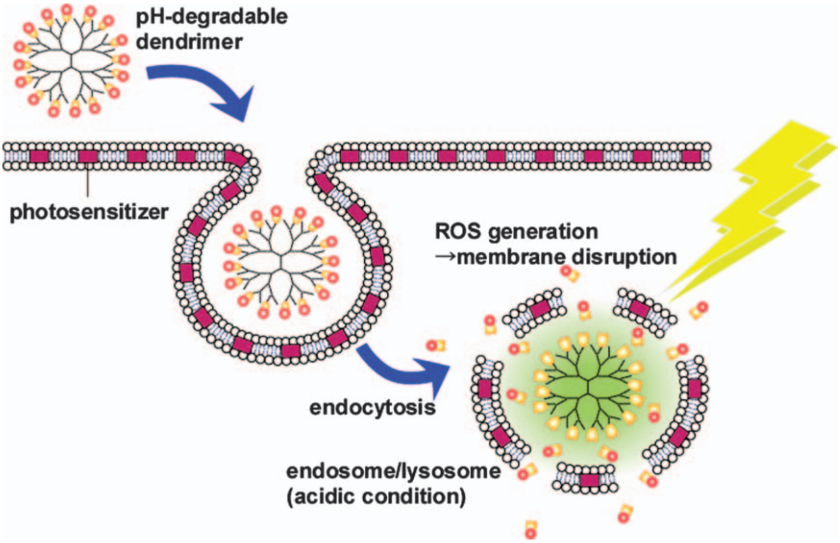

Figure 4.3 An example of drug delivery by photochemical internalization (PCI).

and drug release in the presence of the photosensitizer disulfonated aluminum phthalocyanine (AlPcS2a) was induced by photo-irradiation.[71,72] PCI of this system was effective because the cytotoxicity was much higher than the PDT effect.[71] Dox was conjugated to PAMAM dendrimers *via* amide (stable) and hydrazone (pH-sensitive) bonds (see Section 4.4.3). The hydrazone-linked Dox-dendrimers showed much more effective cytotoxicity than the amide-linked dendrimers,[71] suggesting that cleavable links help the PCI effect (Figure 4.3). Recently, these two groups performed a collaborative study on PCI for Dox delivery into multi-drug-resistant tumor cells. They used polymeric micelles containing DPc. Even though DPc showed PDT effects, cytotoxicity and tumor growth inhibition caused by the combination of DPc and Dox following photo-irradiation were higher than those observed for the same system without Dox. This indicates that the PCI effect is more relevant than the PDT effect. Interestingly, combined PDT and PCI could allow the treatment to exert its effect much more deeply in tumor tissues. In addition, multi-drug resistance (MDR) could be overcome by means of DPc nanoparticles and photo-irradiation. The timing of photo-irradiation was very important, even though the light-induced mechanisms remain to be investigated.[73]

4.3.2 Dendrimers with Photodegradable Moieties

Dendrimers with photodegradable moieties are also useful for photosensitive DDSs. Choi *et al.*[74] reported the conjugation of Dox to a dendrimer *via* a photodegradable linker. Photo-irradiation led to the release of Dox and its cellular uptake, causing the damage of tumor cells.[74] Shabat's group designed photosensitive self-immolative dendrimers composed of a photolabile trigger core, model drug compounds at the termini and self-immolative building blocks (see Section 4.6). The core molecule was activated by photo-irradiation to degrade the building blocks of the dendrimer, and the model drug molecules (pyrene) were released.[75] Thayumanavan's group also reported photodegradable dendritic amphiphilic micelles, having a molecular design similar to the temperature-sensitive dendrimers except for the photodegradable linkers.[42,76] Following photo-irradiation, alkyl chains were cleaved to disassemble the micelle structure. Nile red was rapidly released under photo-irradiation.[76]

4.4 pH-responsive Dendrimers

Although 7.4 is considered as the physiological pH, the human body shows regions of different pH and this variation can be utilized for pH-responsive DDSs. Regarding the gastrointestinal tract, there is a pH difference between the stomach (about pH 2) and the intestine (pH 5–8). The pH of cancer and inflamed tissues is slightly acidic, namely 6.5–7.2. Intra-cellular cytosol, endosome and lysosome pH values are 7.4, 5.0–6.5 and 4.5–5.0, respectively.[6] Therefore, pH-responsive dendrimers may be useful for DDSs.

4.4.1 Dendrimers Containing pH-responsive Moieties

There are many types of pH-sensitive nanoparticles with pH-tunable moieties. Carboxyl and/or tertiary amino groups can function as pH sensors, because their hydrophobicity is altered by protonation and deprotonation.[1–4,6,10,20] Because PAMAM and PPI dendrimers possess many tertiary amines at the branch points, they can respond to pH. Pistolis *et al.*[77] published in 1999 the first report on pH-responsive dendrimers. Release of hydrophobic pyrene molecules from PPI dendrimers was facilitated at low pH, because of a decrease in the inner hydrophobicity of the dendrimers (Figure 4.4A). Gajbhiye *et al.*[78] reported that PEGylated PPI dendrimer could encapsulate the anti-inflammatory drug, aceclofenac, and release it in a pH-dependent manner. They also reported that PEGylated PPI dendrimer could rapidly release encapsulated famotidine, an H_2 receptor antagonist, at low pH.[79] PAMAM dendrimers also solubilized 2-naphthol, nifedipine and nicotinic acid in a pH-dependent manner; and greater solubilities were observed at high pH.[80–82] Tekade *et al.*[83] reported that PEGylated PAMAM dendrimers could encapsulate MTX and all-*trans* retinoic acid (ATRA), and release them depending on pH. Kannaiyan *et al.*[84] prepared PPI-core PAMAM-shell dendrimers able to encapsulate pyrene in a pH-dependent manner. Additionally, it was reported that fluorinated PAMAM dendrimers presented a pH-dependent self-assembling and encapsulated rhodamine B more stably at neutral than at acidic pH.[85] Aspartate-based dendrimers could also solubilize certain drugs, such as naproxen, MTX and histidine, depending on pH.[86] These examples illustrate some pH-sensitive dendrimer candidates.

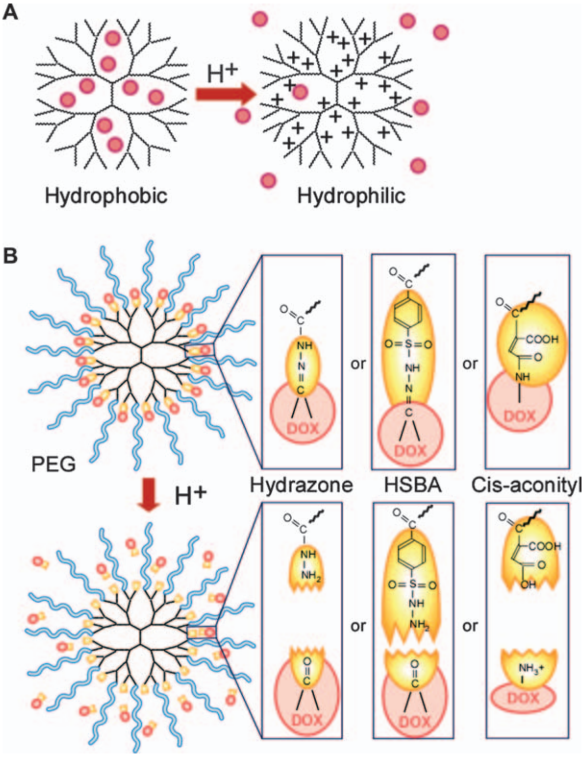

Figure 4.4 The two major types of pH-responsive dendrimers. (A) Drug-encapsulated pH-sensitive dendrimers; drug molecules can be released from these dendrimers at low pH due to the reduced hydrophobicity of the dendrimer. (B) Drug-conjugated PEGylated dendrimers *via* pH-dependent linkages; the linkage can be cleaved to release the drug molecule at low pH.

4.4.2 Dendrimer Assembly with pH-sensing Moieties

Some linear polymer-dendrimer conjugates with pH-sensing moieties assemble in a pH-dependent manner that enables pH-sensitive drug release. These polymers are composed of dendrons containing carboxylic acid or acetal linkages. Since carboxylic acid is protonated at low pH and becomes hydrophobic, the micelle structure changes under acidic conditions.[87] Gillies *et al.*[88,89] synthesized a polyester dendron with a hydrophilic PEG core and hydrophobic trimethoxyphenyl termini *via* acetal linkages. In water, these dendritic polymers formed micelles with a hydrophobic dendron and a hydrophilic PEG surface. Nile red and Dox were stably encapsulated in the dendritic micelles at pH 7.4. In contrast, at low pH the micelles degraded by cleavage of the acetal group and separation of the hydrophobic phenyl groups from the dendron; as a consequence, the drug was released.[88,89] Recently, Liu *et al.*[90] prepared a complex of cationic PAMAM dendrimer with PEG-polyanion block polymer containing lactic acid, *via* electrostatic interaction. The complex was dissociated at low pH because the negative charge of the PEG-polyanion decreased due to protonation. Dox could be loaded into the complex, and was rapidly released at low pH. Interestingly, this complex contained a ligand for hepatocarcinoma, which notably improved the drug action in the *in vitro* and *in vivo* hepatocarcinoma treatment.[90]

4.4.3 Drug-dendrimer Conjugates with pH-responsive Linkages

Dendrimers conjugating drugs *via* a pH-sensitive linkage have been prepared.[10,12,16–18,20] There are two types of pH-degradable linkers between drugs and dendrimers: hydrazone and *cis*-aconityl linkage. These linkages are cleaved at low pH, thus enabling conjugated drugs to be released from dendrimers in tumor tissues and/or in acidic cellular compartments (Figure 4.4B). As discussed in Section 4.3.1, PAMAM dendrimer conjugating Dox *via* a hydrazone linkage exhibited more efficient drug action compared to the amide linked conjugate.[71] Similar results were obtained with drug-conjugated PEGylated PAMAM dendrimers (Figure 4.4B). The hydrazone-linked drug-dendrimer conjugate exhibited higher cytotoxicity than the amide-linked conjugate.[91] These data suggest that drug release from the hydrazone-linked conjugate occurred in acidic endosomes and/or lysosomes. Since PEGylation is indispensable for the biomedical applications, this kind of dendrimer is a potent polymer prodrug.

Bow-tie types of polyester dendrimers incorporating PEG-attached dendrons, and dendrons conjugating Dox *via* hydrazone linkages, were evaluated as pH-dependent DDSs.[92–94] The hydrazone-linked drug-dendrimer conjugates exhibited higher cytotoxicity than the amide-linked conjugates. These polyester dendrimers were found to accumulate in tumor tissues and efficiently inhibit tumor growth with a single dose. The drug efficiency was similar to a commercially available PEGylated liposome containing Dox.[94] Since these bow-tie type dendrimers are difficult to prepare, an improved and simple synthetic method has been developed to produce a dendrimer symmetrically incorporating both PEG and Dox.[95,96] Kaminskas *et al.*[97] reported PEGylated polylysine dendrimers conjugating Dox *via* a hydrazone-like 4-hydrazinosulfonyl benzoic acid (HSBA) linkage (Figure 4.4B). A polylysine dendrimer was modified with a PEG on the alpha amino group and HSBA-linked Dox on the side chain. *In vitro* and *in vivo* assays indicated that the drug action of the dendrimer was similar to that of the PEGylated liposomes containing Dox, but the side effects of the dendrimer were less significant.[98] pH-sensitive Dox-dendrimer conjugates have been modified with ligands such as biotin and galactose.[99,100] Ligand conjugation is useful for active targeting of the pH-sensitive dendrimers.

Zhu *et al.*[101,102] reported the synthesis of PAMAM dendrimers with amino termini partly modified with PEG, and with the residual amino groups subsequently modified with Dox *via* a *cis*-aconityl link. The linkage was pH-sensitive and the cytotoxicity of *cis*-aconityl-linked Dox-dendrimer conjugates was higher than that of succinyl-linked conjugates. The binding ratio and the

PEG length resulted to be very important for the release profiles and the *in vitro* and *in vivo* drug action.[101,102] These studies illustrate how important the release of drug molecules from a dendrimer is for an efficient drug action.

4.5 Redox-responsive Dendritic Polymers

Tissue redox status is a self-regulated internal body stimulus that can be used to trigger drug release from responsive carriers. Glutathione is present inside and outside cells at millimolar and micromolar concentration, respectively.[8,9] This indicates that the intra-cellular environment is much more reducing than the extra-cellular one. This difference between oxidative and reductive environments can be used as a stimulus for site-specific release. In an oxidative environment, thiol groups form disulfide bonds, which are reversibly broken in a reductive environment. This suggests that thiol-containing molecules are useful for the design of redox-responsive dendrimers. Kannan's group reported *N*-acetylcysteine-dendrimer conjugates with disulfide linkages.[103,104] *N*-acetylcysteine is prescribed for neuroinflammation; however, its reaction with cysteine residues of natural proteins causes an extremely low bioavailability. The disulfide linked dendrimer-drug conjugates exhibited much better antioxidant effects than the drug alone.[103,104] Lim *et al.*[105] reported the conjugation of the anticancer drug taxol to PEGylated triazine dendrimers *via* a disulfide bond, in order to improve the therapeutic effect. We synthesized a PEG-attached dendrimer containing cysteine. The disulfide network at the surface of the dendrimer could be degraded under reductive conditions to enhance release of the drug. The permeability of the disulfide network to RB was enhanced in a dithiothreitol solution, which mimics the intra-cellular environment.[106] Excellent reviews on self-immolative dendrimers induced by redox stimuli are available.[107,108]

4.6 Enzyme-responsive Dendritic Polymers

The nature and the amount of proteins in cells and tissues are strictly regulated by controlled gene expression. Since the expression patterns of proteins are different between tissues, certain proteins are possible inducing factors for site-specific drug release. Enzymes in particular can change the chemical composition and/or the conformation of the target molecule. A comprehensive overview of enzyme-responsive DDSs can be found in Chapter 9.

As mentioned previously, Shabat's group designed self-immolative dendrimers containing a photodegradable unit, which degraded under light irradiation leading to release of the drug molecules.[75,107,108] Similarly, enzyme-degradable dendrimers were prepared. The enzyme-labile unit was added to the degradable dendrimers conjugating drug molecules, making them responsive to the catalytic activity (Figure 4.5).[109–113] Shabat's group used a retro-aldol retro-Michael substrate for catalytic antibody 38C2 and phenylacetamide for penicillin G amidase. When the enzymatic substrate was conjugated to the core, a single trigger induced the release of many drug

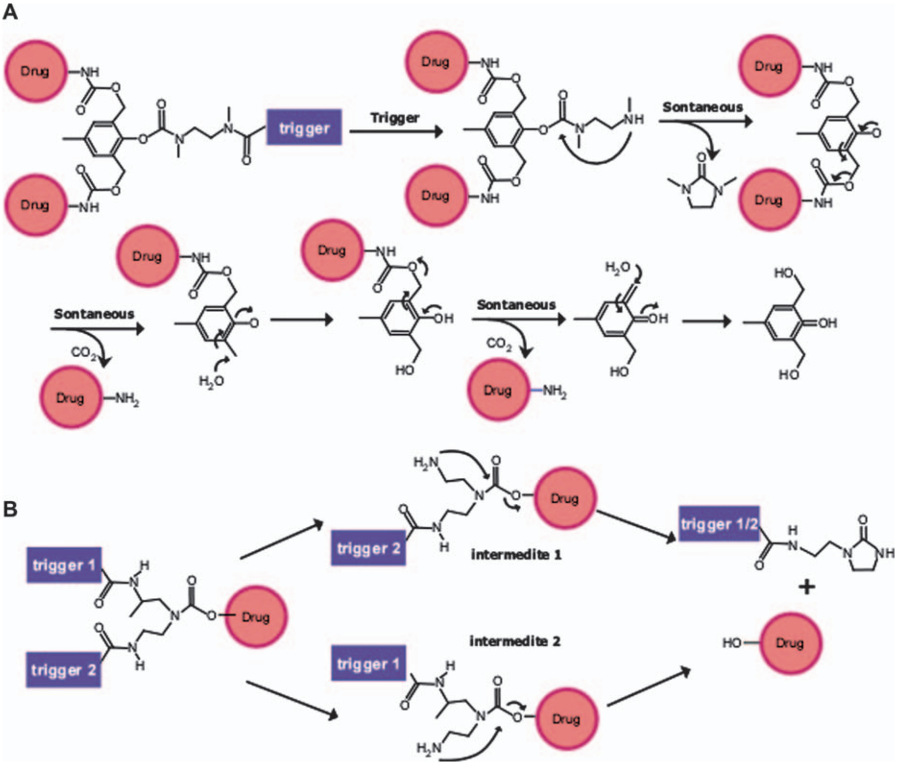

Figure 4.5 Self-immolative dendrimers responding to enzymatic activity, as reported by Shabat's group. (A) Single trigger type: the trigger was conjugated to the core and the drugs to the termini. (B) Multiple triggers type: the triggers were conjugated to the termini and the drug to the core.

molecules conjugated to the dendrimer termini (Figure 4.5A). Several enzyme-degradable dendrimers with Dox and CPT were synthesized. These dendrimers exhibited enzyme-dependent drug release and cytotoxicity.[109] The dendrimer structure played a critical role in the degradation behavior.[110,111] To prevent low solubility in aqueous solution, which is a main cause of resistance to degradation, PEG chains were attached to the dendrimer termini. The PEGylated self-immolative dendrimer of large generation *in vitro* exhibited enhanced drug activity.[110] Furthermore, the dendrimer building block was improved to degrade rapidly, which also resulted in more efficient cytotoxicity of melphalan.[111] When the enzymatic substrates were conjugated to the termini, a multi-enzyme trigger induced the release of the drug molecule conjugated to the dendrimer core (Figure 4.5B). Shabat's group also reported similar multiple enzyme triggered drug release.[112,113] In this case, drug release was induced by both homogeneous and heterogeneous enzymatic activity. Dendrimer generation also contributed to an increase in not only the amount of responsive moieties (triggers), but also in the components to be degraded for the induction of drug release. The former influenced the drug release positively, but the latter influenced drug release negatively. Consequently, a two-armed dendrimer was the most effective for drug release.[112] When heterogeneous enzymatic substrates were attached to the dendrimer termini, a molecular "OR" logic trigger could gate the prodrug activation (Figure 4.5B).[113] These interesting series of systems, which were tested in cell cultures, are based on a novel concept. Detailed biomedical research remains to be conducted for DDSs applications.

As mentioned previously, Thayumanavan's group reported oligo(ethylene glycol)-bound dendritic compounds that exhibited temperature-dependent phase transitions similar to amide group-containing dendrimers, and that formed micelles that released Rhodamine 6G.[42] Enzyme-dependent drug release was reported using such dendritic micelles (Figure 4.6A). An ester

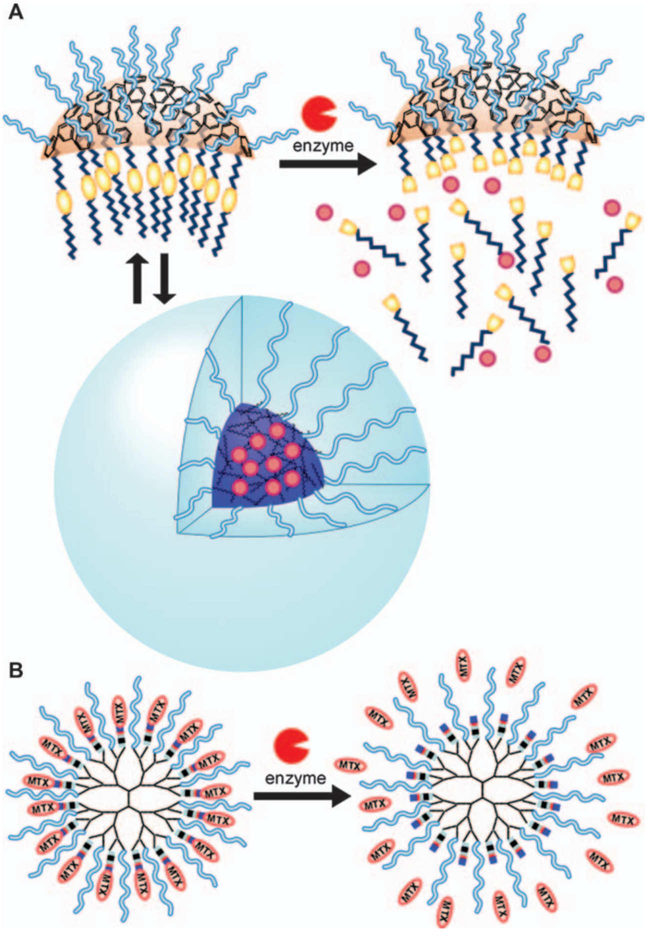

Figure 4.6 Enzyme-sensitive dendritic polymers. (A) Dendrimer assembly containing drug, as reported by Thayumanavan's group. (B) MMP-responsive MTX-conjugated PEGylated dendrimer, as reported by Porter's group.

linkage between the alkyl chain and the dendritic compound was cleaved by esterase, leading to disassembly of the dendritic micelles. Consequently, the encapsulated model drug, pyrene, was released from the dendritic micelles by enzyme activity.[114] Thayumanavan's group also reported protein–protein interaction-dependent drug release using dendritic micelles. Biotin, which binds to avidin, was conjugated to the dendritic polymer. By adding avidin, the dendritic micelles were dissociated and the encapsulated model drugs were released.[115] These papers indicate that the association-dissociation transition of these micelles is sensitive to enzyme activity and protein-absorption.[114,115] It is likely that the temperature-sensitivity of these dendritic micelles contributed to the controlled release. Further study on such drug-loaded micelles, rather than model drug systems, is required.

Kaminskas *et al.*[116] reported drug-conjugated dendrimers *via* a matrix metalloproteinase (MMP)-degradable linkage for MMP-dependent drug release (Figure 4.6B). It is known that some kinds of MMPs are secreted in tumor tissues, in which the conjugated drug release can occur. Dendrimers with PEG and the MMP substrate peptide-linked MTX released the drug in the presence of MMP, suppressing the tumor growth. Interestingly, butoxyl-capping of the MTX-conjugated dendrimers resulted in improved biodistribution and more efficient drug action.[116] The study of such enzyme-dependent drug delivery *via* dendrimers is at an early stage, and more detailed investigations remain to be performed.

4.7 Theragnostic Dendrimers

The stimuli-responsive dendrimers described in previous sections are intended to enhance maximum drug activity and to reduce side effects. When external stimuli (*e.g.* temperature or light) responsive DDS are used, individual differences may occur and a precise spatiotemporal control of the stimuli is required for effective drug delivery. Ideally, the drug action should be monitored to ensure efficient chemotherapy. Therefore, nanocarriers that enable diagnosis as well as therapy, *i.e. theragnosis*, are necessary.[117–119] Baker's group performed a pioneer work on *theragnostic dendrimers*. They focused on the multi-valency of dendrimers, and prepared multi-functional dendrimers conjugating drugs, fluorescent dyes and ligands for the targeting.[120–122] As mentioned previously, Au NPs have photothermogenic properties that are useful for photorelated therapy. Au NPs also have the property of X-ray attenuation, which is useful for X-ray computed tomography (CT), a non-invasive imaging method.[123] Therefore, theragnostic nanoparticles can be produced by the combination of a dendrimer delivery system with Au NPs. PEGylated dendrimers containing Au NPs have been tested for the applications of PTT and CT imaging, and resulted to be useful as *theragnostic dendrimers*.[66,124] More detailed information is provided in a recently published article.[67] Iron oxide nanoparticles (IONP) are useful for magnetic resonance imaging (MRI). Chang *et al.*[125] reported the preparation of IONPs covered with pH-sensitive linked dendrimer-drug conjugates for *theragnostic* treatments. This hybrid material exhibited pH-dependent drug release as well as tumor monitoring properties by MRI.[125] It is expected that theragnostic dendrimer nanoparticles will become more valuable as more information becomes available.

4.8 Conclusion

Dendrimers are unique and well-defined materials. Their molecular weight and chemical composition are theoretically defined, and the characterization of newly synthesized compounds is relatively easy. It is worthwhile to develop functional nanoparticles based on dendritic polymers. Dendrimers are particularly useful for systematic synthesis and the investigation of functional macromolecules. The design of functional dendritic nanoparticles is important for the next generation of DDSs, *i.e.* stimuli-responsive DDSs. This chapter summarizes the various functional dendritic polymers that can be prepared incorporating temperature-, photo-, pH-, redox- and enzyme-sensitive moieties for drug delivery. Improvement of functional dendritic polymers is required to make them more effective *in vivo*. From a practical point of view, a disadvantage of dendrimers is their high cost. Hyperbranched polymers are a useful alternative to dendrimers, because they are simple to synthesize and have a similar globular structure. Temperature-sensitive and pH-sensitive hyperbranched polymers have been reported by several groups.[12,126–131] It is expected that in the future, dendritic and hyperbranched polymers will expand to develop potential novel drug carriers.

Acknowledgements

I thank Ms. Noriko Tano for her help with figure preparation and reference arrangement.

References

1. C. Alarcon de las Heras, S. Pennadam and C. Alexander, *Chem. Soc. Rev.*, 2005, **34**, 276.
2. J. Kost and R. Langer, *Adv. Drug Deliver. Rev.*, 2001, **46**, 125.
3. P. Bawa, V. Pillay, Y. E. Choonara and L. C. du Toit, *Biomed. Mater.*, 2009, **4**, 22001.
4. F. Meng, Z. Zhong and J. Feijen, *Biomacromolecules*, 2009, **10**, 197.
5. M. Bikram and J. L. West, *Expert Opin. Drug Deliv.*, 2008, **5**, 1077.
6. D. Schmaljohann, *Adv. Drug Deliver. Rev.*, 2006, **58**, 1655.
7. C. Alvarez-Lorenzo, L. Bromberg and A. Concheiro, *Photochem. Photobiol.*, 2009, **85**, 848.
8. F. Meng, W. E. Hennink and Z. Zhong, *Biomaterials*, 2009, **30**, 2180.
9. G. Saito, J. A. Swanson and K. D. Lee, *Adv. Drug Deliver. Rev.*, 2003, **55**, 199.

10. A. V. Ambade, E. N. Savariar and S. Thayumanavan, *Mol. Pharmaceut.*, 2005, **2**, 264.
11. D. D. Lasic, *Liposomes: From Physics to Applications*, Elsevier, Amsterdam, 1993.
12. R. Haag and F. Kratz, *Angew. Chem. Int. Ed.*, 2006, **45**, 1198.
13. D. A. Tomalia, A. M. Naylor and W. A. Goddard III, *Angew. Chem. Int. Ed.*, 1990, **29**, 138.
14. D. A. Tomalia, *Prog. Polym. Sci.*, 2005, **30**, 294.
15. D. A. Tomalia, H. Baker, J. Dewald, M. Hall, G. Kallos, S. Martin, J. Roeck, J. Ryder and P. Smith, *Polymer J.*, 1985, **17**, 117.
16. D. Astruc, E. Boisselier and C. Ornelas, *Chem. Rev.*, 2010, **110**, 1857.
17. C. Kojima, *Expert Opin. Drug Deliv.*, 2010, **7**, 307.
18. S. H. Medina and M. E. H. El-Sayed, *Chem. Rev.*, 2009, **109**, 3141.
19. J. B. Wolinsky and M. W. Grinstaff, *Adv. Drug Deliver. Rev.*, 2008, **60**, 1037.
20. R. K. Tekade, P. V. Kumar and N. K. Jain, *Chem. Rev.*, 2009, **109**, 49.
21. C. C. Lee, J. A. MacKay, J. M. Fréchet and F. C. Szoka, *Nat. Biotechnol.*, 2005, **23**, 1517.
22. V. Gajbhiye, P. V. Kumar, R. K. Tekade and N. K. Jain, *Curr. Pharm. Des.*, 2007, **13**, 415.
23. C. M. Paleos, D. Tsiourvas, Z. Sideratou and L. Tziveleka, *Curr. Top. Med. Chem.*, 2008, **8**, 1204.
24. A. D'Emanuele and D. Attwood, *Adv. Drug Deliver. Rev.*, 2005, **57**, 2147.
25. S. Svenson and D. A. Tomalia, *Adv. Drug Deliver. Rev.*, 2005, **57**, 2106.
26. H. Maeda and Y. Matsumura, *Crit. Rev. Ther. Drug Carrier Syst.*, 1989, **6**, 193.
27. H. Maeda, J. Wu, T. Sawa, Y. Matsumura and K. Hori, *J. Control. Release*, 2000, **65**, 271.
28. C. Dufès, I. F. Uchegbu and A. G. Schätzlein, *Adv. Drug Deliver. Rev.*, 2005, **57**, 2177.
29. P. R. Stauffer and S. N. Goldberg, *Int. J. Hyperthermia*, 2004, **20**, 671.
30. M. Kimura, M. Kato, T. Muto, K. Hanabusa and H. Shirai, *Macromolecules*, 2000, **33**, 1117.
31. J. Xu, S. Luo, W. Shi and S. Liu, *Langmuir*, 2006, **22**, 989.
32. Z. Yang, J. Xie, W. Zhou and W. Shi, *J. Biomed. Mater. Res. A*, 2009, **89**, 988.
33. Y. Zhao, X. Fan, D. Liu and Z. Wang, *Int. J. Pharm.*, 2011, **409**, 229.
34. L. Zhu, G. Zhu, M. Li, E. Wang, R. Zhu and X. Qi, *Eur. Polym. J.*, 2002, **38**, 2503.
35. Z. Ge, S. Luo and S. Liu, *J. Polym. Sci. A Polym. Chem.*, 2006, **44**, 1357.
36. T. C. Stover, Y. S. Kim, T. L. Lowe and M. Kester, *Biomaterials*, 2008, **29**, 359.
37. Y. Haba, A. Harada, T. Takagishi and K. Kono, *J. Am. Chem. Soc.*, 2004, **126**, 12760.
38. Y. Haba, C. Kojima, A. Harada and K. Kono, *Angew. Chem. Int. Ed.*, 2007, **46**, 234.

39. Y. Tono, C. Kojima, Y. Haba, T. Takahashi, A. Harada, S. Yagi and K. Kono, *Langmuir*, 2006, **22**, 4920.
40. K. Kono, T. Miyoshi, Y. Haba, E. Murakami, C. Kojima and A. Harada, *J. Am. Chem. Soc.*, 2007, **129**, 7222.
41. K. Kono, E. Murakami, Y. Hiranaka, E. Yuba, C. Kojima, A. Harada and K. Sakurai, *Angew. Chem. Int. Ed.*, 2011, **50**, 6332.
42. S. V. Aathimanikandan, E. N. Savariar and S. Thayumanavan, *J. Am. Chem. Soc.*, 2005, **127**, 14922.
43. D. W. Chang and L. Dai, *J. Mater. Chem.*, 2007, **17**, 364.
44. W. Li, A. Zhang, Y. Chen, K. Feldman, H. Wu and A. D. Schlüter, *Chem. Commun.*, 2008, **2008**, 5948.
45. T. Koide, *Connect. Tissue Res.*, 2005, **46**, 131.
46. D. G. Wallace and J. Rosenblatt, *Adv. Drug Deliver. Rev.*, 2003, **55**, 1631.
47. A. Sano, M. Maeda, S. Nagahara, T. Ochiya, K. Honma, H. Itoh, T. Miyata and K. Fujioka, *Adv. Drug Deliver. Rev.*, 2003, **55**, 1651.
48. C. Kojima, S. Tsumura, A. Harada and K. Kono, *J. Am. Chem. Soc.*, 2009, **131**, 6052.
49. C. Kojima and T. Suehiro, *Chem. Lett.*, 2011, **40**, 1249.
50. T. Suehiro, T. Tada, T. Waku, N. Tanaka, C. Hongo, S. Yamamoto, A. Nakahira and C. Kojima, *Biopolymers*, 2011, **95**, 270.
51. C. Kojima, T. Suehiro, T. Tada, Y. Sakamoto, T. Waku and N. Tanaka, *Soft Matter*, 2011, **7**, 8991.
52. D. E. Dolmans, D. Fukumura and R. K. Jain, *Nat. Rev. Cancer*, 2003, **3**, 380.
53. N. Nishiyama, Y. Morimoto, W. D. Jang and K. Kataoka, *Adv. Drug Deliver. Rev.*, 2009, **61**, 327.
54. N. Nishiyama, H. R. Stapert, G. D. Zhang, D. Takasu, D. L. Jiang, T. Nagano, T. Aida and K. Kataoka, *Bioconjugate Chem.*, 2003, **14**, 58.
55. C. Kojima, Y. Toi, A. Harada and K. Kono, *Bioconjugate Chem.*, 2007, **18**, 663.
56. S. H. Battah, C. E. Chee, H. Nakanishi, S. Gerscher, A. J. MacRobert and C. Edwards, *Bioconjugate Chem.*, 2001, **12**, 980.
57. S. Battah, S. O'Neill, C. Edwards, S. Balaratnam, P. Dobbin and A. J. MacRobert, *Int. J. Biochem. Cell Biol.*, 2006, **38**, 1382.
58. S. Battah, S. Balaratnam, A. Casas, S. O'Neill, C. Edwards, A. Batlle, P. Dobbin and A. J. MacRobert, *Mol. Cancer Ther.*, 2007, **6**, 876.
59. A. Casas, S. Battah, G. Di Venosa, P. Dobbin, L. Rodriguez, H. Fukuda, A. Batlle and A. J. MacRobert, *J. Control. Release*, 2009, **135**, 136.
60. S. Herlambang, M. Kumagai, T. Nomoto, S. Horie, S. Fukushima, M. Oba, T. Nomoto, K. Miyazaki, Y. Morimoto, N. Nishiyama and K. Kataoka, *J. Control. Release*, 2011, **155**, 449.
61. E. Paszko, C. Ehrhardt, M. O. Senge, D. P. Kelleher and J. V. Reynolds, *Photodiagnosis Photodyn. Ther.*, 2011, **8**, 14.
62. P. K. Jain, I. H. El-Sayed and M. A. El-Sayed, *Nanotoday*, 2007, **2**, 18.
63. A. O. Govorov and H. H. Richardson, *Nanotoday*, 2007, **2**, 30.

64. D. Pissuwan, S. M. Valenzuela and M. B. Cortie, *Trends Biotechnol.*, 2006, **24**, 62.
65. Y. Haba, C. Kojima, A. Harada, T. Ura, H. Horinaka and K. Kono, *Langmuir*, 2007, **23**, 5243.
66. Y. Umeda, C. Kojima, A. Harada, H. Horinaka and K. Kono, *Bioconjugate Chem.*, 2010, **21**, 1559.
67. C. Kojima, S. H. Cho and E. Higuchi, *Res. Chem. Intermed.*, 2012, **38**, 1279.
68. P. K. Selbo, A. Weyergang, A. Høgset, O. J. Norum, M. B. Berstad, M. Vikdal and K. Berg, *J. Control. Release*, 2010, **148**, 2.
69. A. Høgset, L. Prasmickaite, P. K. Selbo, M. Hellum, B. Ø. Engesæter, A. Bonsted and K. Berg, *Adv. Drug Deliver. Rev.*, 2004, **56**, 95.
70. H. Cabral, M. Nakanishi, M. Kumagai, W. D. Jang, N. Nishiyama and K. Kataoka, *Pharm. Res.*, 2009, **26**, 82.
71. P. S. Lai, P. J. Lou, C. L. Peng, C. L. Pai, W. N. Yen, M. Y. Huang, T. H. Young and M. J. Shieh, *J. Control. Release*, 2007, **122**, 39.
72. P. S. Lai, C. L. Pai, C. L. Peng, M. J. Shieh, K. Berg and P. J. Lou, *J. Biomed. Mater. Res. A*, 2008, **87**, 147.
73. H. L. Lu, W. J. Syu, N. Nishiyama, K. Kataoka and P. S. Lai, *J. Control. Release*, 2011, **155**, 458.
74. S. K. Choi, T. Thomas, M. H. Li, A. Kotlyar, A. Desai and J. R. Baker Jr., *Chem. Commun.*, 2010, **46**, 2632.
75. R. J. Amir, N. Pessah, M. Shamis and D. Shabat, *Angew. Chem. Int. Ed.*, 2003, **42**, 4494.
76. V. Yesilyurt, R. Ramireddy and S. Thayumanavan, *Angew. Chem. Int. Ed.*, 2011, **50**, 3038.
77. G. Pistolis, A. Malliaris, D. Tsiourvas and C. M. Paleos, *Chem. Eur. J.*, 1999, **5**, 1440.
78. V. Gajbhiye, P. V. Kumar, A. Sharma and N. K. Jain, *Curr. Nanosci.*, 2008, **4**, 267.
79. V. Gajbhiye, P. V. Kumar, R. K. Tekade and N. K. Jain, *Eur. J. Med. Chem.*, 2009, **44**, 1155.
80. M. H. Kleinman, J. H. Flory, D. A. Tomalia and N. J. Turro, *J. Phys. Chem. B*, 2000, **104**, 11472.
81. B. Devarakonda, R. A. Hill and M. M. de Villiers, *Int. J. Pharm.*, 2004, **284**, 133.
82. Y. Cheng and T. Xu, *Eur. J. Med. Chem.*, 2005, **40**, 1384.
83. R. K. Tekade, T. Dutta, V. Gajbhiye and N. K. Jain, *J. Microencapsul.*, 2009, **26**, 287.
84. D. Kannaiyan and T. Imae, *Langmuir*, 2009, **25**, 5282.
85. J. M. Criscione, B. L. Le, E. Stern, M. Brennan, C. Rahner, X. Papademetris and T. M. Fahmy, *Biomaterials*, 2009, **30**, 3946.
86. L. Ouyang, L. Ma, B. Jiang, Y. Li, D. He and L. Guo, *Eur. J. Med. Chem.*, 2010, **45**, 2705.
87. L. Tian and P. T. Hammond, *Chem. Mater.*, 2006, **18**, 3976.

88. E. R. Gillies, T. B. Jonsson and J. M. Fréchet, *J. Am. Chem. Soc.*, 2004, **126**, 11936.
89. E. R. Gillies and J. M. Fréchet, *Bioconjugate Chem.*, 2005, **16**, 361.
90. D. Liu, H. Hu, J. Zhang, X. Zhao, X. Tang and D. Chen, *Chem. Pharm. Bull.*, 2011, **59**, 63.
91. K. Kono, C. Kojima, N. Hayashi, E. Nishisaka, K. Kiura, S. Watarai and A. Harada, *Biomaterials*, 2008, **29**, 1664.
92. H. R. Ihre, O. L. Padilla De Jesús, F. C. Szoka Jr. and J. M. Fréchet, *Bioconjugate Chem.*, 2002, **13**, 443.
93. O. L. Padilla De Jesús, H. R. Ihre, L. Gagne, J. M. Fréchet and F. C. Szoka Jr., *Bioconjugate Chem.*, 2002, **13**, 453.
94. C. C. Lee, E. R. Gillies, M. E. Fox, S. J. Guillaudeu, J. M. J. Fréchet, E. E. Dy and F. F. Szoka, *P. Natl Acad. Sci. USA*, 2006, **103**, 16649.
95. S. J. Guillaudeu, M. E. Fox, Y. M. Haidar, E. E. Dy, F. C. Szoka and J. M. Fréchet, *Bioconjugate Chem.*, 2008, **19**, 461.
96. D. G. van der Poll, H. M. Kieler-Ferguson, W. C. Floyd, S. J. Guillaudeu, K. Jerger, F. C. Szoka and J. M. Fréchet, *Bioconjugate Chem.*, 2010, **21**, 764.
97. L. M. Kaminskas, B. D. Kelly, V. M. McLeod, G. Sberna, D. J. Owen, B. J. Boyd and C. J. H. Porter, *J. Control. Release*, 2011, **152**, 241.
98. L. M. Kaminskas, V. M. McLeod, B. D. Kelly, G. Sberna, B. J. Boyd, M. Williamson, D. J. Owen and C. J. H. Porter, *Nanomedicine*, 2012, **8**, 103.
99. H. Yuan, K. Luo, Y. Lai, Y. Pu, B. He, G. Wang, Y. Wu and Z. Gu, *Mol. Pharmaceut.*, 2010, **7**, 953.
100. J. Huang, F. Gao, X. Tang, J. Yu, D. Wang, S. Liu and Y. Li, *Polym. Int.*, 2010, **59**, 1390.
101. S. Zhu, M. Hong, G. Tang, L. Qian, J. Lin, Y. Jiang and Y. Pei, *Biomaterial.*, 2010, **31**, 1360.
102. S. Zhu, M. Hong, L. Zhang, G. Tang, Y. Jiang and Y. Pei, *Pharm. Res.*, 2010, **27**, 161.
103. R. S. Navath, Y. E. Kurtoglu, B. Wang, S. Kannan, R. Romero and R. M. Kannan, *Bioconjugate Chem.*, 2008, **19**, 2446.
104. Y. E. Kurtoglu, R. S. Navath, B. Wang, S. Kannan, R. Romero and R. M. Kannan, *Biomaterials*, 2009, **30**, 2112.
105. J. Lim, A. Chouai, S. T. Lo, W. Liu, X. Sun and E. E. Simanek, *Bioconjugate Chem.*, 2009, **20**, 2154.
106. C. Kojima, Y. Haba, T. Fukui, K. Kono and T. Takagishi, *Macromolecules*, 2003, **36**, 2183.
107. D. Shabat, *J. Polym. Sci. A Polym. Chem.*, 2006, **44**, 1569.
108. D. V. McGrath, *Mol. Pharmaceut.*, 2005, **2**, 253.
109. M. Shamis, H. N. Lode and D. Shabat, *J. Am. Chem. Soc.*, 2004, **126**, 1726.
110. A. Gopin, S. Ebner, B. Attali and D. Shabat, *Bioconjugate Chem.*, 2006, **17**, 1432.

111. A. Sagi, E. Segal, R. Satchi-Fainaro and D. Shabat, *Bioorg. Med. Chem.*, 2007, **15**, 3720.
112. R. J. Amir and D. Shabat, *Chem. Commun.*, 2004, **2004**, 1614.
113. R. J. Amir, M. Popkov, R. A. Lerner, C. F. Barbas, 3rd and D. Shabat, *Angew. Chem. Int. Ed.*, 2005, **44**, 4378.
114. M. A. Azagarsamy, P. Sokkalingam and S. Thayumanavan, *J. Am. Chem. Soc.*, 2009, **131**, 14184.
115. M. A. Azagarsamy, V. Yesilyurt and S. Thayumanavan, *J. Am. Chem. Soc.*, 2010, **132**, 4550.
116. L. M. Kaminskas, B. D. Kelly, V. M. McLeod, G. Sberna, B. J. Boyd, D. J. Owen and C. J. Porter, *Mol. Pharmaceut.*, 2011, **8**, 338.
117. Y. Cheng, L. Zhao, Y. Li and T. Xu, *Chem. Soc. Rev.*, 2011, **40**, 2673.
118. T. Lammers, F. Kiessling, W. E. Hennink and G. Storm, *Mol. Pharmaceut.*, 2010, **7**, 1899.
119. J. Xie, S. Lee and X. Chen, *Adv. Drug Deliver. Rev.*, 2010, **62**, 1064.
120. I. J. Majoros, T. P. Thomas, C. B. Mehta and J. R. Baker Jr., *J. Med. Chem.*, 2005, **48**, 5892.
121. I. J. Majoros, A. Myc, T. P. Thomas, C. B. Mehta and J. R. Baker Jr., *Biomacromolecules*, 2006, **7**, 572.
122. T. P. Thomas, S. K. Choi, M. H. Li, A. Kotlyar and J. R. Baker Jr., *Bioorg. Med. Chem. Lett.*, 2010, **20**, 5191.
123. E. Boisselier and D. Astruc, *Chem. Soc. Rev.*, 2009, **38**, 1759.
124. C. Kojima, Y. Umeda, M. Ogawa, A. Harada, Y. Magata and K. Kono, *Nanotechnology*, 2010, **21**, 245104.
125. Y. Chang, X. Meng, Y. Zhao, K. Li, B. Zhao, M. Zhu, Y. Li, X. Chen and J. Wang, *J. Colloid Interface Sci.*, 2011, **363**, 403.
126. H. Frey and R. Haag, *Rev. Mol. Biotechnol.*, 2002, **90**, 257.
127. M. Calderon, M. A. Quadir, S. K. Sharma and R. Haag, *Adv. Mater.*, 2010, **22**, 190.
128. H. Liu, Y. Chen and Z. Shen, *J. Polym. Sci. A Polym. Chem.*, 2007, **45**, 1177.
129. Y. Shen, M. Kuang, Z. Shen, J. Nieberle, J. Duan and H. Frey, *Angew. Chem. Int. Ed.*, 2008, **47**, 2227.
130. C. Kojima, K. Yoshimura, A. Harada, Y. Sakanishi and K. Kono, *Bioconjugate Chem.*, 2009, **20**, 1054.
131. C. Kojima, K. Yoshimura, A. Harada, Y. Sakanishi and K. Kono, *J. Polym. Sci. A Polym. Chem.*, 2010, **48**, 4047.

CHAPTER 5

Temperature- and pH-sensitive Polymeric Micelles for Drug Encapsulation, Release and Targeting

ALEJANDRO SOSNIK

The Group of Biomaterials and Nanotechnology for Improved Medicines (BIONIMED), Department of Pharmaceutical Technology, Faculty of Pharmacy and Biochemistry, University of Buenos Aires, 956 Junín St., Buenos Aires CP1113, Argentina and National Science Research Council (CONICET), Buenos Aires, Argentina
Email: alesosnik@gmail.com

5.1 (Bio)pharmaceutic Challenges in Therapeutics

Rational structure-based drug discovery supported by tools such as bioinformatics reduced the number of candidates that enter clinical trials, leading to a substantial diminution of the attrition rate and the cost of drug development.[1] This fact enabled the substantial growth of small pharmaceutical companies,[2] although productivity is relatively low and inconsistent with the extent of investment growth.[3] This outbreak has been accompanied by the emergence and development of technologies aiming to overcome different (bio)pharmaceutical drawbacks. More than 50% of the approved drugs and 70% of the new candidates are poorly water soluble according to the Biopharmaceutic Classification System (BCS).[4–6] Low aqueous solubility represents

---

RSC Smart Materials No. 2
Smart Materials for Drug Delivery: Volume 1
Edited by Carmen Alvarez-Lorenzo and Angel Concheiro
© The Royal Society of Chemistry 2013
Published by the Royal Society of Chemistry, www.rsc.org

a great challenge for formulators that need to bring these new candidates into the pipeline and to ensure good bioavailability of the approved drugs. Low physical and chemical stability are also hurdling the progress of potentially active molecules from the design and synthetic stages to the *in vitro* and *in vivo* evaluation. For example, the self-assembly of drugs into nanoscopic aggregates invisible to the naked eye[7–12] may result in the partial or total loss of the biological activity due to a more limited capacity to cross biological barriers and more elevated toxicity.[9] To minimize the self-aggregation of novel 1-indanone thiosemicarbazones, Glisoni *et al.* recently complexed them with different cyclodextrins.[13] Complexes enabled the reliable evaluation of the activity against the hepatitis C virus (HCV) in Huh7.5 cells containing the full-length and the subgenomic subgenotype 1b HCV replicon.[14]

Motivated by the evolution of nanotechnology, different nanocarriers made of lipids and polymers have been designed and developed to address these limitations.[15,16] Robust platforms were exploited to achieve the temporal and spatial release of drugs, thus constraining the systemic exposure to toxic agents and the appearance of severe adverse effects (*e.g.* doxorubicin and amphotericin B)[17,18] and improving the safety ratio.[15]

Polymeric micelles came out as one of the most versatile nanocarriers due to several unique features: (i) great chemical flexibility to tailor the molecular architecture of the amphiphile and to confer responsiveness to different and multiple stimuli, (ii) capacity to host, solubilize and physico-chemically stabilize poorly water soluble drugs, (iii) ability to accumulate selectively in highly vascularized solid tumors by the so-called enhanced permeation and retention (EPR) effect, and (iv) ability of single amphiphile molecules (unimers) to down-regulate the expression and to inhibit the functional activity of different pumps of the ATP-binding cassette superfamily (ABCs) that are involved in the efflux of drugs against a concentration gradient and consequently in cellular multi-drug resistance (MDR).

Despite their potential applications, polymeric micelles remain clinically uncapitalized. The present chapter overviews the most recent applications of temperature- and pH-responsive polymeric micelles for the encapsulation, release and targeting of drugs.

5.2 Polymeric Micelles

Polymeric micelles are nano-sized (usually <100 nm) structures generated by the spontaneous self-assembly of amphiphilic block copolymers above a given concentration known as critical micellar concentration (CMC).[19] Hydrophobic blocks associate to form an inner core capable of solubilizing lipophilic drugs, while the hydrophilic ones form a corona that comes into direct contact with the external medium, stabilizing the system.[20] The corona also constitutes the interface between the drug reservoir and the release medium, and depending on its properties (*e.g.* microfluidity) and on the drug/corona interaction, the drug release could be facilitated or hampered. In general, when the hydrophilic block is longer than the hydrophobic one, micelles are spherical, while copolymers with longer hydrophobic blocks can give place to micelles of different morphology (*e.g.* rods and lamellae) or to polymeric vesicles (polymersomes).[21] Depending on the molecular arrangement, reverse polymeric micelles with hydrophobic corona and hydrophilic core can be also produced in non-aqueous media.[22] However, only the former are relevant for drug-delivery purposes. The molecular properties of polymeric micelles can be tailored to adjust the size of the core and the nature and strength of core-drug interactions. In addition, the corona can be decorated with specific ligands to facilitate active drug targeting by means of the selective uptake mediated by specific receptors.

Polymeric micelles can be administered by different routes such as oral[23,24] and ocular,[25,26] though parenteral is the most extensively investigated one.[19] Approved conventional surfactants (*e.g.* polyethoxylated castor oil or polysorbate 80) form regular micelles in water and they are profusely employed for drug solubilization.[27] Nevertheless, these pharmaceutical excipients are not deprived of toxic effects. Moreover, when regular micelles undergo dilution to a final concentration below the CMC, they disassemble instantaneously and the drug is released into the medium. Conversely, polymeric micelles are safer for parenteral administration and more stable under dilution, providing more prolonged circulation times. In addition, cores are larger resulting in greater encapsulation capacity.[19]

5.2.1 Micellar Encapsulation

The capacity of polymeric micelles to encapsulate a drug can be expressed by (i) the micelle–water partition coefficient defined as the ratio between the drug concentration inside the micelle and in the aqueous medium,[28,29] (ii) the number of moles solubilized per gram of hydrophobic block, and (iii) the molar solubilization ratio (MSR) that is the molar ratio between the drug and the copolymer. Even though some solubilization capacity can be observed at copolymer concentrations below the CMC,[30] the most substantial solubilization is expected above this point owing to the ability of drug molecules to accommodate within the core. Paterson *et al.*[30] proposed two simple equations to describe the solubilization process below the CMC (Equation 5.1) and above it (Equation 5.2):

If $Cs < \mathrm{CMC}$

$$\frac{S_{apparent}}{S} = 1 + K_{\mathrm{unimer}} \cdot Cs \tag{5.1}$$

If $Cs > \mathrm{CMC}$

$$\frac{S_{apparent}}{S} = 1 + K_{\mathrm{unimer}} \cdot CMC + K_{\mathrm{micelle}} \cdot (Cs - CMC) \tag{5.2}$$

where $S_{apparent}$ is the aqueous solubility of the drug measured in the micellar system, S is the molar intrinsic solubility in pure water, C_S is the copolymer concentration in water, K_{unimer} and K_{micelle} are equilibrium constants describing the solute-unimer ($<$CMC) and solute-micelle ($>$CMC) interactions.

The incorporation capacity of drug molecules by a certain copolymer depends on its molecular weight and its hydrophilic-lipophilic balance (HLB). In general, for similar molecular weights, the lower the HLB is, the greater the encapsulation capacity. Concomitantly, copolymers displaying similar HLB and greater molecular weight tend to display greater encapsulation capacity than those with smaller molecular weight. Moreover, encapsulation is also governed by drug features such as molecular volume or lipophilicity. In other words, the performance of specific amphiphiles needs to be assessed for each single molecule. The ideal solubility of a drug is governed by the intensity of the solute–solute interactions; the stronger these forces, the higher the melting temperature, T_m. Solubilization depends on the generation of strong solute–core interactions (*e.g.* hydrophobic forces) that overcome the solute–solute ones. Thus, drugs displaying low T_m are encapsulated more effectively than those with a greater one. For example, Chiappetta *et al.*[31,32] investigated the solubilization of triclosan (289.5 g/mol; $T_m = 55–57\,^\circ C$) and triclocarban (315.6 g/mol; $T_m = 255\,^\circ C$) in a variety of branched poly(ethylene oxide)-poly(propylene oxide) (PEO-PPO) polymeric micelles. These two anti-bacterial agents display similar molecular structure and molecular weight though very different T_m. The physical stability of the drug-loaded micelles was strongly dependent on the T_m of the encapsulated drug, being high for triclosan and very low for triclocarban. It is also interesting to note that even though the drug–core interaction plays a fundamental role in the encapsulation process, in some cases the interaction of certain hydrophilic functional groups of the drug molecule with the corona can contribute to improve the solubilization performance, as demonstrated with triclosan under different pH conditions.[31]

5.2.2 Preparation Methods

According to (i) the physico-chemical properties of the copolymer and more specifically those of the hydrophobic block and (ii) the properties of the drug, different techniques can be employed to produce drug-loaded polymeric micelles.[21,33] The direct method may comprise the solubilization of the copolymer to obtain polymeric micelles and the subsequent solubilization of the drug that initially remains in suspension and it is gradually incorporated into the micelles until its complete dissolution. When the encapsulation capacity of a certain copolymer with respect to a drug is being assessed, a drug excess is added and the system is allowed to reach the equilibrium for 48–72 h at a constant temperature. Then, the drug excess is removed by filtration and the drug payload quantified. This method is the preferred one because it prevents the use of organic solvents and the implementation of additional operations to remove them. It is commonly used with copolymers of intermediate hydrophobicity that are water soluble and for the encapsulation of drugs with low to intermediate molecular weight. In contrast, when the copolymer is highly hydrophobic and it does not solubilize conveniently in water, both copolymer and drug are primarily solubilized in a water-miscible organic solvent (*e.g.* dimethylformamide or acetone) and poured into water. Then, polymeric micelles are formed upon the elimination of the organic solvent by evaporation or dialysis. The main disadvantage of dialysis is that part of the encapsulated drug can be lost in the dialysis medium, thus leading to lower drug payloads. Alternatively, the drug and the copolymer can be dissolved in a water-immiscible solvent, which is subsequently evaporated. Only then, the film is reconstituted with water to form the drug-loaded micelles.[21] A main constraint of this approach is that highly hydrophobic copolymers can be used in relatively low concentrations between 1 and 2%. Also, the presence of organic solvent residues needs to be quantified to ensure that the remaining concentrations are below the maximum established limits. Other procedures can be applied to fit the properties of the copolymer and the drug. It is worth mentioning though that changes in the technique may result in systems with different drug payloads, micellar size and size distribution and physico-chemical stability.[34,35]

5.2.3 Physical Stability

One of the main drawbacks of polymeric micelles is that they tend to disassemble upon administration and dilution in the biological environment. Disassembled polymeric micelles cannot maintain the encapsulated molecule within the core, and the drug is released into the medium where it can undergo nucleation, crystallization and precipitation. Even though the system is thermodynamically instable below the CMC and will finally disassemble, the kinetics of the process depends on the properties of the copolymer (*e.g.* molecular weight, HLB, core amorphousness or semi-crystallinity and cohesion).[36,37] In general, the stability of relatively hydrophilic copolymers is jeopardized to a greater extent than that of more hydrophobic ones because the gap between the CMC and the final concentration upon dilution is greater. Thus, several works improved the stability of the systems by increasing the hydrophobicity of the amphiphiles.[37] However, the analysis is not so straightforward because the intrinsic properties of the drug may also condition the overall physical stability of the system; drugs displaying stronger solute–solute interactions and higher T_m tend to precipitate faster than those with lower T_m.[31,32] Also, encapsulated drugs may favor or disfavor the aggregation of the amphiphile itself and greater drug–core cohesion may result in higher physical stability when compared to the drug-free micelle.[38] For example, Chiappetta *et al.*[39] showed that the antiretroviral efavirenz (EFV) promotes the self-aggregation of pristine and N-methylated branched PEO-PPO block copolymers (poloxamines). In this regard, it is crucial to monitor the long-term physical stability of the drug-loaded micelles upon dilution in media that are relevant to the clinical use; *e.g.* gastric-mimicking medium.

Two main approaches have been developed to stabilize physically polymeric micelles and to prevent their disassembly upon dilution: (i) core cross-linking, and (ii) corona cross-linking.[40] Both pathways demand the chemical modification of the amphiphile with reactive functional groups and show pros and cons. The physical[41] or chemical[42–45] cross-linking of the core conserves the functionality of the terminal groups exposed on the micellar surface and enables the conjugation of ligands that are useful in active drug targeting. On the other hand, the drug loading capacity and the release rate can be reduced owing to a more densely packed core. Conversely, to cross-link the corona, terminal groups (*e.g.* hydroxyl) are modified and reacted with coupling bifunctional molecules or by free radical polymerization. Depending on the cross-linking density, the corona displays variable permeability, this parameter affecting drug encapsulation and release.[46–49] This is an interesting feature that can be exploited to develop micelles that display rate-controlling coronas and to fine-tune the release kinetics from the drug reservoir. It is worth remarking that to prevent the chemical modification of the drug, the stabilization stage is often carried out before the drug loading. Thus, the chemical modification of the micelle can alter the encapsulation capacity with respect to the pristine copolymer. Moreover, irreversibly cross-linked systems might display problems related to a more limited clearance from the body and they need to be engineered appropriately to ensure biocompatibility and to prevent accumulation.[37] In this context, a number of researchers developed covalently cross-linked polymeric micelles that disassemble *in vivo* by different biological pathways and that are eliminated more effectively.[50–53]

Regardless of the fact that stabilized micelles extend the circulation time under dilution, this phenomenon does not necessarily result in an improved therapeutic index of the drug. Thus, the appropriate balance between effective drug encapsulation and stabilization and drug release needs to be attained.[54] Otherwise a strong core–drug interaction will curtail the gradual release of free drug with an appropriate kinetics. Amphiphiles bearing a semi-crystalline core such as those with hydrophobic blocks made of poly(ε-caprolactone) (PCL) usually withstand better the dilution phenomena than those with amorphous cores (*e.g.* poly(propylene glycol)). However, they are not physically stable in suspension and tend to fuse and cluster into larger aggregates that finally precipitate.[55] To conserve these micelles in the long term, they usually need to undergo freeze-drying, a process that needs to be conducted in the presence of lyo-/cryoprotectants.[56–59] Regardless of the stabilization strategy, the physical stability and the properties of each drug-loaded system need to be comprehensively assessed to understand their behavior *in vivo*. Some pathologies are characterized by the localized increase of the temperature or the decrease of the pH. In this context, nanocarriers can be tailored to release the drug locally upon a change in the microenvironment.

5.3 Temperature-sensitive Polymeric Micelles

Temperature is the most extensively exploited stimulus in the design of environmentally responsive biomaterials, namely smart materials.[60] In addition to the above-mentioned CMC, these amphiphiles display a critical temperature that delimits their ability to self-assemble and it is known as critical micellar temperature (CMT). This parameter depends on intrinsic copolymer features (*e.g.* molecular weight, HLB) and also on the copolymer concentration.

Temperature-responsive amphiphiles can be classified into two main categories, (i) positive and (ii) negative, and they are characterized by an upper critical solution temperature (UCST) and a lower critical solution temperature (LCST), respectively. The latter phenomenon was also coined reverse thermal gelation or RTG behavior by Cohn and collaborators.[61] UCST and LCST indicate a sol-gel transition point. Having expressed this, micellization can be attained at concentrations and temperatures that are far below those required for the generation of a gel. Moreover, low molecular weight derivatives usually micellize, though do not necessarily gel. In general, most of the pharmaceutical applications employ copolymers that undergo micellization upon heating at temperatures close to 37 °C, because polymeric micelles can be obtained under milder conditions.[60] The present section will describe the most relevant temperature-responsive copolymers and their main applications in drug delivery.

5.3.1 Poly(ethylene Oxide)-Poly(propylene Oxide) and Other Polyether Amphiphiles

PEO-PPO block copolymers are the most extensively investigated micelle-forming copolymers.[62–64] One of the most appealing features of PEO-PPO water solutions is that they gel upon heating around 37 °C and they can be used to develop a variety of injectable systems for different biomedical applications.[65,66] Based on their molecular structure, PEO-PPOs are classified into two groups: (i) linear and bifunctional PEO-PPO-PEO triblocks (poloxamers, Pluronic®, Scheme 5.1A) and (ii) X-shaped tetrafunctional derivatives (poloxamine, Tetronic®, Scheme 5.1B). The regular derivatives combine terminal hydrophilic

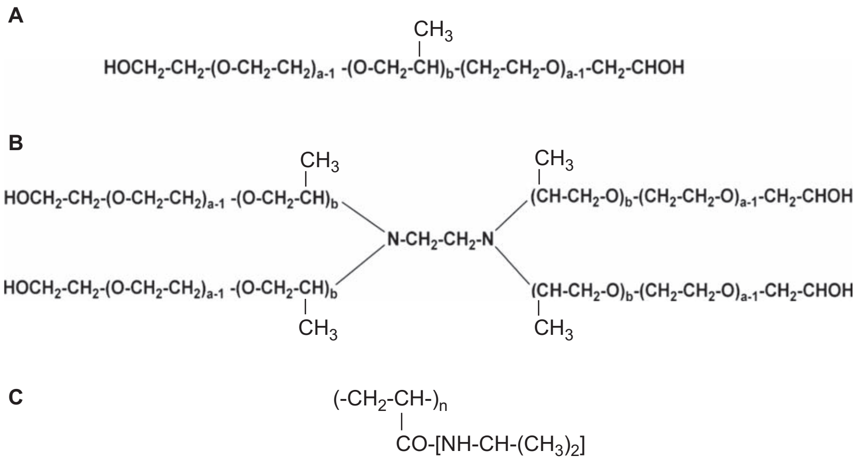

$HOCH_2\text{-}CH_2\text{-}(O\text{-}CH_2\text{-}CH_2)_{a-1}\text{-}(O\text{-}CH_2\text{-}\underset{|}{\overset{CH_3}{CH}})_b\text{-}(CH_2\text{-}CH_2\text{-}O)_{a-1}\text{-}CH_2\text{-}CHOH$

$(\text{-}CH_2\text{-}\underset{CO\text{-}[NH\text{-}CH\text{-}(CH_3)_2]}{CH}\text{-})_n$

Scheme 5.1 General molecular structure of (A) poloxamer, (B) poloxamine and (C) poly(*N*-isopropylacrylamide).

PEO blocks and central PPO ones and form micelles in aqueous medium, being the most relevant as pharmaceuticals. Conversely, there exist reverse-sequential counterparts that display terminal hydrophobic blocks and central hydrophilic ones. In less polar solvents, these derivatives generate reverse micelles that display a hydrophilic core and a hydrophobic corona. PEO-PPOs are biocompatible for topical, oral and parenteral administration[67] and, in general, they have shown good cytocompatibility.[68–71] PEO-PPOs are not biodegradable, though molecules displaying molecular weights below 10–15 kDa can be bioeliminated by renal filtration.[72–74] In addition, polymeric micelles with coronas made of PEO are sterically stabilized (Stealth®) and minimize opsonization and uptake by macrophages, prolonging circulation time *in vivo*.[75]

Poloxamers and poloxamines are commercially available in different molecular weights and EO/PO molar ratios and some linear derivatives were approved by the US Food and Drug Administration (FDA) and the European Medicines Agency (EMA) as pharmaceutical excipients in medicines and medical devices.[76–78] The branched counterparts display two main distinctive features. An ethylenediamine central moiety (and two tertiary amines) that confers the molecule responsiveness to pH[79–81] and enables chemical modification of the core.[39,82] For example, quaternization of poloxamines by means of N-alkylation not only partially suppressed pH-responsiveness, but it also modified the self-aggregation pattern (that resembled poloxamines at low pH), the drug-core affinity and the cytotoxicity.[39,83,84] Even though poloxamines are dually responsive molecules to temperature and pH, they are discussed in this section because the stimulus usually exploited is temperature. However, changes in the aggregation/gelation/drug release under different pH conditions have been reported.[85] Poloxamines display two pK_a values at 3.8–4.0 and 8.0 with minimal changes among derivatives of different molecular weight and HLB.[86] At low pH both amine groups are protonated, coulombic repulsion prevents micellization, and CMT is shifted to a greater temperature.[87] At neutral pH, aggregation increases due to the partial disprotonation of the central group, becoming maximal at $pH > 10–12$ where molecules are completely unprotonated.[87,88] The higher the pH is the greater the aggregation number, the larger the size and the more homogeneous the size distribution of poloxamine micelles.[80] Accordingly, poloxamines display maximum solubilization capacity at $pH > 8–10$. In this framework, the release in biological microenvironments displaying reduced pH could be envisioned.

The mechanism behind the micellization of PEO-PPO and other amphiphilic copolymers is entropy-driven and mainly related to the release of water hydration molecules from the PPO blocks.[89] Thus, the CMC and the CMT depend on the molecular weight and the EO/PO ratio; the greater the HLB and the lower the molecular weight, the higher the CMC and the CMT are.[90] In addition, derivatives of greater molecular weight (and similar HLB) display smaller CMC and CMT.

Since PEO-PPOs are thermo-responsive, the CMC, the micellar size and the size distribution are also strongly dependent on the temperature. At higher temperature, the micellization tendency increases, leading to a smaller CMC and a greater fraction of molecules in micellar form.[91–96] Consequently, the drug encapsulation and solubilization capacity of these copolymers grows with the temperature. Even though PEO-PPOs are non-ionic surfactants, the micellization process can also be affected by the presence of salts and different types of ions that produce salting-out or salting-in phenomena. In general, the greater the concentration of neutral salts, the smaller the CMC and the CMT.[97–100] In this context, some authors proposed a new parameter, namely the critical micelle salt concentration (CMSC), defined as the salt concentration at which micelles begin to form, though this parameter should be determined for every salt type. However, the analysis is not straightforward because extensive studies with different salts suggested that the behavior is not predictable based on the prior art.[101,102]

Most of the research at the interface of PEO-PPOs and drug encapsulation focused on poloxamers.[64] It is worth noting that these developments were intended for a broad spectrum of administration routes, from topical to intravenous. In general, the addition of more amphile molecules above the CMC results in the formation of additional micelles and in the growth of the encapsulation capacity of the micellar system. Considering the relatively high aqueous solubility of PEO-PPOs, concentrations as high as 10–15% can often be obtained. In addition, the use of concentrations above 20–25% enables the generation of physical gels where the drug is primarily encapsulated within the micelles that form 3D networks. This is the reason that Pluronic® F127 has become probably the most extensively investigated of all the poloxamers, a selection that is further supported by the fact that this derivative is currently FDA-approved for use in pharmaceutical products.[64]

Drug-loaded poloxamer micelles were also combined with physical means such as ultrasound to target the release of doxorubicin to tumors.[103–109] Systems accumulated preferentially in the tumor by the EPR effect and then irradiation improved the cellular uptake of the drug. Pitt *et al.*[109] suggested that ultrasound transiently destroys the micelles by cavitation, increasing the drug release in the irradiated area. Ultrasound-triggered release from micelles is tackled in Chapter 6.

In the last years, a few groups investigated more comprehensively the self-aggregation and the capacity of poloxamines to solubilize, stabilize physicochemically and release different drugs.[31,32,39,64,84,110–112] Alvarez-Lorenzo *et al.*[113] assessed the encapsulation of the antifungal griseofulvin in 10% solutions of poloxamine T904 under different pH conditions. The solubility increased three and six times at acid and alkaline pH-values, respectively. A similar behavior has been shown for triclosan in poloxamine T1107 micelles, though solubilization was improved from 2 μg/mL to up to 30 mg/mL (more than 15,000 times).[31] However, this system was more complex owing to the ionization of the drug at $pH > 10$. The most relevant outcome was that triclosan-loaded micelles showed better antibacterial activity than the free drug, even against hospital resistant strains such as methicillin-resistant *Staphylococcus aureus* and vancomycin-resistant *Enterococcus faecalis* and in a

Staphylococcus epidermidis biofilm model. These systems could be effective in the prevention and treatment of topical infections. In another study, a molecularly related drug with an extremely poor water solubility, triclocarban (solubility = 50 ng/mL), was evaluated in poloxamines T1107 and T1307.[32] Both copolymers display similar HLB, though T1307 solubilized the drug more efficiently due to a greater molecular weight and a larger micellar core.

To investigate the chemical stabilization of simvastatin, a hypolipidemic drug that in the stomach is reversibly converted from its absorbable lactonic form to an open carboxylic one (decreasing oral bioavailability), a broad spectrum of drug-loaded poloxamines was prepared.[84] Some derivatives improved the solubility up to 152 times and partially or completely prevented the hydrolysis. In this work, the self-aggregation behavior of N-methylated poloxamine T1107 was assessed for the first time. This chemically modified derivative improved the encapsulation capacity and stability of simvastatin, strongly suggesting a greater drug–core interaction than the pristine derivative.

Our group has recently explored a broad variety of linear and branched PEO-PPOs for the encapsulation of different antiretrovirals employed in the treatment of the human immunodeficiency virus (HIV) infection. EFV is a first-line antiretroviral for the treatment of HIV-infected children above 3 years of age. EFV displays several (bio)pharmaceutic drawbacks such as poor aqueous solubility, low oral bioavailability and high inter- and intra-subject variability. To improve the (bio)pharmaceutic properties of the drug and develop a pediatric formulation, EFV was encapsulated within single and mixed micelles.[114–117] The aqueous solubility of the drug was increased more than 8400 times (from 4 μg/mL to 34 mg/mL).[39,114] Regardless of the great drug payload, the size was usually <100 nm and morphology was spherical (Figure 5.1A).[39,114] Poloxamine T904 showed the best encapsulation capacity of all the investigated copolymers, though it was less physically stable than F127 micelles. Thus, aiming to improve both features F127/T904 mixed micelles were developed.[117] Remarkably, EFV-loaded T904 and F127 micelles were physically stable under strong dilution (up to 1 : 75) over 1 month, at 37 °C.[116] Extensive preclinical investigations of micelles with different composition and size, different drug payload and dose and administration conditions showed a statistically significant increase of the oral bioavailability with respect to a compounded suspension and an oily solution (Figure 5.1B–D).[114,115] The administration of the copolymers did not show any acute adverse effect. A remarkable advantage of poloxamers from a translational perspective over other experimental copolymers is that some of them have been approved as pharmaceutical excipients. Thus they can be used in clinical trials without further evaluations. On the other hand, it should be stressed that poloxamines display two main drawbacks: (i) a more limited variety of derivatives are commercially available and (ii) they are not currently approved as pharmaceutical excipients for the production of medicines. Thus, regardless of the greater encapsulation efficiency of poloxamine T904 with respect to F127, this later copolymer was chosen for the preparation of an EFV-loaded micellar system to be tested regarding oral bioavailability and compared to drug

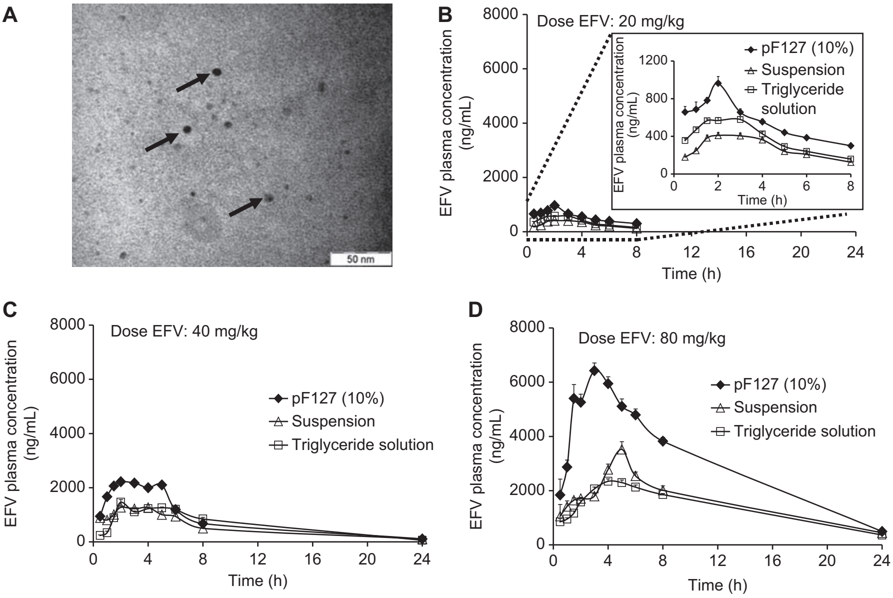

Figure 5.1 (A) Transmission-electron micrograph of EFV-loaded 10% micelles of poloxamine T1307 in buffer (pH 5.0) and negatively stained with 2% phosphotungstic acid. Arrows point out the presence of spherical micelles of variable sizes. (B–D) EFV plasma concentrations after the oral administration of: (A) 20 mg/kg, (B) 40 mg/kg and (C) 80 mg/kg. Results are expressed as mean ± S.E. (n = 8).
(Reproduced from (A) Ref. 114 with permission of Future Medicine and (B–D) Ref. 115 with permission of Elsevier.)

capsules, in a clinical trial with adult healthy volunteers. This versatile platform has also been implemented to investigate the interaction of EFV with the breast cancer resistant protein (BCRP) pump in intestine and central nervous system.[118,119] In this case, the administration route was oral or intravenous.

The blood-brain barrier (BBB) prevents the passage of xenobiotics from plasma into the central nervous system (CNS) and contributes to the generation of one of the most challenging HIV sanctuaries.[120,121] The presence of the virus and the limited access of antiretrovirals may result in HIV-1 encephalitis (HIVE-1), a disease that is more frequent in neonates and children.[122–124] To target EFV to the CNS without the need of expensive chemically modified nanocarriers, recently these EFV-loaded micelles were administered by intranasal route.[125] The CNS bioavailability and the relative exposure index (REI) increased four and five times, respectively, compared to the systems administered intravenously; REI was calculated as the ratio between the area-under-the-curve in CNS and in plasma. In a different application, the ionizable groups of poloxamine were capitalized to complex and stabilize negatively charged DNA,[126] and also to transfect plasmid DNA in skeletal muscle *in vivo*.[127,128]

To overcome different drawbacks, such as the low viscosity of PEO-PPO gels that usually leads to short residence time at the application site *in vivo*, different research groups employed poloxamers as platforms to design a variety of counterparts with improved features. Cohn *et al.*[129–135] improved the macro- and microviscosity of the gels by means of chain extension and *in situ* cross-linking. The same research group introduced cross-linked thermo-responsive nanoshells with interesting features.[136,137] Alvarez-Lorenzo *et al.*[138] grafted poloxamers with poly(acrylic acid) segments to solubilize and chemically stabilize the lactonic form of the antitumoral drug camptothecin; the open carboxylic form is not active. The amphiphiles became dually responsive to temperature and pH. Interestingly, results suggested that the drug was solubilized by both the core and the corona. This aspect deserves a separate comment as it is usually assumed that only drug–core interactions govern the encapsulation capacity of polymeric micelles, but there are a few studies that demonstrated that also drug–corona interactions can contribute to increase the encapsulation capacity of the nanocarrier.[31,138]

Encapsulated drugs can modify the self-assembly of the copolymer. In other words, parameters such as CMC, CMT, aggregation number, cloud point, and micellar size and size distribution can undergo substantial changes in the presence of small drug molecules. It seems that this phenomenon would be more relevant in the case of drugs that hinder the aggregation process. On the other hand, drugs that promote aggregation could be capitalized to improve the properties of amphiphiles displaying poor or incomplete micellization tendency. Most of the research prioritized the study of drug solubilization and did not assess the effect of the drug on the amphiphile aggregation. This incomplete characterization may result in inconsistent and unpredictable data *in vitro* and *in vivo*. Tontosakis *et al.*[139] reported that small *o*-xylene concentrations increase the aggregation of poloxamers. A similar effect was observed with phenol.[140] Conversely, urea hampered the aggregation of Pluronic® P85, leading to the increase of CMC and CMT.[141] Naproxen and indomethacin did not change the CMC of Pluronic® F127, but the size of the micelles and the aggregation numbers decreased sharply.[142] More recently, the pro-aggregation performance of EFV on different pristine and N-alkylated poloxamines has been also described.[39]

A main drawback of PEO-PPOs, regardless of their molecular features, is that owing to the relatively low hydrophobicity and amorphousness of PPO the self-assembly is incomplete. This phenomenon is more remarkable for more hydrophilic counterparts, at 25 °C. Aiming to increase the micellization tendency and reduce the CMC, the group of Attwood replaced PPO by more hydrophobic polyethers such as poly(butylene oxide) (PBO), poly(styrene oxide) (PSO) and poly(phenyl glycidyl ether) (PGO) and reported a prolific bibliography on the aggregation phenomena of various derivatives.[143–157] Different molecular architectures such as A-B diblocks, and A-B-A and B-A-B triblocks, where A and B are the hydrophilic and the hydrophobic component respectively, led to the generation of a broad spectrum of derivatives with unique and improved properties. Due to a greater hydrophobicity, these micelles displayed greater solubilization ability and physical stability than PEO-PPOs. Another aspect that merits consideration is the relative hydrophobicity of the new segment with respect to PPO. For example, PBO is four times more hydrophobic than PPO;[94] thus, 4-fold PEO/PBO ratios are demanded to attain micellization properties similar to those of PEO-PPO copolymers. In addition, as opposed to PPO that is 100% amorphous, PBO, PSO and PGO can undergo crystallization. This difference may demand changes in the preparation procedure, more prolonged solubilization time at low temperature and additional studies to assess their physical stability in suspension and their ability to withstand lyophilization.[153]

In any event, the fact that PEO-PPOs are commercially available and that some of them have already been approved by the main regulatory agencies and that additional ones are under clinical evaluation constitutes a remarkable advantage over other experimental copolymers even if they display improved features.

5.3.2 Poly(ethylene Oxide)-Polyester Block Copolymers

Polyethers are not biodegradable and their bioelimination by renal filtration depends on the molecular weight. Aiming to develop biodegradable amphiphiles and new molecular architectures, poly(ether-ester)s that combine PEG hydrophilic blocks with hydrophobic ones of poly(lactic acid) (PLA) and/or PCL were synthesized and extensively characterized.[158–168] A major advantage of these copolymers is that they can be obtained by ring opening polymerization (ROP) reactions initiated by the corresponding PEG initiator with lactide and ε-caprolactone precursors in the presence of a catalyst. This synthetic pathway results in poly(lactone)-PEG-poly(lactone) block copolymers. Based on the functionality of the initiator (mono-, di- or multifunctional), biomaterials with different architectures were tailored. For example, Salaam *et al.*[169] employed tetrafunctional PEG initiators for the synthesis of 4-star copolymers. As opposed to PEO-PPO-PEO and other polyether triblock amphiphiles that display a central hydrophobic block linked to two terminal hydrophilic ones, when these molecules are synthesized by ROP of lactones employing bifunctional PEG molecules, the hydrophilic block is in the center. This molecular arrangement leads to the generation of "flower-like" micelles, where the looped hydrophilic corona often confers on the system the outlook of flower petals.[170,171] Modifications of the synthetic procedure enabled the preparation of PEG-poly(lactone)-PEG, where the polyester block was in the center of the triblock.[172–175] In this case, PEG-poly(lactone) diblocks were primarily obtained employing a monofunctional PEG and they were coupled with a bifunctional coupling agent (*e.g.* diisocyanate) to render the triblocks. In general, these polymeric micelles display larger cores than those of PEO-PPO, hydrodynamic diameters usually being >30–50 nm. It is worth stressing though that the size is strongly dependent on the molecular weight of the copolymer, the HLB, the copolymer concentration and the block organization along the copolymer backbone. In addition, the core can undergo enlargement upon the incorporation of the drug. Owing to the greater hydrophobicity of PLA and PCL, these nanocarriers fitted for the solubilization of more bulky and hydrophobic drugs such as paclitaxel,[176,177] norfloxacin,[170] rifampicin[178–180] and tacrolimus.[181] Paclitaxel has been the most extensively investigated drug for encapsulation in this kind of polymeric micelle because this antitumoral drug is usually solubilized in surfactants (*e.g.* Cremophor EL) that provoke serious hypersensitivity reactions.

A main limitation of these copolymers is that because of the low solubility of the hydrophobic blocks, polymeric micelles are commonly prepared by the co-solvent method. In addition, copolymer concentrations are small, usually in the 1–2% range. Recently, Moretton *et al.*[178] reported on the development of PCL-PEG-PCL micelles with concentrations as high as 6%. Rifampicin was efficiently encapsulated and the aqueous solubility was increased up to five times.[178] The encapsulation process protected the drug from degradation in acid medium with soluble isoniazid, another potent first-line antituberculosis drug. These systems were proposed as a nanotechnology platform to develop innovative pediatric rifampicin/isoniazid fixed-dose combinations with improved oral rifampicin bioavailability.[180] Another limitation stems from the great re-aggregation tendency shown by these micelles that demand lyophilization in the presence of cryo-/lyoprotectants to stabilize them physically in the long-term range.[179,182,183]

More recently, Cho and Kwon employed dual systems based on (i) PEG-PLA polymeric micelles to encapsulate three poorly water soluble antitumorals: paclitaxel, 17-allylamino-17-demethoxygeldanamycin and rapamycin, and (ii) PEG-PCL micelles to load a carbocyanine dye for the more sensitive imagining of the tumor by near-infrared (Figure 5.2).[184] This strategy known as theranostics (therapeutics + diagnostics) could be useful for intra-operative surgical guidance in oncology.

5.3.3 Poly(*N*-isopropylacrylamide)

Together with PEO-PPOs, poly(isopropylacrylamide) (pNIPAAm) is one of the most popular thermo-responsive smart materials (Scheme 5.1C). From the reports by Tanaka in the late 1970s,[185] a broad spectrum of applications have been described for pristine pNIPAAm and its copolymers, such as diagnostics, separative chemistry, biosensors and drug delivery.[186] Another application of pNIPAAm gels is the engineering of cell sheets developed by Okano and collaborators,[187] which is covered in Chapter 23.

PNIPAAm displays a LCST around 32–33 °C in water, thus it is water soluble below this temperature and water insoluble above it. The mechanism involves the generation of hydrophobic interactions upon heating. This property was capitalized to develop polymeric micelles made of pNIPAAm as the hydrophilic component and different hydrophobic ones.[188] The most common hydrophobic blocks were polystyrene,[189] dimethylacrylamide,[190] alkyl residues,[191] PLA,[192] butylmethacrylate,[193] poly(*N*-vinylimidazole),[194] acrylamide[195] and methylmethacrylate.[196] In addition, pNIPAAm has been

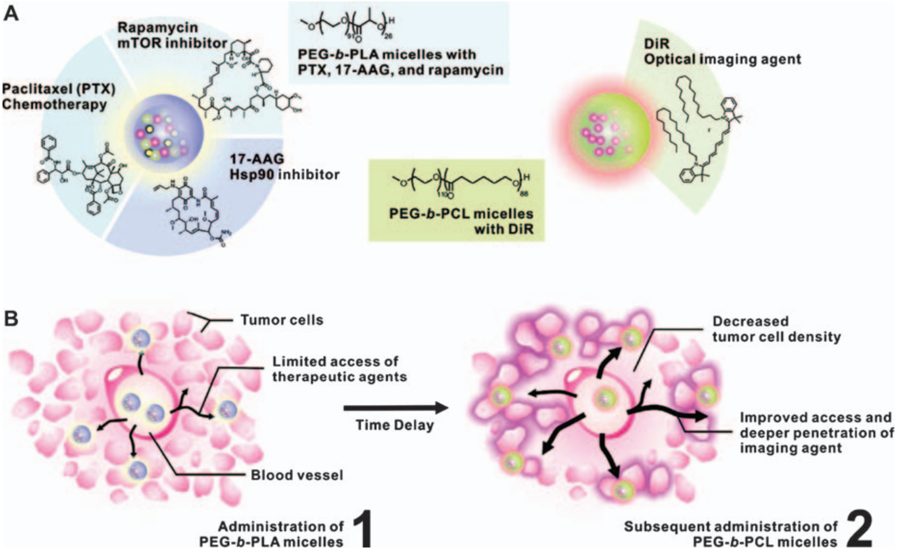
A
Rapamycin
mTOR inhibitor
PEG-*b*-PLA micelles with
PTX, 17-AAG, and rapamycin
Paclitaxel (PTX)
Chemotherapy
17-AAG
Hsp90 inhibitor
PEG-*b*-PCL micelles
with DiR
DiR
Optical imaging agent
B
Tumor cells
Limited access of
therapeutic agents
Time Delay
Blood vessel
Decreased
tumor cell density
Improved access and
deeper penetration of
imaging agent
Administration of
PEG-*b*-PLA micelles
1
Subsequent administration of
PEG-*b*-PCL micelles
2

Figure 5.2 (A) 3-in-1 PEG-PLA micelles containing paclitaxel/17-allylamino-17-demethoxygeldanamycin/rapamycin and PEG-PCL micelles containing a carbocyanine dye. (B) Scheme of the tumor-primed delivery of the carbocyanine dye.
(Reproduced from Ref. 184 with permission of the American Chemical Society.)

copolymerized with hydrophilic monomers to fine-tune the self-aggregation properties and the thermal responsiveness.[197]

The corona is highly hydrated below the LCST and it undergoes dehydration and shrinkage above it. Thus, these micelles can be accumulated in tumors by EPR and the heating and consequent shrinkage promote the fast release of the encapsulated drug in the target tissue/organ (Figure 5.3).[193] The LCST can be fine-tuned to be slightly higher than 37 °C and to release the drug only under hyperthermia.[192,198] For example, Liu *et al.*[195] developed a p(NIPAAm-co-acrylamide)-b-PLA copolymer with LCST of 41 °C for the encapsulation and thermal release of docetaxel. *In vitro* assays indicated that under hyperthermia, micelles were more cytotoxic to different tumor cell lines and less toxic to human umbilical endothelial cells than a standard formulation, indicating the accelerated release of the encapsulated drug. Docetaxel-loaded micelles were more effective *in vivo*.[199,200] When the temperature-dependent transition of NIPAAm is above 37 °C, triggering of drug release *in vivo* requires the use of an external physical stimulus such as ultrasound.

One of the most appealing characteristics of pNIPAAm is the great chemical versatility to tailor novel copolymers with tunable self-assembly, drug encapsulation and release performance. The synthesis of random and block copolymers employing different modalities of free-radical polymerization with chain transfer agents, polycondensation and ring-opening polymerization

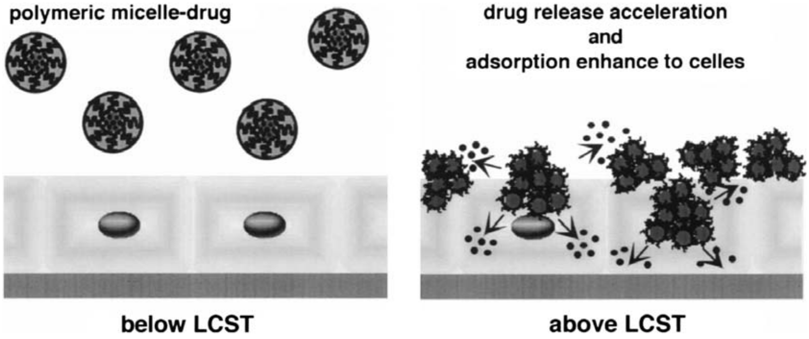

Figure 5.3 Temperature-modulated drug release and interactions between micelles with pNIPAAm as shell-forming segments and cells.
(Reproduced from Ref. 193 with permission of Elsevier.)

enabled the exquisite control of the molecular architecture, the copolymer composition and block arrangement and the physico-chemical properties. For example, the group of Leroux copolymerized NIPAAm, methacrylic acid (MAA) and octadecyl acrylate (ODA).[201] NIPAAm and MAA formed the corona, while ODA formed the core. The incorporation of MAA pH-sensitive blocks resulted in dually responsive systems. Liu *et al.*[202] synthesized pNIPAAm copolymers with poly(lactide-co-glycolide) (PLGA) blocks of different lengths for the encapsulation of doxorubicin. The drug-loading capacity increased with longer PLGA blocks. Interestingly, micelles were stable at 37 °C though they underwent deformation above body temperature leading to the accelerated release of doxorubicin. The synthesis and self-assembly of amphiphiles with more complex architectures such as poly(benzyl ether)-b-pNIPAAm dendritic linear diblocks displaying two collapse stages has also been reported.[203]

To overcome the physical instability of polymeric micelles, Wei *et al.*[196] incorporated a small concentration of 3-(trimethoxysilyl)propyl methacrylate to pNIPAAm micelles in order to cross-link the corona by means of the sol-gel technology. Cross-linked micelles displayed greater encapsulation efficiency and were more physically stable than the non-cross-linked counterparts because they did not re-aggregate upon heating, a behavior that led to a sharp size growth of the non-cross-linked system. In addition, the release rate of encapsulated prednisone was 20 times slower above the LCST. In a more recent work, the same authors decorated the surface with biotin to confer the micelle pretargeting properties in cancer.[204] Similarly, micelles were conjugated with folate for intra-cellular delivery of antitumorals in cells expressing the folate receptor.[205]

The modification of the precursors and the synthetic pathways results in copolymers with different organization of the blocks along the backbone. In this context, molecules where pNIPAAm is flanked by two terminal hydrophobic arms of PCL or PMMA were also synthesized.[206,207] These copolymers formed “flower-like” micelles. When NIPAAm and ε-caprolactone were reacted *via* an atom transfer radical polymerization instead of ring opening polymerization, copolymers having a pNIPAAm-PCL-pNIPAAm structure that self-assembled into regular polymeric micelles.[208] Other groups designed copolymers having more complex molecular arrangements such as graft[209,210] and Y-[211,212] and star-shaped micelles, each system displaying advantages and drawbacks.[213,214] For example, Liu *et al.*[215] synthesized two pNIPAAM graft copolymers with negatively and positively charged backbones made of methacrylic acid and fully quaternized 2-(dimethylamino)ethyl methacrylate, respectively. In water, electrostatic interaction between both copolymers led to the generation of micelles with a polyion complex core and a thermo-responsive corona. The incorporation of azide moieties along the main chain allowed the cross-linking of the core to stabilize the micelles physically. PNIPAAm copolymers were also co-micellized with other types of amphiphiles to produce mixed micelles combining improved physical stability, targeting properties and imaging features.[216–218] Findings suggest that when engineered well, these micelles could be used in diagnosis, targeting and therapy.

As mentioned above, different hydrophobic blocks have been combined with PEG to produce self-assembly amphiphiles. Since pNIPAAm turns from hydrophilic at low temperature to hydrophobic above the LCST, the potential application of PEG-pNIPAAm copolymers has also been explored.[219–222] In general, most of these novel systems capitalized on the same pNIPAAm thermal transition to adjust the release rate of the encapsulated drug, and they have been evaluated *in vitro* and *in vivo*. Even if these works provide further evidence of the versatility of these biomaterials, the use of pNIPAAm and other non-biodegradable polymers by the parenteral route (*e.g.* intravenous) should be appropriately pondered, because *in vitro* cytotoxicity studies are certainly insufficient to ensure their biocompatibility and to demonstrate elimination from the body. In general, these polymers are eliminated by renal filtration as previously described for PEG.[72–74]

Recently, Bertrand *et al.*[223] investigated for the first time the fate of pNIPAAm polymers *in vivo* after intravenous administration. The effect of three key molecular properties, (i) molecular weight, (ii) amphiphilicity and (iii) LCST, on the elimination, the biodistribution and the accumulation was assessed (Table 5.1). In general, the greater the molecular weight, the longer the circulation time is; *e.g.* 30% of the administered dose of a copolymer of molecular weight 40 kDa was in the systemic circulation after 48 h (Figure 5.4).[223] Conversely, the fastest clearance from the bloodstream was observed for copolymers of (i) very low molecular weight (P-5k-NA, 5 kDa) that did not aggregate or (ii) high molecular weight that were insoluble in water (P-40k-L) at 37 °C, the former showing the greatest accumulation in the extravascular space. Copolymers of low molecular weight that formed micelles (P-5k) or of intermediate molecular weight showed intermediate elimination rates. In addition, findings indicated that the glomerular filtration cut-off of pNIPAAm molecules would be approximately 32 kDa; this value being slightly greater than that established for PEG.[72–74] LCST and HLB also affected the process. Nevertheless, data were not always consistent and

Table 5.1 Physico-chemical characteristics of pNIPAAm copolymers. (Adapted from Ref. 223 with permission of Elsevier.)

Polymer	*Initiator (mol%)*	*MAA (mol%)*	*^{14}C-AAm (mol%)*	*M_n (×10^3)*	*M_w/M_n*	*Solubility at 37 °C*	*CAC (mg/L)*
P-40k[a]	0.03	5	1	38.4	1.4	+	260
P-10k	1	5	1	11.5	1.7	+	42
P-5k	8	5	1	6.1	1.4	+	13
P-5k-NA[b]	15	5	1	5.0	1.7	+	330
P-40k-L	0.03	1.5	1	37.3	1.3	–	N.D.

[a]Also contains 5 mol% of cold acrylamide.
[b]Synthesized using non-alkylate initiator.
CAC: Critical Aggregation Concentration. N.D.: Not determined.

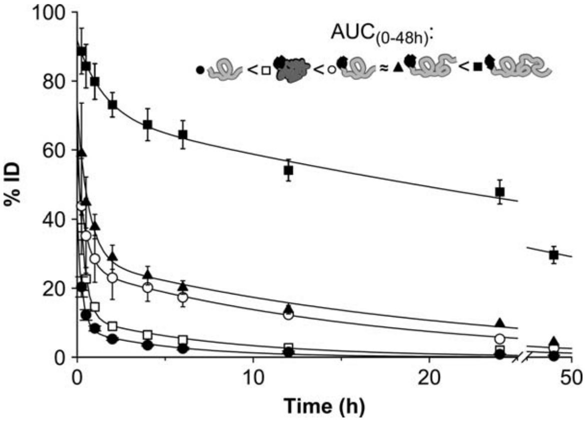

Figure 5.4 Blood level profiles of pNIPAAm copolymers with different molecular features. P-5k (○), P-10k (▲), P-40k (■), P-5k-NA (●) and P-40k-L (□). Mean ± SD ($n=5$–7), %ID represents the remnant percentage of injected dose.
(Reproduced from Ref. 223 with permission of Elsevier.)

clearance from the bloodstream did not necessarily mean elimination from the body. These aspects are very relevant, especially for systems envisioned for multiple administrations and where toxicity due to accumulation could take place. For an extensive overview of the most relevant developments in pNIPAAm micelles, readers are referred to the review of Wei *et al.*[188]

5.3.4 Substitutes of PEG as Hydrophilic Building Block

PEG is the gold-standard hydrophilic building block for the synthesis of thermo-responsive amphiphiles. However, potential substitutes have been proposed to prolong circulation times *in vivo*, especially upon repeated administration owing to the accelerated blood clearance phenomenon mediated by anti-PEG IgM.[224]

Poly[*N*-(2-hydroxypropyl) methacrylamide] (pHPMA) is a highly hydrophilic, biocompatible and non-immunogenic polymer that has been conjugated to a broad variety of hydrophobic blocks.[225–227] Due to the presence of pendant reactive functional groups along the main backbone, drugs can be conjugated for targeting purposes.[228] This functionality was also capitalized to conjugate short hydrophobic residues to pHMA-doxorubicin conjugates (*e.g.* oleoyl, dodecyl, oleic acid and cholesterol), leading to the generation of drug-loaded micelles where the drug was covalently bound to the nanocarrier.[229,230] Besides, pHMA has been reacted with PCL to form pHMA-PCL-pHMA triblocks and star-shaped micelles[231–233] and with pNIPAAm.[234–236]

Polyoxazolines (POs) are polymers obtained by the living cationic ring-opening polymerization of 2-oxazoline.[237] These materials display great chemical flexibility and biocompatibility[238,239] and therefore they have attracted much attention in recent years for the production of vesicles,[240,241] polymeric micelles[242,243] and other drug nanocarriers. The most remarkable advantages over PEG are water solubility, chain flexibility, non-toxicity and more fine-tunable synthesis of derivatives within a very narrow molecular weight range. In addition, due to their chemical versatility they can also be functionalized with hydrophobic moieties to produce self-assembly amphiphilic POs.

The production of drug-loaded micelles may require a final lyophilization stage. Poly(*N*-vinyl-2-pyrrolidone) is a non-ionic, biocompatible and water-soluble synthetic polymer that showed lyoprotectant and cryoprotectant properties. Thus, this polymer represents another alternative to replace PEG in systems that need to undergo lyophilization.[244,245]

5.4 pH-responsive Micelles

pH is another physiological stimulus exploited to design smart polymeric micelles. pH-responsive copolymers usually display pendant ionizable functional groups along the polymer backbone that undergo protonation or deprotonation upon slight changes in the physiological pH.[246,247] The transition between the charged and neutral state leads to changes in the osmotic pressure and to the collapse or the expansion of these polyelectrolyte micelles.

In general, polyelectrolytes are classified into weak polyacids and weak polybases such as poly(acrylic acid) and poly(4-vinylpyridine), respectively. The former undergo the transition in the 4–8 pH range, while the latter at pH > 7–8. In addition, these polymers display a fine balance between ionizable and hydrophobic groups. Thus, when repulsion disappears, the hydrophobic interactions promote self-aggregation.[247] Slight changes of the chemical structure enable the fine-tuning of the self-aggregation performance. For example, the phase transition of poly(acrylic acid) is continuous. Conversely, poly(methacrylic acid) shows a sharper transition due to the stronger hydrophobic interactions generated by the presence of methyl groups.[247] Following this trend, the replacement of methyl by longer alkyl moieties such as ethyl or propyl resulted in more compact conformations at low pH and more pronounced transitions.[248,249] Taking advantage of this feature, core-corona-shell micelles where the polyelectrolyte was conjugated to non-ionic hydrophilic and hydrophobic blocks like PEG and polystyrene, respectively, were also designed.[250,251] The size was governed by the aggregation number and the degree of swelling. The group of Leroux has synthesized a broad variety of copolymers employing methacrylic acid precursors that could be chemically modified to obtain cationic and anionic amphiphiles.[34,252–254]

The incorporation of pH-responsiveness is an interesting tool for the selective release of drugs in pathologies that are characterized by acidosis ($pH < 7.4$), such as ischemia, infection, inflammation and tumoral processes with decreased extra-cellular pH.[254–256] Much lower pH values can be found in intra-cellular compartments (*e.g.* endosomes, lysosomes). Thus, following cellular uptake, these drug-loaded nanocarriers may destabilize endosome membrane and lead to endosomal escape, a pathway that is crucial to ensure the intra-cellular delivery of the encapsulated drug. When the administration route is intravenous, polymeric micelles need to be physically stable at pH 7.4 and to undergo disassembly upon acidification.

pH-sensitive polymeric micelles containing hydrophobic carboxylic acid groups that form the micellar core could also be useful to fine-tune the drug release following oral administration.[254] Under stomach-like conditions, these groups are non-ionized and behave as hydrophobic, retaining the encapsulated drug within the core and minimizing its release. Then, alkalinization in the gut results in (i) deprotonation and expansion of the core due to electrostatic repulsion of carboxylate groups and (ii) weakening of the drug/core interaction that favors the release.[34,257] A fast pH response is essential to ensure the timely release in sites where the residence time is short, such as in the endosomes (30 min.).[254] It is worth noting that the pH-responsiveness of the nanocarrier can be adjusted by changing the composition of the micelle.[258] These systems are more advantageous than drug-copolymer conjugates where the release is governed by the hydrolysis of specific linkages under low pH conditions because the release kinetics is difficult to fine-tune.

Polyaminoacids have also emerged as appealing building blocks for the synthesis of pH-sensitive micelles.[259] Lee *et al.*[21,258] developed mixed micelles of PEG-poly(histidine) and PEG-PLA that were responsive in a pH range between 6.6 and 7.2. These systems were further modified by the incorporation of biotin, a ligand that was exposed on the micellar surface upon the acidification of the system and the ionization of the polyaminoacid, thus resulting in the interaction with the appropriate receptor. In addition, the ionization of poly(histidine) in the core promoted the micellar disassembly and the endosome disruption, improving the cytosolic release of the drug payload after the uptake.[260] Poly(hydroxyethylaspartamide) was another building block used to synthesize pH-responsive amphiphiles with PEG.[261,262] These micelles were assessed to encapsulate amphotericin B employing the solvent evaporation method. Findings showed the improved hematocompatibility of the encapsulated drug. Then, micelles were modified with 11–70% stearic acid to modulate the release rate; the greater the fatty acid content, the slower the release was. Similarly, PEG-poly(aspartic acid) diblocks were used to encapsulate lysozyme and to protect it from release and biodegradation.[263,264] To improve the physical stability, micelles were core-cross-linked through lysine residues using glutaraldehyde. A similar carrier was explored to solubilize and stabilize zinc porphyrin for photodynamic therapy.[265] Cavallaro *et al.*[266] developed derivatives modified with PEG and hexadecylalkylamine as hydrophilic and hydrophobic pendant moieties for encapsulation of paclitaxel, amphotericin B and methotrexate. Poly(lysine) (pLys) is a polycationic polymer that has become an attractive non-viral vector for gene delivery[267] and enhanced cell attachment in tissue engineering scaffolds.[268] Oh and coworkers synthesized a more complex system made of PLA-PEG-pLys copolymers where lysine was N-substituted with 2,3-dimethyl maleic acid.[269] The core was formed by PLA, while the corona and the outer shell by PEG and pLys, respectively. Under low pH (6.5–7.0), maleic acid residues were hydrolyzed exposing a cationic pLys surface that improved the cellular uptake owing to electrostatic interactions with the negatively charged cell surface. Moreover, blending of poly(histidine) in the core provided a mechanism for endosomal escape.

5.5 Translation into Clinics and Perspectives

The great potential of polymeric micelles to encapsulate, release and target drugs and the profuse investigations conducted in the field have led to a rich intellectual property.[16] However, only a few stimuli-responsive micellar systems have reached the clinical phase. Most of these copolymers combine PEG with pAsp, PLA and PPO and exploit the EPR effect to passively target antitumorals and to overcome multi-drug resistance upon intravenous administration (Table 5.2).[270] On the other hand, owing to (i) the great chemical and architectural versatility, (ii) the good encapsulation capacity and (iii) the relatively high physical stability with respect to conventional surfactant micelles, more recent studies have explored their potential administration by alternative routes such as oral, ocular and intra-nasal. Undoubtedly, cancer has led and pushed the nanomedicine research forward. However, the lessons learnt from the extensive experience gained in this field have contributed to envisage the potential translation of these technology platforms for the treatment of infectious diseases like HIV, tuberculose and viral hepatitis. Products for the treatment of cancer are the only ones undergoing more advanced clinical trials and they could become the first approved medicines employing this kind of nanocarrier. In this context, the near future will be decisive to realize the real potential of polymeric micelles.

Table 5.2 Micellar delivery systems under clinical evaluation.

Product	*Amphiphile*	*Encapsulated drug*	*Goal*	*Phase (Country)*	*Company*
NK911		Doxorubicin	Targeting by EPR effect	I for pancreatic, colorectal, leiomyosarcoma, gastric, esophageal and gall bladder	Nippon Kayaku Co., Japan
NK012		SN-38 (active metabolite of irinotecan)		II for breast cancer (USA)	
NK105	PEG-pAsp	Paclitaxel		II for stomach cancer (Japan) I for breast cancer (Japan)	NanoCarrier Co., Japan
NC-6004 (Nanoplatin®)	Coordination bonds of drug with PEG-polyaminoacid copolymer	Cisplatin	Targeting by EPR effect and reduced nephro- and neurotoxicity	II for pancreatic cancer (Asia)	
NC-4016	Coordination bonds of drug with PEG-polyaminoacid copolymer	Oxaliplatin	Targeting by EPR effect and reduced neuropathy	I for solid cancer (EU)	
Genexol-PM	PEG-PLA	Paclitaxel	Solubilization and reduction of Cremophor EL toxicity Targeting by EPR effect	II for breast and lung cancer (USA, Korea) IIa for pancreatic cancer (USA)	Samyang Co., Korea
SP-1049C[a]	Mixed poloxamer micelles	Doxorubicin	Functional inhibition of Pgp efflux pump	II for esophageal and gastroesophageal cancer (USA)	Supratek Pharma Inc., Canada
Efavirenz pediatric aqueous solution	Poloxamer micelles	Efavirenz	Bioavailability improvement Easy dose adjustment and greater patient compliance Reduced inter- and intra-individual variability	Comparative bioavailability study with standard capsule	Faculty of Pharmacy and Biochemistry, University of Buenos Aires

[a]SP-1049C was granted orphan drug designation for the treatment of gastric cancer in 2008.

Acknowledgements

A. Sosnik is a staff member of CONICET and thanks the support of the "Iberoamerican network of new materials for the design of advanced drug-delivery systems in diseases of high socioeconomic impact" (RIMADEL-CYTED).

References

1. J. T. L. Mah, E. S. H. Low and E. Lee, *Drug Discov. Today*, 2011, **16**, 800.
2. L. J. S. Knutsen, *Drug Discov. Today*, 2011, **16**, 476.
3. S. M. Paul, D. S. Mytelka, C. T. Dunwiddie, C. C. Persinger, B. H. Munos, S. R. Lindborg and A. L. Schacht, *Nat. Rev. Drug Discov.*, 2010, **9**, 203.
4. C. Lipinski, *Am. Pharm. Rev.*, 2002, **5**, 82.
5. C. Giliyar, D. C. Fikstad and S. Tyavanagimatt, *Drug Deliv. Technol.*, 2006, **6**, 57.
6. M. Lindenberg, S. Kopp and J. B. Dressman, *Eur. J. Pharm. Biopharm.*, 2004, **58**, 265.
7. P. Taboada, D. Attwood, J. M. Ruso, F. Sarmiento and V. Mosquera, *Langmuir*, 1999, **15**, 2022.
8. P. Taboada, D. Attwood, M. Garcia, M. N. Jones, J. M. Ruso, V. Mosquera and F. Sarmiento, *J. Colloid Interf. Sci.*, 2000, **221**, 242.
9. D. Attwood, E. Boitard, J. P. Dubes and H. Tachoire, *J. Colloid Interf. Sci.*, 2000, **227**, 356.
10. M. A. Cheema, M. Siddiq, S. Barbosa, P. Taboada and V. Mosquera, *J. Chem. Eng. Data*, 2008, **53**, 368.
11. Z. Shervani, H. Etori, K. Taga, T. Yoshida and H. Okabayashi, *Colloid Surface B*, 1996, **7**, 31.
12. R. Glisoni, D. A. Chiappetta, L. M. Finkielsztein, A. G. Moglioni and A. Sosnik, *New J Chem.*, 2010, **34**, 2047.
13. R. Glisoni, D. A. Chiappetta, A. G. Moglioni and A. Sosnik, *Pharm. Res.*, 2012, **29**, 739.
14. R. Glisoni, M. L. Cuestas, V. L. Mathet, J. R. Oubiña, A. G. Moglioni and A. Sosnik, *Eur. J. Pharm. Sci.*, 2012, **47**, 596.
15. P. Couvreur and C. Vauthier, *Pharm. Res.*, 2006, **23**, 1417.
16. A. Sosnik, A. Carcaboso and D. A. Chiappetta, *Recent Pat. Biomed. Eng.*, 2008, **1**, 43.
17. J. Szebeni, F. Muggia, A. Gabizon and Y. Barenholz, *Adv. Drug Deliver. Rev.*, 2001, **63**, 1020.
18. V. P. Torchilin, *Nat. Rev. Drug Discov.*, 2005, **4**, 145.
19. K. Kataoka, A. Harada and Y. Nagasaki, *Adv. Drug Deliver. Rev.*, 2001, **47**, 113.
20. S. R. Croy and G. S. Kwon, *Curr. Pharm. Design*, 2006, **12**, 4669.
21. G. Gaucher, M. H. Dufresne, V. P. Sant, N. Kang, D. Maysinger and J. C. Leroux, *J. Control. Release*, 2005, **109**, 169.

22. M. C. Jones and J. C. Leroux, *Soft Matt.*, 2010, **6**, 5850.
23. L. Bromberg, *J. Control. Release*, 2008, **128**, 99.
24. G. Gaucher, P. Satturwar, M. C. Jones, A. Furtos and J. C. Leroux, *Eur. J. Pharm. Biopharm.*, 2010, **76**, 147.
25. R. C. Nagarwal, S. Kant, P. N. Singh, P. Maiti and J. K. Pandit, *J. Control. Release*, 2009, **136**, 2.
26. A. Ribeiro, A. Sosnik, D. A. Chiappetta, F. Veiga, A. Concheiro and C. Alvarez-Lorenzo, *J. R. Soc. Interface*, 2012, **9**, 2059.
27. R. G. Strickley, *Pharm. Res.*, 2004, **21**, 201.
28. R. Nagarajan, *Polym. Adv. Tech.*, 2001, **12**, 23.
29. G. Riess, *Prog. Polym. Sci.*, 2003, **28**, 1107.
30. I. F. Paterson, B. Z. Chowdhry and S. A. Leharne, *Langmuir*, 1999, **15**, 6187.
31. D. A. Chiappetta, J. Degrossi, S. Teves, M. D'Aquino, C. Bregni and A. Sosnik, *Eur. J. Pharm. Biopharm.*, 2008, **69**, 535.
32. D. A. Chiappetta, J. Degrossi, R. A. Lizarazo, D. L. Salinas, F. Martínez and A. Sosnik, in *Polymer Aging, Stabilizers and Amphiphilic Block Copolymers*, ed. L. Segewicz and M. Petrowsky, Nova Publishers, Hauppauge, NY, 2010, p. 197.
33. M. C. Jones and J. C. Leroux, *Eur. J. Pharm. Biopharm.*, 1999, **48**, 101.
34. V. P. Sant, D. Smith and J. C. Leroux, *J. Control. Release*, 2004, **97**, 301.
35. P. Vangeyte, S. Gautier and R. Jerome, *Colloids Surf. A*, 2004, **242**, 203.
36. D. Maysinger, J. Lovrić, A. Eisenberg and R. Savić, *Eur. J. Pharm. Biopharm.*, 2007, **65**, 270.
37. X.-B. Xiong, A. Falamarzian, S. M. Garg and A. Lavasanifar, *J. Control. Release*, 2011, **155**, 248.
38. J. Lee, E. C. Cho and K. Cho, *J. Control. Release*, 2004, **94**, 323.
39. D. A. Chiappetta, C. Alvarez-Lorenzo, A. Rey-Rico, P. Taboada, A. Concheiro and A. Sosnik, *Eur. J. Pharm. Biopharm.*, 2010, **76**, 24.
40. N. Rapoport, *Colloid Surface B*, 1999, **16**, 93.
41. S. H. Kim, J. P. Tan, F. Nederberg, K. Fukushima, J. Colson, C. Yang, A. Nelson, Y. Y. Yang and J. L. Hedrick, *Biomaterials*, 2010, **31**, 8063.
42. M. Iijima, Y. Nagasaki, T. Okada, M. Kato and K. Kataoka, *Macromolecules*, 1999, **32**, 1140.
43. J. Q. Jiang, B. Qi, M. Lepage and Y. Zhao, *Macromolecules*, 2007, **40**, 790.
44. P. Petrov, M. Bozukov and C. B. Tsvetanov, *J. Mater. Chem.*, 2005, **15**, 1481.
45. J. D. Pruitt, G. Husseini, N. Rapoport and W. G. Pitt, *Macromolecules*, 2000, **33**, 9306.
46. J. Rodríguez-Hernández, F. Chécot, Y. Gnanou and S. Lecommandoux, *Prog. Polym. Sci.*, 2005, **30**, 691.
47. K. H. Bae, S. H. Choi, S. Y. Park, Y. Lee and T. G. Park, *Langmuir*, 2006, **22**, 6380.
48. T. F. Yang, C. N. Chen, M. C. Chen, C. H. Lai, H. F. Liang and H. W. Sung, *Biomaterials*, 2007, **28**, 725.

49. K. H. Bae, Y. Lee and T. G. Park, *Biomacromolecules*, 2007, **8**, 650.
50. Q. Jin, X. Liu, G. Liu and J. Ji, *Polymer*, 2010, **51**, 1311.
51. Y. Kakizawa, A. Harada and K. Kataoka, *J. Am. Chem. Soc.*, 1999, **121**, 11247.
52. M. J. Heffernan and N. Murthy, *Ann. Biomed. Eng.*, 2009, **37**, 1993.
53. S. M. Garg, X. B. Xiong, C. Lu and A. Lavasanifar, *Macromolecules*, 2011, **44**, 2058.
54. A. V. Kabanov and V. Yu. Alakhov, *Critical Rev. Ther. Drug Carrier Syst.*, 2002, **19**, 1.
55. Y. Hu, Y. Ding, Y. Li, X. Jiang, C. Yang and Y. Yang, *J. Nanosci. Nanotechnol.*, 2006, **6**, 3032.
56. A. Richter, C. Olbrich, M. Krause, J. Hoffmann and T. Kissel, *Eur. J Pharm. Biopharm.*, 2010, **75**, 80.
57. Z. L. Yang, X. R. Li, K. W. Yang and Y. Liu, *J. Biomed. Mat. Res. Part A*, 2008, **85**, 539.
58. C. Di Tommaso, C. Como, R. Gurny and M. Möller, *Eur. J. Pharm. Sci.*, 2010, **40**, 38.
59. M. A. Moretton, D. A. Chiappetta and A. Sosnik, *J. R. Soc. Interface*, 2012, **9**, 487.
60. E. S. Gil and S. M. Hudson, *Prog. Polym. Sci.*, 2004, **29**, 1173.
61. D. Cohn, A. Sosnik and A. Levy, *Biomaterials*, 2003, **24**, 3707.
62. S. M. Moghimi and A. C. Hunter, *TIBTECH*, 2000, **18**, 412.
63. H. M. Aliabadi and A. Lavasanifar, *Expert Opin. Drug Del.*, 2006, **3**, 139.
64. D. A. Chiappetta and A. Sosnik, *Eur. J. Pharm. Biopharm.*, 2007, **66**, 303.
65. I. R. Schmolka, *J. Biomed. Mater. Res.*, 1972, **6**, 571.
66. J. Z. Krezanoski, *US Pat.*, 4,188,373, 1980.
67. L. Reeve, in *Handbook of Biodegradable Polymers*, ed. A. Domb, Y. Kost and D. Wiseman, Harwood Academic Publishers, London, UK, 1997, p. 231.
68. A. Sosnik and M. V. Sefton, *Biomaterials*, 2005, **26**, 7425.
69. A. Sosnik, B. Leung, A. P. McGuigan and M. V. Sefton, *Tissue Eng. A*, 2005, **11**, 1807.
70. A. Sosnik, O. F. Khan, M. Butler and M. V. Sefton, in *Hydrogels: Biological Properties and Applications*, ed. R. Barbucci, Springer, 2009, p. 79.
71. B. G. S. Kurkalli, O. Gurevitch, A. Sosnik, D. Cohn and S. Slavin, *Curr. Stem Cell Res. Ther.*, 2010, **5**, 49.
72. E. A. Pec, Z. G. Wout and T. P. Johnston, *J. Pharm. Sci.*, 1992, **81**, 626.
73. J. M. Grindel, T. Jaworski, O. Piraner, R. M. Emanuele and M. Balasubramanian, *J. Pharm. Sci.*, 2002, **91**, 1936.
74. E. V. Batrakova, S. Li, Y. Li, V. Yu. Alakhov, W. F. Elmquist and A. V. Kabanov, *J. Control. Release*, 2004, **100**, 389.
75. S. M. Moghimi, I. S. Muir, L. Illum, S. S. Davis and V. Kolb-Bachofen, *Biochim. Biophys. Acta*, 1993, **1179**, 157.
76. L. E. Bromberg and E. S. Ron, *Adv. Drug Deliver. Rev.*, 1998, **31**, 197.

77. G. Dumortier, J. L. Groissord, F. Agnely and J. C. Chaumeil, *Pharm. Res.*, 2006, **23**, 2709.
78. A. H. Kibbe, *Handbook of Pharmaceutical Excipients*, American Pharmaceutical Association, Washington D.C., 2000, p. 386.
79. J. Dong, B. Z. Chowdhry and S. A. Leharne, *Colloid Surface A*, 2003, **212**, 9.
80. C. Alvarez-Lorenzo, J. Gonzalez-Lopez, M. Fernandez-Tarrio, I. Sandez-Macho and A. Concheiro, *Eur. J. Pharm. Biopharm.*, 2007, **66**, 244.
81. M. Fernandez-Tarrio, C. Alvarez-Lorenzo and A. Concheiro, *J. Thermal. Anal. Calor.*, 2007, **87**, 171.
82. A. Sosnik and M. V. Sefton, *Biomacromolecules*, 2006, **7**, 331.
83. C. Alvarez-Lorenzo, C. A. Rey-Rico, J. Brea, M. I. Loza, A. Concheiro and A. Sosnik, *Nanomedicine-UK*, 2010, **5**, 1371.
84. J. Gonzalez-Lopez, C. Alvarez-Lorenzo, P. Taboada, A. Sosnik, I. Sandez-Macho and A. Concheiro, *Langmuir*, 2008, **24**, 10688.
85. J. K. Armstrong, B. Z. Chowdhry, M. J. Snowden, J. Dong and S. A. Leharne, *Int. J. Pharm.*, 2001, **229**, 57.
86. J. Dong, B. Z. Chowdhry and S. A. Leharne, *Colloid Surface A*, 2003, **212**, 9.
87. J. Dong, B. Z. Chowdhry and S. A. Leharne, *Colloid Surface A*, 2004, **246**, 91.
88. J. Dong, J. Armstrong, B. Z. Chowdhry and S. A. Leharne, *Therm. Acta*, 2004, **417**, 201.
89. P. Alexandridis, J. F. Holzwarth and T. A. Hatton, *Macromolecules*, 1994, **27**, 2414.
90. P. Alexandridis, V. Athanassiou, S. Fukuda and T. A. Hatton, *Langmuir*, 1994, **10**, 2604.
91. Y. Deng, G. Yu, C. Price and C. Booth, *J. Chem. Soc. Faraday Trans.*, 1992, **88**, 1441.
92. G. Yu, Y. Deng, S. Dalton, Q. Wang, D. Attwood, C. Price and C. Booth, *J. Chem. Soc. Faraday Trans.*, 1992, **88**, 2537.
93. P. Linse and M. Malmsten, *Macromolecules*, 1992, **25**, 5434.
94. P. Alexandridis and T. A. Hatton, *Colloid Surface A*, 1995, **96**, 1.
95. P. Alexandridis, T. Nivaggioli and T. A. Hatton, *Langmuir*, 1995, **11**, 1468.
96. T. Nivaggioli, B. Tsao, P. Alexandridis and T. A. Hatton, *Langmuir*, 1995, **11**, 119.
97. N. J. Jain, V. K. Aswal, P. S. Goyal and P. Bahadur, *Colloid Surface A*, 2000, **173**, 85.
98. O. V. Elisseeva, N. A. M. Besseling, L. K. Koopal and M. A. Cohen Stuart, *Langmuir*, 2005, **21**, 4954.
99. K. Nakashima and P. Bahadur, *Adv. Colloid Interfac.*, 2006, **123–126**, 75.
100. K. Patel, P. Bahadur, C. Guo, J. H. Ma, H. Z. Liu, A. Yamashita, A. Khanal and K. Nakashima, *Eur. Polym. J.*, 2007, **43**, 1699.
101. N. K. Pandit and J. Kisaka, *Int. J. Pharm.*, 1996, **145**, 129.

102. G. Mao, S. Sukumaran, G. Beaucage, M. L. Saboungi and P. Thiyagrajan, *Macromolecules*, 2001, **34**, 552.
103. N. Munshi, N. Rapoport and W. G. Pitt, *Cancer Lett.*, 1997, **118**, 13.
104. N. Rapoport, J. N. Herron, W. G. Pitt and L. Pitina, *J. Control. Release*, 1999, **58**, 153.
105. G. A. Husseini, R. I. El-Fayoumi, K. L. O'Neill, N. Y. Rapoport and W. G. Pitt, *Cancer Lett.*, 2000, **154**, 211.
106. G. A. Husseini, N. Y. Rapoport, D. A. Christensen, J. D. Pruitt and W. G. Pitt, *Colloid Surface B*, 2002, **24**, 253.
107. N. Rapoport, *Int. J. Pharm.*, 2004, **277**, 155.
108. Z.-G. Gao, H. D. Fainb and N. Rapoport, *J. Control. Release*, 2005, **102**, 203.
109. D. Stevenson-Abouelnasr, G. A. Husseini and W. G. Pitt, *Colloid Surface B*, 2007, **55**, 59.
110. C. Alvarez-Lorenzo, A. Rey-Rico, A. Sosnik, P. Taboada and A. Concheiro, *Front. Biosci.*, 2010, **E2**, 424.
111. J. Gonzalez-Lopez, I. Sandez-Macho, A. Concheiro and C. Alvarez-Lorenzo, *J. Phys. Chem. C*, 2010, **114**, 1181.
112. P. Parekh, K. Singh, D. G. Marangoni and P. Bahadur, *Colloid Surface B*, 2011, **83**, 69.
113. C. Alvarez-Lorenzo, J. González-López, M. Fernández-Tarrio, M. I. Sández-Macho and A. Concheiro, *Eur. J. Pharm. Biopharm.*, 2007, **66**, 244.
114. D. A. Chiappetta, C. Hocht, C. Taira and A. Sosnik, *Nanomedicine-UK*, 2010, **5**, 11.
115. D. A. Chiappetta, C. Hocht, C. Taira and A. Sosnik, *Biomaterials*, 2011, **32**, 2379.
116. D. A. Chiappetta, C. Hocht and A. Sosnik, *Curr. HIV Res.*, 2010, **8**, 223.
117. D. A. Chiappetta, G. Facorro, E. Rubin de Celis and A. Sosnik, *Nanomedicine: NMB*, 2011, **7**, 624.
118. R. N. Peroni, S. S. Di Gennaro, C. Hocht, D. A. Chiappetta, M. C. Rubio, A. Sosnik and G. F. Bramuglia, *Biochem. Pharmacol.*, 2011, **82**, 1227.
119. R. N. Peroni, C. Hocht, D. A. Chiappetta, S. S. Di Gennaro, M. C. Rubio, A. Sosnik and G. F. Bramuglia, *First World Conference on Nanomedicine and Drug Delivery* (WCN2010), Kottayam, India, April 2010.
120. P. Vivithanaporn, M. J. Gill and C. Power, *Expert Rev. Anti-Infe.*, 2011, **9**, 371.
121. A. Nath and N. Sacktor, *Curr. Opin. Neurol.*, 2006, **19**, 358.
122. L. Crews, C. Patrick, C. L. Achim, I. P. Everall and E. Masliah, *Int. J. Mol. Sci.*, 2009, **10**, 1045.
123. P. K. Dash, S. Gorantla, H. E. Gendelman, J. Knibbe, G. P. Casale, E. Makarov, A. A. Epstein, H. A. Gelbard, M. D. Boska and L. Y. Poluektova, *J. Neurosci.*, 2011, **31**, 3148.
124. K. Grovit-Ferbas and M. E. Harris-White, *Immunol. Res.*, 2010, **48**, 40.

125. D. A. Chiappetta, C. Hocht, J. A. W. Opezzo and A. Sosnik, *Nanomedicine-UK*, 2012, in press.
126. B. Pitard, M. Bello-Roufaï, O. Lambert, P. Richard, L. Desigaux, S. Fernandes, C. Lanctin, H. Pollard, M. Zeghal, P.-Y. Rescan and D. Escande, *Nucleic Acids Res.*, 2004, **32**, e159.
127. C. Roques, K. Bouchemal, G. Ponchel, Y. Fromes and E. Fattal, *J. Control. Release*, 2009, **138**, 71.
128. C. Roques, E. Fattal and Y. Fromes, *J. Gene Med.*, 2009, **11**, 240.
129. D. Cohn, A. Sosnik and A. Levy, *Biomaterials*, 2003, **24**, 3707.
130. D. Cohn and A. Sosnik, *J. Mat. Sci. Mater. Med.*, 2003, **14**, 175.
131. A. Sosnik, D. Cohn, J. San Román and G. A. Abraham, *J. Biomater. Sci. Pol. Edn.*, 2003, **14**, 227.
132. A. Sosnik and D. Cohn, *Biomaterials*, 2004, **25**, 2851.
133. A. Sosnik and D. Cohn, *Biomaterials*, 2005, **26**, 349.
134. D. Cohn, A. Sosnik and S. Garty, *Biomacromolecules*, 2005, **6**, 1168.
135. D. Cohn, G. Lando, A. Sosnik, S. Garty and A. Levi, *Biomaterials*, 2006, **27**, 1718.
136. D. Cohn, H. Sagiv, A. Benyamin and G. Lando, *Biomaterials*, 2009, **30**, 3289.
137. G. Niu, A. Benyamin Djaoui and D. Cohn, *Polymer*, 2011, **52**, 2524.
138. R. Barreiro Iglesias, L. Bromberg, M. Temchenko, T. A. Hatton, A. Concheiro and C. Alvarez-Lorenzo, *J. Control. Rel.*, 2004, **97**, 537.
139. A. Tontisakis, R. Hilfiker and B. Chu, *J. Colloid Interf. Sci.*, 1990, **135**, 427.
140. L. Q. Jiang, Y. Y. Zheng and J. X. Zhao, *Fine Chemicals*, 2001, **18**, 731.
141. P. Alexandridis, V. Athanassiou and T. A. Hatton, *Langmuir*, 1995, **11**, 2442.
142. P. K. Sharma and S. R. Bhatia, *Int. J. Pharm.*, 2004, **278**, 361.
143. W. B. Sun, J. F. Ding, R. H. Mobbs, F. Heatley, D. Attwood and C. Booth, *Colloid Surface*, 1991, **54**, 103.
144. A. D. Bedells, R. M. Arafeh, Z. Yang, D. Attwood, F. Heatley, J. C. Padget, C. Price and C. Booth, *J. Chem. Soc. Faraday Trans.*, 1993, **89**, 1235.
145. Z. Yang, S. Pickard, N. J. Deng, R. J. Barlow, D. Attwood and C. Booth, *Macromolecules*, 1994, **27**, 2371.
146. Y. W. Yang, N. J. Deng, G. E. Yu, Z. K. Zhou, D. Attwood and C. Booth, *Langmuir*, 1995, **11**, 4703.
147. Y. W. Yang, Z. Yang, Z. K. Zhou, D. Attwood and C. Booth, *Macromolecules*, 1996, **29**, 670.
148. C. Booth and D. Attwood, *Macromol. Rap. Comm.*, 2000, **21**, 501.
149. C. Booth, D. Attwood and C. Price, *Phys. Chem. Chem. Phys.*, 2006, **8**, 3612.
150. C. J. Rekatas, S. M. Mai, M. Crothers, M. Quinn, J. H. Collett, D. Attwood, F. Heatley, L. Martini and C. Booth, *Phys. Chem. Chem. Phys.*, 2001, **3**, 4769.

151. M. Crothers, Z. Zhou, N. M. P. S. Ricardo, Z. Yang, P. Taboada, C. Chaibundit, D. Attwood and C. Booth, *Int. J. Pharm.*, 2005, **293**, 91.
152. P. Taboada, G. Velasquez, S. Barbosa, V. Castelletto, S. K. Nixon, Z. Yang, F. Heatley, I. W. Hamley, M. Ashford, V. Mosquera, D. Attwood and C. Booth, *Langmuir*, 2005, **21**, 5263.
153. P. Taboada, G. Velasquez, S. Barbosa, Z. Yang, S. K. Nixon, Z. Zhou, F. Heatley, M. Ashford, V. Mosquera, D. Attwood and C. Booth, *Langmuir*, 2006, **22**, 7465.
154. D. Attwood, Z. Zhou and C. Booth, *Expert Opin. Drug Del.*, 2007, **4**, 533.
155. M. E. N. P. Ribeiro, I. M. Cavalcante, N. M. P. S. Ricardo, S. M. Mai, D. Attwood, S. G. Yeates and C. Booth, *Int. J. Pharm.*, 2009, **369**, 196.
156. M. E. N. P. Ribeiro, I. G. P. Vieira, I. M. Cavalcante, N. M. P. S. Ricardo, D. Attwood, S. G. Yeates and C. Booth, *Int. J. Pharm.*, 2009, **378**, 211.
157. A. Cambón, M. Alatorre-Meda, J. Juárez, A. Topete, D. Mistry, D. Attwood, S. Barbosa, P. Taboada and V. Mosquera, *J. Colloid Interf. Sci.*, 2011, **361**, 154.
158. X. Zhang, J. K. Jackson and H. M. Burt, *Int. J. Pharm.*, 1996, **132**, 195.
159. M. Ramaswamy, X. Zhang, H. M. Burt and K. M. Wasan, *J. Pharm. Sci.*, 1997, **86**, 460.
160. X. Zhang, H. M. Buró, D. Von Hoff, D. Dexter, G. Mangold, D. Degen and A. M. Oktaba, *Cancer Chemother. Pharmacol.*, 1997, **40**, 81.
161. H. M. Burt, X. Zhang, P. Toleikis, L. Embree and W. L. Hunter, *Colloid Surface B*, 1999, **16**, 161.
162. R. T. Liggins and H. M. Burt, *Adv. Drug Deliver. Rev.*, 2002, **54**, 191.
163. T. Y. Kim, D. W. Kim, J. Y. Kim, J. Y. Chung, S. G. Shin, S. C. Kim, D. S. Heo, N. K. Kim and Y. J. Bang, *Clin. Cancer Res.*, 2004, **10**, 3708.
164. S. K. Agrawal, N. Sanabria-DeLong, J. M. Coburn, G. N. Tew and S. R. Bathia, *J. Control. Release*, 2006, **112**, 64.
165. Y. I. Jeong, M. K. Jang and J. W. Nah, *Polym-Korea*, 2009, **33**, 137.
166. L. Sun, L. J. Shen, M. Q. Zhu, C. M. Dong and Y. Wei, *J. Polym. Sci. Pol. Chem.*, 2010, **48**, 4583.
167. L. Calucci, C. Forte, S. J. Buwalda, P. J. Dijkstra and J. Feijen, *Langmuir*, 2010, **26**, 12890.
168. L. Yang, X. Qi, P. Liu, A. El Ghzaoui and S. Li, *Int. J. Pharm.*, 2010, **394**, 43.
169. L. E. Salaam, D. Dean and T. L. Bray, *Polymer*, 2006, **47**, 310.
170. L. Piao, Z. Dai, M. Deng, X. Chen and X. Jing, *Polymer*, 2003, **44**, 2025.
171. W. J. Lin, L. W. Juang and C. C. Lin, *Pharm. Res.*, 2003, **20**, 668.
172. C. Y. Gong, Z. Y. Qian, C. B. Liu, M. J. Huang, Y. C. Gu, Y. J. Wen, B. Kan, K. Wang, M. Dai, X. Y. Li, M. L. Gou, M. J. Tu and Y. Q. Wei, *Smart Mater. Struct.*, 2007, **16**, 927.
173. C. Y. Gong, S. Shi, P. W. Dong, B. Kan, M. L. Gou, X. H. Wang, X. Y. Li, F. Luo, X. Zhao, Y. Q. Wei and Z. Y. Qian, *Int. J. Pharm.*, 2007, **365**, 89.

174. C. Y. Gong, Y. J. Wang, X. H. Wang, X. W. Wei, Q. J. Wu, B. L. Wang, P. W. Dong, L. J. Chen, F. Luo and Z. Y. Qian, *J. Nanoparticle Res.*, 2011, **13**, 721.
175. N. V. Cuong, J. L. Jiang, Y. L. Li, J. R. Chen, S. C. Jwo and M. F. Hsieh, *Cancers*, 2011, **3**, 61.
176. K. Letchford, R. Liggins, K. M. Wasan and H. Burt, *Eur. J. Pharm. Biopharm.*, 2009, **71**, 196.
177. L. Zhang, Y. He, G. Ma, C. Song and H. Sun, *Nanomedicine: NBM*, 2012, in press.
178. M. A. Moretton, R. J. Glisoni, D. A. Chiappetta and A. Sosnik, *Colloid Surface B*, 2010, **79**, 467.
179. M. A. Moretton, D. A. Chiappetta and A. Sosnik, *J. R. Soc. Interface*, 2012, **9**, 487.
180. M. A. Moretton, *PhD thesis, Faculty of Pharmacy and Biochemistry, University of Buenos Aires*, 2013.
181. Y. Wang, C. Wang, S. Fu, Q. Liu, D. Dou, H. Lv, M. Fan, G. Guo, F. Luo and Z. Qian, *Int. J. Pharm.*, 2011, **407**, 184.
182. Y. Hu, Y. Ding, Y. Li, X. Jiang, C. Yang and Y. Yang, *J. Nanosci. Nanotechnol.*, 2006, **6**, 3032.
183. W. Abdelwahed, G. Degobert, S. Stainmesse and H. Fessi, *Adv. Drug Deliver. Rev.*, 2006, **58**, 1688.
184. H. Cho and G. S. Kwon, *ACS Nano*, 2011, **5**, 8721.
185. T. Tanaka, *Phys. Rev. Lett.*, 1978, **40**, 820.
186. H. G. Schild, *Prog. Polym. Sci.*, 1992, **17**, 163.
187. K. Nagase, J. Kobayashi and T. Okano, *J. R. Soc. Interface*, 2009, **6**, S293.
188. H. Wei, S. X. Cheng, X. Z. Zhang and R. X. Zhuo, *Prog. Polym. Sci.*, 2009, **34**, 893.
189. S. Cammas, K. Suzuki, C. Sone, Y. Sakurai, K. Kataoka and T. Okano, *J. Control. Release*, 1997, **48**, 157.
190. X. M. Liu and L. S. Wang, *Biomaterials*, 2004, **25**, 1929.
191. J. E. Chung, M. Yokoyama, K. Suzuki, T. Aoyagi, Y. Sakurai and T. Okano, *Colloid Surface B*, 1997, **9**, 37.
192. N. V. Economidis, D. A. Pena, P. G. Smirniotis, F. Kohori, K. Sakai, T. Aoyagi, M. Yokoyama, M. Yamato, Y. Sakurai and T. Okano, *Colloid Surface B*, 1999, **16**, 195.
193. J. E. Chung, M. Yokoyama, M. Yamato, T. Aoyagi, Y. Sakurai and T. Okano, *J. Control. Release*, 1999, **62**, 115.
194. Z. S. Ge, D. Xie, D. Y. Chen, X. Z. Jiang, Y. F. Zhang, H. W. Liu and S. Liu, *Macromolecules*, 2007, **40**, 3538.
195. M. Yang, Y. T. Ding, L. Y. Zhang, X. P. Qian, X. Q. Jiang and B. R. Liu, *J. Biomed. Mater. Res. A*, 2007, **81A**, 847.
196. H. Wei, C. Cheng, C. Chang, W. Q. Chen, S. X. Cheng, X. Z. Zhang and R. X. Zhuo, *Langmuir*, 2008, **24**, 4564.
197. N. Bertrand, J. G. Fleischer, K. M. Wasan and J. C. Leroux, *Biomaterials*, 2009, **30**, 2598.

198. M. Nakayama, T. Okano, T. Miyazaki, F. Kohori, K. Sakai and M. Yokoyama, *J. Control. Release*, 2006, **115**, 46.
199. B. R. Liu, M. Yang, R. T. Li, Y. T. Ding, X. P. Qian, L. X. Yu and X. Jiang, *Eur. J. Pharm. Biopharm.*, 2008, **69**, 527.
200. B. R. Liu, M. Yang, X. L. Li, X. P. Qian, X. Q. Jiang, Z. T. Shen, Y. Ding and L. Yu, *J. Pharm. Sci.*, 2008, **97**, 3170.
201. J. Taillefer, M. C. Jones, N. Brasseur, J. E. Van Lier and J. C. Leroux, *J. Pharm. Sci.*, 2000, **89**, 52.
202. S. Q. Liu, Y. W. Tong and Y. Y. Yang, *Biomaterials*, 2005, **26**, 5064.
203. Z. S. Ge, S. Z. Luo and S. Y. Liu, *J. Polym. Sci. Pol. Chem.*, 2006, **44**, 1357.
204. Y. Y. Li, X. Z. Zhang, H. Cheng, J. L. Zhu, U. N. Li, S. X. Cheng and R. X. Zhuo, *Nanotechnology*, 2007, **18**, 505101.
205. S. Q. Liu, N. Wiradharma, S. J. Gao, Y. W. Tong and Y. Y. Yang, *Biomaterials*, 2007, **28**, 1423.
206. Y. Y. Li, X. Z. Zhang, J. L. Zhu, H. Cheng, S. X. Cheng and R. X. Zhuo, *Nanotechnology*, 2007, **18**, 215605.
207. C. Chang, H. Wei, C. Y. Quan, Y. Y. Li, J. Liu, Z. C. Wang, S. X. Cheng, X. Z. Zhang and R. X. Zhuo, *J. Polym. Sci. Pol. Chem.*, 2008, **46**, 3048.
208. X. J. Loh, Y. L. Wu, W. T. J. Seow, M. N. I. Norimzan, Z. X. Zhang, F. J. Xu, E. T. Kang, K. G. Neoh and J. Li, *Polymer*, 2008, **49**, 5084.
209. J. X. Zhang, L. Y. Qiu, Y. Jin and K. J. Zhu, *J. Biomed. Mater. Res. A*, 2006, **76A**, 773.
210. J. X. Zhang, L. Y. Qiu, Y. Jin and K. J. Zhu, *Colloid Surface B*, 2005, **43**, 123.
211. Y. Y. Li, X. Z. Zhang, H. Cheng, G. C. Kim, S. X. Cheng and R. X. Zhuo, *Biomacromolecules*, 2006, **7**, 2956.
212. Y. Y. Li, X. Z. Zhang, G. C. Kim, H. Cheng, S. X. Cheng and R. X. Zhuo, *Small*, 2006, **2**, 917.
213. H. Wei, X. Z. Zhang, C. Cheng, S. X. Cheng and R. X. Zhuo, *Biomaterials*, 2007, **28**, 99.
214. H. Wei, W. Q. Chen, C. Chang, C. Cheng, S. X. Cheng, X. Z. Zhang and R. X. Zhuo, *J. Phys. Chem. C*, 2008, **112**, 2888.
215. J. Y. Zhang, Y. M. Zhou, Z. Y. Zhu, Z. S. Ge and S. Y. Liu, *Macromolecules*, 2008, **41**, 1444.
216. C. L. Lo, C. K. Huang, K. M. Lin and G. H. Hsiue, *Biomaterials*, 2007, **28**, 1225.
217. C. L. Lo, K. M. Lin, C. K. Huang and G. H. Hsiue, *Adv. Funct. Mater.*, 2006, **16**, 2309.
218. C. K. Huang, C. L. Lo, H. H. Chen and G. H. Hsiue, *Adv. Funct. Mater.*, 2007, **17**, 2291.
219. M. D. C. Topp, P. J. Dijkstra, H. Talsma and J. Feijen, *Macromolecules*, 1997, **30**, 8518.
220. J. Virtanen, S. Holappa, H. Lemmetyinen and H. Tenhu, *Macromolecules*, 2002, **35**, 4763.

221. W.Q. Zhang, L. Q. Shi, K. Wu and Y. L. An, *Macromolecules*, 2005, **38**, 5743.
222. C. Y. Hong, Y. Z. You and C. Y. Pan, *J. Polym. Sci. Pol. Chem.*, 2004, **42**, 4873.
223. N. Bertrand, J. G. Fisher, K. M. Wasan and J. C. Leroux, *Biomaterials*, 2009, **30**, 2598.
224. T. Ishida, X. Wang, T. Shimizu, K. Nawata and H. Kiwada, *J. Control. Release*, 2007, **122**, 349.
225. J. Kopeček, P. Kopečková, T. Minko and Z. Lu, *Eur. J. Pharm. Biopharm.*, 2000, **50**, 61.
226. C. Konak, B. Ganchev, M. Teodorescu, K. Matyjaszewski, P. Kopeckova and J. Kopecek, *Polymer*, 2002, **43**, 3735.
227. M. Talelli, C. J. F. Rijcken, C. F. van Nostrum, G. Stormand and W. E. Hennink, *Adv. Drug Deliver. Rev.*, 2010, **62**, 231.
228. A. Paul, M. J. Vicent and R. Duncan, *Biomacromolecules*, 2007, **8**, 1573.
229. P. Chytil, T. Etrych, Č. Koňák, M. Šírová, T. Mrkvan, B. Říhová and K. Ulbrich, *J. Control. Release*, 2006, **115**, 26.
230. P. Chytil, T. Etrych, C. Konak, M. Sirova, T. Mrkvan, J. Boucek, B. Rihova and K. Ulbrich, *J. Control. Release*, 2008, **127**, 121.
231. B. S. Lele and J. C. Leroux, *Macromolecules*, 2002, **35**, 6714.
232. S. Lele and J. C. Leroux, *Polymer*, 2002, **43**, 5595.
233. N. Kang and J. C. Leroux, *Polymer*, 2004, **45**, 8967.
234. C. Konåk, D. Oupicky, V. Chytry, K. Ulbrich and M. Helmstedt, *Macromolecules*, 2000, **33**, 5318.
235. C. Y. Hong and C. Y. Pan, *Macromolecules*, 2006, **39**, 3517.
236. M. Hruby, C. Konak, J. Kucka, M. Vetrik, S. K. Filippov, D. Vetvicka, H. Mackova, G. Karlsson, K. Edwards, B. Rihova and K. Ulbrich, *Macromol. Biosci.*, 2009, **9**, 1016.
237. N. Adams and U. S. Schubert, *Adv. Drug Deliver. Rev.*, 2007, **59**, 1504.
238. H. Schlaad, C. Diehl, A. Gress, M. Meyer, D. A. Levent, Y. Nur and A. Bertin, *Macromol. Rapid Commun.*, 2010, **31**, 511.
239. R. Hoogenboom, *Angew. Chem. Int. Ed.*, 2009, **48**, 7978.
240. S. Zalipsky, C. B. Hansen, J. M. Oaks and T. M. Allen, *J. Pharm. Sci.*, 1996, **85**, 133.
241. R. Jordan, K. Martin, J. H. Rader and K. K. Unger, *Macromolecules*, 2001, **34**, 8858.
242. G. Volet, V. Chanthavong, V. Wintgens and C. Amiel, *Macromolecules*, 2005, **38**, 5190.
243. R. Luxenhofer, A. Schulz, C. Roques, S. Li, T. K. Bronich, E. V. Batrakova, R. Jordan and A. V. Kabanov, *Biomaterials*, 2010, **31**, 4972.
244. A. Benahmed, M. Ranger and J. C. Leroux, *Pharm. Res.*, 2001, **18**, 323.
245. L. Luo, M. Ranger, D. G. Lessard, D. Le Garrec, S. Gori, J. C. Leroux, S. Rimmer and D. Smith, *Macromolecules*, 2004, **37**, 4008.
246. A. S. Hoffman, *J. Control. Release*, 1987, **6**, 297.
247. E. S. Gil and S. M. Hudson, *Prog. Polym. Sci.*, 2004, **29**, 1173.

248. S. R. Tonge and B. J. Tighe, *Adv. Drug Deliver. Rev.*, 2001, **53**, 109.
249. N. Murthy, J. R. Robichaud, D. A. Tirrell, P. S. Stayton and A. S. Hoffman, *J. Control. Release*, 1999, **61**, 137.
250. A. S. Lee, V. Butun, M. Vamvakaki, S. P. Armes, J. A. Pople and A. P. Gast, *Macromolecules*, 2002, **35**, 8540.
251. J. F. Gohy, N. Willet, S. Varshney, J. X. Zhang and R. Jerome, *Angew. Chem. Int. Ed.*, 2001, **40**, 3214.
252. M. H. Dufresne, D. Le Garrec, V. Sant, J. C. Leroux and M. Ranger, *Int. J. Pharm.*, 2004, **277**, 81.
253. M. H. Dufresne and J. C. Leroux, *Pharm. Res.*, 2004, **21**, 160.
254. A. E. Felber, M. H. Dufresne and J. C. Leroux, *Adv. Drug Deliver. Rev.*, 2012, **64**, 979.
255. M. Stubbs, P. M. McSheehy, J. R. Griffiths and C. L. Bashford, *Mol. Med. Today*, 2000, **6**, 15.
256. C. F. van Nostrum, *Adv. Drug Deliver. Rev.*, 2004, **56**, 9.
257. Y. Tang, S. Y. Liu, S. P. Armes and N. C. Billingham, *Biomacromolecules*, 2003, **4**, 1636.
258. E. S. Lee, K. Na and Y. H. Bae, *J. Control. Release*, 2003, **91**, 103.
259. C. He, X. Zhuang, Z. Tang, H. Tian and X. Chen, *Adv. Healthcare Mater.*, 2012, **1**, 48.
260. E. S. Lee, K. Na and Y. H. Bae, *Nano Lett.*, 2005, **5**, 325.
261. A. Lavasanifar, J. Samuel and G. S. Kwon, *J. Control. Release*, 2001, **77**, 155.
262. A. Lavasanifar, J. Samuel and G. S. Kwon, *J. Control. Release*, 2002, **79**, 165.
263. A. Harada and K. Kataoka, *Macromolecules*, 1998, **31**, 288.
264. X. Yuan, Y. Yamasaki, A. Harada and K. Kataoka, *Polymer*, 2005, **46**, 7749.
265. G. D. Zhang, N. Nishiyama, A. Harada, D. L. Jiang, T. Aida and K. Kataoka, *Macromolecules*, 2003, **36**, 1304.
266. G. Cavallaro, M. Licciardi, G. Giammona, P. Caliceti, A. Semenzato and S. Salmaso, *J. Control. Release*, 2003, **89**, 285.
267. T. Merdan, J. Kopeček and T. Kissel, *Adv. Drug Deliver. Rev.*, 2002, **54**, 715.
268. E. Ciucurel and M. V. Sefton, *J. Biomater. Sci. Polym. Ed.*, 2011, **22**, 2515.
269. K. T. Oh, D. Kim, H. H. You, Y. S. Ahn and E. S. Lee, *Int. J. Pharm.*, 2009, **376**, 134.
270. C. Alvarez-Lorenzo, A. Sosnik and A. Concheiro, *Curr. Drug Targets*, 2011, **12**, 1112.

CHAPTER 6

Ultrasound-triggered Release from Micelles

WILLIAM G. PITT,*[a] GHALEB A. HUSSEINI[b] AND
LAURA N. KHERBECK[b]

[a] Chemical Engineering Department, Brigham Young University, Provo,
UT84602, USA; [b] American University of Sharjah, Sharjah, UAE
*Email: pitt@byu.edu

6.1 Introduction

The concept of triggered drug release is that a mild stimulus, namely a stimulus that is not harmful to healthy tissues and one that exists only in desired locations or that can be controlled in time and/or space, is required to permeabilize an otherwise impermeable vesicle carrying therapeutics. Ultrasound is such an ideal trigger. Ultrasound does not interact strongly with tissues and, when used appropriately at low intensities, there is no tissue heating or other damage. Ultrasound can be focused from an external device, through the skin and tissue, to the desired target site. There is no scalpel, blood or pain associated with delivery of ultrasound. The delivery of ultrasound can be electronically controlled in time, from a tiny pulse of high intensity, to a series of short pulses in rapid succession over seconds, or to continuous low intensity application for minutes to hours. When compared to other external triggers such as radio frequency (RF) heating and magnetic fields, the temporal and spatial control of high-frequency ultrasound cannot be surpassed. Only focused light can compete in these areas, and the high absorption and scattering of visible light limits its controlled application to relatively short penetration

RSC Smart Materials No. 2
Smart Materials for Drug Delivery: Volume 1
Edited by Carmen Alvarez-Lorenzo and Angel Concheiro
© The Royal Society of Chemistry 2013
Published by the Royal Society of Chemistry, www.rsc.org

depths into the body. While near infrared light can penetrate further than visible light, scattering is still a drawback. By comparison, low-frequency ultrasound can penetrate centimeters into the body with very low scattering. In this aspect it is ideal. As the complementary partner to complete this excellent controlled delivery system, a vehicle is required that can securely sequester the drug and then release it upon application of the ultrasound. For many drugs, a micelle is an ideal match in this partnership.

This chapter reviews the literature regarding the controlled release of therapeutics from micellar carriers using ultrasound (US) as a triggering mechanism. In addition to US, there are other types of external triggering mechanisms mentioned above,[1–3] and several types of passive internal triggering mechanisms such as local pH,[4,5] heat[6] or local biochemistry.[7] We invite the interested reader to consider those stimuli (addressed in other Chapters of this book), especially when comparing the advantages and disadvantages of ultrasound-triggered drug release from micelles. This chapter begins with a description of ultrasound and micelles, then continues with a brief review of conventional micellar drug delivery, and finishes with a thorough review of ultrasonically triggered delivery from micelles and a discussion of the physical mechanisms involved.

6.2 Ultrasound

6.2.1 Physics of Ultrasound

6.2.1.1 Wave Nature of Ultrasound

Ultrasound (US) is simply high-frequency pressure waves, just as audio sound is low-frequency pressure waves. Physicists define US as pressure waves with a frequency of 20 kHz or higher, which is above the common threshold of hearing for humans.[8] As with sound and light waves, ultrasonic waves can be focused on a particular volume that has dimensions as small as about half the wavelength. The speed of sound in water and most tissue is about 1.5 km/s, so the wavelength of 1 MHz US is about 1.5 mm. Thus high-frequency US (>1 MHz) can be focused to fairly small volumes, which is useful for triggering release at precise locations in the body. However, low-frequency US (20 kHz to 200 kHz) is more challenging to focus, not only because the spot size is larger, but the physical size of the transducer is also much larger if focusing is required. For example, the wavelength of 20 kHz US in water is about 7.5 cm, so focal spots cannot be much smaller than 4 cm in diameter, and a decent transducer that can focus adequately would be at least 15 cm in diameter. If the decision of which frequency to use were based on focal volume size, one would select high-frequency US for drug-delivery applications. However, high-frequency US has its own challenges.

The first challenge is the attenuation of the ultrasonic intensity by tissues in the body. This attenuation occurs by both scattering and absorption.[9] Each tissue has its unique attenuation and speed of sound, which have been tabulated.[10,11] The challenge arises because high-frequency US is attenuated more than low-frequency US, and the attenuation increases fairly proportionally to frequency in tissue.[9,12] Thus, although high-frequency US can be focused nicely, its high absorption prevents the penetration deeply into the body, and scattering reduces some of the focal precision endowed by the high frequency. Because the attenuation increases with frequency, the depth of penetration into body tissue is 10 times shorter at 2 MHz than at 200 kHz. High frequencies above 5 MHz simply do not penetrate sufficiently to deliver high-energy densities without the concomitant heating of the tissue (see Section 6.2.1.2). In comparison, low-frequency US is easily propagated through all tissues except bone and lung, and thus is easily delivered to all tissues except lung, bone, marrow and brain. As mentioned, however, the spatial focusing is more problematic. There are advanced techniques that, by using interference between multiple transducers, can create local volumes of focused ultrasound. These techniques are not yet common and are outside of the scope of this Chapter, but they may have important future applications in volume-controlled drug delivery using low-frequency US.

The second main challenge facing high-frequency US is that the key mechanism usually employed as a trigger for ultrasonic drug delivery, called gas bubble cavitation, is much more effective at lower frequencies as will be discussed in Section 6.2.1.3. Thus for drug delivery from a micelle, which usually requires deep tissue penetration and active gas bubble cavitation, low-frequency US is much more practical and is often used in the research lab.

6.2.1.2 *Ultrasonic Heating*

What happens to all of the attenuated energy of high-frequency US? It is converted into heat. Thus ultrasonic heating of tissues increases proportionally to the frequency. Imaging ultrasound employs high frequencies, but only in very short pulses, and thus the average amount of heat deposited in the tissues is low. Nevertheless, there are safety considerations employed to prevent the thermal damage of tissue during diagnostic ultrasonic exposure. The safety level is usually expressed by the Thermal Index (TI), which is the ratio of the applied acoustic power to the power required to raise tissue temperature by 1 °C. For example, an exposure with a TI of 1 would raise tissue temperature by 1 °C and a TI of 3 would raise the temperature by 3 °C. Most diagnostic ultrasound imaging equipment calculates and displays the TI on the screen so as to avoid overheating.

Since the TI is proportional to the heating, as the frequency increases, the TI also increases. For an equivalent exposure intensity (same power density, pulse frequency, pulse length, *etc.*), there would be much more heating at 1 MHz than at 100 kHz. Again consideration of this parameter points to the advantage of lower frequency ultrasound allowing higher intensities and longer durations of exposure.

6.2.1.3 Mechanical Cavitation

Cavitation is the formation and dynamic oscillation of gas bubbles in a liquid, and is a very common and significant phenomenon when ultrasound is applied in any aqueous environment. The oscillating pressure wave causes gas bubbles to expand (as pressure decreases) and contract (as pressure increases) in a cyclic manner. This mechanical movement of the bubble and the surrounding fluid interface creates stresses on nearby cells and vesicles (such as micelles) and causes flow of fluid and movement of particles. Cavitation is generally divided into two general categories – stable and inertial – depending upon the amplitude and nature of the bubble oscillation.

Stable cavitation, also called non-inertial, occurs at relatively low amplitude pressure oscillations and when the frequency of the oscillation does not match the natural resonance frequency of the bubble. In stable cavitation the bubble usually undergoes many repetitive cycles of expansion and contraction without any chaotic behavior. Although there is no violent collapse as is the case with inertial cavitation, the oscillations create fluid flow adjacent to the bubble, called microstreaming.[12,13] Very near the surface of the bubble the fluid velocity gradients are very high, creating a strong local shear stress.[14–16] Stable cavitation is usually detected by listening with a hydrophone to the pressure waves emitted from bubbles as they oscillate. At very low amplitudes, the only oscillations are those matching the frequency of US applied to the bubbles. But as the amplitude increases, non-linear oscillations are formed, which produce emissions at higher harmonics ($2f$, $3f$, $4f$, *etc.*) of the applied ultrasonic frequency f.[12,13,17] As the amplitude increases further, subharmonics ($f/2$, $f/3$, *etc.*) and ultraharmonics ($3f/2$, $5f/2$, $7f/2$, *etc.*) appear. Although the cavitation may remain stable, the appearance of subharmonics usually indicates that the bubbles are near the transition to chaotic behavior associated with collapse cavitation.

Collapse cavitation occurs at relatively large pressure amplitudes or when the resonance frequency of the bubble is near the ultrasonic frequency. It is characterized by large amplitude chaotic (non-repetitive) oscillations that quickly lead to the "collapse" of the gas bubble, which occurs when the momentum of the inward moving spherical wall of water is so great that the opposing pressure from the compressed bubble cannot stop the water from compressing the gas to a supercritical fluid. The temperatures and pressures calculated in such a collapse exceed 5000 K[18,19] and 100 atm.[13] These high temperatures cause dissociation of water and gas molecules into free radicals that can be captured as evidence of and quantification of collapse cavitation.[20–23] The collapsing walls can attain or exceed the speed of sound in air (~340 m/s), creating a spherical shock wave inside the bubble that slams in on itself and then rebounds as a spherical pressure shock wave emanating outward from the site of bubble collapse. The expansion of the supercritical fluid back into gas creates an outward expanding gas bubble. If for some reason the inward collapse or outward expansion is not spherically symmetrical, the bubble will be fragmented into smaller bubbles that also will start to grow and cavitate. Because the inertia of the water (as opposed to the pressure in the bubble) dominates the behavior of these oscillations, this type of cavitation is often called ‘‘inertial cavitation’’. In the past this has been called collapse cavitation and transient cavitation because the bubble existed only transiently before it was ‘‘destroyed’’ by fragmentation.

Needless to say, collapse cavitation is a very violent event, particularly in the near vicinity of the collapse event. The high fluid shear stresses associated with the sudden collapse and rebound of the bubble are thought to be sufficient to damage cell membranes, disrupt liposomes and shear micelles, as illustrated in Figure 6.1. The shock wave can produce compressive and shear stresses in membranes. Free radicals can react with other molecules or with biomolecules in the cells with toxic results. Collapse cavitation has been correlated

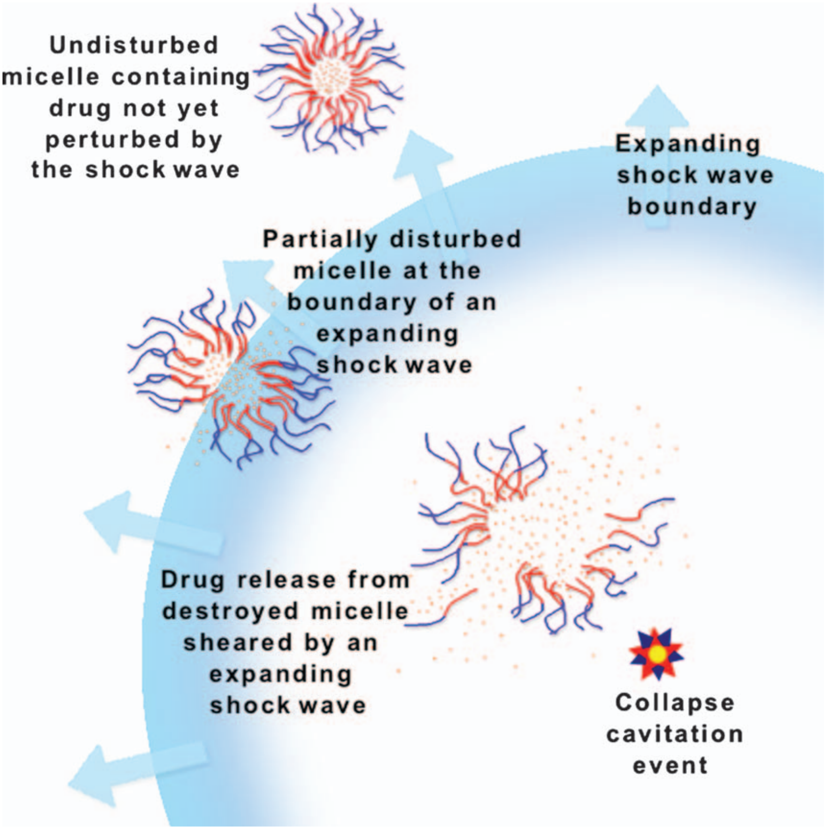
Undisturbed micelle containing drug not yet perturbed by the shock wave
Expanding shock wave boundary
Partially disturbed micelle at the boundary of an expanding shock wave
Drug release from destroyed micelle sheared by an expanding shock wave
Collapse cavitation event

Figure 6.1 Illustration of an expanding shock wave from a collapse cavitation event that causes mechanical disruption of micelles. The compressional shock wave is thought to shear open micelles transiently, thus releasing their contents.

with drug release from liposomes[24,25] and from micelles.[26,27] Collapse cavitation in blood vessels can denude the surface of endothelial cells,[28] permeabilize capillaries[29,30] and even breach the blood-brain barrier.[31–35] Despite these seemingly negative consequences, collapse cavitation does have some positive aspects. Vigorous fluid flow in the region of cavitation enhances the local convective transport of drugs. Also, carefully controlled cavitation is used to transiently open cell membranes (called sonoporation) for gene delivery,[36] for careful breaching of the blood-brain barriers,[31,33] for purposeful destruction of tumors or other unwanted lesions or tissues[37] and for disruption of blood clots.[38–41]

The extent of collapse cavitation can be characterized by measuring the production of free radicals[20,21] and by examining the acoustic emissions.[39,42,43] When listening with a hydrophone, the onset of collapse cavitation is characterized by a sudden increase in the baseline of the acoustic spectrum. The harmonics, subharmonics and ultraharmonics are still present, but they sit on top of a much higher baseline of noise that suddenly appears because of the "white noise" produced in the frequency spectrum by the generation of shock waves.

One of the principal questions in bubble cavitation regards the onset of collapse cavitation. A general observation was that for a given acoustic pressure amplitude, cavitation occurred more readily at lower frequencies. To validate this observation, computer simulations were done to calculate when air bubbles of various sizes would experience inertial cavitation in blood and water.[44] The data showed that the threshold for the onset of inertial cavitation in a field of bubbles with a spectrum of sizes was proportional to the amplitude of the negative pressure cycle (peak negative pressure, p^-), and inversely proportional to the square root of the ultrasonic frequency, f. This supported the observation that as frequency decreased, the inertial cavitation increased. These observations led to the definition of the "Mechanical Index", $\mathrm{MI} = p^- / \sqrt{f}$, where p^- is in MPa and f is in MHz. Along with the Thermal Index, TI, the MI is displayed on most ultrasonic imaging machines, and there are guidelines as to the maximum MI value for safely imaging various tissues, such as fetal tissue, eyes, heart, *etc*.[45,46] The original purpose of MI was to avoid damaging delicate tissues with collapse cavitation events, but the MI can also be used as an indicator of the amount or intensity of collapse cavitation that might be expected if bubbles are already present.

The MI concept was developed for a general distribution of bubbles with a range of sizes, assuming that at least one of those bubbles would have a resonance frequency near the applied frequency. If, however, there is only one bubble size and the objective was to cause collapse cavitation, then it would be important to select the frequency based on the bubble size. Although more rigorous equations are available,[13] a simplified relationship between the resting bubble radius (R_0, radius with no applied pressure) and the resonance frequency, f_{res}, is given by[46] $f_{res} = (3.3m/s)/R_0$. This indicates that a small bubble with a radius of about 1 μm has a resonance frequency of 3.3 MHz. Such small bubbles are used as contrast agents in medical imaging, and imaging instruments operating at about 3.3 MHz would tend to create collapse cavitation, even at low amplitudes.

There are a few other interesting cavitation phenomena that pertain to drug delivery from micelles. The first is the generation of "micro jets" from the collapse of a bubble near a solid surface. The presence of the surface reduces the inward flow of liquid from that direction, resulting in an asymmetric collapse of the bubble in a manner that creates a high-velocity jet of liquid shooting directly at the surface.[12,13] A cell has a sufficiently viscous surface that cavitation near a cell has been observed to shoot a micro jet toward the cell and pierce the cell membrane.[47] It is believed that this mechanism is responsible for the "sonoporation" phenomenon used for ultrasonic gene delivery.[36,47]

A second phenomenon called "acoustic pressure" is caused by the pressure waves emanating from an oscillating bubble.[17,46] The oscillations generate a net force on other objects in the vicinity of the bubble. If the object is denser than the surrounding liquid, the net force is directed toward the bubble, whereas a less dense object feels a force directed away from a bubble. These forces have been observed experimentally.[48] This acoustic pressure is very useful for drug delivery from micelles. In a mixture of bubbles and micelles, the bubbles, which are less dense than water, will push themselves away from each other and spread out. The micelles, which are denser than water, will be pulled toward the nearest bubble. At very short distances the fluid shear rates can approach 10^7 sec^{-1},[16] and these might be sufficient to disrupt the micellar structure.

So far in this discussion of cavitation, the bubbles were assumed already to exist. This is the case when specially engineered bubbles, usually stabilized with a shell of surfactant or protein, are introduced. A common source for these bubbles is the "contrast agent" used in diagnostic sonography. These bubbles are usually from 1 to 5 μm in diameter, so they can be injected into the circulatory system. However the size of the bubbles prevents them from passing from the capillaries into the tissues. Smaller bubbles designed for drug and gene delivery are in development.[49] The existence of bubbles for drug and gene delivery in the extra-capillary space is a desirable research objective, but is difficult to attain.[50] However, new techniques involving the ultrasonic expansion of perfluorocarbon nanoemulsion droplets are being explored.[51–54]

Even in the absence of purposefully introduced bubbles, cavitation can still occur. Most fluids contain dissolved gases, such as oxygen and nitrogen from contact with air. Upon exposure to ultrasound, the negative pressure fluctuations can cause dissolved gasses to nucleate into bubbles that may persist, particularly if they can be stabilized by a layer of surfactants.[13] Such surfactants can be proteins in the blood or extra-capillary space. Thus, it is possible to generate bubbles and then cavitate them *in vitro* or *in vivo*, even in the absence of contrast agents. However, the acoustic intensities required to form bubbles are generally so high that once formed, the bubbles grow by diffusion of more dissolved gas, and then quickly undergo collapse cavitation, fragment into smaller bubbles, grow again and continue the cycle.[12,13] Therefore, vigorous collapse cavitation can occur even when contrast agents or other bubbles are not introduced. In extremely clean and degassed water, the likelihood of bubble formation is decreased.

6.2.1.4 *Acoustic Streaming*

Another mechanical effect, independent of the presence of bubbles, is called "acoustic streaming". This occurs when the very small absorption of ultrasound by the water transfers the momentum from the absorbed sound to the fluid.[12,13] This causes convective flow in the direction of the ultrasound wave propagation. Acoustic streaming happens to a greater extent in colloidal suspensions of cells and protein since these components absorb ultrasound better than pure water. Flows can move as fast as 10 cm s^{-1},[55] but these flows do not have the extreme velocity gradients and shear stresses found in microstreaming and shock waves. The main beneficial effect of acoustic streaming is convective flow and mixing. There are reports of using acoustic streaming to press gas bubbles against blood vessel walls.[56]

6.2.1.5 *Safety*

The TI and MI safety indices described in Sections 6.2.1.2 and 6.2.1.3 were developed in the 1990s to protect delicate tissues from damaging exposure to heat and cavitation stresses. These delicate tissues include the fetus, heart, eye and brain.[46,57–60] In general there is less concern for thermal exposure and cavitation in other tissues because they have redundant architecture (kidneys, liver) or are non-essential (muscles, skin, *etc*.). There are also some reports of petechiae and thermal damage to the skin at high levels of insonation.[61,62] These problems were overcome by introducing different pulse sequences and cooling the transducers.[63,64]

Another topic of concern is that insonation of a tumor with accompanying cavitation might release fragmented portions of the tumor into the circulatory system where they may lodge and grow in other tissues, creating a type of "induced metastasis". Studies designed to reveal ultrasonic enhancement of tumor metastasis found none, even with highly metastatic tumors.[65–67]

6.3 Micelles

6.3.1 Drug Delivery from Micelles

In the science of nanomedicine, one of the most useful carriers for efficient drug delivery is the micelle. Micelles are assemblies of amphiphilic molecules in spheres or rods with diameters ranging from 5 to 100 nm. In aqueous systems, the molecules arrange themselves with their hydrophobic groups toward the interior of the structure and the hydrophilic group toward the surrounding water. Advantages of micelles over other nanocarriers are their easy method of preparation, the simplicity of loading hydrophobic drugs into their core, their stability and the fact that drug release from micelles can be controlled. Micelle stability is related to their critical micelle concentration (CMC), which is the molecular concentration below which the micelle will dissolve. A low CMC indicates that micelles will form readily and remain thermodynamically stable even in relatively low concentration. Once the micelles are diluted below their CMC, the rate of dissolution is related to the size of the amphipathic molecules. Micelles composed of large polymeric molecules take longer to disentangle and dissolve, and thus can persist in their metastable micelle form for minutes.[68,69]

Micelles have been used in pharmaceutical applications for centuries because of their ability to absorb hydrophobic drugs into their core, thus increasing drug loading in traditional aqueous oral formulations. With the advent of technology to introduce micellar formulations directly into the circulatory system (*via* intravenous infusion), it was noted that some formulations suffered from rapid clearance due to their fast uptake by the cells in the mononuclear phagocyte system (MPS). These micellar carriers persisted in circulation longer when coated with agents comprising poly(ethylene glycol) (PEG).[70] The coating agents modified the surface of the colloidal drug carriers such that adsorption of opsonizing proteins was inhibited, so that the cells of the MPS did not recognize and clear the carriers.[71] The ability of PEG-coated particles to inhibit adsorption of proteins depends on the surface density of PEO chains, their length and dynamics.[71] Prolonged circulation resulted in substantial increase of the area under the curve (AUC) of the blood concentration of the therapeutic agent over time.[72]

6.3.1.1 Traditional Surfactant Micelles

Before the advent of synthetic polymers, nearly all pharmaceutical formulations of micelles were composed of natural small surfactant molecules, such as fatty acids, alkyl esters of glycerol, phosphoglycerol esters and other amphiphilic molecules. It was found that the solubility of hydrophobic drugs could be greatly increased by adding these surfactants. These hydrophobic drugs were solubilized in the core of the micelle. The solubility of some amphiphilic drugs could also be increased by the addition of surfactants. These amphiphilic drugs partition to the interface between the hydrophobic core and the hydrophilic corona of the micelle.

With the progress of organic chemistry in the twentieth century, the natural surfactants were supplemented by synthetic surfactants or semi-synthetic surfactants. These new additions broadened the scope of drugs that could be adequately solubilized for oral and intravenous delivery. Surfactants used in micelles are generalized into four categories: anionic (phosphates, carboxylates, sulfates, *etc.*); cationic (usually amine-containing surfactants); zwitterionic (phosphocholines and synthetic surfactants) and non-ionic (ethoxylates, glucosides and more).[73] The charge and chemistry of the hydrophilic headgroup has a large effect on the solubilization capacity and the CMC. In general, the non-ionic surfactants have the greatest solubilization capacity, the anionic surfactants have the least, and cationic and zwitterionic surfactants fall in between.

While some surfactant micelles have very low CMC, polymeric micelles have even lower CMC values.[74] Once the concentration drops below the CMC, surfactant micelles usually dissolve faster than polymeric micelles. Therefore there is a trend to move towards polymeric micelles in new pharmaceutical formulations. To our knowledge there are no reports of ultrasonic-activated drug delivery from traditional non-polymeric micelles. However, that does not preclude the possibility of using surfactant micelles for ultrasonic drug delivery. Natural surfactants may have advantages in safety and biocompatibility.

6.3.1.2 Polymeric Micelles

It is attractive in drug delivery to use polymeric micelles comprised of hydrophobic-hydrophilic block copolymers, with the hydrophilic block containing PEG or other hydrophilic chains. These micelles usually have a spherical, core-like structure with the hydrophobic block forming the core and PEG chains forming the corona. Several types of these copolymers have been proposed. Among them, AB-type block copolymers, such as poly(L-amino)-co-poly (ethylene oxide)[75–78] and ABA-type block copolymers, such as the Pluronics.[79–81] Another class of these copolymers includes poly(ethylene oxide-*b*-isoprene-*b*-ethylene oxide) triblock copolymer, in which the isoprene blocks comprising the core were cross-linked by UV irradiation, rendering micelles stable in blood circulation.[82] As mentioned above, a particularly popular and useful family of polymers for micellar drug delivery is that of Pluronic triblock copolymers of poly(ethylene oxide) (PEO) – poly(propylene oxide) (PPO) – poly(ethylene oxide) (PEO). They are mostly water-soluble, and form micelles at various CMC values, depending on the ratio of PPO to PEO segments.[83] The hydrophobic block forms the core of the micelle and the hydrophilic PEO chains form the corona, resulting in a spherical core-shell structure.

Pluronic P105 is a particularly useful micelle-forming polymer because it easily dissolves in water and yet can carry a good payload of hydrophobic drugs.[84,85] The disadvantage with Pluronic P105 micelles is the relatively high CMC, such that when it is diluted upon intravenous injection, its local concentration drops below the CMC and the micelles start to dissolve.[86] To overcome this problem, the micelles were stabilized by polymerizing an interpenetrating network (IPN) of poly(*N*,*N*-diethylacrylamide) (NNDEA).[87] NNDEA was dissolved into and then polymerized within the Pluronic P105 micelles, which resulted in an IPN that markedly slowed the dissolution of P105 chains from the micelle. Cross-linking the NNDEA network increased micellar stability, such that the micelle could sequester hydrophobic molecules for weeks before total dissolution.[88] Tests were conducted in order to determine whether such stabilization would affect the ability of the micelles to sequester and release doxorubicin (Dox). It has been shown that the amount of drug released and its subsequent re-encapsulation were not very different from the behavior observed for unstabilized micelles, but had the added bonus of slow dissolution of the micelles. The stabilized micelles released Dox by application of 70-kHz ultrasound, as will be discussed in Section 6.3.2.1.[89]

Pluronic copolymers at different aggregation states have been tested as drug carriers.[90–95] Pluronic molecules in the unimeric form (below the CMC) were found to greatly enhance the cytotoxic activity of a wide variety of drugs. Above the CMC, Pluronic molecules form dense micelles with a lipophilic core that encapsulate the drugs within that core.[96] Pluronic and other amphiphilic copolymer micelles are recognized as some of the most novel types of carriers for chemotherapy drugs. The drug is usually introduced into the polymer matrix by mixing, and (in the absence of ultrasound) is slowly released upon the dissolution or degradation of the micelle or by drug diffusing from the micelle.[97] Of particular interest is poly(lactic acid)-b-poly(ethylene glycol) (PLA-b-PEG) since it is biodegradable and biocompatible, and exhibits proper hydrophilic/hydrophobic balance. Its degradation products are non-toxic and can be excreted by the kidneys.[91] Several methods of loading PLA micelles with Dox have been investigated.[98] There are many variations on this structure that employ the hydrolysis of PLA to control drug release.[99–101]

Related to PLA are other polyesters, such as poly(ε-caprolactone) (PCL). For instance, a self-assembled PEG-PCL diblock copolymer micelle was designed to solubilize and deliver the very hydrophobic drug honokiol.[102] PCL micelles have received some recent attention as drug carriers.[103–105] While polymeric micelles are sometimes praised for their high loading capacity for hydrophobic therapeutics,[106] exceeding the maximum loading capacity may cause the drug to precipitate. Furthermore, the aggregation number of the copolymer was found to influence the drug-loading efficiency of the micelle; a greater amount of drug can be incorporated into the core of a micelle with a higher aggregation number.[69]

6.3.1.3 *Drug–Polymer Conjugates*

Drug–polymer conjugates have been a rapidly developing field since they were first proposed in the mid 1970s, and nearly a dozen such carriers have now progressed to the clinical trial stage.[107] These include *N*-(2-hydroxypropyl) methacrylamide (HMPA)-Dox for lung and breast cancers,[108] HPMA-platinate for ovarian cancers and melanomas,[109] poly(ethylene glycol) (PEG)-poly(aspartic acid) (ASP)-Dox micelles for pancreatic cancer[110] and most importantly poly(L-glutamic acid) (PG)-paclitaxel for breast, colorectal, ovarian and lung cancers.[111,112] The latter is in Phase III clinical trials and is on track to become the first drug–polymer conjugate to be used in hospitals.[113] To synthesize drug–polymer conjugates, the chemotherapeutic agents are covalently bonded to a water-soluble polymer. For example PG-paclitaxel is covalently attached to PG *via* an ester bond through the 2′-hydroxyl moiety using a dicyclohexylcarbodiimide (DCC).[111] NMR confirmed the desired conjugation and it was estimated that seven paclitaxel molecules are bonded to each PG chain. The new drug–polymer conjugate suppressed the growth of murine ovarian carcinoma tumors in all 26 mice used in the study. After two months, 96% of the mice remained histologically free of the ovarian carcinoma.[111]

In another study, Nakanishi *et al.*[110] succeeded in synthesizing a PEG-ASP-Dox conjugate. Since this drug-delivery molecule has PEG on its outer surface, it was rendered stealthy and was able to circulate for longer periods of time without being recognized by the MPS.[110] Starting with PEG-NH_2 and the BLA-NCA (the unit of aspartic acid), the synthesis followed three steps: elongation and acetylation, debenzylation and, finally, the partial conjugation to Dox. This carrier showed significant antitumor activities in five different tumor types when compared to free Dox administered in a PBS solution.

Active targeting is also possible with drug–polymer conjugates by attaching a targeting moiety to the polymer. The advantages of drug–polymer conjugates are similar to those of self-assembled micelles and, most importantly, drug–polymer conjugates help overcome multi-drug resistance (MDR). Next we will discuss different targeting techniques that include passive targeting, active targeting and targeting using external stimulus.

6.3.2 Targeting

6.3.2.1 *Passive Targeting*

Blood vessels of healthy tissue have tight inter-endothelial junctions, while tumors often exhibit defective microvasculature with large inter-endothelial gaps. Those gaps result in heightened vascular permeability that allows submicron particles to extravasate beyond the capillaries. Passive targeting is based on the enhanced permeability and retention (EPR) effect that allows extravasation of drug-loaded nanoparticles through such defective microvasculature in tumors. Furthermore, tumors often exhibit poor lymphatic drainage, which reduces clearance of the extravasated carriers from the tumor tissue. Extravasation of nanoparticles does not occur in healthy tissue blood vessels except for specialized tissues such as the liver and kidneys. The accumulation of nanoparticles by the EPR effect requires sufficient circulation time in blood for the particles to collect slowly in the tumor. As mentioned, coating nanoparticles with PEO chains increases the circulation residence time and the amount of accumulation by the EPR effect.[114] Even so, usually less than 5% of the administered dose accumulates in the "targeted" tumor site by passive targeting means.[115]

There are many examples of passive targeting.[104,116–124] For example, Shin *et al.* studied the delivery of several chemotherapeutic agents using a poly(ethylene glycol)-block-poly(lactic acid) (PEG-b-PLA).[116] These agents include poorly soluble antineoplastic molecules such as paclitaxel, etoposide, docetaxel and 17-allylamino-17-demethyoxygeldanamycin (17-AAG). The study also characterized the loading and drug release profiles from micelles encapsulating 2- or 3-drug combinations. All loaded carriers had diameters in the range of 32–39 nm. Using turbidity measurements, 17-AAG was found to reduce drug precipitation, which in turn improves the stability of PEG-b-PLA micelles. Additionally, the study reported that single- and multi-drug micelles released their contents within 12 hours. The study concluded that this new formulation offered an effective method for administering chemotherapy agents with low solubility.

6.3.2.2 *Active Targeting*

There are some situations in which passive targeting is not sufficient, such as for targeting within the circulatory system, or for more specific targeting once the particles have extravasated and there are both healthy and tumorous cells in the extra-capillary space. In this case it is beneficial to attach small site-specific non-antigenic targeting ligands such as folic acid, antibodies, proteins (such as transferrin), sugars or polypeptides.[125–128]

Tumor-specific targeting is possible when the tumor cells express some surface component that is not usually present on normal cells. For example a wide variety of human tumors overexpress folate-binding protein, a glycosylphosphatidylinositol-anchored cell surface receptor for the vitamin folic acid.[129] Another example is the overexpression of the human epidermal growth factor receptor II (HER2) complex on many cancer cells.[130] Micelles can be directed to attach to these cells by conjugating the complementary ligand to the micelle. In many cases, the binding event will stimulate endocytosis of the ligand and its attached vesicle, thus introducing the therapeutic into the tumor, but still within an endosome. Subsequent escape from the endosome is required for maximal drug delivery. The number of ligands can be optimized to increase the efficacy of polymeric drug carriers.[131] Although the accumulation of micelles at the tumor site by passive targeting is largely independent of ligand attachment, ligand-conjugated micelles were found to demonstrate higher tumor fighting activity as compared to non-conjugated ones, which is attributed to direct surface interactions.[132] Furthermore, these targeted carriers can be synthesized to respond to changes in pH, where drug release is accelerated in the intra-cellular acidic environments of endosomes and lysosomes (pH below 4.8).[132,133]

One example of a folate targeted drug–polymer conjugate is the Dox-PLGA-PEG-FOL micelle, assembled by chemically conjugating Dox to the terminal end of PLGA in the diblock copolymer structure of PLGA-b-PEG, and then separately conjugating folate to the terminal end of PEG.[134] Other examples of folated micelles include the amphiphilic block copolymers of methoxy poly(ethylene glycol) (MPEG) and poly(ε-caprolactone) (PCL)[135] and the chondroitin sulfate-Pluronic® 127-folated nanogels, which are capable of inhibiting drug efflux transporters in chemotherapy.[136] To synthesize folated Pluronic P105 micelles (P105-FA), 1,1-carbonyldiimidazole can be used. Such folated Pluronic micelles were able to release Dox using low-frequency ultrasound.[136] Another study used cross-linked Pluronic micelles with folate conjugated to the surface as carriers of Dox and other anticancer drugs to target ovarian cancer. Significant antitumor effects have been observed *in vivo*.[137]

Another option in site-specific drug delivery is to create "immunomicelles" by attaching antibodies or antibody fragments (the Fab' fragment) to the micelles. Monoclonal antibodies can be conjugated, or they can be digested to obtain the Fab' fragment that can be attached by a variety of methods.[126] Polymeric micelles synthesized from polyethylene glycol-phosphatidylethanolamine (PEG-PE) conjugates have been tested and found to show higher accumulation at the tumor site than non-targeted micelles.[138]

Typically, immunomicelles such as 2C5 and 2G4 are tumor-specific, effectively binding to monolayers of antigens corresponding to their ligand.[139] It has been shown that certain monoclonal antibodies, including 2C5, are able to utilize cancer cell surface bound nucleosomes to recognize numerous tumors, but not normal cells.[140–142] Tests conducted with 2C5 labeled with Rhodamine have shown that the immunomicelle recognizes and binds to the surface of human BT20, murine LLC and El4 tumors.[139] The control, which consisted of micelles with no antibody, had practically no association between micelle and tumor cell. Moreover, 2C5-immunomicelles were not found to bind to any healthy cells.[140] Accumulation of 2C5-immunomicelles in murine LLC cells was found to be 30% greater than the accumulation of regular "free" micelles.[140]

In vivo tests confirmed the *in vitro* results above, and showed that micelles targeted with 2C5 monoclonal antibodies are capable of delivering the drug not only to mature tumors with a fully developed vasculature, but also to tumors in the early stages of development as well as to advanced metastatic cancers.[138] Other reports indicate that immunomicelles might be able to deliver the drug to the interior of the tumor cell *via* receptor-mediated endocytosis.[143]

6.3.3 Ultrasound-triggered Release from Micelles

The scenario of an ideal drug-delivery system entails the following: first, a carrier containing the drug would be injected and circulate in the blood. Then, a stimulus would be applied at a controlled location to release the drug. As mentioned, different types of stimuli have been examined, including pH, temperature, electric fields, light and ultrasound. Ultrasound has been found to be a preferred trigger mechanism due to its ability to propagate into deep tissue and to be focused directly on the target tissue.[91]

To date, there are only a few research groups working on ultrasonically controlled drug release from micelles. One is our group at Brigham Young University. Other groups include the Rapoport group at the University of Utah,[144] the Myhr group in Oslo,[145] the Phillips lab at La Trobe University in Victoria, Australia,[146] and the Mokhtari-Dizaji group in Iran.[147] The next sections review this body of literature.

6.3.3.1 *Triggered Release from Micelles* in vitro

Ultrasound triggered drug release from Pluronic P105 micelles was measured under pulsed ultrasound using an ultrasonic exposure chamber with fluorescence detection as illustrated in Figure 6.2. The study[90] examined the

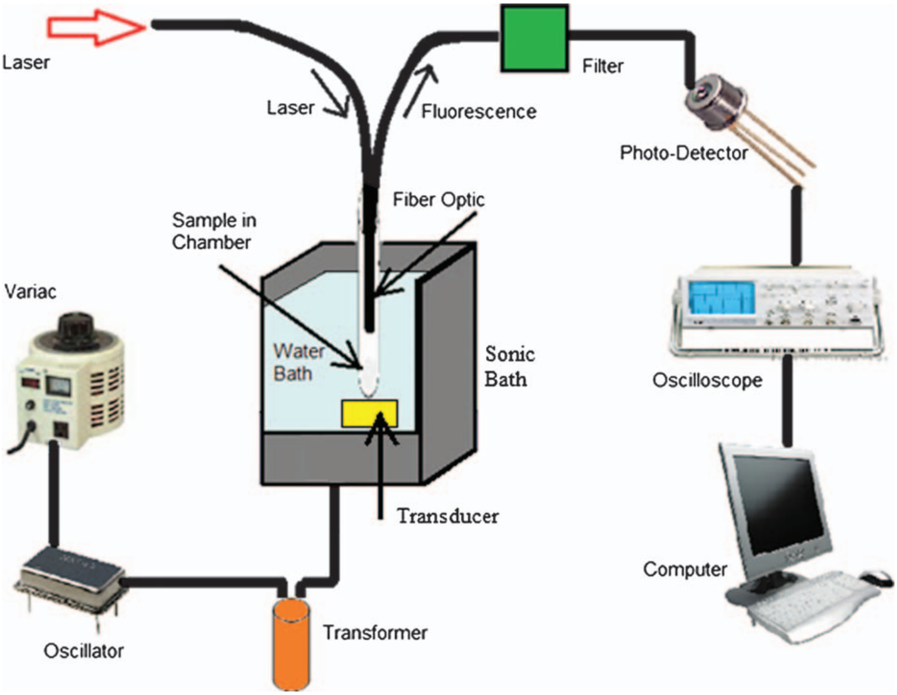

Figure 6.2 Fluorescence detection system with ultrasonic exposure. The intensity of ultrasound in the sonic bath is controlled by the AC voltage from a variac through an oscillator circuit and matching network (transformer). The sample is placed in an acoustically transparent plastic tube in an acoustically intense spot over the transducer. An argon ion laser beam (488 nm) is directed through a fiber optic cable into the sample chamber. The drug fluorescence is collected by a second fiber optic bundle and directed through a 533-nm band pass filter to a silicon photodetector. The detector signal is observed with an oscilloscope, and then digitized with an A/D converter and stored to a computer for post-processing conversion to released drug concentration.

amount of drug released in the low-frequency ultrasound range of 20 to 90 kHz. The analytical measurement in this and most studies employed the fact that many fluorescent molecules exhibit decreased fluorescence intensity when transferred from the hydrophobic core of the micelle to the aqueous environment. In this study, two intrinsically fluorescent drugs were used: Dox and Ruboxyl. The amount released was measured as a function of the applied frequency, and the most release was observed at 20 kHz. The drug release was found to decrease at higher frequencies, even when higher power densities were applied. The results indicated that the role of collapse cavitation in drug release is significant, since the MI increases as frequency decreases. It was also found that drug release increases at lower Pluronic concentrations and decreases if the drug is inserted deeper into the core of the micelle. Finally, the study also established that the drugs are re-encapsulated within the micelle between pulses of ultrasound.[90]

The kinetics of the release and re-encapsulation of Dox from Pluronic P105 micelles was studied using the same fluorescence detection exposure chamber mentioned above.[148] At a power density of 58 mW/cm^2 and a frequency of 20 kHz, experimental results showed that no significant drug release occurred from exposure to ultrasound for less than 0.1 s. This proved to be a threshold time value, above which the amount released was proportional to the pulse length. Furthermore, it was found that re-encapsulation requires a minimum ultrasound "off" phase of 0.1 s. The maximum amount of release and re-encapsulation was observed after around 0.6 s of ultrasound. After fitting the experimental data to several models, it was found that the zero-order release with first-order re-encapsulation kinetics fit the experimental data best.[148] A later study showed no significant difference between the rate constants of acoustic release at 37 °C and 56 °C. However, the release from stabilized micelles proceed significantly slower when compared to non-stabilized micelles.[149]

Further investigation into the kinetics of Dox release from Pluronic P105 micelles was conducted and experimental data fitted to a more complex model that included cavitation events. The first mechanism incorporated into the model was micelle destruction, which caused the release of Dox during insonation. The micelles were destroyed because the collapsing bubble produced shock waves. The second mechanism in the model, the destruction of cavitating nuclei, showed that a small amount of Dox was re-encapsulated, which initiated a slow and partial recovery phase, reassembly of micelles and re-encapsulation of Dox. The third mechanism was the reassembly of micelles and the fourth mechanism was the re-encapsulation of Dox. The latter two mechanisms did not show a dependence on ultrasound, but they were responsible for maintaining a steady-state drug release at a partial level and its re-encapsulation after the insonation ended. In this model, the micellar size distribution was described using a normal distribution.[150]

Experiments have also shown that ultrasound appears to disturb the interpenetrating network of the stabilized micelles, but the time constant of the degradation of the network is very long compared to the time constant related to drug release from micelles.[151] The results were used to deduce degradation kinetics of stabilized Pluronic P105 micelles. The study showed no significant difference between the network degradation time constants after one-hour exposures to 70- and 476-kHz ultrasound.[151]

Studies have also shown that the rate constant of Dox release depends on the degree of stabilization (by cross-linking). However, the re-encapsulation rate constant is roughly the same for stabilized and unstabilized micelles.[152] It has been shown that 70-kHz US releases around 2% of Dox from the core of stabilized Pluronic P105 micelles, whereas 9–10% was released from unstabilized P105 micelles.[26,27]

Later investigations into the thermodynamic characteristics of US-activated drug release from micelles allowed the deduction of thermodynamic activation energy for micelle re-assembly and residual activation energies for micelle destruction. The model showed that residual activation energy decreased as the acoustic intensity increased. Furthermore, higher temperatures were found to increase the rate of micellar destruction, but hindered the re-assembly of micelles.[152]

Artificial neural networks (ANNs) have also been used in modeling this drug-delivery mechanism. As a non-linear modeling technique, ANNs are capable of capturing and estimating the behavior exhibited by a system when exposed to various operating conditions. Some ANN control algorithms have been implemented in model predictive control (MPC).[153,154] ANN-MPC has been shown effectively to model, control and optimize Dox release from Pluronic P105 micelles, with feed-forward neural networks accurately capturing the dynamic behavior involved in Dox release.[97] Additionally, a controller was designed that adjusts the ultrasound frequency, intensity and pulse length in order to ensure a constant rate of Dox release. This controller has then been successfully validated.[155]

Sensitivity analysis using the ANN model of drug release revealed that lower frequencies contribute to the most efficient Dox release, and that the release increases with power density. The latter finding yet again confirms that cavitation plays an important role in US-triggered drug release. Also, according to the model, drug release was not a strong function of temperature, while ANNs indicated that lower copolymer concentrations contribute to a higher rate of drug release.[156]

A solution of diblock copolymeric micelles exposed to high-intensity focused ultrasound has been found to exhibit a decrease in pH. Tests conducted on samples revealed the cause of this phenomenon to be the formation of carboxylic acid dimers and hydroxyl groups. The results suggested that ultrasound induced the hydrolysis reaction of certain organic groups. Those results could be used to develop ultrasound-sensitive block copolymer micelles that have labile chemical bonds in the polymer structure. The idea is that these bonds would then be disrupted by high-intensity focused ultrasound.[157]

6.3.3.2 Triggered Release to Cells in vitro

The effect of high-frequency ultrasonication on the release of Dox from Pluronic micelles, and the subsequent uptake of Dox by cancer cells was studied using promyelocytic leukemia HL-60, ovarian carcinoma (drug-sensitive and multi-drug resistant) and breast cancer MCF-7 cells. Radical trapping was used to quantitate the cavitation events brought about by the high-frequency US. Even short exposure to high-frequency ultrasound was found to greatly increase the rate of cell uptake of the antineoplastic agent.[145,158]

The effectiveness of low-frequency ultrasound for triggering drug release from micelles was examined by exposing HL-60 cells to free Dox and Dox encapsulated in Pluronic P105 micelles.[159] Cells exposed to encapsulated Dox survived much longer than those exposed to free Dox. However, with the application of 70-kHz ultrasound, cells exposed to encapsulated

Dox were killed at a faster rate than those exposed to free Dox. These results indicated that micelles sequestered the drug from the cells prolonging their survival, and that ultrasound released the drug from the carrier.[159]

In order to measure the uptake of Dox by HL-60 cells, 70-kHz ultrasound was pulsed in tone bursts of 0.1 s to 2.0 s duration.[160] The time between the bursts was also varied between 0.1 and 2.0 s. It was found that with constant time intervals between bursts and with a constant total insonation time, the amount of Dox uptake by the cells augmented as the length of insonation increased (up to 3.0 s). The time between bursts had no effect on the amount of uptake of the drug.[160] This indicates that Dox did not return inside the micelles, other than the amount that could have diffused back into the micelles during the period between bursts. The total calculated time to reach 90% of complete uptake was 2.5 seconds of insonation.[159]

Another *in vitro* study employed MDA-MB-231 breast cancer cells in addition to HL-60 cells.[146] This study also employed Dox and P105 micelles, but these micelles were stabilized by the addition of disteroyl-phosphoethanolamine-PEG200 instead of an interpenetrating network. Encapsulation of Dox in these mixed micelles reduced Dox uptake by the MDA-MB-231 cancer cells *in vitro*. Application of 20-kHz ultrasound at 100 W/cm^2 released about 10% of the Dox from the micelles. However, this level of insonation destroyed HL-60 cells *in vitro* at durations of more than 5 s. In contrast, application of 5 s of insonation to the micelles at this power level increased the Dox uptake by HL-60 cells.

The effect of 48-kHz US on the cytotoxicity of cytosine arabinoside to HL-60 cells was examined, and an increase in cell death was observed with insonation. The study ruled out hyperthermia as the cause of death as the temperature increase was less than 0.2 °C. The insonated cells were also analyzed using a scanning electron microscope, which revealed the cells to have a decreased number of microvilli and a disrupted surface. It was concluded that insonation disturbed and modified the cell membrane, thus increasing the amount of drug taken in by the cells.[161] Several other studies have shown similar evidence of sonoporation.[47,162–164] It was also shown that ultrasound formed pores on the cell surface (sonoporation) that allowed the cytoplasm of HL-60 cells to leak out of those pores.[165]

It is also important to mention here that there appears to be a synergistic effect between chemotherapy drugs and ultrasound. A study has shown that exposure to ultrasound that lasted one hour rendered Dox significantly more toxic to Chinese hamster lung cancer.[160] Next we examine literature reporting *in vivo* drug release.

6.3.3.3 Triggered Release in Animal Models

There is a synergistic effect between chemotherapy drugs and ultrasound even in the absence of micelles. Several studies have shown that tumor growth was slowed by exposure to ultrasound and free drug[166] or liposomal drug.[24,145,167,168] For example, our research group used a tumor-bearing rat model to investigate the effect of ultrasound and micellar drugs on tumor growth rate and to determine which frequency works best in the treatment. It was found that the combination of drug and ultrasound resulted in a slower tumor growth rate than free drug without US. It was also found that ultrasound frequency does not affect the growth rate, as 20- and 478-kHz treatments yielded the same results.[159]

Another *in vivo* study was conducted using 42 rats, which were inoculated in each hind leg with a colon carcinogen DHD/K12/TRb tumor cell line. Six weeks after tumor inoculation, Dox encapsulated in stabilized Pluronic P105 micelles was administered weekly by intravenous infusion.[168] Ultrasound was applied about 30 minutes after infusion, allowing time for the micelles to begin accumulating at the tumor site. The study showed that a Dox concentration of 8 mg/kg was lethal within two weeks, while 5.33 and 4.0 mg/kg were lethal within six weeks. Concentrations of 1.33 and 2.67 mg/kg did not cause death. The general results looked promising, as the tumors that were exposed to a combination of encapsulated Dox and US grew slower than the tumors not exposed to ultrasound; some US-treated tumors actually regressed. In treated rats the distribution of Dox to various organs and tissues was measured, and more Dox was found in US-treated tumors than the contralateral untreated tumors. Furthermore, the drug was retained in the tumors longer and in higher concentrations than in other tissues, which suggests drug accumulation by the EPR effect with a maximum in concentration at about 12 hours.[169]

Similar studies have been done in mouse models. Tumors exposed to ultrasound and Dox-containing micelles accumulated a significantly greater amount of micelles than non-insonated tumors.[170] The same study reported that the cardiotoxicity of Dox is reduced by the use of micelles as the encapsulated Dox did not accumulate as much in the heart of the mice. Delivery and effectiveness of 5-fluorouracil (5FU) was also studied in a mouse model of colon cancer.[145] Tumor reduction was significant when the micellar delivery was combined with 20-kHz ultrasound at 3.16 W/cm^2 for 30 minutes.

In another mouse model, this time of breast cancer, ultrasonic frequencies of 28 kHz and 3 MHz were applied simultaneously to the tumor after intravenous administration of Dox in stabilized P105 micelles.[147] The biodistribution of Dox was compared to that when the micelles were not insonated and when free Dox was employed. The Dox concentration in various tissues was measured 24 hours after treatment. The mice receiving micellar Dox with ultrasound had nearly nine times more Dox in their tumors than mice receiving free Dox, and more than three times the amount found in mice receiving micellar Dox without insonation. The Dox concentration in other tissues was less with micellar Dox than with free Dox. This study supports the hypothesis that micellar Dox is extravasated in the tumor, and that insonation of the tumor further increases Dox retention and/or uptake in the tumor tissue. Other studies showed that US alone appears to increase extravasation.[30,171,172]

6.3.3.4 Mechanisms of Ultrasonic-Activated Delivery from Micelles

It is important to examine the mechanism by which micelles deliver anticancer drugs with and without ultrasound. First, micelles slowly and continually release drug. Thus if they collect in a tumor tissue *via* the EPR effect, release will occur to the exterior of the cells. The drug may then diffuse into the cells or enter by other pathways. A second mechanism is that micelles may be taken into the cell by endocytosis, a process by which a cell internalizes macromolecules and fluids from its surroundings. Two types of endocytosis exist: pinocytosis and receptor-mediated endocytosis. Pinocytosis is characterized by the uptake of small droplets of extra-cellular fluid, and any material dissolved in it. Receptor-mediated endocytosis, as the name suggests, utilizes a specific receptor on the cell membrane surface. This receptor binds to the target molecule, or ligand, which in turn sends a signal to the cell membrane to fold in on itself, forming a small vesicle through which the molecule is internalized. Micelles can be labeled with a targeting ligand, such as folate or anti-HER2 mAb, that induces endocytosis of the ligand and its attached micelle.[136]

When ultrasound is applied, additional uptake mechanisms come into play. Firstly, US can enhance the release rate of drug from micelles, which will be discussed thoroughly below. When US induces drug release from micelles, there is a higher concentration of external drug that can diffuse into the cell or enter by pinocytosis. If cavitation events sonoporate the cell membrane, released drug can diffuse directly into the cell, or whole micelles could diffuse in.[96] On a global scale, US appears to enhance extravasation, bringing more micelles into the tumor interstitium.[30,171,172]

Investigation into the mechanisms of ultrasonic drug delivery to cancer cells was conducted in an attempt to elucidate which of these mechanisms was mainly implicated in ultrasonic drug delivery from micelles. First, let's consider the shielding or protection effect that Pluronic P105 micelles have on the drug's cytotoxicity. Below the CMC, one study showed that the uptake of fluorescently labeled Pluronic micelles by HL-60 cells was proportional to the concentration present in the incubation medium.[96] Above the CMC, intracellular uptake of the micelles was far less efficient. These findings led to the conclusion that Pluronic micelles are internalized through fluid-phase endocytosis, rather than by diffusion through plasma membranes. The experiments were conducted using flow cytometry, fluorescence spectroscopy and confocal and fluorescence microscopy.

While US apparently up-regulates endocytosis in endothelial cells[173] and fibroblasts,[174] the increased accumulation of Dox in HL-60 cells was not due to increased endocytosis stimulated by ultrasonication.[175] Rather, it was suspected that sonoporation played the most important role in the process. This led to several hypotheses being proposed as to how ultrasound increases the rate of uptake of the drug by the cells.

One hypothesis states that acoustic streaming, or momentum transfer from sound waves to the biological fluid, and microconvection created by oscillating bubbles of gas in the liquid are responsible for the disruption of the cell membrane. The perturbed cell membrane is rendered more permeable to the drug. This concept has been discussed in Section 2.1.3; briefly, if the bubbles do not exhibit complete collapse during their shrinkage cycle, then stable cavitation creates high velocity gradients. But collapse cavitation also creates high shear stresses, which can sonoporate the cell membrane.[175] The micelles also experience the same high shear stresses. There is a strong correlation between the amount of drug released and subharmonic acoustic emissions, which is attributed to collapse cavitation that disturbs the micelle structure and results in the release of the drug (see Figure 6.1).[27] On a related note, our group has shown that increasing the static pressure suppresses bubble cavitation and drug release,[176] again supporting the hypothesis that bubble cavitation causes drug release. Thus, acoustic streaming and microconvection play very minor roles, if any at all.

Another hypothesis states that exposure to ultrasound increases the concentration of the drug (due to its release from micelles), but does not alter the permeability of the cell membrane. The high concentration outside the cell membrane creates a sufficiently high diffusion gradient for drug uptake by the cells. However, this hypothesis was dismissed when several studies demonstrated that ultrasound does indeed increase the permeability of the cell membrane.[175]

Micelles are transported into cancer cells *via* endocytosis, and the third hypothesis states that ultrasound increases the rate of endocytosis. Experiments have revealed that while ultrasound enhances drug uptake by cells, the rate of endocytosis is not enhanced; so this hypothesis was also dismissed.[175] Some experimental data support the possibility of this hypothesis, in that US does appear to enhance endocytosis in some cell lines,[173,174] but not in all cell lines.[175] Direct experimental uptake of micelles by US-enhanced endocytosis has not yet been observed.

The conclusion of this subsection is that acoustically activated micellar drug-delivery systems are rendered effective due to two main mechanisms. Ultrasound causes drug release from the micelles as it disrupts the core of polymeric micelles, most probably by strong shear stresses; and, additionally, ultrasonic sonoporation has been shown to form micropores in the membranes of cancer cells, which allows released drugs or whole micelles to diffuse passively into the cells.[84] Enhanced endocytosis is a possibility.

Additional studies showed drug uptake could be characterized by Langmuir-type isotherms, which implies that the system has a restricted number of sorption units.[158] Thus, the phenomenon of increased free drug uptake upon sonication could be attributed to new sorption centers being formed as cell structures are perturbed. It could also be that as the equilibrium between the drug inside the cells and the drug outside is shifted, excited drug molecules are generated. This excitation would increase the enthalpy of the drug internalization process.[158]

Once the micelle and drug molecules are taken up by the cell, the objective is for Dox to accumulate in the nucleus, intercalate into the DNA bases and affect many of the cell functions; primarily DNA replication. As a topoisomerase inhibitor, Dox is capable of causing single and double strand breaks in the DNA of treated cells. Therefore, the next paragraph summarizes the results of using the comet assay to measure the amount of DNA damaged.

The comet assay was used to quantify DNA damage by measuring the length and the fraction of broken DNA strands. The pattern of DNA damage indicated the mode of cell death.[177] Experiments were conducted in which cells were treated with various combinations of Dox, US and Pluronic P105 micelles. The cells were sonicated and lysed, then placed in an electrophoresis buffer, which resulted in DNA unwinding, after which electrophoresis was performed. Electrophoresis displayed the migration of intrinsically negative DNA away from the negative electrode and towards the positive electrode. Then a distilled water bath was used to re-anneal the DNA, which was then stained with propidium iodide, a fluorescent dye. Upon analysis, the electrophoresed DNA looks like a comet, with the damaged DNA migrating to form the tail, and undamaged DNA forming the head.[178] The results showed that ultrasound alone caused negligible damage to DNA, whether with or without P105. Dox contained in P105 caused no damage unless US was applied, and free Dox and Dox with ultrasound display various degrees of damage. The rate of DNA damage was higher when a combination of Dox, P105 and US was applied, and a slower rate was observed when Dox and US were used, and there was an even slower rate with free Dox.[175] Another study showed that apoptosis was the mode of cell death in ultrasonic Dox delivery from P105 micelles.[178] The conclusion was reached after examining DNA fragmentation pattern of cells exposure to US and encapsulated Dox.

In summary, polymeric micelles are proven drug carriers that can be activated by ultrasound to release their payload of drugs. By sequestering and then releasing with the ultrasonic trigger, drug delivery can be controlled in time and space so the adverse side effects of chemotherapy can be minimized. Pluronic P105 micelles have been successful in encapsulating and then acoustically releasing at least three chemotherapy agents. These micelles and their stabilized derivatives have also shown promise as viable delivery vehicles *in vitro* and *in vivo*. The question to be answered next is whether these micelles are efficient at higher ultrasonic frequencies that are easy to focus, but are less capable of penetrating deep tissues.

6.4 The Future of Ultrasound-triggered Drug Delivery from Micelles

Definitely the future of ultrasonically activated drug delivery from nanovehicles is bright. Ultrasound presents unprecedented non-invasive control of a fairly effective trigger. In the race to the clinic, ultrasound-triggered release from micelles is in competition with release from liposomes, polymersomes and other nanovehicles. When comparing triggered release from micelles and from liposomes, micelles have advantages in ease of manufacturing (self-assembly) and small size, but they have disadvantages in non-perfect sequestration (drug can slowly leak out) and incomplete release. Researchers and pharmaceutical companies must evaluate and select the best methods in terms of manufacturing cost, quality control, product stability, shelf life, consumer safety and more. As mentioned, the great advantage of the micellar systems is that they are self-assembled, so they are inherently stable and do not disassemble upon prolonged storage. In theory they can be lyophilized and reconstituted by the addition of water or saline, since they self-assemble. There remains much research to perform regarding manufacturing, storage and administration.

It follows, therefore, that for micellar systems to compete with liposomal systems, one needs to develop more effective sequestration in combination with more sensitivity to shear-stress induced release. This is a difficult conundrum to solve. Designing the core to attract the therapeutic more securely would decrease premature leakage, but would make the core less susceptible to rupture by shear stress, keep the therapeutic associated with the hydrophobic sites on the micellar molecules, and increase the rate of re-encapsulation once the micelle recovers from the shear assault. Some creative molecular design will be involved.

Another approach would be to create more cavitation events near the micelles to increase the shear stress on the micelle. For example, one could increase the amount of ultrasonic cavitation by providing extrinsic bubbles, such as perfluoropropane microbubbles that are fairly stable in blood and that are used as ultrasound contrast agents. Even better, the micelles could be attached directly to the surface of the microbubbles using the same conjugation chemistry employed to attach liposomes to microbubbles.[179,180] The size of the gas bubbles restricts delivery to the lumen of the vascular system, but these assemblies could be targeted to collect on diseased tissues of the circulatory system. Then the application of ultrasound could collapse the bubble supporting the micelles, creating high shear stress on the micelles and on the adjacent diseased tissue cells. This scenario would produce more concentrated release since all micelles are guaranteed to be in the immediate vicinity of a collapsing bubble. This delivery technique could be modified for delivery beyond the vascular system by attaching the micelles to nanoemulsions of perfluorocarbon liquids, such as perfluoropentane, stabilized by polymers or other surfactants.[51,52,114,181,182] These assemblies could be built sufficiently small to pass through the fenestrations in the malformed vasculature of tumors and collect in tumor tissues. Once on site, the application of ultrasound could transform the superheated perfluoropentane into a gas bubble in the tissue, which would upon further insonation collapse and rupture the attached micelles.

Needless to say, there are many opportunities for creative science in ultrasound-triggered delivery from micelles. And while the scientific community has not reached a perfect or ideal acoustically activated micellar drug-delivery system, we believe that we are moving forward towards this goal.

References

1. C. S. S. R. Kumar and F. Mohammad, *Adv. Drug Deliver. Rev.*, 2011, **63**, 789.
2. S. Power, M. M. Slattery and M. J. Lee, *Cardiovasc. Inter. Rad.*, 2011, **34**, 676.
3. A. P. Esser-Kahn, S. A. Odom, N. R. Sottos, S. R. White and J. S. Moore, *Macromolecules*, 2011, **44**, 5539.
4. L. H. Lindner and M. Hossann, *Curr. Opin. Drug Disc.*, 2010, **13**, 111.
5. Y. Bae and K. Kataoka, *Adv. Drug Deliver. Rev.*, 2009, **61**, 768.
6. A. Chilkoti, M. R. Dreher, D. E. Meyer and D. Raucher, *Adv. Drug Deliver. Rev.*, 2002, **54**, 613.
7. K. J. Yoon, P. M. Potter and M. K. Danks, *Curr. Med. Chem. Anticancer Agents*, 2005, **5**, 107.
8. K. Ashihara, K. Kurakata, T. Mizunami and K. Matsushita, *Acoust. Sci. Technol.*, 2006, **27**, 12.
9. D. A. Christensen, *Ultrasonic Bioinstrumentation*, Wiley, New York, 1988.
10. S. A. Goss, R. L. Johnston and F. Dunn, *J. Acoust. Soc. Am.*, 1980, **68**, 93.
11. S. A. Goss, R. L. Johnston and F. Dunn, *J. Acoust. Soc. Am.*, 1978, **64**, 423.
12. T. G. Leighton, *Prog. Biophys. Mol. Bio.*, 2007, **93**, 3.
13. C. E. Brennen, *Cavitation and Bubble Dynamics*, Oxford University Press, New York, 1995.
14. J. Wu, *Prog. Biophys. Molec. Biol.*, 2007, **93**, 363.
15. J. R. Wu and W. L. Nyborg, *Adv. Drug Deliver. Rev.*, 2008, **60**, 1103.
16. E. S. Richardson, W. G. Pitt and D. J. Woodbury, *Biophys. J.*, 2007, **93**, 4100.
17. T. G. Leighton, *The Acoustic Bubble*, Academic Press, London, 1994.
18. E. B. Flint and K. S. Suslick, *Science*, 1991, **253**, 1397.
19. W. B. McNamara, Y. T. Didenko and K. S. Suslick, *Nature*, 1999, **401**, 772.
20. L. Somaglino, G. Bouchoux, J. L. Mestas and C. Lafon, *Ultrason. Sonochem.*, 2011, **18**, 810.
21. T. J. Mason, J. P. Lorimer, D. M. Bates and Y. Zhao, *Ultrason. Sonochem.*, 1994, **1**, S91.
22. L. Villeneuve, L. Alberti, J. P. Steghens, J. M. Lancelin and J. L. Mestas, *Ultrason. Sonochem.*, 2009, **16**, 339.
23. G. J. Price, F. A. Duck, M. Digby, W. Holland and T. Berryman, *Ultrason. Sonochem.*, 1997, **4**, 165.
24. A. Schroeder, J. Kost and Y. Barenholz, *Chem. Phys. Lipids*, 2009, **162**, 1–16.
25. A. Schroeder, Y. Avnir, S. Weisman, Y. Najajreh, A. Gabizon, Y. Talmon, J. Kost and Y. Barenholz, *Langmuir*, 2007, **23**, 4019.
26. G. A. Husseini, M. A. Diaz de la Rosa, T. Gabuji, Y. Zeng, D. A. Christensen and W. G. Pitt, *J. Nanosci. Nanotechnol.*, 2007, **7**, 1.

27. G. A. Husseini, M. A. Diaz, E. S. Richardson, D. A. Christensen and W. G. Pitt, *J. Control. Release*, 2005, **107**, 253.
28. D. M. Hallow, A. D. Mahajan and M. R. Prausnitz, *J. Control. Release*, 2007, **118**, 285.
29. C. Y. Lin, Y. L. Huang, J. R. Li, F. H. Chang and W. L. Lin, *Ultrasound Med. Biol.*, 2010, **36**, 1460.
30. S. M. Stieger, C. F. Caskey, R. H. Adamson, S. P. Qin, F. R. E. Curry, E. R. Wisner and K. W. Ferrara, *Radiology*, 2007, **243**, 112.
31. M. A. O'Reilly, A. C. Waspe, M. Ganguly and K. Hynynen, *Ultrasound Med. Biol.*, 2011, **37**, 587.
32. E. E. Cho, J. Drazic, M. Ganguly, B. Stefanovic and K. Hynynen, *J. Cereb. Blood Flow Metab.*, 2011, **31**, 1852.
33. K. Hynynen, *Methods Mol. Biol.*, 2009, **480**, 175.
34. K. Hynynen, *Adv. Drug Del. Rev.*, 2008, **60**, 1209.
35. S. Meairs and A. Alonso, *Prog. Biophys. Mol. Bio.*, 2007, **93**, 354.
36. C. S. Yoon and J. H. Park, *Expert Opin. Drug Deliv.*, 2010, **7**, 321.
37. L. Zhang and Z. B. Wang, *Front. Med. China*, 2010, **4**, 294.
38. M. Fatar, M. Stroick, M. Griebe, A. Alonso, S. Kreisel, R. Kern, M. G. Hennerici and S. Meairs, *Ultrasound Med. Biol.*, 2008, **34**, 1414.
39. A. F. Prokop, A. Soltani and R. A. Roy, *Ultrasound Med. Biol.*, 2007, **33**, 924.
40. A. V. Alexandrov, C. A. Molina, J. C. Grotta, Z. Garami, S. R. Ford, J. Alvarez-Sabin, J. Montaner, M. Saqqur, A. M. Demchuk, L. A. Moye, M. D. Hill, A. W. Wojner, F. Al-Senani, S. Burgin, S. Calleja, M. Campbell, C. I. Chen, O. Chernyshev, J. Choi, A. El-Mitwalli, R. Felberg, S. Ford, Z. Garami, W. Irr, J. Grotta, C. Hall, Y. Iguchi, J. Ireland, L. Labiche, M. Malkoff, L. Morgenstern, E. Noser, N. Okon, P. Piriyawat, D. Robinson, H. Shaltoni, S. Shaw, K. Uchino, F. Yatsu, J. Alvarez-Sabin, J. F. Arenillas, R. Huertas, C. Molina, J. Montaner, M. Ribo, M. Rubiera, E. Santamarina, M. Saqqur, N. Alchtar, F. O'Rourke, S. Hussain, A. Shuaib, E. Abdalla, A. Demchuk, K. Fischer, M. D. Hill, J. Kennedy, J. Roy, K. J. Ryckborst and M. Schebel for the CLOTBUST Investigators, *New Engl. J. Med.*, 2004, **351**, 2170.
41. C. W. Francis, *Echocardiogr-J. Card.*, 2001, **18**, 239.
42. E. Biagi, L. Breschi, E. Vannacci and L. Masotti, *IEEE T. Ultrason. Ferr.*, 2007, **54**, 480.
43. E. Sassaroli and K. Hynynen, *Ultrasound Med. Biol.*, 2007, **33**, 1651.
44. R. E. Apfel and C. K. Holland, *Ultrasound Med. Biol.*, 1991, **17**, 179.
45. S. B. Barnett, G. R. Ter Haar, M. C. Ziskin, H. D. Rott, F. A. Duck and K. Maeda, *Ultrasound Med. Biol.*, 2000, **26**, 355.
46. W. L. Nyborg, *Ultrasound Med. Biol.*, 2001, **27**, 301.
47. P. Prentice, A. Cuschierp, K. Dholakia, M. Prausnitz and P. Campbell, *Nat. Phys.*, 2005, **1**, 107–110.
48. P. Marmottant and S. Hilgenfeldt, *Nature*, 2003, **423**, 153.
49. Y. Wang, X. Li, Y. Zhou, P. Huang and Y. Xu, *Int. J. Pharm.*, 2010, **384**, 148.

50. J. R. Lattin, D. M. Belnap and W. G. Pitt, *Colloid Surface B*, 2012, **89**, 93.
51. P. S. Sheeran, S. Luois, P. A. Dayton and T. O. Matsunaga, *Langmuir*, 2011, **27**, 10412.
52. P. S. Sheeran, V. P. Wong, S. Luois, R. J. McFarland, W. D. Ross, S. Feingold, T. O. Matsunaga and P. A. Dayton, *Ultrasound Med. Biol.*, 2011, **37**, 1518.
53. N. Y. Rapoport, A. L. Efros, D. A. Christensen, A. M. Kennedy and K. H. Nam, *Bubble Sci. Eng. Technol.*, 2009, **1**, 31.
54. R. N. Singh, G. A. Husseini and W. G. Pitt, *Ultrason. Sonochem.*, 2012, **19**, 1120.
55. H. C. Starritt, F. A. Duck and V. F. Humphrey, *Ultrasound. Med. Biol.*, 1989, **15**, 363.
56. M. J. Shortencarier, P. A. Dayton, S. H. Bloch, P. A. Schumann, T. O. Matsunaga and K. W. Ferrara, *IEEE T. Ultrason. Ferr.*, 2004, **51**, 822.
57. M. C. Ziskin and S. B. Barnett, *Ultrasound Med. Biol.*, 2001, **27**, 875.
58. S. B. Barnett, H. D. Rott, G. R. t. Haar, M. C. Ziskin and K. Maeda, *Ultrasound Med. Biol.*, 1997, **23**, 805.
59. S. B. Barnett, G. R. T. Haar, M. C. Ziskin, H. D. Rott, F. A. Duck and K. Maeda, *Ultrasound Med. Biol.*, 2000, **26**, 355.
60. D. Miller, P. Li and W. F. Armstrong, *Echocardiogr-J. Card.*, 2004, **21**, 125.
61. A. M. Rediske, B. L. Roeder, M. K. Brown, J. L. Nelson, R. L. Robison, D. O. Draper, G. B. Schaalje, R. A. Robison and W. G. Pitt, *Antimicrob. Agents Chemother.*, 1999, **43**, 1211.
62. T. Nishioka, H. Luo, M. C. Fishbein, B. Cercek, J. S. Forrester, C. J. Kim, H. Berglund and R. J. Siegel, *J. Am. Coll. Cardiol.*, 1997, **30**, 561.
63. A. M. Rediske, B. L. Roeder, J. L. Nelson, R. L. Robison, G. B. Schaalje, R. A. Robison and W. G. Pitt, *Antimicrob. Agents Chemother.*, 2000, **44**, 771.
64. H. Luo, Y. Birnbaum, M. C. Fishbein, T. M. Peterson, T. Nagai, T. Nishioka and R. J. Siegel, *Thromb. Res.*, 1998, **89**, 171.
65. L. Sicard-Rosenbaum, D. Lord, J. V. Danoff, A. K. Thom and M. A. Eckhaus, *Physical Ther.*, 1995, **75**, 3.
66. L. Sicard-Rosenbaum, J. V. Danoff, J. A. Guthrie and M. A. Eckhaus, *Physical Ther.*, 1998, **78**, 217.
67. D. L. Miller and C. Y. Dou, *J. Ultras. Med.*, 2005, **24**, 349.
68. C. Oerlemans, W. Bult, M. Bos, G. Storm, J. F. W. Nijsen and W. E. Hennink, *Pharm. Res.*, 2010, **27**, 2569.
69. M. C. Jones and J. C. Leroux, *Eur. J. Pharm. Biopharm.*, 1999, **48**, 101.
70. S. Stolnic, L. Illum and S. S. Davis, *Adv. Drug Deliver. Rev.*, 1995, **16**, 195.
71. S. I. Jeon, J. H. Lee, J. D. Andrade and P. G. DeGennes, *J. Colloid Interface Sci.*, 1991, **142**, 149.
72. J. C. Leroux, P. Gravel, L. Balant, B. Volet, B. M. Anner, E. Allemann, E. Doelker and R. Gurny, *J. Biomed. Mater. Res.*, 1994, **28**, 471–481.

73. A. Misra, K. Florence, M. Lalan and T. Shah, in *Colloids in Drug Delivery*, ed. M. Fanun, CRC Press, Boca Raton, FL, 2010.
74. V. P. Torchilin, *Pharm. Res.*, 2007, **24**, 1.
75. G. S. Kwon and K. Kataoka, *Adv. Drug Deliver. Rev.*, 1995, **16**, 295.
76. M. Yokoyama, T. Sugiyama, T. Okano, Y. Sakurai, M. Naito and K. Kataoka, *Pharm. Res.*, 1993, **10**, 895.
77. M. Yokoyama, T. Okano, Y. Sakurai, H. Ekimoto, C. Shibazaki and K. Kataoka, *Cancer Res.*, 1991, **51**, 3229.
78. G. S. Kwon, M. Yokoyama, T. Okano, Y. Sakurai and K. Kataoka, *Pharm. Res.*, 1993, **10**, 970.
79. E. V. Batrakova, S. Li, A. M. Brynskikh, A. K. Sharma, Y. L. Li, M. Boska, N. Gong, R. L. Mosley, V. Y. Alakhov, H. E. Gendelman and A. V. Kabanov, *J. Control. Release*, 2010, **143**, 290.
80. D. Y. Alakhova, N. Y. Rapoport, E. V. Batrakova, A. A. Timoshin, S. Li, D. Nicholls, V. Y. Alakhov and A. V. Kabanov, *J. Control. Release*, 2010, **142**, 89.
81. E. V. Batrakova and A. V. Kabanov, *J. Control. Release*, 2008, **130**, 98.
82. A. Rolland, J. O'Mullane, P. Goddard, L. Brookman and K. Petrak, *J. Appl. Polym. Sci.*, 1992, **44**, 1195.
83. P. Alexandridis, J. F. Holzwarth and T. A. Hatton, *Macromolecules*, 1994, **27**, 2414.
84. G. A. Husseini and W. G. Pitt, *J. Pharm. Sci.*, 2009, **98**, 795.
85. N. Rapoport and K. Caldwell, *Colloid Surface B*, 1994, **3**, 217.
86. N. Munshi, N. Rapoport and W. G. Pitt, *Cancer Lett.*, 1997, **117**, 1.
87. J. D. Pruitt, G. Husseini, N. Rapoport and W. G. Pitt, *Macromolecules*, 2000, **33**, 9306.
88. G. A. Husseini, R. I. El-Fayoumi, K. L. O'Neill, N. Y. Rapoport and W. G. Pitt, *Cancer Lett.*, 2000, **154**, 211.
89. G. A. Husseini, D. A. Christensen, N. Y. Rapoport and W. G. Pitt, *J. Control. Release*, 2002, **83**, 302.
90. G. A. Husseini, G. D. Myrup, W. G. Pitt, D. A. Christensen and N. Y. Rapoport, *J. Control. Release*, 2000, **69**, 43.
91. H. Zhang, H. Xia, J. Wang and Y. Li, *J. Control. Release*, 2009, **139**, 31.
92. N. Rapoport, A. I. Smirnov, A. Timoshin, A. M. Pratt and W. G. Pitt, *Archives Biochem. Biophys.*, 1997, **344**, 114.
93. N. Rapoport, *Colloid Surface B*, 1999, **16**, 93.
94. N. Rapoport and L. Pitina, *J. Pharm. Sci.*, 1998, **87**, 321.
95. N. Y. Rapoport, J. N. Herron, W. G. Pitt and L. Pitina, *J Control. Release*, 1999, **58**, 153.
96. M. D. Muniruzzaman, A. Marin, Y. Luo, G. D. Prestwich, W. G. Pitt, G. Husseini and N. Y. Rapoport, *Colloid Surface B*, 2002, **25**, 233.
97. G. A. Husseini, N. M. Abdel-Jabbar, F. S. Mjalli, W. G. Pitt and A. Al-Mousa, *J. Franklin I*, 2011, **348**, 1276.
98. J. R. Eisenbrey, O. M. Burstein, R. Kambhampati, F. Forsberg, J. B. Liu and M. A. Wheatley, *J. Control. Release*, 2010, **143**, 38.

99. Z. Y. Hu, F. Luo, Y. F. Pan, C. Hou, L. F. Ren, J. J. Chen, J. W. Wang and Y. D. Zhang, *J. Biomed. Mater. Res. A*, 2008, **85A**, 797–807.
100. C. Y. Zhan, B. Gu, C. Xie, J. Li, Y. Liu and W. Y. Lu, *J. Control. Release*, 2010, **143**, 136.
101. Y. Zeng and W. G. Pitt, *J. Biomater. Sci. Polym. Ed.*, 2006, **17**, 591.
102. M. Gou, X. Zheng, K. Men, J. Zhang, B. Wang, L. Lv, X. Wang, Y. Zhao, F. Luo, L. Chen, X. Zhao, Y. Wei and Z. Qian, *Pharm. Res.*, 2009, **26**, 2164.
103. A. S. Mikhail and C. Allen, *Biomacromolecules*, 2010, **11**, 1273.
104. M. L. Forrest, J. A. Yanez, C. M. Remsberg, Y. Ohgami, G. S. Kwon and N. M. Davies, *Pharm. Res.*, 2008, **25**, 194.
105. L. Zheng, M. Gou, S. Zhou, T. Yi, Q. Zhong, Z. Li, X. He, X. Chen, L. Zhou, Y. Wei, Z. Qian and X. Zhao, *Oncol. Rep.*, 2011, **25**, 1557.
106. K. Kataoka, A. Harada and Y. Nagasaki, *Adv. Drug Deliver. Rev.*, 2001, **47**, 113.
107. C. Li and S. Wallace, *Adv. Drug Deliver. Rev.*, 2008, **60**, 886.
108. T. Minko, P. Kopeckova and J. Kopecek, *Int. J. Cancer*, 2000, **86**, 108.
109. M. Campone, J. M. Rademaker-Lakhai, J. Bennouna, S. B. Howell, D. P. Nowotnik, J. H. Beijnen and J. H. M. Schellens, *Cancer Chemother. Pharmacol.*, 2007, **60**, 523.
110. T. Nakanishi, S. Fukushima, K. Okamoto, M. Suzuki, Y. Matsumura, M. Yokoyama, T. Okano, Y. Sakurai and K. Kataoka, *J. Control. Release*, 2001, **74**, 295.
111. C. Li, J. E. Price, L. Milas, N. R. Hunter, S. Ke, D. F. Yu, C. Charnsangavej and S. Wallace, *Clin. Cancer Res.*, 1999, **5**, 891.
112. E. Auzenne, N. J. Donato, C. Li, E. Leroux, R. E. Price, D. Farquhar and J. Klostergaard, *Clin. Cancer Res.*, 2002, **8**, 573.
113. J. W. Singer, S. Shaffer, B. Baker, A. Bernareggi, S. Stromatt, D. Nienstedt and M. Besman, *Anti-Cancer Drug*, 2005, **16**, 243.
114. N. Rapoport, K. H. Nam, R. Gupta, Z. G. Gao, P. Mohan, A. Payne, N. Todd, X. Liu, T. Kim, J. Shea, C. Scaife, D. L. Parker, E. K. Jeong and A. M. Kennedy, *J. Control. Release*, 2011, **153**, 4.
115. Y. H. Bae and K. Park, *J. Control Release*, 2011, **153**, 198.
116. H. C. Shin, A. W. G. Alani, D. A. Rao, N. C. Rockich and G. S. Kwon, *J. Control. Release*, 2009, **140**, 294.
117. S. R. Croy and G. S. Kwon, *Curr. Pharm. Design*, 2006, **12**, 4669.
118. Y. Bae, T. A. Diezi, A. Zhao and G. S. Kwon, *J. Control. Release*, 2007, **122**, 324.
119. Z. G. Gao, H. D. Fain and N. Rapoport, *J. Control. Release*, 2005, **102**, 203.
120. G. Gaucher, M. H. Dufresne, V. P. Sant, N. Kang, D. Maysinger and J. C. Leroux, *J. Control. Release*, 2005, **109**, 169.
121. N. Rapoport, *Prog. Polym. Sci.*, 2007, **32**, 962.
122. G. Kwon, M. Naito, M. Yokoyama, Y. Sakurai, T. Okano and K. Kataoka, *Langmuir*, 1993, **9**, 945.

123. K. Kataoka, T. Matsumoto, M. Yokoyama, T. Okano, Y. Sakurai, S. Fukushima, K. Okamoto and G. S. Kwon, *J. Control. Release*, 2000, **64**, 143.
124. G. S. Kwon, M. Yokoyama, T. Okano, Y. Sakurai and K. Kataoka, *J. Control. Release*, 1994, **28**, 334.
125. B. Stella, S. Arpicco, M. T. Peracchia, D. Desmaele, J. Hoebeke, M. Renoir, J. D'Angelo, L. Cattel and P. Couvreur, *J. Pharm. Sci.*, 2000, **89**, 1452.
126. L. Nobs, F. Buchegger, R. Gurny and E. Allemann, *J. Pharm. Sci.*, 2004, **93**, 1980.
127. S. Hirota and N. Duzgunes, *Curr. Drug Discov. Technol.*, 2011, **8**, 286.
128. P. Ghosh, B. K. Bachhawat and A. Surolia, *Arch. Biochem. Biophys.*, 1981, **206**, 454.
129. R. J. Lee and P. S. Low, *BBA-Biomembranes*, 1995, **1233**, 134.
130. J. Yang, C. H. Lee, J. Park, S. Seo, E. K. Lim, Y. J. Song, J. S. Suh, H. G. Yoon, Y. M. Huh and S. Haam, *J. Mater. Chem.*, 2007, **17**, 2695.
131. A. Hayama, T. Yamamoto, M. Yokoyama, K. Kawano, Y. Hattori and Y. Maitani, *J. Nanosci. Nanotechnol.*, 2007, **8**, 1.
132. Y. Bae, N. Nishiyama and K. Kataoka, *Bioconjugate Chem.*, 2007, **18**, 1131.
133. E. S. Lee, K. Na and Y. H. Bae, *J. Control. Release*, 2003, **91**, 103.
134. H. S. Yoo and T. G. Park, *J. Control. Release*, 2004, **96**, 273.
135. E. K. Park, S. Y. Kim, S. B. Lee and Y. M. Lee, *J. Control. Release*, 2005, **109**, 158.
136. S. J. Huang, S. L. Sun, T. H. Feng, K. H. Sung, W. L. Lui and L. F. Wang, *Eur. J. Pharm. Sci.*, 2009, **38**, 64.
137. N. V. Nukolova, H. S. Oberoi, S. M. Cohen, A. V. Kabanov and T. K. Bronich, *Biomaterials*, 2011, **32**, 5417.
138. A. N. Lukyanov, Z. Gao and V. P. Torchilin, *J. Control. Release*, 2003, **91**, 97.
139. V. P. Torchilin, A. N. Lukyanov, Z. Gao and B. Papahadjopoulos-Sternberg, *P. Natl. Acad. Sci. USA*, 2003, **100**, 6039.
140. L. Z. Iakoubov and V. P. Torchilin, *Oncol. Res.*, 1997, **9**, 439.
141. L. Iakoubov, O. Rokhlin and V. Torchilin, *Immunol. Lett.*, 1995, **47**, 147.
142. L. Z. Iakoubov and V. P. Torchilin, *Cancer Detect. Prev.*, 1998, **22**, 470.
143. J. W. Park, D. B. Kirpotin, K. Hong, R. Shalaby, Y. Shao, U. B. Nielsen, J. D. Marks, D. Papahadjopoulos and C. C. Benz, *J. Control. Release*, 2001, **74**, 95.
144. P. Mohan and N. Rapoport, *Mol. Pharmaceut.*, 2010, **7**, 1959.
145. G. Myhr and J. Moan, *Cancer Lett.*, 2006, **232**, 206.
146. M. Ugarenko, C. K. Chan, A. Nudelman, A. Rephaeli, S. M. Cutts and D. R. Phillips, *Oncol. Res.*, 2009, **17**, 283.
147. H. Hasanzadeh, M. Mokhtari-Dizaji, S. Z. Bathaie and Z. M. Hassan, *Ultrason. Sonochem.*, 2011, **18**, 1165.

148. G. A. Husseini, N. Y. Rapoport, D. A. Christensen, J. D. Pruitt and W. G. Pitt, *Colloid Surface B*, 2002, **24**, 253.
149. G. A. Husseini, M. A. D. de la Rosa, E. O. AlAqqad, S. Al Mamary, Y. Kadimati, A. Al Baik and W. G. Pitt, *J. Franklin I*, 2011, **348**, 125.
150. D. Stevenson-Abouelnasr, G. A. Husseini and W. G. Pitt, *Colloid Surface B*, 2007, **55**, 59.
151. G. A. Husseini, W. G. Pitt, D. A. Christensen and D. J. Dickinson, *J. Control. Release*, 2009, **138**, 45.
152. G. A. Husseini, D. Stevenson-Abouelnasr, W. G. Pitt, K. T. Assaleh, L. O. Farahat and J. Fahadi, *Colloid Surface A*, 2010, **359**, 18.
153. F. S. Mjalli and N. M. Abdel-Jabbar, *Ind. Eng. Chem. Res.*, 2005, **44**, 2125.
154. J. Saintdonat, N. Bhat and T. J. Mcavoy, *Int. J. Control.*, 1991, **54**, 1453.
155. G. A. Husseini, F. S. Mjalli, W. G. Pitt and N. M. Abdel-Jabbar, *Technol. Cancer Res. T*, 2009, **8**, 479.
156. G. A. Husseini, N. M. Abdel-Jabbar, F. S. Mjalli and W. G. Pitt, *Technol. Cancer Res. T*, 2007, **6**, 49.
157. J. Wang, M. Pelletier, H. J. Zhang, H. S. Xia and Y. Zhao, *Langmuir*, 2009, **25**, 13201.
158. A. Marin, H. Sun, G. A. Husseini, W. G. Pitt, D. A. Christensen and N. Y. Rapoport, *J. Control. Release*, 2002, **84**, 39.
159. G. A. Husseini and W. G. Pitt, *J. Nanosci. Nanotechnol.*, 2008, **8**, 2205.
160. K. Tachibana, T. Uchida, K. Tamura, H. Eguchi, N. Yamashita and K. Ogawa, *Cancer Lett.*, 2000, **149**, 189.
161. K. Tachibana, T. Uchida, K. Ogawa, N. Yamashita and K. Tamura, *Lancet*, 1999, **353**, 1409.
162. Y. Zhou, R. E. Kumon, J. Cui and C. X. Deng, *Ultrasound Med. Biol.*, 2009, **35**, 1756.
163. A. van Wamel, K. Kooiman, M. Harteveld, M. Emmer, F. J. ten Cate, M. Versluis and N. de Jong, *J. Control. Release*, 2006, **112**, 149.
164. R. K. Schlicher, J. D. Hutcheson, H. Radhakrishna, R. P. Apkarian and M. R. Prausnitz, *Ultrasound Med. Biol.*, 2010, **36**, 677.
165. P. Loverock, G. Ter Haar, M. G. Ormerod and P. R. Imrie, *Brit. J. Radiol.*, 1990, **63**, 542.
166. B. J. Staples, B. L. Roeder, G. A. Husseini, O. Badamjav, G. B. Schaalje and W. G. Pitt, *Cancer Chemother. Pharmacol.*, 2009, **64**, 593.
167. B. J. Staples, W. G. Pitt, B. Schaalje and B. L. Roeder, 34th Annual Meeting & Exposition of the Controlled Release Society, Long Beach, CA, 2007.
168. J. L. Nelson, B. L. Roeder, J. C. Carmen, F. Roloff and W. G. Pitt, *Cancer Res.*, 2002, **62**, 7280.
169. B. J. Staples, W. G. Pitt, B. L. Roeder, G. A. Husseini, D. Rajeev and G. B. Schaalje, *J. Pharm. Sci.*, 2010, **99**, 3122.
170. N. Y. Rapoport, D. A. Christensen, H. D. Fain, L. Barrows and Z. Gao, *Ultrasonics*, 2004, **42**, 943.

171. S. Samuel, M. A. Cooper, J. L. Bull, J. B. Fowkes and D. L. Miller, *Ultrasound Med. Biol.*, 2009, **35**, 1574.
172. C. Y. Lin, T. M. Liu, C. Y. Chen, Y. L. Huang, W. K. Huang, C. K. Sun, F. H. Chang and W. L. Lin, *J. Control. Release*, 2010, **146**, 291.
173. B. D. Meijering, L. J. Juffermans, A. van Wamel, R. H. Henning, I. S. Zuhorn, M. Emmer, A. M. Versteilen, W. J. Paulus, W. H. van Gilst, K. Kooiman, N. de Jong, R. J. Musters, L. E. Deelman and O. Kamp, *Circ. Res.*, 2009, **104**, 679.
174. J. Hauser, M. Ellisman, H. U. Steinau, E. Stefan, M. Dudda and M. Hauser, *Ultrasound Med. Biol.*, 2009, **35**, 2084.
175. G. A. Husseini, C. M. Runyan and W. G. Pitt, *BMC Cancer*, 2002, **2**, 1.
176. S. B. Stringham, M. A. Viskovska, E. S. Richardson, S. Ohmine, G. A. Husseini, B. K. Murray and W. G. Pitt, *Ultrasound Med. Biol.*, 2009, **35**, 409.
177. D. W. Fairbairn, P. L. Olive and K. L. O'Neill, *Mutation Res.*, 1995, **339**, 37.
178. G. A. Husseini, K. L. O'Neill and W. G. Pitt, *Technol. Cancer Res. T*, 2005, **4**, 707.
179. A. Kheirolomoom, P. A. Dayton, A. F. H. Lum, E. Little, E. E. Paoli, H. Zheng and K. W. Ferrara, *J. Control. Release*, 2007, **118** , 275.
180. A. L. Klibanov, T. I. Shevchenko, B. I. Raju, R. Seip and C. T. Chin, *J. Control. Release*, 2010, **148**, 13.
181. K. Shiraishi, R. Endoh, H. Furuhata, M. Nishihara, R. Suzuki, K. Maruyama, Y. Oda, J. I. Jo, Y. Tabata, J. Yamamoto and M. Yokoyama, *Int. J. Pharm.*, 2011, **421**, 379.
182. N. Y. Rapoport, A. M. Kennedy, J. E. Shea, C. L. Scaife and K. H. Nam, *J. Control. Release*, 2009, **138**, 268.

CHAPTER 7

Smart Polymersomes: Formation, Characterisation and Applications

R. T. PEARSON, M. AVILA-OLIAS, A. S. JOSEPH,
S. NYBERG AND G. BATTAGLIA*

The Krebs Institute, The Department of Biomedical Science, The University of Sheffield, Firth Court, Western Bank, Sheffield, South Yorkshire,
S10 2TN, UK
*Email: g.battaglia@sheffield.ac.uk

7.1 Polymersome Formation

The forces governing amphiphiles in solution adopt a delicate yet robust balance in order to facilitate the spontaneous assembly of supramolecular aggregates. The term amphiphile is derived from the Greek *amphis* meaning both and *philia* meaning love; this describes the mixed relationship that an amphiphilic molecule has with its solvent. More specifically, the molecule is comprised of solvent *phillic* (loving) and solvent *phobic* (hating) sections, which are coupled by strong chemical bonds and are unable to phase separate. If the amphiphile is a polymer and water is the solvent, the most entropically favorable situation for the polymer occurs when the unimers are dispersed throughout the solution, allowing for the maximum number of chain conformations. However, the inability for water molecules to bond with the non-polar, hydrophobic (water hating), sections of the amphiphilic polymer leads to the surrounding water molecules bonding with four adjacent water

---

RSC Smart Materials No. 2
Smart Materials for Drug Delivery: Volume 1
Edited by Carmen Alvarez-Lorenzo and Angel Concheiro
© The Royal Society of Chemistry 2013
Published by the Royal Society of Chemistry, www.rsc.org

molecules. This formation is known as a clathrate (from the Latin *clathratus* meaning cage or lattice) and is entropically unfavorable for the water molecules. In its liquid state, water is a highly dynamic system, rapidly switching between bonding with three and four other water molecules, therefore having an average co-ordination number of 3.5.[1] By forcing the water to adopt a more crystalline co-ordination, the entropy of the system is reduced, resulting in an increase in the free energy. For a very small number of amphiphiles this entropic penalty can be withstood and the individual molecules, or unimers, will remain molecularly dissolved. However, at a crucial concentration, the entropic penalty becomes sufficient for the hydrophobic sections to group together in a process known as the hydrophobic effect.[2,3] This reduces the overall amount of clathrate water present in the system and is known as the critical aggregate concentration (CAC). Often this is referred to as the critical micelle concentration (CMC) due to the micelle being the structure formed from the lowest number of unimers. This value is often quoted for lipid-based amphiphilic systems; however, for polymeric amphiphiles, the concentration is often difficult to measure due to it being so low.[4–6] After a number of amphiphiles have been brought together through hydrophobic forces, the molecule faces another dilemma with regards to its solvation. The close proximity of the chains reduces the volume of water molecules that can bond with the polar hydrophilic sections. This generates a repulsive force between hydrophilic sections as each chain attempts to maximize its interaction volume. However, the stronger hydrophobic force maintains the grouping of the molecules. Therefore, a compromise is achieved between the hydrophobic attraction and the hydrophilic repulsion, resulting in the formation of highly ordered but entropically favorable structures *via* self-assembly. This spontaneous process facilitates the formation of a range of nanoscopic soft matter structures with a vast range of applications. Of the potential structures available, one of the most exciting assemblies is the polymeric vesicle, commonly known as the polymersome.[7] In this next section, we will discuss approaches of forming polymersomes, the current theories of their assembly and methods to control their size.

One of the most common approaches to understanding the structures produced by organized amphiphiles is the molecular packing parameter (p), pioneered by Israelachvili *et al.*[8] Based on the geometric constraints of model lipid molecules assembling, the packing parameter describes the structures formed based on their relative hydrophobic : hydrophilic ratio

$$p = \frac{v}{a_0 l}$$

where v and l are the volume and length of the hydrophobic section, respectively, and a_0 is the interfacial area between the hydrophobic and hydrophilic blocks. The theory states that for values of $p \leq 1/3$ the hydrophilic repulsive forces create highly curved structures known as spherical micelles. These are monolayered particles with all the hydrophobic chains forming a water-free core and the hydrophilic blocks creating a protective corona. Micelles are typically the smallest aggregates seen in any self-assembling system, both in diameter and number of chains per aggregate (N_{agg}). Increasing the relative hydrophobic fraction slightly pushes the packing parameter to $1/3 < p \leq 1/2$; this causes the production of flat monolayers and cylindrical micelles (Figure 7.1). End caps to the cylinder are formed by amphiphiles with higher curvatures, comparable to spherical micelles. This is more favorable than exposing the hydrophobic core and more probable than the cylinder enclosing upon itself and forming a ring or donut structure. For $1/2 < p \leq 1$ the intermolecular curvature is even lower and generates the formation of bilayers or membranes. This is a sandwich-like conformation where the hydrophobic chains create a water-free region between two hydrophilic corona or leaflets. Like the cylindrical micelle, the hydrophobic membrane must be shielded from the water molecules. However, unlike the micelles the formation of highly curved edges to the membrane sheet is far more unfavorable. Therefore, the entire membrane shares the molecular frustration by curving to form an enclosed spherical membrane, trapping a small volume of water within, and forming a structure known as a vesicle. As mentioned previously, when the amphiphilic molecules are polymer chains, this structure is known as a polymersome. Within this range of $1/2 < p \leq 1$ the predicted curvature of the entire

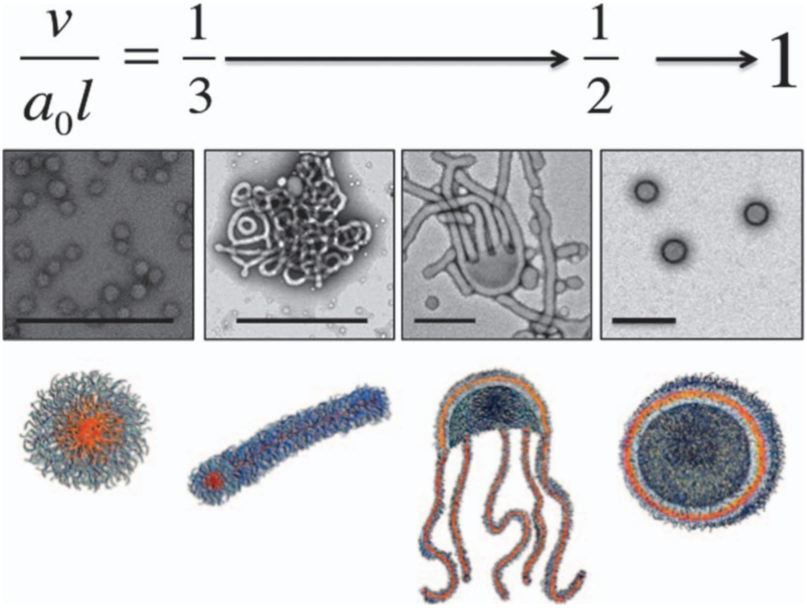
$\frac{v}{a_0 l} = \frac{1}{3} \longrightarrow \frac{1}{2} \longrightarrow 1$

Figure 7.1 The amphiphile packing parameter relates the molecular architecture to the average curvature experienced in a supramolecular assembly. From left to right in descending average molecular curvature, spherical micelles, cylindrical micelles, an intermediate "jellyfish" formation and polymersomes. The TEM scale bars = 200 nm.

membrane ranges from tightly curved around $p = 1/2$, where theoretically small vesicles are formed, and completely planar at $p = 1$, where an infinitely long and wide flat membrane is produced. As mentioned, this latter limit is practically impossible without anchoring the membrane to a substrate in order to satisfy the hydrophobic constraints. The theory provides a simple and roughly reliable model for predicting structures produced by amphiphilic polymers. Along with controlled "living" polymerisation techniques,[9,10] polymersomes can be produced simply by tuning the degree of polymerisation for the relative hydrophilic and hydrophobic volume fractions. Now that the effects of the molecular parameters on the curvature of the resulting structures have been explained, we can crudely divide polymersome formation into two categories: formation from the bulk and formation from solution.

Polymersome formation can be achieved *via* the hydration of a solid film of copolymer. This approach has been transferred directly from lipid vesicle production processes, wherein the polymer is dissolved in a suitable organic solvent and transferred to a vial. The solvent is then driven off before adding water or aqueous buffer to the dry polymer film and left under agitation for the required duration. During this time, the water diffuses into the polymer film, causing it to swell. As water moves into the dry film the copolymer begins to rearrange to generate conformations based on the hydrophobic effect and the molecular packing parameter. Over time, the concentration of water in the film increases and the structures produced evolve from highly ordered lytropic phases to increasingly dispersed mesophases, ending with isotropically dispersed polymersomes (Figure 7.2). The process has been well documented for block copolymer systems.[11–16] Typically, the initial diffusion of water into polymer causes molecular orientation due to the solvation and hydrophobic

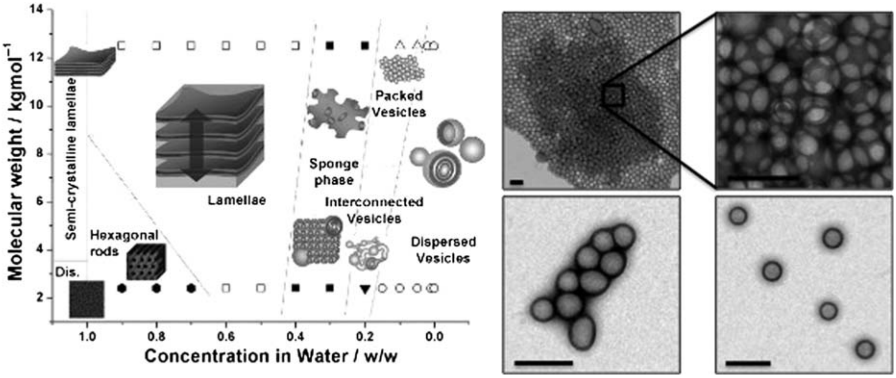

Figure 7.2 A phase diagram showing the structural transitions from solid copolymer films through to dispersed polymersomes for polymer amphiphiles. As discussed, the process of hydrating a dry film of copolymer causes the movement through these phases before reaching dispersed polymersomes. On the right TEM micrographs show the inter-connected "sponge" phase (above) with packed and dispersed polymersomes shown below. Scale bars represent 200 nm.

forces discussed previously. In the case of well-characterised, polymersome forming poly(ethylene oxide)-poly(butylene oxide) (PEO-PBO) diblock copolymers,[12,15] low water content ($\sim$80 wt. % polymer) films adopt a lamellar or hexagonal cylinder structure. This difference is based on molecular weight, where lamellar structures occur for the higher values; this lamellar phase swells with increasing water concentration, characterised by an increase in *d* spacing observed using Small Angle X-Ray Scattering (SAXS). Around 50 wt. % to 30 wt. % polymer these swollen films enter a new set of phases known as the "spongy" or gel phases, which still display some long-range order. The polymer molecular weight, the temperature and final mesophase (micelles or polymersomes) have a huge effect on the structure and properties of this region. Polymersome-forming copolymers produce bicontinuous sponge phases at high molecular weights and cubic packed multi-lamellar vesicles at low molecular weights, whereas micelle-forming PEO-PBO polymers are seen to form a series of close-packed gels with varied optical and mechanical properties based on temperature. As the water content increases further (20 wt. %–10 wt. % polymer) the polymer undergoes a transition from lyotropic gel phases to isotropic dispersed phases. For higher molecular weights, the bicontinuous sponge phase transforms into polymersomes grouped together in a hexagonally close-packed arrangement. The polymersomes then begin to disperse into individual aggregates around 1 wt. % polymer. Lower molecular weight polymersome-forming copolymers transform from cubic packed multi-lamellar vesicles to vesicles that are inter-connected with tubular membranes. These connections are then lost and the polymersomes disperse as single aggregates.

Alternatively, formation of polymersomes can be conducted from homogeneously distributed, molecularly dissolved unimers in a solvent environment suitable for both blocks. The process of self-assembly can then be achieved *via* altering the solvent environment, with parameters such as pH, temperature or water content.[17–26] A common model used to describe homogeneous polymersome formation is a two-step process of nucleation and growth. Firstly, coalescence of copolymer chains occurs *via* the hydrophobic effect, forming small spherical micelle aggregates. Aggregates then grow through a range of architectures of increasingly lower curvatures until spherical polymersomes are formed. Detailed investigations into these intermediate structures have been conducted across various polymer systems.[20,25,27–29] Eisenberg *et al.*[29] studied the micelle-to-vesicle transition of polystyrene-poly(acrylic acid) (PS-PAA) as a function of water to dioxane ratio, and observed the formation of short cylindrical micelles, followed by longer cylindrical micelles, before forming small vesicles at 28 wt. % water. Larger vesicles were seen at higher amounts of water and the whole process is reversible through the addition of dioxane. By studying the kinetics of these transitions and quenching samples at various time points, the same transition of micelles to vesicles *via* cylindrical micelles was observed.[27] The presence of "paddle"-shaped structures comprised of lamellae and cylindrical micelle sections was seen between the pure cylinders and pure polymersome time points. The same group then continued their studies by investigating the effect of changing PS-PAA block lengths on the transition boundaries.[24] Their results correlate with packing factor theory, showing that a longer core-forming block favors the production of polymersomes. pH responsive poly(butadiene)-poly(methacrylic acid) (PBD-PMAA) has been used to study the vesicle-to-micelle transition and the intermediate structures produced as a function of PMAA ionization.[19] Transmission Electron Microscopy (TEM) images taken across the pH range studied show the production of further intermediate species between polymersomes and cylindrical micelles and between cylindrical micelles and spherical micelles; specifically, structures containing a mixture of bilayers and monolayers between polymersomes and cylinders, including the striking "jellyfish" aggregate, a precursor to polymersomes (Figure 7.1). More recently, a study of the self-assembly process was conducted using *in situ* controlled radical polymerisation of poly(glycerol monomethacrylate)–poly(2-hydroxypropyl methacrylate) (PGMA-PHPMA).[30] The HPMA monomer is water soluble up to 13 w/v% at room temperature, but forms an insoluble polymer. Therefore, the evolution of micelles to vesicles was studied in detail by observing the structures produced at prolonged degrees of polymerisation in water. TEM micrographs show the transition from spherical micelles to shorter cylindrical micelles and then to longer cylindrical micelles in accordance with the previous studies mentioned. However, this approach elucidated significantly more information on the transitions from cylindrical micelles to complete vesicles. As the degree of PHPMA polymerisation increases, the cylindrical micelles begin to branch, and the branching points then swell until they eventually contain enough material to form a bilayer surrounded by cylinders, a formation referred to as an "octopus". These octopus structures have been reported previously in a PEO-PBD system by Jain and Bates.[20] The bilayers then curve to produce the jellyfish morphology mentioned earlier, before the bilayer segment of the jellyfish then encloses to form polymersomes. These approaches have elucidated the evolution from spherical micelles to polymersomes as the copolymer curvature reduces. A variety of striking conformations are adopted by polymer amphiphiles as they rearrange to find the minimal energy states between spherical micelles and polymersomes. However, large molecular weight polymeric amphiphiles display reduced molecular exchange kinetics, due to their increased hydrophobicity and weakly segregating inter-digitated membranes,[31,32] thus diminishing the likelihood of bilayer "flip flopping"[33] or unimer insertion/expulsion events.[34] A lack of chain exchange events leads to a kinetically frozen situation in many cases, wherein polymers produce a range of non-ergonomic structures that are "frustrated" with regards to their ideal curvature, but are unable to fuse or exchange with surrounding aggregates and thus remain in an undesired conformation. The reality of this situation from a manufacturing perspective is that large amounts of purification and post-processing are required in order to control the size and yield of the polymersomes produced. These processes have their own limitations and problems to overcome that fall outside the scope of this discussion. Despite these potential processing problems, the polymer membranes of polymersomes offer several advantages over their lipid counterparts. Firstly, the inter-digitated structure leads to greatly improved mechanical properties. For example poly(ethylene oxide)-poly(ethyl ethylene) (PEO-b-PEE) membranes have been shown to display mechanical properties roughly 5–50 times tougher than phosphatidylcholine (PC) membranes.[7] This leads to a much greater ability to withstand typical *in vivo* forces, a topic which will be covered in detail later on. The use of large molecular weight copolymers also provides the advantages of very low CMCs. This reduces problems such as disassembly by dilution.

Each of the two general formation pathways has its advantages and disadvantages. Briefly, rehydration of a polymer film is a slower process with longer time scales for increasing polymer molecular weight, whereas formation from solution is much quicker, but produces a broader range of structures than predicted by the molecular packing parameter due to kinetically trapped formations. Often the decision as to which method to use depends on the application and polymer chemistry. For biomedical applications, the use of organic solvents is highly detrimental to polymersome toxicity. Also the formation method is often determined by the log P of the therapeutic or diagnostic compound to be encapsulated. These interactions with biological systems will be covered in greater detail later in the chapter.

7.2 Polymersomes Characterization

The following section will explore the difficulties and innovations that have been realized in the imaging and analysis of polymersomes as nanoscopic soft-matter structures. Polymersomes and related soft-matter nanotechnology present unique challenges with regards to imaging. Their nanoscopic length scale requires techniques with a spatial resolution of around 200 nm or lower in order to elucidate individual particles. Furthermore, information regarding particle surface topology, domain formation and membrane thickness can require an order of magnitude higher resolution. Alongside this length-scale issue, the requirement of an aqueous environment in order to exist adds an additional difficulty when imaging polymersomes. Conventional light microscopy techniques are continually being refined in terms of spatial resolution. Breakthroughs in lens technology for conventional confocal microscopy and techniques such as Total Internal Reflectance Fluorescence (TIRF)[35,36] and Stimulated Emission Depletion (STED)[37,38] microscopy are pushing the boundaries of optical imaging. Often, these approaches require the presence of fluorescence probes to be incorporated within the polymersome. Regardless, TIRF and STED are capable of sub-200 nm imaging in liquid with good temporal resolution.

Electron microscopy (EM) has always been a steadfast approach to imaging on the nanoscale. The inherently smaller wavelengths of electrons allow for sub-1 nm resolutions to be readily achieved. However, most electron microscopy techniques require the presence of a high vacuum in order to avoid scattering of the electrons. This vacuum creates a problem for polymersome samples, which require the presence of an aqueous environment. In order to circumvent this dilemma whilst maintaining a high degree of spatial resolution, techniques such as cryogenic electron microscopy (CryoEM) and *in situ* liquid electron microscopy are used. CryoEM requires the sample to be rapidly frozen within an aqueous buffer *via* a process known as vitrification. This creates a situation where the sample is suspended within a matrix of solid non-crystalline water. By having a sufficiently thin section of vitrified sample, nanoscale resolution is obtainable. This technique has grown rapidly over the last 20 years in both the life sciences and soft nanotechnology, with many studies on polymersomes using this approach.[20,39–43] The direct imaging of cells and nanoparticles in liquid using electron microscopy often uses the approach of creating a thin layer of liquid between two electron permissive windows.[44,45] This technique is still far from competing with the resolutions achieved by conventional EM or cryogenic EM; however, it shows great promise for imaging aqueous processes in real time.

The techniques discussed so far all require the illumination and detection of electromagnetic radiation. Atomic Force Microscopy (AFM) is able to provide nanoscale imaging in a range of environments by measuring minute deformations in a cantilever.[46–48] The resolution of AFM is determined by the tip architecture, a range of tips are commercially available and many provide subnanometer resolution. Also, topographical, mechanical and chemical data can be obtained using AFM depending on the analysis mode used and the tip chemistry. Each measurement point is converted into a pixel, providing an image where contrast is gained through various perturbations of the tip. AFM has been used to gain morphological and topographical data on polymersomes. For example, a streptavidin functionalized tip was used to observe the formation of biotin domains upon the polymersome surface (Figure 7.3A). A tapping mode was used to measure the force required to detract the tip from the surface of the polymersome. In the presence of biotin, the force required is much greater. Results for each measurement were converted into an image showing the presence of phase-separated domains upon the surface of hydrated nanoscopic polymersomes.[49] A potential drawback of AFM is the requirement of the sample to be anchored to a substrate for analysis. For polymersomes this can be achieved by drying the sample and visualizing the collapsed structures, as shown in Figure 7.3E. Alternatively, in the study discussed above, hydrated polymersomes were imaged by immobilizing biotin-functionalized polymersomes to a streptavidin-coated substrate. This enabled the imaging of stationary polymersomes whilst also allowing the analysis of biotin domains upon the polymersome surface as discussed above.

Imaging is useful for observing morphological changes and providing a visual aid in understanding polymersomes. However, imaging a statistically relevant percentage of the sample is often unfeasible due to a trade-off between resolution and analysis volume/area. There are many other well-established techniques used to gain averaged data from entire samples, and a detailed description falls out of the scope of this discussion. However, we will cover a few commonly used methods in order to outline some of the parameters frequently obtained for polymersomes. Scattering techniques provide a vast

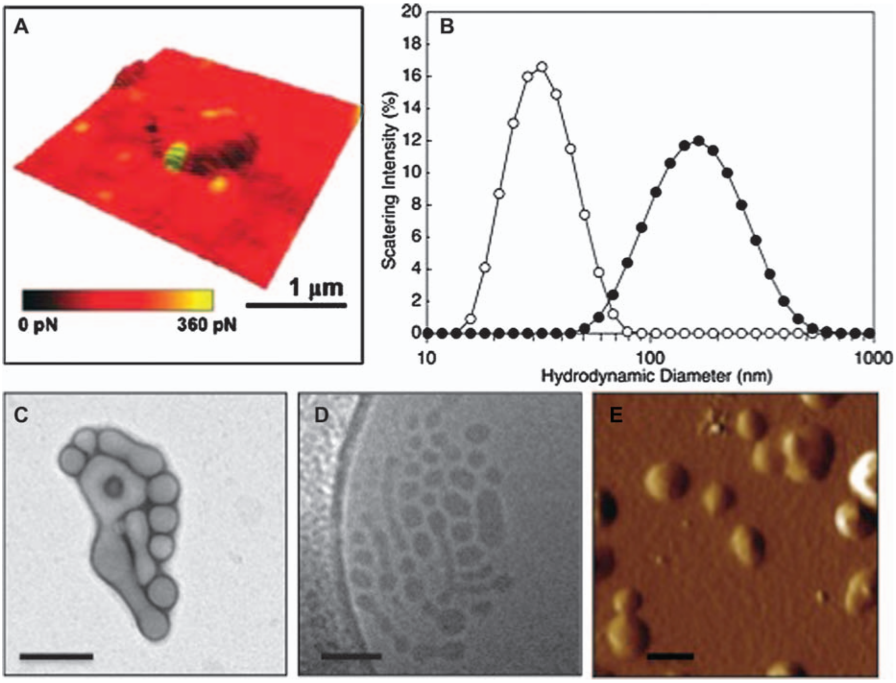

Figure 7.3 Polymersomes analyzed by various techniques: force mapping AFM showing the presence of nanoscopic domains on the surface of the polymersome (A); Dynamic Light Scattering (DLS) showing a typical size distribution for micelles (white points) and polymersomes (black points) (B); and ambient TEM (C), Cryogenic TEM (D) and amplitude mapping AFM (E) of the same sample of polymersomes.

amount of information based on angle-specific elastic interactions between particles and energy sources such as light, X-rays or neutrons. The amount, quality and type of data obtainable by scattering techniques vary with the type of sample and the quality of the energy source. Typically, for polymersomes, information regarding average particle diameter, particle shape, membrane thickness, corona brush depth, amount of bound water and average diffusion coefficient is achievable.[50–53] However, many of these parameters require high-intensity energy sources and long illumination times in order to obtain sufficient data.

As with most analytical approaches, it is often best to use a combination of techniques to characterise polymersomes as fully as possible. Often these techniques are combined with absorbance- or fluorescence-based quantification techniques, frequently in conjunction with chromatography.

Polymersomes are intriguing nanoscopic structures; however, their mimetic nature has driven a huge amount of research into using polymersomes as therapeutic biological delivery systems. The following section will concentrate on the parameters surrounding polymersomes as delivery vectors.

7.3 Polymersomes as Delivery Vectors

Recently, nanotechnology has generated a great deal of interest throughout the biomedical sciences, due to its potential to offer novel approaches to therapeutic and diagnostic drug delivery. Traditional drug formulations are often associated with poor protection of the compound of interest from the biological environments and a lack of controlled release, spatially or temporally. This sometimes results in the need for frequent doses in order to reach a therapeutic effect, which in turn can result in unwanted side effects.

Nanotechnology takes a multi-disciplinary approach to engineer nanoscopic devices that offer enhanced transport and protection of bioactive cargo, increasing the ability to overcome biological barriers and release their cargo at the cellular or subcellular level. Compound delivery by nanoparticles (NPs) is a common nanotechnology approach to enhance drug delivery. The type of nanoparticle is often defined by the material that it is comprised of and the methods of assembly. There is a range of such particles including hard metal nanoparticles (gold, iron), carbon-based NPs (quantum dots, carbon nanotubes) or soft nanotechnology such as lipid nanoparticles (micelles, liposomes) and polymeric nanoparticles (micelles, dendrimers, polymersomes). For this discussion we shall focus primarily on polymersomes as drug-delivery vectors. They are of particular interest due to their ability to encapsulate a range of hydrophilic, hydrophobic and amphiphilic compounds. As mentioned, they display enhanced mechanical properties with respect to lipid systems as a result of the high molecular weight entangled membranes. Also the fully synthetic nature allows for customisable carrier systems. The principal physicochemical characteristics of polymersomes that modulate their behavior across a range of increasingly complex biological systems are highlighted below. Strategies specifically to engineer polymersomes in order to produce enhanced drug-delivery systems are also covered.

Successfully navigating the complex biological barriers experienced by a drug-delivery device is no trivial task. Nevertheless, an ideal system should be able to chaperone the compound of interest through these barriers in order to reach the site of action such as a tissue or a specific group of cells. Therefore, identifying the biological obstacles that a drug-delivery system must overcome is essential for engineering an efficient drug-delivery system. Renal clearance (excretion in the urine after blood filtration by the kidneys) and opsonisation (the passive targeting of foreign bodies by proteins for subsequent recognition by the immune system) are major factors determining the lifetime of nanoparticles in our bodies. These processes are strongly dependent on nanoparticle properties, especially the surface chemistry and size. Nanoparticles with diameters around 100 nm and neutral hydrophilic surface chemistries are generally associated with longer blood circulation times and longer residence times in our bodies.[54,55]

Blood is continuously cleaned *via* filtration by the liver and kidneys, with the consequent excretion of waste products in the feces and urine. Mammalian vessels have an average natural pore size of 5 nm.[56] This means that particles smaller than 5 nm can cross the endothelium easily, equilibrating their concentration in blood and the extra-cellular environment quickly. This can be beneficial for non-specific extra-cellular delivery. However, a similar cut-off is found in the kidneys where only a small fraction of the renal filtrate is reabsorbed back to the blood circulation (water, glucose and small solutes, though often through specific transporters). This indicates that nanoparticles below 10 nm or 50 KDa[56,57] can be efficiently cleared from our bodies *via* the kidneys. Fast renal clearance can be avoided in most cases by engineering NPs bigger than 10 nm in diameter.

As mentioned, another mayor biological obstacle to avoid is opsonisation. Opsonisation is the binding of blood proteins called opsonins to a foreign entity, in this case the nanoparticle, in order to alert the immune system to its presence. Any protein that assists in the immune recognition of a foreign body can be an opsonin. Typically the most common opsonins are immunoglobulins, and complement proteins.[58] However, albumin, fibrinogen and apolipoproteins often work as opsonins.[59] The opsonised particle is subsequently recognized by the immune system; specifically by macrophages of the mononuclear phagocytic system (MPS), also known as the reticuloendothelial system (RES). In most cases, MPS recognition is translated in nanoparticle clearance from the blood, with associated accumulation in liver, lungs and spleen, organs harboring large quantities of MPS macrophages.[60] It has been reported that maintained accumulation of non-biodegradable nanoparticles in MPS organs can lead to toxic effects.[61,62] Blood clearance by opsonisation occurs quickly for nanoparticles greater than 300 nm,[60] within minutes for uncoated nanoparticles[58] and more easily for hydrophobic particles than for hydrophilic ones.[63] Hydrophobic colloids are unstable in aqueous environments such as the blood, and present an enhanced tendency to adsorb proteins in order to reduce contact with the water. On the other hand, hydrophilic particles are surrounded by water molecules, limiting their interactions with other molecules such as proteins. The use of neutral, hydrophilic polyethylene glycol (PEG) (also known as PEO) to coat nanoparticle surfaces is a major strategy in avoiding opsonisation or "fouling". This has been shown to increase blood circulation time of the nanoparticle.[54] For this reason PEGylated systems are usually referred as "stealth" systems. PEG with different molecular weights as well as diverse surface concentrations allows for modification of the non-fouling properties.[64–68] It is generally accepted that a minimum MW of 2000 Da is necessary to impart "stealth" properties to a system.[58] Reasons behind this interesting biological ability can be found in the physico-chemical properties of PEG. PEG is a neutral, water-soluble and flexible polymer.[69] This means that PEG chains in aqueous medium are surrounded by water molecules, creating an ordered water shell between the nanoparticle and the environment. Therefore, a protein trying to interact with a nanoparticle will start to compress the hydrated hydrophilic PEG chains, forcing the removal of water from the system, which is energetically unfavorable. This energy barrier will act against opsonisation, preventing any strong interaction with the nanoparticle.[58]

PEGylation has been used to produce "stealth" liposomes. Nevertheless the percentage of PEG that liposomes can be coated with is restricted to a maximum of 10% in order to maintain the formation of a membrane.[70] It would be preferential to have a greater amount of PEG incorporated in the system. One advantage of polymersomes over liposomes is their synthetic nature. Therefore, the hydrophilic corona can be entirely composed of PEG, subsequently improving nanoparticle protection from opsonization. Also, the increase in amphiphile hydrophilicity can be counteracted by polymerising the hydrophobic block further, resulting in 100% PEG-based polymersomes.[68]

Although PEG is the most commonly used hydrophilic polymer for polymersomes, there are many alternatives available. These include poly(2-methacryloyloxyethyl phosphorylcholine) (PMPC), poly(hydroxyethyl methacrylate) (PHMA),[71] poly(*N*-vinyl pyrrolidone) (PVP)[72] and poly(2-methyl-2-oxazoline) (PMOXA).[73] The concept behind generating "stealth" remains the same, *i.e.* to cover the particle surface with a hydrophilic polymer in order to hinder the adsorption of proteins.[58] It is important to note that the use of such polymers only delays the opsonization of the system for a certain time; adsorption of proteins on the particle surface will eventually happen. Also, it is worth noting the trade-off between "stealth" systems having prolonged circulation lifetimes but reduced cellular uptake (Figure 7.4).[74]

In order to retain the advantage of non-folding polymer coatings whilst simultaneously enhancing cellular uptake the attachment of ligands is often exploited. These are molecules that are recognised strongly by receptors expressed on the cell surface. The attachment of ligands enhances nanoparticle recognition and uptake by cells. Furthermore, using this approach, we can specifically target a tissue or group of cells, provided that they overexpress a biological marker or, better still, present it exclusively. This approach is known

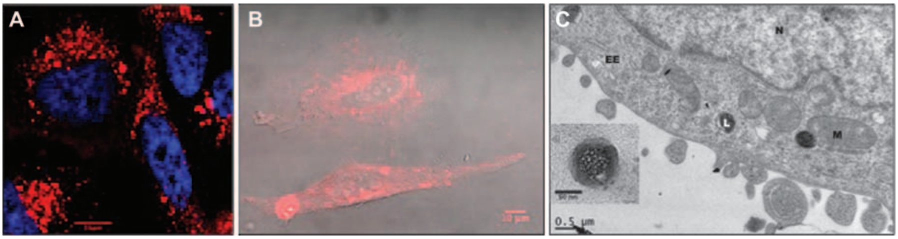

Figure 7.4 Cellular uptake of polymersomes and polymersome-mediated delivery of different compounds into cells. Cellular distribution of rhodamine-labeled polymersomes in HeLa cells after treatment with 1 mg/mL polymersomes for 60 min (nuclei stained in blue) (A); HeLa cells stained in red after 60 min incubation with 1 mg/mL of PMPC polymersomes encapsulating Celluminate® red fluorescent dye (B); TEM micrograph of HeLa cells showing gold nanoparticles distribution trough cell cytoplasm, different organelles and nucleus, after treatment with PMPC polymersomes encapsulating gold nanoparticles for 24 h (C). Insert: TEM micrograph of PMPC polymersomes encapsulating gold nanoparticles 1.4 nm average diameter.

as active targeting. The ability specifically to deliver a therapeutic compound to its site of action is one of the most desirable properties for a drug-delivery system. Specific targeting means that the drug will be concentrated in an area of interest rather than being distributed throughout the body. This reduces side effects derived from interactions between the drug and other areas of the body. In addition it would be possible to reduce the total amount of drug needed since it would accumulate at the desired site. Lower side effects and a lower dose regime result in better patient compliance and reduced costs associated with side effects and multiple dosing. The synthetic nature of polymersomes makes them an ideal vector for active targeting. Examples of biological markers that can be used for active targeting of nanoparticles include the well-studied transferrin and folate receptors, which are overexpressed in tumor cells.[60,75,76] Epidermal growth factor receptors[77,78] have also been recently investigated for tumor targeting. Intra-cellular cell adhesion molecule 1 (ICAM-1)[79] and vascular cell adhesion molecule 1 (VCAM-1)[80] have been used to target endothelial cells in atherosclerotic plaques and inflammatory processes. In recent years, integrins, a family of cell adhesion molecules, have become promising candidates for active targeting since they are implicated in many diseases such as cancer, autoimmune disorders and infectious processes.[81,82]

Once the drug-delivery device has avoided these biological barriers and reached its target site it must interact directly with cells in order to release its cargo. The following section covers the current understanding on nanoparticle interactions leading to cellular internalisation.

Mechanisms of nanoparticle cellular internalisation have mostly been found to be energy-dependent processes, rather than passive diffusion through pores or the membrane.[83] Specifically, endocytosis, the internalisation of fluids, molecules and macromolecules by the controlled deformation of the plasma membrane, has been identified as the primary cellular internalisation pathway for many nanoparticles formulations.[84] Endocytosis and its consequent subcellular sorting is a complex process with multiple cellular pathways often playing interconnecting roles. Understanding these complex mechanisms is key to improving nanoparticle uptake efficiency and to establishing a greater understanding of toxicological effects on the system. Endocytosis is traditionally divided into phagocytosis and pinocytosis. Phagocytosis is almost exclusive to immune cells such as macrophages and neutrophils and is normally reserved for the internalisation of large bodies (>1 μm in diameter). Cells that are able to undergo phagocytosis are often called phagocytes. However, pinocytosis is a process present in almost all eukaryotic cells and it is used for the uptake of particles smaller than 1 μm. Pinocytosis can be further subdivided into several mechanisms defined by the specific lipids and proteins involved in each process. As the particle diameter decreases, it becomes increasingly difficult to correlate its size with a specific pathway of endocytosis. The precise boundary between different pathways is still an area for much debate, and which particular mechanism of uptake remains highly dependent on the type of cell and nanoparticle formulation. For a more detailed summary of parameters affecting drug-delivery system uptake efficiency we direct readers to a recently published review.[85]

In recent years, studies have shown that nanoparticle size is associated with different rates and mechanisms of internalisation. Generally, nanoparticles <100 nm are internalised faster than particles >100 nm.[86,87] In the case of receptor-mediated endocytosis the optimal nanoparticle diameter for cellular uptake has been identified as between 50 and 60 nm.[88–93] Nevertheless these guidelines are strongly affected by other physico-chemical properties of the nanoparticle and hence should be altered for each formulation. When investigating studies on the effects of size on uptake in the literature it is important to define the methods used to calculate optimal nanoparticle size. This can be measured either in terms of speed of uptake or by the total number of nanoparticles internalised within a given time scale. In some cases, the optimal size may vary between the two measurements. Furthermore, as most nanoparticles are designed to be delivery systems, it is important to balance the particle size for uptake with the optimal size for efficient encapsulation of a therapeutic and/or diagnostic compound.

Alongside size, nanoparticle shape plays an important role in the success of a drug-delivery system. Several studies have concluded that spherical nanoparticles are more efficiently internalised than their rod-shaped or cylindrical counterparts across a variety of cell types.[84,90,91,94,95] A reason for this behavior can be found in the fact that spherical particles are characterised by an aspect ratio of one, meaning that orientation has no effect on the physical membrane interactions. Ferrari and Decuzzi[84] found the internalisation time for nanoparticles with aspect ratios approaching unity to be the minimum. Moreover, they observed that particles with large aspect ratios lead to "frustrated endocytosis", where the particles become partially wrapped by the membrane but not successfully internalised. It is reasonable to extend this "frustrated endocytosis" to having negative implications in the toxicological profile of such particles. Prior to this study, Champion and Mitragotri[95] arrived at an interesting conclusion when studying the effect of particle shape on cellular internalisation. They found that the angle experienced between the particle and the cell at the initial contact point, along with the volume of the particle, determines the efficiency of internalisation. Spherical particles are characterised by a cellular contact angle of 45 degrees. Particles with smaller angles correspond to a more elliptical morphology, with the smaller edge oriented towards the cell. This interaction is easily internalised by phagocytes. On the other hand, phagocytes are unable to internalise elongated particles that are parallel to the cell (characterised by contact angles greater than 45 degrees) and will simply spread around them.[95] However, studies by DeSimone *et al.*[96] contradict this trend of less efficient internalisation at increasing aspect ratio. They found higher rates of endocytosis for rod-like nanoparticles compared with cubic-shaped particles. These findings highlight the importance of particle curvature as another parameter that influences cellular uptake of nanoparticles.

To our knowledge, there are no published studies that specifically address the effects of shape on the cellular internalisation of polymersomes. However, Discher and coworkers have studied the shape effects on cellular uptake using block copolymer micelles. These results can be more easily extrapolated to polymersomes than research conducted on hard nanotechnology, such as gold nanoparticles and carbon nanotubes. It was found that spherical micelles and short "rod-like" filomicelles are up-taken more readily by cells than longer filomicelles.[94] However, the filomicelles presented longer circulation times than the spherical micelles, even at μm length scales. Filomicelles remained in blood 10 times longer than their spherical counterparts.[94] Moreover, worm-like micelles were found to have higher drug-loading capacity than spherical formulations due to the higher internal volume of filomicelles.[97] More interestingly, a variation in tissue distribution as a function of micelle shape was observed. Filomicelles tended to accumulate less in healthy tissues than spherical micelles.[98] All these findings underline the importance of the shape in the design of a nanoparticle drug-delivery system.

Due to their nanoscopic length scale, nanoparticles display high surface area to volume ratios. Therefore, in comparison to micron-sized particles, the same number of particles has a much greater surface area with which to interact. Attractive and repulsive forces between nanoparticles and the cellular surface will strongly influence interactions with the plasma membrane and subsequently internalisation. Since the plasma membrane of mammalian cells is covered by anionic polysaccharides called proteoglycans, it presents a net negative charge.[99] Therefore, cationic nanoparticles show a stronger affinity than anionic or neutral particles towards cell membranes. This has driven the design of cationic nanoparticles with the aim to enhance cellular uptake. However, cationic formulations have been related with cytotoxic effects, more often than their anionic and neutral counterparts. This has been demonstrated for a diverse range of nanoparticle formulations including dendrimers,[100,101] gold nanoparticles[102] and liposomes.[103–106]

Battaglia *et al.*[107] studied the effects of charge on the cellular uptake of polymersomes, with complementary results to the aforementioned formulations. Triblock copolymer poly(ethylene oxide)-poly(2-(diisopropylamino) ethyl methacrylate)-poly(2-(dimethylamino) ethyl methacrylate) (PEO-PDPA-PDMAEMA) polymersomes were studied. The neutral (PEO) and the cationic (PDMAEMA) can be tailored during the production of the particles, so that one chemistry or the other is displayed on the outer surface. It was shown that the polymersomes with cationic PDMAEMA exteriors were up-taken faster than neutral PEO polymersomes in human dermal fibroblasts (HDF). However, the cationic formulation induced higher cellular toxicity.[107] The mechanism by which cationic nanoparticles cause this toxicity is still not fully understood. Nevertheless, it is hypothesised that particles with a high density of positive charge will interact with phospholipids in the plasma membrane in such a way as to cause severe membrane damage such as poration.[108,109] Still, there are examples in the literature where the use of cationic polymeric nanoparticles was not related with cytotoxicity. He and coworkers reported that positively charged chitosan-based nanoparticles were up-taken faster than negatively charged counterparts, whilst no toxicity was associated with either formulation in both phagocytic and non-phagocytic cells.[110] Similarly, Simone and colleagues detected no cellular toxicity in HeLa cells after incubation with nanoscale printed cationic particles composed of trimethyloylpropane ethoxylate triacrylate.[96,111]

Although anionic formulations are generally associated with lower cytotoxicity than cationic ones, the negative charge favors the interaction with proteins and other components of the blood and extra-cellular matrix. Strong interactions with proteins can destabilise the nanoparticle structure, promote particle aggregation and finally hinder their ability to be internalised. Interactions of both cationic and anionic nanoparticles with proteins have been observed.[112–116] In either case this interaction can lead to the recognition of the particle by immune system cells and their subsequent clearance from circulation. Moreover, adsorption of proteins onto the surface of nanoparticles may alter the protein structure. As a result, regions of the protein that are usually shielded in the normal configuration become exposed. This phenomenon can have biological consequences such as loss of the protein function and aggregation of proteins upon the nanoparticle. This aggregation can cause the formation of fibrils in a process known as fibrillation.[57,117] Fibrillation is involved in degenerative diseases such as Alzheimer's. Nevertheless, there are still insufficient data to conclude that catalysis of fibrillation by some nanoparticles is associated with the disease.[118] Neutral formulations would therefore appear the most suitable approach to improving nanoparticle blood circulation time, avoiding immune system recognition and interacting with cellular membranes.

Alongside surface charge, an additional consideration regarding surface properties that is becoming a crucial aspect in nanoparticle design is the specific arrangement of domains and the topology of the nanoparticle surface.[119] Battaglia and coworkers have shown that polymersomes with diverse surface topologies can be produced by blending multiple polymersome forming block copolymers.[120,121] Interestingly, it was demonstrated that such topologies are related to drastic changes in the rate of cellular internalisation (Figure 7.5). Blended polymersomes were up-taken more efficiently by the cells than formulations composed of only one block copolymer. More specifically, the formulation that achieved the highest percentage of cells undergoing polymersome internalisation had PMPC-PDPA/PEO-PDPA 25 : 75 molar ratio. However, the total number of polymersomes taken up by the cells was higher for the 75 : 25 molar ratio PMPC-PDPA/PEO-PDPA formulation.[120,121] Moreover, the uptake rates were hardly affected by polymersome diameter for the most efficient blend of polymersomes (25 : 75). This parameter has been shown to strongly influence the uptake when using 100% PMPC-PDPA polymersomes.[120,121] These results suggest that particle topology and the arrangement of chemical groups upon the nanoparticle surface is highly influential in cellular uptake.

Polymersomes show great potential as nanoscopic delivery vectors. Their synthetic nature allows us to engineer the desirable properties of an ideal drug-delivery system. Namely, efficient encapsulation of a therapeutic or diagnostic

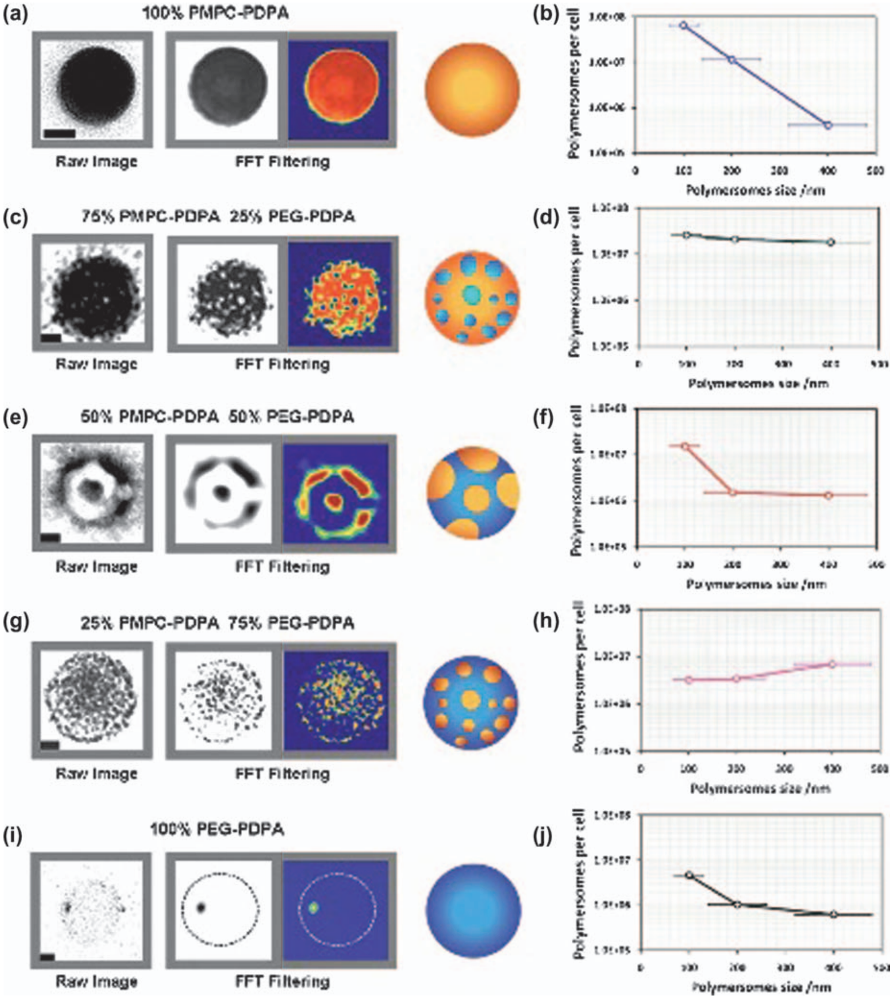

Figure 7.5 Chemical topology has been shown to influence greatly the uptake of polymersomes. TEM micrographs and Fast Fourier Transform filtered images of polymersomes formed by a mixture of two amphiphiles are shown on the left (a, c, e, g and i). When combined in a polymersome, the two chemistries phase separate to form nanodomains. The effects of size and chemical topology on cellular uptake are shown to the right for each composition (b, d, f, h and j).

compound, high cargo retention, sufficient blood circulation times, specific cellular or tissue targeting and non-toxic intra-cellular delivery. Nevertheless nanotechnology is a relatively new field, and as such the long-term impact of this technology *in vivo* will require many more years of investigation. The successful use of polymersomes *in vitro* has driven research into using polymersomes for biomedical applications. The following section covers examples of polymersomes being used as therapeutic and diagnostic aids in medicine and pharmacy. It also covers alternative applications being investigated using polymersomes such as nanoreactors and synthetic organelles.

7.4 Polymersomes in Medicine and Pharmacy

Polymersomes are ideal candidates for many medical applications. For therapeutics they can encapsulate hydrophilic and/or hydrophobic compounds, whilst protecting the molecules from the degradation. They can reduce undesirable side effects by providing targeted drug delivery. Whilst for diagnostics, polymersome encapsulated imaging compounds such as gadolinium, a commonly used Magnetic Resonance Imaging (MRI) contrast agent, have been used. Moreover, polymersomes can encapsulate both therapeutic and diagnostic payloads simultaneously, for an approach known as theranostics.

To date, polymersomes have been used in optical imaging, MRI and ultrasound imaging. Typical limits for these techniques are summarised in Table 7.1. Traditionally, medical imaging is used to provide morphological and functional information on organs for diagnostic purposes. By using polymersomes, useful information can be extended to obtaining higher resolution and monitoring biological pathways and cellular functions *in vivo*.

Traditional *in vivo* nanoparticle-based optical imaging relies on detecting the signal from thousands of nanoparticles that have accumulated in cells. As a result, spatial resolution is much lower in comparison to *in vitro* optical imaging, where one single cell and its internal structures can be observed. Approaches such as window chambers can overcome this limitation by allowing direct observation of the internal biological structure, but this is a highly invasive approach.[123] Optical imaging is often cheaper than alternative medical imaging options such as MRI or PET. However, one main limitation is the poor tissue penetration of light within the visual spectrum. Moreover, tissues autofluorescence occurs within this range; resulting in an increase in background noise and a reduced signal-to-noise ratio. Polymersomes can improve the signal-to-noise ratio by increasing the local concentration of a visual dye to the desired site (*e.g.* after passive or active targeting to tumors). Furthermore, polymersomes for live imaging are often used in conjunction with near infrared fluorophores (NIRF). The longer wavelength allows for greater tissue penetration and reduced background noise. Ghoroghchian and coworkers labeled PEO-PBD polymersomes with (porphinato)zinc(II) (PZn) macrocycles as a NIRF. They showed *in vivo* that polymersomes accumulated

Table 7.1 Limitations of common *in vivo* imaging techniques. Adapted from Kim *et al.*[122]

System	*Penetration depth*	*Resolution*	*Probes*
Optical imaging	<10 cm	1–3 mm	Fluorochromes, photoproteins
MRI	No limit	10–100 μm	Gadolinium, iron oxide particles
PET/SPECT	No limit	1–2 mm	^{18}F, ^{11}C, ^{15}O, ^{99m}TC, ^{111}In
Ultrasound	<20 cm	50 μm	Microbubbles

in tumors at a tissue depth of 1 cm, providing a signal intensity 10 times higher than the background signal.[124] Similarly, Discher and colleagues encapsulated a commercially available lipophilic carbocyanine NIRF DiR in polymersomes based on a blend of PEO-PBD and PAA-PBD. These polymersomes display a surface charge similar to that of red blood cells and a PEO brush that provides stealth properties. *In vivo* biodistribution studies showed that polymersomes can be used successfully to image microvasculature.[125]

MRI is a technique that shares the same principles of Nuclear Magnetic Resonance (NMR) spectroscopy. When a magnetic field of the appropriate radiofrequency is applied to any hydrogen-containing sample (*e.g.* the human body), the spin state of protons will align with said field. When the radiofrequency field is removed, the protons will relax back to a disordered state. This generates a signal that can be translated into a 3D image. Typically, when used *in vivo*, the protons are provided by water. However, it is often necessary to improve contrast between different tissues in order to obtain a higher resolution. This is achieved by applying contrast agents, such as gadolinium, which interfere with the relaxation parameter of the surrounding water, generating higher contrast between locations containing the contrast agent. MRI benefits from contrast agent encapsulation within polymersomes by allowing contrast agent loading in certain tissues, for example tumors.[126] Cheng and coworkers encapsulated gadolinium conjugated to dendrimers (Gd-poly(amido amine), Gd-PAMAM) into porous polymersomes based on PEO-PBD and the degradable poly(ethylene oxide)-polycaprolactone (PEO-PCL). They showed a significant increase in relaxivity when compared to non-porous systems. *In vivo* biodistribution studies on PEO-PBD polymersomes demonstrated sufficient circulation times ($\sim$3.5 h) and afterwards degradation of the vesicles resulted in gadolinium being removed *via* the kidneys.[127,128]

In medical ultrasound imaging, a sound wave with a frequency range of 2–18 MHz is directed towards the desired section of the body to image. Lower frequencies have lower spatial resolution, but a higher tissue penetration in comparison to higher ultrasound frequencies. The sound wave is then reflected back towards its point of origin whenever a change in density is experienced, such as between tissues types. The reflected sound waves are picked up by the detector and then converted into an image based on intensity. One approach to improve contrast between different tissue regions is the administration of microbubbles, such as the Food and Drug Administration (FDA) approved compound Optison. Zhou and coworkers encapsulated microbubbles in poly(ethylene oxide)-poly-DL-lactic acid (PEO-PDLLA) polymersomes. Using a medical ultrasound system, it was shown that the polymersomes were stable and acoustically active. Therefore they are a promising potential ultrasound imaging aid.[129]

In therapeutic applications polymersomes display several advantages over other carrier systems. They facilitate the crossing of bioactive compounds across the many biological barriers that stand between the site of administration and the final target site. The compounds are protected from degradation and immune system clearance within the polymersomes lumen and/or membrane. Furthermore, polymersomes can be engineered to target a specific organ or cell population *via* a combination of passive and active targeting, thus limiting side effects by confining the drug release to the desired site. One major recurrent issue for many anticancer drugs is their low water solubility. Previously, organic solvents have been used to overcome this obstacle. However, they introduce side effects in addition to the ones generated by the drugs themselves. Polymersomes offer an enhanced solution to this solubility problem. Encapsulating such drugs will improve their bioavailability by entrapping the poorly water soluble compounds within water compatible carriers. Furthermore, polymersomes isolate the drug from the body until its arrival and subsequent release. This not only protects the body from potentially harmful side effects, but also shields the drug, thus stopping it from degrading. A therapy is deemed a success when the therapeutic compounds are selectively delivered to the target site, for example a tumor. In order to achieve this, polymersomes should have a blood half-life long enough to reach the tumor site, whilst avoiding the RES, and should deliver their cargo only to the desired cell population or organ. The strategies adopted to prolong blood circulation half-life have been discussed previously. Amongst these, probably the most exploited is the use of PEO-based polymersomes. Solid tumor targeting is achieved by passive targeting combined with active targeting, and sometimes by an externally influenced controlled release to the tumor.

The development of solid tumors is dependent on receiving an adequate nutrient supply. For most tumors this is achieved by the rapid growth of a network of blood vessels, by a process known as angiogenesis. Tumor angiogenesis is characterised by the formation of a chaotic network of rapidly changing vessels. This results in the presence of vessel fenestrations (gaps) up to 700 nm in diameter, significantly bigger than the fenestrations of healthy tissues, which have diameter up to 150 nm (hepatic sinusoid). This difference in diameter allows polymersomes preferentially to escape the blood stream around tumors as opposed to healthy tissues. This also demonstrates an advantage of polymersomes over polymer micelles, which are also used to deliver poorly water soluble compounds. Due to their size, the typically larger polymersomes can selectively extravasate in tumors, whilst micelles can accumulate more readily in several other organs (*i.e.* liver). Alongside this increased permeation, tumors often exhibit lower lymphatic drainage, resulting in greater retention of extra-cellular liquid. This phenomena was firstly described in 1986, and is known as the Enhanced Permeation and Retention effect (EPR).[130] It has also been reported that the intra-tumor pressure is higher than the intra-capillary pressure, and that the pressure is highest at the center of the tumor. This should obstruct the diffusion of particles to tumors. However, this mostly affects low molecular weight drugs, but it appears to have no effect on high molecular weight assemblies such as polymersomes. An example of passive polymersome targeting to tumors was reported by Disher and coworkers.[35,131] They showed how doxorubicin- and paclitaxel-loaded polymersomes efficiently shrank tumors *in vivo*, subsequently proving tumor accumulation of polymersomes. Passive targeting can also be achieved by local administration, *i.e.* intra-tumor delivery of polymersomes. Such an approach was described by Murdoch and coworkers.[132]

Molecules for cellular targeting can be conjugated to polymersomes by two main approaches: attachment to preformed polymersomes or by modifying the copolymer prior to self-assembly. Various chemistries used to functionalise copolymers have recently been reviewed.[133,134] Herein, we will discuss potential and current targeting modifications to polymersome-based cancer therapy. Active targeting is the delivery of a cargo to only a specific target, a cell population or a subset of it. Therefore, active targeting is achieved when a specific targetable marker is overexpressed by the cells of interest, there is a specific binding event between the cell overexpressing the marker and the nanoparticle or the cargo is delivered intra-cellularly. Active targeting increases the amount of therapeutic agent delivered to the desired site and decreases potential side effects, resulting in an overall improved therapeutic efficacy. Another problem related with cancer therapy is known as Multi-drug Resistance (MDR). Cancer cells possess the ability to reduce drug efficacy by several different mechanisms. A typical example is by increasing the efflux of the drug from the cell. This mechanism is mediated by the P-glycoprotein, an ATP-binding cassette-transporter membrane protein. Active targeting alters the normal biodistribution of a drug, at the intra-cellular level, ultimately leading to an improvement in the outcome in the treatment of MDR tumors, as demonstrated by Kiwada and Gibzon[135,136] in their work with liposomes. The advantages of active targeting have been proven *in vitro*. However, to our knowledge, none of the nanocarrier-based formulations approved for medical use *in vivo* adopt active targeting. This is mostly likely due to the trade-off that occurs when "decorating" polymersomes with high molecular weight antibodies. A greater number improves the targeting ability, but also generates faster recognition by immune cells such as macrophages. Nevertheless, active targeting is an attractive and promising approach to improving drug efficiency. Also, as mentioned, the synthetic nature of polymersomes offers many possibilities in terms of conjugation with control over the number and amount of different antibodies that can be conjugated to each vesicle. Due to their biochemical characteristics, tumor specific markers can be actively targeted. For example, Demirgoz and coworkers[137] used the PR b peptide functionalised PEO-PBD to target receptor $\alpha5\beta1$, which is overexpressed by prostate cancer cells. Tumor Necrosis Factor-α (TNFα) was delivered and it was shown that selective *in vitro* targeting was achieved, with internalisation efficiency dependent of surface density of PR b. This resulted in increased therapeutic efficacy compared to free TNFα or untargeted polymersomes. A different approach was chosen by Lecommandoux and coworkers,[138] who prepared polymersomes of poly(γ-benzyl l-glutamate)-hyaluronan (PBLG-HYA). HYA polymer targets CD44, a cell-surface antigen that is overexpressed by certain cancer cells. Polymersomes loaded with doxorubicin were shown to be more effective in controlling tumor growth when compared to free doxorubicin in a mouse model. It was also shown that the encapsulation significantly improved blood half-life of doxorubicin. However, the cited work lacked the control of non-targeted formulation in order to prove a targeted effect.

Finally, tumors can be targeted by controlling the release of the cargo *via* applying an external stimulus such as ultrasound, a magnetic field, or a change in the pH, redox potential or temperature. Tumors have a slightly acidic extracellular environment (pH 6.5–7.2). Therefore pH-sensitive polymersomes have been used selectively to increase the release of therapeutics upon contact with these areas. Agut and coworkers[139] and Chen and coworkers[140] proved how release of anticancer drugs from micelles or polymersomes can be triggered by lowering the pH of the media, while Ahmed and coworkers[35] showed how tumor volume can be effectively shrunk by intravenously delivering pH-sensitive polymersomes loaded with both taxol and doxorubicin. Another approach of stimuli-sensitive release is to exploit temperature. Inflamed tissues such as tumoral tissue have a slightly higher temperature in comparison with healthy tissues. Temperature-sensitive polymers can be applied, sometimes coupled to hyperthermia therapy in order to increase temperature locally and trigger the release of the therapeutic agent as previously reported for liposomes modified with the temperature-sensitive polymer poly(*N*-isopropylacrylamide) PNIPAAm.[141] Other approaches to stimuli-sensitive polymersomes include magnetic field- and ultrasound-sensitive polymersomes. Encapsulating magnetic field-sensitive γFe_2O_3 into poly(butadiene)-poly(glycolic acid) (PBD-PGA) polymersomes or micelles it has been demonstrated that polymersomes can respond to magnetic field and release their cargo.[142]

Gene therapy is defined as the administration of genetic material (DNA or RNA) to target specific cellular processes, either to restore an already suppressed event or to suppress a particular pathological pathway. However, administering genetic material for therapy presents two major challenges. Firstly, genetic material is very susceptible to degradation. This reduces the time available to reach its target site. Secondly, delivery must be as selective as possible in order to limit side effects caused by off-target delivery. Traditionally, the approach used has been either to complex genetic material with polycations or to encapsulate it within lipid carriers, such as commercially available Lipofectamine. The main disadvantages of such approaches are toxicity and the poor circulation times as covered in the previous section. Korobko and coworkers[143,144] complexed DNA with amphiphilic cationic poly-(butadiene-b-*N*-methyl-4-vinyl pyridinium) (PBD-P4VPQI). The system proved to be an efficient approach *in vitro*, but *in vivo* there were problems with non-specific uptake. Brown and colleagues[145] presented another strategy. DNA was encapsulated by polymersomes composed of a triblock copolymer based on PEO, hydrophobic palmitic acid and chains of poly-lysine or poly-ornithine. They showed successful transfection *in vivo* to the lung and liver. However, the system proved to be highly cytotoxic *in vitro*. To encapsulate DNA, Battaglia and coworkers used pH responsive, reversibly cationic (PMPC-PDPA) polymersomes that have been proven to be non-cytotoxic *in vitro*.[146] They efficiently delivered the genetic cargo *in vitro* to Chinese Hamster Ovary (CHO) and primary Human Dermal Fibroblast (HDF) cells. Finally, siRNA was successfully encapsulated in (PEO-PLA) vesicles by Discher and coworkers, who proved the system to be as efficient as Lipofectamine 2000 *in vitro*.[147]

In order to study the biodistribution and the effect of polymersomes in therapy, a new approach is the simultaneous encapsulation of an imaging and a therapeutic agent within the same vesicle, for theranostics. Potentially any imaging technique could be coupled to any therapeutic approach. Recently, Lecommandoux and coworkers encapsulated anticancer compound doxorubicin and the contrast agent Ultra-small Superparamagnetic Iron Oxide (USPIO) into PMTC-PGA polymersomes. They showed vesicles responding to a magnetic field and being driven to the desired site. The magnetic field also controlled the rate of doxorubicin release from polymersomes. Simultaneously, USPIO provided contrast for MRI.[148]

Another growing field of research is the use of polymersomes not just to deliver the therapeutic molecule to the cells, but to potentially replace defective cellular machinery. By taking advantage of the ability of polymersomes to compartmentalise volumes at the nanoscale it is possible to confine certain reactions within the hydrophilic lumen. Polymersomes engineered in this way are known as nanoreactors. With this concept it is theoretically possible to create novel systems such as artificial organelles or fully synthetic cells. The first step involves the loading of polymersomes with an active molecule (such as a protein), capable of performing its reaction within the lumen. A substrate is also added, and the final product diffuses out of the polymersomes. An example of such a system was recently reported by van Hest and coworkers.[149] Using poly[styrene-b-poly-(L-isocyanoalanine(2-thiophen-3-ethyl) amide] PS-PIAT polymersomes, they encapsulated two enzymes that work synergistically to regenerate NADPH, an important cofactor used by cells in the process of generating energy from catabolic reactions. They showed that the system was regenerating NADPH, and that the co-encapsulation of both enzymes was more efficient than surface-anchored reactions.[149] Using the same copolymer (PS-PIAT) Arends *et al.*[150] encapsulated chloroperoxidase within polymersomes, and showed how the kinetics of substrate conversion differed, according to their membrane diffusion rates. This process can be scaled up, with nanoreactors being encapsulated into bigger polymersomes, emulating natural compartmentalization. This was demonstrated by Leccomandoux and coworkers, with nanosized poly(trimethylene carbonate)-b-poly(L-glutamic acid) (PTMC-PGA) polymersomes trapped within giant PEO-PBD polymersomes.[151] One example of producing an artificial organelle was conducted by van Hest and coworkers.[152] The surface of PS-PIAT polymersomes was modified with Tat, a peptide that enhances cellular uptake, while encapsulating Green Fluorescent Protein (GFP) or Horseradish Peroxidase (HRP) allowed the visualisation of the internalised reactor and its activity. Polymersomes were successfully up-taken by cells and it was observed that the HRP-mediated reaction occurred within the cells.[152] Possible applications for these systems range from delivering synthetic organelles for restoring lost cellular functions to the possibility of creating artificial blood that could be stored for long periods of time and transfused with no risk of disease.

References

1. J. D. Smith, C. D. Cappa, K. R. Wilson, R. C. Cohen, P. L. Geissler and R. J. Saykally, *P. Natl. Acad. Sci. USA*, 2005, **102**, 14171.
2. L. R. Pratt, *Annu. Rev. Phys. Chem.*, 2002, **53**, 409.
3. L. R. Pratt, *Annu. Rev. Phys. Chem.*, 1985, **36**, 433.
4. P. Alexandridis and R. J. Spontak, *Curr. Opin. Colloid Interf. Sci.*, 1999, **4**, 130.
5. L. Leibler, H. Orland and J. C. Wheeler, *J. Chem. Phys.*, 1983, **79**, 3550.
6. M. Wilhelm, C. L. Zhao, Y. Wang, R. Xu, M. A. Winnik, J. L. Mura, G. Riess and M. D. Croucher, *Macromolecules*, 1991, **24**, 1033.
7. B. M. Discher, Y. Y. Won, D. S. Ege, J. C. Lee, F. S. Bates and D. E. Discher, *Science*, 1999, **284**, 1143.
8. J. N. Israelachvili, D. J. Mitchell and B. W. Ninham, *J. Chem. Soc. Farad. T 2*, 1976, **72**, 1525.
9. J. Chiefari, Y. K. Chong, F. Ercole, J. Krstina, J. Jeffery, T. P. T. Le, R. T. A. Mayadunne, G. F. Meijs, C. L. Moad, G. Moad, E. Rizzardo and S. H. Thang, *Macromolecules*, 1998, **31**, 5559.
10. J. S. Wang and K. Matyjaszewski, *Macromolecules*, 1995, **28**, 7901.
11. G. Battaglia and A. J. Ryan, *Nat. Mater.*, 2005, **4**, 869.
12. G. Battaglia and A. J. Ryan, *Macromolecules*, 2006, **39**, 798.
13. G. Battaglia and A. J. Ryan, *J. Phys. Chem. B*, 2006, **110**, 10272.
14. I. W. Hamley, S. M. Mai, A. J. Ryan, J. P. A. Fairclough and C. Booth, *Phys. Chem. Chem. Phys.*, 2001, **3**, 2972.
15. J. A. Pople, I. W. Hamley, J. P. A. Fairclough, A. J. Ryan, B. U. Komanschek, A. J. Gleeson, G. E. Yu and C. Booth, *Macromolecules*, 1997, **30**, 5721.
16. G. Wanka, H. Hoffmann and W. Ulbricht, *Macromolecules*, 1994, **27**, 4145.
17. W. Agut, A. Brulet, C. Schatz, D. Taton and S. Lecommandoux, *Langmuir*, 2010, **26**, 10546.
18. J. Z. Du, Y. P. Tang, A. L. Lewis and S. P. Armes, *J. Am. Chem. Soc.*, 2005, **127**, 17982.
19. C. Fernyhough, A. J. Ryan and G. Battaglia, *Soft Matter*, 2009, **5**, 1674.
20. S. Jain and F. S. Bates, *Macromolecules*, 2004, **37**, 1511.
21. H. R. Marsden, L. Gabrielli and A. Kros, *Polym. Chem.*, 2010, **1**, 1512.
22. S. H. Qin, Y. Geng, D. E. Discher and S. Yang, *Adv. Mater.*, 2006, **18**, 2905.
23. C. Sanson, J. F. Le Meins, C. Schatz, A. Soum and S. Lecommandoux, *Soft Matter*, 2010, **6**, 1722.
24. H. W. Shen and A. Eisenberg, *Macromolecules*, 2000, **33**, 2561.
25. L. Shen, J. Z. Du, S. P. Armes and S. Y. Liu, *Langmuir*, 2008, **24**, 10019.
26. M. E. Yildiz, R. K. Prud'homme, I. Robb and D. H. Adamson, *Polym. Adv. Technol.*, 2007, **18**, 427.
27. L. Chen, H. W. Shen and A. Eisenberg, *J. Phys. Chem. B*, 1999, **103**, 9488.
28. Y. Geng, F. Ahmed, N. Bhasin and D. E. Discher, *J. Phys. Chem. B*, 2005, **109**, 3772.

29. H. W. Shen and A. Eisenberg, *J. Phys. Chem. B*, 1999, **103**, 9473.
30. A. Blanazs, J. Madsen, G. Battaglia, A. J. Ryan and S. P. Armes, *J. Am. Chem. Soc.*, 2011, **133**, 16581.
31. S. Creutz, J. vanStam, S. Antoun, F. C. DeSchryver and R. Jerome, *Macromolecules*, 1997, **30**, 4078.
32. Y. Y. Won, H. T. Davis and F. S. Bates, *Macromolecules*, 2003, **36**, 953.
33. T. C. Anglin and J. C. Conboy, *Biochemistry*, 2009, **48**, 10220.
34. S. Creutz, J. van Stam, F. C. De Schryver and R. Jerome, *Macromolecules*, 1998, **31**, 681.
35. F. Ahmed, R. I. Pakunlu, G. Srinivas, A. Brannan, F. Bates, M. L. Klein, T. Minko and D. E. Discher, *Mol. Pharm.*, 2006, **3**, 340.
36. K. N. Fish, *Curr. Protoc. Cytom.*, 2009, **12**, 18.1.
37. T. Muller, C. Schumann and A. Kraegeloh, *ChemPhysChem*, 2012, **13**, 1986.
38. G. Battaglia, C. LoPresti, M. Massignani, N. J. Warren, J. Madsen, S. Forster, C. Vasilev, J. K. Hobbs, S. P. Armes, S. Chirasatitsin and A. J. Engler, *Small*, 2011, **7**, 2010.
39. A. Rank, S. Hauschild, S. Forster and R. Schubert, *Langmuir*, 2009, **25**, 1337.
40. R. Waninge, T. Nylander, M. Paulsson and B. Bergenstahl, *Colloid Surf. B*, 2003, **31**, 257.
41. J. Kuntsche, J. C. Horst and H. Bunjes, *Int. J. Pharm.*, 2011, **417**, 120.
42. A. Lopes, K. Edwards and E. Feitosa, *J. Colloid Interf. Sci.*, 2008, **322**, 582.
43. Y. Y. Won, A. K. Brannan, H. T. Davis and F. S. Bates, *J. Phys. Chem. B*, 2002, **106**, 3354.
44. N. de Jonge, D. B. Peckys, G. J. Kremers and D. W. Piston, *P. Natl. Acad. Sci. USA*, 2009, **106**, 2159.
45. J. M. Yuk, J. Park, P. Ercius, K. Kim, D. J. Hellebusch, M. F. Crommie, J. Y. Lee, A. Zettl and A. P. Alivisatos, *Science*, 2012, **336**, 61.
46. C. W. Yang, I. S. Hwang, Y. F. Chen, C. S. Chang and D. P. Tsai, *Nanotechnol.*, 2007, **18**, No. 084009.
47. F. J. Giessibl, *Rev. Modern Phys.*, 2003, **75**, 949.
48. G. Binnig, C. F. Quate and C. Gerber, *Phys. Rev. Lett.*, 1986, **56**, 930.
49. C. LoPresti, M. Massignani, C. Fernyhough, A. Blanazs, A. J. Ryan, J. Madsen, N. J. Warren, S. P. Armes, A. L. Lewis, S. Chirasatitsin, A. J. Engler and G. Battaglia, *ACS Nano*, 2011, **5**, 1775.
50. T. P. Smart, O. O. Mykhaylyk, A. J. Ryan and G. Battaglia, *Soft Matter*, 2009, **5**, 3607.
51. V. Levi, Q. Ruan, K. Kis-Petikova and E. Gratton, *Biochem. Soc. T*, 2003, **31**, 997.
52. J. Oberdisse, C. Couve, J. Appell, J. F. Berret, C. Ligoure and G. Porte, *Langmuir*, 1996, **12**, 1212.
53. S. L. Li, B. Byrne, J. Welsh and A. F. Palmer, *Biotechnol. Progr.*, 2007, **23**, 278.
54. S. D. Li and L. Huang, *Mol. Pharmaceut.*, 2008, **5**, 496.

55. M. Roser, D. Fischer and T. Kissel, *Eur. J. Pharm. Biopharm.*, 1998, **46**, 255.
56. H. S. Choi, W. Liu, P. Misra, E. Tanaka, J. P. Zimmer, B. I. Ipe, M. G. Bawendi and J. V. Frangioni, *Nat. Biotechnol.*, 2007, **25**, 1165.
57. M. Elsabahy and K. L. Wooley, *Chem. Soc. Rev.*, 2012, **41**, 2545.
58. D. E. Owens and N. A. Peppas, *Int. J. Pharm.*, 2006, **307**, 93.
59. M. A. Dobrovolskaia and S. E. McNeil, *Nat. Nanotechnol.*, 2007, **2**, 469.
60. M. A. Phillips, M. L. Gran and N. A. Peppas, *Nano Today*, 2010, **5**, 143.
61. L. Illum, I. M. Hunneyball and S. S. Davis, *Int. J. Pharm.*, 1986, **29**, 53.
62. M. T. Peracchia, E. Fattal, D. Desmaële, M. Besnard, J. P. Noël, J. M. Gomis, M. Appel, J. d'Angelo and P. Couvreur, *J. Control. Release*, 1999, **60**, 121.
63. H. Carrstensen, R. H. Muller and B. W. Muller, *Clin. Nutr.*, 1992, **11**, 289.
64. J. S. Lee and J. Feijen, *J. Control. Release*, 2012, **161**, 473.
65. C. Giacomelli, V. Schmidt and R. Borsali, *Macromolecules*, 2007, **40**, 2148.
66. B. Shi, C. Fang and Y. Y. Pei, *J. Pharm. Sci.*, 2006, **95**, 1873.
67. T. Waku, M. Matsusaki, T. Kaneko and M. Akashi, *Macromolecules*, 2007, **40**, 6385.
68. P. J. Photos, L. Bacakova, B. Discher, F. S. Bates and D. E. Discher, *J. Control. Release*, 2003, **90**, 323.
69. C. Allen, N. Dos Santos, R. Gallagher, G. N. Chiu, Y. Shu, W. M. Li, S. A. Johnstone, A. S. Janoff, L. D. Mayer, M. S. Webb and M. B. Bally, *Biosci. Rep.*, 2002, **22**, 225.
70. D. E. Discher and A. Eisenberg, *Science*, 2002, **297**, 967.
71. J. H. Teichroeb, J. A. Forrest, L. W. Jones, J. Chan and K. Dalton, *J. Colloid Interf. Sci.*, 2008, **325**, 157.
72. J. Huang, L. Bu, J. Xie, K. Chen, Z. Cheng, X. Li and X. Chen, *ACS Nano*, 2010, **4**, 7151.
73. R. Konradi, B. Pidhatika, A. Muhlebach and M. Textor, *Langmuir*, 2008, **24**, 613.
74. A. Vertut-Doi, H. Ishiwata and K. Miyajima, *Biochim. Biophys. Acta*, 1996, **1278**, 19.
75. D. W. Bartlett, H. Su, I. J. Hildebrandt, W. A. Weber and M. E. Davis, *P. Natl. Acad. Sci. USA*, 2007, **104**, 15549.
76. X. Wang, J. Li, Y. Wang, K. J. Cho, G. Kim, A. Gjyrezi, L. Koenig, P. Giannakakou, H. J. C. Shin, M. Tighiouart, S. Nie, Z. Chen and D. M. Shin, *ACS Nano*, 2009, **3**, 3165.
77. S. R. Kumar, T. P. Quinn and S. L. Deutscher, *Clin. Cancer Res.*, 2007, **13**, 6070.
78. X. Qian, X. H. Peng, D. O. Ansari, Q. Yin-Goen, G. Z. Chen, D. M. Shin, L. Yang, A. N. Young, M. D. Wang and S. Nie1, *Nat. Biotechnol.*, 2008, **26**, 83.
79. J. J. Lin, P. P. Ghoroghchian, Y. Zhang and D. A. Hammer, *Langmuir*, 2006, **22**, 3975.

80. K. A. Kelly, J. R. Allport, A. Tsourkas, V. R. Shinde-Patil, L. Josephson and R. Weissleder, *Circ. Res.*, 2005, **96**, 327.
81. K. N. Sugahara, T. Teesalu, P. P. Karmali, V. R. Kotamraju, L. Agemy, D. R. Greenwald and E. Ruoslahti, *Science*, 2010, **328**, 1031.
82. D. Cox, M. Brennan and N. Moran, *Nat. Rev. Drug Discov.*, 2010, **9**, 804.
83. K. Shapero, F. Fenaroli, I. Lynch, D. C. Cottell, A. Salvati and K. A. Dawson, *Mol. Biosyst.*, 2011, **7**, 371.
84. P. Decuzzi and M. Ferrari, *Biophys. J.*, 2008, **94**, 3790.
85. I. Canton and G. Battaglia, *Chem. Soc. Rev.*, 2012, **41**, 2718.
86. S. Prabha, W. Z. Zhou, J. Panyam and V. Labhasetwar, *Int. J. Pharm.*, 2002, **244**, 105.
87. M. P. Desai, V. Labhasetwar, E. Walter, R. J. Levy and G. L. Amidon, *Pharm. Res.*, 1997, **14**, 1568.
88. S. Zhang, J. Li, G. Lykotrafitis, G. Bao and S. Suresh, *Adv. Mater.*, 2009, **21**, 419.
89. H. Gao, W. Shi and L. B. Freund, *P. Natl. Acad. Sci. USA*, 2005, **102**, 9469.
90. B. D. Chithrani, A. A. Ghazani and W. C. Chan, *Nano Lett.*, 2006, **6**, 662.
91. B. D. Chithrani and W. C. Chan, *Nano Lett.*, 2007, **7**, 1542.
92. S. Z. Hongyan Yuan, *Appl. Phys. Lett.*, 2010, **96**, 1.
93. W. Jiang, B. Y. Kim, J. T. Rutka and W. C. Chan, *Nat. Nanotechnol.*, 2008, **3**, 145.
94. Y. Geng, P. Dalhaimer, S. Cai, R. Tsai, M. Tewari, T. Minko and D. E. Discher, *Nat. Nanotechnol.*, 2007, **2**, 249.
95. J. A. Champion and S. Mitragotri, *P. Natl. Acad. Sci. USA*, 2006, **103**, 4930.
96. S. E. Gratton, M. E. Napier, P. A. Ropp, S. Tian and J. M. DeSimone, *Pharm. Res.*, 2008, **25**, 2845.
97. S. Cai, K. Vijayan, D. Cheng, E. M. Lima and D. E. Discher, *Pharm. Res.*, 2007, **24**, 2099.
98. D. A. Christian, S. Cai, O. B. Garbuzenko, T. Harada, A. L. Zajac, T. Minko and D. E. Discher, *Mol. Pharmaceut.*, 2009, **6**, 1343.
99. D. L. Rabenstein, *Nat. Prod. Rep.*, 2002, **19**, 312.
100. S. Parimi, T. J. Barnes and C. A. Prestidge, *Langmuir*, 2008, **24**, 13532.
101. P. R. Leroueil, S. Hong, A. Mecke, J. R. Baker, B. G. Orr and M. M. Banaszak Holl, *Acc. Chem. Res.*, 2007, **40**, 335.
102. J. Lin, H. Zhang, Z. Chen and Y. Zheng, *ACS Nano*, 2010, **4**, 5421.
103. C. R. Miller, B. Bondurant, S. D. McLean, K. A. McGovern and D. F. O'Brien, *Biochemistry*, 1998, **37**, 12875.
104. C. Kelly, C. Jefferies and S. A. Cryan, *J. Drug Deliv.*, 2011, **2011**, 727241.
105. G. Smistad, J. Jacobsen and S. A. Sande, *Int. J. Pharm.*, 2007, **330**, 14.
106. S. S. Rathore and P. C. Ghosh, *Int. J. Pharm.*, 2008, **350**, 79.
107. A. Blanazs, M. Massignani, G. Battaglia, S. P. Armes and A. J. Ryan, *Adv. Funct. Mater.*, 2009, **19**, 2906.
108. A. Mecke, I. J. Majoros, A. K. Patri, J. R. Baker, M. M. Holl and B. G. Orr, *Langmuir*, 2005, **21**, 10348.

109. T. Kean, S. Roth and M. Thanou, *J. Control. Release*, 2005, **103**, 643.
110. C. He, Y. Hu, L. Yin, C. Tang and C. Yin, *Biomaterials*, 2010, **31**, 3657.
111. S. E. A. Gratton, P. A. Ropp, P. D. Pohlhaus, J. C. Luft, V. J. Madden, M. E. Napier and J. M. DeSimone, *P. Natl. Acad. Sci. USA*, 2008, **105**, 11613.
112. M. Merhi, C. Y. Dombu, A. Brient, J. Chang, A. Platel, F. Le Curieux, D. Marzin, F. Nesslany and D. Betbeder, *Int. J. Pharm.*, 2012, **423**, 37.
113. G. W. Doorley and C. K. Payne, *Chem. Comm.*, 2011, **47**, 466.
114. D. Walczyk, F. B. Bombelli, M. P. Monopoli, I. Lynch and K. A. Dawson, *J. Am. Chem. Soc.*, 2010, **132**, 5761.
115. C. C. You, M. De and V. M. Rotello, *Curr. Opin. Chem. Biol.*, 2005, **9**, 639.
116. G. W. Doorley and C. K. Payne, *Chem. Comm.*, 2012, **48**, 2961.
117. S. Linse, C. Cabaleiro-Lago, W. F. Xue, I. Lynch, S. Lindman, E. Thulin, S. E. Radford and K. A. Dawson, *P. Natl. Acad. Sci. USA*, 2007, **104**, 8691.
118. V. L. Colvin and K. M. Kulinowski, *P. Natl. Acad. Sci. USA*, 2007, **104**, 8679.
119. A. Verma, O. Uzun, Y. Hu, Y. Hu, H. S. Han, N. Watson, S. Chen, D. J. Irvine and F. Stellacci, *Nat. Mater.*, 2008, **7**, 588.
120. C. LoPresti, M. Massignani, C. Fernyhough, A. Blanazs, A. J. Ryan, J. Madsen, N. J. Warren, S. P. Armes, A. L. Lewis, S. Chirasatitsin, A. J. Engler and G. Battaglia, *ACS Nano*, 2011, **5**, 1775.
121. M. Massignani, C. LoPresti, A. Blanazs, J. Madsen, S. P. Armes, A. L. Lewis and G. Battaglia, *Small*, 2009, **5**, 2424.
122. J. H. Kim, K. Park, H. Y. Nam, S. Lee, K. Kim and I. C. Kwon, *Prog. Polym. Sci.*, 2007, **32**, 1031.
123. G. M. Tozer, S. Akerman, N. A. Cross, P. R. Barber, M. A. Björndahl, O. Greco, S. Harris, S. A. Hill, D. J. Honess, C. R. Ireson, K. L. Pettyjohn, V. E. Prise, C. C. Reyes-Aldasoro, C. Ruhrberg, D. T. Shima and C. Kanthou, *Cancer Res.*, 2008, **68**, 2301.
124. P. P. Ghoroghchian, P. R. Frail, K. Susumu, D. Blessington, A. K. Brannan, F. S. Bates, B. Chance, D. A. Hammer and M. J. Therien, *P. Natl. Acad. Sci. USA*, 2005, **102**, 2922.
125. D. A. Christian, O. B. Garbuzenko, T. Minko and D. E. Discher, *Macromol. Rapid Comm.*, 2010, **31**, 135.
126. S. Sharma, U. Paiphansiri, V. Hombach, V. Mailänder, O. Zimmermann, K. Landfester and V. Rasche, *Contrast Media Mol. Imaging*, 2010, **5**, 59.
127. Z. L. Cheng and A. Tsourkas, *Langmuir*, 2008, **24**, 8169.
128. Z. L. Cheng, D. L. J. Thorek and A. Tsourkas, *Adv. Funct. Mater.*, 2009, **19**, 3753.
129. W. Zhou, F. Meng, G. H. Engbers and J. Feijen, *J. Control. Release*, 2006, **116**, e62.
130. J. Fang, H. Nakamura and H. Maeda, *Adv. Drug Deliver. Rev.*, 2011, **63**, 136.

131. F. Ahmed, R. I. Pakunlu, A. Brannan, F. Bates, T. Minko and D. E. Discher, *J. Control. Release*, 2006, **116**, 150.
132. C. Murdoch, K. J. Reeves, V. Hearnden, H. Colley, M. Massignani, I. Canton, J. Madsen, A. Blanazs, S. P. Armes, A. L. Lewis, S. Macneil, N. J. Brown, M. H. Thornhill and G. Battaglia, *Nanomedicine UK*, 2010, **5**, 1025.
133. M. Shi, J. Lu and M. S. Shoichet, *J. Mater. Chem.*, 2009, **19**, 5485.
134. S. Egli, H. Schlaad, N. Bruns and W. Meier, *Polymers*, 2011, **3**, 252.
135. D. Goren, A. T. Horowitz, D. Tzemach, M. Tarshish, S. Zalipsky and A. Gabizon, *Clin. Cancer Res.*, 2000, **6**, 1949.
136. T. Kobayashi, T. Ishida, Y. Okada, S. Ise, H. Harashima and H. Kiwada, *Int. J. Pharm.*, 2007, **329**, 94.
137. D. Demirgoz, T. O. Pangburn, K. P. Davis, S. Lee, F. S. Bates and E. Kokkoli, *Soft Matter*, 2009, **5**, 2011.
138. K. K. Upadhyay, A. K. Mishra, K. Chuttani, A. Kaul, C. Schatz, J. F. Le Meins, A. Misra and S. Lecommandoux, *Nanomed-Nanotechnol.*, 2012, **8**, 71.
139. W. Agut, A. Brulet, C. Schatz, D. Taton and S. Lecommandoux, *Langmuir*, 2010, **26**, 10546.
140. W. Chen, F. H. Meng, R. Cheng and Z. Y. Zhong, *J. Control. Release*, 2010, **142**, 40.
141. H. D. Han, T. W. Kim, B. C. Shin and H. S. Choi, *Macromol. Res.*, 2005, **13**, 54.
142. S. B. Lecommandoux, O. Sandre, F. Checot, J. Rodriguez-Hernandez and R. Perzynski, *Adv. Mater.*, 2005, **17**, 712.
143. A. V. Korobko, C. Backendorf and J. R. C. van der Maarel, *J. Phys. Chem. B*, 2006, **110**, 14550.
144. A. V. Korobko, W. Jesse and J. R. C. van der Maarel, *Langmuir*, 2005, **21**, 34.
145. M. D. Brown, A. Schätzlein, A. Brownlie, V. Jack, W. Wang, L. Tetley, A. I. Gray and I. F. Uchegbu, *Bioconjugate Chem.*, 2000, **11**, 880.
146. H. Lomas, I. Canton, S. MacNeil, J. Du, S. P. Armes, A. J. Ryan, A. L. Lewis and G. Battaglia, *Adv. Mater.*, 2007, **19**, 4238.
147. Y. Kim, M. Tewari, J. D. Pajerowski, S. Cai, S. Sen, J. H. Williams, S. R. Sirsi, G. J. Lutz and D. E. Discher, *J. Control. Release*, 2009, **134**, 132.
148. C. Sanson, O. Diou, J. Thévenot, E. Ibarboure, A. Soum, A. Brûlet,, S. Miraux, E. Thiaudiére, S. Tan, A. Brisson, V. Dupuis, O. Sandre and S. Lecommandoux, *ACS Nano*, 2011, **5**, 1122.
149. S. A. Meeuwissen, A. Rioz-Martínez, G. Gonzalo, M. W. Fraaije, V. Gotor and J. C. M. van Hest, *J. Mater. Chem.*, 2011, **21**, 18923.
150. H. M. de Hoog, M. Nallani, J. J. Cornelissen, A. E. Rowan, R. J. Nolte and I. W. Arends, *Org. Biomol. Chem.*, 2009, **7**, 4604.
151. M. Marguet, O. Sandre and S. Lecommandoux, *Langmuir*, 2012, **28**, 2035.
152. S. F. M. van Dongen, W. P. R. Verdurmen, R. J. R. W. Peters, R. J. M. Nolte, R. Brock and J. C. M. van Hest, *Angew. Chem. Int. Ed.*, 2010, **49**, 7213.

CHAPTER 8

Reduction-sensitive Nanosystems for Active Intracellular Drug Delivery

RU CHENG, FENGHUA MENG, CHAO DENG AND ZHIYUAN ZHONG*

Biomedical Polymers Laboratory, and Jiangsu Key Laboratory of Advanced Functional Polymer Design and Application, Department of Polymer Science and Engineering, College of Chemistry, Chemical Engineering and Materials Science, Soochow University, Suzhou, 215123, P. R. China
*Email: zyzhong@suda.edu.cn

8.1 Introduction

In the past decade, stimuli-responsive nanosystems have received tremendous attention for targeted and triggered drug delivery.[1–3] Among the many different chemical and physical stimuli (pH, temperature, magnetic field, light, *etc.*), redox potential has recently appeared as a unique and fascinating trigger for "active" intra-cellular drug and gene release.[4–6] In contrast to many stimuli such as light and magnetic field that are imposed externally with sophisticated devices, redox is a ubiquitous internal stimulus existing naturally in tumor tissues as well as in cancer cells. It should further be noted that, unlike pH-sensitive nanosystems that are intended to release payloads under mildly acidic endo/lysosomal compartments, reduction-sensitive nanosystems are mostly designed to rapidly dissociate and efficiently release drugs in the cytoplasm and/or the cell nucleus (Figure 8.1).[5]

RSC Smart Materials No. 2
Smart Materials for Drug Delivery: Volume 1
Edited by Carmen Alvarez-Lorenzo and Angel Concheiro
© The Royal Society of Chemistry 2013
Published by the Royal Society of Chemistry, www.rsc.org

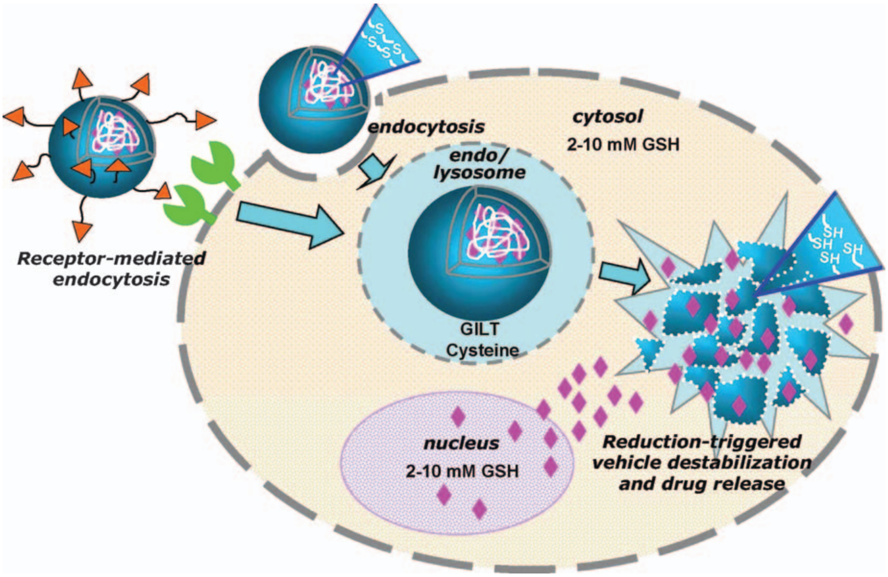

Figure 8.1 Schematic illustration of the intra-cellular trafficking pathway of GSH-responsive nanovehicles including steps of cellular internalization, endosomal escape, reduction-triggered vehicle degradation and drug release. The redox potential of the cytosol is primarily determined by GSH/GSSG, while that of the endo/lysosome is modulated by a specific reducing enzyme GILT and the co-factor cysteine. GSH-responsive nanovehicles may also be partially degraded in the endo/lysosomal compartments.
Reprinted from Ref. 5 with permission of Elsevier.

The design rationale of reduction-sensitive nanosystems usually involves incorporation of disulfide linkage(s) in the polymer main chain, at the polymer side chain or in the cross-linker. The disulfide bonds while stable under an oxidative conditions are rapidly cleaved, at a time scale from minutes to hours, under a reductive environment through thiol-disulfide exchange reactions.[7,8] This quick-response chemical degradation behavior is distinct from common hydrolytically degradable polymers such as aliphatic polyesters and polycarbonates that exhibit gradual degradation kinetics inside the body with degradation times ranging from days to weeks, months or years.[9–11]

The fast and reversible thiol-disulfide exchange reactions play an important role in maintaining proper biological functions of living cells, including stabilization of protein structures, enzymatic activity and redox cycles.[12–14] Glutathione tripeptide (γ-glutamyl-cysteinyl-glycine; GSH) is the most abundant low-molecular-weight biological thiol and GSH/glutathione disulfide (GSSG) is the major redox couple in animal cells.[15] GSH/GSSG is maintained at distinct, non-equilibrium potentials in the mitochondria, the cytoplasm, the nuclei, the secretory pathway and the extra-cellular space.[14] In body fluids (*e.g.* blood), in extra-cellular matrices and on the cell surface, the proteins are rich in stabilizing disulfides as a result of a relatively low redox potential, due to a low concentration of GSH (approximately 2–20 μM). In contrast, inside cells the concentration of GSH is 0.5–10 mM, which is kept reduced by NADPH and glutathione reductase, maintaining a highly reducing environment.[15] It should further be noted that the endosomal compartment is also redox-active and that the redox potential is modulated by a specific reducing enzyme gamma-interferon-inducible lysosomal thiol reductase (GILT) in the co-presence of a reducing agent such as cysteine (but not GSH).[16] Moreover, the redox-active lysosome also contains low-mass iron that is kept in a reduced state (Fe^{2+}) by the acidic interior and high concentrations of thiols such as cysteine within the lysosome.[17] Also of particular interest is that tumor tissues are highly reducing and hypoxic compared with normal tissues,[18] with at least 4-fold higher concentrations of GSH in the tumor tissues over normal tissues.[19]

In order to exert therapeutic effects, many bioactive substances including anticancer drugs, antioxidants, peptide and protein drugs, DNA and siRNA have to be delivered and released into the cellular compartments such as the cytoplasm or cell nucleus.[20,21] For efficient tumor therapy, nanodelivery systems should, therefore, be able to overcome not only extra-cellular barriers (long circulation time, preferential accumulation at diseased sites, selective binding to the targeted cells, *etc.*), but also equally important intra-cellular barriers (such as cellular internalization, endosomal escape or drug release). The reduction-sensitive nanosystems with excellent stability under extra-cellular conditions and in blood, while showing fast degradation under intra-cellular reductive environments, have recently been developed as one of the most ideal platforms for targeted intra-cellular drug delivery. In the past several years, various reduction-sensitive nanosystems have been designed and explored for tumor-targeting "active" intra-cellular drug release.[5] It is anticipated that reduction-sensitive nanosystems will have enormous potential in targeted cancer therapy. In this chapter, we present and discuss recent progress in reduction-sensitive nanosystems, covering polymeric micelles, nanoparticles, capsules, polymersomes and nanogels, for the controlled delivery and release of anticancer drugs (*e.g.* doxorubicin, Dox, and paclitaxel, PTX), photosensitizers, antioxidants, peptide or protein drugs. It should be noted that the contents of this chapter are mostly based on our previous two review articles,[5,6] which are recommended to readers for further study.

8.2 Reduction-sensitive Polymeric Micelles

8.2.1 Reduction-sensitive Shell-sheddable Micelles

In the past two decades, biodegradable micelles based on poly(ethylene glycol)-b-poly(ε-caprolactone) (PEG-PCL) and poly(ethylene glycol)-b-polylactide (PEG-PLA) block copolymers have received much attention for tumor-targeted anticancer drug delivery.[22] However, due to the slow degradation of polyesters, sustained release of drugs over periods of days to weeks *via* a diffusion-controlled mechanism, which often results in reduced drug efficacy, is commonly observed. By contrast, shell-sheddable micelles based on PEG-SS-PCL release Dox quantitatively within 12 h in a reductive environment (10 mM dithiothreitol, DTT) analogous to that of the intra-cellular compartments such as the cytosol and the cell nucleus (Figure 8.2A).[23] Low drug release (<20%) was observed within 24 h for reduction insensitive PEG–PCL micelles under the same conditions as well as for PEG-SS-PCL micelles under non-reductive conditions. PEG-SS-PCL micelles were shown to be sufficiently stable in water, but prone to fast

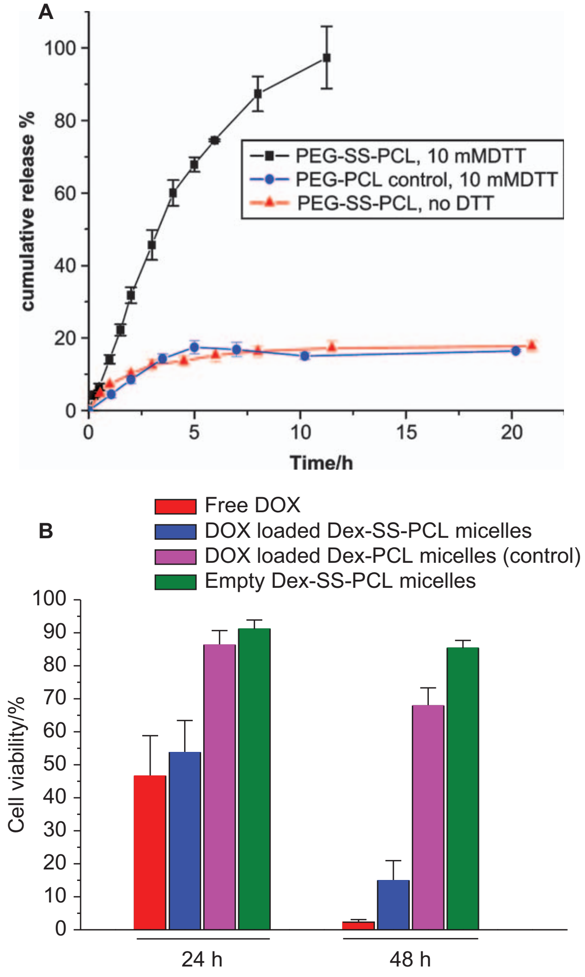

Figure 8.2 Reduction-triggered release of Dox from PEG-SS-PCL micelles (pH 7.4, 50 mM); PEG-PCL micelles were used as a reduction insensitive control (A). Reprinted from reference 23 with permission of Elsevier. Toxicity of Dox-loaded Dex-SS-PCL micelles *versus* Dox-loaded Dex-PCL micelles, free Dox, and empty Dex-SS-PCL micelles in RAW 264.7 cells (B). Dox dosage was 25 μg/mL. The cells were incubated for 24 h or 48 h. Data are presented as the average ± standard deviation ($n = 6$).
Reprinted from Ref. 24 with permission. Copyright (2010) American Chemical Society.

aggregation in the presence of 10 mM dithiothreitol (DTT), due to shedding of the PEG shells through reductive cleavage of the intermediate disulfide bonds. Experiments using a mouse leukemic monocyte macrophage cell line (RAW 264.7) revealed that these shell-sheddable micelles release Dox much faster inside the cells and show a higher antitumor efficacy, as compared to the "traditional" reduction insensitive control. Very similar results were also observed for dextran-SS-PCL block copolymer micelles, in which cell viabilities of about 20 and 70% were recorded for RAW 264.7 cells after 2 days' treatment with Dox-loaded dextran-SS-PCL micelles and Dox-loaded dextran-PCL (reduction-insensitive) micelles, respectively (Figure 8.2B).[24]

The effect of the disulfide content, controlled by varying the weight ratios of PEG-PCL and PEG-SS-PCL block copolymers during preparation of micelles, on reduction-sensitivity, size change, triggered drug release as well as antitumor activity of Dox-loaded PEG-PCL micelles has been evaluated.[25] Intra-cellular drug release from Dox-loaded biodegradable micelles and, accordingly, their therapeutic activity can be precisely controlled by reduction-responsive shedding of hydrophilic shells. This represents a most straightforward and effective approach to control drug release from "traditional" biodegradable micellar carriers. It is interesting to note that bioreducible PEG-PCL micelles maintain good colloidal stability with similar size distributions following shedding off as much as 90% PEG shells. The enhanced drug release upon shedding off shells is likely attributed to formation of drug trafficking channels in the corona, facilitating drug diffusion from the micellar core.

Wang *et al.*[26] discovered that shell-detachable micelles based on disulfide-linked diblock copolymer of PCL and hydrophilic poly(ethyl ethylene phosphate) (PCL-SS-PEEP) display GSH-responsive release of Dox and enable enhanced growth inhibition of A549 tumor cells pretreated with glutathione monoester (GSH-OEt). GSH-OEt is often used to enhance artificially the intra-cellular GSH level. These reduction-sensitive shell-sheddable micelles were shown effectively to overcome the multi-drug resistance (MDR) of cancer cells.[27] In the last few years, many different types of reduction-sensitive shell-sheddable micelles have been designed and explored for controlled drug release. Yoo and Park[28] reported GSH-triggered drug release from camptothecin (CPT)-loaded PEG-SS-poly(γ-benzyl L-glutamate) (PEG-SS-PBLG) micelles, resulting in higher toxicity to SCC7 cancer cells than CPT-loaded PEG-b-PBLG micelles (reduction-insensitive control). Li *et al.*[29] and Shi *et al.*[30] reported that reduction-sensitive PEG-SS-poly(ε-benzyloxycarbonyl-L-lysine) (mPEG-SS-PzLL) and PEG-SS-polyleucine (PEG-SS-Pleu) micelles gave enhanced Dox release in response to 10 mM DTT. Li *et al.*[31] prepared shell-sheddable micelles based on six-armed star-PCL-SS-PEG, which showed an accelerated release of Dox in the presence of 10 mM DTT. Dox-loaded micelles displayed GSH-dependent inhibition effect to MCF-7 cells. Huang and Yan[32] constructed shell-sheddable micelles based on the amphiphilic hyperbranched multi-arm star-PLA-SS-poly(2-ethoxy-2-oxo-1,3,2-dioxaphospholane) (PEP) copolymer, and Oh *et al.*[33] reported the synthesis and reduction-triggered shell-shedding of PEG-SS-PLA micelles.

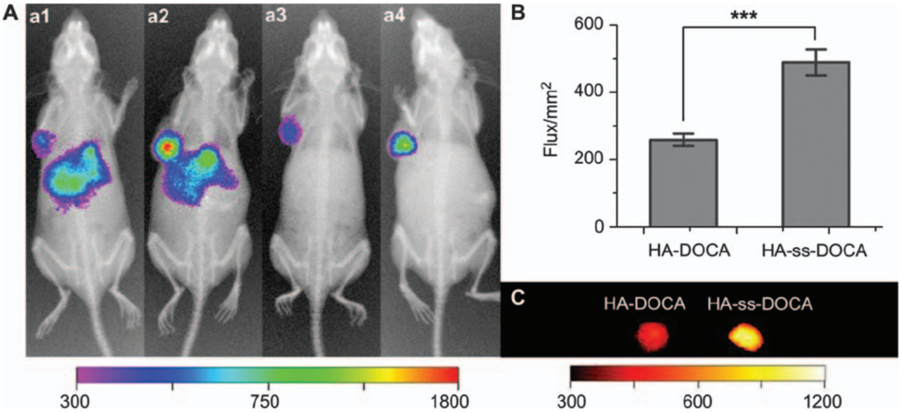

Figure 8.3 *In vivo* imaging of tumor-bearing mice administrated with Cy7-loaded micelles (A). Images taken after administration of HA-DOCA$_{10}$ micelles at 6 hours (a1) and 24 hours (a3) and HA-SS-DOCA$_{10}$ micelles for 6 hours (a2) and 24 hours (a4), respectively. Quantification of the *ex vivo* tumor uptake characteristics of micelles in tumor-bearing mice after 24 hours injection (B). Uptake was expressed as photoflux per mm^2 of tumor. Results were expressed as the mean ± SD from three independent experiments. ***$p < 0.001$. *Ex vivo* fluorescence images of tumors collected at 24 h post-injection of HA-DOCA$_{10}$ micelles and HA-SS-DOCA$_{10}$ micelles (C). Reprinted from Ref. 35 with permission of Elsevier.

Triple-stimuli sensitive micelles of PNIPAM-SS-P(THP-HEMA) have been designed to respond to changes in temperature, pH and redox potential (THP-HEMA: tetrahydropyran (THP)-protected 2-hydroxyethyl methacrylate), which provides a unique possibility to fine-tune the release kinetics of the encapsulated hydrophobic guest molecules.[34] While the pH and redox stimulus separately cause slow or incomplete release of Nile red over a long period of time, combination of both stimuli results in significantly accelerated and more complete release of Nile red.

Hyaluronic acid-SS-deoxycholic acid (HA-SS-DOCA) conjugates self-assemble into redox-sensitive nano-size micelles and rapidly disassemble in the presence of 20 mM GSH.[35] HA-SS-DOCA micelles were taken up by human breast adenocarcinoma cells (MDA-MB-231) *via* HA-receptor mediated endocytosis. *In vivo* studies in tumor-bearing mice showed preferential accumulation of payloads in the tumor site 24 hours following injection (Figure 8.3A). Notably, HA-SS-DOCA micelles displayed enhanced accumulation of Cy7 in the tumor as compared to their reduction-insensitive counterparts (Figure 8.3B and C).

8.2.2 Micelles with Reduction-sensitive Core

Fan *et al.*[36] prepared reductively degradable micelles from amphiphilic graft copolymers of disulfide-containing hydrophobic poly(amido amine) (SS-PAA) and PEG (SS-PAA-g-PEG). Dox was nearly quantitatively released *in vitro* in

10 hours in response to 1 mM DTT, due to reduction-sensitive degradation of the PAA main chain resulting in micelle disassembly, whereas only approximately 25% Dox was released in 24 hours in the absence of DTT. The IC_{50} of the Dox-loaded SS-PAA-g-PEG micelles was determined to be 0.0647 μg/mL for HepG2 cells and 0.0494 mg/mL for HeLa cells, which are only slightly higher than the IC_{50} of free Dox. Huang *et al.*[37] prepared reduction-degradable micelles by conjugating azide-functionalized camptothecin (CPT) and azide-terminated PEG to SS-PAA containing alkyne groups *via* click chemistry (SS-PAA-g-PEG/CPT). At 40 mM DTT, over 85% copolymer was degraded into oligomers and small complexes in 7 days. *In vitro* release studies showed enhanced release of CPT at higher DTT concentration.

Novel reduction-sensitive amphiphilic hyperbranched polyphosphates (HPHDP) have been prepared by self-condensing ring-opening polymerization (SCROP) of 2-[(2-hydroxyethyl)-disulfanyl]ethoxy-2-oxo-1,3,2-dioxaphospholane (Figure 8.4).[38] HPHDP self-assembled into nano-sized micelles with a multi-core/shell structure and a narrow size distribution. Notably, Dox was efficiently transported into the nuclei of tumor cells, resulting in enhanced antitumor efficacy. In a subsequent study, micelles were prepared from amphiphilic hyperbranched block copolyphosphates containing reduction-sensitive hydrophobic core and hydrophilic periphery, which caused faster Dox release and higher proliferation inhibition in GSH-OEt pretreated HeLa cells than in those of the non-treated cells.[39]

GSH-sensitive micelles can be also prepared from amphiphilic copolymers containing disulfide bonds in the hydrophobic segments, which can be broken in response to elevated GSH concentrations leading to the disassembly of micelles and the concomitant enhanced drug release.[40] Although drug release was relatively slow even in the presence of 70 mM GSH, the cytotoxicity of Dox-loaded micelles was positively correlated with the intra-cellular GSH level in MCF-7 cells. Reduction-sensitive micelles based on poly(ethylene oxide)-b-poly(*N*-methacryloyl-*N′*-(t-butyloxycarbonyl)cystamine) (PEO-b-PMABC) diblock copolymers have also shown faster Dox release and higher anticancer efficacy than the reduction-insensitive controls.[41] Other redox-sensitive diselenide-containing block copolymer micelles exhibited a rapid disassembling in response to a low concentration of reducing agent (GSH, 0.01 mg/mL) as well as oxidant (H_2O_2, 0.01% v/v).[42] Very recently, side-chain selenium-containing amphiphilic copolymers were designed to afford oxidation-sensitive micelles that showed fast release of Nile red upon the addition of 0.1% hydrogen peroxide.[43]

8.2.3 Reduction-sensitive Cross-linked Micelles

One practical challenge for micellar carriers is to be stable *in vivo*, and thus to avoid premature drug leakage following intravenous administration.[44] It has been shown that cross-linking of micelles effectively overcomes the instability problem.[45] It should be noted, nevertheless, that overly stable micelles are not ideal either, because the release of drugs may be prohibited once the micelles

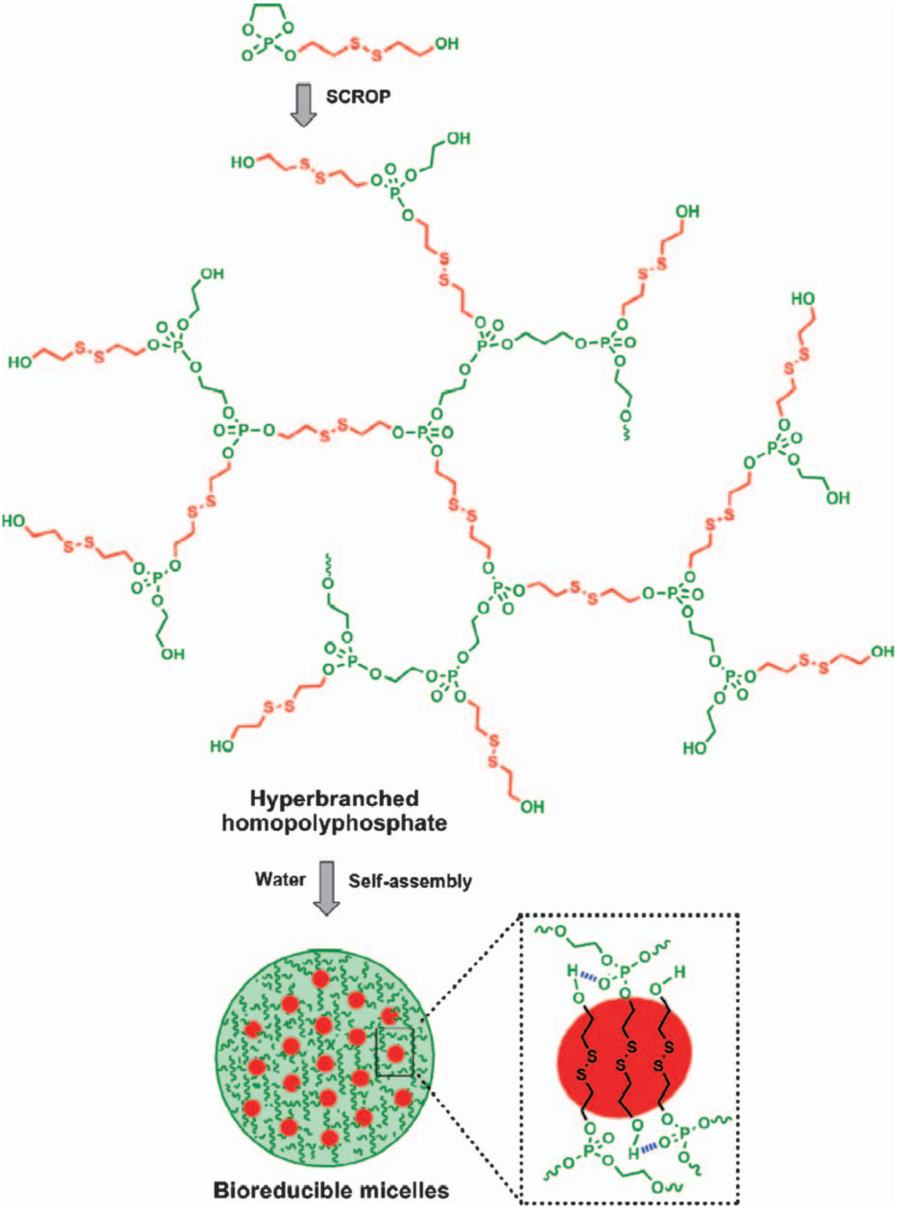
SCROP
Hyperbranched homopolyphosphate
Water
Self-assembly
Bioreducible micelles

Figure 8.4 Synthesis of HPHDP and schematic representation of the self-assembled micelles.
Reproduced from Ref. 38 with permission. Copyright Wiley-VCH Verlag GmbH & Co. KGaA.

arrive at the target sites, resulting in low drug efficacy. The use of intracellularly reversible disulfide cross-links is an attractive strategy to elegantly solve the stability/drug release dilemma of micelles. Bronich *et al.*[46] prepared poly(ethylene oxide)-b-poly(methacrylic acid) (PEO-b-PMA) micelles using divalent metal cations (Ca^{2+}) as templates and cross-linking the ionic cores with cystamine. Interestingly, these micelles showed a high level of Dox loading (50% w/w). *In vitro* release studies demonstrated significant acceleration of Dox release from cystamine-cross-linked micelles when GSH or cysteine were present in the release media, 75% of Dox being released in 1 hour in response to 10 mM GSH. MTT assay revealed that Dox-loaded cystamine-cross-linked micelles were much more cytotoxic to human A2780 ovarian carcinoma cells, with an IC_{50} value at least six times lower as compared to the stably cross-linked control. Stenzel *et al.*[47] obtained stable nucleosides-containing block copolymer micelles by sequential reversible addition-fragmentation chain transfer (RAFT) copolymerization of polyethylene glycol methyl ether methacrylate, 5′-O-methacryloyluridine and bis(2-methacryloyloxyethyl)disulfide (DSDMA, bioreducible cross-linker). In the presence of 0.65 mM DTT, the core-cross-linked (CCL) micelles readily hydrolyzed in less than 1 hour into free block copolymers. As expected, CCL micelles showed a rather slow release of riboflavin (about 30% in 7 hours). By contrast, the addition of 0.65 mM DTT induced fast drug release, with a pattern similar to that of the uncross-linked control (about 60–70% release in 7 hours). Liu *et al.*[48,49] also employed RAFT polymerization to prepare two types of degradable thermo-responsive CCL micelles. In one approach, the double hydrophilic block copolymer, poly(ethylene oxide)-b-poly(*N*-isopropylacrylamide-co-*N*-acryloxysuccinimide), existing as unimers in water at room temperature, formed micelles upon increasing the temperature to above its LCST, which after cross-linking with cystamine yielded stable CCL micelles.[48] The disulfide cross-links could be cleaved in a strong reducing environment. Moreover, these micelles showed tunable swelling/deswelling behavior in response to changes of temperature. In the other approach, CCL micelles were obtained in a one-pot manner *via* RAFT copolymerization of *N*-isopropylacrylamide (NIPAAm) and DSDMA employing poly(*N*-(2-aminoethyl)methacrylamide) as a macro-RAFT agent.[49] These micelles could be disintegrated into unimers upon addition of 15.4 mM DTT. The authors have shown that coronas of CCL micelles could be further functionalized with biocompatible and/or bioactive molecules such as biotin and galactose.

Disulfide cross-linked micelles based on telodendrimers, comprised of a linear PEG and a cysteine-containing dendritic cluster of cholic acids, showed superior drug-loading capacity, enhanced micellar stability, prolonged *in vivo* circulation time and preferential accumulation at the tumor site in nude mice bearing SKOV-3 ovarian cancer xenograft (Figure 8.5A).[50] The release of PTX from micelles while inhibited by cross-linking could be gradually facilitated in a reducing environment. This disulfide cross-linked micellar PTX was shown to be more effective in tumor inhibition than the non-cross-linked counterparts and Taxol (Figure 8.5B).

Dox-conjugated CCL micelles based on *N*-(2-hydroxypropyl)methacrylamide (HPMA) and 2-(2-pyridyldisulfide)ethyl methacrylate (PDSM) block copolymers have been prepared by means of simultaneous Dox conjugation

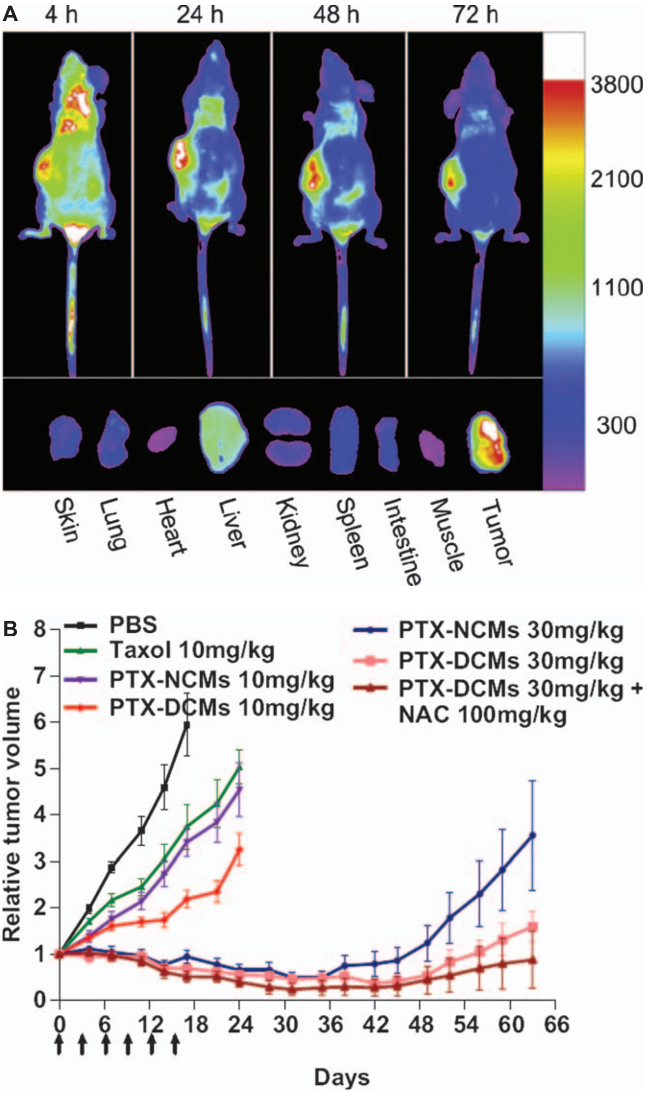

Figure 8.5 *In vivo* and *ex vivo* near infra-red fluorescence (NIRF) optical imaging (A). Top: *In vivo* NIRF optical images of SKOV-3 xenograft bearing mouse were obtained with a Kodak imaging system at different time points after i.v. injection of DCMs co-loaded with PTX and DiD. Bottom: *Ex vivo* NIR image of dissected organs and tumor was obtained at 72 h after injection. *In vivo* antitumor efficacy after intravenous treatment of different PTX formulations in the subcutaneous mouse model of SKOV-3 ovarian cancer (B). Tumor-bearing mice were i.v. treated with PBS (control) and different PTX formulations on days 0, 3, 6, 9, 12 and 15 when tumor volume reached about 100–200 mm^3 ($n = 8$–10).
Reprinted from Ref. 50 with permission of Elsevier.

to the micellar core *via* acid cleavable hydrazone bonds and core-cross-linking *via* reducible disulfide bonds.[51] These micelles disintegrated into unimers upon treatment with tri(2-carboxyethyl)phosphine hydrochloride (TCEP). *In vitro* release studies showed that CCL micelles released 72% and 21% of Dox in 23.5 hours at pH 5.0 and pH 7.4, respectively. Murthy and Heffernan[52] prepared disulfide-cross-linked polyion micelles by electrostatic self-assembly of PEG-poly(L-lysine) (PEG-PLL) block copolymer with negatively charged proteins, both of which contain dithiopyridine functions, followed by disulfide cross-linking. In this way, proteins were chemically tethered to the micellar core *via* a disulfide bond, resulting in a high degree of protein retention under SDS-PAGE. Vaccine delivery systems with ovalbumin and immunostimulatory CpG-DNA were prepared to release the vaccine intra-cellularly through reduction of disulfide cross-links. These micelles were also evaluated as long-circulating enzyme carriers that maintain the enzymatic activity of the antioxidant enzyme catalase within the micelle core.

Shell cross-linked (SCL) micelles have been obtained through self-assembly of PEG-b-poly(L-lysine)-b-poly(L-phenylalanine) triblock copolymers followed by cross-linking of the poly(L-lysine) block with 3,3′-dithiobis(sulfosuccinimidylpropionate) (DTSSP).[53] The release of methotrexate (MTX) from SCL micelles, which demonstrated enhanced stability against sodium dodecyl sulfate (SDS), was greatly retarded as compared to the non-cross-linked counterparts. The rate of drug release from CCL micelles increased as the GSH concentrations in the media rose. The toxicity of MTX-loaded CCL micelles against A549 cells revealed a clear correlation with the intra-cellular GSH levels. Reversible SCL micelles prepared using PEG-b-PPE$_{SH}$-b-PCL triblock copolymer (PPE$_{SH}$: thiol-functionalized polyphosphoester) exhibited enhanced stability against dilution and addition of *N*,*N*′-dimethylformamide.[54] Drug release was retarded by the cross-linking and accelerated in a reductive environment (20 mM DTT). The toxicity of the Dox-loaded SCL micelles against A549 cells became greater with increasing intra-cellular GSH levels, as shown by the MTT assay. We have developed reduction-responsive reversibly cross-linked biodegradable micelles based on PEG-PCL diblock copolymer containing two lipoyl functional groups at their interface (PEG-L$_2$-PCL).[55] These micelles were readily cross-linked by adding 7.6 mol% DTT relative to the lipoyl groups and, after cross-linking, demonstrated a markedly enhanced stability against dilution and physiological salt concentration, as well as organic solvents. By contrast, in the presence of 10 mM DTT, micelles were subject to rapid de-cross-linking. *In vitro* release studies showed minimal release of Dox from cross-linked micelles even at a particularly low micelle concentration (*i.e.* $C < CMC$ of uncross-linked micelles, simulating intravenous injection). In the presence of 10 mM DTT mimicking an intra-cellular reductive environment, sustained release of Dox from cross-linked micelles was achieved, with 75% of Dox released in 9 hours. Another group prepared reversibly cross-linked biodegradable micelles using PEG-PCL block copolymer linked by a peptide comprising three cysteine residues (PEG-Cys3-PCL).[56] The disulfide-stabilized micelles were stable against high dilution. Sustained release was observed *in vitro* below the CMC at 37 °C (<20% release in 24 h), while addition of 1 mM DTT triggered a burst of Dox. Other novel reversible SCL micelles were designed using an alkynylated surfactant cross-linked *via* click reaction with a diazide containing cleavable disulfide, geminal diol or acetal bond.[57] Hydrophobic guests such as pyrene could be readily loaded into the SCL micelles, and the micelles remained robust even after significant dilution to a concentration below the CMC of the surfactant. The entrapped pyrene was, however, completely released from disulfide-cross-linked micelles in *ca.* 1 min. upon addition of just 20 µM DTT. Notably, acid-triggered pyrene release from acetal-cross-linked micelles was found to be much slower. McCormick *et al.*[58] reported the fabrication of SCL micelles from the pH-responsive triblock copolymer, PEO-b-poly(*N*-(3-aminopropyl) methacrylamide)-β-poly(2-(diisopropylamino)ethyl methacrylate) (mPEO-PAPMA-PDPAEMA), which is soluble in water at low pH (<5.0) but self-assembles into micelles above pH 6.0. The micelles were cross-linked with dimethyl 3,3′-dithiobispropionimidate (DTBP). The treatment of SCL micelles with 9.4 mM DTT for 1 h at room temperature resulted in rapid de-cross-linking.

8.3 Reduction-sensitive Polymersomes

Polymersomes (also referred to as polymeric vesicles) have received enormous attention due to their intriguing aggregation phenomena, cell and virus-mimicking dimensions and functions, as well as tremendous potential applications in medicine, pharmacy and biotechnology.[59–61] Several excellent review papers on polymersomes and stimuli-sensitive polymersomes have been published.[2,62,63] The reader is referred to Chapter 7 for further information.

The clinical success of many protein drugs is intimately dependent on the advancement of safe, efficient and economically viable targeted intra-cellular delivery systems. Polymersomes are particularly interesting for intra-cellular protein delivery.[64] We prepared reversibly cross-linked temperature-responsive nano-sized polymersomes (about 220 nm) from water soluble PEO-b-poly(acrylic acid)-b-PNIPAM (PEO-PAA-PNIPAM) triblock copolymers by raising the solution temperature to above the lower critical solution temperature (LCST), followed by cross-linking at the interface using cystamine *via* carbodiimide chemistry.[65] The cross-linked polymersomes, while showing remarkable stability against dilution, organic solvents, high salt conditions and change of temperature in water, were otherwise completely dissociated in 1.5 hours in 10 mM DTT at pH 7.4. Reduction and temperature dual-responsive polymersomes with an elevated LCST of 38–39 °C were obtained by changing the PAA/PNIPAM ratio.[66] These smart polymersomes displayed efficient protein loading under mild conditions, and excellent stability with restrained protein release under physiological conditions due to chemical cross-linking of the polymersome shells. Furthermore, a rapid dis-assembling and protein release was observed under an intra-cellular-mimicking reductive environment and in cancer cells (Figure 8.6). More recently, pH and reduction dual-bioresponsive polymersomes based on poly(ethylene

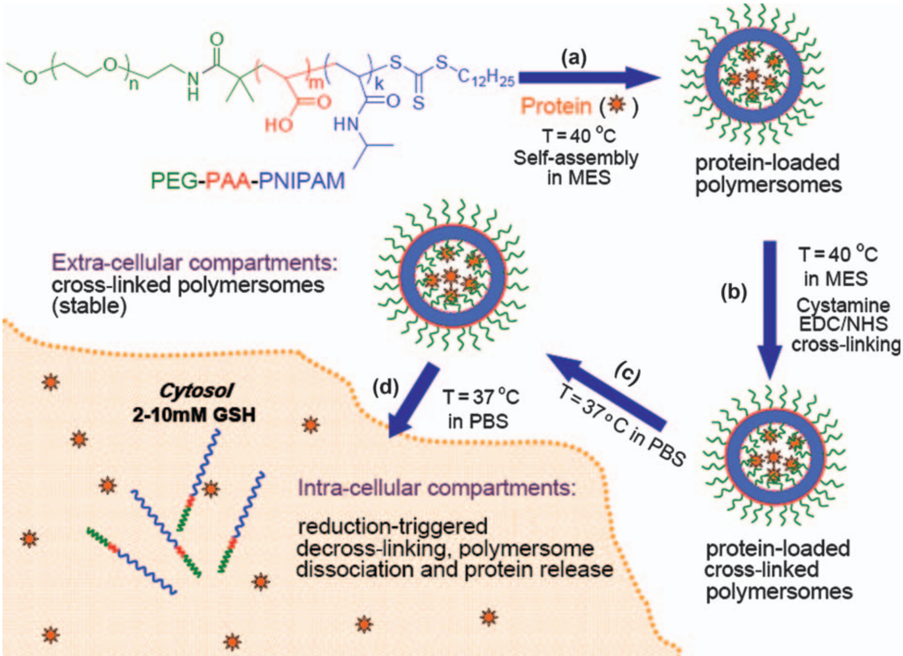
PEG-PAA-PNIPAM
(a)
Protein
T = 40 °C
Self-assembly
in MES
protein-loaded
polymersomes
(b)
T = 40 °C
in MES
Cystamine
EDC/NHS
cross-linking
protein-loaded
cross-linked
polymersomes
(c)
T = 37 °C in PBS
Extra-cellular compartments:
cross-linked polymersomes
(stable)
(d)
T = 37 °C
in PBS
Cytosol
2-10mM GSH
Intra-cellular compartments:
reduction-triggered
decross-linking, polymersome
dissociation and protein release

Figure 8.6 Illustration of reduction and temperature dual-responsive cross-linked polymersomes based on PEG-PAA-PNIPAM triblock copolymers with an elevated LCST for triggered intra-cellular protein release. Protein-loaded polymersomes are readily prepared in mild aqueous conditions (MES, pH 5.5, 20 mM) *via* simply increasing solution temperature to 40 °C (a); protein-loaded polymersomes can be stabilized *via* cross-linking with cystamine by carbodiimide chemistry (b); protein-loaded Cys-cross-linked polymersomes are stable in physiological mimicking conditions (PBS, pH 7.4, 20 mM, 150 mM NaCl, 37 °C) (c); and protein-loaded Cys-cross-linked polymersomes are rapidly disassembled into unimers inside cells (d), resulting in highly efficient intra-cellular protein release.
Reprinted from Ref. 66 with permission of the Royal Society of Chemistry.

glycol)-SS-poly(2-(diethyl amino)ethyl methacrylate) (PEG-SS-PDEA) diblock copolymers facilitated efficient loading of proteins under mild conditions and rapid release of them intracellularly into cancer cells.[67]

Peptide vesicles were formed from the amphiphilic oligopeptide SA2 (Ac-Ala-Cys-Val-Cys-Leu-(Leu/Cys)-Leu-Trp-Glu-Glu-COOH), and stabilized by introducing two or three cysteine units into the hydrophobic domain to enable the establishment of intermolecular disulfide bridges.[68] The *in vitro* release profiles showed that the intermolecular cross-linking of peptides in the vesicles did not affect the calcein release profile. In subsequent studies, water-insoluble phthalocyanines (photosensitizer) were quantitatively loaded into peptide vesicles, which were internalized by cells in their intact form.[69] Incubation in the dark of COS-7 cells with phthalocyanine-loaded peptide vesicles did not result in any cytotoxicity. However, upon illumination, the phthalocyanine-loaded peptide vesicles showed an active photodynamic response towards COS-7 cells, resulting in effective cell killing ($IC_{50} = \sim 2.8$ nM phthalocyanine). Free phthalocyanine and empty peptide vesicles did not show any cytotoxicity.

Reduction-sensitive, robust and biocompatible SSCB[6]VC vesicles were prepared from an amphiphilic cucurbit[6]uril (CB[6]) derivative containing disulfide bonds between hexaethylene glycol units and the CB[6] core.[70] The vesicles were obtained with an average diameter of *ca.* 190 nm by the thin film rehydration method, followed by repeated extrusion through a syringe filter. The vesicles were stable in the presence of 3 μM GSH or 15 μM cysteine. However, complete disruption occurred in 12 hours in response to 5 mM GSH. Notably, these vesicles could be readily decorated with functional moieties such as targeting ligands and imaging probes by using their spermidine conjugates. MTT assays showed that Dox-loaded folate-SSCB[6]VC significantly decreased cell viability as compared to free Dox (28.1% *versus* 52.7%).

8.4 Reduction-sensitive Nanoparticles

Biodegradable nanoparticles have been extensively evaluated *in vitro* and *in vivo* for controlled drug delivery.[71,72] To obtain nanoparticles with high extra-cellular stability and fast intra-cellular drug release, reversibly stabilized multi-functional dextran nanoparticles based on dextran-lipoic acid derivatives (Dex-LAs) were developed (Figure 8.7A).[73] Dextran is a natural analogue of PEG, while lipoic acid is produced naturally in the human body and commonly used as an antioxidant drug for treating diseases such as diabetes and HIV. The nanoparticles after cross-linking with a catalytic amount of DTT were robust against dilution and high salt concentration. The release of Dox was minimal (*ca.* 10%) even under extensive dilution, while over 90% Dox was released in 11 hours in response to 10 mM DTT (Figure 8.7B). Confocal laser scanning microscopy (CLSM) studies using HeLa and RAW264.7 cells revealed a rapid and efficient delivery of Dox into the cell nucleus. MTT assays showed that Dox-loaded cross-linked nanoparticles have a similar efficacy as the non-cross-linked counterparts.

Reduction-sensitive nanoparticles were prepared by introducing disulfide bridges into the side chains of a thermo-sensitive polymer, p(PEG-MEMA-co-Boc-Cyst-MMAm), and simply heating the aqueous solution to above its LCST (LCST varied from 20 to 57 °C depending on copolymer compositions).[74] These nanoparticles remained stable in the presence of 2 μM DTT for 24 hours at 37 °C, but rapidly collapsed in response to 3 mM DTT, likely due to enhanced water solubility after cleavage of disulfide bonds. Disulfide cross-linked PEG-streptavidin hybrid particles from biotin-PEG-b-PPDSM block copolymers have also been obtained.[75] The micellar core functionalization (*e.g.* with a maleimide derivative of a green fluorophore) and cross-linking were carried out concomitantly, to afford fluorescent CCL micelles with a diameter of *ca.* 54 nm and 75 mol% biotin functionality exposed on the micelle corona.

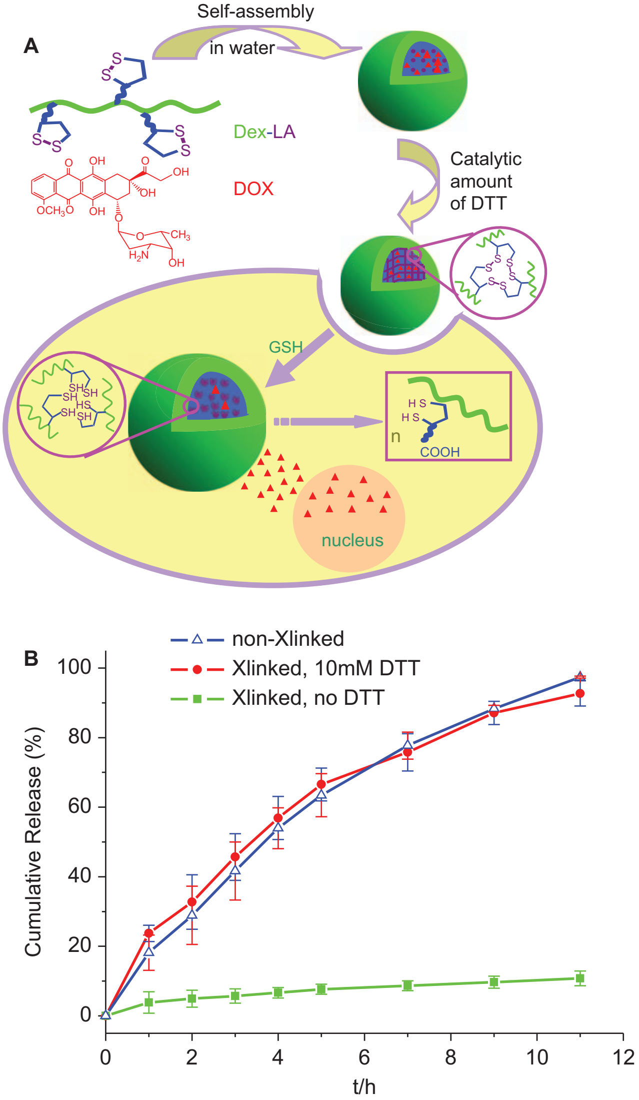

Figure 8.7 Illustration of reversibly stabilized multi-functional dextran nanoparticles (A). Dex-LAs were obtained by coupling lipoic acid to dextran and formed nanoparticles in water; addition of catalytic amount of DTT yielded stable nanoparticles due to cross-linking of the core. In cancer cells, fast de-cross-linking took place owing to a high concentration of glutathione (GSH) tripeptides, triggering a rapid release of encapsulated drugs to the cell nucleus, while the nanoparticles were eventually degraded to non-toxic products, dextran and lipoic acid. (B) Release of Dox from cross-linked dextran nanoparticles (DS 80) in the absence or in the presence of 10 mM DTT at pH 7.4 and 37 °C. Non-cross-linked dextran nanoparticles were used as a control. The experiments were performed in triplicate.
Reproduced from Ref. 73 with permission. Copyright Wiley-VCH Verlag GmbH & Co. KGaA.

The micelles were decorated with streptavidin, yielding polymer–protein hybrid particles with tunable dimensions in the 350 nm–2 μm range. In another study partially thiolated trimethylated chitosan (TMC) and thiolated hyaluronic acid were used to render disulfide-cross-linked positively charged nanoparticles, which resulted to be stable in 0.8 M NaCl.[76] In contrast, particles made from non-thiolated polymers dissociated under the same conditions.

Feng *et al.*[77] reported redox-responsive nanogated mesoporous silica nanoparticles (MSN) obtained by grafting poly(*N*-acryloxysuccinimide) (PNAS) to the pore entrance of MSN particles followed by cross-linking with cystamine. The polymer coating around MSN was uniform and 2 nm thick. The release studies demonstrated that loaded rhodamine B was rapidly released in response to 21.6 mM DTT, in contrast with the slow release in 0.216 mM DTT medium. The release rate of rhodamine B was dependent on the DTT concentration. In comparison, DTT did not induce the release from irreversibly cross-linked ensembles (with 1,6-hexadiamine). In a following study, the authors designed multi-responsive nanogated MSN by immobilizing β-CD to PNAS coated MSN *via* disulfide bonds and then cross-linking with diazo-linker.[78] In the absence of stimuli, no release of entrapped calcein from nanogated MSN was observed, while application of UV, DTT or α-CD resulted in instantaneous release of calcein.

Cysteine was tethered to MSN *via* disulfide bonds (MSN-SS-Cys) to make MSN-based controlled intra-cellular cysteine release systems.[79] There was no leaching of Cys in PBS solution prior to the addition of reducing agents. However, approximately 99, 90, 70 and 60% of Cys was released from MSN-SS-Cys in 30 min following addition of nicotinamide adenine dinucleotide hydride (NADH), DTT, dihydrolipoic acid (DHLA) and GSH, respectively. Toxicity studies showed that MSN-SS–Cys was approximately 444 times more effective in delivering cysteine into HeLa cells than the conventional *N*-acetylcysteine (NAC) approach. In comparison, Cys physisorbed to MSN and Cys tethered to MSN *via* a non-cleavable thioether bond (MSN–Cys) did not show any significant effect on the cell growth inhibition. Intra-cellular cysteine release has also been achieved with ATTO633-labeled cysteine linked to the inner structure of MSN *via* disulfide bridges. High-resolution fluorescence microscopy revealed that endosomal escape is a limiting factor for the redox-triggered release in HuH7 cells of disulfide-bound cysteine from MSN.[80] However, after photochemical rupture of the endosomes by means of a photosensitizer, ATTO633-labeled cysteine was successfully released from MSN into the cytoplasm, indicating that the reducing milieu of the cytoplasm is sufficient to cleave the disulfide bonds.

8.5 Reduction-sensitive Capsules

Hollow capsules are a class of highly versatile vehicles that can be applied for encapsulation and controlled delivery of diverse bioactive molecules including drugs, nucleic acids, peptides and proteins.[81,82] Usually, hollow capsules are fabricated by deposition of interacting polymers, mainly using the layer-by-layer (LbL) technique, onto a sacrificial colloidal template followed by dissolution of the core.[83] The assembly process allows for engineering of capsules including their composition, size, permeability, colloidal stability and surface functionality. Further information on LbL techniques to obtain stimuli-responsive systems can be found in Chapter 17.

Caruso *et al.*[84,85] developed novel reductively degradable capsules based on LbL assembly of thiolated poly(methacrylic acid) (PMA_{SH}) and poly(vinylpyrrolidone) (PVPON) onto silica particles, followed by the cross-linking of the thiol groups in the PMA_{SH} to form stable disulfide bonds, and the dissolution of the sacrificial silica core. PVPON was readily removed *via* disruption of inter-polymer hydrogen bonds in pH 7 buffer, resulting in single-component disulfide cross-linked PMA_{SH} capsules. These capsules were stable in oxidizing conditions, but rapidly disassembled in reducing environments similar to those inside living cells, to release the encapsulated cargo. PMA capsules were applied for *in vitro* and *in vivo* delivery of proteins and peptides for vaccine applications.[86–88] PMA capsules could be efficiently associated with and internalized by monocytes and dendritic cells. PMA capsules loaded with KP9 peptide (a model HIV vaccine peptide) stimulated a significant proportion of the KP9-specific T cells to express simultaneously the cytokines interferon-γ (IFN-γ) and tumor necrosis factor-α (TNF-α). The intravenous vaccination of mice with ovalbumin (OVA) protein- and peptide-loaded PMA_{SH} capsules activated 70-fold and 6-fold the proliferation of OVA-specific CD4 and CD8 T cells, respectively, compared to the equivalent amount of OVA protein administered alone.[88] These bio-destructible capsules were also investigated for intra-cellular delivery of Dox and 5-fluorouracil (5-FU), which were loaded in the form of oleic acid emulsions.[89,90] Dox/oleic acid-loaded capsules released in 100 mM PBS at 37 °C minimal amounts of Dox (<5%) in 24 hours, while in the presence of 5 mM GSH approximately 80% Dox was released in 6 hours. MTT assays revealed that treatment of LIM1215 human colorectal cancer cells with Dox/oleic acid-loaded PMA capsules and 5-FU/oleic acid-loaded capsules resulted in significant cell death (>85%), being more effective than free Dox and 5-FU, respectively. The studies on uptake and intra-cellular fate of PMA_{SH} capsules showed that the internalized capsules were deformed in endocytic compartments and accumulated in late endosomes and lysosomes.[90] Disulfide-stabilized PMA capsules could also be prepared, with up to three polymer layers, *via* a benign method (oxidation free) by sequential deposition of PMA_{SH} and PMA with activated thiol functions, namely 3-carboxy-4-nitrobenzene sulfide and pyridine-2-sulfide.[91] More recently, dual-responsive capsules were developed *via* LbL assembly and click chemistry based on alkyne-modified poly(2-diisopropylaminoethyl methacrylate) (PDPA) and a disulfide-containing biazide cross-linker (Figure 8.8).[92] These dual-responsive capsules showed reversible size changes with pH and released the cargo specifically under pH conditions that mimic those of the intra-cellular acidic compartments.

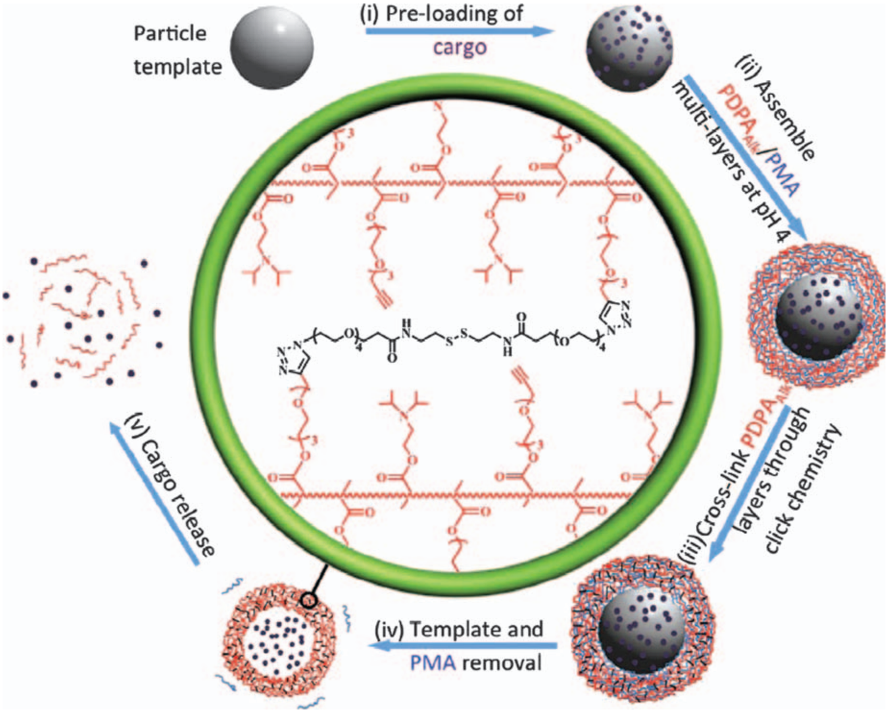
Particle template
(i) Pre-loading of cargo
(ii) Assemble PDPA_{Alk}/PMA multi-layers at pH 4
(iii) Cross-link PDPA_{Alk} layers through click chemistry
(iv) Template and PMA removal
(v) Cargo release

Figure 8.8 Assembly of poly(2-diisopropylaminoethyl methacrylate), PDPA, capsules loaded with therapeutics: (i) preloading of cargo onto a functionally modified SiO_2 particle template; (ii) PDPA alkyne ($PDPA_{Alk}$) and PMA are assembled onto the cargo-loaded SiO_2 particles; (iii) PDPA multi-layers are covalently stabilized by click reaction between the PDPA alkyne moieties and a biazide cross-linker containing a disulfide bond; (iv) the particle template is dissolved, and PMA layers are removed by raising the pH to 7.4, yielding cargo-loaded single-component PDPA capsules; and (v) the cargo release is achieved by changes in pH and redox-potential. Reproduced from Ref. 92 with permission. Copyright Wiley-VCH Verlag GmbH & Co. KGaA.

Kim *et al.*[93] recently reported a novel template-free synthesis approach to reduction-responsive polymer nanocapsules, based on self-assembly of amphiphilic CB[6] followed by shell-cross-linking using a disulfide-containing cross-linker. The resulting capsules had an average diameter of *ca.* 70 nm and a hollow interior, surrounded by an approximately 2.0 nm thickness thin shell. Most nanocapsules collapsed and aggregated after treatment with DTT for 30 min. The encapsulated carboxyfluorescein was quickly released *in vitro* in response to 100 mM DTT. The capsules decorated with galactose showed efficient internalization into HepG2 cells and rapid intra-cellular release of carboxyfluorescein. Zhang *et al.*[94] reported the preparation of reduction-sensitive hollow polyelectrolyte nanocapsules from cysteamine-conjugated chitosan and dextran sulfate by LbL adsorption on β-cyclodextrin functionalized silica spheres, followed by cross-linking of thiols and removal of the silica core. *In vitro* release studies showed significantly enhanced release of bovine serum albumin (BSA) in response to 10 mM GSH.

8.6 Reduction-sensitive Nanogels

Nanogels are biocompatible three-dimensional materials with high water content and sizes ranging from tens of nanometers to submicrons.[95,96] Nanogels can be applied for encapsulation and delivery of various agents including anticancer drugs, proteins, plasmid DNA and imaging probes.[96] Well-defined reduction-sensitive functional nanogels have been obtained by means of inverse mini-emulsion atom transfer radical polymerization (ATRP) and the disulfide–thiol exchange reaction.[97,98] These nanogels were loaded with various water-soluble biomolecules including anticancer drugs, carbohydrates and proteins.[99,100] Dox-loaded disulfide-cross-linked nanogels (drug loading efficiency 50–70%) were essentially non-toxic, but addition of 20 wt.% GSH led to the inhibition of HeLa cells growth. More recently, reduction-sensitive Dox-loaded PEG nanoporous polymer spheres (NPS_{PEG}-Dox) have been prepared through the following steps: (i) loading and immobilization of alkyne or azide-functionalized PEG into MSN templates *via* click chemistry, (ii) click cross-linking of PEG and covalent attachment of Dox through degradable linkers containing disulfide bonds, and (iii) dissolution of the MSN templates.[101] Under reductive conditions (5 mM GSH), the spheres

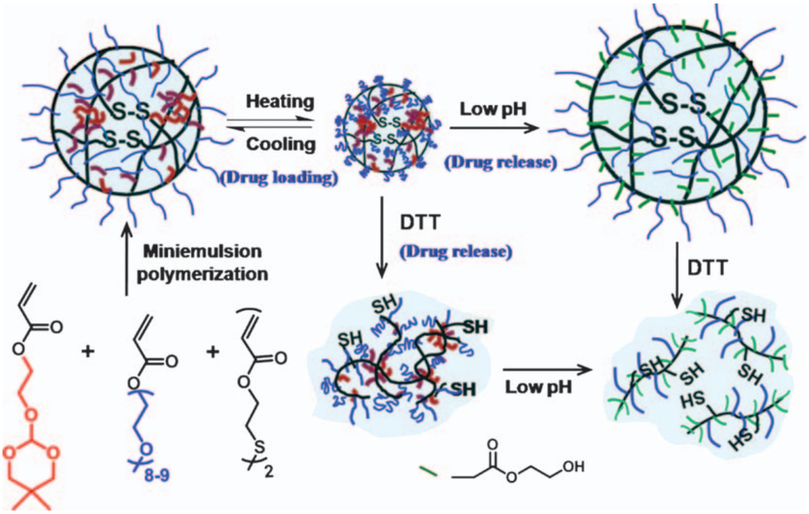

Figure 8.9 Multi-responsive nanogels prepared by miniemulsion copolymerization of monomethyl oligo(ethylene glycol) acrylate (OEGA) and an ortho ester-containing acrylic monomer, 2-(5,5-dimethyl-1,3-dioxan-2-yloxy) ethyl acrylate (DMDEA), using bis(2-acryloyloxyethyl) disulfide (BADS) as a cross-linker. Reprinted from Ref. 103 with permission of Elsevier.

disassembled to release Dox over time. Biocompatible and degradable nanogels (average diameter *ca.* 380 nm) have also been obtained by cross-linking of thiol-functionalized star-shaped poly(ethylene oxide-co-propylene oxide) and linear polyglycidol in inverse mini-emulsion, *via* formation of disulfide bonds.[102] These nanogels were degraded after 6 hours incubation in 10 mM GSH. Finally, temperature, pH and reduction triple-responsive nanogels were obtained *via* miniemulsion copolymerization of monomethyl oligo(ethylene glycol) acrylate (OEGA) and an ortho ester-containing acrylic monomer, 2-(5,5-dimethyl-1,3-dioxan-2-yloxy) ethyl acrylate (DMDEA), using bis(2-acryloyloxyethyl) disulfide (BADS) as a cross-linker (Figure 8.9).[103] The swelling, drug loading and drug release as well as degradation behaviors of nanogels were shown to be facilely controlled by a combination of temperature, pH and reduction conditions.

8.7 Conclusions

The unique disulfide chemistry has enabled development of versatile smart nanosystems that are stable under physiological conditions, but rapidly destabilize under a reducing environment, accomplishing efficient "active" intra-cellular delivery of various therapeutic substances. This superior intra-cellular drug release approach has been shown significantly to enhance drug efficacy, overcome multi-drug resistance (MDR) and/or reduce drug and carrier-associated side effects. The *in vivo* studies have demonstrated that reduction-sensitive reversibly cross-linked nanosystems result in enhanced stability, longer circulation time, improved tumor-targetability and better therapeutic outcomes, as compared to the non-cross-linked controls as well as the free drugs. It is anticipated that reduction-sensitive nanosystems have great potential for targeted cancer therapy.

Acknowledgements

This work was financially supported by research grants from the National Natural Science Foundation of China (NSFC 51103093, 51173126, 20974073, 50973078 and 20874070) and a Project Funded by the Priority Academic Program Development of Jiangsu Higher Education Institutions.

References

1. S. Ganta, H. Devalapally, A. Shahiwala and M. Amiji, *J. Control. Release*, 2008, **126**, 187.
2. F. H. Meng, Z. Y. Zhong and J. Feijen, *Biomacromolecules*, 2009, **10**, 197.
3. V. Torchilin, *Eur. J. Pharm. Biopharm.*, 2009, **71**, 431.
4. G. Saito, J. A. Swanson and K. D. Lee, *Adv. Drug Deliver. Rev.*, 2003, **55**, 199.
5. R. Cheng, F. Feng, F. Meng, C. Deng, J. Feijen and Z. Zhong, *J. Control. Release*, 2011, **152**, 2.

6. F. H. Meng, W. E. Hennink and Z. Y. Zhong, *Biomaterials*, 2009, **30**, 2180.
7. H. F. Gilbert, *Methods Enzymol.*, 1995, **251**, 8.
8. S. Raina and D. Missiakas, *Annu. Rev. Microbiol.*, 1997, **51**, 179.
9. M. Vert, S. M. Li, G. Spenlehauer and P. Guerin, *J. Mater. Sci. Mater. Med.*, 1992, **3**, 432.
10. L. K. Fung and W. M. Saltzman, *Adv. Drug Deliver. Rev.*, 1997, **26**, 209.
11. Y. Ikada and H. Tsuji, *Macromol. Rapid Commun.*, 2000, **21**, 117.
12. A. H. Elias and S. J. Arner, *Eur. J. Biochem.*, 2000, **267**, 6102.
13. D. M. Townsend, K. D. Tew and H. Tapiero, *Biomed. Pharmacotherapy*, 2003, **57**, 145.
14. Y. M. Go and D. P. Jones, *Biochim. Biophys. Acta*, 2008, **1780**, 1273.
15. G. Wu, Y. Z. Fang, S. Yang, J. R. Lupton and N. D. Turner, *J. Nutr.*, 2004, **134**, 489.
16. B. Arunachalam, U. T. Phan, H. J. Geuze and P. Cresswell, *P. Natl. Acad. Sci. USA*, 2000, **97**, 745.
17. T. Kurz, J. W. Eaton and U. T. Brunk, *Antioxid. Redox. Sign.*, 2010, **13**, 511.
18. P. Kuppusamy, M. Afeworki, R. A. Shankar, D. Coffin, M. C. Krishna, S. M. Hahn, J. B. Mitchell and J. L. Zweier, *Cancer Res.*, 1998, **58**, 1562.
19. P. Kuppusamy, H. Li, G. Ilangovan, A. J. Cardounel, J. L. Zweier, K. Yamada, M. C. Krishna and J. B. Mitchell, *Cancer Res.*, 2002, **62**, 307.
20. V. P. Torchilin, *Annu. Rev. Biomed. Eng.*, 2006, **8**, 343.
21. A. Nori and J. Kopecek, *Adv. Drug Deliver. Rev.*, 2005, **57**, 609.
22. K. Kataoka, A. Harada and Y. Nagasaki, *Adv. Drug Deliver. Rev.*, 2001, **47**, 113.
23. H. L. Sun, B. N. Guo, R. Cheng, F. H. Meng, H. Y. Liu and Z. Y. Zhong, *Biomaterials*, 2009, **30**, 6358.
24. H. L. Sun, B. N. Guo, X. Q. Li, R. Cheng, F. H. Meng, H. Y. Liu and Z. Y. Zhong, *Biomacromolecules*, 2010, **11**, 848.
25. W. Wang, H. L. Sun, F. H. Meng, S. B. Ma, H. Y. Liu and Z. Y. Zhong, *Soft Matter*, 2012, **8**, 3949.
26. L. Y. Tang, Y. C. Wang, Y. Li, J. Z. Du and J. Wang, *Bioconjugate Chem.*, 2009, **20**, 1095.
27. Y. C. Wang, F. Wang, T. M. Sun and J. Wang, *Bioconjugate Chem.*, 2011, **22**, 1939.
28. T. Thambi, H. Y. Yoon, K. Kim, I. C. Kwon, C. K. Yoo and J. H. Park, *Bioconjugate Chem.*, 2011, **22**, 1924.
29. H. Y. Wen, H. Q. Dong, W. J. Xie, Y. Y. Li, K. Wang, G. M. Pauletti and D. L. Shi, *Chem. Commun.*, 2011, **47**, 3550.
30. T. B. Ren, W. J. Xia, H. Q. Dong and Y. Y. Li, *Polymer*, 2011, **52**, 3580.
31. T. B. Ren, Y. Feng, Z. H. Zhang, L. Li and Y. Y. Li, *Soft Matter*, 2011, **7**, 2329.
32. J. Liu, Y. Pang, W. Huang, X. Huang, L. Meng, X. Zhu, Y. Zhou and D. Yan, *Biomacromolecules*, 2011, **12**, 1567.

33. B. K. Sourkohi, A. Cunningham, Q. Zhang and J. K. Oh, *Biomacromolecules*, 2011, **12**, 3819.
34. A. Klaikherd, C. Nagamani and S. Thayumanavan, *J. Am. Chem. Soc.*, 2009, **131**, 4830.
35. J. Li, M. Huo, J. Wang, J. Zhou, J. M. Mohammad, Y. Zhang, Q. Zhu, A. Y. Waddad and Q. Zhang, *Biomaterials*, 2012, **33**, 2310.
36. Y. Sun, X. L. Yan, T. M. Yuan, J. Liang, Y. J. Fan, Z. W. Gu and X. D. Zhang, *Biomaterials*, 2010, **31**, 7124.
37. H. Fan, J. Huang, Y. Li, J. Yu and J. Chen, *Polymer*, 2010, **51**, 5107.
38. J. Liu, W. Huang, Y. Pang, P. Huang, X. Zhu, Y. Zhou and D. Yan, *Angew. Chem. Int. Ed.*, 2011, **50**, 9162.
39. J. Liu, Y. Pang, W. Huang, Z. Zhu, X. Zhu, Y. Zhou and D. Yan, *Biomacromolecules*, 2011, **12**, 2407.
40. J. H. Ryu, R. Roy, J. Ventura and S. Thayumanavan, *Langmuir*, 2010, **26**, 7086.
41. P. Sun, D. Zhou and Z. Gan, *J. Control. Release*, 2011, **155**, 96.
42. N. Ma, Y. Li, H. P. Xu, Z. Q. Wang and X. Zhang, *J. Am. Chem. Soc.*, 2010, **132**, 442.
43. H. Ren, Y. Wu, N. Ma, H. Xu and X. Zhang, *Soft Matter*, 2012, **8**, 1460.
44. Y. H. Bae and H. Q. Yin, *J. Control. Release*, 2008, **131**, 2.
45. R. K. O'Reilly, C. J. Hawker and K. L. Wooley, *Chem. Soc. Rev.*, 2006, **35**, 1068.
46. J. O. Kim, G. Sahay, A. V. Kabanov and T. K. Bronich, *Biomacromolecules*, 2010, **11**, 919.
47. L. Zhang, W. G. Liu, L. Lin, D. Y. Chen and M. H. Stenzel, *Biomacromolecules*, 2008, **9**, 3321.
48. J. Y. Zhang, X. Jiang, Y. F. Zhang, Y. T. Li and S. Y. Liu, *Macromolecules*, 2007, **40**, 9125.
49. X. Z. Jiang, S. Y. Liu and R. Narain, *Langmuir*, 2009, **25**, 13344.
50. Y. Li, K. Xiao, J. Luo, W. Xiao, J. S. Lee, A. M. Gonik, J. Kato, T. A. Dong and K. S. Lam, *Biomaterials*, 2011, **32**, 6633.
51. Z. F. Jia, L. J. Wong, T. P. Davis and V. Bulmus, *Biomacromolecules*, 2008, **9**, 3106.
52. M. J. Heffernan and N. Murthy, *Ann. Biomed. Eng.*, 2009, **37**, 1993.
53. A. N. Koo, H. J. Lee, S. E. Kim, J. H. Chang, C. Park, C. Kim, J. H. Park and S. C. Lee, *Chem. Commun.*, 2008, 6570.
54. Y. C. Wang, Y. Li, T. M. Sun, M. H. Xiong, J. A. Wu, Y. Y. Yang and J. Wang, *Macromol. Rapid Comm.*, 2010, **31**, 1201.
55. Y. M. Xu, F. H. Meng, R. Cheng and Z. Y. Zhong, *Macromol. Biosci.*, 2009, **9**, 1254.
56. J. E. Kim, E. J. Cha and C. H. Ahn, *Macromol. Chem. Phys.*, 2010, **211**, 956.
57. S. Y. Zhang and Y. Zhao, *J. Am. Chem. Soc.*, 2010, **132**, 10642.
58. X. W. Xu, A. E. Smith and C. L. McCormick, *Aust. J. Chem.*, 2009, **62**, 1520.
59. D. E. Discher and F. Ahmed, *Annu. Rev. Biomed. Eng.*, 2006, **8**, 323.

60. C. LoPresti, H. Lomas, M. Massignani, T. Smart and G. Battaglia, *J. Mater. Chem.*, 2009, **19**, 3576.
61. F. Meng and Z. Zhong, *J. Phys. Chem. Lett.*, 2011, **2**, 1533.
62. M. H. Li and P. Keller, *Soft Matter*, 2009, **5**, 927.
63. D. A. Christian, S. Cai, D. M. Bowen, Y. Kim, J. D. Pajerowski and D. E. Discher, *Eur. J. Pharm. Biopharm.*, 2009, **71**, 463.
64. G. J. Liu, S. B. Ma, S. K. Li, R. Cheng, F. H. Meng, H. Y. Liu and Z. Y. Zhong, *Biomaterials*, 2010, **31**, 7575.
65. H. F. Xu, F. H. Meng and Z. Y. Zhong, *J. Mater. Chem.*, 2009, **19**, 4183.
66. R. Cheng, F. Meng, S. Ma, H. Xu, H. Liu, X. Jing and Z. Zhong, *J. Mater. Chem.*, 2011, **21**, 19013.
67. J. Zhang, L. Wu, F. Meng, Z. Wang, C. Deng, H. Liu and Z. Zhong, *Langmuir*, 2012, **28**, 2056.
68. A. J. van Hell, D. J. A. Crommelin, W. E. Hennink and E. Mastrobattista, *Pharm. Res.*, 2009, **26**, 2186.
69. A. J. van Hell, M. M. Fretz, D. J. A. Crommelin, W. E. Hennink and E. Mastrobattista, *J. Control. Release*, 2010, **141**, 347.
70. K. M. Park, D. W. Lee, B. Sarkar, H. Jung, J. Kim, Y. H. Ko, K. E. Lee, H. Jeon and K. Kim, *Small*, 2010, **6**, 1430.
71. J. Panyam and V. Labhasetwar, *Adv. Drug Deliver. Rev.*, 2003, **55**, 329.
72. K. S. Soppimath, T. M. Aminabhavi, A. R. Kulkarni and W. E. Rudzinski, *J. Control. Release*, 2001, **70**, 1.
73. Y. L. Li, L. Zhu, Z. Z. Liu, R. Cheng, F. H. Meng, J. H. Cui, S. J. Ji and Z. Y. Zhong, *Angew. Chem. Int. Ed.*, 2009, **48**, 9914.
74. L. H. Li, X. L. Jiang and R. X. Zhuo, *J. Polym. Sci. Pol. Chem.*, 2009, **47**, 5989.
75. Z. Jia, J. Liu, C. Boyer, T. P. Davis and V. Bulmus, *Biomacromolecules*, 2009, **10**, 3253.
76. R. J. Verheul, S. van der Wal and W. E. Hennink, *Biomacromolecules*, 2010, **11**, 1965.
77. R. Liu, X. Zhao, T. Wu and P. Y. Feng, *J. Am. Chem. Soc.*, 2008, **130**, 14418.
78. R. Liu, Y. Zhang and P. Y. Feng, *J. Am. Chem. Soc.*, 2009, **131**, 15128.
79. R. Mortera, J. Vivero-Escoto, I. I. Slowing, E. Garrone, B. Onida and V. S. Y. Lin, *Chem. Commun.*, 2009, 3219.
80. A. M. Sauer, A. Schlossbauer, N. Ruthardt, V. Cauda, T. Bein and C. Brauchle, *Nano Lett.*, 2010, **10**, 3684.
81. B. G. De Geest, N. N. Sanders, G. B. Sukhorukov, J. Demeester and S. C. De Smedt, *Chem. Soc. Rev.*, 2007, **36**, 636.
82. G. B. Sukhorukov, A. L. Rogach, B. Zebli, T. Liedl, A. G. Skirtach, K. Kohler, A. A. Antipov, N. Gaponik, A. S. Susha, M. Winterhalter and W. J. Parak, *Small*, 2005, **1**, 194.
83. A. P. R. Johnston, C. Cortez, A. S. Angelatos and F. Caruso, *Curr. Opin. Colloid Interface Sci.*, 2006, **11**, 203.
84. A. N. Zelikin, J. F. Quinn and F. Caruso, *Biomacromolecules*, 2006, **7**, 27.
85. A. N. Zelikin, Q. Li and F. Caruso, *Chem. Mater.*, 2008, **20**, 2655.

86. S. F. Chong, A. Sexton, R. De Rose, S. J. Kent, A. N. Zelikin and F. Caruso, *Biomaterials*, 2009, **30**, 5178.
87. R. De Rose, A. N. Zelikin, A. P. R. Johnston, A. Sexton, S. F. Chong, C. Cortez, W. Mulholl, F. Caruso and S. J. Kent, *Adv. Mater.*, 2008, **20**, 4698.
88. A. Sexton, P. G. Whitney, S. F. Chong, A. N. Zelikin, A. P. R. Johnston, R. De Rose, A. G. Brooks, F. Caruso and S. J. Kent, *ACS Nano*, 2009, **3**, 3391.
89. S. Sivakumar, V. Bansal, C. Cortez, S. F. Chong, A. N. Zelikin and F. Caruso, *Adv. Mater.*, 2009, **21**, 1820.
90. Y. Yan, A. P. R. Johnston, S. J. Dodds, M. M. J. Kamphuis, C. Ferguson, R. G. Parton, E. C. Nice, J. K. Heath and F. Caruso, *ACS Nano*, 2010, **4**, 2928.
91. S. F. Chong, R. Chandrawati, B. Stadler, J. Park, J. H. Cho, Y. J. Wang, Z. F. Jia, V. Bulmus, T. P. Davis, A. N. Zelikin and F. Caruso, *Small*, 2009, **5**, 2601.
92. K. Liang, G. K. Such, Z. Zhu, Y. Yan, H. Lomas and F. Caruso, *Adv. Mater.*, 2011, **23**, H273.
93. E. Kim, D. Kim, H. Jung, J. Lee, S. Paul, N. Selvapalam, Y. Yang, N. Lim, C. G. Park and K. Kim, *Angew. Chem. Int. Ed.*, 2010, **49**, 4405.
94. S. Shu, X. Zhang, Z. Wu, Z. Wang and C. Li, *Biomaterials*, 2010, **31**, 6039.
95. J. K. Oh, R. Drumright, D. J. Siegwart and K. Matyjaszewski, *Prog. Polym. Sci.*, 2008, **33**, 448.
96. A. V. Kabanov and S. V. Vinogradov, *Angew. Chem. Int. Ed.*, 2009, **48**, 5418.
97. J. K. Oh, C. B. Tang, H. F. Gao, N. V. Tsarevsky and K. Matyjaszewski, *J. Am. Chem. Soc.*, 2006, **128**, 5578.
98. J. K. Oh, S. A. Bencherif and K. Matyjaszewski, *Polymer*, 2009, **50**, 4407.
99. J. K. Oh, D. J. Siegwart and K. Matyjaszewski, *Biomacromolecules*, 2007, **8**, 3326.
100. J. K. Oh, D. J. Siegwart, H. I. Lee, G. Sherwood, L. Peteanu, J. O. Hollinger, K. Kataoka and K. Matyjaszewski, *J. Am. Chem. Soc.*, 2007, **129**, 5939.
101. H. P. Yap, A. P. R. Johnston, G. K. Such, Y. Yan and F. Caruso, *Adv. Mater.*, 2009, **21**, 4348.
102. J. Groll, S. Singh, K. Albrecht and M. Moeller, *J. Polym. Sci. Pol. Chem.*, 2009, **47**, 5543.
103. Z. Y. Qiao, R. Zhang, F. S. Du, D. H. Liang and Z. C. Li, *J. Control. Release*, 2011, **152**, 57.

CHAPTER 9

Enzyme-responsive Drug-delivery Systems

PIER-FRANCESCO CAPONI AND REIN V. ULIJN*

WestCHEM/Department of Pure and Applied Chemistry, The University of Strathclyde, Glasgow, G1 1XL, Scotland, UK
*Email: rein.ulijn@strath.ac.uk

9.1 Introduction

Enzyme-responsive materials (ERMs) are gaining increasing attention as a way to pursue the "magic bullet",[1] conceived more than 100 years ago by Paul Ehrlich, who discovered the first cure against syphilis and was awarded the Nobel Prize in 1908. Initially, this concept relied on the ability to target only (micro-)organisms that participate in or cause a disease, without affecting the host. Nowadays the initial idea has evolved into the need to target certain kinds of tissues, *e.g.* tumors, whilst leaving healthy tissue unaffected. Thanks to progress in crystallization techniques, molecular modeling and protein engineering, a number of classes of enzymes has been discovered to play crucial roles in human body biochemistry and it is known that their disregulation, namely hypo-/hyperexpression, can lead to the development of a range of disease states (Table 9.1). These findings make enzymes useful as markers for diagnosis and highly suitable targets to achieve a selective, effective and localized drug delivery release. Signal amplification is an important and unique property achievable by exploiting enzymatic catalysis, where each enzyme molecule can turn over many substrate molecules (typically $10^6\,\mathrm{min}^{-1}$). ERMs are based on the fact that enzymes can trigger the turnover of a large number of incorporated substrate molecules, which lead to macroscopic change in

RSC Smart Materials No. 2
Smart Materials for Drug Delivery: Volume 1
Edited by Carmen Alvarez-Lorenzo and Angel Concheiro
© The Royal Society of Chemistry 2013
Published by the Royal Society of Chemistry, www.rsc.org

Table 9.1 Examples of diseases that can be generated or detected by disregulation of enzyme activity.

Enzyme name	*Family*	*Role*	*Linked diseases*	*Enzyme malfunction*	*Ref.*
Urokinase	Serine-protease	Participation in thrombolysis and extra-cellular matrix degradation	Vascular diseases, cancer malignity	Anomalous activation	6
Prostatic cancer specific antigen (kallikrein-3)	Serine-protease	Sperm liquefaction	Prostate cancer	Hyperexpression	7
Deubiquitase	Protease	Protein degradation/ trafficking /localization	Tumors, cancers	Enzyme mutation	8
Plasmodium falciparum amidase (PfA-M1)	Amino-peptidase	Hemoglobin digestion	Malaria	Expression by bacteria	9
Nox	Oxidase	Signal transduction, immune functions, hormone biosynthesis	Genome damages, apoptosis	Overexpression	10
Protein kinase	Phospho-transferase	Cell signaling, signal transduction	Alzheimer's syndrome, tumors, cancers	Antagonistic disregulation, hyperexpression	11
Acid lipase	Esterase	Fatty acids metabolism	Fatty liver, Wolman disease	Deficiency	12
Phosphatases	Esterase	Cell signaling, signal transduction, bone formation	Alzheimer's syndrome, tumors, cancers, osteoporosis	Antagonistic disregulation	12,13

physical/chemical properties of the system. It is then no surprise that enzymatic mechanisms are attractive in the field of stimuli-responsive controlled release and a number of approaches have been developed over the last decades.

9.1.1 Exploiting Enzymes in Drug Delivery

The body of literature on exploitation of enzymes in drug delivery is quite large and in the last decade an increase in research activity on ERMs has occurred. Below, other areas where enzymes have been exploited or targeted are briefly discussed and then compared with the ERM approach.

9.1.1.1 Enzyme Inhibitors

In order to target selectively a malfunctioning or harmfully overexpressed enzyme, the most direct and intuitive approach is to synthesize drug molecules that are able to bind and inhibit a specific enzyme (*i.e.* synthetic enzyme inhibitors). For example, kinases are known to be overexpressed and to play a crucial role in the development of tumors. Many examples of kinase inhibitors can be found in drug treatments that have been recently commercialized. For example, imatinib mesylate (Gleevec®) and dasatinib (Sprycel®) are Abelson cytoplasmic tyrosine (ABL) kinase inhibitors and are approved by the Food and Drug Administration (FDA) for use against certain kinds of tumors and leukemia. Studies are currently ongoing to use these drugs in various other malignancies.[2]

Another well-known condition that benefits from the efficacy of targeting enzymes using synthetic inhibitors is acquired immune deficiency syndrome (AIDS). Since the human immunodeficiency virus (HIV) was reported at the beginning of the 1980s,[3] no cure has shown good efficacy until HIV protease inhibitors were discovered and used to treat AIDS in the mid 1990s.[4] The mode of action of this class of drugs is focused on prevention of the correct production of viral proteins that are responsible for the spread of the infection to new cells. These therapies have significantly contributed to increasing the life expectancy and quality of patients.[5] One drawback of this very effective approach is related to the toxicology profiles and pharmacokinetics of new drugs and the long clinical trials that the new molecules have to pass before being approved.

9.1.1.2 Prodrugs

An alternative approach that exploits the functionality of enzymes is the concept of prodrug. A prodrug consists of a drug molecule that is modified with a moiety that makes it inactive. When the moiety is cleaved upon enzymatic catalysis, the pharmaceutical activity of the molecule is restored in the vicinity of the enzyme expression site. This approach is very useful to improve relevant features of already existing drugs (*e.g.* pharmacokinetics, bioavailability), but implicates the chemical modification of the drug molecule. Many prodrugs are currently used, and examples can be found in the excellent review by Rautio *et al.*[14] One example of enzyme triggered prodrug to target cancer tissues reported in 1999[15] is currently undergoing clinical trials.[16] The investigators synthesized an *N*-(2-hydroxypropyl) methacrylamide copolymer and coupled doxorubicin to it *via* a peptide linker. The polymer is internalized by pinocytosis and the peptide linker is cleaved by lysozymes, releasing the drug. In the case of drug–polymer conjugates, the polymer component has an important effect on the properties and the characteristics of the whole delivery system. Most biological applications involve the use of poly(ethylene glycol), PEG, due to its high biocompatibility. However, PEG is suspected to cause complement activation. Alternatives, such as poly(acrylamide) or poly(amino acids), are available and new bio-compatible polymers are under study. The interested reader is referred to an excellent review that has been recently published regarding PEG and other polymers suitable for drug-delivery purposes.[17]

A more sophisticated prodrug approach that is worth mentioning is the so-called antibody directed enzyme prodrug therapy, which is used to increase drug selectivity against tumors. In this approach, monoclonal antibodies for specific tumor receptors are linked to enzymes, *e.g.* carboxypeptidase.[18] The concentration of antibodies is considerably higher in tumor tissues compared to healthy tissues. Thus, if a prodrug is injected, it will be activated by the enzymes achieving cytotoxicity only against tumor cells.[19] This two-step strategy has proven to be effective and is currently undergoing clinical trials. However, it also shows limitations such as the antigenicity of monoclonal antibodies and the difficult control of the concentration and the pharmacokinetics of the drug in the body. Similar techniques have been developed using different carriers to achieve selectivity, such as viral-/gene-directed enzyme prodrug therapy[20] or polymer directed enzyme prodrug.[21]

9.1.1.3 Enzyme-Responsive Materials

The ERM approach is based on responsive polymers that act as carriers able to release the payload only upon the catalytic action of enzymes. An ERM can be defined as a system that undergoes macroscopic changes of physical/chemical properties upon the catalytic action of an enzyme. The response mechanism of ERMs requires, at least, an enzyme sensitive component, that usually is a substrate or a substrate mimic of the enzyme, and a second component that is responsible for changes in the interactions inside the material that can lead to macroscopic transitions. This strategy does not always require modifications of existing drugs, as they can be not chemically but physically entrapped, and it may potentially lower the toxicity of current treatments. Changes in the properties of an ERM can be due to either i) alterations of covalent bonds as occurs, for example, in chemically cross-linked hydrogels or ii) modifications in the balance of combined weak bonds, as in supramolecular assemblies, which involves electrostatic, hydrophobic, steric or π-π interactions, van der Waals forces or hydrogen bonding. Although no clinical trials with ERMs are

Table 9.2 Main advantages (✓) and drawbacks (✗) of some enzyme-related drug-delivery systems. Enzyme inhibitors and prodrugs may show some limitations that can be overcome with ERMs.

	System characteristics			
Functioning mode	*Selectivity*	*Drug biocompatibility*	*Controlled release*	*Amplification*
Enzyme inhibitor	✓	✗	✗	✗
Prodrug	✓	✓	✗	✗
ERM	✓	✓	✓	✓

ongoing yet, there are currently large efforts in developing ERMs useful for drug-delivery applications. In Table 9.2 the main advantages and drawbacks of the different enzyme-related drug-delivery approaches are summarized.

9.1.2 Factors to Consider in the Design of ERMs for Drug Delivery

9.1.2.1 Particle Size

Depending on the enzyme localization, two classes of targets for ERM can be defined: i) extra-cellular enzymes, *i.e.* enzymes that are expressed on cell surface or secreted by target cells; ii) intra-cellular enzymes, *i.e.* enzymes that are not secreted and are only present inside cells. In the first case, the size of the system is not a primary concern but, in the second one, the ERM should have suitable characteristics to allow it to enter into the cells. It is not only the size that matters, but also the shape, the surface chemistry and the overall charge have to be taken into account, particularly if the cellular uptake involves channel proteins or charged pores.[22,23]

Particle size is of capital importance to achieve intravenous (i.v.) delivery to a target. One of the most used mechanisms to achieve passive targeting to tumor tissues is related to the so-called enhanced permeation and retention (EPR) effect.[24] This phenomenon relies on the lack of organization of cancer cells that makes the pores on the blood vessels less tight, allowing bulkier particles to pass through. Moreover, tumoral tissues have a poor lymphatic system, which does not drain efficiently, permitting accumulation of polymer-conjugated drugs. A comprehensive analysis of the relationship between particle size and accumulation in tumor tissue has been recently reported.[25] Furthermore, to avoid a rapid clearance after i.v. administration, the size of the drug carrier should be higher than the renal threshold, which is around 10 nm, but smaller than 100 nm to avoid liver capture. Moreover, since carriers with a particle size less than 100 nm can be enclosed into endocytes, it is clear that the preferable size is between 10 and 100 nm.[26]

Oral and subcutaneous or intra-muscular administration can also be considered. When orally intended, the enzyme-sensitive part of the ERM must be protected from the harsh conditions in the gastro-intestinal tract. For such purpose, pH-responsive polymers that protect the payload from the acid pH of

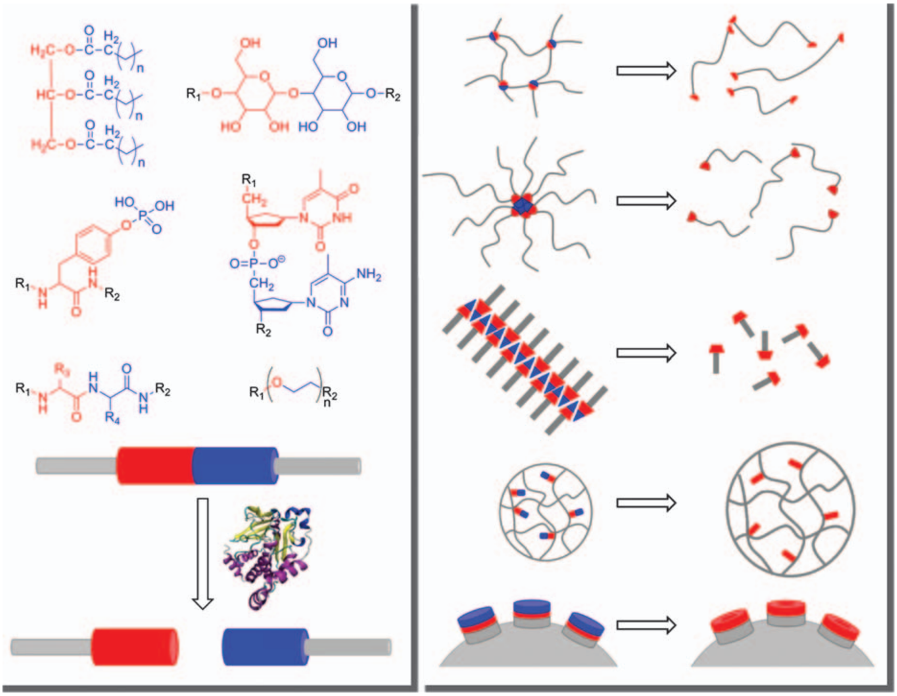

Figure 9.1 Schematic description of the enzyme-sensitive part of ERMs and examples of molecules that are used as enzyme substrates (left) and examples of enzyme-responsive systems useful for drug delivery (right). From top to bottom: degradable hydrogel, disruptive micelle, supramolecular hydrogel, triggered swelling hydrogel and silica nanocontainer.

the stomach, but can expose the enzyme-responsive part to the luminal content of the gut, are particularly suitable. On the other hand, depot systems that are slowly degraded under *in vivo* conditions provide sustained drug release from a single application and for a long time.

Different approaches to selectively target enzymes through ERM will be treated in the next sections. According to the physical and chemical properties of the delivery system, the ERMs are categorized into three groups: hydrogels, micelles and nanocontainers (Figure 9.1).

9.2 Enzyme-responsive Hydrogels

One of the first to recognize the unique properties of gels was Thomas Graham in 1861, a Scottish chemist who is considered the pioneer of studies on colloids.[27] Gels are elastic, three-dimensional structures, constituted of two phases: a network of molecules that defines the properties of the backbone and a liquid phase that is trapped inside it. When the liquid is water, they are commonly named hydrogels; the Greek prefix *hydro*- indicates their high content in water (up to 99% w/w). The nature of the building blocks that constitute the network and the presence of hydrophobic/polar functional groups greatly influences the properties of the gel, particularly the amount of water that the hydrogel can incorporate.[28] Hydrogels can be formed either by chemical cross-linking of polymerizable monomers (*chemical hydrogels*) or by molecules that self-assemble through non-covalent interactions (*physical hydrogels*).[29] Both types can be tailored in order to achieve a number of different particle sizes, from nanometer to centimeter, and potentially administered through a variety of routes, such as i.v. or intra-muscular.

Hydrogels are highly suitable for drug-delivery applications due to some advantageous features: i) a wide range of molecules can be used to form hydrogels, from polymers to naturally occurring building blocks; ii) they provide a semi-wet environment, ideal for biological interactions; iii) they allow small molecules to diffuse freely, while larger (macro)molecules are restricted in mobility; and iv) they can be designed to change physical properties, resulting in swelling or dissolution, in response to certain stimuli.[30]

Although it does not fulfill the definition of ERM (in fact, this system does not respond directly to the catalytic action of enzymes, but to glucose concentration), a pioneering system that combines the versatility of enzymes with the responsiveness of hydrogels was developed by Kost and coworkers to control the release of insulin as a function of glucose concentration.[31] Glucose oxidase (GOx), catalase and insulin were trapped inside both cross-linked and non-cross-linked poly(2-hydroxyethylmethacrylate-co-*N*,*N*-dimethylaminoethyl methacrylate) hydrogels. Simulating *in vivo* conditions, GOxs converted the glucose that diffused into the hydrogels in gluconic acid, causing the swelling and the consequent release of insulin. Catalases were included to provide oxygen to the oxidation reaction. It was found that the release rate of insulin was glucose-concentration dependent, and that the non-cross-linked hydrogels provided better release profiles. This concept, first reported in 1985,[32] is still actively researched today.[33]

9.2.1 Chemically Cross-linked Hydrogels

Many strategies have been reported to achieve chemical cross-linking, among which radical polymerization, high-energy irradiation and chemical reaction with complementary groups are quite common.[34] Also enzymatic methods have been used to create covalently cross-linked hydrogels.[35]

9.2.1.1 Degradable Hydrogels

There are many examples of enzymatic-degradable hydrogels in literature. Most of them involve the use of natural molecules, such as polysaccharides and polypeptides, either on their own or in combination with biocompatible synthetic polymers, such as PEG. These hydrogels are designed to degrade only in the presence of specific enzymes, making them suitable for controlled release purposes (Figure 9.2).

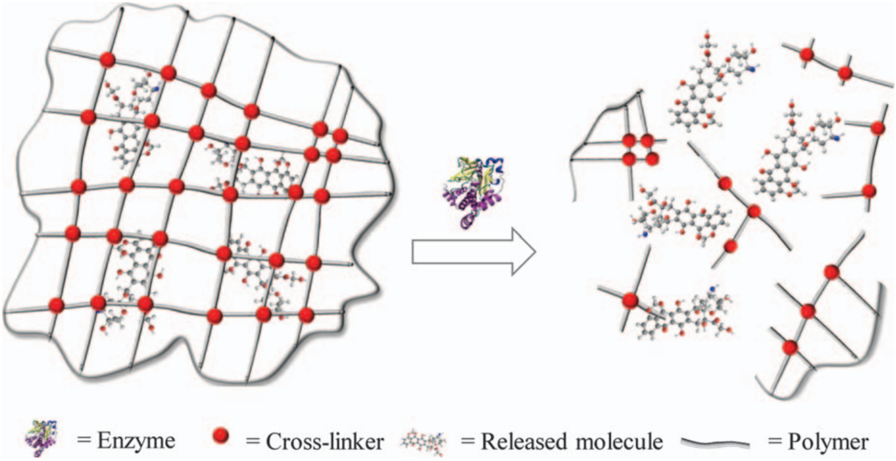

Figure 9.2 Schematic representation of a hydrogel with cross-linkers designed to behave as enzymatically degradable substrates. Upon cleavage of the substrate the hydrogel degrades, leading to the release of the payload.

Table 9.3 Composition and enzyme-responsiveness of some degradable hydrogels described in Section 9.2.1.1.

	Polymer	*Cross-linker*	*Enzyme*	*Released molecule*
1	Acrylate derivative[36,37]	Azo linker[36]	Oxidoreductase[36]	Drugs[36,37]
2	Dextran[38]	Dextran[37]	Transferase[37]	Fluorophore[38]
3	PEG[39]	Peptide[38,39]	Hydrolase[38,39]	Protein[39]

A system designed for site-specific drug release in the colon was reported in 1995 by Shantha *et al.*[36] The hydrogel contained azoaromatic moieties as cross-linking agents that stabilize the gel, avoiding its degradation by acidic pH of the stomach. These gels are easily degraded by azoreductases produced by the microbial flora of the large intestine, *via* reduction of azo-compounds in the presence of NADPH. In this way, after degradation of the azoaromatic moieties, the pH-responsive hydrogel is able to swell in the neutral-alkaline conditions of the colon, leading to the release of the drug (Table 9.3, Entry 1).

Also for colon-targeted drug delivery, Kim and Oh[37] used a dextran-based polymer cross-linked with acrylic acid, to obtain a dextranase/pH degradable hydrogel. Dextranases are naturally occurring enzymes in the colon that hydrolyze dextran to smaller oligosaccharides. As a model payload, the anti-inflammatory drug 5-aminosalicylic acid was used. Under *in vitro* simulated colon conditions, an increase in 5-aminosalicylic acid release rate was recorded when the hydrogels were exposed to the enzyme and the cleavage of the α-1,6 dextran bonds led to the swelling and degradation of the hydrogels (Table 9.3, Entries 1 and 2). Lévesque and Soichet[38] reported on a dextran-based hydrogel with a backbone functionalized with *p*-maleimidophenyl isocyanate to avoid the presence of hydrolysable esters. The system was cross-linked with a modified peptide sequence, which is a substrate for the matrix metalloproteinase 2 gelatinase A (MMP-2), an enzyme overexpressed in some disease conditions, such as arthritis, osteolysis and metastasis. This hydrogel was stable under physiological conditions but degraded, releasing the payload molecules, upon the action of MMP-2 (Table 9.3, Entries 2 and 3).

PEG-based hydrogels cross-linked by thiolene photopolymerization of a peptidic enzyme substrate were developed by Anseth and coworkers.[39] The peptide sequence was selectively cleaved by human neutrophil elastase (HNE), a protease that is expressed in inflammation sites. The rate of hydrogel degradation can be tailored by adjusting the peptide substrate, the peptide reaction constant and the concentration of HNE. Indeed, the payload, albumin bovine serum and carbonic anhydrase, was released at different rates depending on the hydrogel composition and on the kinetics of the enzymatic cleavage (Table 9.3, Entry 3).

9.2.1.2 Triggered Swelling Hydrogels

An alternative strategy to obtain an enzyme-responsive cross-linked hydrogel is to anchor pendant enzyme-sensitive moieties. In this way, the starting polymeric structure stays intact, and the macroscopic transition is expressed as a swelling/change of the material. Chemically cross-linked polyethylene glycol acrylamide (PEGA) hydrogels have been designed by Thornton *et al.* to allow different levels of accessibility to three proteases that differ in substrate selectivity.[40] The hydrogels were functionalized with peptidic sequences, made of zwitterionic peptides flanked by oppositely charged amino acids that have a high affinity only for one kind of protease. After the enzymatic cleavage of the sequence, the hydrogel swelled due to the specific interaction of the target enzyme with the peptide sequence and the removal of anionic aspartic acid groups. Fluorescently labeled dextran and avidin were used as payload in order to monitor the diffusion and the release profiles upon swelling. This system was further developed by functionalizing PEGA hydrogels with peptide sequences that, after enzymatic cleavage, provided the beads with a different overall charge.[41] Using this approach, it was possible selectively to release oppositely charged proteins, such as albumin and avidin, taken advantage of the electrostatic repulsion between the payload and the hydrogel. This example shows that the release mechanism may be matched to the properties of the payload. An optimization of this system was possible by increasing the charge density of the pendant amino acid sequences attached to the polymer, adding zwitterionic branched peptide actuators.[42] In this way, a controlled release of the payload was obtained upon the catalytic activity of proteases on micro-sized hydrogel particles under physiological conditions; the increased overall charge allowed the beads not to be affected by salt concentration in solution. This system enables the loading of a model drug taking benefit of pH-responsive swelling of the hydrogel and the release only upon the action of a specific enzyme. However, it should be noted that a more biocompatible matrix would be required for translation to therapeutics.

Another interesting example in which enzyme substrates are exploited to achieve specificity for drug delivery was reported by Tauro *et al.*[43] A cross-linked poly(ethylene glycol) diacrylate was functionalized with pendant peptide sequences that are substrate for matrix metalloproteases (MMPs). Platinum, a well-known chemotherapy agent, was complexated with the Lys[†]-containing peptide. The release of platinum was influenced by the peptide sequence chosen as substrate of MMP; the higher the peptide-MMP affinity, the faster the release was. Moreover, *in vitro* experiments on a malignant glioma cell line showed significant decrease of cellular proliferation in the presence of the platinum-containing hydrogels and MMPs. Differently from the systems reported above, the performance of these hydrogels does not rely on the polymer swelling to trigger the drug release. Instead, the platinum ions are held in place forming complexes with the charged Lys residues, which are cleaved by the enzyme, releasing the payload.

9.2.1.3 Supramolecular Hydrogels

Supramolecular assemblies consist of molecules that are held together by non-covalent links, such as electrostatic interactions, hydrogen bonds, π-stacking, van der Waals forces, hydrophobic interactions or combinations thereof, in aqueous or organic media.[44] In the last decade a strong interest in the possibility of using enzymes to trigger supramolecular assembly/disassembly has been raised.

A common strategy to form a supramolecular hydrogel consists of modifying a drug molecule with a precursor of a hydrogelator functionalized with an enzyme-sensitive trigger. For example, the analgesic and antipyretic drug acetaminophen (paracetamol) was covalently linked to a fatty acid through a lipase cleavable linker.[45] Enzyme addition after gelation led to cleavage of ester linker and to drug release. Curcumin, a hydrophobic drug, was also incorporated in the hydrogel network to be released under the same conditions as acetaminophen, creating a multi-drug release system (Table 9.4, Entry 1). This technique can be adapted to incorporate a drug into the hydrophobic core of hydrogel fibers.[46] A low molecular weight hydrogelator, amygdalin (a glycoside present in Nature), was synthesized exploiting enzyme catalysis. Under physiological conditions, lipases triggered the fibre disassembly and the release of curcumin (Table 9.4, Entry 2).

A two-stage release system, triggered by enzyme and pH, has been reported by Van Bommel *et al.*[47] 6-Aminoquinoline (AQ) was incorporated through an enzyme cleavable linker, Phe, into a cyclohexane trisamide scaffold functionalized with two ethylene glycol units. The linker was not accessible for the enzyme when the hydrogel was in the assembled state. In response to a pH or

---

[†] All the amino acids will be referred to using the following three-letter codes: Alanine (Ala); Arginine (Arg); Asparagine (Asn); Aspartic acid (Asp); Cysteine (Cys); Glutamic acid (Glu); Glycine (Gly); Histidine (His); Isoleucine (Ile); Leucine (Leu); Lysine (Lys); Methionine (Met); Phenylalanine (Phe); Proline (Pro); Serine (Ser); Threonine (Thr); Tyrosine (Tyr); Valine (Val).

Table 9.4 Composition and enzyme-responsiveness of some supramolecular hydrogels described in Section 9.2.1.3.

	Starting material	*Enzyme-sensitive component*	*Enzyme*	*Response*	*Ref.*
1	Apn[a]-O-[C]$_n$	Apn-O∼C	Lipase	Gel-to-sol, release of Apn and curcumin	45
2	Amygdalin-O-[C]$_n$	Amygdalin-O∼C	Lipase	Gel-to-sol, release of curcumin	46
3	G[a]-Phe-AQ	G∼Phe∼AQ	α-chymotrypsin	Gel-to-sol, release of AQ	47
4	Taxol-(Phe)$_2$-Lys-*p*Tyr	*p*Tyr	Phosphatase	Sol-to-gel, diffusion of taxol	48
5	Fmoc-*p*Tyr	*p*Tyr	Phosphatase	Sol-to-gel	51
6	Fmoc-Phe-*p*Tyr	*p*Tyr	Phosphatase	Micelles to fibers	52
7	(Phe)$_4$-Cys-Gly-Leu-(Asp)$_2$	Gly∼Leu	Matrix Metallo Protease-9	Sol-to-gel	53
8	Naph-(Phe)$_2$-Gly-Glu-Tyr	Tyr/*p*Tyr	Kinase/Phosphatase	Gel-to-sol/ sol-to-gel	54
9	Lys-(Arg)$_2$-Ala-Ser-Val-Ala-Gly-Lys-[C$_{12}$](NH$_2$)	Ser/*p*Ser	Kinase/Phosphatase	Gel-to-sol/sol-to-gel, release of doxorubicin	55
10	Fmoc-Tyr-Leu-OMe	O∼Me	Subtilisin	Sol-to-gel	56

[a] Apn = Acetaminophen, G = gelling scaffold

temperature change, the gel fibers dissociated into individual molecules that were cleaved by α-chymotrypsin, resulting in the release of the loaded drug (Table 9.4, Entry 3). Gao *et al.*[48] designed a hydrogel precursor based on taxol, a well-established antineoplastic agent. Drug molecules were covalently linked to a peptide motif (naphthalene-Phe-Phe-Lys) that can self-assemble, and a group (phosphorylated tyrosine; *p*Tyr) that is cleavable by an enzyme. Upon the action of phosphatases, the phosphate group was removed and the precursor transformed into the hydrogelator, which self-assembled leading to the formation of a nanofibrous gel. The taxol-functionalized gel fibers preserved the therapeutic efficiency of the drug. Dephosphorylation/phosphorylation may be a powerful stimulus to control self-assembly by means of the changes in the electrostatic interactions that occur when the anionic phosphate groups are removed or added (Table 9.4, Entry 4). The latter two systems can be considered as prodrug/ERM combinations. An alternative strategy to the direct incorporation of drugs within the gelator system, which partially applies to the example just described, is to use peptides building blocks to obtain supramolecular hydrogels. Peptide-based hydrogels (PBH) have recently generated great interest for applications in the drug-delivery field, *e.g.* injectable implants for subcutaneous and intra-ocular sustained release.[49,50] The main advantage of using peptides is that they are natural building blocks and hence inherently biocompatible, an essential aspect for biological applications. A number of ERMs based on PBH have been developed, although to the best of our knowledge only one example of enzyme-triggered drug release from PBH has been reported to date. Some of these ERMs are summarized below.

In a pioneering work on PBH published in 2004, Xu and coworkers[51] reported how enzymes can trigger the formation of gels starting from simple building blocks, such as *N*-(fluorenylmethyloxycarbonyl) (Fmoc) amino acids. This concept has been further developed by a number of research groups (Table 9.4, Entry 5). Sadownik *et al.*[52] reported on micelle (see Section 9.3) to fiber transition upon enzymatic dephosphorylation of Fmoc-Phe-*p*Tyr (Table 9.4, Entry 6). This approach may serve to transform, upon catalysis in the presence of overexpressed enzymes, micelles with drug molecules loaded in the hydrophobic cores into gels around a target area, for isolation of the damaged cells and controlled release of the payload. However, this concept remains to be tested for its suitability under *in vivo* conditions. The strategy of selective isolation of the target area, *e.g.* cancer tissue, surrounding it with a hydrogel was previously reported by Yang *et al.*[53] using another enzyme. They designed a nonapeptide amphiphile to be a substrate for MMP. After enzymatic reaction, the peptide was cleaved in the expected position. Then, the self-assembly motif led to hydrogelation due to interactions driven by the four repeating Phe units (Table 9.4, Entry 7).

Reversibility is also achievable using enzymes. Kinases and phosphatases are ideal enzymes to create reversible systems, due to their antagonistic behavior and biological relevance (Table 9.1). To achieve phosphorylation with kinase, adenosine-5′-triphosphate (ATP) must be present in the medium, because it is the source of phosphate that the enzyme uses to phosphorylate amino acids. ATP can be seen as the "fuel" that drives the reaction having both the enzymes present. Xu and coworkers[54] studied a pentapeptidic hydrogelator (naphthalene-Phe-Phe-Gly-Glu-Tyr) and observed a gel-sol transition when kinases and ATP were added to the hydrogel; the phosphorylation of Tyr residues led to a more hydrophilic molecule. Reversibly, adding phosphatases the Tyr residues became dephosphorylated and the gel was restored. Importantly, they succeeded in testing this system *in vivo* in a mouse model, suggesting new applications for the engineering of biomaterials useful in drug delivery (Table 9.4, Entry 8). Very recently, a similar approach has been reported by Stupp and coworkers.[55] Using the same antagonistic enzymes, they developed a system that forms filamentous nanostructures upon dephosphorylation and disassembles upon phosphorylation. A nonapeptide, containing one serine unit, covalently attached to a C_{12} chain was synthesized. To assess the feasibility of drug release from such a system, they incorporated doxorubicin into the fibers and studied the cytotoxicity against tumor cells that secrete kinases. Not only did they observe a faster release from the phosphorylated peptide (not self-assembled), but also a higher level of toxicity against cells only when kinases were present. Despite some problems of doxorubicin leaking, these self-assembled systems represent a big step forward toward the biomedical applications of enzyme-triggered release PBH systems (Table 9.4, Entry 9).

The control of the hydrogel structure is quite critical because it can greatly influence the network properties and, consequently, the drug-release process. This challenge can be overcome by studying the enzyme role in the self-assembly, and understanding the dynamics of this process. In this sense, Hirst *et al.*[56] evaluated hydrogels obtained by the aggregation of several Fmoc-dipeptides capped with methyl ester functionalities, which occurs when they are hydrolyzed by subtilisin. The molecular order of the hydrogels increased, resulting in stiffer networks, as the enzyme concentration raised, suggesting that the enzyme plays an important role in the self-assembly process and in the structure of the resultant hydrogel (Table 9.4, Entry 10). This knowledge suggests a route to processing these gels for regulating the release profile.

All the systems described in this section are good candidates for sustained or controlled drug delivery-applications, as well as interesting platforms to shield molecules with poor water solubility inside hydrogels.

9.3 Enzyme-responsive Micelles

Micelles are structures formed by surfactants, *e.g.* phospholipids, where a hydrophilic head is in contact with the water while a hydrophobic tail hides inside, giving the overall spherical shape. For drug-delivery purposes, micelles are often made of amphiphilic copolymers or conjugates of hydrophobic/polar polymers with polar/hydrophobic biomolecules.

The enzyme-responsive micelles that are described in this chapter have sizes in the nm range, which is generally suitable for administration purposes of carriers intended to enter into contact with either extra-cellular or intra-cellular enzymes. Moreover, the physico-chemical properties of micelles are very appealing for applications in the drug-delivery field due to the possibility to load hydrophobic drugs in the core and, hence, to lead to lower drug cytotoxicity, extended half-life time and tumor accumulation.[57] Enzyme-responsive micelles can be categorized into two classes, according to their physical response upon catalytic action of the enzyme, as described in the next sections.

9.3.1 Disruptive Enzyme-responsive Micelles

In this category we placed all the enzyme-responsive micelles that, after enzymatic reaction, lose the original structure of the micelle-composing molecules (unimers). Namely, the enzyme selectively cleaves a bond which divides the molecular structure into two or more parts that are not able to self-assemble any more (Figure 9.3). A conceptually similar approach to prodrugs is to bond the drug molecules through a linker to a polymer chain, which should not affect the effectiveness of the drug. Uhrich and coworkers[58] designed an amphiphilic macromolecule with a hydrophobic component, a C_{12} chain, and a hydrophilic moiety, a PEG chain, attached to a mucic acid backbone, which is conjugated to the drug through a hydrazone linker. The macromolecule was designed to be biocompatible and biodegradable (in less than 6 days) when

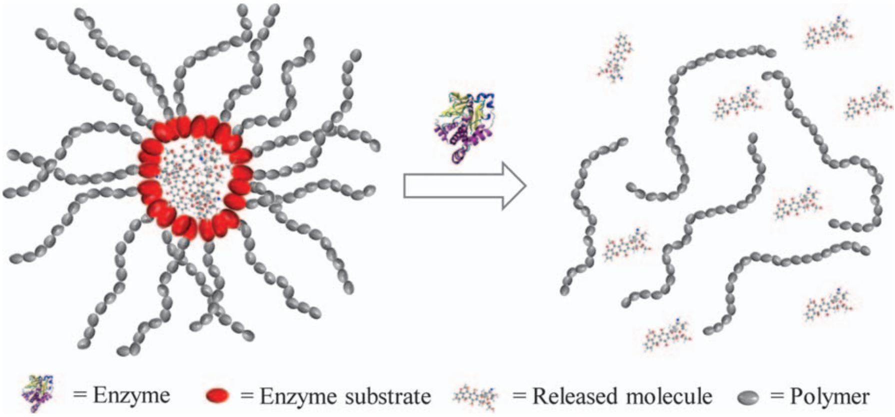

Figure 9.3 Schematic representation of a disruptive enzyme-responsive micelle. The enzyme substrate plays a critical role in the self-assembly process. Upon enzymatic catalysis, the polymeric structure is modified and the interactions leading to self-assembly are lost; as a result the structure disassembles and the payload is released.

Table 9.5 Composition and enzyme-responsiveness of some disruptive enzyme-responsive micelles described in Section 9.3.1.

	Polymer	*Enzyme substrate*	*Enzyme*	*Released molecule*	*Ref.*
1	PEG-[C_{12}](Mucic acid)$_4$	Hydrazone linker	Pancreatic lipase	Doxorubicin	58
2	PLA-b- PEG/PLA-b-PNIPAM	PLA	Lipase	Ibuprofen	59
3	(Ala)$_2$-Lys-Leu-Val-(Phe)$_2$-PEG	Phe$\sim$Phe	α-chymotrypsin	Amyloid peptide fragments	60
4	*co*-poly(n butyl acrylate) -polystyrene-b-poly(Glu-co-Ala)	Ala$\sim$Ala	Elastase, thermolysin	Amino acid fragments	61
5	OEG-polyester	Ester chains	Proteinase K	Doxorubicin and rifampin	62
6	Dendrons	Ester linker	Porcine liver esterase	Pyrene	63

exposed to pancreatic lipase. In contrast, the macromolecule was stable for weeks in the absence of enzyme (Table 9.5, Entry 1). The release of doxorubicin was mainly intra-cellular and pH driven.

Another potential drug-delivery system based on lipase-degradable micelles was reported by Shi and coworkers.[59] The micelles were formed by two diblock copolymers, poly(lactide)-block-poly(ethylenglycol) (PLA-b-PEG) and poly(lactide)-block-poly(*N*-isopropylacrilamide) (PLA-b-PNIPAM). When the temperature exceeded the low critical solution temperature (LCST) of PNIPAM, a PLA-PNIPAM-PEG core-shell-corona structure was formed.

The PEG corona enabled an adjustable diffusion of lipase, an enzyme able to degrade PLA and hence to trigger the release of ibuprofen from the micelles (Table 9.5, Entry 2).

Castelletto *et al.*[60] reported on a polymer-peptide conjugate that self-assembled forming micelles; the corona being formed by PEG and the core by a heptapeptide containing two β-alanines and hydrophobic amino acids that form helical structures. Upon exposure to α-chymotrypsin, the peptide sequence was cleaved and the micelles fell apart. The amino acid sequence chosen contained a self-recognition motif that can specifically bind to amyloid protein. The authors suggested that this method could be used in the future to develop an enzyme-responsive peptide delivery system for therapeutics or diagnostics (Table 9.5, Entry 3).

Heise and coworkers[61] exploited the selectivity of a protease to cleave a polypeptide diblock copolymer. In this case the peptides (poly(L-Glu) with variable amounts of L-Ala) are used as corona, while the core is formed by hydrophobic poly(*N*-butyl acrylate)-co-polystyrene. Exposure to proteases led to a degradation rate that was proportional to the content in Ala of the polymeric peptide, which opens the possibility to design copolymers with tunable degradation times. Moreover, by incorporating different peptide sequences, it is possible to design materials that may be triggered by different target peptidases. The enzyme/substrate specificity guarantees that the ERM only responds to one specific enzyme, while it remains unaltered when exposed to other enzymes (Table 9.5, Entry 4).

Another way to obtain disruptive micelles is to use polymers that are themselves substrates of enzymes. Wang *et al.*[62] synthesized amphiphilic alternating polyester polymers, containing oligo(ethylene glycol) (OEG) pendant chains to minimize non-specific interactions. Micelles containing doxorubicin and rifampin released the drugs at a higher rate in the presence of proteinase K and at pH 5.5. Both enzymatic and acid hydrolysis enabled the cleavage of polymer backbone, resulting in micelle degradation. In the absence of enzymes only 10% of the drug was released. Moreover, *in vitro* studies showed that the micelles were able to penetrate into cancer cells and to release doxorubicin, providing higher antitumoral efficacy than the drug alone (Table 9.5, Entry 5).

Disruptive micelles were also obtained from amphiphilic dendrimers that contain an enzyme cleavable ester moiety between the hydrophobic and hydrophilic units. These dendrimers self-assembled as a result of the orthogonal placement of hydrophilic and lipophilic units in every repeating unit of the dendrimer.[63] Upon esterase exposure, the micellar aggregates disassembled (Table 9.5, Entry 6).

9.3.2 Switchable Micelles

A common feature of switchable micelles is that the disassembling process occurs without disrupting the original composition of the polymer. All available prototypes are based on the catalytic activity of phosphatases, which highlights the great interest that this class of enzymes, together with their antagonistic counterparts, kinases, is generating (as seen in Section 9.2.1.3). The first two examples were reported in close succession in 2009. Hawker and coworkers[64] prepared water soluble block-copolymers by copolymerization of polyethylene glycol (PEG) macroinitiator with vinyl monomers bearing an enzymatically cleavable solubilizing moiety, namely phosphate groups. These copolymers self-assemble under physiological conditions upon action of phosphatases that removed the solubilizing phosphate moieties from the vinyl polymer backbone, which turned out to be hydrophobic. Consequently, the polymer became amphiphilic and formed colloidal nanoaggregates. The enzymatic reaction occurred slowly and the dephosphorylation was not complete after 7 days, probably due to the self-assembly of the polymer after only a partial conversion, which does not allow the enzymes to cleave all the phosphate moieties. Kühnle and Börner[65] synthesized a poly(ethylene oxide)-block-peptide copolymer (PEO-peptide conjugate). The peptide segment had a primary structure with five repeating units of threonine and valine diads ($(\text{Thr-Val})_5$), which have a strong tendency to form β-sheets aggregates in water. This behavior was suppressed by introducing three phosphothreonines into the $(\text{Thr-Val})_5$ peptide aggregation domain. After the addition of phosphatase in the solution, the transition from random coils to β-sheets in overall fibrillar structures was achieved. Therefore, in this case the formed structures are not micelles.

A dual-responsive phosphatase/temperature material has recently been developed starting from poly(2-isopropyl-2-oxazoline) chains that were functionalized with Fmoc-*p*Tyr, which is known to self-assemble upon dephosphorylation.[66,67] This structure, besides combining the numerous advantages of the starting polymer chain, such as stealth behavior and low toxicity profiles, adds to the system the temperature responsiveness. The enzymatic dephosphorylation and thus the micelle formation were reported to be faster compared to the ones described above – full dephosphorylation was achieved within one hour – due to the presence of only one phosphate group per polymer chain. Fmoc allowed monitoring the reaction by spectroscopy, but it could be replaced by a more biocompatible molecule, ideally purely peptidic. When the temperature exceeded the LCST, the hydrophilic corona became hydrophobic and collapsed around the hydrophobic core formed by Fmoc-Tyr, considerably reducing the particle size of the micelles. The temperature responsiveness was reversible, a feature that could be used to enhance tissue-targeting or help in loading the payload.

Another way to exploit phosphatases consists in employing the enzyme to trigger the disassembly of the micelles instead of the self-assembly of polymers.[68] The hydrophilic block copolymer methoxy-poly(ethylene glycol)-block-poly(L-lysine hydrochloride) (PEG-b-PLKC) can interact with negatively charged molecules, such as ATP, through the cationic PLKC block. The ionic interactions physically bind ATP and PLKC together, incorporating the hydrophobic functionality of adenosine, turning the polymer amphiphilic and leading to self-assembly as micelles. Upon enzymatic dephosphorylation, the

ATP is degraded to adenosine and single charged phosphate groups, which are not able to bind anymore to PLKC, and then the micelles fall apart.

Although the systems reported in this section have not yet been tested as drug-delivery systems, the great amount of work that has been done in the last few years on this topic makes us believe that in the near future the current limitations of these systems will be overcome and applications will be feasible.

9.4 Enzyme-responsive Silica Nanocontainers

Enzyme-responsive silica nanocontainers (SN) are mesoporous supports that can host molecules to be released upon the catalytic action of enzymes (Figure 9.4). Silica mesoporous systems have a number of advantages for drug delivery, such as high loading capacity due to their large pore volume, biocompatibility and stability. They also provide good protection of the payload molecules because silica is not affected by external stimuli, such as pH or temperature.[69] Silica particles have been used to sustain drug release,[70] but what makes these systems really interesting is the possibility to "cap" the pores with stimuli-responsive molecules that allow the release of the payload under certain conditions. The first example of silica support with capped pores was

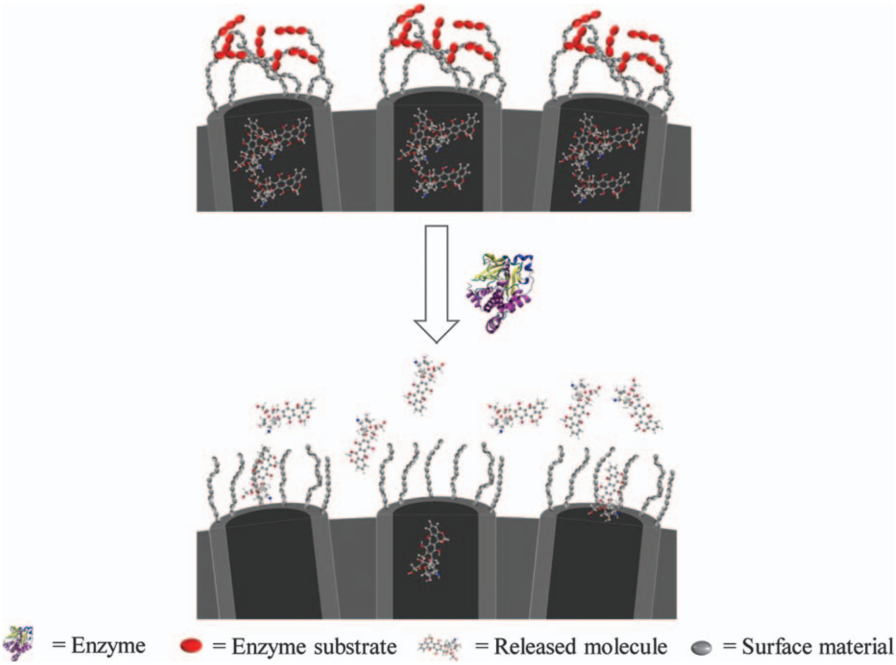

Figure 9.4 Schematic representation of an enzyme-responsive silica nanocontainer. Mesoporous particles are functionalized with enzyme substrates, which obstruct the pores due to steric hindrance or weak interactions. Upon enzyme catalysis, the substrates are removed from the particles and the payload is released.

reported in 2003 by Mal *et al.*,[71] who realized a light-sensitive reversible gate system through the photodimerization of coumarin. After this first study, a number of systems responsive to pH,[72] temperature[73] or antibody-antigen interactions[74] were developed. There is still a paucity of *in vivo* studies about biocompatibility of silica nanoparticles and how specific characteristics of the material, *e.g.* particle size, may influence the toxicity.[75,76] Comprehensive information on smart drug delivery from silica nanoparticles can be found in Chapter 15.

Since enzyme-responsive SNs are quite recent – the first one was described in 2008 by Patel *et al.*[77] – most of the reports are still proof-of-concept studies with materials not yet used in drug delivery. In this first example, the authors functionalized mesoporous silica particles, having ~400 nm diameter and 2 nm pore diameter, to obtain a linker composed by ethylene glycol with a free azide group terminus. Following the loading of the luminescent probe rhodamine B by diffusion, the particles were incubated with α-cyclodextrin for one day, and then the pendant azide groups were ''clicked'' on adamantyl stoppers with pendant alkyne groups to obtain a [2]rotaxane. Two different adamantyl stoppers were synthesized; the first one had an ester linker susceptible to esterase catalysis, while the second was an amide analogue used as a control. After exposure to porcine liver esterase, it was found that rhodamine B was released only from the particles with the ester linked stopper, while no release was detected for the control. With the removal of the stopper, the α-cyclodextrin molecules became free, not being threaded any longer, leaving the pore open and allowing the diffusion of the luminescent probe (Table 9.6, Entry 1).

Another example exploiting cyclodextrins has been reported by Kim and coworkers,[78] who used smaller particles (~60 nm diameter) with the same pore size (2.5 nm diameter). A similar functionalization strategy was applied; first the surface was coated with alkyne groups, and then the cyclodextrins were ''clicked'' on the surface after the loading of the fluorescent calcein. Under exposition to α-amylase, an enzyme that catalyses the degradation of starch into sugar cleaving the α-1,4-glycosidic bond, the nanoparticles released calcein from the pores. No calcein release was noticed when the particles were not exposed to the enzyme or incubated with its denaturated form. Moreover, they synthesized a second population of dextran-based functionalized particles that had a different linker, containing an ester bond, without major changes in the

Table 9.6 Composition and enzyme-responsiveness of the coatings of some silica nanocontainers described in Section 9.4.

	Surface material	*Enzyme substrate*	*Enzyme*	*Released molecule*
1	Saccharide[77–80]	Ester linker[77,78]	Esterase[77,78,80]	Fluorophore[77–84]
2	Peptide[81,82,84]	Glycosidic bond[77–80]	Glycosyl hydrolase[77–80]	Oligonucleotide[84,85]
3	Oligonucleotide[84,85]	Peptide[81–84]	Protease[81–84]	
4		Oligonucleotide[85]	Nuclease[85]	

functionalization strategy. After exposure to lipases, the ester was cleaved and the calcein was released (Table 9.6, Entries 1 and 2).

A lactose-derivative disaccharide was used by Bernardos *et al.*[79] to functionalize particles having 2.4 nm average pore diameter. In this study, before coating the SNs, the mesopores were loaded with the $[Ru(bipy)_3]Cl_2$ dye to monitor the release upon enzymatic catalysis. The release took place upon the catalytic action of β-D-galactosidase, able to cleave the 1→4 glycosidic bond between β-D-galactose and β-D-glucose monosaccharides in the lactose structure. After the rupture of the bond, the bulky disaccharide that was sterically hindering the release of $[Ru(bipy)_3]Cl_2$ disappeared. This process occurred under conditions that resemble those at which β-D-galactosidase is located in the intestine. The performance of this system was also tested simulating the pH conditions of the gastrointestinal tract. At the acid pH of the stomach or at pH 7.5 of the gut, negligible dye release was noticeable in absence of the enzyme. Finally, the system was tested for selectivity against other enzymes, *e.g.* proteases, and no significant loss of payload was observed (Table 9.6, Entries 1 and 2). This system was further developed by functionalizing the surface of the particles (100–200 nm diameter and 2.3 nm pore diameter) with different starch derivates, composed by various mixtures of polysaccharides.[80] When exposed to pancreatin, a mixture of amylases and lipases extracted from the pancreas, the particles exhibited a controlled release of the payload molecules. The release rate depended on the composition of saccharides used to functionalize the surface. Finally, the starch-functionalized particles that showed the best release profile were tested in *in vitro* and *ex vivo* assays using doxorubicin as guest molecule instead of $[Ru(bipy)_3]Cl_2$. *In vitro* experiments confirmed that the release of the drug only occurred when the enzyme was present in the dissolution medium. *Ex vivo* assays showed that the nanocontainers were internalized by the cells through endocytosis, and then transported to the autolysosomes where enzymes able to degrade saccharides are present. After incubation of cancer cells with this enzyme-responsive doxorubicin-loaded SN, a decrease in cell viability and an increase in cell death were observed (Table 9.6, Entries 1 and 2).

Thornton and Heise[81] used a protease cleavable Fmoc-tetrapeptide sequence to functionalize the surface of silica particles (5 μm diameter, 30 nm pore diameter) using fluorescein isothiocyanate (FITC) functionalized dextran, rhodamin B and fluorescein as model payloads to test the ability to trap molecules of various molecular weights. The particles were functionalized with two tetrapeptides with different affinity for two proteases: elastase and thermolysin. Due to the hydrophobic and π-π interactions and to the steric hindrance of the Fmoc moieties, in the absence of enzyme the pores were closed and the payload was retained. Upon exposure to the two proteases, the tetrapeptides were cleaved at a rate that depended on the substrate specificity for the selected protease and on the enzyme concentration, and the dyes were released in a controlled manner (Table 9.6, Entries 1, 2 and 3).

Coll *et al.*[82] reported another example in which peptide sequences act as enzyme-responsive gate guardians. Different peptides of various lengths were synthesized and used as substrate of proteolytic enzymes from *Streptomyces griseus* after trapping a dye inside the SNs (~100 nm diameter, 0.9 nm pore diameter). The length of the peptide sequence determined its efficiency to cap the gate and to trigger the release upon the catalytic action of enzyme. The enzyme-responsive SNs coated with the longest peptide (18 amino acids) showed zero-order release before exposure to enzyme, while with the particles functionalized with shorter (11 and 6 amino acids) sequences a significant leakage was observed (Table 9.6, Entries 1, 2 and 3).

The avidin/biotin interaction was also exploited to design enzyme-responsive SNs.[83] The particle surface was modified with biotin and, after trapping fluorescein in the pores, avidin was added to the solution. Due to the strong interactions between biotin and avidin, the pores closed and no leakage of fluorescein was noticed. Upon exposure to trypsin, a protease that can digest avidin, amounts close to 100% of the payload were released in less than three hours. To further prove that the avidin/biotin interaction was closing the pores, the release of dye was monitored at higher temperatures, at which this interaction became weaker. Under these conditions, fluorescein was gradually released (Table 9.6, Entries 1 and 3).

So far, all the SNs reported above exploited enzyme catalysis to cleave one part of the molecule coating the surface, preventing steric hindrance or self-assembly interactions. Another strategy that uses the total degradation of coating molecules to trigger the release has been recently reported by Hanagata and coworkers. Particles of 500 nm diameter and a pore size between 2.4 and 2.6 nm diameter were loaded with fluorescein and then coated by layer-by-layer deposition of a negatively charged oligodeoxinucleotide and positively charged poly(L-Lys).[84] Upon *in vitro* exposure to α-chymotrypsin, the release of fluorescent dyes and genes was triggered due to degradation of the polymer (Table 9.6, Entries 1, 2 and 3). In a subsequent study,[85] the SNs were coated only with the oligodeoxinucleotide. Deoxyribonuclease was able to degrade the model gene and to provoke the release of fluorescein. This approach, besides exploiting non-covalent interactions to coat the particles, allows the triggered release of a second molecule, *i.e.* an oligonucleotide (Table 9.6, Entries 1, 2, 3 and 4).

9.5 Conclusion

Enzymes offer a number of advantages as potential tools to improve drug delivery. They are often involved in the development of diseases, making them extremely useful to address one of the biggest challenges of drug delivery: selectivity. The examples treated in this chapter illustrate how the versatility of enzymes offers multiple approaches to trigger drug release. Indeed, possible strategies involve degradation, self-assembly, disassembly, cleavage and swelling, upon the catalytic action of enzymes, which lead to the release of drugs. There are several examples in which the release system was entirely composed of natural building blocks, of naturally occurring building blocks conjugated to synthetic materials or of solely synthetic materials. The development of new biocompatible materials is exerting a very important effect on the advances made in ERM for biomedical applications, and most recent research relies on the availability of materials that show low cytotoxicity profiles or are even FDA approved. The majority of the research discussed in this chapter is currently in the 'proof of concept' stage. These systems help to uncover the design rules for ERM and clearly demonstrate the versatility due to the modularity of these systems. Over time, applications in drug delivery are likely to become a clinical reality.

References

1. P. Ehlrich, *Lancet*, 1907, **2**, 351.
2. a) K. R. Schultz, W. P. Bowman, A. Aledo, W. B. Slayton, H. Sather, M. Devidas, C. Wang, S. M. Davies, P. S. Gaynon, M. Trigg, R. Rutledge, L. Burden, D. Jorstad, A. Carroll, N. A. Heerema, N. Winick, M. J. Borowitz, S. P. Hunger, W. L. Carroll and B. Camitta, *J. Clin. Oncol.*, 2009, **27**, 5175. b) H. Kantarjian, N. P. Shah, A. Hochhaus, J. Cortes, S. Shah, M. Ayala, B. Moiraghi, Z. Shen, J. Mayer, R. Pasquini, H. Nakamae, F. Huguet, C. Boqué, C. Chuah, E. Bleickardt, B. Bradley-Garelik, C. Zhu, T. Szatrowski, D. Shapiro and M. Baccarani, *N. Eng. J. Med.*, 2010, **362**, 2260.
3. R. C. Gallo and L. Montagnier, *Nature*, 1987, **326**, 435.
4. D. D. Richman, D. M. Margolis, M. Delaney, W. C. Greene, D. Hazuda and R. J. Pomerantz, *Science*, 2009, **323**, 1304.
5. D. D. Richman, *Nature*, 2001, **410**, 995.
6. H. A. Chapman, P. Bertozzi and J. J. Reilly, *CHEST*, 1988, **93**, 1256.
7. D. S. Smith, P. A. Humphrey and W. J. Catalona, *Cancer*, 1997, **80**, 1853.
8. S. Singhal, M. C. Taylor and R. T. Baker, *BMC Biochem.*, 2008, **9**, S3.
9. P. J. Rosenthal, *J. Exp. Biol.*, 2003, **206**, 3735.
10. J. M. Matés, C. Pérez-Gómez and I. Núñez De Castro, *Clinical Biochem.*, 1999, **32**, 595.
11. B. J. Clodfelder-Miller, A. A. Zmijewska, G. V. W. Johnson and R. S. Jope, *Diabetes.*, 2006, **55**, 3320.
12. M. Freeman, L. Kuiken, J. B. Ragland and S. M. Sabesin, *Lipids*, 1976, **12**, 433.
13. F. Liu, Z. Liang and C. X. Gong, *Panminerva Med.*, 2006, **48**, 97.
14. J. Rautio, H. Kumpulainen, T. Heimbach, R. Oliyai, D. Oh, T. Järvinen and J. Savolainen, *Nat. Rev. Drug Discov.*, 2008, **7**, 255.
15. P. A. Vasey, S. B. Kaye, R. Morrison, C. Twelves, P. Wilson, R. Duncan, A. H. Thomson, L. S. Murray, T. E. Hilditch, T. Murray, S. Burtles, D. Fraier, E. Friegerio and J. Cassidy, *Clin. Cancer Res.*, 1999, **5**, 83.
16. Y. Singh, M. Palombo and P. J. Sinko, *Curr. Med. Chem.*, 2008, **15**, 1802.
17. K. Knop, R. Hoogenboom, D. Fischer and U. S. Schubert, *Angew. Chem. Int. Ed.*, 2010, **49**, 6288.

18. M. P. Napier, S. K. Sharma, C. J. Springer, K. D. Bagshawe, A. J. Green, J. Martin, S. M. Stribbling, N. Cushen, D. O'Malley and R. H. J. Begent, *Clin. Canc. Res.*, 2000, **6**, 765.
19. V. T. DeVita, T. S. Lawrence and S. A. Rosenberg, ed., *Cancer: Principles and Practice of Oncology*, WoltERM Kluwer/Lippincott Williams & Wilkins, Philadelphia, 8th edn, 2008.
20. a) Z. Ram, K. W. Culver, S. Walbridge, R. M. Blaese and E. H. Oldfield, *Cancer Res.*, 1993, **53**, 83. b) S. Schepelmann and C. J. Springer, *Curr. Gene Ther.*, 2006, **6**, 647.
21. a) R. Satchi, T. A. Connors and R. Duncan, *Br. J. Cancer*, 2001, **85**, 1070. b) Y. Singh, M. Palombo and P. J. Sinko, *Curr. Med. Chem.*, 2008, **15**, 1802.
22. S. M. Moghimi, A. C. Hunter and C. J. Murray, *FASEB J.*, 1995, **19**, 311.
23. J. A. Champion, Y. K. Katare and S. Mitragotri, *J. Control. Release*, 2007, **121**, 3.
24. H. Maeda, J. Wu, T. Sawa, Y. Matsumura and K. Hori, *J. Control. Release*, 2000, **65**, 271.
25. K. Greish, *J. Drug Target.*, 2007, **15**, 271.
26. M. Goldberg, R. Langer and X. Jia, *J. Biomater. Sci. Polymer Ed.*, 2007, **18**, 241.
27. a) T. Graham, *J. Chem. Soc.*, 1862, **15**, 216. b) T. Graham, *P. Roy. Soc. Lond.*, 1864, **13**, 335.
28. M. Hamidi, A. Azadi and P. Rafiei, *Adv. Drug. Deliver. Rev.*, 2008, **60**, 1638.
29. F. Carpi and E. Smela, ed., *Biomedical Applications of Electroactive Polymer Actuators*, John Wiley & Sons Ltd, 2009.
30. R. V. Ulijn, N. Bibi, V. Jayawarna, P. D. Thornton, S. J. Todd, R. J. Mart, A. M. Smith and J. E. Gough, *Mater. Today*, 2007, **10**, 40.
31. T. Traitel, Y. Cohen and J. Kost, *Biomaterials*, 2001, **21**, 1679.
32. J. Kost, T. A. Horbett, B. D. Ratner and M. Singh, *J. Biomed. Mater. Res.*, 1985, **19**, 1117.
33. W. Zhao, H. Zhang, Q. He, Y. Li, J. Gu, L. Li, H. Li and J. Shi, *Chem. Comm.*, 2011, **47**, 9459.
34. W. E. Hennink and C. F. van Nostrum, *Adv. Drug. Deliver. Rev.*, 2002, **54**, 13.
35. J. J. Sperinde and L. G. Griffith, *Macromolecules*, 2000, **33**, 5476.
36. K. L. Shantha, P. Ravichandran and K. P. Rao, *Biomaterials*, 1995, **16**, 1313.
37. I. S. Kim and I. J. Oh, *Arch. Pharm. Res.*, 2005, **28**, 983.
38. S. G. Lévesque and M. S. Soichet, *Bioconjugate Chem.*, 2007, **18**, 874.
39. A. A. Aimetti, A. J. Machen and K. S. Anseth, *Biomaterials*, 2009, **30**, 6048.
40. P. D. Thornton, R. Mart and R. V. Ulijn, *Adv. Mater.*, 2007, **19**, 1252.
41. P. D. Thornton, R. J. Mart, S. J. Webb and R. V. Ulijn, *Soft Matter*, 2008, **4**, 821.

42. T. O. McDonald, H. Qu, B. R. Saunders and R. V. Ulijn, *Soft Matter*, 2009, **5**, 1728.
43. J. R. Tauro, B. S. Lee, S. S. Lateef and R. A. Gemeinhart, *Peptides*, 2008, **29**, 1965.
44. G. M. Whitesides and B. Grzybowsky, *Science*, 2002, **295**, 2418.
45. P. K. Vemula, G. A. Cruikshank, J. M. Karp and G. John, *Biomaterials*, 2009, **30**, 383.
46. P. K. Vemula, J. Li and G. John, *J. Am. Chem. Soc.*, 2006, **128**, 8932.
47. K. J. C. Van Bommel, M. C. A. Stuart, B. L. Feringa and J. Van Esch, *Org. Biomol. Chem.*, 2005, **3**, 2917.
48. Y. G. Gao, Y. Kuang, Z. F. Guo, Z. Guo, I. J. Krauss and B. Xu, *J. Am. Chem. Soc.*, 2009, **131**, 13576.
49. A. Altunbas, S. J. Lee, S. A. Rajasekaran, J. P. Schneider and D. J. Pochan, *Biomaterials*, 2011, **32**, 5906.
50. L. Liang, X. D. Xu, C. S. Chen, J. H. Fang, F. G. Jiang, X. Z. Zhang and R. X. Zhuo, *J. Biomed. Mater. Res. B Appl. Biomater.*, 2010, **93B**, 324.
51. Z. Yang, H. Gu, D. Fu, P. Gao, J. K. Lam and B. Xu, *Adv. Mater.*, 2004, **16**, 1440.
52. J. W. Sadownik, J. Leckie and R. V. Ulijn, *Chem. Comm.*, 2011, **47**, 728.
53. Z. Yang, M. Ma and B. Xu, *Soft Matter*, 2009, **5**, 2546.
54. Z. Yang, G. Liang, L. Wang and B. Xu, *J. Am. Chem. Soc.*, 2006, **128**, 3038.
55. M. J. Webber, C. J. Newcomb, R. Bitton and S. I. Stupp, *Soft Matter*, 2011, **7**, 9665.
56. A. R. Hirst, S. Roy, M. Arora, A. K. Das, N. Hodson, P. Murray, S. Marshall, N. Javid, J. Sefcik, J. Boekhoven, J. H. van Esch, S. Santabarbara, N. T. Hunt and R. V. Ulijn, *Nat. Chem.*, 2010, **2**, 1089.
57. E. Blanco, E. A. Bey, C. Khemtong, S. E. Yang, J. Setti-Guthi, H. Chen, C. W. Kessinger, K. A. Carnevale, W. G. Bornmann, D. A. Boothman and J. Gao, *Cancer Res.*, 2010, **70**, 3896.
58. L. S. del Rosario, B. Demirdirek, A. Harmon, D. Orban and K. E. Uhrich, *Macromol. Biosci.*, 2010, **10**, 415.
59. C. Wu, R. Ma, H. He, L. Zhao, G. Gao, Y. An and L. Shi, *Macromol. Biosci.*, 2009, **9**, 1184.
60. V. Castelletto, J. E. McKendrick and I. W. Hamley, *Langmuir*, 2010, **26**, 11624.
61. G. J. M. Habraken, M. Peeters, P. D. Thornton, C. E. Koning and A. Heise, *Biomacromolecules*, 2011, **12**, 3761.
62. W. Wang, J. Ding, C. Xiao, Z. Tang, D. Li, J. Chen, X. Zhuang and X. Chen, *Biomacromolecules*, 2011, **12**, 2466.
63. M. A. Azagarsamy, P. Sokkalingam and S. Thayumanavan, *J. Am. Chem. Soc.*, 2009, **131**, 14185.
64. J. A. Amir, S. Zhong, D. J. Pochan and C. J. Hawker, *J. Am. Chem. Soc.*, 2009, **131**, 13949.
65. H. Kühnle and H. G. Börner, *Angew. Chem. Int. Ed.*, 2009, **48**, 6431.

66. P. F. Caponi, X. P. Qiu, F. Vilela, F. M. Winnik and R. V. Ulijn, *Polym. Chem.*, 2011, **2**, 306.
67. a) Z. Yang and B. Xu, *Chem. Comm.*, 2004, **21**, 2424. b) Z. Yang, H. Gu, D. Fu, P. Gao, J. K. Lam and B. Xu, *Adv. Mater.*, 2004, **16**, 1440.
68. C. Wang, Q. Chen, Z. Wang and X. Zhang, *Angew. Chem. Int. Ed.*, 2010, **49**, 8612.
69. Y. W. Yang, *Med. Chem. Comm.*, 2011, **2**, 1033.
70. a) D. Schmaljohann, *Adv. Drug Deliver. Rev.*, 2006, **58**, 1655. b) M. Vallet-Regi, F. Balas and D. Arcos, *Angew. Chem. Int. Ed.*, 2007, **46**, 7548.
71. N. K. Mal, M. Fujiwara and Y. Tanaka, *Nature*, 2003, **421**, 350.
72. a) A. Bernardos, E. Aznar, C. Coll, R. Martínez-Máñez, J. M. Barat, M. D. Marcos, F. Sancenón and J. Soto, *J. Control. Release*, 2008, **131**, 181. b) S. Angelos, Y. W. Yang, N. M. Khashab, J. F. Stoddart and J. I. Zink, *J. Am. Chem. Soc.*, 2009, **131**, 11344.
73. Q. Fu, G. V. R. Rao, L. K. Ista, Y. Wu, B. P. Andrezejewski, L. A. Sklar, T. L. Ward and G. P. López, *Adv. Mater.*, 2003, **15**, 1262.
74. E. Climent, A. Bernardos, R. Martínez-Máñez, A. Maquieira, M. D. Marcos, N. Pastor-Navarro, R. Puchades, F. Sancenón, J. Soto and P. Amorós, *J. Am. Chem. Soc.*, 2009, **131**, 14075.
75. a) K. O. Yu, C. M. Grabinski, A. M. Schrand, R. C. Murdock, W. Wang, B. Gu, J. J. Schlager and S. M. Hussain, *J. Nanopart. Res.*, 2009, **11**, 15. b) D. B. Warheit, T. R. Webb, V. L. Colvin, K. L. Reed and C. M. Sayes, *Toxicol. Sci.*, 2007, **95**, 270.
76. a) G. Xie, J. Sun, G. Zhong, L. Shi and D. Zhang, *Arch. Toxicol.*, 2010, **84**, 183. b) W. Lin, Y. Huang, X. D. Zhou and Y. Ma, *Tox. Appl. Pharmacol.*, 2006, **217**, 252.
77. K. Patel, S. Angelos, W. R. Dichtel, A. Coskun, Y. W. Yang, J. I. Zink and J. F. Stoddart, *J. Am. Chem. Soc.*, 2008, **130**, 2382.
78. C. Park, H. Kim, S. Kim and C. Kim, *J. Am. Chem. Soc.*, 2009, **131**, 16614.
79. A. Bernardos, E. Aznar, M. D. Marcos, R. Martínez-Máñez, F. Sancenón, J. Soto, J. M. Barat and P. Amorós, *Angew. Chem. Int. Ed.*, 2009, **48**, 5884.
80. A. Bernardos, L. Mondragón, E. Aznar, M. D. Marcos, R. Martínez-Máñez, F. Sancenón, J. Soto, J. M. Barat, E. Pérez-Payá, C. Guillem and P. Amorós, *ACS Nano*, 2010, **4**, 6353.
81. P. D. Thornton and A. Heise, *J. Am. Chem. Soc.*, 2010, **132**, 2024.
82. C. Coll, L. Mondragón, R. Martínez-Máñez, F. Sancenón, M. D. Marcos, J. Soto, P. Amorós and E. Pérez-Payá, *Angew. Chem. Int. Ed.*, 2011, **50**, 2138.
83. A. Schlossbauer, J. Ketch and T. Bein, *Angew. Chem. Int. Ed.*, 2009, **48**, 3092.
84. Y. Zhu, W. Meng, H. Gao and N. Hanagata, *J. Phys. Chem.*, 2011, **115**, 13630.
85. Y. Zhu, W. Meng and N. Hanagata, *Dalton Trans.*, 2011, **40**, 10203.

CHAPTER 10

Bioresponsive Polyplexes and Micelleplexes

CAMERON ALEXANDER AND
FRANCISCO FERNANDEZ TRILLO*

School of Pharmacy, University of Nottingham, Nottingham,
NG7 2RD, UK
*Email: francisco.fernandez-trillo@nottingham.ac.uk

10.1 Introduction

The delivery of therapeutic biomacromolecules such as nucleic acids (NAs) is problematic for many reasons, not least of which is their size. While most therapeutic proteins and nucleic acid oligomers are less than 20 nm in hydrodynamic radius, these molecules are still of a much greater size than "standard" drugs, and present severe challenges for any carrier system to gain entry into a target cell.[1] For gene therapy constructs such as plasmid DNA, or mammalian artificial chromosomes, the sizes can reach micron dimensions, and thus conventional encapsulation and conjugation strategies cannot be employed. Accordingly, a number of methods for condensation of NAs and other biomacromolecules have been developed, many of which employ polyelectrolyte complexation strategies to screen or eliminate charge–charge repulsion and hence collapse polyanionic nucleotide strands.

The wealth of literature on polyelectrolyte complexes (often termed "polyplexes") of nucleic acids with cationic species is beyond the scope of this chapter, and interested readers are referred to specialized reviews.[2–8] In any case, a few points are worthy of note to inform the discussion on responsive

---

RSC Smart Materials No. 2
Smart Materials for Drug Delivery: Volume 1
Edited by Carmen Alvarez-Lorenzo and Angel Concheiro
© The Royal Society of Chemistry 2013
Published by the Royal Society of Chemistry, www.rsc.org

polyplexes. In the absence of condensing carrier molecules, which are polycationic in nature, nucleic acids can be easily degraded by enzymes such as DNAses or RNAses within seconds of being injected into the bloodstream.[9,10] Therefore, in order to improve the delivery properties across these barriers and increase the stability of nucleic acids against enzymatic degradation, the biotherapeutic needs to be stabilized as well as condensed. A number of studies have shown that polycations are better for nucleic acids delivery than cationic lipids in several aspects. Polycations confer i) relatively small complex size and narrow size distribution;[11] ii) high stability against nucleases; iii) ease of manipulation of physical factors (*e.g.* hydrophilicity and charge); and iv) feasibility of changing polycationic polymer structure by chemical modification or copolymerization with proper monomers in order to achieve higher efficiency or cell targeting without loss in activity.[2]

Various synthetic polycations, *e.g.* poly(ethylene imine) (PEI),[12] and polyamidoamine (PAMAM) dendrimers,[13,14] have been proposed for delivering DNA encoding genes of interest, after formulation of DNA polyplexes, and increasingly these systems are being modified or optimized for small interfering ribonucleic acid (siRNA) delivery too. However, for all the "conventional" polycations, the need for strong condensation of a nucleic acid to retain polyplex stability conflicts with the requirement for unpackaging of the biotherapeutic at the target site. As a consequence, stimuli- and/or bioresponsive polyplexes continue to be a major research goal in many laboratories.

In principle, for successful synthetic gene delivery to take place, the carrier vectors must inherently have some form of stimuli response. This is because in order to promote release of complexed NA at target site, the gene carrier must undergo a change in a property triggered by the environment it is in, which allows the NA to escape. Typically this change in state is needed to take place as a function of subtle modifications in the biochemistry at the intended subcellular location. For instance, it is well known that the pH in the endosome drops to 5.5–6.0, while in the lysosome it can become as low as pH 4.5. Because the endosome is the most likely route for nano-sized polyplexes to be internalized, the most widely used synthetic vectors have relied on the pH-responsive polymers that can change their degree of protonation, such as PEI,[12] poly(dimethyl amino ethyl methacrylate) (pDMAEMA)[15,16] or histidine-rich peptides.[17] This protonation is normally associated with a buffering capacity that promotes the proton uptake by endosomal ATPases, and an increase in the concentration of chloride ions. This in turn induces a change in the osmolarity of the endosome, which, coupled with the swelling of the polymer network due to internal charge repulsion, leads to the destabilization of the endosomal vesicle. This phenomenon has become known as the "proton-sponge" effect.[18] Other systems, such as several fusogenic peptides, undergo a pH-dependent change in hydrophilicity, conferring amphiphilicity, membrane-disruptive properties and capacity to form pores or destabilize membranes.[5] In addition to pH, the change in glutathione concentration inside cells (approx 100-fold compared to that in the plasma),[19] or the local increase of the temperature in a target tissue,[20,21] have also been considered as biostimuli to enhance gene delivery.

In this chapter we describe synthetic gene vectors that have been designed to exploit these subtle changes in physiological conditions for promoting physical changes in the vector structure and function, leading in turn to an increase in gene delivery efficiency.

10.2 pH-responsive Polyplexes

As described earlier, most synthetic gene delivery vehicles are pH responsive, and have the ability to protonate in the endosome to promote efficient transit to the cytosol and/or the nuclei. The detailed mechanisms of endosomal escape by pH responsive polyplexes are beyond the scope of this chapter, so we focus primarily on synthetic gene delivery vehicles that take advantage of changes in pH to promote specific alterations in properties. These include systems that decrease in stability through depolymerization or cross-links cleavage, and thus exhibit a reduction in affinity towards the NA or the loss of a protective corona layer. This latter effect was reported independently by the groups of Park and Kataoka for the delivery of oligodeoxynucleotides (ODNs) to mammalian cells (Figure 10.1). PEG was conjugated to ODN using a phosphoramidate,[22] or a β-thiopropionate,[23] and the recovery of the free NA at pH 5 could be monitored using HPLC. An increase in gene knockdown was observed for these conjugates when compared to a non-cleavable conjugate.[24] In order to increase uptake by HUH-7 cells, lactose was conjugated to the distal end of the PEG chain,[24,25] and growth inhibition of tumor spheroids could be demonstrated using poly(L-lysine) (PLL) or branched PEI (b-PEI) as polycations to complex the cleavable PEG-NA conjugates.[26] Using the same strategy, the group of Mahato was able to improve the pharmacokinetic properties of galactose functionalized PEG-ODN conjugates in rats, without the use of a polycation.[27]

The same principle was investigated by Wagner *et al.*[28] for the systemic delivery of pDNA (plasmid cytomegalovirus-luciferase gene reporter, pCMV-Luc) to severe combined immunodeficiency (SCID) mice. PEG was conjugated to PLL *via* a hydrazone linkage (Figure 10.2a), and polyplexes incorporating b-PEI to aid endosomal escape and transferring (Tf) or epidermal growth factor (EGF) to increase targeting were prepared. Cleavable polyplexes were significantly more efficient in transfecting K562, Neuro2 and Renca-EGFR

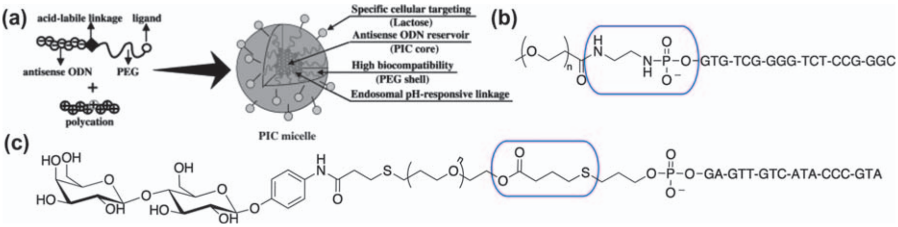

Figure 10.1 Scheme of a pH-responsive polyion complex (PIC) micelle, indicating some relevant properties for gene delivery, reproduced from Ref. 24 with permission from Wiley-VCH Verlag (a), and structures of PEG-ODNs (b) and pH-sensitive linkage (c).

cells. *In vivo*, a 10-fold increase in transfection into SCID mice bearing subcutaneous HUH-7 hepatocellular carcinoma was observed, when compared to the targeted non-cleavable shielded and the non-shielded polyplexes. The same chemistry has been used more recently by Kataoka and coworkers to prepare PLL-PEG conjugates (Figure 10.2b) that were able to deliver pDNA containing a luciferase reporter across a wide range of cell lines.[29] The authors suggested that by partially reacting the hydrazides of a poly(aspartic acid) (p(Asp)) derivative, PEG-(pAsp-hydrazide)-PLL copolymers with a dual pH response could be obtained. While PLL amines are expected to be permanently charged during endocytic uptake and processing, hydrazides (p$K_a \sim 5$) will protonate in the endosome, in a similar fashion to PEI or histidine-rich peptides, providing gene vectors with a higher capacity to reach the cytosol.

In a related strategy to provide a removable "corona" for gene carriers, Wagner *et al.*[30] reported the use of pH-sensitive ketal linkers to prepare PEG-b-PEI conjugates (Figure 10.2c) for the delivery of pCMV-Luc to K562 and Renca-EGFR cells *in vitro*, while Li and coworkers described pH-sensitive PEG-pDMAEMA conjugates (Figure 10.2d), using the same chemistry, that were able to deliver pDNA to 293T cells.[31] In this case, preparing an acid labile PEGylated atom transfer radical polymerization (ATRP) initiator provides an easy way to control pDMAEMA chain length in the conjugates. In a similar fashion, PEG-cholesterol conjugates were synthesized by Miller and coworkers, using an oxime linker (Figure 10.2e).[32] Systemic administration of a liposomal formulation incorporating these pH-sensitive conjugates to deliver siRNA to hepatitis B virus (HBV) transgenic mice resulted in up to 3-fold suppression of markers of HBV replication.

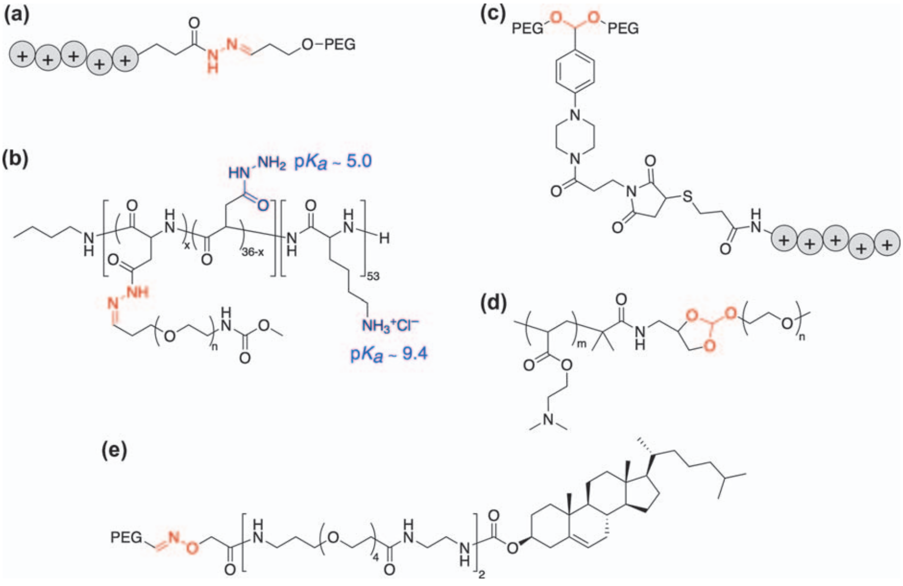

Figure 10.2 Representative pH-sensitive gene vectors. The pH-responsive linkers are highlighted in red.

While all of these examples relied on the cleavage of a pH-sensitive linker to remove the PEGylated corona and increase transfection efficiency once polyplexes are internalized, Bae and coworkers employed pH-sensitive block-copolymers to coat the surface of pDNA/b-PEI polyplexes, increasing in this way the biocompatibility.[33] Poly(sulfonamide) (PSD), a sulfonamide-based pH-responsive polymer,[34] protonates at endosomal pH so that the PEG-PSD corona is removed inside the endosome. An increase of transfection efficiency was observed for these coated pH-sensitive polyplexes when transfection of A2780 carcinoma cells was done at pH 6.6.

A similar shielding strategy has been described by Kataoka *et al.*[35] to improve the transfection efficiency of a di(ethylene imine) derivative of p(Asp), p(Asp-DET), in HUVEC cells. In this case, positively charged p(Asp-DET) was reacted with succinic anhydride or *cis*-aconitic anhydride, to mask its positive charge and produce negatively charged polymers (Figure 10.3). These negatively charged polymers were used to coat p(Asp-DET) polyplexes

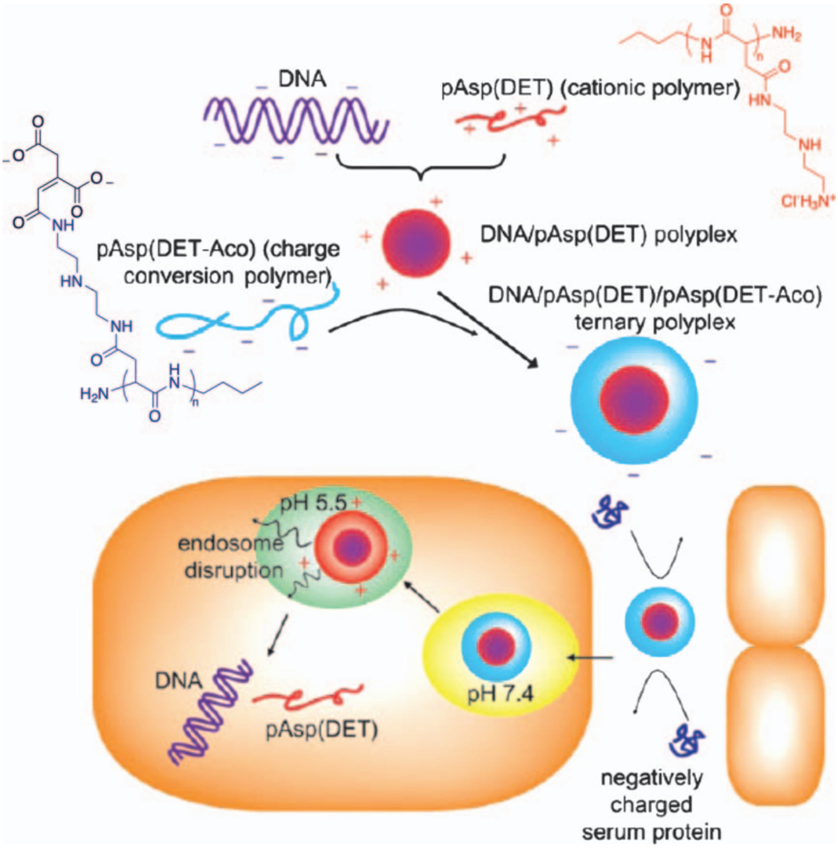
DNA
pAsp(DET) (cationic polymer)
NH2
HN
NH
Cl⁻H3N⁺
DNA/pAsp(DET) polyplex
pAsp(DET-Aco) (charge conversion polymer)
H2N
DNA/pAsp(DET)/pAsp(DET-Aco) ternary polyplex
pH 5.5
endosome disruption
DNA
pAsp(DET)
pH 7.4
negatively charged serum protein

Figure 10.3 Scheme of a charge-conversion ternary polyplex with an endosome-disrupting function, and structure of the representative synthetic components.
Adapted from Ref. 35 with permission from Wiley-VCH Verlag.

containing a luciferase reporter, resulting in overall negatively charged particles with high stability in serum and low cytotoxicity, when compared to non-coated polyplexes. Once internalized, maleic amides degraded at weakly acidic pH (5.5), unmasking the positively charged amines of p(Asp-DET), and deshielding the polyplex. In addition, the buffering capacity was significantly enhanced with the increase in p(Asp-DET) concentration, leading to endosomal escape and an improvement in transfection when compared to the non-shielded polyplex.

pH-Sensitive linkers can be employed to improve the biocompatibility of synthetic gene delivery vectors. For instance, PEI, one of the most widely adopted synthetic gene delivery vectors for laboratory transfections, has several limitations: Its high cation content can lead to extremely stable polyplexes, which may not be able to release the complexed DNA under the slightly acidic conditions of the endosome, a requisite for efficient delivery. On the other hand, PEI has a high cytotoxicity, often associated to its membrane disruption ability.[36] Decreasing the molar mass and the degree of branching can reduce cytotoxicity, normally at the expense of decreasing its transfection efficiency as well.[37] Alternatively, conjugation with neutral polymers such as PEG has been described as a way to increase PEI biocompatibility and reduce its toxicity.[38] In this regard, Kim and coworkers described cross-linking of low molecular weight (Mw) b-PEI (1.8 kDa) using glutaraldehyde to generate materials able to efficiently deliver pCMV-Luc to 293 T cells and A7R5 cells.[39] Imine cross-linked b-PEI could be degraded at endosomal pH (5.4) and resulted in significantly less toxicity than 25 kDa b-PEI with similar transfection efficiencies. A similar approach was independently reported by the groups of Wagner and Kwon, using ketals in this case to cross-link PEI.[40,41] These pH-sensitive polycations have shown efficiency in the delivery of both pDNA and siRNA across a range of mammalian cells.[42,43]

Rozema *et al.*[44] proposed a masking strategy, using pH-sensitive maleic amides, to reduce the toxicity of melittin, a cationic membrane-active peptide. At neutral pH, the lysines of melittin were covalently acylated with 2-propionic-3-methylmaleic anhydride, stopping its membrane disruption properties. This pH-sensitive conjugate could deliver a phosphorodiamidate morpholino oligonucleotide (PMO) that allowed for the recovery of luciferase expression in HeLa-Luc/705 cells.

10.3 Reducible Polyplexes

Under normal conditions, there is a difference in the reduction potential between the extra-cellular environment and the cytosol,[19] which can be used to reduce disulfide linkages. This reduction has been exploited as a trigger to provide polyplexes with improved stability and circulation times outside the target cells, while offering minimized toxicity and controlled delivery once internalized.

Some of these principles were early illustrated by Behr and coworkers, with the templated complexation of pDNA with a cysteine-based cationic detergent.[45] Using a detergent : pDNA 1 : 1 charge ratio, individual anionic pCMV-Luc molecules were cooperatively collapsed into small spherical polyplexes (20–30 nm), that were then "fixed" by spontaneous oxidation of the cysteine moieties. These polyplexes were more stable to serum nucleases than naked pDNA. On the other hand, the negative charge (–40 mV) of these particles prevented fast uptake by BNL Cl.2 murine hepatocytes, which lead to marginal gene expression. Transfection efficiency for this type of stimuli-responsive polyplexes could be improved increasing the N/P ratio to 3 at the expense of producing larger particles ($>$500 nm),[45] which could be further improved by tailoring the length of the hydrophobic chain of the detergent (C10 $<$ C14 $<$ C16).[46] Keeping the size of these polyplexes small, while maintaining a negative or neutral charge, was considered advantageous in order to overcome some of the physiological barriers present *in vivo*. Therefore, the authors suggested that performing pDNA complexation under thermodynamic control, using N/P ratios close to 1, would lead to small-size polyplexes. Decoration of the surface of the particles with targeting ligands such as folate,[47,48] or arginine-glycine-aspartic acid (RGD) peptides,[49] led to an increase in uptake that did not correlate with an increase in transfection efficiency. On the other hand, the introduction of a transfection helper such as 1,2-dioleoyl-sn-glycero-3-phosphoethanolamine (DOPE),[50] and performing transfection experiments in the presence of chloroquine led to an expression of pCMV-Luc in endothelial cells comparable to that of b-PEI control (Figure 10.4).[49] A similar templating strategy was developed by Hagstrom and coworkers for the condensation of pDNA into particles of small size ($<$150 nm), which were able to induce luciferase expression in NIH/3T3 cells, with a 100-fold increase in gene expression when compared with similar complexes prepared from non-templated polymers.[51]

Low Mw peptides derived from Lys residues have been shown to be active gene delivery vectors, which can be optimized through controlled synthesis. In order to overcome some of their limitations, such as stability in blood, the group of Rice reported the preparation of reducible derivatives of tryptophan-lysine (Trp-Lys_{19}) that could condense pDNA and spontaneously oxidize to yield stable polyplexes,[52–55] in a similar fashion to the cationic lipids described by Behr and coworkers.[49] Several factors such as the number of cysteine (Cys),[52] length of the peptide,[53] the presence of histidine as a buffering residue to promote endosomal escape,[53] the strength of the S-S bond,[55] the presence of D-aminoacids[55] or the introduction of targeting ligands were investigated.[55] In general, reducible polyplexes were more stable against sonicative shear than those prepared with the parent compound, with increasing stability as a function of the number of cross-links, and polyplex sizes could be kept below 100 nm. Cys-Lys_4-Cys was the smallest peptide able to produce stable polyplexes with efficient transfection activity *in vitro*, while the presence of histidine residues allowed for transfection in the absence of chloroquine. Targeting to hepatocytes *in vivo* could be achieved using a combination of a cross-linkable peptide that incorporated a glycan as a targeting ligand, a PEGylated peptide and a backbone peptide. In addition, the half-life of DNA in the liver could be extended up to 2 h using a backbone peptide composed of D-amino acids.[55]

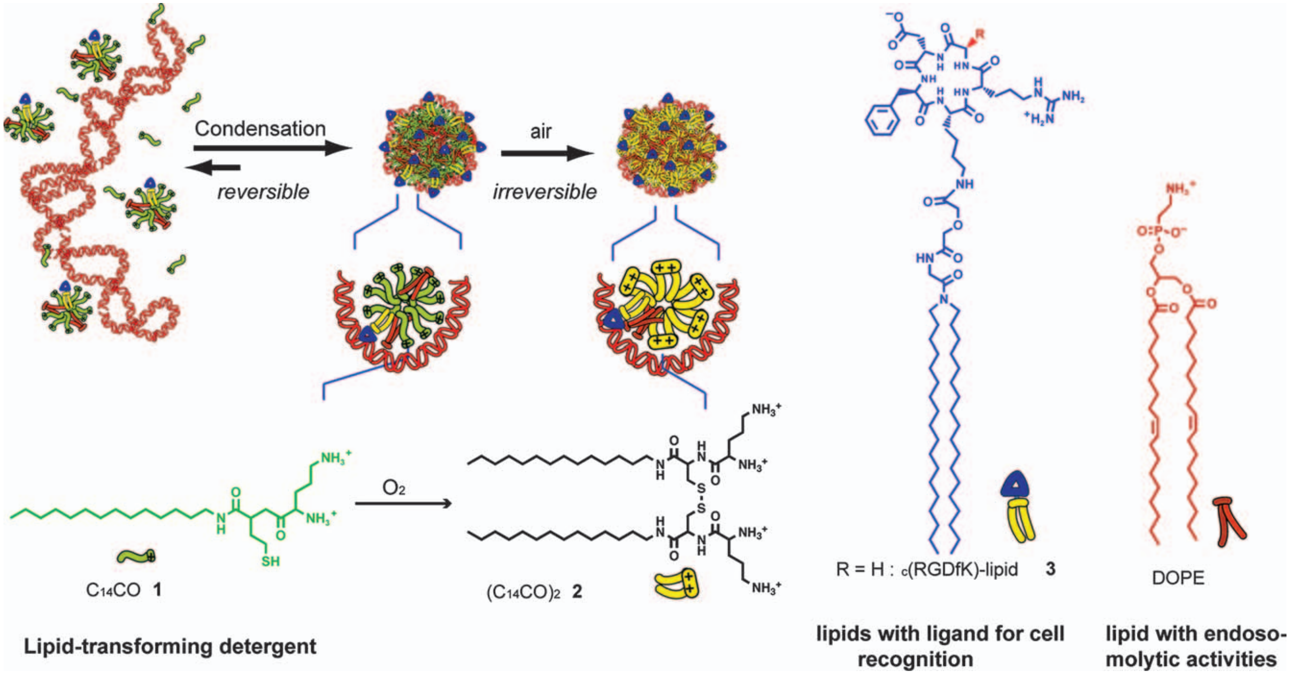
Condensation
reversible
air
irreversible
O2
C14CO 1
(C14CO)2 2
Lipid-transforming detergent
R = H : c(RGDfK)-lipid 3
DOPE
lipids with ligand for cell recognition
lipid with endosomolytic activities

Figure 10.4 Templated complexation of pDNA with 1 equivalent of cysteine-based cationic detergent (**1**) in the presence of DOPE and integrin-targeting lipid (**3**). Polyplexes are stabilized by oxidation of the detergent into a lipid-like molecule **2**, leading to stable and cRGD-decorated DNA complexes.
Adapted from Ref. 49. Copyright (2009) American Chemical Society.

A similar strategy has been employed by the groups of Preece and Seymour to produce reducible gene delivery vehicles. In this approach, using Cys-Lys$_{10}$-Cys as the parent peptide, linear reductively cleavable polycations (RPCs) were prepared in a first step by oxidative condensation, which were then used to complex pDNA at different N/P ratios.[56,57] Factors such as polymer length,[56] peptide length,[58] presence of histidine residues[58–60] and pK_a of the starting peptide[60] were thoroughly investigated (Figure 10.5). In all cases, the authors showed that the enhancement in gene expression by these RPCs is related to intra-cellular levels of glutathione, which is the major endogenous antioxidant produced by the cells, confirming the responsiveness of the materials. These systems are able to deliver not only pDNA but also siRNA,[58,59] which due to its smaller size and its mode of action requires gene vectors different from pDNA. Introducing histidine residues allows for transfection to be performed in the absence of reagents to facilitate endosomal escape such as cationic lipid 1,2-dioleoyl-3-trimethylammonium-propane (DOTAP) or chloroquinone. In order to produce neutral polyplexes with increased potential for *in vivo* applications, the authors coated some of the polyplexes with an amine reactive poly(2-hydroxypropylacrylamide) (pHPMA), introducing basic fibroblast growth factor (bFGF) to improve uptake by human retinoblastoma 911 cells.[56] Targeting can be performed alternatively using a peptide derived from *Plasmodium falciparum* circumporozoite protein, which is attached to the terminal end of the RPCs and allows not only for an increase in uptake, but for selectivity towards hepatocytes.[59] These peptidic RPCs have been recently described by Fabre *et al.*[61] as useful synthetic vectors to deliver pDNA to HUH-7 and HeLa cell lines and to

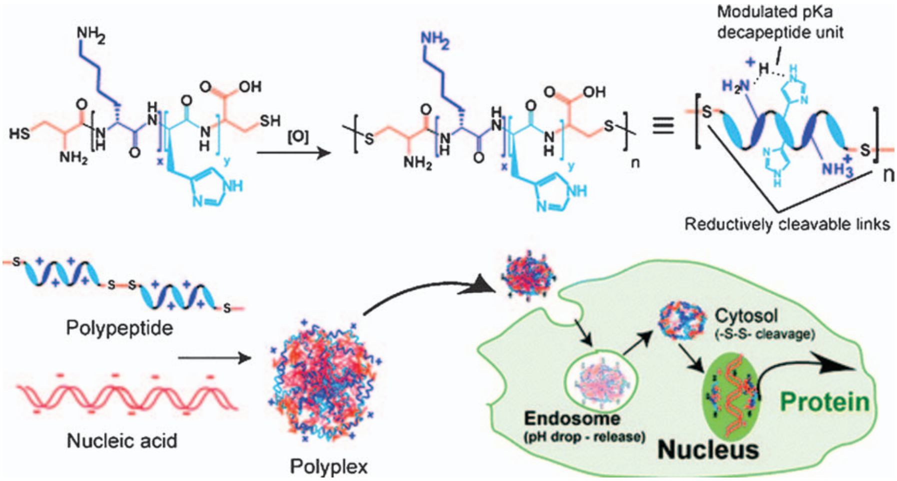

Figure 10.5 Structure of polypeptidic linear reducible cleavable polycation (RPC) vectors incorporating histidine residues for endosomal escape, and scheme of their response once internalized.
Reproduced from Ref. 60 with permission of The Royal Society of Chemistry.

post-mitotic rabbit corneal endothelial cells using luciferase as a reporter. PLL or non-reducible polyplexes were unstable in the presence of negatively charged fusogenic peptides based on the amino terminus of the hemmaglutinin subunit 2 (HA2) moiety of influenza virus hemagglutinin.[62,63] On the other hand, reducible polyplexes could be coated with these fusogenic peptides, leading to increased endosomal escape and higher transfections.

The group of Oupicky has reported a similar strategy to prepare polyplexes based on TAT-peptide, the amino acid residues 47–57 of the transactivating transcriptional activator protein from human immunodeficiency virus (HIV-1). This peptide has the ability to translocate across cell membranes in a receptor- and temperature-independent manner, making it a good candidate to investigate gene delivery vehicles.[64,65] Luciferase expression in B16F10, HeLa and EA.hy926 cell lines for TAT-based polyplexes was strongly dependent on the presence of chloroquine, suggesting uptake *via* an endosomal route and a reduced capacity to escape the endosome for these vectors when compared to b-PEI.[66] In a similar fashion, Oupicky and coworkers reported RPCs containing different ratios of a histidine-rich peptide and nuclear localization sequence peptide to modulate intra-cellular trafficking of transfected siRNA and primary RNA transcripts (pri-miRNA). This way, RNAs could be delivered to the nuclei with low toxicity.[67]

As described earlier, low Mw linear PEI (l-PEI, 800–2000 Da) has significantly fewer cytotoxic effects than high Mw b-PEI (f.i. 25 kDa), but its ability as gene delivery vector is limited, probably because of its reduced size, which leads to a lower capacity to compact NAs into well-defined polyplexes. In order to improve the potential of low Mw l-PEI, Lee and coworkers reported that cross-linking of l-PEI (800 Da) with reducible linkers (Figure 10.6) could increase its transfection efficiency in CHO cells, using pCMV-Luc as a reporter.[68] Transfection, depending on the cross-linking reagent, the extent of conjugation and the N/P ratio, could be increased up to similar levels compared to those of 25 kDa b-PEI, while retaining biocompatibility. In a related work, Goepferich *et al.*[69] reported cross-linking of l-PEI (2 kDa) using a similar strategy and evaluated its transfection efficiency across seven different cell lines using enhanced green fluorescent protein (EGFP) as a reporter. The same polymers were later employed to complex siRNA and reduce EGFP expression in CHO-K. Uptake of reducible polyplexes was lower than for b-PEI, but their responsiveness allowed for better transfection efficiencies.[70] A similar strategy has been recently employed by the group of Yeo to deliver pEGFP or pBR322 to NIH/3T3 and M109 cells lines.[71] Reducible cross-linked l-PEI (2.5 kDa) was able to condense pDNAs into small polyplexes (approx. 100 nm) that were coated with hyaluronic acid to yield neutral polyplexes with high transfection efficiencies in the presence of serum proteins.

In order to prepare synthetic gene delivery vectors with low toxicity a series of closely related polymers based on *N*,*N*′-cystaminebisacrylamide have been reported by the groups of Engbergsen, Wan Kim, Oupicky and Cho.[72–80] Michael addition of different primary amines to the acrylamide moieties in *N*,*N*′-cystaminebisacrylamide yielded reducible gene delivery vectors. This

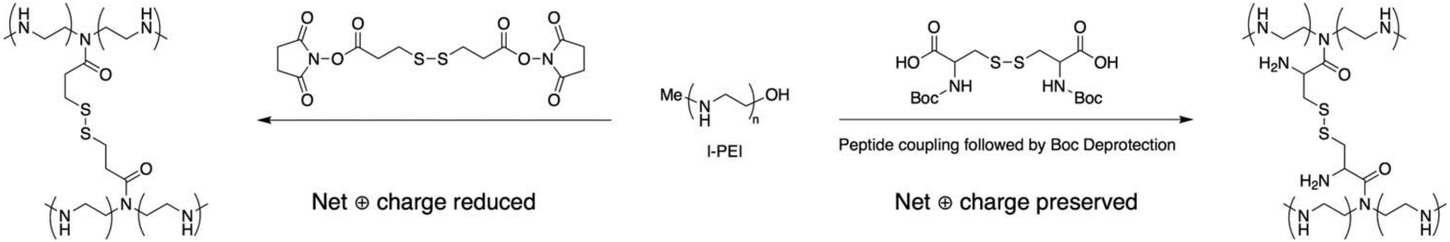
l-PEI
Peptide coupling followed by Boc Deprotection
Net ⊕ charge reduced
Net ⊕ charge preserved

Figure 10.6 Synthesis of reducible b-PEI using reducible cross-linkers.

approach can be easily modified and allows for the introduction of different functionalities, such as secondary amines and imidazoles with buffering capacities,[73–75,80] alcohols and ethers,[74] or aliphatic primary amines to increase DNA binding affinity.[76] Reducible polymers based on 1,6-diaminohexane were able to deliver prostaglandin E2 (PGE2)-modified siRNA promoting Fas gene silencing and inhibition of cardiomyocyte apoptosis *in vitro*,[77] while those based on spermine were able to deliver pEGFP to the lungs of ICR mice.[80]

For synthetic gene delivery vectors to be successful in the clinic, not only should they be stable towards polyion exchange and nucleases, but aggregation in the presence of serum proteins should be prevented. As described earlier, this can be achieved by using polyplexes with neutral or negative surface charge. The group of Kataoka proposed the application of double hydrophilic block copolymers incorporating a cationic block that can effectively induce complexation of negatively charged polymers such as pNAs, to form core-shell type polyplexes with a hydrophilic corona, also known as polyion complex (PIC) micelles. PEG was chosen as the hydrophilic corona based on its biocompatibility and low toxicity and, in this way, PIC micelles using PLL as the cationic polymer and pDNA were prepared.[81] In order to improve the stability of the polyplex towards the extra-cellular environment, and induce the release of the pDNA once internalized, the core of the polyplex was reversibly cross-linked using two different disulfide cross-linkers. Transfection was dependent on the degree of cross-linking, and PIC micelles from pDNA[82] or siRNA were reported.[83] Also, the authors showed that depending on the degree of cross-linking, a specific N/P ratio has to be chosen to get small well-defined polyplexes.[84] In order to promote uptake and enhance luciferase expression in HeLa cells, RGD peptides were conjugated to the surface of the PIC micelles.[85] Using VEGF as the targeting ligand, and choosing the right degree of cross-linking to allow enhanced stability and sustained release, antiangiogenic pDNA could be delivered *in vivo* to the tumor vasculature of a subcutaneous pancreatic tumor model implanted in Balb/c nude mice.[86]

Reducible linkers have also been described as useful moieties to promote removal of components that can limit transfection efficiency once polyplexes are internalized. Seymour *et al.*[87] reported coating of reducible polyplexes made from small l-PEI-based RPCs with p(HPMA) using a reducible bond. This way, the p(HPMA) corona was removed once internalized, leading to an increase in transfection of A549 cells with pGL3 when compared with a non-reducible coating. Kataoka and coworkers reported a similar strategy to conjugate PEG to a di(ethylene imine) derivative of p(Asp) *via* a reducible linker, and efficiently transfect HeLa cells with pGL3 luciferase reporter in the presence of serum and without the need of chloroquinone.[88]

Conjugation of small NAs, such as siRNA or antisense oligodeoxynucleotide (asODN), to PEG *via* a reducible linker can provide a way to improve their pharmacokinetic properties in a reversible manner. This was illustrated by the group of Kataoka with the conjugation of PEG to asODN (Figure 10.7), which was then complexed with b-PEI or PLL to yield PIC micelles with a removable PEG corona. These polyplexes were able to reduce luciferase expression in

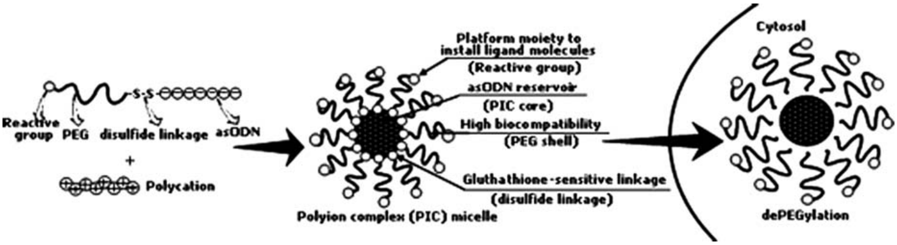

Figure 10.7 Schematic illustration of a reducible PIC micelle and some of its relevant properties for gene delivery.
Reproduced from Ref. 89. Copyright (2005) American Chemical Society.

HUH-7 cells to a greater extent than a non-reducible PEG-asODN-b-PEI polyplex.[89] Using a similar approach, the same group has recently reported reducible PEG-siRNA conjugates that were used to template the precipitation of calcium phosphate into well-defined nano-sized hybrid particles with similar effects in luciferase expression in HUH-7 cells.[90]

The group of Park has reported closely related polyelectrolyte complexes of reducible PEG-siRNA to knockdown VEGF expression.[91] Using b-PEI to complex the PEG-siRNA block copolymer, well-defined polyelectrolyte complexes micelles were produced that could provide protection for siRNA *in vivo*, without significant induction of siRNA-mediated immunostimulation. Passive targeting to the tumor site leads to successful suppression of tumor growth of prostate cancer cells in female mice.[92] Alternatively, KALA, an amphipathic peptide with endosomal disruptive properties,[93] was used to complex PEG-siRNA conjugates. Similar gene inhibition to that exhibited by b-PEI/siRNA could be observed with lower toxicity.[94] Additionally, using a KALA derivative modified with cysteine residues at both termini, RPCs were produced that could complex the reducible PEG-siRNA conjugates and yield polyplexes with increased stability against heparin, which was used as a model polyion.[95]

Because of its reduced size when compared with pDNA, polyplexes made with siRNa are more susceptible to exchange with large polyions leading to higher instability *in vivo*. Increasing the overall length of the siRNA by the introduction of overhangs[96] has been proposed to improve its stability. The groups of Kwon and Park independently reported the polymerization of thiol-modified double-stranded siRNAs as a way of reversibly increasing the molar mass of the siRNA without affecting its final properties.[97,98] Polymerized siRNA was complexed with b-PEI, resulting in polyplexes more stable against polyanion displacement and RNAses in serum. In addition, polyplexes made with reducible polymerized siRNA were able to induce greater gene knockdown in different cell lines.

A different way to increase reversibly the length of siRNA has been reported by Kataoka *et al.*[99] To produce multimeric siRNA, a thiol derivative was conjugated to the backbone of p(Asp) using a reducible linker, and then was complexed with a di(ethylene imine)-p(Asp) derivative, similar to that previously reported by the same group.[88] In such a way, molar mass was increased without the need to conjugate to an antisense strand, as in the previous two examples. These polyplexes showed a potent inhibition of luciferase expression in B16F10-Luc cells without cytotoxicity or immunogenicity.

10.4 Thermo-responsive Polyplexes

The application of temperature to control the delivery of NAs was first introduced by Yokoyama, Okano and others with the delivery of pDNA (pCMV-lacZ) to COS-1 cells by poly(*N*-isopropylacrylamide (NIPAAm)-co-2-(dimethylamino)ethyl methacrylate (DMAEMA)-co-butylmethacrylate (BMA).[100,101] The ability of random copolymers of NIPAAm and DMAEMA to complex pCMV-lacZ and deliver it to NIH/OVCAR-3 cells had already been reported by Hennink and coworkers,[102] but the effect of changing the temperature in transfection was not investigated at that point. In their work, Yokoyama *et al.*[103] introduced BMA as a comonomer in order to decrease the lower critical solution temperature (LCST) of the polymer to 21 °C, and to improve transfection efficiency. Transfection with thermo-responsive polyplexes showed increased β-galactosidase activity, when a hypothermic shock (3 h at 20 °C) was introduced halfway through the incubation of cells under normal conditions (37 °C) (Figure 10.8). This effect was not observed in the case of p(DMAEMA), which showed reduced transfection upon cooling, probably due to a lower metabolic activity at lower temperature. The authors also showed that the timing of the hypothermic shock was important, and an incubation time at 37 °C prior to lowering the temperature was needed, in order to prevent delivery of encapsulated pDNA before uptake of the polyplexes by the cells. It was also concluded that complexes formed at temperatures above

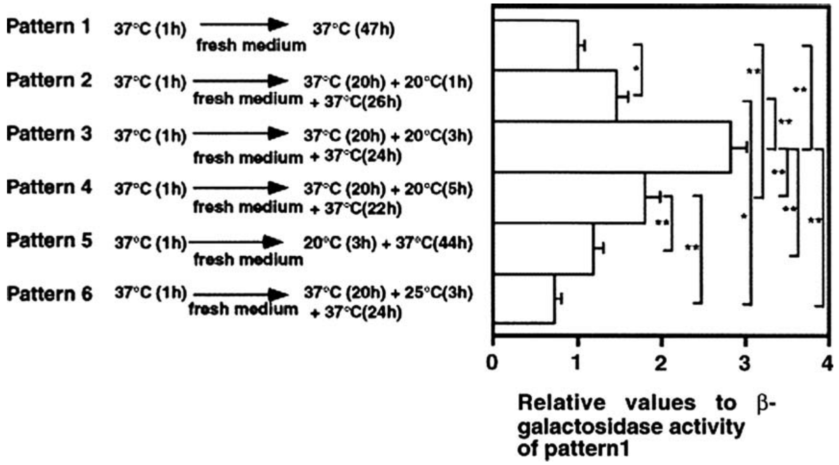

Figure 10.8 Effect of incubation temperature and temperature cycle on gene expression using p(NIPAAm-co-DMAEMA-co-BMA) as the gene vector. *P < 0.01, **P < 0.001.
Reproduced from Ref. 100 with permission of Elsevier.

the LCST increase transfection efficiency probably due to the formation of tighter complexes, which are taken up more efficiently by cells with a lower degree of enzymatic DNA degradation.

Thermo-responsive polymers have also been conjugated to PEI in order to reduce its toxicity and modulate gene transfection as a function of the temperature. For instance, the group of Pişkin reported the synthesis of PEI-*g*-pNIPAAm, by attaching acid-functionalized pNIPAAm to the terminal amine of PEI.[104] As PEI toxicity and transfection efficiency are known to depend on the Mw and branching of PEI, the authors modified 2 and 25 kDa b-PEI and 25 kDa l-PEI to yield polymers with LCSTs in the 35–40 °C range. While b-PEI (25 kDa) showed the best results in terms of uptake by HeLa cells of a green fluorescent expressing plasmid (pEGFP-N2), complexes prepared with l-PEI (25 kDa) showed the highest transfection efficiency without inducing significant toxicity. l-PEI-*g*-pNIPAAm was latter evaluated with smooth muscle cells, and its transfection efficiency improved by introducing a hypothermic shock (28 °C for 45 min) after an initial incubation at 37 °C. Preliminary *in vivo* evaluation of both b-PEI and l-PEI (25 kDa) polyplexes with 5-week old female nude mice revealed that, by cooling the injection area, the amount of GFP expressed subcutaneously could be increased.[105]

Polycationic systems of this class have been employed in order to understand what "design" elements govern efficiency in the delivery of DNA. For this purpose, a PEI-*g*-pNIPAAm derivative (LCST 32 °C) and several poly(DMAEMA-co-NIPAAm-co-hexyl acrylate (HA)) copolymers (LCST ranging from 22 to 50 °C) were prepared and compared to b-PEI (25 kDa).[106] Gel retardation experiments showed that, while b-PEI-*g*-pNIPAAm had a higher affinity for pX61 at temperatures higher than the LCST, high Mw p(DMAEMA-co-NIPAAm-co-HA) copolymer showed reduced affinity above the LCST. All polymers showed toxicity to C2C12 cells, but this toxicity was significantly reduced when the polymers were complexed with pX61 (N/P 2–4), except in the case of the high Mw p(DMAEMA-co-NIPAAm-co-HA) copolymer.[107] In addition, all polymers were able to promote fast uptake of YOYO-1 labeled pX61, but only b-PEI-*g*-pNIPAAm was efficient in transfecting a plasmid encoding GFP in this cell line. This complex showed enhanced GFP expression when a period of 1 h transfection below the LCST was introduced, in agreement with Pişkin's and Yokoyama's observations.[103–105]

Lower molar mass NA such as ODN or siRNA can be synthetically prepared, which allows for covalent conjugation as an alternative for polyplex preparation. This was the strategy taken up by Maeda *et al.*[108,109] for the delivery of a synthesized ODN containing the antisense sequence for the ribosomal binding site of the mRNA encoding EGFP. 3′- and 3′,5′-Methacryloyl-modified ODNs were independently copolymerized with NIPAAm (1 : 4000 ratio) and antisense activity evaluated as a function of temperature. Interestingly, the copolymers were unable to inhibit the expression of EGFP unless the temperature was decreased to below the LCST of the polymer (33 °C, assay performed at 27 °C). It was proposed by the authors that the polymer would collapse above the LCST shielding the ODN and preventing the ribosome from binding to the antisense sequence. In addition, 3′,5′ derivatives provided a better shielding and protected ODN from nucleases at 37 °C.

All of these examples show the potential that thermo-responsive gene delivery vehicles have for the smart delivery of NAs. However, they all rely on local hypothermia, which is difficult to achieve *in vivo* with high spatial resolution. On the other hand, locoregional hyperthermia, that is, the local increase of the temperature in a target tissue, is an approved method to improve drug delivery, especially in tumors.[20,21] Selective heating of the tissue, among other effects, increases the blood flow and the permeability of the area allowing for the extravasation of macromolecules. It was reasoned by Wagner and coworkers that, by designing PEI-*g*-PNIPAAm copolymers with LCSTs between 37 and 42 °C, improved transfection efficiencies should be obtained, without the induction of hyperthermic associated toxicity. By applying short hyperthermic cycles (30 min at 42 °C followed by 30 min at 37 °C, up to four cycles) luciferase expression in Neuro2A cells could be enhanced almost two orders of magnitude when compared to cells transfected at physiological temperature.[110] The authors showed that hyperthermic shock had a bigger impact in transfection when applied during incubation, with marginal effect on the uptake of the polyplexes. Based on these observations, the authors suggested that thermo-responsive polyplexes were probably taken up as larger particles when the temperature was increased, in agreement with the aggregation experiments done in the absence of cells. These larger aggregates led to bigger quantities of PEI trapped in the endosome, so that endosomal disruption by the proton sponge effect was more likely to happen, leading to higher transfection. Similar effects were observed in A/J mice bearing a syngeneic Neuro2A neuroblastoma tumor subcutaneously.[111] Hyperthermic treatment of the tumors right after intra-peritoneal injection of the polyplexes improved pDNA accumulation in the tumor tissue, improved luciferase expression and, interestingly, improved selectivity towards the tumors, for those thermo-responsive polyplexes. However, these polyplexes still showed reduced gene expression when compared to PEI complexes, probably arising from the fact that they tend to form irreversible aggregates with sizes in the μm range. Therefore, they accumulate in the tumor vessels, but are not as likely to diffuse into the tumor tissue.

While some of these reports approach thermo-responsive delivery of NAs in a variety of ways, several common conclusions can be drawn (Figure 10.9): i) preparing thermo-responsive polyplexes above the LCST provides tighter complexes and improved shielding of the complexed NAs; ii) temperature above LCST seems to have a positive effect on thermo-responsive polyplexes uptake, probably by promoting passive endocytosis of larger particles, and increasing the amount of polycation "loaded" into the endosome; and iii) incubation of thermo-responsive polyplexes within cells at temperatures below the LCST provides a mean to weaken NA-polymer interactions within the endosome. As a result, polycations are able to act as proton sponges, leading to endosomal disruption and allowing endosomal escape. In addition, weaker NA-polymer interactions are expected to lead to higher accessibility for transcription enzymes.

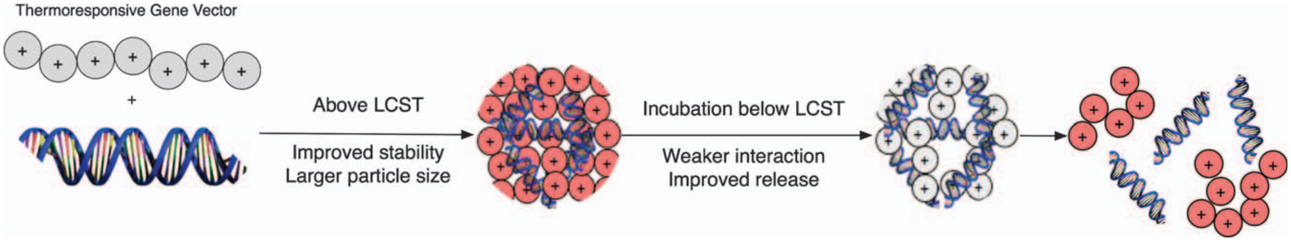
Thermoresponsive Gene Vector
+
Above LCST
Improved stability
Larger particle size
Incubation below LCST
Weaker interaction
Improved release

Figure 10.9 Schematic view of the mode of action of thermo-responsive polyplexes.

Following these principles, other polycationic carriers such as chitosan,[112,113] polyarginine[114] and thermo-responsive polymers such as pluronics[115,116] or poly([2-(2-methoxyethoxy)ethyl methacrylate] copolymers[117,118] have also been investigated.

10.5 Other Stimuli-responsive Polyplexes

The group of Rotello developed a light-regulated system to release DNA in mouse embryonic cells.[119] Positively charged dimethylethylammonium moieties were conjugated to the surface of the nanoparticles using an *o*-nitrobenzyl ester linkage. *o*-Nitrobenzyl ester is a biocompatible photolabile group, that has long-term stability under ambient light, but can be removed quickly and efficiently by UV light (>350 nm) with low side effects on biological systems.[120,121] This way, the surface charge of the nanoparticles could be changed to negative, leading to destabilization of the DNA-nanoparticle complex and release of the DNA (Figure 10.10).

Using light cleavable (6-nitropiperonyloxymethyl)-caged thymidine residues,[122] a masking strategy was developed by Dieters *et al.*[123] to control luciferase expression in mouse fibroblasts. A phosphorothioate DNA antisense agent, previously reported to target the *Renilla* luciferase reporter gene,[124] was modified with three or four light-responsive phosphorothioates, and luciferase expression in NIH or 3T3 mouse fibroblasts measured before and after brief UV irradiation at 365 nm. Luciferase expression was significantly reduced for those antisense DNAs with cleavable residues and spatial control over gene expression could be achieved.

A different response to light was investigated by Lee and coworkers in the delivery of asODNs to block expression of EGFR2 in breast carcinoma cells.[125] asODNs were hybridized onto ODNs immobilized on the surface of gold nanorods. Controlling the aspect ratio (3.5) the absorption of gold nanorods could be tuned to the near infrared (NIR) wavelength range

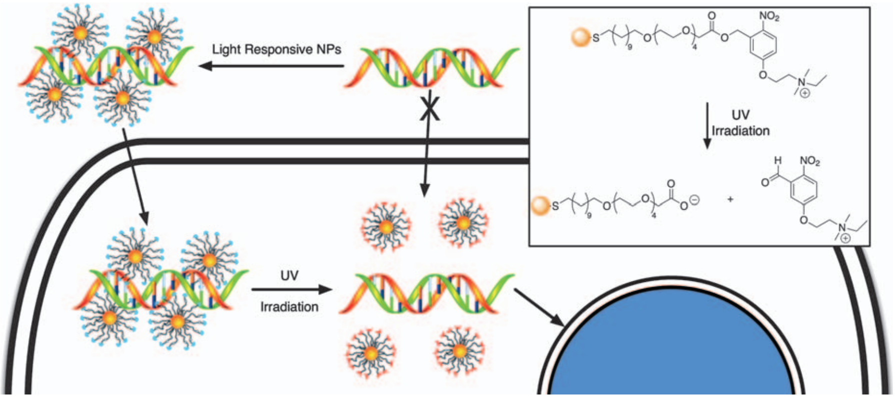

Figure 10.10 Schematic illustration of the release of DNA from light-responsive nanoparticles upon UV irradiation within the cell. The insert shows a scheme of light-induced charge inversion on the surface of the nanoparticles. Adapted from Ref. 119 with permission of Elsevier.

(758 nm) so that upon excitation of the particles with a laser, minimal disruption of the carcinoma cells was caused. Local heating around the gold nanorods during laser excitation triggered melting of the dsODN and release of the asODN in a spatially controlled fashion. A similar strategy was employed by Reich *et al.*[126] for the knockdown of GFP expression in mouse endothelial cells C166-GFP. In this case, dsRNA was immobilized onto 40 nm gold nanoparticles, and then coated with a TAT-modified lipid, in order to improve uptake and endosomal escape. The S-Au bond is cleaved upon laser excitation at 800 nm, leading to the release of the RNA and efficient gene inhibition with spatial control.

10.6 Dual Responsive Polyplexes

Possibly the best approach to achieve virus-like behavior, and therefore similar transfection efficiencies to viral systems, is the combination of more than one stimulus in the delivery of NAs. In this regard, Rozema and coworkers reported the combination of pH and reducible stimuli for the delivery of siRNA to hepatocytes *in vivo*;[127] namely, conjugation of siRNA to the backbone of an amphipathic poly(vinyl ether) *via* a disulfide bond. The primary amines in the polymer backbone were masked using a PEGylated carboxy dimethylmaleic anhydride, to increase circulation time, and an *N*-acetylgalactosamine carboxy dimethylmaleic anhydride derivative, to improve hepatocyte targeting. As a consequence, the activity of the polymer was masked until it reached the endosome, where pH-sensitive maleic amides degraded, promoting endosomal escape and the delivery of the siRNA under the reducing conditions in the cytosol. The efficiency of gene knockdown was assessed using two endogenous genes in mouse liver, apolipoprotein B (*apoB*) and peroxisome proliferator-activated receptor alpha (*ppara*), leading to clear phenotypic changes such as reduction in serum cholesterol by *apoB* knockdown, and significant increase in serum triglycerides after delivery of *ppara* siRNA polyconjugate. A similar strategy was employed by Wagner *et al.*[128] for the delivery of siRNA to Neuro2A-eGFPLuc cells. In this case, melittin was conjugated to a PEGylated polycation (PLL or PEI) *via* a reducible linker and its membrane activity masked using maleic amides. This way, luciferase expression could be efficiently inhibited even in the case of PLL, which has no endosomal activity on its own.

The synthesis of virus-like particles that incorporate pH-sensitive and reducible moieties for the delivery of pDNA (gWIZ-Luc) *in vitro* has recently been reported.[129] Reducible polyplexes made from peptidic RPCs were coated with pH-responsive polymers, bearing acetal linkers (Figure 10.11).[60] Once internalized by A549 and bEND.3 cells, pH-sensitive coatings were degraded leading to increased luciferase expression when compared to non-pH-sensitive coated polyplexes. This approach proved highly modular, with the ability to tune peptide affinity towards DNA and their endosomal activity, the stability of the pH-sensitive coating or the introduction of targeting ligands to improve uptake, opening the path to gene delivery vectors with viral-mimetic activity. A similar strategy has recently been

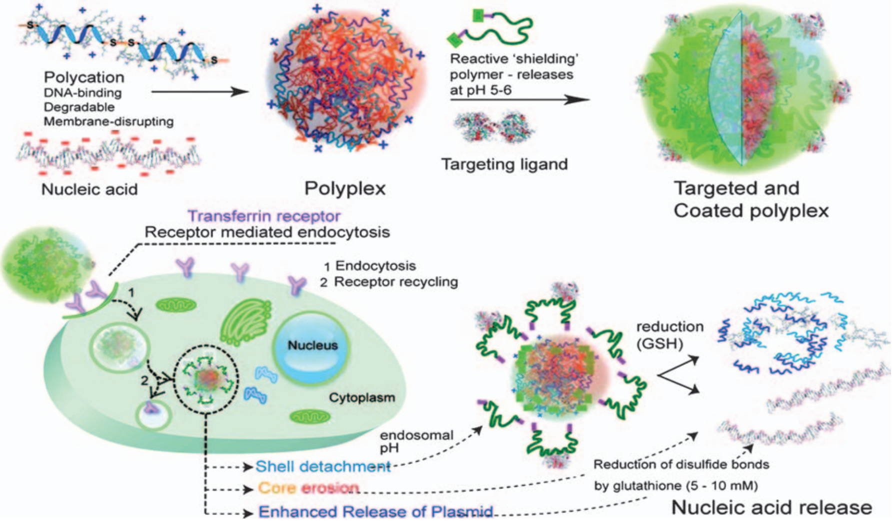
Polycation
DNA-binding
Degradable
Membrane-disrupting
Nucleic acid
Polyplex
Reactive 'shielding' polymer - releases at pH 5-6
Targeting ligand
Targeted and Coated polyplex
Transferrin receptor
Receptor mediated endocytosis
1 Endocytosis
2 Receptor recycling
1
2
Nucleus
Cytoplasm
reduction (GSH)
endosomal pH
Shell detachment
Core erosion
Enhanced Release of Plasmid
Reduction of disulfide bonds by glutathione (5 - 10 mM)
Nucleic acid release

Figure 10.11 Schematic view of reducible polyplexes with pH-cleavable coatings. Reproduced from Ref. 129. Copyright (2012) American Chemical Society.

described by Shi and coworkers for the delivery of pDNA to 293T cells *in vitro*.[130] Lys_{15} peptides were PEGylated *via* a reducible linker, and the resulting conjugates cross-linked with glutaraldehyde. The imine cross-linked polyplexes could be degraded under the acidic conditions of the endosome, leading to transfection efficiencies similar to b-PEI, as measured using a luciferase and a GFP reporter.

10.7 Conclusions

In this chapter we have selected some examples that demonstrate the breadth and depth of studies into bioresponsive polyelectrolyte complexes for nucleic acid delivery. There has been considerable progress in refining the chemistries of these systems to respond to a variety of biological stimuli, and similar improvements in pharmaceutical formulation strategies such that nucleic acids can be packaged and released with high efficiency. At the same time, there have been advances in the study of biological pathways and processing mechanisms and, although the details of trafficking routes such as those leading from endosomal uptake through to cytosolic release are still not completely understood, there is nevertheless much new insight from which pharmaceutical scientists can gain inspiration. It should be stressed that, at present, none of the bioresponsive polyplexes described can outperform viral gene vectors in terms of improved transfection efficiency, although synthetic systems do have the advantage of non-infectivity. Improved understanding of the mechanisms by which these new gene carriers operate will greatly facilitate the design of "next-generation" materials, which combine the design-in properties of synthetic systems with improved transfection, and perhaps scale-up to practical use in the clinic.

Cell Lines Mentioned in this Chapter

Organism	*Designation*	*Details*
Human	293T	Kidney Epithelial
Human	911	Retinoblastoma
Human	A2780	Ovarian Epithelial Carcinoma
Human	A549	Epithelial Lung Carcinoma
Human	EA.hy926	Endothelial
Human	HeLa	Cervical Epithelial Carcinoma
Human	HUH-7	Hepato Cellular Carcinoma
Human	HUVEC	Endothelial
Human	K562	Erythromyeloblastoid Leukemia
Human	NIH/OVCAR-3	Endothelial Ovariy adenocarcinoma
Mouse	B16F10	Epithelial Melanoma
Mouse	bEND.3	Brain endothelioma
Mouse	BNL Cl.2	Hepatocytes
Mouse	C166	Endothelial
Mouse	C2C12	Muscle Myoblast
Mouse	CHO-K	Ovarian Epithelial
Mouse	M109	Lung Carncinoma
Mouse	Neuro2	Neuroblastoma
Mouse	Neuro2A	Neuroblastoma
Mouse	NIH/3T3	Fibroblast
Mouse	Renca	Renal Cortical Adenocarcinoma
Rat	A7R5	Muscle Fibroblast

References

1. J. P. Magnusson, A. O. Saeed, F. Fernández-Trillo and C. Alexander, *Polym. Chem.*, 2010, **2**, 48.
2. S. Li and L. Huang, *Gene Ther.*, 2000, **7**, 31.
3. K. Taira, K. Kataoka and T. Niidome, ed., *Non-viral Gene Therapy*, Springer Verlag, Heidelberg, 2005.
4. C. Dufès, I. F. Uchegbu and A. G. Schatzlein, *Adv. Drug Deliver. Rev.*, 2005, **57**, 2177.
5. M. E. Martin and K. G. Rice, *AAPS J.*, 2007, **9**, E18.
6. S. Y. Wong, J. M. Pelet and D. Putnam, *Progr. Polym. Sci.*, 2007, **32**, 799.
7. D. N. Nguyen, J. J. Green, J. M. Chan, R. Langer and D. G. Anderson, *Adv. Mater.*, 2009, **21**, 847.
8. J. Nguyen and F. C. Szoka, *Acc. Chem. Res.*, 2012, **45**, 1153–1162.
9. Y. T. A. Chim, J. K. W. Lam, Y. Ma, S. P. Armes, A. L. Lewis, C. J. Roberts, S. Stolnik, S. J. B. Tendler and M. C. Davies, *Langmuir*, 2005, **21**, 3591.
10. P. R. Dash, M. L. Read, L. B. Barrett, M. A. Wolfert and L. W. Seymour, *Gene Ther.*, 1999, **6**, 643.
11. S. Li and L. Huang, *Gene Ther.*, 1997, **4**, 891.
12. O. Boussif, F. Lezoualc'h, M. A. Zanta, M. D. Mergny, D. Scherman, B. Demeneix and J. P. Behr, *P. Natl Acad. Sci. USA*, 1995, **92**, 7297.

13. D. A. Tomalia, H. Baker, J. Dewald, M. Hall, G. Kallos, S. Martin, J. Roeck, J. Ryder and P. Smith, *Polym. J.*, 1984, **17**, 117.
14. J. F. Kukowska-Latallo, A. U. Bielinska, J. Johnson, R. Spindler, D. A. Tomalia and J. R. Baker, *P. Natl Acad. Sci. USA*, 1996, **93**, 4897.
15. J. Y. Cherng, P. van de Wetering, H. Talsma, D. J. A. Crommelin and W. E. Hennink, *Pharm. Res.*, 1996, **13**, 1038.
16. P. van de Wetering, J. Y. Cherng, H. Talsma and W. E. Hennink, *J. Control. Release*, 1997, **49**, 59.
17. C. Pichon, C. Gonçalves and P. Midoux, *Adv. Drug Deliver. Rev.*, 2001, **53**, 75.
18. J. P. Behr, *Chimia*, 1997, **51**, 34.
19. A. Meister and M. E. Anderson, *Annu. Rev. Biochem.*, 1983, **52**, 711.
20. H. D. Suit and M. Shwayder, *Cancer*, 1974, **34**, 122.
21. E. D. Hager, in *Hyperthermia in Cancer Treatment: A Primer*, ed. G. F. Baronzio and E. D. Hager, Springer, Boston, MA, 2006, p. 167.
22. J. H. Jeong, S. W. Kim and T. G. Park, *Bioconjugate Chem.*, 2003, **14**, 473.
23. M. Oishi, S. Sasaki, Y. Nagasaki and K. Kataoka, *Biomacromolecules*, 2003, **4**, 1426.
24. M. Oishi, F. Nagatsugi, S. Sasaki, Y. Nagasaki and K. Kataoka, *ChemBioChem*, 2005, **6**, 718.
25. M. Oishi, Y. Nagasaki, K. Itaka, N. Nishiyama and K. Kataoka, *J. Am. Chem. Soc.*, 2005, **127**, 1624.
26. M. Oishi, Y. Nagasaki, N. Nishiyama, K. Itaka, M. Takagi, A. Shimamoto, Y. Furuichi and K. Kataoka, *ChemMedChem*, 2007, **2**, 1290.
27. L. Zhu, Z. Ye, K. Cheng, D. D. Miller and R. I. Mahato, *Bioconjugate Chem.*, 2008, **19**, 290.
28. G. F. Walker, C. Fella, J. Pelisek, J. Fahrmeir, S. Boeckle, M. Ogris and E. Wagner, *Mol. Ther.*, 2005, **11**, 418.
29. M. P. Xiong, Y. Bae, S. Fukushima, M. L. Forrest, N. Nishiyama, K. Kataoka and G. S. Kwon, *ChemMedChem*, 2007, **2**, 1321.
30. V. Knorr, L. Allmendinger, G. F. Walker, F. F. Paintner and E. Wagner, *Bioconjugate Chem.*, 2007, **18**, 1218.
31. S. Lin, F. Du, Y. Wang, S. Ji, D. Liang, L. Yu and Z. Li, *Biomacromolecules*, 2008, **9**, 109.
32. S. Carmona, M. R. Jorgensen, S. Kolli, C. Crowther, F. H. Salazar, P. L. Marion, M. Fujino, Y. Natori, M. Thanou, P. Arbuthnot and A. D. Miller, *Mol. Pharmaceut.*, 2009, **6**, 706.
33. V. A. Sethuraman, K. Na and Y. H. Bae, *Biomacromolecules*, 2006, **7**, 64.
34. S. I. Kang and Y. H. Bae, *J. Control. Release*, 2002, **80**, 145.
35. Y. Lee, K. Miyata, M. Oba, T. Ishii, S. Fukushima, M. Han, H. Koyama, N. Nishiyama and K. Kataoka, *Angew. Chem. Int. Ed.*, 2008, **47**, 5163.
36. S. M. Moghimi, P. Symonds, J. C. Murray, A. C. Hunter, G. Debska and A. Szewczyk, *Mol. Ther.*, 2005, **11**, 990.
37. L. Parhamifar, A. K. Larsen, A. C. Hunter, T. L. Andresen and S. M. Moghimi, *Soft Matter*, 2010, **6**, 4001.

38. A. Kichler, *J. Gene Med.*, 2004, **6**, S3.
39. Y. H. Kim, J. H. Park, M. Lee, Y. H. Kim, T. G. Park and S. W. Kim, *J. Control. Release*, 2005, **103**, 209.
40. V. Knorr, V. Russ, L. Allmendinger, M. Ogris and E. Wagner, *Bioconjugate Chem.*, 2008, **19**, 1625.
41. M. S. Shim and Y. J. Kwon, *Biomacromolecules*, 2008, **9**, 444.
42. M. S. Shim and Y. J. Kwon, *Bioconjugate Chem.*, 2009, **20**, 488.
43. M. S. Shim and Y. J. Kwon, *J. Control. Release*, 2009, **133**, 206.
44. D. B. Rozema, K. Ekena, D. L. Lewis, A. G. Loomis and J. A. Wolff, *Bioconjugate Chem.*, 2003, **14**, 51.
45. T. Blessing, J. S. Remy and J. P. Behr, *P. Natl Acad. Sci. USA*, 1998, **95**, 1427.
46. E. Dauty, J. S. Remy, T. Blessing and J. P. Behr, *J. Am. Chem. Soc.*, 2001, **123**, 9227.
47. E. Dauty, J. S. Remy, G. Zuber and J. P. Behr, *Bioconjugate Chem.*, 2002, **13**, 831.
48. G. Zuber, L. Zammut-Italiano, E. Dauty and J. P. Behr, *Angew. Chem. Int. Ed. Engl.*, 2003, **42**, 2666.
49. G. Zuber, M. Dontenwill and J. P. Behr, *Mol. Pharmaceut.*, 2009, **6**, 1544.
50. I. M. Hafez, N. Maurer and P. R. Cullis, *Gene Ther.*, 2001, **8**, 1188.
51. V. S. Trubetskoy, V. G. Budker, L. J. Hanson, P. M. Slattum, J. A. Wolff and J. E. Hagstrom, *Nucleic Acids Res.*, 1998, **26**, 4178.
52. D. L. McKenzie, K. Y. Kwok and K. G. Rice, *J. Biol. Chem.*, 2000, **275**, 9970.
53. D. L. McKenzie, E. Smiley, K. Y. Kwok and K. G. Rice, *Bioconjugate Chem.*, 2000, **11**, 901.
54. Y. Park, K. Y. Kwok, C. Boukarim and K. G. Rice, *Bioconjugate Chem.*, 2002, **13**, 232.
55. K. Y. Kwok, Y. Park, Y. Yang, D. L. McKenzie, Y. Liu and K. G. Rice, *J. Pharm. Sci.*, 2003, **92**, 1174.
56. D. Oupicky, A. L. Parker and L. W. Seymour, *J. Am. Chem. Soc.*, 2002, **124**, 8.
57. M. L. Read, K. H. Bremner, D. Oupicky, N. K. Green, P. F. Searle and L. W. Seymour, *J. Gene Med.*, 2003, **5**, 232.
58. M. L. Read, S. Singh, Z. Ahmed, M. Stevenson, S. S. Briggs, D. Oupicky, L. B. Barrett, R. Spice, M. Kendall, M. Berry, J. A. Preece, A. Logan and L. W. Seymour, *Nucleic Acids Res.*, 2005, **33**, e86.
59. M. Stevenson, V. Ramos-Perez, S. Singh, M. Soliman, J. A. Preece, S. S. Briggs, M. L. Read and L. W. Seymour, *J. Control. Release*, 2008, **130**, 46.
60. R. Nasanit, P. Iqbal, M. Soliman, N. Spencer, S. Allen, M. C. Davies, S. S. Briggs, L. W. Seymour, J. A. Preece and C. Alexander, *Mol. BioSyst.*, 2008, **4**, 741.
61. A. L. Parker, L. Eckley, S. Singh, J. A. Preece, L. Collins and J. W. Fabre, *BBA-Gen. Subjects*, 2007, **1770**, 1331.

62. J. D. Lear and W. F. DeGrado, *J. Biol. Chem.*, 1987, **262**, 6500.
63. D. V. Zhelev, N. Stoicheva, P. Scherrer and D. Needham, *Biophys. J.*, 2001, **81**, 285.
64. S. Ruben, A. Perkins, R. Purcell, K. Joung, R. Sia, R. Burghoff, W. A. Haseltine and C. A. Rosen, *J. Virol.*, 1989, **63**, 1.
65. C. Rudolph, C. Plank, J. Lausier, U. Schillinger, R. H. Müller and J. Rosenecker, *J. Biol. Chem.*, 2003, **278**, 11411.
66. D. Soundara Manickam, H. S. Bisht, L. Wan, G. Mao and D. Oupicky, *J. Control. Release*, 2005, **102**, 293.
67. U. L. Rahbek, K. A. Howard, D. Oupicky, D. S. Manickam, M. Dong, A. F. Nielsen, T. B. Hansen, F. Besenbacher and J. Kjems, *J. Gene Med.*, 2008, **10**, 81.
68. M. A. Gosselin, W. Guo and R. J. Lee, *Bioconjugate Chem.*, 2001, **12**, 989.
69. M. Breunig, U. Lungwitz, R. Liebl and A. Goepferich, *P. Natl Acad. Sci. USA*, 2007, **104**, 14454.
70. M. Breunig, C. Hozsa, U. Lungwitz, K. Watanabe, I. Umeda, H. Kato and A. Goepferich, *J. Control. Release*, 2008, **130**, 57.
71. P. Xu, G. K. Quick and Y. Yeo, *Biomaterials*, 2009, **30**, 5834.
72. L. V. Christensen, C. W. Chang, W. J. Kim, S. W. Kim, Z. Zhong, C. Lin, J. F. J. Engbersen and J. Feijen, *Bioconjugate Chem.*, 2006, **17**, 1233.
73. C. Lin, Z. Zhong, M. C. Lok, X. Jiang, W. E. Hennink, J. Feijen and J. F. J. Engbersen, *J. Control. Release*, 2006, **116**, 130.
74. C. Lin, Z. Zhong, M. C. Lok, X. Jiang, W. E. Hennink, J. Feijen and J. F. J. Engbersen, *Bioconjugate Chem.*, 2007, **18**, 138.
75. J. Hoon Jeong, L. V. Christensen, J. W. Yockman, Z. Zhong, J. F. J. Engbersen, W. Jong Kim, J. Feijen and S. Wan Kim, *Biomaterials*, 2007, **28**, 1912.
76. M. Ou, X. L. Wang, R. Xu, C. W. Chang, D. A. Bull and S. W. Kim, *Bioconjugate Chem.*, 2008, **19**, 626.
77. S. H. Kim, J. H. Jeong, M. Ou, J. W. Yockman, S. W. Kim and D. A. Bull, *Biomaterials*, 2008, **29**, 4439.
78. S. H. Kim, J. H. Jeong, T. I. Kim, S. W. Kim and D. A. Bull, *Mol. Pharmaceut.*, 2009, **6**, 718.
79. J. Chen, C. Wu and D. Oupicky, *Biomacromolecules*, 2009, **10**, 2921.
80. D. Jere, J. E. Kim, R. Arote, H. L. Jiang, Y. K. Kim, Y. J. Choi, C. H. Yun, M. H. Cho and C. S. Cho, *Biomaterials*, 2009, **30**, 1635.
81. S. Katayose and K. Kataoka, *Bioconjugate Chem.*, 1997, **8**, 702.
82. K. Miyata, Y. Kakizawa, N. Nishiyama, A. Harada, Y. Yamasaki, H. Koyama and K. Kataoka, *J. Am. Chem. Soc.*, 2004, **126**, 2355.
83. Y. Kakizawa, A. Harada and K. Kataoka, *Biomacromolecules*, 2001, **2**, 491.
84. S. Matsumoto, R. J. Christie, N. Nishiyama, K. Miyata, A. Ishii, M. Oba, H. Koyama, Y. Yamasaki and K. Kataoka, *Biomacromolecules*, 2009, **10**, 119.

85. M. Oba, K. Aoyagi, K. Miyata, Y. Matsumoto, K. Itaka, N. Nishiyama, Y. Yamasaki, H. Koyama and K. Kataoka, *Mol. Pharmaceut.*, 2008, **5**, 1080.
86. M. Oba, Y. Vachutinsky, K. Miyata, M. R. Kano, S. Ikeda, N. Nishiyama, K. Itaka, K. Miyazono, H. Koyama and K. Kataoka, *Mol. Pharmaceut.*, 2010, **7**, 501.
87. R. C. Carlisle, T. Etrych, S. S. Briggs, J. A. Preece, K. Ulbrich and L. W. Seymour, *J. Gene Med.*, 2004, **6**, 337.
88. S. Takae, K. Miyata, M. Oba, T. Ishii, N. Nishiyama, K. Itaka, Y. Yamasaki, H. Koyama and K. Kataoka, *J. Am. Chem. Soc.*, 2008, **130**, 6001.
89. M. Oishi, T. Hayama, Y. Akiyama, S. Takae, A. Harada, Y. Yamasaki, F. Nagatsugi, S. Sasaki, Y. Nagasaki and K. Kataoka, *Biomacromolecules*, 2005, **6**, 2449.
90. M. Zhang, A. Ishii, N. Nishiyama, S. Matsumoto, T. Ishii, Y. Yamasaki and K. Kataoka, *Adv. Mater.*, 2009, **21**, 3520.
91. S. H. Kim, J. H. Jeong, S. H. Lee, S. W. Kim and T. G. Park, *J. Control. Release*, 2006, **116**, 123.
92. S. H. Kim, J. H. Jeong, S. H. Lee, S. W. Kim and T. G. Park, *J. Control. Release*, 2008, **129**, 107.
93. T. B. Wyman, F. Nicol, O. Zelphati, P. V. Scaria, C. Plank and F. C. Szoka, *Biochemistry*, 1997, **36**, 3008.
94. S. H. Lee, S. H. Kim and T. G. Park, *Biochem. Bioph. Res. Co.*, 2007, **357**, 511.
95. H. Mok and T. G. Park, *Biopolymers*, 2008, **89**, 881.
96. A. L. Bolcato-Bellemin, M. E. Bonnet, G. Creusat, P. Erbacher and J. P. Behr, *P. Natl Acad. Sci. USA*, 2007, **104**, 16050.
97. S. Y. Lee, M. S. Huh, S. Lee, S. J. Lee, H. Chung, J. H. Park, Y. K. Oh, K. Choi, K. Kim and I. C. Kwon, *J. Control. Release*, 2010, **141**, 339.
98. H. Mok, S. H. Lee, J. W. Park and T. G. Park, *Nat. Mater.*, 2010, **9**, 272.
99. H. Takemoto, A. Ishii, K. Miyata, M. Nakanishi, M. Oba, T. Ishii, Y. Yamasaki, N. Nishiyama and K. Kataoka, *Biomaterials*, 2010, **31**, 8097.
100. M. Kurisawa, M. Yokoyama and T. Okano, *J. Control. Release*, 2000, **69**, 127.
101. M. Yokoyama, M. Kurisawa and T. Okano, *J. Artif. Organs*, 2001, **4**, 138.
102. W. L. Hinrichs, N. M. Schuurmans-Nieuwenbroek, P. van de Wetering and W. E. Hennink, *J. Control. Release*, 1999, **60**, 249.
103. M. Kurisawa, M. Yokoyama and T. Okano, *J. Control. Release*, 2000, **68**, 1.
104. M. Türk, S. Dinçer, I. G. Yuluğ and E. Pişkin, *J. Control. Release*, 2004, **96**, 325.
105. M. Türk, S. Dinçer and E. Pişkin, *J. Tissue Eng. Regener. Med.*, 2007, **1**, 377.

106. B. R. Twaites, C. de Las Heras Alarcón, D. Cunliffe, M. Lavigne, S. Pennadam, J. R. Smith, D. C. Górecki and C. Alexander, *J. Control. Release*, 2004, **97**, 551.
107. B. R. Twaites, C. de Las Heras Alarcón, M. Lavigne, A. Saulnier, S. S. Pennadam, D. Cunliffe, D. C. Górecki and C. Alexander, *J. Control. Release*, 2005, **108**, 472.
108. M. Murata, W. Kaku, T. Anada, Y. Sato, M. Maeda and Y. Katayama, *Chem. Lett.*, 2003, **32**, 986.
109. M. Murata, W. Kaku, T. Anada, Y. Sato, T. Kano, M. Maeda and Y. Katayama, *Bioorg. Med. Chem. Lett.*, 2003, **13**, 3967.
110. A. Zintchenko, M. Ogris and E. Wagner, *Bioconjugate Chem.*, 2006, **17**, 766.
111. A. Schwerdt, A. Zintchenko, M. Concia, N. Roesen, K. Fisher, L. H. Lindner, R. Issels, E. Wagner and M. Ogris, *Hum. Gene Ther.*, 2008, **19**, 1283.
112. S. Sun, W. Liu, N. Cheng, B. Zhang, Z. Cao, K. Yao, D. Liang, A. Zuo, G. Guo and J. Zhang, *Bioconjugate Chem.*, 2005, **16**, 972.
113. Z. Mao, L. Ma, J. Yan, M. Yan, C. Gao and J. Shen, *Biomaterials*, 2007, **28**, 4488.
114. N. Cheng, W. Liu, Z. Cao, W. Ji, D. Liang, G. Guo and J. Zhang, *Biomaterials*, 2006, **27**, 4984.
115. S. H. Choi, S. H. Lee and T. G. Park, *Biomacromolecules*, 2006, **7**, 1864.
116. S. H. Lee, S. H. Choi, S. H. Kim and T. G. Park, *J. Control. Release*, 2008, **125**, 25.
117. J. Yang, P. Zhang, L. Tang, P. Sun, W. Liu, P. Sun, A. Zuo and D. Liang, *Biomaterials*, 2010, **31**, 144.
118. R. Zhang, Y. Wang, F. S. Du, Y. L. Wang, Y. X. Tan, S. P. Ji and Z. C. Li, *Macromol. Biosci.*, 2011, **11**, 1393.
119. G. Han, C. C. You, B. J. Kim, R. S. Turingan, N. S. Forbes, C. T. Martin and V. M. Rotello, *Angew. Chem. Int. Ed.*, 2006, **45**, 3165.
120. J. H. Kaplan, B. Forbush and J. F. Hoffman, *Biochemistry*, 1978, **17**, 1929.
121. D. M. Rothman, M. E. Vázquez, E. M. Vogel and B. Imperiali, *Org. Lett.*, 2002, **4**, 2865.
122. H. Lusic, D. D. Young, M. O. Lively and A. Deiters, *Org. Lett.*, 2007, **9**, 1903.
123. D. D. Young, H. Lusic, M. O. Lively, J. A. Yoder and A. Deiters, *ChemBioChem*, 2008, **9**, 2937.
124. Y. Xu, H. Y. Zhang, D. Thormeyer, O. Larsson, Q. Du, J. Elmén, C. Wahlestedt and Z. Liang, *Biochem. Biophys. Res. Commun.*, 2003, **306**, 712.
125. S. E. Lee, G. L. Liu, F. Kim and L. P. Lee, *Nano Lett.*, 2009, **9**, 562.
126. G. B. Braun, A. Pallaoro, G. Wu, D. Missirlis, J. A. Zasadzinski, M. Tirrell and N. O. Reich, *ACS Nano*, 2009, **3**, 2007.

127. D. B. Rozema, D. L. Lewis, D. H. Wakefield, S. C. Wong, J. J. Klein, P. L. Roesch, S. L. Bertin, T. W. Reppen, Q. Chu, A. V. Blokhin, J. E. Hagstrom and J. A. Wolff, *P. Natl Acad. Sci. USA*, 2007, **104**, 12982.
128. M. Meyer, A. Philipp, R. Oskuee, C. Schmidt and E. Wagner, *J. Am. Chem. Soc.*, 2008, **130**, 3272.
129. M. Soliman, R. Nasanit, S. R. Abulateefeh, S. Allen, M. C. Davies, S. S. Briggs, L. W. Seymour, J. A. Preece, A. M. Grabowska, S. A. Watson and C. Alexander, *Mol. Pharmaceut.*, 2012, **9**, 1.
130. X. Cai, C. Dong, H. Dong, G. Wang, G. M. Pauletti, X. Pan, H. Wen, I. Mehl, Y. Li and D. Shi, *Biomacromolecules*, 2012, **13**, 1024.

CHAPTER 11

Advances in Drug-delivery Systems Based on Intrinsically Conducting Polymers

MANISHA SHARMA,[a] DARREN SVIRSKIS[a] AND
SANJAY GARG*[b]

[a] School of Pharmacy, Faculty of Medical and Health Sciences, University of Auckland, New Zealand; [b] School of Pharmacy and Medical Sciences, University of South Australia, Adelaide, Australia
*Email: Sanjay.Garg@unisa.edu.au

11.1 Introduction

Intrinsically conducting polymers (ICPs) are organic polymers with unique capabilities including the conductance of electricity. In 2000, the Nobel Prize in Chemistry was awarded to Heeger, MacDiarmid and Shirakawa for the pioneering work they achieved discovering and developing ICPs in the late 1970s. In over three decades since, research into the properties and abilities of these materials has exploded. There has been a movement of late from fundamental science into more applied areas, with ICPs finding use in integrated circuits, light-emitting devices, electromagnetic shielding, antistatic coatings, corrosion inhibitors, functional coatings, field effect transistors and sensing devices.[1,2] ICPs have been used in the biomedical setting as biosensors and devices for nerve regeneration and wound healing, and have an increasing interest as components in drug-delivery systems (DDS).[3–5] The contribution this group of materials can make to drug delivery is the ability to electrically

RSC Smart Materials No. 2
Smart Materials for Drug Delivery: Volume 1
Edited by Carmen Alvarez-Lorenzo and Angel Concheiro
© The Royal Society of Chemistry 2013
Published by the Royal Society of Chemistry, www.rsc.org

tune drug release rates depending on patient need. The release of drugs from ICP-based DDS can be modified using electrical signaling to alter the redox state of the ICP, which leads to subsequent changes in polymer charge and volume.[5] Polypyrrole (PPy) is the most investigated ICP for drug-delivery purposes; however, other ICPs including PPy derivatives,[6] polyanaline (PANI)[7] and PEDOT (poly(3,4-ethylenedioxythiophene))[8] have also been used.

11.2 Polymerisation

ICPs are polymerised through oxidation of monomer units. Oxidation, as represented in Figure 11.1, can be achieved either chemically or electrochemically. An increasing range of monomers and functionalised monomers have been used to form various polymers with different properties.[2] The final polymer product is not only the result of the monomer selected, but is also influenced by the dopant anions used (A^-), the rate and extent of polymerisation, the concentration of reactants, temperature, stirring and the physical setup of the electrochemical cell.[9]

Common chemical oxidants include ferric chloride and ammonium persulfate. However, it is difficult to control the rate and extent of polymerization chemically, and often electrochemical approaches are used. By using a set current to cause oxidation, the rate and the extent of polymerization are controlled by the magnitude and the time interval that the current flows for, respectively. Keeping other parameters constant, more rapid polymerization results in relatively irregular polymers, with rougher surfaces, more porous structure and lower densities.[10–12] For drug-delivery purposes, polymerization conditions must be optimized not only for drug loading, but also to provide ideal polymer morphology as this will influence the mobility of drug in the polymer and the release profiles. Although the efficiency of electrochemical oxidation is less than 100%, the total amount of current passed during polymerisation will dictate the quantity of polymer formed. This can provide a rough estimation, and efficiency appears to change with the total thickness of polymer produced, but reported estimates of charge density of 240 mC cm^{-2} to 600 mC cm^{-2} are required to produce a 1 μm thickness of PPy.[12–14]

To create an electrochemical cell for polymerization either two or three electrodes can be used; a working electrode, a counter electrode and optionally a reference electrode. Both the working and the counter electrodes should be clean, inert materials so as not to take part in any electrolysis reaction themselves. The working electrode surface is the site of polymer formation, and the surface material can influence the initial polymerization reaction. However,

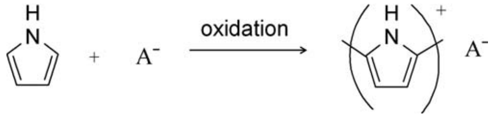

Figure 11.1 Polypyrrole polymerization.

while this influences very thin polymer films, the influence of the material is lost in the formation of thicker films, as the newly forming polymer is laid down on the existing polymer.[15] Ideally the voltage generated in the cells is monitored using a reference electrode (commonly a silver/silver chloride or saturated calomel electrode), to ensure the polymer is not exposed to too large a voltage. Excessive voltage results in overoxidation and subsequent loss of conductivity and reversible redox activity.[14,16] During synthesis, solutions are usually left unstirred, since stirring can negatively influence the deposition of insoluble oligomer units onto the growing polymer film.[17]

As displayed in Figure 11.1 the newly formed polymer is in the oxidized form with positive charges distributed along the backbone, with a single positive charge every three to four subunits.[18–21] These positive charges must be balanced by anionic dopant molecules for the successful formation of the polymer. The dopant anion selected will have a major influence on the morphology, properties and the function of the polymers produced.[17,18] For example, keeping other variables constant, the same PPy films prepared with chloride ions (Cl^-) were two to eight times thicker than those prepared using *p*-toluene sulfonate (pTS) or poly(styrene sulfonate) (PSS), with PPy-Cl having the roughest surface and PPy-PSS the smoothest surface.[22]

11.3 Properties

11.3.1 Conductivity

ICPs, as the name suggests, conduct electricity. The degree of conductivity usually falls into the range commonly associated with the semi-conductors. The conductivity is due to the uninterrupted π-conjugated backbone. The level of conductivity is variable and ultimately it depends on mobility of the electrons to carry charge along the polymer.[1,23] In the oxidized state, electrons have been removed from the ICP backbone leaving "holes". Surrounding mobile electrons are able to move into these holes effectively shifting the hole along the polymer backbone explaining the resultant conductivity. The regularity and degree of branching of the polymer backbone are, therefore, major determinants to conductivity.

11.3.2 Stability

Various ICPs display differing levels of stability. PPy is regarded as relatively stable in the oxidized form.[17,18,24] There are very few reports on the stability of ICP based DDS,[25] and this is an area that will require more in-depth investigation in the future. Conductivity has been used as a marker for stability.[26–29] The dopant used influences stability; PPy films prepared with pTS have been shown to be more stable than PPy prepared with ClO_4^-, BF_4^-, NO_3^-[26] or with dodecyl sulfate.[27] Temperature plays an important role in environmental breakdown. With increasing temperatures, conductivity has been shown to reduce in shorter time periods.[26,28,29] Truong *et al.*[27] found that for PPy-*p*TS stored at 150 °C in air, the conductivity began to fall immediately. However, when the same polymer films were stored in oxygen-free environment at 150 °C there was no decrease in conductivity after 3 days. Subsequent introduction of oxygen resulted in an immediate decline in conductivity. The reaction between PPy and oxygen seems to be accelerated at high temperatures, leading to an irreversible loss of conjugation and consequently of conductivity.[26] This has been examined by FTIR where the appearance of a band at $1690\,cm^{-1}$, characteristic of α, β-unsaturated ketones, indicates the irreversible oxidation at the β′-position of PPy.[30]

11.3.3 Biosensing

ICPs biosensing capabilities are constantly being developed.[3,31,32] Immobilized enzymes on ICP films form amperometric biosensing devices with the ability to signal a concentration-based response to glucose,[33–35] cholesterol,[36] lactate[37] or urea.[38] Looking forward, it may be possible to combine the biosensing and the drug-delivery capabilities of ICPs, creating a single material with the ability to self-tune the rate of drug release as a function of a sensed change in the local environment.[39]

11.3.4 Solubility

While oligomers of ICP monomers may be soluble, the polymer products are almost always insoluble due to strong inter- and intra-molecular forces.[23] However, soluble PPy can be produced through chemical polymerization by doping with sulfate anions.[40] Chemical modification of the monomer units has also been used to produce PPy with limited solubility.[41] These approaches have resulted in solubility in some organic solvents, however the polymers remain insoluble in water.

11.4 Characterization

Several techniques are frequently utilised to characterize ICPs including Infrared and Raman spectroscopy, Atomic Force Microscopy and Cyclic Voltammetry. Here we briefly discuss these techniques and how they can be used to assess the ability of ICPs to act as DDS.

11.4.1 Infrared (IR) and Raman Spectroscopy

Infrared (IR) and Raman spectroscopy are complementary techniques that are used to examine the vibration, stretching and bending of intra-molecular bonds. These techniques allow for ICP identification,[12,42–44] can give an indication of doping levels[45,46] and can be used to detect overoxidation of PPy,[44] and enable the identification of dopants or other molecules that may be present in the ICP.[12,42,44,47]

11.4.2 Atomic Force Microscopy

Atomic Force Microscopy (AFM) is a useful surface probing technique that has been utilised to assess both the surface characteristics and volume changes in ICP films.[5,48–51] The surface features are important as they can influence drug release and biological interactions, including cell adhesion.[22] Out-of-plane volume changes of PPy films have been linked to drug release[5] and, therefore, the assessment of this feature by means of AFM is highly useful.

11.4.3 Cyclic Voltammetry

Cyclic Voltametry (CV) is an electrochemical technique used to assess reversible electroactivity and to determine the potentials at which the redox state of the polymer can be switched. During CV analysis, the potential is increased or decreased between two set points, at a predetermined scan rate, while the current is measured. By constructing potential *vs.* current plots, useful information can be extracted. When a redox active material or species, including an ICP, is examined, peaks may be observed correlating to oxidation or reduction processes. A peak represents current flow into or out of the material, indicating reduction or oxidation, respectively. By integrating the area under each peak, the amount of charge passed during the redox process can be calculated. The peak's position roughly indicates the potentials at which oxidation or reduction occurs. As a change in the redox state can be utilized to trigger drug release, this technique provides information on the potentials required to force such a change. An ideal reversible system exhibits very little difference between the potential at which oxidation and reduction occur.[52] However, ICPs typically show significant separation between broad oxidation and reduction peaks (Figure 11.2).[16]

11.5 Biocompatibility

For biomedical applications the biocompatibility of ICPs must be considered. Polypyrrole is the ICP that has been most widely investigated for biomedical applications and is regarded as biocompatible.[3,47] As ICP synthesis requires the presence of anionic dopants, it is not only the biocompatibility of the polymer be considered, but also that of the entire system. Specific dopants can be used to promote the biocompatibility of the polymer.[53] However, while some dopants are capable of imparting desirable functionality into the polymer, they should be avoided for biomedical applications due to their toxicity. Ideally a biologically inert dopant molecule will be used, however it may be possible to use a non-biocompatible dopant for synthesis, and to impart desired functionality, and subsequently exchange it out of the polymer.

In addition to the dopants used, the physical properties of the material, including morphology and mechanics, can modify biocompatibility.[49,54] As seen in the polymerization section, the physical properties of the polymer can be controlled to some degree depending on the synthesis conditions employed.

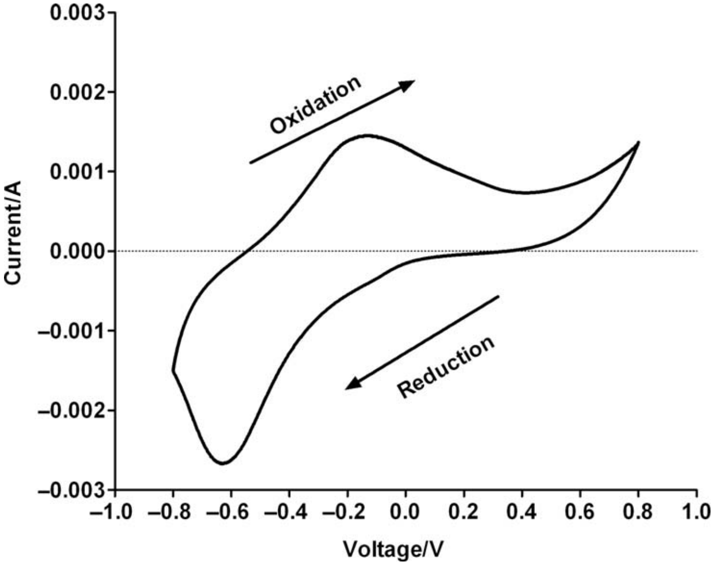

Figure 11.2 Cyclic voltammogram of PPy doped with dodecyl benzene sulfonate cycled in 0.1 M $NaNO_3$ between +0.8 V and −0.8 V at a scan rate of 50 mV s^{-1}.

Another way to improve the biocompatibility is by modifying the surface of the ICP after polymerization.[55] The electrical stimulation used to regulate drug release from ICP-based DDS can also be used to modify cell behavior and, thus, the biocompatibility.[56,57] As ICP-based DDSs advance toward clinical applications, the biocompatibility aspects of these systems need to be more completely investigated.

11.6 Mechanisms for Controlled Drug Release

In a broad sense, modifiable drug delivery from ICPs is achieved by utilizing either alterations in electrostatic forces or volume, as ICPs undergo a change in redox state. Hydrophilic–hydrophobic interactions also play a role, but have not been fully investigated. Frequently, it is a combination of these different mechanisms that results in drug incorporation as well as release. However, for the purposes of explanation, electrostatic forces and volume changes will be discussed separately.

11.6.1 Utilizing Electrostatic Forces in ICPs

When the redox state of an ICP is altered, there is an accompanying change in the charge of the polymer backbone. PPy is positively charged in the oxidized state (PPy^+) and neutral in the reduced state (PPy^0). In the simplest scenario, a negatively charged drug can be used as the dopant anion during polymerization. Subsequent reduction of PPy^+ to PPy^0 leads to a loss of electrostatic attraction between the anionic drug and the polymer, and the excess negative charge along with diffusion drive drug release.[58] Often, however, polymer is not formed or desired polymer properties are not attained when using a drug as the dopant anion. To overcome this, an ideal anionic dopant can be selected and, if it is mobile, following polymerization it can be exchanged out of the polymer by redox cycling in favor of an anionic drug.[10] The anionic drug is subsequently available for release on reduction of the polymer.

The release of cationic drugs can also be controlled through electrostatic forces. If an ICP is prepared with an immobile anion, when the polymer is reduced from PPy^+ to PPy^0, a net negative charge remains due to the immobilized anions. This feature can be utilized to load the polymer with a cationic drug. Subsequently, if the polymer is oxidized back to PPy^+, the cationic drug is expelled out of the polymer due to electrostatic repulsion.[59] Clearly the utilization of electrostatic forces is somewhat limited in requiring the drug to be charged. When selecting candidate drugs, attention must be paid to their pK_a and to the pH of the intended environment of the ICP based delivery system.

11.6.2 Volume Changes in ICPs

When the redox state of the polymer changes, the charge of the polymer backbone is also altered. These changes in polymer charge need to be balanced and solvated ions move into and/or out of the polymer.[48] In predicting alterations in volume of an ICP, the polymer structure and the mobility of ions in and around the polymer must be considered. Expansion or shrinkage of the polymer can be designed to occur solely on either oxidation or reduction of the polymer, or a mixed response may be observed.

If PPy was prepared with an immobile anion (often large and multi-charged), when PPy shifts from the oxidized state (PPy^+) to the reduced state (PPy^0), there is a net negative charge in the polymer due to the presence of the immobile anion. This net negative charge is balanced by an influx of mobile cations and thus the polymer expands. Subsequent oxidation of the polymer from PPy^0 to PPy^+ results in a net positive charge, which causes the mobile cations to be expelled out and the polymer to shrink. This phenomenon is referred to as cation driven actuation. Conversely, if PPy is polymerized with a mobile anion, as PPy is reduced from PPy^+ to PPy^0 a net negative charge evolves in the polymer. Some of the anion will therefore be expelled out, and the polymer will shrink. It follows that expansion of the polymer will occur on oxidation of PPy^0 back to PPy^+ and the re-entry of the solvated anions into the polymer bulk. The situation described is referred to anion driven actuation. Such clear cation driven or anion driven actuations are rarely seen since they require precise control over ionic species present in the polymer and surrounding environment. Certainly in *in vivo* environments or environments mimicking the *in vivo* situation a broad mix of species is present. In this situation mixed-ion actuations are likely to be observed, where both anions and cations are mobile to enter and exit the polymer.[60]

11.7 Drug-delivery Systems

In the last two decades many different ICP based DDSs have been described in both academic literature and as intellectual property. Recent work has described combinations of ICPs with other biomaterials to enhance the performance of the DDS. For easy understanding, this section has been divided according to the method of drug loading and the mechanism of drug release. The following categories are presented; reservoir systems, actuating devices, matrix systems and miscellaneous systems.

11.7.1 Reservoir Systems

Reservoir systems have been quite successful for controlled release of therapeutic agents as they can provide zero-order kinetics for longer periods. Youngnam *et al.*[61] detailed the preparation of a reservoir type drug delivery system by encapsulating a growth factor in PPy. Two approaches were used to encapsulate the biomolecule. In the first approach, neural growth factor (NGF) was absorbed into mesoporous silica nanoparticles (MSNs) by electrostatic interactions between free silanol groups on the wall of the pores and the positively charged amine groups on the NGF at neutral pH (Figure 11.3). The particles were then used as a template on a clean indium tin oxide (ITO) surface for PPy or COOH-PPy electropolymerization at a constant +0.7 V to form PPy/MSN-NGF composites. Carboxylation was used to impart hydrophilicity to the polymer. The inorganic MSNs provide a protective shell to the biological agent against *in vivo* degradation and thus enhances stability and increases therapeutic effect. In the second approach NGF was immobilized into the porous PPy films applying the *N*-hydroxysuccinimide (NHS), ethyl-3-(3-dimethyl-aminopropyl) carbodiimide hydrochloride (EDC) coupling

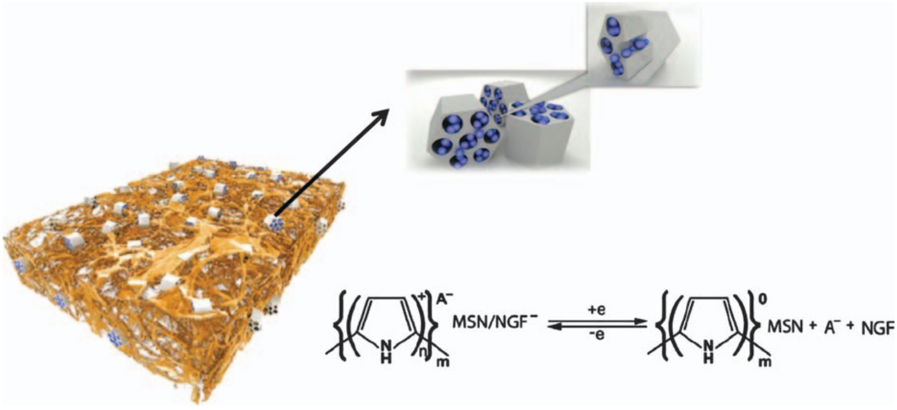

Figure 11.3 Schematic representation of MSN particles assembled within PPy. Application of electric potential releases NGF from PPy/MSN-NGF composites by redox cycling.
(Reproduced with the permission of IOPScience from Ref. 62.)

reaction. The PPy films were made porous by dissolving the MSN templates in 20% hydrofluoric acid for 24 hours. Delivery systems prepared by both methods were tested for their efficacy to promote proliferation of PC 12 cells. *In vitro* release of NGF from PPy/MSN-NGF composites was observed with and without electrical stimulation. Cells grown on electrically stimulated composites showed 40% greater proliferation and neurite extension, compared to nerve cells cultured without stimulation. This was further confirmed by SEM analysis, which showed increased attachment and neurite extensions as shown in Figure 11.4.[62]

Similarly, various conducting polymer based reservoir-type devices have been investigated by Carlsson *et al.*[63] The devices include a conducting polymer element and a substance incorporating element, *i.e.* a drug reservoir assembled together on to the substrate. The release of the drug from the reservoir is characterized by the redox property of the ICPs. On application of the appropriate potential, the ICPs can switch between oxidized and reduced states. This redox change is also accompanied by a volume change and, as a result, a significant amount of the solvent and associated ions can be dragged in and out of the ICPs. However, the applications of such kinds of devices in drug delivery are limited by the fact that many drugs are uncharged or are hydrophobic in nature.

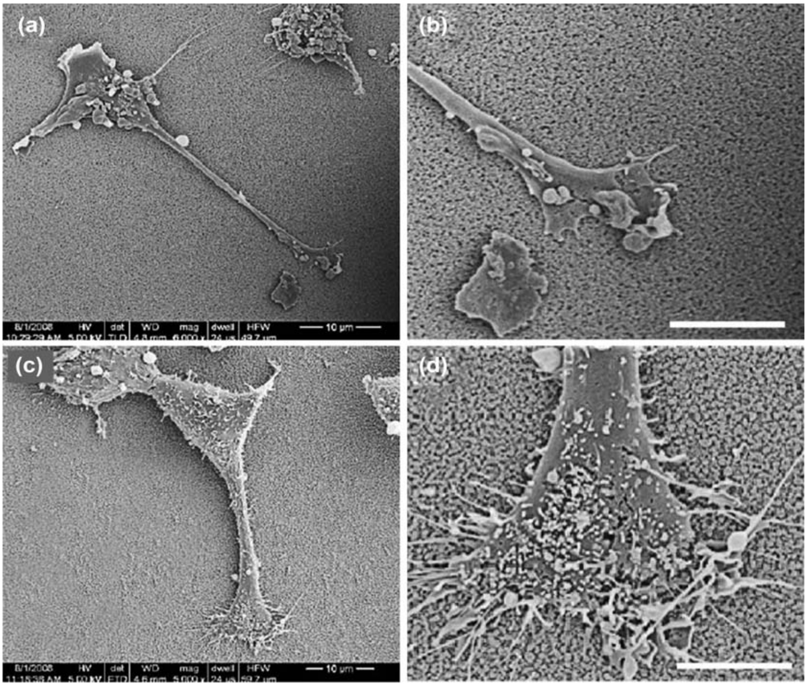
(a)
(b)
(c)
(d)
8/1/2008 HV det WD mag dwell HFW
10 μm
8/1/2008 HV det WD mag dwell HFW
10 μm

Figure 11.4 SEM images of cells and neuritis cultured on unstimulated (a and b) and electrically stimulated (c and d) PPy/MSN-NGF composites. (Reproduced with permission of IOPScience from Ref. 62.)

11.7.1.1 Microchips

Over the past decade there has been much interest in the application of microfabrication technology to drug delivery. Ge *et al.*[64] developed a microchip by electrochemically depositing a drug-doped PPy film onto gold microelectrode arrays. Such reservoir based microchips have numerous advantages such as the ablility to release multiple drugs at a given time, small size, and the ability to release small precise amount of drug and provide pulsatile drug release. Each microchip consisted of gold microelectrodes microfabricated on a silicon substrate. Each of the gold microelectrodes can be controlled individually. PPy containing drug (sulfosalicyclic acid) was electropolymerized on gold microelectrodes by galvanostatic polymerization using a current density of $2.5\,\mathrm{mA\,cm^{-2}}$ for 800 s. The study showed that over 2 to 4 hours, 100% of loaded sulfosalicylic acid was released on electrical stimulation. However, when a second layer of PPy was electropolymerized onto the chip, the bilayer setup prevented spontaneous release of the drug from the microchip, and stimulated pulsatile release of drug was achieved over a period of several days.[64]

11.7.2 Actuating Devices

11.7.2.1 Peristaltic Pumps

The general structure of an ICP actuating device comprises a closed fluid delivery channel (drug reservoir) with inlet and outlet ports, an ICP as an actuator and a controller to regulate the expansion and contraction of actuators. Morgan *et al.*[65] discloses a conducting polymer actuating peristaltic pump for the delivery of a therapeutic agent to selected sites. The peristaltic pump consists of a flexible tubing, the outer surface of which is composed of the electroactive polymer actuators. The conducting polymers, when electrically stimulated, generate a mechanical force or movement. This dimensional change occurs due to the transfer of ions into and out of the polymer, therefore causing expansion and contraction of the polymer. As a result, the fluid from the reservoir is conveyed from one end of the flexible tube to the other, imparting a peristaltic pumping action. The developed device could be in the form of an endocardial medical lead or catheter. Similarly, Cannell *et al.*[66] reported the development of a "micropump", a microfabricated pumping device for the delivery of drugs. The device consists of a drug reservoir, an actuator made of conducting polymer arranged within the reservoir and an electrode array, which acts as a controller. The electrode array facilitates phased cyclic actuation of the conducting polymer to effect the peristaltic pumping action. Particularly polypyrrole, polypyrrole derivatives and polyaniline are used as actuating elements because, compared to other materials, they have low voltage requirements (1–5 volts). The micropump can be integrated with a microprocessor to provide refined control for drug delivery. Therefore dosages can be altered externally to the patient's body by means of a processor and a wireless interface.[66] Such pumps also have application as infusion devices for infusing liquid medications such as insulin for the treatment of diabetes, opiates infusion for use in severe pain, local infusion of drugs for cancer chemotherapy, infusion of stimulants for the treatment of heart failure or arrhythmia and infusion of drugs for seizure treatment.[67]

11.7.2.2 Microneedle-based Nanoactuators

Microneedles represent a breakthrough technology in drug delivery, science. These can be inserted into the skin without any pain to create micrometer size pathways across the skin to deliver the drug molecules. Gabriela *et al.*[68] reported the development of a multiplexed novel drug delivery system consisting of an array of microneedles coupled with conducting polymer nanoactuators for the controlled release of therapeutic molecules. The device consists of several components as shown in the Figure 11.5. PPY act as the actuating element after it has been electrodeposited on the gold sputtered polycarbonate membrane. The release characteristics of the developed device were evaluated by loading the reservoir with the dye methylene green. On application of a negative potential, the PPy membrane switches to the reduced relaxed state, resulting in closure of the pores with no dye release. On switching the membrane to the oxidized state by applying positive potential, the

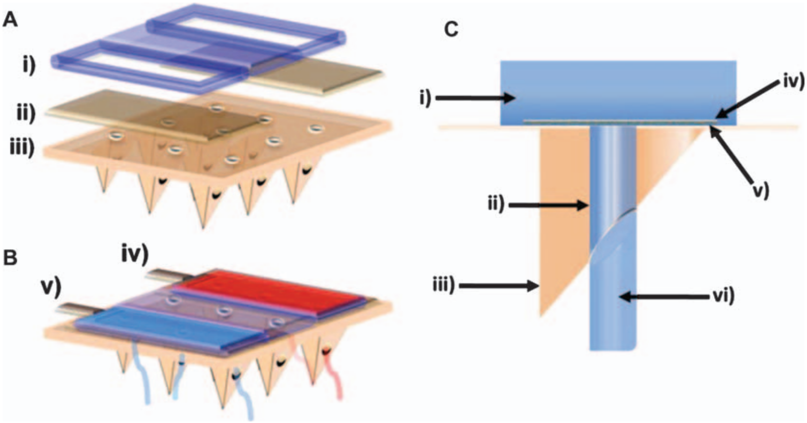

Figure 11.5 (A) Schematic representation of the microneedle-based multi-plexed drug-delivery system. The main components are (i) hollow microneedle array, (ii) gold-sputtered polycarbonate membrane electrodeposited with dodecylbenzenesulfonate-doped polypyrrole (PC/Au/PPy/DBS) and (iii) polydimethylsiloxane (PDMS) reservoir. (B) Schematic illustration of the assembled dual-channel drug-delivery system outlining the reservoirs for (iv) drug 1 and (v) drug 2. (C) Schematic of main components of single microneedle during drug delivery: (i) reservoir, (ii) lumen (342 μm diameter), (iii) hollow microneedle, (iv) Au/PPy/DBS nanoporous membrane, (v) PC membrane and (vi) the released drug.
(Reproduced with permission from Ref. 67.)

membrane contracted thereby facilitating the opening of the pores, allowing the dye to flow through the membrane. The actual actuation of the PPy membrane was well demonstrated and was stable for up to 10 actuating cycles. This type of microdevice provides an avenue for targeted therapy where the drug doses can be modulated according to the patient's conditions.

11.7.2.3 Smart Membranes

Smart membranes are delivery devices specifically designed to achieve pulsatile release of drugs on electrical stimulation. Jeon *et al.*[69] developed nanoporous PPy membranes doped with dodecylbenzenesulfonate (DBS). The PPy was electropolymerized on anodized aluminium oxide (a hard template to create porous PPy). PPy/DBS exhibits a very large volume change (up to 35%) depending on the electrochemical state and has excellent biocompatibility. The polymeric membrane was actuated by altering the electrochemical state. The activating potential is less than 1.1 V, which is relatively low compared to the voltage, required for the operation of an artificial heart (*c.a.* 3 V). The actuation of the pore size was successfully demonstrated by an *in situ* AFM study; a reduction in pore size was observed in the reduced state, while the pore size increased in the oxidized state (Figure 11.6). These smart membranes showed a quick response time (less than 10 s) and pulsatile drug release, and therefore could have potential application in emergency conditions such as angina pectoris, migraine and hormone-related disorders, which requires precise and on-demand drug delivery.[69]

11.7.2.4 Hydrogel-conducting Polymer Composites (Electro-conductive Hydrogels)

The combination of the electrically switchable properties of conducting polymers and the swelling/deswelling capabilities of hydrogels, make these composite materials an exciting prospect for various biomedical purposes, including drug delivery. Tsai *et al.*[70] fabricated a cylindrical electro-conductive hydrogel to investigate the electro-tunable release of the drug indomethacin. The ICP polyaniline was co-blended with poly(vinyl alcohol) and cross-linked with diethyl acetamidomalonate to form a polymeric hydrogel system. The drug entrapment efficiency of the polymeric hydrogel ranged from 65 to 70%. On application of different electrical potentials, between +0.3 V and +5.0 V for 60 seconds, cumulative drug release ranged from 4.7 to 25.2% after four release cycles respectively. It was observed that there was an increase in the percentage of drug released with an increase in the applied potential difference. However, a constant drug release was obtained between +1.5 V and +3.5 V. The electro-stimulated release of indomethacin was associated with the degree of cross-linking, the polymeric ratio and the drug content. The main mechanism of indomethacin release was ascribed to the erosion of the hydrogel upon exposure to electrical stimulation.[70] Similarly, Torresi *et al.*[71] blended

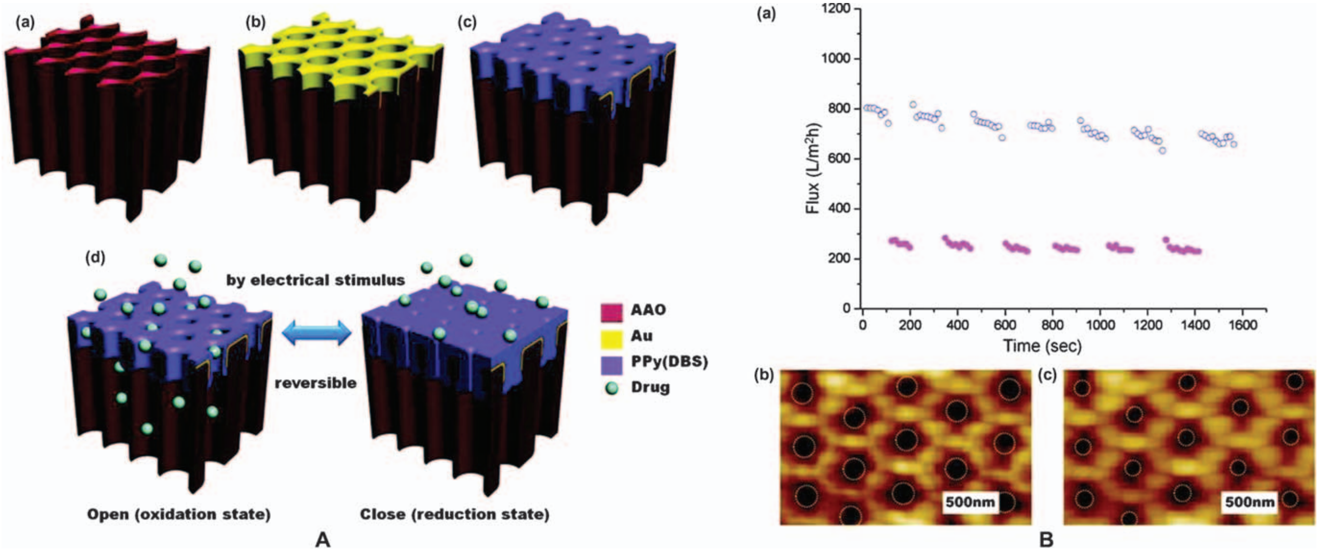
(a)
(b)
(c)
(d)
by electrical stimulus
reversible
Open (oxidation state)
Close (reduction state)
AAO
Au
PPy(DBS)
Drug
A
(a)
Flux (L/m^{2}h)
0
200
400
600
800
1000
1200
Time (sec)
0
200
400
600
800
1000
1200
1400
1600
(b)
(c)
500nm
500nm
B

Figure 11.6 (A) Schematic representation of smart electro-responsive nanoporous membrane.[72] (a) Fabrication of anodized aluminium oxide (AAO) membrane. (b) Thermal deposition of thin gold (Au) layer on the AAO membrane. (c) Polypyrrole was electropolymerized on the Au layer. (d) Reversible change of pore size between oxidation and reduction states on electrical stimulation. (B) *In situ* flux and AFM results of a membrane with initial pore diameter of 200 nm at two different electrochemical states. (a) *In situ* flux *versus* time. Data points were taken every 15 s. Open (blue) and closed (magenta) circles indicate the oxidization and reduction states. (b, c) Figure represents the *in situ* AFM height images corresponding to the oxidization and reduction states. (Reproduced with the permission of Elsevier from Ref. 68.)

polyacrylamide hydrogel with PPy electrochemically to characterize the controlled release of model drug safranin. The synthesis parameters were optimized using a fractional factorial design. The hydrogel was quite stable under neutral pH conditions, which is essential for *in vivo* applications. Sirivat and Chansai[72] developed blends of PPy and poly(acrylic acid) doped with an anionic drug for transdermal delivery. Such stimuli-responsive hydrogels exhibit great potential for triggered drug therapy.

11.7.3 Matrix Type

Dubois-Rande *et al.*[73] described an implantable metallic stent for the prevention of post-angioplastic restenosis. The stent was coated with conducting polymer with an encapsulated antisense oligoneuclotide to selectively inhibit the expression of genes preventing the proliferation of smooth muscle cells on the arterial wall. The polymerization of the ICP onto the stent is two stage processes. In the first stage the ICPs is electropolymerized directly on to the metallic support in presence of another hydrophilic polymer like polyethylene glycol, polyvinylpyrrolidone or polyethylene oxide. This is followed by stage two where the oligoneucleotide is attached to the polymer by oxidation or reduction. The presence of hydrophilic polymers in the polymer matrix enhances the permeability of the polymer to anionic molecules such as oligonucleotides. Oligoneucleotides have a very short life as they are rapidly digested by nucleases in the body. Therefore, the present invention is advantageous as it protects the oligoneuclotides in the polymer matrix and delivers them on the desired site where they can act effectively. *In-vivo* studies were carried out in New Zealand rabbits and the coated stents were implanted in abdominal aorta. After 15 days the artery was removed and histology was performed. It was observed that there was no thrombus formation and the proliferative layer which covered the stent was more organized and had a layer of endothelial cells on the top. This shows that the stents were well tolerated after implantation.[73] A similar device has been described by Jager *et al.*[74] Medical devices such as catheters, guidewires, pacemakers and defibrillators coated with conducting polymer doped with therapeutic molecule have proved quite effective.

Minteer and Ulyanova[75] are inventors on a patent which also discussed similar matrix type devices and their method of fabrication. The patent classifies the therapeutic agent as an imprint molecule (IM) and the conducting polymer as an electroactive molecularly imprinted polymer (EMIP). The release of the drug molecule at the target location is dependent upon the change in electro-conformation of the conducting polymer on the application of electric potential. The state of the art defines the IM incorporated into the polymer during electropolymerization occupies a three dimensional space, the binding site, within the EMIP. The IM is encapsulated within the polymer matrix and is held by various electrical and mechanical forces without the formation of any covalent chemical bound. Such a device has wide application in drug delivery and biosensing.

Weber *et al.*[76] reported the development of implantable drug delivery device for localized drug delivery, specifically to the interior of the blood vessel. The device is also equipped with a sensor that detects the presence of any lesions or plaques on the interior of the vessels. By combining sensing and drug delivery elements the drug can be delivered by the electroactive polymer matrix according to the conditions in the local environment.

11.7.4 Miscellaneous Devices

11.7.4.1 Implantable Electrodes

Cochlear implants consist of an electrode array implanted into the scala tympani of the cochlea to electrically stimulate spiral ganglionic neurons (SGNs) and, therefore, provide auditory perception to individuals with hearing loss. However, such implants can themselves cause loss of residual hair cells and apoptosis of SGNs due to the delivered charge. To overcome this problem Richardson *et al.*[77] developed an electrode array in which PPy encapsulating therapeutic neutrophins (NT3) was coated on to the implantable electrodes. The developed electrode array is presented in the Figure 11.7. Neutrophins have protective effects and prevent the loss of SGNs. About 2 ng of NT3 was encapsulated in the electrode array and was able to release 0.1 ng/day with electrical stimulation when implanted into deafened guinea pig cochleae. The electrode array not only provided electrical stimulation but was also able to deliver the trophic agents to the SGNs preventing its degeneration after hearing loss.

11.7.4.2 Nanostructured Conducting Polymers for Drug Delivery Systems

To date functionalized nanostructured conducting polymer surfaces have gained much interest in the field of DDS. Various methods such as hard-templates and soft-templates have been introduced in the synthesis of conducting polymer micro- or nanostructures.[78] The references cited here particularly highlight the specific attributes in the synthesis of nanostructured surfaces and their application to drug delivery. Luo and Cui[79] developed electrically controlled DDS based on sponge-like nanostructured PPy. They utilized self-assembled polystyrene nanobeads as the hard template for forming nanostructures. After electropolymerization of PPy, the template was removed leaving nanopores in the PPy film. The proposed system can load multiple drug molecules in the polymer backbone during PPy polymerization as a dopant, and a second drug can be loaded into the nanostructures inside the polymer film. These nanostructures then can be sealed by electroploymerizing a second thin layer of PPy on top. This kind of system therefore significantly improves the drug loading capacity as the overall effective surface area of the film is increased and the initial burst effect is prevented by the bilayer. Upon electrical stimulation, drug molecules incorporated in the backbone were released *via* a

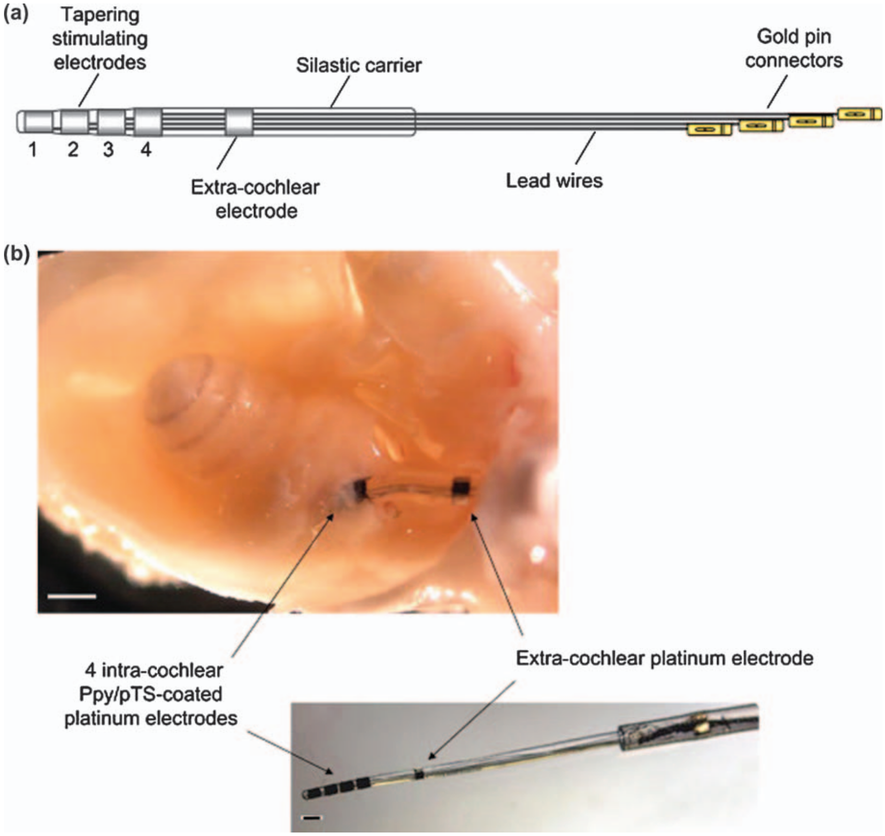
(a)
Tapering stimulating electrodes
Silastic carrier
Gold pin connectors
1
2
3
4
Extra-cochlear electrode
Lead wires
(b)
4 intra-cochlear Ppy/pTS-coated platinum electrodes
Extra-cochlear platinum electrode

Figure 11.7 Four-ring platinum electrode array for implantation in guinea pigs (GP). (a) The electrode array consisted of four active electrodes individually wired for stimulation as electrode pairs and an extra-cochlear electrode as a marker for insertion depth. Diagram is not drawn to scale. (b) An electrode array coated with Ppy/pTS implanted into a GP cochlea. The fourth electrode can be seen protruding from the cochleostomy in this example. The fifth uncoated platinum extra-cochlear electrode is also visible. (Reproduced with permission from Ref. 76.)

dedoping process, while those physically encapsulated in the nanopores were squeezed out owing to the actuation of the nanoporous film. This kind of drug delivery system has applicability in cases where delivery of a combination of drugs is necessary.

The actuation of conducting polymer nanotubes is another approach that has been used to achieve controlled release.[80,81] An advantage of this approach is that drug loading and release can be achieved regardless of whether or not the drug is charged. Nanotubes consist of an open lumen enclosed by a cylindrical ICP layer. The lumen can be filled with drug. Presumably, drug release is achieved by electrically altering the permeability of drug through the ICP wall.

Sirivisoot *et al.*[81] used multi-walled carbon nanotubes grown out of anodized titanium (MWNT-Ti) as a template to electrodeposit PPy by cyclic voltammetry. PPy was doped with therapeutic agents such as penicillin/streptomycin or dexamethasone. Drug release was studied on application of a negative voltage. The results showed a controllable biphasic release profile and the cumulative amount released was about 80% after 5 cycles of the applied voltages at a scan rate of 0.1 Vs^{-1}.

Abidian *et al.*[80] developed conducting polymer nanotubes utilizing biodegradable poly(L-lactide) (PLLA) or poly(lactide-co-glycolide) (PLGA) as templates onto gold coated silicon wafers as a substrate. The drug (dexamethasone) was incorporated into the template. The biodegradable polymer was electrospun onto the substrate, followed by electropolymerization of conducting polymer (PEDOT). The PLLA/PLGA nanofibers were then dissolved creating nanotubular PEDOT. The nanotubes were electrically actuated by applying a positive potential of 1 V. With the electrical stimulation of nanotubes the release of bioactives can be precisely controlled and achieved for 58 days. Later the approach was transformed into an implantable medical device capable of controlled delivery of bioactives.[82] Such devices can be useful, in the manufacture of improved microelectromechanical systems (MEMS), electrode-based devices for long-term implantation in the central nervous system (CNS), development of new generation of cardiac, musculoskeletal-electrophysiological devices, and implantable electrical and biomolecule sensors and drug delivery devices.

Ferain *et al.*[83] disclosed the development of a drug eluting nanowire array. The nanoscopic sized wire in the array is available in two configurations. In one configuration it is a conductive metallic wire, made up of metals including Cu, Pt, Au, Ni or Pd coated with conducting polymer doped with drug molecules. In the second configuration the array is present as hollow nanoscopic wire formed from electroactive conjugated polymer, containing a therapeutic molecule. Such types of nanowire array can be incorporated into stimulation electrodes at the interface with biological tissues. They can act to reduce both nerve damage and contact impedance. Impedance is reduced as the capillary like structure of the nanowires increases the real area to geometric area ratio of the electrode in contacts. Such systems also provide an accurate and controlled local drug delivery and therefore are suitable for neurological disorders related to spinal cord injuries.

11.8 Demonstration of Biological Applications

The exciting potential of ICPs to achieve tunable drug delivery is frequently described in the literature; this is slowly becoming a reality in biological systems. Ge *et al.*[84] developed a novel dual stimuli responsive nanoparticle system in which the rates of drug release can electrically controlled. Polypyrrole nanoparticles loaded with drug molecules were prepared by an emulsion polymerization technique. These nanoparticles are then suspended in a temperature sensitive hydrogel, which is a liquid at low temperature but becomes a gel at body temperature. They successfully demonstrated the in-vivo drug release in mice by applying an external electric field. Similarly cochlear implants loaded with neutrophins as developed by Richardson *et al.*[77] have demonstrated their *in-vivo* effectiveness in delivering neurotrophic agents neurons in a controlled manner to preserve their activity. In addition the electrical stimulation provided by the implant minimizes the degeneration of SGNs after hearing loss. Implantable heart valve prosthetic devices including annuloplasty rings and bands coated with ICPs when implanted in animals exhibited a tremendous reduction in inflammation and pannus formation.[85] As DDS based on ICPs become more sophisticated and reliable we will see an increasing number of reports moving these systems from the lab bench into biological models. To date, these delivery systems have found use where local delivery of drug is required. Before these systems can be applied to a wider range of medical conditions the level of drug that can be loaded and released must be increased. This will allow the systemic delivery of drug and will demonstrate the versatility of ICPs to act as a drug delivery platform which can be used to treat a range of health conditions.

11.9 Conclusions

ICP based devices are beginning to fulfill their exciting potential in drug delivery science. The inherent redox properties and the actuation behavior on electrical stimulation make ICPs a promising platform for delivering drugs at a controlled rate to desired locations. The rate of drug release can be modulated according to an individual patient's condition. Apart from reservoir and matrix systems, nanostructured systems such as nanotubes, nanowires, nanofibers and nanofilms appear to be promising, as increased surface area allows enhanced loading of the therapeutic molecule. These nanostructured ICPs can be appropriately functionalized or tagged and can act as excellent biosensing materials. ICP-hydrogel composites combine the swelling properties of hydrogels and the electroactivity of ICPs making them a versatile tool for delivering drugs at a controlled rate. On-demand release of drug is possible from these smart polymers by simply switching between redox states. With the novel technologies discussed in this chapter practical applications of ICPs are imminent. Hence research and development is currently exploring further applications of these interesting materials in drug delivery and biomedical science.

References

1. B. Norden and E. Krutmeijer, *The Nobel Prize in Chemistry, 2000: Conductive polymers*. http://www.nobelprize.org/nobel_prizes/chemistry/laureates/2000/advanced-chemistryprize2000.pdf (Accessed in March 25, 2009).
2. J. Schultze and H. Karabulut, *Electrochim. Acta*, 2005, **50**, 1739.
3. S. Geetha, C. R. Rao, M. Vijayan and D. Trivedi, *Anal. Chim. Acta*, 2006, **568**, 119.

4. R. Richardson, B. Thompson, S. Moulton, C. Newbold, M. G. Lum, A. Cameron, G. Wallace, R. Kapsa, G. Clark and S. O'Leary, *Biomaterials*, 2007, **28**, 513.
5. D. Svirskis, B. E. Wright, J. Travas-Sejdic, A. Rodgers and S. Garg, *Electroanalysis*, 2010, **22**, 439.
6. L. L. Miller and Q. X. Zhou, *Macromolecules*, 1987, **20**, 1594.
7. L. M. Lira and S. I. Cordoba de Torresi, *Electrochem. Commun.*, 2005, **7**, 717.
8. M. R. Abidian, D. H. Kim and D. C. Martin, *Adv. Mater.*, 2006, **18**, 405.
9. D. Svirskis, J. Travas-Sejdic, A. Rodgers and S. Garg, *J. Control. Release*, 2010, **146**, 6.
10. K. Kontturi, P. Pentti and G. Sundholm, *J. Electroanal. Chem.*, 1998, **453**, 231.
11. J.-M. Pernaut and J. R. Reynolds, J. Phys. Chem. *B*, 2000, **104**, 4080.
12. R. Wadhwa, C. F. Lagenaur and X. T. Cui, *J. Control. Release*, 2006, **110**, 531.
13. A. F. Diaz and J. I. Castillo, *J. Chem. Soc., Chem. Commun.*, 1980, **9**, 397.
14. B. C. Thompson, S. E. Moulton, J. Ding, R. Richardson, A. Cameron, S. O'Leary, G. G. Wallace and G. M. Clark, *J. Control. Release*, 2006, **116**, 285.
15. J. Li and E. Wang, *Synth. Met*, 1994, **66**, 67.
16. G. G. Wallace, G. M. Spinks, L. A. Kane-Maguire and P. R. Teasdale, *Conductive electroactive polymers: Intelligent polymer systems*. 3rd ed., CRC Press, Boca Raton FL, 2009.
17. L. L. Miller, B. Zinger and Q.-X. Zhou, *J. Am. Chem. Soc.*, 1987, **109**, 2267.
18. T. Vernitskaya and O. Efimov, *Russ. Chem. Rev.*, 1997, **66**, 443.
19. E. Genies and J. Pernaut, *Synth. Met.*, 1984/5, **10**, 117.
20. M. Hepel and F. Mahdavi, *Microchem. J.*, 1997, **56**, 54.
21. K. Kanazawa, A. Diaz, R. Geiss, W. Gill, J. Kwak, J. Logan, J. Rabolt and G. Street, *J. Chem. Soc., Chem. Commun.*, 1979, **19**, 854.
22. J. M. Fonner, L. Forciniti, H. Nguyen, J. D. Byrne, Y.-F. Kou, J. Syeda-Nawaz and C. E. Schmidt, *Biomed. Mater.*, 2008, **3**, 034124.
23. T. A. Skotheim and J. Reynolds, *Conjugated Polymers: Theory, Synthesis, Properties and Characterization*. 3rd ed., CRC Press, Boca Raton FL, 2007.
24. P. Burgmayer and R. W. Murray, *J. Phys. Chem.*, 1984, **88**, 2515.
25. D. Svirskis, B. E. Wright, J. Travas-Sejdic, A. Rodgers and S. Garg, *Sens. Actuators B*, 2010, **151**, 97.
26. M. Brie, R. Turcu and A. Mihut, *Mater. Chem. Phys.*, 1997, **49**, 174.
27. V. T. Truong, B. C. Ennis, T. G. Turner and C. M. Jenden, *Polym. Int.*, 1992, **27**, 187.
28. K. J. Waynne and G. B. Street, *Macromolecules*, 1985, **18**, 2361.
29. A. Kaynak, *Fibers Polym*, 2009, **10**, 590.
30. A. Kaynak, L. Rintoul and G. A. George, *Mater. Res. Bull.*, 2000, **35**, 813.
31. J. B. Spires, H. Peng, D. E. Williams, B. E. Wright, C. Soeller and J. Travas-Sejdic, *Biosens. Bioelectron.*, 2008, **24**, 928.

32. H. Peng, L. Zhang, C. Soeller and J. Travas-Sejdic, *Biomaterials*, 2009, **30**, 2132.
33. Y. M. Uang and T. C. Chou, *Electroanalysis*, 2002, **14**, 1564.
34. S. Tirkes, L. Toppare, S. Alkan, U. Bakir, A. Onen and Y. Yagci, *Int. J. Biol. Macromol.*, 2002, **30**, 81.
35. M. Quinto, I. Losito, F. Palmisano and C. G. Zambonin, *Anal. Chim. Acta*, 2000, **420**, 9.
36. J. L. Besombes, S. Cosnier, P. Labbe and G. Reverdy, *Anal. Chim. Acta*, 1995, **317**, 275.
37. S. Cosnier, M. Fontecave, C. Innocent and V. Niviere, *Electroanalysis*, 1997, **9**, 685.
38. S. Komaba, M. Seyama, T. Momma and T. Osaka, *Electrochim. Acta*, 1997, **42**, 383.
39. C. L. Bayer and N. A. Peppas, *J. Control. Release*, 2008, **132**, 216.
40. Q. Lu, *Microchi. Acta*, 2010, **168**, 205.
41. P. Audebert, P. Aldebert, N. Girault and T. Kaneko, *Synth. Met*, 1993, **53**, 251.
42. A. Merz and A. Haimerl, *Synth. Met*, 1988, **25**, 89.
43. S. Lamprakopoulos, D. Yfantis, A. Yfantis, D. Schmeisser, J. Anastassopoulou and T. Theophanides, *Synth. Met*, 2004, **144**, 229.
44. V. Bajpai, P. He and L. Dai, *Adv. Funct. Mater.*, 2004, **14**, 145.
45. Y. C. Liu, *Electroanalysis*, 2003, **15**, 1134.
46. J. Sui, J. Travas-Sejdic, S. Y. Chu, K. C. Li and P. A. Kilmartin, *J. Appl. Polym. Sci.*, 2009, **111**, 876.
47. Y. Xiao, J. Che, C. M. Li, C. Q. Sun, Y. T. Chua, V. S. Lee and J. H. Luong, *J. Biomed. Mater. Res. Part A*, 2007, **80A**, 925.
48. E. Smela and N. Gadegaard, *Adv. Mater.*, 1999, **11**, 953.
49. A. Gelmi, M. J. Higgins and G. G. Wallace, *Biomaterials*, 2010, **31**, 1974.
50. M. J. Higgins, S. T. McGovern and G. G. Wallace, *Langmuir*, 2009, **25**, 3627.
51. K. J. Gilmore, M. Kita, Y. Han, A. Gelmi, M. J. Higgins, S. E. Moulton, G. M. Clark, R. Kapsa and G. G. Wallace, *Biomaterials*, 2009, **30**, 5292.
52. G. Denuault, M. Sosna and K. J. Williams, in *Handbook of Electrochemistry*, ed. C. G. Zoski, Elsevier, Amsterdam, 2007, p. 443.
53. R. T. Richardson, A. K. Wise, B. C. Thompson, B. O. Flynn, P. J. Atkinson, N. J. Fretwell, J. B. Fallon, G. G. Wallace, R. K. Shepherd, G. M. Clark and S. J. O'leary, *Biomaterials*, 2009, **30**, 2614.
54. D. D. Ateh, H. A. Navsaria and P. Vadgama, *J. R. Soc. Interface*, 2006, **3**, 741.
55. Y. Li, K. G. Neoh, L. Cen and E. T. Kang, *Biotechnol. Bioeng.*, 2003, **84**, 305.
56. G. Wallace and L. Kane-Maguire, *Adv. Mater.*, 2002, **14**, 953.
57. G. Shi, M. Rouabhia, Z. Wang, L. H. Dao and Z. Zhang, *Biomaterials*, 2004, **25**, 2477.
58. A. Boyle, E. Genies and M. Fouletier, *J. Electroanal. Chem.*, 1990, **279**, 179.

59. Q. X. Zhou, L. L. Miller and J. R. Valentine, *J. Electroanal. Chem.*, 1989, **261**, 147.
60. R. Kiefer, S. Y. Chu, P. A. Kilmartin, G. A. Bowmaker, R. P. Cooney and J. Travas-Sejdic, *Electrochim. Acta*, 2007, **52**, 2386.
61. Y. Cho, R. Shi, A. Ivanisevic and R. Borgens, WO 20111002947 A1, 2011.
62. Y. Cho, R. Shi, A. Ivanisevic and R. Ben Borgens, *Nanotechnology*, 2009, 20.
63. D. Carlsson, M. Krogh, M. Skoglund and T. Landy, WO 20091096822 A1, 2009.
64. D. Ge, X. Tian, R. Qi, S. Huang, J. Mu, S. Hong, S. Ye, X. Zhang, D. Li and W. Shi, *Electrochim. Acta*, 2009, **55**, 271.
65. K. L. Morgan, A. M. Shelchuk, J. D. Snell, N. Holmström and J. R. Helland, United States Patent 7397166, 2008.
66. M. B. Cannell, R. P. Cooney, P. Kilmartin, C. Soeller and J. Travas-sejdic, United States Patent 0061870, 2010.
67. L. A. Couvillon Jr., P. M. Nicholas and M. S. Banik, United States Patent 0065500 A1, 2005.
68. G. Valdés-Ramírez, J. R. Windmiller, J. C. Claussen, A. G. Martinez, F. Kuralay, M. Zhou, N. Zhou, R. Polsky, P. R. Miller, R. Narayan and J. Wang, *Sens. Actuators B*, 2012, **161**, 1018.
69. G. Jeon, S. Y. Yang, J. Byun and J. K. Kim, *Nano Lett.*, 2011, **11**, 1284.
70. T. S. Tsai, V. Pillay, Y. E. Choonara, L. C. Du Toit, G. Modi, D. Naidoo and P. Kumar, *Polymers*, 2011, **3**, 150.
71. R. C. Barthus, L. M. Lira and S. I. Torresi, *J. Braz. Chem. Soc*, 2008, **19**, 630.
72. P. Chansai and A. Sirivat, *Advances in Science and Technology*, 2008, **57**, 170.
73. J. L. Dubois-Rande, T. Le Doan, M. C. Pham, B. Piro, E. Teiger and J. P. Tenu, United States Patent 6468304, 2002.
74. E. Jager, D. Carlsson, M. Skoglund, M. Krogh and A. Selbing, United States Patent 20100016957 A1, 2010.
75. S. Minteer and J. Ulyanova, United States Patent 0077461 A1, 2007.
76. J. Weber, K. Harrison and A. Flanagan, United States Patent 0137155 A1, 2011.
77. R. T. Richardson, A. K. Wise, B. C. Thompson, B. O. Flynn, P. J. Atkinson, N. J. Fretwell, J. B. Fallon, G. G. Wallace, R. K. Shepherd, G. M. Clark and S. J. O'Leary, *Biomaterials*, 2009, **30**, 2614.
78. L. Xia, Z. Wei and M. Wan, *J. Colloid Interface Sci.*, 2010, **341**, 1.
79. X. Luo and X. T. Cui, *Electrochem. Commun.*, 2009, **11**, 1956.
80. M. R. Abidian, D. H. Kim and D. C. Martin, *Adv. Mater.*, 2006, **18**, 405.
81. S. Sirivisoot, R. Pareta and T. J. Webster, *Nanotechnology*, 2011, **22**, 085101.
82. D. C. Martin and M. R. Abidian, United States Patent 0097280 A1, 2008.
83. E. Ferain, D. Magnin, S. Demoustier-champagne, M. A. Thil, J. Delbeke and I. Colin, United States Patent 0233226 A1, 2010.
84. J. Ge, E. Neofytou, T. J. Cahill, R. E. Beygui and R. N. Zare, *ACS Nano*, 2012, **6**, 227.
85. E. A. Mensah, M. J. Capps, C. M. Coppin and J. M. Gross, United States Patent 7740656 B2, 2010.

CHAPTER 12

UV and Near-IR Triggered Release from Polymeric Micelles and Nanoparticles

MANUEL ALATORRE-MEDA,*[a]
CARMEN ALVAREZ-LORENZO,[b] ANGEL CONCHEIRO[b]
AND PABLO TABOADA*[a]

[a] Departamento de Física de la Materia Condensada, Facultad de Física, Universidad de Santiago de Compostela, 15782-Santiago de Compostela, Spain; [b] Departamento de Farmacia y Tecnología Farmacéutica, Facultad de Farmacia, Universidad de Santiago de Compostela, 15782-Santiago de Compostela, Spain
*Email: manuel.alatorre@usc.es; pablo.taboada@usc.es

12.1 Introduction

Strong efforts are being expended in the drug-delivery field to design nano- or microvehicles (referred to as nano-/microcarriers) that can protect, transport and release dose-active therapeutic molecules on demand to any desired site of action, thus achieving greater efficiency/safety ratios.[1] Among the different kinds of carriers proposed for oral, transdermal, mucosal and parenteral routes,[2] polymeric drug-delivery systems (DDSs) are especially suited to release a wide range of therapeutic agents, comprising from small-molecule drugs to biomacromolecules like proteins, DNA and RNA.[3–5] Recent approaches pursue the design and implementation of DDSs capable of controlling the site, timing and duration of drug release, allowing in turn the remote, non-invasive,

---

RSC Smart Materials No. 2
Smart Materials for Drug Delivery: Volume 1
Edited by Carmen Alvarez-Lorenzo and Angel Concheiro
© The Royal Society of Chemistry 2013
Published by the Royal Society of Chemistry, www.rsc.org

repeatable and reliable switching of therapeutic agent flux (with negligible release in the ‘‘off’’ state).[6,7] To accomplish this aim, the DDS should integrate components responsive to well-focused triggering stimuli.

Triggering mechanisms for drug-delivery applications can be induced by either i) interaction between a ‘‘smart’’ material and changes in its surrounding environment related to the progression of the disease or to certain functions/biorhythms (*e.g.* changes in temperature, pH and/or concentration of some substances);[8–13] or ii) external stimuli (such as magnetic and electric fields, heat, compression, ultrasound or light) whose intensity can be controlled by an operator or by the patient him/herself.[14–22] Although most efforts have been dedicated to systems that respond to changes in pH[9,10] and temperature,[11–13] light irradiation is receiving growing attention as photoregulated activation and transport of bioactive materials is better understood.[14,18–24]

This chapter focuses on phototriggered polymeric DDSs, with a special emphasis on light-sensitive micelles and nanoparticles. Approaches proved to be useful for imparting these systems with the desired light-responsiveness and the underlying drug release mechanisms are analyzed in detail. Polymeric systems in which the light responsiveness arises from the presence of photosensitive groups/ligands in the polymeric structure are comprehensively discussed. Other kinds of photosensitive systems such as those that combine polymers with inorganic or metallic nanoparticles are covered elsewhere in the present book, mainly in Chapters 13 and 15.

12.2 UV and Near-IR Light Irradiation

Light-responsiveness is receiving increasing attention owing to the possibility of developing DDSs sensitive to electromagnetic irradiation, particularly in the UV, visible and near-IR ranges.[18] Light is a particularly attractive stimulus for drug delivery because it provides a precise, temporal (*i.e.* by adjusting the intensity and duration of exposure) and spatial (*i.e.* by adjusting the irradiation wavelength and beam diameter) control over the activation and release of therapeutic agents. The present section is devoted to the interactions of light with the biological tissues and how they can affect the use of light as a triggering stimulus for drug delivery and related applications. UV and near-IR light irradiation are particularly addressed.

12.2.1 UV-visible Light

Far- (*ca.* 10–200 nm) and near-UV (*ca.* 200–400 nm) have been proposed as triggering stimuli for a plethora of applications including drug delivery,[25] cosmetics[26] and agriculture.[27] Irradiation at these regions presents pros and cons depending on the selected wavelength. Far-UV light ($\lambda < 200$ nm) offers the possibility of provoking irreversible changes in polymeric carriers with a concomitant almost instantaneous drug release,[28] which might be beneficial for certain applications. Far-UV irradiation is energetic enough to ionize, saturate and cleave covalent bonds (with energies of the order of 100 kcal mol^{-1}) of the polymer by laser ablation;[29,30] however, it might also be destructive for active molecules and tissues, which makes these wavelengths unsuitable for therapeutic purposes.[31] By contrast, irradiation at longer wavelengths (>200 nm) and continuous wave (CW) lasers are known to preserve the integrity of both drugs and tissues to a higher extent.[32,33] In these cases, the mild radiation acts over chromophores and optically active dyes present in the nanocarrier, producing either reversible[34] or irreversible structural and/or permeability changes.[35,36] Although much safer than far-UV, the irradiation with near-UV ($\lambda > 200$ nm) of optically active dyes in direct contact with skin might be dangerous, because irreversible photobleaching of dyes constitutes a source of active degradation products such as highly toxic radicals.[35] One additional disadvantage of UV light is that it cannot penetrate deeper than 1 cm into the body, since it is absorbed by endogenous components such as oxy- and deoxy-hemoglobin, lipids and water.[15,37,38] Hence, the usefulness of light irradiation below 650 nm is limited to trigger drug release for topical treatment of pathological processes on skin and mucosa, or in the external layers of some internal organs.[15]

12.2.2 Near-IR light

Near-IR has proven to be a promising tool for triggered drug delivery, *in vivo* imaging[39–41] and photothermal cancer treatment,[14,15,18] overcoming many of the drawbacks of UV and visible light irradiation. A key advantage of using light in the near-IR window (650–900 nm) is its minimal absorption by skin and tissues, enabling penetration into the body up to 10 cm because hemoglobin (the principal absorber of visible light), water and lipids (the principal absorbers of infrared light) have low absorption in this region.[42,43] Moreover, near-IR light does not cause a significant heating in the application area. Therefore, it can be useful for triggering drug release in areas of the body with difficult accessibility. Near-IR irradiation of nanocarriers that absorb in this region can be exploited to induce structure/conformation changes or to increase the local temperature, as the nanocarrier transforms the incoming energy into heat. Both effects lead to changes in the nanocarrier's permeability that can tune cargo release rate.[44,45] Some organic chromophores can simultaneously absorb two photons of low-energy near-IR light, and undergo the same chemical transformations as upon absorption of one photon of high-energy UV light.[46,47]

To construct efficient near-IR-triggered DDSs, it is essential to design materials that can be used safely without injuring tissues. Near-IR triggered materials must preferentially be irradiated with continuous-wave power flux in the range of 0.1 to 10 W cm^{-2} in order to avoid side-effect damage to organs and tissues. Based on ocular tests, the American National Standards Institute (ANSI) published in 1993 the maximum permissible exposures (MPEs) to laser light irradiation. In the case of a light source that is not collimated (*e.g.* light emitted by a fiber optic cable, which spreads in a conical fashion), the MPE for 700 nm light from a continuous wave source is 200 mW cm^{-2} steradian (sr)$^{-1}$ for long exposures, and as high as 10 W cm^{-2}sr^{-1} for exposures no longer than a second. For collimated light, acceptable levels are much lower: 0.2 mW cm^{-2} for extended exposures or 2 mW cm^{-2} if the exposure is not above 1 s. For longer wavelengths, higher power fluxes are permissible. When ultrafast laser pulses are applied, the MPE depends on the pulse duration and the interval between pulses, as well as on the light wavelength.[48]

12.3 Mechanisms of Light-triggered Release

There exist several mechanisms to achieve a phototriggered and photo-controllable release of a cargo from a nanocarrier, which may involve partial or complete destruction and recycling of the DDS.[49]

A) *Photo-isomerization* is related to a conformational change around a bond, usually a double bond, that is restricted in rotation. This phenomenon can be irreversible (due to the cleavage of the chromophore group upon photo-induced structural transformation) or reversible (the photo-excited molecules undergo internal rearrangements). This latter process predominantly involves a *trans* to *cis* isomerization upon irradiation (*e.g.* in azobenzenes, which have a -N=N- group with phenyl rings on either side), or the generation of charged species (*e.g.* the conversion of spiropyrane to merocyanine). Photo-isomerization is usually accompanied by a change in the hydrophilic/hydrophobic balance of the photo-excitable molecules. Thus, if these molecules are assembled in a nanocarrier, light can serve as a remote trigger for particle disassembly and drug release.[50]

B) *Polymer backbone photodegradation* enables light-triggered drug delivery through the ablation of polymeric chains, which causes the disassembly of the DDS. Degradation of polymers in small fragments may facilitate the clearance from the body.

C) *Photo-cross-linking or photopolymerization* may lead to the cargo release upon irradiation of polymerizable double bonds either directly or in the presence of a radical initiator/sensitizer. The procedure causes shrinking of the nanostructure, disruption of the initial packing of the molecules and formation of pores throughout the DDS.[51] The opposite process *photodecross-linking* (rupture of light-sensitive cross-links) also increases the porosity of the DDS network and induces the release of the payload.

D) *Photosensitization-induced oxidation* implicates the generation of a strong oxidizing agent, singlet oxygen, upon illumination of a sensitizer molecule included in the DDS either as a loaded agent or as a part of the structure. Irradiation at an appropriate wavelength causes the disruption of the nanocarrier.[52]

E) *Photo-excitation*. Photo-induced release can also be attained by exploiting the ability of metal nanoparticles to absorb light efficiently due to coherent oscillation of conduction band electrons in strong resonance with certain frequencies of light (which depend on nanoparticle size, shape, level of aggregation and composition).[53] Photo-excitation of metal nanostructures results in the formation of a heated electron gas that rapidly cools down by exchanging energy with the nanoparticle lattice.[54] Metal nanoparticles can reach temperatures well above 600–800 °C,[55] which induce significant thermal and mechanical stresses in the structure of the nanocarriers, leading to their rupture and subsequent payload release. Moreover, the nanoparticles rapidly transmit the energy to the surrounding medium causing localized heating, although the increase in temperature is limited to a few degrees.

12.4 Light-sensitive Polymeric DDSs

Light has long been recognized as an external stimulus and applied to modulate the aggregation features of conventional surfactants,[56–60] but is still scarcely exploited as a trigger for drug release from polymeric DDSs, compared to other stimuli like changes in pH and temperature.[8–13] In this section, strategies applied to make polymeric carriers sensitive to light are described.

12.4.1 Light-sensitive Polymeric Micelles

Polymeric micelles are particularly attractive core-shell nanocarriers.[19,61] Amphiphilic block copolymers (BCPs) spontaneously self-assemble in block-selective solvents when the BCP concentration surpasses the critical micelle concentration (CMC).[8,61–63] In aqueous medium, the hydrophobic blocks associate to form the core of the polymeric micelles primarily by hydrophobic interactions to minimize contact with water, although electrostatic interactions[64,65] and stereocomplex formation[66] can also be important. Meanwhile, the hydrophilic blocks of the copolymers form the shell of the micelles, stabilizing the micellar structure. Drugs can be loaded by physical means or chemical conjugation, resulting in an enhancement in the apparent solubility.[67] BCP micelles are more advantageous for drug delivery than conventional micelles, due to their larger cores enabling higher solubilization capacity[68] and physical stability (slower dissociation upon dilution) even at concentrations well below their CMC. Such stability extends their circulation time in blood.[65,69,70]

The application of polymeric micelles as DDSs was pioneered by the group of Ringsdorf in 1984.[71] In the early 1990s, Kataoka *et al.*[72] developed drug-conjugated block copolymer micelles, and Kabanov *et al.*[73] incorporated non-covalently linked drugs inside micellar cores. Nowadays, polymeric micelles (typically in the size range of 10–50 nm) are extensively studied as drug nanocarriers since they can fulfill most requirements for selective drug delivery.[74–76] In particular, they enable the formulation of hydrophobic drugs in aqueous medium, avoiding the use of toxic adjuvants like ethanol or Cremophor EL, increase drug bioavailability avoiding their rapid clearance by liver and/or kidneys and passively target the drug to certain tissues (for example, tumors) by means of the enhanced permeability and retention (EPR) effect.[77,78] The interest in polymeric micelles is accentuated by the possibility of modulating drug release by external stimuli, mainly ultrasound (addressed in Chapter 6) and light irradiation.[18] For polymeric micelles to be light-responsive, their constituting BCPs must incorporate/conjugate chemical groups reactive/sensitive to light.[79] In line with the triggering mechanisms described in Section 12.3, photoresponsive polymeric micelles can be grouped into four different categories depending on the photo-induced structural changes that cause the cargo release: a) a shift in the hydrophilic/hydrophobic balance of the BCPs, b) a break of block junctions within the BCPs, c) a BCP chain degradation process or d) a reversible cross-linking reaction (Figure 12.1).[61] The release of the loaded guest molecules does not necessarily require complete micelle disassembly, but a structural rearrangement to allow the diffusion of the cargo out of the micelle. These strategies can also be applied to other types of polymeric nanostructures.

12.4.1.1 Shifts of the Hydrophilic/Hydrophobic Balance

This approach consists in incorporating a chromophore in the block copolymer chain to render its hydrophilic/hydrophobic balance sensitive to illumination.

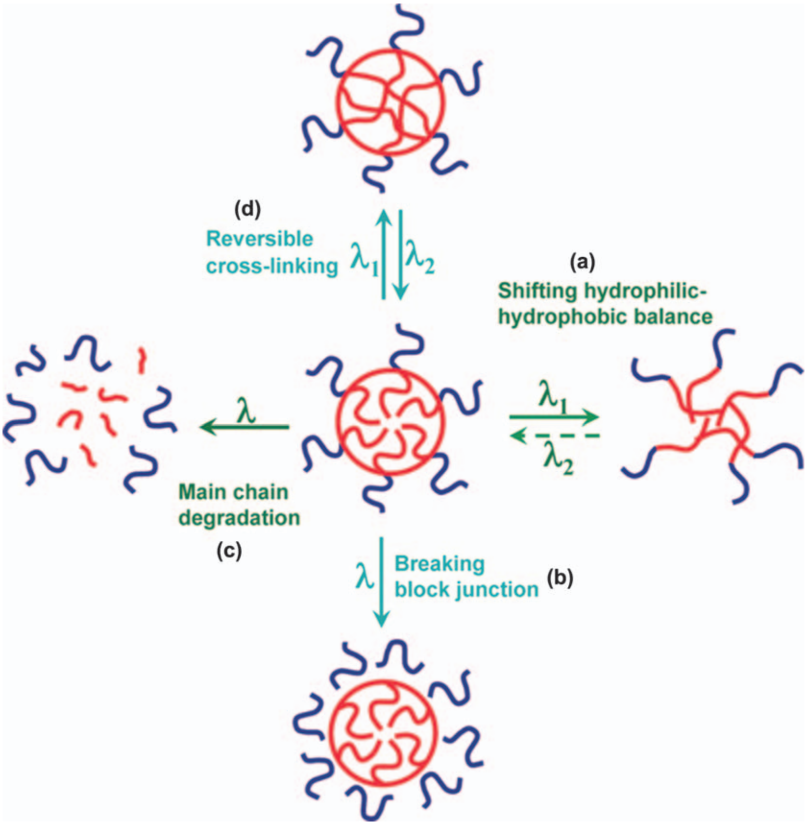
(d)
Reversible
cross-linking
λ1
λ2
(a)
Shifting hydrophilic-
hydrophobic balance
λ1
λ2
λ
Main chain
degradation
(c)
λ
Breaking
block junction
(b)

Figure 12.1 Schematic view of the different mechanisms by which light alters the structure of a sensitive copolymer micelle.
Reproduced from Ref. 61. Copyright (2012) American Chemical Society.

The photo-isomerization leads to a change in both the net dipole moment and the water solubility of the hydrophobic block, giving rise to micelle destabilization and subsequent disassembly by bringing the BCP concentration below its CMC. The key concept to photo-induced dissociation of polymeric micelles is that the isomer formed upon irradiation should have a significantly higher polarity than the non-irradiated, more stable isomer form. This process enables the release of molecules encapsulated inside the polymeric micelles at a chosen time and location. Both reversible and irreversible dissociation of BCP micelles upon irradiation with UV, visible or near-IR light have been achieved.[18,62,79] Nevertheless, a photo-induced shift of the hydrophilic/hydrophobic balance does not always result in an easy dissociation of micelles, provided that photo-induced changes are also coupled to structural parameters such as the block composition and polymer chain length.[61] If the photoreaction is reversible, the initial balance can be restored upon exposure to light at a different wavelength, and the micelle can be reassembled in solution (Figure 12.2).

Two different photoreactions enable micelle disassembly: those implying removal of pendant photochromic moieties upon photo-induced cleavage reaction (that transforms the hydrophobic block into a hydrophilic one, resulting in a permanent structural change that triggers the release);[18,19] and those that involve a change in the block copolymer polarity keeping attached the chromophore (Figure 12.2(a) and (b)). Photochemical groups involved in the first type of reactions include UV-activated pyrene,[80,81] *o*-nitrobenzyl (ONB)[82,83] and coumarin (both UV and near-IR-activated).[84,85] The hydrophobic blocks have the common feature of possessing an aryl methylester group linked to the chain backbone. In all cases, the photoreaction cleaves the photochromic moieties and converts the hydrophobic block into a hydrophilic one by forming carboxylic groups. For controlled drug-delivery purposes, it may be advantageous that the photoreaction does not involve the cleavage of the chromophore from the polymer, because the released compounds may lead to toxicity problems. Photochemical groups that do not cleave upon photoreaction are, for example, azobenzene, spiropyran, dithienylethene, diazonaphthoquinone (DNQ), stilbene, cinnamoyl, fulgides and triphenylmethane leucohydroxide.[18] Most of them cause UV-induced dissociation of polymeric micelles through a photo-isomerization process, which can be reversed under visible light, such as *trans*-*cis* isomerization of azobenzene and stilbene, isomerization of spiropyran and spirooxazines to merocyanine, conversion between ring-open and ring-closed forms of dithienylethene and fulgide or isomerization of cynnamoyl groups to more hydrophilic species due to electric charge generation or dimerization (Figure 12.3). By contrast, DNQ groups display a Wolf-rearrangement reaction (*i.e.* a conversion of an α-diazo-ketone group into a ketene one) that is irreversible. Triphenylmethane leucohydroxide undergoes a charge generation process under UV irradiation, which is only reversible under certain temperature conditions.

The first demonstration of the interest of photocontrollable BCP micelles based on shifts of the hydrophilic/hydrophobic balance as DDSs dates back to 2004,[34,86] when Zhao and coworkers reported the reversible dissociation of

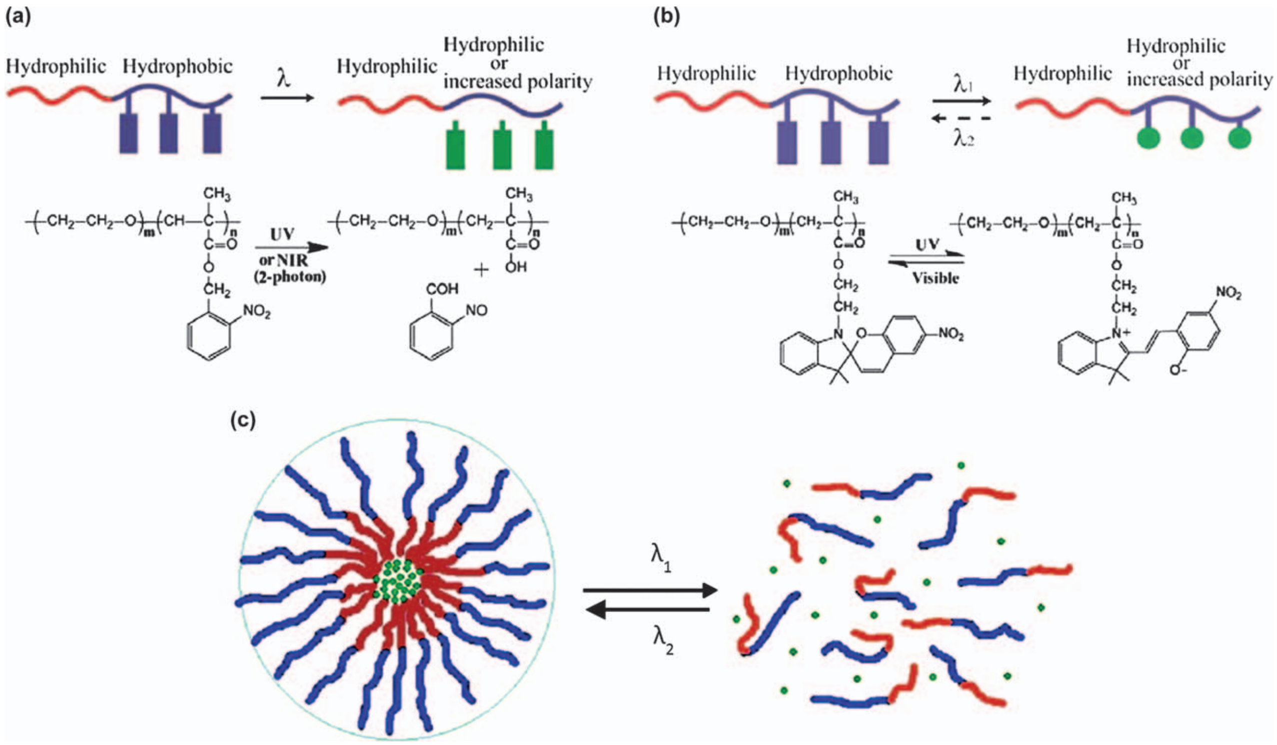
(a)
Hydrophilic
Hydrophobic
λ
Hydrophilic
Hydrophilic
or
increased polarity
UV
or NIR
(2-photon)
COH
NO
NO$_2$
(b)
Hydrophilic
Hydrophobic
λ$_1$
λ$_2$
Hydrophilic
Hydrophilic
or
increased polarity
UV
Visible
NO$_2$
O-
N+
(c)
λ$_1$
λ$_2$

Figure 12.2 Photo-induced shifting of the hydrophilic/hydrophobic balance in a block copolymer with *o*-nitrophenyl units that are removed after irradiation (a); with spiropyran units without removal of the photochromic moieties (b) (adapted from Ref. 61. Copyright (2012) American Chemical Society); and schematic view of the reversible micelle disassembly/reassembly process thereby produced (c).
(Reproduced from Ref. 47. Copyright (2005) American Chemical Society).

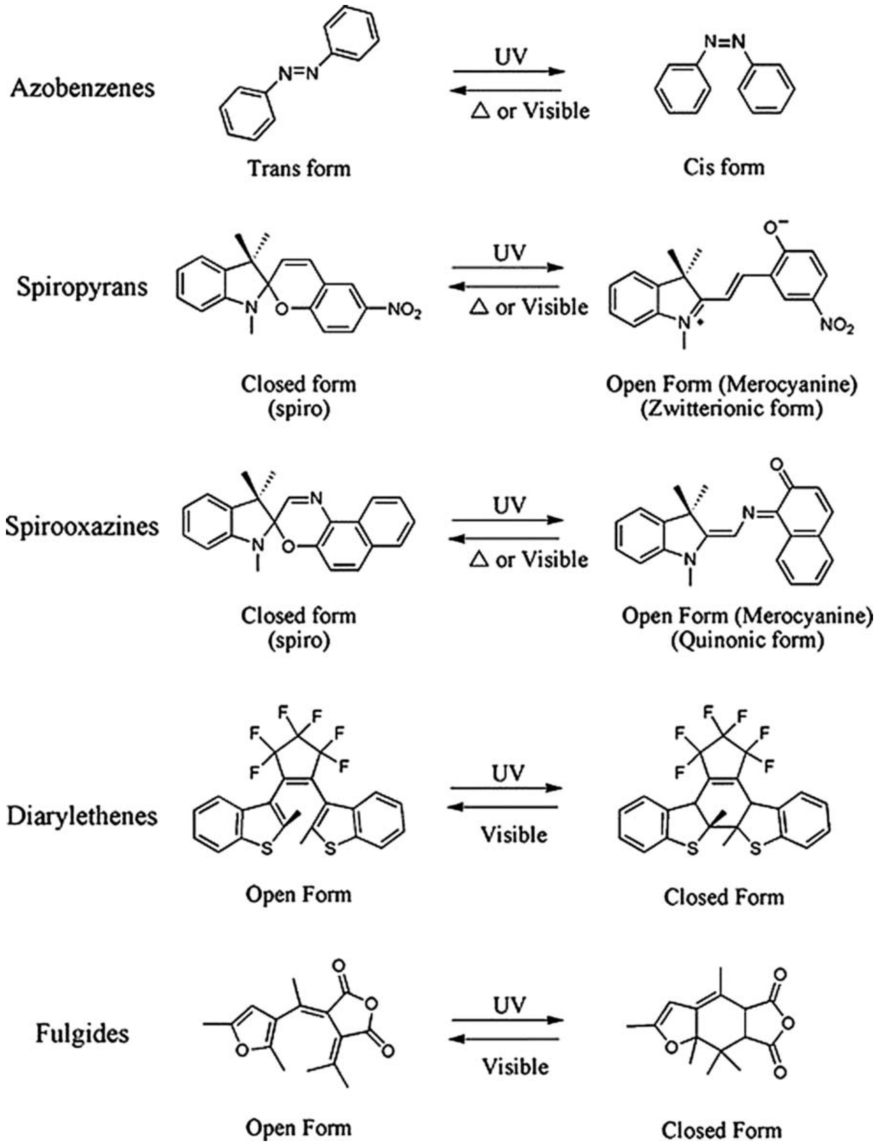
Azobenzenes
N=N
UV
△ or Visible
N=N
Trans form
Cis form
Spiropyrans
N
O
NO2
UV
△ or Visible
O⁻
N⁺
NO2
Closed form (spiro)
Open Form (Merocyanine) (Zwitterionic form)
Spirooxazines
N
O
N
UV
△ or Visible
O
N=
N
Closed form (spiro)
Open Form (Merocyanine) (Quinonic form)
Diarylethenes
F F F F F F
S S
UV
Visible
F F F F F F
S S
Open Form
Closed Form
Fulgides
O O O
UV
Visible
O O O
Open Form
Closed Form

Figure 12.3 Some photochromic moieties that exhibit reversible photoswitching. Reproduced from Ref. 21 with permission of The Royal Society of Chemistry.

micellar aggregates of azobenzene-containing polymethacrylate and poly(*tert*-butyl acrylate) (PAzoMA-b-PtBA) upon exposure to UV and visible light irradiation. The polymers with azobenzene groups in the *trans* form aggregated as core-shell micelles or vesicles depending on the preparation conditions. Upon illumination of a micellar solution with UV light (360 nm), *trans* azobenzene groups were converted to *cis* isomers, which resulted in a large increase in the polarity of the PAzoMA block and caused the micellar disruption. When the singly dispersed block copolymer chains were irradiated with visible light (440 nm), the reverse *cis*-*trans* isomerization restored the initial polymeric micelles. Two conditions have to be met to guarantee reversible UV light-induced micellar dissociation: i) the azobenzene group conjugated to the hydrophobic block should have a small (close to zero) dipole moment in the *trans* form and a considerably higher dipole moment in the *cis* form in order to ensure a significant change in polarity upon irradiation; and ii) the hydrophilic block should be weakly hydrophilic. The commitment of these two conditions can make the light-induced shift of the hydrophilic/hydrophobic balance great enough to achieve the reversible change in the aggregation state.[34,86] However, there are cases in which the *trans*-*cis* isomerization proves to be unfavorable for micellar disruption. For example, if azobenzene is *para*-substituted with an electron-donor and an electron-acceptor group,[87,88] the stable *trans* form actually has a greater dipole moment than the *cis* one, which implies that upon UV or visible irradiation the *trans*-*cis* isomerization would result in a decrease in polarity for the hydrophobic block, making the dissociation of BCP micelles unlikely to occur.[19]

Liu and Jiang[89] took benefit of the solubility change in azobenzene derivatives to induce the formation of micelles in a non-polar organic medium by using a complexable polymer pair consisting of poly(4-phenylazomaleinanil-co-4-vinylpyridine) (AzoMI-VPy) and polybutadiene with a terminal carboxy group.[89] The hydrogen bonding between the pyridyl and carboxy groups enabled the formation of "graft-like" inter-polymer complexes in toluene. The "graft copolymer" was toluene-soluble when the azobenzene units of AzoMIVPy were in the *trans* conformation. Under UV irradiation, the azobenzene units were isomerized into the polar *cis* form, which caused a decrease in the solubility of the AzoMI-VPy chains and the assembly in core-shell structures of the photo-induced amphiphilic "graft copolymer". This process was found to be reversible, namely following irradiation with visible light, the azobenzene returned to the *trans* form and the micelles quickly disassociated into transparent inter-polymer complexes.[89] The *cis*-*trans* isomerization was also used to modify (normally, to increase) the lower critical solution temperature (LCST) of thermo-sensitive polymers. Since the *cis* conformer is more hydrophilic, these polymers could be used to produce temperature and light dual responsive micellar systems.[90]

Extending this approach to other photochromic molecules, Lee *et al.*[91] reported BCPs that undergo reversible aggregation based on the photoisomerization between spiropyran and merocyanine.[91] The BCP was composed of poly(ethylene oxide) (PEO) as the hydrophilic block and a polymethacrylate bearing spiropyran moieties (PSPMA) as the hydrophobic block. Upon UV irradiation (365 nm), spiropyran was isomerized to charged merocyanine, which increased the polarity of the polymethacrylate block and led to micelle dissociation. Subsequent exposure to visible light (620 nm) caused merocyanine to transform again in spiropyran and then the polymer micelles could be

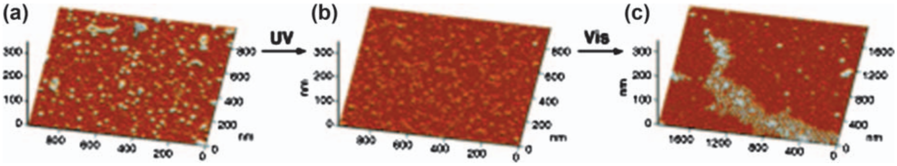

Figure 12.4 Atomic force microscopy (AFM) height images of PEO-b-PSPMA solutions spin-coated on mica under various conditions: PEO-b-PSPMA micelles (a); PEO-b-PSPMA micelles after 365-nm UV exposure for 30 min. showing micelle disassembly (b); and PEO-b-PSPMA micelles after 365-nm UV exposure for 30 min. followed by 620-nm visible-light exposure for 120 min. demonstrating micelle reassembly (c). Reproduced from Ref. 91 with permission of Wiley. Copyright (2007).

reconstituted (Figure 12.4).[91] Encapsulated coumarin 102, a hydrophobic dye, was released under UV irradiation, and some dye molecules were re-entrapped by the micelles reformed upon visible light exposure. As compared to the *trans*-*cis* isomerization of azobenzene, the conversion of spiropyran to charged merocyanine induces a larger increase in polarity for the hydrophobic micelle core-forming block.

Irreversible micelle disruption was demonstrated by Zhao *et al.*[80] with an amphiphilic diblock copolymer composed of PEO and poly(1-pyrenylmethyl methacrylate) (PPyMA). Upon UV irradiation of PEO-b-PPyMA micelles in aqueous medium, the photosolvolysis of pyrenylmethyl esters took place, cleaving 1-pyrenemethanol from the polymer and converting the ester groups to carboxylic acid ones. By this way, the hydrophobic PPyMA is converted to the hydrophilic poly(methacrylic acid) (PMAA). The concept was validated employing a BCP composed of PEO and poly(2-nitrobenzylmethyl methacrylate) (PNBMA).[92] By this case, the photolysis of 2-nitrobenzyl groups resulted in the cleavage of 2-nitrosobenzaldehyde from the polymer, transforming the hydrophobic PNBMA into hydrophilic PMAA and triggering the micellar dissociation (Figure 12.5).[49] Nile red was released upon the photoinduced micelle dissociation (80% after 420 s of irradiation), while no release was observed in the absence of UV irradiation. This micellar system also released the dye *via* two-photon near-IR, but at a much slower rate due to the low efficiency of two-photon absorption of 2-nitrobenzene. Remarkably, the possibility of using light to control the release rate of encapsulated molecules by varying the irradiation intensity was demonstrated.[92] Other controlled release processes employing the cleavage of different chromophore groups conjugated to BCPs to produce irreversible micelle disruption were reported later on.[93,94]

Conjugation of aromatic drugs to the hydrophobic block of an amphiphilic copolymer through photocleavable links may enable the light triggering of simultaneous micellar dissociation and drug release at a chosen time and location. For example, the anticancer drug 5-fluoruracil was covalently linked to the coumarin side groups on the hydrophobic block of a diblock copolymer through a UV-induced cyclo-addition process. Drug release from micelles of this copolymer occurred upon shorter-wavelength UV irradiation.[95] Using a

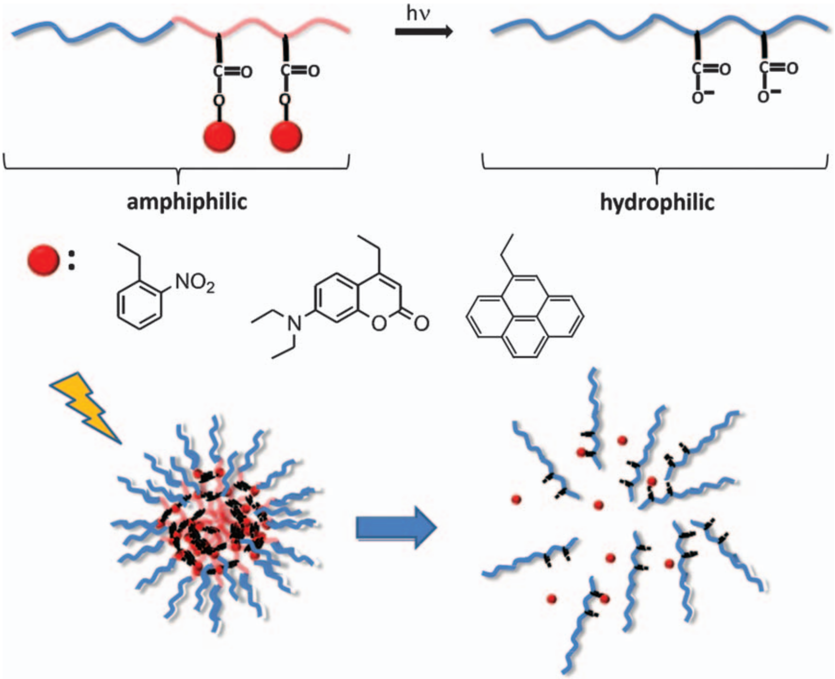

Figure 12.5 Block copolymer with masked carboxyl groups undergoing amphiphilic to hydrophilic switch upon light exposure and examples of light-sensitive protecting groups are shown at the top. The amphiphilic block-copolymer micelles disassembly upon irradiation is represented at the bottom. Reprinted from Ref. 49 with permission of Elsevier.

similar approach, Johnson *et al.*[96] synthesized brush-like nanosystems through polymerization of norbornene-containing macromonomers followed by covalent binding of doxorubicin using "click" chemistry. The linkage also contained the photo-uncaging ONB moiety that could be triggered by UV light to release the drug.[96]

The disruption of BCP micelles by near-IR light (especially in the window of 650–900 nm) is particularly attractive for biomedical applications since near-IR has a deeper penetration through water and tissues and is less detrimental to healthy cells than UV, as commented previously.[97] Some organic chromophores can simultaneously absorb two photons of low-energy near-IR light, and undergo the same chemical transformation as upon absorption of one photon of high-energy UV light. That is the case of *o*-nitrobenzyl esters and coumarin derivatives, the latter presenting larger two-photon absorbing cross-sections.[97] Application of near-IR light to release hydrophobic molecules from BCP micelles dates back to 2005.[47] Goodwin and coworkers used the Wolf rearrangement reaction of DNQ, which can be activated by one-photon UV or two-photon near-IR absorption, to photocontrol the dissociation of micelles formed by an amphiphilic polymer with a short poly(ethylene glycol)

(PEG) chain and a hydrocarbon tail bearing the DNQ group at the end. Upon two-photon near-IR absorption, Nile red previously loaded in the polymeric micelles was released to the aqueous medium as a result of the Wolf rearrangement that converted the hydrophobic DNQ to the hydrophilic 3-indenecarboxylate, leading to micelle disruption and concomitant cargo release.[47] Later, this DNQ-based system was modified by incorporation of dendritic polyester between the PEG and DNQ moieties, which allowed incorporation of various DNQ molecules per dendrimer.[98] The use of two-photon near-IR absorption as energy source has been further tested.[46,92,99] Although this approach is a suitable alternative to the highly energetic UV irradiation, in most of the cases it proved to be slow and inefficient due to the typically low two-photon-absorbing cross sections of the chromophores, which compelled to explore other near-IR-based approaches.[19] Recently, a novel strategy that uses a continuous-wave diode near-IR laser to disrupt BCP micelles and trigger the release of their ''payloads'' has been developed (Figure 12.6). By encapsulating NaYF4 : TmYb upconverting nanoparticles (UCNPs) inside micelles of PEO-block-poly(4,5-dimethoxy-2-nitrobenzyl methacrylate) and exposing the micellar solution to 980 nm light, photons in the UV region were emitted by the UCNPs, which, in turn, were absorbed by *o*-nitrobenzyl groups in the micellar core-forming block. The activation of the

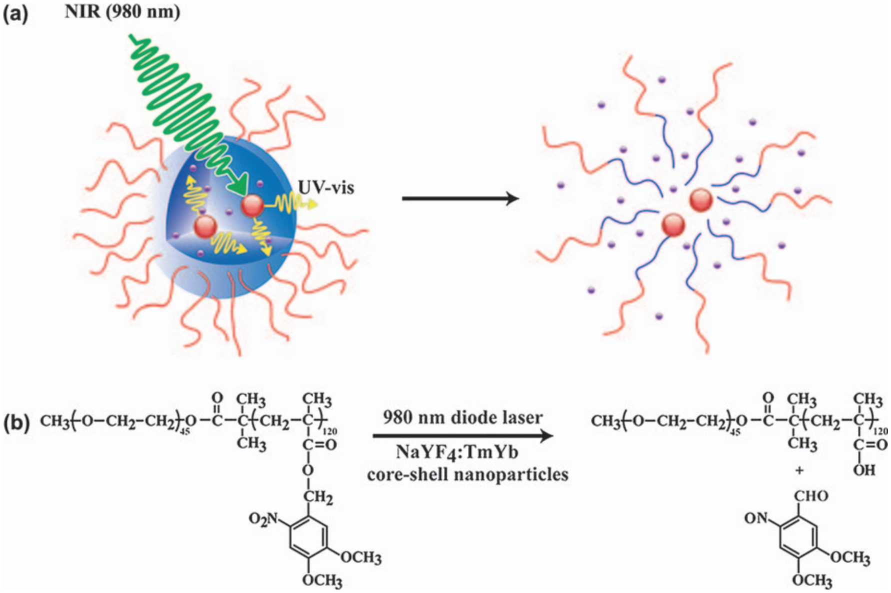

Figure 12.6 Schematic view of how near-IR light excitation of UCNPs can trigger dissociation of BCP micelles (a) and near-IR light-triggered photocleavage of PEO-b-PNBMA copolymer in the presence of NaYF4 : TmYb upconverting nanoparticles (UCNPs) (b).
Reproduced from Ref. 100. Copyright (2011) American Chemical Society.

photocleavage reaction leads to the dissociation of the BCP micelles and the subsequent release of co-loaded hydrophobic species.[100] This micellar system took advantage of the intense emission of NaYF4 : TmYb nanoparticles at 333–355 nm when excited by 980 nm near-IR light. It is worth stressing that this approach seems to be suitable for other systems because the photoreactions explored for the triggered release from polymeric micelles, even those requiring the use of UV or visible light, can be activated by near-IR light *via* excitation and emission of UCNPs.

12.4.1.2 Breakage of Block Junctions

Polymeric micelles can also be disrupted using light to separate the hydrophilic and hydrophobic blocks far apart by breaking block junctions. However, this approach is not the most suitable to achieve a photocontrolled release of the encapsulated cargo, provided that the breakage of the block junction basically removes the hydrophilic corona from the hydrophobic core but does not guarantee the core dissociation. That is, while the hydrophilic chains become dissolved in the aqueous solution, the micelle core can remain intact forming a nanoparticle that retains the payload (Figure 12.7).[94]

ONB-based moieities,[82,83] truxillic acid derivatives[101] and inserted azobenzene-cyclodextrin (CD) complexes[102,103] may serve as photocleavable block junctions. Constructs containing azobenzene-cyclodextrin (CD) complexes are particularly interesting for drug delivery, since they can undergo a reversible dissociation through a photoswitchable host-guest interaction between α-CD and the azo groups. Upon UV light irradiation to induce the *trans*-*cis* isomerization of azobenzene, the azobenzene-CD junction is broken. The junction can be restored upon visible light irradiation that induces the reverse *cis*-*trans* azobenzene isomerization (Figure 12.8).[102] This approach has

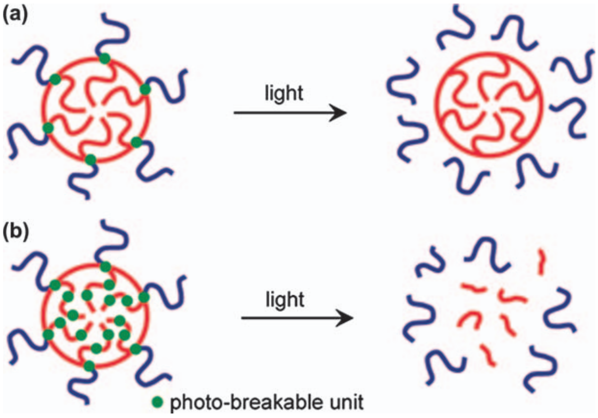

Figure 12.7 Effect of light on the behavior of micelles formed by block copolymers that contain one photobreakable group at only the block junction (a) or many of them on the hydrophobic block (b).
Reproduced from Ref. 94. Copyright (2011) American Chemical Society.

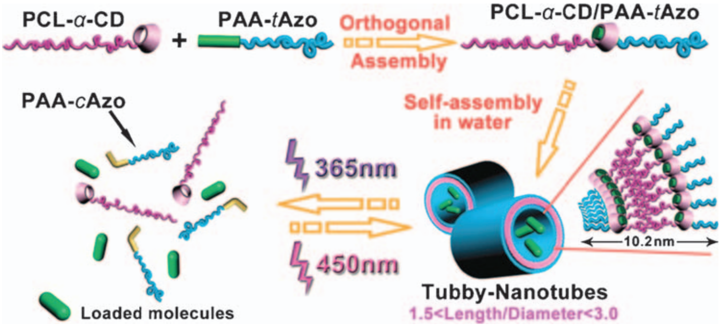

Figure 12.8 Structure of PCL-α-CD and PAA-*t*Azo, and scheme of the assembly/disassembly of light-responsive nanotubes on the basis of orthogonal host–guest interactions. PCL and PAA stand for poly(caprolactone) and poly(acrylic acid), respectively.
Reproduced from Ref. 102 with permission of The Royal Society of Chemistry.

been applied to achieve a photocontrollable exposure of functional groups used as targeting ligands to trigger the selective uptake of polymeric constructs by cancerous cells,[103] or to control the extent of interactions between polymer chains in polymer blends to regulate sol-gel phase transitions and cargo release.[104]

12.4.1.3 Main Chain Degradation

Photocleavable moieties can be inserted into the main chain of the hydrophobic blocks to cause a fast photo-induced degradation of the polymeric chain and, hence, of the micelle (Figure 12.7b).[94] Photolysis of pendant protecting groups (self-immolative groups) can trigger a cascade of cyclization and rearrangement reactions resulting in the degradation of the polymer chain backbone[85,105] and subsequent micelle disruption.[106,107] This approach has been applied to triblock copolymers bearing PEO blocks at both extremes and a photoresponsive hydrophobic middle block.[94,108] In one case, the hydrophobic polyurethane-based block possessed an ONB group in each repeating unit, which could be degraded in small segments upon UV light irradiation, thus leading to the rupture of the micelle core and subsequent cargo release.[94] In another case, the hydrophobic middle block contained not only an ONB group, but also a redox-cleavable disulfide functionality in each repeating unit.[108] The formed BCP micelles could undergo fast photodegradation upon UV exposure or slow degradation due to the reducing agent dithiothreitol (DTT).

12.4.1.4 Reversible Cross-linking

The instability of polymeric micelles in body fluids upon injection caused by strong and sudden dilution can result in premature release of the cargo. A well-known strategy to avoid this problem is the chemical cross-linking of the polymeric chains inside the micelle,[109–111] but such increased stability can make drug diffusion from micelles too slow at the target site. To overcome this problem, reversible photo-cross-linking of the micelles by irradiation at certain wavelength may be particularly useful. Destabilization can take place under irradiation with light of a different wavelength (Figure 12.9). To reach this goal, the photodimerization reaction through the cyclo-addition of coumarin-based groups under UV light at $\lambda > 310$ nm, and the subsequent cleavage of cyclobutane bridges under UV light at $\lambda < 260$ nm has been exploited.[112] Cinnamic acid can be also used for this purpose.[113,114]

In 2007, Zhao and coworkers designed a random copolymer with PEO and a hydrophobic block of 4-methyl-(7-(methacryloyl)oxy-ethyloxy) coumarin and methyl methacrylate (P(CMA-co-MMA)).[115] In aqueous medium, the dimerization degree of the photoresponsive groups of PEO_{112}-b-P(CMA_8-co-MMA_{20}) micelles varied between 20 and 80% depending on the wavelength of the UV light, altering the cross-linking density of the micellar core (Figure 12.9). This behavior could also be observed in non-aqueous micellar solutions. For example, in acidic organic medium THF/CH_2Cl_2 (1/1 v/v), shell-cross-linked,

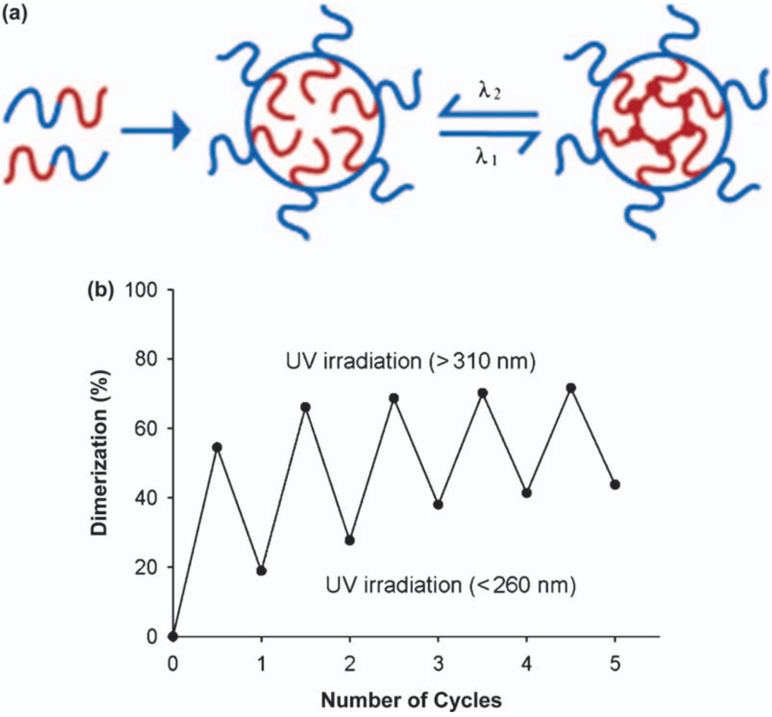

Figure 12.9 a) Schematic representation of block copolymer micelles that can be reversibly cross-linked and de-cross-linked by light at two different wavelengths. b) Changes in photodimerization degree of PEO_{112}-b-P(CMA_8-co-MMA_{20}) copolymer in solution subjected to alternating irradiations at two wavelengths.
Adapted from Ref. 115. Copyright (2007) American Chemical Society.

reverse micelles (SCRM) were obtained from copolymers composed of poly(dimethylaminoethyl methacrylate) (PDMAEMA) as the hydrophilic block, and a random copolymer of coumarin methacrylate and methyl methacrylate (P(CMA-co-MMA)) as the hydrophobic block. This micellar structure allowed the growth of additional layers of PDMAEMA at the surface of the micelles, resulting in robust polymer nanoparticles. The grafting of the hydrophilic PDMAEMA chains rendered the SCRMs soluble in water at pH7 and room temperature, the solubility being sensitive to changes in these variables. Importantly, these new nanoparticles retained the light-responsiveness imparted by the coumarin moieties of the P(CMA-co-MMA) block.[116] This responsiveness, reflected as a reversible stability, is crucial for the dual stable/non-stable behavior that the micelles must exhibit when circulating in the body fluids. Namely, the micelles must be stable enough to resist dilution and minimize interactions with the biological medium (*e.g.* hydrolysis and enzymatic degradation) in order to avoid the release at first stages of body internalization (*e.g.* when travelling through the bloodstream),[117,118] but they need to be disrupted for releasing the drug once they reach the target.[84] Importantly, different from chemical cross-links that may impair the biodegradability, physical cross-links may be more friendly for cells and tissues.[119]

The reversible photocross-linking approach can be exploited in combination with other external stimuli. For instance, temperature/pH-responsive and photoresponsive groups/blocks inside a unique polymeric chain may provide multiple switching capability to BCPs.[120–123] As an example, a dually responsive block copolymer with PEO, as the hydrophilic block, and an acrylate-based block bearing ONB units, as the thermo-responsive hydrophobic block, can form micelles encapsulating Nile red at a temperature above the LCST of the hydrophobic block. Upon continuous UV irradiation for 180 min., the ONB groups are cleaved and the LCST of the thermo-responsive block increases by 11 °C, causing micelle dissociation. Further increase in the temperature above the LCST of the new thermo-responsive block caused the micelles to be reformed and re-encapsulate the dye (Figure 12.10).[61] Using a similar approach, He *et al.*[120] demonstrated the dual responsiveness (to temperature and light) of a diblock copolymer composed of PEO and a coumarin-containing poly[2-(2-methoxyethoxy)ethyl methacrylate] (PMEO$_2$MA) block, which formed core-cross-linked micelles upon simultaneous heating of the solution above the LCST of PMEO$_2$MA and exposure to UV light at $\lambda > 310$ nm. Upon subsequent cooling below the LCST, the cross-links prevented the micelles from disassembly, giving rise to nanogel particles with hydrophilic core and shell and phototunable size.[120]

12.4.2 Polymeric Vesicles

Self-assembly of amphiphilic BCPs can lead, under certain circumstances,[124] to the formation of vesicle-type structures consisting of a bilayer surrounding an aqueous core (Figure 12.11), which were named "polymersomes" by Discher *et al.*[125] in 1999 due to their resemblance to liposomes. The possibility of

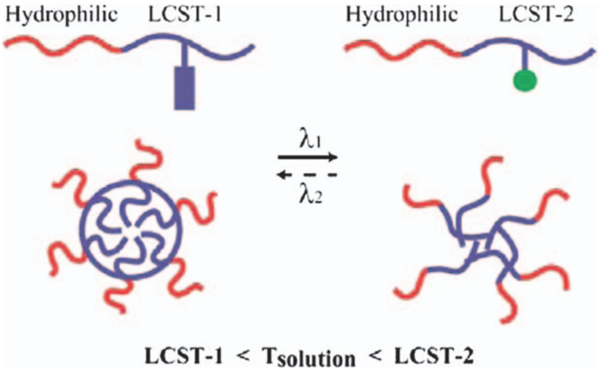

Figure 12.10 Photo-induced micelle disassembly due to an increase in the LCST of thermal sensitive blocks caused by a photoreaction (reversible or irreversible).
Reproduced from Ref. 61. Copyright (2012) American Chemical Society.

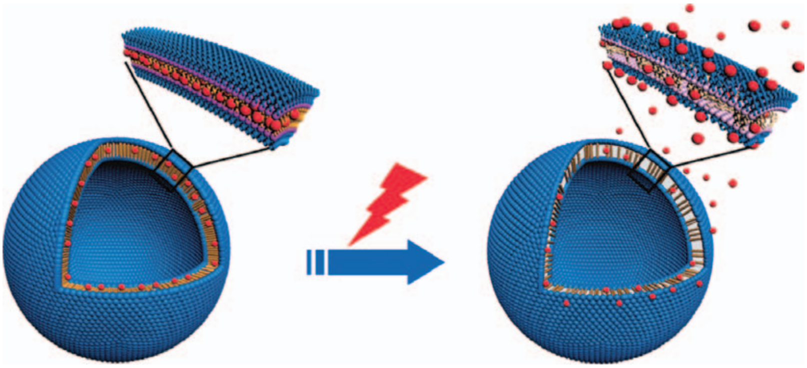

Figure 12.11 Structure of a polymersome and schematic view of the photocontrolled release of the hydrophobic cargo loaded into the bilayer.
Reproduced from Ref. 126. Copyright (2012) American Chemical Society.

polymersomes formation depends on the polymer composition, the mutual affinity between the copolymer blocks and the solvent and the preparation conditions (*e.g.* ionic strength of the medium or temperature).[124] Polymersomes can be obtained through different methods, including electroformation, rehydration and direct dissolution into water.[126,127]

The attractiveness of polymersomes for encapsulation lies in both the availability of biodegradable polymers and the feasibility of tailoring the bilayer properties.[125,128,129] Compared to lipidic vesicles, polymersomes are considered to be more rigid, stable and versatile,[130,131] and this can be further enhanced by cross-linking of the polymer network.[132] Polymersomes may simultaneously be used as carriers of hydrophobic (accommodated in the bilayer) and hydrophilic (accommodated in the aqueous interior) drugs.[62,133,134] Apart from biodegradation through hydrolysis,[133,135] oxidation-[136,137] or reduction-responsive processes[138,139] and stimuli like changes in pH[140–142] and temperature,[143–145] drug release from polymersomes can be triggered by light exposure following the same strategies described for polymeric micelles (Figure 12.11).[126] This outstanding flexibility opens a broad range of opportunities for their use in biomedical applications.[126,146,147]

As reported for micelles, azobenzene derivatives are suitable to induce morphological changes in BCP vesicles upon light irradiation. Han *et al.*[148] reported on the photocontrolled swelling/shrinking transitions of micron-sized, light-sensitive vesicles formed by a diblock copolymer of poly(*N*-isopropylacrylamide)-block-poly(6-[4-(4-pyridyazo)phenoxy] hexylmethacrylate) (PNIPAM-b-PAzPy) in water/tetrahydrofuran medium.[148] The vesicles were found to swell upon UV-light irradiation as a result of the *trans*-to-*cis* photoisomerization of the azopyridine groups; meanwhile, they returned to their original dimensions when visible light irradiation restored the *trans* form. The degree of swelling could be controlled by adjusting the density of UV light power, opening a novel way to transform light energy to mechanical energy. Moreover, since the diblock copolymer also presented pH- (PAzPy) and temperature- (PNIPAM) responsive functional groups,[148] other applications can be envisioned. Employing a similar approach, Lin *et al.*[149] reported on the photo-induced rearrangement in water/tetrahydrofuran medium of vesicles formed by a diblock copolymer of PEO and polymethacrylate with photochromic azopyridine moieties in the side groups.[149] Upon different periods of UV light irradiation (from 10 to 60 min.), the vesicles underwent a cyclic process from fusion, damage and defect formation to disruption, disintegration and rearrangement. This behavior has two main advantages: i) the defects produced along the bilayer increase the permeability of vesicular membranes; and ii) the disruption of the vesicular membrane is expected to promote the exchange of substances between the outside and the inside of the vesicles. Therefore, controlled release of encapsulated chemical species could be achieved by adjusting the extent of photo-induced change in the morphology of vesicles. The release process can be inhibited at any moment by irradiation with visible light.[149] Photocontrolled self-assembly/disassembly has also been reported for supramolecular polymer nanocontainers obtained through the electrostatic association between an azobenzene-containing surfactant (AzoC10) and a double-hydrophilic block ionomer composed of PEG and PAA.[150] The block ionomer complex self-assembles in aqueous solution and forms vesicle-like aggregates consisting of a PEG corona and a PAA shell associated with the azobenzene-containing surfactant. When irradiated at 360 nm, the azobenzene groups photo-isomerized, enabling the release of the guest substances. After irradiation at 440 nm, the guest molecule was partially re-encapsulated.[150] Pursuing the same goal but employing a multi-stimuli strategy, Jin and coworkers explored the possibility of forming *trans*-azobenzene-CD inclusion complexes either to tune the complete disassembly of polymer vesicles[151] or to control the type of self-assembled nanostructure (*i.e.* vesicle or micelle) present in the solution.[152] PEO-b-poly(2-(diethylamino)ethyl methacrylate-co-6-(4-phenylazo phenoxy)hexyl methacrylate formed vesicles in aqueous solution at pH 8.[151,152] On adjusting the pH to 3, a transition from vesicles to micelles occurred.[152] A similar transition was also realizable on addition of β-CD at pH 8, followed by an alternating irradiation of the solution with UV and visible light that triggered a *trans*-to-*cis* isomerization of azobenzene units and, consequently, a reversible micelle-to-vesicle conversion.[151,152] Structural transitions from micelles to vesicles and *vice versa* were also observed by Liu and coworkers subjecting mixed systems of poly(4-phenylazomaleinanil-co-4-vinylpyridine) (AzoMI-VPy) and polybutadiene with a terminal carboxy group (CPB) to UV light irradiation.[89] The AzoMI-VPy/CPB mixture formed "graft-like" inter-polymer complexes in toluene due to the hydrogen-bonding interaction between carboxylic acid and pyridine. The complexes were soluble in toluene when the azobenzene units of AzoMI-VPy were in the *trans* conformation. However, under UV light irradiation, the azobenzene units adopted the polar *cis* conformation, making the AzoMI-VPy chains aggregate into core–shell micelles. The core of these micelles, composed of pyridyl groups, was cross-linked with 1,4-diiodobutene at room temperature. The cross-linked micelles responded to the light irradiation with reversible and remarkable morphological changes. Namely, visible light led to the formation of hollow spheres as a result of intense swelling of the core with the *cis*-to-*trans* azobenzene isomerization, and UV light caused the hollow spheres to return to micelles as a result of isomerization in the opposite direction. Importantly, this reversible optical switching of the micelle–vesicle transition was achieved employing common, readily prepared polymers.[89]

Azobenzene-mediated light photo-isomerization has also been employed for triggering an extremely rapid cargo release from polymersomes. The basic principle to induce a rapid release is to cause frustrations in the membrane, as proved for asymmetric polymersomes in which each leaflet consisted of a different type of diblock copolymer.[153] One of the copolymers (PEG-b-PBD) was insensitive to any remote stimulus, whereas the second one located in the outer part of the membrane was a liquid-crystalline (LC) polymer containing azobenzene mesogens (PEG-b-PMAzo444).[153] The *trans* to *cis* isomerization of the azobenzene groups upon UV irradiation induced a nematic (N) to isotropic (I) phase transition in the LC polymer, which modified the conformation from extended to coiled state.[154] That conformational change altered the membrane curvature and led to the polymersome bursting (Figure 12.12). Heat or electric or magnetic fields could also be employed as remote stimuli, provided that one of the two leaflets of the membrane was composed of suitably designed LC copolymers.[155,156]

Light-triggered delivery from polymersomes can also be achieved using other methodologies and chromophores. For example, Jiang *et al.*[157] described the assembly of PEG-terminated triphenylmethane dye into vesicles in the absence of UV irradiation. Upon UV irradiation, the photochromic triphenylmethane

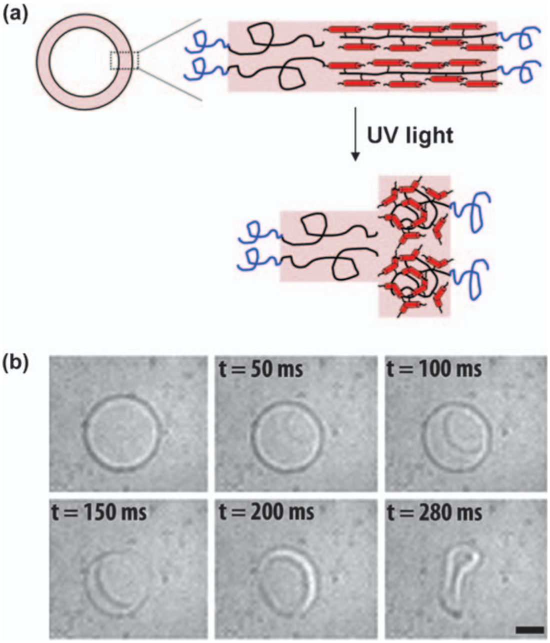

Figure 12.12 Scheme of a polymersome depicting the conformation, within the bilayer of the vesicle, of PEG-b-PBD in the coil-coil state and PEG-b-PMAzo444 in a rod-like conformation (corresponding to a nematic state) in the absence of UV light and in coiled conformation (isotropic state) under UV illumination (a). The isomerization of the mesogenic groups induces a conformational change of the polymer backbone with a subsequent increase in the bilayer curvature. Snapshots of a polymersome bursting under UV illumination (b). The first image shows the vesicle before illumination. Time $t = 0$ corresponds to pore nucleation. The other images show the same vesicle as the pore grows (Scale bar, 5 μm). Reproduced from Ref. 153 with permission of the National Academy of Sciences.

was ionized to a cationic form, leading to the disassembly of the vesicles. The cation thermally recovered its electrically neutral form, and the disassembled species could reform the vesicles. The reverse reaction was temperature-controlled and could be speeded up by heating.[157] Employing spiropyran as chromophore, Huang and coworkers prepared vinylpyridine-based BCP vesicles.[158] When located inside the vesicle membrane wall, isomerization of colorless spiropyran to colored merocyanine upon UV irradiation prompted both an increased photostability of the vesicles and a quantum yield enhancement of the chromophore fluorescence.[158] Based on the reversible color and on other changes in physical and chemical properties of spiropyran, these materials have already found interesting applications in data recording, optical and electrical switching and signal processing at the molecular level.[159–162] Harvesting of light energy to produce local heating and membrane budding in polymersomes was performed by Robbins *et al.*[163] Polymersomes made of a

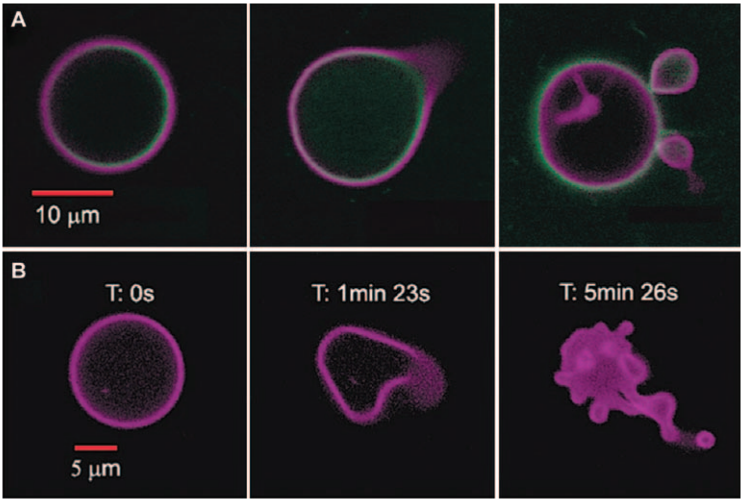

Figure 12.13 Confocal micrographs of polymersomes with PZn2 (purple) in the membrane and iron-free apoferritin (HSAF) in the interior. BODIPY-FL-labeled HSAF + PZn2 vesicle imaged using two lasers simultaneously (488, 543 nm) (A) and unlabeled HSAF + PZn2 vesicle imaged using three lasers simultaneously (488, 543, 633 nm), where PZn_2 absorbs strongly (B).
Reproduced from Ref. 163. Copyright (2009) American Chemical Society.

polyethylene oxide-polybutadiene BCP (PEO_{30}-b-PBD_{46}), incorporating horse spleen ferritin (HSF) or iron-free apoferritin (HSAF) in their aqueous interior and a porphyrin-based meso-to-meso ethyne-bridge bis[(porphinato)zinc] (PZn_2) chromophore in their membrane, were found to undergo vesicle shape changes upon exposure to light at different wavelengths. The synergy between the protein and the chromophore led to a photo-initiated destruction of this tertiary system (Figure 12.13). The broad range of wavelengths (including near-IR) that may induce the vesicle deformation suggests a local membrane heating mediated by electronically and vibrationally excited porphyrin molecules.[163]

Photocleavage of BCPs has also been explored to disrupt vesicles. For example, a diblock copolymer of PEG and poly(caprolactone) joined by a photocleavable 2-nitrophenylalanine moiety (PEG-2NPA-PCL) has been used to prepare vesicles that show UV-driven drug release.[164] When exposed to light and as the release proceeded, the vesicles diminished the size owing to a thickening and gradual collapse of the membrane, coupled with the expulsion of aqueous contents. Also utilizing photocleavable junction units between polymer blocks, Cabane *et al.*[165] prepared and tested poly(methyl caprolactone)-ONB-PAA (PMCL-ONB-PAA) based vesicles as smart, triggerable nanocarriers. These vesicles were found to disintegrate upon UV irradiation, yielding small micellar-like structures and simultaneously releasing their

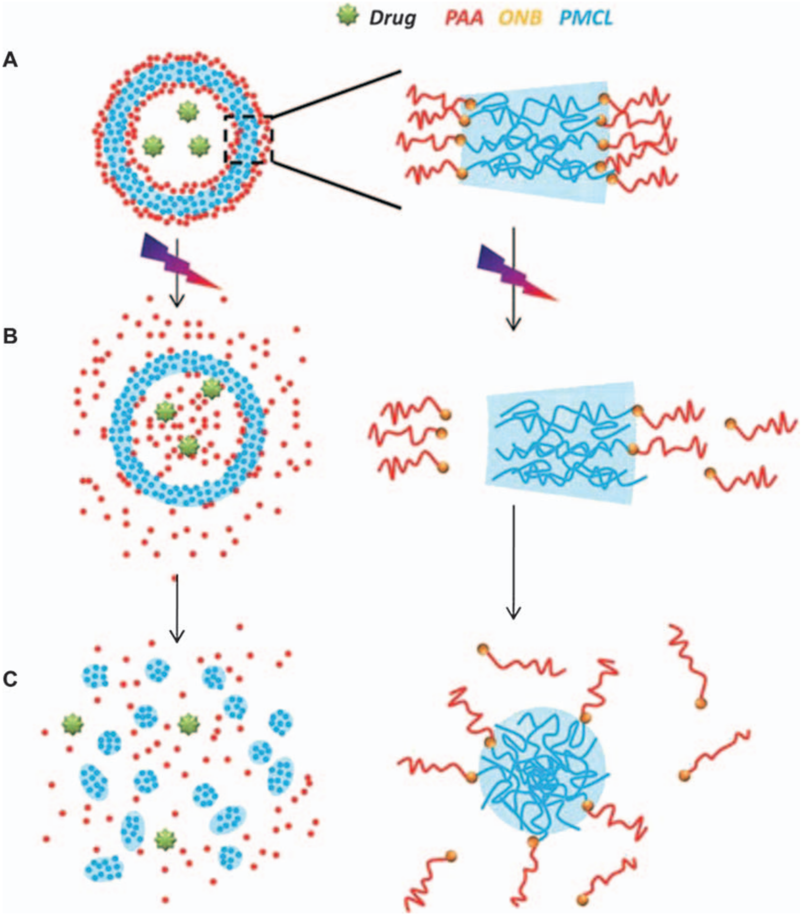

Figure 12.14 Steps of the photocleavage of the assembled polymer chains forming the vesicle membranes (A). Upon UV exposure, the corona PAA chains are cleaved, *i.e.* separated from the PMCL that form the core of the membrane (B). As a consequence, the vesicle membrane is destroyed and the payload released (C).
Reproduced from Ref. 165 with permission of The Royal Society of Chemistry.

payload (Figure 12.14). The versatility of this system was confirmed for low molecular weight molecules (fluorescein and ATTO655 dye) and proteins (enhanced green fluorescent protein), which were released in a controlled manner by varying the UV intensity.[165] Finally, Zhao and coworkers developed cross-linked BCP vesicles capable of expanding in response to temperature while preserving their structural integrity.[121] Large vesicles formed by a coumarin-containing BCP of poly[2-(dimethylamino)ethyl methacrylate] (PDMAEMA) and PNIPAM were subjected to corona cross-linking through dimerization of coumarin upon UV irradiation at temperatures above the

PNIPAM's LCST. Vesicles with a low cross-linking density (~5 mol% of coumarin units in the corona-forming block) showed large (~700%) and reversible volume transitions upon cooling from 40 to 20 °C. Coined as "soft coronal cross-linking", this approach represents an attractive strategy for designing polymer vesicles for delivery purposes.[166] The key point is to produce a lightly cross-linked corona capable of both retaining the vesicle structure and allowing the swelling of vesicle membrane under certain circumstances to enable drug release. Polymers whose water solubility can be switched by other stimuli such as light and pH can also be used to prepare vesicles of this kind.[121]

12.4.3 Polymeric Nano-/microparticles

Polymeric particles such as single and multi-layered capsules, micro-/nanogels and solid nano-/microspheres are widely studied in the pharmaceutical field.[28,45,167,168] These particles display interesting features related to the stabilization, protection and delivery of labile, active compounds.[169,170] Different from micelles and vesicles, they can be prepared not only from block and branched copolymers[169,170] but also from linear, biocompatible polymers like natural chitosan,[171,172] alginate,[173,174] gelatin,[175,176] albumin,[177,178] polylactic acid (PLA),[179,180] poly(lactic-co-glycolic) acid (PLGA),[181,182] PCL[183,184] and poly(cyanoacrylate) (PCA),[185,186] as well as combinations with other materials such as PEG.[181,184,185] To obtain the particles, it is possible to start from monomers applying heterogeneous (such as emulsion) polymerization methods, or from pre-formed polymers, mainly applying coacervation/precipitation, layer-by-layer (LbL) assembly or grafting to a secondary polymer.[187–192]

12.4.3.1 Polymeric Capsules

Polymeric capsules are nano-/microparticles that consist of a polymeric wall (single or multi-layered) that surrounds a liquid core (either an oil or an aqueous solution, depending on the synthetic procedure).[26,193] Capsules allow the entrapment of drug molecules either inside the inner compartment or along the layer(s) of the polymeric shell. Drug encapsulation can be done i) by incorporation into sacrificial components that act as templates for the capsule formation and that when are removed, the solid or solubilized drug molecule remains in the cavity of the capsule (which is especially useful when the compound cannot permeate the polymeric shell);[194–196] and ii) by loading the molecules of interest into pre-fabricated capsules upon reversible chemical (decross-linking/depolymerization) or physical (rupture, melting or increase in porosity of the shell wall) changes in the membrane permeability that are commonly produced by external stimuli.[28,197] The approaches prompting changes in membrane permeability can also be used to trigger the release from the capsules (Figure 12.15). Triggers that can be used to accelerate the release include variations in pH, ionic strength and temperature;[198–200] exposure to enzymes,[201,202] ultrasound,[203–205] microwaves[206,207] and light[14,28]

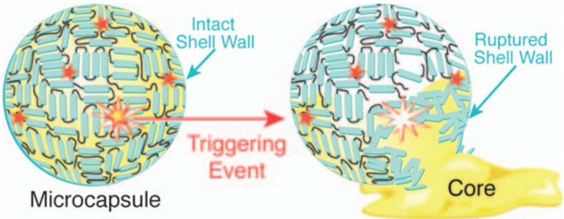

Figure 12.15 Scheme of a stimuli-responsive microcapsule that contains a sensitive element (depicted as a star) that can be activated to trigger the cargo release from the capsule.
Reproduced from Ref. 105. Copyright (2010) American Chemical Society.

and application of a mechanical force.[36,208,209] Capsules can be made sensitive to UV and near-IR light by incorporation of sensitive polymers,[32,210] functional dyes,[211,212] metal nanoparticles[44,213,214] and nanotubes.[215] In the next paragraphs, we will exclusively focus on capsules made of light-responsive polymers.

As occurs with micelles and polymersomes, light irradiation can lead to reversible changes in the capsule permeability because of chromophore isomerization cycles in the polymer chain. Likewise, light irradiation can also produce irreversible changes and rupture in the capsule shell by bond cleavage and occurrence of phase transitions or changes in the structural arrangement of the wall-forming polymers as a result of the increase in vibrational energy (heat) produced by absorbed light. In this regard, concerns about the potential toxicity of the constituting capsule elements upon rupture have to be considered.[33] To the best of our knowledge, encapsulation and release from photoresponsive polymer-based capsules have only been achieved by using UV light irradiation. Studies dealing with near-IR-sensitive capsules report hybrid constructs, *i.e.* polymeric capsules containing inorganic elements such as metal nanoparticles,[44,213,214] carbon nanotubes[215] or near-IR-reactive dyes.[35]

Light-triggerable capsules were prepared by Kono *et al.*[216] from partly cross-linked PAA, polyethylenimine (PEI) and a copolymer of acrylic acid and bis(4-(dimethylamino)phenyl)(4-vinylphenyl)-methyl leucohydroxide. Upon UV irradiation, the triphenylmethane derivative dissociated into an ion pair, thereby generating electrostatic charges. The permeation of an encapsulated anionic molecule, *p*-toluenesulfonate, through the capsule membrane was enhanced significantly after 10 min. of irradiation. Permeation decreased when the irradiation was stopped, because of the re-association of the triphenylmethane derivative by thermal recovery.[216] Light-induced capsule release was also described by Schärtl *et al.*,[217] who functionalized polyorganosiloxane nanoparticles with nitrocinnamate photochemical switches in order to build and disassemble the microcapsules shell walls using light. After assembly, the nanoparticles were cross-linked with UV light in a water/oil/water emulsion to create the microcapsule shell wall through the reaction of cinnamate groups in a

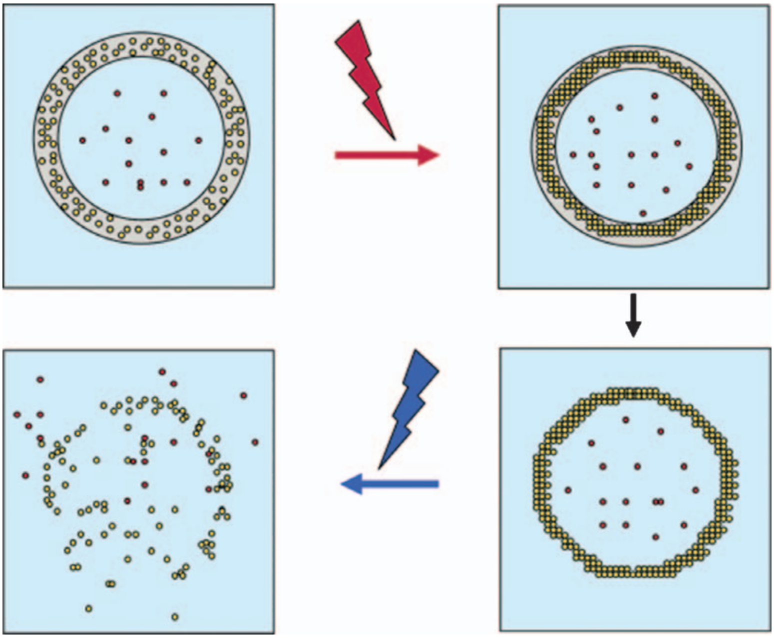

Figure 12.16 Scheme of microcapsules prepared by photocross-linking of photoreactive nanoparticles within the oil layer of water/oil/water emulsion droplets as a template, and controlled destruction by UV irradiation which causes the release of their contents.
Reproduced from Ref. 217. Copyright (2005) American Chemical Society.

reversible 2 + 2 photocyclo-addition. Destruction of the microcapsules and release of the cargo was successfully achieved by photocleavage of the dimer linkages at 254 nm (Figure 12.16).[217] However, the process was quite slow since photo-addition and photodissociation required several hours. Park *et al.*[218] used photocross-linking as a means to achieve rhodamine B release from LbL nanocapsules prepared with benzophenone modified-poly(allylamine hydrochloride) and poly(sodium-4-styrenesulfonate) (PAH-BP/PSS). The release rate could readily be controlled by the photocross-linking density of the PAH chains; the permeability of the (PAH-BP/PSS) hollow shells being reduced by *ca.* 50% after 3 min. of UV irradiation.[218]

Photo-induced structural changes in the polymeric shell have been applied to encapsulate and release fluorescently labeled dextran molecules from an azobenzene-substituted LbL construct of $[PAH/PAZO]_n/PVS$, where PAZO and PVS stand for poly(1-4[4-3(3carboxy-4-hydroxyphenyl-azo)benzenesulfonamido]-1,2-ethanedyil) and poly(vinyl) sulfonate, respectively. Irradiation caused shell shrinkage coupled with an increase in the wall permeability, which facilitated the encapsulation. The longer the irradiation time, the greater the encapsulation yield was found to be. Although annealing effects were excluded, the permeability changes were found to be irreversible.[32] PAZO-based microcapsules have also been formed by precipitation polymerization using monodisperse silica particles with trapped acetonitrile as templates, the silica particles being removed by hydrofluoric acid etching. Acetonitrile evaporation created pore channels in the shell. The *cis* azobenzene conformation under UV light exposure gave rise to larger pore diameters than *trans* azobenzene, allowing a faster loading and release of rhodamine B according to a pure Fickian diffusion mechanism.[219]

Photo-acid generation is another recognized method for light-induced encapsulation and release.[210] Koo and coworkers employed the LbL technique to prepare microcapsules with walls containing photo-acid generators (PAGs). Upon exposure to UV light, the PAGs were activated and the decrease in the pH caused by the release of protons triggered the swelling of the microcapsules. The microcapsules could be opened and closed *via* alternate exposure to UV light and washing with neutral water. Prolonged exposure led to breakage of the capsules and caused rapid release of the entrapped substances (Figure 12.17).[210]

Multi-responsive capsules have also been developed. As an example, Landfester *et al.*[220] reported controlled release *via* multiple stimuli (pH-, UV light- or temperature-induced) of a dye molecule from polyurethane nanocapsules formed by an aqueous core and azo bonds located at the polymeric shell. Depending on the stimulus, the release occurred in minutes (UV light), hours (temperature) or days (pH), revealing the high versatility of the capsules.

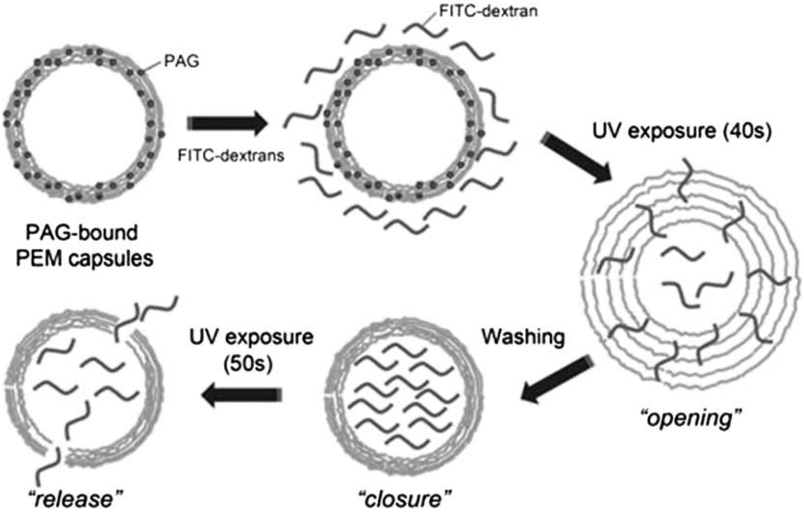

Figure 12.17 Encapsulation of fluorescein isothiocyanate-labeled dextran (FITC-dextran) into PAG-bound polyelectrolyte multi-layer capsules and subsequent cargo release from the capsules brought about by UV irradiation.
Reproduced from Ref. 210 with permission of The Royal Society of Chemistry.

This new generation of triggered nanocapsules might be particularly suitable when a selective release of a drug or a catalyzer is required.[28,220,221]

12.4.3.2 Nanogels

Nanogels are aqueous dispersions of chemically or physically cross-linked polymer particles of nanoscale sizes that imbibe water without dissolving. Current approaches for the preparation of nanogels can be divided into four broad categories, namely i) physical self-assembly of interactive polymers; ii) polymerization of monomers in a homogeneous phase or in a heterogeneous environment; iii) cross-linking of pre-formed polymers; and iv) template-assisted nanofabrication.[187,189,222–224] Nanogels are regarded as very promising drug-delivery carriers considering their high stability in solution and, more importantly, the feasibility to respond to internal and external stimuli, changing on demand some of their physico-chemical properties (*e.g.* volume, water content, refractive index, network permeability or hydrophilicity).[225–228] Drugs can be loaded into nanogels by physical entrapment,[229] covalent conjugation[230] or controlled self-assembly.[231] Controlled release can be achieved *via* different pathways, such as i) diffusion throughout the network;[232] ii) erosion of the network through intra-molecular degradation or rupture of inter-molecular bonds;[233] or iii) volume phase transitions induced by a physical stimulus.[234] Depending on the composition, light-responsive nanogels can be broadly divided into two groups: those made with light-responsive polymers bearing photo-active groups (such as azobenzene, spirobenzopyran or cinnamonyl) and those composed of a polymeric network (typically temperature-responsive) and inorganic particles (typically of a metal). The first group is analyzed below, the second one in Chapter 13.

Purely polymeric, light-responsive nanogels have scarcely been studied for drug-delivery applications as compared to hybrid nanogels. This is presumably because the irradiation necessary for inducing the phase transition is either UV or visible short wavelength light, both of which are not as friendly for cells and tissues as the near-IR light employed when working with hybrid systems. As mentioned previously, near-IR irradiation (within the so-called "friendly window") can induce a phase transition in hybrid nanogels thanks to the absorptivity of the inorganic component, which transforms the incoming energy into heat and enables the cargo release by modifying to suitable extents the permeability of the polymeric network.[44,45,235–237]

Using coumarin-containing block copolymers, Zhao's group proposed a strategy to make a stable, compatible nanogel with easy on-site release.[120,123] Photoresponsive nanogel particles were made of a double hydrophilic block copolymer (DHBCP) composed of PEO and PMEO$_2$MA.[120] At temperatures above LCST, the polymer aggregates were photocross-linked *via* dimerization of coumarin under UV light ($\lambda > 310\,\text{nm}$). After cooling down, the nanogel particles could undergo a reverse photocleavage reaction under UV light ($\lambda < 260\,\text{nm}$) leading to swelling with a volume increase of up to ~90%. The size of the nanogel particles and the rate of cargo release was photo-controllable through the reversible photocross-linking and de-cross-linking

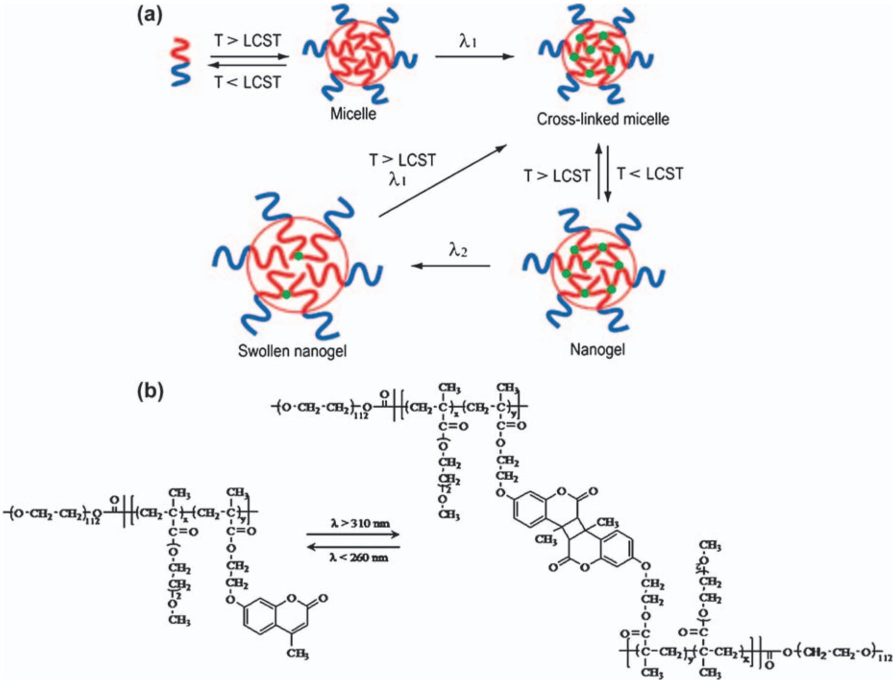

Figure 12.18 Scheme of the preparation and photocontrolled volume change of nanogels (a) and structure of the block copolymer bearing coumarin groups useful for the reversible photocross-linking reactions (b). Reprinted from Ref. 120. Copyright (2009) American Chemical Society.

reaction of coumarin (Figure 12.18).[120] Nanogels with a highly cross-linked core released dipyridamole at a slower rate than after de-cross-linking.[120] In a subsequent publication this research group reported both core- and shell-cross-linked nanogels.[123] Reverse photocleavage of coumarin dimers under UV light ($\lambda < 260$ nm) caused notable changes in the size, which were more relevant than for the nanogels with only cross-linked core or only cross-linked shell.[123] Photocross-linkable coumarin-based block copolymer nanogels have also been prepared with one of the blocks being pH-responsive, enabling a double control of the nanogel size.[238]

Photocontrollable nanogels have also been developed taking benefit from the self-aggregation of an azo-dextran polymer through π stacking interactions.[239] The nanogels were loaded with rhodamine B and aspirin and their release pattern depended on the isomerization of the azobenzene group. The release rate was slow when the azo moiety was in the *trans* configuration. By contrast, the *trans*-*cis* photo-isomerization led to the disruption of the polymer stacking and accelerated the release of the contents. The release rate was also found to be increasingly faster for longer irradiation times and higher contents of azo groups in the nanogel.[239] Alternatively, photocleavage of ONB groups has been shown to be able to trigger the swelling and degradation of gel particles;[240] for example, poly(4,5-dimethoxy-2-nitribenzyl methacrylate) nanoparticles, obtained by a free radical miniemulsion polymerization process, could transform into the hydrophilic poly(methacrylic acid) to trigger the release of the cargo (Nile red).[241]

The combination of light and other stimuli can be exploited for a fine tuning of the release. Landfester's group prepared dual stimuli-responsive hydroxyethyl methacrylate-co-methacrylic acid (poly(HEMA-co-MAA)) microgel particles by inverse miniemulsion copolymerization, using two photodegradable cross-linkers containing nitrophenyl units.[242] Microgel degradation, necessary for the release of the protein myoglobin, depended on light wavelength and intensity (UV light induced the cleavage of the photolabile cross-linking points), while the pH of the medium determined the ionization of MAA and thus the degree of swelling (Figure 12.19). This particular combination of stimuli led to the attainment of a fast, controlled degradation (induced by irradiation) and a slow, controlled release (induced by pH changes), which allowed an on-demand delivery of myoglobin.[242] The same approach has been implemented to create dual enzyme and light-responsive nanogels composed of acrylamide and a dextran-nitrobenzyl-acrylate cross-linker.[243] Partial enzymatic cleavage of the dextran backbones resulted in nanogel swelling; while irradiation with UV light induced either swelling or complete degradation of the nanogel depending on the irradiation time. Hence, a two-step degradation profile could be attained by the combination of the two orthogonal stimuli.[243]

In addition to drug delivery, light-sensitive nanogels have also been designed for other biomedical purposes. Photoresponsive nanogels formed by the self-assembly of spiropyrane-bearing pullulan (SpP) can act as artificial molecular chaperones.[244] The solution properties of these nanogels are controlled by photostimulation *via* isomerization between hydrophobic spiropyrane and hydrophilic merocyanine. The activity of citrate synthase significantly increases when the amphiphilicity of SpP nanogels is switched by photostimulation.[244] Also, nanogels bearing cinnamate moieties at the surface can be used to

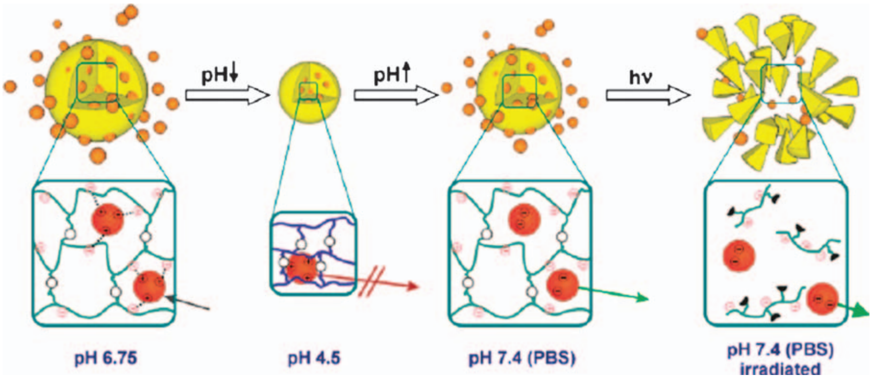

Figure 12.19 Schematic representation of double stimuli-responsive photodegradable p(HEMA-co-MAA) microgels.
Reproduced from Ref. 242. Copyright (2011) American Chemical Society.

fabricate autonomous self-healing coatings.[245] For example, nanoparticles prepared by miniemulsion copolymerization and surface functionalized with cinnamate groups were used to form films by drop-casting. Then, light was applied to induce an inter-particle photocross-linking through dimerization of the previously incorporated cinnamate groups. The resultant films showed high swellability, homogeneous ordering, efficient photoreactivity and marked affinity for different additives.[245]

12.4.3.3 Solid Polymeric Nanoparticles

Solid matrices with sizes between 10 and 200 nm and different levels of porosity, capable of holding molecules inside their structure or embedded along their surface,[246] can be prepared by different methods including solvent evaporation, coacervation, spray drying, ionic gelation, microfluidics and supercritical fluids precipitation.[247] In contrast to micellar aggregates, polymeric nanoparticles have an outstanding ability to maintain the structural integrity in diverse environments, which is appealing for a broad variety of applications.[248,249] The possibility of designing nanoparticles able to disassemble in a controlled fashion upon the application of a stimulus (*i.e.* light irradiation) further increases their interest in the biomedical field. In general, the materials and the procedures employed to endow capsules with light-sensitivity can also be adapted to these micro-/nanospheres.

Photo-irradiation may serve to regulate the sizes of polymeric nanoparticles.[250] For example, self-assembled nanoparticles of polymers containing cinnamic acid blocks, obtained by applying a solvent mixing method, proved to undergo reversible size changes upon irradiation with 280 nm (50% shrinking) and 254 nm (75% swelling) UV light.[251] The diameter changes were attributed to a [2 + 2] cyclo-addition formation (cross-linking) and cleavage of the cinnamate groups,[251] as further confirmed even in the presence of PEG (Figure 12.20). In the latter case, the photocross-linking induced a size decrement of up to 30% in the nanoparticles depending on the grafting degree and molecular weight of PEG. Such a size decrement of the nanoparticles gave rise to an increase in PEG chain density, notably decreasing non-specific protein adsorption. These water-dispersible and photoresponsive nanoparticles might be useful as functional carriers for drug-delivery systems and biological diagnosis devices.[113] Polymeric nanoparticles containing azobenzenes[252] and 1,2-dithienylethene derivative pendant groups[253] have also demonstrated a similar size tunability under UV light irradiation.

Formation of photosensitive polymeric nanoparticles can readily be achieved by ionic self-assembly of oppositely charged polyelectrolytes, such as cationic chitosan and an anionic photosensitive pyrene derivative.[28,254] Nile red-loaded particles released the cargo when irradiated with UV light. Contrary to what was originally expected, the dye release was mediated by particle shrinking rather than by particle disassembly. This behavior was attributed to the cross-linking of chitosan by butanoic acid generated after the removal of pyrene groups. Although to a lower extent, dye release was also observed upon

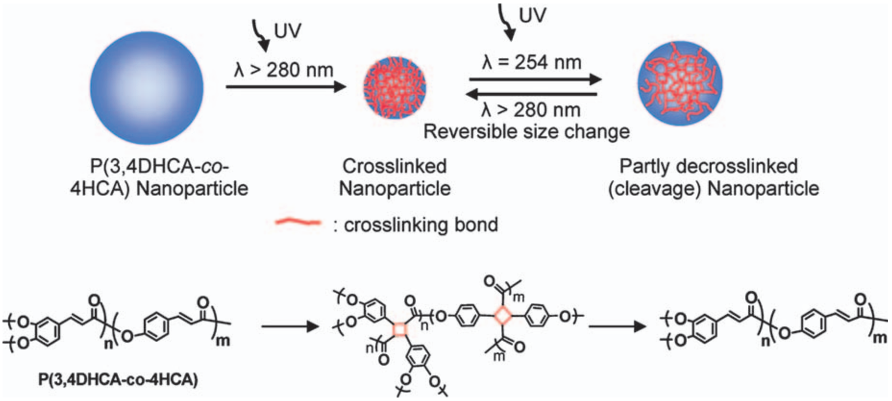

Figure 12.20 Scheme of the size changes undergone by P(3,4DHCA-co-4HCA) (DHCA, dihydroxycinnamic acid; HCA, hydrodycinnamic acid) nanoparticles under UV irradiation, which causes a [2+2] cycloaddition (cross-linking) first and then a deformation (cleavage). Reproduced from Ref. 251. Copyright (2008) American Chemical Society.

irradiation with near-IR light thanks to the two-photon absorbance of the pyrene derivative.[254] Switchable drug release can also be obtained by photodissociation of photolabile groups, which leads to particle disassembly. That is the case of fluorescent dyes encapsulated in polymer nanoparticles made of a triblock copolymer of poly(pyrenylmethyl methacrylayte)-b-polystyrene-b-poly(ethylene oxide).[81] UV irradiation resulted in the photodissociation of 1-pyrenemethanol units from the polymer backbone, resulting in breakage of the particles and subsequent release of the cargo.[81] Photolabile, cross-linkable cationic nanoparticles of ONB- and methacrylate-functionalized PEI have been tested as gene carriers.[255] The polymer consists of three functional domains: a cationic one to form polyplexes with DNA, a cross-linking domain to retain the DNA within the polyplex and a photolabile domain to release the DNA when irradiated with light of an appropriate wavelength. The cross-linked particles provided a 3-fold enhanced transfection efficiency compared to similarly prepared non-cross-linked particles.[255]

Cargo release can also be attained from light-responsive nanoparticles through polymer degradation. Removal of pendant protecting groups from polymers can trigger a cascade of cyclization and rearrangement reactions that results in degradation of the polymer chain backbone.[85,105–107] Almutairi *et al.*[99] reported a light-sensitive self-immolative polymer containing a quinine-methide backbone and photocleavable nitrobenzyl alcohol groups as the triggers. The polymeric nanoparticles were formed *via* a single emulsion method, encapsulating Nile red. Irradiation with 350 nm light resulted in a burst release (67% in 60 s), while near-IR irradiation caused a slower release (Figure 12.21).[99] This system has been further improved to achieve efficient polymer disassembly upon near-IR irradiation.[85]

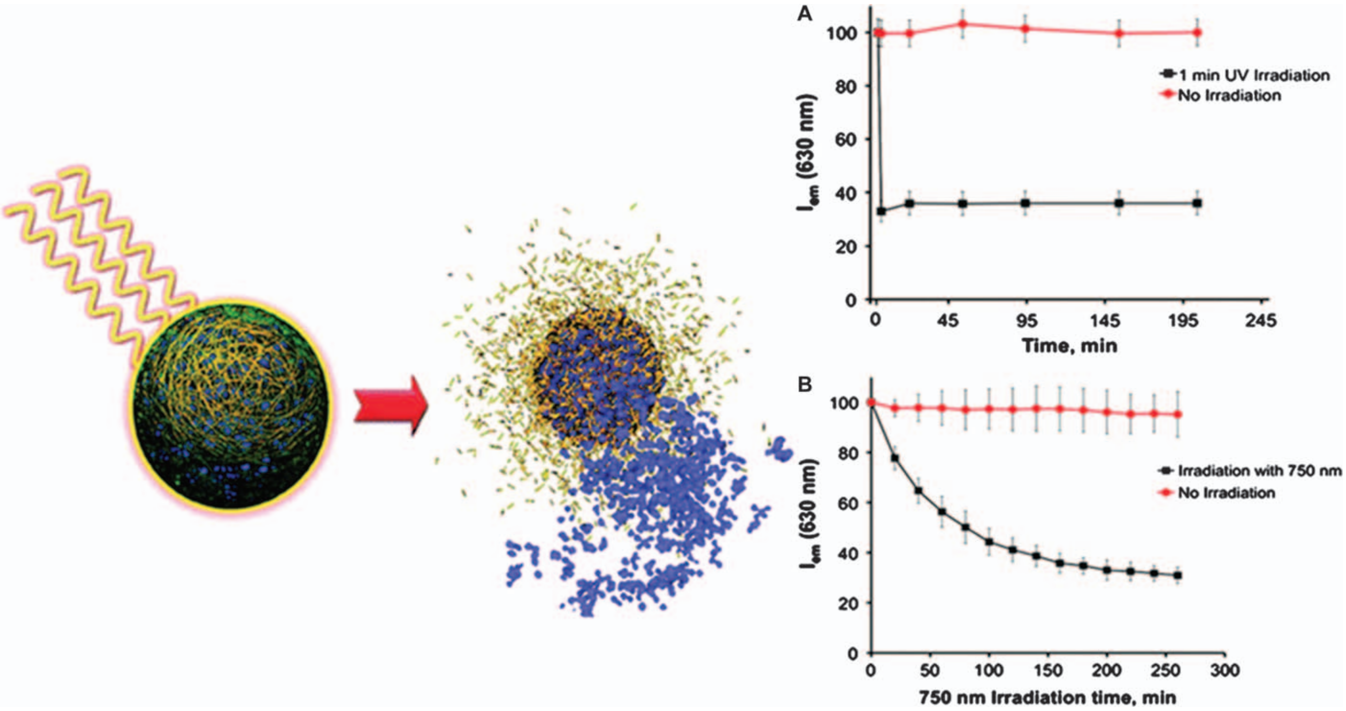

Figure 12.21 Light-triggered degradation of polymeric particles and release of Nile red upon UV irradiation at 300–400 nm (A) and near-IR irradiation at 750 nm (B). The plots show the fluorescence intensity inside the polymeric particles.
Reproduced from Ref. 99. Copyright (2010) American Chemical Society.

Photo-induced targeting of polymeric nanoparticles to diseased cells and tissues has recently been reported. Kohane *et al.*[256] described the use of light to trigger nanoparticles binding in specific illuminated areas. The design comprised drug-loaded nanoparticles whose surface was covalently modified with the amino acid sequence YIGSR, which adheres to the β1 integrins present on all cell surfaces. This peptide was linked to the caging group 4,5-dimethoxy-2-nitrobenzyl (DMNB), rendering it biologically inert.[257] Illumination with UV light (365 nm) triggered the release of the caging group from the ligand and allowed the particles to bind cells. In contrast to other reports where nanoparticles had been triggered by light to produce single drug release events,[55,258] this approach resulted in the deposition of the carrier at the desired site.[256] This and other similar systems allowed tissue targeting without specific markers (Figure 12.22).[103,256] Furthermore, this methodology can be employed with highly specific ligands.

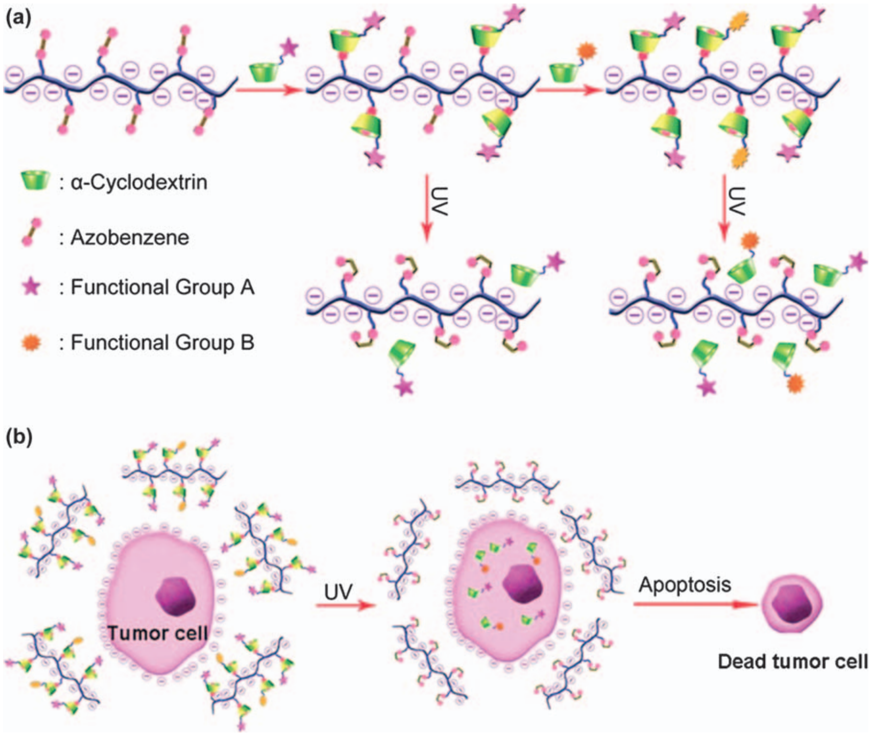

Figure 12.22 Scheme of an anionic polymer bearing side azobenzene that forms inclusion complexes with cyclodextrins conjugated to functional moieties (including drugs). The polymer can inhibit the loaded drug being up-taken by normal cells. Under UV irradiation, the complexes are broken and can be internalized by tumor cells.
Reproduced from Ref. 103 with permission of Wiley. Copyright (2011).

12.5 Conclusion and Outlook

Either alone or combined with other triggering stimuli, light-responsiveness constitutes a very promising approach for developing advanced DDSs such as micelles, vesicles and nanoparticles capable of modulating drug release at the target site. Despite the advances made in the last years to optimize light-responsive polymer-based drug carriers for tentative therapeutic applications, considerable efforts are still needed to translate them into clinical practice. The most challenging issues include:

1. *Design and synthesis of new biocompatible polymeric materials that fulfill the requirements of generally recognized safe compounds*. In this regard, most studies reported so far have been focused on proving the concept or principle of light-induced responsiveness while taking little care about polymer toxicity. Then, more efforts have to be performed to provide new biocompatible polymers. Recent works reporting near-IR two-photon light-responsive polymeric micelles composed of copolymers formed by PEO and poly(glutamic) acid (PGA) blocks bearing either spiropyran[259] or coumarin side groups[260] constitute important achievements in this direction. Polymeric materials must also be designed to host large amounts of payloads, to be stable in the blood for a long time without undesired leakage and to accumulate selectively in targeted tissues or cells. The choice of the photochromic moieties whose reactions trigger the micelle/particle disruption must also be an important factor to be considered in order to minimize the toxicity.
2. *Design and synthesis of new chromophore groups with larger two-photon absorption cross sections*. Provided that near-IR is preferred to UV and visible light for biomedical applications, there is a need to develop both new chromophore groups with larger two-photon absorption cross sections and new experimental procedures to reduce the utilization of high power density-lasers currently required for efficient near-IR-triggered drug release. Near-IR triggered disassembly of a low amount of photochromic groups leading to significant increases in the LCST of the micelle core-forming block[61] or the use of continuous-wave near-IR light excitation of UCNPs to activate the photoreactions requiring UV or visible light[100] can be suitable choices to resolve the wavelength issue.
3. *In vivo evaluation of the performance of light-responsive polymeric delivery systems*. Currently, most of the developed systems were only tested *in vitro*; hence, these studies must be supplemented with *in vivo* tests in order to progress toward the clinical use of these DDSs.

Acknowledgements

Work supported by MICINN (SAF2011-22771), Xunta de Galicia (10CSA203013PR) and FEDER.

References

1. J. Kost and R. Langer, *Adv. Drug Deliver. Rev.*, 2001, **46**, 125.
2. I. Silverstein, *Chem. Eng. News*, 2011, **89**, 8.
3. D. N. Nguyen, J. J. Green, J. M. Chan, R. Longer and D. G. Anderson, *Adv. Mater.*, 2009, **21**, 847.
4. M. L. Rogers and R. A. Rush, *J. Control. Release*, 2012, **157**, 183.
5. S. De Koker, B. N. Lambrecht, M. A. Willart, Y. van Kooyk, J. Grooten, C. Vervaet, J. P. Remon and B. G. De Geest, *Chem. Soc. Rev.*, 2011, **40**, 320.
6. C. L. Bayer and N. A. Peppas, *J. Control. Release*, 2008, **132**, 216.
7. C. Vauthier and D. Labarre, *J. Drug Del. Sci. Tech.*, 2008, **18**, 59.
8. C. Alvarez-Lorenzo and A. Concheiro, *Mini-Rev. Med. Chem.*, 2008, **8**, 1065.
9. M. Guo, Y. Yan, X. Liu, H. Yan, K. Liu, H. Zhang and Y. Cao, *Nanoscale*, 2010, **2**, 434.
10. T. C. Lai, Y. Bae, T. Yoshida, K. Kataoka and G. S. Kwon, *Pharm. Res.*, 2010, **27**, 2260.
11. W. Wang, H. Liang, R. C. Al Ghanami, L. Hamilton, M. Fraylich, K. M. Shakesheff, B. Saunders and C. Alexander, *Adv. Mater.*, 2009, **21**, 1809.
12. C. Huang, Y. Zhou, Y. Jin, X. Zhou, Z. Tang, X. Guo and S. Zhou, *J. Mater. Chem.*, 2011, **21**, 5660.
13. X. J. Loh, N. Vu Phuong Nam, N. Kuo and J. Li, *J. Mater. Chem.*, 2011, **21**, 2246.
14. B. P. Timko, T. Dvir and D. S. Kohane, *Adv. Mater.*, 2010, **22**, 4925.
15. C. Oerlemans, W. Bult, M. Bos, G. Storm, J. F. W. Nijsen and W. E. Hennink, *Pharm. Res.*, 2010, **27**, 2569.
16. T. Hoare, B. P. Timko, J. Santamaria, G. F. Goya, S. Irusta, S. Lau, C. F. Stefanescu, D. Lin, R. Langer and D. S. Kohane, *Nano Lett.*, 2011, **11**, 1395.
17. G. Jeon, S. Y. Yang, J. Byun and J. K. Kim, *Nano Lett.*, 2011, **11**, 1284.
18. C. Alvarez-Lorenzo, L. Bromberg and A. Concheiro, *Photochem. Photobiol*, 2009, **85**, 848.
19. Y. Zhao, *J. Mater. Chem.*, 2009, **19**, 4887.
20. M. S. Yavuz, Y. Cheng, J. Chen, C. M. Cobley, Q. Zhang, M. Rycenga, J. Xie, C. Kim, K. H. Song, A. G. Schwartz, L. V. Wang and Y. Xia, *Nature Mater.*, 2009, **8**, 935.
21. F. Ercole, T. P. Davis and R. A. Evans, *Polym. Chem.*, 2010, **1**, 37.
22. J. M. Schumers, C. A. Fustin and J. F. Gohy, *Macromol. Rapid Comm.*, 2010, **31**, 1588.
23. D. Lohmann and K. Petrak, *Crit. Rev. Ther. Drug*, 1989, **5**, 263.
24. L. C. Kennedy, L. R. Bickford, N. A. Lewinski, A. J. Coughlin, Y. Hu, E. S. Day, J. L. West and R. A. Drezek, *Small*, 2011, **7**, 169.
25. P. Bawa, V. Pillay, Y. E. Choonara and L. C. du Toit, *Biomed. Mater.*, 2009, **4**, No. 022001.

26. A. P. Esser-Kahn, S. A. Odom, N. R. Sottos, S. R. White and J. S. Moore, *Macromolecules*, 2011, **44**, 5539.
27. S. P. Friedman, *Eur. J. Soil Sci.*, 1997, **48**, 523.
28. M. F. Bedard, B. G. De Geest, A. G. Skirtach, H. Mohwald and G. B. Sukhorukov, *Adv. Colloid Interfac.*, 2010, **158**, 2.
29. A. Vogel and V. Venugopalan, *Chem. Rev.*, 2003, **103**, 577.
30. L. V. Zhigilei, P. B. S. Kodali and B. J. Garrison, *J. Phys. Chem. B*, 1998, **102**, 2845.
31. P. E. Dyer and R. Srinivasan, *Appl. Phys. Lett.*, 1986, **48**, 445.
32. M. Bedard, A. G. Skirtach and G. B. Sukhorukov, *Macromol. Rapid Comm.*, 2007, **28**, 1517.
33. K. Katagiri, A. Matsuda and F. Caruso, *Macromolecules*, 2006, **39**, 8067.
34. X. Tong, G. Wang, A. Soldera and Y. Zhao, *J. Phys. Chem. B*, 2005, **109**, 20281.
35. A. G. Skirtach, A. A. Antipov, D. G. Shchukin and G. B. Sukhorukov, *Langmuir*, 2004, **20**, 6988.
36. M. F. Bedard, A. Munoz-Javier, R. Mueller, P. del Pino, A. Fery, W. J. Parak, A. G. Skirtach and G. B. Sukhorukov, *Soft Matt.*, 2009, **5**, 148.
37. P. Juzenas, A. Juzeniene, O. Kaalhus, V. Iani and J. Moan, *Photochem. Photobiol. Sci.*, 2002, **1**, 745.
38. J. Klohs, A. Wunder and K. Licha, *Basic Res. Cardiol.*, 2008, **103**, 144.
39. V. Ntziachristos, J. Ripoll, L. H. V. Wang and R. Weissleder, *Nature Biotechnol.*, 2005, **23**, 313.
40. Y. Jiang, N. N. Horimoto, K. Imura, H. Okamoto, K. Matsui and R. Shigemoto, *Adv. Mater.*, 2009, **21**, 2309.
41. M. P. Melancon, M. Zhou and C. Li, *Accounts Chem. Res.*, 2011, **44**, 947.
42. R. Weissleder, *Nat. Biotechnol.*, 2001, **19**, 316.
43. C. R. Simpson, M. Kohl, M. Essenpreis and M. Cope, *Phys. Med. Biol.*, 1998, **43**, 2465.
44. A. G. Skirtach, P. Karageorgiev, M. F. Bédard, G. B. Sukhorukov and H. Möhwald, *J. Am. Chem. Soc.*, 2008, **130**, 11572.
45. M. N. Antipina and G. B. Sukhorukov, *Adv. Drug Del. Rev.*, 2011, **63**, 716.
46. J. Babin, M. Pelletier, M. Lepage, J. F. Allard, D. Morris and Y. Zhao, *Angew. Chem. Int. Ed.*, 2009, **48**, 3329.
47. A. P. Goodwin, J. L. Mynar, Y. Ma, G. R. Fleming and J. M. J. Fréchet, *J. Am. Chem. Soc.*, 2005, **127**, 9952.
48. Z136.1-1993, *American National Standards Institute, Laser Institute Orlando, FL*, 1993.
49. N. Fomina, J. Sankaranarayanan and A. Almutairi, *Adv. Drug Del. Rev.*, 2012, **64**, 1005.
50. K. Kano, Y. Tanaka, T. Ogawa, M. Shimomura, Y. Okahata and T. Kunitake, *Chem. Lett.*, 1980, **4**, 421.
51. S. L. Regen, A. Singh, G. Oehme and M. Singh, *Biochem. Biophys. Res. Commun.*, 1981, **101**, 131.

52. V. C. Anderson and D. H. Thompson, *BBA-Biomembranes*, 1992, **1109**, 33.
53. B. G. Prevo, S. A. Esakoff, A. Mikhailovsky and J. A. Zasadzinski, *Small*, 2008, **4**, 1183.
54. S. Link and M. A. El-Sayed, *Int. Rev. Phys. Chem.*, 2000, **19**, 409.
55. G. Wu, A. Mikhailovsky, H. A. Khant, C. Fu, W. Chiu and J. A. Zasadzinski, *J. Am. Chem. Soc.*, 2008, **130**, 8175.
56. J. Y. Shin and N. L. Abbott, *Langmuir*, 1999, **15**, 4404.
57. Y. Einaga, O. Sato, T. Iyoda, A. Fujishima and K. Hashimoto, *J. Am. Chem. Soc.*, 1999, **121**, 3745.
58. C. T. Lee, K. A. Smith and T. A. Hatton, *Macromolecules*, 2004, **37**, 5397.
59. J. Eastoe and A. Vesperinas, *Soft Matter*, 2005, **1**, 338.
60. Y. P. Wang, N. Ma, Z. Q. Wang and X. Zhang, *Angew. Chem. Int. Ed.*, 2007, **46**, 2823.
61. Y. Zhao, *Macromolecules*, 2012, **45**, 3647.
62. C. J. F. Rijcken, O. Soga, W. E. Hennink and C. F. van Nostrum, *J. Control. Release*, 2007, **120**, 131.
63. A. V. Kabanov, P. Lemieux, S. Vinogradov and V. Alakhov, *Adv. Drug Del. Rev.*, 2002, **54**, 223.
64. A. Harada and K. Kataoka, *Science*, 1999, **283**, 65.
65. D. A. Chiappetta, C. Alvarez-Lorenzo, A. Rey-Rico, P. Taboada, A. Concheiro and A. Sosnik, *Eur. J. Pharm. Biopharm.*, 2010, **76**, 24.
66. N. Kang, M. E. Perron, R. E. Prud'homme, Y. Zhang, G. Gaucher and J. C. Leroux, *Nano Lett.*, 2005, **5**, 315.
67. N. Rapoport, *Progr. Polym. Sci.*, 2007, **32**, 962.
68. J. Xu and S. Liu, *Soft Matter*, 2008, **4**, 1745.
69. G. S. Kwon, *Crit. Rev. Ther. Drug*, 2003, **20**, 357.
70. D. A. Chiappetta and A. Sosnik, *Eur. J. Pharm. Biopharm.*, 2007, **66**, 303.
71. H. Bader, H. Ringsdorf and B. Schmidt, *Angew. Makromol. Chem.*, 1984, **123**, 457.
72. M. Yokoyama, G. S. Kwon, T. Okano, Y. Sakurai, T. Seto and K. Kataoka, *Bioconjugate Chem.*, 1992, **3**, 295.
73. A. V. Kabanov, V. P. Chekhonin, V. Y. Alakhov, E. V. Batrakova, A. S. Lebedev, N. S. Melik-Nubarov, S. A. Arzhakov, A. V. Levashov, G. V. Morozov, E. S. Severin and V. A. Kabanov, *FEBS Lett.*, 1989, **258**, 343.
74. V. P. Torchilin, *J. Control. Release*, 2001, **73**, 137.
75. C. Allen, D. Maysinger and A. Eisenberg, *Colloid Surface B*, 1999, **16**, 3.
76. M. L. Adams, A. Lavasanifar and G. S. Kwon, *J. Pharm. Sci.*, 2003, **92**, 1343.
77. H. Maeda, J. Wu, T. Sawa, Y. Matsumura and K. Hori, *J. Control. Release*, 2000, **65**, 271.
78. J. S. Kloover, M. A. den Bakker, H. Gelderblom and J. P. van Meerbeeck, *Brit. J. Cancer*, 2004, **90**, 304.
79. Y. Zhao, *Chem. Record*, 2007, **7**, 286.
80. J. Jiang, X. Tong and Y. Zhao, *J. Am. Chem. Soc.*, 2005, **127**, 8290.

81. S. Menon and S. Das, *J. Polym. Sci. A Polym. Chem.*, 2011, **49**, 4448.
82. J. M. Schumers, J. F. Gohy and C. A. Fustin, *Polym. Chem.*, 2010, **1**, 161.
83. P. Theato, *Angew. Chem. Int. Ed.*, 2011, **50**, 5804.
84. J. He and Y. Zhao, *Dyes Pigments*, 2011, **89**, 278.
85. N. Fomina, C. L. McFearin, M. Sermsakdi, J. M. Morachis and A. Almutairi, *Macromolecules*, 2011, **44**, 8590.
86. G. Wang, X. Tong and Y. Zhao, *Macromolecules*, 2004, **37**, 8911.
87. A. Natansohn and P. Rochon, *Chem. Rev.*, 2002, **102**, 4139.
88. T. Ikeda, *J. Mater. Chem.*, 2003, **13**, 2037.
89. X. K. Liu and M. Jiang, *Angew. Chem. Int. Ed.*, 2006, **45**, 3846.
90. K. Sugiyama and K. Sono, *J. Appl. Polym. Sci.*, 2001, **81**, 3056.
91. H. I. Lee, W. Wu, J. K. Oh, L. Mueller, G. Sherwood, L. Peteanu, T. Kowalewski and K. Matyjaszewski, *Angew. Chem. Int. Ed.*, 2007, **46**, 2453.
92. J. Q. Jiang, X. Tong, D. Morris and Y. Zhao, *Macromolecules*, 2006, **39**, 4633.
93. J. M. Schumers, O. Bertrand, C. A. Fustin and J. F. Gohy, *J. Polym. Sci. A Polym. Chem.*, 2012, **50**, 599.
94. D. Han, X. Tong and Y. Zhao, *Macromolecules*, 2011, **44**, 437.
95. Q. Jin, F. Mitschang and S. Agarwal, *Biomacromolecules*, 2011, **12**, 3684.
96. J. A. Johnson, Y. Y. Lu, A. O. Burts, Y. H. Lim, M. G. Finn, J. T. Koberstein, N. J. Turro, D. A. Tirrell and R. H. Grubbs, *J. Am. Chem. Soc.*, 2011, **133**, 559.
97. T. Furuta, S. S. H. Wang, J. L. Dantzker, T. M. Dore, W. J. Bybee, E. M. Callaway, W. Denk and R. Y. Tsien, *Proc. Natl Acad. Sci. USA*, 1999, **96**, 1193.
98. J. L. Mynar, A. P. Goodwin, J. A. Cohen, Y. Ma, G. R. Fleming and J. M. J. Frechet, *Chem. Comm.*, 2007, 2081.
99. N. Fomina, C. McFearin, M. Sermsakdi, O. Edigin and A. Almutairi, *J. Am. Chem. Soc.*, 2010, **132**, 9540.
100. B. Yan, J. C. Boyer, N. R. Branda and Y. Zhao, *J. Am. Chem. Soc.*, 2011, **133**, 19714.
101. H. Yang, L. Jia, Z. Wang, A. Di-Cicco, D. Lévy and P. Keller, *Macromolecules*, 2011, **44**, 159.
102. Q. Yan, Y. Xin, R. Zhou, Y. Yin and J. Yuan, *Chem. Comm.*, 2011, **47**, 9594.
103. W. Xiao, W. H. Chen, X. D. Xu, C. Li, L. Zhang, R. X. Zhuo and X. Z. Zhang, *Adv. Mater.*, 2011, **23**, 3526.
104. C. Alvarez-Lorenzo, S. Deshmukh, L. Bromberg, T. A. Hatton, I. Sández-Macho and A. Concheiro, *Langmuir*, 2007, **23**, 11475.
105. A. P. Esser-Kahn, N. R. Sottos, S. R. White and J. S. Moore, *J. Am. Chem. Soc.*, 2010, **132**, 10266.
106. A. Sagi, R. Weinstain, N. Karton and D. Shabat, *J. Am. Chem. Soc.*, 2008, **130**, 5434.
107. M. A. DeWit and E. R. Gillies, *J. Am. Chem. Soc.*, 2009, **131**, 18327.
108. D. Han, X. Tong and Y. Zhao, *Langmuir*, 2012, **28**, 2327.

109. C. Cheng, K. Qi, D. S. Germack, E. Khoshdel and K. L. Wooley, *Adv. Mater.*, 2007, **19**, 2830.
110. S. Y. Park and M. H. Park, *Langmuir*, 2007, **23**, 6788.
111. Y. Li, I. Akiba, S. Harrisson and K. L. Wooley, *Adv. Funct. Mater.*, 2008, **18**, 551.
112. S. R. Trenor, A. R. Shultz, B. J. Love and T. E. Long, *Chem. Rev.*, 2004, **104**, 3059.
113. D. Shi, M. Matsusaki and M. Akashi, *Bioconjugate Chem.*, 2009, **20**, 1917.
114. D. Shi, M. Matsusaki and M. Akashi, *J. Control. Release*, 2011, **149**, 182.
115. J. Jiang, B. Qi, M. Lepage and Y. Zhao, *Macromolecules*, 2007, **40**, 790.
116. J. Babin, M. Lepage and Y. Zhao, *Macromolecules*, 2008, **41**, 1246.
117. H. Chen, S. Kim, W. He, H. Wang, P. S. Low, K. Park and J. X. Cheng, *Langmuir*, 2008, **24**, 5213.
118. H. Chen, S. Kim, L. Li, S. Wang, K. Park and J. X. Cheng, *Proc. Natl Acad. Sci. USA*, 2008, **105**, 6596.
119. Y. Kakizawa and K. Kataoka, *Adv. Drug Del. Rev.*, 2002, **54**, 203.
120. J. He, X. Tong and Y. Zhao, *Macromolecules*, 2009, **42**, 4845.
121. J. He, X. Tong, L. Tremblay and Y. Zhao, *Macromolecules*, 2009, **42**, 7267.
122. Q. Jin, X. Liu, G. Liu and J. Ji, *Polymer*, 2010, **51**, 1311.
123. J. He, B. Yan, L. Tremblay and Y. Zhao, *Langmuir*, 2011, **27**, 436.
124. E. B. Zhulina, M. Adam, I. LaRue, S. S. Sheiko and M. Rubinstein, *Macromolecules*, 2005, **38**, 5330.
125. B. M. Discher, Y. Y. Won, D. S. Ege, J. C. M. Lee, F. S. Bates, D. E. Discher and D. A. Hammer, *Science*, 1999, **284**, 1143.
126. J. Dong, Y. Zeng, Z. Xun, Y. Han, J. Chen, Y. Y. Li and Y. Li, *Langmuir*, 2012, **28**, 1733.
127. J. Juarez, P. Taboada, M. A. Valdez and V. Mosquera, *Langmuir*, 2008, **24**, 7107.
128. T. Azzam and A. Eisenberg, *Angew. Chem. Int. Ed.*, 2006, **45**, 7443.
129. M. H. Li and P. Keller, *Soft Matter*, 2009, **5**, 927.
130. D. E. Discher and F. Ahmed, *Annu. Rev. Biomed. Eng.*, 2006, **8**, 323.
131. D. E. Discher and A. Eisenberg, *Science*, 2002, **297**, 967.
132. I. W. Hamley, *Soft Matter*, 2005, **1**, 36.
133. F. Ahmed, R. I. Pakunlu, A. Brannan, F. Bates, T. Minko and D. E. Discher, *J. Control. Release*, 2006, **116**, 150.
134. D. E. Discher, V. Ortiz, G. Srinivas, M. L. Klein, Y. Kim, D. Christian, S. Cai, P. Photos and F. Ahmed, *Progr. Polym. Sci.*, 2007, **32**, 838.
135. F. Ahmed and D. E. Discher, *J. Control. Release*, 2004, **96**, 37.
136. A. Napoli, M. Valentini, N. Tirelli, M. Muller and J. A. Hubbell, *Nat. Mater.*, 2004, **3**, 183.
137. A. Napoli, H. Bermudez and J. A. Hubbell, *Langmuir*, 2005, **21**, 9149.
138. S. Cerritelli, D. Velluto and J. A. Hubbell, *Biomacromolecules*, 2007, **8**, 1966.

139. A. Klaikherd, S. Ghosh and S. Thayumanavan, *Macromolecules*, 2007, **40**, 8518.
140. F. Liu and A. Eisenberg, *J. Am. Chem. Soc.*, 2003, **125**, 15059.
141. F. Chécot, J. Rodríguez-Hernández, Y. Gnanou and S. Lecommandoux, *Biomol. Eng.*, 2007, **24**, 81.
142. H. C. Chiu, Y. W. Lin, Y. F. Huang, C. K. Chuang and C. S. Chern, *Angew. Chem. Int. Ed.*, 2008, **47**, 1875.
143. Y. Li, B. S. Lokitz and C. L. McCormick, *Angew. Chem. Int. Ed.*, 2006, **45**, 5792.
144. Y. Li, A. E. Smith, B. S. Lokitz and C. L. McCormick, *Macromolecules*, 2007, **40**, 8524.
145. K. E. Gebhardt, S. Ahn, G. Venkatachalam and D. A. Savin, *J. Colloid Interf. Sci.*, 2008, **317**, 70.
146. J. C. M. Lee, H. Bermudez, B. M. Discher, M. A. Sheehan, Y. Y. Won, F. S. Bates and D. E. Discher, *Biotechnol. Bioeng.*, 2001, **73**, 135.
147. F. Meng, G. H. M. Engbers and J. Feijen, *J. Control. Release*, 2005, **101**, 187.
148. K. Han, W. Su, M. Zhong, Q. Yan, Y. Luo, Q. Zhang and Y. Li, *Macromol. Rapid Comm.*, 2008, **29**, 1866.
149. L. Lin, Z. Yan, J. S. Gu, Y. Y. Zhang, Z. Feng and Y. L. Yu, *Macromol. Rapid Comm.*, 2009, **30**, 1089.
150. Y. Wang, P. Han, H. Xu, Z. Wang, X. Zhang and A. V. Kabanov, *Langmuir*, 2010, **26**, 709.
151. Q. Jin, G. Liu, X. Liu and J. Ji, *Soft Matter*, 2010, **6**, 5589.
152. Q. Jin, C. Luy, J. Ji and S. Agarwal, *J. Polym. Sci. A Polym. Chem.*, 2012, **50**, 451.
153. E. Mabrouk, D. Cuvelier, F. Brochard-Wyart, P. Nassoy and M. H. Li, *Proc. Natl Acad. Sci. USA*, 2009, **106**, 7294.
154. M. H. Li, P. Auroy and P. Keller, *Liquid Cryst.*, 2000, **27**, 1497.
155. P. G. de Gennes, *Soft Matter*, 2005, **1**, 16.
156. Y. L. Yu and T. Ikeda, *J. Photoch. Photobio. C*, 2004, **5**, 247.
157. Y. Jiang, Y. Wang, N. Ma, Z. Wang, M. Smet and X. Zhang, *Langmuir*, 2007, **23**, 4029.
158. C. Q. Huang, Y. Wang, C. Y. Hong and C. Y. Pan, *Macromol. Rapid Comm.*, 2011, **32**, 1174.
159. F. M. Raymo and S. Giordani, *J. Am. Chem. Soc.*, 2001, **123**, 4651.
160. D. A. Parthenopoulos and P. M. Rentzepis, *Science*, 1989, **245**, 843.
161. A. Kocer, M. Walko, W. Meijberg and B. L. Feringa, *Science*, 2005, **309**, 755.
162. Y. Ito, N. Sugimura, O. H. Kwon and Y. Imanishi, *Nature Biotech.*, 1999, **17**, 73.
163. G. P. Robbins, M. Jimbo, J. Swift, M. J. Therien, D. A. Hammer and I. J. Dmochowski, *J. Am. Chem. Soc.*, 2009, **131**, 3872.
164. J. S. Katz, S. Zhong, B. G. Ricart, D. J. Pochan, D. A. Hammer and J. A. Burdick, *J. Am. Chem. Soc.*, 2010, **132**, 3654.

165. E. Cabane, V. Malinova, S. Menon, C. G. Palivan and W. Meier, *Soft Matter*, 2011, **7**, 9167.
166. A. V. Kabanov and V. A. Kabanov, *Adv. Drug Deliver. Rev.*, 1998, **30**, 49.
167. S. De Koker, L. J. De Cock, P. Rivera-Gil, W. J. Parak, R. Auzely Velty, C. Vervaet, J. P. Remon, J. Grooten and B. G. De Geest, *Adv. Drug Deliver. Rev.*, 2011, **63**, 748.
168. M. Delcea, H. Möhwald and A. G. Skirtach, *Adv. Drug Deliver. Rev.*, 2011, **63**, 730.
169. K. S. Soppimath, T. M. Aminabhavi, A. R. Kulkarni and W. E. Rudzinski, *J. Control. Release*, 2001, **70**, 1.
170. F. Delie and M. J. Blanco-Prieto, *Molecules*, 2005, **10**, 65.
171. M. de la Fuente, M. Ravina, P. Paolicelli, A. Sanchez, B. Seijo and M. J. Alonso, *Adv. Drug Deliver. Rev.*, 2010, **62**, 100.
172. S. Al-Qadi, A. Grenha and C. Remunan-Lopez, *Carbohydr. Polym.*, 2011, **86**, 25.
173. B. Mu, P. Liu, X. R. Li, P. C. Du, Y. Dong and Y. J. Wang, *Mol. Pharmaceut.*, 2012, **9**, 91.
174. P. Lertsutthiwong and P. Rojsitthisak, *Pharmazie*, 2011, **66**, 911.
175. F. L. Cao, B. Y. Ding, M. Sun, C. Y. Guo, L. Zhang and G. X. Zhai, *Drug Del.*, 2011, **18**, 545.
176. K. Ofokansi, G. Winter, G. Fricker and C. Coester, *Eur. J. Pharm. Biopharm.*, 2010, **76**, 1.
177. L. Yang, F. Cui, D. M. Cun, A. Tao, K. Shi and W. H. Lin, *Int. J. Pharm.*, 2007, **340**, 163.
178. E. Markovsky, N. Koroukhov and G. Golomb, *Nanomedicine*, 2007, **2**, 545.
179. I. M. Martins, S. N. Rodrigues, M. F. Barreiro and A. E. Rodrigues, *Ind. Eng. Chem. Res.*, 2011, **50**, 13752.
180. J. L. Bourges, S. E. Gautier, F. Delie, R. A. Bejjani, J. C. Jeanny, R. Gurny, D. BenEzra and F. F. Behar-Cohen, *Invest. Ophth. Vis. Sci.*, 2003, **44**, 3562.
181. S. Pamujula, S. Hazari, G. Bolden, R. A. Graves, D. D. Chinta, S. Dash, V. Kishore and T. K. Mandal, *J. Pharm. Pharmacol.*, 2012, **64**, 61.
182. J. L. Italia, D. K. Bhatt, V. Bhardwaj, K. Tikoo and M. N. V. R. Kumar, *J. Control. Release*, 2007, **119**, 197.
183. R. A. Tuli, T. R. Dargaville, G. A. George and N. Islam, *J. Pharm. Sci.*, 2012, **101**, 733.
184. D. S. Lin, Y. Y. Huang, Q. Jiang, W. D. Zhang, X. Y. Yue, S. T. Guo, P. Xiao, Q. Du, J. F. Xing, L. D. Deng, Z. C. Liang and A. J. Dong, *Biomaterials*, 2012, **32**, 8730.
185. J. Nicolas, D. Brambilla, O. Carion, T. Pons, I. Maksimovic, E. Larquet, B. Le Droumaguet, K. Andrieux, B. Dubertret and P. Couvreur, *Soft Matter*, 2011, **7**, 6187.
186. G. G. Yordanov and C. D. Dushkin, *Colloid Polym. Sci.*, 2010, **288**, 1019.
187. J. K. Oh, R. Drumright, D. J. Siegwart and K. Matyjaszewski, *Progr. Polym. Sci.*, 2008, **33**, 448.

188. M. Motornov, Y. Roiter, I. Tokarev and S. Minko, *Progr. Polym. Sci.*, 2010, **35**, 174.
189. A. V. Kabanov and S. V. Vinogradov, *Angew. Chem. Int. Ed.*, 2009, **48**, 5418.
190. G. Decher, *Science*, 1997, **277**, 1232.
191. B. Staedler, A. D. Price and A. N. Zelikin, *Adv. Funct. Mater.*, 2011, **21**, 14.
192. I. Luzinov, S. Minko and V. V. Tsukruk, *Soft Matter*, 2008, **4**, 714.
193. H. N. Yow and A. F. Routh, *Soft Matter*, 2006, **2**, 940.
194. B. Sukhorukov Gleb, in *Carrier-Based Drug Delivery*, ed. S. Svenson, American Chemical Society, Washington DC, 2004, vol. 879, pp. 249–266.
195. S. Sivakumar, V. Bansal, C. Cortez, S. F. Chong, A. N. Zelikin and F. Caruso, *Adv. Mater.*, 2009, **21**, 1820.
196. Y. J. Wang and F. Caruso, *Chem. Mater.*, 2005, **17**, 953.
197. G. B. Sukhorukov, A. A. Antipov, A. Voigt, E. Donath and H. Mohwald, *Macromol. Rapid Comm.*, 2001, **22**, 44.
198. C. Y. Gao, S. Leporatti, S. Moya, E. Donath and H. Möhwald, *Chem.-Eur. J.*, 2003, **9**, 915.
199. C. Déjugnat and G. B. Sukhorukov, *Langmuir*, 2004, **20**, 7265.
200. J. Heuvingh, M. Zappa and A. Fery, *Langmuir*, 2005, **21**, 3165.
201. T. Borodina, E. Markvicheva, S. Kunizhev, H. Möhwald, G. B. Sukhorukov and O. Kreft, *Macromol. Rapid Comm.*, 2007, **28**, 1894.
202. O. Kreft, A. G. Skirtach, G. B. Sukhorukov and H. Möhwald, *Adv. Mater.*, 2007, **19**, 3142.
203. B. G. De Geest, A. G. Skirtach, A. A. Mamedov, A. A. Antipov, N. A. Kotov, S. C. De Smedt and G. B. Sukhorukov, *Small*, 2007, **3**, 804.
204. A. G. Skirtach, B. G. De Geest, A. Mamedov, A. A. Antipov, N. A. Kotov and G. B. Sukhorukov, *J. Mater. Chem.*, 2007, **17**, 1050.
205. D. G. Shchukin, D. A. Gorin and H. Möhwald, *Langmuir*, 2006, **22**, 7400.
206. D. A. Gorin, D. G. Shchukin, A. I. Mikhailov, K. Kohler, S. A. Sergeev, S. A. Portnov, I. V. Taranov, V. V. Kislov and G. B. Sukhorukov, *Tech. Phys. Lett.*, 2006, **32**, 70.
207. L. L. del Mercato, E. Gonzalez, A. Z. Abbasi, W. J. Parak and V. Puntes, *J. Mater. Chem.*, 2011, **21**, 11468.
208. A. Fery and R. Weinkamer, *Polymer*, 2007, **48**, 7221.
209. V. V. Lulevich, I. L. Radtchenko, G. B. Sukhorukov and O. I. Vinogradova, *J. Phys. Chem. B*, 2003, **107**, 2735.
210. H. Y. Koo, H. J. Lee, J. K. Kim and W. S. Choi, *J. Mater. Chem.*, 2010, **20**, 3932.
211. X. Tao, J. B. Li and H. Mohwald, *Chem. Eur. J.*, 2004, **10**, 3397.
212. M. F. Bedard, S. Sadasivan, G. B. Sukhorukov and A. Skirtach, *J. Mater. Chem.*, 2009, **19**, 2226.
213. B. Radt, T. A. Smith and F. Caruso, *Adv. Mater.*, 2004, **16**, 2184.
214. R. Palankar, A. G. Skirtach, O. Kreft, M. Bedard, M. Garstka, K. Gould, H. Möhwald, G. B. Sukhorukov, M. Winterhalter and S. Springer, *Small*, 2009, **5**, 2168.

215. S. J. Pastine, D. Okawa, A. Zettl and J. M. J. Fréchet, *J. Am. Chem. Soc.*, 2009, **131**, 13586–13587.
216. K. Kono, Y. Nishihara and T. Takagishi, *J. Am. Chem. Soc.*, 2009, **131**, 13586.
217. X. Yuan, K. Fischer and W. Schärtl, *Langmuir*, 2005, **21**, 9374.
218. M. K. Park, S. Deng and R. C. Advincula, *Langmuir*, 2005, **21**, 5272.
219. X. Wang, Y. Yang, Y. Liao, Z. Yang, M. Jiang and X. Xie, *Eur. Polym. J.*, 2012, **48**, 41.
220. E. M. Rosenbauer, M. Wagner, A. Musyanovych and K. Landfester, *Macromolecules*, 2010, **43**, 5083.
221. A. G. Skirtach, A. M. Yashchenok and H. Moehwald, *Chem. Comm.*, 2011, **47**, 12736.
222. K. Raemdonck, J. Demeester and S. De Smedt, *Soft Matter*, 2009, **5**, 707.
223. N. Sanson and J. Rieger, *Polym. Chem.*, 2010, **1**, 965.
224. K. Landfester and A. Musyanovych, in *Chemical Design of Responsive Microgels*, ed. A. R. Pich and W. Richtering, Springer, Heidelberg, 2010, pp. 39–63.
225. N. Morimoto, M. Nomura Shin-ichiro, N. Miyazawa and K. Akiyoshi, in *Polymeric Drug Delivery II*, ed. S. Svenson, American Chemical Society, New York, 2006, pp. 88–101.
226. G. R. Hendrickson, M. H. Smith, A. B. South and L. A. Lyon, *Adv. Funct. Mater.*, 2010, **20**, 1697.
227. M. Oishi and Y. Nagasaki, *Nanomedicine*, 2010, **5**, 451.
228. L. Zha, B. Banik and F. Alexis, *Soft Matter*, 2011, **7**, 5908.
229. K. Akiyoshi, S. Kobayashi, S. Shichibe, D. Mix, M. Baudys, S. Wan Kim and J. Sunamoto, *J. Control. Release*, 1998, **54**, 313.
230. T. K. Bronich, S. Bontha, L. S. Shlyakhtenko, L. Bromberg, T. A. Hatton and A. V. Kabanov, *J. Drug Target.*, 2006, **14**, 357.
231. K. Ogawa, S. Sato and E. Kokufuta, *Langmuir*, 2007, **23**, 2095.
232. D. Missirlis, R. Kawamura, N. Tirelli and J. A. Hubbell, *Eur. J. Pharm. Sci.*, 2006, **29**, 120.
233. J. K. Oh, D. J. Siegwart, H. I. Lee, G. Sherwood, L. Peteanu, J. O. Hollinger, K. Kataoka and K. Matyjaszewski, *J. Am. Chem. Soc.*, 2007, **129**, 5939.
234. D. Wu and M. Wan, *J. Pharm. Pharm. Sci.*, 2008, **11**, 32.
235. T. Kawano, Y. Niidome, T. Mori, Y. Katayama and T. Niidome, *Bioconjugate Chem.*, 2009, **20**, 209.
236. T. Nakamura, A. Tamura, H. Murotani, M. Oishi, Y. Jinji, K. Matsuishi and Y. Nagasaki, *Nanoscale*, 2010, **2**, 739.
237. W. Wu, J. Shen, P. Banerjee and S. Zhou, *Biomaterials*, 2010, **31**, 7555.
238. Q. Jin, G. Liu and J. Li, *Eur. Polym. J.*, 2010, **46**, 2120.
239. S. Patnaik, A. K. Sharma, B. S. Garg, R. P. Gandhi and K. C. Gupta, *Int. J. Pharm.*, 2007, **342**, 184.
240. D. Klinger and K. Landfester, *Soft Matter*, 2011, **7**, 1426.
241. D. Klinger and K. Landfester, *Macromol. Rapid Comm.*, 2011, **32**, 1979.
242. D. Klinger and K. Landfester, *Macromolecules*, 2011, **44**, 9758.

243. D. Klinger and K. Landfester, *J. Polym. Sci. A Polym. Chem.*, 2012, **50**, 1062.
244. T. Hirakura, Y. Nomura, Y. Aoyama and K. Akiyoshi, *Biomacromolecules*, 2004, **5**, 1804.
245. P. Froimowicz, D. Klinger and K. Landfester, *Chem. Eur. J.*, 2011, **17**, 12465.
246. L. Brannon-Peppas, *Int. J. Pharm.*, 1995, **116**, 1.
247. A. C. Lima, P. Sher and J. F. Mano, *Expert Opin. Drug Deliver.*, 2012, **9**, 231.
248. M. Das, H. Zhang and E. Kumacheva, *Annu. Rev. Mater. Res.*, 2006, **36**, 117.
249. K. Landfester, *Angew. Chem. Int. Ed.*, 2009, **48**, 4488.
250. I. Willerich and F. Gröhn, *Macromolecules*, 2011, **44**, 4452.
251. D. Shi, M. Matsusaki, T. Kaneko and M. Akashi, *Macromolecules*, 2008, **41**, 8167.
252. B. Yu, X. Jiang, R. Wang and J. Yin, *Macromolecules*, 2010, **43**, 10457.
253. S. J. Lim, C. J. Carling, C. C. Warford, D. Hsiao, B. D. Gates and N. R. Branda, *Dyes Pigments*, 2011, **89**, 230.
254. W. Cui, X. Lu, K. Cui, J. Wu, Y. Wei and Q. Lu, *Nanotechnol.*, 2011, 22.
255. M. S. Kim, J. Gruneich, H. Jing and S. L. Diamond, *J. Mater. Chem.*, 2010, **20**, 3396.
256. T. Dvir, M. R. Banghart, B. P. Timko, R. Langer and D. S. Kohane, *Nano Lett.*, 2010, **10**, 250.
257. G. C. R. Ellis-Davies, *Nature Meth.*, 2007, **4**, 619.
258. D. V. Volodkin, A. G. Skirtach and H. Moehwald, *Angew. Chem. Int. Ed.*, 2009, **48**, 1807.
259. V. K. Kotharangannagari, A. Sánchez-Ferrer, J. Ruokolainen and R. Mezzenga, *Macromolecules*, 2011, **44**, 4569.
260. S. Kumar, J. F. Allard, D. Morris, Y. L. Dory, M. Lepage and Y. Zhao, *J. Mater. Chem.* 2012, **22**, 7252.

Subject Index

Abbreviation DDS = drug delivery systems
Page numbers in **bold** refer to figures/tables
Page numbers prefixed by 1. refer to Volume One
Page numbers prefixed by 2. refer to Volume Two

AAc. *see* polyacrylic acid
AAm (acrylamide). *see* polyacrylamide
AB/ABA-type block copolymers 1.157
ABC. *see* accelerated blood clearance phenomenon
ABCs (ATPase ATP-binding cassette superfamily) 1.116
Abelson cytoplasmic tyrosine (ABL) kinase inhibitors 1.234
ABLATE study, colorectal liver metastases 1.69, 1.70, **1.70**
accelerated blood clearance (ABC) phenomenon 1.132, 1.84, 1.86, 1.9
acetazolamide 2.238–40, **2.241**
acetylcholine 2.100
acetylcysteine 1.105
acoustic pressure, ultrasound 1.154
acoustic streaming, ultrasound 1.155, 1.167–8
acquired immune deficiency syndrome. *see* HIV/AIDS
acrylamide (AAm). *see* polyacrylamide
acrylic acid (AAc). *see* polyacrylic acid
acryloylthioureido phenylboronic acid (ATPBA) 2.327, **2.328**
activation-modulated DDS 1.2, **1.3**, 2.243, **2.244**
active excipients 1.3
active pharmaceutical ingredients, evolution 1.1
active targeting
  polymersomes 1.191, 1.198, 1.199
  reduction-sensitive nanosystems 1.210, 1.227
  ultrasound-responsive DDSs 1.160–1
actuating devices, intrinsically conducting polymers 1.292–6, **1.293**, **1.295**
acute toxicity, definitions 2.104
adamantyl capped pores 1.249, 2.79
adeno-associated virus (AAV) delivery systems 2.190
AESH (aminoethanthiol) **2.172**
ATP (adenosine-triphosphate) 1.243, 1.247–8, 1.257
ATPase ATP-binding cassette superfamily (ABCs) 1.116
administration routes
  enzyme-responsive materials 1.236–7
  hydrogels 1.238
  polymeric micelles 1.122
adrenalin **2.278**
adriamycin (ADR) 1.96
adsorption, isolated polymer phase transitions 1.12

advanced excipients 1.4–9, **1.5**, **1.7**, **1.8**
aerosol/spray-drying 2.65, 2.72
α. *see* alpha
affinity-controlled release, hydrogels. *see* imprinted hydrogels
AFM (atomic force microscopy) 1.186, **1.187**, 1.287, **1.314**
AFP (α-fetoprotein) 2.277–9, **2.279**, **2.280**
age factors, patients 1.9
age-related macular degeneration 1.100
aggregation properties
  anionic nanoparticles 1.194
  polymeric micelles 1.123, 1.126
AIBN (azobisisobutyronitrile) **2.172**, 2.203
AIDS. *see* HIV/AIDS
albumin 1.189, 1.240
alginates
  cell/tissue delivery systems **2.292**, 2.292–3
  dual responsive hydrogels 2.172
  layer-by-layer assemblies 2.125
  pH responsive microgels 2.158
  tissue engineering 2.293
alkyl acrylamide homopolymers/copolymers 2.199
alkylhalides 2.95
all-*trans* retinoic acid (ATRA) 1.102
α-amino acid based hydrogels 2.199–203, **2.201–3**, 2.224
  cisplatin 2.211–17, **2.212**, **2.213**, **2.215**, **2.216**
  future perspectives 2.221–4, **2.222–3**
  pH/ion-responsive 2.204–9, **2.207–10**, 2.210, 2.213, 2.214, 2.222
  pilocarpine 2.217–21, **2.218**, **2.219**, **2.220**
  swelling properties 2.204, **2.207**, 2.209, 2.211, 2.214, 2.217, **2.218**, 2.219, 2.221–2, **2.222**
  syntheses **2.203**, 2.203–4, **2.205**
  temperature responsive 2.209–11, 2.213, 2.221
α,β-poly(hydroxyethyl aspartamide-g-maleic anhydride) (PHEA-g-MA) 2.157–8
α-chymotrypsin 2.271, **2.272**
α-fetoprotein (AFP) 2.277–9, **2.279**, **2.280**
α-folate receptors (FR) 2.67
alternating magnetic fields (AMFs) 2.72, 2.75
aluminum phthalocyanine 1.101
Alzheimer's disease 1.20, 1.194, **1.233**, 2.100
American National Standards Institute (ANSI) 1.306–7
amino acid biomimetics 2.181, 2.182. *see also* α-amino acid based hydrogels; elastin-like recombiners
aminoethanthiol (AESH) **2.172**
aminopropyl methacrylamide (APMA) 2.333–5
aminopropyl triethoxy silane (APTES) 2.326
aminopropyl trimethoxysilane (ATMS) 2.74–5, 2.327
aminoquinoline (AQ) 1.241
aminosalicylic acid 1.239
ammonium persulfate (APS) 2.203
amphiphiles 1.179–80, **1.181**, 1.182
amphiphilic block copolymers. *see* block copolymers
amphiphilic hyperbranched polyphosphates (HPHDP) 1.214, **1.215**
amphiphilic micelles 1.308–17, **1.309**, **1.315–16**, **1.319**, 1.320–7, 2.41–4, **2.42**, **2.43**
amphiphilic oligopeptides 1.220
amphoteric hydrogels 2.208–9, 2.211, **2.212**
amphotericin B 1.80, 1.134–5, 2.99–100
amplitude mapping, polymersomes **1.187**
AND logic gates 2.80
angiogenesis, tumors 1.198. *see also* vascularisation

animal models
  biochemical-responsive DDS 1.21
  carbon nanotubes 2.107
  enzyme-responsive DDS 1.19
  low temperature sensitive
    liposomes 1.38, 1.60–2, 1.64
  magnetic nanoparticles 2.57, **2.58**
  polyplexes 1.258–9
  ultrasound triggered 1.165–6
anion driven actuation,
  polypyrrole 1.289
anionic hydrogels 2.204–8, **2.207**
anionic nanoparticles 1.193, 1.194
anisotropy, cell sheet
  engineering 2.303, 2.306
ANNs (artificial neural
  networks) 1.164
ANSI (American National Standards
  Institute) 1.306–7
anthracyclines 2.97. *see also*
  doxorubicin
anti-apoptotic gene delivery 2.300
antibiotics 2.189. *see also specific
  drugs by name*
antibodies
  biochemical-responsive DDS 1.21
  biomolecule-sensitive
    hydrogels 2.262
  enzyme prodrug therapy 1.235
anticancer drugs. *see*
  chemotherapeutic agents
antiepileptic drugs 2.57, **2.58**
antifungal agents 2.99–100. *see also
  specific drugs by name*
antigens 1.9, 1.21
  biomolecule-sensitive
    hydrogels 2.272–6, **2.275**, **2.276**
  mesoporous silica nanoparticles
    2.79
anti-inflammatory drugs. *see also
  specific drugs by name*
  carbon nanotubes 2.100
  pH triggered drug release 2.129,
    2.161
antimicrobial therapy 2.189. *see also
  specific drugs by name*
antisense oligonucleotides 1.84, 2.6
APMA (aminopropyl
  methacrylamide) 2.333–5
apolar solvents 2.232
apolipoproteins 1.189
approved excipients, FDA 1.122
APS (ammonium persulfate) 2.203
APTES (aminopropyl triethoxy
  silane) 2.326
AQ (aminoquinoline) 1.241
area under the curve (AUC)
  pH sensitive liposomes 1.89
  timolol 2.237
  ultrasound-responsive
    DDSs 1.156
arginineglycine-aspartic acid (RGD)
  peptides 1.262, 2.96
arthritis 1.240
artificial neural networks
  (ANNs) 1.164
asbestos 2.107–8
ascorbic acid 2.156–7
aspartic acid 1.159
aspirin 1.332, **2.326**
ATMS (aminopropyl
  trimethoxysilane) 2.74–5, 2.327
atom transfer radical polymerization
  (ATRP) 1.226, 2.271, 2.296, 2.321,
  2.323, 2.325–6
atomic force microscopy
  (AFM) 1.186, **1.187**, 1.287, **1.314**
ATP (adenosine-triphosphate)
  1.243, 1.247–8, 1.257
ATPase ATP-binding cassette
  superfamily (ABCs) 1.116
ATPBA (acryloylthioureido
  phenylboronic acid) 2.327, **2.328**
ATRA (all-*trans* retinoic acid) 1.102
ATRP (atom transfer radical
  polymerization) 1.226, 2.271,
  2.296, 2.321, 2.323, 2.325–6
AUC. *see* area under the curve
Au NPs. *see* gold nanoparticles
autoimmune diseases 2.98. *see also*
  immune responses
avidin 1.108, 1.240, 1.251, 2.79

azobenzene 1.307, 1.310, 1.313–14, 1.330–2, 1.334, **1.337**
  layer-by-layer assemblies 2.138
  light responsive hydrogels 2.251, **2.252**, 2.253
  light-sensitive polymeric micelles 1.317–18, **1.318**
  light-sensitive polymeric vesicles 1.322–3
azobisisobutyronitrile (AIBN) **2.172**, 2.203
AzoMI-VPy (poly(4-phenylazomaleinanil-co-4-vinylpyridine) 1.313

bacterial infections. *see* infected tissues
bacteriorhodopsin, polymer grafting 2.338, **2.338**
BADS (bis(2-acryloyloxyethyl) disulfide) **1.226**, 1.227
basic fibroblast growth factor (bFGF) 1.264
BBB (blood–brain barrier) 1.125, 1.153
B-cell lymphoma 2 (Bcl-2) 2.300, **2.301**
BCMs. *see* block copolymer micelles
BCPs. *see* block copolymers
BCRP (breast cancer resistant protein) pump 1.125
BCS (Biopharmaceutic Classification System) 1.115
bilayers, lipid 1.34–5, **1.35**, 1.36, 1.42–3
binding agents 1.20–21
Bingel cyclopropanation 2.95
biochemical-responsive DDSs **1.17**, 1.19–21, 2.229. *see also* biomolecule-sensitive hydrogels
biocompatibility
  carrier systems 2.63
  cell/tissue delivery systems **2.292**, 2.292–3
  liposomes 2.121
  mesoporous silica nanoparticles 2.80–1
  polymer grafting 2.336
  polypyrrole 1.287–8
biodegradability, hydrogels 2.171–2
biofilms 2.316, 2.341
biofouling, combination products 2.341
bioinformatics 1.115
bioinspired networks 2.235–40, **2.236**, **2.237**, **2.238**, **2.239**
bilayers, lipid. *see* lipid bilayers
biologic primary modes of action 2.314
biological barriers 1.188, 1.197–8
biological interfaces, layer-by-layer assemblies 2.142–4
biological models, carbon nanotubes 2.106–7
biological stimuli. *see* internal stimuli
biomacromolecules 1.6
biomarkers, disease states 1.191, 2.262, 2.277–9, **2.279**
biomaterials
  definitions 1.4
  evolution 1.4, 1.5, **1.5**, 1.5–6
  first generation 1.4
  second generation 1.5
  third generation 1.6–7, **1.8**
biomedical implants. *see* implants
biomimetics 2.180–1, 2.320
biomolecular imprinting 2.277–9, **2.278**, **2.279**
biomolecule-sensitive hydrogels 2.229, 2.261–2, **2.282**, 2.282–5, **2.283**, **2.284**
  design strategies 2.262–4, **2.263**, **2.264**
  DNA sensitive **2.282**, 2.282
  glucose-sensitive 2.264–70, **2.265**, **2.267–9**
  imprinted 2.276–9, **2.278**, **2.279**
  nanoparticles 2.279–81
  protein-sensitive 2.270–6, **2.272–3**, **2.275–6**

biopersistence, carbon nanotubes 2.105, 2.108
Biopharmaceutic Classification System (BCS) 1.115
biosensing, intrinsically conducting polymers 1.286
biotin 1.108, 1.130, 1.134, 1.186, 1.251
bipolar disorder 2.222–4, **2.223**
bis (2-acryloyloxyethyl) disulfide (BADS) **1.226**, 1.227
block copolymer micelles (BCMs) 2.120, 2.127, 2.128, 2.131, 2.136, **2.136–7**
block copolymers (BCPs) 1.14, 1.194, 2.44, 2.96
  light-sensitive polymeric micelles 1.308–17, **1.309**, **1.315–16**, **1.319**, 1.320–7
  light-sensitive polymeric vesicles **1.321**, **1.324–6**
  magnetic nanoparticles 2.50–1, **2.51**
  phototriggered micelles/ nanoparticles 1.327–31, **1.332**
  surface modification **2.39**, 2.39–40
block junctions, light-sensitive micelles **1.317**, 1.317–18
blood circulation half-life, liposomes **1.46**
blood vessel fenestrations. *see* enhanced permeability and retention effect
blood–brain barrier (BBB) 1.125, 1.153
BMA (butyl methacrylate) 2.164
Boltzmann factor 2.245
bone morphogenetic proteins (BMPs) 2.192
bottom up approaches, DDSs 2.40
bovine serum albumin (BSA) 2.157, 2.249
breast cancer
  carbon nanotubes 2.96, 2.98–9
  doxorubicin **1.68**, 1.68–9
  pH responsive nanogels 2.159
  pH sensitive liposomes **1.87**, 1.88, 1.90
  ultrasound triggered 1.158, 1.164, 1.165, 1.166
breast cancer resistant protein (BCRP) pump 1.125
bright field optical microscopy 2.281
Brownian relaxation 2.35–6
brushes, polymer 2.296, **2.297**, 2.304, **2.305**, 2.320, **2.322**, 2.323, 2.325–38, **2.327**
brush-like nanosystems 1.315
butyl methacrylate (BMA) 2.164
butoxyl-capped pores 1.108

calcein 1.249–50
calmodulin (CaM) 2.284–5
camptothecin (CPT) 1.100, 1.212
  carbon nanotubes 2.99
  dendrimers, smart 1.106
  magnetic nanoparticles **2.53**, 2.53–4
  mesoporous silica nanoparticles 2.67, 2.75, 2.81
  pH responsive nanogels 2.160
cancer cells. *see* chemotherapy drugs; tumor cells
Candida spp. 2.100, 2.336
canine model of cancer 1.64
capped pores. *see also* corking
  adamantyl 1.249, 2.79
  dendrimers, smart 1.108
  layer-by-layer assemblies 2.125, **2.126**
  mesoporous silica nanoparticles 2.65, 2.66, 2.74–80
  silica nanocontainers 1.248–9
capsules, polymeric. *see also* hollow capsules; nanocapsules
  layer-by-layer assemblies 2.118, 2.120, **2.122**, 2.122, **2.123**, 2.132, **2.133**, **2.139**
  phototriggered 1.327–31, **1.328–30**

carbon nanotubes (CNTs) 2.90–3, **2.91**, **2.93**, 2.110
  encapsulation properties 2.100–3, **2.102**
  external attachment of drugs 2.96–100
  functionalization 2.91–7, **2.91**, 2.102–3, **2.103**, 2.106
  toxicity/environmental impacts 2.104–10, **2.106**
carbonic anhydrase inhibitors 2.238–40
carboplatin 1.71, 2.97–8, 2.102
carboxyfluoroscene (CF) 1.53–4, **1.54**
carboxylic acid 2.204–8, **2.207**, 2.211, **2.212**, 2.262
carboxymethyl-chitosan (CMCS) 1.89–90
cardiomyopathy 1.50
catalase 1.238
catalysts, toxicity 2.105–6, 2.108
catheters, combination products 2.319, 2.320, 2.325, 2.329
cation driven actuation 1.289
cationic nanoparticles, cytotoxicity 1.193–4
cavitation, ultrasound. *see* gas bubble cavitation
CBER (Center for Biologics Evaluation and Research) 2.315
CDs. *see* cyclodextrins
CDER (Center for Drug Evaluation and Research) 2.315
CDRH (Center for Devices and Radiological Health) 2.315
cefazolin 2.130, 2.189
cell delivery systems 2.290–1, 2.307
  cell sheet engineering 2.295–307, **2.295**, **2.297–302**, **2.304–6**
  polymeric materials used 2.291–4, **2.292**
  thermo-responsive polymers 2.294–5
cell lines, table of abbreviations **1.276**
cell membranes
  permeability 1.9
  poration damage 1.193
  stress and strain parameters 1.43
  ultrasound effects 1.165, 1.167, 1.168
cell orientation, sheet engineering 2.303–7, **2.305**, **2.306**
cell-penetrating peptides (CPP) 1.87
cell sheet engineering 2.295–307, **2.295**, **2.297–302**, **2.304–6**
cell sorting 2.33
cells, as biomaterials 1.6
cellular uptake
  carbon nanotubes 2.92
  nanoparticles 1.191–2, 2.78–9
  polymersomes **1.190**, 1.191–2, 1.194, **1.195**
cellulose derivatives 2.173
Center for Biologics Evaluation and Research (CBER) 2.315
Center for Devices and Radiological Health (CDRH) 2.315
Center for Drug Evaluation and Research (CDER) 2.315
ceramic combination products 2.317
CF (carboxyfluorescein) 1.53–4, **1.54**
chain transfer agents (CTA) 2.296, **2.297**
charge-shifting polymers 2.128, **2.128**
chemical bonding, combination products 2.320
chemical hydrogels 1.238–44, **1.239**, **1.242**
chemical initiation, polymer grafting 2.325–8
chemical polymer hydrogels
  cross-linkage 2.185–8, **2.186**
  elastin-like recombinamers **2.184**, 2.184–5
chemotherapy drugs 1.4. *see also specific drugs by name*
  α-amino acid based hydrogels 2.200, 2.211–17
  carbon nanotubes 2.99
  delivery from micelles 1.167–9
  elastin-like recombinamers 2.188–9, **2.189**, 2.193
  gold nanoparticles 2.3

  low temperature sensitive liposome 1.34
  magnetic nanoparticles 2.46–8, **2.48**
  mesoporous silica nanoparticles 2.72
  pH sensitive liposomes 1.87–9
  polymersomes 1.198
  risk-benefit ratios 2.63
  synergistic effects **2.20**
  ultrasonography synergistic effect 1.165–6
  zero premature release 2.64, 2.65
CHEMS (cholesteryl hemisuccinate) 1.81
chitosan (CHIT)
  cysteamine-conjugated 1.225–6
  dual responsive hydrogels 2.172, 2.173
  imprinted hydrogels 2.248
  layer-by-layer assemblies 2.121, 2.125, 2.129, 2.132, 2.141–2
  nanoparticles 1.193, 1.225–6
  pH responsive microgels 2.158, **2.159**
chloroquine 2.103
chloroquinone 1.264
cholesterol 1.46, 1.81
cholesteryl hemisuccinate (CHEMS) 1.81
chromatography, polymersomes 1.187
chromophores
  amphiphilic block copolymers 1.309–17
  phototriggered micelles/nanoparticles 1.328
chronic toxicity, definition 2.104
cinnamic acid 1.319
ciprofloxacin 2.341
cis-aconityl pH-responsive dendrimers **1.103**, 1.104–5
cisplatin
  α-amino acid based hydrogels 2.200, 2.202, 2.211–17, **2.212–13**, **2.215–16**
  carbon nanotubes 2.97–8, 2.101–2
  low temperature sensitive liposomes 1.71
  pH sensitive liposomes **1.85**, 1.89
  polymeric micelles **1.136**
cis–trans isomerization
  light-sensitive polymeric micelles 1.310, 1.313, 1.317, **1.318**
  light-sensitive polymeric vesicles 1.323
clathrates 1.180
clay nanoplatelets 2.119
CLDPD (CMCS-cationic liposome-coated DNA/protamine/DNA complexes) 1.90
clearance, filomicelles 1.193. *see also* accelerated blood clearance (ABC) phenomenon
cleavable linkers, carbon nanotubes 2.98
click chemistry 1.214, 1.224, **1.225**, 1.226
  elastin-like recombinamers 2.185
  layer-by-layer assemblies 2.125, 2.142
  light-sensitive polymeric micelles 1.315
  mesoporous silica nanoparticles 2.79
  silica nanocontainers 1.249
clinical trials
  changed criteria for 1.115
  doxorubicin 1.64–9, **1.66**, **1.68**, 1.70, **1.70**
  new excipients 1.7, 1.8
cloud point. *see* lower critical temperature of dissolution
CMC. *see* critical micellar concentration
CMCS (carboxymethyl-chitosan) 1.89–90
CMSC (critical micelle salt concentration) 1.123
CNTs. *see* carbon nanotubes
coacervates 2.181

coating, combination products 2.320
cochlear implants 1.297, **1.298**, 1.300
collagen
  mimics 1.99
  phase transitions 1.11
  tissue engineering 2.293
collapse cavitation, ultrasound 1.151–5, **1.152**, 1.168, 1.170
collapse transition, phase transitions 1.12–13
colloid templates
  layer-by-layer assemblies **2.119**
  magnetic nanoparticles 2.50, **2.51**
colorectal cancer
  α-amino acid based hydrogels 2.200
  animal models 1.166
  hollow capsules 1.224
  layer-by-layer assemblies 2.144
  oxaliplatin 2.98
combination products 2.313–17, **2.315**
  design strategies **2.342**
  drug-incorporation 2.318–25, **2.319**, **2.322**, **2.323**, **2.324**
  future perspectives 2.341–2
  materials used 2.317–18
  responsive surfaces 2.325–41, **2.326–32**, **2.334–5**, **2.337–8**
combination therapy 2.92
competitive displacement 2.229
  biochemical-responsive DDS 1.20–21
  imprinted hydrogels 2.240–2
composite drug-delivery membranes 2.56–9, **2.57–9**
composition-structure-property relationships 1.34, 1.35, 1.36, 1.40–51, **1.40**, **1.41**, **1.44–6**, **1.48**, **1.49**
compounding 2.318, **2.319**
concanavalin A 1.20
conductivity. *see* intrinsically conducting polymers
configurational biomimesis approach 2.238
conformational imprinting. *see* molecularly imprinted polymers
conjugate released gentamicins 1.19
conjugation properties, dendrimers 1.96
contact lenses, soft 2.235–40, **2.236**, **2.237**, **2.239**
continuous wave (CW) lasers 1.306
contrast agents
  carbon nanotubes 2.101
  magnetic resonance
    imaging 2.73–4
controlled drug release
  chemical hydrogels 1.238
  intrinsically conducting
    polymers 1.288–9
co-patterning, tissue-mimicking cell sheets 2.301–3, **2.302**
copolymer poloxamines 1.193
copper-oxicam complexes 2.200
coprecipitation, magnetic nanoparticles 2.37–8
core–corona nanostructures 2.191
core cross-linking
  polymeric micelles 1.119–20
  reduction-sensitive
    nanosystems 1.214–19, **1.215**, **1.217**
core-shell nanoparticles 2.171
corking 2.101–2, **2.102**. *see also* capped pores
cornea reconstruction 2.296–7
corneal epithelial cells 2.300
corona cross-linking 1.119–20
corona discharge **2.322**
co-solvent methods 1.128
cost-effectiveness, DDSs 1.25
Coulomb interactions 1.12
coumarin 1.249, 1.314, 1.315, 1.319, 1.326
coupled phase transitions 1.14
covalent bonds, molecularly imprinted polymers 2.230

covalent functionalization, carbon nanotubes 2.91, 2.93–5
CPPs (cell-penetrating peptides) 1.87
CPT. *see* camptothecin
creatinine 2.240, 2.242
critical micellar concentration (CMC) 1.156–8, 1.180
  light-sensitive polymeric micelles 1.308, 1.310
  polymeric micelles 1.116–19, 1.122–3, 1.126, 1.167
  reduction-sensitive nanosystems 1.219
critical micellar temperature (CMT), polymeric micelles 1.120–1, 1.122, 1.123, 1.126
critical micelle salt concentration (CMSC) 1.123
critical solubility temperature (CST), polymers 1.21–2. *see also* lower critical temperature of dissolution; upper critical solution temperature
cross-linkage. *see also* PEGylation
  α-amino acid based hydrogels 2.200, 2.204, **2.205**, 2.206, **2.209**, 2.209, 2.220, 2.221
  biomolecule-sensitive hydrogels 2.263–4, **2.264**, 2.271, 2.274, **2.284**
  chemical hydrogels 1.238, 1.238–44, **1.239**, **1.242**
  combination products, drug/medical devices 2.320
  dual-responsive hydrogels 2.170
  elastin-like recombinamers 2.185–8, **2.186**
  glucose-sensitive hydrogels 2.267–8
  hydrogels 2.235, 2.236
  imprinted hydrogels 2.238, 2.245, **2.246**, 2.248
  light-sensitive polymeric micelles 1.318–20, **1.319**
  micelles 1.163, 1.218, 1.319–20
  molecularly imprinted polymers 2.231, 2.232, 2.234–5
  polymer grafting 2.330
  polymeric capsules 1.307, 1.328–9, **1.329**
  polymeric micelles 1.119–20, 1.130, 1.135, 1.157
  poly(*N*-acryloxysuccinimide) 2.78
  reduction-sensitive nanosystems 1.214–19, **1.215**, **1.217**
cross-talk, cellular 2.297
cryogenic electron microscopy (CryoEM) 1.185, **1.187**
Cryptococcus neoformans 2.100
crystallization, phase transitions 1.13
CTA (chain transfer agents) 2.296, **2.29**
CTAB (hexadecyltrimethylammonium bromide) 2.6
curcumin 1.241
CW (continuous wave) lasers 1.306
cyclic voltametry (CV) 1.287, **1.288**
cyclo-addition reactions, carbon nanotubes 2.95
cyclodextrins (CDs) 1.116, 1.249
  combination products 2.320
  layer-by-layer assemblies **2.127**, 2.127
  mesoporous silica nanoparticles 2.75–6, 2.80
cylindrical nanoparticles 1.192
cystamine 2.78
cystaminebisacrylamide 1.265–6
cysteamine-conjugated chitosan-based nanoparticles 1.225–6
cysteine 1.105, 1.223, **1.263**, 1.264
cytokines 2.297
cytosine arabinoside 1.165
cytosine-phosphate-guanosine (CpG)-gold nanoparticles 2.6
cytosol
  pH 1.16
  reduction-sensitive nanosystems **1.211**, 1.211
cytotoxicity. *see* toxicology

daidzein 1.97
dapsone 2.100
dasatinib 1.234
daunorubicin (DNR) 2.125
DBS (dodecylbenzenesulfonate) 1.294
DBT (dibenzothiophenes) 2.248
DCC (dicyclohexylcarbodiimide) 1.158
DCM (dilated cardiomyopathy) 2.297
DDSs. *see* drug delivery systems
DEAA (diethylacrylamide) 2.236
DEAMA (diethylaminoethyl methacrylate) 2.265, 2.280, 2.281, 2.291
Debye theory 2.34, 2.36
defect group functionalization 2.93, 2.94
defences, bodily 1.37. *see also* immune responses
definitions
  biomaterials 1.4
  combination products 2.314
  enzyme-responsive materials 1.235
  gene therapy 1.200
  intelligent DDS 1.15–16
  nanogels/microgels 2.154
  new excipients 1.7
  pharmaceutical excipients 1.4
  prodrugs 1.234
  toxicity 2.104
  ultrasound 1.149
degradable hydrogels, enzyme-responsive 1.238–40, **1.239**
delayed-release 1.2
dendrimer-phthalocyanine (DPc) 1.100
dendrimers, smart 1.94–6, 1.109
  cytotoxicity 1.193
  enzyme-responsive 1.105–8, **1.106**, **1.107**
  layer-by-layer assemblies 2.129
  photoresponsive 1.100–2, **1.101**
  pH-responsive 1.102–5, **1.103**
  polyamidoamine **1.95**
  redox-responsive 1.105
  temperature-responsive 1.96–9, **1.97**
  theragnostic 1.108–9
deoxyribonucleic acid. *see* DNA
dephosphorylation/phosphorylation 1.242
dermal contact, carbon nanotubes 2.105, 2.108
device primary mode of action 2.315
dexamethasone 2.100, 2.192
dextran
  hydrogels **1.239**
  layer-by-layer assemblies 2.121, 2.129, 2.131, 2.132
  pH responsive nanogels 2.160
  temperature-responsive hydrogels 2.165
dextran-lipoic acid derivatives (Dex-LAs) 1.221–3, **1.222**
dextranases 1.239
DHLA (dihydrolipoic acid) 1.223
diabetic treatment. *see* glucose-sensitive hydrogels
diagnosis. *see* theranostics
diazonaphthoquinone (DNQ) 1.310, 1.315–16
diazoresin 2.125
dibenzothiophenes (DBT) 2.248
dichloromethane 2.102
diclofenac 1.24
dicyclohexylcarbodiimide (DCC) 1.158
diethylacrylamide (DEAA) 2.236
diethylaminoethyl methacrylate (DEAMA) 2.265, 2.280, 2.281, 2.291
diffusion-controlled drug release 2.124–5
DIGNITY breast cancer study **1.68**, 1.68–9, **1.70**, 1.70
dihydrolipoic acid (DHLA) 1.223
dilated cardiomyopathy (DCM) 2.297
diltiazem hydrochloride (DIL-HCl) 2.157

DIM (D-phenylalanine) **2.242**
dimethylacrylamide
  (DMAAm) 2.240
  dual responsive hydrogels 2.171
  polymer grafting 2.335
  temperature-responsive
    hydrogels 2.164
dimethylaminoethyl methacrylate
  (DMAEMA) 2.336, 2.337,
  2.337
dimethyl-1,3-dioxan-2-yloxy) ethyl
  acrylate (DMDEA) **1.226**, 1.227
dimethylformamide (DMF) 2.215,
  2.216
dimethyl sulfoxide (DMSO) 2.211,
  2.212, 2.215
dimyristoyl phosphatidic acid
  (DMPA) 2.131
dimyristoylphosphatidylcholine
  (DMPC) 1.45
dioleoylphosphatidylcholine
  (DOPC) 1.81
dioleoylphosphatidyl-ethanolamine
  (DOPE) 1.81, 1.262
dioleoyl-3-trimethylammonium-
  propane (DOTAP) 1.264
dipalmitoyl phosphatidyl choline
  (DPPC) 1.43, 1.71
  composition–structure–property
    relationships 1.45, 1.47
  lipid membrane components **1.41**,
    1.41–2
  low temperature-sensitive
    liposome **1.54**, 1.54
  permeability **1.48**, 1.49
  in vitro performance-in-
    service 1.54–6, **1.55**, 1.57, 1.58
dipalmitoyl-*sn*-glycero-3-
  phosphoglyceroglycerol
  (DPPGOG) 1.71
direct sidewall functionalization,
  carbon nanotubes 2.93, 2.94–5
disease-responsive DDS 1.15–25,
  1.17, **1.22**, 2.161
disregulation, enzyme activity 1.232,
  1.233
disruptive enzyme-responsive
  micelles 1.244–6, **1.245**
distearoyl phosphatidyl choline,
  (DSPC) 1.44, 1.47
distearoyl phosphatidyl ethanolamine
  lipid membrane components **1.41**,
    1.41–2, 1.50–1
  low temperature-sensitive
    liposomes 1.54, **1.54**
  in vitro performance-in-
    service **1.57**, 1.57, 1.57–8, 1.59
disulfonated aluminum
  phthalocyanine 1.101
dithionite assay, low temperature-
  sensitive liposome 1.54–6, **1.55**
dithiothreitol (DTT) 1.212, 1.214,
  1.216, 1.218, 1.219, 1.221–3, **1.222**,
  1.225, 2.78
DLS. *see* dynamic light scattering
DMAEMA (dimethylaminoethyl)
  methacrylate) 2.336, 2.337, **2.337**
DMDEA (dimethyl-1,3-dioxan-2-
  yloxy) ethyl acrylate) **1.226**, 1.227
DMF (dimethylformamide) 2.215,
  2.216
DMAAm. *see* dimethylacrylamide
DMPA (dimyristoyl phosphatidic
  acid) 2.131
DMPC
  (dimyristoylphosphatidylcholine)
  1.45
DMSO (dimethyl sulfoxide) 2.211,
  2.212, 2.215
DNA damage, ultrasound
  triggered 1.168–9
DNA delivery systems. *see* gene
  delivery
DNA sensitive sol–gel transition
  systems 2.282, **2.282**
DNQ (diazonaphthoquinone) 1.310,
  1.315–16
DNR (daunorubicin) 2.125
docetaxel 1.129
dodecylbenzenesulfonate
  (DBS) 1.294
dopamine 2.293

DOPC (dioleoylphosphatidylcholine) 1.81
DOPE (dioleoylphosphatidylethanolamine) 1.81, 1.262
dosage forms, evolution/development 1.1–4, **1.3**
DOTAP (dioleoyl-3-trimethylammonium-propane) 1.264
DPPC. *see* dipalmitoyl phosphatidyl choline
DPPGOG (dipalmitoyl-sn-glycero-3-phosphoglyceroglycerol) 1.71
double-walled carbon nanotubes (DWCNTs) 2.92, 2.103, **2.103**, 2.104, 2.110
doxorubicin 1.80
  carbon nanotubes 2.96–7
  dendrimers, smart 1.96, 1.100, 1.101, 1.103–4, 1.106
  enzyme-responsive DDS 1.235, 1.243, **1.245**, 1.246
  gold nanoparticles 2.3, 2.10, 2.20
  layer-by-layer assemblies 2.142
  magnetic responsive DDS 2.42, **2.42**, 2.46, 2.139–40, **2.140**
  mesoporous silica nanoparticles 2.68, 2.71, 2.72, 2.74, 2.81
  pH responsive DDS **1.85**, **1.87**, 1.88, 2.160
  polymeric micelles 1.130, 1.133, **1.136**, 1.157–8, 1.160
  polymersomes 1.198–9, 1.199–200, 1.201
  production 1.51–2, **1.52**
  reduction-sensitive DDS 1.213–14, 1.216, 1.216–18, 1.224, 1.226–7
  shell-sheddable micelles 1.210–11, **1.211**, 1.212
  temperature-responsive DDS 1.34, 1.39, **1.49**, 1.49–50, 2.167
  ultrasound triggered 1.159, 1.162–9
  in vitro performance-in-service 1.56–60, **1.56**, **1.57**, **1.59**
  in vivo performance-in-service 1.60–9, **1.62**, **1.63**, **1.66**, **1.68**
DPc (dendrimer-phthalocyanine) 1.100
D-phenylalanine (DIM) **2.242**
DPPC (dipalmitoyl phosphatidyl choline) 1.71
drug delivery systems (DDSs), general information
  advanced 1.4–9, **1.7**, **1.8**
  carrier systems **2.64**
  evolution 1.1–4, **1.3**
  future perspectives 1.25
  intelligent 1.15–25, **1.17**, **1.22**
  main approaches **1.3**
  stimuli responsive
    networks 1.9–15, **1.10**, **1.15**. *see also specific stimuli by name*
drug dissolution test 1.2
drug efflux pumps 1.9, 1.82, 1.125, 2.71–2
drug-eluting devices. *see* combination products
drug excipients. *see* excipients
drug-loaded soft contact lenses 2.235–40, **2.236**, **2.237**, **2.239**
drug partition coefficients, imprinted hydrogels 2.238
drug–polymer conjugates 1.158–9, 1.235
drug primary mode of action 2.314
drug release rates. *see* release rate
drug resistance. *see* multi-drug resistance
drug trapping liposomes 1.51
DSPC (distearoyl phosphatidyl choline) 1.44, 1.47
DTT (dithiothreitol) 1.212, 1.214, 1.216, 1.218–19, 1.221–3, **1.222**, 1.225, 2.78
dual-responsive DDS. *see also* synergistic effects
  hydrogels 2.154, 2.170–3
  mesoporous silica
    nanoparticles 2.71, 2.79–80
  polyelectrolyte complexes 1.274–5
Durapores poly(vinylidene difluoride) membranes 2.292, 2.297, **2.299**, 2.307

dynamic light scattering (DLS)
  elastin-like recombinamers 2.192
  polymersomes **1.187**
dysopsonins 2.41, 2.131

EB (electron-beam) irradiation 2.296
EBA (ethylene-bisacrylamide) 2.200, 2.204, **2.205**
ECM (extra-cellular matrix) 2.290–1, 2.294, **2.295**, 2.297, **2.298**, 2.303
EDC (ethyl- 3-(3-dimethyl-aminopropyl) carbodimide hydrochloride) 1.290–1
EDS, *see* equilibrium degree of swelling
efavirenz (EFV) 1.119, 1.124–5, **1.125**, 1.126, **1.136**
efflux pumps 1.9, 1.82, 1.125, 2.71–2
EGF. *see* epidermal growth factor
Ehrlich, Paul 1.232
Ehrlich tumors 1.89
elastic modulus liposomes 1.46, **1.46**
elastin, biomimetics 2.181
elastin-like recombinamers (ELRs) 2.181–3, **2.182**, **2.183**, 2.195–6
  hydrogels **2.184**, 2.184–90, **2.186**, **2.189**
  nanoparticles 2.190–5, **2.191**, **2.194**, **2.195**
electric field responsive DDS **1.22**, 1.24–5, 2.100
electroactive molecularly imprinted polymers (EMIP) 1.296
electrochemical responsive drug release 2.134–5, **2.135**
electro-conductive hydrogels 1.294–6. *see also* intrinsically conducting polymers
electrodes, implantable 1.297, **1.298**, 1.300
electron microscopy 1.185, **1.187**, 2.94, 2.101
electron-beam irradiation 2.296
electron-beam lithography 2.338
electron microscopy. *see* transmission electron microscopy
electronic properties, carbon nanotubes 2.92
electrophilic addition, carbon nanotubes 2.95
electrophoretic deposition (EPD) 2.56
electrospraying 2.193
electrostatic forces, intrinsically conducting polymers 1.288–9
elimination assessments, new excipients 1.7
elimination mechanisms, carbon nanotubes 2.108–9
ELRs. *see* elastin-like recombinamers
EMA (European Medicines Agency) 1.122
EMIP (electroactive molecularly imprinted polymers) 1.296
emulsion polymerization techniques 1.299
encapsulating membranes, lipid bilayers 1.43–7, **1.44**
encapsulation properties
  carbon nanotubes 2.100–3, **2.102**
  dendrimers, smart 1.96
  polymeric micelles 1.117–18, 1.123
encephalitis 1.125
endocytosis 1.86, 1.167, 1.168, 1.191, 1.192, 2.105
endoscopic submucosal dissection (ESD) 2.296–7, **2.299**
endosome, pH 1.16, 1.257
endovascular stents 2.316
engineering 1.4, **1.5**
  cell/tissue delivery systems 2.293–4
  low temperature sensitive
    liposomes 1.36–51, **1.38–41**, **1.44–6**, **1.48–9**
enhanced permeability and retention (EPR) effect 1.3, 1.9, 1.81, **1.82**, 1.167
  carbon nanotubes 2.99
  dendrimers, smart 1.96
  elastin-like recombinamers 2.188, **2.189**
  gold nanoparticles 2.2

enhanced permeability and retention (EPR) effect (*continued*)
  low temperature-sensitive liposome 1.37–8, **1.38**, 1.62, 1.73
  mesoporous silica nanoparticles 2.67
  new excipients 1.9
  and particle size 1.236
  pH-sensitive liposomes 1.81, **1.82**, 1.87
  polymeric micelles 1.116
  polymersomes 1.198–9
  ultrasound-responsive DDSs 1.23, 1.159–60
entangled membranes, polymersomes 1.188
Enterococcus faecalis 1.123–4
entropy-driven micellization mechanisms 1.122
entropy-driven polymersomes 1.180
environmental impacts/interactions
  carbon nanotubes **2.106**, 2.109–10
  dual responsive hydrogels 2.171
enzymatic degradation, gastrointestinal tract 1.2
enzyme cross-linkage, elastin-like recombiners 2.187
enzyme delivery, polymersomes 1.201
enzyme inhibitors 1.234
enzyme-responsive materials (ERMs) **1.17**, 1.18–19, 1.232–6, 1.251–2
  advantages/drawbacks **1.236**
  biomolecule-sensitive hydrogels 2.270–2, **2.272**
  dendrimers, smart 1.105–8, **1.106**, **1.107**
  drug design 1.236–7, **1.237**
  enzyme disregulation **1.233**
  glucose-sensitive hydrogels 2.264–5, **2.265**
  gold nanoparticles 2.20–1
  hydrogels 1.237–44, **1.239**, **1.242**
  layer-by-layer assemblies 2.141–2, **2.143**
  mesoporous silica nanoparticles 2.71, 2.79
  micelles 1.244–8, **1.245**
  silica nanocontainers **1.248**, 1.248–51, **1.249**
EPD (electrophoretic deposition) 2.56
epidermal growth factor (EGF)
  carbon nanotubes 2.98
  pH sensitive liposomes 1.89
  receptor active targeting 1.191
epilepsy 2.57, **2.58**
epirubicin 2.99
EPR effect. *see* enhanced permeability and retention effect
equilibrium degree of swelling (EDS), α-amino acid based hydrogels 2.204, 2.206–11, **2.207**, **2.208**, **2.210**, 2.214, 2.217, **2.218**, 2.219, 2.221–2, **2.222**
equilibrium polymerization, phase transitions 1.12
ERMs. *see* enzyme-responsive materials
erythrocytes, stress and strain parameters 1.43
erythromycin 2.160
Escherichia coli 2.335, 2.337
ESD (endoscopic submucosal dissection) 2.296–7, **2.299**
estrogen anchored pH-sensitive liposomes 1.86, **1.87**
ethosuximide 2.57, **2.58**
ethoxzolamide 2.238–40
ethyl- 3-(3-dimethyl-aminopropyl) carbodiimide hydrochloride (EDC) 1.290–1
ethylene-bisacrylamide (EBA) 2.200, 2.204, **2.205**
ERMs. *see* enzyme-responsive materials
ethylene glycol (EG) 2.236, **2.236**, 2.265
ethylenediamine 1.122, 1.133–4
European Medicines Agency (EMA) 1.122

excipients. *see also* drug delivery systems
  active/passive 1.3
  advanced 1.4–9, **1.5**, **1.7**, **1.8**
  evolution 1.1, 1.2
excretion. *see* elimination
explodable systems, layer-by-layer assemblies 2.122, 2.129, 2.138
extended-release DDS 1.2, 2.122, 2.125, **2.126**
external attachment of drugs, carbon nanotubes 2.91, 2.96–100, 2.101
external stimuli-responsive DDSs 1.96, 1.305, 2.2, **2.76**, 2.154. *see also* light-responsive DDS; temperature-responsive DDS
extra-cellular matrix (ECM) 2.290–1, 2.294, **2.295**, 2.297, **2.298**, 2.303
extrusion procedures, liposomes 1.51

FA. *see* folate/folic acid
FDA. *see* Food and Drug Administration
feedback-modulated DDSs 1.2, **1.3**, 2.243, **2.244**
fenestrations, tumor. *see* enhanced permeability and retention effect
fiber paradigm, pulmonary toxicology 2.107
fibrillation 1.194
fibrin 2.293
fibrinogen 1.189
field-effect transistor (FET) gates 2.266
filomicelles, clearance 1.193
first generation
  biomaterials 1.4
  excipients 1.2
first order phase transitions 1.11–12
5-fluorouracil (5-FU) 1.96, 1.166
5-fluorouracilhexyl-carbamoyl fluorouracil (HCFU) 2.166
flame treatment, polymer grafting **2.322**
flow dynamics, carbon nanotubes (CNTs) 2.92
flower-like micelles 1.127, 1.130–1
fluorescein 2.75
fluorescein isothiocyanate (FITC) 2.74
fluorescent resonance energy transfer (FRET) mechanism 2.21
fluorination, carbon nanotubes 2.95
Fmoc-Phe-*p*Tyr 1.243
folate/folic acid (FA) 1.160
  binding protein 1.160
  carbon nanotubes 2.96–7, 2.98
  gold nanoparticles 2.3
  mesoporous silica
    nanoparticles 2.67–8
  polyplexes 1.262
  tumor cell receptors 1.191
Food and Drug Administration (FDA) 1.197, 1.234
  approved excipients 1.122
  Office of Combination
    Products 2.314–15, **2.315**
force mapping, Atomic Force Microscopy **1.187**
fouling. *see* opsonisation
FR (α-folate receptors) 2.67
free-radical graft polymerization 2.321, **2.323**, 2.323–4
free radicals, ultrasound-triggered 1.152, 1.153
freeze-drying
  pH-sensitive liposomes 1.89
  polymeric micelles 1.120
FRET (fluorescent resonance energy transfer) 2.21
frustrated endocytosis 1.192, 2.105
fullerenes 2.101–2, **2.102**, 2.102
functional monomers 2.230, 2.231, 2.238
  biomolecule-sensitive 2.276
  drug-loaded soft contact
    lenses 2.235, 2.236
  pH-responsive 2.251
  stimuli-responsive imprinted
    networks 2.245
  temperature-responsive 2.245–6

functionalization
  carbon nanotubes 2.91–7, **2.91**, 2.102–3, **2.103**, 2.106
  combination products 2.325–38, **2.326–32**, **2.334–5**, **2.337–8**
  plasma polymerization 2.339–41
fusogenic liposomes 1.82–3, 1.86
future perspectives
  α-amino acid based hydrogels 2.221–4, **2.222–3**
  combination products 2.341–2
  imprinted hydrogels 2.254
  mesoporous silica nanoparticles 2.81–2
  ultrasound-responsive DDSs 1.169–70

gadolinium 1.196, 1.197, 2.73, 2.101
galactose 2.144
gamma ray polymer grafting **2.322**, 2.323–4, **2.329**, 2.329–38
gammainterferon-inducible lysosomal thiol reductase (GILT) **1.209**, 1.210
gas bubble cavitation 1.150–5, **1.152**, 1.163, 1.168, 1.170. *see also* microbubbles
gastrointestinal tract
  doxorubicin toxicity 1.50
  drug release in 1.239
  enzyme-responsive materials 1.236–7
  pH responsive DDS 1.16, 1.102, 2.129, 2.154, 2.155
gate effects, imprinted hydrogels 2.240, 2.242, **2.248**, 2.248–9. *see also* capped pores
gel phases. *see* phase transitions
gene delivery (for gene therapy) 1.4. *see also* RNA
  cell/tissue delivery systems 2.300
  elastin-like recombinamers 2.190, 2.192
  gold nanoparticles 2.6, **2.8**, 2.16–17, **2.18**
  layer-by-layer assemblies 2.124, 2.126, 2.135
  magnetic nanoparticles 2.48–50, **2.50**
  mesoporous silica nanoparticles 2.71–2
  pH-sensitive liposomes **1.85**, 1.89–90
  phase transitions 1.11–12
  polymeric micelles 1.135
  polymersomes 1.200
  polyplexes 1.256–8, 1.261–7, **1.263**, 1.269–70, **1.273**, 1.273–4
  ultrasound-sensitive systems 1.154
gene silencing effect 2.13
genotoxicity. *see also* toxicology
  carbon nanotubes 2.109, 2.110
  definitions 2.104
  new excipients 1.9
gentamicin 2.130
GFP (green fluorescent protein) 1.201
giant unilamellar vesicles (GUVs) 1.35, 1.43, 1.44, **1.45**. *see also* low temperature sensitive liposomes
GILT (gammainterferon- inducible lysosomal thiol reductase) **1.209**, 1.210
G-insulin (synthetic glycosylated insulin) 2.291
glass transitions 1.13
glaucoma 2.203, 2.211, 2.236. *see also* pilocarpine
glucose oxidase (GOD) 1.238
  combination products **2.340**
  glucose-sensitive hydrogels **2.265**, 2.265
  insulin cell/tissue delivery systems 2.291
glucose-responsive DDS. *see also* insulin
  biomolecule-sensitive hydrogels 2.262, 2.264–70, **2.265**, **2.267–9**
  combination products 2.339–40, **2.340**
  layer-by-layer assemblies 2.141
  nanocarriers 1.20

glutathione tripeptide (g-glutamyl-cysteinyl-glycine) 1.209, **1.209**. *see also* redox-responsive drug release
glycerylphosphorylcholine 1.34–5, **1.35**, 1.43, 1.46, 1.47
glycine-proline-(hydroxy)proline (Gly-Pro-Pro (Hyp)) 1.99
glycolphosphatidylethanolamine conjugates 1.161
glycosidases 1.19
GOD. *see* glucose oxidase
gold nanoparticles 2.1–7, **2.3**, **2.4**, **2.5**, 2.7, **2.8**, 2.23
  carbon nanotubes 2.101–2
  cytotoxicity 1.193
  dendrimers, smart 1.108
  enzyme-responsive 2.20–1
  glutathione-responsive 2.10, **2.12**
  layer-by-layer assemblies 2.119–20, **2.120**, 2.137–8
  light-responsive DDSs 1.23
  mesoporous silica nanoparticles 2.77
  pH-responsive DDS **2.9**, 2.9–10, **2.11**
  photo-active/photodynamic 2.10–14, **2.13**, **2.15**
  photothermal therapy 1.100, 2.14–20, **2.16**, **2.17**, **2.18**, **2.19**
  surface modification 2.39
  synergistic effects **2.20**, 2.20
  temperature-responsive DDS 1.22
  theranostics 2.21–3, **2.22**, **2.23**
Golgi apparatus 1.16
graft copolymers 1.313, 1.323
grafting-from/to 2.321. *see also* polymer grafting
Graham, Thomas 1.237
green fluorescent protein (GFP) 1.201
griseofulvin 1.123
growth factors
  electric field responsive DDS 1.25
  hepatocyte 2.298, **2.300**
  layer-by-layer assemblies 2.142–3
guar gum 2.165
GUVs. *see* giant unilamellar vesicles
gyrase subunit B (GyrB) 2.285

Halobacterium halobium 2.338
HB (hypocrellin B) 2.138
Hc (hysteresis coercivity) 2.37
HCC (hepatocellular carcinoma) 1.65–8, **1.66**, 1.258–9
HCFU (5-fluorouracilhexyl-carbamoyl fluorouracil) 2.166
HDF. *see* human dermal fibroblast
HDPE (high-density polyethylene) 2.220–1
HEAA (hydroxyethyl acrylamide) 2.240
HEAT study, HepatoCellular Carcinoma 1.67–8, **1.70**, 1.70
heating, ultrasound 1.150. *see also* temperature-responsive DDS
helix-to-random coil transitions 1.11–12
HEMA. *see* hydroxyethylmethacrylate
hemoglobin **2.276**
Henderson–Hasselbalch equation 2.206
heparin 2.125, 2.284, **2.284**
hepatitis C virus (HCV) 1.116
hepatocarcinoma 1.104
hepatocellular carcinoma (HCC) 1.65–8, **1.66**, 1.258–9
hepatocyte growth factor (HGF) 2.298, **2.300**
hepatocytes
  cell/tissue delivery systems 2.293
  tissue-mimicking cell sheets **2.302**, 2.302
HER2 complex (human epidermal growth factor receptor) 1.160
hexadecyltrimethylammonium bromide (CTAB) 2.6
hexamethylamine 2.102
hierarchical delivery systems, layer-by-layer assemblies 2.122–3, **2.123**

high-affinity binding sites **2.232**, 2.234, 2.235, 2.236. *see also* imprinted hydrogels
high-density polyethylene (HDPE) 2.220–1
high-energy radiation 2.187
high frequency ultrasound (HIFU) 1.70, **1.70**, 1.149–50
high-frequency magnetic field (HFMF) 2.35, **2.43**, **2.55**, **2.56**, **2.57**. *see also* magnetic nanoparticles
high-performance liquid chromatography (HPLC) **1.258**
high-resolution transmission electron microscopy (HRTEM) 2.54, **2.55**
histamine H1-receptor 2.238
histidine monomers **2.205**, 2.208–9, **2.209**, 2.218, 2.219, **2.219**, 2.220
histidine-rich peptides 1.257, 1.262
HIV-1 encephalitis (HIVE-1) 1.125
HIV/AIDS 1.124–5, 1.234
HLB. *see* hydrophilic-lipophilic balance
HNE (human neutrophil elastase) 1.240
hollow capsules
  reduction-sensitive
    nanosystems 1.223–6, **1.225**
  layer-by-layer assemblies 2.118
hollow vesicles 2.194–5, **2.195**
homeostasis, and DDSs 1.3
hormones, bodily release 2.153–4
horse spleen ferritin (HSF) 1.325
horseradish peroxidase (HRP) 1.201
HPC (hydroxypropylcellulose) 2.173
HPHDP (hyperbranched polyphosphates) 1.214, **1.215**
HPLC (high-performance liquid chromatography) **1.258**
HPMA (hydroxypropyl methacrylamide) 1.158, 2.265
HRP (horseradish peroxidase) 1.201
HRTEM (high-resolution transmission electron microscopy) 2.54, **2.55**
HSBA (hydrazinosulfonyl benzoic acid) **1.103**, 1.104
HSF (horse spleen ferritin) 1.325
human dermal fibroblast (HDF) 1.200, 2.303, 2.304, **2.304**, 2.306
human epidermal growth factor receptor II (HER2) complex 1.160
human immunodeficiency virus. *see* HIV/AIDS
human neutrophil elastase (HNE) 1.240
human serum albumin (HSA) 2.41, 2.131
human umbilical vein endothelial cells (HUVECs) 2.303
hydrazone **1.103**, 1.104–5
hydrazinosulfonyl benzoic acid (HSBA) **1.103**, 1.104
hydrogel collapse transition 1.12
hydrogel-conducting polymer composites 1.294–6
hydrogels 2.154, 2.173–4. *see also* α-amino acid based hydrogels; biomolecule-sensitive hydrogels; microgels; nanogels
  affinity-controlled
    release 2.235–43, **2.236–9**, **2.241–3**
  chemical 1.238–44, **1.239**, **1.242**
  conformational
    imprinting 1.14–15
  dual responsive 2.154, 2.170–3
  elastin-like recombinamers **2.184**, 2.184–90, **2.186**
  enzyme-responsive
    materials 1.237–44, **1.239**, **1.242**
  pH-responsive 1.18, 2.154, **2.155**, 2.155–61, **2.156**, **2.159**, 2.173–4
  physical 1.238, **2.184**, 2.184, 2.188
  properties 2.200
  temperature-responsive 2.154, **2.161**, 2.161–9, **2.162**, **2.163**, **2.166**, **2.169**, 2.173–4
hydrogen bonds 1.12, 1.19
hydrolases 1.19

hydrolysis
  imprinted hydrogels 2.242–3
  layer-by-layer assemblies 2.125–9, **2.127**, **2.128**
  phase transitions 1.14
hydrophilic building blocks 1.132–3
hydrophilic particles 1.189
hydrophilic poly(*N*-acryloylmorpholine) (PAcMo) 2.304
hydrophilic/hydrophobic balance
  α-amino acid based hydrogels 2.210
  light-sensitive micelles 1.309–20, **1.311**, **1.314**, **1.315**, **1.317**
  switching 2.154
  temperature-responsive hydrogels 2.162, **2.163**
hydrophilic-lipophilic balance (HLB), polymeric micelles 1.118, 1.122, 1.127
hydrophobic colloids 1.189
hydrophobic effect 1.35, 1.180, 1.183
hydrophobic interactions 1.12
hydrophobic poly(*N*-butyl acrylate)-co-polystyrene 1.246
hydroxyethyl acrylamide (HEAA) 2.240
hydroxyethylmethacrylate (HEMA) 2.236, 2.238, 2.240, 2.242-3, 2.291–3
hydroxyl radicals 2.187
hydroxypropylcellulose (HPC) 2.173
hydroxypropyl methacrylamide (HMPA) 1.158, 2.265
hyperbranched polyphosphates 1.214, **1.215**
hyperthermia 2.174. *see also* temperature-responsive DDS
  dendrimers, smart 1.96
  elastin-like recombinamers 2.193–4
  imprinted hydrogels 2.247
  mesoporous silica nanoparticles 2.73
  temperature-responsive nanogels 2.166
  theory 2.33, 2.34–7, **2.35**, **2.36**
  ultrasound triggered 1.165
hypocrellin B (HB) 2.138
hypo-/hyperexpression, enzymes 1.232, **1.233**
hypoxia, tumor cells 1.210
hysteresis coercivity (Hc) 2.37

IBAM (isobutylamide) group 1.98
ibuprofen
  layer-by-layer assemblies 2.132
  magnetic nanoparticles 2.42
  upper critical solution temperature 2.169
ICAM-1 (intra-cellular cell adhesion molecule 1) 1.191
ICPs. *see* intrinsically conducting polymers
IM (imprint molecules) 1.296
imaging compounds **2.41**
imatinib mesylate 1.234
imidazole 2.242–3, **2.243**
immune responses 1.9
  autoimmune diseases 2.98
  elastin-like recombinamers 2.190, 2.195
  low temperature-sensitive liposomes 1.37
  to medical devices 2.316
  opsonins 1.189
immunoglobulins 1.189, 2.272–3
immunomicelles 1.161
implantable electrodes 1.297, **1.298**, 1.299, 1.300
implants, biomedical
  biomaterials 1.5
  intrinsically conducting polymers 1.297, **1.298**, 1.299, 1.300
  layer-by-layer assemblies 2.142
  opportunistic bacteria 2.316
imprint molecules (IM) 1.296

imprinted hydrogels 2.228–9, 2.235–43, **2.236–9**, **2.241–3**
  biomolecule-sensitive 1.21, 2.229, 2.276–9, **2.278**, **2.279**
  light-responsive 2.251–4, **2.252**, **2.253**, **2.254**, 2.254
  molecular imprinting 2.229–35, **2.230**, **2.232**, **2.234**
  pH-responsive 2.249–51, **2.250**
  stimuli-responsive networks 2.243–5, **2.244**
  temperature-responsive 2.245–9, **2.246–8**
  see also molecularly imprinted polymers
in vitro performance-in-service, mesoporous silica nanoparticles 2.73
in vivo performance-in-service, polymeric micelles 1.131–2, **1.132**
indium tin oxide (ITO) 1.290, 2.134
indomethacin 1.126, 1.294
induced fit, molecularly imprinted polymers 2.235
induced metastasis, ultrasound-triggered 1.155
industrial revolution 1.2
inertial cavitation, ultrasound 1.152
infected tissues
  gold nanoparticles 2.3
  and implantable devices 2.316
  layer-by-layer assemblies 2.130, **2.131**
  pH changes 1.83, 1.134
  temperature-responsive DDS 2.154
inflamed tissues
  carbon nanotubes 2.98
  enzyme-responsive DDS 1.19
  pH changes 1.16, 1.83, 1.134
  responses to medical devices 2.316
infrared (IR) spectroscopy 1.286
infrared radiation 1.23
inhalation, carbon nanotubes 2.105, 2.107–8
inorganic mesoporous silica. *see* mesoporous silica nanoparticles
inorganic shells **2.39**, 2.40
insulin 1.238. *see also* glucose-responsive DDS
  cell/tissue delivery systems 2.290–3, **2.292**
  combination products 2.339–40, **2.340**
  competitive binding 2.229
  electric field responsive DDS 1.24
  layer-by-layer assemblies 2.141
  pH responsive microgels 2.156
  synthetic glycosylated 2.291
integrins 1.191
intelligent DDS. *see* stimuli-responsive DDSs
interdisciplinary research
  biomaterials 1.6
  excipients 1.4
internal stimuli-responsive DDSs. *see* self-regulated DDS
interpenetrating polymer networks (IPNs) 1.157, 2.330
  biomolecule-sensitive hydrogels 2.271, **2.272**, 2.274, **2.275**, **2.276**
  dual-responsive hydrogels 2.173
  imprinted hydrogels 2.246
  polymer grafting 2.331, 2.333
  temperature-responsive hydrogels 2.165
intra-cellular cell adhesion molecule 1 (ICAM-1) 1.191
intra-ocular lens implantation 2.316
intravascular release
  doxorubicin **1.62**, 1.62–4, **1.63**
  hypothesis 1.72–3
intrinsically conducting polymers (ICPs) 1.283–5, **1.290**, 1.290–9, 1.300. *see also* polypyrrole
  biocompatibility 1.287–8
  biological applications 1.299–300
  characterization 1.286–7, **1.288**
  conducting polymer nanotubes 1.297–9
  controlled drug release mechanisms 1.288–9

DDS **1.290**, 1.290–9, **1.291**, **1.293**, **1.295**, **1.298**
electric field-responsive DDS 1.25
properties 1.285–6
inverse temperature transition (ITT) 2.182
inverted hexagonal phase, pH sensitive liposomes 1.86
inverted micelles 1.36
ionic interactions, cross-linkage 2.188
ion-responsive DDSs 1.16–18, **1.17**
α-amino acid-based hydrogels 2.202, 2.204–9, **2.207**, **2.208**, **2.209**, 2.210
IPNs. *see* interpenetrating polymer networks
iron oxide nanoparticles (IONP) 1.108. *see also* magnetic nanoparticles
iron-free apoferritin (HSAF) **1.325**, 1.325
irradiation, polymer grafting **2.322**, 2.323, 2.324, 2.329–38, **2.338**
ischemia, pH changes 1.134
isobutylamide (IBAM) group 1.98
isoprene 1.157
isothermal titration calorimetry (ITC) 2.330
isotherms, Langmuir type 1.168
isotropic (random) phase liquid crystals 1.13
ITT (inverse temperature transition) 2.182

jellyfish aggregate, polymersomes **1.181**, 1.184
Jurkat cells 2.98

KALA polyplexes 1.268
ketoprofen 2.100
ketotifen 2.238
kinases/kinase inhibitors 1.19, 1.234, 1.243, 1.247
knob elastin-like recombinamers 2.193
Kupffer cells 1.37

L-phenylalanine (LIM) 2.208, **2.242**, 2.242
L-pyroglutamic acid (Pga) 2.247
L-valine. *see* valine
laser light irradiation 1.306–7
layer-by-layer (LbL) assemblies 2.117
biological interfaces 2.142–4
biological stimuli 2.141–2, **2.143**
constituents/architectures 2.119–23, **2.120–3**
diffusion-controlled DDS 2.124–5
drug incorporation strategies 2.123–4
electrochemical/redox-responsive DDS 2.134–5, **2.135**
hydrolytic degradation 2.125–9, **2.127**, **2.128**
light-triggered DDS 2.137–9, **2.139**
magnetic field triggered DDS 2.139–40, **2.140**
pH-triggered DDS 2.129–32, **2.130**, **2.131**, **2.132**
salt-triggered DDS 2.132, **2.132**, **2.133**, 2.133–4
substrates/templates 2.117–18, **2.119**
temperature-responsive DDS 2.136–7, **2.136–7**
ultrasound-responsive DDSs 2.140–1
LCST. *see* lower critical temperature of dissolution
LDPE (low density polyethylene) 2.336, **2.337**, 2.337
leakiness, tumor cell blood vessels 1.37–8, **1.38**. *see also* enhanced permeability and retention effect
lectins
biochemical-responsive DDS 1.20
competitive binding 2.229
concanavalin A 2.268–70, **2.269**, 2.277, **2.280**, **2.281**
glucose-sensitive hydrogels 2.266–70

leukocytes, stress and strain parameters 1.43
ligand-anchored pH-sensitive liposomes 1.86, **1.87**
ligand-driven active targeting 1.3
ligand exchange method 2.39, **2.39**
light-responsive DDS **1.22**, 1.23–4. *see also* near-infrared; photodynamic therapy; ultraviolet light-responsive DDS
  dendrimers, smart 1.100–2, **1.101**
  gold nanoparticles 2.10–14, **2.13**
  imprinted hydrogels 2.251–4, **2.252**, **2.253**, **2.254**
  layer-by-layer assemblies 2.137–9, **2.139**
  mesoporous silica nanoparticles 2.70, 2.77–8
  polymer grafting 2.338
  polymeric micelles 1.304–5, 1.308–20, **1.309**, **1.311**, **1.312**, **1.314–19**
  polymeric nano-/microparticles 1.327–37, **1.328–30**, **1.332**, **1.333**, **1.335–7**, 1.338
  polymeric vesicles 1.320–7, **1.321**, **1.324–6**
  polyplexes **1.273**, 1.273–4
  release mechanisms 1.307–8
LIM (L-phenylalanine) 2.208, **2.242**, 2.242
lipases, enzyme-responsive DDS 1.19
lipid bilayers
  encapsulating membrane 1.43–7, **1.44**
  light-sensitive polymeric vesicles 1.322
  low temperature-sensitive liposome **1.41**
lipids as smart materials 1.33–6, **1.35**
  nanoparticles 1.188. *see also* liposomes; micelles
lipofectamine 1.200, 1.201
liposomes. *see also* low temperature sensitive liposomes
  comparison with polymersomes 1.190
  cytotoxicity 1.193
  elastic modulus 1.46, **1.46**
  elastin-like recombinamers 2.194
  enzyme-responsive DDS 1.19
  layer-by-layer assemblies 2.119, 2.120–1
  self-assembly 1.94
  thermo-sensitive 2.46, **2.47**
liquid crystals, phase transitions 1.13
liquid electron microscopy 1.186
liquid–liquid phase transitions 1.13
lithium α-amino acid based hydrogels 2.222–4, **2.223**
living radical polymerization (LRP) 2.296
local drug release systems, cell sheet engineering 2.298–301. *see also* targeted drug delivery
localized surface plasmon resonance (LSPR) 2.20
logic gates, AND 2.80
low density polyethylene (LDPE) 2.336, **2.337**, 2.337
low temperature-sensitive liposomes (LTSL) 1.33–6, **1.35**, 1.72–4
  future perspectives 1.69–74
  production 1.51–2, **1.52**
  reverse engineering 1.36–51, **1.38–41**, **1.44–6**, **1.48**, **1.49**
  in vitro performance-in-service 1.53–60, **1.54**
  in vivo performance-in-service 1.60–9, **1.62–3**, **1.66**, **1.68**
lower critical temperature of dissolution (LCST)
  α-amino acid based hydrogels 2.199, 2.204, 2.210
  biomolecule-sensitive hydrogels 2.262–3, **2.263**, 2.275, 2.277
  combination products 2.325–6
  core-cross-linked micelles 1.216
  dendrimers, smart 1.96–7, 1.98, 1.99
  dual-responsive hydrogels 2.173

  elastin-like recombinamers 2.181, 2.187
  glucose-sensitive hydrogels 2.266, 2.267
  gold nanoparticles 2.17
  layer-by-layer assemblies 2.137
  light-sensitive polymeric micelles 1.313, 1.320
  light-sensitive polymeric vesicles **1.321**
  magnetic nanoparticles 2.44, 2.45, 2.46
  mesoporous silica nanoparticles 2.69, 2.70
  micro-patterned surfaces 2.302
  phototriggered micelles/nanoparticles 1.338
  PNIPAAm/PMAA films 2.136
  polymer grafting 2.331, 2.336
  polymeric micelles 1.121, 1.126, 1.129
  polyplexes 1.269, 1.270, 1.271
  reduction-sensitive nanosystems 1.219, **1.220**
  switchable micelles 1.247
  temperature-responsive hydrogels 2.161, **2.161–3**, 2.162–7
  temperature-sensitive polymers 1.21–2
low-frequency ultrasound 1.149–50
low-permeability barrier layers 2.125
L-phenylalanine (LIM) 2.208, **2.242**, 2.242
L-pyroglutamic acid (Pga) **2.172**, 2.247
LRP (living radical polymerization) 2.296
LSPR (localized surface plasmon resonance) 2.20
LTSL. *see* low temperature-sensitive liposomes
luciferase 1.259, 1.261, 1.265, 1.267–8, 1.271
lung cancer 1.158
lung toxicology, fiber paradigm 2.107
L-valine. *see* valine
lysine residues 1.135, 1.262, 1.264
lysosomes 1.16, 2.100
lysosomotropic micelles 1.18

MAA. *see* methacrylic acid
macroradicals 2.187
macular degeneration 1.100
Mag-Dye@MSNs 2.74
magnetic nanoparticles (MNPs) 2.32–4, **2.33**, **2.48**, 2.59–60
  amphiphilic/organic 2.41–4, **2.42**, **2.43**
  composite membranes 2.56–9, **2.57**, **2.58**, **2.59**
  hyperthermia theory 2.33, 2.34–7, **2.35**, **2.36**
  mesoporous silica 2.51–4, **2.52**, **2.53**, 2.72–5
  nanoshells 2.50–6, **2.51**, **2.52**, **2.53**, **2.55**, **2.56**
  surface modification **2.38**, 2.38–40, **2.39**
  synthesis 2.37–8
  temperature-responsive DDS **2.44**, 2.44–50, **2.45–7**
magnetic resonance imaging (MRI) 2.33
  carbon nanotubes 2.101
  dendrimers 1.108
  imaging compounds 1.196
  mesoporous silica nanoparticles 2.66, 2.73–4
  pH-sensitive liposomes 1.90
  polymersome imaging compounds **1.196**, 1.197
  rat fibrosarcoma model 1.60–1
magnetic-responsive DDSs **1.22**, 1.24
  α-amino acid based hydrogels 2.222
  layer-by-layer assemblies 2.139–40, **2.140**
  polymersomes 1.200
main chain degradation, light-sensitive micelles 1.318

malaria **1.233**
maleic acid residues 1.135
manganese prophyrins 1.71
materials matrix, low temperature sensitive liposome **1.40**
materials science 1.4, **1.5**
  combination products 2.317
matrix metalloproteinases (MMPs) 1.239, 1.241, 2.21
  biomolecule-sensitive hydrogels 2.283–4
  dendrimers, smart 1.108
matrix type intrinsically conducting polymers 1.296–7
maximum permissible exposures (MPE) to laser light irradiation 1.306–7
MBA (methylene-bisacrylamide) 2.200, 2.204, **2.205**
MBAA biomolecule-sensitive hydrogels 2.274, **2.275**
MCM-41 mesoporous silica 2.48, **2.49**
MDR. *see* multi-drug resistance
ME (mercaptoethanol) 2.78
mechanical cavitation, ultrasound 1.150–5, **1.152**, 1.163, 1.168, 1.170. *see also* microbubbles
mechanical index (MI), ultrasound 1.153, 1.155
medicated contact lenses, soft 2.235–40, **2.236**, **2.237**, **2.239**
melanoma 1.158, 2.214, **2.215**, 2.216, **2.216**
melphalan dendrimers, smart 1.106
membrane elastic modulus liposomes 1.46, **1.46**
membranes
  bilayers. *see* lipid bilayers
  biocompatible **2.292**, 2.292–3
  composite drug-delivery 2.56–9, **2.57–9**
  phase transitions 1.14
memorization
  imprinted hydrogels 2.243–4
  responsive polymers 1.14–15
MEMS (microelectromechanical systems) 1.299
mercaptoethanol (ME) 2.78
mesoporous silica nanoparticles (MSNPs) 1.223, 1.290, 2.63–6
  biocompatibility 2.80–1
  future perspectives 2.81–2
  layer-by-layer assemblies 2.119
  magnetic 2.42, **2.43**, 2.46–8, **2.48**, **2.49**, 2.51–4, **2.52**, **2.53**, 2.72–5
  multifunctionality 2.66, **2.67**, 2.74
  polymeric coatings 2.68–72
  stimuli-responsive DDSs 2.75–80, **2.76**
  targeting agents 2.66–8
mesothelioma 2.108
metal-based drugs 2.200. *see also* carboplatin; cisplatin; oxaliplatin
metal combination products 2.317
metal-enhanced fluorescence (MEF) **2.132**
metallic stents 1.296–7
metastases
  α-amino acid based hydrogels 2.200
  enzyme-responsive DDS 1.240
  ultrasound-triggered 1.155
methacrylic acid (MAA) 2.157
  α-amino acid-based hydrogels **2.208**, 2.208
  drug-loaded soft contact lenses 2.236
  glucose-sensitive hydrogels 2.265
  imprinted hydrogels **2.236**, 2.240, 2.248
  monomers 2.203
  pH-responsive hydrogels **2.250**, 2.251
  pH-responsive microgels 2.156, 2.158
  pH-responsive nanogels 2.159–60
  polymer grafting 2.329
  temperature-responsive hydrogels 2.165, 2.245–6, **2.246**
methacryloylethyl *p*-aminobenzoate 2.242–3

methacryloyloxy ethyl phosphorylcholine (MPC) 2.271
methicillin 1.123–4
methicillin-resistant *Staphylococcus aureus*. *see* MRSA
methotrexate (MTX) 1.218
  carbon nanotubes 2.98
  dendrimers, smart 1.96, 1.102, **1.107**
  gold nanoparticles 2.3, **2.4**
  light responsive hydrogels **2.252**
  mesoporous silica nanoparticles 2.68
  polymeric micelles 1.135
methoxy poly(ethylene glycol) (MPEG) 1.160, 1.247–8
methyl methacrylate 1.319, 1.320
methyl tetrazolium test (MTT) 2.160
methylene-bisacrylamide 2.200, 2.204, **2.205**
methylmethacrylate (MMA) 2.251–4
metoprolol tartarate 2.156
MI (mechanical index), ultrasound 1.153, 1.155
micelles 1.181
  amphilic 1.308–17, **1.309**, **1.315–16**, **1.319**, 1.320–7, 2.41–4, **2.42**, **2.43**
  biochemical-responsive DDS 1.20
  comparison with liposomes 1.169–70
  delivery mechanisms 1.167–9
  dendrimers, smart 1.107, **1.107**
  elastin-like recombinamers 2.193, 2.194–5
  enzyme-responsive DDS 1.19, 1.244–8, **1.245**
  formation 1.183
  gene delivery 1.18
  layer-by-layer assemblies 2.120
  low temperature sensitive liposomes 1.36
  phase transitions 1.14
  polymeric. *see* polymeric micelles
  self-assembly 1.94, **1.181**
  temperature-responsive DDS 1.22
  ultrasound-responsive DDSs 1.155–9
Michael-type addition reaction 2.283
miconazole 2.319
micro jets 1.154
microbial colonies (biofilms) 2.316, 2.341
microbubbles. *see also* gas bubble cavitation
  layer-by-layer assemblies 2.118
  polymersome imaging compounds 1.197
microcapsules. *see* capsules
microchips
  intrinsically conducting polymers 1.292
  magnetic nanoparticles 2.57, **2.58**
microcontact printing 2.302
microelectromechanical systems (MEMS) 1.299
microencapsulation, cell/tissue delivery systems 2.290–1, **2.292**, 2.292–3
micro-fabricated thermo-responsive surfaces 2.301–7, **2.302**, **2.304**, **2.305**, **2.306**
microgels
  definitions 2.154
  pH-responsive 2.156–8
  temperature-responsive 2.163–5
microgrooved polydimethylsiloxane (PDMS) 2.303
microneedles **1.293**, 1.293–4
microorganism-triggered DDS
  enzyme-responsive 1.19
  pH responsive 1.16
microparticles, polymer. *see* polymer nano-/microparticles
micro-patterned surfaces, cell sheet engineering 2.302, **2.302**, **2.304**, **2.305**
micropipet manipulation 1.43, 1.44, 1.47
micropumps 1.292–3
MIPs. *see* molecularly imprinted polymers
mitochondria 2.100
mitomycin C 2.99

MMA (methylmethacrylate) 2.251–4
MMPs. *see* metalloproteinases
MNPs. *see* magnetic nanoparticles
model predictive control (MPC), ultrasound-responsive DDSs 1.164
models, carbon nanotubes 2.106–7
Modified Robbins Device (MRD) 2.332
modified Stõber method 2.65
molar solubilization ratio (MSR) 1.117
molecular weight, elastin-like recombinamers 2.187
molecularly imprinted polymers (MIPs) 2.229–35, **2.230**, **2.232**, **2.234**
  biochemical-responsive 1.21, 2.229, 2.276–9, **2.278**, **2.279**
  covalent bonds 2.230
  responsive polymers 1.14–15
  see also imprinted hydrogels
monoclonal antibodies 1.88, 1.161, 2.97
mononuclear phagocyte system (MPS) 1.156, 1.189
monooleoylphosphatidylcholine (MOPC) 1.48
monostearoylphosphatidylcholine (MSPC) **1.41**, 1.41–2, 1.54–6
  low temperature-sensitive liposome 1.53, **1.54**, **1.55**
  in vitro performance-in-service 1.57, **1.57**, 1.58, 1.59
mortars, evolution 1.2
MPC. *see* model predictive control
MPC (methacryloyloxy ethyl phosphorylcholine) 2.271
MPE. *see* maximum permissible exposures
MPEG (methoxy poly(ethylene glycol)) 1.160, 1.247–8
MPS (mononuclear phagocyte system) 1.156, 1.189
MRI. *see* magnetic resonance imaging
MSNPs. *see* mesoporous silica nanoparticles
MRSA (methicillin-resistant *Staphylococcus aureus*)
  combination products, drug/medical devices 2.329
  polymer grafting 2.331–2
MSPC. *see* monostearoylphosphatidylcholine
MSR (molar solubilization ratio) 1.117
MTT (methyl tetrazolium test) 2.160
MTX. *see* methotrexate
mucosal epithelial cell sheets 2.297, **2.299**
multi-drug release system, supramolecular hydrogels 1.241
multi-drug resistance (MDR) 1.82, 1.89, 2.1
  carbon nanotubes 2.97
  dendrimers, smart 1.101
  drug–polymer conjugates 1.159
  mesoporous silica nanoparticles 2.72
  polymeric micelles 1.116
  polymersomes 1.199
  reduction-sensitive nanosystems 1.212, 1.227
  tumours 1.9
multifunctionality
  carbon nanotubes 2.91, **2.91**, **2.93**, 2.94, 2.99, 2.101
  mesoporous silica nanoparticles 2.66, **2.67**, 2.74
multilayered cardiomyocyte sheets 2.303
multiple stimuli responsive polymer-based hydrogels. *see* α-amino acid based hydrogels
multi-walled carbon nanotubes (MWCNTs) 2.90, 2.92
  encapsulation properties 2.101
  environmental impacts 2.104, 2.110
  external attachment of drugs 2.96–7, 2.99–100
  toxicity 2.104, 2.106, 2.107, 2.108
myoblast sheets 2.297, **2.300**, 2.300, **2.301**

myocardial infarction 2.298, 2.300, 2.303
Myocet 1.34

NADPH (nicotinamide adenine dinucleotide phosphate) 1.201, 1.210, 1.239
NaAlg (sodium alginate) 2.158. *see also* alginates
nalidixic acid 2.333–7, **2.335**, **2.337**
N-alkyl acrylamide homopolymers 2.199
nanocaps/gates 2.74–5, 2.77, 2.79–80. *see also* capped pores
nanocapsules 1.34, 2.41, 2.118
nanocarriers, glucose-responsive 1.20
nanocontainers
  carbon 2.100–3, **2.102**
  silica **1.248**, 1.248–51, **1.249**. *see also* mesoporous silica nanoparticles
nanogels
  definitions 2.154
  magnetic nanoparticles 2.58, 2.59, **2.59**
  pH-responsive 2.158–61
  phototriggered 1.331–4, **1.332**, **1.333**
  reduction-sensitive **1.226**, 1.226–7
  temperature-responsive DDS 1.22, 2.166–7
  tumor-targeted delivery 1.18
nanoparticles 1.188. *see also* dendrimers; gold nanoparticles; liposomes; mesoporous silica nanoparticles; micelles; polymer nanoparticles; polymersomes
  biomolecule-sensitive hydrogels 2.279–81
  cellular internalisation mechanism 1.191–2
  elastin-like recombinamers 2.190–5, **2.191**, **2.194**, **2.195**
  low temperature sensitive liposomes 1.62
  organic 2.41–4, **2.42**, **2.43**
  reduction-sensitive nanosystems 1.221–3, **1.222**
nanopores 1.59–60
nanoreactors 1.201
nanoshells, magnetic nanoparticles 2.50–6, **2.51**, **2.52**, **2.53**, **2.55**, **2.56**
nano-straws, carbon nanotubes 2.101
nanostructured conducting polymers 1.297–9
nanotechnology 1.3, 1.188, 1.195
nanothermometers 2.101
nanowire arrays 1.299
naproxen 1.126
nature-designed materials 1.5
$NaYF_4$ **1.316**, 1.316–17
NBA (nitrobenzyl methacrylate) 2.326
Néel relaxation 2.36
near infrared fluorophores (NIRF) 1.196–7
near-infrared radiation (NIR) 1.23, 1.305–7
  carbon nanotubes 2.92
  gold nanoparticles 2.14
  layer-by-layer assemblies 2.138
  micelles/nanoparticles 1.338
  nanogels 1.331
  polymeric micelles 1.315, 1.316
  solid polymeric nanoparticles 1.335
nematic (parallel alignment) phase, liquid crystals 1.13
neural growth factor (NGF) 1.290, **1.290**
neurotrophins 1.25, 1.297
new excipients 1.7–8, **1.8**
nicotinamide adenine dinucleotide phosphate (NADPH) 1.201, 1.210, 1.239
N-hydroxysuccinimide (NHS) 1.290–1
NIR. *see* near-infrared radiation
NIRF (near infrared fluorophores) 1.196–7

N-isopropylacrylamide (NIPAAm) 1.216
  α-amino acid based hydrogels 2.204, **2.205**, 2.206, 2.220, 2.221, 2.222
  biomolecule-sensitive hydrogels 2.271, 2.274, 2.277, 2.281
  cell sheet engineering 2.296, **2.297**
  dendrimers, smart 1.97, 1.98
  dual-responsive hydrogels 2.170, 2.172
  glucose-sensitive hydrogels 2.266
  plasma polymerization 2.339
  polymer grafting 2.327, **2.330**, 2.334, 2.335
  temperature-responsive hydrogels 2.163–5, **2.166**, 2.245–6, **2.246**
  temperature-responsive nanogels 2.167
N-isopropylmethacrylamide (NIPMAM) 2.58
nitrobenzyl methacrylate (NBA) 2.326
nitroxide-mediated (NMRP) radical polymerization 2.321, 2.323
N-methylated poloxamines 1.124, **1.125**
Nobel Prize in Chemistry (2000) 1.283
non-covalent functionalization
  carbon nanotubes 2.91, 2.95–6
  molecularly imprinted polymers 2.230, 2.232
noradrenalin **2.278**
norfloxacin
  imprinted hydrogels 2.237–8, **2.238**, **2.239**
  polymer grafting 2.335
nosocomial infections 2.316
NNDEA (poly(*N,N*-diethylacrylamide) 1.157
N-succinyl-DOPE 1.81
nucleic acids (NAs). *see* gene delivery
nucleophilic addition, carbon nanotubes 2.95
nucleopores poly(carbonate) membrane 2.292
N-vinylcaprolactam 2.167
N-vinylimidazole (NVIm) 2.242–3, **2.243**
N-vinylpyrrolidone (NVP) 2.240, 2.266

octopus structures, polymersomes 1.184
oil-in-water emulsions 2.118
oligodeoxynucleotides (ODNs) 1.258, 1.258
oligo(ethylene glycol) (OEG) **1.226**, 1.246, 1.98, 1.99, 1.107
oligonucleotides 1.84, 1.220, 1.296, 2.6
1D crystallization phase transitions 1.12
o-nitrobenzyl (ONB) 1.310, 1.315, 1.317, 1.318, 1.320, 1.325, 1.332
ophthalmic drug delivery 2.235–40, **2.236**, **2.237**, **2.239**
opportunistic bacteria 2.316. *see also* infected tissues
opsonisation 1.37, 1.189, 2.109
optical imaging, polymersome compounds **1.196**, 1.196–7
Optison 1.197
OR logic triggers 1.107
oral administration
  enzyme-responsive materials 1.236–7
  pH-responsive hydrogels 2.155
oral mucosal epithelial cell sheets 2.297, **2.299**
organelles, artificial 1.201
organic nanoparticles 2.41–4, **2.42**, **2.43**
organic polymers, phase transitions 1.14
organic solvents 1.218, 2.171
  anticancer drugs 1.198
  elastin-like recombinamers 2.188
  layer-by-layer assemblies 2.121–2
organic-inorganic hybrids, combination products 2.317–18

orientation, cell sheet
  engineering 2.303–7, **2.305**, **2.306**
osteolysis, enzyme-responsive
  DDS 1.240
osteoporosis **1.233**
ovalbumin (OVA) protein 1.224
ovarian cancer
  carbon nanotubes 2.98–9
  reduction-sensitive
    nanosystems 1.216, **1.217**
  ultrasound triggered DDS 1.164,
    1.158–9, 1.160
oxaliplatin
  carbon nanotubes 2.97–8, 2.99
  dual responsive hydrogels 2.173
  polymeric micelles **1.136**
oxidation/oxidative stress. *see also*
  reactive oxygen species
  biochemical-responsive DDS 1.20
  carbon nanotubes 2.94, 2.108
  phase transitions 1.14
  photosensitization-induced
    oxidation 1.307
  polypyrrole **1.284**, 1.284–5
oxidative photodynamic
  therapy 1.100
oxidoreductases 1.20

PAA. *see* polyacrylic acid
PAAm. *see* polyacrylamide
packing factor theory 1.180, **1.181**,
  1.184
paclitaxel (taxol) 2.98–9
  dendrimers, smart 1.96, 1.105
  electric field responsive DDS 1.25
  layer-by-layer assemblies 2.118
  pH responsive nanogels 2.160
  polymeric micelles 1.128 drug,
    1.135, **1.136**
  polymersomes 1.198–9, 1.200
  reduction-sensitive
    nanosystems 1.216
  supramolecular hydrogels 1.242
PAcMo (poly(*N*-
  acryloylmorpholine) **2.305**
PAGs (photo-acid generators) 1.330
PAH (poly(alylamine hydrochloride)
  2.120, 2.138, 2.141–2
palmitoyloleoylphosphatidylcholine
  (POPC) **1.55**, 1.55–6
PAMAM (polyamidoamine)
  dendrimers 1.94, **1.95**, 1.98, 1.101,
  1.102, 1.103–4, 1.257
p-aminobenzoate (PAP) 2.242–3
pancreatic cancer 2.67
pancreatic islets, microencapsulated
  2.290–1, **2.292**, 2.292–3
pancreatin 1.250
PANI (polyanaline) 1.25, 1.294
paracetamol 2.251, 2.252, **2.254**
parenteral drug applications 1.6,
  1.117, 1.122
Parkinson's disease 2.293
PARP (poly(ADP-ribose)
  polymerase) **2.216**, 2.217
particle size. *see* size factors
Passerini condensation 2.186
passive excipients 1.3
passive targeting. *see* enhanced
  permeability and retention effect
patterning, tissue-mimicking cell
  sheets 2.301–3, **2.302**,
  2.304, **2.305**
PAZO (poly(1-4[4-3(3carboxy-4-
  hydroxyphenyl-azo)benzene-
  sulfonamido]- 1,2-ethanediyl)
  1.329–30
PBA (phenylboronic acid) 2.266,
  2.267, **2.268**
PBD (poly-butadiene) 1.184, 1.200
PBH (peptide-based hydrogels)
  1.242–3
PBLG-HYA (poly(g-benzyl
  l-glutamate)-hyaluronan)
  1.199–200
PBMA (poly(n-butyl
  methacrylate) 2.302, **2.302**
PBO (poly(butylene oxide) 1.126–7
PCI (photochemical
  internalization) 1.100–1, **1.101**
PCL (poly(caprolactone) 1.120,
  1.160, 1.212, 1.128, **1.318**, 2.6

PCL-SS-PEEP (poly(ethyl ethylene phosphate) 1.212
PDADMAC (poly(diallyldimethylammonium chloride) 2.124
PDEAEMA (poly(2-(diethylamino)-ethyl methacrylate) **1.225**, 2.70, **2.155**, 2.155, 2.195
PDMA (poly(*N,N*-dimethylacrylamyde) 2.326
PDMAEMA (poly(dimethyl amino ethyl methacrylate) 1.257, 1.320, **2.155**, 2.155, **2.156**, 1.257, 1.320
PDMS (polydimethylsiloxane) 2.303, 2.319
PDT. *see* photodynamic therapy
PE (phosphatidylethanolamine) 1.83, 1.84, 1.86
PEDOT (poly(3,4-ethylenedioxythiophene) 1.25, 1.284, 1.299
PEGylation (polyethylene glycol) 1.3, 1.9
  accelerated blood clearance phenomenon 1.9, 1.84
  α-amino acid based hydrogels 2.200, 2.221
  biochemical-responsive DDS 1.20
  biomolecule-sensitive hydrogels 2.262, 2.271–2, **2.283**, 2.280, 2.281, 2.283–4
  dendrimers 1.97
  elastin-like recombinamers 2.187
  enzyme-responsive materials 1.235
  gold nanoparticles **2.4**, 2.4
  hydrogels **1.239**, 1.240
  hydrophilic particles 1.189
  imprinted hydrogels 2.238
  layer-by-layer assemblies 2.128
  light-sensitive polymeric micelles 1.313, **1.314**
  light-sensitive polymeric vesicles 1.325
  low temperature-sensitive liposomes 1.62
  magnetic nanoparticles 2.41, 2.44–5, **2.45**, 2.56, 2.57
  mesoporous silica nanoparticles 2.68, 2.81
  micelles 1.134–5, 1.158
  multi-walled carbon nanotubules 2.97
  pH-responsive microgels 2.156, 2.157
  pH-sensitive liposomes 1.183, 1.184, 1.185
  polyelectrolyte complexes 1.258, 1.267
  polyester block copolymers 1.127–8
  polymeric micelles 1.118, **1.121**, 1.121–7, **1.125**, **1.129**
  polymersomes 1.189–90, 1.193, 1.197, 1.198
  poloxamines 1.119
  reduction-sensitive nanosystems 1.210, 1.212, 1.214, 1.216, 1.219–20, **1.220**
  switchable micelles 1.247
  temperature-responsive nanogels 2.166
  ultrasound-triggered release 1.156, 1.157, 1.159
  see also stealth properties
PEI (poly(ethylene imine) 1.257, 1.261, 1.265, **1.266**, 2.70, 2.71, 2.75–6, 2.118
PEMs. *see* polyelectrolyte multilayers
pendant glucose (poly(2-glucosyloxyethyl methacrylate), (PGEMA) 2.268–70, **2.269**, 2.280, 2.281, **2.281**
PEO (poly(ethylene oxide). *see* PEGylation
peptide-based hydrogels (PBH) 1.242–3
peptides, therapeutic
  elastin-like recombinamers 2.189–90
  pH-sensitive liposome delivery **1.85**, 1.90

perfluoropentane 1.170
peristaltic pumps 1.292–3
permeability changes, DDSs 1.40, 1.47–9, **1.48**, 2.228
PET (polyethylene terephthalate) 2.56, 2.57
PGA (poly(l-glutamic acid) **2.172**, 2.247
P-glycoprotein 1.9, 1.199, 2.71–2
PGMA-PHPMA (poly(glycerol monomethacrylate)–poly(2-hydroxypropyl methacrylate) 1.184
PGO (poly(phenyl glycidyl ether) 1.126–7
pH-responsive DDS 1.2, 1.16–18, **1.17**
  α-amino acid based hydrogels 2.202, 2.204–9, **2.207–10**, 2.210, 2.213, 2.214, 2.222
  biomolecule-sensitive hydrogels 2.261–2, 2.263, 2.270
  carbon nanotubes 2.103
  dendrimers, smart 1.102–5, **1.103**
  dual-responsive hydrogels 2.170–3
  elastin-like recombinamers 2.193, **2.194**
  electric field-responsive DDS 1.24
  glucose-sensitive hydrogels **2.265**, 2.265
  gold nanoparticles **2.9**, 2.9–10, **2.11**
  hydrogels 2.154, **2.155**, 2.155–61, **2.156**, **2.159**
  hydrolytically-induced drug release 2.243
  imprinted hydrogels 2.249–51, **2.250**
  insulin cell/tissue delivery systems 2.291
  layer-by-layer assemblies 2.129–32, **2.130**, **2.131**, **2.132**
  low temperature-sensitive liposomes 1.38
  mesoporous silica nanoparticles 2.70, 2.75–7
  micelles, polymeric 1.122, 1.133–5
  poly(butadiene)–poly(methacrylic acid) 1.184
  polymer grafting **2.331**
  polymersomes 1.200
  polyplexes 1.257, **1.258–60**, 1.258–61, 1.274, **1.275**
  ultrasound triggered 1.164
pH-sensitive liposomes 1.80–6, 1.90–1
  cancer therapy applications **1.83**
  passive accumulation in tumor cells **1.82**
  therapeutic applications 1.87–90
  uptake/intra-cellular delivery **1.84**, 1.86–7, **1.87**
phagocytosis 1.191, 1.192
pharmaceutical companies 1.115
phase transitions. *see also* lower critical temperature of dissolution; upper critical temperature of dissolution
  α-amino acid based hydrogels 2.204, 2.206–11, **2.207**, **2.208**, **2.210**, 2.214, 2.217–19, **2.218**, 2.221–2, **2.222** 209
  biomolecule-sensitive hydrogels 2.262–4, **2.263**, **2.264**, 2.274, **2.276**, **2.278**
  dendrimers, smart 1.96–7
  dual-responsive hydrogels 2.171
  enzyme-responsive hydrogels 1.240–1
  glucose-sensitive hydrogels **2.269**
  imprinted hydrogels 2.233, 2.235, 2.236, 2.242–7, **2.247**, **2.248**
  interpenetrating networks 2.173
  polymeric micelles 1.121
  polymersomes 1.183
  stimuli-responsive networks 1.11–14, **1.15**, 2.245
  temperature-responsive hydrogels 2.161, 2.181

PHEA-g-MA (α,β-poly(hydroxyethyl aspartamide-g-maleic anhydride) 2.157–8
PHEMA (poly(AA-co-AM-co-NVP-co-HEMA-co-PEG200DMA) 2.238, **2.239**, 2.240
phenylalanine 2.208, **2.242**, 2.242
phenylboronic acid (PBA) 2.266, **2.267**, **2.268**
PHMA (poly(hydroxyethyl methacrylate) 1.190, 1.238
phosphatases 1.19, 1.243, 1.246–8
phosphatidylethanolamine (PE) 1.83, 1.84, 1.86
phosphorylation 1.242
photo-acid generators (PAGs) 1.330
photo-active gold nanoparticles 2.10–14, **2.13**. *see also* light-responsive DDS
photochemical internalization (PCI) 1.100–1, **1.101**
photocross-linking, polymeric capsules 1.307, 1.328–9, **1.329**
photodegradable moieties 1.101–2
photodynamic therapy (PDT)
  dendrimers, smart 1.100, 1.101
  gold nanoparticles **2.13**, 2.14, **2.15**
  oxidative 1.100. *see also* reactive oxygen species
  polymeric micelles 1.135
photo-excitation 1.307–8
photo-isomerization 1.307, 1.310, **1.312**
photolithography technique 2.304, **2.305**
photoluminescence 2.92
photo responsive DDS. *see* light responsive DDS
photosensitization 1.100–2, 1.307, 2.14
photothermal therapy (PTT) 1.100
  carbon nanotubes 2.92
  gold nanoparticles 2.14–20, **2.16**, **2.17**, **2.18**, **2.19**
  layer-by-layer assemblies 2.138
pHPMA (2-hydroxypropylacrylamide) 1.133, 1.264, 2.173
physical hydrogels 1.238, **2.184**, 2.184, 2.188
physically cross-linked elastin-like recombinamers 2.188
physics of ultrasound 1.149–5, **1.152**
PIC (polyion complex) micelles **1.258**, 1.267, **1.268**
pilocarpine 2.203, 2.211, 2.217–21, **2.218**, **2.219**, **2.220**
pinocytosis 1.167, 1.191
PLA (poly(lactic acid) 1.127, 1.128, 1.158, 1.245, 2.128
placental growth factor (PlGF) 2.301
plasma polymerization 2.325
  polymer grafting **2.322**, **2.324**, 2.324–5
  surface modification 2.339–41
Plasmodium falciparum 1.264
plastic crystals, phase transitions 1.13
platinum 1.241
platinum-based anticancer drugs 2.97–8, 2.100–2. *see also* carboplatin; cisplatin; oxaliplatin
PLGA (poly(lactide-co-glycolide) 1.299, 2.160, 2.291, 2.293
PLL (poly(L-lysine) 2.121, **2.121**, 2.130, 2.134–5, **2.135**, 1.259, **1.259**
PLLA (poly(L-lactide) 1.299
Pluronic F-127 2.6, 2.96
pluronic polymers 1.157, 1.160, 1.161–3, **1.162**, 1.164, 1.167, 1.169
PMAA. *see* poly(methacrylic acid)
PMOA. *see* primary mode of action (PMOA)
PMOXA (poly(2-methyl-2-oxazoline) 1.190
PMPC (poly(2-methacryloyloxyethyl phosphorylcholine) 1.190, 1.194, 1.200
PNH (poly(*N*-isopropylacrylamide-co-2-hydroxyethyl methacrylate) **2.172**
PNIPAAm. *see* poly(isopropylacrylamide)
PNVCL (poly(*N*-vinylcaprolactam) **2.162**, 2.166–7

POs (polyoxazolines) 1.133
poloxamers/poloxamine **1.121**, 1.121–6, **1.125**
poly(AA-co-AM-co-NVP-co-HEMA-co-PEG200DMA) (PHEMA) 2.238, **2.239**, 2.240
polyacrylamide (PAAm) 2.158, 2.164, 2.170, 2.199, 2.248
  biomolecule-sensitive hydrogels 2.271, 2.274
  cell sheet engineering 2.303
  dual responsive hydrogels 2.173
  enzyme-responsive materials 1.235
  layer-by-layer assemblies 2.141
  upper critical solution temperature 2.168–9
polyacrylic acid (PAA) 1.133, **1.239**, 2.339, **2.340**
  α-amino acid based hydrogels **2.208**, 2.208
  biomolecule-sensitive hydrogels 2.277, 2.281
  cell/tissue delivery systems 2.293
  drug-loaded soft contact lenses 2.236
  functional monomers 2.203, 2.231
  imprinted hydrogels 2.237, **2.247**
  layer-by-layer assemblies 2.118
  light responsive hydrogels 2.251
  light-sensitive polymeric micelles **1.318**
  mesoporous silica nanoparticles 2.70
  pH responsive hydrogels **2.155**, 2.155, **2.156**, 2.249
  polymer grafting 2.329–30, **2.330**, **2.331**, 2.333, **2.338**, 2.338
poly(acryloylmorpholine) (PAcMo) **2.305**
poly(acryloxysuccinimide) 2.78
poly(ADP-ribose) polymerase (PARP) **2.216**, 2.217
poly(allylamine hydrochloride) (PAH) 2.120, 2.138, 2.141–2
polyamidoamine (PAMAM) dendrimers 1.94, **1.95**, 1.98, 1.101, 1.102, 1.103–4, 1.257
poly(aminoethyl)methacrylamide) 1.216
polyaminoacids 1.134, 1.235
poly(ampholyte) hydrogels 2.208–9, 2.211, **2.212**
polyanaline (PANI) 1.25, 1.294
poly(β-amino esters) 2.125–6
poly(g-benzyl l-glutamate)-hyaluronan (PBLG-HYA) 1.199–200
polybutadiene 1.313
poly-butadiene (PBD) 1.184, 1.200
poly(butyl methacrylate) (PBMA) 2.302, **2.302**
poly(butylene oxide) (PBO) 1.126–7
poly(caprolactone (PCL) 1.120, 1.160, 1.212, 1.128, **1.318**, 2.6
poly(carboxylic acids) 2.129
poly(carboxymethyl-β-cyclodextrin) **2.127**
polycarboxy-4-hydroxyphenyl-azobenzenesulfonamidoethanedyil (PAZO) 1.329–30
poly(diallyldimethylammonium chloride) (PDADMAC) 2.124
poly(2-(diethylamino)ethyl methacrylate) (PDEAEMA) **1.225**, 2.70, **2.155**, 2.155, 2.195
poly(dimethylacrylamyde) (PDMA) 2.326
poly(*N,N*-dimethyl aminoethyl methacrylate) (PDMAEMA) 1.257, 1.320, **2.155**, 2.155, **2.156**
polydimethylsiloxane (PDMS) 2.303, 2.319
polyelectrolyte complexes (polyplexes) 1.256–8, 1.275
  charge-conversion ternary **1.260**
  dual-responsive 1.274–5
  light-responsive **1.273**, 1.273–4
  pH-responsive **1.258**, 1.258–61, **1.259**, **1.260**, 1.274, **1.275**
  reducible 1.261–9, **1.263**, **1.264**, **1.266**, **1.268**, 1.274
  temperature-responsive **1.269**, 1.269–73, **1.272**

polyelectrolyte multilayers (PEMs) 2.118–29, **2.120**, **2.121**, 2.133–5, 2.137–41, 2.143–4
poly(ethyl ethylene phosphate) (PCL-SS-PEEP) 1.212
poly(3,4-ethylenedioxythiophene) (PEDOT) 1.25, 1.284, 1.299
polyethylene glycol. *see* PEGylation
poly(ethylene imine) (PEI) 1.257, 1.261, 1.265, **1.266**, 2.70, 2.71, 2.75–6, 2.118
poly(ethylene oxide). *see* PEGylation
polyethylene terephthalate (PET) 2.56, 2.57
poly(l-glutamic acid) (PGA)) **2.172**, 2.247
poly(L-glutamic acid) (PG)-paclitaxel 1.158, 2.130
poly(glycerol monomethacrylate)–poly(2-hydroxypropyl methacrylate) (PGMA-PHPMA) 1.184
poly(hydroxyethyl methacrylate) (PHMA) 1.190, 1.238
poly(hydroxyethylaspartamide) 1.134
poly(hydroxypropyl methacrylate) (PHPMA) 1.133, 1.264, 2.173
polyion complex (PIC) micelles **1.258**, 1.267, **1.268**
poly(isopropylacrylamide) (PNIPAAm) 1.200, **1.269**, 1.269, 2.171, **2.171**. *see also* temperature-responsive DDS
  α-amino acid based hydrogels 2.199
  biomolecule-sensitive hydrogels 2.262–3, 2.275, 2.277
  cell/tissue delivery systems 2.291
  cell sheet engineering **2.295**, 2.295–6, 2.303, 2.304, **2.305**
  cell/tissue delivery systems 2.294–5
  combination products 2.323
  dendrimers, smart 1.96–7, 1.98
  dual-responsive hydrogels **2.172**, 2.172, 2.173
  glucose-sensitive hydrogels 2.266, 2.267, **2.267**
  imprinted hydrogels 2.246, 2.248
  layer-by-layer assemblies 2.120, 2.129–30, **2.130**, 2.136, 2.137
  magnetic nanoparticles **2.45**, 2.58, **2.59**
  mesoporous silica nanoparticles 2.69, 2.70
  plasma polymerization 2.339
  polymer grafting 2.325–6, **2.326**, **2.330**, 2.330, **2.331**, **2.332**, 2.333, **2.334**
  polymeric micelles 1.128–32, **1.130**, **1.132**
  shell-sheddable micelles 1.213
  temperature-responsive hydrogels 2.163–5
  temperature-responsive nanogels 2.166, 2.167
  tissue-mimicking cell sheets **2.302**, 2.302
poly(lactic acid) (PLA) 1.127, 1.128, 1.158, 1.245, 2.128
poly(L-lactide) (PLLA) 1.299
poly(L-lactide)-co-NIPAAm 1.98
poly(lactide-co-glycolide) (PLGA) 1.299, 2.160, 2.291, 2.293
poly(lactone)-PEG-poly(lactone) block copolymers 1.127
poly(L-lysine (PLL) 2.121, **2.121**, 2.130, 2.134–5, **2.135**, 1.259, **1.259**
polymer backbone photodegradation 1.307
polymer blends 1.13
polymer brushes 2.296, **2.297**, 2.304, **2.305**, 2.320, **2.322**, 2.323, 2.325–38, **2.327**
polymer capsules. *see* capsules
polymer coatings
  combination products, drug/medical devices 2.320
  mesoporous silica nanoparticles 2.68–72
polymer combination products 2.317

polymer grafting
  cell sheet engineering **2.295**, 2.295–6, **2.297**
  combination products 2.320–5, **2.322**, **2.323**, **2.324**
  responsive surfaces 2.325–38, **2.326–32**, **2.334–5**, **2.337–8**
polymer membranes 2.290. *see also* cell/tissue delivery systems
polymer micelles 1.115–20
  clinical applications 1.135, **1.136**
  comparison with polymersomes 1.198
  light-sensitive 1.308–20, **1.309**, **1.311**, **1.312**, **1.314–19**
  pH-responsive 1.122, 1.133–5
  preparation methodology 1.118–19
  reduction-sensitive 1.210–19, **1.211**, **1.213**, **1.215**, **1.217**
  temperature-responsive 1.120–33, **1.121**, **1.125**, **1.129**, **1.130**, **1.132**
  ultrasound-responsive 1.157–8
polymer nano-/microparticles 1.188, 1.327–37, **1.328–30**, **1.332–3**, **1.335–7**. *see also* dendrimers; micelles; polymersomes
polymer threading, membrane phase transitions 1.11
polymer vesicles. *see* polymersomes
polymerisation process **1.284**, 1.284–5
polymer–polymer interactions 1.12
polymers, general information 1.2, 1.94
  as drug delivery systems **1.7**, 1.15–25, **1.17**, **1.22**
  evolution 1.6
  phase transitions 1.11–14
  temperature-responsive DDS 1.72
  therapeutic functionality 1.9
  thermosensitive **1.97**, 1.97–8
polymer–solvent interactions 1.12
polymersomes 1.117
  cellular uptake **1.190**, 1.191–2, 1.194, **1.195**
  characterization 1.185–7, **1.187**, 1.188
  comparison with liposomes 1.190
  comparison with polymer micelles 1.198
  as delivery vectors 1.188–96, **1.195**
  formation 1.179–85, **1.181**, **1.182**
  light-sensitive 1.320–7, **1.321**, **1.324–6**
  medical applications **1.196**, 1.196–201
  reduction-sensitive nanosystems 1.219–21, **1.220**
polymethacrylate bearing spiropyran moieties (PSPMA) 1.313, **1.314**
poly(methacrylic acid) (PMAA) 1.224, 2.130, **2.131**
  light-sensitive polymeric micelles 1.314
  pH responsive hydrogels **2.155**, 2.155–7, 2.159
  polymer grafting 2.326
poly(methacryloyloxyethyl phosphorylcholine) (PMPC) 1.190, 1.194, 1.200
poly(methyl-2-oxazoline) (PMOXA) 1.190
polymorphic liposomes 1.82–3
poly(*N,N*-diethylacrylamide) (NNDEA) 1.157
poly(*N*-isopropylacrylamide). *see* poly(isopropylacrylamide
poly(*N*-isopropylacrylamide- co-2-hydroxyethyl methacrylate) (PNH) **2.172**
poly(2-nitrobenzylmethyl methacrylate) (PNBMA) 1.314, **1.315**
poly(*N*-tertbutylacrylamide-co-acrylamide/maleic acid) 2.249
poly(*N*-vinyl pyrrolidone) (PVP) 1.190
poly(*N*-vinylcaprolactam) (PNVCL) **2.162**, 2.166–7
poly(*N*-vinylisobutyramide) 1.98
poloxamines 1.193
polyoxazolines (POs) 1.133

polypeptides, phase transitions 1.11
poly(phenyl glycidyl ether) (PGO) 1.126–7
poly(4-phenylazomaleinanil-co-4-vinylpyridine) (AzoMI-VPy) 1.313
polyplexes. *see* polyelectrolyte complexes
polypropylene (PP)
  plasma polymerization 2.339
  polymer grafting 2.317, 2.329–33, **2.330**, **2.331–2**, **2.334–5**, 2.335
poly(propylene glycol) 1.120
poly(propylene oxide) (PPO) 1.157–8
polypropyleneimine (PPI) dendrimer 1.97, 1.198, 1.102
polypyrrole (PPy) 1.283. *see also* intrinsically conducting polymers
  actuating devices **1.293**, 1.293–4, 1.294, **1.295**
  cyclic voltammetry 1.287, **1.288**
  electro-conductive hydrogels 1.296
  electrostatic forces 1.288–9
  implantable electrodes 1.297
  microchips 1.292
  nanostructured conducting polymers 1.297–9
  polymerization **1.284**, 1.284–5
  reservoir systems 1.290–2, **1.290**, **1.291**
  solubility 1.286
  stability 1.285–6
  volume changes 1.289
poly(1-pyrenylmethyl methacrylate) (PPyMA) 1.314
polysaccharide-based nanogels 2.160
polysaccharides 2.41
polystyrene (PS) 2.326
polystyrene beads 2.195
poly(styrene oxide) (PSO) 1.126–7
polystyrene sulfonate (PSS) 2.120, 2.124, 2.125, **2.126**
polystyrene-poly(acrylic acid) (PS-PAA) 1.183
poly(sulfonamide) (PSD) 1.260
poly(trimethylene carbonate)- b-poly(L-glutamic acid) (PTMC-PGA) polymersomes 1.201
polyurethane catheters 2.319
poly(vinyl alcohol) (PVA) 2.141, 2.173, 2.266
poly(vinyl) sulfonate 1.329–30
poly(vinylidene difluoride) (PVDF) 2.292, 2.297, **2.299**, 2.307
poly(4-vinylpyridine) 1.133, 2.70
poly(vinylpyrrolidone) (PVPON) 1.224
poly(VPGVG) (poly(Val-Pro-Gly-Val-Gly) 2.181, 2.191, 2.192. *see also* elastin-like recombinamers
POPC (palmitoyloleoylphosphatidylcholine) **1.55**, 1.55–6
pores, capped. *see* capped pores
posterior capsule opacification 2.316
PP. *see* polypropylene
PPI (polypropyleneimine) 1.97, 1.198, 1.102
PPO (poly(propylene oxide) 1.157–8
PPy. *see* polypyrrole
PPyMA (poly(1-pyrenylmethyl methacrylate) 1.314
precipitation, magnetic nanoparticles 2.37–8
prednisone 2.100
presoaking, combination products 2.318, 2.319, **2.319**
pressure waves, ultrasound 1.149, 1.154
primary mode of action (PMOA), combination products 2.314–15, **2.315**, 2.318, 2.341
principle of precaution, carbon nanotubes 2.105, 2.110
processing–structure–function relationships **1.8**
processing–structure–property relationships 1.4, 1.5–6
prodrugs 1.234–5
promyelocytic leukemia, ultrasound triggered 1.164
proof-of-principle experiments 2.102
property-composition-structure relationships 1.34, 1.35, 1.36, 1.40–51, **1.40–1**, **1.44–6**, **1.48–9**
propyl 1.134
prostate cancer 1.64–5, **1.233**

protease inhibitors 1.234
proteases 1.19
protein-based materials, biomimetics 2.181. *see also* elastin-like recombinamers
proteins
  folding, biomolecule-sensitive hydrogels 2.284
  nanoparticle interactions 1.194
  reduction-sensitive nanosystems 1.219
  therapeutic 1.256, 2.189
protein-sensitive hydrogels 2.270–6, **2.272**, **2.273**, **2.275–6**
proteoglycans 1.193
proton gradients, layer-by-layer assemblies 2.134
proton-sponge effect 1.257, 2.81
PS. *see* polystyrene
PSD (poly(sulfonamide)) 1.260
PSO (poly(styrene oxide)) 1.126–7
PSPMA (polymethacrylate bearing spiropyran moieties) 1.313, **1.314**
PSS (polystyrene sulfonate) 2.120, 2.124, 2.125, **2.126**
PTMC-PGA (poly(trimethylene carbonate)-*b*-poly(L-glutamic acid) polymersomes 1.201
PTT. *see* photothermal therapy
pulmonary toxicology, fiber paradigm 2.107
PVA (poly(vinyl alcohol) 2.141, 2.173, 2.266
PVP (poly(*N*-vinyl pyrrolidone) 1.190
PVDF (poly(vinylidene difluoride)) 2.292, 2.297, **2.299** , 2.307
PVPON (poly(vinylpyrrolidone) 1.224
PVS (poly(vinyl) sulfonate) 1.329–30
pyrene 1.108, 2.130–1
pyroglutamic acid (Pga) 2.247

quantum dots (QDs) **2.38**

radical polymerization 2.185
radio frequency ablation (RFA) 1.65–8, **1.66**, 1.96
radioactive substances **1.85**
RAFT. *see* reversible addition fragmentation transfer
Raman spectroscopy 1.286, 2.92
rapamycin 2.215
rate-programmed drug release. *see* release rate
reactive oxygen species (ROS). *see also* oxidation
  carbon nanotubes 2.106, 2.109
  photodynamic therapy 2.14
  photothermal therapy 1.100
receptor-mediated endocytosis 1.167
receptor specific ligands 1.82
recognition, responsive polymers 1.14–15
redox cycling, intrinsically conducting polymers **1.290**
redox-responsive drug release **1.17**, 1.21, 1.210, 1.223, 1.288
  dendrimers, smart 1.105
  gold nanoparticles 2.10, **2.12**
  intrinsically conducting polymers 1.283, 1.291, 1.295
  layer-by-layer assemblies 2.134–5
  mesoporous silica nanoparticles 2.78–9
  nanovehicles **1.209**, 1.210, 1.214
reducible cleavable polycation (RPC vectors) **1.264**, 1.265
reducible polyelectrolyte complexes (polyplexes) 1.261–9, **1.263**, **1.264**, **1.266**, **1.268**, 1.274
reducing agents, layer-by-layer assemblies 2.135
reduction-sensitive nanosystems 1.208–10, **1.209**, 1.227
  hollow capsules 1.223–6, **1.225**
  nanogels **1.226**, 1.226–7
  nanoparticles 1.221–3, **1.222**
  polymeric micelles 1.210–19, **1.211**, **1.213**, **1.215**, **1.217**
  polymersomes 1.219–21, **1.220**
regenerative medicine 2.295, 2.296–8. *see also* cell/tissue delivery systems
relative exposure index (REI), polymeric micelles 1.125

release rate, drug 1.2
  enzyme-responsive DDS 1.240
  evolution **1.3**
  layer-by-layer assemblies 2.122, 2.125, **2.126**
  supramolecular hydrogels 1.242
renal clearance, drug delivery systems 1.188–9
renal thresholds, particle size 1.236
reservoir systems, intrinsically conducting polymers **1.290**, 1.290–2, **1.291**
residual catalysts, toxicity 2.105–6, 2.108
resistance. *see* multi-drug resistance
responsive imprinted networks 2.229. *see also* molecular imprinting
restenosis 2.316
reticulo-endothelial (RES) system 1.81, 2.41
  gold nanoparticles 2.3–4
  mesoporous silica nanoparticles 2.68
  opsonin recognition 1.189
reverse engineering, low temperature sensitive liposomes 1.36–51, **1.38–41**, **1.44–6**, **1.48–9**
reversible addition fragmentation transfer (RAFT)
  cell sheet engineering 2.296, **2.297**, 2.304
  polymerization 1.216, 2.321
reversible cross-linking, light-sensitive polymeric micelles 1.318–20, **1.319**
reversible-deactivation radical polymerization 2.321
reversible photoswitching **1.314**, **1.315**. *see also* switching
  polymeric micelles **1.312**, 1.313, 1.317, **1.318**
  polymeric vesicles **1.321**, 1.322
RFA (radio frequency ablation) 1.65–8, **1.66**, 1.96
RGD (arginine–glycine–aspartic acid) peptides 1.262, 2.96
rhodamine 6G 1.99, **1.107**, 1.107
rhodamine B 1.102, 1.161, 1.223, 1.249, 1.332, 2.48
rifampicin
  combination products 2.319
  enzyme-responsive DDS 1.246
  polymeric micelles 1.128
ring opening polymerization (ROP) reactions 1.127
risk–benefit ratios, chemotherapy drugs 2.63
RNA. *see also* gene delivery
  cell/tissue delivery systems 2.300
  gene delivery 1.265
  gold nanoparticles 2.6
  mesoporous silica nanoparticles 2.71–2
  polyplexes 1.268
rod-shaped
  nanoparticles 1.192
  polymersomes 1.193
ROP (ring opening polymerization) reactions 1.127
ROS. *see* reactive oxygen species
RPC (reducible cleavable polycation) vectors **1.264**, 1.265
ruboxyl 1.162–3
ruthenium 2.200

saccharide-sensitive polymer brushes 2.327, **2.328**
safety assessments, drug delivery systems 1.25
  molecularly imprinted polymers 2.234
  new excipients 1.7, 1.8
  phototriggered micelles/nanoparticles 1.338
  ultrasound 1.155
safranin 1.296
salt-triggered release, layer-by-layer assemblies **2.132**, 2.132, **2.133**, 2.133–4
saporin-conjugated dendrimers 1.100

SAXS (small angle X-Ray scattering) 1.183
scaffold-based cell/tissue delivery systems 2.293–4
scanning electron microscopy (SEM) 1.44, **1.44**, **1.291**, 1.291
scattering techniques 1.186–7
scCO_2 (supercritical CO_2) 2.319
SCID (severe combined immunodeficiency) mice 1.258–9
SCL (shell cross-linked) micelles 1.218
SCRM (shell-cross-linked reverse micelles) 1.319–20
SDF-1. *see* stromal-derived factor-1
second generation
  biomaterials 1.5
  excipients 1.2
second order phase transitions 1.11–12
self-assembly
  elastin-like recombinamers 2.188, 2.191, 2.192, 2.194, 2.195, 2.199–200
  hydrogels 1.238
  light-sensitive polymeric vesicles 1.322–3
  lipids 1.33, 1.34
  liposomes/micelles 1.94
  magnetic nanoparticles 2.40, **2.43**
  micelles 1.169
  molecularly imprinted polymers 2.230, 2.232
  polymeric micelles 1.116
  polymersomes 1.179–85, **1.182**
  polysaccharide-based nanogels 2.160
  shell cross-linked micelles 1.218
  solid polymeric nanoparticles 1.334
  supramolecular hydrogels 1.242, 1.243
self-regulated DDS 1.96, 1.305, 2.154
  layer-by-layer assemblies 2.141–2
  mesoporous silica nanoparticles **2.76**
SEM (scanning electron microscopy) 1.44, **1.44**, **1.291**, 1.291
sequestering agents, polymers 1.9
sequestration, micelles 1.169–70
severe combined immunodeficiency (SCID) mice 1.258–9
SGNs (spiral ganglionic neurons) 1.297, 1.300
shape
  carbon nanotubes 2.92, 2.110
  nanoparticles 1.192–3
  polymersomes 1.193
shear-stress induced release, micelles 1.170
shell cross-linked (SCL) micelles 1.218
shell-cross-linked reverse micelles (SCRM) 1.319–20
shell-sheddable micelles, reduction-sensitive 1.210–13, **1.211**, **1.213**
signal amplification, enzyme-responsive materials 1.232
signal-to-noise ratio, polymersome imaging compounds 1.196
silane coupling chemistry 2.69
silane monolayers **2.322**
silica nanocontainers (SN) **1.248**, 1.248–51, **1.249**. *see also* mesoporous silica nanoparticles
silicon brushes, polymer 2.327
simvastatin 1.124
single-crystal shell drug nanocarriers 2.54–6, **2.55**, **2.56**
single-walled carbon nanotubes (SWCNTs) 2.90, 2.92, 2.100
  encapsulation properties 2.101
  environmental impacts 2.110
  external attachment of drugs 2.96–7
  layer-by-layer assemblies 2.119
  toxicity/environmental impacts 2.104, 2.106, 2.107, 2.108
size factors
  carbon nanotubes 2.105
  enzyme-responsive materials 1.236–7

- size factors (*continued*)
  - mesoporous silica nanoparticles 2.65
  - nanoparticles 1.191–2
  - proteins, therapeutic 1.256
  - switching 2.154
- skeletal myoblast sheets 2.297, **2.300**, **2.301**
- skin contact, carbon nanotubes 2.105, 2.108
- small angle X-Ray scattering (SAXS) 1.183
- small interfering ribonucleic acid (siRNA) 1.257
- small unilamellar vesicles (SUVs) 1.34
- smart membranes, intrinsically conducting polymers 1.294, **1.295**. *see also* stimuli responsive DDS
- snap-top systems 2.78
- sodium alginate (NaAlg) 2.158. *see also* alginates
- soft contact lenses 2.235–40, **2.236**, **2.237**, **2.239**
- soft coronal cross-linking 1.327
- sol–gel phase transitions 1.13
- sol–gel technology 1.130
- solid polymeric nanoparticles 1.334–7, **1.335**, **1.336**, **1.337**
- solid tumor targeting 1.198
- solubility, drugs 1.115
- solvents. *see also* organic solvents
  - combination products 2.319
  - dimethylformamide 2.215, **2.216**
  - imprinted hydrogels **2.242**, 2.242, 2.248
  - molecularly imprinted polymers 2.232
  - polymer–solvent interactions 1.12
- sonoporation 1.153, 1.165, 1.167, 1.168. *see also* ultrasound
- SOPC (stearoyl-2-oleoyl-*sn*-glycero-3-phosphocholine) 1.34–5, **1.35**, 1.43, 1.46, 1.47
- spatial conformation, polymer chains 2.229
- spherical
  - nanoparticles 1.192
  - polymersomes 1.193
- spike-wave discharges (SWD) 2.57, **2.58**
- spiral ganglionic neurons (SGNs) 1.297, 1.300
- spiropyran 1.307, 1.310, **1.311**, 1.313, 1.314, 1.324, 1.333–4, 1.338
- spongy phases, polymersomes 1.183
- SPR (surface plasmon resonance) effects 2.14
- spray-drying 2.65, 2.72
- stability, intrinsically conducting polymers 1.285–6
- stacking devices, cell sheet engineering **2.306**
- *Staphylococcus aureus*. *see also* MRSA
  - combination products **2.340**, 2.341
  - layer-by-layer assemblies 2.130
  - polymer grafting 2.336
  - polymeric micelles 1.123–4
  - wounds 1.19
- star-shaped micelles 1.131
- Staundinger, Hermann 1.6
- stealth systems 1.38, 1.50. *see also* PEGylation; PHMA; PMOXA; PMPC; PVP
  - lipid membrane components 1.42
  - mesoporous silica nanoparticles 2.68–9
  - pH-sensitive liposomes 1.84, **1.85**, 1.90
  - polymersomes 1.197
  - switchable micelles 1.247
- stents 1.296–7, 2.316
- stearoyl-2-oleoyl-*sn*-glycero-3-phosphocholine (SOPC) 1.34–5, **1.35**, 1.43, 1.46, 1.47
- stimulated emission depletion (STED) microscopy 1.185
- stimuli responsive DDS 2.229. *see also specific DDS*
  - combination products 2.321
  - general information 1.9–25, **1.10**, **1.17**, **1.22**

stress and strain parameters, cell membranes 1.43
stromal-derived factor-1 (SDF-1)
  cytokines 2.297–8
  regenerative medicine **2.300**
structure-property-composition relationships 1.34–6, 1.40–51, **1.40**, **1.41**, **1.44–6**, **1.48**, **1.49**
substrates, layer-by-layer assemblies 2.117–18, **2.119**
sugar-induced release. *see* glucose-responsive DDS
supercritical CO_2 ($scCO_2$) 2.319
superparamagnetism 2.34
supramolecular hydrogels 1.241–4, **1.242**
surface area-to-volume ratios
  mesoporous silica nanoparticles 2.65
  nanoparticles 1.193
surface chemistry, carbon nanotubes 2.106, 2.109
surface functionalization. *see* functionalization
surface modification
  magnetic nanoparticles **2.38**, 2.38–40, **2.39**
  plasma polymerization 2.339–41
surface plasmon resonance (SPR) effects 2.14
surface topologies, polymersomes 1.194, **1.195**
surfactant micelles 1.156–7
surfactants 2.171
SUVs (small unilamellar vesicles) 1.34
SWCNTs. *see* single-walled carbon nanotubes
SWD (spike-wave discharges) 2.57, **2.58**
swelling–collapse phenomenon 1.12. *see also* equilibrium degree of swelling; phase transitions
swelling solvents, combination products 2.319, **2.319**
switching. *see also* magnetic nanoparticles; reversible photoswitching
  α-amino acid based hydrogels 2.200
  enzyme-responsive DDS 1.243
  hydrophilic/hydrophobic state 2.154
  imprinted hydrogels 2.245
  mesoporous silica nanoparticles 2.75, 2.79, 2.79–80
  micelles 1.246–8
  size/shape 2.154
  solid polymeric nanoparticles 1.335
  temperature-responsive DDS 2.136
synergistic effects. *see also* dual-responsive DDS
  chemotherapy drugs/ultrasound 1.165–6
  cisplatin/temsirolimus **2.216**, 2.216–17
  combination products 2.316
  gold nanoparticles **2.20**, 2.20
  magnetic nanoparticles 2.42
  mesoporous silica nanoparticles 2.71, 2.72, 2.73
  pH/redox-stimulated DDS 1.213
synthetic glycosylated insulin (G-insulin) 2.291
synthetic metals, electric field responsive DDS 1.25

tamoxifen 2.118, 2.159
Tanaka equation 2.244–5
targeted drug delivery 2.1. *see also* active targeting; *specific DDS*
  cancer chemotherapeutics 2.3
  cell sheet engineering 2.298–301
  mesoporous silica nanoparticles 2.66–8
  nanogels 1.18
  ultrasound-responsive DDSs 1.159–61

Tarzan-swing mechanism 2.234
TAT (transactivator of transcription) 1.88, 1.265
taxol. *see* paclitaxel
TCEP (tri(2-carboxyethyl)phosphine hydrochloride) 1.218
TCPS (tissue culture polystyrene) dishes 2.295–6
TEM. *see* transmission electron microscopy
temperature-responsive DDS **1.17**, 1.21–4, **1.22**. *see also* hyperthermia; low temperature-sensitive liposomes; photothermal therapy; poly(isopropylacrylamide)
  α-amino acid based hydrogels 2.202, 2.209–11, 2.213, 2.214, 2.221
  biomolecule-sensitive hydrogels 2.261–2, 2.277
  cell/tissue delivery systems 2.294–5, **2.295**, **2.297–302**, **2.304–6**
  dendrimers, smart 1.96–9, **1.97**
  dual responsive hydrogels 2.170–3
  elastin-like recombinamers 2.193–4
  glucose-sensitive hydrogels **2.267**
  hydrogels 2.154, **2.161**, 2.161–9, **2.162–3**, **2.166**, **2.169**
  hydrolytically induced drug release 2.243
  imprinted hydrogels 2.245–9, **2.246–8**
  layer-by-layer assemblies **2.136–7**, 2.136–7
  liposomes 2.46, **2.47**
  magnetic nanoparticles **2.44**, 2.44–50, **2.45–7**
  mesoporous silica nanoparticles 2.69, 2.70
  micelles, polymeric 1.120–33, **1.121**, **1.125**, **1.129**, **1.130**, **1.132**
  moieties 1.98–9
  polyelectrolyte complexes **1.269**, 1.269–73, **1.272**
  polymer grafting **2.331**, 2.334
  polymersomes 1.200
  upper critical solution temperature 2.168–9, **2.169**
template extraction, molecularly imprinted polymers 2.233, **2.234**
templates, layer-by-layer assemblies 2.117–18, **2.119**
temsirolimus 2.202, 2.203, 2.215, 2.216, **2.216**, 2.217, 2.224
tetrahydropyran (THP)-protected 2-hydroxyethyl methacrylate) 1.213
tetramethylpiperidinyl-1-oxy (TEMPO) 2.323
TGF-β1 (transforming growth factor beta 1) 2.125
theophylline 2.100, 2.240, 2.251
theranostics
  carbon nanotubes 2.91
  dendrimers, smart 1.108–9
  enzymes in 1.232
  gold nanoparticles 2.21–3, **2.22**, **2.23**
  magnetic nanoparticles **2.41**
  pH-sensitive liposomes 1.90
  polymeric micelles 1.128
  polymersomes 1.196
therapeutic index, drug 1.120
therapeutic neutrophins 1.297
therapeutic proteins 1.256, 2.189
thermal decomposition, magnetic nanoparticles **2.38**, 2.38
thermal index (TI) 1.150, 1.155
thermal responsiveness. *see* temperature-responsive DDS
ThermoDox. *see* doxorubicin
thermodynamic characterization, ultrasound-responsive DDSs 1.163–4
thermodynamic phase transitions 1.14
thermoseeds 2.73
thiolated poly(methacrylic acid) (PMASH) 1.224
thiolates 2.5

thiol-disulfide exchange reactions 1.209
thiophene fluorophore 2.160
thioundecyl-tetraethyleneglycoestero-nitrobenzylethyldimethylammonium bromide (TUNA) 2.77–8
thioundecyltetraethyleneglycolcarboxylate (TUEC) 2.77–8
third generation
  biomaterials 1.6–7, **1.8**
  excipients 1.2
THP (tetrahydropyran-protected 2-hydroxyethyl methacrylate) 1.213
three dimensional networks
  α-amino acid based
    hydrogels 2.200
  layer-by-layer assemblies 2.143–4
three dimensional (3D) tissues 2.291, 2.293, 2.303, **2.304**. *see also* cell/tissue delivery systems
thrombin-sensitive peptide linkers 1.19
time-controlled release. *see* release rate
time-dependent tumor cell death 2.167
timolol 2.236, **2.237**, 2.237
TIRF (total internal reflectance fluorescence) 1.185
tissue culture polystyrene (TCPS) dishes 2.295–6
tissue engineering 2.293–4. *see also* cell/tissue delivery systems
tissue-mimicking cell sheets. *see* cell sheet engineering
TNF (tumor necrosis factor) 1.199, **2.5**
topoisomerase inhibitors 1.169. *see also* doxorubicin
total internal reflectance fluorescence (TIRF) 1.185
toxicology 2.1
  capsules, polymeric 1.328
  carbon nanotubes 2.92, 2.97–8, 2.104–10
  cisplatin hydrogels 2.214–17, 2.200
  cross-linked micelles 1.216
  enzyme inhibitors 1.234
  fiber paradigm 2.107
  layer-by-layer assemblies 2.140
  light-sensitive polymeric micelles 1.310
  lipofectamine 1.200
  nanoparticles 1.193–4
  new excipients 1.9
  pH-responsive nanogels 2.160
  pilocarpine 2.220–1
  polyelectrolyte complexes 1.270
  reduction-sensitive nanosystems 1.218
  switchable micelles 1.247
  see also toxicology
transactivator of transcription (TAT) 1.88, 1.265
trans–cis isomerization
  light-responsive hydrogels 2.251, 2.252
  light-sensitive polymeric micelles 1.310, 1.313, 1.314, 1.317, **1.318**
  light-sensitive polymeric vesicles 1.323
  phototriggered micelles/nanoparticles 1.332
transdermal drug delivery, layer-by-layer assemblies 2.144
transferrin receptors, tumor cells 1.191
transforming growth factor beta 1 (TGF-β1) 2.125
transglutaminase 2.271, 2.187
transition temperature, liposomes 1.47
translocation, carbon nanotubes 2.108
transmission electron microscopy (TEM)
  elastin-like recombinamers 2.192
  lipid bilayers **1.44**, 1.44
  polymersomes **1.182**, 1.184, 1.185, **1.187**, **1.190**
trans-to-*cis* photoisomerization
  light-sensitive polymeric vesicles 1.322

tri(2-carboxyethyl)phosphine hydrochloride (TCEP) 1.218
triclocarban 1.118, 1.124
triclosan 1.118, 1.123
trimethyloylpropane ethoxylate triacrylate 1.194
tumor cells
  biochemical-responsive DDS 1.20, 1.21
  enzyme-responsive DDS 1.19
  enzyme disregulation **1.233**
  low temperature-sensitive liposomes 1.34, 1.37, **1.38**, 1.39
  magnetic-responsive DDSs 1.24
  nanogels 1.18
  passive accumulation 1.81, **1.82**
  pH 1.16, 1.83, 1.134, 2.70, 2.129, 2.155, 2.158–61
  reduction-sensitive nanosystems 1.210
  stress and strain parameters 1.43
  temperature-responsive nanogels 2.166
  ultrasound-responsive DDSs 1.23, 1.159–61
  vascularisation 1.37, **1.38**, 1.61, 1.63–4, 1.198
tumor diagnosis. *see* theranostics
tumor markers 2.262, 2.277–9, **2.279**
tumor necrosis factor (TNF) 1.199, **2.5**
TUEC (thioundecyltetraethyleneglycolcarboxylate) 2.77–8
TUNA (thioundecyltetraethyleneglycoestero-nitrobenzylethyldimethylammonium bromide) 2.77–8
TUNEL assay, gold nanoparticles **2.8**
two photon near-IR absorption 1.316
two-step model 1.183

UCST. *see* upper critical solution temperature
Ugi condensation 2.186
ultra-small superparamagnetic iron oxide (USPIO) 1.201
ultrasonication 2.95
ultrasound imaging compounds **1.196**, 1.196, 1.197
ultrasound-responsive DDSs **1.22**, 1.23, 1.148–9
  future perspectives 1.169–70
  layer-by-layer assemblies 2.140–1
  micelles 1.155–9
  physics of ultrasound 1.149–5, **1.152**
  polymeric micelles 1.123, 1.157–8
  targeting tumor cells 1.159–61
  triggered release from micelles 1.161–9, **1.162**
ultraviolet light-responsive DDSs 1.23, 1.305–7
  gold nanoparticles 2.14
  imprinted hydrogels 2.251, 2.252
  layer-by-layer assemblies 2.139
  mesoporous silica nanoparticles 2.70, 2.77–8
  micelles/nanoparticles 1.330, 1.338
  nanogels 1.331
  polymer grafting **2.322**, 2.323
  polymeric micelles 1.313, 1.314, 1.315
  polymeric vesicles 1.322, 1.323–4
  solid polymeric nanoparticles 1.334, **1.336**
United States Pharmacopoeia (USP), 21-National Formulary 1.2
upper critical solution temperature (UCST)
  dual responsive hydrogels 2.173
  magnetic nanoparticles 2.44
  polymeric micelles 1.121
  temperature-responsive hydrogels **2.161**, 2.161, 2.168–9, **2.169**
  temperature-sensitive polymers 1.21–2
Urry's model 2.181
USPIO (ultra-small superparamagnetic iron oxide) 1.201

vaginal pH 1.18
valine residues 2.200–1, 2.203, **2.205**, 2.206, **2.207**, **2.210**, 2.211, 2.213, **2.213**, 2.214, 2.219–21, **2.219**, **2.220**
Val-Pro-Gly-Xaa-Gly (VPGXG) 2.181, 2.182. *see also* elastin-like recombinamers
valproic acid 2.224
van der Waals interactions 1.12
  carbon nanotubes 2.95
  enzyme-responsive DDS 1.19
  lipid bilayers 1.43
vancomycin
  elastin-like recombinamers 2.189
  polymer grafting 2.329–33, **2.331**, **2.332**, **2.334**
  polymeric micelles 1.123–4
vascular cell adhesion molecule 1 (VCAM-1) 1.191
vascular diseases, enzyme disregulation **1.233**
vascular endothelial growth factor (VEGF)
  biomolecule-sensitive hydrogels 2.284, 2.285
  cell sheet engineering 2.306
  polyelectrolyte complexes 1.268
  regenerative medicine 2.298, **2.300**, 2.301
vascularization
  tissue-mimicking cell sheets 2.303, 2.306
  tumor cells 1.37, **1.38**, 1.61, 1.63–4, 1.198
VCAM-1 (vascular cell adhesion molecule) 1.191
VEGF. *see* vascular endothelial growth factor
vesicle area dilation experiment **1.45**
vesicles
  elastin-like recombinamers 2.194, **2.195**
  fenestrations. *see* enhanced permeability and retention effect
  hollow 2.194–5, **2.195**
  light-sensitive polymeric 1.320–7, **1.321**, **1.324–6**
  lipid bilayers 1.43
  phase transitions 1.14
vesicle-to-micelle transitions 1.184
vinyl hydrogels 2.200–3, **2.201–2**
viscoelasticity, biomaterials 1.6
VPGXG (Val-Pro-Gly-Xaa-Gly) 2.181, 2.182. *see also* elastin-like recombinamers
volume changes, intrinsically conducting polymers 1.289. *see also* swelling–collapse phenomenon

water solubility, drugs 1.115
wave nature, ultrasound 1.149–50
wet chemical polymer grafting **2.322**
wet-chemical synthesis, mesoporous silica nanoparticles 2.65
wild-type myoblast sheets **2.301**
window chambers, optical imaging 1.196
Wolf rearrangement reaction 1.315–16
Wolman disease **1.233**
worm-like micelles 1.193
wounds
  enzyme-responsive DDS 1.19
  pH 1.16–18, 2.155

X-ray contrast agents. *see* contrast agents

zero premature release, chemotherapy drugs 2.64, 2.65
zinc porphyrin 1.135
zwitterionic ligands 2.10
zwitterionic peptide linkers 2.272, **2.273**

Smart Materials for Drug Delivery
Volume 2

Downloaded on 01/09/2013 10:27:01.

Downloaded on 01/09/2013 10:27:01.

RSC Smart Materials

Series Editor:
Hans-Jörg Schneider, *Saarland University, Germany*
Mohsen Shahinpoor, *University of Maine, USA*

Titles in this Series:
1: Janus Particle Synthesis, Self-Assembly and Applications
2: Smart Materials for Drug Delivery: Volume 1
3: Smart Materials for Drug Delivery: Volume 2

How to obtain future titles on publication:
A standing order plan is available for this series. A standing order will bring delivery of each new volume immediately on publication.

For further information please contact:
Book Sales Department, Royal Society of Chemistry, Thomas Graham House,
Science Park, Milton Road, Cambridge, CB4 0WF, UK
Telephone: +44 (0)1223 420066, Fax: +44 (0)1223 420247
Email: booksales@rsc.org
Visit our website at www.rsc.org/books

Downloaded on 01/09/2013 10:27:01.

Smart Materials for Drug Delivery

Volume 2

Carmen Alvarez-Lorenzo
University of Santiago de Compostela, Spain
Email: carmen.alvarez.lorenzo@usc.es

Angel Concheiro
University of Santiago de Compostela, Spain
Email: angel.concheiro@usc.es

RSC Publishing

Downloaded on 01/09/2013 10:27:01.

RSC Smart Materials No. 3

ISBN: 978-1-84973-878-1
ISSN: 2046-0066

A catalogue record for this book is available from the British Library

© The Royal Society of Chemistry 2013

All rights reserved

Apart from fair dealing for the purposes of research for non-commercial purposes or for private study, criticism or review, as permitted under the Copyright, Designs and Patents Act 1988 and the Copyright and Related Rights Regulations 2003, this publication may not be reproduced, stored or transmitted, in any form or by any means, without the prior permission in writing of The Royal Society of Chemistry or the copyright owner, or in the case of reproduction in accordance with the terms of licences issued by the Copyright Licensing Agency in the UK, or in accordance with the terms of the licences issued by the appropriate Reproduction Rights Organization outside the UK. Enquiries concerning reproduction outside the terms stated here should be sent to The Royal Society of Chemistry at the address printed on this page.

The RSC is not responsible for individual opinions expressed in this work.

Published by The Royal Society of Chemistry,
Thomas Graham House, Science Park, Milton Road,
Cambridge CB4 0WF, UK

Registered Charity Number 207890

For further information see our web site at www.rsc.org

Printed in the United Kingdom by Henry Ling Limited, Dorchester, DT1 1HD, UK

Downloaded on 01/09/2013 10:27:02.

Foreword

In recent years smart materials have found new and promising applications as drug carriers for delivery of new therapeutic agents. At a time when present uses of drug delivery have become rather difficult to launch commercially because of the pressure from generic drug delivery systems, smart materials provide new applications, especially in the treatment of diseases where present formulations have not found good use. Indeed, intelligent biomaterial carriers have attracted significant interest because of the promise to respond to physiological conditions of the body, but also to respond to elevated quantities of analytes responsible for a particular disease.

The present book is a welcome addition to the field of smart polymers and comes to fill a major need in the use of smart materials as carriers for drug delivery. As we read the various chapters it becomes apparent that the editors, Professors Carmen Alvarez-Lorenzo and Angel Concheiro of the University of Santiago de Compostela, have set specific goals for this book and have spent numerous days trying to edit the chapters and balance the book. Their goals are to highlight the design, characterization and investigation of the next generation of "intelligent" or smart polymeric structures and biohybrids that can be used for drug delivery and can "communicate" with their surrounding environment.

The use of smart polymer carriers is a natural approach to the solution of many delivery problems as the discovery and delivery of drugs to cure chronic diseases have been achieved by a combination of intelligent material design and advances in nanotechnology. In particular, there has been considerable work in preparing nanostructured biomaterials for various applications, such as carriers for controlled and targeted drug delivery, micropatterned devices, systems for biological recognition, and others. Since many drugs act as protagonists or antagonists to different chemicals in the body, a delivery system that can respond to the concentrations of certain molecules in the body is

---

RSC Smart Materials No. 3
Smart Materials for Drug Delivery: Volume 2
Edited by Carmen Alvarez-Lorenzo and Angel Concheiro
© The Royal Society of Chemistry 2013
Published by the Royal Society of Chemistry, www.rsc.org

Downloaded on 01/09/2013 10:27:02.

invaluable. For this purpose, intelligent therapeutics or "smart drug delivery" call for the design of the next generation of responsive devices and materials, both from purely synthetic materials as well as through combination of natural and biological molecules with synthetic materials.

In other advanced pharmaceutical applications, biomimetic materials, especially polymeric networks, capable of biological recognition can be prepared by designing interactions between the building blocks of biocompatible networks and the desired specific ligands and by stabilizing these interactions by a three-dimensional structure. In addition, biomimetic methods are now used to build biohybrid systems or even biomimetic materials (mimicking biological recognition) for drug targeting and tissue engineering devices. Additionally, micro- and nanofabrication techniques have enabled the development of novel biomedical systems, sensors and delivery devices that can improve the therapeutic effect of drugs, such as micro- and nanoscale needles, pumps, valves, and implantable drug delivery devices. These advances are expertly presented in this book.

Why do we observe such an explosion in research in this field now? The development of nanoparticulate systems for biological applications has taken a level of sophistication never before seen in the field of biomedicine. Using intelligent polymers, it is now possible to design new devices for intelligent diagnostics, therapeutics, molecular communication, etc. Such systems can be employed for auto-feedback action, whereby the biomaterial can be designed to rapidly respond to changes in the external biological conditions. This idea may be used to study biological communication and develop novel biological machines. This book presents new molecular techniques which are used to design new biomaterials based on star polymers, symmetric structures of inorganic and organic materials, dendrimers, self-assembled monolayers and biological/synthetic constructs.

In view of the growing need in biological, biomolecular and biomedical engineering for scientists with a broad, but strong, background in materials engineering and biological sciences, this book will promote the investigation and utilization of novel macromolecular structures, biohybrid systems and biopolymers with ability to interact with or recognize external phenomena associated with biological or physiological solutions. The book incorporates educational and research components with emphasis on the synthesis, design, development and analysis of novel structures useful in the biomedical, biochemical, cellular and related fields.

Nanostructured materials have thus created great excitement in research and industrial circles because of numerous and diverse applications in electronic devices, automobile engines, industrial catalysts, and cosmetics. To date, and despite their great promise, applications of nanophase materials in the biomedical field (other than in drug delivery) have been close to nonexistent. Undoubtedly, the capability of synthesizing and processing nanomaterials with tailored structures and enhanced properties provides tremendous opportunities for designing novel biomaterials of exceptional promise for biomedical applications.

Downloaded on 01/09/2013 10:27:02.

Finally, the book addresses some of the novel applications of intelligent materials which can be used in electronic devices. This raises exciting possibilities for combining microelectronics and biotechnology to develop new technologies with unprecedented power and versatility. Thus, in recent years we have seen an explosion in the field of novel microfabricated and nanofabricated devices for drug delivery.

This book covers all the areas addressed above in a most thorough way. Various mechanisms of triggering drug delivery are addressed in a number of chapters. After a careful introduction of the importance of intelligent polymers in drug delivery by the editors Carmen Alvarez-Lorenzo and Angel Concheiro, expert reviews of temperature and pH-sensitive liposomes are presented by David Needham of Duke University and S. P. Vyas and associates of Dr. Harisingh Gour University. The corresponding behavior of temperature and pH-sensitive micelles is addressed by C. Kojima of Osaka Prefecture University. William Pitt and associates of the University of Utah address interesting and important applications of ultrasound-triggered release from micelles.

Polymersomes are a relatively new class of important intelligent polymer structures that can be used in drug delivery. This subject is expertly addressed by Giuseppe Battaglia of the University of Sheffield. Two important aspects of intelligent systems utilize reduction-sensitive nanosystems mostly for intracellular drug delivery, as carefully presented by R. Cheng, F. Meng, C. Deng and Z. Zhong of Soochow University, and enzyme-responsive drug delivery systems, as described by P. F. Caponi and R. V. Ulijn of the University of Strathclyde.

In subsequent chapters, the editors have tried to present important biological applications of all these smart materials. For example, Cameron Alexander and associates from the University of Nottingham address the use of bioresponsive polyplexes and micelleplexes, while the editors give a detailed analysis of our latest knowledge on UV and near-IR triggered release from nanoparticles. Another important triggering mechanism is heating via remote irradiation of gold nanoparticles-based systems, which is addressed by E. K. Lim and associates of Yonsei University. Finally, magnetic-responsive nanoparticles for drug delivery are expertly presented by Ting-Yu Liu of the National Taiwan University and associates.

Recent advances in nanoscale systems based on inorganic materials that are finding applications in drug delivery are presented by Maria Vallet-Regi of the Complutense University (silica nanoparticles) and Gerard Tobias and Emmanuel Flahaut of CMAB-CSIC, Barcelona, Spain and the University Paul Sabatier (smart carbon nanotubes). The use of smart layer-by-layer films is a powerful new method with important applications in drug delivery and is expertly discussed by S. Sukhishvili and S. Pavlukhina of Stevens Institute of Technology.

In the next few chapters, the editors have elected to present new applications of intelligent hydrogels, a subject of major interest to the medical and pharmaceutical fields. Thus, Francesco Puoci and Manuela Curcio of the University

Downloaded on 01/09/2013 10:27:02.

of Calabria discuss temperature- and pH-responsive hydrogels, Jose Carlos Rodriguez-Cabello and associates of the University of Valladolid address elastin-like hydrogels and self-assembled nanostructures, while Mario and Ilaria Casolaro discuss multiple stimuli-responsive hydrogels. The editors Carmen Alvarez-Lorenzo and Angel Concheiro offer an expert presentation of molecularly-imprinted hydrogels and associated techniques. These materials appear to have great promise for a variety of applications. Finally, T. Miyata of Kansai University discusses the latest advances in biomolecule-sensitive hydrogels.

In the development of smart biomaterials, it is often desired to attain spatial control of cells and related biological organisms. Numerous surface micro- and/or nanofabrication techniques have been developed in order to create a material for regulating cell functions for application in tissue engineering, microbiosensors, and other applications requiring a desired pattern of response from the cells. Teruo Okano and H. Takahashi of the Tokyo Women's Medical University present a thorough review of the latest research on intelligent surfaces for cell and tissue delivery. The book ends with another chapter written by the editors Carmen Alvarez-Lorenzo and Angel Concheiro that addresses an important area for current and future applications, that of drug/medical device combination products. Often these combination products are designed with possible stimuli-responsive eluting surfaces and promise to exhibit recognitive characteristics.

I think that all researchers in the field of drug delivery will find this new book a very valuable addition in the field and will use it for many years to come. I know I will.

Nicholas A. Peppas, ScD, NAE, IOM, FBSE
The University of Texas at Austin
Austin, Texas, USA

Downloaded on 01/09/2013 10:27:03.

Preface

Writing a book is an adventure, in words of Winston Churchill. Editing a book is not lesser adventure. It is both a challenging and a rewarding task. We put a foot in this adventure when Prof. Hans-Jörg Schneider encouraged us to think about a book project for the RSC Series on Smart Materials with a focus on Drug Delivery; the second foot was put when the RSC Publications Committee approved our proposal. The design and application of stimuli-responsive materials is a growing field that benefits from contributions of people from diverse backgrounds all around the world. Numerous drug delivery systems with advanced performances based on the features of smart materials have come up in the last years. A wide range of materials with diverse structure, their processing for creating carriers of varied architecture, and the responsiveness to physiological variables, to illness markers or to external stimuli useful for triggering or switching on/off drug release are addressed in the present book. In addition to small synthetic drugs, other classes of therapeutic molecules or even cells are covered. A balance between novelty and clinical possibilities was the criterion followed to choose the contents, which were organized as a function of the carrier architecture and the stimulus that activates the release. Drug-device combination products were also taken into account. An effort has been made to not be lost in the particular details, but to prioritize the general concepts that are behind the design and functioning of intelligent drug delivery systems.

It was truly rewarding when the invited contributors answered very positively to the book project. We are in debt with all of them for their efforts on writing comprehensive as well as educational chapters, covering in detail the state-of-the-art in each assigned topic. Our acknowledgement goes also to Prof. Nicholas Peppas for his always encouraging comments and the kind foreword, and to the people of the RSC editorial office, particularly Mrs. Alice Toby-Brant, for providing an invaluable help with formal and not so formal aspects.

RSC Smart Materials No. 3
Smart Materials for Drug Delivery: Volume 2
Edited by Carmen Alvarez-Lorenzo and Angel Concheiro
© The Royal Society of Chemistry 2013
Published by the Royal Society of Chemistry, www.rsc.org

We finally would like to thank the readers of this book, from who we will be very happy to receive comments and feedback. Working in the interface between stimuli responsiveness and drug delivery is itself a tricky and long adventure, but along the path outstanding advances for therapeutics are already becoming a reality. We hope that this text would serve as a guide for the beginners in the field and as a multidisciplinary meeting point for researchers involved in quite diverse areas.

Carmen Alvarez-Lorenzo
Angel Concheiro
Department of Pharmacy and Pharmaceutical Technology
Faculty of Pharmacy, University of Santiago de Compostela
15782-Santiago de Compostela (Spain)

Downloaded on 01/09/2013 10:27:03.

Downloaded on 01/09/2013 10:27:05.

Contents

Volume 1

Chapter 1 From Drug Dosage Forms to Intelligent Drug-delivery Systems: a Change of Paradigm 1

C. Alvarez-Lorenzo and A. Concheiro

1.1 Evolution of Drug Dosage Forms 1
1.2 Advanced Excipients 4
1.3 Stimuli-responsive Components 9
  1.3.1 Phase Transitions 11
  1.3.2 Memorization of the Conformation. Molecular Imprinting and Recognition 14
1.4 Intelligent Drug-delivery Systems 15
  1.4.1 pH- and/or Ion-responsive DDSs 16
  1.4.2 Enzyme-responsive DDSs 18
  1.4.3 Biochemical-responsive DDSs 19
  1.4.4 Glutathione-responsive DDSs 21
  1.4.5 Temperature-responsive DDSs 21
  1.4.6 Ultrasound-responsive DDSs 23
  1.4.7 Light-responsive DDSs 23
  1.4.8 Magnetic-responsive DDSs 24
  1.4.9 Electric Field-responsive DDSs 24
1.5 Conclusions and Future Aspects 25
Acknowledgements 26
References 26

RSC Smart Materials No. 3
Smart Materials for Drug Delivery: Volume 2
Edited by Carmen Alvarez-Lorenzo and Angel Concheiro
© The Royal Society of Chemistry 2013
Published by the Royal Society of Chemistry, www.rsc.org

Downloaded on 01/09/2013 10:27:05.

Chapter 2 Materials Science and Engineering of the Low Temperature Sensitive Liposome (LTSL): Composition-Structure-Property Relationships That Underlie its Design and Performance 33
David Needham and Mark W. Dewhirst

2.1 Introduction 33
  2.1.1 Lipids as "Smart Materials" 33
  2.1.2 Micelles, Bilayers and Inverted Micelles 36
2.2 Reverse Engineering the LTSL 36
  2.2.1 Define the Function 37
  2.2.2 LTSL Component Design 39
  2.2.3 Materials Choice and CSP Relationships 40
  2.2.4 Composition-Structure-Properties of Each Component 42
2.3 Production 51
2.4 Performance-in-Service 53
  2.4.1 Performance-in-Service: *in vitro* 53
  2.4.2 Performance-in-Service: *in vivo* (Preclinical) 60
  2.4.3 Performance-in-Service: *in vivo* (Canine and Human Clinical Trials) 64
2.5 Future Prospects 69
  2.5.1 New ThermoDox® Trials and Preclinical Studies 70
  2.5.2 Other Drugs 70
  2.5.3 Other New Thermal-sensitive Formulations (Lipids and Polymers) 71
2.6 Concluding Remarks 72
  2.6.1 The Drug-delivery Problem 72
  2.6.2 A New Paradigm for Local Drug Delivery: Drug Release in the Bloodstream 72
  2.6.3 New Horizons 73
Acknowledgements 74
References 74

Chapter 3 pH-sensitive Liposomes in Drug Delivery 80
Shivani Rai Paliwal, Rishi Paliwal and Suresh P Vyas

3.1 Introduction 80
3.2 pH-sensitive Liposomes as Smart Drug Carriers 82
3.3 Uptake and Intra-cellular Delivery of Therapeutic Agents from pH-sensitive Liposomes 86
3.4 Therapeutic Applications of pH-sensitive Liposomes 87
  3.4.1 Cancer Chemotherapy 87
  3.4.2 Gene Delivery 89
  3.4.3 Tumor Diagnosis 90

Downloaded on 01/09/2013 10:27:05.

3.5 Conclusion 90
References 91

Chapter 4 Smart Dendrimers 94
Chie Kojima

4.1 Introduction 94
4.2 Temperature-responsive Dendrimers 96
  4.2.1 Dendrimers Containing Thermo-sensitive Polymers 97
  4.2.2 Dendrimers Containing Thermo-sensitive Moieties 98
  4.2.3 Collagen-mimic Dendrimers 99
4.3 Photoresponsive Dendrimers 100
  4.3.1 Dendrimers for Photochemical Internalization 100
  4.3.2 Dendrimers with Photodegradable Moieties 101
4.4 pH-responsive Dendrimers 102
  4.4.1 Dendrimers Containing pH-responsive Moieties 102
  4.4.2 Dendrimer Assembly with pH-sensing Moieties 103
  4.4.3 Drug-dendrimer Conjugates with pH-responsive Linkages 104
4.5 Redox-responsive Dendritic Polymers 105
4.6 Enzyme-responsive Dendritic Polymers 105
4.7 Theragnostic Dendrimers 108
4.8 Conclusion 109
Acknowledgements 109
References 109

Chapter 5 Temperature- and pH-sensitive Polymeric Micelles for Drug Encapsulation, Release and Targeting 115
Alejandro Sosnik

5.1 (Bio)pharmaceutic Challenges in Therapeutics 115
5.2 Polymeric Micelles 116
  5.2.1 Micellar Encapsulation 117
  5.2.2 Preparation Methods 118
  5.2.3 Physical Stability 119
5.3 Temperature-sensitive Polymeric Micelles 120
  5.3.1 Poly(ethylene Oxide)-Poly(propylene Oxide) and Other Polyether Amphiphiles 121
  5.3.2 Poly(ethylene Oxide)-Polyester Block Copolymers 127

5.3.3 Poly(*N*-isopropylacrylamide) 128
5.3.4 Substitutes of PEG as Hydrophilic Building Block 132
5.4 pH-responsive Micelles 133
5.5 Translation into Clinics and Perspectives 135
Acknowledgements 137
References 137

Chapter 6 Ultrasound-triggered Release from Micelles 148
William G. Pitt, Ghaleb A. Husseini and Laura N. Kherbeck

6.1 Introduction 148
6.2 Ultrasound 149
6.2.1 Physics of Ultrasound 149
6.3 Micelles 155
6.3.1 Drug Delivery from Micelles 155
6.3.2 Targeting 159
6.3.3 Ultrasound-triggered Release from Micelles 161
6.4 The Future of Ultrasound-triggered Drug Delivery from Micelles 169
References 171

Chapter 7 Smart Polymersomes: Formation, Characterisation and Applications 179
R. T. Pearson, M. Avila-Olias, A. S. Joseph, S. Nyberg and G. Battaglia

7.1 Polymersome Formation 179
7.2 Polymersomes Characterization 185
7.3 Polymersomes as Delivery Vectors 188
7.4 Polymersomes in Medicine and Pharmacy 196
References 202

Chapter 8 Reduction-sensitive Nanosystems for Active Intracellular Drug Delivery 208
Ru Cheng, Fenghua Meng, Chao Deng and Zhiyuan Zhong

8.1 Introduction 208
8.2 Reduction-sensitive Polymeric Micelles 210
8.2.1 Reduction-sensitive Shell-sheddable Micelles 210
8.2.2 Micelles with Reduction-sensitive Core 213
8.2.3 Reduction-sensitive Cross-linked Micelles 214

Downloaded on 01/09/2013 10:27:05.

Downloaded on 01/09/2013 10:27:05.

8.3 Reduction-sensitive Polymersomes 219
8.4 Reduction-sensitive Nanoparticles 221
8.5 Reduction-sensitive Capsules 223
8.6 Reduction-sensitive Nanogels 226
8.7 Conclusions 227
Acknowledgements 227
References 227

Chapter 9 Enzyme-responsive Drug-delivery Systems 232
Pier-Francesco Caponi and Rein V. Ulijn

9.1 Introduction 232
  9.1.1 Exploiting Enzymes in Drug Delivery 234
  9.1.2 Factors to Consider in the Design of ERMs for Drug Delivery 236
9.2 Enzyme-responsive Hydrogels 237
  9.2.1 Chemically Cross-linked Hydrogels 238
9.3 Enzyme-responsive Micelles 244
  9.3.1 Disruptive Enzyme-responsive Micelles 244
  9.3.2 Switchable Micelles 246
9.4 Enzyme-responsive Silica Nanocontainers 248
9.5 Conclusion 251
References 252

Chapter 10 Bioresponsive Polyplexes and Micelleplexes 256
Cameron Alexander and Francisco Fernandez Trillo

10.1 Introduction 256
10.2 pH-responsive Polyplexes 258
10.3 Reducible Polyplexes 261
10.4 Thermo-responsive Polyplexes 269
10.5 Other Stimuli-responsive Polyplexes 273
10.6 Dual Responsive Polyplexes 274
10.7 Conclusions 275
Cell Lines Mentioned in this Chapter 276
References 276

Chapter 11 Advances in Drug-delivery Systems Based on Intrinsically Conducting Polymers 283
Manisha Sharma, Darren Svirskis and Sanjay Garg

11.1 Introduction 283
11.2 Polymerisation 284

Downloaded on 01/09/2013 10:27:05.

11.3 Properties 285
  11.3.1 Conductivity 285
  11.3.2 Stability 285
  11.3.3 Biosensing 286
  11.3.4 Solubility 286
11.4 Characterization 286
  11.4.1 Infrared (IR) and Raman Spectroscopy 286
  11.4.2 Atomic Force Microscopy 287
  11.4.3 Cyclic Voltammetry 287
11.5 Biocompatibility 287
11.6 Mechanisms for Controlled Drug Release 288
  11.6.1 Utilizing Electrostatic Forces in ICPs 288
  11.6.2 Volume Changes in ICPs 289
11.7 Drug-delivery Systems 290
  11.7.1 Reservoir Systems 290
  11.7.2 Actuating Devices 292
  11.7.3 Matrix Type 296
  11.7.4 Miscellaneous Devices 297
11.8 Demonstration of Biological Applications 299
11.9 Conclusions 300
References 300

Chapter 12 UV and Near-IR Triggered Release from Polymeric Micelles and Nanoparticles 304
Manuel Alatorre-Meda, Carmen Alvarez-Lorenzo, Angel Concheiro and Pablo Taboada

12.1 Introduction 304
12.2 UV and Near-IR Light Irradiation 305
  12.2.1 UV-visible Light 305
  12.2.2 Near-IR light 306
12.3 Mechanisms of Light-triggered Release 307
12.4 Light-sensitive Polymeric DDSs 308
  12.4.1 Light-sensitive Polymeric Micelles 308
  12.4.2 Polymeric Vesicles 320
  12.4.3 Polymeric Nano-/microparticles 327
12.5 Conclusion and Outlook 338
Acknowledgements 338
References 339

Subject Index 349

Volume 2

Chapter 13 Remotely Triggered Drug Release from Gold Nanoparticle-based Systems **1**
Eun-Kyung Lim, Kwangyeol Lee, Yong-Min Huh and Seungjoo Haam

13.1 Introduction 1
13.2 Gold Nanoparticle-based DDSs 2
13.3 Activatable DDSs Based on Gold Nanoparticles 7
  13.3.1 pH-responsive Au-based DDSs 9
  13.3.2 Glutathione-mediated Au-based DDSs 10
  13.3.3 Photo-active and/or Photodynamic Au-based DDSs 10
  13.3.4 Photothermally Mediated Au-based DDSs 14
  13.3.5 Enzymatically Activated Au-based DDSs 20
13.4 Gold Nanoparticle-based Theranostic Systems 21
13.5 Conclusions and Outlook 23
References 23

Chapter 14 Magnetic-responsive Nanoparticles for Drug Delivery **32**
San-Yuan Chen, Shang-Hsiu Hu and Ting-Yu Liu

14.1 Introduction 32
14.2 Hyperthermia Theory of the Magnetic Field 34
14.3 Synthesis and Surface Modification of Magnetic Nanoparticles 37
  14.3.1 Synthesis of Magnetic Nanoparticles 37
  14.3.2 Surface Modification of Magnetic Nanoparticles 38
14.4 Magnetic Nanocarriers for Drug Delivery 40
  14.4.1 Amphiphilic Micelles and Organic Nanoparticles 41
  14.4.2 Temperature-responsive Magnetic Nanocarriers 44
14.5 Nanocarriers with a Magnetic Shell as DDSs 50
  14.5.1 Polymer Drug Carriers with Magnetic Nanoparticle Shells 50
  14.5.2 Mesoporous Silica Capped with Iron-oxide Nanoparticles 51
  14.5.3 Magnetic Single-crystal Shell Drug Nanocarriers 54

Downloaded on 01/09/2013 10:27:05.

Downloaded on 01/09/2013 10:27:05.

14.6 Magnetic-responsive Composite Drug-delivery Membranes 56
14.7 Conclusion 59
References 60

Chapter 15 Smart Drug Delivery from Silica Nanoparticles 63
Montserrat Colilla and María Vallet-Regí

15.1 Introduction 63
15.2 Multi-functionality of Mesoporous Silica Nanoparticles to Design Smart DDSs 66
- 15.2.1 Targeting Agents 66
- 15.2.2 Polymeric Coatings 68
- 15.2.3 Magnetic Nanoparticles 72
- 15.2.4 Stimuli-responsive Drug Delivery 75

15.3 Biocompatibility of Mesoporous Silica Nanoparticles 80
15.4 Future Prospects 81
References 82

Chapter 16 Smart Carbon Nanotubes 90
Gerard Tobias and Emmanuel Flahaut

16.1 Introduction 90
- 16.1.1 Carbon Nanotubes: Structure and Properties 90
- 16.1.2 Carbon Nanotubes in Drug Delivery 91

16.2 Functionalization of Carbon Nanotubes for Biomedical Applications 93
- 16.2.1 Covalent Functionalization 93
- 16.2.2 Non-covalent Functionalization 95

16.3 External Attachment of Drugs onto Carbon Nanotubes 96
- 16.3.1 Delivery of Doxorubicin with Carbon Nanotubes 96
- 16.3.2 Delivery of Platinum-based Drugs with Carbon Nanotubes 97
- 16.3.3 Delivery of Other Anticancer Drugs by Carbon Nanotubes 98
- 16.3.4 Delivery of Other Drugs by Carbon Nanotubes 99

Downloaded on 01/09/2013 10:27:05.

16.4 Encapsulation of Drugs Inside Carbon Nanotubes 100
- 16.4.1 Carbon Nanotubes as Nanocontainers 100
- 16.4.2 Drug Delivery with Filled Carbon Nanotubes 101

16.5 Toxicity and Environmental Impact of Carbon Nanotubes 104
- 16.5.1 Introduction to Toxicity of Carbon Nanotubes 104
- 16.5.2 Main Characteristics of Carbon Nanotubes in Terms of Toxicity Investigation 105
- 16.5.3 Biological Models 106
- 16.5.4 Inhalation 107
- 16.5.5 Contamination through the Skin 108
- 16.5.6 Translocation 108
- 16.5.7 Mechanisms of Protection and Elimination 108
- 16.5.8 Genotoxicity 109
- 16.5.9 Environmental Impact of Carbon Nanotubes 109

16.6 Conclusions 110

References 110

Chapter 17 Smart Layer-by-Layer Assemblies for Drug Delivery 117
Svetlana Pavlukhina and Svetlana Sukhishvili

17.1 Introduction 117

17.2 LbL Substrates and Templates 117

17.3 LbL Constituents and Architectures 119

17.4 Drug Incorporation Strategies within LbL Assemblies 123

17.5 Drug Release Strategies 124
- 17.5.1 Diffusion-controlled Release 124
- 17.5.2 Hydrolytic Degradation 125
- 17.5.3 pH-triggered Release 129
- 17.5.4 Salt-triggered Release 133
- 17.5.5 Electrochemical and Redox-activated Release 134
- 17.5.6 Temperature-triggered Release 136
- 17.5.7 Light-triggered Release 137
- 17.5.8 Magnetic Field-triggered Release 139
- 17.5.9 Ultrasound-triggered Release 140
- 17.5.10 Application of Biological Stimuli 141

17.6 LbL Interfacing Biology 142

Acknowledgements 144

References 144

Downloaded on 01/09/2013 10:27:05.

Chapter 18 pH- and Temperature-responsive Hydrogels in Drug Delivery **153**
Francesco Puoci and Manuela Curcio

18.1 Introduction 153
18.2 pH-responsive Hydrogels for Drug Delivery 155
 18.2.1 pH-responsive Microgels 156
 18.2.2 pH-responsive Nanogels 158
18.3 Temperature-responsive Hydrogels for Drug Delivery 161
 18.3.1 LCST Hydrogels 162
 18.3.2 UCST Hydrogels 168
18.4 Dually Responsive Hydrogels for Drug Delivery 170
18.5 Conclusion 173
Acknowledgements 174
Reference 174

Chapter 19 Elastin-like Hydrogels and Self-assembled Nanostructures for Drug Delivery **180**
José Carlos Rodríguez-Cabello, Israel González de Torre and Guillermo Pinedo

19.1 Introduction 180
19.2 Elastin-like Recombinamers (ELRs) 181
19.3 ELRs-based Drug-delivery Systems 183
 19.3.1 ELRs-based Hydrogels 184
 19.3.2 ELRs Nanoparticles 190
19.4 Conclusion and Future Perspectives 195
References 196

Chapter 20 Multiple Stimuli-responsive Hydrogels Based on α-Amino Acid Residues for Drug Delivery **199**
Mario Casolaro and Ilaria Casolaro

20.1 Introduction 199
20.2 Syntheses 203
20.3 Swelling Properties 204
 20.3.1 Effect of pH and Ions 204
 20.3.2 Effect of the Temperature 209
20.4 Drug Delivery from α-Amino Acid Hydrogels 211
 20.4.1 Loading and Release of Cisplatin 211
 20.4.2 Cytotoxicity of Cisplatin-loaded Hydrogels 214
 20.4.3 Loading and Release of Pilocarpine 217
 20.4.4 Cytotoxicity of Pilocarpine-loaded Hydrogels 220

Downloaded on 01/09/2013 10:27:05.

20.5 Outlook for the Future 221
20.6 Conclusion 224
References 225

Chapter 21 Molecularly Imprinted Hydrogels for Affinity-controlled and Stimuli-responsive Drug Delivery 228
C. Alvarez-Lorenzo, C. González-Chomón and A. Concheiro

21.1 Introduction 228
21.2 Molecular Imprinting Technology 229
21.3 Imprinted Hydrogels 235
  21.3.1 Affinity-controlled Release from Bioinspired Networks 235
  21.3.2 Competitive Displacement Release 240
  21.3.3 Hydrolytically Induced Drug Release 242
21.4 Stimuli-responsive Imprinted Networks 243
  21.4.1 Temperature-sensitive Imprinted Hydrogels 245
  21.4.2 pH-sensitive Imprinted Gels 249
  21.4.3 Light-responsive Imprinted Networks 251
21.5 Conclusions and Future Aspects 254
Acknowledgements 254
References 255

Chapter 22 Biomolecule-sensitive Hydrogels 261
Takashi Miyata

22.1 Introduction 261
22.2 Strategies for Designing Biomolecule-sensitive Hydrogels 262
22.3 Glucose-sensitive Hydrogels 264
  22.3.1 Glucose-sensitive Hydrogels Using Enzymatic Reaction 264
  22.3.2 Glucose-sensitive Hydrogels Using Phenylboronic Acid 266
  22.3.3 Glucose-sensitive Hydrogels Using Lectin 266
22.4 Protein-sensitive Hydrogels 270
  22.4.1 Enzyme-sensitive Hydrogels 270
  22.4.2 Antigen-sensitive Hydrogels 272
22.5 Biomolecule-sensitive Hydrogels Prepared by Molecular Imprinting 276
22.6 Biomolecule-sensitive Hydrogel Particles 279
22.7 Other Biomolecule-sensitive Hydrogels 282
22.8 Conclusion 285
References 285

Downloaded on 01/09/2013 10:27:05.

Chapter 23 Intelligent Surfaces for Cell and Tissue Delivery **290**
Hironobu Takahashi and Teruo Okano

23.1 Introduction 290
23.2 Overview of Polymeric Materials for Cell/Tissue Delivery 291
  23.2.1 Self-regulating Insulin Delivery System as a Substitute for Cell Transplantation 291
  23.2.2 Microencapsulation of Cells with Polymeric Membranes for Cell Delivery 292
  23.2.3 Scaffold-based Cell/Tissue Delivery in Tissue Engineering 293
23.3 The Intelligence of Thermo-responsive Polymers for Cell/Tissue Delivery 294
  23.3.1 Thermo-responsive Poly(*N*-isopropylacrylamide) 294
  23.3.2 Thermo-responsive Encapsulation of Cells for Cell Delivery 294
23.4 Thermo-responsive Surface for Cell Sheet-based Tissue Delivery 295
  23.4.1 Cell Sheet Engineering for Scaffold-free Cell/Tissue Delivery Systems 295
  23.4.2 Thermo-responsive Polymer Grafting on Cell Culture Substrates 295
  23.4.3 Cell Sheet-based Tissue Delivery in Regenerative Medicine 296
  23.4.4 Local Drug Release Technique with Cell Sheet Transplantation 298
  23.4.5 Micro-fabricated Thermo-responsive Surfaces for Delivery of Tissue-mimicking Cell Sheets 301
23.5 Conclusions 307
References 307

Chapter 24 Drug/Medical Device Combination Products with Stimuli-responsive Eluting Surface **313**
C. Alvarez-Lorenzo and A. Concheiro

24.1 Combination Products 313
24.2 Benefits of Combining Medical Devices and Drugs/Biological Products 316
24.3 Materials for Medical Devices 317
24.4 Procedures to Incorporate Drugs 318
  24.4.1 Compounding 318
  24.4.2 Impregnation Using a Swelling Solvent 319

24.4.3 Coating 320
24.4.4 Drug Chemically Bonded to the Surface 320
24.4.5 Polymer Grafting to the Device Surface 321
24.5 Responsive Surfaces for Drug Loading/Controlled Release 325
24.5.1 Polymers Grafted by Means of Chemical Initiators 325
24.5.2 Polymers and Networks Grafted Applying Radiation 329
24.5.3 Surface Modification Applying Plasma Techniques 339
24.6 Conclusions and Future Aspects 341
Acknowledgements 342
References 342

Subject Index **349**

Downloaded on 01/09/2013 10:27:05.

Downloaded on 01/09/2013 10:27:05.

Downloaded on 01/09/2013 10:27:05.

CHAPTER 13

Remotely Triggered Drug Release from Gold Nanoparticle-based Systems

EUN-KYUNG LIM,[a] KWANGYEOL LEE,[b]
YONG-MIN HUH[c] AND SEUNGJOO HAAM*[a]

[a] Department of Chemical and Bimolecular Engineering, Yonsei University, Seoul, 120-749, Republic of Korea; [b] Department of Chemistry, Korea University, Seoul, 136-701, Republic of Korea; [c] Department of Radiology, Yonsei University, Seoul, 120-752, Republic of Korea
*Email: haam@yonsei.ac.kr

13.1 Introduction

Non-specific delivery of drugs is accompanied by unwanted side effects such as drug-resistance and toxicity, mainly because the amount of drug that reaches the target site is much smaller than the administered dose. Enhancement of drug efficacy would require increasing the dose. Therefore, the concept of targeted drug delivery has been engendered by the necessity to improve the therapeutic efficiency and to reduce the side effects, and various drug-delivery approaches are being developed. In particular, nanoparticles can be surface-modified to enable the conjugation of drug molecules and to improve the solubility, the stability and the pharmacokinetics of drugs.[1–7] They can also take the form of a hollow container to load drug molecules in the center void. Nanoparticles can passively accumulate in tumor tissues to a higher extent than

RSC Smart Materials No. 3
Smart Materials for Drug Delivery: Volume 2
Edited by Carmen Alvarez-Lorenzo and Angel Concheiro
© The Royal Society of Chemistry 2013
Published by the Royal Society of Chemistry, www.rsc.org

Downloaded on 01/09/2013 10:27:05.

in normal tissues by enhanced permeability and retention (EPR) effect.[8–10] Tumor blood vessels are generally characterized by abnormalities such as a relatively high proportion of proliferating endothelial cells because of the rapid vascularization to provide oxygen and nutrients for fast-growing tumors. The combination of leaky vasculature and poor lymphatic drainage leads to accumulation of nanoparticles in the target site, and this passive tumor targeting by the EPR effect has been the mainstream strategy for the delivery of nanoparticle-based drug-delivery systems. Nanoparticles can be made much more target-specific by conjugation of targeting moieties such as antibodies or aptamers. This unprecedented targeting ability, which is unknown for conventional drugs, makes nanoparticles effectively deliver drugs to the target site, while significantly mitigating side effects.[11–17]

Recently, activatable nanoparticles have been designed to deliver drugs to the target sites at accurate timing or condition; these systems can control drug discharge by specific stimuli (external or internal) through chemical and/or physical changes. External stimuli such as temperature, light and magnetic field, and internal stimuli including pH and biological ions and molecules, are often used to trigger drug release or to induce physical or chemical effects leading to disease treatment.[13,18–25] Gold nanoparticles provide a great opportunity in this field due to their unique properties from size- and shape-dependent surface plasmon resonance. They are easily formed in various sizes and shapes with a great monodispersity, and most importantly they are non-toxic and biocompatible.[2,26–30] Gold nanoparticles can be heated by irradiating with NIR light and it is extremely easy to introduce targeting molecules, drugs and other biomolecules on their surface. These properties facilitate a variety of approaches for developing drug-delivery systems (DDSs) able to control drug release at remote sites.[2,28] In this chapter, we describe various types of gold nanoparticles useful for drug delivery as well as theranostic systems. Especially, we focus on activatable DDSs based on gold nanoparticles capable of triggering drug release by external or internal stimuli.

13.2 Gold Nanoparticle-based DDSs

Delivery systems for drugs, proteins, DNA and RNA based on gold nanoparticles are attracting great attention because of advantages such as simple synthesis, easily tunable size, facile surface modification, versatile conjugation with biomolecules and biocompatibility (Figure 13.1).[31–35] These features allow the loading of therapeutic agents or biomolecules by covalent or non-covalent conjugation.[35–49]

For tumor delivery, gold nanoparticles should be modified with molecules that target cancer-specific markers and strongly interact with receptors overexpressed on the cancer cells in order to accomplish active detection and enhanced delivery to the target site.[50–60] Proteins, peptides, nucleic acids

Downloaded on 01/09/2013 10:27:05.

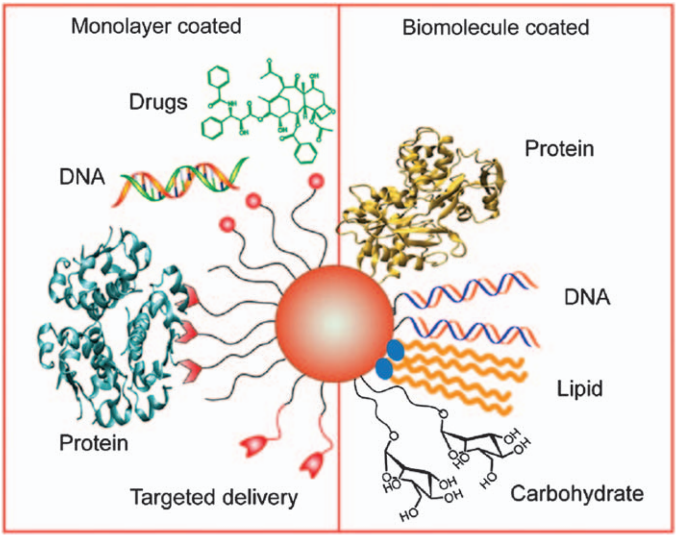

Figure 13.1 Scheme of the two AuNP surface structures commonly employed for drug delivery.
Reproduced from Ref. 32 with permission of Elsevier.

(aptamers), vitamins or carbohydrates are extensively employed as targeting moieties.[54,60] For example, doxorubicin (Dox)-loaded and folate-modified poly(ethyleneglycol) (PEG)-functionalized gold nanoparticles (FOL-PEG-gold nanoparticles) showed much higher toxicity for cancerous cells than for HFF cells, suggesting that these nanocarriers have high potential to be used in targeted cancer therapy.[61] The nanoscale size of gold nanoparticles with a high surface-to-volume ratio provides a versatile platform for attachment of a number of drugs through covalent and non-covalent interactions.[32] Chen *et al.*[62] conjugated methotrexate (MTX), as a chemotherapeutic agent, onto gold nanoparticles (Figure 13.2) and showed that the accumulation of MTX is faster and higher in tumor cells treated with MTX-gold nanoparticles than in those treated with free MTX. MTX-gold nanoparticles showed tumor growth suppression whereas MTX alone had no antitumor effect, indicating that MTX-gold nanoparticles are much more effective than free MTX in cancer treatment.[62] Similarly, antibacterial drug-capped gold nanoparticles showed good antibacterial effect against various strains of Gram-positive and Gram-negative bacteria, such as *S. aureus*, *M. luteus*, *E. coli* and *P. aeruginosa*.[35]

Gold nanoparticle-based systems, however, can be caught during circulation by the reticulo-endothelial (RES) system to accumulate in the liver and spleen, depending on their size and surface characteristics.[63–65] To avoid RES capture,

Downloaded on 01/09/2013 10:27:05.

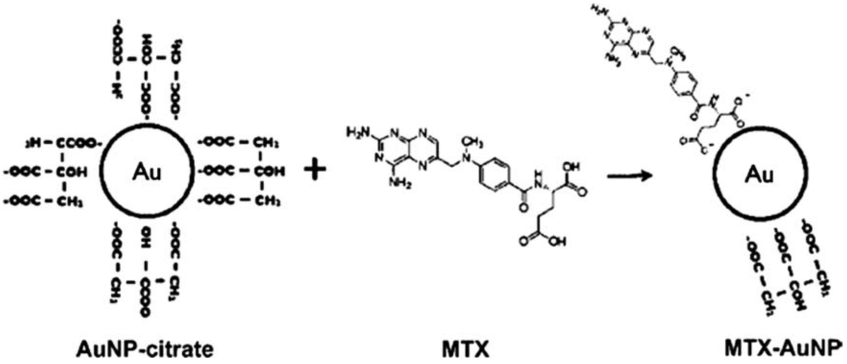
Au
+
MTX
Au
AuNP-citrate
MTX-AuNP

Figure 13.2 Conjugation of methotrexate (MTX) to the surface of an AuNP. Reproduced from Ref. 62 with permission of the American Chemical Society.

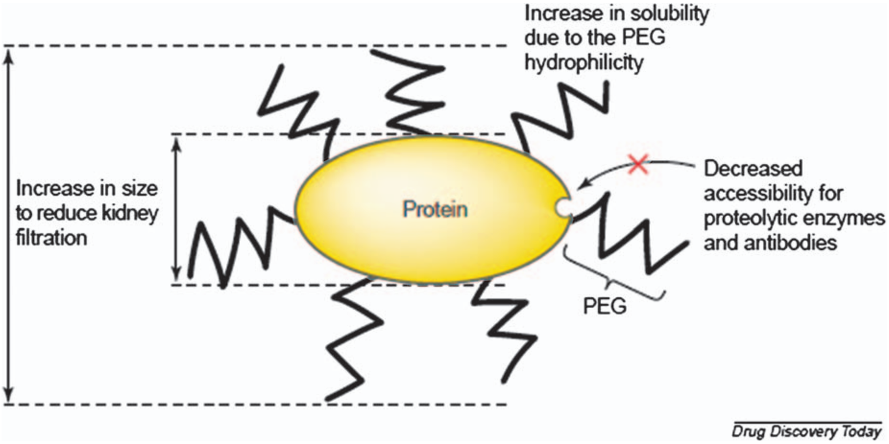
Increase in solubility due to the PEG hydrophilicity
Increase in size to reduce kidney filtration
Protein
Decreased accessibility for proteolytic enzymes and antibodies
PEG
Drug Discovery Today

Figure 13.3 Main advantages of the PEGylated proteins. The polymer, PEG, shields the protein surface from degrading agents by steric hindrance. Moreover, the increased size of the conjugate decreases the kidney clearance. Reproduced from Ref. 67 with permission of Elsevier.

hydrophilic polymers such as PEG are attached onto the surface of gold nanoparticles. It is well known that PEG creates a highly water-bound barrier resulting from hydrogen bonding between the oxygen atoms of PEG and water, and thereby the surface density and the chain length of PEG on the nanoparticle surface could prevent opsonization and, thus, MPS uptake (Figure 13.3).[58,59,66–68] PEGylated gold nanoparticles exhibit excellent stability under physiological conditions, minimal interaction with biomacromolecules

Downloaded on 01/09/2013 10:27:05.

and specific molecular recognition due to the steric hindrance. Therefore, hydrophobic dyes/drugs loaded inside the hydrophilic barrier are released only upon contact with the target cell.[66,68]

Gold nanoparticles (AuNP) can be stabilized by thiolates *via* strong Au-S bonds between weak acidic Au and the weak thiolate base as follows:[69,70]

$$(\mathrm{RS})_n\mathrm{AuNP} + m\mathrm{R'SH} \rightarrow (\mathrm{RS})_{n\text{-}m}(\mathrm{R'S})_m\mathrm{AUNP} + m\mathrm{RSH} \tag{13.1}$$

Using this approach, oligonucleotides, peptides, drugs and PEG can be incorporated onto gold nanoparticles.[49,59,71–73] Paciotti *et al.*[58] reported that PEG can be bonded to Au *via* Au-S bond-forming PEG-SH molecule and the resulting PEGylated Au nanoparticles exhibited an increased residence time in blood circulation (Figure 13.4). Other polymers have also been used to increase

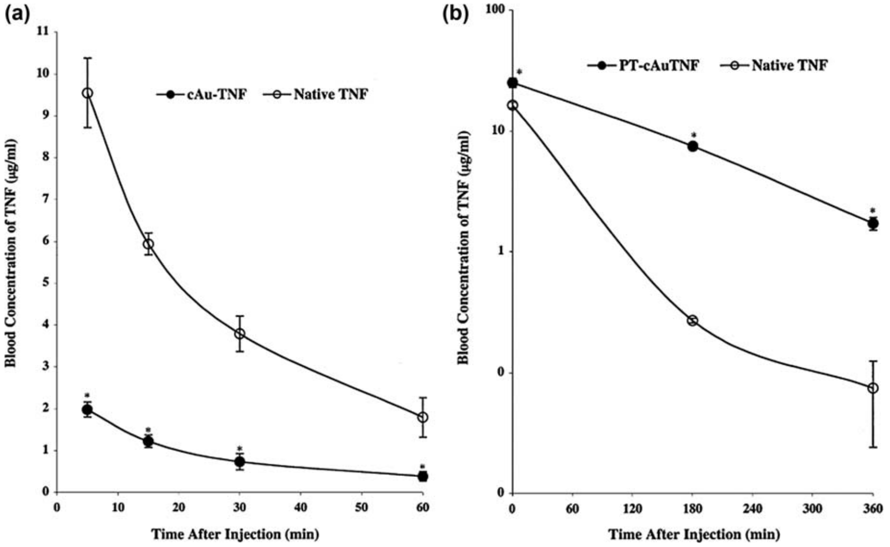

Figure 13.4 (a) Pharmacokinetic profiles of native tumor necrosis factor (TNF) and cAu-TNF vector in MC-38 tumor-burdened C57/BL6 mice ($n = 3$/group/time point), that were intravenously injected with 10 µg of either native TNF or cAu-TNF vector. At the indicated time points the mice were anesthetized and bled through the retro-orbital sinus, and the blood was diluted 1:1 with PBS containing $1\,\mathrm{mg\,mL^{-1}}$ heparin. TNF concentration was determined using an enzyme immunoassay. $*p < 0.05$ cAu-TNF *versus* native TNF. (b) Pharmacokinetic profiles of native TNF and PT-cAu-TNF vector in MC-38 tumor-burdened C57/BL6 mice. Mice were bled at 5, 180 and 360 min after the injection, and the blood samples were analyzed as described above. Data are presented as the mean ± SEM blood concentration from three mice/time point. $*p < 0.1$ $**p < 0.05$ *versus* native group.
Reproduced from Ref. 59 with permission of Informa Healthcare.

Downloaded on 01/09/2013 10:27:05.

the circulation time of nanoparticles. For example, a highly biocompatible drug carrier based on gold nanorods has been prepared by exchanging hexadecyltrimethylammonium bromide (CTAB) with polycaprolactone dithiol (PCL-diSH) and Pluronic F-127.[73]

Gold nanoparticles have also been actively investigated as an alternative nanocarrier for siRNA delivery,[74,75] due to their high stability in saline solution, easy binding of complementary nucleic acid and compatibility with cells and tissues.[49,54,74–95] Recently, thiol-modified antisense oligonucleotides were directly conjugated onto gold nanoparticles (Au-ASODN composites; ASNPs) to be used in regulation of protein expression in cells.[89] The affinity constants of ASNPs for complementary nucleic acid are much higher than that of unmodified oligonucleotides. The nucleic acids in ASNPs are less susceptible to degradation by nucleases, and hence ASNPs are more efficient intra-cellular oligonucleotide carriers than conventional transfection agents. Gold nanoparticles chemically modified with polymers and/or amino acids, including primary and quaternary amine moieties, can act as scaffolds for effective DNA binding with subsequent condensation.[43,74,75,92,96–101] In a recent study, siRNA–PEG/gold polyelectrolyte complexes were tested for intra-cellular delivery of siRNA. These amine-functionalized gold nanoparticles can electrostatically interact with PEGylated siRNA. The PEG moiety improves the stability of the nanoparticle dispersions by protecting them from uncontrollable aggregation, and favors a more efficient internalization into human prostate carcinoma cells compared to that achieved by polyelectrolyte complexes with siRNA alone.[74] Recently, formulations of uniform siRNA-loaded nanoparticles PEI/siRNA/PEI-AuNP were prepared by deposition of siRNA on gold nanoparticles *via* a layer-by-layer technique by ionic interaction.[54] The homogeneity in the size and the amount of siRNA loaded that can be achieved are greatly beneficial to siRNA-based therapy.[54,102]

Recent reports show that the polyvalent attachment of drugs and imaging agents onto DNA-gold nanoparticles results in enhanced cellular uptake and activity. Cytosine-phosphate-guanosine (CpG)-gold nanoparticles have been shown to act as polyvalent immunostimulatory nanoagents by inducing production of proinflammatory cytokines (TNF-α and IL-6) (Figure 13.5).[59] Moreover, 6-mercaptopurine-9-β-D-ribofuranoside (6-MPR) – the most widely utilized antileukemic and anti-inflammatory drugs – incorporated onto gold nanoparticles (6-MPR-gold nanoparticles) has shown a substantially increased antiproliferative effect against K-562 leukemia cells, compared to the drug in typically administered free form. This effect is attributed to an enhanced intracellular transport followed by the subsequent release in lysosomes.[47]

DNA-gold nanoparticles can also be used for the delivery of hydrophobic chemotherapeutic agents (Figure 13.6).[49] Lipid-DNA-gold nanoparticles appear as a hybrid-based gene-delivery system able to render better transfection efficiency and reduced cytotoxicity, by taking advantage of the features of both gold nanoparticles and liposomes as gene-delivery vehicles. These lipid-DNA-gold nanoparticle hybrid delivery systems require smaller lipid concentration to achieve low cytotoxicity with higher efficiency than a lipid-only delivery system.[88]

Downloaded on 01/09/2013 10:27:05.

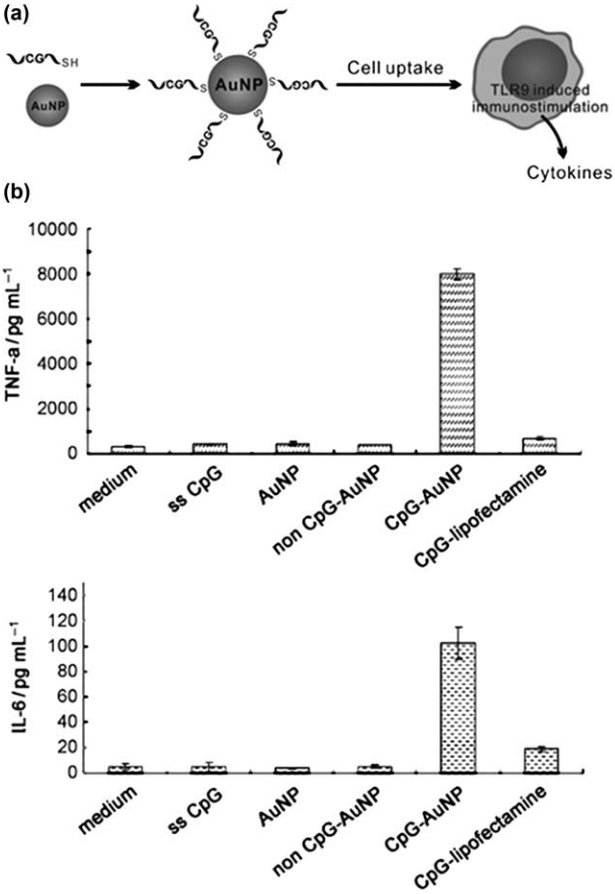

Figure 13.5 a) Assembly of CpG-conjugated AuNPs and their immunostimulatory effects, and b) CpG-AuNP conjugates stimulate the secretion of cytokines. RAW264.7 cells were treated with the indicated materials at a DNA concentration of 0.05 mM. An equal molar concentration of AuNPs was used as control. The concentrations of TNF-α and IL-6 in culture media were measured at 8 h (TNF-α) or 24 h (IL-6) by an ELISA method. Results are expressed as the mean ± SD of three determinations. Reproduced from Ref. 94 with permission of Wiley.

13.3 Activatable DDSs Based on Gold Nanoparticles

Stimuli-responsive DDSs are mainly designed to provide the drug concentration within its therapeutic window to target site. The internal and external stimuli include temperature, light, pH, specific enzymes activity and reactive oxygen species (ROS). The physical and chemical changes caused by the stimulus in the container may reversibly trigger the drug release.[20,87,103–105]

Downloaded on 01/09/2013 10:27:05.

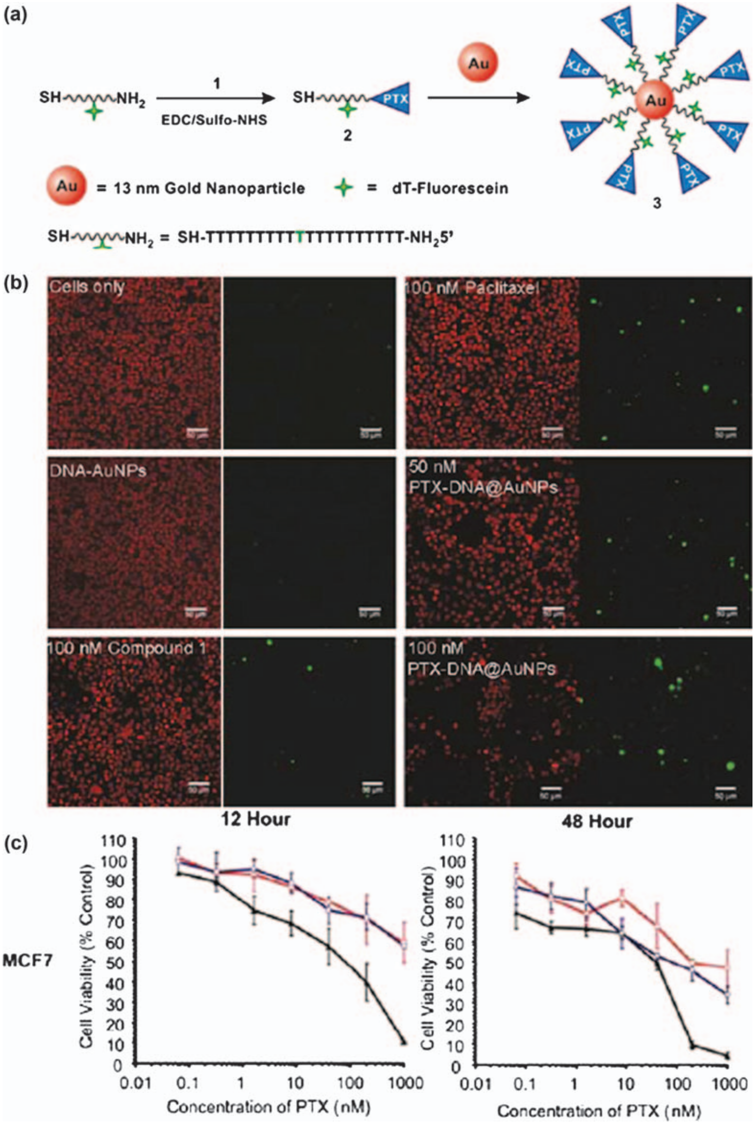

Figure 13.6 a) Synthesis of PTX-DNA@AuNP conjugates, b) TUNEL assay testing activity of PTX-DNA@AuNPs in MCF7 cells TUNEL (green) and counter-stain (red) images of cells left untreated, DNA-AuNPs, 10 nM of free paclitaxel and compound 1, and PTX-DNA@AuNPs at the equivalent paclitaxel concentrations of 50 and 100 nM. Scale bars correspond to 50 μm. After treatment by PTX-DNA@AuNPs for 48 h, significant numbers of TUNEL-positive cells and reduced populations are observed in both tested cell lines. c) Cytotoxicity profiles of PTX-DNA@AuNPs (black circles) at equivalent paclitaxel dose with MCF7 are present in the top, middle and bottom panels, respectively (n = 6).
Reproduced from Ref. 49 with permission of the American Chemical Society.

Downloaded on 01/09/2013 10:27:05.

13.3.1 pH-responsive Au-based DDSs

Tumors develop unique microenvironments with an extra-cellular pH more acidic (pH 5–6) than that found in blood and healthy tissues (pH 7.4), because the increased glycolysis and plasma membrane proton-pump activity leads to an enhanced production and release of lactic acid to the extra-cellular regions. The pH in endosome and lysosome is even at 5.0–5.5 (Figure 13.7).[23,106–115]

The pH-responsive drug carriers release drug in response to acidic condition due to: i) cleavage of linkages, such as hydrazone, between drug and the nanocarrier, or ii) change of internal structure (shrinking-swelling or protonation) (Figure 13.8).[116,117] For example, Au-P(LA-Dox)-b-PEG-OH/FA nanoparticles exhibited pH-triggered drug-release properties useful for tumor-targeted drug

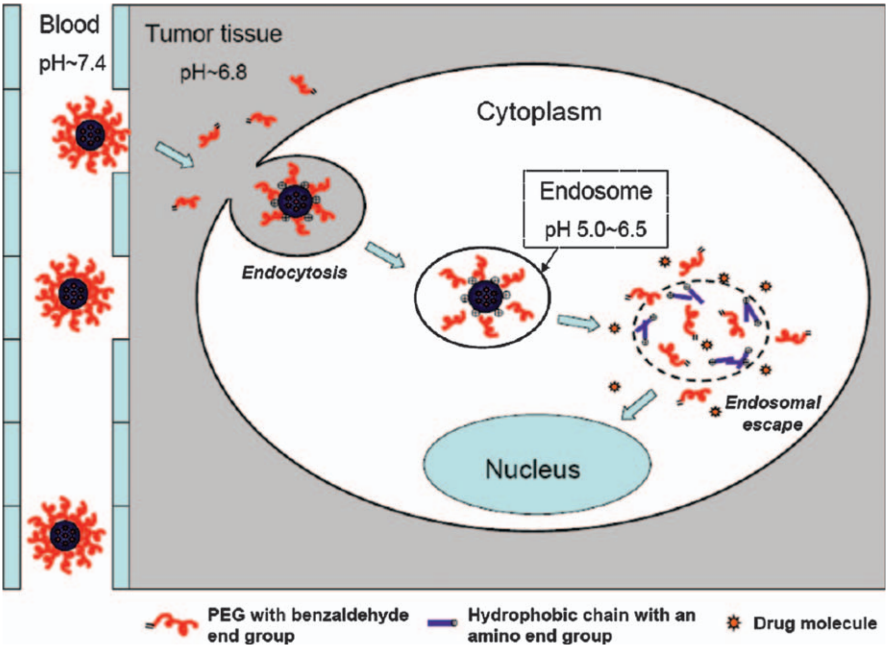

Figure 13.7 Scheme of a multi-functional drug carrier with tumor-targeting capability and intra-cellular delivery ability due to the pH-dependent progressive hydrolysis of a chemical bond, *e.g.* benzoic-imine, in the carrier-forming polymer. The particle has a PEG corona to obtain prolonged circulation in the blood. A suitable particle size would make the carrier accumulate in tumor tissue by means of the EPR effect. Under the weak acidic condition in a tumor, the particle surface becomes positively charged due to partial hydrolysis of the main linker, facilitating cellular uptake through adsorptive endocytosis. Subsequently, in the more acidic environment of the endosome, the complete hydrolysis of the main bond causes the particle to dissociate and destabilize the endosomal membrane to release the drugs rapidly into the cytoplasm. Reproduced from Ref. 106 with permission of the American Chemical Society.

Downloaded on 01/09/2013 10:27:05.

delivery. The anticancer drug doxorubicin (Dox) was covalently conjugated onto the hydrophobic inner shell by acid-cleavable hydrazone linkage (Figure 13.8a).[116] The rate and amount of Dox released from Au-P(LA-Dox)-b-PEG-OH/FA NPs were strongly influenced by pH condition; Dox was abruptly released when the hydrazone linkage was cleaved by hydrolysis in medium of pH 5.3 to 6.6. More than 90% of Dox was released at 48 h in pH 5.3 medium, while only ~15% of Dox was released for the same time at pH 7.4 (Figure 13.8b). These Au-P(LA-Dox)-b-PEG-OH/FA NPs showed high cytotoxicity against the 4T1 mouse mammary carcinoma cell-line with targeting ability, indicating their potential for chemotherapy.

13.3.2 Glutathione-mediated Au-based DDSs

The design of glutathione (GSH)-responsive DDSs relies on the dramatic difference between intra-cellular and extra-cellular GSH concentrations.[118–120] Disulfide linkages can be broken in the presence of intra-cellular GSH. Gold nanoparticles with thiol-modified drugs can exhibit exchange reactions between Au-S-R and glutathione, inducing the efficient dissociation of the drug from the gold nanoparticles.[31,32,121–124] However, it is difficult to control reactivity of the disulfide linkage, because this linkage exchange can also be caused by cysteines of serum proteins in the bloodstream. Recent studies have demonstrated GSH-mediated intra-cellular release of a thiolated hydrophobic dye (HSBDP) from monolayer-functionalized gold nanoparticles. The release rate of HSBDP was 8-fold greater than that of the tripeptide, suggesting that the exchange in thiol groups is responsible for releasing HSBDP ligands from the gold nanoparticles surface (Figure 13.9a,b).[125] In addition, a novel cyclodextrin-covered gold nanoparticle (AuNP) carrier has been developed for non-covalent encapsulation of an anticancer drug. The surface of the AuNPs was functionalized with cyclodextrin *via* disulfide linkages, and the cyclodextrin moieties formed pockets effective for loading of hydrophobic drugs (Figure 13.9c,d).[124]

13.3.3 Photo-active and/or Photodynamic Au-based DDSs

Recently, research efforts have been focused on developing light-sensitive systems for remote-controlled release of drugs.[2,32,69,70,73,126–136] General aspects on this topic can be consulted in Chapter 11. Light provides a highly orthogonal external stimulus, allowing spatiotemporal control of drug release. DDSs have been designed by conjugating with drugs and carriers *via* photo-cleavable bonds (Figure 13.10).[137–139] The drug is not active while attached to the carrier. Photo-irradiation causes the cleavage of the bonds and the drug is trigger-released.[2,137–140]

Gold nanoparticles (AuNPs) for photo-controlled release of 5-fluorouracil have been prepared by conjugating the drug to the particles (Au_PCFU) through a photoresponsive *o*-nitrobenzyl linkage. The Au_PCFU also contained a mixed monolayer of zwitterionic ligands that provided water

Downloaded on 01/09/2013 10:27:05.

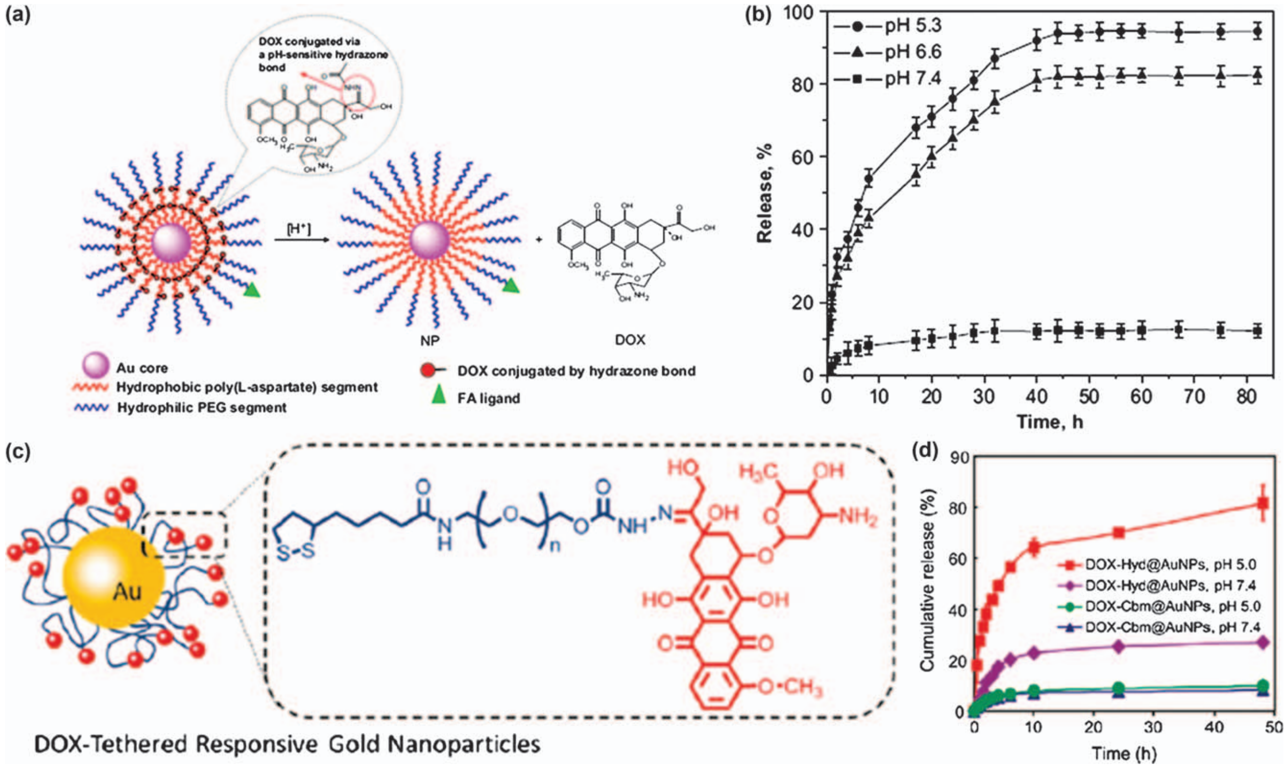

Figure 13.8 a) Schematic illustration of an Au-P(LA-Dox)-b-PEG-OH/FA NP and its pH-triggered drug release; b) Dox release profiles from the Au-P(LA-Dox)-b-PEG-OH/FA NPs at 37°C. Reproduced from Ref. 116 with permission of Elsevier; c) scheme of doxorubicin (Dox)-tethered responsive gold nanoparticles; and d) quantitative analyses of the *in vitro* release of doxorubicin at 37°C from doxorubicin-tethered AuNPs at pH 7.4 and in acetate buffer at pH 5.0.
Reproduced from Ref. 117 with permission of the American Chemical Society.

Downloaded on 01/09/2013 10:27:05.

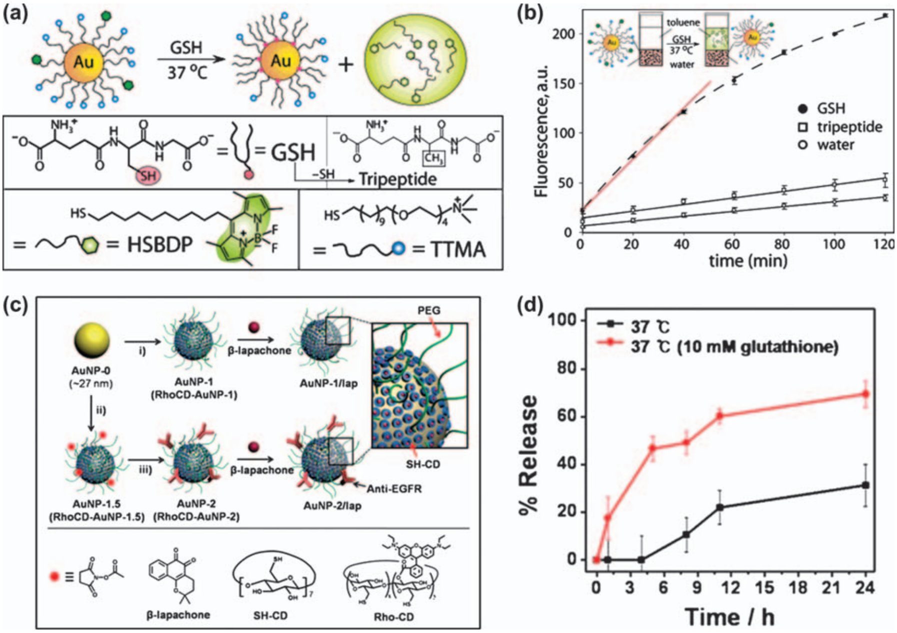
(a)
Au
GSH
37 °C
Au
+
SH
= GSH
-SH
Tripeptide
CH3
HS
= HSBDP
HS
= TTMA
(b)
toluene
GSH
37 °C
water
GSH
tripeptide
water
Fluorescence, a.u.
time (min)
0
50
100
150
200
0
20
40
60
80
100
120
(c)
AuNP-0
(~27 nm)
i)
AuNP-1
(RhoCD-AuNP-1)
β-lapachone
AuNP-1/lap
PEG
ii)
AuNP-1.5
(RhoCD-AuNP-1.5)
iii)
AuNP-2
(RhoCD-AuNP-2)
β-lapachone
AuNP-2/lap
Anti-EGFR
SH-CD
β-lapachone
SH-CD
Rho-CD
(d)
37 ℃
37 ℃ (10 mM glutathione)
% Release
Time / h
0
20
40
60
80
100
0
3
6
9
12
15
18
21
24

Figure 13.9 a) Schematic depiction of the GSH-mediated surface monolayer exchange reaction which triggers the release of the payload, in this case a hydrophobic dye, from AuNPs; b) *in vitro* release of HSBDP mediated by GSH. Samples of nanoparticles were incubated at 37 °C in pure water, in tripeptide (10 mM) and in GSH (10 mM), and the fluorescence spectra of the toluene phase were recorded. The fluorescence intensities at 507 nm of the toluene phase were plotted against the incubation time. The slopes were 2.5 (initial period), 0.33 and 0.24 for the GSH, tripeptide and water, respectively. Reproduced from Ref. 124 with permission of the American Chemical Society; c) functionalization of AuNP carriers with β-lapachone, using: i) SH-CD and mPEG-SH for AuNP-1 RhoCD and mPEG-SH for RhoCD-AuNP-1); ii) SH-CD, mPEG-SH and NHS-PEG-SH for AuNP-1.5 (RhoCD, mPEG-SH, NHS-PEG-SH or RhoCD-AuNP-1.5) and iii) anti-EGFR; and d) effect of glutathione concentration on the release of β-lapachone from AuNP-1/lap in HEPES buffer solution (pH 7.4). Reproduced from Ref. 125 with permission of the Royal Society of Chemistry.

solubility and prevented premature cellular uptake (Figure 13.10a).[138] Cell viability studies showed an IC_{50} of 0.7 μM upon irradiation of Au_PCFU, whereas no significant death was observed for cells treated with only light or with only Au_PCFU (Figure 13.10b).[138] In another example, the surface of the gold nanoparticles was functionalized with the photoresponsive linker thioundecyl-tetraethyleneglycolester-o-nitrobenzylethyldimethyl ammonium bromide (TUNA). The drug release rate could be easily controlled by low-power photo-irradiation under biocompatible and physiological conditions (Figure 13.10c–d).[139] Furthermore, the Au-S and the S-S bonds can be cleaved not only by an intra-cellular physiological thioldisulfide bond exchange

Downloaded on 01/09/2013 10:27:05.

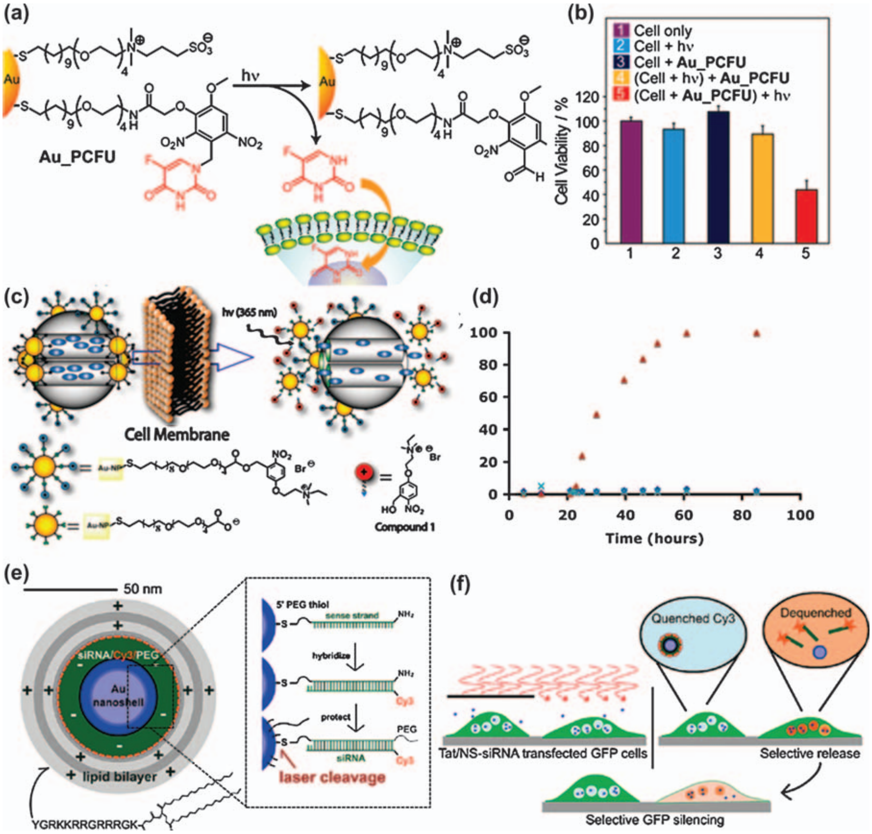
(a)
Au
hν
Au_PCFU
(b)
1 Cell only
2 Cell + hν
3 Cell + Au_PCFU
4 (Cell + hν) + Au_PCFU
5 (Cell + Au_PCFU) + hν
Cell Viability / %
120
100
80
60
40
20
0
1
2
3
4
5
(c)
hν (365 nm)
Cell Membrane
Compound 1
(d)
100
80
60
40
20
0
0
20
40
60
80
100
Time (hours)
(e)
50 nm
siRNA/Cy3/PEG
Au nanoshell
lipid bilayer
YGRKKRRGRRRGK
5' PEG thiol
sense strand
hybridize
protect
PEG
siRNA
Cy3
laser cleavage
(f)
Quenched Cy3
Dequenched
Tat/NS-siRNA transfected GFP cells
Selective release
Selective GFP silencing

Figure 13.10 a) Photochemical reaction of Au_PCFU and delivery of payload to cells, and b) effect of different conditions on the viability of MCF-7 cells. The concentration of Au_PCFU used was 1 µM, and the light exposure time was 20 min.; c) upon UV irradiation, the photolabile linker on the PR-AuNPs was cleaved, changing the surface charge property (zeta-potential) of these gold nanoparticles from positive to negative. The charge repulsion between the AuNPs and MSN would then uncap the mesopores and allow the release of guest molecules; d) controlled release profile of fluorescein from PR-AuNPs-MSN after UV irradiation (▲), in the dark (×) and from fluorescein-loaded MSN without the AuNPs cap (◆); e) diagram of Tat-lipid-coated NS-siRNA used for transfection and selective release of siRNA and scheme of the siRNA construct used; and f) scheme of gene knockdown using laser. Reproduced from Refs. 137–139 with permission of the American Chemical Society.

reaction, but also by applying sufficient energy. For example, the Au-S bond of siRNA conjugated to the surface of a gold nanoshell can be cleaved using NIR laser, enabling the controlled release of siRNA from the cell-internalized gold nanoshell and the gene (GFP) silencing effect (Figure 13.10e–f).[137]

Downloaded on 01/09/2013 10:27:05.

Photodynamic therapy (PDT) is another emerging, externally activatable, strategy for cancer treatment. Photosensitizer (PS) molecules are activated by UV or visible light, and this leads to the generation of oxidizing oxygen species (reactive oxygen species, ROS) in a confined space. The overproduced ROS causes a deleterious effect in cancer cells, by damaging DNA, RNA and protein.[2,141–145] PS molecules are inherently fluorescent and thus can be used for imaging. For this reason, PDT has recently been evaluated as a possible theranostic strategy for various forms of cancer.[141]Au-based PDT systems have also been developed by conjugation of hydrophobic photosensitizing agents, such as phthalocyamine (Pc), to PEGylated gold nanoparticles.[142] Again the PEG moieties inhibited colloidal aggregation in physiological condition, thus providing the stability of the nanoparticles dispersion. The *in vivo* results showed that AuNP-Pc4 accumulated into the target tumor within 2 hours without adverse effect, while the accumulation of free Pc4 molecules up to a therapeutically useful concentration usually takes about 2 days. This demonstrates the usefulness of Au nanoparticles in developing effective PDT systems. Furthermore, targeted PDT systems are also possible by attaching suitable targeting moieties to the nanoparticle surface and, importantly, by confining the light irradiation focus to the tumor site only. This would in turn lead to an efficient cancer therapy without damage to normal tissues (Figure 13.11).[141]

13.3.4 Photothermally Mediated Au-based DDSs

Photothermal therapy (hyperthermia) of cancer is an attractive therapeutic modality that consists in increasing the temperature (>43 °C) at a desired site by photo-irradiation.[32,69,70,73,126–136] Generated heat kills cancer cells within the localized irradiated area with minimal healthy tissue damage, unlike the conventional chemotherapy and the gene therapy. Furthermore, it could be utilized to control the release rate of drugs from delivery systems to reach a synergistic effect.[146]

13.3.4.1 Photothermal Effect of Gold Nanoparticles

The unique surface plasmon resonance (SPR) effects of gold nanoparticles, which converts absorbed light to heat, can be used for photothermal therapy.[70,73,126,128–130,133,147] Gold nanoparticles of various shapes absorb light in a broad spectrum range, from near UV to NIR. When a gold nanoparticle is irradiated, the absorbed light *via* SPR rapidly transforms into thermal energy, causing local temperature increases, which are high enough to produce irreversible damage to photogenes, cancer cells and tumor tissues. To be efficient as photothermal therapeutic agents, gold nanoparticles should have SPR in the NIR range in order that the light is minimally absorbed by biological molecules such as hemoglobin and water (Figure 13.12).[148] The wavelength of maximal absorption and the intensity of the SPR bands of the gold nanoparticles can be easily tailored by changing their shape, size, morphology and composition (Figure 13.13).[149]

Downloaded on 01/09/2013 10:27:05.

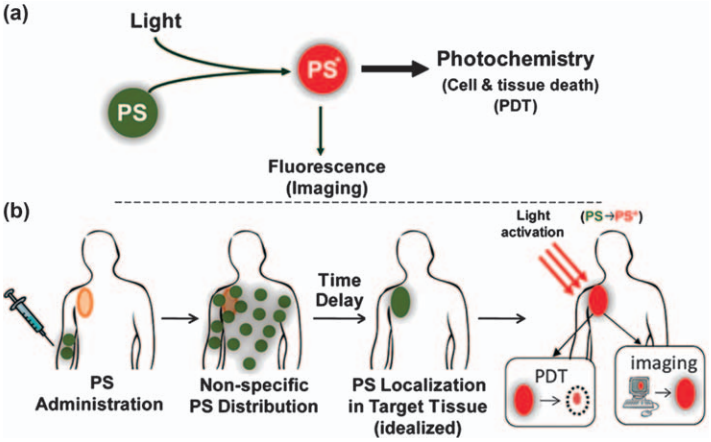

Figure 13.11 a) Schematic view of the photodynamic therapy (PDT) where PS is a photo-activatable multi-functional agent, which upon light activation can serve as both an imaging agent and a therapeutic agent, and b) sequence of administration, localization and light activation of the PS for PDT and for fluorescence imaging.
Reproduced from Ref. 141 with permission of the American Chemical Society.

There are already data about the feasibility of gold-nanorod (rod-shaped gold nanoparticle)-mediated NIR photothermal therapy for destruction of tumors.[132,149] The absorption peak of gold nanorods is easily tunable to the NIR region by varying their aspect ratio (length/width). Recently, Haam *et al.* developed thiolated dextran modified gold nanorods (DEX-GNRs) for targeted photothermal therapy, and demonstrated their ability ot kill target cells under NIR light irradiation.[70] When exposed to NIR laser 808 nm, the temperature of a DEX-GNRs solution increased from 24 °C to 48–52 °C. The *in vitro* experiments using NIR light showed a significant cell-killing efficacy, even with a low gold concentration and a low-power light source.

13.3.4.2 Photothermally Triggered Drug Release

Gold nanoparticles are largely used as activatable carriers with photothermal properties that can lead to a triggered release of the drug in a localized area. As mentioned earlier, gold nanoparticles can have a strong and tunable surface plasmon absorption in the NIR range, by which heat is generated for hyperthermal therapy of cancer.[32,69,70,73,126–136,147] Furthermore, induced heat can trigger the release drugs from gold nanoparticle-based drug carriers by changing the shape of the gold nanoparticles and by affecting the chemical and/or physical properties of the surface-bound moieties.[29,150–156] In particular, gold nanorods undergo shape transformation to spherical nanoparticles due to the induced heat after the absorption of NIR, which affects the binding of biomolecules conjugated to their surface (Figure 13.14).[150] Then, the release of

Downloaded on 01/09/2013 10:27:05.

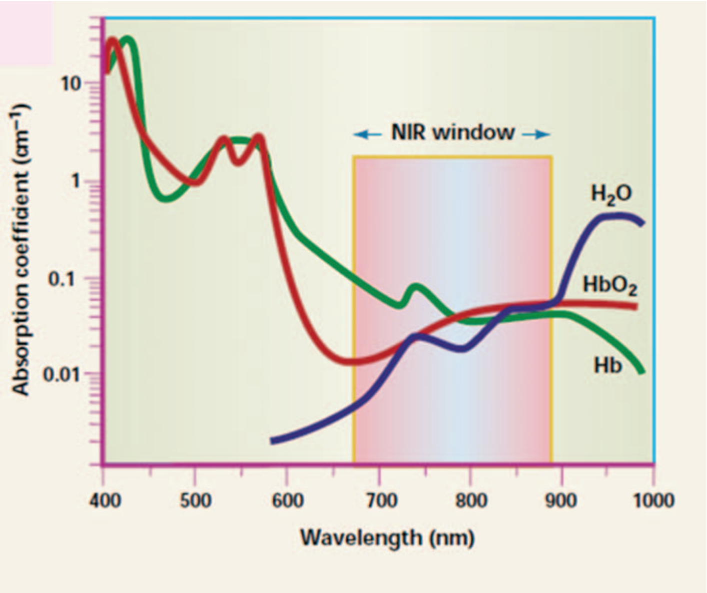

Figure 13.12 The NIR window is ideally suited for *in vivo* imaging because of the minimal light absorption by hemoglobin (<650 nm) and water (>900 nm). Reproduced from Ref. 148 with permission of Nature Publishing Groups.

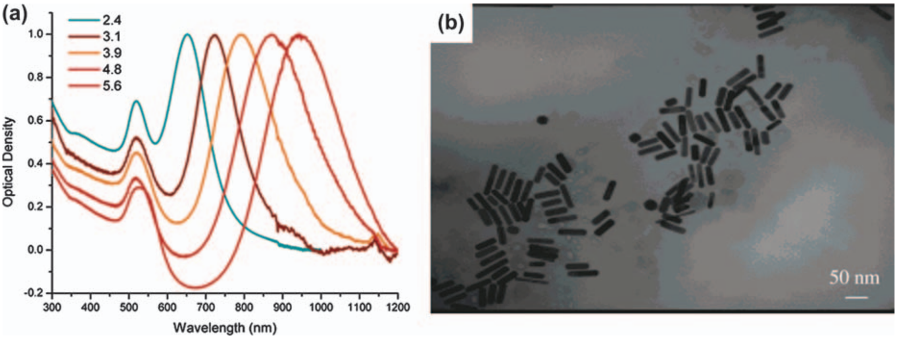

Figure 13.13 a) Surface plasmon absorption spectra of gold nanorods of different aspect ratio, and b) TEM image of nanorods of aspect ratio 3.9 (their absorption spectrum is shown as the orange curve in panel a). Reproduced from Ref. 149 with permission of the American Chemical Society.

siRNA bound *via* Au-S bond can be regulated by NIR irradiation; the changes in the shapes of the gold nanorods are accompanied by the dissociation of siRNA from Au.[29,134,155,156] Utilizing the Au nanorod shape change, two distinct DNA oligonucleotides can be selectively released from gold nanorods

Downloaded on 01/09/2013 10:27:05.

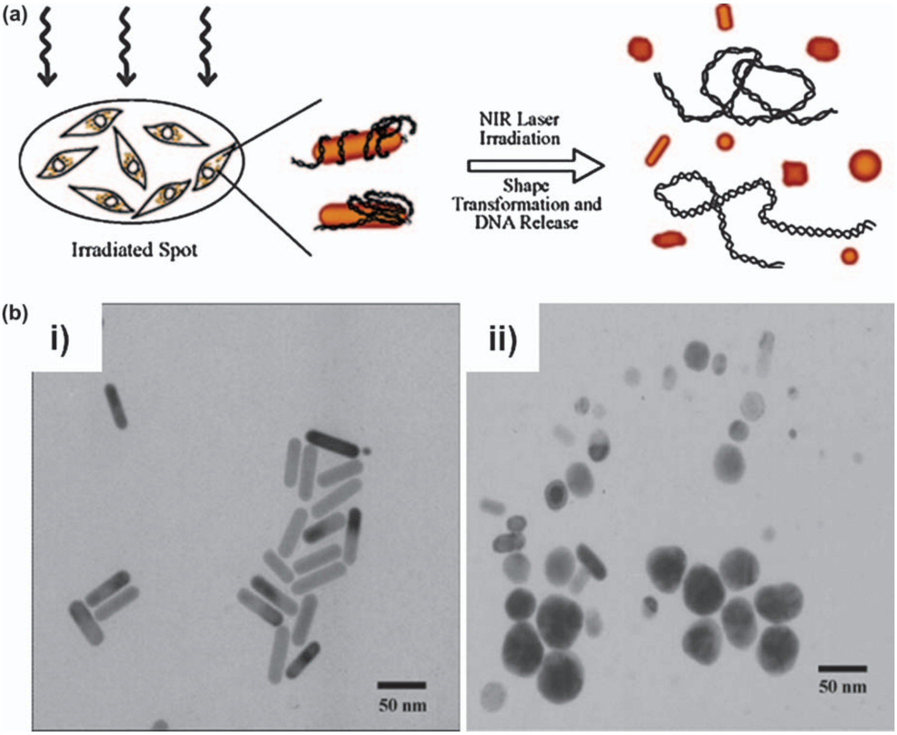

Figure 13.14 a) Scheme of the effect of NIR laser irradiation spot (3.5 mm in diameter) on cells containing EGFP-GNR conjugates (left). After laser irradiation, the gold nanorods of EGFP-GNR conjugates undergo a shape transformation that results in the release of EGFP DNA (right), and b) typical TEM images of EGFP-GNR conjugates i) before and ii) after irradiation with laser beam (79 μJ/pulse for 60 s).
Reproduced from Ref. 150 with permission of the American Chemical Society.

that melt under different wavelength light; namely *via* selective laser-induced melting of the nanorods. This strategy might be further developed for the realization of multiple-drug-delivery techniques (Figure 13.15).[154]

Gold nanoparticles can be coated with thermally responsive polymers that change their volume due to the heat induced by the NIR absorption. Specifically, drug molecules can be trapped inside a hollow Au container and the volume contraction of the thermally responsive polymer or liposome on the Au container may lead to the release of the drug.[20,157–175] Thermally responsive polymers used for this purpose exhibit a decreased water-solubility as the temperature increases, due to their characteristic of having lower critical solution temperature (LCST).[176–180] At lower temperature, water molecules form hydrogen bonds with hydrophilic segments of the polymer, enabling its dissolution in water. By contrast, at higher temperature, hydrophobic

Downloaded on 01/09/2013 10:27:05.

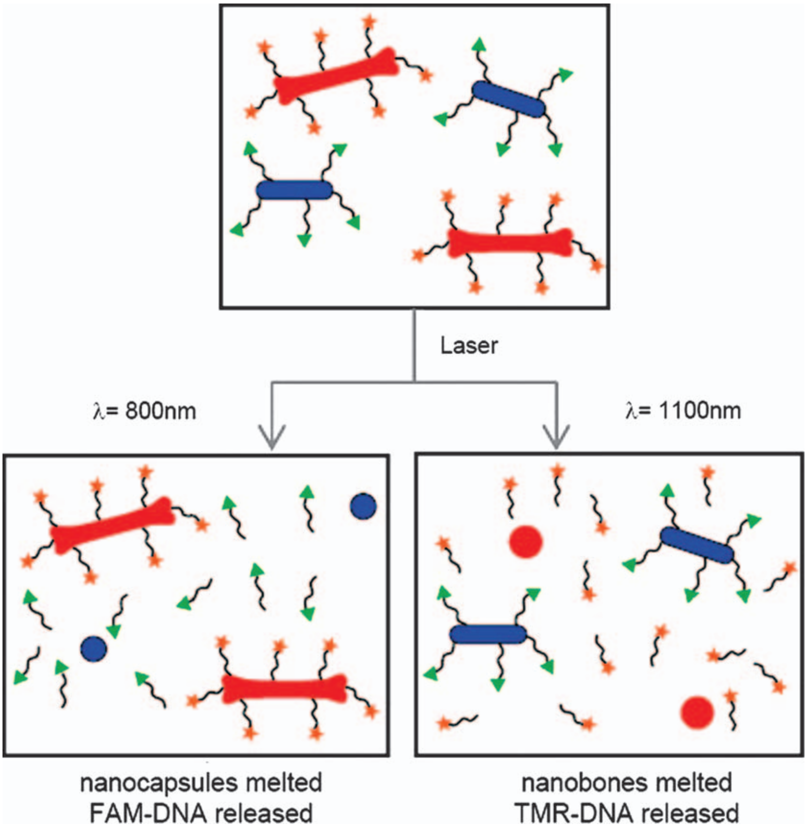

Figure 13.15 Overview of selective release after laser irradiation of DNA-conjugated nanocapsules (blue ovals) and nanobones (red bones). Exposure to $\lambda = 800$ nm irradiation (left) melts the nanocapsules, which then selectively release the DNA (labeled with FAM, green triangles). On the other hand, exposure to $\lambda = 1100$ nm irradiation (right) melts the nanobones, selectively releasing the DNA (labeled by TMR, orange stars).
Reproduced from Ref. 154 with permission of the American Chemical Society.

interactions between hydrophobic segments of the polymer become strengthened (Figure 13.16).[136]

Among many other temperature-responsive polymers, poly(*N*-isopropylacrylamide) (pNIPAAm) is the most extensively studied because its LCST is in the 25–32 °C range, *i.e.* near physiological temperature, and can be shifted to higher or lower temperatures by incorporating hydrophilic or hydrophobic segments.[158,162,173] Gold nanocages can be modified with various phase-change materials such as 1-tetradecanol or pNIPAAm for controlling the release applying NIR laser irradiation (Figure 13.17).[173] When these gold nanocages

Downloaded on 01/09/2013 10:27:05.

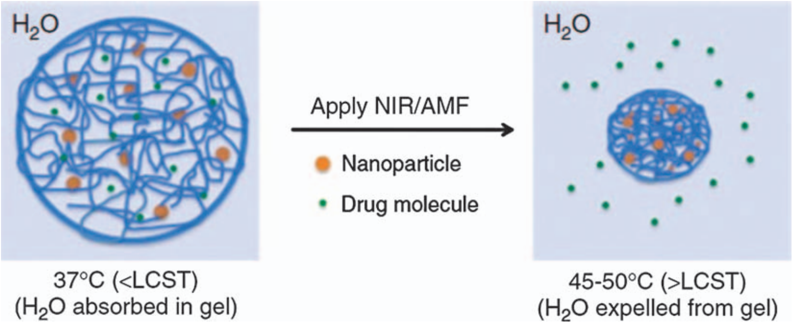
H_2O
Apply NIR/AMF
Nanoparticle
Drug molecule
H_2O
37°C (<LCST)
(H_2O absorbed in gel)
45-50°C (>LCST)
(H_2O expelled from gel)

Figure 13.16 Schematic view of the drug delivery from a temperature-responsive polymer with LSCT.
Reproduced from Ref. 136 with permission of Wiley.

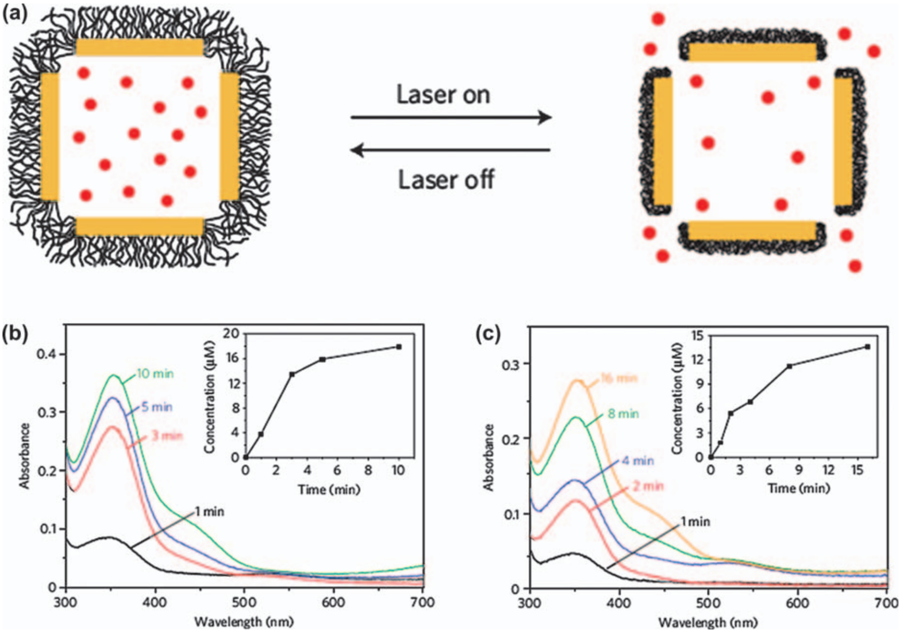

Figure 13.17 a) Schematic illustration of the drug release mechanism from AuNCs coated with a smart copolymer, and, below, absorption spectra of alizarin-PEG released from the copolymer-covered AuNCs b) by heating at 42 °C for 1, 3, 5 and 10 min and c) upon exposure to a pulsed NIR laser for 1, 2, 4, 8 and 16 min at 10 mW cm^{-2}. The insets show the accumulated concentrations of alizarin-PEG released from the AuNCs.
Reproduced from Ref. 173 with permission of Nature Publishing Group.

Downloaded on 01/09/2013 10:27:05.

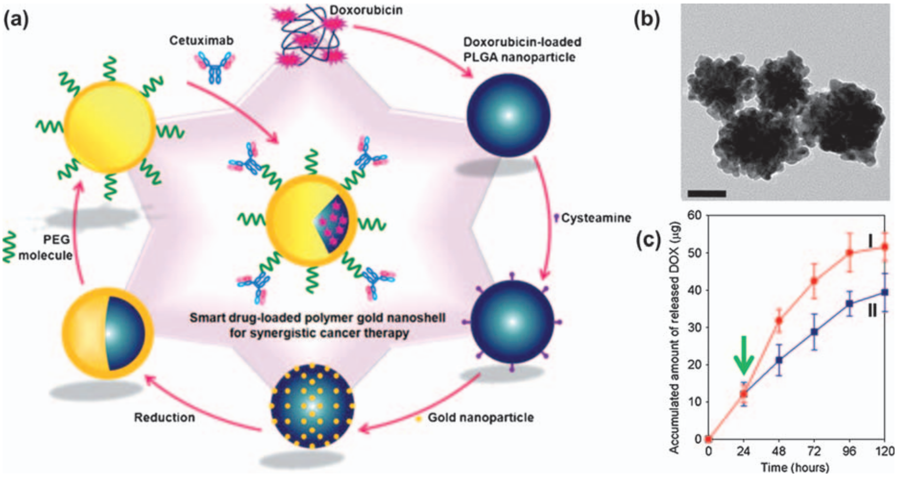
(a)
Doxorubicin
Cetuximab
Doxorubicin-loaded PLGA nanoparticle
PEG molecule
Cysteamine
Smart drug-loaded polymer gold nanoshell for synergistic cancer therapy
Reduction
Gold nanoparticle
(b)
(c)
Accumulated amount of released DOX (μg)
0
10
20
30
40
50
60
I
II
0
24
48
72
96
120
Time (hours)

Figure 13.18 a) Scheme of the preparation of multi-functional drug-loaded gold nanoshells (DPGNS) for synergistic cancer therapy, b) TEM images of DPGNS (scale bar: 50 nm) and c) Dox release patterns from I) DPGNS and II) DPGNS irradiated by NIR laser (green arrow indicates onset of NIR irradiation with 820 nm and 15 W cm^{-2} for 10 min) for 120 h. Reproduced from Ref. 172 with permission of Wiley.

are NIR irradiated matching their localized surface plasmon resonance (LSPR) peak, the absorbed light is converted into heat. As the temperature increases above the LCST, modified polymer chains collapse and thus the drugs are released. With the laser turned off, the polymer chains change back to the extended form due to a lowered temperature, and drug release is interrupted. Furthermore, the drug release can be controlled by the on-and-off modulation of the external NIR laser.

Recently, Haam *et al.*[172] developed a novel nanotherapeutic system consisting of a poly(lactic-co-glycolic acid) (PLGA) matrix containing Dox as a chemotherapeutic agent and a gold over-layer on a polymer matrix (Figure 13.18). This system provides synergistic therapeutic effects as compared with the effects of the individual treatments. Upon irradiation with NIR light, Dox can be abruptly released from polymer matrix leading to high cancer cell toxicity as well as to photothermal ablation because of the increase in the local temperature.

13.3.5 Enzymatically Activated Au-based DDSs

Specific enzymatic cleavage of protein substrates, typically peptide cleavage, can be utilized for effective drug delivery. Drug can be trigger-released from the carrier by the cleavage of specific peptide sequence in the presence of

Downloaded on 01/09/2013 10:27:05.

specific enzymes (cathepsin B, caspase) or protein antigens such as matrix metalloproteinases (MMPs), when drug and drug carrier are conjugated *via* peptide linker.[21,31,32,111,181–184] MMPs can be used as important cancer-specific markers, because of their overproduction in the cancer cells. General aspects on enzyme-responsive DDSs can be found in Chapter 9.

An enzymatic-sensitive gold nanosystem (AuNP) has been prepared through the anchoring of fluorescence dye (Cy5.5) molecules *via* MMP-cleavable peptide substrate to gold nanoparticles.[182] The Cy5.5 dyes are self-quenched by the Fluorescent Resonance Energy Transfer (FRET) mechanism. In the presence of MMPs, a high Cy5.5-fluorescence signal intensity is caused by the de-quenching effect that occurs after the cleavage of the Cy5.5-substrate peptide sequence by MMPs.[182] These systems might be further developed into activatable DDSs by using a drug instead of fluorescent dye (Cy5.5).

13.4 Gold Nanoparticle-based Theranostic Systems

Gold nanoparticles have been studied as imaging contrast agents due to their optical properties.[129,185–187] Recently, gold nanoparticles have received much attention as computed tomography (CT) imaging agents because they exhibit an enhanced absorption coefficient, which results in 2.7 times higher contrast than typical iodine agents.[131,187–189] Enzyme-sensitive or peptide specific probes based on optical properties of gold nanoparticles have been developed for tumor localization and metastasis imaging. Xia *et al.*[184,190] modified the surface of gold nanocages with dye-labeled peptides, which are cleavable by MMPs (Figure 13.19). When no MMP-2 protease was present, the emission from the dye was quenched by the above-mentioned FRET process. Upon exposure to the active MMPs, dye molecules were released from the gold nanocages resulting in strong fluorescence emission.[184,190]

Gold nanorods can be also utilized as photothermal agents, in addition to the roles of optical tracers or imaging contrast agents (absorbance, photoacoustic or optical coherence tomography imaging).[2,20,32,127,129,151,185,190–200] Integrin-targeting gold nanorods have been evaluated both *in vitro* and *in vivo* regarding their utility in NIR optical imaging for glioblastoma, demonstrating their theranostic ability. Gold nanorods were employed as absorption imaging and photothermal therapeutic agents with excellent tumor-targeting ability (Figure 13.20).[129] It appears that gold nanoparticles are well suited for theranostic systems enabling diagnosis and therapy simultaneously, which can serve as optical tracers or contrast agents, kill cancer cells through the photothermal effect, and furthermore remotely control drug release by an external stimulus.[129]

Downloaded on 01/09/2013 10:27:05.

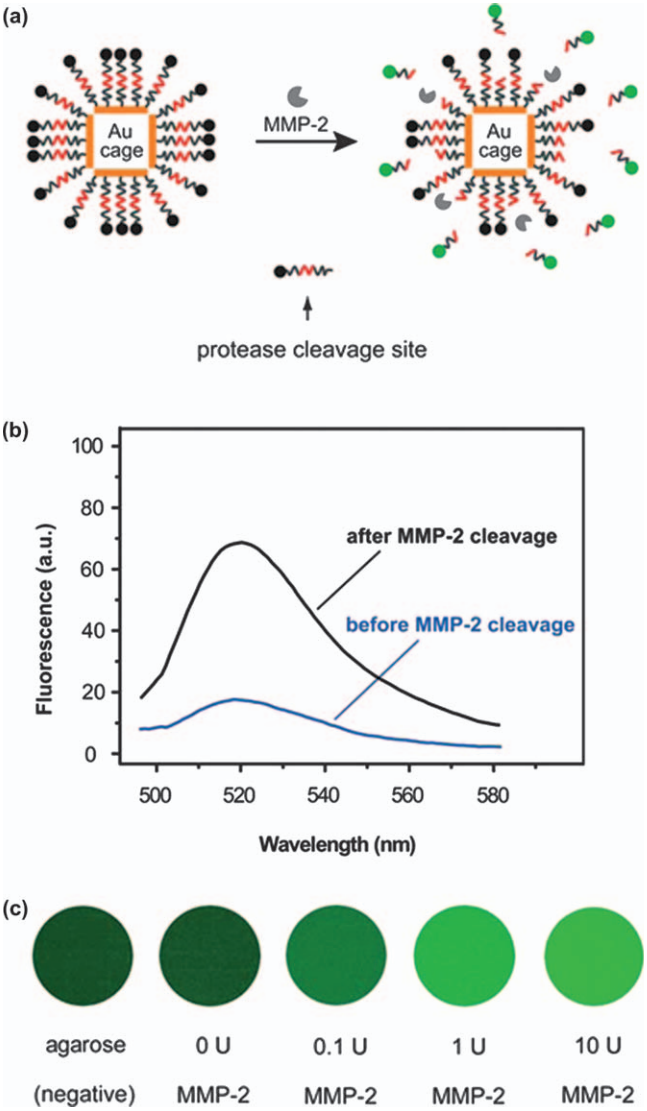

Figure 13.19 a) Scheme of a dual probe that could be activated by an enzyme. The probe comprises Au nanocage and fluorescent dyes linked together through enzyme-cleavable peptides. The fluorescence emission from the dyes is initially quenched by the Au nanocage. Upon the cleavage of the peptide and the release of the dye from the surface of the Au nanocage, the fluorescence of the dye is recovered, b) fluorescence spectra of FITC–GKGPLGVRGC–cage before and after incubation for 3 h with 1 U (72 ng mL^{-1}) MMP-2 at 37 °C, and c) fluorescence of FITC-GKGPLGVRGC-cage incubated with different concentrations of MMP-2 at 37 °C for 12 h. The sample was mixed with 1.5% agarose to form a gel for imaging.
Reproduced from Ref.184 with permission of the Royal Society of Chemistry.

Downloaded on 01/09/2013 10:27:05.

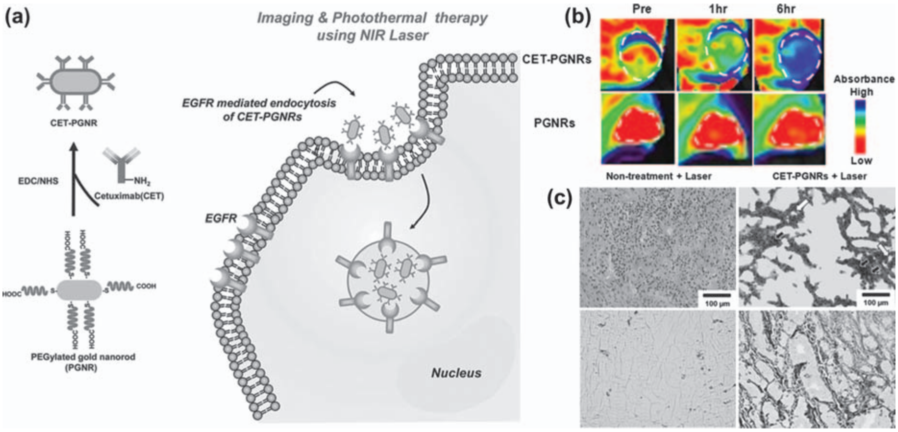
(a)
Imaging & Photothermal therapy using NIR Laser
CET-PGNR
EDC/NHS
Cetuximab(CET)
NH_2
HOOC
COOH
PEGylated gold nanorod (PGNR)
EGFR mediated endocytosis of CET-PGNRs
EGFR
Nucleus
(b)
Pre
1hr
6hr
CET-PGNRs
PGNRs
Absorbance
High
Low
Non-treatment + Laser
CET-PGNRs + Laser
(c)
100 μm
100 μm

Figure 13.20 a) Scheme of cetuximab-conjugated polyethylene glycol PEGylated gold nanorods (CET-PGNRs) as near-infrared (NIR) absorption imaging and photothermal therapeutic agents for treatment of epithelial cancer, b) *in vivo* non-invasive NIR absorption images of real-time tumor specificity of CET-PGNRs and PGNRs. The white dotted circles indicate the tumor regions, and c) Hematoxylin and silver staining eosin. Tumor region was characterized by extensive pyknosis (black arrows) and cell vacuolization (white arrows) only in mice treated with CET-PGNRs after NIR laser irradiation ($\lambda = 808$ nm, 1 W cm^{-2}). Reproduced from Ref. 129 with permission of Wiley.

13.5 Conclusions and Outlook

Gold nanoparticles are promising materials for designing advanced DDSs with the following major advantages: i) the ease with which their sizes and shapes can be controlled during synthesis, ii) the well-established protocols for surface modification with therapeutic agents and biological molecules such as targeting moieties, and iii) the photothermal effect. Gold nanoparticles can further serve as optical tracers or contrast agents for a variety of imaging and diagnostic techniques due to their unique optical properties. Furthermore, gold nanoparticle-based DDSs can regulate the release of drugs by various triggering (external or internal) stimuli, which can facilitate an effective drug delivery to the target site, while reducing unwanted side effects such as toxicity and drug-resistance. The theranostic potential of these systems may greatly contribute to a better understanding of the disease and to the development of more effective cures.

References

1. U. Bilati, E. Allemann and E. Doelker, *Eur. J. Pharm. Sci.*, 2005, **24**, 67.
2. B. Duncan, C. Kim and V. M. Rotello, *J. Control. Release*, 2010, **148**, 122.

3. S. Jin and K. Ye, *Biotechnol. Prog.*, 2007, **23**, 32.
4. M. Shi, K. Ho, A. Keating and M. S. Shoichet, *Adv. Funct. Mater.*, 2009, **19**, 1689.
5. R. Singh and J. W. Lillard Jr., *Exp. Mol. Pathol.*, 2009, **86**, 215.
6. V. P. Torchilin, *Adv. Drug Deliver. Rev.*, 2006, **58**, 1532.
7. O. Veiseh, J. W. Gunn and M. Zhang, *Adv. Drug Deliver. Rev.*, 2010, **62**, 284.
8. Y. Matsumura and H. Maeda, *Cancer Res.*, 1986, **46**, 6387.
9. N. Nasongkla, E. Bey, J. Ren, H. Ai, C. Khemtong, J. S. Guthi, S. F. Chin, A. D. Sherry, D. A. Boothman and J. Gao, *Nano Lett.*, 2006, **6**, 2427.
10. K. T. Oh, H. Yin, E. S. Lee and Y. H. Bae, *J. Mater. Chem.*, 2007, **17**, 3987.
11. S. K. Balasubramanian, J. Jittiwat, J. Manikandan, C. N. Ong, L. E. Yu and W. Y. Ong, *Biomaterials*, 2010, **31**, 2034.
12. D. Pissuwan, T. Niidome and M. B. Cortie, *J. Control. Release*, 2011, **149**, 65.
13. K. Sato, K. Yoshida, S. Takahashi and J. Anzai, *Adv. Drug Deliver. Rev.*, 2011, **63**, 809.
14. D. Shi, N. M. Bedford and H. S. Cho, *Small*, 2011, **7**, 2549.
15. C. Sun, J. S. Lee and M. Zhang, *Adv. Drug Deliver. Rev.*, 2008, **60**, 1252.
16. J. D. Byrne, T. Betancourt and L. Brannon-Peppas, *Adv. Drug Deliver. Rev.*, 2008, **60**, 1615.
17. O. Veiseh, J. W. Gunn and M. Zhang, *Adv. Drug Deliver. Rev.*, 2010, **62**, 284.
18. M. Delcea, H. Mohwald and A. G. Skirtach, *Adv. Drug Deliver. Rev.*, 2011, **63**, 730.
19. N. Graf and S. J. Lippard, *Adv. Drug Deliver. Rev.*, 2012, **64**, 993.
20. T. Kim, Y. M. Huh, S. Haam and K. Lee, *J. Mater. Chem.*, 2010, **20**, 8194.
21. R. D. la Rica, D. Aili and M. M. Stevens, *Adv. Drug Deliver. Rev.*, 2012.
22. F. Meng, Z. Zhong and J. Feijen, *Biomacromolecules*, 2009, **10**, 197.
23. S. M. Moghimi, A. C. Hunter and J. C. Murray, *FASEB J.*, 2005, **19**, 311.
24. M. S. Shim and Y. J. Kwon, *Adv. Drug Deliver. Rev.*, 2012, 64 1043.
25. V. Vergaro, F. Scarlino, C. Bellomo, R. Rinaldi, D. Vergara, M. Maffia, F. Baldassarre, G. Giannelli, X. Zhang, Y. M. Lvov and S. Leporatti, *Adv. Drug Deliver. Rev.*, 2011, **63**, 847.
26. D. N. Heo, D. H. Yang, H. J. Moon, J. B. Lee, M. S. Bae, S. C. Lee, W. J. Lee, I. C. Sun and I. K. Kwon, *Biomaterials*, 2012, **33**, 856.
27. E. Jang, E. K. Lim, J. Choi, J. Park, Y. J. Huh, J. S. Suh, Y. M. Huh and S. Haam, *Cryst. Growth Des.*, 2012, **12**, 37.
28. A. Kumar, H. Ma, X. Zhang, K. Huang, S. Jin, J. Liu, T. Wei, W. Cao, G. Zou and X. J. Liang, *Biomaterials*, 2012, **33**, 1180.
29. D. Pissuwan, T. Niidome and M. B. Cortie, *J. Control. Release*, 2011, **149**, 65.
30. Y. Xia, W. Li., C. M. Cobley, J. Chen, X. Xia, Q. Zhang, X. Yang, E. C. Cho and P. K. Brown, *Accounts. Chem. Res.*, 2011, **44**, 914.

Downloaded on 01/09/2013 10:27:05.

Downloaded on 01/09/2013 10:27:05.

31. S. Rana, A. Bajaj, R. Mout and V. M. Rotello, *Adv. Drug Deliver. Rev.*, 2012, **64**, 200.
32. P. Ghosh, G. Han, M. De, C. K. Kim and V. M. Rotello, *Adv. Drug Deliver. Rev.*, 2008, **60**, 1307.
33. J. D. Gibson, B. P. Khanal and E. R. Zubarev, *J. Am. Chem. Soc.*, 2007, **129**, 11653.
34. J. R. Hwu, Y. S. Lin, T. Josephrajan, M. H. Hsu, F. Y. Cheng, C. S. Yeh, W. C. Su and D. B. Shieh, *J. Am. Chem. Soc.*, 2009, **131**, 66.
35. A. Nirmala Grace and K. Pandian, *Colloid Surface. A*, 2007, **297**, 63.
36. J. M. Bergen, H. A. von Recum, T. T. Goodman, A. P. Massey and S. H. Pun, *Macromol. Biosci.*, 2006, **6**, 506.
37. G. L. Burygin, B. N. Khlebtsov, A. N. Shantrokha, L. A. Dykman, V. A. Bogatyrev and N. G. Khlebtsov, *Nanoscale Res. Lett.*, 2009, **4**, 794.
38. P. J. S. Chakraborty, S. Dey, V. Shanker, Z. A. Ansari, S. P. Singh and P. Chakrabarti, *J. Colloid Interface Sci.*, 2011, **355**, 402.
39. Y. H. Chen, C. Y. Tsai, P. Y. Huang, M. Y. Chang, P. C. Cheng, C.;H. Chou, D. H. Chen, C. R. Wang, A. L. Shiau and C. L. Wu, *Mol. Pharmaceut.*, 2007, **4**, 713.
40. L. Hosta, M. Pla-Roca, J. Arbiol, C. Lopez-Iglesias, J. Samitier, L. J. Cruz, M. J. Kogan and F. Albericio, *Bioconjugate Chem.*, 2009, **20**, 138.
41. J. R. Hwu, Y. S. Lin, T. Josephrajan, M. H. Hsu, F. Y. Cheng, C. S. Yeh, W. C. Su and D. B. Shieh, *J. Am. Chem. Soc.*, 2009, **131**, 66.
42. B. K. Jena and C. R. Raj, *Biosens. Bioelectron.*, 2008, **23**, 1285.
43. H. M. Joshi, D. R. Bhumkar, K. Joshi, V. Pokharkar and M. Sastry, *Langmuir*, 2006, **22**, 300.
44. C. K. Kim, P. Ghosh, C. Pagliuca, Z. J. Zhu, S. Menichetti and V. M. Rotello, *J. Am. Chem. Soc.*, 2009, **131**, 1360.
45. X. Li, J. Guo, J. Asong, M. A. Wolfert and G. J. Boons, *J. Am. Chem. Soc.*, 2011, **133**, 11147.
46. V. S. Murthy, J. N. Cha, G. D. Stucky and M. S. Wong, *J. Am. Chem. Soc.*, 2004, **126**, 5292.
47. P. Podsiadlo, V. A. Sinani, J. H. Bahng, N. W. S. Kam, J. Lee and N. A. Kotov, *Langmuir*, 2008, **24**, 568.
48. Y. Shen, E. Jin, B. Zhang, C. J. Murphy, M. Sui, J. Zhao, J. Wang, J. Tang, M. Fan, E. V. Kirk and W. J. Murdoch, *J. Am. Chem. Soc.*, 2010, **132**, 4259.
49. X. Q. Zhang, X. Xu, R. Lam, D. Giljohann, D. Ho and C. A. Mirkin, *ACS Nano*, 2011, **5**, 6962.
50. B. Asadishad, M. Vossoughi and I. Alemzadeh, *Ind. Eng. Chem. Res.*, 2010, **49**, 1958.
51. J. M. Bergen, H. A. von Recum, T. T. Goodman, A. P. Massey and S. H. Pun, *Macromol. Biosci.*, 2006, **6**, 506.
52. G. L. Burygin, B. N. Khlebtsov, A. N. Shantrokha, L. A. Dykman, V. A. Bogatyrev and N. G. Khlebtsov, *Nanoscale Res. Lett.*, 2009, **4**, 794.

Downloaded on 01/09/2013 10:27:05.

53. S. Dhar, W. L. Daniel, D. A. Giljohann, C. A. Mirkin and S. J. Lippard, *J. Am. Chem. Soc.*, 2009, **131**, 14652.
54. M. Y. Lee, S. J. Park, K. Park, K. S. Kim, H. Lee and S. K. Hahn, *ACS Nano*, 2011, **5**, 6138.
55. C. A. J. Lin, T. Y. Yang, C. H. Lee, S. H. Huang, R. A. Sperling, M. Zanella, J. K. Li, J. L. Shen, H. H. Wang, H. I. Yeh, W. J. Parak and W. H. Chang, *ACS Nano*, 2009, **3**, 395.
56. S. Manju and K. Sreenivasan, *J. Colloid Interface Sci.*, 2012, **368**, 144.
57. S. M. Moghimi, A. C. Hunter and J. C. Murray, *Pharmacol. Rev.*, 2001, **53**, 283.
58. G. F. Paciotti, D. G. I. Kingston and L. Tamarkin, *Drug Dev. Res.*, 2006, **67**, 47.
59. G. F. Paciotti, L. Myer, D. Weinreich, D. Goia, N. Pavel, R. E. McLaughlin and L. Tamarkin, *Drug Deliv.*, 2004, **11**, 169.
60. A. G. Tkachenko, H. Xie, D. Coleman, W. Glomm, J. Ryan, M. F. Anderson, S. Franzen and D. L. Feldheim, *J. Am. Chem. Soc.*, 2003, **125**, 4700.
61. B. Asadishad, M. Vossoughi and I. Alemzadeh, *Ind. Eng. Chem. Res.*, 2010, **49**, 1958.
62. Y. H. Che, C. Y. Tsai, P. Y. Huang, M. Y. Chang, P. C. Cheng, C.H. Chou, D. H. Chen, C. R. Wang, A. L. Shiau and C. L. Wu, *Mol. Pharmaceut.*, 2007, **4**, 713.
63. X. Gao, Y. Cui, R. M. Levenson, L. W. Chung and S. Nie, *Nat. Biotechnol.*, 2004, **22**, 969.
64. J. R. Hwu, Y. S. Lin, T. Josephrajan, M. H. Hsu, F. Y. Cheng, C. S. Yeh, W. C. Su and D. B. Shieh, *ACS Nano*, 2010, **4**, 4559.
65. V. Torchilin, *Adv. Drug Deliver. Rev.*, 2011, **63**, 131.
66. A. Kopwitthaya, K. T. Yong, R. Hu, I. Roy, H. Ding, L. A. Vathy, E. J. Bergey and P. N. Prasad, *Nanotechnology*, 2010, **21**, 315101.
67. Y. F. Li and C. Chen, *Small*, 2011, **7**, 2965.
68. T. Niidome, M. Yamagata, Y. Okamoto, Y. Akiyama, H. Takahashi, T. Kawano, Y. Katayama and Y. Niidome, *J. Control. Release*, 2006, **114**, 343.
69. E. Boisselier and D. Astruc, *Chem. Soc. Rev.*, 2009, **38**, 1759.
70. R. Choi, J. Yang, J. Choi, E. K. Lim, E. Kim, J. S. Suh, Y. M. Huh and S. Haam, *Langmuir*, 2010, **26**, 17520.
71. M. C. Franchini, J. Ponti, R. Lemor, M. Fournelle, F. Broggi and E. Locatelli, *J. Mater. Chem.*, 2010, **20**, 10908.
72. X. Li, D. Liu and Z. Wang, *Biosens. Bioelectron.*, 2011, **26**, 2329.
73. E. Kim, J. Yang, J. Choi, J. S. Suh, Y. M. Huh and S. Haam, *Nanotechnology*, 2009, **20**, 365602.
74. S. H. Lee, K. H. Bae, S. H. Kim, K. R. Lee and T. G. Park, *Int. J. Pharm.*, 2008, **364**, 94.
75. Y. Lee, S. H. Lee, J. S. Kim, A. Maruyama, X. Chen and T. G. Park, *J. Control. Release*, 2011, **155**, 3.

Downloaded on 01/09/2013 10:27:05.

76. M. Ahmed, Z. Deng, S. Liu, R. Lafrenie, A. Kumar and R. Narain, *Bioconjugate. Chem.*, 2009, **20**, 2169.
77. A. C. Bonoiu, S. D. Mahajan, H. Ding, I. Roy, K. T. Yong, R. Kumar, R. Hu, E. J. Bergey, S. A. Schwartz and P. N. Prasad, *P. Natl. Acad. Sci. USA*, 2009, **106**, 5546.
78. A. Elbakry, A. Zaky, R. Liebl, R. Rachel, A. Goepferich and M. Breunig, *Nano Lett.*, 2009, **9**, 2059.
79. P. S. Ghosh, C. K. Kim, G. Han, N. S. Forbes and V. M. Rotello, *ACS Nano*, 2008, **2**, 2213.
80. G. Han, C. T. Martin and V. M. Rotello, *Chem. Biol. Drug. Des.*, 2006, **67**, 78.
81. C. Hu, Q. Peng, F. Chen, Z. Zhong and R. Zhuo, *Bioconjugate Chem.*, 2010, **21**, 836.
82. H. Jaganathan and A. Ivanisevic, *J. Mater. Chem.*, 2011, **21**, 939.
83. J. S. Lee, J. J. Green, K. T. Love, J. Sunshine, R. Langer and D. G. Anderson, *Nano Lett.*, 2009, **9**, 2402.
84. D. Li, P. Li, G. Li, J. Wang and E. Wang, *Biomaterials*, 2009, **30**, 1382.
85. Y. Liu and S. Franzen, *Bioconjugate Chem.*, 2008, **19**, 1009.
86. C. M. McIntosh, E. A. Esposito, A. K. Boal, J. M. Simard, C. T. Martin and V. M. Rotello, *J. Am. Chem. Soc.*, 2001, **123**, 7626.
87. G. Qiao, L. Zhuo, Y. Gao, L. Yu, N. Li and B. Tang, *Chem. Commun.*, 2011, **47**, 7458.
88. W. K. Rhim, J. S. Kim and J. M. Nam, *Small*, 2008, **4**, 1651.
89. N. L. Rosi, D. A. Giljohann, C. S. Thaxton, A. K. Lytton-Jean, M. S. Han and C. A. Mirkin, *Science*, 2006, **312**, 1027.
90. K. K. Sandhu, C. M. McIntosh, J. M. Simard, S. W. Smith and V. M. Rotello, *Bioconjugate Chem.*, 2002, **13**, 3.
91. V. Sokolova and M. Epple, *Angew. Chem. Int. Ed.*, 2008, **47**, 1382.
92. M. Stobiecka and M. Hepel, *Biomaterials*, 2011, **32**, 3312.
93. M. Thomas and A. M. Klibanov, *P. Natl. Acad. Sci. USA*, 2003, **100**, 9138.
94. M. Wei, N. Chen, J. Li, M. Yin, L. Liang, Y. He, H. Song, C. Fan and Q. Huang, *Angew. Chem. Int. Ed.*, 2012, **51**, 1202.
95. J. K. Wong, S. P. Yip and T. M. Lee, *Small*, 2012, **8**, 214.
96. B. K. Jena and C. R. Raj, *Biosens. Bioelectron.*, 2008, **23**, 1285.
97. J. S. Lee, J. J. Green, K. T. Love, J. Sunshine, R. Langer and D. G. Anderson, *Nano Lett.*, 2009, **9**, 2402.
98. C. C. Chen, C. H. Hsu and P. L. Kuo, *Langmuir*, 2007, **23**, 6801.
99. P. S. Ghosh, C. K. Kim, G. Han, N. S. Forbes and V. M. Rotello, *ACS Nano*, 2008, **2**, 2213.
100. C. Hu, Q. Peng, F. Chen, Z. Zhong and R. Zhuo, *Bioconjugate Chem.*, 2010, **21**, 836.
101. T. Niidome, K. Nakashima, H. Takahashi and Y. Niidome, *Chem. Commun.*, 2004, 1978.
102. A. Elbakry, A. Zaky, R. Liebl, R. Rachel, A. Goepferich and M. Breunig, *Nano Lett.*, 2009, **9**, 2059.

Downloaded on 01/09/2013 10:27:05.

103. D. A. Fluri, C. Kemmer, M. Daoud-El Baba and M. Fussenegger, *J. Control. Release*, 2008, **131**, 211.
104. E. Gullotti and Y. Yeo, *Mol. Pharm.*, 2009, **6**, 1041.
105. D. Pornpattananangkul, S. Olson, S. Aryal, M. Sartor, C. M. Huang, K. Vecchio and L. Zhang, *ACS Nano*, 2010, **4**, 1935.
106. C. Ding, J. Gu, X. Qu and Z. Yang, *Bioconjugate Chem.*, 2009, **20**, 1163.
107. J. R. Casey, S. Grinstein and J. Orlowski, *Nat. Rev. Mol. Cell Biol.*, 2010, **11**, 50.
108. J. Z. Du, X. J. Du, C. Q. Mao and J. Wang, *J. Am. Chem. Soc.*, 2011, **133**, 17560.
109. L. E. Gerweck and K. Seetharaman, *Cancer Res.*, 1996, **56**, 1194.
110. T. Goda, Y. Goto and K. Ishihara, *Biomaterials*, 2010, **31**, 2380.
111. E. Gullotti and Y. Yeo, *Mol. Pharmaceut.*, 2009, **6**, 1041.
112. H. Mok, J. W. Park and T. G. Park, *Bioconjugate Chem.*, 2008, **19**, 797.
113. Y. Shen, E. Jin, B. Zhang, C. J. Murphy, M. Sui, J. Zhao, J. Wang, J. Tang, M. Fan, E. V. Kirk and W. J. Murdoch, *J. Am. Chem. Soc.*, 2010, **132**, 4259.
114. F. Zhan, W. Chen, Z. Wang, W. Lu, R. Cheng, C. Deng, F. Meng, H. Liu and Z. Zhong, *Biomacromolecules*, 2011, **12**, 3612.
115. L. Zhou, R. Cheng, H. Tao, S. Ma, W. Guo, F. Meng, H. Liu, Z. Liu and Z. Zhong, *Biomacromolecules*, 2011, **12**, 1460.
116. M. Prabaharan, J. J. Grailer, S. Pilla, D. A. Steeber and S. Gong, *Biomaterials*, 2009, **30**, 6065.
117. F. Wang, Y. C. Wang, S. Dou, M. H. Xiong, T. M. Sun and J. Wang, *ACS Nano*, 2011, **5**, 3679.
118. M. E. Anderson, *Chem. Biol. Interact.*, 1998, **111–112**, 1.
119. D. P. Jones, J. L. Carlson, J. Vino, C. Mody, J. Cai, M. J. Lynn and J. P. Sternberg, *Free Radic. Biol. Med.*, 2000, **28**, 625.
120. H. Sies, *Free Radic. Biol. Med.*, 1999, **27**, 916.
121. X. J. Cai, H. Q. Dong, W. J. Xia, H. Y. Wen, X. Q. Li, J. H. Yu, Y. Y. Li and D. L. Shi, *J. Mater. Chem.*, 2011, **21**, 14639.
122. R. Hong, G. Han, J. M. Fernandez, B. J. Kim, N. S. Forbes and V. M. Rotello, *J. Am. Chem. Soc.*, 2006, **128**, 1078.
123. A. N. Koo, H. J. Lee, S. E. Kim, J. H. Chang, C. Park, C. Kim, J. H. Park and S. C. Lee, *Chem. Commun.*, 2008, 6570.
124. C. Park, H. Youn, H. Kim, T. Noh, Y. H. Kook, E. T. Oh, H. J. Park and C. Kim, *J. Mater. Chem.*, 2009, **19**, 2310.
125. R. Hong, G. Han, J. M. Fernandez, B. J. Kim, N. S. Forbes and V. M. Rotello, *J. Am. Chem. Soc.*, 2006, **128**, 1078.
126. R. Bardhan, W. Chen, C. Perez-Torres, M. Bartels, R. M. Huschka, L. L. Zhao, E. Morosan, R. G. Pautler, A. Joshi and N. J. Halas, *Adv. Funct. Mater.*, 2009, **19**, 3901.
127. J. Chen, M. Yang, Q. Zhang, E. C. Cho, C. M. Cobley, C. Kim, C. Glaus, L. V. Wang, M. J. Welch and Y. Xia, *Adv. Funct. Mater.*, 2010, **20**, 3684.

Downloaded on 01/09/2013 10:27:05.

128. J. Chen, D. Wang, J. Xi, L. Au, A. Siekkinen, A. Warsen, Z. Y. Li, H. Zhang, Y. Xia and X. Li, *Nano Lett.*, 2007, **7**, 1318.
129. J. Choi, J. Yang, D. Bang, J. Park, J. S. Suh, Y. M. Huh and S. Haam, *Small*, 2012, **8**, 746.
130. J. Choi, J. Yang, E. Jang, J. S. Suh, Y. M. Huh, K. Lee and S. Haam, *Anti-cancer Agent Me.*, 2011, **11**, 953.
131. P. Huang, L. Bao, C. Zhang, J. Lin, T. Luo, D. Yang, M. He, Z. Li, G. Gao, B. Gao, S. Fu and D. Cui, *Biomaterials*, 2011, **32**, 9796.
132. X. Huang, W. Qian, I. H. El-Sayed and M. A. El-Sayed, *Lasers Surg. Med.*, 2007, **39**, 747.
133. J. Kang, J. Yang, J. Lee, S. J. Oh, S. Moon, H. J. Lee, S. C. Lee, J.H. Son, D. Kim, K. Lee, J. S. Suh, Y. M. Huh and S. Haam, *J. Mater. Chem.*, 2009, **19**, 2902.
134. W. Lu, G. Zhang, R. Zhang, L. G. Flores 2nd, Q. Huang, J. G. Gelovani and C. Li, *Cancer Res.*, 2010, **70**, 3177.
135. D. Pissuwan, S. M. Valenzuela and M. B. Cortie, *Trends Biotechnol.*, 2006, **24**, 62.
136. L. E. Strong and J. L. West, *Wires. Nanomed. Nanobi.*, 2011, **3**, 307.
137. S. S. Agasti, A. Chompoosor, C. C. You, P. Ghosh, C. K. Kim and V. M. Rotello, *J. Am. Chem. Soc.*, 2009, **131**, 5728.
138. G. B. Braun, A. Pallaoro, G. Wu, D. Missirlis, J. A. Zasadzinski, M. Tirrell and N. O. Reich, *ACS Nano*, 2009, **3**, 2007.
139. J. L. Vivero-Escoto, I. I. Slowing, C. W. Wu and V. S. Y. Lin, *J. Am. Chem. Soc.*, 2009, **131**, 3462.
140. G. Han, C. C. You, B. J. Kim, R. S. Turingan, N. S. Forbes, C. T. Martin and V. M. Rotello, *Angew. Chem. Int. Ed.*, 2006, **118**, 3237.
141. J. P. Celli, B. Q. Spring, I. Rizvi, C. L. Evans, K. S. Samkoe, S. Verma, B. W. Pogue and T. Hasan, *Chem. Rev.*, 2010, **110**, 2795.
142. Y. Cheng, J. D. Meyers, A. M. Broome, M. E. Kenney, J. P. Basilion and C. Burda, *J. Am. Chem. Soc.*, 2011, **133**, 2583.
143. D. C. Hone, P. I. Walker, R. Evans-Gowing, S. FitzGerald, A. Beeby, I. Chambrier, M. J. Cook and D. A. Russell, *Langmuir*, 2002, **18**, 2985.
144. M. Misawa and J. Takahashi, *Nanomedicine*, 2011, **7**, 604.
145. K. R. Weishaupt, C. J. Gomer and T. J. Dougherty, *Cancer Res.*, 1976, **36**, 2326.
146. J. You, R. Zhang, G. Zhang, M. Zhong, Y. Liu, C. S. Van Pelt, D. Liang, W. Wei, A. K. Sood and C. Li, *J. Control. Release*, 2012, **158**, 319.
147. J. Lee, J. Yang, H. Ko, S. J. Oh, J. Kang, J. H. Son, K. Lee, S. W. Lee, H. G. Yoon, J. S. Suh, Y. M. Huh and S. Haam, *Adv. Funct. Mater.*, 2008, **18**, 1.
148. R. Weissleder, *Nat. Biotechnol.*, 2001, **19**, 316.
149. X. Huang, I. H. El-Sayed, W. Qian and M. A. El-Sayed, *J. Am. Chem. Soc.*, 2006, **128**, 2115.
150. C. C. Chen, Y. P. Lin, C. W. Wang, H. C. Tzeng, C. H. Wu, Y. C. Chen, C. P. Chen, L. C. Chen and Y. C. Wu, *J. Am. Chem. Soc.*, 2006, **128**, 3709.

151. H. C. Huang, S. Barua, G. Sharma, S. K. Dey and K. Rege, *J. Control. Release*, 2011, **155**, 344.
152. H. Huang, S. Barua, D. B. Kay and K. Rege, *ACS Nano*, 2009, **3**, 2941.
153. T. R. Kuo, V. A. Hovhannisyan, Y. C. Chao, S. L. Chao, S. J. Chiang, S. J. Lin, C. Y. Dong and C. C. Chen, *J. Am. Chem. Soc.*, 2010, **132**, 14163.
154. A. Wijaya, S. B. Schaffer, I. G. Pallares and K. Hamad-Schifferli, *ACS Nano*, 2009, **3**, 80.
155. S. E. Lee, G. L. Liu, F. Kim and L. P. Lee, *Nano Lett.*, 2009, **9**, 562.
156. J. Xie, S. Lee and X. Chen, *Adv. Drug Deliver. Rev.*, 2010, **62**, 1064.
157. J. Chen, M. Yang, Q. Zhang, E. C. Cho, C. M. Cobley, C. Kim, C. Glaus, L. V. Wang, M. J. Welch and Y. Xia, *Adv. Funct. Mater.*, 2010, **20**, 3684.
158. M. Das, N. Sanson, D. Fava and E. Kumacheva, *Langmuir*, 2007, **23**, 196.
159. Y. Jin and X. Gao, *J. Am. Chem. Soc.*, 2009, **131**, 17774.
160. J. H. Kim and T. R. Lee, *Chem. Mat.*, 2004, **16**, 3647.
161. J. H. Kim and T. R. Lee, *Drug Dev. Res.*, 2006, **67**, 61.
162. W. Li, X. Cai, C. Kim, G. Sun, Y. Zhang, R. Deng, M. Yang, J. Chen, S. Achilefu, L. V. Wang and Y. Xia, *Nanoscale*, 2011, **3**, 1724.
163. L. Paasonen, T. Laaksonen, C. Johans, M. Yliperttula, K. Kontturi and A. Urtti, *J. Control. Release*, 2007, **122**, 86.
164. L. Paasonen, T. Sipilä, A. Subrizi, P. Laurinmäki, S. J. Butcher, M. Rappolt, A. Yaghmur, A. Urtti and M. Yliperttul, *J. Control. Release*, 2010, **147**, 136.
165. D. Pissuwan, S. M. Valenzuela and M. B. Cortie, *Trends Biotechnol.*, 2006, **24**, 62.
166. B. Radt, T. A. Smith and F. Caruso, *Adv. Mater*, 2004, **16**, 2184.
167. P. Rai, S. Mallidi, X. Zheng, R. Rahmanzadeh, Y. Mir, S. Elrington, A. Khurshid and T. Hasan, *Adv. Drug Deliver. Rev.*, 2010, **62**, 1094.
168. S. R. Sershen, S. L. Westcott, N. J. Halas and J. L. West, *J. Biomed. Mater. Res.*, 2000, **51**, 293.
169. L. E. Strong and J. L. West, *J. Biomed. Mater. Res.*, 2011, **3**, 307.
170. Q. Wei, J. Ji and J. Shen, *Macromol. Rapid Commun.*, 2008, **29**, 645.
171. G. Wu, A. Mikhailovsky, H. A. Khant, C. Fu, W. Chiu and J. A. Zasadzinski, *J. Am. Chem. Soc.*, 2008, **130**, 8175.
172. J. Yang, J. Lee, J. Kang, S. J. Oh, H. J. Ko, J. H. Son, K. Lee, J. S. Suh, Y. M. Huh and S. Haam, *Adv. Mater.*, 2009, **21**, 4339.
173. M. S. Yavuz, Y. Cheng, J. Chen, C. M. Cobley, Q. Zhang, M. Rycenga, J. Xie, C. Kim, K. H. Song, A. G. Schwartz, L. V. Wang and Y. Xia, *Nat. Mater.*, 2009, **8**, 935.
174. J. You, R. Zhang, G. Zhang, M. Zhong, Y. Liu, C. S. van Pelt, D. Liang, W. Weie, A. K. Sood and C. Li, *J. Control. Release*, 2012, **158**, 319.
175. M. Q. Zhu, L. Q. Wang, G. J. Exarhos and A. D. Q. Li, *J. Am. Chem. Soc.*, 2004, **126**, 2656.
176. J. E. Chung, M. Yokoyama, T. Aoyagi, Y. Sakurai and T. Okano, *J. Control. Release*, 1998, **53**, 119.

Downloaded on 01/09/2013 10:27:05.

Downloaded on 01/09/2013 10:27:05.

177. J. E. Chung, M. Yokoyama and T. Okano, *J. Control. Release*, 2000, **65**, 91.
178. A. S. Hoffman, *Adv. Drug Deliver. Rev.*, 2002, **43**, 3.
179. Y. Qiu and K. Park, *Adv. Drug Deliver. Rev.*, 2001, **53**, 321.
180. P. Shum, J. M. Kim and D. H. Thompson, *Adv. Drug Deliver. Rev.*, 2001, **53**, 273.
181. M. Egeblad and Z. Werb, *Nat. Rev. Cancer*, 2002, **2**, 161.
182. S. Lee, E. J. Cha, K. Park, S. Y. Lee, J. K. Hong, I. C. Sun, S. Y. Kim, K. Choi, I. C. Kwon, K. Kim and C. H. Ahn, *Angew. Chem. Int. Ed.*, 2008, **47**, 2804.
183. M. Oishi, A. Tamura, T. Nakamura and Y. Nagasaki, *Adv. Funct. Mater.*, 2009, **19**, 827.
184. X. Xia, M. Yang, L. K. Oetjen, Y. Zhang, Q. Li, J. Chen and Y. Xia, *Nanoscale*, 2011, **3**, 950.
185. A. M. Alkilany, L. B. Thompson, S. P. Boulos, P. N. Sisco and C. J. Murphy, *Adv. Drug Deliver. Rev.*, 2012, **64**, 190.
186. P. Rai, S. Mallidi, X. Zheng, R. Rahmanzadeh, Y. Mir, S. Elrington, A. Khurshid and T. Hasan, *Adv. Drug Deliver. Rev.*, 2010, **62**, 1094.
187. I. C. Sun, D. K. Eun, H. Koo, C. Y. Ko, H. S. Kim, D. K. Yi, K. Choi, I. C. Kwon, K. Kim and C. H. Ahn, *Angew. Chem. Int. Ed.*, 2011, **50**, 9348.
188. D. Kim, Y. Y. Jeong and S. Jon, *ACS Nano*, 2010, **4**, 3689.
189. I. C. Sun, D. K. Eun, J. H. Na, S. Lee, I. J. Kim, I. C. Youn, C. Y. Ko, H. S. Kim, D. Lim, K. Choi, P. B. Messersmith, T. G. Park, S. Y. Kim, I. C. Kwon, K. Kim and C. H. Ahn, *Chemistry*, 2009, **15**, 13341.
190. Y. Xia, W. Li, C. M. Cobley, J. Chen, X. Xia, Q. Zhang, M. Yang, E. C. Cho and P. K. Brown, *Acc. Chem. Res.*, 2011, **44**, 914.
191. J. Choi, J. Yang, E. Jang, J. S. Suh, Y. M. Huh, K. Lee and S. Haam, *Anticancer Agents Med. Chem.*, 2011, **11**, 953.
192. S. M. Janib, A. S. Moses and J. A. MacKay, *Adv. Drug Deliver. Rev.*, 2010, **62**, 1052.
193. H. Liu, D. Chen, L. Li, T. Liu, L. Tan, X. Wu and F. Tang, *Angew. Chem. Int. Ed.*, 2011, **50**, 891.
194. G. D. Moon, S. W. Choi, X. Cai, W. Li, E. C. Cho, U. Jeong, L. V. Wang and Y. Xia, *J. Am. Chem. Soc.*, 2011, **133**, 4762.
195. J. Park, J. Yang, E. K. Lim, E. Kim, J. Choi, J. K. Ryu, N. H. Kim, J. S. Suh, J. I. Yook, Y. M. Huh and S. Haam, *Angew. Chem. Int. Ed.*, 2012, **51**, 945.
196. J. H. Park, G. von Maltzahn, L. L. Ong, A. Centrone, T. A. Hatton, E. Ruoslahti, S. N. Bhatia and M. J. Sailor, *Adv. Mater.*, 2010, **22**, 880.
197. S. Shukla, A. Priscilla, M. Banerjee, R. R. Bhonde, J. Ghatak, P. V. Satyam and M. Sastry, *Chem. Mater.*, 2005, **17**, 5000.
198. G. von Maltzahn, A. Centrone, J. H. Park, R. Ramanathan, M. J. Sailor, T. A. Hatton and S. N. Bhatia, *Adv. Mater.*, 2009, **21**, 3175.
199. M. K. Yu, J. Park and S. Jon, *Theranostics*, 2012, **2**, 3.
200. J. Zhu, K. T. Yong, I. Roy, R. Hu, H. Ding, L. Zhao, M. T. Swihart, G. S. He, Y. Cui and P. N. Prasad, *Nanotechnology*, 2010, **21**, 285106.

CHAPTER 14

Magnetic-responsive Nanoparticles for Drug Delivery

SAN-YUAN CHEN,*[a] SHANG-HSIU HU[a] AND
TING-YU LIU[b]

[a] Department of Materials Science and Engineering, National Chiao Tung University, Taiwan, ROC; [b] Institute of Polymer Science and Engineering, National Taiwan University, Taipei 10617, Taiwan, ROC
*Email: sanyuanchen@mail.nctu.edu.tw

14.1 Introduction

Smart materials responsive to multiple environmental stimuli may offer advanced performances in the drug-delivery field. Nanometric carriers (*e.g.* nanoparticles, NPs) able to control the release of therapeutic agents have received wide attention because they provide two relevant advantages, namely high delivery efficiency and site-specific therapy, compared with traditional dosage forms. Given these advantages, many smart structures that integrate active drug molecules have been designed to optimize the release profiles. In addition to slow, zero-order release patterns, the stimuli-responsive systems may provide pulsatile profiles mimicking the natural release of biological molecules, such as insulin or thyroxine, in the body.[1] In addition to drug-delivery applications, nanocarriers are also of high interest for nanoscale chemistry. Irrespective of the application, external trigger of the release of a controlled dose of the encapsulated cargo at a specific time and location is highly beneficial. Therefore, many responsive drug carriers have been reported that respond to specific stimuli, such as temperature,[2,3] pH,[4] electric field,[5]

RSC Smart Materials No. 3
Smart Materials for Drug Delivery: Volume 2
Edited by Carmen Alvarez-Lorenzo and Angel Concheiro
© The Royal Society of Chemistry 2013
Published by the Royal Society of Chemistry, www.rsc.org

ultrasound[6,7] and magnetic field[8–11] to deliver drugs in a therapeutically desirable manner. Some external stimuli, such as light, electric signals or mechanical forces, require a physical contact with the drug carrier to trigger drug release, which may be difficult to attain in practice. Furthermore, real-time response upon a short-duration stimulus is also hard to achieve for most stimuli-responsive polymeric materials, which is especially critical for urgent treatments. Some of these drawbacks could be overcome by magnetic-responsive materials used in conjunction with localized heating.[12,13] Drug delivery *via* magnetic-sensitive materials can be guided or triggered by a non-contact force (an external high-frequency magnetic field), which is superior to traditional stimuli such as pH or temperature. Through a magnetism-based method (such as the application of an external magnet), the magnetic carriers loaded with the pharmaceutical agents can be guided to the site-specific target, and then provide a sustained drug release under external magnetic stimulation (Figure 14.1). In addition, a high-frequency magnetic field can increase the temperature of magnetic nanoparticles (MNPs), which could be useful for creating local hyperthermia suitable for cancer therapy.

Nanocarriers encapsulating MNPs can be designed to deliver the drug to a specific disease site, releasing the therapeutically effective dose to the right region at the right time using a magnetic field.[14–16] MNPs, especially those using iron oxide, offer several other advantages for biomedical applications including magnetic resonance imaging (MRI), cell sorting and hyperthermia,

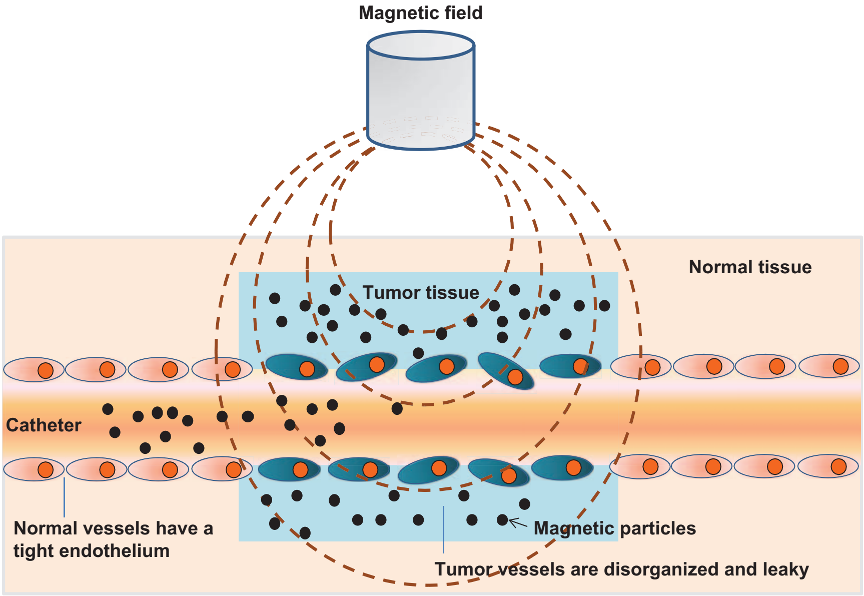
Magnetic field
Normal tissue
Tumor tissue
Catheter
Normal vessels have a tight endothelium
Magnetic particles
Tumor vessels are disorganized and leaky

Figure 14.1 Magnetic-responsive carriers loaded with pharmaceutical agents can be guided to target tissues and trigger drug release through the application of an externally applied magnetic field.
Reproduced from Ref. 12 with permission of Elsevier.

because they do not have the multiple domains found in larger magnets; the unit-cell spins of the entire nanoparticle line up and act as a single "super" spin that aligns more perfectly with the applied field, giving rise to a higher magnetic sensitivity. This "superparamagnetism", which is unique to NPs, provides a stronger magnetic response than bulk magnetism, exhibiting a fast response to a magnetic/temperature stimulus. In addition, combinations of nano-sized iron oxide particles with biocompatible polymers lead to drug nanocarriers that not only exhibit multiple functions, but also are more readily biodegraded in and cleared from the body. In the following sections, the current status and knowledge about the nanoscale hybrid systems that have been developed to exploit magnetic-responsive NPs for drug delivery are analyzed in detail.[17–20]

14.2 Hyperthermia Theory of the Magnetic Field

Having a magnetic core or shell as a part of a colloidal nanoparticle offers three opportunities: the MNPs can be attracted to a region with a high magnetic field H; they may experience internal stress as non-uniform distortion arises from magnetic forces; and they can be heated by a non-contact magnetic field. The attracting field can be either direct current (DC) or alternating current (AC) since the magnetic body force is the gradient of the magnetic internal energy density as follows:

$$\text{Magnetic internal energy density} = 1/2\chi\mu_o H^2 \tag{1}$$

In this expression, χ is the susceptibility and μ_o the permeability of vacuum. Therefore, high-susceptibility materials are desirable for magnetic localization. On the other hand, the heating field is always AC, typically in the radio-frequency (RF) range of $10^4 \sim 10^5$ Hz. Because an AC field can generate an eddy current, induction heating is always feasible for any conductor, but it becomes more efficient for a magnetic material in which magnetic hysteresis causes additional energy dissipation. To maximize the sum of eddy current (joule) heating and magnetic heating, a relatively high electrical resistivity and large magnetic coercivity (mainly due to the resistance to domain wall movement) are required. Nanomagnets suitable for nanocolloids are, however, superparamagnetic, *i.e.* a single-domain ferromagnet free to switch following a quasi-static field without apparent coercivity. Thus, nanomagnets contribute little to coercivity, and the energy dissipation must come from some sort of internal or boundary "friction" that does not prevent switching, but drags the magnetic moment letting it lag behind the AC field. In a linear-response medium, the Debye theory describes this lag in terms of relaxation time, τ. It then follows that maximal dissipation occurs when τ^{-1} is commensurate with the frequency f, *i.e.* $2\pi f\tau \sim 1$, because when $2\pi f\tau << 1$, there is no lag, but when $2\pi f\tau >> 1$, the moment stops to respond. Therefore, effective heating can be obtained by tuning the frequency to the range of $2\pi f\tau \sim 1$; under this condition, more heat can be generated by driving the field harder (higher H) and faster (higher f). Lastly, magnetic distortion can be caused by either a DC or an AC field, as long as the frequency is not much higher than the resonance frequency.[21]

Under magnetic heating, the temperature of the magnetic nanocolloid solution gradually rises to reach a steady state with several (up to tens) degrees Celsius higher than room temperature. At this temperature, the heat input from the MNPs equals the heat loss at the external boundary (*e.g*. container, fixtures and surfaces). Because the energy input to heat up the water comes entirely from the heat generated in the magnetic particles, the heating rate R_M of the MNPs can be calculated from the expression:

$$V_M R_M C_M = (1 - V_M) R_W C_W \tag{2}$$

R_W being the heating rate of water, V_M the volume fraction of MNPs relative to the solution, and C_W and C_M the volumetric specific heat of water and the MNPs, respectively. Assuming that magnetic heating involves isolated, independent nanoparticles only, the heating effects of MNPs subjected to AC magnetic fields are from two sources: Brownian and Néel relaxations (Figure 14.2), and their relative contributions strongly depend on the particle size. NPs with a core diameter less than 30 nm are usually composed of a single domain, and their magnetization relaxation is governed by the combined effects of the rotational external (Brownian) and internal (Néel) diffusion of the particle magnetic moment.[22] First, the particle may tumble, causing frictional heating at the particle–water interface. The relaxation time, τ_B, for this mode can be estimated as the time required for Brownian motion over a characteristic distance of the order of one particle diameter. Brownian relaxation is due to thermal orientational fluctuations of the grain itself in the carrier fluid, with the magnetic moment being locked onto the crystal anisotropy axis. The characteristic time, τ_B, for Brownian relaxation is given by the expression:

$$\tau_B = 3\eta V_H / kT \tag{3}$$

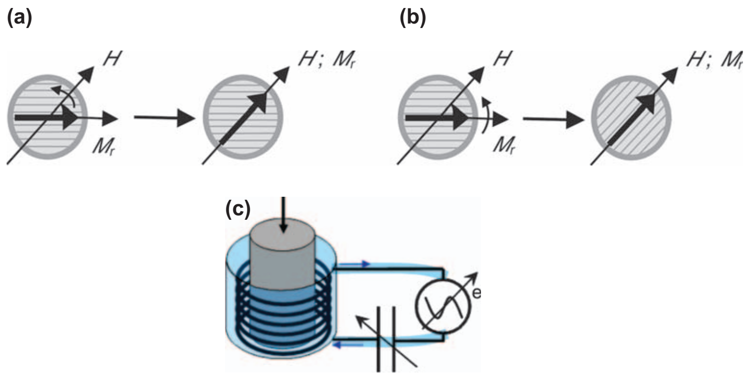

Figure 14.2 Intrinsic (Néel, a) and extrinsic (Brownian, b) remagnetization mechanism and equipment of high-frequency magnetic field (HFMF, c). Reproduced from Ref. 21 with permission of American Chemical Society.

where η is the viscosity of the carrier fluid, k is the Boltzmann constant, T is the temperature and V_H is the hydrodynamic volume of the particle.[21]

Brownian relaxation may not be responsible for the frictional heating of the MNPs. Friction may also arise from spin rotation without crystal-lattice rotation. Néel relaxation refers to the internal thermal rotation of the particle magnetic moment within the crystal. The relaxation time, τ_N, for this mode (Néel relaxation) is the reciprocal of the spin flipping rate, which is of the order of $\nu_D \exp(-KV/kT)$. Here, ν_D is the Debye frequency of the order of 10^{12} s^{-1}, and KV is the energy barrier for coherent spin flipping, which may be of magnetocrystalline or shaped origin. As the two relaxation mechanisms take place in parallel, the effective relaxation time, τ, can be estimated from the following relationship:

$$1/\tau = 1/\tau_N + 1/\tau_B \tag{4}$$

and, then, the shorter time determines the dominant mechanism of relaxation.

The inductive heating (hyperthermia) in AC magnetic fields, in which the thermal energy from a hysteresis loss of magnetic materials depends on the type of the remagnetization process, has been the subject of many studies in recent years. Hyperthermia from the magnetic drug-carriers induced by AC magnetic fields can trigger drug release or enable thermal therapy. When a ferromagnetic material is magnetized by an increasing applied field and then the field is decreased, the magnetization does not follow the initial magnetization curve obtained during the increase (Figure 14.3). This irreversibility or hysteresis can occur in ferromagnetic or ferroelectric materials. An example of a full or major hysteresis curve (or loop), *i.e.* M is taken to near M_s, is shown in Figure 14.3a. At extremely high applied fields, the magnetization (M) approaches the saturation value, M_s. Then, if the field is decreased to zero, the M *vs.* H curve does not follow the initial profile, but instead lags behind and when $H = 0$ again a remanent magnetization persists (the remanence M_r). If the field is now applied

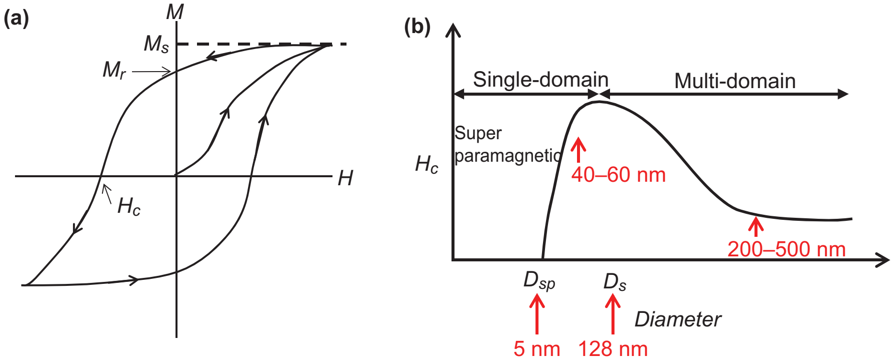

Figure 14.3 Full-loop hysteresis curve (a), where M_s is the saturation magnetization, M_r is the remanent magnetization (at $H = 0$) and H_c is the coercivity; and the relationship between the particle size and hysteresis coercivity (b). Reproduced from Ref. 22 with permission of John Wiley and & Sons.

in the inverse direction (a negative field), M is forced to zero at a field magnitude called hysteresis coercivity, H_c. Increasing this negative field further forces the magnetization toward saturation in the negative direction. Symmetric behavior of this hysteresis curve is obtained as H is varied widely between large positive and negative values. Hysteresis could be said to be due to internal friction. Hence, the area inside the loop corresponds to the magnetic energy that is dissipated while circling the loop.

The inductive heating effect in the AC magnetic field depends on the size of the MNPs, which means that saturation magnetization (Ms) and hysteresis coercivity (Hc) are very important factors in magnetic-responsiveness of NPs. Fe_3O_4, for example, exhibits superparamagnetic behavior (H_c is near zero) when the particle size is lower than 5 nm. Moreover, H_c reaches a maximum when the particle size is 128 nm, *i.e.* the critical point between single-domain and multi-domain iron particles. H_c becomes saturated when the particle size is higher than 200 nm (Figure 14.3b). Thus, the heating ability of each ferrite increases as the areas of the hysteresis loops and the frequency of the alternating magnetic field increase.

14.3 Synthesis and Surface Modification of Magnetic Nanoparticles

14.3.1 Synthesis of Magnetic Nanoparticles

Several methods have been widely investigated, including coprecipitation, thermal decomposition, sol-gel reaction, electrochemical reaction, flow injection synthesis, sonochemical synthesis, constrained environments, polyol method, flame method, photochemical method and mechanical milling. Several compounds, comprising organic monomers, organic polymers, inorganic components and bioactive molecules, can be used as stabilizers. Two commonly used synthesis procedures are described below.

14.3.1.1 Coprecipitation

The precipitation in aqueous media without organic stabilizing agents was the first controlled process. In this method, magnetic iron oxides (Fe_3O_4 or γ-Fe_2O_3) are prepared using a mixture of $FeCl_3$ and $FeCl_2$ in a pH range of 8 to 14. Nucleation appears above the critical supersaturation species concentration. The coprecipitation process is easy to implement, but the size distribution of the obtained magnetite particles is wide. When the ratio of $[Fe^{2+}]/[Fe^{3+}]$ is fixed at 2/3 and the amount of iron ions in the solution varies from 12.5 to 250 mmol, the crystallinity reduces and particle size decreases to about 8 nm.[23] Size control of magnetite NPs with high crystallinity and ferromagnetic properties could be successfully achieved using coexisting anions. An increase in the size of the NPs was observed at high pressures, which may be explained by the change in the Gibbs free energy value during crystallization from a homogeneous supersaturated solution.

14.3.1.2 Thermal Decomposition

Iron oxide NPs of high quality have been obtained by hydrolysis and oxidation or neutralization of mixed metal hydroxides in a high-temperature solution. The properties of the MNPs can be modulated through the control of reaction conditions, including the nature of the solvent, temperature, time and concentration and molar ratio of reactants. Monodisperse magnetic nanocrystals have been synthesized through the thermal decomposition of organometallic compounds in high-boiling organic solvents containing stabilizing surfactants.[24–27] The hydrophobic NPs can be transformed into hydrophilic NPs by adding bipolar surfactants. For example, iron oxide NPs with uniform size between 5 and 30 nm were successfully prepared through the "heating up" thermal decomposition method, using decanoic acid and carefully tuning the heating rate.[28] Figure 14.4 illustrates the preparation of magnetite nanocrystals (Fe_3O_4) applying the thermal decomposition synthesis method and using $Fe(acac)_3$ [*i.e.* tris(acetylacetonato) iron(III)], tri-octylamine and oleic acid at the relatively low temperature of 200 °C.[28–30]

14.3.2 Surface Modification of Magnetic Nanoparticles

Without a surface coating, the oil-soluble MNPs are not easy to use for biological applications. Therefore, the native hydrophobic surface ligands must

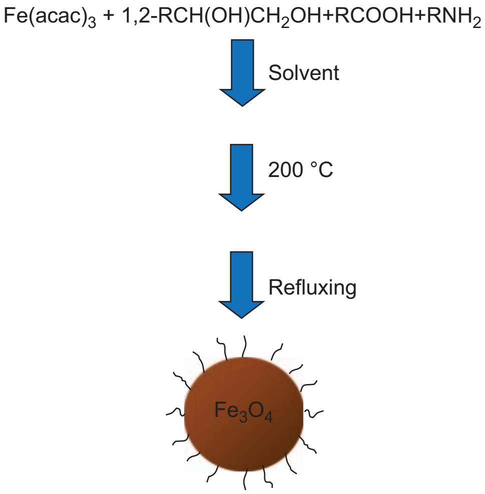

Figure 14.4 Reaction of Fe-(acac)$_3$ with surfactants applying a high-temperature decomposition method to yield monodisperse Fe_3O_4 nanoparticles. Reproduced from Ref. 28 with permission of American Chemical Society.

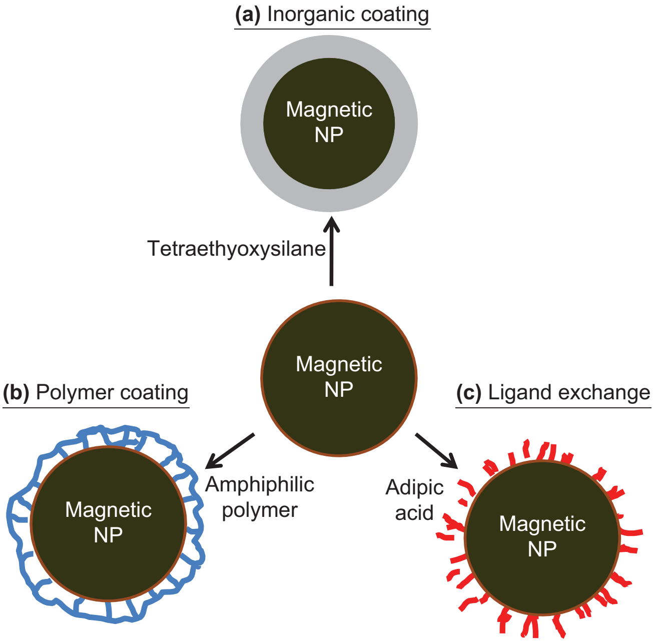

Figure 14.5 Scheme of three types of surface modification of magnetic nanoparticles: inorganic surface coating with an amorphous silica shell (a), amphiphilic polymer coating on the magnetic nanoparticles (b), and ligand exchange to replace native surface ligands (c). These routes provide polar or charged functional groups onto the outer surface of the NP enhancing water solubility.
Reproduced from Ref. 34 with permission of Springer.

be modified not only to stabilize them against aggregation both in a biological medium and in a magnetic field, but also to minimize the remanent magnetization. Based on this concept, surface ligands of other NPs such as quantum dots (QDs) and gold NPs enable an easy adaptation of the previously developed surface-engineering methods to the MNPs. In the paragraphs below, three approaches to modify hydrophobic NPs in order to make them soluble in aqueous biological buffers are discussed (Figure 14.5).

In the ligand exchange method, hydrophobic surface ligands are replaced with amphiphilic ligands containing head-groups that bind the MNP surface, and hydrophilic tails that interact with the aqueous solvent.[31] There are widely available, compatible ligands that can be applied in this convenient water-solubilization procedure.[32] However, a key drawback is the risk of desorption of labile ligands from the MNP surface. Incomplete surface coverage is likely to lead to NP aggregation, inefficient conjugation with biomolecules, and desorption of the bioconjugated surface ligand. These stability problems can reduce the overall biological functionality of the MNPs.

Another solubilization strategy to retain hydrophobic ligands on the MNP surface is the adsorption (coating) of amphiphilic polymers, such as polyacrylic acid copolymers,[33] PEG-derived phospholipids[34] and amphiphilic polyanhydrides. Amphiphilic polymers used for the encapsulation of MNPs contain hydrophobic segments (mostly hydrocarbons), that intercalate and interact with the alkyl tails of the native MNP surface ligands by means of the multivalency effect, and hydrophilic segments (PEG or multiple charged groups) that cause the overall MNP–polymer constructs to be soluble in aqueous buffer. Biodegradable amphiphilic polymers originally designed for drug delivery are also used to encapsulate MNPs for *in vivo* applications, because the components of the construct, namely the core material (Fe_3O_4/Fe_2O_3), the surface ligands (oleic acid) and the polymer coating (polyethylacrylic-polypropylacrylic acid), are biocompatible.

It is also possible to modify the surface of MNPs creating an inorganic shell, typically consisting of silica or gold, according to one of the following procedures: precipitation and reaction at the NP surface, or deposition of preformed colloids onto the NP surface.[35] The formation of silica shells involves the base-catalyzed hydrolysis of alkoxides of tetraethoxysilane (TEOS), followed by condensation of the resulting silanol groups. The advantages of using silica include biocompatibility, ease of bioconjugation and stability *in vivo* (biostability). Xia and coworkers employed a sol-gel approach for the direct surface coating of MNPs with amorphous silica through the hydrolysis and condensation of TEOS, and observed a concentration-dependent shell thickness which ranged from 2 to 100 nm.[36]

14.4 Magnetic Nanocarriers for Drug Delivery

Recent advances in nanotechnology have improved the ability specifically to tailor the features and properties of MNPs for therapeutic applications. MNP-based drug carriers composed of an iron oxide core and a polymeric shell with a specific tumor-targeting ligand are particularly promising for enhanced tumor delivery of therapeutic agents. The use of an external magnetic field to localize the therapeutic agents to the desired sites is a modern technology in the design of drug-delivery systems (DDSs). MNPs enable minimization of the amounts of cytotoxic drugs in the systemic circulation and of unwanted side effects. Incorporation of MNPs in organic or inorganic matrices make them able to be (i) visualized, since superparamagnetic NPs are used as contrast agents in MRI; (ii) heated under a magnetic field to trigger drug release or to produce hyperthermia/ablation of cells; and (iii) guided or held in place as magnetic vectors by a magnetic field gradient toward a certain location, to act as targeted DDSs (Figure 14.6).[7]

The MNPs carriers combine intrinsic magnetic properties with drug-loading capability and biochemical features that can be bestowed by means of suitable modifications. Preparation methods of NPs generally fall into the category of the so-called “bottom up” approach, in which materials are formed from atoms or molecules in a controlled manner that is thermodynamically regulated by means such as self-assembly. Depending on the synthesis procedure, particles or capsules can be obtained. Core-shell NPs may be produced with a core of

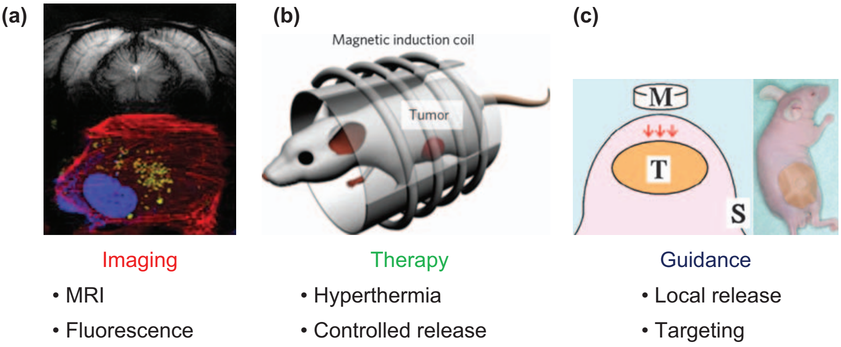

Figure 14.6 Magnetic nanoparticles for biomedical applications: imaging and diagnosis (a), therapy (b) and guidance (c).
Reproduced from Ref. 37 with permission of Elsevier.

magnetic iron oxide (usually Fe_3O_4 or γ-Fe_2O_3) and a shell of a polymer (dextran, PLGA or PVA) and/or a non-polymer (silica or metals). The drug is covalently attached to the surface or entrapped or adsorbed within the pores of the magnetic carrier (polymer or mesoporous silica). Nanocapsules refers to magnetic vesicular systems in which the drug is confined to an aqueous or oily cavity, usually prepared by the reverse micelle procedure, and surrounded by an organic membrane (*i.e.* magnetoliposomes) or encapsulated within a hollow inorganic capsule. The MNP surface can be functionalized with carboxyl and amine groups, biotin, streptavidin and antibodies. Coating the NPs with neutral hydrophilic compounds, such as polyethylene glycol (PEG), polysaccharides or dysopsonins (human serum albumin, HSA), can increase the circulatory half-life from minutes to hours or days. A similar effect can be achieved choosing the particle size to avoid the action of the reticuloendothelial system.[38,39]

14.4.1 Amphiphilic Micelles and Organic Nanoparticles

Amphiphilic polymers self-assembling into micelles are being broadly investigated as coatings of MNPs. The addition of ligands, such as tetradecylphosphonate and PEG-2-tetradecylether, induces the formation of micelles around the NP with the hydrophilic PEG end of the ligand contributing to the water solubility. Similarly, water-soluble iron oxide NPs can be prepared using a micelle-based coating of either amphiphilic PEG-phospholipids or poly(maleic anhydride-alt-1-octadecene)-PEG block copolymers.[40,41] Owing to hydrophobic interactions, multiple MNPs are confined in the micelles formed by the amphiphilic polystyrene-poly(acrylic acid) (PS-PAA) block copolymer.[42] Similarly, the evaporation of organic solutions containing polylactide-PEG block copolymers generates micelles that trap the MNPs at the hydrophobic core. A recent report proposed a newly designed, multi-functional PLGA nanostructure incorporating monodisperse MNPs for MRI, QDs for fluorescence

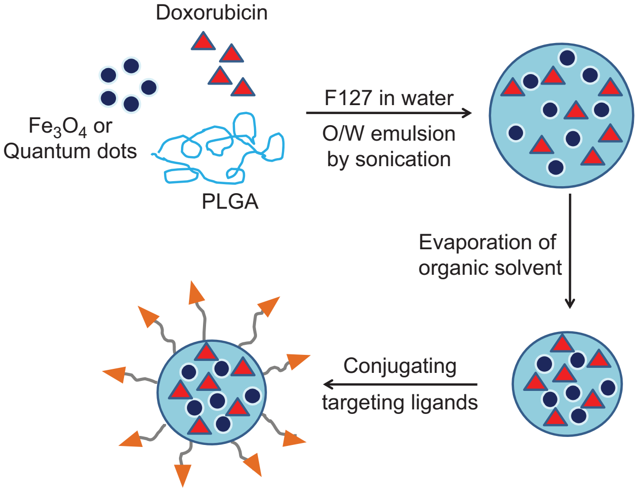

Figure 14.7 Procedure to obtain multi-functional magnetic nanocarriers. Reproduced from Ref. 43 with permission of John Wiley & Sons.

visualization, and doxorubicin as a therapeutic agent (Figure 14.7). Multifunctional magnetic nanocarriers (100–200 nm) were prepared from an oil-in-water emulsion using a non-ionic amphiphilic surfactant under sonication, followed by solvent evaporation. Incorporation of cancer-specific targeting agents at the surface of the MNPs opens the possibility of enhancing the therapeutic efficacy through a synergistic strategy: the nanoconstructs are manipulated by a magnetic field and concentrated near cancer cells, and the ligands force the adhesion/penetration into the cancer cells (Figure 14.7).[43]

Diffusion of drug molecules from the nanocarriers to the environment is thermodynamically unavoidable under a high concentration gradient. Therefore, after administration, there is a risk of premature leakage and, thus, of undesired clinical complications including reduced drug levels at the required site. To minimize this problem, magnetic nanocarriers were designed and constructed by preparing iron oxide NPs with drug molecules embedded in an ultra-thin but dense silica nanoshell (SAIO@SiO_2) (Figure 14.8). The nanoshell acts as a physical barrier to prevent undesirable drug release before reaching the target sites. For this purpose, a mixture of iron oxide NPs and amphiphilic polymer PVA was employed to form cores that can entrap hydrophilic or hydrophobic drugs, PVA acting as a glue among the NPs.[44]

The silica-coated core-shell (SAIO@SiO_2) nanocarriers exhibited real-time response to an external magnetic field, triggering burst drug release when the cores partially disintegrate under the stimulus. When the stimulus stopped, the core structure was recovered and a relatively slow and linear release was immediately restored (Figure 14.9). *In vitro* tests showed that, in the absence of a magnetic field, non-coated MNPs (SAIO) released 90% ibuprofen in 48 hours, while minimal release was observed for SAIO@SiO_2 nanocarriers.

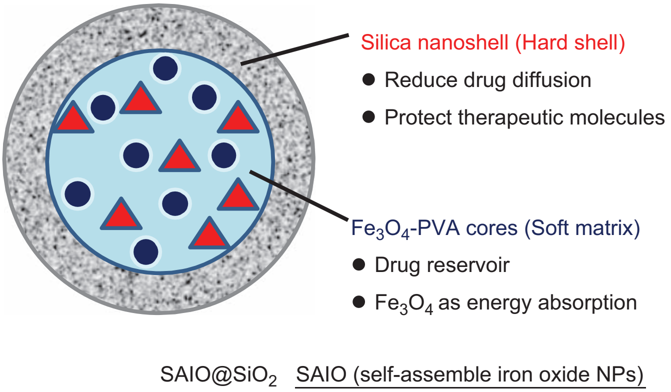
Silica nanoshell (Hard shell)
● Reduce drug diffusion
● Protect therapeutic molecules
Fe_3O_4-PVA cores (Soft matrix)
● Drug reservoir
● Fe_3O_4 as energy absorption
$SAIO@SiO_2$
SAIO (self-assemble iron oxide NPs)

Figure 14.8 Structure of a self-assemble iron oxide/silica core-shell ($SAIO@SiO_2$) nanocarrier for magnetically controlled drug release.
Reproduced from Ref. 44 with permission of John Wiley & Sons.

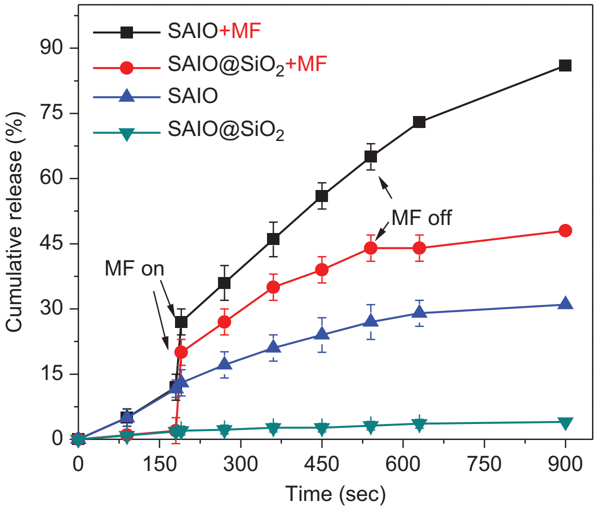

Figure 14.9 Natural and HFMF-triggered release profiles of ibuprofen from SAIO and $SAIO@SiO_2$ nanocarriers. The $SAIO@SiO_2$ nanocarriers released less drug than SAIO nanoparticles (+MF represents the application of a high-frequency magnetic field).
Reproduced from Ref. 44 with permission of John Wiley & Sons.

Application of the magnetic field led to a burst release from both the coated and the non-coated MNPs (Figure 14.9). With stimuli of different duration, the amount of drug released from the nanocarriers showed a linear increase with time. Interestingly, ibuprofen release profiles from the $SAIO@SiO_2$ nanocarriers followed zero-order kinetics even under the magnetic stimulus. In other words, despite there being a burst at the beginning of the application of the high-frequency magnetic field, ibuprofen release from the SAIO@SiO_2 nanocarriers can still be well regulated.[44]

14.4.2 Temperature-responsive Magnetic Nanocarriers

Since body temperature is nearly constant, a small change can serve as an environmental stimulus. Temperature-responsive soft materials used in conjunction with localized heating (*e.g. via* hyperthermia) are therefore prime candidates for biomedical applications under magnetic stimuli. One important application of magnetically and thermally responsive smart nanomaterials for remotely controlled drug delivery is illustrated in Figure 14.10.[45]

14.4.2.1 Thermal-responsive Polymers and Carriers

Like all materials, polymers manifest thermodynamic structural transitions along with associated physical or chemical responses. Biomedical applications may benefit from the behavior of polymer-water solutions that are stable below a so-called lower critical solution temperature (LCST) and that, when heated above the LCST, partition into two phases: water and a polymer-rich phase. This behavior is in contrast to the phase separation below an upper critical solution temperature (UCST) that is more commonly encountered in non-polymer systems. Among block copolymers, the most studied are the poly(ethylene oxide)-poly(propylene oxide)-poly(ethylene oxide) (PEO-PPO-PEO) triblock copolymers, commercialized as Pluronics® (BASF) or Poloxamers® (ICI). PEO, also known as PEG, is frequently present as a

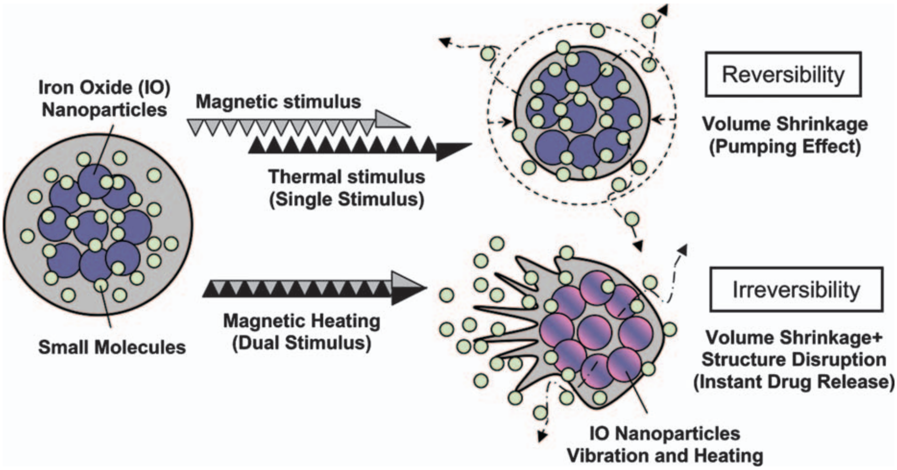
Iron Oxide (IO) Nanoparticles
Small Molecules
Magnetic stimulus
Thermal stimulus (Single Stimulus)
Magnetic Heating (Dual Stimulus)
Reversibility
Volume Shrinkage (Pumping Effect)
Irreversibility
Volume Shrinkage+ Structure Disruption (Instant Drug Release)
IO Nanoparticles Vibration and Heating

Figure 14.10 Drug release mechanisms under magnetic heating: gentle magnetic heating causes temperature-responsive polymer to shrink, squeezing drug out from the nanoparticle, while intense magnetic heating additionally causes the rupture of the nanoparticle, triggering a burst-like drug release. Reproduced from Ref. 45 with permission of Elsevier.

biocompatible hydrophilic coating on NPs to improve their *in vivo* circulation; PPO, in contrast, is more hydrophobic. The PEO and the PPO blocks can self-segregate into hydrophilic and hydrophobic domains, respectively. These aspects are covered in detail in Chapter 5. Above the LCST, inter-chain aggregation occurs, forming alternating PEO and PPO layers arranged into micelles, cylinders, lamellas or other supramolecular structures. Stabilized supramolecular structures of PEO-PPO-PEO (*via* chemical cross-linking, physical entanglement with another inter-penetrating polymer network or adsorption onto a water/oil interface) undergo a volumetric transition at the LCST due to water solubilization/rejection in the PPO layer.[45] Some examples of polymer-based temperature-responsive colloidal particles are given in Table 14.1; most of them dilate below the LCST and shrink above the LCST, with a radius ratio typically ranging from 2 to 5. Post-formation cross-linking adds stability to the colloids, without substantially affecting their thermal response.[45–47]

Magnetic heating of the temperature-responsive nanocarriers above the LCST induces aggregation and size shrinkage to squeeze out hydrophilic drugs. These magnetic, thermal-responsive, drug-targeting carriers have several advantages, such as: (i) the LCST of the outer shell can be designed to be above human body temperature (37 °C); (ii) the magnetic carrier can be targeted to a specific site; (iii) the encapsulated drug can be released in response to heat generated by an alternative magnetic field; and (iv) the polymer carrier is bioeliminable. Magnetic dual-functional nanospheres composed of magnetic iron oxide NPs embedded in a thermo-sensitive Pluronic F-68/F-127 matrix have been successfully synthesized by an *in situ* coprecipitation process. The thermo-sensitive polymer undergoes a fast structural change when a short exposure to high-frequency magnetic field causes rapid heating. During the stimulus duration, considerable volume shrinkage of the nanospheres (2.3-fold in diameter) occurs, and an instantaneous release of the encapsulated drug

Table 14.1 Volume change (%) and temperature transition (°C) of various temperature-responsive drug carriers. Reproduced from Ref. 45 with permission of Elsevier.

Materials	*Volume changes (%)*	*Transition temperature (°C)*
PNIPAAm/iron oxide nanobeads	~85	35
PNIPAAm microspheres	~83	35
Au/Boltorn H40-NIPAAm nanoparticles	~64	32
Pluronic® F-127/iron oxide nanoparticles	~78	20–25
Pluronic® F-127 nanocapsules	~97	26
Pluronic® F-127/heparin nanocapsules	~99	25
Pluronic® F-127/poly(ethylenimine) nanocapsules	92–97	21
Au/Pluronic® F-127 core-shell nanocapsules	~96	18
Pluronic® F-127/PEG nanocapsules	~89	23
Pluronic® F-68 nanocapsules	~98	40
Pluronic® F-68/iron oxide nanocapsules	~94	40
Pluronic® F-68/iron oxide nanocapsules	~94	40

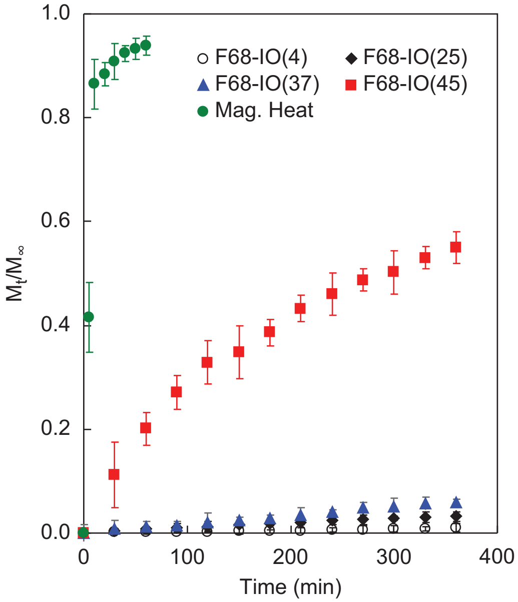

Figure 14.11 Cumulative release of a model drug (vitamin B12) from F-68–IO nanocapsules at various temperatures. The rapid release rate at 45 °C is mostly due to nanocapsule shrinkage. The much faster burst-like release during magnetic heating is due to rupture of the nanocapsule. Reproduced from Ref. 45 with permission of Elsevier.

(vitamin B12) is induced. The drug release profiles shown in Figure 14.11 are quite convenient: very slow at 4 °C and 25 °C, modest at 37 °C (below the LCST), much faster at 45 °C (above the LCST) and bursting upon magnetic heating, with a release rate at least 100-fold higher than that of 25 °C.[45,48]

Thermo-sensitive magnetic liposomes have been designed to combine biological and physical targeting mechanisms for use in hyperthermia-triggered drug release (Figure 14.12). Folate-targeted doxorubicin-containing magnetic liposomes showed encapsulation efficiencies of approximately 85% and 24% for doxorubicin and MNPs (~10 nm), respectively. Magnetic hyperthermia at 42.5 and 43.5 °C synergistically increased the cell killing ability. These results suggest that an integrated concept of biological and physical drug targeting, triggered drug release and hyperthermia based on magnetic field can be used advantageously for thermo-chemotherapy of cancer.[49]

14.4.2.2 Mesoporous Inorganic Magnetic Nanocarriers for Drug Delivery

In addition to organic polymers, inorganic mesoporous silica has several attractive features, such as stable mesoporous structure, large surface area, tunable pore size and volume and well-defined surface properties (further

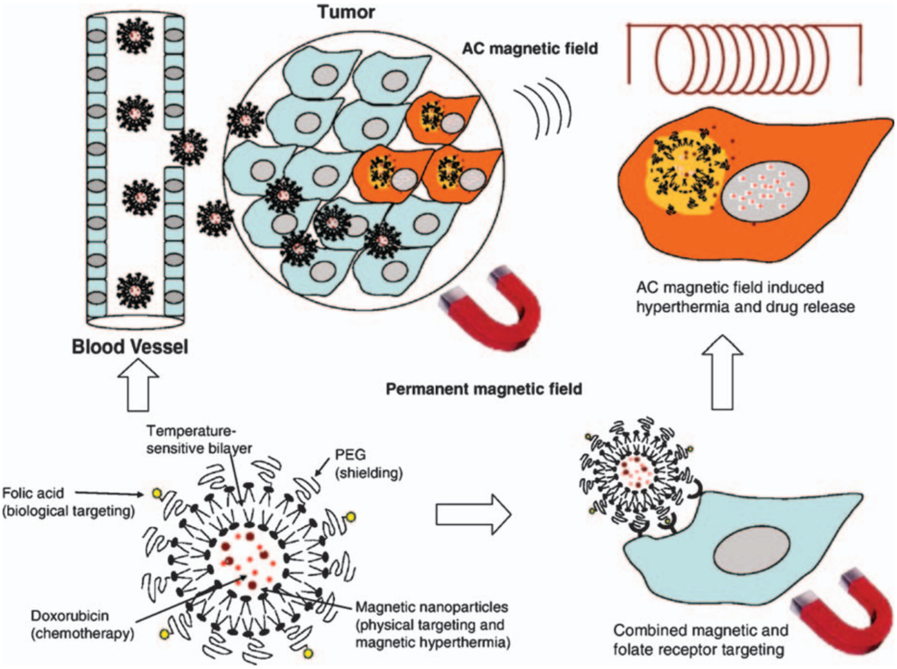
Tumor
AC magnetic field
Blood Vessel
AC magnetic field induced
hyperthermia and drug release
Permanent magnetic field
Temperature-
sensitive bilayer
PEG
(shielding)
Folic acid
(biological targeting)
Doxorubicin
(chemotherapy)
Magnetic nanoparticles
(physical targeting and
magnetic hyperthermia)
Combined magnetic and
folate receptor targeting

Figure 14.12 Multi-functional temperature-sensitive magnetic liposomes containing doxorubicin can be targeted physically by magnetic field and biologically by folic acid to tumor cells. Drug release is triggered by hyperthermia upon local application of an AC magnetic field on the tumor tissue.
From Ref. 49 with permission of Elsevier.

information is available in Chapter 15). Drugs can be loaded onto mesoporous silica along with MNPs, forming multi-functional mesoporous silica-MNP platforms (Figure 14.13) useful for diagnostics or monitoring (*via* fluorescence image and MRI) and delivery of therapeutics to tumors.[50] Hydrophobic monodisperse iron oxide NPs were synthesized *via* high-temperature organic phase methods and transferred, upon evaporation of the organic solvent, to an aqueous phase containing an amphiphilic surfactant. Thick mesoporous silica shells (100–200 nm) were grown around the water solubilized iron oxide NPs using TEOS, at a controlled temperature (65–80 °C). Afterward, fluorescein isothiocyanate (FITC) dye was conjugated to the pore walls and to the particle surface. To prevent NPs aggregation during loading of hydrophobic drugs, the surfaces were modified with trihydroxysilylpropyl methylphosphonate to inhibit inter-particle hydrogen bonding between the surface silanol groups. Using a clinical MRI instrument, the aqueous NPs can produce hypointense (negatively enhanced) T2-weighted MRI. In this case, a high NP concentration was needed to achieve MRI contrast enhancement, because few MNPs were loaded and the thick silica shell reduces the interaction of MNPs

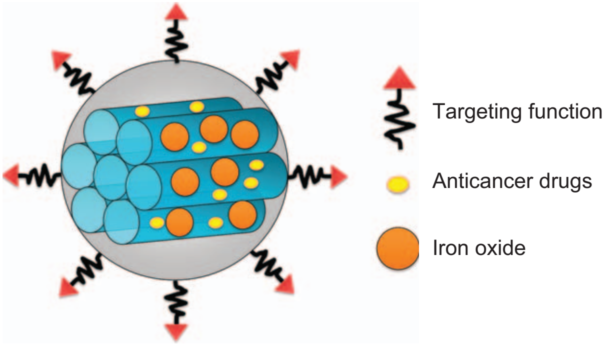

Figure 14.13 Multi-functional nanoparticle showing iron oxide nanocrystals encapsulated within mesoporous silica, hydrophobic anticancer drugs stored inside the pores, and surface modification with phosphonate and folic acid targeting ligands.
From Ref. 50 with permission of the American Chemical Society.

with water molecules. These carriers were able to load the anticancer drugs camptothecin and paclitaxel and to induce their uptake by cancer cells *in vitro*.[50]

More recently, a number of investigations have focused on nanocarriers made of a nanoporous silica matrix, known as MCM-41. The therapeutic or biologically active molecules are filled and anchored into the nanopores of the silica NPs. Drug diffusion can be modulated by adding capping molecules that open/close the entrance of the pores as a function of certain stimuli. These ideas have been applied to fabricate multi-functional nanoprobes for imaging live cancer cells by co-encapsulation of QDs and magnetite NPs within organically modified silica. The biocompatible magnetic nanocarriers containing dye molecules were suitable for optical tracking of basic processes at the cellular level. In particular, $(Zn_{0.4}Fe_{0.6})Fe_2O_4$ NPs were incorporated inside porous nanocarriers having molecular valves that consist of a thread and a capping molecule, which closes the silica pores to keep the drug inside (Figure 14.14).[51] When an external alternating magnetic field was applied, the heat generation and the subsequent pressure built up inside the porous NPs caused the rapid removal of the molecular valves and the release of the cargo. Under a pulsed magnetic field, the release of a fluorescent dye (Rhodamine B) occurred in each pulse in a staircase-like fashion.[51]

14.4.2.3 Magnetic Nanocarriers for Gene Therapy

Gene therapy may represent a very effective approach to correct aberrant cell signaling that induces uncontrolled cell growth and tumor formation. The purpose of the delivery of DNA molecules to cancer cells is to insert or to

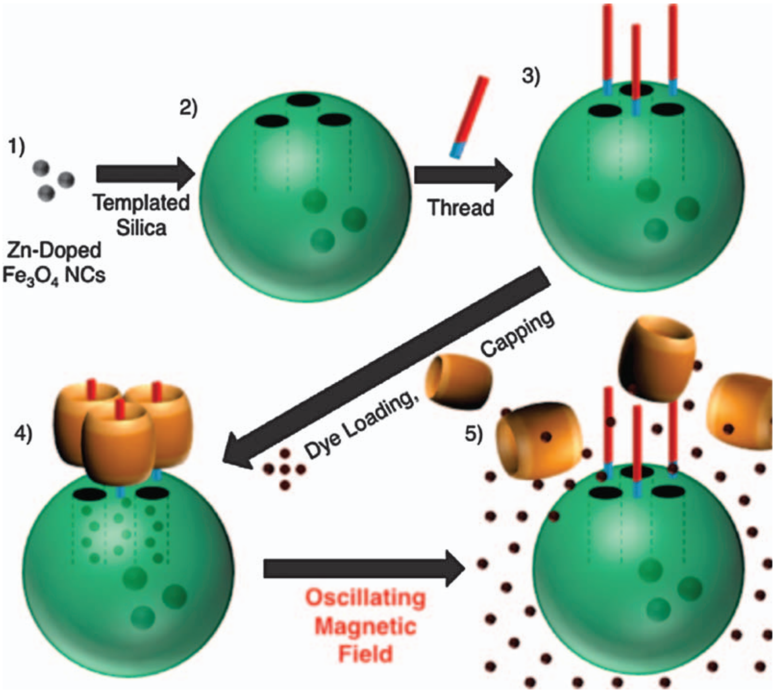

Figure 14.14 Scheme of a magnetically triggered drug release system. The particles and machines are not drawn to scale.
Reproduced from Ref. 51 with permission of the American Chemical Society.

modify a gene in order to solve a dysfunction. A variety of vectors, including viruses, cell-based systems and synthetic vectors, have been tested for DNA delivery. MNPs offer a novel approach to gene therapy which is known as "magnetofection".[52] Recently, Mok and coworkers reported magnetic nanovectors composed of an iron oxide core coated with three different functional molecules: polyethyleneimine (PEI), siRNA and chlorotoxin (Figure 14.15).[53] Nanovectors with a size of 60 nm exhibited long-term stability and good magnetic properties. The PEI was blocked on the vectors with citraconic anhydride to increase the biocompatibility and to elicit a pH-sensitive cytotoxic effect in the acidic tumor microenvironment. Furthermore, DNA encoding green fluorescent protein (GFP) was used for optical monitoring of gene expression, when mice bearing C6 rat glioma xenograft flank tumors were treated with DNA-loaded chlorotoxin-activated iron-oxide nanovectors.[54] The accumulation in the tumor sites was monitored using MRI and analyzed by histology. Furthermore, the uptake into cells was confirmed through gene expression using Xenogen and confocal fluorescence imaging.

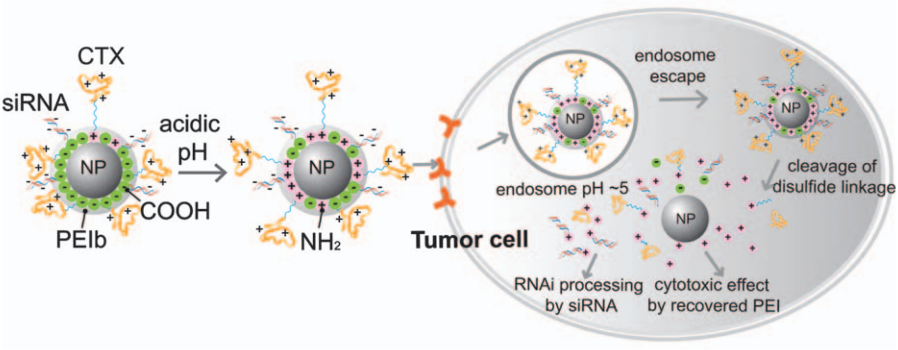

Figure 14.15 Scheme of the intra-cellular uptake, intra-cellular trafficking and processing of magnetic nanovectors for delivering gene into tumor cells. Reproduced from Ref. 53 with permission of the American Chemical Society.

14.5 Nanocarriers with a Magnetic Shell as DDSs

14.5.1 Polymer Drug Carriers with Magnetic Nanoparticle Shells

Various nanocarriers or vesicles can be prepared using self-assembly of amphiphilic block-copolymers and MNPs, regulating solvent-nanoparticle and polymer-nanoparticle interactions (Figure 14.16).[55] Three distinct structures can be obtained: a) core-shell type polymer assemblies, in which NPs are arranged at the interface between the polymer core and the shell (magneto-core shell), b) polymer micelles with NPs homogeneously incorporated (magneto-micelles), and c) polymersomes densely packed with NPs (magneto-polymersomes). Furthermore, the morphology and the size of the nanoparticle-encapsulating polymer assemblies significantly affect their magnetic relaxation properties, emphasizing the importance of the self-assembling structure and nanoparticle arrangement.[55]

Magnetoresponsive smart capsules can also be fabricated by a colloid-templating technique (Figure 14.17). Magnetite (Fe_3O_4) NPs were selectively deposited on a template surface by aqueous solution deposition using Pd catalysts. Hollow capsules were obtained by removal of the template core. Alternating magnetic fields were used to control the timing and dose of repeatedly released cargo from such vesicles by locally heating the membrane, which changed its permeability without major effects on the environment.[56]

Magnetic-sensitive particles were also prepared using Fe_3O_4/poly(allylamine) (Fe_3O_4/PAH) to construct a shell that breaks under a given magnetic stimulus. Depending on the duration of the stimulus, the magnetic-sensitive shell structure showed relatively slow release to burst-like behavior. Thus, release rate of encapsulated active substances can be tuned according to the time of

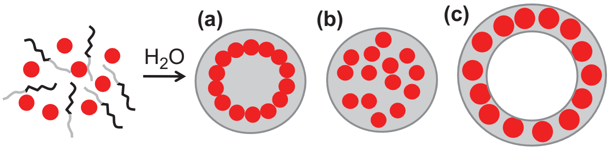

Figure 14.16 Self-assembly of nanoparticles and block copolymers: magneto-core shell assemblies formed when DMF/THF mixture (96.8% DMF) was used as the initial solvent for polymers and nanoparticles (a), magneto-micelles assembled in THF (b) and magneto-polymersomes assembled in dioxane/THF (96.8% dioxane) (c).
Reproduced from Ref. 55 with permission of the American Chemical Society.

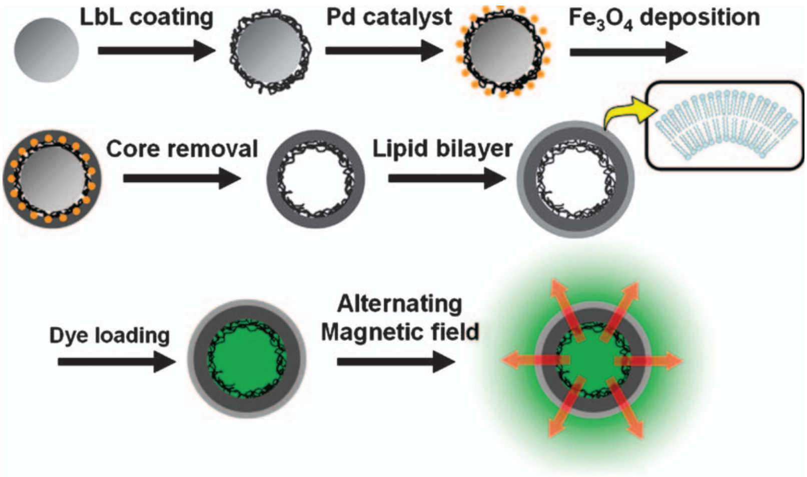

Figure 14.17 Preparation process and release of substances from magneto-responsive hybrid capsules. Nanoscale triggered release from liposomes, through magnetic actuation of iron oxide nanoparticle containing membranes, allows control over the released dose in space and time.
Reproduced from Ref. 57 with permission of the American Chemical Society.

exposition to the magnetic field. Furthermore, the magnetic-sensitive nanocapsules allowed a rapid uptake by tumor cells suggesting a potential for effective delivery of anticancer drugs.[57]

14.5.2 Mesoporous Silica Capped with Iron-oxide Nanoparticles

Nanosystems based on mesoporous inorganic silica nanoparticles (MSNs) may result in leakage-free, site-specific delivery, sustained release and imaging capability. Such is the case of the systems formed by MCM-41 type

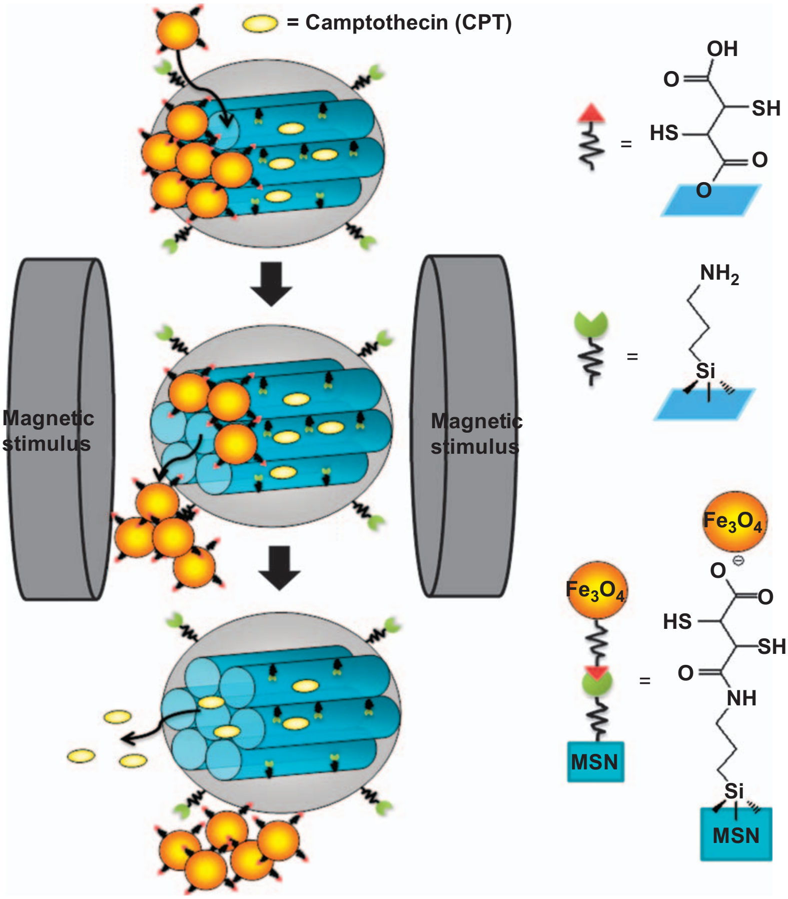

Figure 14.18 Scheme of the synthesis and the structure of the Fe_3O_4 NPs-capped mesoporous silica drug nanocarriers. The drug release from MSN@Fe_3O_4 nanocarriers can be remotely controlled under a magnetic stimulus. Reproduced from Ref. 58 with permission of the Royal Society of Chemistry.

mesoporous silica loaded with drug molecules, and with the pores chemically capped with Fe_3O_4 NPs (Figure 14.18).[58]

The MCM-type silica matrix was first functionalized with 3-aminopropyltrimethoxy silane to add amine groups along the silica surface (Figure 14.19(a)). (S)-(+)-Camptothecin was filled into the pores by soaking in DMSO for 48 h and drying under a vacuum for 24 h. Camptothecin-loaded amine-MSNs were covalently capped with *meso*-2,3-dimercaptosuccinic acid functionalized superparamagnetic iron oxide NPs (DMSA-Fe_3O_4 NPs; Figure 14.18). The resultant camptothecin-loaded MSN@Fe_3O_4 nanocarriers (~100 nm; Figure 14.19(b)) were well suspended in distilled water for more than 24 h without using any surfactant. The capped Fe_3O_4 NPs formed a dense

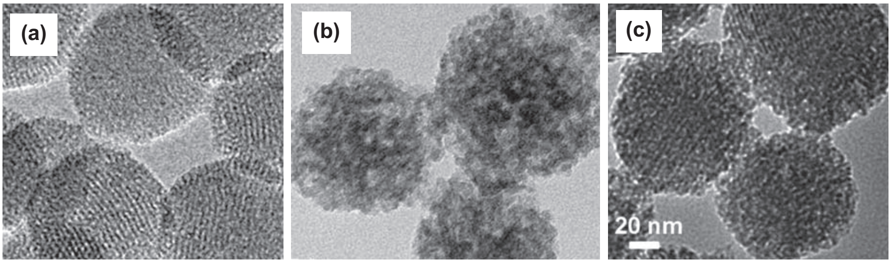

Figure 14.19 TEM images of mesoporous silica nanoparticles (a), Fe_3O_4 NPs-capped mesoporous silica nanocarriers ($MSN@Fe_3O_4$)Fe_3O_4 NPs before (b) and after (c) the magnetic field was applied.
Reproduced from Ref. 58 with permission of the Royal Society of Chemistry.

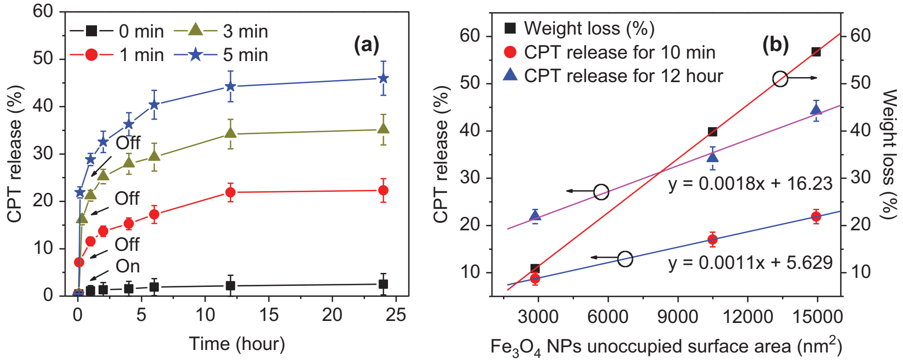

Figure 14.20 Camptothecin released from MSN and $MSN@Fe_3O_4$ nanocarriers triggered by magnetic stimulus for 1–5 min. (a). The $MSN@Fe_3O_4$ nanocarriers showed no drug leakage compared to MSN nanoparticles. A linear relationship was observed between the weight loss of Fe_3O_4 NPs and the Fe_3O_4 NP unoccupied surface area of MSN (b). A similar relationship can be established between the amount of camptothecin released and the Fe_3O_4 NPs unoccupied surface area of MSN at 10 min. and 12 hours of release test.
Reproduced from Ref. 58 with permission of the Royal Society of Chemistry.

and uniform layer tightly bound to the MSN surface without any signs of removal from the surface upon vigorous stirring in distilled water. With a magnetic trigger (Figure 14.19(c)) the Fe_3O_4 nanocaps can be removed from the surface of mesoporous silica vehicles due to the breaking of chemical bonds, subsequently leading to a fast-response drug release.

Without a magnetic stimulus, only a negligible amount of drug (0.2%) was released from the $MSN@Fe_3O_4$. The application of the stimulus for 5 minutes caused the cumulative drug release to increase up to 21.9% (Figure 14.20(a)) and, when the stimulus was removed, some of the Fe_3O_4 NPs fell from the surface of the MSN, increasing the surface area exposure and resulting in an increased camptothecin elution. After 24 hours, the cumulative release was 45.9%. This nanocarrier offers tunable release profiles depending on the strength and the time period of magnetic induction. Further estimation on the exposed surface area of the MSN upon magnetic stimulus was calculated using the equation[58]

$$W = P \cdot 4\pi R^2 \cdot \rho \cdot h = 4/3 \cdot \pi r^3 \cdot \rho \cdot N \tag{5}$$

where W represents the total weight of Fe_3O_4 NPs in an MSN@Fe_3O_4 nanocarrier, P is the random probability of 64% (for a randomly packed configuration of the nanocaps on a given MSN surface area), R is the MSN radius, ρ is the density ($5.17\,g\,cm^{-3}$), h is the thickness and r is the radius of the Fe_3O_4 NPs, and N is the number of Fe_3O_4 NPs on the surface of an MSN nanoparticle. On this basis, the exposed surface area can be correlated in a quantitative manner with the weight change of the nanocarriers after being subjected to the magnetic stimulus for various time spans (Figure 14.20(b)). The transverse relaxivity, r_2, of the MSN@Fe_3O_4 nanocarriers was *ca.* $121.57\,s^{-1}mM^{-1}$ Fe, which is larger than that reported for the mesoporous silica NPs decorated with magnetite nanocrystals. Therefore, MSN@Fe_3O_4 nanocarriers could perform well as a T_2-type magnetic resonance contrast enhancement agent for cell or molecular imaging. In addition, the MSN@Fe_3O_4 nanocarriers demonstrate fairly high cell uptake efficiency. Taking into account these features together with its versatile magnetic manipulation, this new type of MSN@Fe_3O_4 nanosystem can be considered a new class of multi-functional nanodevice with combined tunable drug release and nanoimaging modalities for a variety of biomedical uses.[58]

14.5.3 Magnetic Single-crystal Shell Drug Nanocarriers

Magnetic core-shell nanocarriers (15–23 nm) can be obtained surrounding a drug core with a single crystalline iron oxide shell (Figure 14.21). With such a unique core-shell configuration, drug molecules encapsulated in the core with an outer single-crystalline thin iron oxide shell can be protected from damage by harsh environment, and prevented from uncontrollable release due to natural diffusion of molecules upon delivery. Micrographs of high-resolution transmission electron microscopy (HRTEM) (Figure 14.21(a)) show a relatively dense, single-crystal shell with an orderly arranged crystal lattice, characteristic of magnetite (Fe_3O_4). Such a highly ordered arrangement of the crystal lattice in the shell structure is relatively unique and results from a self-assembly of the iron oxide salt in the presence of the drug. The amount of a fluorescence dye released from the core-shell nanospheres under a high-frequency magnetic field increased with the time of exposure, showing a maximum at 180 seconds (Figure 14.22(a)). When the nanospheres were exposed to a 60-second high-frequency magnetic field, kept away from the field for another 120 seconds and then exposed again to the field, repeatable release profiles were obtained by the action of the magnetic stimulus (Figure 14.22(b)).

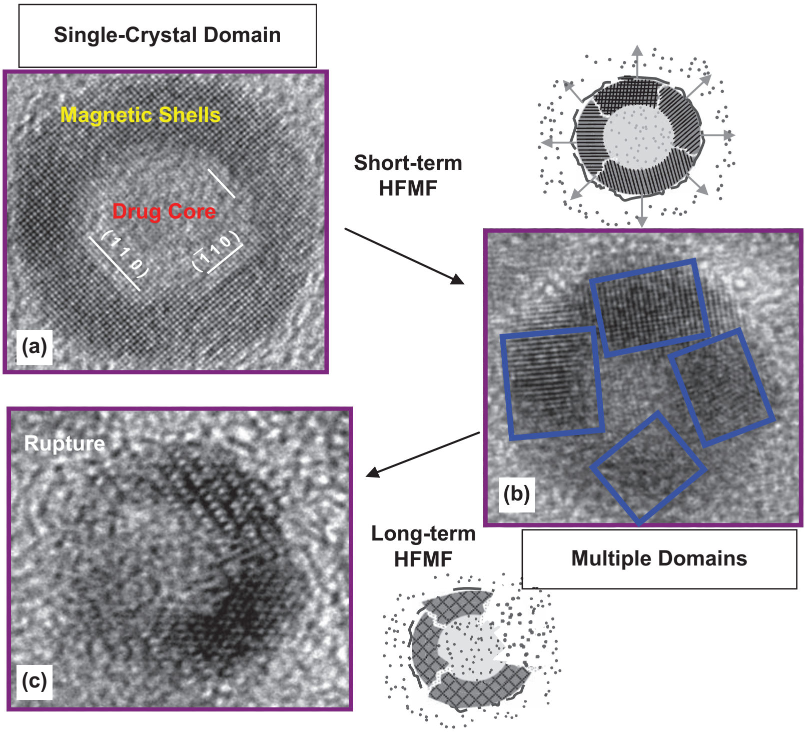

Figure 14.21 TEM images and schematic illustration of a magnetic nanocarrier with thin shell before (a) and while applying HFMF (b). Vibration enlarges the dimension of the nanofaults, making dye molecules easy to release out. The change in the dimension of the nanofaults is physically reversible upon a short-term field exposure. By contrast, under long-term exposure, the nanofaults receive a sufficient amount of the energy to rupture the thin shell permanently (c).
Reproduced from Ref. 59 with permission of Elsevier.

Negligible amounts of dye molecules were released in the absence of the stimulus. This simple test indicates that the shell was reversibly closed right after the field was removed, and that the dye molecules were physically enclosed inside the core phase again, completely avoiding uncontrolled diffusion. The changes in the structure of these core-shell nanocarriers are depicted in Figure 14.21. After a short exposure to the stimulus, *i.e.* 60 seconds, the single-crystal nanoshell underwent lattice deformation as a result of atomic rearrangement, forming nano-sized polycrystals of varying orientations. Boundaries between the nano-polycrystal developed, and such boundaries, which are prone to lead to nanocrevices under continuing stimulus, likely provided conduits for the dye molecules. In other words, while being subjected to the magnetic field for a short period (Figure 14.21(b)), crevices or cracks in a nanometric scale evolved along the boundary region of the thin shell because of the magnetically induced vibration, permitting the dye molecules to be easily

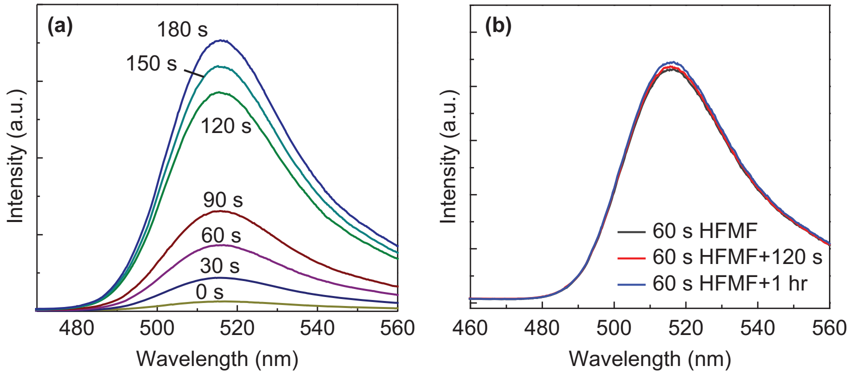

Figure 14.22 Emission spectra of dye-loaded PVP-modified Silica/Fe_3O_4 core-shell nanospheres (15 mg per 10 mL water) after applying HFMF from 30 s to 180 s (a) and when exposed to HFMF for 60 s, kept away from the field for another 120 s and then exposed again to the field (b). A negligibly small amount of the dye molecule is further released from the nanospheres for a time period of 120 s in the absence of the stimulus. Reproduced from Ref. 59 with permission of Elsevier.

released. The change in the dimension of the nanocrevices is physically reversible to a certain degree upon a short-term field exposure. However, under long-term exposure, the nano-crevices further enlarge in scale as a nanometric crack propagates along the spherical shell structure, which ultimately leads to irreversible deformation, *i.e.* rupture of the shell (Figure 14.21(c)), while absorbing a sufficient amount of magnetic energy, resulting in an increase in both pore volume and surface area. The variation in the crystal lattice orientation of the single-crystal iron oxide nanoshell upon magnetic stimulation may be a result of the thermally induced atomic re-arrangement, in which the free or surface energy of the single-crystal shell is reduced to form polycrystal-like structures with varying orientations. Additionally, the drug-loaded NPs were efficiently uptaken and rapidly released the drug in a well-controllable manner within the cells. This observation illustrates the prevention of premature leakage and the precise release of the required molecule for therapeutic purposes under the action of the magnetic field.[59]

14.6 Magnetic-responsive Composite Drug-delivery Membranes

Magnetic field-sensitive nanocarriers capable of delivering active agents in a controllable manner can be used as building blocks to form nanoporous membranes, that can be driven under a given electric field to aggregate onto flexible electrodes. Taking advantage of electrophoretic deposition (EPD) methods, a flexible drug-delivery device was designed and fabricated onto an electrically conductive flexible polyethylene terephthalate (PET) substrate.

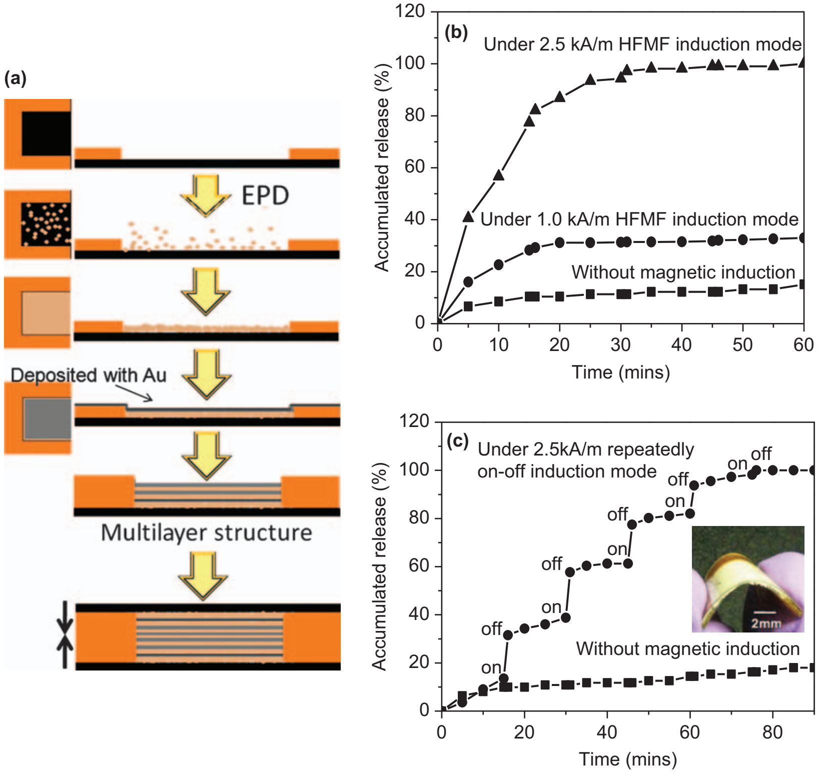

Figure 14.23 Schematic flowchart of the preparation of a multi-layer membrane for a drug-delivery chip (a), drug release (b) and pulse release (c) profiles from the ESM-containing core-shell nanoparticles. Magnetic field triggers fast release, while minimal release is observed without the magnetic induction treatment.
Reproduced from Ref. 60 with permission of Elsevier.

Figure 14.23 illustrates the preparation procedure of a uniform and nanoporous membrane.[60] The membranes were used to fabricate a drug-delivery chip with sandwich structure, consisting of PET-ethosuximide-loaded membrane-PET for the controlled delivery of this antiepileptic drug. Ethosuximide has long been used as the first-choice therapeutic agent to ameliorate clinical spike-wave discharge (SWD) occurrences. The chip showed a variety of release profiles (*e.g.* slow, sustained, stepwise and burst release profiles) depending on the mode of magnetic operation. When the magnetic field was removed, the release instantly ceased; the process being reversible.[60]

A preliminary *in vivo* study was carried out with Long-Evans rats that display spontaneous SWDs. The frequency of the SWDs was recorded after intra-peritoneal administration of saline solution, ethosuximide solution or ethosuximide-Fe_3O_4@SiO_2 particles dispersion, and the implantation of a magnetically induced ethosuximide-chip (Figure 14.24). A significant reduction

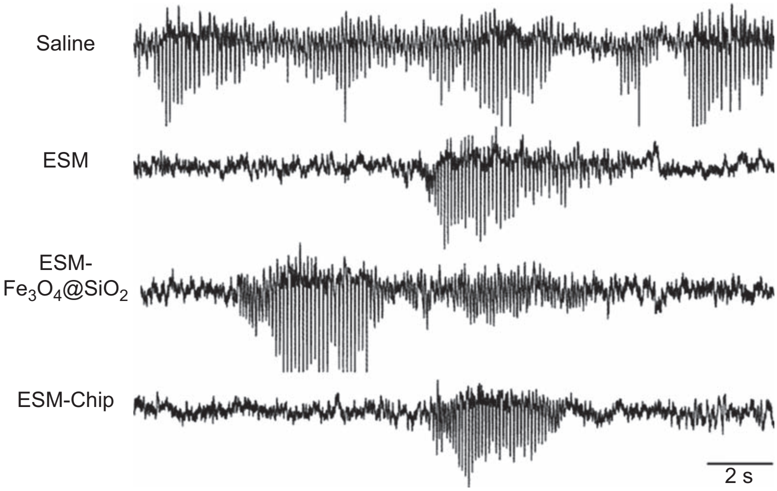

Figure 14.24 Spontaneous spike-wave discharges (SWDs) recorded after intraperitoneal administration of saline solution, ethosuximide (ESM) solution, ESM-containing nanoparticles (ESM-Fe_3O_4@SiO_2) dispersion and implantation of the ESM-chip.
Reproduced from Ref. 60 with permission of Elsevier.

in the number and total duration of spontaneous SWDs was recorded for the rats bearing the chip when subjected to the same magnetic induction as *in vitro*, indicating the usefulness of the chip for ethosuximide delivery. The flexible, membrane-like drug-delivery chip may offer advantages over conventional drug-delivery devices, improving dosing precision and ease of operation, and enabling more versatile elution patterns and better compliance.

Another magnetic composite membrane has been prepared combining multiple engineered MNPs (the sensor entity) with thermo-sensitive PNIPAAm-based nanogels (the switching entity), which enables rapid, repeatable and tunable drug delivery upon the application of an external oscillating magnetic field (Figure 14.25). To facilitate an effective *in vivo* triggering, nanogels were engineered to remain swollen (*i.e.* in the "off" state) at physiological temperature by copolymerizing NIPAAm with *N*-isopropylmethacrylamide (NIPMAM) and acrylamide (AAm). The ratio between the monomers was chosen with the aim of maximizing the size change from the swollen to the collapsed state and, thus, of optimizing the membrane pore opening when triggered. The ability of the membrane constituents and the composite membrane to be triggered at physiologically relevant temperatures was evaluated using both thermal and magnetic stimuli. Nanogels dispersed in PBS shrink from ~750 nm to ~350 nm upon heating from the physiological temperature to 50 °C, with >90% of the total deswelling transition completed at 43 °C. Thermal triggering of the nanogel-containing membrane was tested by placing it between two chambers of a glass flow cell submerged in a water bath, and evaluating the flux of sodium fluorescein between the chambers (*i.e.* across

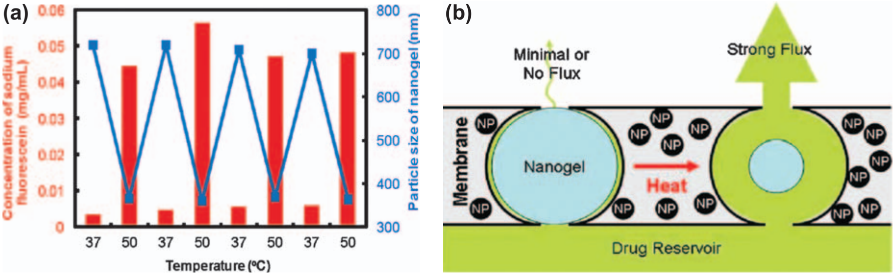

Figure 14.25 Stimulus-responsive membrane triggering *in vitro*: changes in the particle size (blue data, right y-axis) of dispersed nanogels and flux of sodium fluorescein through the nanogel-loaded membranes (red data, left y-axis) as a function of temperature (a); and proposed mechanism of the membrane functioning (b).
Reproduced from Ref. 61 with permission of the American Chemical Society.

the membrane) as a function of time and temperature. An approximately 20-fold higher flux of sodium fluorescein occurred at temperature exceeding the volume phase transition temperature (~40 °C) of the nanogels (Figure 14.25(a)). The fluorescein flux could be switched on and off over multiple thermal cycles with high reproducibility, suggesting that the nanogel phase transition inside the membrane pores was fully reversible. The magnetic triggering of the composite membrane is shown in Figure 14.25(b). The MNPs embedded in the membrane heated inductively when subjected to an external oscillating magnetic field. Upon application of a magnetic field at the right frequency and amplitude, the water inside the semi-adiabatic flow cell heated from 37 °C to 42 °C over the course of 10 min, reaching the steady state. Heat generated by magnetic induction was transferred to the adjacent thermosensitive nanogels, causing the nanogels to shrink and permitting drug diffusion out of the device. As in the thermally activated experiments, a 10- to 20-fold differential flux was observed between the "off" and "on" states. Furthermore, multiple on-off cycles could be performed without significantly changing the permeability of the membrane in the "off" state. This reproducibility suggests that magnetically triggered physical distortion of the device does not play a significant role in accelerating drug release from membrane-based devices.[61]

14.7 Conclusion

The magnetic drug carriers show outstanding switching on/off of the release *via* the addition and removal of an external high-frequency magnetic field, respectively. Real-time responses can be obtained. Furthermore, the magnetic drug carriers can be surface modified with ligands for active targeting delivery and used as MRI contrast agents for cell-tracking. Combining magnetic-responsive NPs that exhibit a rapid response to the magnetic field with intelligent polymers allows for site-specific or cell-based drug delivery with considerably improved therapeutic efficacy. We envision that these NPs will play a significant role in the development of a new generation of site-selective, controlled-release drug-delivery nanodevices and other carrier formats.

References

1. A. C. R. Grayson, I. S. Choi, B. M. Tyler, P. P. Wang, H. Brem, M. J. Cima and R. Langer, *Nat. Mater.*, 2003, **2**, 767.
2. Z. Hu and X. Xia, *Adv. Mater.*, 2004, **16**, 305.
3. X. Z. Zhang, D. Q. Wu and C. C. Chu, *Biomaterials*, 2004, **25**, 3793.
4. M. Das, S. Mardyani, W. C. W. Chan and E. Kumacheva, *Adv. Mater.*, 2006, **18**, 80.
5. M. R. Abidian, D. H. Kim and D. C. Martin, *Adv. Mater.*, 2006, **18**, 405.
6. B. G. De Geest, A. G. Skirtach, A. A. Mamedov, A. A. Antipov, N. A. Kotov, S. C. De Smedt and G. B. Sukhorukov, *Small*, 2007, **3**, 804.
7. H. J. Kim, H. Matsuda, H. Zhou and I. Honma, *Adv. Mater.*, 2006, **18**, 3083.
8. E. R. Edelman, J. Kost, H. Bobeck and R. Langer, *J. Biomed. Mater. Res.*, 1985, **19**, 67.
9. J. Kost, J. Wolfrum and R. Langer, *J. Biomed. Mater. Res.*, 1987, **21**, 1367.
10. J. Kost, R. Noecker, E. Kunica and R. Langer, *J. Biomed. Mater. Res.*, 1985, **19**, 935.
11. Z. Lu, M. D. Prouty, Z. Guo, V. O. Golub, C. S. S. R. Kumar and Y. M. Lvov, *Langmuir*, 2005, **21**, 2042.
12. J. Fricker, *Drug Discov. Today*, 2001, **6**, 387.
13. T. Y. Liu, S. H. Hu, K. H. Liu, D. M. Liu and S. Y. Chen, *J. Magn. Magn. Mater.*, 2006, **304**, e397.
14. T. D. Dziubla, M. C. Torjman, J. I. Joseph, M. Murphy-Tatum and A. M. Lowman, *Biomaterials*, 2001, **22**, 2893.
15. H. Storrie and D. J. Mooney, *Adv. Drug Deliver. Rev.*, 2006, **58**, 500.
16. O. C. Farokhzad and R. Langer, *ACS Nano*, 2009, **3**, 16.
17. S. H. Hu, Y. Y. Chen, T. C. Liu, T. H. Tung, D. M. Liu and S. Y. Chen, *Chem. Commun.*, 2011, **47**, 1776.
18. S. H. Hu and Xiaohu Gao, *J. Am. Chem. Soc.*, 2010, **132**, 7234.
19. S. H. Hu, K. T. Kuo, W. L. Tung, D. M. Liu and S. Y. Chen., *Adv. Funct. Mater.*, 2009, **19**, 3396.
20. S. H. Hu, T. Y. Liu, H. Y. Huang, D. M. Liu and S. Y. Chen, *J. Nanosci. Nanotechnol.*, 2009, **9**, 866.
21. J. P. Fortin, C. Wilhelm, J. Servais, C. Ménager, J. C. Bacri and F. Gazeau, *J. Am. Chem. Soc.*, 2007, **129**, 2628.
22. C. M. Sorensen, in *Nanoscale Materials in Chemistry*, ed. K. J. Klabunde, Wiley-Interscience, New York, 2001, p. 169.
23. C. H. Griffiths, M. P. Ohoro and T. W. Smith, *J. Appl. Phys.*, 1979, **50**, 7108.
24. C. B. Murray, D. J. Norris and M. G. Bawendi, *J. Am. Chem. Soc.*, 1993, **115**, 8706.

25. Z. A. Peng and X. G. Peng, *J. Am. Chem. Soc.*, 2001, **123**, 183.
26. L. H. Qu, Z. A. Peng and X. G. Peng, *Nano Lett.*, 2001, **1**, 333.
27. M. A. Hines and P. Guyot-Sionnest, *J. Phys. Chem.*, 1996, **100**, 468.
28. S. Sun, H. Zeng, D. B. Robinson, S. Raoux, P. M. Rice, S. X. Wang and G. Li, *J. Am. Chem. Soc.*, 2004, **126**, 273.
29. T. Hyeon, S. S. Lee, J. Park, Y. Chung, N. Bin and H. Na, *J. Am. Chem. Soc.*, 2001, **123**, 12798.
30. J. Park, K. J. An, Y. S. Hwang, J. G. Park, H. J. Noh, J. Y. Kim, J. H. Park, N. M. Hwang and T. Hyeon, *Nat. Mater.*, 2004, **3**, 891.
31. Y. W. Jun, Y. M. Huh, J. S. Choi, J. H. Lee, H. T. Song, S. Kim, S. Yoon, K. S. Kim, J. S. Shin, J. S. Suh and J. Cheon, *J. Am. Chem. Soc.*, 2005, **127**, 5732.
32. A. K. Gupta, R. R. Naregalkar, V. D. Vaidya and M. Gupta, *Nanomedicine UK*, 2007, **2**, 23.
33. J. W. M. Bulte and D. L. Kraitchman, *NMR Biomed.*, 2004, **17**, 484.
34. Y. X. J. Wang, S. M. Hussain and G. P. Krestin, *Eur. Radiol.*, 2001, **11**, 2319.
35. A. P. Philipse, M. P. B. Vanbruggen and C. Pathmamanoharan, *Langmuir*, 1994, **10**, 92.
36. Y. Lu, Y. D. Yin, B. T. Mayers and Y. N. Xia, *Nano Lett.*, 2002, **2**, 183.
37. M. Arruebo, R. Fernández-Pacheco, M. R. Ibarra and J. Santamaría, *Nano Today*, 2007, **2**, 22.
38. H. S. Choi, W. Liu, P. Misra, E. Tanaka, J. P. Zimmer, B. I. Ipe, M. G. Bawendi and J. V. Frangioni, *Nat. Biotechnol.*, 2007, **25**, 1165.
39. R. Weissleder, A. S. Lee, A. J. Fischman, P. Reimer, T. Shen, R. Wilkinson, R. J. Callahan and T. J. Brady, *Radiology*, 1991, **181**, 245.
40. N. Nitin, L. E. W. LaConte, O. Zurkiya, X. Hu and G. Bao, *Biol. Inorg. Chem.*, 2004, **9**, 706.
41. R. D. Corato, A. Quarta, P. Piacenza, A. Ragusa, A. Figuerola, R. Buonsanti, R. Cingolani, L. Manna and T. Pellegrino, *J. Mater. Chem.*, 2008, **18**, 1991.
42. A. K. Gupta and M. Gupta, *Biomaterials*, 2005, **26**, 3995.
43. J. Kim, J. E. Lee, S. H. Lee, J. H. Yu, J. H. Lee, T. G. Park and T. Hyeon, *Adv. Mater.*, 2008, **20**, 478.
44. S. H. Hu, W. L. Tung, C. F. Liao, D. M. Liu and S. Y. Chen, *Adv. Funct. Mater.*, 2008, **18**, 2946.
45. T. Y. Liu, S. H. Hu, D. M. Liu, S. Y. Chen and I. W. Chen, *Nano Today*, 2009, **4**, 52.
46. Y. Kadam, U. Yerramilli, A. Bahadur and P. Bahadur, *Colloid Surface. B*, 2011, **83**, 49.
47. P. Khullar, A. Mahal, V. Singh, T. S. Banipal, G. Kaur and M. S. Bakshi, *Langmuir*, 2010, **26**, 11363.
48. T. Y. Liu, K. H. Liu, D. M. Liu, S. Y. Chen and I. W. Chen, *Adv. Funct. Mater.*, 2009, **19**, 616.
49. P. Pradhan, J. Giri, F. Rieken, C. Koch, O. Mykhaylyk, M. Döblinger, R. Banerjee, D. Bahadur and C. Plank, *J. Control. Release*, 2010, **142**, 108.

50. M. Liong, J. Lu, M. Kovochich, T. Xia, S. G. Ruehm, A. E. Nel, F. Tamanoi and J. I. Zink, *ACS Nano*, 2008, **2**, 889.
51. C. R. Thomas, D. P. Ferris, J. H. Lee, E. Choi, M. H. Cho, E. S. Kim, J. F. Stoddart, J. S. Shin, J. Cheon and J. I. Zink, *J. Am. Chem. Soc.*, 2010, **132**, 10623.
52. S. L. Sun, Y. L. Lo, H. Y. Chen and L. F. Wang, *Langmuir*, 2012, **28**, 3542.
53. H. Mok, O. Veiseh, C. Fang, F. M. Kievit, F. Y. Wang, J. O. Park and M. Zhang, *Mol. Pharmaceut.*, 2010, **7**, 1930.
54. F. M. Kievit, O. Veiseh, C. Fang, N. Bhattarai, D. Lee, R. G. Ellenbogen and M. Zhang, *ACS Nano*, 2010, **4**, 4587.
55. R. J. Hickey, A. S. Haynes, J. M. Kikkawa and S. J. Park, *J. Am. Chem. Soc.*, 2011, **133**, 1517.
56. K. Katagiri, M. Nakamura and K. Koumoto, *ACS Appl. Mater. Inter.*, 2010, **2**, 768.
57. S. H. Hu, C. H. Tsai, C. F. Liao, D. M. Liu and S. Y. Chen, *Langmuir*, 2008, **24**, 11811.
58. P. J. Chen, S. H. Hu, C. S. Hsiao, Y. Y. Chen, D. M. Liu and S. Y. Chen, *J. Mater. Chem.*, 2011, **21**, 2535.
59. S. H. Hu, S. Y. Chen, C. S. Hsiao and D. M. Liu, *Adv. Mat.*, 2008, **20**, 2690–2695.
60. W. C. Huang, S. H. Hu, K. H. Liu, S. Y. Chen and D. M. Liu, *J. Control. Release*, 2009, **139**, 221.
61. T. Hoare, J. Santamaria, G. F. Goya, S. Irusta, D. Lin, S. Lau, R. Padera, R. Langer and D. S. Kohane, *Nano Lett.*, 2009, **9**, 3651.

CHAPTER 15

Smart Drug Delivery from Silica Nanoparticles

MONTSERRAT COLILLA[a,b] AND
MARÍA VALLET-REGÍ*[a,b]

[a] Departamento de Química Inorgánica y Bioinorgánica, Facultad de Farmacia, Universidad Complutense de Madrid. Plaza Ramón y Cajal s/n, 28040 Madrid, Spain; [b] Networking Research Center on Bioengineering, Biomaterials and Nanomedicine (CIBER-BBN), Madrid, Spain
*Email: vallet@farm.ucm.es

15.1 Introduction

One of the main challenges for the biomedical scientific community is the design of novel drug-delivery systems (DDSs) able to transport an effective amount of cargo specifically to the target cell and/or tissue.[1] Currently, most clinically used drugs in oral or systemic administration are low-molecular-weight compounds that exhibit short half-lives in the bloodstream and a high overall clearance rate. Therefore, high initial drug doses are needed to maintain therapeutic concentrations over a prolonged time period. In addition, these drugs are distributed within the body and unspecifically interact with both defected and healthy tissues. As a consequence, only small amounts of the drug reach the target site and the therapy is associated with limited efficacy and side effects. This is particularly important in oncology, where the risk-benefit ratio associated with chemotherapy is often unmanageable. Targeted DDSs that transport an effective drug dose to the cells and tissues is a good alternative to overcome this shortcoming. An ideal smart DDS must satisfy important requirements: i) the carrier material must be biocompatible;

RSC Smart Materials No. 3
Smart Materials for Drug Delivery: Volume 2
Edited by Carmen Alvarez-Lorenzo and Angel Concheiro
© The Royal Society of Chemistry 2013
Published by the Royal Society of Chemistry, www.rsc.org

ii) high loading and protection capability of desired drug molecules; iii) "zero premature release" of drug molecules before reaching its target; iv) cell type or tissue specificity and site targeting ability; v) efficient cellular uptake; vi) effective endosomal escape; and vii) controllable release rate to achieve an effective local concentration.

In the last years, different approaches have been developed to design smart DDSs able to provide site-specific and stimuli-responsive controlled drug release. Drug-delivery nanocarriers based on organic platforms that have been used include dendrimers,[2] liposomes,[3] polymers[4,5] and virus-like particles[6] (Figure 15.1). Recently, inorganic nanoparticles, such as gold,[7] semiconductor nanocrystals,[8] superparamagnetic nanoparticles[9] and silicon[10] and silica-based materials[11,12] have been investigated as promising candidates for drug delivery. Inorganic nanoparticles are receiving considerable attention due to their increased mechanical strength, chemical stability, biocompatibility and resistance to microbial attack as compared to their organic equivalents.[11,13,14] In addition, the ceramic matrix efficiently protects entrapped guest molecules against enzymatic degradation or denaturation induced by pH and temperature as no swelling or porosity changes take place as a response to environmental variations.

Among the different types of inorganic nanoparticles, mesoporous silica nanoparticles (MSNPs) have emerged as promising drug-delivery carriers. After the introduction of mesoporous materials in the drug-delivery arena in 2001,[15] MSNPs are receiving growing scientific attention for their potential applications in the biotechnology and nanomedicine fields.[16–26] The synthesis of MSNPs can be carried out by using two different approaches. The first one is

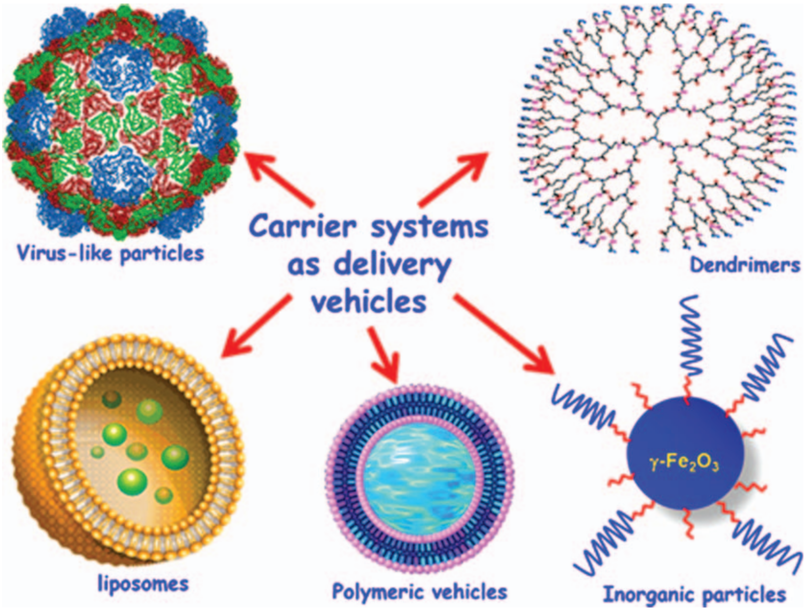

Figure 15.1 Some carrier systems used as release vehicles for smart drug delivery.

the so-called "modified Stöber method", which consists in the condensation of silica under basic medium in the presence of cationic surfactants as structure directing agents.[27] The second strategy is the aerosol-assisted synthesis, which allows using not only cationic but also anionic and non-ionic surfactants to obtain MSNPs.[28–32] The surfactant removal usually leads to materials with cylindrical mesopores arranged in a two-dimensional hexagonal fashion, characteristic of MCM-41 type materials.[33] MSNPs exhibit distinctive and advantageous textural and structural features, such as high surface area (*ca.* $1000\,m^2\,g^{-1}$) and pore volume (*ca.* $1\,cm^3\,g^{-1}$), stable mesostructure, tunable pore diameter (2–10 nm), two functional surfaces (exterior particle and inner pore faces) and tunable particle size. The nanoparticle size in the range of interest for targeted intra-cellular delivery applications falls into the 50–200 nm range, since larger particles cannot easily bypass physical membranes in the body, and smaller MSNPs are difficult to synthesize due to their inherent mesoporosity. As the particle size has been demonstrated to play a pivotal role in the nanoparticle distribution and behavior in living systems,[34–36] narrow particle size distributions are preferred. Therefore, wet-chemical synthesis methods are generally more beneficial than other physical methods such as spray-drying, which commonly lead to a relatively wide particle size distribution with non-negligible fractions of fine and larger particles. The unique hexagonally ordered pore structures of MSNPs offer the possibility of obtaining a "perfect" capping of mesopore channels. This is essential for certain applications, for instance the delivery of toxic antitumor drugs, which requires "zero release" before reaching the targeted cells or tissues. Then, drug release would take place at specific sites after application of a suitable stimulus, in the so-called stimuli-responsive delivery systems.

The features of MSNPs make them excellent candidates to develop smart DDSs. However, when aiming at smart drug delivery for specific applications in biomedicine, diverse moieties have to be incorporated into the nanosystem to provide it with multi-functionality. Thus, MSNPs can be modified by targeting moieties, such as peptides, antibodies or simple molecules such as folic acid to deliver specifically the desired drugs into unhealthy cells. Moreover, it is possible to cover the outer surface of MSNPs with polymeric coatings. At this point, MSNPs can be given "stealth" properties by functionalizing their external surface with biocompatible polymers, thus preventing the removal of MSNPs from blood circulation by the mononuclear phagocytic system. It is also possible to coat MSNPs with stimuli-responsive polymers able to control the delivery of the cargo in response to the application of a determined stimulus. Moreover, the combination of MSNPs and polymers could permit the delivery of nucleic acids for gene-therapy purposes. Magnetic nanoparticles can be combined with MSNPs to design magnetic nanocomposites that could be guided to the target organ or tissue by application of an external magnetic field. In addition, magnetic NPs could act as thermoseeds for hyperthermia treatment, which in combination with chemotherapy would increase the antitumor effect of the system. Magnetic NPs can also be used as nanocaps that block the pore entrances and allow drug delivery from mesochannels after their removal by application of an external magnetic field. Magnetic NPs could also permit magnetic resonance imaging (MRI) to be performed. Finally, it is possible to incorporate molecular nanogates as mesopore capping agents to create gate-keeping properties, *i.e.* capping the pore openings to prevent physically adsorbed cargo desorbing from the carrier before reaching the target cells. The drug release would be triggered by a given stimulus that produces the removal of the nanogates.

In this chapter we illustrate the different approaches developed so far to design and improve the behavior of MSNPs as multi-functional drug-delivery platforms. The results regarding the *in vitro* and *in vivo* biocompatibility of these nanosystems are also reviewed.

15.2 Multi-functionality of Mesoporous Silica Nanoparticles to Design Smart DDSs

MSNPs have an internal surface, *i.e.* the inner part of the mesoporous cavities, and an external surface, *i.e.* the external face of the nanoparticle. This remarkable feature permits the selective functionalization of the internal and external surface of MSNPs with different functional groups or biologically active molecules. Commonly, the functionalization of the mesopore walls of MSNPs is performed by using co-condensation or one-step methods, which allow homogeneously incorporating several functional groups during the synthesis step. The co-condensation method of a tetraalkoxysilane, $(RO)_4Si$, and one or more organoalkoxysilanes, $(RO)_3SiR'$, has been widely employed to synthesize mesoporous organic-inorganic hybrid materials.[37,38] Thus, a wide range of functional groups have been introduced to MSNPs to adsorb drug molecules or covalently attach fluorophores.[16,39] Usually, the fluorophore is pre-reacted with an aminosilane that is subsequently used in the co-condensation synthesis, yielding inherently fluorescent MSNPs for cell imaging.[40–46]

However, as previously mentioned, when aiming at targeted smart drug delivery, additional moieties have to be incorporated into MSNPs to provide them with multi-functional properties, as schematically depicted in Figure 15.2. The different possibilities reported to date are described in the next sections.

15.2.1 Targeting Agents

Cell targeting is a key issue in cases such as cancer therapy, where the lack of specificity of antitumor drugs results in adverse side effects and limited effectiveness due to unspecific action on healthy cells. Much research effort is being committed to develop MSNPs with cell-targeting capability to deliver specifically the desired drugs to unhealthy cells. Tumor targeting can be mainly achieved through the combined effect of passive and active targeting strategies. The leaky vasculature and poorly operational lymph system of tumors allow MSNPs exiting the blood vessels and accumulating at the tumor site by passive

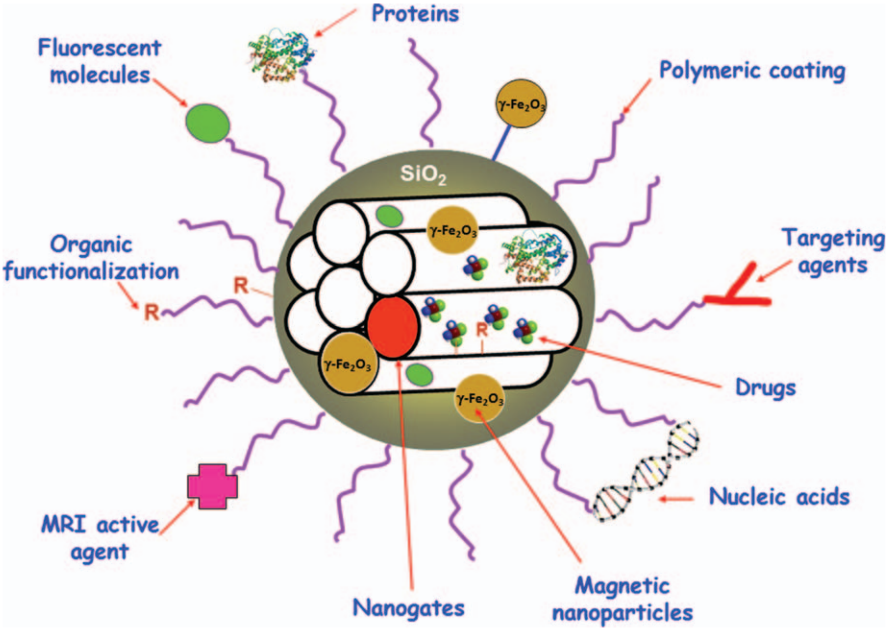

Figure 15.2 Multi-functionality and cargo loading possibilities of mesoporous silica nanoparticles.

targeting, *via* the enhanced permeability and retention (EPR) effect.[47–49] The diffusion rate in the extra-cellular spaces of the tumor is governed by the size and the surface charge of the particles. On the other hand, active targeting aims at facilitating the interaction of MSNPs with cancer cells, retaining the nanocarrier into the tumor site and facilitating the cellular uptake. The selectivity is a function of the ability of the NPs to be internalized by the targeted cell population. Several strategies have been proposed to chemically graft different targeting ligands, such as sugars,[50–54] monoclonal antibodies,[55,56] DNA aptamers[57,58] or folic acid (FA),[39,40,46,50,59–63] to the external surface of MSNPs. These systems are supported in the ability of the targeting agents selectively to bind receptors that are overexpressed on the cancer cell surface to trigger receptor-mediated endocytosis. Among these possibilities, the functionalization of MSNPs with FA has emerged as an attractive alternative for targeted drug delivery[64] because α-folate receptor (FR) is up-regulated in various types of human cancer cells.[65,66] Successful *in vitro* cell-specific drug delivery to cancer cells using MSNPs functionalized with FA has been reported.[40] Thus, the cytotoxicity of MSNPs-FA loaded with the antitumor drug camptothecin (CPT) was higher in cell lines overexpressing FR, such as pancreatic PANC-1 cancer cells (60% cell death based on a viability assay), than in control non-cancerous cells such as foreskin fibroblast HFF (30% cell death). Moreover, the cytotoxicity of the FA-modified and unmodified drug-loaded MSNPs was similar for the HFF since these cells do not overexpress the receptors. These results showed that FA modification to the MSNPs can increase the particle uptake and deliver more drug to the cancer cells, but not to the non-cancerous fibroblast. Similar numbers were reported by Zhu *et al.*,[57] who investigated the effect of doxorubicin (Dox)-loaded MSNPs, which were surface functionalized with aptamer conjugates, on cell viability in cancerous HeLa cells (40% viability) and healthy QGY7703 cells (60% viability). Recently, Rosenholm *et al.*[60] attached methotrexate (MTX), an antitumor drug structurally similar to FA, to the surface of MSNPs. MTX exerted a dual function, acting as targeting ligand and cytotoxic agent. MTX-loaded MSNPs induced an apoptotic cell death of about 33% after 72 h in the cancerous HeLa cell line, compared to non-cancerous HEK293 cells where no apoptosis over the control was observed.

In the last two years, Zink's group has provided noteworthy advances this landscape by carrying out *in vivo* studies of targeted *versus* non-targeted MSNPs. These authors reported for the first time that MSNPs were effective for antitumor drug delivery and that the tumor suppression was significant in a subcutaneous human breast cancer xenograft in mice.[62] In the study, the subcutaneous tumors in mice were virtually eliminated by treating with CPT-loaded MSNPs or CPT-loaded FA-modified-MSNPs. More recently, the same research group reported the efficacy of MSNPs using two different human pancreatic cancer xenografts on different mouse species.[63] Significant tumor-suppression effects were achieved with CPT-loaded MSNPs. Dramatic improvement of the potency of tumor suppression was obtained by surface modifying MSNPs with FA.

15.2.2 Polymeric Coatings

The aim of using polymers of different chemical nature to cover MSNPs is two-fold. The first consists in grafting a certain polymer to the MSNPs to increase their blood circulation lifetimes, by minimizing both their binding to blood proteins and their uptake by human macrophages. The second strategy regards the covalent link of stimuli-responsive polymers to MSNPs to control the release of the cargo "on demand" obeying the application of a certain stimulus (pH, temperature, light, *etc.*).

15.2.2.1 "Stealth" Properties

Huge protein adsorption onto MSNPs under physiological conditions is a major concern and must be avoided because it would decrease the targetability of the particles as well as increase their recognition as foreign bodies by the defense mechanisms (the reticuloendothelial system, RES), which would lead to rapid clearance from the blood circulation. Moreover, protein adsorption onto MSNPs may affect their toxicity. The functionalization with certain polymers, such as polyethylene glycol (PEG), a process known as PEGylation, has been a widely used approach to provide MSNPs with "stealth" properties, *i.e.* decreased protein adsorption (opsonization) capability. This characteristic promotes the EPR effect of MSNPs at the tumor site, and their blood circulation half-lives are prolonged.[67–69] The "stealth" features of PEGylated particles are generally attributed to the steric hindrance and repulsion effects of PEG chains against blood proteins and macrophages, which are closely correlated to the PEG molecular weight, surface chain density and conformation.[70,71] One major challenge is to find the optimal PEG molecular weight and chain density on MSNPs to minimize both their binding to blood proteins and their uptake by human macrophages.[72] He *et al.*[69] investigated the influence of PEG molecular weight and packing density on the adsorption of serum proteins to MSNPs, whose PEG chains were linked to the MSNPs using silane coupling chemistry. The results derived from this work revealed that PEG molecular weights of 10–20 kD were optimal for minimizing non-specific protein adsorption. Furthermore, the optimum PEG molecular weight may be a function of the used chemistry to covalently link PEG to the MSNP surface. Recently, the same research group carried out *in vivo* assays to evaluate the effect of PEGylation of MSNPs on the *in vivo* biodistribution and urinary excretion by tail-vein injection in ICR mice.[73] The results indicated that PEGylated MSNPs escaped more easily from capture by liver, spleen and lung tissues, possessed longer blood-circulation lifetime, and were more slowly biodegraded and correspondingly had a lower excreted amount of degradation products in the urine compared to non-PEGylated MSNPs.

15.2.2.2 Stimuli-responsive Capability

It is possible to covalently link stimuli-responsive polymers to MSNPs with the aim of regulating the transport of encapsulated cargo. When a stimulus, such as a change of pH, temperature, light, redox potential, *etc.* is applied, the physicochemical properties of the polymer change, which allows the delivery of the drug out of the mesopores.

The attachment of *temperature-responsive polymers*, such as poly(*N*-isopropylacrylamide) (PNIPAAm) and its derivatives, onto the surface of MSNPs has been reported in the recent years.[74–77] PNIPAAm changes its molecular chain conformation in response to temperature in aqueous environments.[78] Thus, the molecular chains of PNIPAAm are hydrated below the lower critical solution temperature (LCST) of 32 °C, resulting in an extended chain conformation that prevents the departure of the drugs loaded inside the mesopore channels. When the temperature increases above the LCST, the polymer chains dehydrate resulting in a collapsed conformation, pore opening and subsequently release of the cargo. An increase in the LCST so that collapse occurs under physiological conditions would be desirable for biomedical applications. This can be achieved by performing modifications of the polymer composition by copolymerization with other monomers such as acrylamide[79,80] or *N*-isopropylmethacrylamide.[81,82] Very recently, Baeza *et al.*[83] have presented a novel nanodevice able to perform remotely controlled release of small molecules and proteins in response to an alternating magnetic field. This device is based on MSNPs with iron oxide nanocrystals encapsulated inside the silica matrix and decorated on the outer surface with a thermo-responsive copolymer of poly(ethylenimine)-b-poly(*N*-isopropylacrylamide) (PEI/NIPAAm). The polymer structure was designed with a double purpose: to act as temperature-responsive gatekeeper for the drugs hosted inside the mesopores, and to retain proteins in the polymer shell by electrostatic or hydrogen bond interactions. The nanosystem retains the different cargos at low temperature (20 °C) and delivers the entrapped molecules when the temperature exceeds 35–40 °C following different release kinetics.

Another method consists in covalently linking *pH-responsive polymers* to the external surface of MSNPs, which act as smart nanoshells able to regulate the release of guest molecules. Liu *et al.*[84] reported the grafting of poly(4-vinyl pyridine) on the mesoporous silica surface to create a nanoshell that acts as pH-sensitive barrier controlling the release of the molecules trapped inside the pores. Poly(acrylic acid) (PAA) grafted MSNPs have also been prepared, demonstrating that the drug release rate was pH dependent and increased with the decrease of pH due to the fact that the protonization of PAA weakens the interactions with the drug.[85,86] It is also possible to design pH-responsive nanocontainers that exhibit the opposite release behavior. In alkaline solution, the polymer chains are extended, the mesopore entrances are open and the drug is released. On the contrary, in acidic medium the compact polymer layers block the pores and hinder the drug diffusion out of the channels. However, in certain pathologies such as cancer, where targeted smart drug delivery is especially relevant, the external pH of cancerous tissues is usually lower than that of the surrounding healthy tissues.[87] Consequently, suitable cancer therapies demand the development of acid-triggered delivery systems that release the drugs under acidic conditions and impede drug release at physiological pH. With this goal in mind, Sun *et al.*[88] have recently shown the preparation of novel pH-responsive nanodevices consisting in poly(2-(diethylamino)ethyl methacrylate) (PDEAEMA) grafted to MSNPs. In acidic medium, the tertiary amine in PDEAEMA easily obtains a proton, forming a quaternary ammonium and the protonated chains adopt an extended (soluble) conformation, allowing release of the cargo. Conversely, in neutral or alkaline solution, the polymer is in the collapsed (insoluble) state due to the hydrophobic interaction of polymer chains, impeding the diffusion of the drug out of the pores.

Another innovative approach consists in anchoring a *light-responsive polymer* on the pore outlets of MSNPs.[89] This strategy relies upon the fact that the incorporation of hydrophobic or hydrophilic monomers into the PNIPAAm backbone can lead to a decrease or an increase in the LCST, respectively. Therefore, when monomers bearing a light-responsive moiety such as azobenzene and 2-nitrobenzyl groups were incorporated in the PNIPAAm backbone, the resultant polymers were light-responsive. Their LCST could be easily modulated by applying UV irradiation, which makes the polarity of the light-responsive moieties change. Thus, upon UV irradiation, the polymer modifies its conformation from collapsed to coil state, so that the gate is opened and subsequently the entrapped molecules escape out of the pores.

Enzyme-responsive polymers have also been linked to MSNPs to provide them with bioresponsive drug-delivery capability using the antitumor drug Dox.[90] The authors first electrostatically adsorbed an acrylamide to the MSNP surface and then used the acryl groups to synthesize a covalently cross-linked PEG-based polymer shell. They characterized MSNPs Dox-eluting properties *in vitro* and demonstrated that the polymer-coated MSNPs release the entrapped drug in response to proteases present at a tumor site *in vivo*, resulting in cellular apoptosis.

Very recently, Chang *et al.*[91] reported the grafting of *dual-stimuli-responsive polymers* to MSNPs. Core-shell MSNPs with thermo-/pH-coupling sensitivity were synthesized using the MSNPs as the core and a cross-linked poly(*N*-isopropylacrylamide-co-methacrylic acid) (P(NIPAAm-co-MAA)) polymer as the outer shell. The temperature-sensitive volume phase transition (VPTT) could be precisely regulated by the molar ratio of MAA to NIPAAm and the concentration of NaCl. The amount of drug released was small below the VPTT and increased above such value, the system exhibiting an apparent thermo-/pH-response controlled drug release.

15.2.2.3 DNA and siRNA Delivery

Polymer coatings of MSNPs can be used for delivering nucleic acids, such as DNA and siRNA, for gene-therapy purposes. The advantage of using MSNPs for gene delivery lies in the possibility of combining the binding of nucleic acid molecules on the outer surface of the particles and the incorporation of drugs into the mesoporous cavities, permitting the dual delivery of nucleic acids and drugs. Radu *et al.*[92] reported the grafting of second generation (G2) poly(amido amine) (PAMAM) dendrimers to MSNPs. A plasmid DNA (pEGFPC1) that codes for an enhanced green fluorescence protein, forms a complex with the G2-PAMAM dendrimers on the MSNPs, thus preventing the enzymatic cleavage of the DNA and facilitating its entry into the cells.

Polyethyleneimine (PEI) coated MSNPs have also been used to deliver siRNA and DNA constructs.[93,94] In these reports, PEI binds to the surface of MSNPs *via* electrostatic interactions. The cellular uptake of the PEI-coated MSNPs is considerably increased compared to unmodified MSNPs. The positively charged PEI electrostatically binds siRNA or DNA, enhances the particle uptake by cells, and facilitates the endosomal escape of the nucleotide being released. High-molecular-weight PEI (25 kD) increases the toxicity of the MSNPs for cells, but also causes a higher siRNA and DNA delivery efficacy. The 10 kD PEI polymer was demonstrated to retain high cellular uptake and transfection efficiency while reducing or even eliminating cationic MSNPs cytotoxicity. The PEI coating of the MSNPs does not affect their capability to host and release drug molecules, providing a dual delivery system.[93,94]

Meng *et al.*[95] have recently reported a PEI-coated MSNPs system that delivers a siRNA to overcome the drug resistance of a cancer cell line and simultaneously release encapsulated antitumor drugs. Overexpression of drug efflux transporters such as P-glycoprotein (Pgp) is one of the major mechanisms for multiple drug resistance (MDR) in cancer cells. This new approach to overcome drug resistance in cancer cells is based on a synergistic co-delivery strategy that utilizes a siRNA to silence the expression of efflux transporter together with Dox as chemotherapeutic agent. MSNPs were functionalized with a phosphonate group, which allows electrostatic binding of Dox to the porous interior. Dox release was achieved by acidification of the medium under abiotic and biotic conditions. In addition, phosphonate modification allows exterior coating with PEI, which endows the MSNPs contemporaneously to deliver Pgp siRNA. The dual delivery of Dox and siRNA in KB-V1 cells was capable of increasing the intra-cellular as well as the intra-nuclear drug concentration, to levels exceeding those achieved with the free Dox or with the drug being delivered by MSNPs in the absence of siRNA.[95] These results demonstrate that it is possible to use MSNPs as smart platforms to effectively deliver a siRNA that knocks down gene expression of a drug exporter, which can be used to improve drug sensitivity to a chemotherapeutic agent.

15.2.3 Magnetic Nanoparticles

Magnetic NPs constitute a valuable family of nanomaterials consisting of typical magnetic elements such as iron, nickel, cobalt, manganese, chromium and gadolinium, as well as their chemical compounds. They exhibit attractive features, such as high values of saturation magnetization and magnetic susceptibility, which make them suitable for different bionanotechnological applications.[96–99] Magnetic NPs can be synthesized with controlled size from a few to tens of nanometers, which means that they can interact with diverse biological entities (cells, viruses, proteins, *etc.*). In addition, magnetism of magnetic NPs permits their manipulation by an external magnetic field gradient to selective target and accumulation in the desired organs or tissues inside the body.[100,101] And, last but not least, magnetic NPs can respond to the action of alternating magnetic fields (AMFs), leading to the transfer of energy from the field to the particle. Thus, the magnetic NPs could be used to transmit certain amounts of thermal energy into tumor cells, which constitutes the principle of antitumor therapy by hyperthermia.[102,103] Among magnetic NPs, colloidal superparamagnetic iron oxide materials, such as magnetite (Fe_3O_4) or its oxidized form maghemite (γ-Fe_2O_3), are gaining attention as they offer high potential for several biomedical applications. Further information on magnetic-responsive DDSs can be consulted in Chapter 14.

Different approaches have been developed to synthesize magnetic MSNPs, including impregnation and reduction, reverse microemulsion, phase transfer and aerosol or spray-drying.[104–107] In the following sections we focus on the use of magnetic NPs within MSNPs that serve as thermoseeds for hyperthermia treatment. The development of magnetic MSNPs for magnetic resonance imaging (MRI) is also described. Finally, we tackle the possibility of attaching magnetic NPs to block the pore openings of MSNPs, which can be removed by application of an external magnetic field that triggers the cargo release.

15.2.3.1 Thermoseeds for Hyperthermia

Hyperthermia as antitumor therapy consists of heating a tumor region to inhibit the regulatory and growth processes of cancerous cells with the aim of destroying them or making them more sensitive to the effects of radiation and antineoplastic drugs. The incorporation of a sufficient amount of maghemite (γ-Fe_2O_3) nanoparticles encapsulated within a mesoporous silica matrix has led to materials that can reach temperatures in the range of hyperthermia under the action of alternating magnetic fields.[104,108,109] This would permit the synergistic combination of hyperthermia and chemotherapy for cancer treatment. Both the mesoporous order and the magnetic properties of the resulting material can be tailored by varying the type of surfactant employed, the surfactant/silica molar ratio and the amount of encapsulated magnetic NPs. The capability of these highly magnetic MSNPs to cause magnetic hyperthermia upon exposure to a low-frequency alternating magnetic field has been demonstrated *in vitro* using human cells of cancerous nature.[110] Magnetic hyperthermia experiments showed the ability to control the temperature rise in the cell culture environment upon treatment with magnetic MSNPs and AMF exposure, thus generating heat that severely compromises cell survival. Maximum temperature in magnetic microspheres suspensions increased to a range above 42 °C as a function of the amounts of particles exposed to AMF. Cell culture experiments showed that, by adjusting the amount of magnetic MSNPs and the time of exposure to AMF, heat treatments of mild to very high intensities could be achieved. Cell viability dropped as a function of the intensity of the heat treatment achieved by magnetic MSNPs and AMF exposures. The possibility of fine-tuning the heating power output, together with efficient uptake by tumor cells *in vitro*, makes magnetic MSNPs promising agents for hyperthermia combined with intra-cellular delivery of chemotherapeutic drugs.

15.2.3.2 Magnetic Resonance Imaging (MRI)

Molecular imaging aims at visualizing molecules and molecular processes that take place at a cellular level. MRI is one of the most powerful non-invasive techniques used in clinical medicine that allows visualizing the internal structure and the functions of the body.[111] MRI uses the magnetic spins of hydrogen nuclei aligned by a powerful external magnetic field. Two independent relaxation processes occur in MRI: longitudinal relaxation, denoted T_1, and transverse relaxation, denoted T_2. MRI agents produce image contrast by affecting the relaxation properties of water protons and they are classified as a function of the different contrast mechanism. T_1 contrast agents generate a positive image by increasing the longitudinal relaxation rates of surrounding water protons. The most common T_1 contrast agents are Gd(III) chelating complexes. T_2 contrast agents generate a negative image contrast by increasing the transverse relaxation rates of water protons. T_2 contrast agents are mainly superparamagnetic nanoparticles, being the most used iron oxide NPs, which can be strongly magnetized under an external magnetic field and lead to a considerable distortion of the local magnetic field. Mesoporous silica is a good carrier for the metal because its high porosity permits water to move freely in and out of the frame; the rigidity of the frame hampers the rotational movement of the metal and improves the relaxation of water. Thus, the incorporation Gd(III) compounds into MSNPs has been proposed as a good strategy to design improved MRI contrast agents.[112–115]

Moreover, the combination of magnetic NPs and MSNPs has been demonstrated to be a good method to design multi-functional platforms with MRI capability. Mou and coworkers[116,117] reported the synthesis of a multi-functional fluorescent, magnetic and porous silica nanocomposite called Mag-Dye@MSNs, which consisted of silica-coated core/shell superparamagnetic iron oxide NPs co-condensed with fluorescein isothiocyanate (FITC)-incorporated MSNPs. Mag-Dye@MSNs can label human mesenchymal stem cells through endocytosis efficiently for MRI *in vitro* and *in vivo*, as demonstrated by using a clinical 1.5-T MRI system with requirements of simultaneous low incubation dosage of iron, low detection cell numbers and short incubation time. Sanchez and coworkers[105] reported a facile preparation method of hybrid silica/spinel iron oxide composite microspheres built with superparamagnetic NPs for MRI hyperthermia. A hybrid mesoporous matrix enabled the transport of bioactive molecules for *in vivo* biomedical applications. The reported nanohybrid materials exhibit interesting behavior for hyperthermia and an effective T_2 effect for MRI applications.

Hyeon and coworkers[118–120] reported the synthesis of highly versatile nanocomposite nanoparticles by decorating the external surface of dye-doped MSNPs with multiple magnetite nanocrystals. The superparamagnetic property of the magnetite nanocrystals enabled the nanoparticles to be used as a contrast agent in MRI, and the dye molecules in the silica framework imparted optical imaging modality. Integrating a multitude of magnetite nanocrystals on the silica surface resulted in remarkable enhancement of magnetic resonance signal due to the synergistic magnetism. The anticancer drug Dox could be loaded in the pores and induced efficient cell death. *In vivo* passive targeting and accumulation of the nanoparticles at the tumor sites was confirmed by both T_2 magnetic resonance and fluorescence imaging. Furthermore, apoptotic morphology was clearly detected in tumor tissues of mice treated with Dox-loaded nanocomposite nanoparticles, demonstrating that Dox was successfully delivered to the tumor sites and its anticancer activity was retained. The same research group has recently developed multi-functional core-shell structured MSNPs for simultaneous magnetic resonance and fluorescence imaging, cell targeting and photodynamic therapy (PDT) as a promising material for cancer diagnosis and therapy.[121]

15.2.3.3 Stimuli-responsive Nanogates

Magnetic NPs can be covalently linked to pore entrances of MSNPs, acting as nanocaps that hinder the leak of the drug out of the channels. The application of a particular stimulus, such as a magnetic field or a change in pH or redox potential, promotes the removal of nanocaps, which allows the cargo to be released "on demand".

Chen *et al.*[122] reported the pore capping of MSNPs with Fe_3O_4 magnetic nanoparticles. MSNPs were first functionalized with 3-aminopropyltrimethoxysilane (APTS) and then loaded with the antitumor drug CPT. Afterwards, the mesopore entrances were capped through amidation of the APTS bound at the pore surface with *meso*-2,3-dimercaptosuccinic acid functionalized iron oxide superparamagnetic NPs (average diameter of 5.6 nm). The application of a magnetic field provoked the removal of the Fe_3O_4 nanocaps by cleaving of chemical bonds, and triggered the drug release. Recently, the group of Vallet-Regí[123] has reported the use of alternating magnetic fields (AMF) as an external release trigger to develop "on-off" stimuli-responsive drug-delivery systems. For this purpose, oligonucleotide-modified MSNPs encapsulating iron oxide superparamagnetic NPs were loaded with the model molecule fluorescein. Then, the pore entrances were capped with iron oxide magnetic nanocrystals functionalized with complementary strands, which acted as gatekeepers. DNA duplex was selected to display a melting temperature of 47 °C, which corresponds to the upper limit of therapeutic magnetic hyperthermia. The magnetic-responsive release of this system was tested by exposure of the fluorescein-loaded system to an AMF. Once the temperature reached 47 °C, the pore channels were uncapped and the cargo molecule was released. This system acts as a reversible gatekeeper, because the cargo release is triggered when the temperature is increased but hindered when the temperature is stabilized at 37 °C. The "on-off" behavior makes this system a potential smart drug-delivery device, with promising biomedical applications such as the synergistic combination of chemotherapy and hyperthermia for cancer treatment.

15.2.4 Stimuli-responsive Drug Delivery

The mushrooming expansion of MSNPs as stimuli-responsive DDSs aims at avoiding the premature release of drug molecules before reaching the target cells or tissue (Figure 15.3).[16,20,25,40,41,124–129] For this purpose, the available channels of MSNPs are used as drug reservoirs and different molecular nanogates are utilized to block the pore entrances and avoid untimely departure of the cargo. The application of an internal or external stimulus provokes the opening of the nanocap and triggers the drug release (Figure 15.3). The different stimuli that have been used as triggers and the gatekeeping possibilities are summarized in the following sections.

15.2.4.1 pH

The pH is an attractive release trigger because some tissues in the body, such as tumors or inflamed tissues, as well as endosomal cell compartments, have a more acidic pH than blood or healthy tissues. Park *et al.*[130] reported the controlled release of molecules from MSNPs by using a pH-sensitive polyethyleneimine/cyclodextrin (PEI/CD) polypseudorotaxane motif. The

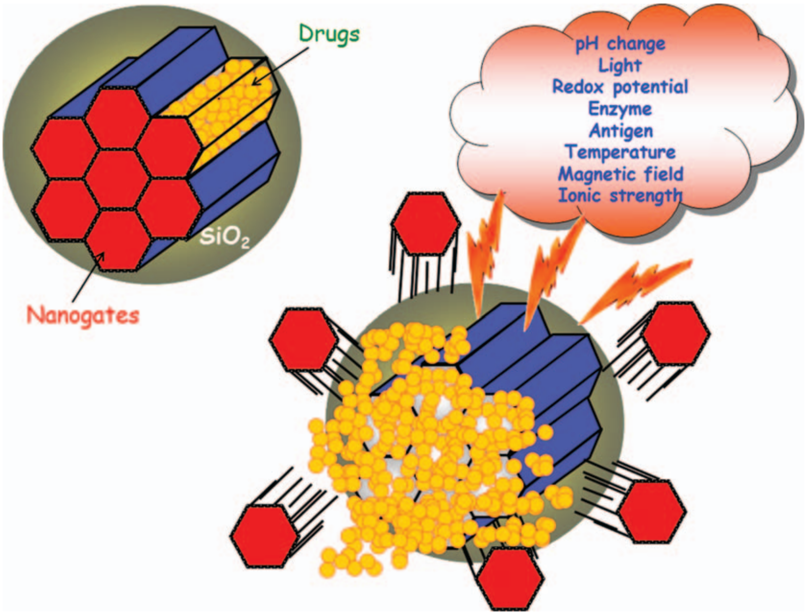

Figure 15.3 External and internal stimuli suitable for smart drug delivery from mesoporous silica nanoparticles.

mesopores were filled with a guest molecule (calcein) and then blocked by threading of CDs onto the surface-grafted PEI chains at pH 11. At pH 5.5, calcein molecules were released from the pores by the reversible dethreading of CDs from the PEI chain. Zink and coworkers have reported the potential application of CDs in the development of pH-sensitive nanovalves.[25,26,124,127] In 2009, they introduced a new category of MSNPs consisting of hollow mesoporous silica nanoparticles capped by supramolecular machines based on CDs.[131] These authors prepared pH-responsive nanovalves controlled by a supramolecular system containing α-CD rings interacting by hydrogen bonds with anilinoalkane stalks that were tethered to the silica surface. When the α-CD rings were complexed with the stalk at neutral pH, the α-CDs were located near the nanopore openings, blocking the leakage of cargo molecules previously loaded in the nanopores and the hollow interior of the particle. When the nitrogen atoms on the aniline residues were protonated at lower pH, the binding affinities between the α-CD rings and the stalks decreased, releasing the α-CDs and allowing the cargo molecules to escape. The same research group reported a system based on the function of β-CD nanovalves that were also responsive to the endosomal acidification.[132] In some recent works, the same group investigated the opposite recognition, *i.e.* the β-CD rings were immobilized and the stalks were movable.[133] In this case, the removable rhodamine B/benzidine stalks acted as nanopistons and moved in and out of the cylindrical cavities provided by the β-CD rings in response to changes in pH.

A different approach consists in the incorporation of nanocaps tethered to the mesopore entrances of MSNPs through acid cleavable chemical bonds. Thus, gold[134] and Fe_3O_4 nanoparticles[135] have been used as blocking caps to control the transport of cargo from MSNPs through a reversible pH-dependent boronate ester bond, which is hydrolyzed under acid pH. Acid-labile acetal linker has also been reported as a pH-responsive nanogated ensemble by capping the pores of MSNPs with gold NPs through the formation of pH-sensitive bonds.[136]

Recently, Chen *et al.*[137] have developed an imaginative pH-responsive release system based on DNA nanoswitch-controlled organization of gold NPs attached to MSNPs. In this system, the hybridization and dehybridization of DNA between strands 1 and 2 were controlled by the adjustment of the pH of the aqueous media. This structural transformation allows unlocking and closing the mesopore outlets, leading to the controlled release of loaded molecules from pore voids at acid conditions.

15.2.4.2 Light

Since processes involving light activation are rapid and directional, light-responsive MSNPs permit low invasiveness in biological systems. Fujiwara *et al.*[138,139] reported for the first time that the uptake, storage and release of organic molecules in MCM-41 could be regulated through the photo-controlled and reversible inter-molecular dimerization of coumarin derivatives attached to the pore entrances. Later, they developed a multi-functional, fully controlled storage and release system by attaching azobenzene groups on the mesopore outlets.[140] The release of guest molecules included in the pores of mesoporous silica was promoted by simultaneous irradiation with UV and VIS light, which made the azobenzene molecules act as both impellers and nanogates. The reversible *cis*-*trans* photo-isomerization of azobenzene substituents on the pore surface by a rotation-inversion mechanism causes a stirring action that accelerates the diffusion of the guest from the mesopores.

Zink and coworkers[141] have reported the use of light-operated mechanized MSNPs whose operation is based on the high binding affinity in aqueous solution between β-CD and *trans*-azobenzene derivatives and low, if any, binding between β-CD and *cis*-azobenzene derivatives.[141] Irradiating with 351 nm light causes the isomerization of azobenzene to the *cis* conformation and, therefore, pore uncapping. An alternative strategy proposed by Park *et al.*[142] consisted of covalently linking β-CDs on the surface of MSNPs through a photocleavable *o*-nitrobenzyl ester moiety. Upon exposure to UV light, the guest molecules were released from the pore by removal of the CD gatekeeper.[142]

Lin and coworkers[143] described the use of gold nanoparticles as light-sensitive gatekeepers by surface attachment through the photoresponsive linker thioundecyl-tetraethyleneglycoestero-nitrobenzylethyldimethylammonium bromide (TUNA). Upon UV irradiation, TUNA transforms in the negatively charged thioundecyltetraethyleneglycolcarboxylate (TUEC), leading to the dissociation of the AuNPs from the MSNP surface due to charge repulsion. Thus, an uncapping of the mesopores occurred and the release of guest molecules took place.[143] In a recent study, sulforhodamine 101 was loaded inside the mesopores of mercaptopropyl-functionalized MSNPs and the cargo molecules were entrapped by $Ru(bpy)_2(PPh_3)$-moieties, coordinated to mercaptopropyl functional groups.[144] Upon irradiation with visible light ($\lambda = 455$ nm), Ru-S coordination bonds were cleaved, triggering the release of capping species and loaded molecules.

15.2.4.3 Redox Potential

Another interesting approach is to take advantage of the different redox potentials between the intra-cellular and the extra-cellular space as internal stimuli to trigger the release from MSNPs. Following this premise, different redox potential-responsive release systems have been developed, consisting in using different nanocaps, such as CdS,[145] Fe_3O_4[146] or Au[147] nanoparticles, covalently linked to the MSNPs through chemically labile disulfide linkages. The removal of the nanocaps and the subsequent release of the entrapped cargo were achieved by cleaving such linkages with disulfide-reducing agents, such as dithiothreitol (DTT) or mercaptoethanol (ME). Liu *et al.*[148] reported the use of cross-linked poly(*N*-acryloxysuccinimide) attached at the pore entrance of MSNPs. After loading the dye molecules into MSNPs, the openings were blocked by adding cystamine, a disulfide-based bifunctional primary amine, which allows polymer chains to be cross-linked through the reaction with *N*-oxysuccinimide groups along the polymer chain. The presence of DTT cleaved the disulfide bond of the cystamine, causing a disruption in the polymeric network and leading to the redox potential driven delivery. More recently, the immobilization of collagen on the outer surface of MSNPs by disulfide bonds, which can be cleaved with various reducing agents, has been accomplished.[54]

Zink *et al.*[149] reported the fabrication of snap-top systems using MSNPs functionalized with rotaxanes incorporating disulfide bonds in their stalks, which are encircled by curcurbit[6]uril or α-CD rings. Upon exposition to DTT, there is a reductive cleavage of disulfide bonds in the stalks, resulting in the snapping of the stalks of the rotaxanes and leading to the cargo release from MSNPs. A similar approach carried out by Kim *et al.*[150] involved glutathione-induced intra-cellular release of cargos from MSNPs with CD gatekeepers covalently linked onto the particle surface *via* a disulfide unit. However, different studies have revealed that the medium in endosomes is slightly reductive or even oxidative.[151] Therefore, the contact to the cytosol is essential for cleavage of the disulfide linkages and release of the cargo. The use of photo-active compounds to open the endosome is one prospect to tackle this challenge.[152,153] Bein and coworkers demonstrated that there was no release of disulfide-bound dye from MSNPs endocytosed by cells.[154] Inefficient endosomal escape is generally a bottleneck for molecular delivery into the cytoplasm. However, after photochemical rupture of the endosomes by means of a photosensitizer, MSNPs successfully released disulfide-bound dye into the cytoplasm, showing that the reducing milieu of the cytoplasm is enough to cleave the disulfide linkages.

15.2.4.4 Enzymes

The design of enzyme-responsive nanocaps blocking the pores of MSNPs is another attractive prospect, since there is an anomalous increase of enzymatic presence or activity in some diseased tissues. Zink and coworkers[155] functionalized the pore outlets of MSNPs with a [2]rotaxane capped with an ester-linked adamantyl stopper. The system released its cargo after addition of porcine liver esterase, which induced dethreading of the [2]rotaxane due to hydrolysis of the adamantyl ester. CDs have been also attached on the MSNPs surface *via* "click chemistry" reactions. The addition of α-amilase catalyzed the hydrolysis of these groups, allowing the release of molecules entrapped into the mesopores.[156] Bein and coworkers reported the attachment of avidin caps on biotinylated MSNPs.[157] The addition of the protease trypsin provoked the hydrolysis of the attached avidin and the release of the entrapped cargo. Martínez-Máñez and coworkers[158] described the capping of MSNPs with lactose and the selective uncapping in the presence of enzyme β-D-galactosidase. The same research group functionalized the MSNPs surface with saccharide derivatives and the cargo release was achieved by enzymatic hydrolysis in the presence of pancreatin or β-D-galactosidase in pure water, and also in intra-cellular media by lysosomal enzymes.[159]

15.2.4.5 Antigens

A groundbreaking strategy consists in using the highly specific antibody-antigen interaction as a powerful switchable method to develop tailor-made MSNPs for controlled release functions. Thus, Martínez-Máñez and coworkers[160] reported the functionalization of the pore outlets of MSNPs with a certain hapten able to be recognized by an antibody that acts as a nanoscopic cap. The opening protocol and delivery of the entrapped cargo relies on the highly effective displacement reaction involving the presence in the solution of the antigen to which the antibody is selective.

15.2.4.6 Dual Stimuli

Dual-controlled or multi-responsive controlled delivery systems are those able to respond to two or more inputs in either an independent or a synergistic way. Martínez-Máñez and coworkers[161] reported the attachment of suitable polyamines on the MSNP surface to obtain dual stimuli-responsive gate-like ensembles. The release of the cargo entrapped inside the mesoporous matrix was triggered by changes in pH or by the presence of certain anions. The same research group described the functionalization of the pore outlets of MSNPs with boronic acid functionalized gold nanoparticles acting as nanocaps. These

AuNPs were linked to the surface of saccharide-functionalized MSNPs through the formation of boronate ester bonds, which are hydrolyzed under acidic conditions ($pH = 3$). The nanosystem exhibited an "on-off" response due to the reversibility of the boronate bond formation. Furthermore, the metallic nanoparticles could be heated by laser irradiation at 1064 nm (266 mJ) causing a plasmon-resonance light-induction release due to the thermal boronate bond cleavage. Angelos *et al.*[162] demonstrated that dual-stimuli controlled release MSNPs could also be used as AND logic gates. These molecular machines were designed to operate in tandem with one another in such a way that the dual-controlled nanoparticle systems function as AND logic gates. In this case, two different molecular machines were mounted on the mesoporous silica surface, azobenzene as light-activated nanoimpellers and [2]pseudorotaxanes as pH-responsive nanovalves. The two systems can act separately, but only the simultaneous activation of both molecular machines conducts to the load release, showing that these kinds of devices could not only be used in drug-delivery applications, but also could perform simple logic operations. Liu *et al.*[163] reported a multi-responsive supramolecular capped mesoporous silica system by grafting β-CD-bearing polymer on the surface of mesoporous silica and cross-linking by the addition of disulfide groups to form a polymeric network that blocked the pore entrances. The nanodevice was able to release its cargo in response to three different stimuli: UV light (causing the isomeric transformation of azobenzene groups), presence of α-CD (as competitive ligands to displace β-CD) and addition of disulfide reductive agents such as DTT (to cleave the disulfide bond between β-CD and polymer main chains). In a very recent work Chen *et al.*[164] described the synthesis of dual stimuli-responsive vehicles by attaching self-complementary duplex DNA to the pore openings of MSNPs, which resulted in a cap for trapping guest molecules. The duplex DNA cap could be either denatured by heating or hydrolyzed by endonucleases, thus opening the nanopores and releasing the cargo.

15.3 Biocompatibility of Mesoporous Silica Nanoparticles

The application of MSNPs as smart DDSs in nanomedicine requires researching their cellular uptake and biocompatibility *in vitro*, and their toxicity, biodistribution and clearance *in vivo*. The cellular uptake of MSNPs can be investigated by grafting fluorescent dye molecules to the MSNPs, which enables visualizing the nanosystems by fluorescence and confocal microscopy.[165] Cellular uptake of MSNPs and their good biocompatibility have been confirmed by several research groups using both healthy and cancer cell lines.[17,91,165,166] No cellular toxicity is observed up to 100 $\mu g\ mL^{-1}$ for unmodified MSNPs with 100 nm of particle size,[62,94,166–168] which is above the effective particle concentration needed for most therapeutic treatments. The cellular uptake and cytotoxicity of MSNPs depend on the particle size, shape, surface charge and functional groups, as reported by different groups.[17,26,169]

Cells staining assays together with the fluorescently labeled MSNPs permits the study of the cellular uptake mechanisms and the particle location inside the cells. Small MSNPs (<200 nm) are generally taken up by endocytosis. Further details of the different endocytosis mechanisms for MSNPs can be found in recent reviews.[17,169] Summing up, the internalization of MSNPs through endocytosis results in the formation of vesicles that capture the nanoparticles in the extra-cellular environment. Then, these vesicles undergo a complex series of fusion events directing the internalized MSNPs to the cytosolic compartment. The series of events after the MSNPs have been endocytosed can be divided into the following sequence: the material is first transported to primary endosomes followed by transport to sorting endosomes. From sorting endosomes, a fraction of the MSNPs are directed back to the cell exterior through recycling endosomes, while the remaining fraction is transported to secondary endosomes, which fuse with the acidic lysosomes. The MSNPs end up inside these acidic ($pH \approx 4.5$) organelles in cells. It has also been demonstrated that nanoparticles with surface groups that can be protonated assist the "proton sponge effect", which leads to the endosomal escape of the uptaken particles.[93] This permits the membrane impermeable molecules such as hydrophilic drugs, DNA and siRNA to be released from the membrane-bounded endosomes and travel to their effective sites.

Several studies of the *in vivo* toxicity, biodistribution and clearance of MSNPs in animal models have been reported.[62,168,170] MSNPs of hollow and MCM-41 types (100 nm) have shown very good long-term (>1 month) biocompatibility in mice.[62] The *in vivo* toxicity of MSNPs is related to the injection method. The size and surface functional groups and charges of the particles greatly affect the biodistribution and pharmacokinetics.[171–173] For instance, positively charged MSNPs have a much faster clearance rate than negatively charged ones. Moreover, as previously described (Section 15.2.2.1) it is possible to coat MSNPs with PEG to increase their *in vivo* circulation time, preventing their removal by phagocytes. Therefore less PEG-coated MSNPs are trapped in the reticuloendothelial system (RES) of the liver and spleen. *In vivo* degradation and urinary excretion of MSNPs have also been observed in several cases. As commented in Section 15.2.1, one key factor to consider when designing *in vivo* drug-delivery platforms is the targeting of diseased organs or tissues. Thus, targeting of MSNPs with moieties that selectively bind cell surface receptors to trigger receptor-mediated endocytosis increases the cellular uptake of the nanosystems.[39,42,55,174] The *in vivo* capability of delivering anti-cancer drugs, such as CPT or Dox, for tumor shrinking has been also demonstrated with human xenografts in mice.[62,175]

15.4 Future Prospects

MSNPs have become excellent nanoplatforms to design smart DDSs for nanomedicine. The development of multi-functional stimuli-responsive drug-delivery nanodevices requires the design of nanocarriers addressing: biocompatibility and absence of toxicity of all its components, biocompatible trigger stimuli and efficiency to target the suitable cells or tissues, considering the enormous complexity of the human body. Significant achievements derived from *in vitro* experiments have been made during the last decade. In addition, *in vivo* findings are encouraging from the perspective of moving the MSNPs platforms into clinical trials. Nevertheless, we are just at the beginning of a groundbreaking scientific journey and much research work remains to be done to allow the transit from bench to bedside.

References

1. J. Shi, A. R. Votruba, O. C. Farokhzad and R. Langer, *Nano Lett.*, 2010, **10**, 3223.
2. J. Khandare, M. Calderón, N. M. Dagia and R. Haag, *Chem. Soc. Rev.*, 2012, **41**, 2824.
3. V. P. Torchilin, *Nat. Rev. Drug Discov.*, 2005, **4**, 145.
4. R. Haag and F. Kratz, *Angew. Chem. Int. Ed.*, 2006, **45**, 1198.
5. K. T. Oh, H. Yin, E. S. Lee and Y. H. Bae, *J. Mater. Chem.*, 2007, **17**, 3987.
6. Y. Ma, R. J. M. Nolte and J. J. L. M. Cornelissen, *Adv. Drug Deliver. Rev.*, 2012, **24**, 811.
7. P. Ghosh, G. Han, M. De, C. K. Kim and V. M. Rotello, *Adv. Drug Deliver. Rev.*, 2008, **60**, 1307.
8. A. M. Smith, H. Duan, A. M. Mohs and S. Nie, *Adv. Drug Deliver. Rev.*, 2008, **60**, 1226.
9. C. Sun, J. S. H. Lee and M. Zhang, *Adv. Drug Deliver. Rev.*, 2008, **60**, 1252.
10. E. J. Anglin, L. Cheng, W. R. Freeman and M. J. Sailor, *Adv. Drug Deliver. Rev.*, 2008, **60**, 1266.
11. C. Barbé, J. Bartlett, L. Kong, K. Finnie, H. Q. Lin, M. Larkin, S. Calleja, A. Bush and G. Calleja, *Adv. Mater.*, 2004, **16**, 1959.
12. Y. Piao, A. Burns, J. Kim, U. Wiesner and T. Hyeon, *Adv. Funct. Mater.*, 2008, **18**, 3745.
13. W. Tan, K. Wang, X. He, X. J. Zhao, T. Drake, L. Wang and R. P. Bagwe, *Med. Res. Rev.*, 2004, **24**, 621.
14. D. Avnir, T. Coradin, O. Lev and J. Livage, *J. Mater. Chem.*, 2006, **16**, 1013.
15. M. Vallet-Regí, A. Rámila, R. P. del Real and J. Pèrez-Pariente, *Chem. Mater.*, 2001, **13**, 308.
16. M. Vallet-Regí, F. Balas and D. Arcos, *Angew. Chem. Int. Ed.*, 2007, **46**, 7548.
17. J. L. Vivero-Escoto, I. I. Slowing, B. G. Trewyn and V. S. Y. Lin, *Small*, 2010, **18**, 1952.
18. Y. Zhao, J. L. Vivero-Escoto, I. I. Slowing, B. G. Trewyn and V. S. Y. Lin, *Expert Opin. Drug Deliv.*, 2010, **7**, 1013.
19. J. M. Rosenholm, C. Sahlgren and M. Lindén, *Nanoscale*, 2010, **2**, 1870.

20. M. Vallet-Regí, E. Ruiz-Hernández, B. González and A. Baeza, *J. Biomater. Tissue Eng.*, 2011, **1**, 6.
21. J. Liu, X. Jiang, C. Ashley and C. J. Brinker, *J. Am. Chem. Soc.*, 2009, **131**, 7567.
22. M. Vallet-Regí, M. Colilla and B. González, *Chem. Soc. Rev.*, 2011, **40**, 596.
23. C. E. Ashley, E. C. Carnes, G. K. Phillips, D. Padilla, P. N. Durfee, P. A. Brown, T. N. Hanna, J. Liu, B. Phillips, M. B. Carter, N. J. Carroll, X. Jiang, D. R. Dunphy, C. L. Willman, D. N. Petsev, D. G. Evans, A. N. Parikh, B. Chackerian, W. Wharton, D. S. Peabody and C. J. Brinker, *Nat. Mater.*, 2011, **10**, 389.
24. M. Vallet-Regí and E. Ruiz-Hernández, *Adv. Mater.*, 2011, **23**, 5177.
25. M. W. Ambrogio, C. R. Thomas, Y. L. Zhao, J. I. Zink and J. F. Stoddart, *Accounts Chem. Res*, 2011, **44**, 903.
26. Z. Li, J. C. Barnes, A. Bosoy, J. F. Stoddart and J. I. Zink., *Chem. Soc. Rev.*, 2012, **41**, 2590.
27. M. Grün, I. Lauer and K. K. Unger, *Adv. Mater.*, 1997, **9**, 254.
28. Y. F. Lu, H. Y. Fan, A. Stump, T. L. Ward, T Rieker and C. J. Brinker, *Nature*, 1999, **398**, 223.
29. C. J. Brinker, Y. F. Lu, A. Sellinger and H. Y. Fan, *Adv. Mater.*, 1999, **11**, 579.
30. D. Arcos, A. López-Noriega and E. Ruiz-Hernández, *Chem. Mater.*, 2009, **21**, 1000.
31. M. Colilla, M. Manzano, I. Izquierdo-Barba, M. Vallet-Regí, C. Boissiére and C. Sanchez, *Chem. Mater.*, 2010, **22**, 1821.
32. C. Boissiére, D. Grosso, A. Chaumonnot, L. Nicole and C. Sanchez, *Adv. Mater.*, 2011, **23**, 599.
33. C. T. Kresge, M. E. Leonowicz, W. J. Roth and J. C. Vartuli, *Nature*, 1992, **359**, 710.
34. W. H. Suha, Y. H. Suh and G. D. Stucky, *Nano Today*, 2009, **4**, 27.
35. O. C. Farokhzad and R. Langer, *ACS Nano*, 2009, **3**, 16.
36. Y. S. Lin and C. L. Haynes, *J. Am. Chem. Soc.*, 2010, **132**, 4834.
37. F. Hoffmann, M. Cornelius, J. Morell and M. Fröba, *Angew. Chem. Int. Ed.*, 2006, **45**, 3216.
38. F. Hoffmann and M. Fröba, *Chem. Soc. Rev.*, 2011, **40**, 608.
39. J. M. Rosenholm, A. Meinander, E. Peuhu, R. Niemi, J. E. Eriksson, C. Sahlgren and M. Lindén, *ACS Nano*, 2009, **3**, 197.
40. M. Liong, J. Lu, M. Kovochich, T. Xia, S. G. Ruehm, A. E. Nel, F. Tamanoi and J. I. Zink, *ACS Nano*, 2008, **2**, 889.
41. M. Liong, S. Angelos, E. Choi, K. Patel, J. F. Stoddart and J. I. Zink, *J. Mater. Chem.*, 2009, **19**, 6251.
42. I. I. Slowing, B. G. Trewyn and V. S. Y. Lin, *J. Am. Chem. Soc.*, 2006, **128**, 14792.
43. Y. S. Lin, C. P. Tsai, H. Y. Huang, C. T. Kuo, Y. Hung, D. M. Huang, Y. C. Chen and C. Y. Mou, *Chem. Mater.*, 2005, **17**, 4570.

44. Y. S. Lin, S. H. Wu, Y. Hung, Y. H. Chou, C. Chang, M. L. Lin, C. P. Tsai and C. Y. Mou, *Chem. Mater.*, 2006, **18**, 5170.
45. J. Lu, M. Liong, S. Sherman, T. Xia, M. Kovochich, A. E. Nel, J. I. Zink and F. Tamanoi, *Nanobiotechnol.*, 2007, **3**, 89.
46. J. M. Rosenholm, E. Peuhu, J. E. Eriksson, C. Sahlgren and M. Lindén, *Nano Lett.*, 2009, **9**, 3308.
47. F. M. Muggia, *Clin. Cancer Res.*, 1999, **5**, 7.
48. H. Maeda, G. Y. Bharate and J. Daruwalla, *Eur. J. Pharm. Biopharm.*, 2009, **71**, 409.
49. V. Torchilin, *Adv. Drug Deliver. Rev.*, 2011, **63**, 131.
50. J. Gu, W. Fan, A. Shimojima and T. Okubo, *Small*, 2007, **3**, 1740.
51. I. Y. Park, I. Y. Kim, M. K. Yoo, Y. J. Choi, M. H. Cho and C. S. Cho, *Int. J. Pharm.*, 2008, **359**, 280.
52. D. Brevet, M. Gary-Bobo, L. Raehm, S. Richeter, O. Hocine, K. Amro, B. Loock, P. Couleaud, C. Frochot, A. Morére, P. Maillard, M. García and J. O. Durand, *Chem. Commun.*, 2009, 1475.
53. O. Hocinea, M. Gary-Bobo, D. Breveta, M. Maynadierd, S. Fontanel, L. Raehma, S. Richetera, B. Loock, P. Couleaud, C. Frochot, C. Charnay, G. Derrien, M. Smaïhi, A. Sahmoune, A. Morère, P. Maillard, M. García and J. O. Duranda, *Int. J. Pharm.*, 2010, **402**, 221.
54. Z. Luo, K. Cai, Y. Hu, L. Zhao, P. Liu, L. Duan and W. Yang, *Angew. Chem. Int. Ed.*, 2011, **50**, 640.
55. C. P. Tsai, C. Y. Chen, Y. Hung, F. H. Chang and C. Y. Mou, *J. Mater. Chem.*, 2009, **19**, 5737.
56. M. M. J. Kamphuis, A. P. R. Hohnston, F. K. Duch, H. H. Dam, R. A. Evans, A. M. Scout, E. C. Nice, J. K. Heath and F. Caruso, *J. Am. Chem. Soc.*, 2010, **132**, 15881.
57. C. L. Zhu, X. Y. Song, W. H. Zhou, H. H. Yang, Y. H. Wen and X. R. Wang, *J. Mater. Chem.*, 2009, **19**, 7765.
58. V. C. Ozalp, F. Eyidogan and H. A. Oktem, *Pharmaceuticals*, 2011, **4**, 1137.
59. V. Lebret, L. Raehm, J. O. Durand, M. Smaihi, M. H. V. Werts, M. Blanchard-Desce, D. Methy-Gonnod and C. Dubernet, *J. Sol-Gel Sci. Techn.*, 2008, **48**, 32.
60. J. M. Rosenholm, E. Peuhu, L. T. Bate-Eya, J. E. Eriksson, C. Sahlgren and M. Lindén, *Small*, 2010, **6**, 1234.
61. L. S. Wang, L. C. Wu, S. Y. Lu, L. L. Chang, I. T. Teng, C. M. Yang and J. A. Ho, *ACS Nano*, 2010, **4**, 4371.
62. J. Lu, M. Liong, Z. Li, J. I. Zink and F. Tamanoi, *Small*, 2010, **6**, 1794.
63. J. Lu, Z. Li, J. I. Zink and F. Tamanoi, *Nanomed-Nanotechnol.*, 2012, **8**, 212.
64. P. S. Low, W. A. Henne and D. D. Doonerweerd, *Acc. Chem. Res.*, 2008, **41**, 120.
65. J. Sudimack and R. J. Lee, *Adv. Drug Deliver. Rev.*, 2000, **41**, 147.
66. H. Elnakat and M. Ratean, *Adv. Drug Deliver. Rev.*, 2004, **56**, 1067.

67. G. R. Harper, M. C. Davies, S. S. Davis, T. F. Tadros, D. C. Taylor, M. P. Irving and J. A. Waters, *Biomaterials*, 1991, **12**, 695.
68. M. V. Francesco and P. Gianfranco, *Drug Discov. Today*, 2005, **10**, 1451.
69. Q. He, J. Zhang, J. Shi, Z. Zhu, L. Zhang, W. Bu, L. Guo and Y. Chen, *Biomaterials*, 2010, **31**, 1085.
70. D. E. Owens III and N. A. Peppas, *Int. J. Pharm.*, 2006, **307**, 93.
71. P. M. Claesson, E. Blomberg, J. C. Froberg, T. Nylander and T. Arnebrant, *Adv. Colloid. Interf. Sci.*, 1995, **57**, 161.
72. F. P. Kathleen and H. C. H. Esther, *Trends Biotechnol.*, 2008, **26**, 552.
73. Q. He, Z. Zhang, F. Gao, Y. Li and J. Shi, *Small*, 2011, **7**, 271.
74. Y. Z. You, K. K. Kalebaila, S. L. Brock and D. Oupický, *Chem. Mater.*, 2008, **20**, 3354.
75. J. H. Park, Y. H. Lee and S. G. Oh, *Macromol. Chem. Phys.*, 2007, **208**, 2419.
76. S. Zhu, Z. Zhou, D. Zhang, C. Jin and Z. Li, *Micropor. Mesopor. Mat.*, 2007, **106**, 56.
77. Y. Zhu, S. Kaskel, T. Ikoma and N. Hanagata, *Micropor. Mesopor. Mat.*, 2009, **123**, 107.
78. Q. Fu, R. Rao, T. L. Ward, Y. Lu and G. P. López, *Langmuir*, 2007, **23**, 170.
79. K. Nagase, J. Kobayashi, A. Kikuchi, Y. Akiyama, H. Kanazawa and T. Okano, *Langmuir*, 2007, **23**, 9409.
80. A. Zintchenko, M. Ogris and E. Wagner, *Bioconjugate Chem.*, 2006, **17**, 766.
81. M. Keerl, V. Smirnovas, R. Winter and W. Richtering, *Macromolecules*, 2008, **41**, 6830.
82. T. Hoare, J. Santamaría, G. F. Goya, S. Irusta, D. Lin, S. Lau, R. Padera, R. Langer and D. S. Kohane, *Nano Lett.*, 2009, **9**, 3651.
83. A. Baeza, E. Guisasola, E. Ruiz-Hernández and M. Vallet-Regí, *Chem. Mater.*, 2012, **24**, 517.
84. R. Liu, P. Liao, J. Liu and P. Feng, *Langmuir*, 2011, **27**, 3095.
85. C. Y. Hong, X. Li and C. Y. Pan, *J. Mater. Chem.*, 2009, **19**, 5155.
86. L. Yuan, Q. Tang, D. Yang, J. Z. Zhang, F. Zhang and J. Hu, *J. Phys. Chem. C*, 2011, **115**, 9926.
87. K. Engin, D. B. Leeper, J. R. Cater, A. J. Thistlethwaite, L. Tupchong and J. D. Mcfarlane, *Int. J. Hypertherm.*, 1995, **11**, 211.
88. J. T. Sun, C. Y. Hing and C. Y. Pan, *J. Phys. Chem. C*, 2010, **114**, 12481.
89. J. Lai, X. Mu, Y. Xu, X. Wu, C. Wu, C. Li, J. Chen and Y. Zhao, *Chem. Commun.*, 2010, **46**, 7370.
90. N. Singh, A. Karambelkar, L. Gu, K. Lin, J. S. Miller, C. S. Chen, M. J. Sailor and S. N. Bhatia, *J. Am. Chem. Soc.*, 2011, **133**, 19582.
91. B. Chang, X. Sha, J. Guo, Y. Jiao, C. Wang and W. Yang, *J. Mater. Chem.*, 2011, **21**, 9239.
92. D. R. Radu, C. Y. Lai, K. Jeftinija, E. W. Rowe, S. Jeftinija and V. S. Y. Lin, *J. Am. Chem. Soc.*, 2004, **126**, 13216.

93. T. Xia, M. Kovochich, M. Liong, H. Meng, S. Kabehie, S. George, J. I. Zink and A. E. Nel, *ACS Nano*, 2009, **3**, 3273.
94. C. Hom, J. Lu, M. Liong, H. Luo, Z. Li, J. I. Zink and F. Tamanoi, *Small*, 2010, **6**, 1185.
95. H. Meng, M. Liong, T. Xia, Z. Li, Z. Ji, J. I. Zink and A. E. Nel, *ACS Nano*, 2010, **4**, 4539.
96. A. K. Gupta and M. Gupta, *Biomaterials*, 2005, **26**, 3995.
97. J. R. McCarthy and R. Weissleder, *Adv. Drug Deliver. Rev.*, 2008, **60**, 1241.
98. S. Laurent, D. Forge, M. Port, A. Roch, C. Robic, L. Vander Elst and R. N. Muller, *Chem. Rev.*, 2008, **108**, 2064.
99. A. G. Roca, R. Costo, A. F. Rebolledo, S. Veintemillas-Verdaguer, P. Tartaj, T. González-Carreño, M. P. Morales and C. J. Serna, *J. Phys. D Appl. Phys.*, 2009, **42**, 224002.
100. A. Lübbe, C. Bergemann, J. Brock and D. G. J. McClure, *Magn. Magn. Mater.*, 1999, **194**, 149.
101. R. Bardhan, W. X. Chen, M. Bartels, C. Pérez-Torres, M. F. Botero, R. W. McAninch, A. Contreras, R. Schiff, R. G. Pautler, N. J. Halas and A. Joshi, *Nano Lett.*, 2010, **10**, 4920.
102. F. K. H. van Landeghem, K. Maier-Hauff, A. Jordan, K. T. Hoffmann, U. Gneveckow, R. Scholz, B. Thiesen, W. Bruck and A. von Deimling, *Biomaterials*, 2009, **30**, 52.
103. C. Vauthier, N. Tsapis and P. Couvreur, *Nanomedicine-UK*, 2011, **6**, 99.
104. E. Ruiz-Hernández, A. López-Noriega, D. Arcos, I. Izquierdo-Barba, O. Terasaki and M. Vallet-Regí, *Chem. Mater.*, 2007, **19**, 3455.
105. B. Julián-López, C. Boissière, C. Chanéac, D. Grosso, S. Vasseur, S. Miraux, E. Duguet and C. Sanchez, *J. Mater. Chem.*, 2007, **17**, 1563.
106. J. Li, S. Z. Qiao, A. H. Hu and G. Q. Lu, *Small*, 2011, **7**, 425.
107. J. Deng, Y. Cai, Z. Sun and D. Zhao, *Chem. Phys. Lett.*, 2011, **510**, 1.
108. E. Ruiz-Hernández, A. López-Noriega, D. Arcos and M. Vallet-Regí, *Solid State Sci.*, 2008, **10**, 421.
109. D. Arcos, V. Fal-Miyar, E. Ruiz-Hernández, M. García-Hernández, M. L. Ruiz-González, J. González-Calbet and M. Vallet-Regí, *J. Mater. Chem.*, 2012, **22**, 64.
110. F. M. Martín-Saavedra, E. Ruíz-Hernández, A. Boré, D. Arcos, M. Vallet-Regí and N. Vilaboa, *Acta Biomater.*, 2010, **6**, 4522.
111. E. Terreno, D. D. Castelli, A. Viale and S. Aime, *Chem. Rev.*, 2010, **110**, 3019.
112. Y. S. Lin, Y. Hung, J. K. Su, R. Lee, C. Chang, M. L. Lin and C. Y. Mou, *J. Phys. Chem. B*, 2004, **108**, 15608.
113. K. M. L. Taylor, J. S. Kim, W. J. Rieter, H. An, W. Lin and W. Lin, *J. Am. Chem. Soc.*, 2008, **130**, 2154.
114. K. M. L. Taylor-Pashow, J. Della Rocca, R. C. Huxford and W. Lin, *Chem. Commun.*, 2010, **46**, 5832.
115. S. Li, H. Liu, L. Li, N. Q. Luo, R. H. Cao, D. H. Chen and Y. Z. Shao, *Appl. Phys. Lett.*, 2011, **98**, 093704.

116. H. M. Liu, S. H. Wu, C. W. Lu, M. Yao, J. K. Hsiao, Y. Hung, Y. S. Lin, C. Y. Mou, C. S. Yang, D. M. Huang and Y. C. Chen, *Small*, 2008, **4**, 619.
117. S. H. Wu, Y. S. Lin, Y. Hung, Y. H. Chou, Y. H. Hsu, C. Chang and C. Y. Mou, *ChemBioChem*, 2008, **4**, 53.
118. J. E. Lee, N. Lee, H. Kim, J. Kim, S. H. Choi, J. H. Kim, T. Kim, I. C. Song, S. P. Park, W. K. Moon and T. Hyeon, *J. Am. Chem. Soc.*, 2010, **132**, 552.
119. J. E. Lee, D. J. Lee, N. Lee, B. H. Kim, S. H. Choi and T. Hyeon, *J. Mater. Chem.*, 2011, **21**, 16869.
120. J. E. Lee, N. Lee, T. Kim, J. Kim and T. Hyeon, *Acc. Chem. Res.*, 2011, **44**, 893.
121. F. Wang, X. Chen, Z. Zhao, S. Tang, X. Huang, C. Lin, C. Cai and N. Zheng, *J. Mater. Chem.*, 2011, **21**, 11244.
122. P. J. Chen, S. H. Hu, C. S. Hsiao, Y. Y. Chen, D. M. Liu and S. Y. Chen, *J. Mater. Chem.*, 2011, **21**, 2535.
123. E. Ruiz-Hernández, A. Baeza and M. Vallet-Regí, *ACS Nano*, 2011, **5**, 1259.
124. S. Saha, K. C. F. Leung, T. D. Nguyen, J. F. Stoddart and J. I. Zink, *Adv. Funct. Mater.*, 2007, **17**, 685.
125. B. G. Trewyn, S. G. Giri, I. I. Slowing and V. S. Y. Lin, *Chem. Commun.*, 2007, 3236.
126. I. I. Slowing, J. L. Vivero-Escoto, C. W. Wu and V. S. Y. Lin, *Adv. Drug Deliver. Rev.*, 2008, **60**, 1278.
127. K. K. Cotí, M. E. Belowich, M. Liong, M. W. Ambrogio, Y. A. Lau, H. A. Khatib, J. I. Zink, N. M. Khashab and J. F. Stoddart, *Nanoscale*, 2009, **1**, 16.
128. M. Manzano, M. Colilla and M. Vallet-Regí, *Expert Opin. Drug Deliv.*, 2009, **6**, 1383.
129. M. Manzano and M. Vallet-Regí, *J. Mater. Chem.*, 2010, **10**, 5593.
130. C. Park, K. Oh, S. C. Lee and C. Kim, *Angew. Chem. Int. Ed.*, 2007, **46**, 1455.
131. L. Du, S. Liao, H. A. Khatib, J. F. Stoddart and J. I. Zink, *J. Am. Chem. Soc.*, 2009, **131**, 15136.
132. H. Meng, M. Xue, T. Xia, Y. L. Zhao, F. Tamanoi, J. F. Stoddart, J. I. Zink and A. E. Nel, *J. Am. Chem. Soc.*, 2010, **132**, 12690.
133. Y. L. Zhao, Z. Li, S. Kabehie, Y. Y. Botros, J. F. Stoddart and J. I. Zink, *J. Am. Chem. Soc.*, 2010, **132**, 13016.
134. E. Aznar, C. Coll, M. D. Marcos, R. Martínez-Máñez, F. Sancenón, J. Soto, P. Amorós, J. Cano and E. Ruiz, *Chem. Eur. J.*, 2009, **15**, 6877.
135. Q. Gan, X. Lu, Y. Yan, J. Qian, H. Zhou, X. Lu, J. Shi and C. Liu, *Biomaterials*, 2011, **32**, 1932.
136. R. Liu, Y. Zhang, X. Zhao, A. Agarwal, L. J. Mueller and P. Feng, *J. Am. Chem. Soc.*, 2010, **132**, 1500.
137. L. Chen, J. Di, C. Cao, Y. Zhao, Y. Ma, J. Luo, Y. Wen, W. Song, Y. Song and L. Jiang, *Chem. Commun.*, 2011, **47**, 2850.
138. N. K. Mal, M. Fujiwara and Y. Tanaka, *Nature*, 2003, **421**, 350.

139. N. K. Mal, M. Fujiwara, Y. Tanaka, T. Taguchi and M. Matsukata, *Chem. Mater.*, 2003, **15**, 3385.
140. S. Angelos, E. Choi, F. Vögtle, L. de Cola and J. I. Zink, *J. Phys. Chem. C*, 2007, **111**, 6589.
141. D. P. Perris, Y. L. Zhao, N. M. Khashab, H. A. Khatib, J. F. Stoddart and J. I. Zink, *J. Am. Chem. Soc.*, 2009, **131**, 1686.
142. C. Park, K. Lee and C. Kim, *Angew. Chem. Int. Ed.*, 2009, **48**, 1275.
143. J. L. Vivero-Escoto, I. I. Slowing, C. W. Wu and V. S. Y. Lin, *J. Am. Chem. Soc.*, 2009, **131**, 3462.
144. N. Z. Knežević, B. G. Trewyn and V. S. Y. Lin, *Chem. Commun.*, 2011, **47**, 2817.
145. C. Y. Lai, B. G. Trewyn, D. M. Jeftinija, K. Jeftinija, S. Xu, S. Jeftinija and V. S. Y. Lin, *J. Am. Chem. Soc.*, 2003, **125**, 4451.
146. S. Giri, B. G. Trewyn, M. P. Stellmaker and V. S. Y. Lin, *Angew. Chem., Int. Ed.*, 2005, **44**, 5038.
147. F. Torney, B. G. Trewyn, V. S. Y. Lin and K. Wang, *Nat. Nanotechnol.*, 2007, **2**, 295.
148. R. Liu, X. Zhao, T. Wu and P. Feng, *J. Am. Chem. Soc.*, 2008, **130**, 14418.
149. M. W. Ambrogio, T. A. Pecorelli, K. Patel, N. M. Khashab, A. Trabolsi, H. A. Khatib, Y. Y. Botros, J. I. Zink and J. F. Stoddart, *Org. Lett.*, 2010, **12**, 3304.
150. H. Kim, S. Kim, C. Park, H. Lee, H. J. Park and C. Kim, *Adv. Mater.*, 2010, **22**, 4280.
151. C. D. Austin, X. Wen, L. Gazzard, C. Nelson, R. H. Scheller and S. J. Scales, *P. Natl Acad. Sci. USA*, 2005, **102**, 17987.
152. K. G. de Bruin, C. Fella, M. Ogris, E. Wagner, N. Ruthardt and C. Bräuchle, *J. Control. Release*, 2008, **130**, 175.
153. S. Febvay, D. M. Marini, A. M. Belcher and D. E. Clapham, *Nano Lett.*, 2010, **10**, 2211.
154. A. M. Sauer, A. Schlossbauer, N. Ruthardt, V. Cauda, T. Bein and C. Bräuchle, *Nano Lett.*, 2010, **10**, 3684.
155. K. Patel, S. Angelos, W. R. Dichtel, A. Coskun, Y. W. Yang, J. I. Zink and J. F. Stoddart, *J. Am. Chem. Soc.*, 2008, **130**, 2382.
156. C. Park, H. Kim, S. Kim and C. Kim, *J. Am. Chem. Soc.*, 2009, **131**, 16614.
157. A. Schlossbauer, J. Kecht and T. Bein, *Angew. Chem. Int. Ed.*, 2009, **48**, 3092.
158. A. Bernardos, E. Aznar, M. D. Marcos, R. Martínez-Máñez, F. Sancenón, J. Soto, J. M. Barat and P. Amorós, *Angew. Chem. Int. Ed.*, 2009, **48**, 5884.
159. A. Bernardos, L. Mondragón, E. Aznar, M. D. Marcos, R. Martínez-Máñez, F. Sancenón, J. Soto, J. M. Barat, E. Pérez-Payá, C. Guillem and P. Amorós, *ACS Nano*, 2010, **4**, 6353.
160. E. Climent, A. Bernados, R. Martínez-Máñez, A. Maquieira, M. D. Marcos, N. Pastor-Navarro, R. Puchades, F. Sancenón, J. Soto and P. Amorós, *J. Am. Chem. Soc.*, 2009, **131**, 14075.

161. R. Casasús, E. Climent, M. D. Marcos, R. Martínez-Máñez, F. Sancenón, J. Soto, P. Amorós, J. Cano and E. Ruiz, *J. Am. Chem. Soc.*, 2008, **130**, 1903.
162. S. Angelos, Y. W. Yang, N. M. Khashab, J. F. Stoddart and J. I. Zink, *J. Am. Chem. Soc.*, 2009, **131**, 11344.
163. R. Liu, Y. Zhang and P. Feng, *J. Am. Chem. Soc.*, 2009, **131**, 15128.
164. C. Chen, J. Geng, F. Pu, X. Yang, J. Ren and X. Qu, *Angew. Chem. Int. Ed.*, 2011, **50**, 882.
165. J. Lu, M. Liong, J. I. Zink and F. Tamanoi, *Small*, 2007, **3**, 1341.
166. S. P. Hudson, R. F. Padera, R. Langer and D. S. Kohane, *Biomaterials*, 2008, **29**, 4045.
167. C. R. Thomas, D. P. Ferris, J. H. Lee, E. Choi, M. H. Cho, E. S. Kim, J. F. Stoddart, J. S. Shin, J. Cheon and J. I. Zink, *J. Am. Chem. Soc.*, 2010, **132**, 10623.
168. J. Lu, E. Choi, F. Tamanoi and J. I. Zink, *Small*, 2008, **4**, 421.
169. S. H. Wu, Y. Hung and C. Y. Mou, *Chem. Commun.*, 2011, **47**, 9972.
170. X. Huang, L. Li, T. Liu, N. Hao, H. Liu, D. Chen and F. Tang, *ACS Nano*, 2011, **26**, 5390.
171. J. S. Souris, C. H. Lee, S. H. Cheng, C. T. Chen, C. S. Yang, J. A. A. Ho, C. Y. Mou and L. W. Lo, *Biomaterials*, 2010, **31**, 5564.
172. M. M. van Schooneveld, E. Vucic, R. Koole, Y. Zhou, J. Stocks, D. P. Cormode, C. Y. Tang, R. E. Gordon, K. Nicolay, A. Meijerink, Z. A. Fayad and W. J. M. Mulder, *Nano Lett.*, 2008, **8**, 2517.
173. Q. He and J. Shi, *J. Mater. Chem.*, 2011, **21**, 5845.
174. D. P. Ferris, J. Lu, C. Gothard, R. Yanes, C. R. Thomas, J. C. Olsen, J. F. Stoddart, F. Tamanoi and J. I. Zink, *Small*, 2011, **7**, 1816.
175. H. Meng, M. Xue, T. Xia, Z. Ji, D. Tarn, J. I. Zink and A. E. Nel, *ACS Nano*, 2011, **5**, 4131.

CHAPTER 16

Smart Carbon Nanotubes

GERARD TOBIAS*[a] AND EMMANUEL FLAHAUT[b]

[a] Institut de Ciència de Materials de Barcelona (ICMAB-CSIC), Campus UAB, 08193-Bellaterra, Barcelona, Spain; [b] Centre Interuniversitaire de Recherche et d'Ingénierie des Matériaux, Université Paul Sabatier, CIRIMAT - UMR CNRS 5085, 31062 Toulouse Cedex 9, France
Email: flahaut@chimie.ups-tlse.fr
*Email: gerard.tobias@icmab.es

16.1 Introduction

16.1.1 Carbon Nanotubes: Structure and Properties

Carbon nanotubes (CNTs) are quasi-one-dimensional structures that can be described as graphene layers rolled up to form seamless cylinders.[1] Depending on the number of layers, CNTs can be classified as single-walled CNTs (SWCNTs),[2] when their structure is formed by a single layer, or multi-walled CNTs (MWCNTs), when their structure is formed by several concentric layers.[1] The structure of each layer consists of sp^2 hybridized carbon atoms in a hexagonal network with in-plane σ bonds and out-of-plane π orbitals.[3] This particular structure is responsible for CNTs' and graphene's unique physical, chemical and mechanical properties, which are of interest for a wide variety of applications, ranging from reinforcement in composite materials, sensors or energy storage to drug-delivery systems (DDSs). The length of CNTs is typically in the region of micrometers with diameters that usually range from about 0.8 to 2 nm, in the case of SWCNTs, and from 2 to 100 nm, in the case of MWCNTs. Defect-free CNTs are almost chemically inert. Being an advantage for some applications, this chemical inertness together with their intrinsic poor

---

RSC Smart Materials No. 3
Smart Materials for Drug Delivery: Volume 2
Edited by Carmen Alvarez-Lorenzo and Angel Concheiro
© The Royal Society of Chemistry 2013
Published by the Royal Society of Chemistry, www.rsc.org

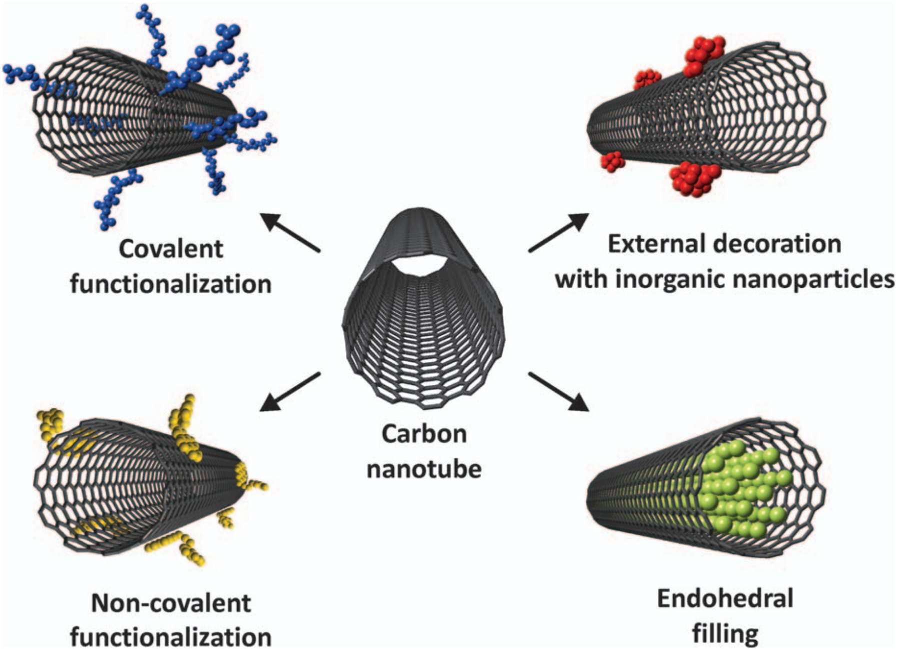
Covalent functionalization
External decoration with inorganic nanoparticles
Carbon nanotube
Non-covalent functionalization
Endohedral filling

Figure 16.1 Schematic representation of strategies for the functionalization of carbon nanotubes.

dispersibility in most solvents (both organic and water-based) represents a major challenge towards their practical application. Furthermore, as-produced SWCNTs and few-layered MWCNTs align parallel to each other forming bundles, due to van der Waals interactions, which further agglomerate into entangled networks. In this context, the functionalization of CNTs is a key step towards increasing their dispersibility, reactivity, processability and biocompatibility. The functionalization of CNTs allows the modification of the structural framework and the creation of supramolecular complexes.[4] The main strategies employed for the modification of CNTs can be classified into four groups: covalent functionalization, non-covalent functionalization, external decoration with inorganic materials and endohedral filling.[5–9] For biomedical applications and in particular for the development of novel CNT-based DDSs, either covalent or non-covalent functionalization is essential. Furthermore, it is also possible to apply two or more functionalization strategies on a given specimen of CNTs resulting in CNTs bearing multiple functionalities. A schematic representation of these four functionalization strategies is presented in Figure 16.1.

16.1.2 Carbon Nanotubes in Drug Delivery

CNTs may play a role in the biomedical field and have been advocated as promising candidates in the areas of drug delivery, diagnosis and therapy. Due to their needle-like shape, CNTs possess an enhanced capacity to penetrate cellular membranes and better flow dynamics than that of spherical nanoparticles, and can carry multiple moieties at high density because of their large specific surface area.[10] Functionalized CNTs are flexible structures that might bend, allowing interaction with cells through multiple binding sites.[11] Furthermore, it is possible to take advantage of their tubular shape and simultaneously encapsulate a chosen payload in their interior, whilst the external walls can be functionalized to render them dispersible, biocompatible and even targetable.

The intrinsic electronic (and optical) properties of CNTs allow their monitoring (detection and imaging) in biological tissues by means of several spectroscopic techniques, including Raman,[12–14] photoluminescence[15–17] and photo-acoustic imaging.[18] The electronic properties of CNTs can also be exploited for therapeutic purposes *via* photothermal therapy, since SWCNTs strongly absorb light in the near-infrared (NIR) range (800–1600 nm).[19,20] The emission range of SWCNTs is within 800 to 2000 nm, covering the transparency window of biological tissues (800–1400 nm). Therefore, CNTs can be utilized for multiple imaging by merely taking advantage of their intrinsic properties. Photoluminescence and Raman spectroscopy greatly complement each other since the former is sensitive to individual semi-conducting nanotubes, whereas specific signals for both semi-conducting and metallic nanotubes (even in bundles) are obtained for the latter. Despite MWCNTs being less attractive in terms of optical properties compared to SWCNTs, they present different sizes and dispersibility properties and therefore should still be regarded as potentially useful for drug delivery. Double-walled CNTs (DWCNTs) keep a morphology very close to that of SWCNTs, but the outer wall can be functionalized without any modification of the inner one.

If we want to use CNTs as a new platform for drug delivery, the first questions that we need to answer are: are they biocompatible? Are they toxic? Early studies reported that as-prepared CNTs were toxic, but it was later shown that the toxicity was actually likely to be due to the presence of catalytic particles or long nanotubes.[21] Although pharmacological studies are still in progress, there is a general consensus within the scientific community that purified, short and well-dispersed nanotubes are indeed rather biocompatible. Nevertheless, since the toxicity and the environmental impact of CNTs are key points for any new development in the area of drug delivery, these aspects are addressed in Section 16.5 at the end of the chapter.

The rational design of DDSs employing nanotechnological approaches allows addressing and overcoming some limitations of "free" drugs. In this context, the development of smart CNTs has the potential of moving a step forward compared to conventional drugs. For instance, the use of CNTs could improve the formulation of poorly water-soluble drugs, allow targeted delivery reducing side effects and even enable the co-delivery of two or more drugs for combination therapy. Furthermore by taking advantage of the different *in vivo* microenvironments, smart nanotubes can be designed to trigger the release of drugs *via* endogenous stimuli, such as a change in the pH or in the local

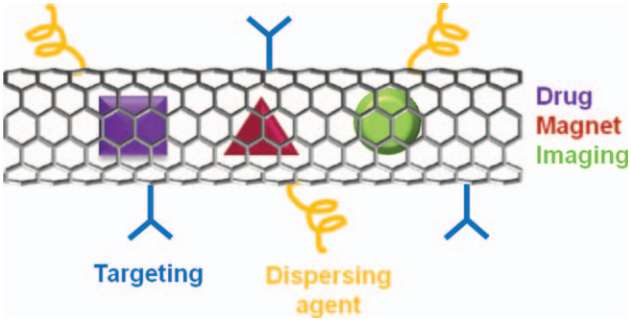

Figure 16.2 Scheme of a smart carbon nanotube bearing multiple functionalities.

temperature. Drug release could also be controlled *via* an external stimulus (magnetic field, irradiation, *etc*.). In the search for smart nanomaterials, one can design multi-functional nanotubes, which, apart from carrying the chosen drug, can contain targeting and dispersing agents, nanoparticles for imaging, a magnet for hyperthermia and so on. A schematic representation of such smart nanotubes is presented in Figure 16.2.

16.2 Functionalization of Carbon Nanotubes for Biomedical Applications

The use of CNTs for biomedical applications is hampered by their intrinsic hydrophobicity, which hinders their dispersibility in aqueous media and hence may compromise their biocompatibility. Therefore, the external sidewalls of the CNTs need to be functionalized to render them dispersible. This can be achieved by either covalent or non-covalent functionalization.[5–8,22] Both methods have their own advantages and disadvantages that must be carefully considered depending on each specific application. When using CNTs as DDSs the functionalization of the pristine material also plays a key role in rendering them suitable for the attachment of both drugs and targeting agents. The different functionalization approaches are now discussed.

16.2.1 Covalent Functionalization

Covalent functionalization of CNTs has been widely used to improve their dispersibility, to conjugate a wide variety of moieties including biomolecules and polymers and to tailor their properties for specific applications. The main advantage of this approach is the stability of the chemical bond, which indeed overpasses any of the functionalization strategies based on non-covalent interactions. The strategies for covalent functionalization of CNTs can be classified into two groups: direct sidewall functionalization and defect group functionalization.

Direct sidewall functionalization is based on the rehybridization of sp^2 carbon atoms of the CNT backbone into an sp^3 configuration to form covalent bonds with the attacking species. We will refer to defect group functionalization when the desired functionalities are attached to intentionally created defects or pre-existing chemical groups on the CNT scaffold. The major drawback of both covalent approaches is the disturbance of the CNT tubular structure leading to a modification or degradation of their intrinsic properties, such as electronic and optical ones, which are sometimes employed to detect the CNT-based DDSs in the biological environment. The main difference between these complementary approaches is that defect functionalization is primarily located (at low defect density creation) at the CNT tips where oxidation is favored compared to the sidewall, as opposed to direct sidewall functionalization where the functionalities are installed on the CNT sp^2 network, *i.e.* along the outer wall. Both strategies have been used to design CNTs for diverse applications including the development of multi-functional drug nanocarriers.

16.2.1.1 Defect Group Functionalization

The most common approach for the generation of defects on the CNT structure is oxidation by liquid-phase (*i.e.* refluxing in HNO_3), gas-phase (*i.e.* O_2) or even electrochemical oxidation. It has been proved that the oxidation process starts at topological defects of the sp^2 network and the CNT tips (which ideally are two hemifullerenes) because these are more reactive towards oxidative chemical attacks than a perfect sp^2 carbon network, due to the strong curvature (pentagons). Hence, the oxidation process yields oxygen-bearing groups, initially in the intrinsic defects and the CNT tips, but increasing the duration or the energy of the treatment also results in the creation of new defects in the CNT scaffold (sidewall). The oxidative process results in the creation of carboxylic groups and other oxygen-bearing functionalities.[23] These functional groups created at the CNT surface serve as a starting point for further derivatization. Removal of the amorphous carbon impurities has been shown to be an essential step for an efficient sidewall functionalization using nitric acid.[24] Among the different derivatization strategies, the esterification and amidation of carboxylic acid groups have been extensively investigated to anchor drugs and other biomolecules. The analysis of functionalized CNTs is typically performed by spectroscopic techniques, widely used for the characterization of organic compounds, such as Raman, infrared (IR), ultraviolet (UV) and nuclear magnetic resonance (NMR), which provide information about the bulk materials. Nowadays, electron microscopy techniques, initially used for the characterization of inorganic materials, valuably complement the spectroscopic analysis providing local information and even allowing in some cases the visual detection of the organic moieties down to the atomic scale.[25]

16.2.1.2 Direct Sidewall Functionalization

The synthetic routes developed during the last years following this approach are numerous. One of the first sidewall functionalization reactions was fluorination. The fluorinated CNTs serve as a starting point in many reactions where fluorine atoms are later replaced and derivatized using, for instance, Grignard or organolithium reagents. Following the same idea, CNTs have also been chlorinated, brominated and iodinated. Among the different methods for direct sidewall functionalization, cyclo-addition reactions deserve special attention since they are being widely employed to render CNTs dispersible and for the attachment of biomolecules. These include, for instance, the carbene cyclo-addition to pristine CNTs, the 1,3-dipolar cyclo-addition reaction or the so-called Bingel cyclopropanation. Both electrophilic and nucleophilic additions have also been employed to modify the CNT structure. For instance, electrophilic addition of alkylhalides results in the formation of alkyl and hydroxyl groups, and as an example of the latter, nucleophilic addition of amine-based nucleophiles leads to amino-functionalized CNTs. Other methods for direct sidewall functionalization include radical additions with diazonium salts, ozonolysis, plasma activation and mechano-chemical functionalization.

Both defect and direct sidewall functionalization are being employed for the attachment of drugs and other molecules onto the CNT skeleton to allow their integration in biological systems. In summary, there has been an extensive effort in developing routes towards the covalent functionalization of CNTs both at the sidewalls and at the tips. These efforts in combination with the organic chemistry toolbox have led to tailor-made properties for various applications in many fields in nanotechnology.

16.2.2 Non-covalent Functionalization

Non-covalent functionalization of CNTs consists of the adsorption or wrapping of various functional molecules on the tubular surface. This approach is based on π-π stacking, van der Waals or charge-transfer interactions. Therefore its main interest resides in the fact that it preserves the extended π-network of the tubes and, therefore, retains the intrinsic electronic and optical properties of the CNTs, which might be employed for their visualization in the biological medium. Most of the research on non-covalent functionalization has aimed to achieve the dispersion of CNTs by the exfoliation of bundles to obtain individual CNTs, which are otherwise very difficult to disperse homogeneously in order to form a stable suspension. In the past few years preparation of highly stable suspensions of individually dispersed nanotubes has been achieved, in both aqueous and organic media.

Typically, the functionalization involves ultrasonication in a solvent followed by centrifugation and filtration. Ultrasonication produces a high-shear environment that results in the formation of gaps or spaces at the bundle ends. These gaps are unstable, so in the absence of a dispersing agent the nanotubes reattach through van der Waals attraction. When a dispersing agent is present, these spaces or gaps at the bundle ends are propagated by the dispersant adsorption, ultimately separating the individual nanotubes from the bundle.[26]

A wide range of compounds have been used for the non-covalent functionalization of CNTs, including surfactants, polymers, biomolecules and polynuclear aromatic molecules.[27] Besides, CNTs have also been modified with ionic liquids, dyes, macrocyclic host molecules and phosphines, among others. Depending on their final application, these non-covalently functionalized CNTs have been used in some cases for further modification with biomolecules, inorganic nanoparticles, organic moieties, *etc*.

16.3 External Attachment of Drugs onto Carbon Nanotubes

CNTs are being explored as delivery vehicles for a wide range of biomolecules.[11,28–31] Apart from drugs, on which this chapter is focused, biomacromolecules such as proteins, DNA and RNA have also been conjugated to CNTs. Several drug molecules have been attached either covalently or through π-π interactions on the surface of both SWCNTs and MWCNTs. Multi-functional CNTs have been developed not only to include the chosen drugs, but to also bear targeting ligands such as antibodies,[17,19,32,33] folic acid[20,34] and peptides.[35,36] Among the different drugs that have been attached to CNTs, special attention has been paid to doxorubicin and platinum-based anticancer drugs.

16.3.1 Delivery of Doxorubicin with Carbon Nanotubes

Doxorubicin is a widely used anthracycline anticancer drug efficient against a wide range of tumors, including breast, stomach, ovary, bladder and thyroid gland cancer, as well as several types of lymphoma and leukemia.[37] Anthracyclines intercalate with DNA causing disruption of transcription and replication. The first report of the use of CNTs as carriers for doxorubicin showed, in 2007, that a high-loading of drug could be conjugated onto the surface of SWCNTs (4 g of drug per gram of nanotubes).[36] The SWCNTs were initially dispersed with poly(ethylene glycol) terminated with a lipid chain, which was then linked to doxorubicin. This binding is pH dependent and favors drug release in endosomes and lysosomes, as well as in tumor micro-environment (with a pH lower than that of healthy tissues). Their multi-walled counterparts have been employed in a similar manner using the block copolymer Pluronic F127 to suspend the CNTs in water. An enhanced antitumoral effect was observed towards human breast cancer cells *in vitro* compared to the free drug and to the doxorubicin-Pluronic F127 complex.[38] Smart DDSs for targeted delivery of doxorubicin using CNTs have been developed by means of multiple functionalization. The peptide arginine-glycine-aspartic acid (RGD) was conjugated to doxorubicin-loaded SWCNTs to act as a targeting ligand in order to impart recognition of moieties for integrin receptors.[36] Targeted delivery to cancer cells and controlled release of doxorubicin has been achieved by functionalization of SWCNTs with polysaccharides and folic acid.[39–41] Folic acid receptors tend to be overexpressed in the surface of cancer cells. Dual targeting *via* combination of both active (folate) and passive (iron) targeting agents has been achieved with a CNT nanocarrier that contains doxorubicin, folate and iron (magnetic material).[40,42] The targeted delivery was assisted with an external magnetic field to guide the CNTs to the specific site. High drug loading, pH-dependent controlled release and good delivery efficiency could be achieved with this CNTs-based DDS. Another approach that is receiving great attention in terms of targeting consists of the conjugation of monoclonal antibodies. Triple functionalization of SWCNTs with doxorubicin (as therapeutic agent), fluorescein (to facilitate their detection) and monoclonal antibody (for targeting) was recently reported for cancer therapy.[43] The monoclonal antibody assisted in the effective binding of the nanocarrier to the cancer cells by recognition of the tumor marker (carcinoembryonic antigen).

Tumors treated with anthracyclines, such as doxorubicin, might become multi-drug resistant to several structurally related drugs,[44] which is a major obstacle for a successful chemotherapeutical treatment. Recently, poly(ethylene glycol)-conjugated MWCNTs have been reported as efficient doxorubicin delivery systems for overcoming multi-drug resistance. The functionalized CNTs accumulated with the same efficiency in multi-drug resistant cells (generated by growth in a medium with doxorubicin) compared to non-multi-drug resistant tumor cells.

16.3.2 Delivery of Platinum-based Drugs with Carbon Nanotubes

Platinum-based anticancer drugs rank second in terms of delivery of chemotherapeutic agents using CNTs as vectors. Cisplatin, oxaliplatin and carboplatin have all been either conjugated to the external walls of CNTs or encapsulated within their cavities. Research on platinum coordination complexes as anticancer drugs began with the discovery, back in the 1960s, that some platinum compounds inhibit bacterial cell division. Further studies revealed that they also inhibit tumor cell growth. Platinum-based complexes hydrolyse in the cells leading to positively charged platinum cations, which coordinate to the nitrogen atoms of the adenine and guanine bases of DNA. DNA duplication is hindered in this way, because cells are unable to repair the distorted DNA helix leading to cell apoptosis.[45] The highest antitumor activity was exhibited by cisplatin (*cis*-diamminedichloroplatinum (II); *cis*-$[Pt(NH_3)Cl_2]$. Cisplatin has been employed for the treatment of several types of cancers, including metastatic testicular and ovarian cancers as well as advanced bladder cancer.[46] The initial studies on delivery of both doxorubicin and cisplatin, using CNTs as DDSs, took place in 2007. In a similar approach to the initial studies with doxorubicin, SWCNTs were dispersed by means of a lipid-polyethylene chain bearing a platinum (IV) compound as a prodrug to deliver cisplatin (cytotoxic drug of platinum (II) compound).[47] The inert platinum (IV) complex, attached *via* peptide linkages, becomes activated upon reduction to the platinum (II) form in the cell endosomes. The lower pH environment in the endosomes induces the reduction and release of cisplatin, thus killing the testicular carcinoma cells used to establish the efficacy of the system. The CNTs loaded with the platinum complex are taken into the cancer cells by endocytosis and reside in the endosomes. The cytotoxic effect when using CNTs as DDSs is over 100-fold higher than that of the molecule administered alone. A prodrug of platinum (IV) was employed since the direct use of platinum (II) is limited by its deactivation upon administration. This is due to the sensitivity of platinum (II)-based molecules to intra-cellular glutathione levels.[48] This problem can be overcome by employing complexes of platinum in a higher oxidation state (IV), as described, which become reduced to the active antitumoral platinum (II) form upon entering the cells.

Later, CNTs have been conjugated not only with a platinum-based drug (or prodrug) but also with targeting agents, such as folic acid, in a multi-modal approach.[34] The targeted delivery of the resulting construct showed a higher toxicity towards folate receptor positive cells compared to folate receptor negative cells. *In vivo* and *in vitro* studies have also been performed with CNTs bearing cisplatin and epidermal growth factor (EGF).[49] The CNTs are directed to overexpressed epidermal growth factor receptors on squamous carcinoma cells (head and neck). Tumor growth was inhibited much more rapidly in mice treated with cisplatin-loaded CNTs bearing EGF compared to CNTs with the same drug but without EGF. Although to a lesser extent, other platinum-based chemotherapeutic agents, such as carboplatin and oxaliplatin, have also been delivered by CNTs. The former has been encapsulated inside the cavity of CNTs and will be discussed in Section 16.4.2. Oxaliplatin is another important platinum-based anticancer drug employed for treatment of colorectal cancer[46] that has recently been tested in photothermal therapy using CNTs.[50] The local effect of oxaliplatin on colorectal cancer cells was aided with photothermal heating to 42 °C applying infrared radiation.

16.3.3 Delivery of Other Anticancer Drugs by Carbon Nanotubes

CNTs have also been employed for the delivery of other anticancer drugs apart from doxorubicin and platinum-based antitumoral agents. In this section some representative examples are discussed.

Early studies on the use of CNTs for the delivery of methotrexate were performed in 2006.[51] Methotrexate is an inhibitor of folic acid biosynthesis, which slows the proliferation of cells. Since cancer cells present a rapid proliferation, methotrexate appeared to be a promising drug for cancer treatment. Nowadays, its main use resides in the treatment of autoimmune and inflammatory diseases.[52] Initial studies with Jurkat cells incubated up to 72 h showed that methotrexate remains active upon conjugation to CNTs.[51] Later on, the anticancer activity of the molecule conjugated to CNTs *via* cleavable linkers, peptide and ester bonds was investigated. An enhanced anticancer activity was found when using the peptide linker compared to the ester-bonded conjugates and to the free drug. Proteases overexpressed in tumor cells were responsible for the selective cleavage of the linker.[53]

The use of cleavable linkers has also been investigated with other drugs, such as paclitaxel (commercialized as Taxol), both *in vitro* and *in vivo*. Paclitaxel, a natural product mainly used for the treatment of metastatic breast and ovarian cancers,[54] was conjugated to poly(ethylene glycol) functionalized SWCNTs *via* ester cleavable bonds. Biodistribution and pharmacokinetic studies revealed a higher tumor uptake of paclitaxel when incorporated in CNTs compared to the free drug, and also longer blood circulation half-life.[55] The tumor uptake of this DDS is likely due to the EPR effect, since no targeting moieties had been conjugated. A rapid dissociation and excretion of the paclitaxel molecules carried to liver and spleen was observed, thus reducing the toxicity of the conjugate. This result highlights the potential of CNTs for systemic administration of chemotherapeutic agents. In another study, multi-functional CNTs were developed for the delivery of a taxoid prodrug (derivative from paclitaxel) also containing tumor-recognition modules (biotin and a spacer). The prodrug attached to CNTs *via* a cleavable linker is activated to its cytotoxic form inside the tumor cells, upon internalization and intra-cellular drug release.[56] The conjugate showed specificity to cancer cells that overexpress biotin receptors on their surface. The cytotoxicity of the conjugate was ascribed to the released taxoid molecules inside the cancer cells.

Following the concept described for oxaliplatin, MWCNTs bearing mitomycin C have also been developed as delivery systems aided by photothermal annealing.[50] Mitomycin C is an ancillary anticancer agent that is mainly used in combination with other drugs for the treatment of breast, stomach, cervical, bladder, head, neck and lung cancers.[57] After being activated in cells, mitomycin C cross-links between DNA strands blocking its synthesis.

The antitumor activity of 10-hydroxycamptothecin covalently conjugated to MWCNTs has been investigated both *in vivo* and *in vitro*. Camptothecin and its analogues act by inhibiting the enzyme topoisomerase I, which plays a key role in DNA replication. The developed DDS results in high concentration in tumor sites and longer blood circulation compared to the free drug. Therefore, a better anticancer activity is achieved by using CNTs for the delivery.[58]

Recently, CNTs have been used for the delivery of epirubicin, an anthracycline chemotherapeutic agent similar to doxorubicin that is employed for the treatment of several types of solid tumors. Actually epirubicin and doxorubicin present the same molecular formulae and only differ in the spatial orientation of one of the hydroxyl groups.[59] Epirubicin has been conjugated to MWCNTs *via* non-covalent supramolecular functionalization. A higher epirubicin loading could be achieved by a previous oxidation of the CNTs by an acid treatment. The nanocarriers released the drug faster in acidic medium than in neutral medium. Furthermore, an enhanced concentration at tumor sites was achieved when using CNTs than when administering free epirubicin.

16.3.4 Delivery of Other Drugs by Carbon Nanotubes

Although anticancer drugs have been the main focus for the development of DDSs based on CNTs, other active substances have also been conjugated to them. For instance the delivery of amphotericin B, a natural antifungal agent,[60] incorporated to CNTs presents several advantages. This drug has a low solubility in aqueous media, which might be responsible for its toxicity.

The attachment to MWCNTs allows the modulation of amphotericin B activity and prevents the aggregation of the drug molecules.[61] A fluorescent probe anchored to the tubular structure of the CNTs facilitates the detection and the monitoring of the cellular uptake. The functionalized CNTs behave as nano-needles, crossing the membranes of mammalian cells without toxic effects. Furthermore, amphotericin B delivered by CNTs maintains the antifungal activity against several pathogens, including *Candida albicans*, *Candida parapsilosis* and *Cryptococcus neoformans*.

The delivery of anti-inflammatory drugs using CNTs as nanocarriers has also been studied. Dexamethasone,[62] ketoprofen[63] and dapsone[64] have been conjugated to SWCNTs (dexamethasone) and MWCNTs (ketoprofen, dapsone). Dexamethasone is a member of the prednisone class (synthetic analogues of cortisol/cortisone) with greater potency and longer half-life than prednisone itself and, thus, is widely used in rheumatic/inflammatory disorders.[65] The delivery of dexamethasone through electrical stimuli has been achieved using CNTs as the carrier. By tuning the potential applied to the system, it is possible to modulate the cellular uptake of dexamethasone and the drug release rate.[62] The use of electric stimulus for the release of drugs is valid for both SWCNTs and MWCNTs.[63] An enhanced release of ketoprofen has been reported when applying a potential to ketoprofen-loaded MWCNTs. A matrix of a polymeric network has been employed to create the electro-sensitive delivery systems. Recently, the anti-inflammatory and antimicrobial drug dapsone has been conjugated to MWCNTs.[64] In this case no external stimulus has been employed to modulate the delivery of the drug. Prolonged incubation of cells with the nanocarrier (over three days) resulted in cell apoptosis without oxidative stress. In contrast, oxidative stress was observed when the cells were incubated with free dapsone.

Alzheimer's disease is associated to the loss of neurons.[66] SWCNTs have been tested as drug carriers for the delivery of acetylcholine to the brain for the treatment of this pathology.[67] Lysosomes are identified as the pharmacological target organelles for SWCNTs, and mitochondria are the toxicological target. Thus, the amount of drug-loaded SWCNTs should be carefully regulated to enable a preferential accumulation in lysosomes, compared to mitochondria.

Alginate microspheres filled with CNTs have been developed as drug carriers for theophylline. The CNTs prevented the leakage of theophylline and provided a more sustained drug-release profile. The cytocompatibility of the alginate microspheres was not affected by the presence of CNTs in their structure.[68] CNTs functionalized with carboxylic acid groups have also been employed to improve the hydrosolubility of carvedilol, a poorly water-soluble drug used for the treatment of hypertension.[69]

16.4 Encapsulation of Drugs Inside Carbon Nanotubes

16.4.1 Carbon Nanotubes as Nanocontainers

Soon after the report on MWCNTs by Iijima in 1991,[1] Pederson and Broughton[70] predicted on the basis of computer simulations that open-ended nanotubes should act as "nano-straws" and draw in molecules from vapor or fluid phases. In the following years several groups reported on the encapsulation of materials into MWCNTs. These initial studies focused on the encapsulation of inorganic materials due to their ease of detection by means of electron microscopy techniques. In the case of SWCNTs it was not until five years after their discovery, back in 1993,[2] that they were filled with materials such as $RuCl_3$ and fullerene C_{60}.[71,72] Nowadays it is possible to encapsulate a large variety of materials including inorganic salts,[73] organic molecules,[74] fullerenes,[72] metals[75] and water.[76] Unprecedented structures and properties have been observed for the encapsulated material, which can also alter the properties of the SWCNTs.[74,77,78] Thanks to advances in electron microscopy it is nowadays possible to determine the structure that both inorganic and organic materials adopt once confined within the CNT walls.[73,79] Filled CNTs encounter applications in different fields, ranging, for instance, from nanoelectronics to the biomedical field. Within the latter, filled CNTs are envisaged as promising agents for *in vivo* imaging and tumor targeting. SWCNTs containing Gd^{3+} have been studied for magnetic resonance imaging (MRI),[80] and I_2@SWCNTs have been reported as X-ray contrast agents.[81] Radionuclide-filled SWCNTs allow ultrasensitive imaging *in vivo* and the delivery of an unprecedented radiodose density, and therefore present potential for both diagnosis and treatment.[82] Furthermore, a nanothermometer for temperature control in biological environments is also being developed with copper iodide filled tubes.[83]

16.4.2 Drug Delivery with Filled Carbon Nanotubes

The containment of materials into CNTs is gaining increasing attention for the development of multi-functional DDSs, because the cavity can be filled with therapeutic and/or imaging cargos, whilst the outer surface can be modified to improve their dispersibility, biocompatibility and site-selectivity. The containment of the chosen drug into CNTs presents some advantages compared to delivery through external attachment. On the one hand, the carbon shell protects the encapsulated drug from interaction with the external environment, which in some cases might lead to the inactivation or even decomposition of the drug molecules. On the other hand, a controlled discharge of the cargo might be achieved *via* either an *in situ* or an *ex situ* stimulus.

The encapsulation of drugs has been studied from both experimental and theoretical points of view. Platinum-based chemotherapeutic agents have not only been anchored to the external CNT surface, but also filled into the inner cavities of CNTs. Initial modeling on the viability of drug encapsulation, performed with three different orientations of cisplatin, showed that the minimum radius of the CNT host must be at least 4.785 Å to allow the loading of this polar molecule.[84] Subsequently, cisplatin has been experimentally filled into CNTs. The resulting DDSs developed with shortened CNTs inhibited the viability of breast and prostate cancer cells.[85,86] A higher cisplatin loading has recently been achieved by using functionalized gold nanoparticles to block the ends of the MWCNTs.[87] Other platinum-based compounds have been developed due to the side effects associated with the use of cisplatin, which include nausea, vomiting, hearing loss and nerve and kidney damage. Carboplatin, available since 1989, presents reduced side effects compared to cisplatin and is effective, for instance, for ovarian and lung carcinomas.[46] The reversible filling-release process of carboplatin into MWCNTs has been investigated *in vitro*.[88] The structure of the drug molecule is retained once confined within the CNT cages. Carboplatin-loaded CNTs effectively suppressed the growth of bladder cancer cells, whereas unfilled, open-ended CNTs barely affected their growth.

Research is currently being devoted in finding routes that would allow a triggered discharge of the encapsulated payload. A series of proof-of-principle experiments by different groups have shown that it is indeed possible to achieve a controlled discharge of material from CNTs by external stimuli *via* a high voltage[89] or current density,[90] or from a change in the local environment of the nanocarrier.[91] Bulk filling of carbon nanotubes always results in the presence of material both inside and outside their tubular structure. A simple and effective methodology to seal soluble materials inside open-ended SWCNTs using fullerene C_{60} molecules has recently been reported.[89,90] The strong affinity that C_{60} molecules have towards the inner CNT cavities[72,92] allows them to act as sealing agents. These are insoluble in water[89] but can be removed, at least partially, using organic solvents such as dichlorobenzene,[93] toluene–ethanol (4 : 1)[94] or dichloromethane.[90] Following this approach, the anticancer drug hexamethylamine has been encapsulated inside SWCNTs by blocking the ends with fullerenes. The discharge of both the fullerenes and the drug is performed by treating the nanocarrier systems with dichloromethane.[90] In order to realize the release of the encapsulated payloads in aqueous media, relevant for biological applications, the fullerenes need to be functionalized.[91] A pH-triggered release in aqueous media is possible by using, for instance, dimethylamino functionalized fullerenes (f-C_{60}) as "corks" (Figure 16.3).

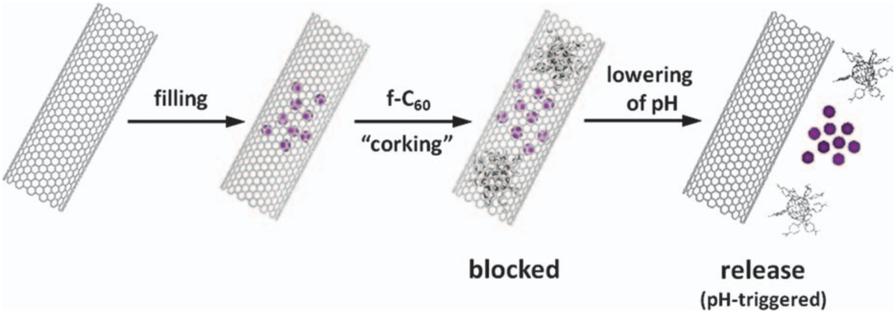

Figure 16.3 Schematic representation of the process for the encapsulation, "corking" and pH-triggered release of the encapsulated payload from SWCNTs. Adapted from Ref. 91.

The removable corks isolate the encapsulated material from the external media when the pH is that of a healthy tissue, but become soluble upon getting in contact with an acidic medium, thus allowing the release of the encapsulated compounds.[91] Both bulk (UV-Vis) and local (HRTEM) data confirm the successful containment and pH-sensitive release of the cargo. Recently another approach based on molecular dynamic simulations has been proposed for the controlled release of drugs from CNTs. This consists of encapsulating the chosen payload and carbonated water inside the CNTs. The discharge of the drug would take place by laser heating of the nanocarrier, which would result in the emission of carbon dioxide that would increase the inner pressure pushing the drug molecules outside the tubular cavities.[95]

Double-functionalized double-walled CNTs have also been evaluated for gene delivery. A plasmid coding for the production of a fluorescent protein was anchored to the outer wall of the nanotubes, while the inside was filled with chloroquine, a lysosomotropic compound. After incorporation into the cells, the pH decrease inside the lysosomes allowed the release of chloroquine from the nanotubes, leading to the rupture of the lysosomes and the release of the nanotubes directly into the cytoplasm, from where the plasmid could finally reach the nucleus (Figure 16.4).[96]

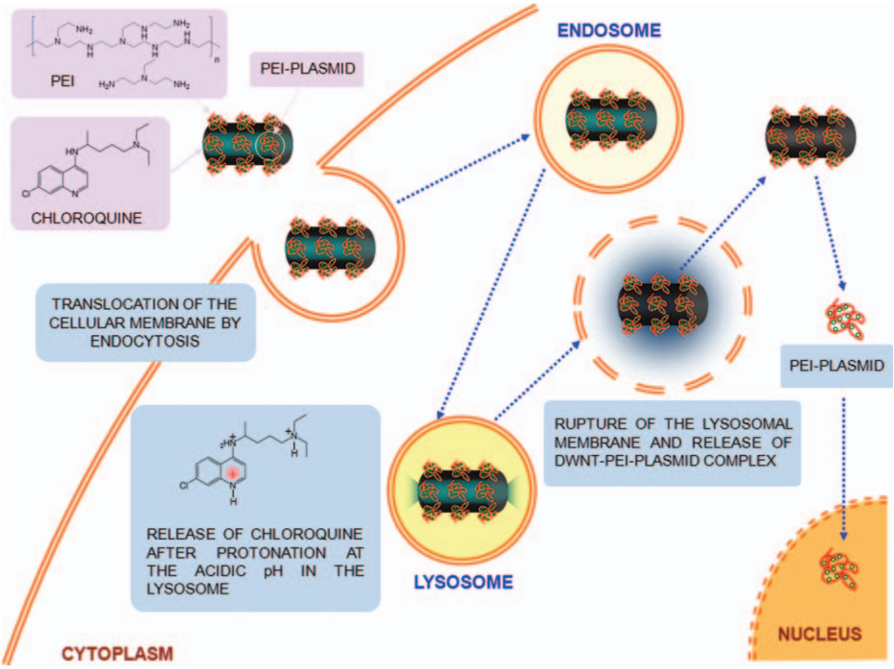
PEI
PEI-PLASMID
CHLOROQUINE
ENDOSOME
TRANSLOCATION OF THE CELLULAR MEMBRANE BY ENDOCYTOSIS
PEI-PLASMID
RUPTURE OF THE LYSOSOMAL MEMBRANE AND RELEASE OF DWNT-PEI-PLASMID COMPLEX
RELEASE OF CHLOROQUINE AFTER PROTONATION AT THE ACIDIC pH IN THE LYSOSOME
LYSOSOME
NUCLEUS
CYTOPLASM

Figure 16.4 Scheme of the intra-cellular trafficking of double-functionalized carbon nanotubes to deliver gene material to the nucleus.
Reproduced from Ref. 96 with permission of Elsevier.

16.5 Toxicity and Environmental Impact of Carbon Nanotubes

Because of the many applications of CNTs, questions are raised about their potential toxicity. Their annual production is now reaching thousands of tons per year, and concerns exist about their safe handling and use by workers. Dissemination in the environment could also happen during different steps of their life cycle, from their production to their processing, use and finally during disposal or recycling. In this section, the state-of-the-art in the field of toxicity and ecotoxicity of carbon nanotubes is revised.

16.5.1 Introduction to Toxicity of Carbon Nanotubes

As the number of industrial applications of CNTs increases constantly with the production capacity at the worldwide level (estimated to be around 4000 tons in 2012, and more than 12,000 in 2016),[97] it is reasonable to ask the question of their potential impact on both human health and the environment. It is important to consider that the number of different kinds of CNTs (SWCNTs, DWCNTs, MWCNTs) and different synthesis routes (arc-discharge, laser ablation, (catalytic) chemical vapor deposition (C-CVD)) make the investigation of the toxicity of CNTs more complex, and comparison of the results already published almost impossible. CNTs are most of the time not found as individual objects but in the form of bundles, or more likely as large micrometric agglomerates. All specimens contain different levels of residual catalyst(s), depending on the synthesis route and purification steps that they may have undergone. Usual purification treatments involve the combination of acids and oxidizing agents, which lead to at least partial functionalization of the outer wall, making the treated samples more hydrophilic. SWCNTs and DWCNTs usually form long and flexible bundles (typically hundreds of micrometers) while MWCNTs are generally shorter (tens of micrometers) and more rigid. MWCNTs also have more surface defects, which enhances their chemical reactivity. The specific surface area of CNTs can range from a few tens of square meters per gram in the case of densely packed MWCNTs to just below 1000 $m^2 g^{-1}$ in the case of SWCNTs and DWCNTs (the theoretical limit being 1300 $m^2 g^{-1}$ in the case of individual closed SWCNTs).[98,99]

Toxicity is generally defined as the degree to which a substance can harm. It can be acute or chronic. Acute toxicity involves harmful effects in an organism through a single or short-term exposure. Chronic toxicity is the ability of a substance or mixture of substances to cause harmful effects over an extended period, usually upon repeated or continuous exposure. Genotoxicity corresponds to alterations of the cell genetic material (DNA); its effects are usually not visible in the short-term range and it is thus an indicator of potential long-term effects (mutagenesis, carcinogenesis). Genotoxicity is a very important indicator for the investigation of the toxicity in general, because it deals with low-dose exposures, at which no toxicity is normally evidenced.

The main exposure routes for dry CNTs are first inhalation and then dermal contact. Ingestion is generally considered to be accidental, although it is in fact more or less related to inhalation because some inhaled particles leave the respiratory system and reach the stomach from the upper airways (*via* the mucociliary escalator). Injection in the bloodstream is envisaged, but would not be accidental (biological applications such as imaging, targeted cell delivery, hyperthermia, *etc*.).

After entry into the body, and depending on the route, migration to other organs could be possible. This would be especially true if the nanoparticles are able to reach the blood circulation. Typical target organs would then be the liver, the spleen and the kidneys, as well as the cardiovascular system in general. It has also been reported that nanoparticles could reach the brain *via* the olfactory nerve,[100] although there is currently no *in vivo* evidence in the case of CNTs. The different routes of exposure and the potential toxicity of CNTs are described below. The ‘‘principle of precaution’’ should be applied, and therefore gloves and a lab coat should be worn at any time as well as an adapted (FFP3 type) disposable dust mask.

16.5.2 Main Characteristics of Carbon Nanotubes in Terms of Toxicity Investigation

CNTs are usually not perfect cylindrical tubes made of pure sp^2 carbon, as they are often pictured. Their shape can vary from short and straight (typical for arc-discharge MWCNTs) to long and flexible (SWCNTs, DWCNTs). Their diameter can range from one nanometer (SWCNTs, DWCNTs) to *ca*. 100 nm (large MWCNTs). They can be individual (rare) or most likely gathered into bundles. The diameter of the bundles can vary from a few nanometers to hundreds of nanometers. Inter-connections between the bundles are very often observed (web-like material). Bundles can agglomerate themselves to form much larger particles. The size and shape of nanoparticles are very important parameters because they will determine the mobility within the body, and the likelihood of being cleared or not (biopersistence): it is well known (and rather intuitive) that fibers are less mobile than spherical particles. In terms of length, macrophages will not manage to eliminate particles longer than them (about a few tens of micrometers for humans, depending on the organ where they are located), leading to what is called frustrated phagocytosis. Since CNTs can be more or less agglomerated, such an agglomeration will also play a role in terms of biological interaction.

The chemical composition of CNTs can vary strongly depending on their purity. Whatever the synthesis technique, they usually still contain some catalyst (typically transition metals, such as Fe, Co or Ni, as well as other additives, including Y, Mo, S, *etc*.). The amount of residual catalyst can vary from a few tens of wt. % in as-prepared materials to a few ppm in highly purified CNTs. In purified samples, it is generally assumed that the residual catalyst is encapsulated in graphitized shells or within the CNTs and cannot

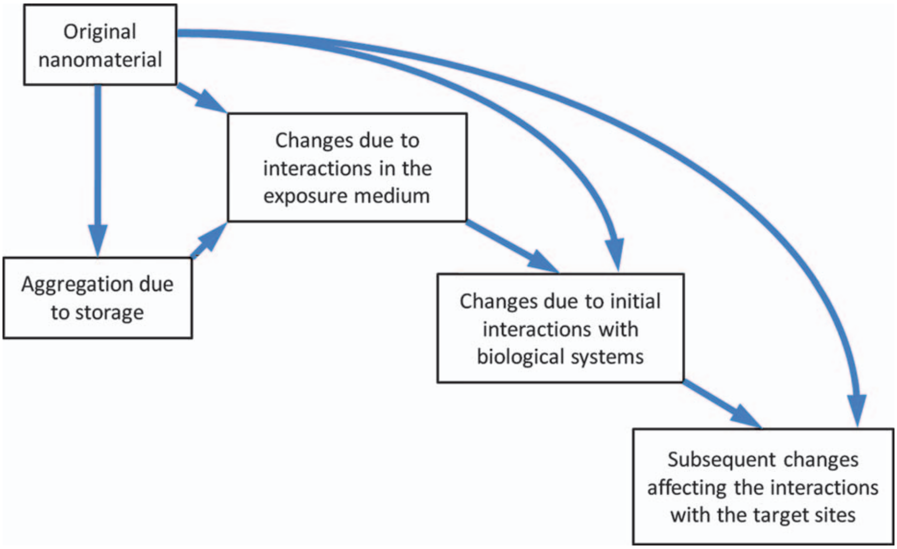
Original nanomaterial
Changes due to interactions in the exposure medium
Aggregation due to storage
Changes due to initial interactions with biological systems
Subsequent changes affecting the interactions with the target sites

Figure 16.5 Potential modifications of particles due to interactions with the environment.
Adapted from Ref. 103.

directly interact with the environment.[101,102] The presence of such metals can favor the production of free radicals such as reactive oxygen species (ROS), which can themselves modulate different biological functions.

Other parameters such as the specific surface area and the surface chemistry are also very important; for the same weight of CNTs, the available surface can vary strongly. Functionalization of CNTs can be deliberate – for example, in the case of targeted delivery, or to stabilize a suspension by addition of surfactants– or not – when it occurs during purification – and will control the interface with biological environments, because of the resulting surface charge or modification of wettability, for example. The interactions of the CNTs with their local environment may vary with time and will subtly affect the interaction with the target sites (Figure 16.5).[103]

In the case of the toxicity of nanoparticles, the relevant unit to quantify the exposure is probably the number of particles, and not the weight or even not the specific surface area. A simple comparison between MWCNTs and SWCNTs shows that the same weight of material can correspond to very different amounts of individual objects.[104]

16.5.3 Biological Models

Toxicity can be assessed by means of both *in vitro* and *in vivo* experiments. In the case of *in vitro* assays, cell cultures, usually immortalized cancer cells, but also primary cultures or even stem cells, are exposed to suspensions of CNTs. The way the suspension is prepared (with or without addition of a surfactant, dispersion by sonication with a bath or a tip, *etc.*) and exposed to the cells is very important. In the case of *in vivo* assays, the animals (mice, rats, worms, amphibians, fishes, *etc.*) are exposed either to aerosols (inhalation) or mainly to suspensions of CNTs, which will be administrated according to different protocols depending on the study (intra-tracheal instillation, injection, contact with the skin, *etc.*). It must be noted that the transposition of the toxicity results from animals (or even worse from cells) to humans is very delicate, but the data are, however, very useful for the sake of comparison in a given system and with given experimental conditions. As an example, it is sometimes even difficult to transpose from rats to mice.

In the case of suspensions, the main issue concerns their stability. This question has been widely studied worldwide and the general approach is the addition of a surfactant in order to stabilize the CNTs in the liquid. The main problem is that all commonly used surfactants are toxic to a certain extent and thus cannot be used in the presence of living cells or animals for *in vitro* or *in vivo* investigations, or must be used at such low concentrations that they do not really play anymore the role there are supposed to play. Although a few natural surfactants such as proteins,[105] starch,[106] gum arabic[107] or sugar derivatives[108] have been investigated, the stability of the suspensions in the presence of living organisms is often very different (fast destabilization leading to flocculation). It is also extremely important to keep in mind that when nanoparticles eventually reach the target cells, their surface is very likely to be rather different from what it was initially, due to the unpredictable adsorption of many biological compounds (proteins) all along the way: in the end, what the cells see can be very different from the initial bare surface of the starting nanoparticle.[109]

16.5.4 Inhalation

Among respiratory tract cells, the lung (alveolar) cells are the most studied. Only one paper has been published so far about the *in vivo* impact on the nose.[110] The target respiratory cells in the lungs are the epithelial cells and the macrophages. In particular, epithelial cells provide a selective and permeable interface between the lumen and the underlying tissue, for exchange of gases and other molecules. The intra-tracheal instillation of mice with suspensions of SWCNTs, purified or not,[111] led to an inflammatory response in the alveolar area. Granuloma (spheroidal accumulation of immune cells trying to destroy a foreign substance) were observed after 90 days of exposure due to frustrated phagocytosis, *i.e.* impossibility for the macrophages to destroy or remove the CNTs. Similar observations were reported (still with SWCNTs), but the granuloma vanished after three months.[112] The influence of the length of the CNTs was investigated and it was shown, in the case of MWCNTs, that the shorter the length the better the distribution in the lungs.[113] Recent studies have compared CNTs and asbestos because of the well known "fiber paradigm" in pulmonary toxicology: fibers that are long (longer than the cells of the lung, which usually get rid of fibers and other dusts – that is, usually longer than about 15 μm), thin (thin enough to enter the lungs – less than about 5 μm) and biopersistent in the lungs are likely to lead to mesothelioma. Poland *et al.*[21] have used peritoneal injection to compare the effect of different kinds of MWCNTs (different diameters, different lengths) with amosite, a known pathogenic form of asbestos. The results suggest that long and straight MWCNTs may be pathogenic in the same manner as amosite, but the small number of animals used in this study (three) may moderate the conclusions, although this model was commonly used in the case of asbestos. Recent publications by the same authors suggest that CNTs shorter than *ca.* 5 μm would be safe, as they could escape the lung through the stomata of the parietal pleura and thus be evacuated.[114] In another study involving mesothelial cell cultures, it was also shown that non-purified SWCNTs induced the activation of molecular pathways associated with oxidative stress,[115] similarly to asbestos. In this case, it can clearly be questioned whether the oxidative stress came from the CNTs themselves or from residual catalyst.[116]

16.5.5 Contamination through the Skin

It is generally admitted that nanoparticles do not cross a healthy dermis and may only accumulate in the upper layers of the epidermis, although they may reach the dermis along hair follicles.[117] Only a few examples of skin penetration are available (case of Ag nanoparticles),[118] but none refer to CNTs. *In vitro* cytotoxicity of CNTs *vs.* keratinocytes was, however, shown.[119] Oxidative stress, alterations of cellular membrane, internalization and production of pro-inflammatory cytokines were also described after *in vitro* exposure of human epidermal keratinocytes to MWCNTs.[120]

16.5.6 Translocation

After the CNTs have entered the body, they could travel following different routes depending on the entry point (movements from one organ to another are referred to as translocation) but also mainly on their physico-chemical characteristics. The main route for translocation is *via* the bloodstream. Objects recognized as non-self by the immune system usually end up in the liver or the kidneys if they can be transported there, and could possibly be excreted (eliminated) from the body. In the general case, CNTs will just accumulate (biopersistence) if they cannot be excreted.

16.5.7 Mechanisms of Protection and Elimination

Foreign particles are usually intercepted by macrophages; namely, cells present in all tissues, the role of which is to phagocytose (engulf and then digest) cellular debris and pathogens, as well as to stimulate lymphocytes and other immune cells to respond to the pathogens. Taking into account the small size of macrophages as compared to that of CNTs aggregates, bundles or even individual CNTs, macrophages usually do not manage to get rid of the CNTs by phagocytosis. However, they try to do so and thus release reactive oxygen species (ROS), enzymes, cytokines (interferons), *etc.* and agglomerate around them to isolate them from the body. Mechanisms involved in the inflammatory response by macrophages have been described recently.[121] Proteins present in the blood and most biological fluids (complement system – innate immunity) play a similar role by "labeling" the CNTs (opsonization)[122] and possibly generating some inflammation reactions. The complement system strongly interacts with the leukocytes. These natural phenomena have deleterious consequences on the surrounding tissues: inflammation in the first instance and, often, formation of granuloma (commonly observed in the lungs after exposure to CNTs). Each target organ has its own phagocytic cells (Kupffer cells in the liver, Langerhans cells in the skin, *etc.*).

As soon as CNTs are in contact with a biological fluid, their surface chemistry is likely to be modified very quickly by adsorption of proteins (complement system,[122] surfactants,[123] *etc.*[109]); this adsorption can be very specific[122,123] and is likely to be dynamic and subject to affinity of the molecules for the surface of the CNTs (pristine or functionalized). It is thus obvious that the surface chemistry of the CNTs plays a very important role.

16.5.8 Genotoxicity

Genotoxicity deals with gene alterations and mutations, and corresponds to the "hidden risk" during classical toxicity investigations because the consequences (mutagenic, carcinogenic effects) only appear after a long period of time and are thus not observed during the assay. Genotoxicity was only scarcely investigated in the case of human studies. A few papers by Muller *et al.*, however, suggest a potential genotoxicity of MWCNTs and report chromosomal alterations in human epithelial cells[124] or the observation of micronuclei after exposure of rat liver epithelial cells (immortalized).[125] In the latter case, it was shown that the chemical purity of the MWCNTs specimens played an important role. Therefore purification and shortening strategies that preserve the tubular structure of the CNTs with a low degree of structural defects are needed.[102,126] Recent publications also confirm the potential genotoxicity of CNTs.[127,128]

16.5.9 Environmental Impact of Carbon Nanotubes

The potential use of CNTs in commercial products (*e.g.* sports equipment such as tennis rackets, baseball bats or bikes, flat-screen displays, additives in tires and automobile industry) begs the question of their fate at the end of their life cycle. If the impact of CNTs on human health has been under investigation already for a few years now, it is noteworthy that the environmental impact has almost not been taken into account at all. Only a few publications are currently available. A few studies on different aquatic organisms exposed to CNTs are available: aquatic worms exposed to SWCNTs,[129] estuarine copepods exposed to SWCNTs,[130] freshwater crustaceans (*Daphnia magna*) exposed to functionalized SWCNTs,[131] cladocerans and amphipods exposed to raw and oxidized MWCNTs,[132] zebrafish embryos (*Danio rerio*) exposed to SWCNTs and DWCNTs,[133] trout exposed to dispersed SWCNTs in the presence of a surfactant[134] and amphibian larvae (*Ambystoma mexicanum*, *Xenopus laevis*) exposed to DWCNTs.[135,136] In the last case, no genotoxic effects could be observed. The influence of CNTs on marine species has only scarcely been investigated[137] since seawater is a more complex environment, and the presence of dissolved salts is not in favor of proper dispersion of CNTs. All of these studies indicate that exposure to CNTs leads to biological disorders at different levels, usually from or above 10 mg L^{-1}, which is much higher than what could be reasonably found in the environment (or this could only be very localized, and accidental).[138] To minimize the environmental impact CNTs wastes should be burnt. Due to the potentially very high specific surface area of CNTs, they could act as vectors for pollutants adsorbed on their surface, such as polycyclic aromatic hydrocarbons (PAH), ions, *etc.*, even if they themselves do not show any significant sign of toxicity.

16.6 Conclusions

Although the development of carbon nanotubes as DDSs is still in its infancy, their potential to improve the performance of "free" drugs has been highlighted with several examples through this chapter. Both *in vitro* and *in vivo* studies reveal that the delivery of a chosen payload with carbon nanotubes results in an enhanced therapeutic effect and/or in a reduced toxicity of the therapeutically active molecule. The tubular shape of CNTs allows the delivery of biomolecules *via* two complementary approaches, namely by anchoring the drug to the external sidewall through either covalent or non-covalent functionalization, and by encapsulating the chosen payload into the inner cavity. There is currently no consensus about the toxicity of CNTs, although *ca.* 1700 papers have already been published on this topic within only the last eight years. Despite the worldwide effort devoted to this field of research, the huge variety of CNTs types, shapes, compositions, sizes, surface functionalizations, *etc.* make it very difficult to answer this simple question: "are CNTs toxic?" The "principle of precaution" should not stop all research in this area, but only draw the attention to a more responsible attitude for people working on their synthesis or manipulating them, and industrials willing to include them in consumer products.

References

1. S. Iijima, *Nature*, 1991, **354**, 56.
2. S. Iijima and T. Ichihashi, *Nature*, 1993, **363**, 603.
3. R. Saito, G. Dresselhaus and M. S. Dresselhaus, *Physical Properties of Carbon Nanotubes*, Imperial College Press, London, 1998.

4. D. M. Guldi and N. Martín, *Carbon Nanotubes and Related Structures: Synthesis, Characterization, Functionalization and Applications*, Wiley-VCH, Berlin, 2010.
5. A. Hirsch and O. Vostrowsky, *Top. Curr. Chem.*, 2005, **245**, 193.
6. D. Tasis, N. Tagmatarchis, A. Bianco and M. Prato, *Chem. Rev.*, 2006, **106**, 1105.
7. N. Karousis, N. Tagmatarchis and D. Tasis, *Chem. Rev.*, 2010, **110**, 5366.
8. M. Prato, K. Kostarelos and A. Bianco, *Acc. Chem. Res.*, 2007, **41**, 60.
9. G. Tobias, E. Mendoza and B. Ballesteros, in *Encyclopedia of Nanotechnology*, ed. B. Bhushan, Springer, Heidelberg, 2012, Part 7, p. 911.
10. K. Kostarelos, *Nat. Biotech.*, 2008, **26**, 774.
11. Z. Liu, S. Tabakman, K. Welsher and H. Dai, *Nano Res.*, 2009, **2**, 85.
12. D. A. Heller, S. Baik, T. E. Eurell and M. S. Strano, *Adv. Mater.*, 2005, **17**, 2793.
13. A. M. Rao, E. Richter, S. Bandow, B. Chase, P. C. Eklund and K. A. Williams, *Science*, 1997, **275**, 187.
14. Y. Xiao, X. Gao, O. Taratula, S. Treado, A. Urbas and R. D. Holbrook, *BMC Cancer*, 2009, **9**, 351.
15. P. Cherukuri, S. M. Bachilo, S. H. Litovsky and R. B. Weisman, *J. Am. Chem. Soc.*, 2004, **126**, 15638.
16. M. J. O'Connell, S. M. Bachilo, C. B. Huffman, V. C. Moore, M. S. Strano, E. H. Haroz, K. L. Rialon, P. J. Boul, W. H. Noon and C. Kittrell, *Science*, 2002, **297**, 593.
17. K. Welsher, Z. Z. Liu, D. D and H. Dai, *Nano Lett.*, 2008, **8**, 586.
18. A. D. L. Zerda, C. Zavaleta, S. Keren, S. Vaithilingam, S. Bodapati and Z. Liu, *Nat. Nanotechnol.*, 2008, **3**, 557.
19. P. Chakravarty, R. Marches, N. S. Zimmerman, A. D. E. Swafford, P. Bajaj, I. H. Musselman, P. Pantano, R. K. Draper and E. S. Vitetta, *P. Natl Acad. Sci. USA*, 2008, **105**, 8697.
20. N. W. S. Kam, M. O'Connell, J. A. Wisdom and H. Dai, *P. Natl Acad. Sci. USA*, 2005, **102**, 11600.
21. C. A. Poland, R. Duffin, I. Kinloch, A. Maynard, W. A. H. Wallace, A. Seaton, V. Stone, S. Brown, W. MacNee and K. Donaldson, *Nat. Nanotechnol.*, 2008, **3**, 423.
22. Y. Zhang, Y. Bai and B. Yan, *Drug Discov. Today*, 2010, **15**, 428.
23. A. Kuznetsova, I. Popova, J. T. Yates, M. J. Bronikowski, C. B. Huffman, J. Liu, R. E. Smalley, H. H. Hwu and J. G. Chen, *J. Am. Chem. Soc.*, 2001, **123**, 10699.
24. L. Shao, G. Tobias, C. G. Salzmann, B. Ballesteros, S. Y. Hong, A. Crossley, B. G. Davis and M. L. H. Green, *Chem. Commun.*, 2007, 5090.
25. S. Y. Hong, G. Tobias, B. Ballesteros, F. El Oualid, J. C. Errey, K. J. Doores, A. I. Kirkland, P. D. Nellist, M. L. H. Green and B. G. Davis, *J. Am. Chem. Soc.*, 2007, **129**, 10966.
26. M. S. Strano, V. C. Moore, M. K. Miller, M. J. Allen, E. H. Haroz, C. Kittrell, R. H. Hauge and R. E. Smalley, *J. Nanosci. Nanotechnol.*, 2003, **3**, 81.

27. D. A. Britz and A. N. Khlobystov, *Chem. Soc. Rev.*, 2006, **35**, 637.
28. G. Pastorin, *Pharm. Res.*, 2009, **26**, 746.
29. S. K. Vashist, D. Zheng, G. Pastorin, K. Al-Rubeaan, J. H. T. Luong and F. S. Sheu, *Carbon*, 2011, **49**, 4077.
30. Y. Rosen and N. M. Elman, *Expert Op. Drug Deliver.*, 2009, **6**, 517.
31. A. M. A. Elhissi, W. Ahmed, I. U. Hassan, V. R. Dhanak and A. D'Emanuele, *J. Drug Deliv.*, 2012, **2012**, 837327.
32. Z. Liu, X. Li, S. M. Tabakman, K. Jiang, S. Fan and H. Dai, *J. Am. Chem. Soc.*, 2008, **130**, 13540.
33. M. R. McDevitt, D. Chattopadhyay, B. J. Kappel, J. S. Jaggi, S. R. Schiffman, C. Antczak, J. T. Njardarson, R. Brentjens and D. A. Scheinberg, *J. Nucl. Med.*, 2007, **48**, 1180.
34. S. Dhar, Z. Liu, J. Thomale, H. Dai and S. J. Lippard, *J. Am. Chem. Soc.*, 2008, **130**, 11467.
35. Z. Liu, W. B. Cai, L. N. He, N. Nakayama, K. Chen, X. M. Sun, X. Y. Chen and H. J. Dai, *Nat. Nanotechnol.*, 2007, **2**, 47.
36. Z. Liu, X. Sun, N. Nakayama and H. Dai, *ACS Nano*, 2007, **1**, 50.
37. J. Nadas and D. Sun, *Expert Op. Drug Discov.*, 2006, **1**, 549.
38. H. Ali-Boucetta, K. T. Al-Jamal, D. McCarthy, M. Prato, A. Bianco and K. Kostarelos, *Chem. Commun.*, 2008, 459.
39. X. Zhang, L. Meng, Q. Lu, Z. Fei and P. J. Dyson, *Biomaterials*, 2009, **30**, 6041.
40. E. Heister, V. Neves, C. Lamprecht, S. R. P. Silva, H. M. Coley and J. McFadden, *Carbon*, 2012, **50**, 622.
41. L. J. Meng, X. K. Zhang, Q. H. Lu, Z. F. Fei and P. J. Dyson, *Biomaterials*, 2012, **33**, 1689.
42. R. Li, R. Wu, L. Zhao, Z. Hu, S. Guo and X. Pan, *Carbon*, 2011, **49**, 1797.
43. E. Heister, V. Neves, C. Tîlmaciu, K. Lipert, V. S. Beltrán and H. M. Coley, *Carbon*, 2009, **47**, 2152.
44. G. Szakács, J. K. Paterson, J. A. Ludwig, C. Booth-Genthe and M. M. Gottesman, *Nat. Rev. Drug Discov.*, 2006, **5**, 219.
45. D. Wang and S. J. Lippard, *Nat. Rev. Drug Discov.*, 2005, **4**, 307.
46. J. Lokich, *Cancer Invest.*, 2001, **19**, 756.
47. R. P. Feazell, N. Nakayama-Ratchford, H. Dai and S. J. Lippard, *J. Am. Chem. Soc.*, 2007, **129**, 8438.
48. E. Wong and C. M. Giandomenico, *Chem. Rev.*, 1999, **99**, 2451.
49. A. A. Bhirde, V. Patel, J. Gavard, G. Zhang, A. A. Sousa and A. Masedunskas, *ACS Nano*, 2009, **3**, 307.
50. N. H. Levi-Polyachenko, E. J. Merkel, B. T. Jones, D. L. Carroll and J. H. S. Iv, *Mol. Pharmaceut.*, 2009, **6**, 1092.
51. G. Pastorin, W. Wu, S. Wieckowski, J. P. Briand, K. Kostarelos and M. Prato, *Chem. Commun.*, 2006, 1182.
52. J. Swierkot and J. Szechinski, *Pharmacol. Rep.*, 2006, **58**, 473.
53. C. Samori, H. Ali-Boucetta, R. Sainz, C. Guo, F. M. Toma and C. Fabbro, *Chem. Commun.*, 2010, 1494.
54. N. H. Oberlies and D. J. Kroll, *J. Nat. Prod.*, 2004, **167**, 129.

55. Z. Liu, K. Chen, C. Davis, S. Sherloc, Q. Cao, X. Chen and H. Dai, *Cancer Res*., 2008, **68**, 6652.
56. J. Chen, S. Chen, X. Zhao, L. V. Kuznetsova, S. S. Wong and I. Ojima, *J. Am. Chem. Soc*., 2008, **130**, 16778.
57. W. D. Bradner, *Cancer Treat. Rev*., 2001, **27**, 35.
58. Y. Pommier, *Nat. Rev. Cancer*, 2006, **6**, 789.
59. Z. Chen, D. Pierre, H. He, S. Tan, C. Pham-Huy and H. Hong, *Int. J. Pharm*., 2011, **405**, 153.
60. M. Kleinberg, *Int. J. Antimicrob. Agents*, 2006, **27**, S12.
61. W. Wu, S. Wieckowski, G. Pastorin, M. Benincasa, C. Klumpp and J. P. Briand, *Angew. Chem., Int. Ed*., 2005, **44**, 6358.
62. S. Naficy, J. M. Razal, G. M. Spinks and G. G. Wallace, *Sens. Actuators A*, 2009, **155**, 120.
63. J. S. Im, B. C. Bai and Y. S. Lee, *Biomaterials*, 2010, **31**, 1414.
64. G. D. Vukovic, S. Z. Tomic, A. D. Marinkovic, V. Radmilovic, P. S. Uskokovic and M. Colic, *Carbon*, 2010, **48**, 3066.
65. T. Rhen and J. A. Cidlowski, *N. Engl. J. Med*., 2005, **353**, 1711.
66. E. D. Roberson and L. Mucke, *Science*, 2006, **314**, 781.
67. Z. Yang, Y. Zhang, Y. Yang, L. Sun, D. Han and H. Li, *Nanomedicine NMB*, 2010, **6**, 427.
68. X. Zhang, Z. Hui, D. Wan, H. Huang, J. Huang and H. Yuan, *Int. J. Biol. Macromol*., 2010, **47**, 389.
69. Y. Li, T. Wang, J. Wang, T. Jiang, G. Cheng and S. Wang, *Appl. Surf. Sci*., 2011, **257**, 5663.
70. M. R. Pederson and J. Q. Broughton, *Phys. Rev. Lett*., 1992, **69**, 2689.
71. J. Sloan, J. Hammer, M. Zwiefka-Sibley and M. L. H. Green, *Chem. Commun*., 1998, 347.
72. B. W. Smith, M. Monthioux and D. E. Luzzi, *Nature*, 1998, **396**, 323.
73. R. R. Meyer, J. Sloan, R. E. Dunin-Borkowski, A. I. Kirkland, M. C. Novotny, S. R. Bailey, J. L. Hutchison and M. L. H. Green, *Science*, 2000, **289**, 1324.
74. T. Takenobu, T. Takano, M. Shiraishi, Y. Murakami, M. Ata, H. Kataura, Y. Achiba and Y. Iwasa, *Nat. Mater*., 2003, **2**, 683.
75. J. Y. Chen, A. Kutana, C. P. Collier and K. P. Giapis, *Science*, 2005, **310**, 1480.
76. K. Koga, G. T. Gao, H. Tanaka and X. C. Zeng, *Nature*, 2001, **412**, 802–805.
77. J. Lee, H. Kim, S. J. Kahng, G. Kim, Y. W. Son, J. Ihm, H. Kato, Z. W. Wang, T. Okazaki, H. Shinohara and Y. Kuk, *Nature*, 2002, **415**, 1005.
78. M. Wilson, *Nano Lett*., 2004, **4**, 299.
79. M. Koshino, T. Tanaka, N. Solin, K. Suenaga, H. Isobe and E. Nakamura, *Science*, 2007, **316**, 853.
80. B. Sitharaman, K. R. Kissell, K. B. Hartman, L. A. Tran, A. Baikalov, I. Rusakova, Y. Sun, H. A. Khant, S. J. Ludtke, W. Chiu, S. Laus, E. Tóth, L. Helm, A. E. Merbach and L. J. Wilson, *Chem. Commun*., 2005, 3915.

81. J. M. Ashcroft, K. B. Hartman, K. R. Kissell, Y. Mackeyev, S. Pheasant, S. Young, P. A. W. V. d. Heide, A. G. Mikos and L. J. Wilson, *Adv. Mater.*, 2007, **19**, 573.
82. S. Y. Hong, G. Tobias, K. T. Al-Jamal, B. Ballesteros, H. Ali-Boucetta, S. Lozano-Perez, P. D. Nellist, C. Finucane, S. J. Mather, M. L. H. Green, K. Kostarelos and B. G. Davis, *Nat. Mater.*, 2010, **9**, 485.
83. A. Vyalikh, A. U. B. Wolter, S. Hampel, D. Haase, M. Ritschel, A. Leonhardt, H. J. Grafe, A. Taylor, K. Krämer, B. Büchner and R. Klingeler, *Nanomedicine UK*, 2008, **3**, 321.
84. T. A. Hilder and J. M. Hill, *Nanotechnology*, 2007, **27**, 275704.
85. C. Tripisciano, K. Kraemer, A. Taylor and E. Borowiak-Palen, *Chem. Phys. Lett.*, 2009, **478**, 200.
86. A. Guven, I. A. Rusakova, M. T. Lewis and L. J. Wilson, *Biomaterials*, 2012, **33**, 1455.
87. J. Li, S. Q. Yap, S. L. Yoong, T. R. Nayak, G. W. Chandra, W. H. Ang, T. Panczyk, S. Ramaprabhu, S. K. Vashist, F. S. Sheu, A. Tan and G. Pastorin, *Carbon*, 2012, **50**, 1625.
88. S. Hampel, D. Kunze, D. Haase, K. Krämer, M. Rauschenbach and M. Ritschel, *Nanomedicine UK*, 2008, **3**, 175.
89. L. Shao, T. W. Lin, G. Tobias and M. L. H. Green, *Chem. Commun.*, 2008, 2164.
90. Y. Ren and G. Pastorin, *Adv. Mater.*, 2008, **20**, 2031.
91. P. Luksirikul, B. Ballesteros, G. Tobias, M. G. Moloney and M. L. H. Green, *Carbon*, 2010, **48**, 1912.
92. H. Ulbricht, G. Moos and T. Hertel, *Phys. Rev. Lett.*, 2003, **90**, 095501.
93. F. Simon, H. Peterlik, R. Pfeiffer, J. Bernardi and H. Kuzmany, *Chem. Phys. Lett.*, 2007, **445**, 288.
94. J. Fan, M. Yudasaka, R. Yuge, D. N. Futaba, K. Hata and S. Iijima, *Carbon*, 2007, **45**, 722.
95. V. V. Chaban and O. V. Prezhdo, *ACS Nano*, 2011, **5**, 5647.
96. V. Sanz, C. Tilmacaru, B. Soula, E. Flahaut, H. M. Coley, S. R. P. Silva and J. McFadden, *Carbon*, 2011, **49**, 5348.
97. http://www.nanowerk.com/spotlight/spotid=23118.php, accessed May, 2012.
98. E. Flahaut, R. Bacsa, A. Peigney and C. Laurent, *Chem. Commun.*, 2003, 1442.
99. A. Peigney, C. Laurent, E. Flahaut, R. R. Bacsa and A. Rousset, *Carbon*, 2001, **39**, 507.
100. G. Oberdorster, Z. Sharp, V. Atudorei, A. Elder, R. Gelein, W. Kreyling and C. Cox, *Inhal. Toxicol.*, 2004, **16**, 437.
101. E. Flahaut, F. Agnoli, J. Sloan, C. O'Connor and M. L. H. Green, *Chem. Mater.*, 2002, **14**, 2553.
102. B. Ballesteros, G. Tobias, L. Shao, E. Pellicer, J. Nogués, E. Mendoza and M. L. H. Green, *Small*, 2008, **4**, 1501.

103. SCENIHR (Scientific Committee on Emerging and Newly Identified Health Risks), *Risk assessment of products of nanotechnologies*, European Commission, Brussels, 2009.
104. C. Laurent, E. Flahaut and A. Peigney, *Carbon*, 2010, **48**, 2994.
105. V. Zorbas, A. Ortiz-Acevedo, A. Dalton, M. M. Yoshida, G. R. Dieckmann, R. K. Draper, R. H. Baughman, M. Jose-Yacaman and I. H. Musselman, *J. Am. Chem. Soc.*, 2004, **126**, 7222.
106. A. Star, D. W. Steuerman, J. R. Heath and J. F. Stoddart, *Angew. Chem., Int. Ed.*, 2002, **41**, 2508.
107. R. Bandyopadhyaya, E. Nativ-Roth, O. Regev and R. Yerushalmi-Rozen, *Nano Lett.*, 2002, **2**, 25.
108. V. Datsyuk, P. Landois, J. Fitremann, A. Peigney, A. M. Galibert, B. Soula and E. Flahaut, *J. Mater. Chem.*, 2009, **19**, 2729.
109. A. E. Nel, L. Mädler, D. Velegol, T. Xia, E. M. V. Hoek, P. Somasundaran, F. Klaessig, V. Castranova and M. Thompson, *Nat. Mater.*, 2009, **8**, 543.
110. L. D. Gabory, R. Bareille, R. Daculsi, B. L'Azou, E. Flahaut and L. Bordenave, *Rhinology*, 2011, **49**, 45.
111. C. W. Lam, J. T. James, R. McCluskey and R. L. Hunter, *Toxicol. Sci.*, 2004, **77**, 126.
112. D. B. Warheit, B. R. Laurence, K. L. Reed, D. H. Roach, G. A. Reynolds and T. R. Webb, *Toxicol. Sci.*, 2004, **77**, 117.
113. J. Muller, F. Huaux, N. Moreau, P. Misson, J. F. Heilier, M. Delos, M. Arras, A. Fonseca, J. B. Nagy and D. Lison, *Toxicol. Appl. Pharmacol.*, 2005, **207**, 221.
114. K. Donaldson, F. Murphy, A. Schinwald, R. Duffin and C. A. Poland, *Nanomedicine UK*, 2011, **6**, 143.
115. M. Pacurari, X. J. Yin, J. Zhao, M. Ding, S. S. Leonard, D. Schwegler-Berry, B. S. Ducatman, D. Sbarra, M. D. Hoover, V. Castranova and V. Vallyathan, *Environ. Health Persp.*, 2008, **116**, 1211.
116. V. E. Kagan, Y. Y. Tyurina, V. A. Tyurin, N. V. Konduru, A. I. Potapovich, A. N. Osipov, E. R. Kisin, D. Schwegler-Berry, R. Mercer, V. Castranova and A. A. Shvedova, *Toxicol. Lett.*, 2006, **165**, 88.
117. J. Lademann, H. Weigmann, C. Rickmeyer, H. Barthelmes, H. Schaefer, G. Mueller and W. Sterry, *Skin Pharmacol. Appl. Skin Physiol.*, 1999, **12**, 247.
118. F. F. Larese, F. D'Agostin, M. Crosera, G. Adami, N. Renzi and M. Bovenzi, *Toxicology*, 2009, **255**, 33.
119. A. R. Murray, E. Kisin, S. S. Leonard, S. H. Young, C. Kommineni, V. E. Kagan, V. Castranova and A. A. Shvedova, *Toxicology*, 2009, **257**, 161.
120. N. A. Monteiro-Rivier, R. J. Nemanich, A. O. Inman, Y. Y. Wang and J. E. Riviere, *Toxicol. Lett.*, 2005, **155**, 377.
121. E. Meunier, A. Coste, D. Olagnier, H. Authier, L. Lefèvre, C. Dardenne, E. Flahaut and B. Pipy, *Nanomedicine NMB*, 2012, 8, 987.

122. C. Salvador-Morales, E. Flahaut, E. Sim, J. Sloan, M. L. H. Green and R. B. Sim, *Mol. Immunol.*, 2006, **43**, 193.
123. C. Salvador-Morales, P. Townsend, E. Flahaut, C. Venienbryan, A. Vlandas and M. L. H. Green, *Carbon*, 2007, **45**, 607.
124. J. Muller, I. Decordier, P. H. Hoet, N. Lombaert, L. Thomassen, F. Huaux, D. Lison and M. Kirsch-Volders, *Carcinogenesis*, 2008, **29**, 427.
125. J. Muller, F. Huaux, A. Fonseca, J. B. Nagy, N. Moreau, M. Delos, E. Raymundo-Piñero, F. Béguin, M. Kirsch-Volders, I. Fenoglio, B. Fubini and D. Lison, *Chem. Res. Toxicol.*, 2008, **21**, 1698.
126. G. Tobias, L. Shao, C. G. Salzmann, Y. Huh and M. L. H. Green, *J. Phys. Chem. B*, 2006, **110**, 22318.
127. H. K. Lindberg, G. C. M. Falck, S. Suhonen, M. Vippola, E. Vanhala, J. Catalán, K. Savolainen and H. Norppa, *Toxicol. Lett.*, 2009, **186**, 166.
128. M. Naya, N. Kobayashi, K. Mizuno, K. Matsumoto, M. Ema and J. Nakanishi, *Regul. Toxicol. Pharmacol.*, 2011, **61**, 192.
129. E. Petersen, Q. Huang and W. Weber, *Environ. Health Persp.*, 2008, **116**, 496.
130. R. C. Templeton, P. L. Ferguson, K. M. Washburn, W. A. Scrivens and G. T. Chandler, *Environ. Sci. Technol.*, 2006, **40**, 7387.
131. A. P. Roberts, A. S. Mount, B. Seda, J. Souther, R. Qiao, S. Lin, P. C. Ke, A. M. Rao and S. J. Klaine, *Environ. Sci. Technol.*, 2007, **41**, 3025.
132. A. J. Kennedy, M. S. Hull, J. A. Steevens, K. M. Dontsova, M. A. Chappell, J. C. Gunter and C. A. Weiss, *Environ. Toxicol. Chem.*, 2008, **27**, 1932.
133. J. Cheng, E. Flahaut and S. Cheng, *Environ. Toxicol. Chem.*, 2007, **26**, 708.
134. C. Smith, B. Shaw and R. Handy, *Aquat. Toxicol.*, 2007, **82**, 94.
135. F. Mouchet, P. Landois, E. Flahaut, E. Pinelli and L. Gauthier, *Nanotoxicology*, 2007, **1**, 149.
136. F. Mouchet, P. Landois, E. Sarremejean, G. Bernard, P. Puech, E. Pinelli, E. Flahaut and L. Gauthier, *Aquat. Toxicol.*, 2008, **87**, 127.
137. K. W. Kwok, K. M. Leung, E. Flahaut, J. Cheng and S. H. Cheng, *Nanomedicine UK*, 2010, **5**, 951.
138. F. Gottschalk, T. Sonderer, R. W. Scholz and B. Nowack, *Environ. Sci. Technol.*, 2009, **43**, 9216.

CHAPTER 17

Smart Layer-by-Layer Assemblies for Drug Delivery

SVETLANA PAVLUKHINA AND
SVETLANA SUKHISHVILI*

Department of Chemistry, Chemical Biology and Biomedical Engineering,
Stevens Institute of Technology, Hoboken, NJ 07030, USA
*Email: ssukhish@stevens.edu

17.1 Introduction

Localized drug delivery can significantly enhance treatment effectiveness, while reducing adverse reaction and systemic toxicity effects. Layer-by-layer (LbL) assemblies provide an ideal, versatile platform for constructing novel systems to achieve such localized drug delivery.[1–4] Importantly, LbL constructs can support both prolonged release of functional compounds, as well as stimuli-responsive, on-demand delivery. A combination of these functions becomes highly desirable for designing novel drug-delivery systems. While our recent review concerned delivery of biologically active molecules from LbL films, *i.e.* from 2D matrices,[3] this chapter focuses on the progress made within the last 3–4 years in development of LbL-based delivery systems with both 2D and 3D geometries.

17.2 LbL Substrates and Templates

An important feature of the LbL technique is its ability to create conformal coatings on planar or colloidal substrates of virtually any shape and surface

---

RSC Smart Materials No. 3
Smart Materials for Drug Delivery: Volume 2
Edited by Carmen Alvarez-Lorenzo and Angel Concheiro
© The Royal Society of Chemistry 2013
Published by the Royal Society of Chemistry, www.rsc.org

chemistry.[5] Planar, low-roughness substrates are usually used as model surfaces during exploration of fundamentals of LbL film construction, such as film composition, thickness and morphology. Examples of the most commonly used planar substrates include silicon wafers, glass, quartz, gold and mica. In the case of biomedical implant devices, surfaces of titanium or titanium alloys can also be considered locally flat. The charge of the surfaces determines the possibility of film deposition and growth.[6,7] If a specific LbL system cannot be directly deposited on a substrate, the surface can be pretreated with a precursor layer. This treatment takes advantage of the fact that many solid surfaces are negatively charged and enable adsorption of polycations, such as poly(ethylene imine) (PEI). Moreover, the use of polyelectrolytes grafted onto a planar inorganic substrate with different chain conformations as a template for depositing polyelectrolyte multilayers (PEMs) may be promising for creation of nanoscale patterns in the resulting multilayer films.[8]

Deposition of LbL films on colloidal substrates was demonstrated more than a decade ago. Since then, solid organic particles (polystyrene and melamine formaldehyde), inorganic particles ($CaCO_3$ and $MnCO_3$),[9] gold nanoparticles (AuNP)[10] and even cells[11] have been used as core materials. After multilayer deposition, the core-shell structures can be used "as is", or the core can be dissolved to leave hollow polymeric capsules.[12] For construction of hollow capsules, inorganic materials are often preferable because of their ability to dissolve in mild aqueous media, compared to severe conditions used for dissolution of organic particles. Applicable templates and their properties were discussed in a recent review.[13]

The size and shape of the capsules is usually determined by the template used for deposition. In a very recent example illustrated in Figure 17.1, the use of colloidal crystal templates in LbL deposition enabled the construction of highly ordered 3D LbL structures.[14] In addition, anisotropic micro- and nanostructures have recently been prepared by LbL coating of anisotropically shaped template particles.[15,16]

One way to prepare micro- and nanocapsules is the use of oil-in-water emulsions as cores for multilayer deposition.[17,18] For example, sequential assembly of PEI and polyacrylic acid (PAA) at the surface of toluene-loaded polyglutamate shells led to particle stabilization, and resulted in robust containers useful for storage and delivery of water-insoluble compounds.[17] Lipid droplets have also been used as templates and, when covered by protein-polysaccharide films, showed better protection against oxidation.[19] Another interesting application of LbL is deposition of a protein shell at an air–liquid interface. In this case, stable microbubbles coated with chemically reduced lysozyme that retained its antimicrobial activity have been demostrated.[20]

Templates for LbL deposition can be made from the cargo itself, since many high-potency drugs including some anticancer agents, such as paclitaxel and tamoxifen, have low solubility in water.[21–24] This approach assured extremely high encapsulation efficacy. For example, aqueous suspensions of poorly soluble drugs were sonicated to obtain 100–200 nm cores, and then coated by PEM shells.[23,24]

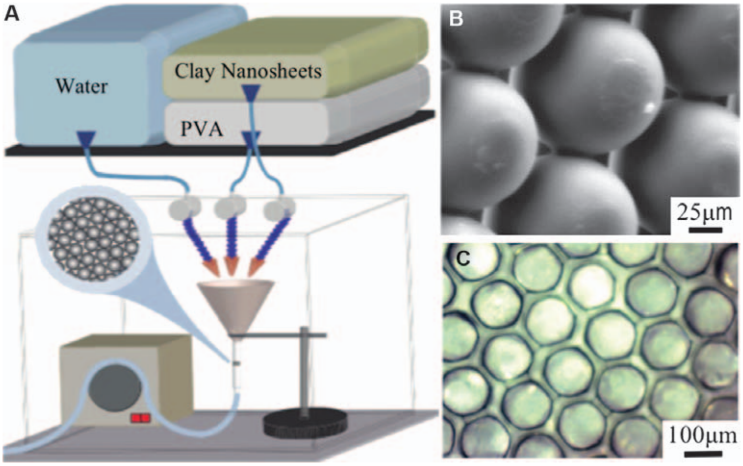

Figure 17.1 (A) 3D LbL setup used to deliver alternating solutions *via* solenoid valves through a colloidal crystal template (CCT) secured within silicone tubing and accelerated by a peristaltic pump. (B) SEM image of the annealed polystyrene CCT. (C) Optical microscopy image of the LbL clay nanocomposite on the CCT.
Reprinted with permission from Ref. 14. Copyright (2012) American Chemical Society.

17.3 LbL Constituents and Architectures

A broad variety of LbL film constituents used in varying deposition conditions enable tuning film composition, functionality, stability and permeability. Driving forces for LbL assembly include electrostatic interactions, hydrogen bonding, covalent attachment and even biological key-lock interactions. Therefore, constituents of LbL assemblies comprise polyelectrolytes, proteins and peptides,[25–30] polysaccharides,[31] DNA,[32,45–47] anticancer drugs,[33] inorganic nanoparticles,[33–35] carbon nanotubes,[36] micelles[37] and even viruses.[38] Moreover, liposomes or degradable particles can also be incorporated within LbL films as film components.[39,40] Importantly, components that are incompatible in bulk mixtures can be incorporated within different strata of the LbL film, and the distance between those strata can be controlled at the nanoscale.[41]

Incorporation of inorganic materials such as AuNPs,[42] single-walled carbon nanotubes (SWCNs),[43] silica nanoparticles or clay nanoplatelets[44,45] within the LbL assemblies increase their mechanical strength and stiffness. Mechanical properties of the capsules are important, since they regulate capsule stability and integrity. Without such stabilization, all-polymer PEM capsules can deform during intra-cellular uptake and lose a significant fraction of incorporated bioactive molecules.[46]

Figure 17.2 shows an example of how the amount of AuNPs deposited within each assembly layer can be controlled by the deposition conditions.[41]

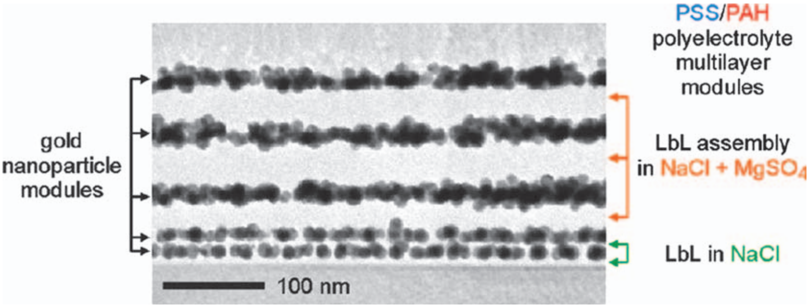

Figure 17.2 Cross-section TEM image of heterogeneous LbL assembly of AuNPs and polyelectrolytes (PSS and PAH). The spacer PEMs comprise $(PAH/PSS)_{4.5}$. The bottom two AuNP modules were assembled from dip coating solutions with 1 M NaCl. Solutions with 0.05 M of "auxiliary" $MgSO_4$ in 0.80 M NaCl were used for the assembly of the top three AuNP modules.
Reprinted with permission from Ref. 41. Copyright (2012) American Chemical Society.

Stratification of AuNPs within LbL films is achieved *via* assembly of polystyrene sulfonate (PSS)/poly(allylamine hydrochloride) (PAH) spacer layers. The AuNPs and PEM modules appear, respectively, as dark and light strata in the cross-sectional transmission electron microscopy (TEM) image.

Amphiphilic block copolymer micelles (BCMs) can endow films with functional hydrophobic domains addressable through environmental stimuli. These domains can serve as depots for efficient uptake of small hydrophobic molecules, and provide for on-demand, stimuli-responsive release. Progress in constructing pH- and temperature-responsive 2D LbL assemblies *via* inclusion of BCMs with responsive cores is summarized in a recent review.[37] In parallel efforts, responsive BCMs were assembled in 3D geometry; *i.e.* they were included within walls of hollow capsules constructed entirely from pH-responsive BCMs.[47] This approach broadens the application of LbL assemblies for encapsulation and release of diverse bioactive substances, as the resultant capsules combine the advantages of 2D LbL assemblies of polymeric micelles (*i.e.* their capability to load and controllably deliver hydrophobic molecules) with those of LbL capsules (*i.e.* availability of the capsule interior for hydrophilic drug compounds). Moreover, additional functionality has recently been endowed to LbL films or capsules by assembly of DNA-grafted poly(*N*-isopropylacrylamide) (PNIPAAm) micelles within PEMs, and the resultant assemblies could be degraded by the addition of an enzyme DNAse.[48] Chemical composition of the micellar shells assembled within capsule walls can also be used to load functional compounds. For example, polystyrene-block-poly(acrylic acid) BCMs incorporated within capsule walls enabled selective trapping of positively charged water-soluble compounds.[49]

Besides micelles, other well-known vesicles for loading of functional compounds are liposomes that can entrap drugs in the interior aqueous cavities, or in the lipid phase of their shells. Combination of liposomes and LbL technology is advantageous due to their biocompatibility, simplicity of preparation and well-known routes for drug incorporation and delivery.[50] For example, liposomes have recently been used as templates for LbL assembly resulting in LbL capsules.[51,52] In particular, positively charged chitosan (CHIT) was deposited onto negatively charged liposomes, followed by deposition of anionic dextran sulfate (DEXS) or DNA. Functional molecules of different charge, such as 1-hydroxy pyrene-3,6,8-trisulfonic acid, alendronate or glucose, could then be encapsulated and trapped within liposome-templated capsules.[53] Moreover, encapsulation of magnetic nanoparticles in the interior of the unilamellar liposomes covered with LbL assemblies opens opportunities for controlling drug delivery through the application of magnetic or electric fields.[54]

An interesting recent report describes assembly of liposomes at the surface of poly(L-lysine) (PLL)/PSS PEMs. This phenomenon was explained by the ability of PLL to diffuse within the films and stabilize the liposome vehicles during the film construction.[55] Figure 17.3 illustrates the mechanism of stabilization of adsorbed liposomes by PLL diffusion (A) and shows relative vesicle adsorption as a function of the number of deposited underlying PLL/PSS layers (B), when the entire underlying PEM (uPEM) serves as a reservoir for PLL diffusion to the surface.[55] Inclusion of liposomes with LbL assemblies provides an ideal environment for liposome-entrapped bioactive molecules. In 3D geometry, such assembly results in liposome-containing capsules (capsosomes), which can additionally entrap different types of bioactive compounds within capsule interiors.[39]

LbL assembly is often performed using aqueous solutions, without exposure to organic solvents. This represents a significant advantage for inclusion of many bioactive molecules, such as proteins and nucleic acids, which tend to

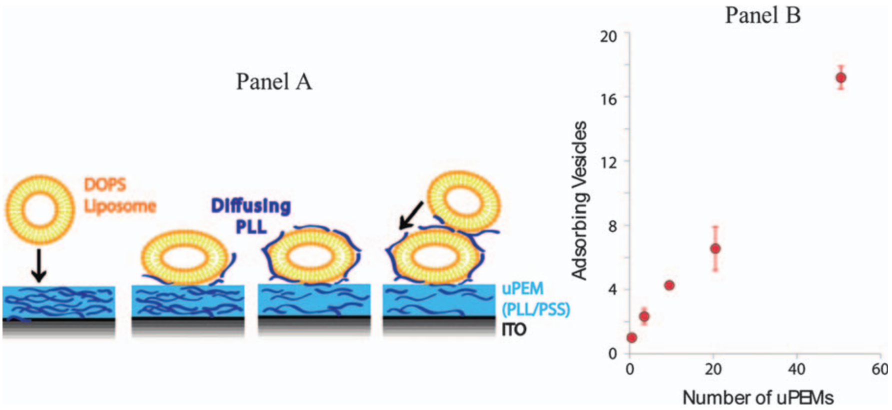

Figure 17.3 Panel A. Stabilization of adsorbed liposome vehicles by PLL diffusion. Panel B. Relative vehicle absorption as a function of number of deposited underlying PLL/PSS layers (uPEMs).
Reprinted with permission from Ref. 55. Copyright (2011) American Chemical Society.

denature in non-aqueous media. However, organic solvents can also be used to tune the composition of LbL films during film buildup.[56] Moreover, organic solvents can be advantageously used in reverse-phase LbL (RP-LbL) capsule construction, when PEMs are deposited from organic solutions. This approach enables encapsulation and release of water-soluble molecules using the aqueous interior of 3D LbL assemblies. For example, the polymeric shell of LbL-coated agarose microbeads expanded upon exposure to an aqueous solution, while the microbead remained suspended within the interior of the LbL capsule wall (Figure 17.4). These "inflated" capsules may be useful for localization and delivery of two different drugs from microcapsules.[57]

In recent years further progress has been made with more complex biomolecule delivery from capsules with compartmental architectures. In one exciting example, self-exploding LbL-coated gel beads released their interior as a result of degradation of smaller-size microcapsules, followed by an increase in the osmotic pressure and the rupture of LbL bead shells.[58] The degradation time (or explosion time) could be conveniently regulated by the cross-linking density of the gel network.[58] Such advanced hierarchical structures are very promising for time-controlled release of biologically

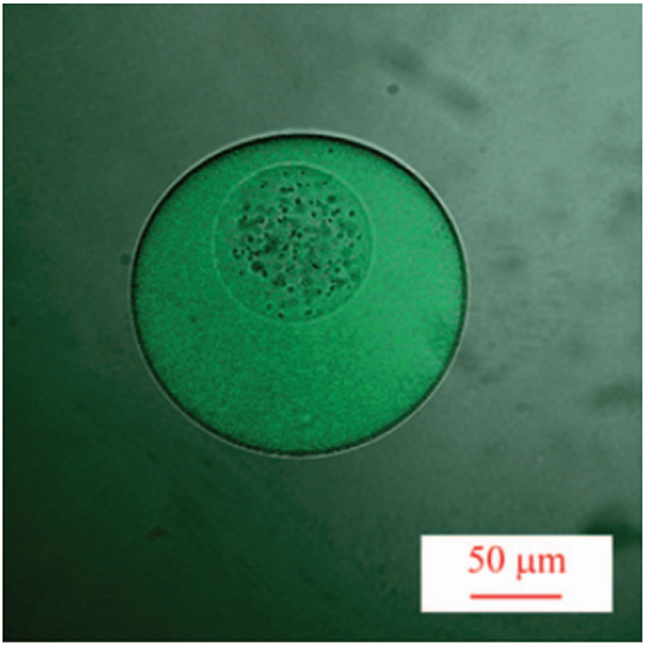

Figure 17.4 Confocal image of inflated microcapsules. Blue-PS microcapsules were trapped within the agarose microbead, and fluorescein isothiocyanate (FITC)-dextran (Mw 2000 kDa) is trapped inside the inflated LbL microcapsule.
Reproduced from Ref. 57 with permission from The Royal Society of Chemistry.

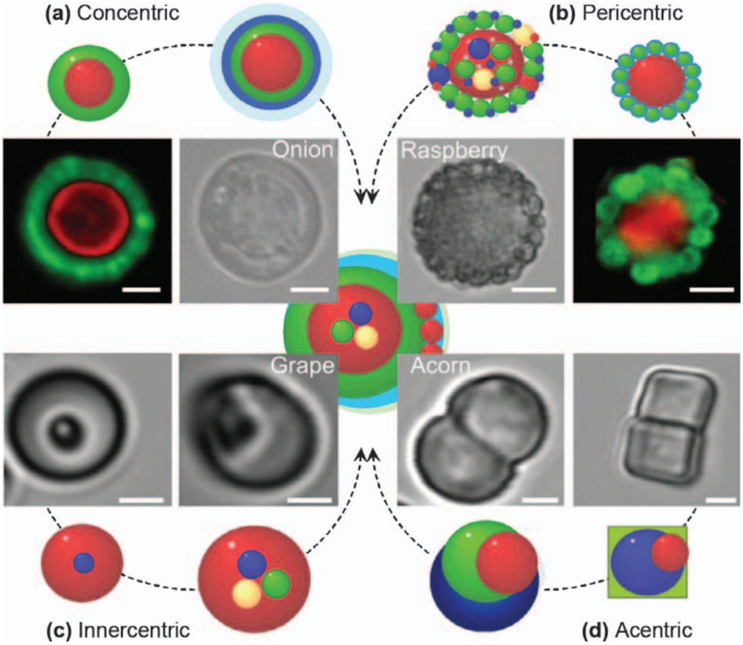

Figure 17.5 Multi-compartment microcapsules: a) concentric, b) pericentric, c) innercentric and d) acentric. The structure in the middle incorporates all four approaches.
Reproduced from Ref. 61 by permission of John Wiley & Sons, Inc.

active molecules. Another example of hierarchical delivery systems includes LbL assemblies of mesoporous compartments which demonstrated multi-step, self-regulated release of different encapsulated compounds.[59,60] Preparation of more complex multi-compartmental capsules for simultaneous delivery of multiple drugs has also been achieved.[61] Figure 17.5 shows a schematic illustration of the structure of capsules with advanced hierarchical functionalities. For example, an enzyme and its substrate can be simultaneously incorporated in the same capsule.[61]

17.4 Drug Incorporation Strategies within LbL Assemblies

Often, bioactive molecules are incorporated within films as a component. In this scenario, drug can be uniformly loaded with the entire film, and the amount loaded can be simply and advantageously controlled by the number of PEM layers or the film thickness. In some cases, bioactive molecules are complexed with oppositely charged macromolecules, prior to assembly within LbL architectures.[62,63] LbL assemblies can also be loaded with functional molecules at the post-assembly step.[64,65] For the success of such an approach, the interactions between infiltrating molecules with LbL films and the mesh size of the LbL matrix should be considered.

For 3D LbL assemblies, drugs can be incorporated in the shell of capsules or trapped within their internal cavity. The mesh size and the permeability of the LbL films and capsules are important for biomolecules trapping and can be controlled by environmental conditions such as pH, temperature or ionic strength. Polyelectrolyte multilayer capsules consisting of poly(diallyldimethylammonium chloride) PDADMAC and PSS were shown either to swell or to shrink in water at elevated temperatures depending on the polyelectrolyte forming the outer layer rather than on the total number of layers.[66,67] Shrinkage of the PDADMAC/PSS microcapsules resulted in denser and more mechanically stable structures.[68,69] This thermally induced shrinkage of the capsule walls allows incorporation of hydrophilic solutes within the capsules.[68]

Bioactive molecules can be a part of the template used for LbL deposition. Templates for LbL constructions can be either insoluble particles of pure drugs,[21–24] or non-drug templates loaded with biologically active compounds. The latter approach has been used for the encapsulation of DNA,[70–72] proteins[73,74] and siRNA.[75] Dissolution of the core material yields functional capsules containing the loaded compound dissolved within their interiors. Depending on the ratio between the molecular sizes of the entrapped compound and the mesh size of the capsule wall, encapsulated material can then either controllably diffuse out of the capsule, or remain trapped within the capsule interior compartment.

17.5 Drug Release Strategies

LbL assemblies can support either "passive" delivery of loaded compounds (occurring due to drug diffusion or hydrolytic film degradation), or release of functional compounds in response to stimuli. Stimuli-responsive drug release can occur as a result of desorption of a drug from LbL films, enhanced permeability of multilayer films, or decomposition of the entire film/capsule wall. The stimuli can be divided into three categories: chemical (pH, ionic strength, solvent), physical (light, electric or magnetic field, temperature and mechanical stimuli) or biological, responding to the presence of bioactive compounds.[76] Very often, at physiologic conditions, external stimuli become useful.[77] It is also useful to construct pulsatile delivery systems responding in an on-off manner to applied stimuli.

17.5.1 Diffusion-controlled Release

Release of functional molecules of low molecular weight is often regulated by their concentration gradient between the film and the environment. In this diffusion-controlled release scenario, recent studies established correlations between film porosity, pore size and rate of loaded molecule diffusion.[78] Several functional molecules (for example, cationic and anionic molecules) can also be co-loaded and simultaneously released from the film through this elution-based mechanism.[79] Specifically, this has been demonstrated with two model molecules – anionic methyl orange and cationic rhodamine 6G – which were incorporated within the PEM film through adsorption to positively and negatively charged groups provided within the film by the assembled polyampholytes.[79] Simultaneous delivery of hydrophobic and hydrophilic molecules from LbL-covered surfaces by a diffusion mechanism has also been reported.[80]

One of the problems frequently met with controlled release relying exclusively on diffusion is that loaded functional compounds leach out of LbL films in a short period of time. For many biomedical applications, it is desirable to extend the release time for at least several days or weeks to increase therapeutic dose and diminish risk of toxicity. A promising approach to slow down diffusion of drugs from LbL films is the insertion of low-permeability barrier layers within PEM films. This approach was first demonstrated for hydrolytically degradable PEM films though the insertion of PAH/PAA or other barrier layers.[81] Release profiles can also be tailored by capping the films with diazoresin and PSS barrier layers (Figure 17.6 a and b).[79] Very recently, it has been shown that incorporation of graphene oxide as a barrier layer within hydrolytically degradable protein-containing films extends the release profile to as long as 30 to 90 days.[82]

Diffusion-controlled delivery of functional molecules has also shown promising for biological applications with 3D LbL constructs. Specifically, CHIT/alginate capsules loaded with the anticancer drug daunorubicin (DNR) within their interiors effectively induced the apoptosis of BEI-7402 tumor cells. The release profile followed diffusion-controlled kinetics with complete release from 2 to 6 h.[83] In another case, LbL capsules with heparin at both the PEM wall and in the hollow interior acted as centers for binding of growth factors (such as TGF-β1), and prolonged the release of bioactive molecules. TGF-β1 burst release was followed by its sustained release over several days without affecting its biological activity.[84] Moreover, heparin-containing capsules can be incorporated within a gelatin tissue engineered cryogel scaffold without changing its properties.

17.5.2 Hydrolytic Degradation

Hydrolytic degradation of LbL constituents is often explored as a means to release molecules that are either incorporated within LbL films, or trapped within LbL capsules. The use of micelles,[85] nanoparticles,[86,40] polycyclodextrins[63] and prodrugs in alternation with polyions is reported for hydrolysis-based delivery of bioactive molecules. In addition to the above assemblies, which rely on non-covalent interactions, fabrication of degradable multilayer films and capsules *via* "click" chemistry has recently been explored.[87,88]

A series of biocompatible cationic poly(β-amino esters) is frequently used as a degradable component for multilayer construction. Films containing this

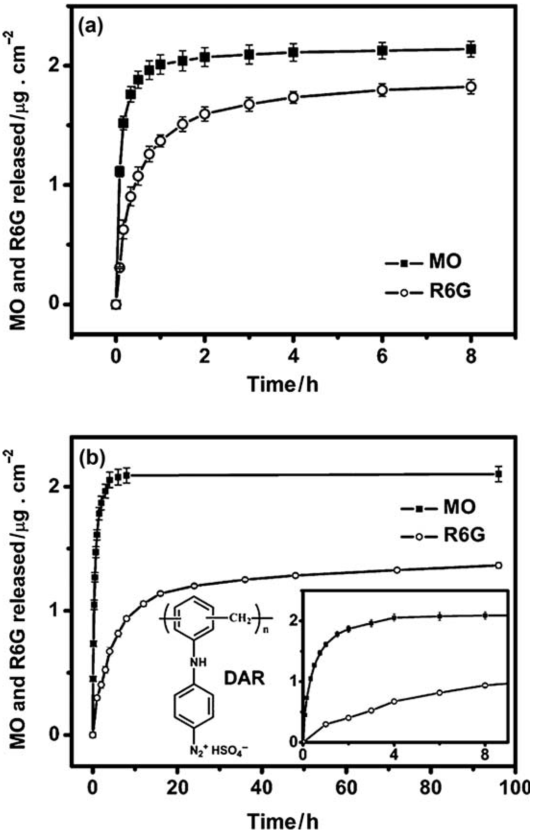

Figure 17.6 Time-dependent simultaneous release profiles of methyl orange (MO) and cationic rhodamine 6G (R6G) molecules from PAH-D-CO2 microgels containing amine and carbamate groups assembled with PSS in a $(PAH\text{-}D\text{-}CO_2/PSS)_{10}$ film (a), and a $(PAH\text{-}D\text{-}CO_2/PSS)_{10}$ film capped with a cross-linked diazoresin (DAR) and PSS barrier layer (b). Inset in (b) shows the release profile during the first 9 h.
Reprinted with permission from Ref. 79. Copyright (2010) American Chemical Society.

degradable polycation can incorporate and release various individual drugs,[89–92] or multiple therapeutic agents, including gentamicin, vancomycin and/or diclofenac.[93–95] Hydrolytically degradable poly(β-amino ester)/DNA PEMs deposited at planar substrates and at the surface of poly(styrene) particles hold significant promise for DNA vaccine delivery.[92,96,97,91,98] Importantly, since the hydrolytic degradation rate of poly(β-amino ester) depends on the hydrophobicity, charge density and strength of ionic pairing within PEM film,[99,100] degradation of LbL films can be controlled by molecular parameters, as well as by the conditions of film assembly.

Many drugs are, however, hard to include directly within LbL assemblies at the step of film assembly, because of their small size and few functional groups.

Several approaches have been used to overcome this challenge. In one approach, small drugs (such as ciprofloxacin, flurbiprofen and diclofenac) have been bound within polymeric cyclodextrins, offering the negatively charged groups of the drug free to be assembled with a range of degradable polycations within LbL films.[63,94] Figure 17.7 illustrates this approach, in which bioactive molecules were included within the cyclodextrin units of the polymer to promote their assembly within the film. The release profiles were shown to be independent of the type of incorporated agents and were governed by hydrolytic degradation of the polycations.[63] However, in this approach, bioactive molecules remained bound within cyclodextrin interiors even after release of the functional molecules to the solution. In another recent study, BCMs were used for pre-loading of hydrophobic drugs (paclitaxel and diclofenac) prior to their assembly with a hydrolytically degradable polycation, and resultant PEMs controllably released drugs to *in vitro* cultured cells.[85]

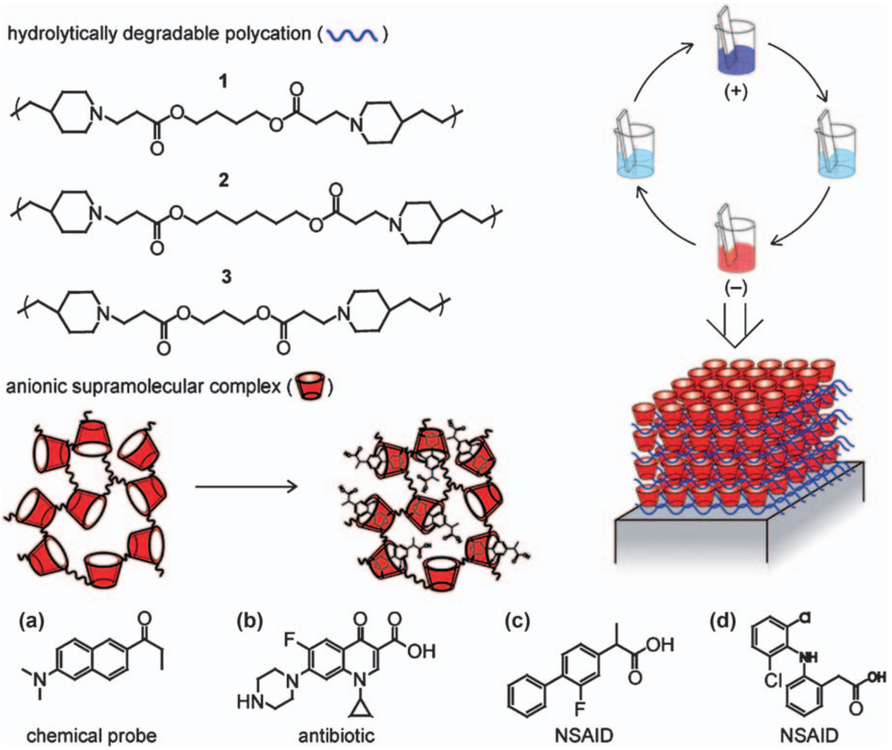
hydrolytically degradable polycation ( )
1
2
3
anionic supramolecular complex ( )
(+)
(–)
(a)
chemical probe
(b)
antibiotic
(c)
NSAID
(d)
NSAID

Figure 17.7 LbL assembly of hydrolytically degradable polycations and anionic supramolecular complexes. Poly(carboxymethyl-β-cyclodextrin) in combination with small bioactive molecules was used as the anionic supramolecular complex. (a) Fluorescent chemical probe prodan; (b) ciprofloxacin; and (c) and (d) non-steroidal anti-inflammatory drugs (NSAIDs) flurbiprofen and diclofenac.
Reproduced from Ref. 63 by permission of John Wiley & Sons, Inc.

Hydrolysable components can also be a part of a drug carrier. For example, hydrolysable poly(ethylene oxide)-block-poly(caprolactone) (PEO-b-PCL) BCMs were used as containers for drug inclusion within LbL assemblies.[101] Hydrogen-bonded films of triclosan-loaded PEO-b-PCL BCMs and PAA rapidly deconstructed to release micelles upon exposure to physiologic conditions, yet the film decomposition rate could be decreased *via* thermal cross-linking of the film.[101] In another example, hydrolysable nanoparticles (*i.e.* poly(lactic acid) nanoparticles (PLA NPs)) were included within PLA NP/PEI films, and shown to support prolonged release of pyrene from the films.[40] Nanoparticles of poly(DL-lactic-co-glycolic acid) were also included within PEMs and used for multiple drug delivery.[86]

An interesting type of degradable LbL assembly includes "charge-shifting" polymers, which change ("shift") their charge rather than chain length during degradation.[102,103] For example, LbL films containing citraconate-modified PAH were stable at neutral pH, but degraded producing positively charged PAH in weakly acidic conditions.[103] Changes in the polymer net charge within the layers promoted film disintegration (Figure 17.8). Such LbL films show longer degradation times compared to traditional degradable films whose degradation occurs through main chain cleavage.

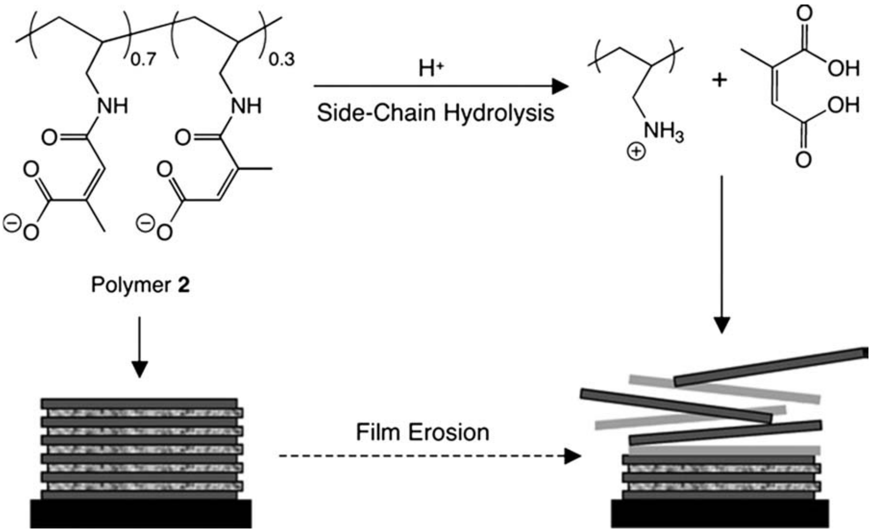

Figure 17.8 Hydrolysis of the citraconic amide side chains of anionic "charge-shifting" polymer 2 under acidic conditions yields cationic poly(allylamine). Anionic polymer 2 in combination with polycations can be used to fabricate polyelectrolyte multilayers. Time-dependent changes in the net charge of polymer 2 promote film disintegration and the release of cationic film components.
Reproduced from Ref. 103 with permission from The Royal Society of Chemistry.

In a different approach, a drug is bound to the polymer matrix *via* a hydrolysable bond.[104,105] LbL assemblies of CHIT with a prodrug – paclitaxel conjugated with hyaluronic acid (HA) *via* succinate ester linkage – showed selective release of paclitaxel, while polymer matrices remained stable.[104] Similar release, triggered by hydrolysis of a prodrug linkage with the film, was demonstrated for hydrogen-bonded PAA/glucocorticoid-poly(*N*-vinylpyrrolidone) (PVPON) multilayers, in which hydrolysis of a prodrug hydrazone linkage was enhanced under acidic pH.[105] In both examples, the released drug retained its therapeutic activity.

While the above strategies are used for continuous, time-extended release, burst and/or pulsed on-demand release can be beneficial for some biomedical applications, where it could minimize the development of antibiotic resistance or long-term toxicity. An interesting "explodable" system recently reported is based on dextran–hydroxyethyl methacrylate (dex-HEMA) microgels coated with PEM films that were impermeable to the degradation products of dex-HEMA.[106] Degradation of dex-HEMA caused a buildup of inner pressure within the microcontainer, eventually leading to the rupture of the PEM coatings and the burst release of encapsulated protein.[106,107]

17.5.3 pH-triggered Release

Developing LbL-based systems with built-in pH sensitivity is useful for several routes including delivery of (a) proteins and peptides through the gastrointestinal tract, (b) anticancer drugs to tumor cells or (c) anti-inflammatory drugs to inflamed tissues. In all these cases, local pH variations in specific tissues are used as a trigger to deliver enhanced amounts of drugs. pH variations induce increased drug flux either from the LbL film itself (which could be a part of an LbL capsule or a planar coating deposited at the surface of a biomedical implant), or from the interior of the LbL capsules.

pH response is usually realized through inclusion of weak polyelectrolytes (wPEs) within LbL films. At pH values different from the film assembly pH, such LbL assemblies can change their swelling degree or mesh size (and therefore their permeability characteristics), or even decompose.[108,109] For example, hydrogen-bonded LbL films demonstrate pH-sensitivity as a result of deprotonation of poly(carboxylic acids) at increased pH values.[110] Another study describes application of dendrimer/poly(methacrylic acid) (PMAA) LbL films stabilized by a combination of hydrogen bonding and electrostatic pairing, for pH-triggered rapid drug release.[111]

A significant challenge in constructing biologically relevant pH-responsive coatings is tuning the film response within the pH range close to physiological conditions. One example of such tuning has been demonstrated for hydrogen-bonded films containing temperature-responsive polymers. Decomposition pH of these LbL assemblies could be tuned by varying deposition and/or post-assembly temperature.[112] Specifically, when PNIPAAm/PMAA films prepared at different temperatures were exposed to solutions of increasing pH at the same temperature, they exhibited different pH stability. The critical pH of film

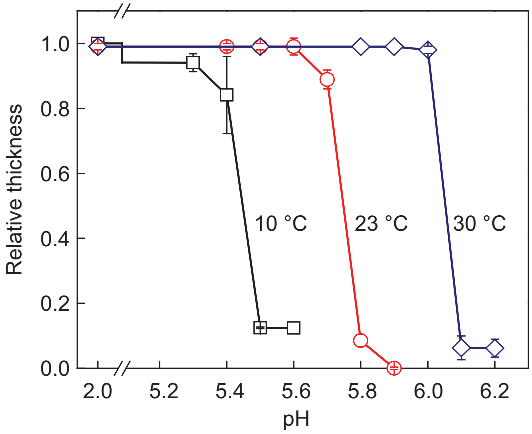

Figure 17.9 pH-triggered disintegration of hydrogen-bonded PNIPAAm/PMAA films deposited at 10 °C (squares), 23 °C (circles) or 30 °C (diamonds) and destructed in solutions at 23 °C.
Reprinted with permission from Ref. 112. Copyright (2009) American Chemical Society.

disintegration (pH_{crit}) at 23 °C increased from 5.5 to 5.8 and 6.1 for assembly temperatures 10, 23 and 30 °C, respectively (Figure 17.9). These systems might be useful as temperature-triggered drug-release delivery systems.

The pH-decomposable films can also be stabilized within a broad pH range through thermal, chemical or photochemical cross-linking of film components.[113,114] In one example, chemical cross-linking of hydrogen-bonded PMAA/PVPON, followed by PVPON release, resulted in hydrogel-like PMAA coating, which could be reversibly loaded with various functional compounds.[114] Importantly, such films can retain bioactive molecules at pH 7.4, and release their contents upon pH lowering. Recently, films of this type were saturated with an electrostatically interacting antimicrobial peptide, and they released the peptide in response to the local pH lowering associated with bacterial infection (Figure 17.10A).[65] As the pH decreased, the peptide L5 was released faster from ethylenediamine (EDA)-stabilized $(PMAA)_{10}$ hydrogels (Figure 17.10B), retaining its antibacterial activity (Figure 17.10C and D). Cross-linking of LbL films of a different type has also been used to tune the critical pH of film disintegration to neutral values of pH, as demonstrated for multilayers of PAH-porphyrin conjugate and thiol-modified PAA.[115]

Electrostatically assembled multilayer films containing wPEs were also used for controlled release of charged dyes *via* pH changes.[111,116,117] Similarly, release of antibiotics, such as cefazolin and gentamicin, from electrostatically assembled films of poly(L-glutamic acid) (PLGA) and PLL has also been triggered *via* pH changes.[118] Importantly, released antibiotics retained their antibacterial activity against *Staphylococcus aureus*.[118] A model hydrophobic compound, pyrene, was also incorporated within electrostatically assembled

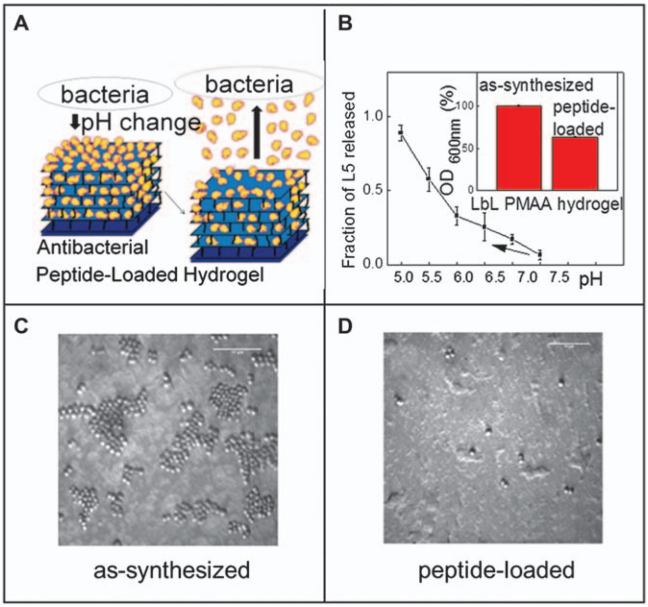

Figure 17.10 (A) Scheme illustrating release of peptide L5 from the LbL films due to pH lowering during bacterial growth. (B) Effect of pH on retention of peptide within the film. The inset shows normalized optical density of *S. epidermidis* measured at 600 nm (OD600) in tryptic soy broth (TSB) after incubation for 4 h in the presence of the as-synthesized or peptide-loaded hydrogels. Surface coverage by *S. epidermidis* of $(PMAA)_{10}$ as-synthesized (C) and peptide-loaded (D) after incubation for 4 h in the TSB medium.
Adapted with permission from Ref. 65. Copyright (2010) American Chemical Society.

films of amphiphilic BCMs, and films showed pH-dependent release of pyrene owing to the pH response of core-forming polymer blocks.[119]

For LbL capsules, changes in shell charge and permeability control the release of loaded molecules from the wall or the interior of the capsule, respectively. Biomimetic LbL capsules built from human serum albumin (HSA) and a zwitterionic lipid, L-α-dimyristoyl phosphatidic acid (DMPA) were permeable to dextran (40 kDa) at pH 4.8 and lower, but impermeable at pH 7.4 or higher[120] as a result of pH-induced charge changes in HSA and DMPA, also causing conformational reorganization of HSA. Permeability of hydrogen-bonded capsules of PVPON, poly(*N*-vinylcaprolactam) (PVCL) or PNIPAAm with tannic acid (TA) towards FITC-labeled polysaccharides was also controlled by pH variations resulting in changes in multilayer total charge.[121] Usually, the release of encapsulated cargo from capsules is promoted by an increase in the density of charges of the same sign. For example, lysozyme was retained within PAH/PAA capsules at pH 7.4, but was released at pH 2 due to repulsions between lysozyme and pH-induced positive charges in PAH chains.[122] In another system useful for oral delivery of protein drugs, release of bovine serum albumin from microcapsules of CHIT and DEXS was suppressed at pH 1.4, but occurred very rapidly at pH 7.4 as a result of a decrease of the positive charges on CHIT.[123] Capsules constructed from non-degradable polymers, poly(4-vinylpyridine hydrochloride) (PVP) and PSS, also allowed encapsulation of HSA in the pH range 6–6.8 where capsule walls were highly swollen, and HSA release at $pH > 6.8$ where capsule walls dissolved.[124] pH-responsive capsules from organomodified clay layers sandwiched between PDADMAC and PSS have shown release of ibuprofen ($pK_a = 4.4$) at low pH, as a result of desorption of electrostatically bound ibuprofen from clay nanosheets at acidic pH values.[125]

Some interesting systems with dual response (with pH used as one stimulus) have also been reported. Release of FITC-dextran from intra-cellularly degradable polyelectrolyte capsules was simultaneously mediated by pH and by an enzyme. Such microcapsules are attractive candidates for local delivery of drugs to target tissues.[126] Paramagnetic microcapsules composed of CHIT and citrate-modified metal oxide nanoparticles have also provided pH-sensitive release of methylene blue (MB).[127] When the MB-adsorbed magnetic microspheres were placed in solutions of pH 7 or 10, no significant amount of the dye was released even after 48 h. However, at pH 4 almost all MB was released from the loaded microspheres in 48 h due to weakening interactions between the assembled molecules.[127]

Recently, pH and salt stimuli were used to regulate singlet oxygen generation efficiency of the porphine-based fluorophore (Por^{4-}) within LbL films through spacing of Por^{4-} and Ag clusters with pH- and salt-responsive (PAA)/poly(diallyl-dimethylammonium chloride) (PDDA) bilayers (Figure 17.11).[128] The approach could be used to control the activity of oxygen-producing species in photodynamic therapy.[128]

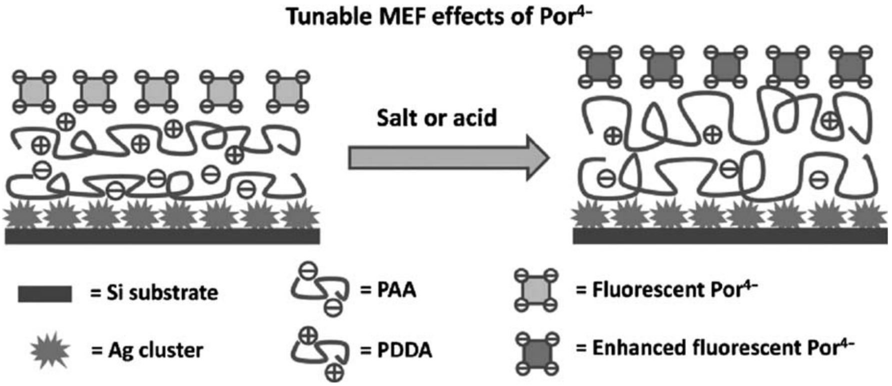

Figure 17.11 Schematic of tunable metal-enhanced fluorescence (MEF) effects as influenced by ionic strength or pH.
Reproduced from Ref. 128 by permission of John Wiley & Sons, Inc.

17.5.4 Salt-triggered Release

In contrast to polyelectrolyte gels, PEM films usually swell with increasing ionic strength. Salt ions weaken the interactions between polycations and polyanions within the layers, and also contribute to increase the osmotic pressure within the films. At a certain critical ionic strength multilayers can dissolve. The influence of salt concentration on permeability and morphology of electrostatically assembled multilayers,[129–131] as well as the mechanism of swelling and dissolution of PEM films,[132] are well known. However, salt has the opposite effect on PEMs containing hydrophobic polymers.[133] For example, the presence of salt in solution triggered an increase in hydrophobic interactions within the PSS/polycation capsule wall, resulting in capsule shrinkage.[133] Figure 17.12 shows an interesting example of salt-induced fusion of PEM capsules composed of PDADMAC and PSS, in which salt enhanced molecular mobility of assembled polyelectrolytes and enabled capsule fusion.[134] Such an approach is promising for constructing various artificial vesicles, including artificial cells.

Increased concentrations of small ions can also be used to trigger release of functional molecules from LbL assemblies. Salt-induced release of MB from PLGA/PLL multilayers, for example, has been demonstrated.[135] While complete release of MB in deionized water was accomplished within several hours, only a

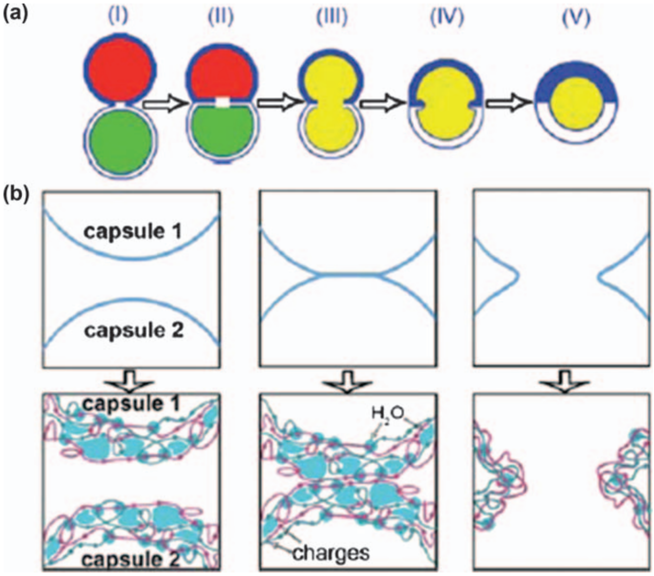

Figure 17.12 Fusion mechanism of microcapsules (a), and the magnified view of the interfacial areas. (b) (I) Salt creates defects and pores in the contacting membranes; (II) pores enlarge by lateral tension; (III) the inner contents of neutral polymers mix; and (IV–V) the polyelectrolyte molecules in the membranes do not mix.
Reproduced from Ref. 134 with permission from The Royal Society of Chemistry.

few minutes were required for the dye release in buffered solution.[135] The mechanism of release in this case most likely includes direct displacement of MB from the binding sites in the film.

17.5.5 Electrochemical and Redox-activated Release

Application of electrical signals is an attractive way to control drug delivery *via* remote stimuli. The approach is simple, safe and inexpensive. However, special attention should be paid to the susceptibility of drugs to be oxidated or reducted, and to the effect of applied current on the behavior of tissue and cells. It was found, for example, that current densities larger than 0.57 A m^{-2} induce death of myoblast cells cultured directly on the microelectrodes within 2 min of exposure.[136]

The manipulation of PEM stability and controlled release of functional molecules is enabled by the effect of the electric field on the charge and/or the oxidation state of the film. For example, the formation and stability of biocompatible PLL/heparin multilayers depend on the applied potential.[137] The application of a voltage to a multilayer-coated indium tin oxide (ITO) electrode resulted in on/off switching of heparin elution from the films.[137] Similarly, release of porphyrin from PAH/PAA LbL film was achieved by application of electrode potential +1.2 V or higher.[138] PLL/DNA films fabricated at 0 V were stable in pH 7.4 buffer, but dissolved slowly under applied potential higher than 1.8 V. However, dissolution was much quicker if a bias potential of 1.2 V was applied during film fabrication.[139] Moreover, electrochemical release has been demonstrated with films of electro-active nanoparticles. LbL films containing such nanoparticles dissolved due to a change in the oxidation state of the nanoparticles, resulting in release of film constituents.[140] This work demonstrates the rich potential of electrochemical techniques to control dissolution kinetics of LbL coatings.[139]

Significant attention has been paid to explorations of the mechanism of PEM modification upon the application of an external current. The process was explained by pH changes occurring in the vicinity of the electrode as a result of the electrolysis of water and the migration of ions within the film, in response to the applied potential.[139,141] A proton gradient is established next to the electrode as a result of the application of the electric field (the longer the distance from the electrode, the lower the proton concentration). A decrease in pH by more than 1 unit was observed at the distance up to 20 μm from the electrode in water after application of 4 A m^{-2} current for 1.5 s, while in buffer the extent of the pH change was narrowed to the submicrometer range.[136] The produced protons neutralize charge on weak anionic groups within PEMs, leading to disruption of polyanion/polycation ionic pairs, and eventually to release of free polyelectrolytes in the bulk solutions. Charge misbalance also occurs as a result of proton absorption, and the excess of positive charge is compensated by counter-ions migrating within the films.[141] This can result in elevated osmotic pressure, formation of cavities in the assembly and film detachment. In one example, electrochemically triggered release of dye molecules from liposomes embedded within PLL/PLGA multilayers

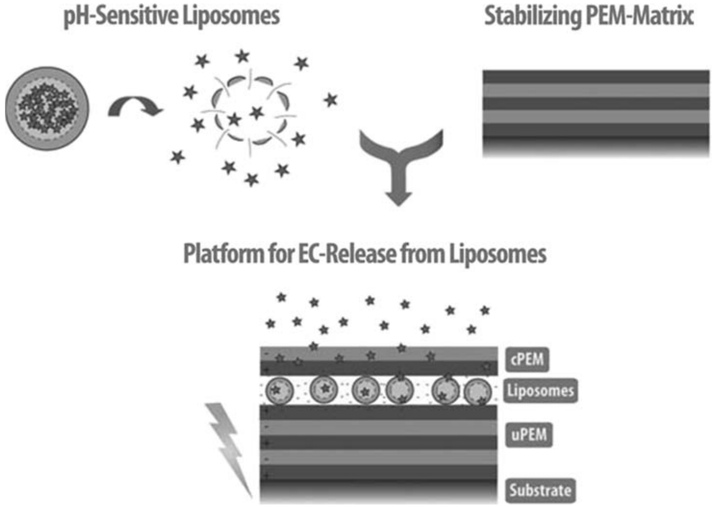

Figure 17.13 Schematics of LbL films containing pH-sensitive liposomes for electrochemically triggered release of the liposome content. The platform includes the underlying PEM (uPEM), the vesicles and the covering PEM (cPEM).
Reproduced from Ref. 142 by permission of John Wiley & Sons, Inc.

(Figure 17.13) occurred due to protonation of the negatively charged phosphatidyl serine head groups of the lipids, leading to destabilization and rupture of the vesicular assembly.[142] Another hypothesis on the mechanism of electrochemical degradation includes the formation of gases at the electrode surface. For example, oxygen is produced during water electrolysis, and chloride ions present in the vicinity of the electrode might also be oxidized to form Cl_2.[141] Gases, produced and accumulated under the PEM films, can form bubbles and eventually lead to delamination of PEMs from surfaces.[141]

Another way of changing the molecular charge within LbL films is through changing redox state of film constituents. In one example, LbL organometallic capsules change their permeability in response to chemical oxidation with $FeCl_3$.[143] Another promising route to control PEM permeability is cleavage of disulfide bonds by the addition of a reducing agent (such as dithiothreitol), or by reducing agents existing in Nature, such as the reducing conditions of a cell membrane.[144–146] For example, the cellular concentration of glutathione was found to regulate degradation of the disulfide-cross-linked PMAA shell, causing release of a peptide from the capsule shell.[147] LbL films of a hyperbranched poly(amido amine) containing bioreducible disulfide bonds have also been applied for DNA delivery.[148] The release dynamics of DNA could be controlled by the type of binding of DNA within LbL constructs. When DNA was included within LbL as DNA-polycation complex, rather than unbound DNA chains, faster DNA delivery was achieved.[148] These results are promising for controlled gene delivery and tissue engineering applications.

17.5.6 Temperature-triggered Release

Temperature-induced hydrophilic-to-hydrophobic polymer phase transitions have also been used to control drug delivery. One approach to achieve highly efficient temperature-control delivery of functional compounds from LbL films is to include temperature-responsive micelles within multilayers. Often, these systems contain PNIPAAm, a biocompatible polymer with a lower critical solution temperature (LCST) of ~32 °C. One example of constructing temperature-responsive assemblies using PNIPAAm-containing BCMs is hydrogen-bonded films of PVPON-b-PNIPAAm micelles assembled with PMAA (Figure 17.14).[149] A decrease in temperature below the LCST of PNIPAAm led to the solubilization of micellar core blocks and the acceleration of the release of incorporated small hydrophobic molecules.[149]

Multilayers of cationic BCMs poly(2-(dimethylamino)ethyl methacrylate)-block-PNIPAAm (PDMA-b-PNIPAAm) with PSS showed temperature-controlled switching between the hydrophobic and hydrophilic state of

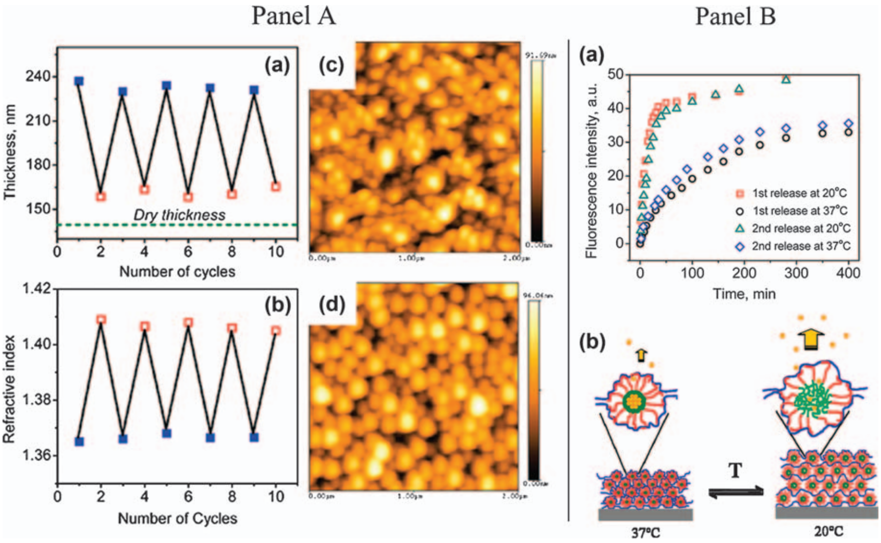

Figure 17.14 Panel A. Temperature-induced swelling/deswelling of hydrogen-bonded films of PVPON-b-PNIPAAm micelles assembled with PMAA. *In situ* ellipsometry measurements of thickness (a) and refractive index (b) of a $(BCM/PMAA)_4$ film in 0.01 M phosphate buffer of pH 5.0 at 20 °C (filled squares) and 45 °C (open squares), and AFM images taken for film dried at 45 °C (c), as well as for wet film at 20 °C (d). Panel B. (a) Release kinetics of pyrene from a $[BCM/PMAA]_{10}$ film in 30 mL of pH 5.0 buffer solution at 20 and 37 °C. Pyrene release was monitored by measuring fluorescence intensity of pyrene accumulated in solution ($\lambda_{ex} = 338$ nm, $\lambda_{em} = 373$ nm). (b) Schematic representation of reversible temperature-triggered swelling of BCM/PMAA films.
Reprinted with permission from Ref. 149. Copyright (2009) American Chemical Society.

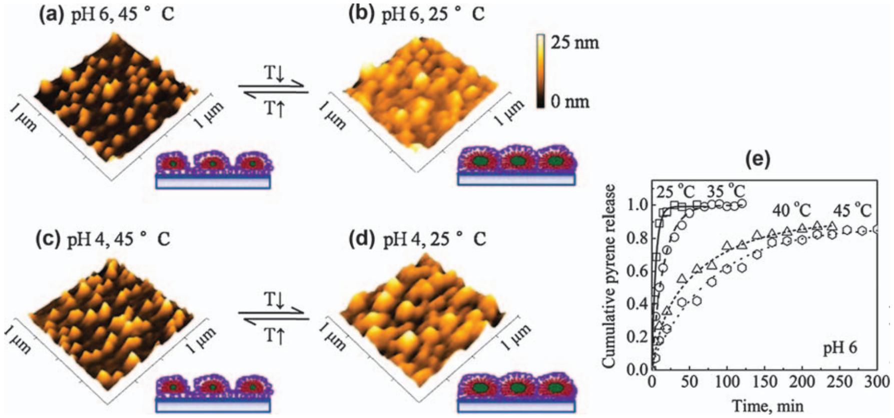

Figure 17.15 Surface morphology of wet BCM/PSS single bilayer films after 5 min exposure to 0.01 M phosphate buffer solutions at (a) pH 6, 45 °C, (b) pH 6, 25 °C, (c) pH 4, 45 °C and (d) pH 4, 25 °C observed by *in situ* AFM. (e) Release profile of pyrene dye from (BCMpyr/PSS)$_{10}$ film in 0.01 M phosphate buffer solution at pH 6 as followed by the intensity at 374 nm with excitation wavelength of $\lambda_{ex} = 333$ nm. pH of aqueous solutions was adjusted to 6, and temperature was controlled at 25 °C (squares), 35 °C (circles), 40 °C (triangles) and 45 °C (hexagons).
Reprinted with permission from Ref. 150. Copyright (2011) American Chemical Society.

assembled micellar cores.[150] Similar reversible switching between hydrophobic and hydrophilic states of the film-assembled micelles was recently reported for a different system.[151] Temperature-controlled film swelling/deswelling was also used to regulate the release of a micelle-loaded pyrene dye, whose release rate increased at temperatures below the LCST of PNIPAAm (Figure 17.15).[150] Very recently, hydrogen-bonded multilayers of micelles of the pH- and the temperature-responsive block copolymer, poly[2-(*N*-morpholino)ethylmethacrylate-block-2-(diisopropylamino)ethyl methacrylate] (PMEMA-b-PDPA) and tannic acid (TA) releasing pyrene have also been reported.[152]

Alternatively, temperature response can be endowed to LbL films *via* inclusion of liposomes as multilayer constituents.[50] Heating liposome-containing PEMs above the phase transition temperature of the constituent lipid of ~41 °C resulted in an increase of lipid bilayer permeability and release rate of vesicle-encapsulated molecules. Moreover, the response was reversible, and release of functional molecules could be interrupted by lowering the temperature below 41 °C.[50]

17.5.7 Light-triggered Release

The use of light as a remote trigger for drug delivery is attractive as it provides spatial and temporal control of bioactive molecule release.[153] Important parameters for such controlled drug delivery are interaction of external radiation with light-sensitive molecules and/or metal nanoparticles incorporated within coatings. The delivery profiles of bioactive compounds can be tuned by light wavelength and power.[154,155] Incorporation of gold nanorods within PEMs, for example, provides wavelength-selective response of LbL assemblies in the visible and near infrared (NIR) regions.[156] A combination of exceptional mechanical and optical properties of carbon nanotubes (with absorption in broad spectral infrared and visible range) also makes them attractive candidates as functional blocks for LbL assemblies capable of light-triggered release of bioactive molecules.[36] NIR light is promising for *in vivo* applications, as it penetrates deeper biological tissues, and is less damaging to cells compared to visible light.

In the case of plasmonic nanostructures assembled within multilayer films, the response is achieved through photothermal effects, *i.e.* local heating generated as the result of light absorption and scattering by metal nanoparticles. This process can result in changes in PEM permeability and/or in film rupture, depending on the incident intensity of light, the size of the nanoparticles and their absorption characteristics. For example, AuNPs do not have NIR absorption, but an NIR absorption band emerges with core/shell structures or gold aggregates (*e.g.* obtained by adding salt ions).[157] In earlier studies, fast release of functional molecules from AuNP-containing LbL capsules *via* NIR irradiation was realized as a result of high thermal stress and shell rupture.[158–160] In more recent studies, the use of aggregates of AuNPs enabled not only "explosions" of the capsules to be avoided, but also membrane permeability to be reversibly controlled. The shells permeability was decreased after the laser was turned off and subsequently increased when the laser was turned on[161] (Figure 17.16). In another example of reversible response, films and capsule-included films of biocompatible polymers (HA and PLL) containing aggregates of AuNPs released their cargo under stimulation with NIR as a result of light-triggered changes in film permeability.[162]

Incorporation of chemical photosensitive groups within LbL assemblies is another promising approach for constructing capsules for reversible encapsulation and release of molecules of interest. For example, capsules containing photoactive groups such as azobenzene moieties are good candidates for encapsulation of heat-sensitive molecules (proteins and DNAs), which might denature in conditions of extreme heat generation, often caused by interaction of light with plasmonic nanostructures. Light can also induce greater mobility of molecules within LbL assemblies, and this phenomenon can be used as a tool for encapsulation of molecular cargo. For example, light-induced shrinking of capsules made of PAH, poly{1-[4-(carboxy-4-hydroxyphenylazo)benzenesulfoamido]-1,2-ethanediyl, sodium salt} and poly(vinylsulfonate), was used for encapsulation of fluorescent dextran.[163]

Several interesting examples exist of the use of light to activate release of therapeutic species from LbL microcapsules. For example, when taken up by cells, ALG/CHIT capsules containing entrapped drug for photodynamic therapy, hypocrellin B (HB), remained biocompatible in the absence of radiation, but became highly cytotoxic after irradiation with UV light as a result of oxygen-containing radicals produced by HB.[164] In another example,

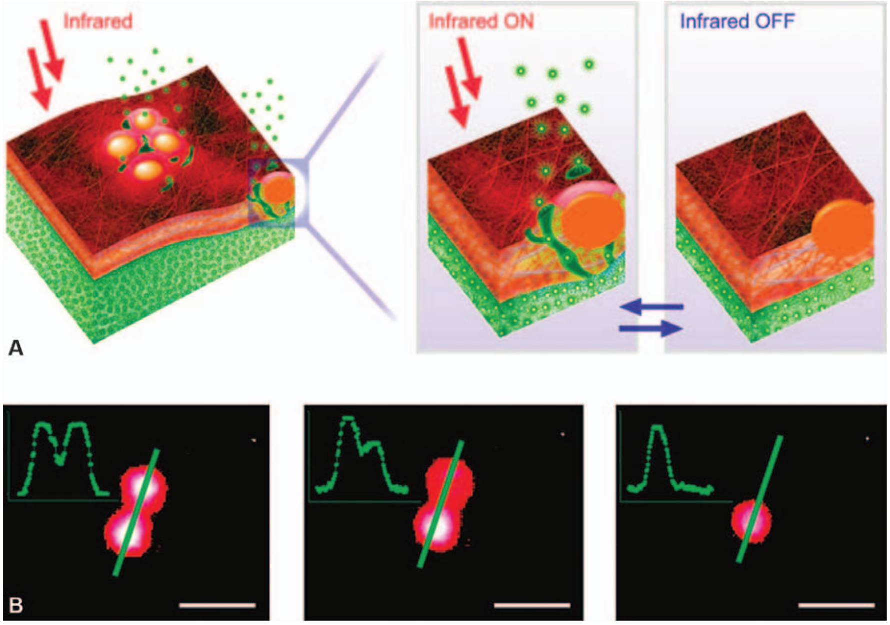

Figure 17.16 Remote release from microcapsules. (A) Schematics of nanoparticle functionalized polyelectrolyte layers opening channels upon laser illumination; (B) a polymeric microcapsule shell acts as a reversible nanomembrane. After the second illumination the microcapsule completely releases its content (right).
Reprinted with permission from Ref. 161. Copyright (2008) American Chemical Society.

porphyrin included within PEM capsule walls as a light absorbing agent endowed the capsule walls with the capability to deform under 532 nm laser irradiation in the presence of an oxidizing agent, a feature that could be useful for drug release.[165] Finally, another interesting approach describes the use of light to produce protons from microencapsulated photo-acid generating compounds. Specifically, the UV-light-triggered pH lowering resulted in microcapsule swelling and release of the entrapped drugs.[166]

17.5.8 Magnetic Field-triggered Release

At high-frequency magnetic field (HFMF) of 50–360 kHz, magnetic nanoparticles produce heat and promote stress development in the polymer multilayers that can result in changes in PEM permeability due to nanocavities development or even multilayer rupture.[167,168] For instance, the amount of doxorubicin (Dox) released from (Fe_3O_4 NP/PAH)$_4$ capsules under a magnetic stimulus is significantly higher than from the same capsules in the absence of magnetic field (Figure 17.17).[167] In another interesting example, LbL films of magnetic nanoparticles on oil droplets allow drug loading in the oil core and

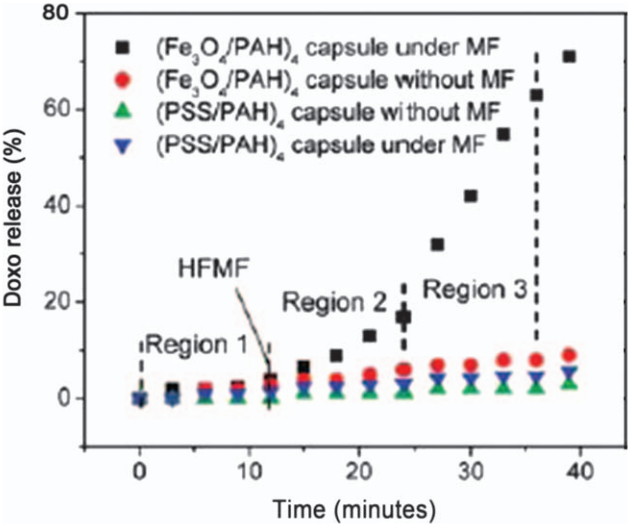

Figure 17.17 Doxorubicin release profiles of $(Fe_3O_4/PAH)_4$ capsules triggered by a HFMF, from 12 to 39 min (black squares). The control groups of $(PSS/PAH)_4$ capsules without magnetic iron incorporation under HFMF (blue triangle) and without HFMF (green triangle), and $(Fe_3O_4/PAH)_4$ capsules without HFMF treatment (red circles) are also shown.

Reprinted with permission from Ref. 167. Copyright (2008) American Chemical Society.

are promising for magnetically driven delivery of biomolecules.[169] Importantly, magnetically sensitive alginate-templated LbL microshells constructed for Dox delivery were less cytotoxic than Dox itself.[170] In addition to release through damage or rupture of the capsule walls, drug release can also occur due to a phase transition in the lipid membrane caused by heating of magnetic nanoparticles under magnetic stimuli, such as in the case of capsules composed of polyelectrolytes, magnetic nanoparticles and lipids.[171] Finally, microparticles with dual response to magnetic fields and laser radiation have been recently constructed by simultaneous incorporation of iron oxide and gold nanoparticles within LbL shells.[172]

17.5.9 Ultrasound-triggered Release

Ultrasound can also be used as a promising means for treatment and drug delivery.[173] Disruption of polymer layers under ultrasound treatment is due to the shear forces between the fluid layers. High power ultrasonic treatment (120 or 500 W, 20 kHz) of PAH/PSS[174,175] and Fe_3O_4 NP/PAH/PSS [175] capsules disrupted capsule walls and released the encapsulated material even at short (5 s) sonication times. PEMs with magnetite nanoparticles enable magnetic-field-assisted targeting of capsule to the desired site before ultrasonic treatment.[175]

It is important to minimize the intensity and time of ultrasound exposure to the safety level of a few W cm^{-2}.[176] Improved sensitivity of drug carriers to the ultrasound has been achieved, for example, by inclusion of ZnO nanoparticles within PAH/PSS capsules. In addition, incorporation of ZnO nanoparticles significantly increases their stiffness.[177] Under the same power and time of treatment conditions, the capsule wall disintegrated to much smaller shell residues as the fraction of ZnO nanoparticles within the multilayers increased.[177]

17.5.10 Application of Biological Stimuli

17.5.10.1 Sugar-induced Release

Engineering glucose-sensitive materials that release insulin in response to elevated levels of glucose in blood are central in the treatment of diabetes. Sensitivity of these materials to glucose is often provided through inclusion of a glucose-binding boronic moiety. Glucose-responsive LbL films and capsules were constructed by including, for example, glucose oxidase, lectin and phenylboronic acid.[178,179] LbL films of poly(vinyl alcohol) (PVA) and poly(acrylamide-co-3-(acrylamido)phenylboronic acid) have demonstrated sensitivity to 5–30 mM of glucose *via* enhanced film decomposition.[180] However, these films slowly decomposed even in the absence of glucose.[180] LbL capsules stable at normal glucose level (5 mM) were constructed from PSS and a copolymer containing phenylboronic acid moieties.[181] These capsules decomposed within 5 min in the presence of 27 mM glucose.[181] Another glucose-sensitive LbL system includes films and capsules built from PVA-borate and CHIT.[182] These capsules disintegrated within several hours in the presence of 25 mM glucose, and additionally allowed efficient loading of Dox for a combined targeting and treatment of cancer cells, which have higher glucose content.[182]

17.5.10.2 Enzymatic Degradation

PEMs susceptible to degradation by enzymes have also been explored. The fact that polypeptides and polysaccharides degrade into non-toxic, non-immunogenic monomeric products makes them specifically promising candidates for enzymatic drug delivery. For example, LbL films of CHIT and HA degradable by lysozyme and hyaluronidase have been constructed.[183] The rate of degradation of these films, as well as other biocompatible PLL/DNA multilayers,[184] could be significantly lowered by covalent cross-linking.[183] In the latter system, degradation of PLL/DNA film resulted in release of DNA. As in the case of hydrolytically degradable assembly, stability, permeability and degradation of enzymatically degradable LbL assemblies were strongly influenced by the nature of the polymers, as was demonstrated for PLL/HA and PAH/HA capsules stabilized by carbodiimide chemistry.[185] Higher sensitivity of the PLL/HA capsules to degradation by hyaluronidase was explained by weaker interactions between the polyelectrolytes as compared to the PAH/HA systems.[185]

Since the rate of enzymatic degradation depends on enzyme concentrations, multilayers can be advantageously used to regulate local enzyme concentration through enzyme adsorption at the LbL surface.[73] Larger amounts of chitosanase were adsorbed – for example at the DEXS-topped/CHIT multilayer – as a result of electrostatic interactions, as compared to CHIT-topped multilayer, leading to faster enzymatic degradation of the membrane of the capsules.[73] In another example, the degradation rate of DNA/PDADMAC films was controlled by the concentration of Ca^{2+} and Mg^{2+} affecting activity of DNase I.[186]

Control over incorporation depth of a drug within a multilayer, as well as over its released dose, can be achieved *via* a combination of enzymatic sensitivity with click-chemistry. For example, Dox was conjugated to alkyne-functionalized PLGA ($PLGA_{Alk}$). $PLGA_{Alk}$ and $PLGA_{Alk}$Dox were assembled with PVPON within LbL films at planar and colloidal silica templates. After film stabilization using diazide cross-linkers and PVPON release, Dox-loaded capsules were degraded enzymatically, showing sustained release of Dox over 2 h and *in vitro* anticancer activity.[88] Similar to hydrolytic degradation, the prodrug approach was also applied to enzymatically degrade LbL assemblies. For example, assembly of a Dox-polymer conjugate within LbL films at the surfaces of gold nanoparticles produced capsules responsive to the presence of lysosomal enzyme cathepsin B. Release of Dox selectively occurred from Dox-polymer conjugates with a specific amino acid sequence of an oligopeptide spacer, while the release rate was negligible in the case of linkers with a random amino acid sequence.[187] Enzymatic fragmentation of a model fluorescently labeled prodrug entrapped within biodegradable DEXS/poly-L-arginine (pARG) multilayers produced fluorescently labeled peptide fragments, and this occurred exclusively after capsule uptake by living cells, as the result of degradation by intra-cellular proteases (Figure 17.18).[188] In contrast, prodrug entrapped within non-degradable PAH/PSS capsules was not released after an incubation period of several days (Figure 17.18).[188] Enzymatic degradation of DEXS/pARG capsules was also used to deliver antigens and vaccines.[189,190]

17.6 LbL Interfacing Biology

Versatility and multi-functionality of LbL assemblies make them promising for coating of a broad variety of interfaces, and especially surfaces of biomedical devices.[191,192] Specific examples include coatings of biomedical implants, arteries, catheters and vessels. LbL assemblies with desired chemical composition, molecular architecture and mechanical properties can be constructed, which regulate surfaces interactions with cells and/or deliver bioactive compounds to surrounding tissues. For example, incorporation of growth factors within films of synthetic hydrolytically degradable polymers and/or biologically derived oppositely charged polyelectrolytes (such as heparin sulfate and chondroitin sulfate) significantly enhanced proliferation of

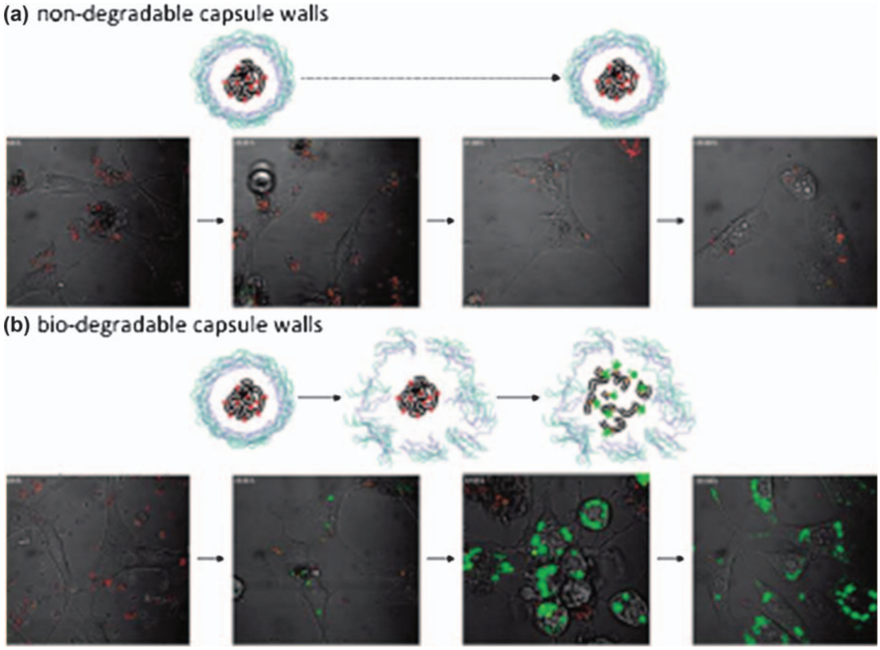
(a) non-degradable capsule walls
(b) bio-degradable capsule walls

Figure 17.18 Confocal microscope images taken immediately and during 2 h after addition of (a) non-degradable PSS/PAH or (b) degradable DEXS/pARG capsules loaded with a model fluorescently labeled prodrug to embryonic NIH/3T3 fibroblasts.
Reprinted with permission from Ref. 188. Copyright (2009) American Chemical Society.

MC3T3 preosteoblast cells.[193] In another example, LbL assemblies of PLL/pDNA[194] and CHIT/pDNA[195] on titanium significantly improved surface interactions with fibroblast and osteoblast cells, respectively. PEMs can also be used selectively to enrich cells *in vitro*. Fetal liver cells were successfully enriched and maintained by the PLGA/PLL surface coatings.[196] Specific modes of interaction between LbL coatings and biological matter are not yet completely understood, and significant advancement in the field can be achieved through additional experimentation.

Apart from their use as functional coatings, PEMs can also be used for growth and detachment of cell sheets.[197] The approach includes building a non-degradable support film (such as PAH/PSS) on top of a sacrificial precursor film, and the use of this construct as a substrate for cell growth. The sacrificial precursor film degrades in mild conditions, resulting in detachment of PEM-supported cell sheets.[197] This approach shows great potential for tissue repair and evaluation of novel therapeutic agents.

The field of 3D LbL assemblies has continued to flourish and evolve towards interfacing biology. A significant advantage of these multi-functional, responsive 3D constructs is that they can be conveniently targeted to specific cells or tissues *via* their surface modification with a ligand. For example, specific recognition of galactose-containing microcapsules by membrane galactose receptors has been reported.[198] Polyelectrolyte capsules expressing an antigen have also been used for targeting the delivery to colon cancer cells.[199]

One promising and not yet sufficiently explored application of PEMs is their use as skin patches for transdermal drug delivery. For example, LbL-based skin patches with film-incorporated ovalbumin (ova) and cytosine–phosphate diester–guanine-rich (CpG) oligonucleotides, enabled transdermal release of both biomolecules to Langerhans cells in two different time scales – with rapid release of ova, and sustained release of CpG.[200] Considering the relative simplicity and rapid progress made in the area of functional and stimuli-responsive LbL materials, this approach shows great potential for LbL-based delivery systems.

Acknowledgements

This research project has been partly supported by the National Science Foundation through grant #CBET-0708379. The authors thank Thomas Cattabiani (Stevens Institute of Technology) for his helpful comments on the chapter.

References

1. M. Delcea, H. Möhwald and A. G. Skirtach, *Adv. Drug Deliver. Rev.*, 2011, **63**, 730.
2. S. De Koker, L. J. De Cock, P. Rivera-Gil, W. J. Parak, R. Auzély Velty, C. Vervaet, J. P. Remon, J. Grooten and B. G. De Geest, *Adv. Drug Deliver. Rev.*, 2011, **63**, 748.
3. S. Pavlukhina and S. Sukhishvili, *Adv. Drug Deliver. Rev.*, 2011, **63**, 822.
4. K. Ariga, Y. M. Lvov, K. Kawakami, Q. Ji and J. P. Hill, *Adv. Drug Deliver. Rev.*, 2011, **63**, 762.
5. K. Ariga, J. P. Hill and Q. Ji, *Phys. Chem. Chem. Phys.*, 2007, **9**, 2319.
6. D. Zhou, A. Bruckbauer, M. Batchelor, D. J. Kang, C. Abell and D. Klenerman, *Langmuir*, 2004, **20**, 9089.
7. C. Peng, Y. S. Thio and R. A. Gerhardt, *Langmuir*, 2012, **28**, 84.
8. P. Laurent, G. Souharce, J. Duchet-Rumeau, D. Portinha and A. Charlot, *Soft Matter*, 2012, **8**, 715.
9. C. Déjugnat and G. B. Sukhorukov, *Langmuir*, 2004, **20**, 7265.
10. G. Schneider and G. Decher, *Nano Lett.*, 2004, **4**, 1833.
11. B. Neu, A. Voigt, R. Mitlöhner, S. Leporatti, C. Gao, E. Donath, H. Kiesewetter, H. Möhwald, H. Meiselman and H. Bäumler, *J. Microencapsulation*, 2001, **18**, 385.
12. C. S. Peyratout and L. Dähne, *Angew. Chem. Int. Ed.*, 2004, **43**, 3762.
13. A. G. Skirtach and O. Kreft, in *Nanotechnology in Drug Delivery*, M. M. de Villiers, P. Aramwit and G. S. Kwon (eds.), Springer, New York, 2009, p. 545.

14. C. M. Andres, M. L. Fox and N. A. Kotov, *Chem. Mater.*, 2012, **24**, 9.
15. O. Shchepelina, V. Kozlovskaya, E. Kharlampieva, W. Mao, A. Alexeev and V. V. Tsukruk, *Macromol. Rapid Commun.*, 2010, **31**, 2041.
16. O. Shchepelina, V. Kozlovskaya, S. Singamaneni, E. Kharlampieva and V. V. Tsukruk, *J. Mater. Chem.*, 2010, **20**, 6587.
17. X. Teng, D. G. Shchukin and H. Möhwald, *Adv. Funct. Mater.*, 2007, **17**, 1273.
18. X. R. Teng, D. G. Shchukin and H. Möhwald, *Langmuir*, 2008, **24**, 383.
19. Y. H. Cho, E. A. Decker and D. J. McClements, *Langmuir*, 2010, **26**, 7937.
20. F. Cavalieri, M. Ashokkumar, F. Grieser and F. Caruso, *Langmuir*, 2008, **24**, 10078.
21. H. Ai, S. A. Jones, M. M. de Villiers and Y. M. Lvov, *J. Control. Release*, 2003, **86**, 59.
22. X. Qiu, S. Leporatti, E. Donath and H. Möhwald, *Langmuir*, 2001, **17**, 5375.
23. Z. Zheng, X. Zhang, D. Carbo, C. Clark, C. A. Nathan and Y. Lvov, *Langmuir*, 2010, **26**, 7679.
24. A. Agarwal, Y. Lvov, R. Sawant and V. Torchilin, *J. Control. Release*, 2008, **128**, 255.
25. J. S. Rudra, K. Dave and D. T. Haynie, *J. Biomater. Sci. Polym. Ed.*, 2006, **17**, 1301.
26. O. Etienne, C. Gasnier, C. Taddei, J. C. Voegel, D. Aunis, P. Schaaf, M. H. Metz-Boutigue, A. L. Bolcato-Bellemin and C. Egles, *Biomaterials*, 2005, **26**, 6704.
27. A. Guyomard, E. Dé, T. Jouenne, J. J. Malandain, G. Muller and K. Glinel, *Adv. Funct. Mater.*, 2008, **18**, 758.
28. F. Boulmedais, B. Frisch, O. Etienne, P. Lavalle, C. Picart, J. Ogier, J. C. Voegel and P. Schaaf, *Biomaterials*, 2004, **25**, 2003.
29. A. Shukla, K. E. Fleming, H. F. Chuang, T. M. Chau, C. R. Loose, G. N. Stephanopoulos and P. T. Hammond, *Biomaterials*, 2010, **31**, 2348.
30. O. Etienne, C. Picart, C. Taddei, Y. Haikel, J. L. Dimarcq, P. Schaaf, J. C. Voegel, J. A. Ogier and C. Egles, *Antimicrob. Agents Chemother.*, 2004, **48**, 3662.
31. F. J. Pavinatto, L. Caseli and O. N. Oliveira, *Biomacromolecules*, 2010, **11**, 1897.
32. D. M. Lynn, *Soft Matter*, 2006, **2**, 269.
33. N. Reum, C. Fink-Straube, T. Klein, R. W. Hartmann, C. M. Lehr and M. Schneider, *Langmuir*, 2010, **26**, 16901.
34. K. Katagiri, K. Koumoto, S. Iseya, M. Sakai, A. Matsuda and F. Caruso, *Chem. Mater.*, 2009, **21**, 195.
35. J. P. deRocher, P. Mao, J. Y. Kim, J. Han, M. F. Rubner and R. E. Cohen, *ACS Appl. Mater. Interfaces*, 2012, **4**, 391.
36. A. M. Yashchenok, D. N. Bratashov, D. A. Gorin, M. V. Lomova, A. M. Pavlov, A. V. Sapelkin, B. S. Shim, G. B. Khomutov, N. A. Kotov, G. B. Sukhorukov, H. Möhwald and A. G. Skirtach, *Adv. Funct. Mater.*, 2010, **20**, 3136.

37. Z. Zhu and S. A. Sukhishvili, *J. Mater. Chem.*, 2012, **22**, 7667.
38. P. J. Yoo, K. T. Nam, J. Qi, S. K. Lee, J. Park, A. M. Belcher and P. T. Hammond, *Nat. Mater.*, 2006, **5**, 234.
39. B. Städler, R. Chandrawati, K. Goldie and F. Caruso, *Langmuir*, 2009, **25**, 6725.
40. Y. H. Jiao, Y. Li, S. Wang, K. Zhang, Y. G. Jia and Y. Fu, *Langmuir*, 2010, **26**, 8270.
41. N. D. Bassim, W. J. Dressick, K. P. Fears, R. M. Stroud, T. D. Clark and D. Y. Petrovykh, *J. Phys. Chem. C*, 2012, **116**, 1694.
42. M. F. Bédard, A. Munoz-Javier, R. Mueller, P. del Pino, A. Fery, W. J. Parak, A. G. Skirtach and G. B. Sukhorukov, *Soft Matter*, 2009, **5**, 148.
43. B. S. Shim, J. Zhu, E. Jan, K. Critchley, S. Ho, P. Podsiadlo, K. Sun and N. A. Kotov, *ACS Nano*, 2009, **3**, 1711.
44. E. Kharlampieva and V. Kozlovskaya, B. Wallet, V. V. Shevchenko, R. R. Naik, R. Vaia, D. L. Kaplan and V. V. Tsukruk, *ACS Nano*, 2010, **4**, 7053.
45. Z. Tang, N. A. Kotov, S. Magonov and B. Ozturk, *Nat. Mater.*, 2003, **2**, 413.
46. A. Muñoz Javier, O. Kreft, M. Semmling, S. Kempter, A. G. Skirtach, O. T. Bruns, P. del Pino, M. F. Bedard, J. Rädler, J. Käs, C. Plank, G. B. Sukhorukov and W. J. Parak, *Adv. Mater.*, 2008, **20**, 4281.
47. T. Addison, O. J. Cayre, S. Biggs, S. P. Armes and D. York, *Langmuir*, 2010, **26**, 6281.
48. F. Cavalieri, A. Postma, L. Lee and F. Caruso, *ACS Nano*, 2009, **3**, 234.
49. X. Li, T. Lu, J. Zhang, J. Xu, Q. Hu, S. Zhao and J. Shen, *Acta Biomater.*, 2009, **5**, 2122.
50. D. V. Volodkin, P. Schaaf, H. Mohwald, J. C. Voegel and V. Ball, *Soft Matter*, 2009, **5**, 1394.
51. Z. S. Haidar, R. C. Hamdy and M. Tabrizian, *Biomaterials*, 2008, **29**, 1207.
52. Z. S. Haidar, R. C. Hamdy and M. Tabrizian, *Biomaterials*, 2010, **31**, 2746.
53. Y. Fukui and K. Fujimoto, *Langmuir*, 2009, **25**, 10020.
54. J. F. Pereira da Silva, A. Gomes, A. Rank, J. Kronenberger, M. Fritz, Winterhalter and Y. Ramaye, *Langmuir*, 2009, **25**, 6793.
55. N. Graf, E. Thomasson, A. Tanno, J. Vörös and T. Zambelli, *J. Phys. Chem. B*, 2011, **115**, 12386.
56. H. Zhang, Z. Wang, Y. Zhang and X. Zhang, *Langmuir*, 2004, **20**, 9366.
57. J. Bai, S. Beyer, W. C. Mak and D. Trau, *Soft Matter*, 2009, **5**, 4152.
58. B. G. De Geest, S. De Koker, K. Immesoete, J. Demeester, S. C. De Smedt and W. E. Hennink, *Adv. Mater.*, 2008, **20**, 3687.
59. Q. Ji, M. Miyahara, J. P. Hill, S. Acharya, A. Vinu, S. B. Yoon, J. S. Yu, K. Sakamoto and K. Ariga, *J. Am. Chem. Soc.*, 2008, **130**, 2376.
60. Q. Ji, S. Acharya, J. P. Hill, A. Vinu, S. B. Yoon, J. S. Yu, K. Sakamoto and K. Ariga, *Adv. Funct. Mater.*, 2009, **19**, 1792.

61. M. Delcea, A. Yashchenok, K. Videnova, O. Kreft, H. Möhwald and A. G. Skirtach, *Macromol. Biosci.*, 2010, **10**, 465.
62. M. Dimitrova, C. Affolter, F. Meyer, I. Nguyen, D. G. Richard, C. Schuster, R. Bartenschlager, J. C. Voegel, J. Ogier and T. F. Baumert, *P. Natl. Acad. Sci. USA*, 2008, **105**, 16320.
63. R. C. Smith, M. Riollano, A. Leung and P. T. Hammond, *Angew. Chem.*, 2009, **121**, 9136.
64. G. B. Sukhorukov, D. V. Volodkin, A. M. Gu and A. I. Petrov, *J. Mater. Chem.*, 2004, **14**, 2073.
65. S. Pavlukhina, Y. Lu, A. Patimetha, M. Libera and S. Sukhishvili, *Biomacromolecules*, 2010, **11**, 3448.
66. K. Köhler, D. G. Shchukin, H. Möhwald and G. B. Sukhorukov, *J. Phys. Chem. B*, 2005, **109**, 18250.
67. K. Köhler, H. Möhwald and G. B. Sukhorukov, *J. Phys. Chem. B*, 2006, **110**, 24002.
68. C. Déjugnat, K. Köhler, M. Dubois, G. B. Sukhorukov, H. Möhwald, T. Zemb and P. Guttmann, *Adv. Mater.*, 2007, **19**, 1331.
69. R. Palankar, A. G. Skirtach, O. Kreft, M. Bédard, M. Garstka, K. Gould, H. Möhwald, G. B. Sukhorukov, M. Winterhalter and S. Springer, *Small*, 2009, **5**, 2168.
70. A. N. Zelikin, A. L. Becker, A. P. R. Johnston, K. L. Wark, F. Turatti and F. Caruso, *ACS Nano*, 2007, **1**, 63.
71. A. N. Zelikin, Q. Li and F. Caruso, *Angew. Chem. Int. Ed.*, 2006, **45**, 7743.
72. A. D. Price, A. N. Zelikin, Y. Wang and F. Caruso, *Angew. Chem. Int. Ed.*, 2009, **48**, 329.
73. Y. Itoh, M. Matsusaki, T. Kida and M. Akashi, *Biomacromolecules*, 2006, **7**, 2715.
74. A. Yu, Y. Wang, E. Barlow and F. Caruso, *Adv. Mater.*, 2005, **17**, 1737.
75. A. Elbakry, A. Zaky, R. Liebl, R. Rachel, A. Goepferich and M. Breunig, *Nano Lett.*, 2009, **9**, 2059.
76. B. G. De Geest, N. N. Sanders, G. B. Sukhorukov, J. Demeester and S. C. De Smedt, *Chem. Soc. Rev.*, 2007, **36**, 636.
77. B. P. Timko, T. Dvir and D. S. Kohane, *Adv. Mater.*, 2010, **22**, 4925.
78. M. C. Berg, L. Zhai, R. E. Cohen and M. F. Rubner, *Biomacromolecules*, 2006, **7**, 357.
79. X. Wang, L. Zhang, L. Wang, J. Sun and J. Shen, *Langmuir*, 2010, **26**, 8187.
80. U. Manna and S. Patil, *Langmuir*, 2009, **25**, 10515.
81. K. C. Wood and H. F. Chuang, R. D. Batten, D. M. Lynn and P. T. Hammond, *P. Natl. Acad. Sci. USA*, 2006, **103**, 10207.
82. J. Hong, N. J. Shah, A. C. Drake, P. C. Demuth, J. B. Lee, J. Chen and P. T. Hammond, *ACS Nano*, 2012, **6**, 81.
83. B. Han, B. Shen, Z. Wang, M. Shi, H. Li, C. Peng, Q. Zhao and C. Gao, *Polym. Adv. Technol.*, 2008, **19**, 36.

84. L. J. De Cock, O. De Wever, S. Van Vlierberghe, E. Vanderleyden, P. Dubruel, F. De Vos, C. Vervaet, J. P. Remon and B. G. De Geest, *Soft Matter*, 2012, **8**, 1146.
85. B. S. Kim, R. C. Smith, Z. Poon and P. T. Hammond, *Langmuir*, 2009, **25**, 14086.
86. T. Soike, A. K. Streff, C. Guan, R. Ortega, M. Tantawy, C. Pino and V. P. Shastri, *Adv. Mater.*, 2010, **22**, 1392.
87. B. G. De Geest, W. Van Camp, F. E. Du Prez, S. C. De Smedt, J. Demeester and W. E. Hennink, *Macromol. Rapid Commun.*, 2008, **29**, 1111.
88. C. J. Ochs, G. K. Such, Y. Yan, M. P. van Koeverden and F. Caruso, *ACS Nano*, 2010, **4**, 1653.
89. H. F. Chuang, R. C. Smith and P. T. Hammond, *Biomacromolecules*, 2008, **9**, 1660.
90. J. S. Moskowitz, M. R. Blaisse, R. E. Samuel, H. P. Hsu, M. B. Harris, S. D. Martin, J. C. Lee, M. Spector and P. T. Hammond, *Biomaterials*, 2010, **31**, 6019.
91. C. M. Jewell and D. M. Lynn, *Adv. Drug Deliver Rev.*, 2008, **60**, 979.
92. S. L. Bechler and D. M. Lynn, *Biomacromolecules*, 2012, **13**, 542.
93. S. Y. Wong, J. S. Moskowitz, J. Veselinovic, R. A. Rosario, K. Timachova, M. R. Blaisse, R. C. Fuller, A. M. Klibanov and P. T. Hammond, *J. Am. Chem. Soc.*, 2010, **132**, 17840.
94. A. Shukla, R. C. Fuller and P. T. Hammond, *J. Control. Release*, 2011, **155**, 159.
95. N. J. Shah, M. L. Macdonald, Y. M. Beben, R. F. Padera, R. E. Samuel and P. T. Hammond, *Biomaterials*, 2011, **32**, 6183.
96. J. Zhang, L. S. Chua and D. M. Lynn, *Langmuir*, 2004, **20**, 8015.
97. E. M. Saurer, C. M. Jewell, J. M. Kuchenreuther and D. M. Lynn, *Acta Biomater.*, 2009, **5**, 913.
98. E. M. Saurer, R. M. Flessner, S. P. Sullivan, M. R. Prausnitz and D. M. Lynn, *Biomacromolecules*, 2010, **11**, 3136.
99. J. Zhang, N. Fredin, J. Janz and B. Sun, *Langmuir*, 2006, **22**, 239.
100. R. C. Smith, A. Leung, B. S. Kim and P. T. Hammond, *Chem. Mater.*, 2009, **21**, 1108.
101. B. S. Kim, S. W. Park and P. T. Hammond, *ACS Nano*, 2008, **2**, 386.
102. J. Zhang and D. M. Lynn, *Adv. Mater.*, 2007, **19**, 4218.
103. X. Liu, J. Zhang and D. M. Lynn, *Soft Matter*, 2008, **4**, 1688.
104. B. Thierry, P. Kujawa, C. Tkaczyk, F. M. Winnik, L. Bilodeau and M. Tabrizian, *J. Am. Chem. Soc.*, 2005, **127**, 1626.
105. Y. Cao and W. He, *Biomacromolecules*, 2010, **11**, 1298.
106. B. G. De Geest, C. Déjugnat, G. B. Sukhorukov, K. Braeckmans, S. C. De Smedt and J. Demeester, *Adv. Mater.*, 2005, **17**, 2357.
107. B. G. De Geest, S. De Koker, J. Demeester, S. C. De Smedt and W. E. Hennink, *J. Control. Release*, 2009, **135**, 268.
108. S. T. Dubas and J. B. Schlenoff, *Macromolecules*, 2001, **34**, 3736.

109. T. Mauser, C. Déjugnat and G. B. Sukhorukov, *Macromol. Rapid Commun.*, 2004, **25**, 1781.
110. E. Kharlampieva, V. Kozlovskaya and S. A. Sukhishvili, *Adv. Mater.*, 2009, **21**, 3053.
111. S. Tomita, K. Sato and J. Anzai, *J. Colloid Interface Sci.*, 2008, **326**, 35.
112. A. Zhuk, S. Pavlukhina and S. A. Sukhishvili, *Langmuir*, 2009, **25**, 14025.
113. S. Y. Yang and M. F. Rubner, *J. Am. Chem. Soc.*, 2002, **124**, 2100.
114. E. Kharlampieva, I. Erel-Unal and S. A. Sukhishvili, *Langmuir*, 2007, **23**, 175.
115. J. Niu, F. Shi, Z. Liu, Z. Wang and X. Zhang, *Langmuir*, 2007, **23**, 6377.
116. T. Serizawa, D. Matsukuma and M. Akashi, *Langmuir*, 2005, **21**, 7739.
117. H. Sato, R. Okuda, A. Sugiyama, M. Hamatsu and J. I. Anzai, *Mater. Sci. Eng. C*, 2009, **29**, 1057.
118. B. Jiang and B. Li, *Int. J. Nanomedicine*, 2009, **4**, 37.
119. M. G. Kellum, C. A. Harris, C. L. Mccormick and S. E. Morgan, *J. Polym. Sci. A Polym. Chem.*, 2010, **49**, 1104.
120. Z. An, H. Möhwald and J. Li, *Biomacromolecules*, 2006, **7**, 580.
121. V. Kozlovskaya, E. Kharlampieva, I. Drachuk, D. Cheng and V. V. Tsukruk, *Soft Matter*, 2010, **6**, 3596.
122. Y. Wang and F. Caruso, *Chem. Mater.*, 2006, **18**, 4089.
123. S. Shu, C. Sun, X. Zhang, Z. Wu, Z. Wang and C. Li, *Acta Biomater.*, 2010, **6**, 210.
124. C. Basset, C. Harder, C. Vidaud and C. Déjugnat, *Biomacromolecules*, 2010, **11**, 806.
125. P. Chaturbedy, D. Jagadeesan and M. Eswaramoorthy, *ACS Nano*, 2010, **4**, 5921.
126. B. G. De Geest, R. E. Vandenbroucke, A. M. Guenther, G. B. Sukhorukov, W. E. Hennink, N. N. Sanders, J. Demeester and S. C. De Smedt, *Adv. Mater.*, 2006, **18**, 1005.
127. B. Mu, P. Liu, Y. Dong and C. Lu, *J. Polym. Sci. A Polym. Chem.*, 2010, **48**, 3135.
128. N. Ma, F. Tang, X. Wang, F. He and L. Li, *Macromol. Rapid Commun.*, 2011, **32**, 587.
129. A. A. Antipov, G. B. Sukhorukov and H. Mo, *Small*, 2003, **19**, 2444.
130. A. Fery, B. Schöler, T. Cassagneau and F. Caruso, *Langmuir*, 2001, **17**, 3779.
131. R. A. McAloney, M. Sinyor, V. Dudnik and M. C. Goh, *Langmuir*, 2001, **17**, 6655.
132. H. Mjahed, J. C. Voegel, B. Senger, A. Chassepot, A. Rameau, V. Ball, P. Schaaf and F. Boulmedais, *Soft Matter*, 2009, **5**, 2269.
133. C. Gao, H. Möhwald and J. C. Shen, *ChemPhysChem*, 2004, **5**, 116.
134. R. Zhang, K. Köhler, O. Kreft, A. Skirtach, H. Möhwald and G. Sukhorukov, *Soft Matter*, 2010, **6**, 4742.
135. Y. Zhong, C. F. Whittington, L. Zhang and D. T. Haynie, *Nanomedicine NBM*, 2007, **3**, 154.

136. M. Gabi, T. Sannomiya, A. Larmagnac, M. Puttaswamy and J. Vörös, *Integr. Biol.*, 2009, **1**, 108.
137. F. Boulmedais, C. S. Tang, B. Keller and J. Vörös, *Adv. Funct. Mater.*, 2006, **16**, 63.
138. H. Sato, Y. Takano and K. Sato, and J. Anzai, *J. Colloid Interface Sci.*, 2009, **333**, 141.
139. L. Diéguez, N. Darwish, N. Graf, J. Vörös and T. Zambelli, *Soft Matter*, 2009, **5**, 2415.
140. K. C. Wood, N. S. Zacharia, D. J. Schmidt, S. N. Wrightman, B. J. Andaya and P. T. Hammond, *P. Natl. Acad. Sci. USA*, 2008, **105**, 2280.
141. O. Guillaume-Gentil, N. Graf, F. Boulmedais, P. Schaaf, J. Vörös and T. Zambelli, *Soft Matter*, 2010, **6**, 4246.
142. N. Graf, F. Albertini, T. Petit, E. Reimhult, J. Vörös and T. Zambelli, *Adv. Funct. Mater.*, 2011, **21**, 1666.
143. Y. Ma, W. F. Dong, M. A. Hempenius, H. Möhwald and G. J. Vancso, *Nat. Mater.*, 2006, **5**, 724.
144. S. Shu, X. Zhang, Z. Wu, Z. Wang and C. Li, *Biomaterials*, 2010, **31**, 6039.
145. D. T. Haynie, N. Palath, Y. Liu, B. Li and N. Pargaonkar, *Langmuir*, 2005, **21**, 1136.
146. B. Li and D. T. Haynie, *Biomacromolecules*, 2004, **5**, 1667.
147. S. F. Chong, A. Sexton, R. De Rose, S. J. Kent, A. N. Zelikin and F. Caruso, *Biomaterials*, 2009, **30**, 5178.
148. J. Blacklock, G. Mao, D. Oupický and H. Möhwald, *Langmuir*, 2010, **26**, 8597.
149. Z. Zhu and S. A. Sukhishvili, *ACS Nano*, 2009, **3**, 3595.
150. L. Xu, Z. Zhu and S. A. Sukhishvili, *Langmuir*, 2011, **27**, 409.
151. S. Utsel, E. E. Malmström, A. Carlmark and L. Wågberg, *Soft Matter*, 2010, **6**, 342.
152. I. Erel, H. E. Karahan, C. Tuncer, V. Bütün and A. L. Demirel, *Soft Matter*, 2012, **8**, 827.
153. P. Rai, S. Mallidi, X. Zheng, R. Rahmanzadeh, Y. Mir, S. Elrington, A. Khurshid and T. Hasan, *Adv. Drug Deliver. Rev.*, 2010, **62**, 1094.
154. X. Tao, J. Li and H. Möhwald, *Chem. Eur. J.*, 2004, **10**, 3397.
155. A. G. Skirtach, A. A. Antipov, D. G. Shchukin and G. B. Sukhorukov, *Langmuir*, 2004, **20**, 6988.
156. A. G. Skirtach, P. Karageorgiev, B. G. De Geest, N. Pazos-Perez, D. Braun and G. B. Sukhorukov, *Adv. Mater.*, 2008, **20**, 506.
157. M. F. Bédard, D. Braun, G. B. Sukhorukov and A. G. Skirtach, *ACS Nano*, 2008, **2**, 1807.
158. B. Radt, T. A. Smith and F. Caruso, *Adv. Mater.*, 2004, **16**, 2184.
159. A. S. Angelatos, B. Radt and F. Caruso, *J. Phys. Chem. B*, 2005, **109**, 3071.
160. B. G. De Geest, A. G. Skirtach, T. R. M. De Beer, G. B. Sukhorukov, L. Bracke, W. R. G. Baeyens, J. Demeester and S. C. De Smedt, *Macromol. Rapid Commun.*, 2007, **28**, 88.

161. A. G. Skirtach, P. Karageorgiev, M. F. Bédard, G. B. Sukhorukov and H. Möhwald, *J. Am. Chem. Soc.*, 2008, **130**, 11572.
162. D. V. Volodkin, M. Delcea, H. Möhwald and A. G. Skirtach, *ACS Appl. Mater. Interfaces*, 2009, **1**, 1705.
163. M. Bédard, A. G. Skirtach and G. B. Sukhorukov, *Macromol. Rapid Commun.*, 2007, **28**, 1517.
164. K. Wang, Q. He, X. Yan, Y. Cui, W. Qi, L. Duan and J. Li, *J. Mater. Chem.*, 2007, **17**, 4018.
165. M. F. Bédard, S. Sadasivan, G. B. Sukhorukov and A. Skirtach, *J. Mater. Chem.*, 2009, **19**, 2226.
166. H. Y. Koo, H. J. Lee, J. K. Kim and W. S. Choi, *J. Mater. Chem.*, 2010, **20**, 3932.
167. S. H. Hu, C. H. Tsai, C. F. Liao, D. M. Liu and S. Y. Chen, *Langmuir*, 2008, **24**, 11811.
168. H. Ai, *Adv. Drug Deliver. Rev.*, 2011, **63**, 772.
169. Y. Han, D. Radziuk, D. Shchukin and H. Moehwald, *Macromol. Rapid Commun.*, 2008, **29**, 1203.
170. J. Liu, Y. Zhang, C. Wang, R. Xu, Z. Chen and N. Gu, *J. Phys. Chem. C*, 2010, **114**, 7673.
171. K. Katagiri, M. Nakamura and K. Koumoto, *ACS Appl. Mater. Interfaces*, 2010, **2**, 768.
172. D. A. Gorin, S. A. Portnov, O. A. Inozemtseva, Z. Luklinska, A. M. Yashchenok, A. M. Pavlov, A. G. Skirtach, H. Möhwald and G. B. Sukhorukov, *Phys. Chem. Chem. Phys.*, 2008, **10**, 6899.
173. M. N. Antipina and G. B. Sukhorukov, *Adv. Drug Deliver. Rev.*, 2011, **63**, 716.
174. A. G. Skirtach, B. G. De Geest, A. Mamedov, A. A. Antipov, N. A. Kotov and G. B. Sukhorukov, *J. Mater. Chem.*, 2007, **17**, 1050.
175. D. G. Shchukin, D. A. Gorin and H. Möhwald, *Langmuir*, 2006, **22**, 7400.
176. S. B. Barnett, G. R. Ter Haar, M. C. Ziskin, H. D. Rott, F. A. Duck and K. Maeda, *Ultrasound Med. Biol.*, 2000, **26**, 355.
177. T. A. Kolesnikova, D. A. Gorin, P. Fernandes, S. Kessel, G. B. Khomutov, A. Fery, D. G. Shchukin and H. Möhwald, *Adv. Funct. Mater.*, 2010, **20**, 1189.
178. K. Sato, K. Yoshida, S. Takahashi and J. I. Anzai, *Adv. Drug Deliver. Rev.*, 2011, **63**, 809.
179. W. Qi, L. Duan and J. Li, *Soft Matter*, 2011, **7**, 1571.
180. Z. Ding, Y. Guan, Y. Zhang and X. X. Zhu, *Soft Matter*, 2009, **5**, 2302.
181. B. G. De Geest, A. M. Jonas, J. Demeester and S. C. De Smedt, *Langmuir*, 2006, **22**, 5070.
182. U. Manna and S. Patil, *ACS Appl. Mater. Interfaces*, 2010, **2**, 1521.
183. C. Picart, A. Schneider and O. Etienne, J. Mutterer, P. Schaaf, C. Egles, N. Jessel and J. C. Voegel, *Adv. Funct. Mater.*, 2005, **15**, 1771.
184. K. Ren, J. Ji and J. Shen, *Bioconjugate Chem.*, 2006, **17**, 77.
185. A. Szarpak, D. Cui, F. Dubreuil, B. G. De Geest, L. J. De Cock, C. Picart and R. Auzély-Velty, *Biomacromolecules*, 2010, **11**, 713.

186. T. Serizawa, M. Yamaguchi and M. Akashi, *Angew. Chem. Int. Ed.*, 2003, **42**, 1115.
187. G. F. Schneider, V. Subr, K. Ulbrich and G. Decher, *Nano Lett.*, 2009, **9**, 636.
188. P. Rivera-Gil, S. De Koker, B. G. De Geest and W. J. Parak, *Nano Lett.*, 2009, **9**, 4398.
189. S. De Koker, B. G. De Geest, S. K. Singh, R. De Rycke, T. Naessens, Y. Van Kooyk, J. Demeester, S. C. De Smedt and J. Grooten, *Angew. Chem. Int. Ed.*, 2009, **48**, 8485.
190. S. De Koker, T. Naessens, B. G. De Geest, P. Bogaert, J. Demeester, S. De Smedt and J. Grooten, *J. Immunol.*, 2010, **184**, 203.
191. V. Gribova, R. Auzely-Velty and C. Picart, *Chem. Mater.*, 2012, **24**, 854.
192. H. Kerdjoudj, N. Berthelemy, F. Boulmedais, J. F. Stoltz, P. Menu and J. C. Voegel, *Soft Matter*, 2010, **6**, 3722.
193. M. L. Macdonald, N. M. Rodriguez, N. J. Shah and P. T. Hammond, *Biomacromolecules*, 2010, **11**, 2053.
194. J. J. J. P. van den Beucken, M. R. J. Vos, P. C. Thüne, T. Hayakawa, T. Fukushima, Y. Okahata, X. F. Walboomers, N. A. J. M. Sommerdijk, R. J. M. Nolte and J. A. Jansen, *Biomaterials*, 2006, **27**, 691.
195. Y. Hu, K. Cai, Z. Luo, R. Zhang, L. Yang, L. Deng and K. D. Jandt, *Biomaterials*, 2009, **30**, 3626.
196. H. A. Tsai, R. R. Wu, I. C. Lee, H. Y. Chang, C. N. Shen and Y. C. Chang, *Biomacromolecules*, 2010, **11**, 994.
197. A. Chassepot, L. Gao, I. Nguyen, A. Dochter, F. Fioretti, P. Menu, H. Kerdjoudj, C. Baehr, P. Schaaf, J.-Claude Voegel, F. Boulmedais, B. Frisch and J. Ogier, *Chem. Mater.*, 2012, **24**, 930.
198. F. Zhang, Q. Wu, Z. C. Chen, M. Zhang and X. F. Lin, *J. Colloid Interface Sci.*, 2008, **317**, 477.
199. C. Cortez, E. Tomaskovic-Crook, A. P. R. Johnston, B. Radt, S. H. Cody, A. M. Scott, E. C. Nice, J. K. Heath and F. Caruso, *Adv. Mater.*, 2006, **18**, 1998.
200. X. Su, B. S. Kim, S. R. Kim, P. T. Hammond and D. J. Irvine, *ACS Nano*, 2009, **3**, 3719.

CHAPTER 18

pH- and Temperature-responsive Hydrogels in Drug Delivery

FRANCESCO PUOCI* AND MANUELA CURCIO

Department of Pharmaceutical Sciences, University of Calabria, Edificio Polifunzionale, Arcavacata di Rende (CS), 87036 Italy
*Email: francesco.puoci@unical.it

18.1 Introduction

Over the past two decades, controlled drug-delivery research has been focused on two main challenges. The first one was to obtain sustained zero-order release of therapeutic agents over a prolonged period of time. This goal has been achieved for a wide range of systems, including matrices with controllable swelling,[1] diffusion[2] or erosion rate.[3] Even though these systems are therapeutically advantageous over the conventional systems, they are not always effective from a pharmacological point of view because they remain insensitive to the biorhythms and the pathological changes in the body. The need to obtain materials able to respond to changes in the local environment prompted the second challenge, which aims to fabricate stimuli-responsive materials able to respond to changes in temperature, pH or concentration of specific molecules.[4] The purpose is to synchronize drug release profiles with the modifications of physiological conditions and to mimic the behavior of macromolecular systems constituting living tissues, *i.e.* proteins, polysaccharides and nucleic acids, which are stable along a wide range of external parameters, such as pH or temperature, but undergo drastic conformational changes upon narrow variation of these variables around a given critical point.[5] Release of hormones is an important example of the ability of the body to respond to the variation of

---

RSC Smart Materials No. 3
Smart Materials for Drug Delivery: Volume 2
Edited by Carmen Alvarez-Lorenzo and Angel Concheiro
© The Royal Society of Chemistry 2013
Published by the Royal Society of Chemistry, www.rsc.org

the surrounding environment; in fact, in this process, a baseline release is combined with pulsed, one-shot type release within a short time range.[6,7] The distinguishing characteristic of the stimuli-responsive materials is their ability to undergo rapid changes in their microstructure from a hydrophilic to a hydrophobic state, which are triggered by small perturbations in the environment. The macroscopic changes that occur are reversible; namely, the materials are capable of returning to the initial state when the trigger is removed.[8,9]

Soft materials, such as hydrogels, have attracted great attention in the field of smart drug-delivery systems, due to their versatility and their unique properties, such as the high water content and soft and rubbery consistency that make them similar to natural tissues. Depending on the preparation method, hydrogels with different sizes and shapes can be obtained. Microgels are cross-linked hydrogel particles that are confined to small dimensions, while nanogels are characterized by their submicron size. Microgels and nanogels have a high water content, a large surface area for multi-valent bioconjugation and an interior network for the incorporation of therapeutics. These unique properties offer great potential for their utilization in many fields, such as tissue engineering,[10] bionanotechnology[11] and drug delivery.[12] If synthesized with suitable functionalities, the so-called "smart" or "intelligent" hydrogels can be obtained. These kinds of materials are able to modify their size/shape through abrupt changes in the physical nature of the network in response to external or internal stimuli. Externally controlled stimuli, such as temperature, light, pressure, sound and electric and magnetic fields, are produced with the help of different stimuli-generating devices, ultimately resulting in pulsed drug delivery.[13] Internally regulated systems, however, include those responding to the variations of internal body parameters, such as temperature, pH, ionic strength, redox state and specific molecular recognition events. They are also known as self-regulated devices, and the release rate is controlled by a feedback mechanism produced within the body that leads to structural changes in the polymer network, without any external intervention.

Hydrogels able to respond to pH and temperature signals have been the most widely investigated. This is firstly because many physiological and pathological conditions are accompanied by variations of pH and/or temperature. Modifications of pH are indeed found along the gastrointestinal tract and in certain tissues, tumoral and infected areas and subcellular compartments, while the body temperature can be altered by several pathological conditions, including infections and other diseases. Secondly, pH and temperature can be easily registered or even manipulated under both *in vitro* and *in vivo* conditions.[14,15] It follows that hydrogels able to dramatically respond to one or both of these signals are very useful in biomedical applications such as controlled release of drugs. This chapter is an overview of the recent research on pH- and temperature-sensitive micro- and nanogels, principally, and their application as drug carriers. Dually pH- and temperature-responsive materials and their potential use as drug-delivery systems are also discussed.

18.2 pH-responsive Hydrogels for Drug Delivery

pH-responsive materials are polyelectrolytes characterized by bearing ionizable weak acidic or basic moieties attached to a hydrophobic backbone able to swell or collapse in response to the pH variation in the surrounding environment. Poly(acrylic acid) (PAA) and poly(methacrylic acid) (PMAA) are commonly used polyacids, while poly(*N*,*N*′-dimethyl aminoethyl methacrylate) (PDMAEMA) and poly(*N*,*N*′-diethyl aminoethyl methacrylate) (PDEAEMA) are typical examples of pH-sensitive polybases (Figure 18.1). If a pH variation around the pK_a value of the functional group occurs, electrostatic repulsive forces are generated, leading to an increase in the hydrodynamic volume of the polymeric hydrogel (*i.e.* swelling). For example, the carboxylic pendant groups of PAA accept protons at pH below its pK_a (4.28), releasing them at greater pH values. As a consequence, when the hydrogel passes from a deionized to an ionized state, the increase in hydrophilicity and the repulsion among equally charged groups make the network increase its hydrodynamic volume and, hence, the degree of swelling (Figure 18.2a). The opposite behavior is observed for PDMAEMA; *i.e.*, the hydrogel. The hydrogel enhances its hydrodynamic volume at low pH, when the amino groups are protonated, becoming swollen (Figure 18.2b).

The most common application of the pH-sensitive hydrogels is the oral delivery of drugs and peptides, due to their ability to respond to the abrupt pH modification that occurs from the stomach (pH 2) to the intestine (pH 5–8).[16] However, their properties can be exploited in many other physiological or pathological conditions characterized by changes in pH. Thus, they are potentially useful for the targeting of drugs to tumor cells, because the extracellular space of cancer tissues has a pH range from 6.5 to 7.2, thus slightly lower than the healthy pH 7.4,[17,18] or in the treatment of chronic wounds that exhibit pH values ranging from 7.4 and 5.4.[19] The most recent research about

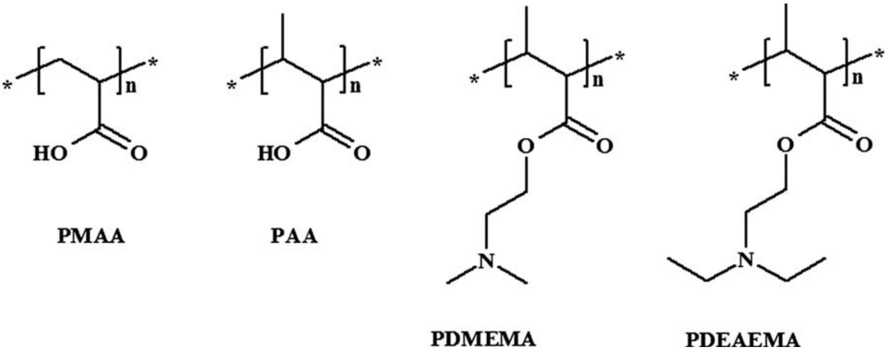

Figure 18.1 Structure of some polyacids (poly(methacrylic acid) (PMAA) and poly(acrylic acid) (PAA), and polybases (poly(*N*,*N*′-dimethyl aminoethyl methacrylate) (PDMAEMA) and poly(*N*,*N*′-diethyl aminoethyl methacrylate) (PDEAEMA), commonly used for preparing pH-responsive networks.

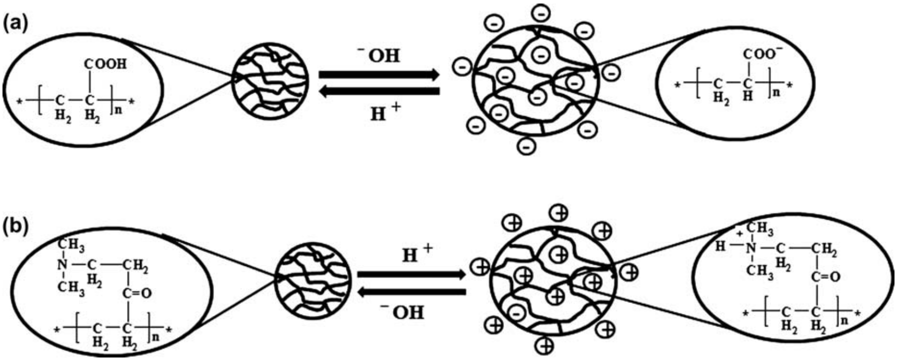

Figure 18.2 Schematic view of the effect of a pH change on the swelling of poly(acrylic acid), PAA, (a) and poly(*N*,*N*′-dimethyl aminoethyl methacrylate), PDMAEMA, (b) hydrogels.

pH-responsive hydrogels with particular attention to their applicability as drug-delivery systems is summarized below.

18.2.1 pH-responsive Microgels

Most anionic pH-responsive microgels are based on PAA and its derivatives, and mostly intended for oral drug administration. Morishita *et al.*[20] prepared pH-responsive microparticles based on poly(methacrylic acid-g-ethylene glycol) (PMAA-g-EG) to be used as carriers of insulin. Due to the chemical nature of the hydrogel, insulin release was significantly retarded in acidic media, while rapid release occurred under neutral/basic conditions. In a more recent work,[21] pH-responsive hydrogels based on methacrylic acid (MAA) grafted on poly(ethylene oxide)-poly(vinylpyrrolidone) (PEO-PVP) networks were synthesized by means of electron beam irradiation. The grafted hydrogels showed pH- and composition-dependent swelling behavior. The suitability of these gels as matrix materials for stimuli-responsive sustained-release drug formulations was evaluated by performing *in vitro* assays with an antihypertensive drug, metoprolol tartarate, at pH 1.2 and 7.4. The extent of drug release was found to be pH-dependent and the kinetics, after fitting the profiles to Korsemeyer and Peppas's equation, indicated that the anomalous diffusion was the main release mechanism. The applicability of pH-responsive poly(methacrylic acid-co-ethylene glycol dimethacrylate) (PMAA-co-EGDMA) hydrogel microparticles as intelligent delivery carriers for ascorbic acid was also demonstrated.[22] A drastic change in the swelling ratio of these microparticles was observed at pH 5. As the MAA proportion in the hydrogel increased, a greater degree of swelling was observed at pH above 5. It was found that the loading efficiency of the ascorbic acid into the hydrogel was affected more by the degree of swelling than by the hydrogel/ascorbic acid electrostatic interactions. The (PMAA-co-EGMA) microgels showed a pH-sensitive release behavior. Thus, at pH 4, almost no ascorbic acid permeated through the microgels, while at pH 6 relatively high permeability was observed. pH-sensitive hydrogels based on MAA and poly(ethylene glycol) (PEG) macromonomer were prepared inside soft gelatin capsules to entrap diltiazem hydrochloride (DIL · HCl).[23] Four different copolymer compositions were tested in terms of swelling behavior and release profile at pH 1, simulating the acid pH of the stomach, and at pH 7, simulating the higher pH environment of the intestine. Hydrogels with intermediate compositions resulted to be effective in protecting the drug against the harsh medium of the stomach and allowed release at the higher pH of the intestine. At neutral pH, the slow protonation of the carboxylic groups of MAA led to an increase of the swelling degree and enabled zero-order drug release over a long period of time, making the capsules suitable for oral drug administration.

The swelling degree and the pH range at which the conformational changes take place may be easily modulated by introducing hydrophobic elements in the PMAA backbone. The first example of this evidence dates back to 1997, when Philippova *et al.*[24] prepared *n*-alkyl acrylates of PAA ($n = 8$, 12, 18), demonstrating that the swelling transition shifts to alkaline pH with increasing hydrophobicity of the gel, as previously observed by Siegel for other methacrylate-based hydrogels.[25] This was explained by the stabilization of the network in the collapsed state by hydrophobic aggregation of *n*-alkyl side chains. In a more recent work, hydrophobically modified hydrogels of PMAA were prepared by free radical copolymerization of MAA and diallyl methyl hexadecyl ammonium salts (CC16) in aqueous solution.[26] The presence of hydrophobic segments significantly reduces the degree of swelling at low pH, while the opposite effect is observed at high pH. If compared to hydrogels of PMAA solely or hydrophobically modified with poly(acrylic acid-2-ethylhexyl ester), the proposed systems showed a more remarkable reduction and increase of the swelling degree at low and high pH, respectively, indicating that the presence of CC16 confers higher sensitivity to pH changes.

Besides non-biodegradable synthetic materials, various natural polymers, such as proteins (albumin and gelatin) and polysaccharides (CH, hyaluronic acid, alginate, agar), have also shown pH-responsive behavior.[27,28] In most cases, these natural macromolecules are chemically modified to combine their useful properties with other suitable functionalities and have been proposed in the development of pH-sensitive drug-delivery devices due to their biocompatibility, biodegradability and resemblance with the macromolecular environment of the extra-cellular matrix.[29] An example of such synthetic strategy included the development of a pH-responsive hydrogel based on methacrylate derivatized bovine serum albumin (BSA).[30] In this work, polymerizable acrylic groups were inserted in BSA structure by functionalization with methacrylic anhydride. Several pH-responsive microbeads, showing a narrow size distribution range, spherical shape and porous surface, were obtained varying the amount of the proteic macromonomer and sodium methacrylate. The suitability of these materials as oral drug carriers was confirmed by evaluating water affinity and drug release profiles in media simulating gastrointestinal fluids. In another work,[31] α,β-poly(hydroxyethyl aspartamide-g-maleic anhydride) (PHEA-g-MA) has been cross-linked *via* gamma irradiation to obtain pH-responsive hydrogels able to release therapeutic proteins. Since the dimensions of the encapsulated molecule are comparable to those of the network mesh, a pulsatile release profile can be achieved by a pH/ionic strength "switch". The possibility of tuning the network mesh size simply by changing the irradiation conditions makes (PHEA-g-MA) hydrogels able to be adapted to the delivery demands of molecules of different sizes.

As mentioned above, pH-responsive hydrogels can also be prepared with polysaccharides; alginate and chitosan (CH) are the most frequently used anionic and cationic macromolecules, respectively. A series of pH-responsive graft copolymers of sodium alginate (NaAlg) – a polyanionic polysaccharide originally extracted from brown seaweed algae – with itaconic acid (IA) were synthesized obtaining pH-responsive NaAlg-g-IA microspheres to be used as carriers of nifedipine.[32] Another example is a new approach for enhancing the dissolution and the oral bioavailability of silymarin by means of NaAlg-based pH-responsive hydrogel encapsulating poly(D,L-lactic-co-glycolic acid) (PLGA) nanoparticles. The microspheres showed promising biodegradability and desirable sustained release profiles of silymarin in addition to enhanced silymarin overall dissolution.[33]

CH is an *N*-deacetylated derivative of chitin and one of the most abundant polysaccharides in Nature. El-Sherbiny and Smith[34] reported on the carboxymethylation of CH followed by photo-induced graft copolymerization with poly(ethylene glycol) acrylate (PEGA) in a mild aqueous medium. Some of the resulting copolymers were cross-linked using methylene bisacrylamide (MBA) to develop pH-responsive hydrogel matrices to be used as carriers for the oral controlled release of 5-fluorouracil (Figure 18.3). Ampholitic and pH-responsive hydrogels can also be prepared *via* copolymerization of CH with MAA and acrylamide (AAm) under gamma-radiation.[35] These hydrogels can be suitable for site-specific antibiotic delivery in the stomach. Similarly, monodisperse core-shell microcapsules based on cross-linked CH membrane with acid-triggered burst release properties have been developed for stomach-specific drug delivery.[36] In neutral medium (pH 7.1), the microcapsules maintain a good spherical shape and structural integrity; while in acidic medium (pH 1.5 or 4.7), the microcapsules decompose rapidly and release the encapsulated contents completely in time periods varying from 39 s to 22 min.

18.2.2 pH-responsive Nanogels

pH-sensitive nanogels have been proposed as devices for cancer drug targeting, due to the significant drop in the pH value of the tumor tissues (pH in the range of 5–6), as compared to normal tissues, and exploiting the enhanced permeability and retention (EPR) mechanism, which allows nanocarriers to concentrate in solid tumors.[37] Once accumulated at the tumor site, nanogels can act as local drug depots depending on the carrier

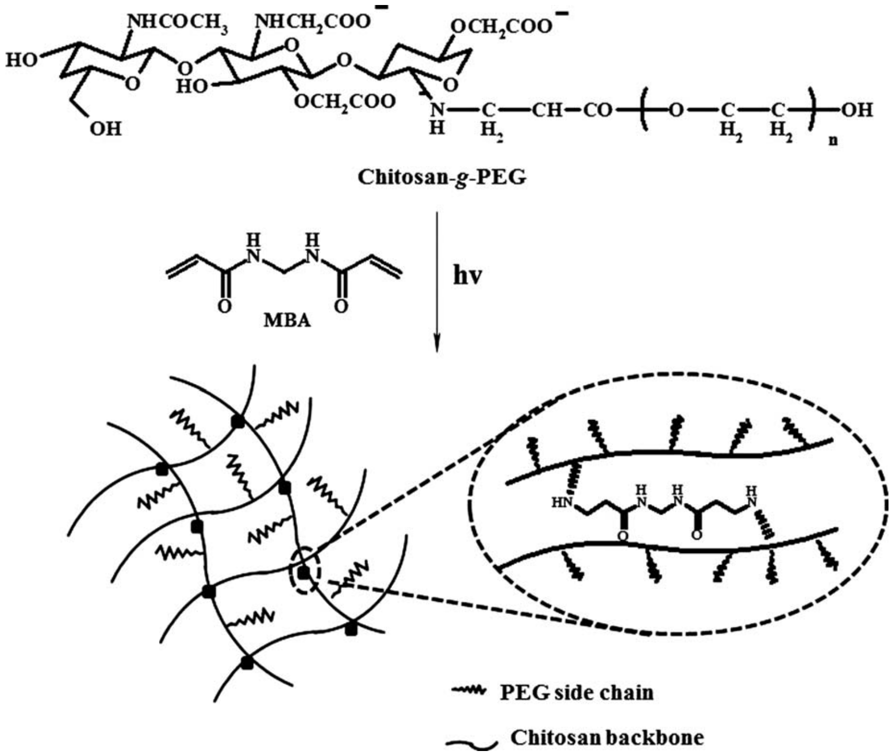

Figure 18.3 Preparation of hydrogels of chitosan (CH)-g-PEG cross-linked with methylene bisacrylamide (MBA).
Adapted from Ref. 34 with permission of Elsevier.

composition.[38] For example, poly(ε-caprolactone)-based nanoparticles have been shown to be able to increase the local concentration of tamoxifen in estrogen receptors positive breast cancer,[39] while pH-sensitive nanogels based on poly(β-amino ester)s can boost the delivery of the anticancer drug paclitaxel to tumor cells.[40] These biodegradable and pH-responsive nanogels have shown a higher efficacy in killing cancer cells than the free drug.

In 2002 Robinson and Peppas[41] investigated the pH-responsive behavior of (PMAA-g-EG) nanospheres obtained by applying a photo-initiated free-radical precipitation polymerization method. It was found that the nanospheres undergo a volume phase transition when the pH ranged from 3.3 to 7.5 and that particle size distribution and swelling degree were highly influenced by the MAA/EG molar feed ratio and the amount of cross-linking agent. Nanogels based on (PMAA-g-PEG) have also been prepared by a thermally initiated free radical dispersion polymerization method.[42] The effects of various reaction parameters, including quantity of monomer, temperature, and initiator, cross-linker and co-stabilizer concentrations, on the preparation of these materials were investigated. Moreover, Argentiere and coworkers[43] studied the mechanism involved in the uptake and release of bioactive molecules from stimuli-responsive nanogels synthesized by emulsion copolymerization of MAA and methyl acrylate. These nanospheres were loaded with thiophene fluorophore (hydrophobic) and doxorubicin (Dox, cationic). The release profiles were mainly affected by the chemical nature of the encapsulated drugs, suggesting that these nanogels could target drugs to basic or acidic compartments within the body depending on the chemical structure of the drug.

Polysaccharide-based nanogels are attracting increasing attention.[44,45] An example of this kind of materials includes the development of self-assembled structures from pullulan acetate sulfadimethoxine conjugates, which may be useful as anticancer drug-delivery systems responsive to tumor extra-cellular pH.[46] Nanocarriers for targeting of tumors have been also prepared by graft polymerization of NIPAAm with CH.[47] Camptothecin, an alkaloid effective in the treatment of colorectal cancer and ovarian cancer,[48] was loaded on PNIPAAm/CH nanoparticles and the drug release profiles were investigated *in vitro*. Camptothecin-loaded nanogels showed a drastically enhanced cytotoxicity at pH 6.8 compared to that at healthy pH. Subsequent *in vivo* experiments on mice were carried out with paclitaxel-loaded nanoparticles.[49] Methyl tetrazolium test (MTT) and fluorescence microscopy confirmed that PNIPAAm/CH nanoparticles rapidly released the drug in tumor surroundings, while drug release was minimal in healthy tissues. Mice treated with paclitaxel-loaded nanoparticles experienced a small decrease in body weight, but a significant tumor regression which was complete for more than 50% of the mice. Nanogels of CH-g-PNIPAAm have also been tested as pH-responsive delivery systems of oridonin. MTT assay and cellular morphological analyses showed that the cell growth inhibition by oridonin-loaded nanogels was higher at pH 6.5 than at pH 7.4.[50] On the other hand, pH-responsive core-shell nanoparticles based on hydroxyethyl cellulose (HEC) and PMAA networks were prepared *via* one-step copolymerization of MAA and MBA on HEC template in water.[51] The nanoparticles were stable in a wide pH range (0.7–11.5), and their size, structure and pH-responsiveness could be adjusted by varying the reaction parameters, *i.e.* HEC/MAA ratio and pH of the medium.

The ability of hydrogels to respond to changes in pH can also be exploited to prepare colon-targeted drug-delivery devices. Pectin nanogels cross-linked with glutaraldehyde released the drug more rapidly in simulating colon fluid than in simulating gastric or intestine fluids. The release can be further accelerated in the presence of a pectinolytic enzyme. Cytotoxicity studies have shown that the nanogel itself had no apparent inhibitory effect on cells.[52] pH-sensitive nanoparticles composed of glycidyl methacrylate (GMA)-derivatized dextran (DEX) and AA have also been shown able to load erythromycin and to release the drug rapidly in simulating intestinal fluid, as the network is enzymatically degraded and swollen.[53] Nanospheres based on polymeric mixtures of poly(lactic-co-glycolic) acid (PLGA) and a pH-sensitive methacrylate copolymer combined controlled release features of biodegradable polymers with responsiveness to the colon pH.[54] The nanospheres loaded with budesonide exerted more efficient anti-inflammatory effects in a trinitrobenzenesulfonic acid-induced colitis rat model than conventional enteric microparticles. In addition, the colon targeting properties, systemic bioavailability and specific uptake by the inflamed colon mucosa were evaluated using coumarin-6-loaded nanospheres. The nanospheres showed strongly pH-dependent drug release properties, with a rapid release at acidic and neutral pH followed by a sustained release phase at pH 7.4. *In vivo* experiments revealed the superior therapeutic efficiency of budesonide-loaded nanospheres in alleviating the symptoms of trinitrobenzenesulfonic acid-induced colitis.

18.3 Temperature-responsive Hydrogels for Drug Delivery

Together with pH, body temperature changes are the most widely used triggering signals for both site-specific therapy and pulsatile drug release.[4,55–57] An increase in body temperature can occur as a consequence of a disease state, *e.g.* during fever, or can result from a modulated external heat source (*e.g.* in the form of heat-triggered subdermal implants). Polymers that, in an aqueous solution, exhibit abrupt changes when temperature varies below or above body temperature are very interesting for biomedical applications.[58,59] The study of temperature-responsive gels started in 1978, when Tanaka reported the thermodynamics underlying the collapse of the polymer network in polyacrylamide gels.[60] Temperature-sensitive hydrogels are characterized by a critical solution temperature at which the network exhibits a volume phase transition, causing a sudden modification in the solvation state.[61] The critical solution temperature can be defined as the temperature at which the polymer undergoes a phase transition from a soluble state (*i.e.* random coil form) to an insoluble state (*i.e.* collapsed or globule form) (Figure 18.4). Positive temperature polymers become soluble upon heating and have an upper critical solution temperature (UCST). By contrast, negative temperature polymers become insoluble upon heating and are characterized by a low critical solution temperature (LCST).[62,63] Once the polymers are cross-linked, the solvation

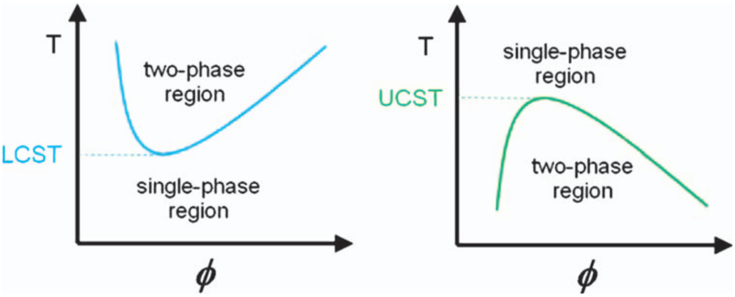

Figure 18.4 Temperature *vs.* polymer volume fraction (ϕ) phase diagrams of LCST and UCST polymers.
Reproduced from Ref. 62.

changes are transmitted to the hydrogel as an abrupt modification in the degree of swelling.[62,64] Such changes in the mesh size of the network alter the diffusional path of the solutes (*e.g.* drug molecules) trapped in the hydrogels and are the basis of the temperature-switchable drug release systems. Representative examples of LCST and UCST hydrogels for drug delivery are presented and discussed in the next sections.

18.3.1 LCST Hydrogels

Generally, an increase in temperature is accompanied by an enhancement of the polymer solubility, but LCST hydrogels exhibit the opposite behavior because the volume phase transition is driven by hydrophobic interactions among the polymer chains. At temperatures below the LCST, the hydrogel is swollen, but a brusque phase transition occurs when the temperature increases above the LCST. As the temperature rises, the hydrophobic segments are strengthened, thus resulting in shrinking of the hydrogels.[65] From a thermodynamic point of view, the polymer association at the LCST is due to a gain in entropy (ΔS), compared to the one-phase polymer-water system (which involves hydrogen bonding), with respect to the increase in the enthalpy (ΔH). This results in a negative free energy (ΔG), which facilitates the hydrophobic interactions between polymer chains and makes the water–polymer association unfavorable.[64,66] A common characteristic of most LCST polymers is the presence of hydrophobic alkyl groups. Typical LCST synthetic polymers are based on poly(*N*-isopropylacrylamide) (PNIPAAm),[67,68] poly(*N*,*N*′-diethylacrylamide) (PDEAAm),[69] poly(*N*-vinylcaprolactam) (PNVCL)[70,71] and poly(methylvinylether) (PMVE)[72] (Figure 18.5).

The temperature-sensitivity of these systems is affected by the size, architecture and mobility of alkyl side groups.[73,74] The main mechanisms of drug release from LCST hydrogels are illustrated in Figure 18.6.[75] Hydrophilic drugs incorporated into the hydrogels are released faster when in the swollen state (below the LCST) (Figure 18.6A).[76,77] More hydrophobic drugs may be squeezed from the collapsed gel (Figure 18.6B). Some heterogeneous gels may form a dense skin layer of the hydrophobic collapsed polymer component, while the core remains in the swollen state (Figure 18.6C), the skin being responsible for regulating drug release kinetics.

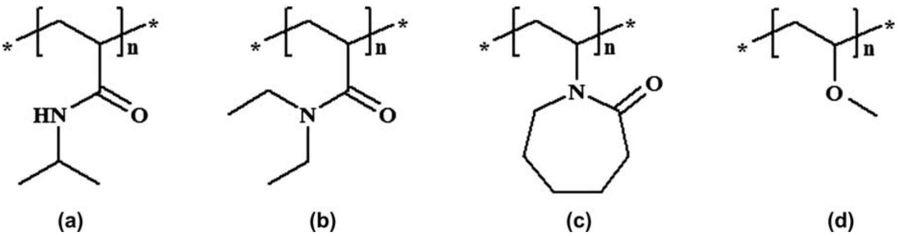

Figure 18.5 Structure of poly(*N*-isopropyl acrylamide), PNIPAAm (a), poly(*N*,*N*′-diethylacrylamide), PDEAAm (b), poly(*N*-vinylcaprolactam), PNVCL (c), and poly(methylvinylether), PMVE (d).

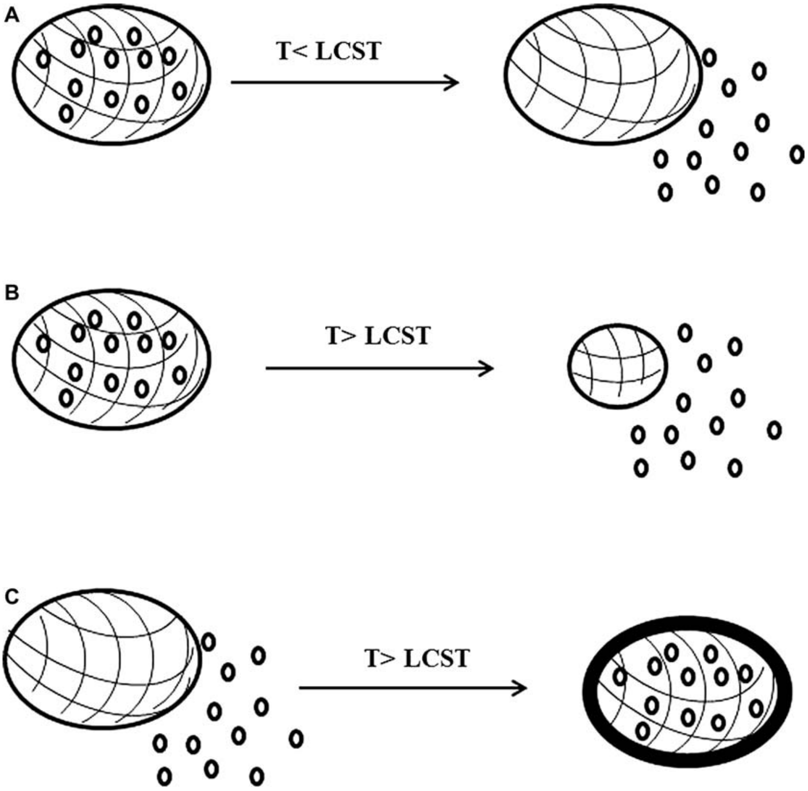

Figure 18.6 Mechanisms of drug release from thermo-sensitive hydrogels: swelling-promoted diffusion (A), shrinking-promoted squeezing (B) and outer layer (skin) barrier-controlled drug diffusion (C).
Adapted from Ref. 75 with permission of Elsevier.

In the drug-delivery field, the LCST polymers have received more attention than the UCST ones. Some representative examples of drug-delivery devices based on micro- and nano-sized LCST hydrogels are presented below.

18.3.1.1 LCST Microgels

PNIPAAm is the most widely studied and used synthetic temperature-responsive polymer in drug delivery, owing to the fact that its LCST (32 °C) is close to body temperature.[77,78] This means that the hydrogel chains hydrate at temperatures below 32 °C to form an expanded structure with a large mesh size enabling water diffusion, while above 32 °C these chains dehydrate to form a shrunken structure with a small mesh size. The LCST of temperature-responsive polymers can be adjusted to the desired value by modulating the ratio of hydrophilic and hydrophobic moieties in the network.[79] Copolymerization of NIPAAm with hydrophilic monomers in the hydrogel structure favors interactions with water, leading to an increase of the LCST of the copolymer.[80–83] Hoffman's group[84–86] reported the LCST behavior of a series of copolymers of NIPAAm with relatively hydrophilic comonomers such as AA, or with relatively hydrophobic comonomers such as *N*-butylacrylamide and *N*-tertbutylacrylamide. Increasing the content in hydrophilic comonomer content raises the LCST value of the copolymer. It was verified, however, that copolymerization of NIPAAm with acrylate-type comonomers can lead to gels possessing relatively weak thermo-sensitivity.[86] Therefore, the comonomer choice needs to be as careful as possible to preserve the functionality of the hydrogel.[87]

Acrylamide is often copolymerized with NIPAAm to obtain thermo-responsive materials with enhanced LCST.[88] PNIPAAm-co-AAm exhibits a phase transition temperature of around 36 °C, which makes this copolymer very useful in biomedical applications. Microspheres of PNIPAAm-co-AAm have been prepared by chemical cross-linking of amide groups with glutaraldehyde, using a concentrated copolymer solution at a temperature lower than the LCST.[89] These microspheres undergo a rapid volume change as a response to temperature modifications, which also have an effect on the drug release kinetics. Nevertheless, the hydrophilicity and the molecular weight of the tested drugs (propranolol, lidocaine, vitamin B12) also affect their release profiles. A similar hydrogel structure, consisting of *N*,*N*′-dimethylacrylamide (DMAAm) and NIPAAm, has been grafted onto polypropylene (PP) surfaces applying γ-ray irradiation in order to improve the hemocompatibility and the drug elution features of PP when used as a component of medical devices.[90] Due to the presence of DMAAm in the polymeric structure, the LCST shifted from 32 to 37 °C. The (PP-g-DMAAm)-g-NIPAAm films adsorbed serum albumin but not fibrinogen, and had significantly lower hemolytic and thrombogenic activity. The DMAAm promoted the loading of norfloxacin when the hydrogel layer was swollen; as the NIPAAm shrank, a sustained delivery occurred at body temperature. Grafting of responsive brushes and hydrogels on the surface of medical devices is extensively tackled in Chapter 24.

Copolymerization of NIPAAm with hydrophobic monomers, such as *N*-butyl methacrylate (BMA), may render hydrogels that exhibit "on-off" drug release profile when the temperature increases.[91–93] The "off" phase is ascribable to the formation of a dense skin-type layer on the hydrogel surface when the temperature is higher than the LCST. This barrier is generated by the faster collapse of the gel at the surface than at the interior, and its thickness is regulated *via* the length of the methacrylate alkyl side chain.[94] A popular polymer belonging to the NIPAAm family is PDEAAm. Its LCST can range from 25 to 35 °C[95] but, contrary to PNIPAAm, is dependent on the tacticity of the polymer.[96] DEAAm copolymerized with AA in the presence of MBA as cross-linking agent renders hydrogels with an LCST of 37.5 °C, which is close to human physiological temperature.[97] Pulsatile swelling behavior in distilled water at temperatures alternating between 20 and 60 °C has been proved to be reversible. Furthermore, due to the presence of AA hydrophilic moieties, these hydrogels could respond to pH changes.

Temperature-responsive hydrogels have also been synthesized combining proteins and polysaccharides with synthetic polymers, extending the concept of stimuli-responsive systems and their potential application. Huang *et al.*[98] prepared a series of hydrogels with both thermo-responsive and completely biodegradable properties through free radical polymerization of NIPAAm and a DEX macromer containing multiple hydrolytically degradable oligolactate-2-hydroxyethyl methacrylate units. The hydrogels showed an LCST at approximately 32 °C. The swelling and the degradation strongly depended on the temperature and on the hydrogel composition. These features together with the molecular size of the drugs notably determined drug release kinetics. Another interesting work reports on the development of hydrogel beads from droplets of DEX-MA and PNIPAAm dispersions deposited on superhydrophobic surfaces.[99] The beads showed temperature-responsive swelling and such responsiveness enabled to tune the release rate of BSA and insulin.

Interpenetrating polymer networks (IPNs) based on guar gum and PNIPAAm, prepared *via* redox radical polymerization, exhibited faster deswelling rates than PNIPAAm hydrogels.[100] The network of guar gum improves the temperature sensitivity and permeability of PNIPAAm hydrogels. Another polysaccharide-based temperature-responsive hydrogel was prepared by cross-linking of azide-modified cellulose and alkyne-modified poly(*N*-isopropylacrylamide-co-hydroxylethyl methacrylate) (PNIPAAm-co-HEMA) in the presence of Cu(I) catalyst.[101] The PNIPAAm-co-HEMA/cellulose hydrogels had a porous structure and exhibited temperature-dependent swelling ratio, deswelling and reswelling kinetics.

Proteins have also been used to prepare temperature-responsive networks. For example, methacrylate BSA can act as protein cross-linking agent for the synthesis of microgels with spherical shape,[102] while hydrolyzed methacrylated gelatin can be employed as pro-hydrophilic monomer/cross-linker in order to obtain biodegradable microbeads with LCST close to body temperature.[103] Also, gelatin-based thermo-responsive spherical microgels can be obtained through radical grafting of NIPAAm and MBA on native gelatin backbone (Figure 18.7).[104] These microgels exhibit a small increase in LCST, up to 34.6–34.8 °C, as the gelatin content in the network increases. Drug release experiments carried out at various temperatures confirmed an increase in the diffusion rate at temperature below the LCST.

In general, grafting of PNIPAAm from hyaluronic acid (HA) and gelatin reduces the gelation temperature and increases the hydrophilicity.[105] Drug release experiments revealed that drug release rate decreases as follows: PNIPAAm > HA with grafted PNIPAAm chains (HPN) > HPN further grafted with gelatin (HPNG) hydrogels. Drug accumulation studies in bladder tissue indicated that the HPNG hydrogels led to a considerable increase in the cisplatinum concentration without any adverse change in urothelium.

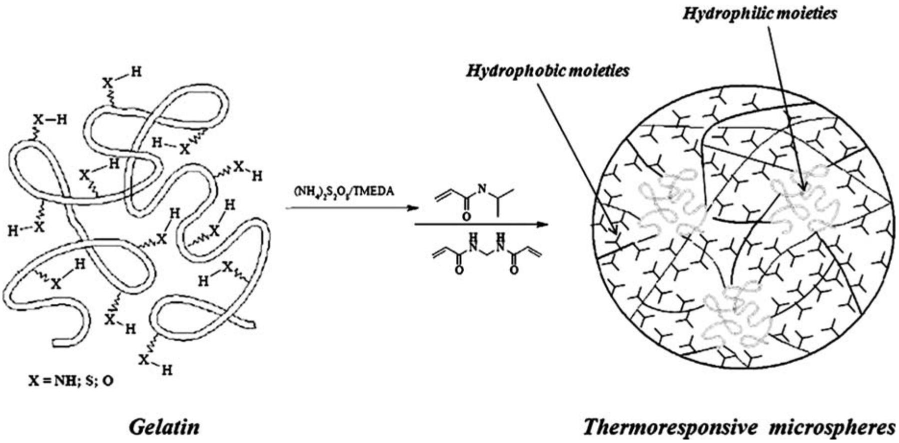

Figure 18.7 Preparation of thermo-responsive microspheres by means of free radical grafting of NIPAAm and MBA on native gelatin.
Adapted from Ref. 104 with permission of Elsevier.

18.3.1.2 LCST Nanogels

Tumors have a slightly elevated temperature by about 1–2 °C in comparison to normal tissue due to increased cellular activity. Furthermore, tumor vasculature has greater thermal sensitivity than the normal vasculature, which makes the cancer cells unable to withstand temperatures above 40 °C. These features have led to the development of a local treatment called hyperthermia, which consists in increasing the temperature of solid tumors at 40–45 °C.[106] Thus, a key challenge for the use of thermo-responsive hydrogels is to modulate their LCST around the temperature of the tumor or the temperature used for hyperthermia treatment of cancer.[107]

Gulati *et al.*[108] investigated the hemocompatibility of PNIPAAm-PEG based nanoparticles (200 nm, low polydispersity and LCST of 40–41°C) and the influence of PEG on the interactions with cells. The nanoparticles showed nearly 83% encapsulation efficiency for Dox and temperature-dependent release. The presence of PEG resulted in high hemocompatibility and reduced protein adsorption by more than 50% in comparison to non-PEG-containing nanoparticles. Hydrophilic nanospheres based on NIPAAm and vinyl pyrrolidone (VP), encapsulating a bioactive derivative of 5-fluorouracil-hexyl-carbamoyl fluorouracil (HCFU), have been also prepared.[109] The HCFU-loaded nanospheres were found to be stable in whole blood, having a negligible toxicity towards the red blood cells. Moreover, cytotoxicity assays in Mia-Paca 3 pancreatic cancer cell line showed an increase in antitumor activity over a period of 72 h.

PNVCL has not been studied as intensively as PNIPAAm, but it also possesses very interesting properties for medical and biotechnological applications. It is soluble in water and organic solvents and biocompatible, and exhibits a transition temperature at 33 °C, *i.e.* within the settings of these applications.[110] *N*-vinylcaprolactam has been copolymerized with methyl methacrylate by free radical polymerization, using hydrogen peroxide and L-ascorbic acid as redox initiators, in o/w microemulsion containing sodium dodecyl sulfate. Copolymers were of less than 50 nm size with spherical morphology and possessed phase transition temperature close to body temperature.[111] IC_{50} on B16F10 melanoma cell lines was in the 0.01–0.1 mg mL^{-1} range. An increase in polymer concentration was not harmful for the cell survival, suggesting that these systems can be useful as drug-delivery devices. PNVCL has been also used to prepare thermo-responsive graft nanoparticles (TRC-NPs) by grafting from CH.[112] The TRC-NPs showed an LCST at 38 °C and a prominent release above the LCST, and were non-toxic to an array of cell lines in the concentration range of 100–1000 μg mL^{-1}. 5FU-loaded nanoparticles showed comparatively higher toxicity to cancer cells than to the healthy ones.

Dually temperature- and magnetic-responsive systems may play a relevant role in cancer treatment. Specific aspects of magnetic-responsive systems are covered by Chapter 14. PNIPAAm-CH based nanohydrogels containing Fe_3O_4 nanoparticles are biocompatible and exhibit different LCST depending on the polymer/nanoparticle ratio.[113,114] Superparamagnetic nanoparticles (200 nm) decorated with a PNIPAAm thermo-responsive shell have been tested as carriers for Dox.[115] These nanosystems, which exploit the temperature-responsive behavior of the PNIPAAm polymeric shell for controlling drug loading and release, were able to provide time-dependent tumor cell death as Dox was released. Moreover, comparative studies of the Dox-loaded nanosystems in the presence and absence of an external magnet demonstrated an increment in cell accumulation and toxicity when magnetically guided. Dox was also used to test drug loading capacities and the release behavior of magnetic hydrogel nanospheres based on (PNIPAAm-co-AA)/Fe_3O_4.[116] Due to the presence of NIPAAm, AA and colloidal magnetite nanoparticles, the resulting hydrogel nanospheres exhibited temperature- and pH-responsiveness, and superparamagnetic properties. *In vitro* release experiments revealed a faster release of drug at pH 5.3 (37 °C) than at pH 7.4 (either at 25 °C or at 37 °C). Dox-loaded magnetic hydrogel nanospheres provided *in vitro* an enhanced anticancer effect, compared to the free drug.

In a recent work,[117] thermo-sensitive and magnetic nanocarriers were prepared by grafting PNIPAAm on the surface of silica (SiO_2)-coated Fe_3O_4 nanoparticles. The nanoparticles reversibly adsorbed proteins at temperatures above the LCST, through hydrophobic interactions between NIPAAm and BSA chains. Cytotoxicity studies carried out on Chinese hamster ovary (CHO-K1) cells evidenced that PNIPAAm-grafted nanoparticles at a concentration of 0.5 mg mL^{-1} were biocompatible for 48 h, and caused minor cytotoxicity after 72 h of incubation. These PNIPAAm-grafted nanoparticles did not induce by themselves any morphological change in the cells after exposure for 108 h.

18.3.2 UCST Hydrogels

As mentioned above, positive temperature hydrogels shrink at low temperature and swell at higher temperature than the UCST. The driving force of this phase transition is the enthalpic effect, associated to the balance between intra- and inter-molecular forces and solvation.[118] Thus, unlike the LCST materials, the volume phase transition of UCST hydrogels is driven by hydrogen bond formation; namely, at lower temperature, the hydrogel forms an intermolecular complex *via* hydrogen bonding forces between polymer chains, maintaining the particles in a collapsed state. On the contrary, when temperature increases, these bonds are weakened and the gel rapidly swells to the maximum possible extent.[119] Thus, to exhibit UCST in aqueous medium, the interactions between polymer chains must be stronger than those between water and polymer moieties at low temperature. On the basis of these considerations, positive temperature hydrogels can be obtained by engineering hydrogen bonding and/or electrostatic interactions within the polymer chains. For example, poly(*N*,*N*-dimethylaminoethyl methacrylate), which is a typical LCST polymer, exhibits a UCST-type behavior in the presence of trivalent counter-ions that increase polymer/polymer interactions by means of electrostatic bridging between the charged polymer segments.[120] Many polymers and copolymers, such as PAAm-PAA[121,122] and PAAm-BMA,[123] are positively temperature dependent. Nevertheless, in the literature, few examples of the use of this kind of material for drug delivery have been reported, probably because they require that the drug loading is carried out at relatively high temperature, which complicates drug formulation and may be harmful for labile conventional and biopharmaceutical drugs.[124]

Drug delivery systems that provide slow release at basal temperature and faster release at a higher temperature may be suitable to feed-back regulate drug delivery when pathological processes, such as inflammation or cancer, occur.[125] UCST hydrogels are suited to this necessity because of their ability to perform rapid/slow drug release at high/low temperatures. Core-shell hydrogel microspheres with positively thermo-responsive behavior have been developed according to the three-step mechanism depicted in Figure 18.8: i) preparation of monodisperse poly(acrylamide-co-styrene) seeds applying emulsifier-free emulsion polymerization, ii) formation of polyacrylamide or poly[acrylamide-co-(butyl methacrylate)] shells on the microsphere seeds by means of free radical polymerization and iii) interpenetration of the shell network with poly(acrylic acid) to obtain core-IPN shell microspheres.[126] The microspheres exhibited tunable swelling kinetics as a function of temperature: at temperatures below the UCST they were in the shrunken state due to complex formation by hydrogen bonding between PAA and PAAm, while above the transition temperature, the microspheres swelled because of the rupture of the hydrogen bonds.

In a more recent work, poly(acrylic acid)-g-β-cyclodextrin (PAA-g-β-CD) and PAAm were employed in the synthesis of IPNs with a UCST of

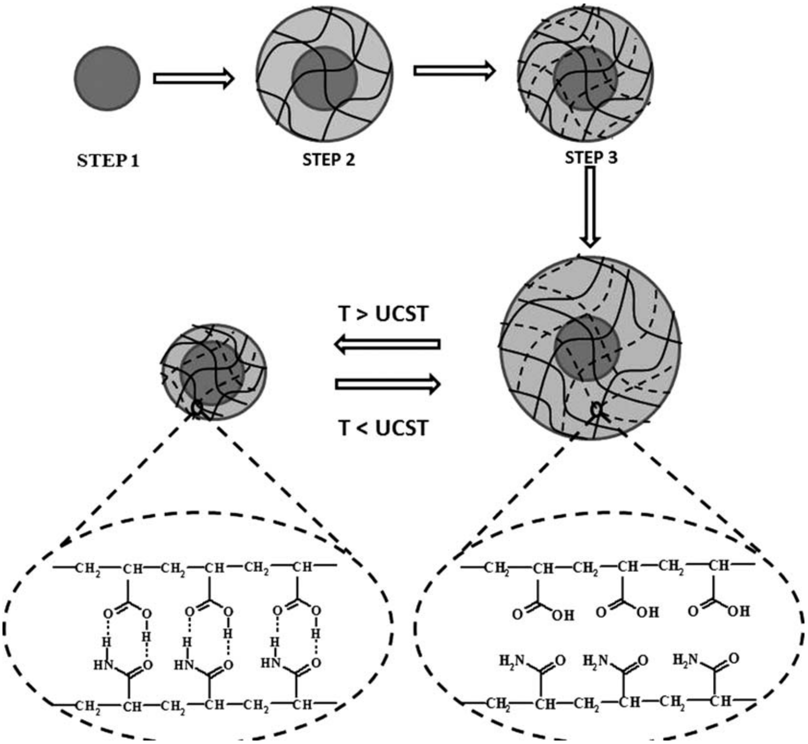

Figure 18.8 Synthesis of UCST core-shell microgels: 1) monodisperse poly(acrylamide-co-styrene) (PAAm-co-St) seeds are prepared by emulsifier-free emulsion polymerization, 2) poly(acrylamide) or poly(acrylamide-co-butyl methacrylate) shells are formed on the seeds by free-radical polymerization and 3) poly(acrylic acid) is interpenetrated to obtain poly(acrylamide)/poly(acrylic acid) PAAm/PAAc IPN shells. The PAAm/PAAc-based IPN microspheres are swollen at temperatures below the UCST due to the dissociation of the PAAm/PAAc complexes, while they shrink at temperatures above UCST because of hydrogen bonding interactions between PAAm and PAAc.
Adapted from Ref. 126 with permission of John Wiley & Sons, Inc.

approximately 35 °C.[127] Ibuprofen release profiles, obtained at 25 and 37 °C, confirmed the positive-temperature drug release pattern from the IPNs. In comparison with IPNs prepared without β-CD, the presence of β-CD enhanced drug loading, delayed drug release and improved the control of the response rate. Polymers with ureido groups can also undergo UCST-type phase transitions under physiological conditions, and have potential applicability in the drug-delivery field.[128] Poly(allylurea) copolymers, even at low concentration, showed UCST behavior at pH 7.5 in 150 mM NaCl. Similar thermo-sensitivity was observed with copolypeptides consisting of L-citrulline having an ureido group.

18.4 Dually Responsive Hydrogels for Drug Delivery

The development of materials able to respond simultaneously to pH and temperature signals opens the possibility of preparing delivery systems that exhibit an amplification of the response to the stimuli and a more precise control of the targeting and release kinetics when the pathology is accompanied by changes in these two variables. These materials can also be useful for independent regulation of the release of two or more drugs (*e.g.*, one drug as a function of pH and another in response to temperature changes).[4,129]

A potential application of dually responsive materials is the development of anticancer drug-delivery systems, as certain malignancies can lead to an increase in temperature and to a decrease in extra-cellular pH around the tumor site. The most immediate synthetic approach to obtain this kind of material is the copolymerization of a temperature-sensitive monomer, *e.g.* NIPAAm, with a pH-responsive one, namely AA. The dependence of the critical temperature of PNIPAAm on the presence of ionizable monomers in the network may be an obstacle to the efficient combination of pH and temperature-sensitive components,[82,130,131] although the design of new monomers or synthetic routes can help to overcome this problem.[14,85] For example, PNIPAAm-co-PAA copolymers can be prepared with a low polydispersity by means of RAFT copolymerization, rendering physical hydrogels that exhibit sharp response to narrow variations of temperature or pH.[132,133] The phase transitions are induced by changes in both the protonation of the carboxylic acid groups of PAA, motivated by pH modifications, and in the interactions with water of PNIPAAm regulated by temperature. Copolymerization with a hydrophobic monomer, such as butyl acrylate, increases the pH at which gelation can occur. It was found that PNIPAAm-co-PAA maintains the bioactivity of basic fibroblast growth factor following storage at 37 °C and can provide pH-dependent sustained release of vascular endothelial growth factor.[133] These features make these polymers suitable for use in injectable depot drug-delivery systems.

Regarding chemically cross-linked networks, combination of ionic and hydrophobic co-monomers in a NIPAAm hydrogel was shown to be useful for the loading of a polypeptide drug without degradation, taking benefit of the temperature-responsive swelling/collapse, and to deliver it to the desired location owing to the pH-responsiveness.[134] The copolymerization of NIPAAm with a small proportion of a monomer with amino groups (*N*-aminopropyl methacrylamide) provided hydrogels able to take up and release an anionic divalent molecule reversibly in response to small changes in pH, temperature and ionic strength. Furthermore, these stimuli altered not only the physical conformation of the polymer chains in the network, but also the strength of the electrostatic interactions with the target molecule. It has been shown that, when multiple contact points are required for the binding of a molecule, the spatial conformation of the ionic groups in the network determines the possibility of establishing such multiple point interactions and, consequently, the overall affinity of the hydrogel for the target molecule. It has been shown that, for such hydrogels/target molecules combinations, the amount of drug loaded and, more importantly, the amount released strongly depended on the concentration of the target molecule in the medium; namely, if the released drug remains in the surrounding of the hydrogels without being absorbed/taken by the cells, the release stops. Such a feedback mechanism of regulating drug release would allow a quite constant drug concentration to be kept at the application site.[129]

Hydrogels in the format of core-shell nanoparticles, *e.g.* (PNIPAAm-co-PAA)-β-polycaprolactone loaded with anticancer drugs, have been prepared under supercritical carbon dioxide environment, thus avoiding the use of organic solvents or any other additives, such as surfactants.[135] Grafting of IPNs of PNIPAAm and PAA to polymeric medical devices has been shown to be an efficient way of endowing the surface of the device with both temperature- and pH-sensitivity, useful for drug loading and controlled release.[136] Another synthetic approach consisted in the copolymerization of *N*-ethylpyrrolidine methacrylate with DMAA and a low amount of bisacrylamide. The obtained hydrogels showed a double sensitivity to pH and temperature and a pulsatile behavior in response to both stimuli, although the high phase transition temperature (around 80 °C) may limit their practical use.[137] Rapid pH-/temperature-responsive cationic hydrogels have been obtained with a (PNIPAAm-co-DMAEMA) backbone network and grafted (PNIPAAm-co-DMAEMA) side chains.[138] In these comb-type grafted hydrogels, the mobile grafted (PNIPAAm-co-DMAEMA) chains can easily swell and shrink as environmental pH and/or temperature changes occur (Figure 18.9). The grafted (PNIPAAm-co-DMAEMA) chains prevent the formation of a dense skin layer on the surface of comb-type hydrogels; as a result, the comb-type hydrogels show intense response to temperature/pH stimuli.

The main limitation in the use of pH- and thermo-responsive hydrogels constituted by acrylic monomers is their non-biodegradability. To open the path to new applications and to minimize concerns about environmental contamination, great attention is being focused on the design of hydrogels that combine acrylic derivatives and biodegradable components, such as polypeptides and natural macromolecules, or that even solely use the biodegradable

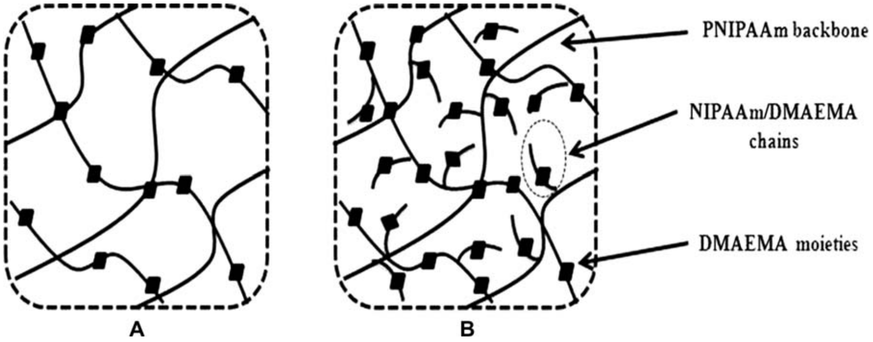

Figure 18.9 Scheme of normal-type (A) and comb-type (B) grafted P(NIPAm-co-DMAEMA) hydrogels.
Adapted from Ref. 138 with permission.

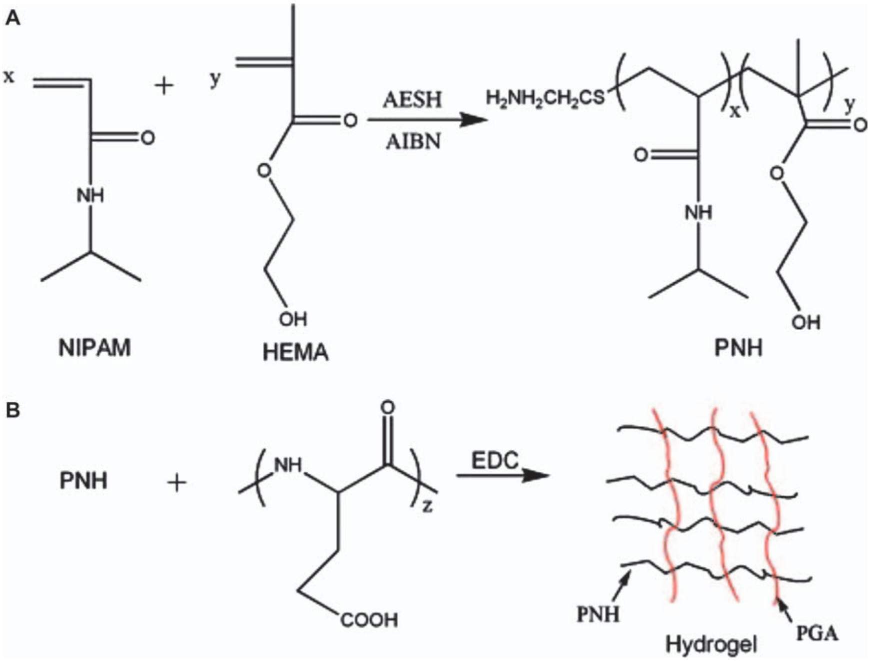

Figure 18.10 Synthesis of hydrogels based on temperature-sensitive poly(*N*-isopropylacrylamide-co-2-hydroxyethyl methacrylate) (PNH), by free radical polymerization initiated with 2,2′-azoisobutyronitrile (AIBN) and 2-aminoethanthiol (AESH) (A), and on pH-sensitive poly(l-glutamic acid) (PGA), through chemical coupling between the carboxylic groups in the PGA and the hydroxyl groups in the PNH using 1-ethyl-3-(3-dimethylaminopropyl) carbodiimide hydrochloride (EDC) (B).
Reproduced from Ref. 139 with permission of Elsevier.

components. For example, PNIPAAm-co-HEMA has been combined with biodegradable and pH-sensitive poly(L-glutamic acid) to prepare hydrogels suitable for the controlled release of hydrophilic drugs (Figure 18.10).[139] In the presence of the enzyme proteinase K, the hydrogels degrade at a rate that can be tuned by the composition of the network. Biodegradable double-responsive hydrogels have also been obtained from amphiphilic polyaspartamides containing *N*,*N*-diisopropylaminoethyl pendent groups.[140]

Polysaccharides have also been used in the preparation of dually responsive systems, by inserting thermo-responsive moieties in the polysaccharide backbone. For example, beads of alginate and PNIPAAm cross-linked by calcium ions provided temperature- and pH-dependent indomethacin release profiles.[141] Further coating of the beads with CH and alginate enabled a more sustained release.[142] Such particles were also partially mineralized with calcium phosphate in order to improve their biocompatibility with bone tissue.[143] There are a number of papers that report on the combination of NIPAAm and CH. P(CH-g-NIPAAm) copolymers show temperature and pH sensitivity and are able to regulate the release of drugs, such as coenzyme A, as a function of both variables.[144] Dually responsive CH grafted with PAA, poly(vinyl alcohol) (PVA), poly(hydroxypropyl methacrylate) (PHPMA) and gelatin has been tested for oral drug delivery.[145] Oxytetracycline release profiles from the hydrogels depended on the content in monomers, the γ-ray radiation dose applied to form the network and the pH of release medium. IPNs of PNIPAAm and CH have been prepared by free radical polymerization and cross-linking of NIPAAm in CH solutions, followed by immersion in glutaraldehyde solutions of various concentrations (0 to 0.7 vol. %). The amount of CH in the IPNs, which was proportional to the glutaraldehyde concentration used for the cross-linking, notably affected the thermodynamics (*i.e.* temperature, enthalpy, heat capacity and width of the transition) of the IPN phase transitions, due to the subdivision of the PNIPAAm network in microdomains that find it difficult to participate in the transitions. Changes in pH from 8 to 3 caused remarkable modifications in the ionization degree of CH, but only a minor increase in the transition temperature, from 32 to 36 °C. CH provided the IPNs with high affinity for anionic drugs, such as a diclofenac. The IPNs with low cross-linked CH showed the higher temperature-sensitive release patterns. In contrast, the temperature did not significantly affect the release rate from the most cross-linked CH IPNs, in which the PNIPAAm microdomains were smaller and the volume phase transitions less sharp.[146]

Cellulose derivatives, particularly hydroxypropylcellulose (HPC) with an LCST at 41 °C, have also been tested in the synthesis of dually responsive hydrogels. HPC-PAA nanoparticles with semi-IPN structure, in which proton-accepting HPC forms complexes with the proton-donating PAA, exhibited stimuli-responsive drug delivery.[147] Depending on the chemical composition and the degree of cross-linking, the temperature-responsive behavior of the HPC-PAA gel particles can be shifted from LCST to UCST property, and their sizes can be modified from 100 nm to 1 μm in a controllable way. Hydrophilic antitumor drug oxaliplatin was successfully loaded in the particles, forming platinum-PAA complexes, maintaining a high anticancer activity. On the other hand, hydrogels of AA and AA-grafted HPC exhibited pH-dependent swelling and drug release, temperature-dependent transmittance and composition-dependent biodegradability.[148]

18.5 Conclusion

Smart pH- and temperature-sensitive chemically cross-linked hydrogels, exhibiting tunable release rates, are an important class of materials that find unique applications in biomedical and pharmaceutical fields and have undergone tremendous progress in the past few decades. Micro- and nano-sized particles are among the most suitable formats for stimuli-responsive drug-delivery systems, because of their rapid responsiveness under *in vivo* conditions. Micro-sized materials are mainly intended for oral administration or subcutaneous implantation, while the nano-sized hydrogels can reach profound tissues and be exploited to target drug release towards tumor cells or other pathological conditions. Other formats such as layers of the cross-linked hydrogels applied as *in situ* photopolymerized coatings on conventional drug-delivery systems (*e.g*. pellets and tablets)[149,150] or medical devices (see Chapter 24) also offer attractive performances. pH-responsive hydrogels are made of polyelectrolytes and operate by widening of the mesh size when repulsive forces among the polymer chains arise due to the ionization. Negative and positive temperature-sensitive hydrogels have been shown useful for the preparation of carriers able to regulate drug release under hyperthermia conditions, caused by a pathological state or by the application of a heat source external to the body. Hydrogels that combine both pH- and temperature-responsiveness respond to the stimuli in a more specific and amplified way, which enables a more precise control of the site and the rate at which the release should occur. In summary, although the application of smart materials to the drug-delivery field is still quite recent, the many elegant approaches already developed make foreseeable that, in the next years, novel pH- and temperature-responsive materials able to face up to the numerous challenges that biomedical use demands, including the improvement of responsiveness, mechanical strength, biocompatibility and biodegradability, will appear.

Acknowledgements

Financial support of Regional Operative Program (ROP) Calabria ESF 2007/2013 – IV Axis Human Capital – Operative Objective M2 – Action D.5 is gratefully acknowledged.

References

1. S. Shukla, A. K. Bajpai and J. Bajpai, *Macromol. Res.*, 2003, **11**, 273.
2. N. A. Peppas and A. R. Khare, *Adv. Drug Deliver. Rev.*, 1993, **11**, 1.
3. D. S. Katti, S. Lakshmi, R. Langer and C. T. Laurencin, *Adv. Drug Deliver. Rev.*, 2002, **54**, 933.
4. C. Alvarez-Lorenzo and A. Concheiro, *Mini-Rev. Med. Chem.*, 2008, **8**, 1065.
5. J. F. Mano, *Adv. Eng. Mater.*, 2008, **10**, 515.
6. G. Brabant and K. Prank, *Trends Endocrinol. Metabol.*, 1992, **3**, 183.
7. R. A. Siegel and C. G. Pitt, *J. Control. Release*, 1995, **33**, 173–188.
8. P. Gupta, K. Vermani and S. Garg, *Drug Discov. Today*, 2002, **7**, 569.
9. J. Kost and R. Langer, *Adv. Drug. Deliver. Rev.*, 2001, **46**, 125.
10. R. Langer and J. P. Vacanti, *Science*, 1993, **260**, 920.
11. N. A. Peppas, J. Z. Hilt, A. Khademhosseini and R. Langer, *Adv. Mater.*, 2006, **18**, 1345.
12. R. Langer, *Science*, 2001, **293**, 58.
13. C. Alvarez-Lorenzo, L. Bromberg and A. Concheiro, *Photochem. Photobiol.*, 2009, **85**, 848.
14. M. Ebara, M. Yamato, M. Hirose, T. Aoyagi, A. Kikuchi, K. Sakai and T. Okano, *Biomacromolecules*, 2003, **4**, 344.

15. J. Weidner, *Drug Discov. Today*, 2001, **6**, 1239.
16. A. T. Florence and D. Attwood, *Physicochemical Principles of Pharmacy*, Macmillan Press, London, 3rd edn, 1998.
17. P. Vaupel, F. Kallinowski and P. Okunieff, *Cancer Res.*, 1989, **49**, 6449.
18. E. K. Rofstad, B. Mathiesen, K. Kindem and K. Galappathi, *Cancer Res.*, 2006, **66**, 6699.
19. J. Dissemond, M. Witthoff, T. C. Brauns, D. Harberer and M. Gros, *Hautarzt*, 2001, **54**, 959.
20. M. Morishita, A. M. Lowman, K. Takayama, P. Nagai and N. A. Peppas, *J. Control. Release*, 2002, **81**, 25.
21. A. Mohanan, B. Vishalakshi, R. Narayana Charyulu, N. M. Harish and S. Ganesh, *Int. J. Polym. Mater.*, 2009, **58**, 32.
22. E. Lee, K. Kim, M. Choi, Y. Lee, J. W. Park and B. Kim, *Drug Deliv.*, 2010, **17**, 573.
23. G. Frutos, A. Prior-Cabanillas, R. París and I. Quijada-Garrido, *Acta Biomater.*, 2010, **6**, 4650.
24. O. E. Philippova, D. Hourdet, R. Audebert and A. R. Khokhlov, *Macromolecules*, 1997, **30**, 8278.
25. R. A. Siegel, *Adv. Polym. Sci.*, 1993, **109**, 233.
26. D. G. Gao, J. Z. Ma and H. Q. Guo, *New J. Chem.*, 2010, **34**, 2034.
27. T. Coviello, P. Matricardi, C. Marianecci and F. Alhaique, *J. Control. Release*, 2007, **119**, 5.
28. B. Blanco-Fernández, M. López-Viota, A. Concheiro and C. Alvarez-Lorenzo, *Carbohydr. Polymers*, 2011, **85**, 765.
29. J. F. Mano, G. A. Silva, H. S. Azevedo, P. B. Malafaya, R. A. Sousa, S. S. Silva, L. F. Boesel, J. M. Oliveira, T. C. Santos, A. P. Marques, N. M. Neves and R. L. Reis, *J. R. Soc. Interface*, 2007, **4**, 999.
30. F. Iemma, U. G. Spizzirri, F. Puoci, R. Muzzalupo, S. Trombino, R. Cassano, S. Leta and N. Picci, *Int. J. Pharm.*, 2006, **312**, 151.
31. C. LoPresti, V. Vetri, M. Ricca, V. Fodera, G. Tripodo, G. Spadaro and C. Dispenza, *React. Funct. Polym.*, 2011, **71**, 155.
32. N. Isiklan, M. Inal, F. Kursun and G. Ercann, *Carbohydr. Polym.*, 2011, **84**, 933.
33. I. M. El-Sherbiny, M. Abdel-Mogib, A. A. M. Dawidar, A. Elsayed and H. D.C. Smyth, *Carbohydr. Polym.*, 2011, **83**, 1345.
34. I. M. El-Sherbiny and H. D. C. Smythv, *Carbohydr. Res.*, 2010, **345**, 2004.
35. M. F. A. Taleb, *Polym. Bull.*, 2008, **61**, 341.
36. L. Liu, J. P. Yang, X. J. Ju, R. Xie, Y. M. Liu, W. Wang, J. J. Zhang, C. H. Niu and L. Y. Chu, *Soft Matter*, 2011, **7**, 4821.
37. S. M. Moghimi, A. C. Hunter and J. C. Murray, *Pharmacol. Rev.*, 2001, **53**, 283.
38. I. Brigger, C. Dubernet and P. Couvreur, *Adv. Drug Deliver. Rev.*, 2002, **54**, 631.
39. J. S. Chawla and M. M. Amiji, *Int. J. Pharm.*, 2002, **249**, 127.
40. D. Shenoy, S. Little, R. Langer and M. Amiji, *Mol. Pharm.*, 2005, **2**, 357.
41. D. N. Robinson and N. A. Peppas, *Macromolecules*, 2002, **35**, 3668.

42. L. Deng, X. He, A. Li, Q. Yang and A. Dong, *J. Nanosci. Nanotechnol.*, 2007, **7**, 626.
43. S. Argentiere, L. Blasi, G. Morello and G. Gigli, *J. Phys. Chem. C*, 2011, **115**, 16347.
44. J. K. Oh, D. I. Lee and J. M. Park, *Prog. Polym. Sci.*, 2009, **34**, 1261.
45. M. D. Moya-Ortega, C. Alvarez-Lorenzo, A. Concheiro and T. Loftsson, *Int. J. Pharm.*, 2012, **428**, 152.
46. K. Na and Y. H. Bae, *Pharm. Res.*, 2002, **19**, 681.
47. F. Li, W. Hong, Z. Hui, L. Fei, Y. Tie-hong, G. Chun-hu and Y. Qian, *Carbohydr. Polym.*, 2008, **73**, 390.
48. H. T Chris, W. John and G. A. Susan, *Biochim. Biophys. Acta*, 1998, **1400**, 107.
49. F. Li, W. Hong, Z. Hui, L. Fei, G. Chun-hu and Y. Qian, *Carbohydr. Polym.*, 2009, **77**, 773.
50. C. Duan, D. Zhang, F. Wang, D. Zheng, L. Jia, F. Feng, Y. Liu, Y. Wang, K. Tian, F. Wang and Q. Zhang, *Int. J. Pharm.*, 2011, **409**, 252.
51. Y. Zhang, Q. Jin, Y. Chen and J. Zhao, *J. Nanopart. Res.*, 2011, **13**, 4451.
52. C. Chang, Z. Wang, C. Y. Quan, H. Cheng, S. X. Cheng, X. Z. Zhang and R. X. Zhuo, *J. Biomater. Sci. Polym. Ed.*, 2007, **18**, 1591.
53. H. Zhang, H. Wu, L. Fan, F. Li, C. Gu and M. Jia, *Polym. Composites*, 2009, **30**, 1243.
54. A. Makhlof, Y. Tozuk and H. Takeuchi, *Eur. J. Pharm. Biopharm.*, 2009, **72**, 1.
55. K. A. Anal, *Recent Pat. Endocr. Metab. Immune Drug Discov.*, 2007, **1**, 83.
56. Z. Liusheng, B. Brittany and A. Frank, *Soft Matter*, 2011, **7**, 5908.
57. A. K. Bajpai, S. K. Shukla, S. Bhanu and S. Kankane, *Prog. Polym. Sci.*, 2008, **33**, 1088.
58. L. E. Bromberg and E. S. Ron, *Adv. Drug Deliver. Rev.*, 1998, **31**, 197.
59. E. S. Gil and S. M. Hudson, *Prog. Polym. Sci.*, 2004, **29**, 1173.
60. T. Tanaka, *Phys. Rev. A: Atomic Mol. Opt. Phys.*, 1978, **17**, 763.
61. L. Klouda and A. G. Mikos, *Eur. J. Pharm. Biopharm.*, 2008, **68**, 34.
62. M. A. Ward and T. K. Georgiou, *Polymers*, 2011, **3**, 1215.
63. B. Schmaljohann, *Adv. Drug. Deliver. Rev.*, 2006, **58**, 1655.
64. V. Y. Grinberg, A. S. Dubovik, D. V. Kuznetsov, N. V. Grinberg, A. Y. Grosberg and T. Tanaka, *Macromolecules*, 2000, **33**, 8685.
65. Y. Qiu and K. Park, *Adv. Drug. Deliver. Rev.*, 2001, **53**, 321.
66. P. Bawa, V. Pillay, Y. E. Choonara and L. C du Toit, *Biomed. Mater.*, 2009, **4**, 1.
67. H. G. Schild, *Prog. Polym. Sci.*, 1992, **17**, 163.
68. Z. M. O. Rzaev, S. Dincer and E. Piskin, *Prog. Polym. Sci.*, 2007, **32**, 534.
69. I. Idziak, D. Avoce, D. Lessard, D. Gravel and X. X. Zhu, *Macromolecules*, 1999, **32**, 1260.
70. K. Van Durme, S. Verbrugghe, F. E. Du Prez and B. Van Mele, *Macromolecules*, 2004, **37**, 1054.

71. E. E. Makhaeva, H. Tenhu and A. R. Khokhlov, *Macromolecules*, 1998, **31**, 6112.
72. L. M. Mikheeva, N. V. Grinberg, A. Y. Mashkevich, V. Y. Grinberg, L. T. M. Thanh, E. E. Makhaeva and A. R. Khokhlov, *Macromolecules*, 1997, **30**, 2693.
73. S. Chaterji, I. K. Kwon and K. Park, *Prog. Polym. Sci.*, 2007, **32**, 1083.
74. S. Sershen and J. West, *Adv. Drug Deliver. Rev.*, 2002, **54**, 1225.
75. L. E. Bromberg and E. S. Ron, *Adv. Drug Deliver. Rev.*, 1998, **31**, 197.
76. A. S. Hoffman, *Artif. Organs*, 1995, **19**, 458.
77. H. G. Schild, *Prog. Polym. Sci.*, 1992, **17**, 163.
78. Y. Guan and Y. J. Zhang, *Soft Matter*, 2011, **7**, 6375.
79. H. Feil, Y. H. Bae, J. Feijen and S. W. Kim, *Macromolecules*, 1993, **26**, 2496.
80. H. Feil, Y. H. Bae, J. Feijen and S. W. Kim, *Macromolecules*, 1992, **25**, 5528.
81. M. Irie, *Adv. Polym. Sci.*, 1993, **110**, 49.
82. M. Shibayama and T. Tanaka, *Adv. Polym. Sci.*, 1993, **109**, 1.
83. M. A. Lago, V. Ya. Grinberg, T. V. Burova, A. Concheiro and C. Alvarez-Lorenzo, *J. Funct. Biomater.*, 2011, **2**, 373.
84. J. H. Priest, R. J. Murray, R. J. Nelson and A. S. Hoffman, in *Reversible Polymeric Gels and Related Systems*, ed. P. S. Russo, ACS Symposium Series, vol. 350, American Chemical Society, Washington DF, 1987, pp. 255–264.
85. G. Chen and A. S. Hoffman, *Nature*, 1995, **373–375**, 49.
86. G. Chen and A. S. Hoffman, *Macromol. Chem. Phys.*, 1995, **195**, 1251.
87. R. Yoshida, K. Sakai, T. Okano and Y. Sakurai, *J. Biomater. Sci. Polym. Ed.*, 1994, **6**, 585.
88. D. E. Meyer, B. C. Shin, G. A. Kong, M. W. Dewhirst and A. Chilkoti, *J. Control. Release*, 2001, **74**, 213.
89. G. Fundueanu, M. Constantin and P. Ascenzi, *Acta Biomater.*, 2009, **5**, 363.
90. A. Contreras-García, E. Bucio, A. Concheiro and C. Alvarez-Lorenzo, *J. Bioact. Compat. Pol*, 2011, **26**, 405.
91. Y. H. Bae, T. Okano and S. W. Kim, *Pharm. Res.*, 1991, **8**, 531.
92. Y. H. Bae, T. Okano and S. W. Kim, *Pharm. Res.*, 1991, **8**, 624.
93. R. Yoshida, K. Sakai, T. Okano and Y. Sakurai, *J. Biomater. Sci. Polym. Ed.*, 1994, **6**, 585.
94. Y. Okuyama, R. Yoshida, K. Sakai, T. Okano and Y. Sakurai, *J. Biomater. Sci. Polym. Ed.*, 1993, **4**, 545.
95. Y. Qiu and K. Park, *Adv. Drug. Deliver. Rev.*, 2001, **53**, 321.
96. M. Nakayama, T. Okano, T. Miyazaki, F. Kohori, K. Sakai and M. Yokoyama, *J. Control. Release*, 2006, **115**, 46.
97. H. Liu, M. Liu, S. Jin and S. Chen, *Polym. Int.*, 2008, **57**, 1165.
98. X. Huang and T. L. Lowe, *Biomacromolecules*, 2005, **6**, 2131–2139.
99. A. C. Lima, W. Song, B. Blanco-Fernandez, C. Alvarez-Lorenzo and J. F. Mano, *Pharm. Res.*, 2011, **28**, 1294.

100. X. Li, W. Wu and W. Liu, *Carbohydr. Polym.*, 2008, **71**, 394.
101. J. Zhang, X. D. Xu, D. Q. Wu, X. Z. Zhang, R. X. Zhuo and Ren-Xi, *Carbohydr. Polym.*, 2009, **77**, 583.
102. F. Iemma, U. G. Spizzirri, F. Puoci, G. Cirillo, M. Curcio, O. I. Parisi and N. Picci, *Colloid Polym. Sci.*, 2009, **287**, 779.
103. M. Curcio, F. Puoci, U. G. Spizzirri, F. Iemma, G. Cirillo, O. I. Parisi and N. Picci, *AAPS PharmSciTech*, 2010, **11**, 652.
104. M. Curcio, U. G. Spizzirri, F. Iemma, F. Puoci, G. Cirillo, O. I. Parisi and N. Picci, *Eur. J. Pharm. Biopharm.*, 2010, **76**, 48.
105. J. P. Chen, Y. L. Leu, C. L. Fang, C. H. Chen and J. Y. Fang, *J. Pharm. Sci.*, 2011, **100**, 655.
106. M. W. Dewhirst, L. Prosnitz, D. Thrall, D. Prescott, S. Clegg, C. Charles, J. MacFall, G. Rosner, T. Samulski, E. Gillette and S. LaRue, *Semin. Oncol.*, 1997, **24**, 616–625.
107. A. Chilkoti, M. R. Dreher, D. E. Meyer and D. Raucher, *Adv. Drug Deliver. Rev.*, 2002, **54**, 613.
108. N. Gulati, R. Rastogi, A. K. Dinda, R. Saxena and V. Koul, *Colloid Surface B*, 2010, **79**, 164.
109. A. K. Verma, A. Chanchal and A. Maitra, *Ind. J. Exp. Biol.*, 2010, **48**, 1043.
110. E. E. Makhaeva, H. Tenhu and A. R. Khokhlov, *Macromolecules*, 1998, **31**, 6112.
111. S. Shah, A. Pal, R. Gude and S. Devi, *Eur. Polym. J.*, 2010, **46**, 958.
112. N. S. Rejinold, K. P. Chennazhi, S. V. Nair, H. Tamura and R. Jayakumar, *Carbohydr. Polym.*, 2011, **83**, 776.
113. Q. Yuan, R. Venkatasubramanian, S. Hein and R. D. K. Misra, *Acta Biomater.*, 2008, **4**, 1024.
114. M. K. Jaiswal, R. Banerjee, P. Pradhan and D. Bahadur, *Colloid Surface B*, 2010, **81**, 185.
115. S. Deka, A. Quarta, R. Di Corato, A. Riedinger, R. Cingolani and T. Pellegrino, *Nanoscale*, 2011, **3**, 619.
116. T. Fan, M. Li, X. Wu, M. Li and Y. Wu, *Colloid Surface B*, 2011, **88**, 593.
117. Y. H. Lien, T. M. Wu, J. H. Wu and J. W. Liao, *J. Nanopart. Res.*, 2011, **13**, 5065.
118. C. Vasile and A. K. Kulshreshtha, *Handbook of Polymer Blends and Composites*, Rapra Technology Ltd, Shawbury, UK, 2003.
119. T. Okano, *Adv. Polym. Sci.*, 1993, **110**, 179–197.
120. F. A. Plamper, A. Schmalz, M. Ballauff and A. H. E. Muller, *J. Am. Chem. Soc.*, 2007, **129**, 14538.
121. D. E. Owens, Y. Jian, J. E. Fang, B. V. Slaughter, Y. H. Chen and N. A. Peppas, *Macromolecules*, 2007, **40**, 7306.
122. C. Echeverria, D. Lopez and C. Mijangos, *Macromolecules*, 2009, **42**, 9118.
123. H. Katono, A. Maruyama, K. Sanui, T. Okano and Y. Sakurai, *J. Control. Release*, 1991, **16**, 215.
124. C. He, S. W. Kim and D. S. Lee, *J. Control. Release*, 2008, **127**, 189.

125. Y. Shin, J. H. Chang, J. Liu, R. Williford, Y. K. Shin and G. J. Exarhos, *J. Control. Release*, 2001, **73**, 1.
126. X. C. Xiao, L. Y. Chu, W. M. Chen, S. Wang and Y. Lin, *Adv. Funct. Mater.*, 2003, **13**, 847.
127. Q. Wang, S. Li, Z. Wang, H. Liu and C. Li, *J. Appl. Polym. Sci.*, 2009, **111**, 1417.
128. N. Shimada, H. Ino, K. Maie, M. Nakayama, A. Kano and A. Maruyama, *Biomacromolecules*, 2011, **12**, 3418.
129. C. Alvarez-Lorenzo and A. Concheiro, *J. Control. Release*, 2002, **80**, 247.
130. C. Ramkisson-Ganorkar, A. Gutowska, F. Liu, M. Baudys and S. W. Kim, *Pharm. Res.*, 1999, **16**, 819.
131. W. F. Lee and W. Y. Yuan, *J. Appl. Polym. Sci.*, 2000, **77**, 1760.
132. X. Yin, A. S. Hoffman and P. S. Stayton, *Biomacromolecules*, 2006, **7**, 1381.
133. J. C. Garbern, A. S. Hoffman and P. S. Stayton, *Biomacromolecules*, 2010, **11**, 1833.
134. M. Baudys, A. Serres, C. Ramkissoon and S. W. Kim, *J. Control. Release*, 1997, **48**, 304.
135. L. Zhang, R. Guo, M. Yang, X. Jiang and B. Liu, *Adv. Mater.*, 2007, **19**, 2988.
136. F. Muñoz-Muñoz, J. C. Ruiz, C. Alvarez-Lorenzo, A. Concheiro and E. Bucio, *Eur. Polym. J.*, 2009, **45**, 1859.
137. N. Gonzalez, C. Elvira and J. San Roman, *Macromolecules*, 2005, **38**, 9298.
138. J. Zhang, R. Xie, S. B. Zhang, C. J. Cheng, X. J. Ju and L. Y. Chu, *Polymer*, 2009, **50**, 2516.
139. C. Zhao, X. Zhuang, P. He, C. Xiao, C. He, J. Su, X. Chen and X. Jing, *Polymer*, 2009, **50**, 4308.
140. J. R. Moon and Ji-Heung Kim, *Macromol. Res.*, 2008, **16**, 489.
141. J. Shi, N. M. Alves and J. F. Mano, *Macromol. Biosc.*, 2006, **6**, 358.
142. J. Shi, N. M. Alves and J. F. Mano, *J. Biomed. Mater. Res. B*, 2008, **84B**, 595.
143. J. Shi, L. Liu, X. Sun, S. Cao and J. F. Mano, *Macromol. Biosci.*, 2008, **8**, 260.
144. B. L. Guo, J. F. Yuan and Q. Y. Gao, *Polym. Int.*, 2008, **57**, 463.
145. H. H. Sokker, A. M. Abdel Ghaffar, Y. H. Gad and A. S. Aly, *Carbohydr. Polym.*, 2009, **75**, 222.
146. C. Alvarez-Lorenzo, A. Concheiro, A. S. Dubovik, N. V. Grinberg, T. V. Burova and V. Ya. Grinberg, *J. Control. Release*, 2005, **102**, 629.
147. Y. Chen, D. Ding, Z. Mao, Y. He, Y. Hu, W. Wu and X. Jiang, *Biomacromolecules*, 2008, **9**, 2609.
148. Z. Zhang, L. Chen, C. Zhao, Y. Bai, M. Deng, H. Shan, X. Zhuang, X. Chen and X. Jing, *Polymer*, 2011, **52**, 676.
149. M. Mayo-Pedrosa, C. Alvarez-Lorenzo, I. Lacík, R. Martinez-Pacheco and A. Concheiro, *J. Pharm. Sci.*, 2007, **96**, 93.
150. M. Mayo-Pedrosa, N. Cachafeiro-Andrade, C. Alvarez-Lorenzo, R. Martinez-Pacheco and A. Concheiro, *Eur. Polym. J.*, 2008, **44**, 2629.

CHAPTER 19

Elastin-like Hydrogels and Self-assembled Nanostructures for Drug Delivery

JOSÉ CARLOS RODRÍGUEZ-CABELLO,*
ISRAEL GONZÁLEZ DE TORRE AND
GUILLERMO PINEDO

G.I.R. BIOFORGE (Group for Advanced Materials and
Nanobiotechnology), Universidad de Valladolid, Edificio I + D,
Paseo de Belén, 11, 47011-Valladolid, Spain
*Email: roca@bioforge.uva.es

19.1 Introduction

Nature has always provided humans with all types of resources and, in particular, supplies a vast amount of protein-based materials that present outstanding properties. Nowadays, researchers of different disciplines such as materials science and biology are combining efforts in the design of advanced materials that exhibit naturally occurring properties. This has led to the birth of a new and evolving science called biomimicry or biomimetics. Mimicking natural sophisticated materials sets challenging goals and, although significant progress has been made, there is still a lot to learn from the organizational principles employed by Nature. Translating these hierarchical concepts into synthetic, bio-inspired structures would lead to new, high-performance, types of products.

RSC Smart Materials No. 3
Smart Materials for Drug Delivery: Volume 2
Edited by Carmen Alvarez-Lorenzo and Angel Concheiro
© The Royal Society of Chemistry 2013
Published by the Royal Society of Chemistry, www.rsc.org

Materials scientists are mimicking Nature to obtain synthetic proteins with the properties of natural macromolecules. Protein-based polymers offer a set of interesting physical, chemical and biological features. Their component units, the amino acids, provide a broad range of specific characteristics since they can be hydrophobic or hydrophilic, and bear aromatic, cationic, anionic or neutral groups. By changing the sequence design, complex secondary structures as different as α helices, β turns or β sheets can be obtained. This chapter provides an overview of the features and applications in drug delivery of elastin-like recombinamers (ELRs), a new family of protein-based polymers that mimic natural elastin.

19.2 Elastin-like Recombinamers (ELRs)

Elastin is a major component of the extra-cellular matrix and it can be found in many tissues such as skin, lung, artery, ligament and cartilage, conferring them with elasticity. Recombinant techniques allow one to obtain protein-based materials that exhibit some features found in natural proteins together with other properties of technological interest. One of the most interesting protein-based materials is the family of the so-called elastin-like recombinamers (ELRs), which have recently focused the attention of many researchers due to their ability to form a variety of structures, such as nanoparticles, nanofibers, films or hydrogels.[1–3] This versatility along with biocompatibility, bioactivity and smart behavior make ELRs unsurpassable candidates for biomedical applications, including implants and drug-delivery systems (DDSs).[4] ELRs are genetically engineered biopolymers exhibiting stimuli-responsiveness, based on repeats of the pentapeptide sequence Val-Pro-Gly-Xaa-Gly, where Xaa is any natural amino acid except proline. The most widely studied is poly(VPGVG), namely poly(Val-Pro-Gly-Val-Gly). All functional ELRs present a reversible phase transition in response to changes in temperature.[5] In aqueous solution below a certain temperature, *i.e.* the transition temperature (T_t) or lower critical solution temperature (LCST), the polymer chains remain disordered, relatively extended with a random coil conformation and fully hydrated.[6] The hydrophobic hydration is characterized by an ordered clathrate-like water structure surrounding the apolar moieties of the polymer. This structure is somewhat similar to that described for crystalline gas hydrates, although it is more heterogeneous and of varying perfection and stability.[7,8] When temperature surpasses the T_t, according to Urry's model the polymer chains hydrophobically fold and undergo a conformational transition that leads to phase separation. The resultant "coacervate" is composed of about of 63% water and 37% polymer.[9] In the folded state, the polymer chain adopts a dynamic, regular, non-random structure called a β spiral, which involves one type II β turn per pentamer stabilized by intra-spiral, inter-turn and inter-spiral hydrophobic contacts.[5] The process begins with the formation of filaments composed of three-stranded dynamic polypeptide β-spirals, which grow up to hundreds of nanometers before settling into a visible separated state (Figure 19.1).[5,10] This process is completely reversible (*i.e.* lowering the temperature below Tt, the

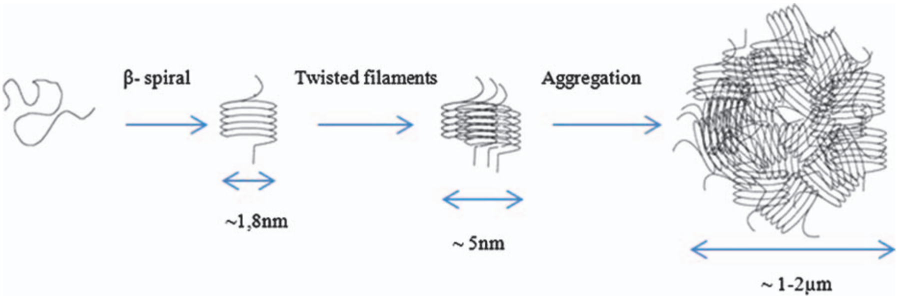

Figure 19.1 Steps of the inverse temperature transition of elastin-like polymers. From left to right: β-spiral structure, formation of twisted filaments or supercoil of β-spiral and aggregation into microaggregates.

initial state is recovered) and has an associated latent heat, ΔHt,[5] which is the result of the combination of the disruption of the water structure and the folding and stabilization owing to the Van der Waals interactions.[11] One VPGVG sequence is enough to permit the transition from random coil to ordered β turn, but higher molecular weight polymers are required to obtain materials presenting useful properties.[12]

Common proteins undergo unfolding and denaturalization when temperature rises. The shift described above from a disordered to an ordered state upon heating is the base of the inverse temperature transition (ITT). At this point, the reader might think that this behavior is not possible, because it seems to violate the second law of thermodynamics. However, this apparent mystery can be solved if the system as a whole is considered; namely, not only the protein but also the water surrounding it. When the system moves to the ordered state, the increase in order of the protein component is less than the decrease in order of the water component. Thus, the second law of thermodynamics is indeed satisfied.

It has been proven that the amino acids sequence has a great influence on the ITT of ELRs.[13] Substitutions of the amino acid at the fourth position (Xaa) of the pentamer modify the values of T_t, to an extent that depends on the polarity of the amino acid side chain. As a rule of thumb, an increase in the polarity decreases the hydrophobic hydration, which causes an increase in T_t and a decrease in ΔHt. The transition temperature can also be altered by physiological variables, such as pH, salt concentration or presence of certain ions or molecules.[14]

As mentioned above, most of the ELRs are based on the general formula (VPGXG), where X represents any natural or modified amino acid except proline. All polymers with this structure are functional, *i.e.* all show smart behavior with sharp responsiveness. However, the achievement of functional ELRs by means of the substitution of any of the other amino acids in the pentamer is not so straightforward. For example, the proline cannot be substituted, and the first glycine cannot be replaced with any natural amino acid other than L-alanine. This is because the type II β-turn per pentamer involves this glycine together with the proline in the folded state of the polymer. The presence of bulky moieties in amino acids with L chirality impedes the formation of the β-turn, and the resulting polymer is not functional. Thus, the substitution by alanine is the only possibility reported that still leads to a functional polymer, though even in this case the resulting polymer shows significantly different and out-of-trend mechanical and thermal properties. Another strategy for tuning the features of ELRs is to synthesize them through genetic engineering to obtain multi-block copolymers.

19.3 ELRs-based Drug-delivery Systems

The efficacy of pharmacological treatments is constricted by inadequate pharmacokinetics and/or systemic toxicity of some drugs.[15] Targeted drug delivery using a suitable carrier can increase the plasma half-life, minimize the systemic toxicity and improve the local efficacy of the therapeutic agent.[16] An alternative to systemic drug administration is the localized delivery from an immobile matrix that is implanted in the tissue of interest. Drug diffusion into the target organ or tissue reduces the need of repetitive administrations, and overcomes systemic barriers associated with the traditional delivery approaches.

A narrow control of the composition and the size of the carrier is crucial for the biocompatibility and effectiveness of the systemic target delivery. Thus, the possibility of synthesizing ELRs with accurate and low polydispersity molecular weight biocompatibility and controlled degradation makes them exceptional carrier components for systemic and targeted drug delivery. Many DDSs based on ELRs have been designed in the form of nanostructures (aggregates, micelles), films and hydrogel networks, which can regulate drug release through diffusion, erosion or swelling mechanisms (Figure 19.2).[17]

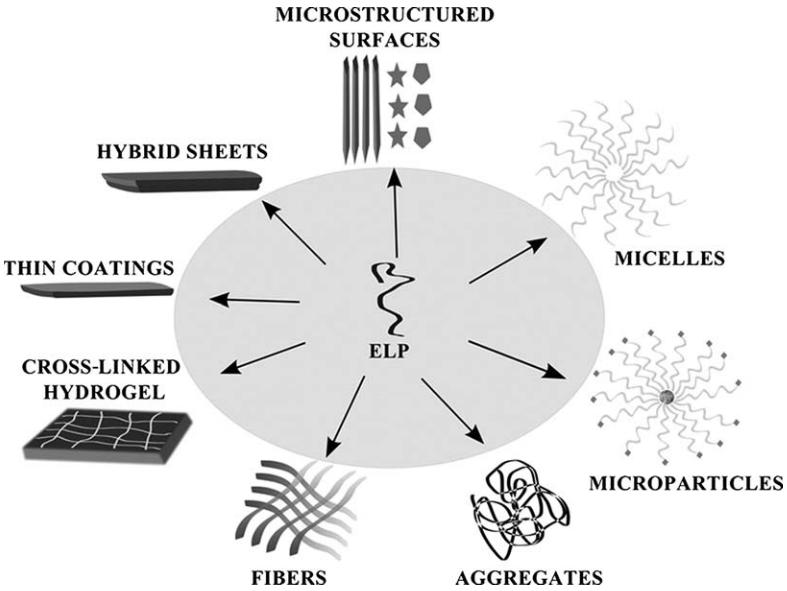

Figure 19.2 Some structures of elastin-based systems useful for drug delivery.

19.3.1 ELRs-based Hydrogels

In the last four decades, hydrogels have been used for biomedical and pharmaceutical applications, mainly due to the high water content, resemblance of natural tissues, biocompatibility and stimuli-responsiveness of some of them.[18,19] In fact, they were the first biomaterials designed to be applied in the human body.[20]

Hydrogels can be classified into two large groups according to the way the network is formed: reversible or physical, and permanent or chemical (Figure 19.3). In a reversible or physical hydrogel the network is held together by molecular entanglements, Coulomb forces, H-bonding or hydrophobic interactions.[21,22] Usually physical hydrogels are not homogeneous and present clusters of molecular entanglements (areas of high cross-linking density and low water swelling) and hydrophobically or ionically associated domains. Chain loops and free chain ends also create transitory network defects. Permanent or chemical hydrogels are covalently cross-linked networks and may contain clusters spread within regions of low cross-linking density and

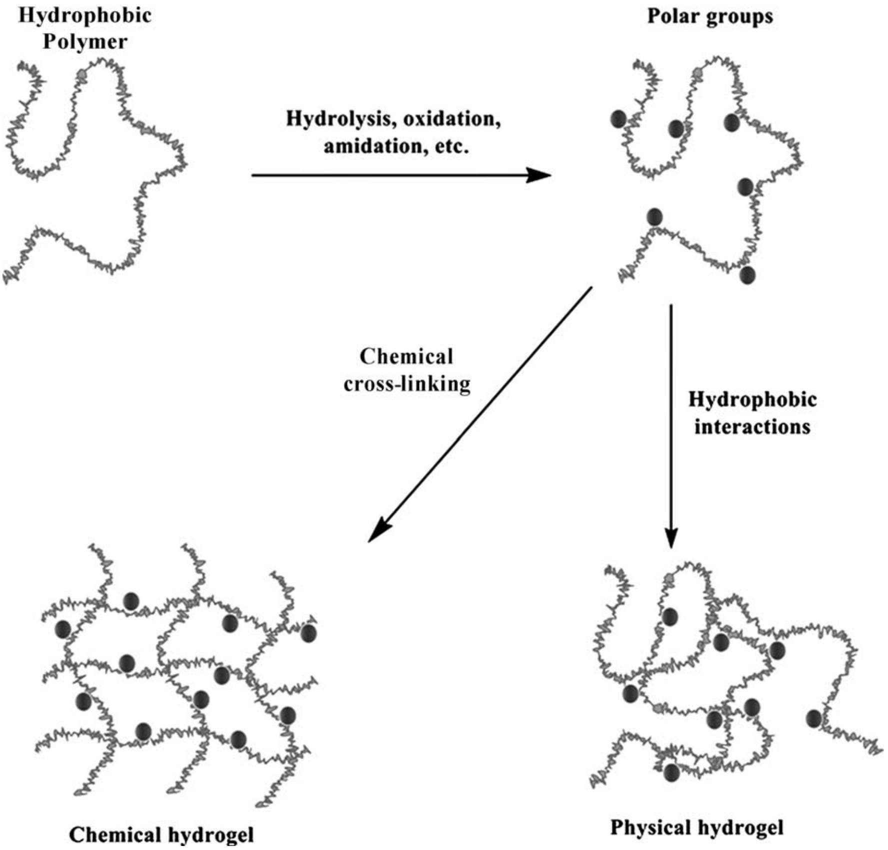
Hydrophobic Polymer
Polar groups
Hydrolysis, oxidation, amidation, etc.
Chemical cross-linking
Hydrophobic interactions
Chemical hydrogel
Physical hydrogel

Figure 19.3 Schematic view of the formation of some physical and chemical polymer hydrogels.

high water swelling. Free chain ends also cause defects in the gel and do not contribute to the elasticity of the networks.

Most traditional methods of hydrogel synthesis do not permit an exact control of the sequence, the chain length and the three-dimensional structure and, thus, some deficiencies in the mechanical properties, and delayed or slow response times to external stimuli might appear.[23] To overcome these problems many strategies have been developed and numerous polypeptide-based responsive hydrogels have been designed, including networks formed from block copolypeptides,[24] recombinant segments of elastin, silk and collagen[7,25] and recombinant triblock copolymers of a random polypeptide sequence flanked by two coiled-coil blocks.[26,27] Protein segments can be introduced to provide degradability, temperature-induced phase transition and sensitivity to biologically active molecules.[28–30] All these strategies can provide very close control over the length and the molecular weight of the proteins that will form the hydrogel network. Thus, hydrogels bearing functional proteins in their structures have huge potential applications in nanotechnology, microfabrication, tissue engineering and drug delivery.

ELRs can be cross-linked at exact places along the skeletal structure of the polypeptide.[31,32] Usually these cross-linking sites correspond to lysine residues spaced and repeated after a concrete number of amino acids, which can react with amine-reactive molecules such as glutaraldehyde, disuccinimidyl suberate or hexamethylene diisocianate. Through chemoselective cross-linking of dried thin films of ELRs, the stiffness of the hydrogel network can be controlled.[33] Recently, click-chemistry has been applied to form ELRs networks avoiding the use of organic solvents.[34] Nevertheless, hydrogels formed in water have a less uniform structure presumably due to phase transitions, which do not occur in organic media.

19.3.1.1 Chemically Cross-linked ELRs Hydrogels

ELRs hydrogels are quite attractive due to the versatility of the genetic techniques to incorporate active amino acids as guest residue (X) in the elastin base unit (VPGXG) and to render biologically active sequences that can provide unique properties. The formed hydrogels maintain the sensitivity to environmental changes in temperature, pH and light exposition.[35,36]

Four typical cross-linking strategies can be applied to obtain ELRs hydrogels, as follows (Figure 19.4).[37]

a) *Radical polymerization*. Chemically cross-linked hydrogel networks can be synthesized by radical polymerization of ELRs derivatized with polymerizable (vinyl, acrylic, alkyne) groups. The polymerization can be induced using chemical initiators like peroxides, which usually are not cytotoxic, or UV light. The remnant chemical initiator and its degradation products have to be removed (usually by diffusion in an appropriate medium) from the hydrogel network before any *in vivo* application.

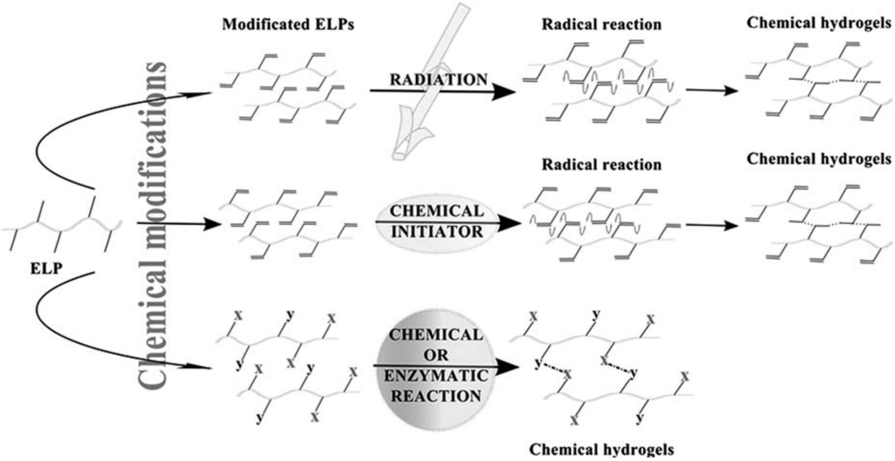

Figure 19.4 Typical strategies to cross-link elastin-like recombinamers (ELRs).

b) *Chemical reaction of complementary groups*. Functional groups of ELRs (amine, alcohol, thiol and acid) can be used to form hydrogels through covalent bonds with complementary groups, involving, for example, the reaction of an aldehyde with an amine or with a hydrazide, or even a Michael reaction of an acrylate and a primary amine or a thiol to form a secondary amine or a sulfide.[38] Some different types of condensation reactions can also be applied to hydrogels formation, such as the Passerini condensation, in which a carboxylic acid and an aldehyde or a ketone react with an isocyanide, or the Ugi condensation by adding an amine to the same reaction mixture to yield an α-(acylamino) amide.[39,40] Some of these reactions can be used for rapid cross-linking and *in situ* gelling, due to the short reaction time (in certain cases even less than 6 minutes)[41] and the versatility to form different kinds of bonds.[42,43] Other cross-linkers can be used to slowly form hydrogel networks (gelling time greater than 30 minutes).[44] Two typical procedures are used for ELRs chemical cross-linking. The first one consists of the prefunctionalization of the ELRs with a cross-linker agent, avoiding the use of small molecules that could be cytotoxic. This procedure has the inconvenience of requiring one or more reactions to functionalize the ELRs, which involve the use of non-biocompatible solvents or cytotoxic chemical agents. Once the ELRs have been modified, the gelation reaction can be carried out in aqueous medium. The second procedure involves the direct reaction of functional groups (amine, alcohol, thiol and acid) of ELRs with homo- or hetero-bifunctionalized molecules. As a drawback, this kind of gelation process has to be carried out in non-biocompatible conditions (organic solvents or chemical additives) and for this reason the obtained gels have to be washed intensely under biofriendly conditions.

c) *High-energy irradiation*. Vinyl and other unsaturated groups can be polymerized when high-energy radiation, principally gamma radiation and electron beam, is applied. The radiation can induce radicals on ELRs derivatized with vinyl groups (caused by, for instance, homolytic C-H bond dissociation) but may also cause the radiolysis of water molecules and the formation of hydroxyl radicals, which can react with ELRs chains to form macroradicals.[45] The reaction between the macroradicals on different chains of ELRs leads to the formation of covalent bonds. Usually, the irradiation is carried out in an inert atmosphere in order to avoid the macroradicals reacting with air oxygen. The greater the irradiation dose, the higher the cross-linking density and thus the smaller the degree of swelling that the VPGXG-based hydrogels can display in water. The degree of swelling also depends on temperature due to the sensitivity of the polymer to this variable.[46,47] Network formation by means of high-energy radiation has the advantage of occurring under mild conditions (room temperature and physiological pH) and in the absence of chemical cross-linkers which could be toxic.

d) *Cross-linking using enzymes*. The use of enzymes to trigger gelation of PEG-based hydrogels has been widely reported.[48,49] By contrast, the application of this approach to ELRs is still quite scarce and only a few examples of ELRs cross-linked by transglutaminase[50] and collagen enzymatically cross-linked with tailored ELRs[51,52] can be found in the bibliography. Transglutaminases catalyze the formation of bonds between glutamine and lysine residues of the proteins. These enzymes need Ca^{2+} ions for their activity.[53] The gelation reaction usually takes between 5 and 30 minutes, depending on the protein structure and the enzyme concentration. The enzyme-controlled gelation occurs under mild conditions and is, therefore, very cell-friendly.

Both aqueous and organic media can be used to form ELRs networks; the cross-linking in an organic solvent rendering hydrogels with a more uniform structure due to the absence of transitions. Conversely, in water the behavior of the ELRs molecules is governed by the LCST.[31] Some organic solvents, such as tris-succinimidyl aminotriacetate, can react with the lysine residues of different ELRs chains to form a network. The cross-linking confers the hydrogel with structural stability, being insoluble in water even upon cooling.

Concentration, molecular weight and lysine content of ELRs are key parameters for hydrogel formation. Below a critical concentration,[33] the hydrogel network is not formed due to the lack of inter-molecular contacts. ELRs with high molecular weight are more prone to establish an elevated number of inter-molecular contacts that promote the network formation. ELRs with a high content in lysine are the most used to prepare hydrogel networks, because of the suitability of the amino group of lysine to form covalent bonds between ELRs chains.

The chemical cross-linking strategy has some important advantages, for instance the covalent bonds avoid hydrogel network dilution and prevent components diffusing out from the place where the hydrogel is implanted.

Furthermore, relevant features of the hydrogel, such as gelation time, network pore size, stiffness and degradability, can be narrowly controlled through the nature and the concentration of the cross-linker agent. Labile chemical linkages can also be formed in order to be broken under physiological conditions, either enzymatically or chemically.[37] As a drawback, chemical cross-linking usually requires organic solvents and reagents that have to be exhaustively removed after synthesis of the network.

19.3.1.2 Physically Cross-linked ELRs Hydrogels

Several strategies can be applied to prepare physically cross-linked ELRs hydrogels. Some are described below.

a) *Cross-linking by ionic interactions*. Polymers with acid groups can be cross-linked by calcium ions at room temperature and physiological pH. The hydrogels are destabilized by extraction of calcium ions using a chelating agent.[54] ELRs modified with monosaccharide residues can be cross-linked by means of ionic/coordination interactions in the presence of potassium ions, since the ionic radius perfectly fits into the free space established by six oxygen atoms of the glucose residues of various polymer chains.
b) *Self-assembly of amphiphilic blocks and graft copolymers*. Hydrogels can be obtained through aggregation among hydrophobic segments of multiblock copolymers of ELRs. The hydrophobic functionalities are provided by amino acids like alanine (Ala), leucine (Leu), isoleucine (Ile), valine (Val), phenylalanine (Phe), tryptophan (Thp), tyrosine (Tyr) or methionine (Met).

19.3.1.3 Applications of ELRs Hydrogels

The ELRs hydrogels are attractive for a wide range of purposes, such as protein purification, biosensing, tissue engineering and, mainly, drug delivery. Many different therapeutic agents can be encapsulated in ELRs hydrogels, *e.g*. peptides, antibiotics, antitumor drugs, anti-inflammatory agents, and so on.

Anticancer Therapy

Systemic administration of anticancer drugs has the problem that, although the active principle reaches the site of action, the healthy tissues are exposed to the toxic effects of the drug. To overcome this limitation, two peculiarities of tumors can be exploited: i) the irregularity of their vasculature, which leads to leaky sections, increasing the global permeability; and ii) the lack of a functional lymphatic drainage. Thus, the drugs diffuse better from blood vessels to tumor tissues than to healthy ones and, once the drug is inside the tumor, it is not efficiently cleared (Figure 19.5). This enhanced retention and permeability effect (EPR) can be exploited using ELRs to encapsulate drugs for targeted delivery, as demonstrated for example with doxorubicin.[55] Cell internalization of ELRs-based constructs can be increased using a cell-penetrating peptide and

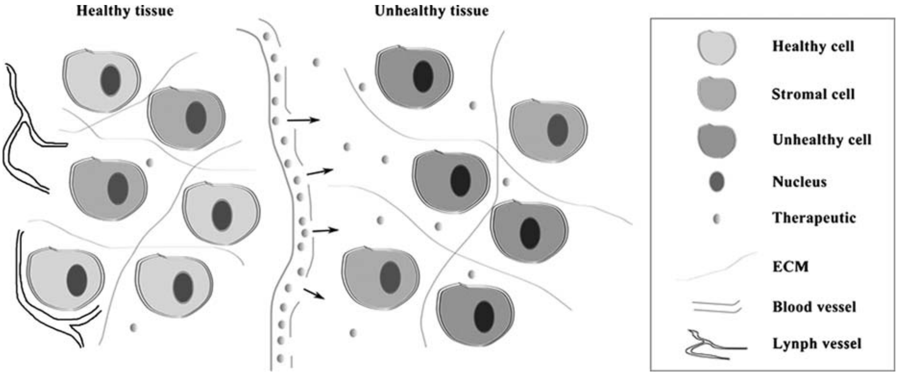

Figure 19.5 Schematic view of the passive targeting of a systemic drug-delivery system to cancer cells, based on the differences between tumor and healthy tissue morphologies.

taking benefit of the hyperthermia induced phase transition. The ELRs vector introduces doxorubicin into the cytoplasm and kills cells by apoptosis. When the treatment is combined with hyperthermia, the cytotoxicity rises up to 20-fold, which proves the usefulness of ELRs for the thermal targeting of doxorubicin. Xenografts of FaDu were used to evaluate *in vivo* the accumulation of ELRs in solid tumors grown in nude mice.[56] Greater tumor penetration and more homogeneous distribution were observed in thermally treated tumors, suggesting that the combination of temperature-sensitive ELRs with mild hyperthermia improve the anticancer therapy).

Antimicrobial Therapy

Controlled release of antibiotics is another field of application of ELRs, particularly in orthopedics. It has been shown that vancomycin and cefazolin can be homogeneously entrapped in freeze-dried ELRs hydrogels, simply by pre-soaking the networks in drug solutions of different concentration. The hydrogels can sustain the release of both drugs, keeping their bioactivity.[57] The size and the physico-chemical features of the encapsulated molecules strongly determine the entrapment efficiency and the subsequent release pattern. Drug loading in high drug concentration solutions caused the networks to exhibit burst release of vancomycin, but not of cefazolin. The concentration of ELRs used to prepare the constructs also play an important role in the release rate of high-molecular-weight drugs (*e.g.* vancomycin), but not in the case of small molecules (*e.g.* cefazolin).

Peptide Delivery

Therapeutic peptides and proteins are susceptible to degradation by endogenous proteases located in the gastrointestinal tract and other tissues and exhibit a poor tissue and cellular membrane permeability. Thus, site specific and controlled delivery of these bioactive macromolecules is of great interest.[58] Some ELRs have been tested as carriers of therapeutic peptides. In particular, they have been attached to cell-penetrating peptides to enhance the intracellular delivery.[59]

Gene Therapy

Gene therapy is a promising strategy for the treatment of many diseases, but the development of an efficient and safe gene delivery vector is still a great challenge.[58] Kim *et al.*[60] have developed an ELRs-mediated adeno-associated virus (AAV) delivery system for transduction to fibroblasts and human neural stem cells (hNSCs). The ELRs used in this study are based on the well-known pentapeptide sequence VPGVG and on a novel variant of the AAV; the AAV-v3.45. ELRs were absorbed on a tissue culture polystyrene surface (TCPS) and AAV-v3.45 was immobilized onto the ELRs. The amount of ELRs adsorbed on the TCPS determined the surface morphology, roughness and wettability, which are key factors in the modulation of cellular transduction. ELR-mediated AAV delivery significantly enhanced the transfection efficiency in fibroblasts and hNSCs, which have great potential for use in tissue engineering and in neurodegenerative disorder treatments. In the case of nude plasmid DNA, the polymer concentration, the cure time of the hydrogels and the ionic strength of the medium had notorious influence on the diffusivity of the DNA through the networks.[58]

19.3.2 ELRs Nanoparticles

ELRs block copolymers can form nano- or micro-sized structures that could be directly injected into the systemic circulation without the risk of blocking blood vessels.[61–63] The mimicking of natural elastin provides ELRs with the peculiarity of "hiding" from the immune system. In other words, the immune system just ignores these polymers because it is unable to distinguish them from natural elastin. Furthermore, the biodegradation products are just natural amino acids.

19.3.2.1 Preparation and Properties

ELRs leading to the formation of nanoparticles are normally synthesized as amphiphile diblock and triblock; namely one or more building blocks are hydrophilic and the other(s) are hydrophobic. This is achieved by substituting the amino acid X in the guest position at the pentamer VPGXG. If X is glutamic acid (abbreviated as E), this block will be hydrophilic, but if X is valine and the third amino acid is substituted by alanine (abbreviated as A), the block will be hydrophobic. When an aqueous solution of an ELR multiblock copolymer is heated above the T_t, the copolymer chains orientate themselves in a way that the hydrophobic blocks are taken off from the aqueous environment in order to reach a state of minimum free energy. This process results in the formation of core–corona nanostructures, with the corona composed of the hydrophilic blocks and the core formed by the hydrophobic blocks. That is the case of the block copolymer comprising an E-block of [(VPGVG)$_2$-(VPGEG)-(VPGVG)$_2$] and an A-block of VPAVG monomer.[64] Both blocks are thermo-sensitive and, additionally, the E-block is pH responsive; at pH above 4.5, *i.e.* the pK_a of the carboxylic acid group; the glutamic acid is deprotonated and the polymer loses the ITT to become "soluble" at any temperature. At acid pH, it is possible to obtain an amphiphilic block copolymer with the E-block soluble in water at any temperature, while the A-block becomes insoluble above the characteristic T_t. Under these conditions, the polymer shows polar and apolar domains and readily forms micelles, which are good carriers for poorly soluble drugs entrapped within the hydrophobic cores.

Herrero-Vanrell *et al.*[4] characterized the self-assembly process of poly(VPAVG). This polymer aggregates at 30.7 °C forming nano- or micro-structures, but does not re-dissolve until the temperature is undercooled down to 8.8 °C (Figure 19.6). This hysteresis phenomenon is explained by the fact that during the cooling process, the reverse dissolution of the poly(VPAVG) aggregates is strongly hindered by the lack of water molecules between amide groups, which are directly bound together causing stabilization of the folded structure.[65] The hysteresis is a very interesting feature for drug delivery, as it allows the formation of drug-loaded particles at a certain temperature, and then the particles can be cooled down to the physiological conditions and

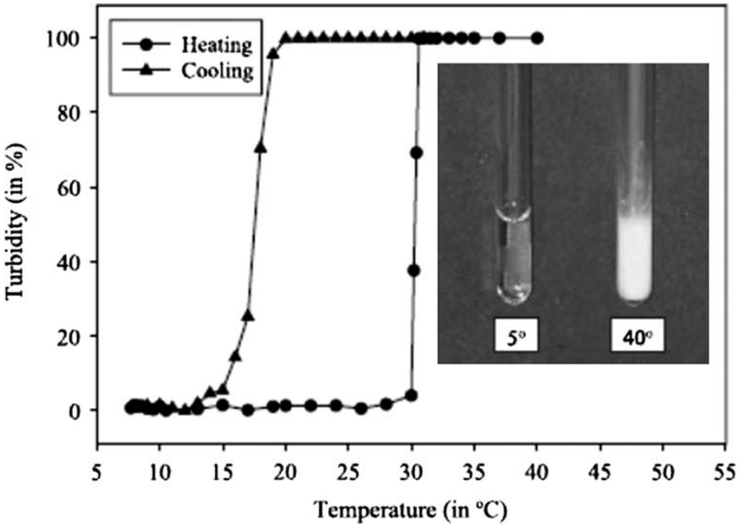

Figure 19.6 Turbidity *vs.* temperature profiles of poly(VPAVG) showing aggregation when the solution is heated, and dissolution when cooling down. The temperature at which turbidity reaches 50% is assumed to be the transition temperature.
Reproduced from Ref. 4 with permission of Elsevier.

injected into the patient. The size and the shape of the particles can be characterized using dynamic light scattering (DLS), static light scattering (SLS) and transmission electron microscopy (TEM) techniques.[66,67]

19.3.2.2 Applications of ELRs Nanoparticles

Self-assembled ELRs have been tested for the delivery of a wide range of products, such as genes, proteins and therapeutic agents. Bessa *et al.*[68] showed that recombinant ELR $(VPAVG)_{220}$ can render stable nanoparticles of 237.5 nm diameter suitable for the delivery of bone morphogenetic proteins (BMPs). The particles were formed exploiting the thermo-responsive self-assembly of the material, by resuspending lyophilized polymer in cold phosphate buffer saline (PBS), followed by incubation at 37 °C for 30 min. The growth factors were loaded into the particles by simple addition to the cold polymer solution. The particles encapsulated significant amounts of BMP-2 or BMP-14 with high efficiency as a result of the hydrophobic interactions between the polymer and the growth factors.[68] The release of both BMPs followed a two-stage release profile, consisting of an initial rapid release in the first 24 h (due to a rapid swelling), followed by a slower release for 14 days. The growth factors retained their activity, as shown by the induction of alkaline phosphatase (ALP) activity and osteogenic mineralization in C2C12 cells.

Rodriguez Cabello's group also explored the use of self-assembled ELRs nanoparticles for controlled release of dexamethasone phosphate. Poly(VPAVG) formed particles above its transition temperature (30 °C), which kept their integrity until a strong cooling was applied. These nanoparticles were able to encapsulate important amounts of dexamethasone phosphate when the self-assembling process occurred in a co-solution of polymer and drug. The release was sustained for about 30 days.[4] ELRs have also been reported as gene vectors. Chen *et al.*[69] have designed a polyplex based on K_8-ELR (1-60) to transfect MCF-7 cells. The block copolymers were composed of a cationic block from oligolysine (VGK_8G) and an ELR block with 60 repetitive penta-peptide units [$(VPGXG)_{60}$; X being Val, Ala and Gly in a 5 : 2 : 3 ratio]. The cationic block provided the binding place for the plasmid DNA, in such a way that the pDNA remains in the core of the nanoparticles, while the ELR block forms a protecting shell. K_8-ELR (1-60) condensed pDNA at a cation to anion (N/P) ratio above 0.25 with a particle size (measured by DLS) in the 32.4 to 115.5 nm range, showing minimal cytotoxicity and successful transduction of MCF-7 cells.

Recently, Sun *et al.*[70] have described a novel targeted drug carrier comprising the knob domain of a fiber protein from adenovirus 5 fused with an ELR diblock capable of self-assembling into a micellar structure. These polypeptide nanoparticles target a unique uptake mechanism, which is differentially expressed throughout the body. The chosen ELR diblock contained two motifs with different transition temperature, which assemble into nanoparticles at physiological temperature. It was demonstrated, by non-denaturing-PAGE, that the purified knob-ELRs form dimers and trimers, which is a property of the native knob/fiber protein. To examine the functionality of the knob-ELRs, their uptake was assessed in a hepatocyte cell line that expresses the adenovirus serotype 5 fiber and the knob receptor, the coxsackievirus and adenovirus receptor (CAR). It was found that both plain ELR and knob-ELR can attach to the outside of the cells. Nevertheless, more internalization and localization into lysosomes was attained by the knob-ELR complex. These results prove that large fusion proteins can be assembled by diblock ELRs, without the need of bioconjugate chemistry, which simplifies the design of targeted drug carriers.

ELRs micelles have also been evaluated as carriers of antitumoral agents.[71] McDaniel *et al.*[72] conjugated the C-terminus of the ELRs with doxorubicin that self-assembled into nanostructures able to promote tumor regression on a mouse model. The sequestration of doxorubicin within the core of the forming nanoparticles may limit the toxicity to healthy tissues, while targeting the drug to the tumor *via* the EPR effect.

Electrospraying is also useful for generating ELRs nanoparticles with potential application in drug delivery. Wu *et al.*[73] reported the preparation of 300–400 nm nanoparticles, dissolving ELRs in trifluoroethanol and doxorubicin in trifluoroethanol : ethanol 25 : 1 vol/vol mixture. Two ELRs of different molecular weight were tested, with peptide sequence SKGPG-(VGVPGIGVPGIGVPGEGVPGIGVPG)$_8$WPC and SKGPG(VGVPGIG-VPGIGVPGEGVPGIGVPG)$_{32}$-WPC(GGC)$_7$. These sequences contained glutamic acid residues with the aim that the charged amino acids i) promote the formation of nanoparticles in electrospraying *via* Coulombic repulsion and ii) enable the tuning of the T_t and, thus, of the drug release rate as a function of pH (Figure 19.7). During the electrospraying process, the solution is accelerated across a voltage gradient and the solvents are rapidly evaporated, leading to the formation of solid particles that can be collected from the target surface. Varying the experimental conditions (flow rate, spraying voltage) different morphologies could be achieved such as particles with tails, fibers and nanospheres. The morphology was also strongly affected by the molecular weight and the concentration of the ELR. Spherical particles were preferentially obtained using ELRs of low molecular weight. Once immersed in buffer medium, particles exposed to pH 6.5 and 7.5 rapidly dissolved, while at pH 2.5 the particles remain as a coacervate phase. This caused the particles incubated at pH 5.5 or 7.5 and 37 °C (below their T_t) to display nearly complete release of doxorubicin after only 15 min. In contrast, particles incubated at pH 2.5 and 37 °C (above their T_t) reached a plateau at 70% released. The other 30% of drug remained trapped in the ELR coacervate, but could be released upon return to solubility at pH 7.5.

An alternative to the administration of preformed particles consists in exploiting the thermal responsiveness of ELRs with T_t between 37 and 42 °C (limit temperature for mild hyperthermia) to form the particles into the body.[72] For example, a solution of ELR was injected into mice bearing human ovarian carcinoma, and the tumor was heated up to 42 °C in order

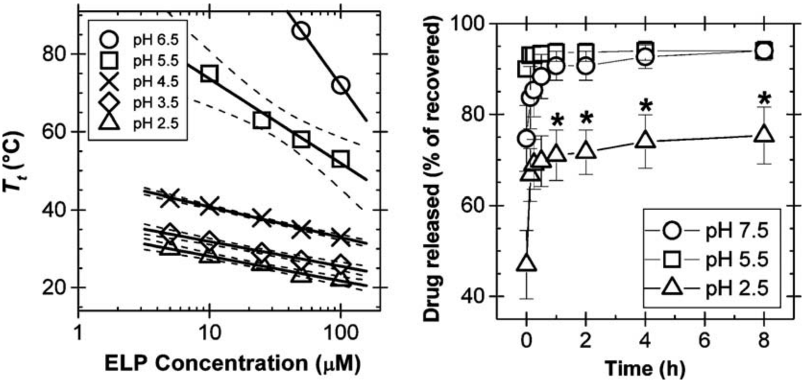

Figure 19.7 pH-dependent transition temperature of low-molecular-weight (17.8 kD) ELR as a function of concentration at various pHs. A best-fit line and 95% confidence interval are presented. Cumulative drug release from the elastin-like recombinamer (ELR) nanoparticles at 37 °C (n = 3) is shown in the plot on the right. *Significant ($p < 0.05$, ANOVA-Tukey) difference in comparison to either pH 7.5 or pH 5.5.
Reproduced from Ref. 73. Copyright 2009 American Chemical Society.

to trigger the coacervation of ELR in the tumor. In this way, active targeting to solid tumors can be achieved just by focused local hyperthermia.

Recently, Martín *et al.*[64] have reported the possibility of obtaining micelles and vesicles from the spontaneous self-assembly of ELRs. Three different ELRs (E50A40, E50A40E50 and E100A40) were investigated, all of them based on the same composing blocks but with different lengths and architecture. The E block was [(VPGVG)$_2$-(VPGEG)-(VPGVG)$_2$]n and the A block was (VPAVG)n. ELRs were solubilized in water at 4 °C, filtered through a 0.45 μm pore membrane and then heated up to 60 °C. The ELR E50A40 adopted micellar structure upon heating, while the other two ELRs self-assembled into hollow vesicles. Therefore, the molecular architecture of the ELRs, namely the block arrangement and length, is determinant for the self-assembled structure. The typical structure of these hollow vesicles is shown in Figure 19.8. In aqueous solution the hydrophilic segment is expressed both on the inside and the outside of the hydrophobic membrane, forming a hydrated hydrophilic corona. Theoretically, the elasticity, permeability and mechanical stability are determined by the membrane thickness, which can be controlled by the molecular weight of the hydrophobic block of the copolymer.[74] Compared to liposomes (see Chapters 2 and 3 in this book), the membrane of the hollow vesicles is in general thicker, stronger and tougher due to the higher molecular weight of the components. Thus, the hollow vesicles may be more stable than conventional liposomes. Perhaps the most striking potential application of the ELRs vesicles is in the suitability of their inner cavity for the encapsulation of hydrophilic therapeutic agents. While micelles are adequate for the entrapment

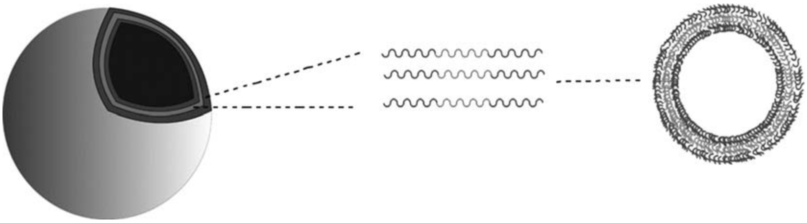

Figure 19.8 Structure of a hollow vesicle formed by self-assembly of an amphiphilic elastin-like recombinamer (ELR) triblock copolymer.

of hydrophobic molecules, the hollow vesicles can encapsulate hydrophilic ones in the cavity and hydrophobic molecules in the hydrophobic bilayer.

An alternative to self-assembly to obtain hollow vesicles is the coating of polystyrene beads with ELRs, followed by cross-linking of the ELRs and the dissolution of the beads. Such hollow spheres have been tested by Dash *et al.*[75] as depots for gene delivery. One ELR, containing a hydrophobic block and a cross-linking block, was used. The hydrophobic block was composed of sequences derived from human exons 20 and 24, while the cross-linking domain was derived from exons 21 and 23. The hollow spheres were obtained through three sequential processes: coating, cross-linking and dissolution of the core. Polystyrene beads were sulfonated to create negative surface charges and then used as a template. Sulfonate polystyrene beads were coated with the ELR and incubated in media with different concentrations of mTGase for cross-linking. Finally, polystyrene beads were dissolved using THF to obtain the hollow spheres. Polyplexes were prepared, using poly(2-dimethyl-aminoethylmethacrylate) (PDMAEMA)-block-poly ethylene glycol methyl ether methacrylate (PEGMEMA)/ethylene dimethacrylate (EDGMA) copolymer and pCMV-GLuc plasmid in PBS. A polyplex of pCMV-GFP was prepared following a similar procedure. The polyplexes may protect pDNA against endosomal degradation. Both pDNA and polyplexes were efficiently loaded inside the hollow spheres, but the loading yield was higher when the polyplex was used. The pDNA alone is loaded by diffusion and not through a charge interaction; in fact, both hollow spheres and pDNA are negatively charged. The higher efficiency of polyplex loading is likely due to i) reduction of pDNA size when complexed with a polymer, ii) electrostatic interaction between positively charged polyplex and negatively charged hollow spheres and iii) diffusion. The release of polyplexes from the hollow spheres was minimal, but it remarkably increased when a protease and elastase treatment was applied. This high pDNA loading capability and the transfection ability of the released polyplexes highlight the interest of the hollow spheres as nucleic acid depots.

19.4 Conclusion and Future Perspectives

Elastin-like recombinamers are excellent biocompatible candidates to form part of DDSs since they are “invisible” for the human immune system and can be easily degraded. The self-assembling property of ELRs in response to environmental changes makes them hugely attractive for the fabrication of nanodevices that can load the drug during the hydrophobic aggregation above T_t, target the drug to specific organs and tissues, and modulate subsequent release. The carriers can degrade at a suitable rate if an appropriate amino acid sequence for the polymer is selected. Hydrophilic drugs can also be loaded within ELR hollow nanoparticles. Furthermore, the ELRs may be convenient to prepare injectable implants that form long-time biocompatible depots for easier treatment of diseases like diabetes or other chronic pathologies. Novel ELRs can provide more environmentally sensitive DDSs suitable for cancer treatment and gene therapy. Nevertheless, for these applications to become a reality much research is still needed.

References

1. L. Huang, R. A. McMillan, R. P. Apkarian, B. Pourdeyhimi, V. P. Conticello and E. L. Chaikof, *Macromolecules*, 2000, **33**, 2989.
2. M. R. Dreher, A. J. Simnick, K. Fischer, R. J. Smith, A. Patel, M. Schmidt and A. Chilkoti, *J. Am. Chem. Soc.*, 2008, **130**, 687.
3. L. Martin, M. Alonso, A. Girotti, F. J. Arias and J. C. Rodriguez-Cabello, *Biomacromolecules*, 2009, **10**, 3015.
4. R. Herrero-Vanrell, A. C. Rincon, M. Alonso, V. Reboto, I. T. Molina-Martinez and J. C. Rodriguez-Cabello, *J. Control. Release*, 2005, **102**, 113.
5. D. W. Urry, *Angew. Chem. Int. Ed.*, 1993, **32**, 819.
6. P. L. San Biagio, F. Madonia, T. L. Trapane and D. W. Urry, *Chem. Phys. Lett.*, 1988, **145**, 571.
7. D. W. Urry, *J. Phys. Chem. B*, 1997, **101**, 11007.
8. J. C. Rodriguez-Cabello, M. Alonso, T. Perez and M. M. Herguedas, *Biopolymers*, 2000, **54**, 282.
9. D. W. Urry, T. L. Trapane and K. U. Prasad, *Biopolymers*, 1985, **24**, 2345.
10. M. Manno, A. Emanuele, V. Martorana, P. L. San Biagio, D. Bulone, M. B. Palma-Vittorelli, D. T. McPherson, J. Xu, T. M. Parker and D. W. Urry, *Biopolymers*, 2001, **59**, 51.
11. J. C. Rodriguez-Cabello, J. Reguera, M. Alonso, T. M. Parker, D. T. McPherson and D. W. Urry, *Chem. Phys. Lett.*, 2004, **388**, 127.
12. H. Reiersen, A. R. Clarke and A. R. Rees, *J. Mol. Biol.*, 1998, **283**, 255.
13. A. Ribeiro, F. J. Arias, J. Reguera, M. Alonso and J. C. Rodriguez-Cabello, *Biophys. J.*, 2009, **97**, 312.
14. B. Li, D. O. V. Alonso and V. Daggett, *J. Mol. Biol.*, 2001, **305**, 581.
15. R. Satchi-Fainaro, R. Duncan and C. Barnes, in *Polymer Therapeutics II*, Springer, Berlin, 2006, p. 1.
16. R. Langer and D. A. Tirrell, *Nature*, 2004, **428**, 487.
17. R. Langer and N. Peppas, *J. Macromol. Sci. C*, 1983, **23**, 61.
18. A. S. Hoffman, *Adv. Drug Deliver. Rev.*, 2002, **54**, 3.
19. N. A. Peppas, *J. Control. Release*, 2000, **68**, 135.
20. J. Kopecek, *Biomaterials*, 2007, **28**, 5185.

21. D. Campoccia, P. Doherty, M. Radice, P. Brun, G. Abatangelo and D. F. Williams, *Biomaterials*, 1998, **19**, 2101.
22. G. D. Prestwich, D. M. Marecak, J. F. Marecek, K. P. Vercruysse and M. R. Ziebell, *J. Control. Release*, 1998, **53**, 93.
23. J. Kopeček and J. Yang, *Polym. Int.*, 2007, **56**, 1078.
24. A. P. Nowak, V. Breedveld, L. Pakstis, B. Ozbas, D. J. Pine, D. Pochan and T. J. Deming, *Nature*, 2002, **417**, 424.
25. J. T. Prince, K. P. McGrath, C. M. DiGirolamo and D. L. Kaplan, *Biochem.*, 1995, **34**, 10879.
26. W. A. Petka, J. L. Harden, K. P. McGrath, D. Wirtz and D. A. Tirrell, *Science*, 1998, **281**, 389.
27. C. Xu, V. Breedveld and J. Kopecek, *Biomacromolecules*, 2005, **6**, 1739.
28. K. Ulbrich, J. Strohalm and J. Kopecek, *Biomaterials*, 1982, **3**, 150.
29. C. Wang, J. I. Kopecek and R. J. Stewart, *Biomacromolecules*, 2001, **2**, 912.
30. T. Miyata, N. Asami and T. Uragami, *Nature*, 1999, **399**, 766.
31. R. A. McMillan, K. L. Caran, R. P. Apkarian and V. P. Conticello, *Macromolecules*, 1999, **32**, 9067.
32. R. A. McMillan and V. P. Conticello, *Macromolecules*, 2000, **33**, 4809.
33. K. Trabbic-Carlson, L. A. Setton and A. Chilkoti, *Biomacromolecules*, 2003, **4**, 572.
34. J. Patterson, M. M. Martino and J. A. Hubbell, *Mater. Today*, 2010, **13**, 14.
35. J. C. Rodríguez-Cabello, M. Alonso, L. Guiscardo, V. Reboto and A. Girotti, *Adv. Mater.*, 2002, **14**, 1151.
36. J. C. Rodriguez-Cabello, J. Reguera, A. Girotti, M. Alonso and A. M. Testera, *Progr. Polym. Sci.*, 2005, **30**, 1119.
37. W. E. Hennink and C. F. van Nostrum, *Adv. Drug Deliver. Rev.*, 2002, **54**, 13.
38. T. R. Hoare and D. S. Kohane, *Polymer*, 2008, **49**, 1993.
39. A. E. J. de Nooy, G. Masci and V. Crescenzi, *Macromolecules*, 1999, **32**, 1318.
40. A. E. J. de Nooy, D. Capitani, G. Masci and V. Crescenzi, *Biomacromolecules*, 2000, **1**, 259.
41. X. Z. Shu, S. Ahmad, Y. Liu and G. D. Prestwich, *J. Biomed. Mater. Res. A*, 2006, **79A**, 902.
42. P. Bulpitt and D. Aeschlimann, *J. Biomed. Mater. Res.*, 1999, **47**, 152.
43. C. Hiemstra, L. J. van der Aa, Z. Zhong, P. J. Dijkstra and J. Feijen, *Macromolecules*, 2007, **40**, 1165.
44. S. K. Hahn, E. J. Oh, H. Miyamoto and T. Shimobouji, *Int. J. Pharm.*, 2006, **322**, 44.
45. N. A. Peppas, *Hydrogels in Medicine and Pharmacy: Vol. 1 Fundamentals*, CRC Press, Boca Raton, 1986.
46. J. Lee, C. W. Macosko and D. W. Urry, *Macromolecules*, 2001, **34**, 4114.
47. J. Lee, C. W. Macosko and D. W. Urry, *Biomacromolecules*, 2001, **2**, 170.
48. J. J. Sperinde and L. G. Griffith, *Macromolecules*, 2000, **33**, 5476.
49. J. J. Sperinde and L. G. Griffith, *Macromolecules*, 1997, **30**, 5255.
50. M. K. McHale, L. A. Setton and A. Chilkoti, *Tissue Eng.*, 2005, **11**, 1768.

51. Y. Garcia, N. Hemantkumar, R. Collighan, M. Griffin, J. C. Rodriguez-Cabello and A. Pandit, *Tissue Eng. A*, 2009, **15**, 887.
52. Y. Garcia, R. Collighan, M. Griffin and A. Pandit, *J. Mater. Sci. Mater. Med.*, 2007, **18**, 1991.
53. E. Westhaus and P. B. Messersmith, *Biomaterials*, 2001, **22**, 453.
54. P. Gacesa, *Carbohydr. Polym.*, 1988, **8**, 161.
55. G. L. Bidwell III, I. Fokt, W. Priebe and D. Raucher, *Biochem. Pharmacol.*, 2007, **73**, 620.
56. W. Liu, M. R. Dreher, D. C. Chow, M. R. Zalutsky and A. Chilkoti, *J. Control. Release*, 2006, **114**, 184.
57. S. B. Adams, M. F. Shamji, D. L. Nettles, P. Hwang and L. A. Setton, *J. Biomed. Mater. Res. B*, 2009, **90B**, 67.
58. Z. Megeed, J. Cappello and H. Ghandehari, *Adv. Drug Deliver. Rev.*, 2002, **54**, 1075.
59. G. L. Bidwell III and D. Raucher, *Adv. Drug Deliver. Rev.*, 2010, **62**, 1486.
60. J. S. Kim, H. S. Chu, K. I. Park, J. I. Won and J. H. Jang, *Gene Ther.*, 2011, **19**, 329.
61. R. Gref, A. Domb, P. Quellec, T. Blunk, R. H. Müller, J. M. Verbavatz and R. Langer, *Adv. Drug Deliver. Rev.*, 1995, **16**, 215.
62. S. J. Douglas, S. S. Davis and L. Illum, *Crit. Rev. Ther. Drug Carrier Syst.*, 1987, **3**, 233.
63. W. Kim, J. Thévenot, E. Ibarboure, S. Lecommandoux and E. L. Chaikof, *Angew. Chem. Int. Ed.*, 2010, **49**, 4257.
64. L. Martín, E. Castro, A. Ribeiro, M. Alonso and J. C. Rodriguez-Cabello, *Biomacromolecules*, 2012, **13**, 293.
65. P. Schmidt, J. Dybal, J. C. Rodriguez-Cabello and V. Reboto, *Biomacromolecules*, 2005, **6**, 697.
66. W. Brown, *Light Scattering: Principles and Development*, Clarendon Press, Oxford, 1996.
67. W. Burchard, *Adv. Polym. Sci.*, 1983, **48**, 1.
68. P. C. Bessa, R. Machado, S. Nurnberger, D. Dopler, A. Banerjee, A. M. Cunha, J. C. Rodriguez-Cabello, H. Redl, M. van Griensven, R. L. Reis and M. Casal, *J. Control. Release*, 2010, **142**, 312.
69. T. H. Chen, Y. Bae and D. Y. Furgeson, *Pharm. Res.*, 2008, **25**, 683.
70. G. Sun, P. Y. Hsueh, S. M. Janib, S. Hamm-Alvarez and J. Andrew MacKay, *J. Control. Release*, 2011, **155**, 218.
71. M. R. Dreher, D. Raucher, N. Balu, O. Michael Colvin, S. M. Ludeman and A. Chilkoti, *J. Control. Release*, 2003, **91**, 31.
72. J. R. McDaniel, D. J. Callahan and A. Chilkoti, *Adv. Drug Deliver. Rev.*, 2010, **62**, 1456.
73. Y. Wu, J. A. MacKay, J. R. McDaniel, A. Chilkoti and R. L. Clark, *Biomacromolecules*, 2009, **10**, 19.
74. B. M. Discher, Y. Y. Won, D. S. Ege, J. C. M. Lee, F. S. Bates, D. E. Discher and D. A. Hammer, *Science*, 1999, **284**, 1143.
75. B. C. Dash, S. Mahor, O. Carroll, A. Mathew, W. Wang, K. A. Woodhouse and A. Pandit, *J. Control. Release*, 2011, **152**, 382.

CHAPTER 20

Multiple Stimuli-responsive Hydrogels Based on α-Amino Acid Residues for Drug Delivery

MARIO CASOLARO* AND ILARIA CASOLARO

Department of Pharmaceutical and Applied Chemistry, University of Siena,
Via Aldo Moro 2, I-53100 Siena, Italy
*Email: mario.casolaro@unisi.it

20.1 Introduction

Cross-linked synthetic polymers that can incorporate a significant amount of water are of increasing interest in drug delivery. Hydrogels can be used to load drugs and to release them slowly over time or to trigger release in response to a wide variety of chemical and physical stimuli. Recently, multiple stimuli-responsive polymer-based systems have attracted significant attention. Functional hydrogels sensitive to pH and temperature can mimic the responsive macromolecules found in Nature and have great potential in the biomedical field.[1,2]

An important group of water-soluble, non-ionic polymers, which form thermo-reversible gels with expanding-contracting properties over a wide range of temperature, is that of *N*-alkyl acrylamide homopolymers and copolymers with or without acidic/basic ionizable comonomers.[3–5] Among these, poly(*N*-isopropylacrylamide) (pNIPAAm) has received considerable attention, since its lower critical solution temperature (LCST) of 32 °C approaches normal body temperature,[5–11] and it can be increased/decreased by the incorporation

RSC Smart Materials No. 3
Smart Materials for Drug Delivery: Volume 2
Edited by Carmen Alvarez-Lorenzo and Angel Concheiro
© The Royal Society of Chemistry 2013
Published by the Royal Society of Chemistry, www.rsc.org

of hydrophilic (charged)/hydrophobic comonomers, respectively.[4,12] Macromolecular extension and contraction can be magnified by constructing three-dimensional networks, which may be suitable as switches for drug-delivery devices.[13–16] Hydrogels can be made from virtually any water-soluble polymer, encompassing a wide range of chemical compositions, bulk physical properties and physical formats, including slabs, microparticles, nanoparticles, coatings and films. Their porous structure can be easily tuned by controlling the cross-link density of the gel matrix and the affinity of the components for the aqueous environment. Porosity strongly influences the loading of small drug molecules and macromolecules and their subsequent release through the network at a rate dependent on the diffusion coefficient.[16] As a result, hydrogels are commonly used in the clinical practice and experimental medicine for a wide range of applications, including tissue engineering and regenerative medicine,[17] diagnostics,[18] separation of biomolecules or cells[19] and barrier materials to regulate biological adhesion.[20]

In recent years, the potential applications of polyelectrolyte hydrogels as carriers of metal-based drugs have been explored.[21] Platinum and ruthenium coordination compounds are currently the most promising metal-based chemotherapeutics, and some of them are being intensively studied in clinical trials to fight metastases and colon cancer.[22] Some new drugs based on platinum- and copper-oxicam complexes have been reported as anticancer agents.[23,24] Among the antitumor agents, cisplatin is commonly used in clinical practice for the treatment of a variety of solid tumors, even though many severe toxic side effects arise.[25] Recent strategies aimed at overcoming some drawbacks of cisplatin consist in developing platforms for chemotherapy that deliver the drug to the local environment of the tumor for extended periods of time. These platforms are based on polyelectrolyte hydrogels carrying functional groups able to form liable complexes with Pt(II)-species.[21,26–28] The cisplatin entrapped or complexed in polymeric systems has a reduced systemic toxicity and an increased activity. There is a large body of information about the *in vivo* compatibility after subcutaneous implantation of synthetic polymers, such as poly(acrylic acid) and poly(methyl methacrylate), and about the ability of carboxylic acid groups to form hydrogen bonds with the glycoprotein coating the mucosal surfaces.[29] To improve these features and to create more attachment sites for a wide range of therapeutics, some vinyl hydrogels containing α-amino acid residues have recently been proposed as novel polymeric compounds to get tunable drug delivery rates.[28,30–33] Hydrogels carrying selected moieties of L-valine, L-leucine, L-phenylalanine or L-histidine can be obtained from the corresponding acrylic and methacrylic monomers (Table 20.1).

Free radical polymerization of acrylate and methacrylate monomers may render linear and cross-linked polymers. The latter can be obtained with a variety of cross-linking densities by using suitable cross-linking agents, such as *N*,*N*′-ethylene-bisacrylamide (EBA), *N*,*N*′-methylene-bisacrylamide (MBA) or poly(ethyleneglycol)diacrylate (PEG-DA). The hydrogels based on L-valine residues enabled cisplatin-coordination and a tunable release rate.[28] The valine

Table 20.1 Structure of the vinyl monomers used for preparing α-amino acid-based hydrogels.

Name	*Acrylates*	*Methacrylates*
N-acryloyl-L-valine	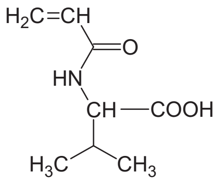	
N-methacryloyl-L-leucine		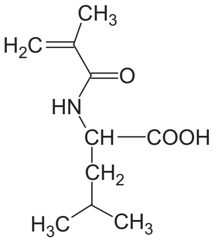
N-acryloyl-L-phenylalanine	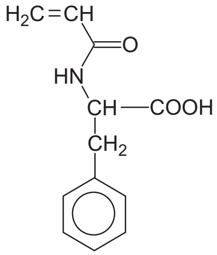	
N-acryloyl-L-histidine	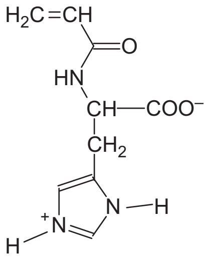	
N-methacryloyl-L-histidine		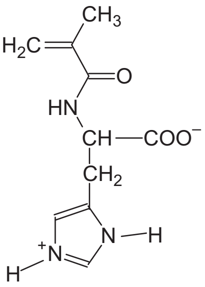

Table 20.1 (*Continued*)

Name	*Acrylates*	*Methacrylates*
N-isopropylacrylamide	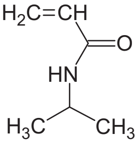	
Cross-linking agents:		
N,*N*′-methylene-bisacrylamide (MBA)	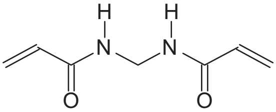	
N,*N*′-ethylene-bisacrylamide (EBA)	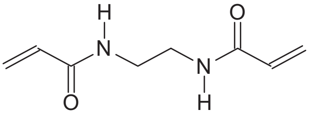	
Poly(ethyleneglycol)diacrylate (PEG-DA-258, M_n 258; PEG-DA-575, M_n 575)	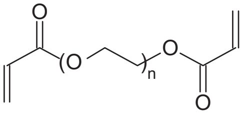	

moiety contains, besides the carboxylic group, amido and isopropyl groups in a conformation that resembles that of the NIPAAm. As a result, it provides the polymer networks with pH-, ion- and temperature-responsiveness in aqueous solution. The interaction between the Pt(II)-species and the hydrogel allows a chemically controlled release along with the diffusion-controlled mechanism. The research already carried out has been focused on elucidating the role of the cross-linking density on the ability of the hydrogels to load cisplatin by presoaking in drug solutions, to regulate the release to aqueous medium at various pHs and temperatures, and to modulate the cytotoxic properties of the drug. The pharmacological efficacy of the Pt(II)-species released from the hydrogels has been compared with that of cisplatin in solution. Moreover, from an interesting point of view in clinical practice, the synergic effect of cisplatin with temsirolimus (macrolid antibiotic) has also been considered.[28] The temsirolimus is a rapamycin ester used as immunosuppressor in the prevention of transplant rejection,[34,35] which is not cytotoxic by itself, but could synergistically increase the cytotoxicity of cisplatin.

As a matter of fact, different drugs able to interact ionically with the ionized functional of the α-amino acid moieties may be incorporated into the gel matrix. The strength of the link of the drug regulates the release rate from the hydrogel, as observed for pilocarpine loaded on vinyl hydrogels containing

L-histidine and L-valine residues.[36] Pilocarpine is a water-soluble drug widely used in glaucoma therapy.[37] Since the molecule contains an imidazole ionizable group, it can interact with the carboxylic acid groups of the polymer and subsequently be released in a stimuli-responsive way from the hydrogel. These systems may be useful as ophthalmic inserts (in the line of the Ocusert-pilocarpine device) due to their valuable properties regarding cytocompatibility and good optical transmission in the swollen state.[38,39] The inserts provide an increased contact time with the conjunctival tissue, to ensure a prolonged delivery through the cornea. Compared with other polymeric ophthalmic devices, the reported hydrogel platforms may have the additional advantages of responding to external stimuli, like changes in temperature, which could be used to trigger the release of the complexed drug under specific ocular circumstances.[40] This chapter focuses on recent developments and future trends of the α-amino acid-based hydrogels as drug-delivery (cisplatin, temsirolimus, pilocarpine) systems for cancer and glaucoma therapy, and as platforms for lithium ion delivery to the brain for bipolar disorder management.

20.2 Syntheses

Stimuli-responsive polyelectrolytes formed by a vinyl backbone and bearing suitable functional groups can be obtained through free radical polymerization of monomers dissolved in suitable organic and/or aqueous media, in the presence of a suitable initiator such as azobisisobutyronitrile (AIBN) or ammonium persulfate (APS) (Scheme 20.1). The corresponding hydrogels can be obtained *via* a similar route of synthesis but with the addition of cross-linking agents. Commercially available or purposely synthesized monomers can be used. Usually, vinyl monomers containing α-amino acid residues are prepared by acylation of the appropriate amino acid with acryloyl or methacryloyl chloride in alkaline solution.[41–43] After neutralization with concentrated hydrochloric acid, the monomers may be crystallized with an analytic grade purity, as shown by potentiometric, calorimetric and spectroscopic (^{1}H NMR and FT-IR) methods. In most cases, white crystals are obtained from aqueous (acrylic monomers) or benzenic (methacrylic monomers) solutions. The monomers are stable under atmospheric moisture conditions and can be stored for several months at low temperature. The

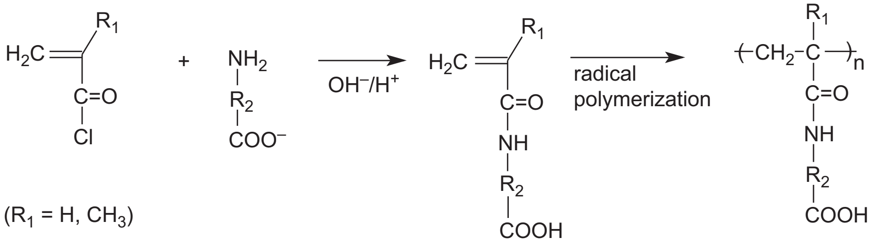

Scheme 20.1 Synthetic pathway to obtain polymers of α-amino acids.

structure of some synthetic monomers used for the preparation of the linear (soluble) polymers and cross-linked (swellable) hydrogels is shown in Table 20.1.

Linear and cross-linked copolymers with various compositions have been obtained by copolymerization of the α-amino acid vinyl monomers together with the well-known NIPAAm to communicate the LCST feature.[6,11,41,44,45] The acid-base titration of the ionizable groups in the copolymers indicated that the comonomers had been effectively incorporated at the feed ratios and randomly distributed along the macromolecules.[46] Hydrogels were obtained adding cross-linking agents, like MBA,[47] EBA[28,30–33] and PEG-DA (Table 20.1), PEG-DA leading to more porous materials. In all cases, the polymerization was carried out in water with various cross-linker proportions. Copolymer hydrogels were obtained neither when PEG-DA was incorporated at low concentration, nor when only α-amino acid vinyl monomers (without cross-linking agent) were used. Thus, only the hydrogels containing 12 mol.% of cross-linking agent and incorporating NIPAAm:synthetic monomer at a 90 : 10 molar ratio were prepared for further studies (Table 20.2). The hydrogels were treated with hydrochloric acid solution (which caused the networks to collapse), washed, dried and cut as small pieces for the subsequent experiments.

20.3 Swelling Properties

Several stimuli, namely ionic strength, specific ions, pH, temperature and electric field, can trigger swollen/collapsed phase transitions of the hydrogels, the swelling behavior strongly depending on the nature of the amino acid residues and the cross-linking degree. In the following sections, the main properties of anionic (carboxylic acid) and amphoteric hydrogels that may be useful for the design of stimuli-responsive drug-delivery systems will be considered.[30–33]

20.3.1 Effect of pH and Ions

20.3.1.1 Anionic (Carboxylic Acid) Hydrogels

Anionic hydrogels can be prepared from acrylates containing L-valine or L-phenylalanine residues and methacrylates carrying the L-leucine moiety. The α-amino acid monomers can also be copolymerized with NIPAAm to tune the temperature-responsiveness.[28,30,47]

The ionization of the carboxylic acid group along with the ionic strength of the medium play a relevant role in the swelling/deswelling of the polymer. Uncharged NIPAAm units decrease the basicity constant (log *K*) of the carboxylate anion, because of the reduced coulombic forces on the uptake of protons. Compared to the free amino acids, the log *K* of the COO^- groups was greater in the corresponding polymers.[41,42,44–46] As a rule, the log *K* value observed in the polymers is “apparent”, *i.e.* it depends on the degree of

Table 20.2 Compositions of monomers in the α-amino acid-based hydrogels.

	Monomer composition (mol. %)						*Amount of cross-linking agent (mol. %)*[a]			
Name of the hydrogel samples	*NIPAAm*	*AVa*	*MAL*	*PHE*	*HIS*	*MHIS*	*MBA*	*EBA*	*PEG-DA-258*	*PEG-DA-575*
AVa-1		100						1		
AVa-2		100						2		
AVa-5		100						5		
NIP-MAL-1	94		6				1			
NIP-MAL-2	94		6				2			
NIP-MAL-5	94		6				5			
NIP-MAL-10	94		6				10			
PHE-9				100				9		
NIP-PHE-2	90			10				2		
HIS-5					100			5		
HIS-10					100			10		
NIP-HIS-1	92				8			1		
NIP-HIS-9	92				8			9		
MHIS-2						100		2		
NIP-MHIS-2	92					8		2		
NIP-MHIS-10	92					8		10		
NIP-AVa-PEG-258	90	10							12	
NIP-AVa-PEG-575	90	10								12
NIP-PHE-PEG-258	90			10					12	
NIP-MHIS-PEG-258	90					10			12	

[a] mol.% of cross-linking agent compared to the moles of monofunctional monomer(s).

AVa-1, AVa-2, AVa-5: homopolymeric hydrogels with *N*-acryloyl-L-valine and cross-linked with 1, 2 and 5 mol.% of EBA;

NIP-MAL-1, NIP-MAL-2, NIP-MAL-5, NIP-MAL-10: copolymeric hydrogels of NIPAAm and *N*-methacryloyl-L-leucine and cross-linked with 1, 2, 5 and 10 mol.% of MBA;

PHE-9, NIP-PHE-2: homopolymeric and copolymeric hydrogels of *N*-acryloyl-L-phenylalanine and NIPAAm and cross-linked with 9 and 2 mol.% of EBA;

HIS-5, HIS-10, NIP-HIS-1, NIP-HIS-9: homopolymeric and copolymeric hydrogels of *N*-acryloyl-L-histidine and NIPAAm and cross-linked with 5, 10, 1 and 9 mol.% of EBA;

MHIS-2, NIP-MHIS-2, NIP-MHIS-10: homopolymeric and copolymeric hydrogels of *N*-methacryloyl-L-histidine and NIPAAm and cross-linked with 2, 2 and 10 mol.% of EBA;

NIP-AVa-PEG-258, NIP-AVa-PEG-575: copolymeric hydrogels of *N*-acryloyl-L-valine and NIPAAm and cross-linked with 12 mol.% of PEG-DA-258 and PEG-DA-575;

NIP-PHE-PEG-258: copolymeric hydrogel of *N*-acryloyl-L-phenylalanine and NIPAAm and cross-linked with 12 mol.% of PEG-DA-258;

NIP-MHIS-PEG-258: copolymeric hydrogel of *N*-methacryloyl-L-histidine and NIPAAm and cross-linked with 12 mol.% of PEG-DA-258.

protonation of the whole macromolecule.[48] The polymers show a polyelectrolyte behavior either in the linear or in the cross-linked gel form. Generally, the log K linearly decreases as the degree of protonation increases according to the modified Henderson–Hasselbalch equation:[49]

$$\log K = \log K^{\circ} + (n-1)\log[(1-\beta)/\beta]$$

where β is the degree of protonation of the whole macromolecule, and log K° is the value of the basicity constant at $\beta = 0.5$. The n value is related to the magnitude of the electrostatic interaction and to the hydrophilicity of the polymer; n values greater than 1 suggest a decreasing log K upon protonation.[48]

The presence of NIPAAm in the linear and cross-linked copolymers leads to a further decrease in both log K° and polyelectrolyte effect. In copolymers with charges randomly distributed, the uncharged NIPAAm moieties shield the charges along the macromolecule, reducing the electrostatic effect.[46] When the proportion of charged units is very low, log K° approaches the lower value of the corresponding non-macromolecular analogue. Moreover, the protonation data of the linear polymer analogues is expected to help to explain also the protonation process of the hydrogels, since the hydrophilic-hydrophobic balance of the functional groups modulates the phase transitions. For example, a sharp decrease in the equilibrium degree of swelling (EDS) of hydrogels carrying the L-valine residues (AVa) is observed when the pH decreases to values close to that of the critical degree of protonation of the carboxylate anion.[28,41] At that pH, the degree of protonation is 0.66 and enables the collapse of the macromolecular coil due to the fact that the hydrophobic interactions between the isopropyl groups can outweigh the repulsive electrostatic interactions of the partially ionized polymer (which otherwise lead to the more extended and hydrated conformation). For example, at pH ∼ 4 the AVa-1, AVa-2 and AVa-5 hydrogels abruptly collapsed in acetate buffer (Figure 20.1). At pH > 4, the charge density of the network became higher and the EDS increased. As estimated from the log K of the linear polymer analogue, the charge density of the COO^{-} group reached about 100% at pH 7.4 and about 34% at pH 4.[41] The greater EDS of AVa-1 hydrogel is explained by its lower degree of cross-linking.

The pH of the phase transition becomes slightly higher in media of low ionic strength, due to an increase in the basicity constant of the carboxylate group. The EDS/pH plots for the AVa-2 and AVa-5 hydrogels in two different buffers (acetate 0.05 M in water and acetate 0.01 M in 0.15 M NaCl) are reported in Figure 20.1.[36] As can be seen in that plot, and in more detail in Figure 20.2, the higher the ionic strength, the lower the EDS was. A sharp decrease in EDS occurred as the concentration of NaCl in the medium raised up to 0.15 M (the 0.9% physiological saline solution). Beyond that concentration, the changes were less marked and reached a plateau. The NaCl concentration at which the EDS stabilized depended on the pH of the medium (Figure 20.2). As the pH decreased approaching the log K value, the effect of the salt on the EDS was sharper. Namely, a higher concentration of salt led to a further collapse at

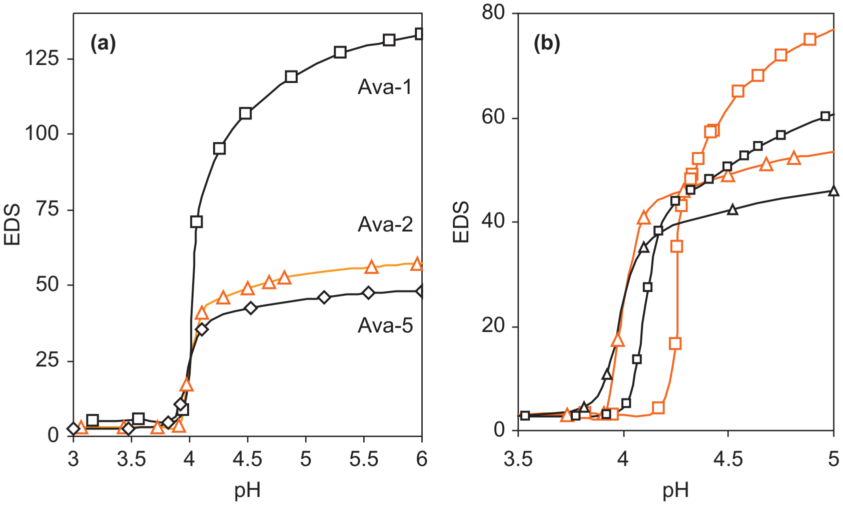

Figure 20.1 Dependence of the equilibrium degree of swelling (EDS) on pH for (a) the AVa-1, AVa-2 and AVa-5 hydrogels at 25 °C in 0.15 M ionic strength (NaCl) medium, and (b) the AVa-2 (red lines) and AVa-5 (dark lines) hydrogels at 25 °C in different ionic strength media: 0.05 M acetate buffer (squares) and 0.01 M acetate buffer in 0.15 M NaCl (triangles). Reproduced from Ref. 36 with permission of Elsevier.

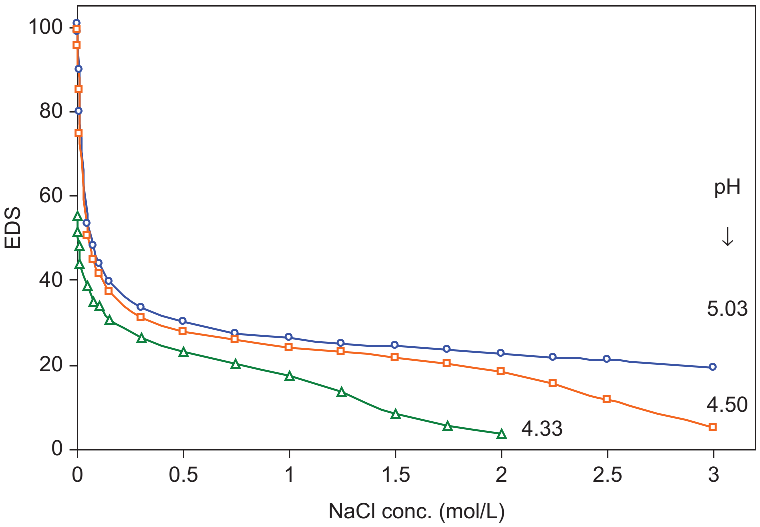

Figure 20.2 Dependence of the EDS of AVa-5 hydrogels on the ionic strength (sodium chloride concentration, mol L^{-1}) at three different pH values and 25 °C.

lower hydration states, as occurred for uncharged hydrogels based on NIPAAm and for charged hydrogels containing different α-amino acid (L-phenylalanine) residues.[30,50] It is worth mentioning the behavior of hydrogels containing L-phenylalanine residues. The homopolymeric PHE-9 hydrogels showed greater EDS than that of the copolymeric NIP-PHE-2 hydrogels, despite the latter having a lower cross-link density. Therefore, the presence of more negative charges improves the swelling and the further shrinking phenomenon.[30]

20.3.1.2 Amphoteric Hydrogels

Acrylates and methacrylates of L-histidine, which have both positive and negative charges regularly inserted on each monomer unit, are particularly suitable for preparing poly(ampholyte) hydrogels.[31–33,51] The imidazole nitrogen of histidine is the main one responsible for the buffering capacity of proteins in the physiological range of pH. It is also able to interact with various metal ions and appears to constitute the principal site for metal binding in proteins.[52] Unlike the above-described carboxylic acid-containing polymers, the ampholyte hydrogels swell less at intermediate pH, but can swell as much as the former ones at extreme pH. The dependence of the EDS of the acrylate (HIS-5 and HIS-10) and methacrylate (MHIS-2) hydrogels on the pH value is shown in Figure 20.3.[31,33]

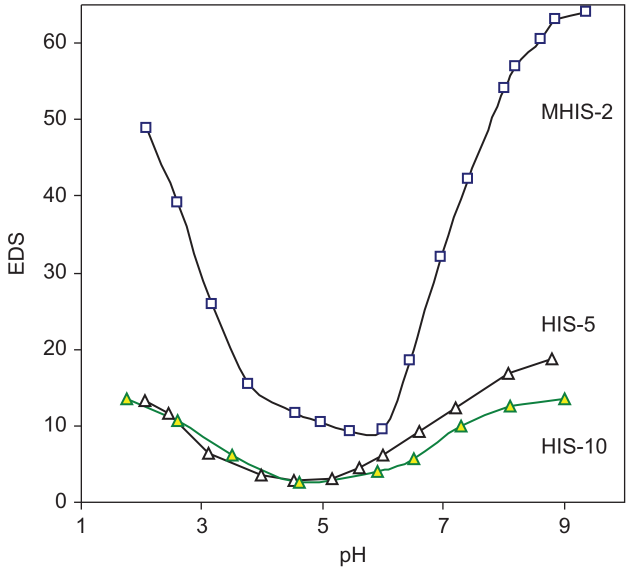

Figure 20.3 Dependence of the EDS of the acrylate (HIS-5 and HIS-10) and methacrylate (MHIS-2) hydrogels on pH in 0.15 M NaCl and 25 °C.

Table 20.3 Basicity constants (log K°) of the histidine monomers and of the linear and cross-linked related polymers (25 °C in 0.15 M NaCl).

Compound	*log* $K_1^{\circ a}$	*log* $K_2^{\circ a}$	n_1^a
Hist	6.48		
MHist	6.88		
Poly(Hist)	7.64	2.3	2.22
Poly(MHist)	7.53	2.0	1.49
Poly(Hist-co-NIPAAm)	7.11	2.9	1.76
HIS-5	7.60	2.4	1.96
HIS-10	7.74	2.9	1.66
MHIS-2	7.66	2.5	1.29

[a] $\log K_i = \log K_i^\circ + (n_i - 1)\log[(1\text{-}\beta)/\beta]$; β represents the degree of protonation.

The pattern of the EDS/pH plot of the cross-linked polymers closely resembles the dependence observed for the reduced viscosity of the corresponding un-cross-linked soluble polymer analogues.[31,33] The charges also determine the hydration process; at high pH, the EDS was maximum, meaning that carboxylate anions lead to greater solvation shells compared to those observed for the "onium" ion at strongly acid pH. At the isoelectric point, the gel shrinks to its minimum hydration. This result is in agreement with the conformational change observed in the linear macromolecule;[31] in fact, the extension of the macromolecular coil at high/low pH is due to not only charge repulsion, but also to the magnitude of the hydration shell of the ionized groups. The cross-linking density also plays a role in the swelling process of the polymer network (Figure 20.3). In the whole range of pH considered, an increase in the cross-linking density leads to a decrease of the EDS.

On the other hand, the EDS/pH plots of the different hydrogels practically overlapped each other at low pH, despite having different basicity constants (Table 20.3). In fact, log K_2° of HIS-10 is higher than that of HIS-5; thus, at the same low pH value, a greater protonation is expected for HIS-10 than for HIS-5 due to the presence of more positively charged groups. Thus, if both networks had an equal cross-linking density, HIS-10 should swell more. However, the EDSs were almost the same because the positive net charge is compensated by a higher cross-linking density. The relative differences of the log K may clarify the small shift of the minimum EDS value of HIS-10 at higher pH, as the isoelectric point slightly increases.

The addition of certain anions and cations provokes a phase-transition from the swollen to the collapsed state when the critical salt concentration is surpassed. The phase-transition occurs at lower salt concentration when the pH of the medium makes the hydrogel have low charge density.[32,50]

20.3.2 Effect of the Temperature

In general, the EDS of α-amino acid hydrogels decreases as the temperature increases. Under physiological pH and salt conditions (namely 0.15 M NaCl in acetate and PBS buffers), the EDS shows a linear decreasing pattern as the

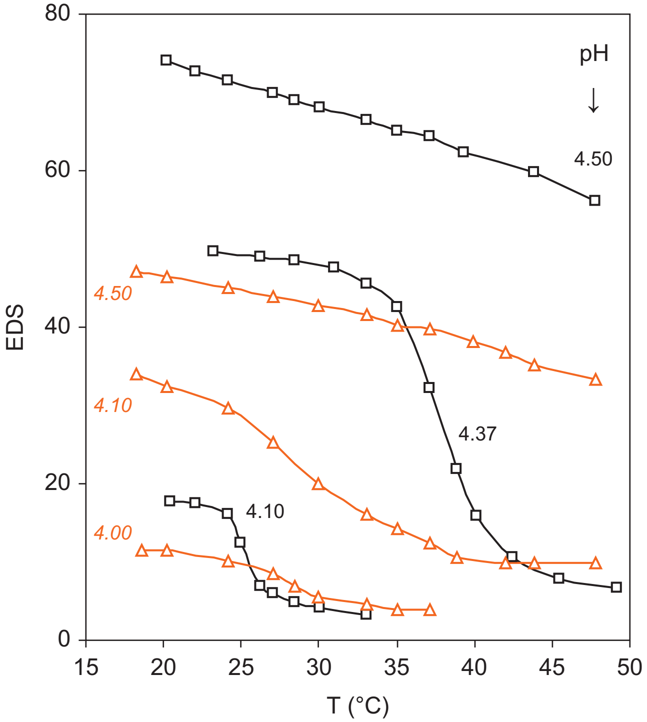

Figure 20.4 Dependence of the EDS of the AVa-2 hydrogel on temperature in acetate buffers of different pH (squares: 0.05 M acetate in water; red triangles: 0.01 M acetate in 0.15 M NaCl).
Reproduced from Ref. 36 with permission of Elsevier.

temperature increases in the 15–50 °C range, when the pH is above the log *K* of the functional group (Figure 20.4). Any increase in pH shifts the shrunk region of the hydrogel to higher temperatures, and no sharp inflection point is detected. That means that the ionic/ionizable groups make the macromolecule retain its hydrophilicity despite the increase in temperature up to 50 °C.[28,30–33] This behavior was observed for both anionic (carboxylic acid) and amphoteric hydrogels, owing to the electrostatic repulsion exerted by the ionized groups preventing the hydrogel from shrinking in the range of the temperature considered.[28,36]

As the pH decreases approaching the critical value of 4, the hydrophilic–hydrophobic forces become competitive, and the sensitivity of the hydrogels to temperature increases. The hydrophobic forces outweigh the electrostatic ones and an increase in temperature causes a brusque collapse. The temperature that triggers the phase transition becomes lower as the pH becomes close to 4 (Figure 20.4). This is common behavior of the temperature-sensitive polymers that show lower LCST as hydrophobic moieties are incorporated;[12] the opposite is true for the incorporation of hydrophilic substituents, which lead to a greater phase-transition temperature that vanishes at high charge density. From a practical point of view, the hydrogel AVa-2 may be a good candidate for drug delivery, because its sensitivity to various stimuli that may trigger the release of a drug through a change in the degree of swelling. In the next section, some examples of the potential application of the α-amino acid hydrogels for the controlled release of cisplatin and pilocarpine for cancer and glaucoma therapy, respectively, are analyzed.[28,36]

20.4 Drug Delivery from α-Amino Acid Hydrogels

The hydrogels containing α-amino acid residues have been mainly evaluated as platforms for controlled release of novel synthetic metal-based anticancer drugs, such as Pt^{2+}-complexes, Ru^{2+}-coordination compounds, Cu^{2+}-oxicam complexes or cisplatin.[21–24] The carboxylic acid and the basic amino groups of the polymers make the chemical binding of the drug possible, this interaction being responsible for the control of the release. Moreover, the electrostatic interaction of the drugs with the proposed platforms may serve for the loading/release of other ionic water-soluble organic molecules, such as pilocarpine.[36,37]

20.4.1 Loading and Release of Cisplatin

Hydrogels swollen above the critical pH were loaded by immersion in a cisplatin aqueous solution and then the release of Pt(II) in PBS pH 7.4 medium was monitored *via* the colorimetric assay with *o*-PDA.[53] Because of the strong coordinating ability of the imidazole sp^2-nitrogen in the poly(ampholyte)s, the release of the metal was difficult. The anionic (carboxylic acid) hydrogels released more Pt(II)-species. The amount of complexed Pt(II)-species was stoichiometric in both hydrogels, but the different interactions between the metal center and the ionized functional groups explains the differences in release rate. In all cases, when the swollen hydrogels were immersed in a cisplatin solution, a progressive deswelling occurred due to the slow reaction of the platinum(II)-species with the functional groups of the polymer to form complexes.[21] A ligand:Pt(II)-metal center 2:1 stoichiometric ratio was shown for both the linear and the cross-linked polymers from viscometric and swelling data, respectively.[26,28] The EDS of the hydrogels swollen in deionized water regularly decreased upon the stepwise addition of a stock cisplatin solution. The minimum EDS value was obtained at a cisPt/AVa molar ratio close to 0.5, *i.e.* the stoichiometric value. This stoichiometry was confirmed by the weight increase of the hydrogel after washing and drying. The interaction of the Pt(II)-species with the carboxylic groups neutralizes the polymer charges and leads to the collapse of the network. In the dry form, the Pt(II)-loaded hydrogels had the appearance of yellowish, tightly compact particles. The FTIR spectra in the neutral, ionized and Pt(II)-complexed forms were compared to monitor the interaction between the COO^- groups and the aminated Pt(II)-species.[26,28] In the case of the AVa-2 hydrogel, the broadband at 1580 cm^{-1} of the COO^- stretching of the ionized networks split into two bands at 1610 cm^{-1} (Pt-coordinated COO^{-}) and 1515 cm^{-1} (N-H amide II frequencies) after complex formation.[28] Similar spectra were recorded for AVa-1 and AVa-5 hydrogels and also for the PHE-9 hydrogel.[26] The Pt(II)-species were not able to form stable complexes with copolymer hydrogels with NIPAAm, because of the greater distance between adjacent COO^{-} groups from different monomer units, which are separated by uncharged and randomly distributed NIPAAm monomers. Any shield of the COO^{-} groups leads to a lack in the coordination ability, as observed for the linear and the cross-linked NIP-PHE-2 polymers.[26] The spectra also revealed that the NH_3 of cisplatin remains linked to the Pt(II)-coordinated species. This indicates that the chloride ion acts as the leaving group and is responsible for the improvement of the Pt(II)-coordination.[28]

Since the solubility in water of cisplatin (0.25% w/w) is quite limited, additional loading experiments were carried out using a drug solution prepared in a water:DMSO mixture (98.4:1.6, v/v).[27] The DMSO strongly coordinated the cisPt(II)-species, leading to reduced or lacking cytotoxic effect upon its release from the hydrogel.[26] The amount of Pt(II)-complex species released in PBS pH 7.4 buffer strongly depended on the initial cisplatin stock solution used for the loading. Hydrogels loaded by immersion in cisplatin solution containing DMSO released three times more cisplatin than those loaded in aqueous solution. Nevertheless, in both cases, the cumulative release had a biphasic pattern, with a burst in the first few hours followed by a sustained release that fitted a near zero-order kinetics (Figure 20.5).[26] The hydrogels containing the

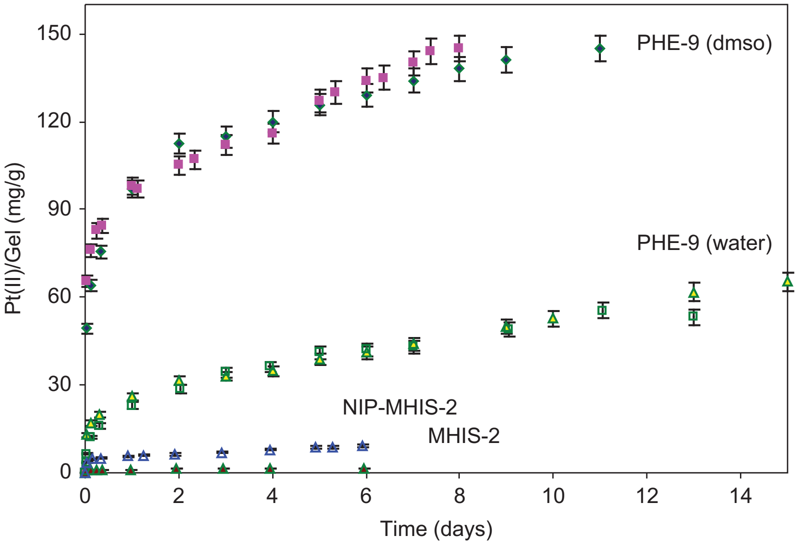

Figure 20.5 Release profiles in PBS buffer (pH 7.4 and 25 °C) of Pt(II)-species from the carboxylic acid hydrogel PHE-9 loaded with cisplatin in water and in water/DMSO solution, and from the amphoteric MHIS-2 and NIP-MHIS-2 hydrogels.

L-valine residues sustained the release for more than one week,[28] according to a zero-order release kinetics, which may be desirable from certain applications.[54]

The effect of the temperature on the amount of Pt(II) released from hydrogels containing L-valine residues was evaluated in different buffer solutions (Figure 20.6). Triggering the release of the drug in response to the temperature at desired pH values might be a further advantage of the hydrogels. At 25 °C the release rate of the Pt(II)-species was constant for the first four days. An increase in temperature up to 36°C accelerated drug release from the AVa-2 hydrogel, showing a burst in the first few hours followed by a flatter release pattern. This behavior is explained by the shrinking phenomenon caused by the temperature.[55] The presence of amido and isopropyl functional groups in the AVa-2 hydrogel, which resemble those of the classical temperature-sensitive pNIPAAm, together with the Pt(II)-carboxylic coordinated groups, renders this system responsive to temperature even at pH greater than the log K° value of the hydrogel. At 25 °C the hydrogel is strongly solvated, but quickly loses the water molecules upon the increase in temperature. This causes the gel to shrink and the Pt(II)-species to squeeze out from the polymeric network. It is noteworthy that as the release proceeded, the swelling of the hydrogel increased. Moreover, the effect of temperature on the cisplatin-loaded hydrogel was less evident at lower pH. Unlike the abrupt

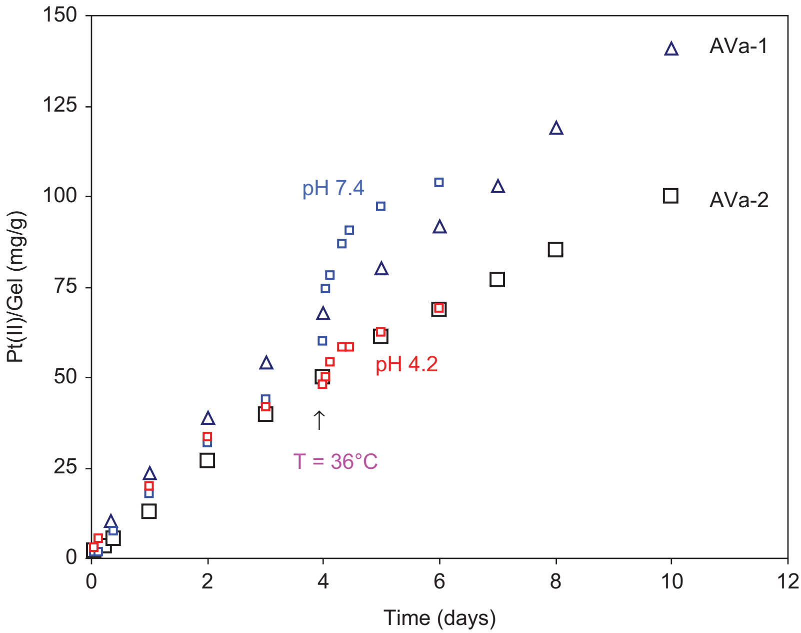

Figure 20.6 Release profiles in PBS buffer at 25 °C of Pt(II)-species from the AVa-1 (triangles) and AVa-2 (squares) hydrogels. The increase in temperature to 36 °C in the tests with AVa-2 hydrogels at different pH values (blue squares, pH 7.4; red squares, pH 4.2) is indicated with an arrow.

pH- and temperature-responsiveness shown by the AVa-2 hydrogel at pH close to 4, the Pt(II)-species anchored to the hydrogel decreased the EDS by themselves, resulting in a less intense shrinking phenomenon at pH 4.2 (Figure 20.6).

In the case of the AVa hydrogels, besides the swelling-controlled drug release, a further mechanism should be considered.[26,28] When a dry hydrogel is immersed in a favorable solvent, the polymer undergoes a transition from an unperturbed (glassy) to a solvated (rubbery) state, with an increase in macromolecular mobility due to a chain extension and in free volume for transport through the gel.[54] The zero-order release arises when the constant rate of solvent front penetration is much smaller than the drug diffusion rate in the swollen gel.[56] Together with the diffusion-controlled step, a chemically controlled release mechanism related to the breakage of coordinated Pt(II)-hydrogel bond has to be considered. The Pt(II)-species released are subjected to a concentration-dependent diffusion that is related to the strength of the binding of the complex species with the coordinating groups inside the network. The stepwise binding cleavage and diffusion of the Pt(II)-species from the inner to the external interface of the hydrogel can provide a broad range of delivery time scales. Thus, the release rate of the Pt(II)-species depends on the dissociation strength of the Pt(II)-gel coordinate bonds and on the mesh size of the network. For the same content in AVa monomer, the less cross-linked AVa-1 hydrogel released the Pt(II)-species faster (slope 15.0 mg g^{-1} per day) than the AVa-2 hydrogel (11.7 mg g^{-1} per day), which indicates that the diffusion process is more favorable through the networks that have a greater mesh size.[28,56] The PHE-9 hydrogel (with a greater cross-linking density) showed even lower slope in the near zero-order release phase (2.7 mg g^{-1} per day).[26]

20.4.2 Cytotoxicity of Cisplatin-loaded Hydrogels

The cytotoxic effect of the Pt(II)-species released from the hydrogels was compared to that of the native cisplatin by using the Me665/2/21 melanoma cell line. The cells were cultured at 37 °C in RPMI 1640 medium supplemented with 10% heat-inactivated fetal calf serum, 2 mM L-glutamine and 50 mg L^{-1} gentamicin, in a humidified atmosphere containing 5% CO_2. In all cases, the cells were treated with cisplatin-loaded hydrogels of small particle size without previous sterilization. The experiments were carried out at cisplatin concentrations close to those found in the plasma of patients with solid tumors treated with this drug; namely 1 μg mL^{-1} of native cisplatin, corresponding to 0.67 μg mL^{-1} or 3.3 μM of Pt. In the experiments with the hydrogel PHE-9, the cells were treated with 30 μg mL^{-1} of the hydrogel, which were loaded in aqueous medium and contained 8.7 μg mL^{-1} or 45 μM of Pt. These hydrogels are the ones that provide the slower release rate and thus melanoma cells received a dose of Pt(II) comparable to that of native cisplatin (0.51 μg mL^{-1} or 2.6 μM released within the first 3 h; Figure 20.5). The cisplatin released from the hydrogel induced a remarkable apoptotic cell death, as evaluated by cell loss, cell detachment from the monolayer and increased activity of caspase-3/7 (Table 20.4).[26]

Table 20.4 Viable and detached Me665/2/21 melanoma cells (1.5×10^6) after being treated for 72 h with native cisplatin (1 μg mL^{-1}) or with cisplatin-loaded PHE-9 hydrogels (30 μg mL^{-1}). The percentages of detached cells on total cells in control (untreated) and in hydrogels loaded by immersion in cisplatin solution in water: DMSO were minor, ranging from 2 to 5%. Mean ± standard error; $n = 3$–5. ND = non-detectable.

Sample	*Total cell number ($\times10^{-6}$)*	*Detached cells (%)*
Control	12.04 ± 0.68	ND
Cisplatin	3.02 ± 0.44	80.8 ± 1.2
Hydrogel-Cisplatin (in water)	3.00 ± 0.38	77.0 ± 4.9
Hydrogel-Cisplatin (in water : DMSO)	11.22 ± 0.44	ND

By contrast, no effect on cell growth and viability was observed with the same hydrogel PHE-9 when loaded with cisplatin from a water/DMSO mixture, although it released a higher amount of Pt(II)-species (Figure 20.5). In the latter case, the loss of activity of the Pt(II)-species released from the hydrogel may be attributed to its exclusion from the cells, because of the steric hindrance of charged Pt(II)-complex species interacting with DMSO molecules. Moreover, the presence of DMSO in the Pt(II)-complex species could suppress the intercalation between the two DNA strands.[57] Solvolysis reactions of cisplatin in DMSO might be expected to form primarily monofunctional DNA adduct.[58] Different Pt(II)-species can be released from the same hydrogel PHE-9; unlike the Pt(II)-species released from PHE-9 loaded in aqueous solution, the adduct containing a DMSO molecule has reduced ability to bind double-stranded DNA and, therefore, its toxicity is lower.[57] The electrospray MS and FT-IR spectra confirmed the composition and the structure of the Pt(II)-DMSO adduct;[26] the prevailing peak at m/z = 343 was consistent with the $Pt(NH_3)_2Cl(DMSO)$ species, and two strong S=O stretching bands at 1028 cm^{-1} and 1124 cm^{-1} confirmed the presence of DMSO. Unlike the cisplatin solution in water, both the loading solution of cisplatin in water/DMSO and the samples of release medium with Pt(II)-species coming from the hydrogel evidenced the presence of one DMSO molecule linked to Pt(II), because of the replacement of a chloride leaving group. This leads to the hypothesis that, once linked, the DMSO molecule remains stably complexed. Thus, the affinity of Pt(II) for sulfur donor ligands makes DMSO unsuitable for use in biological studies of the mechanism of action of platinum antitumor drugs, and the experiments employing this molecule in mixtures of DMSO with other solvents must be strongly discouraged. By contrast, no biological problems were observed for hydrogels that were loaded in DMF solutions. In fact, the synergic effect of cisplatin with temsirolimus was tested after loading of the hydrogels in DMF, due to the insolubility of temsirolimus in water. Temsirolimus, a rapamycin analogue acting through the mammalian target of rapamycin (mTOR) inhibition,[34] is an approved immunosuppressive agent that is under investigation as a potential anticancer drug when combined with other

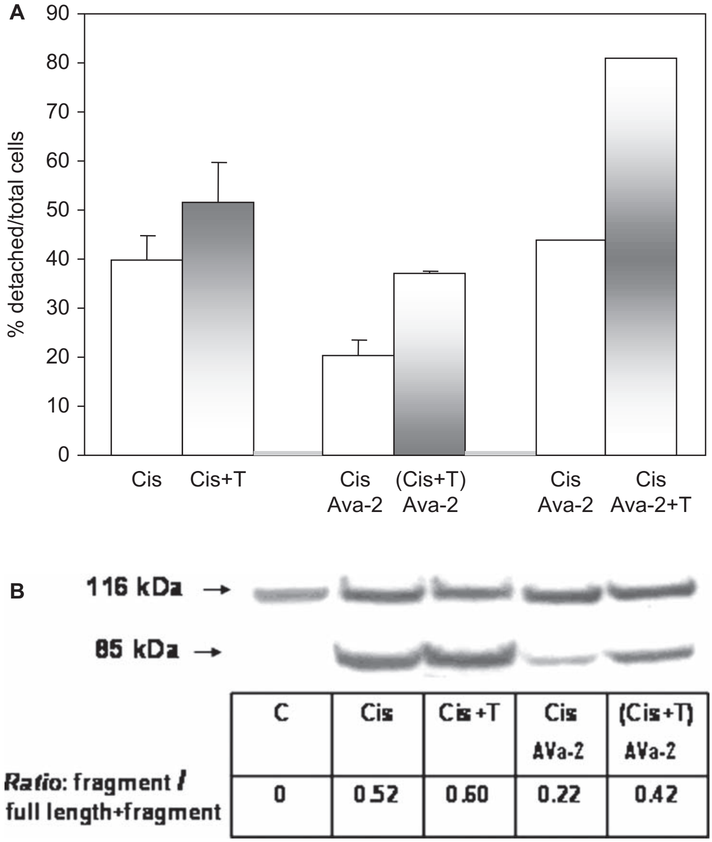

	C	Cis	Cis+T	Cis AVa-2	(Cis+T) AVa-2
Ratio: fragment / full length+fragment	0	0.52	0.60	0.22	0.42

Figure 20.7 Me665/2/21 melanoma cells were treated for 48 h with cisplatin with or without temsirolimus, in diverse experimental conditions where drugs are in the native forms (codes Cis and Cis + T), both loaded in AVa-2 hydrogel from DMF solution (codes Cis AVa-2 and (Cis + T) AVa-2) or cisplatin loaded in the hydrogel from aqueous solution and temsirolimus remains in native form (codes Cis AVa-2 and Cis AVa-2 + T); (**A**) cell death is expressed as percentage of floating cells on total cells; (**B**) Western blot of PARP protein and densitometric analysis of the bands; PARP cleavage is expressed as the ratio between fragments (85 kDa) and total protein (full length + fragment).
Reproduced from Ref. 28 with permission of Elsevier.

cytotoxic drugs.[59] Used in a wide range of concentrations (1–1000 nM) on Me665/2/21 melanoma cells, temsirolimus alone exerts a moderate inhibition of proliferation with no sign of cell death. On the contrary, in the combined treatment with cisplatin and temsirolimus, the latter increases cisplatin cytotoxicity acting through a moderate synergy (Figure 20.7, panel A).

When melanoma cells were treated with cisplatin/temsirolimus-loaded AVa-2 hydrogel, the synergic effect was much higher, and the contribution of temsirolimus almost doubled the cytotoxic response of the hydrogel loaded with cisplatin alone.[28] In these experiments, both cisplatin and temsirolimus were loaded in DMF and, under such conditions, the release of cisplatin is slower and the cytotoxic response is lower than that observed for the native drug. The synergistic cytotoxic effect was more remarkable when the native temsirolimus was combined with cisplatin-loaded AVa-2 hydrogel (Figure 20.7, panel A). The extent of apoptotic cell death was confirmed by Western blot analysis of the caspase-dependent proteolysis of the nuclear enzyme poly(ADP-ribose) polymerase (PARP). PARP cleavage is a hallmark of apoptosis, and the ratio between the cleaved moiety and the total protein (full length + fragment) strictly mirrors the extent of both cell death and activation of caspase-3/7. The extent of PARP proteolysis was much higher in the co-treatment cisplatin + temsirolimus, in conditions where both the drugs are delivered from the AVa-2 hydrogel (Figure 20.7, panel B).[28]

20.4.3 Loading and Release of Pilocarpine

Suitable drug carriers for the ocular therapy of glaucoma are being searched for with the aim of increasing the efficacy of the topically administered drugs.[60–64] Pilocarpine is an imidazole derivative with parasympathomimetic activity that has been used in the treatment of chronic open-angle glaucoma and acute angle-closure glaucoma for over 100 years. It is also used to reduce the possibility of glare at night from lights in patients who underwent implantation of phakic intra-ocular lenses. The most common concentration for this application is 1%, the weakest therapeutic concentration. The high water solubility of the drug makes it have low ocular bioavailability due to low permeability and short residence time of the aqueous solution in the precorneal area. For glaucoma treatment, pilocarpine is administered as drops of 3% solution and, less frequently, as gels or controlled release inserts (Ocusert Pilo).[38] Hydrogels are gaining interest as platforms for ocular drug delivery.[60–63] Sinko and coworkers[64] developed fast-forming hydrogels containing thiol groups for controlled ocular delivery of pilocarpine and evaluated the subsequent pupillary constriction. Hydrogels based on α-amino acid residues suitable for pilocarpine delivery should incorporate anionic or zwitterionic residues able to interact electrostatically with the drug.[36] Besides the three carboxylic acid hydrogels based on L-valine described above, two more networks bearing L-histidine residues with different zwitterionic charge density were evaluated. During the loading process, the swelling degree of AVa hydrogels progressively decreased (Figure 20.8) due to the partial charge neutralization caused by the electrostatic interactions between the negatively ionized groups of the hydrogel and the positively ionized nitrogen of pilocarpine.

The initial sharper decrease of the EDS of AVa-2 hydrogels as drug concentration increases in the loading solution is ascribed to the ionic interaction of the pilocarpine hydrochloride with the negatively ionized gel. Nevertheless, the complexes are not expected to have a high stability constant, and relatively high amounts of pilocarpine are needed to reach a stoichiometric break-point. Theoretically, neutralization should occur at a pilocarpine

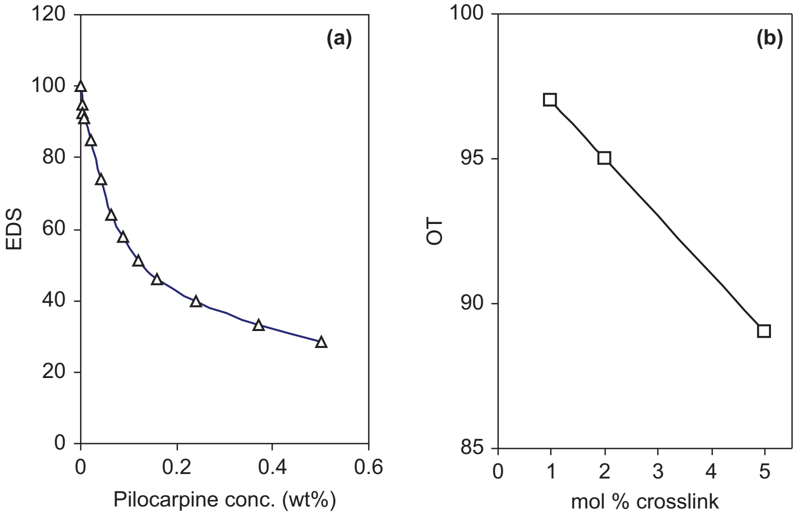

Figure 20.8 Dependence of (a) the EDS, in deionized water at 25 °C, of the AVa-2 hydrogel on pilocarpine concentration (wt.%), and (b) the optical transmission (OT) on the cross-linking density of the pilocarpine-loaded AVa hydrogels in PBS buffer (pH 7.4).
Reproduced from Ref. 36 with permission of Elsevier.

concentration of 0.02 wt.%, but the experimental end-point was observed at 5–10 times greater pilocarpine concentrations. The low stability hypothesis was confirmed by the FT-IR spectra of the AVa-2 gel in the ionized form and after forming complexes with protonated pilocarpine. The small shifts of characteristic bands belonging to pilocarpine and the C=O stretching of the gel were indicative of weak interaction. Overall, once pilocarpine is loaded into the gel, the low electrostatic interaction facilitates the release. Transmittance at 480 nm of the pilocarpine-loaded AVa hydrogels swollen in PBS pH 7.4 linearly decreased as the cross-link density raised (Figure 20.8). The lower swelling of the hydrogels at acid pH resulted in a greater opacity. The hydrogels were loaded by immersion in an aqueous solution (3 wt.%) of pilocarpine hydrochloride for one week. Once loaded, the hydrogels were filtered, washed with distilled water and dried. In all cases, they showed a relevant weight increase due to the incorporation of the drug. The greater the EDS in the loading solution, the higher was the amount of pilocarpine loaded. The release of pilocarpine in PBS pH 7.4 buffer was monitored for one week (Figure 20.9).[36] After a burst in the first few hours, due to the physically entrapped pilocarpine, sustained release profiles were observed.

The total amount of released pilocarpine depended on the nature of the hydrogel. The zwitterionic hydrogel HIS-5 almost stopped the release after 24 h, with less than 200 mg of drug released per gram of dry gel (Figure 20.9). The less ionized NIP-HIS-1 hydrogel released around 400 mg pilocarpine g^{-1} of dry gel. A greater amount of drug, around 600 mg g^{-1}, was released from the

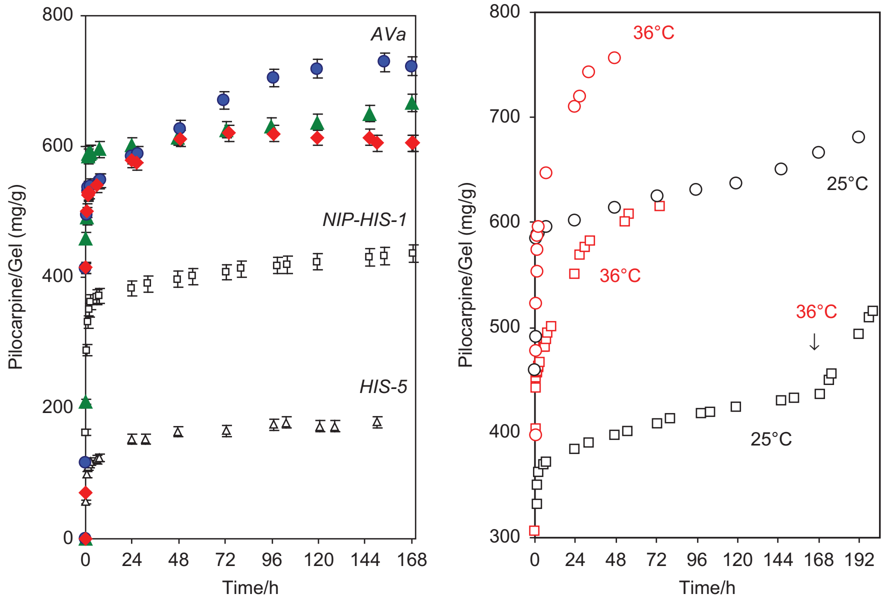

Figure 20.9 Release profiles of pilocarpine in PBS buffer pH 7.4 from the hydrogels: (left) HIS-5, NIP-HIS-1 and AVa (AVa-1, blue circles; AVa-2, green triangles; AVa-5, red squares) at 25 °C; and (right) NIP-HIS-1 (dark squares with pulse of temperature, and red squares at 36 °C) and AVa-2 at 25 °C (dark circles) and 36 °C (red circles).
Reproduced from Ref. 36 with permission of Elsevier.

AVa hydrogels due to their higher affinity for the drug during the loading. Thus, the different releasing pattern may be ascribed to the different electrostatic interaction between the pilocarpine and the ionized groups into the network. Pilocarpine has a log K of 7.2;[65] hence at pH 7.4 the drug is mostly in neutral or positively ionized form. As the pilocarpine comes inside the zwitterionic hydrogel HIS-5, there may be electrostatic repulsions with the positively ionized imidazole residues of the hydrogel, despite the presence of negative carboxylate charges. These latter groups may weakly interact with the protonated drug. Moreover, the low swelling of the HIS-5 gel leads to a small amount of physically loaded pilocarpine. On the other hand, the smaller number of charges and the greater swelling of the NIP-HIS-1 hydrogel (because of a lower cross-linking density) made the loading of pilocarpine two times higher. Furthermore, after the burst, the hydrogels sustained the release for one week. This behavior was also reported for the release of ferulic acid from the zwitterionic hydrogels.[32] As a matter of fact, the presence of carboxylate anions of greater log K in the AVa hydrogels clearly showed the relevant role of the electrostatic interactions. All AVa hydrogels incorporated similar amounts of pilocarpine despite the relative EDS value being different. The AVa-5 swelled three times more than the HIS-5 hydrogel. After the initial burst effect, the less cross-linked AVa-1 hydrogel showed a greater release slope over six days.

As the cross-link density increased, the slope decreased. These findings indicate that through the selection of the α-amino acid monomer and the cross-linking density, the design of tailor-made hydrogels able to fit the efficacy and safety requirements of specific applications may be possible.

The effect of temperature in the 25 to 36 °C range was evaluated for NIP-HIS-1 and AVa-2 hydrogels (Figure 20.9).[36] The increase in temperature notably accelerated pilocarpine release and increased the total amount of drug released, particularly in the case of NIP-HIS-1 hydrogel. This behavior is correlated to the shrinking phenomenon occurring in temperature-sensitive hydrogels.[55,66] In the NIP-HIS-1 gel, the presence of NIPAAm led to a lower solvation at 36 °C. This caused the gel to shrink and the pilocarpine molecules to be gradually squeezed out from the polymeric network. The AVa-2 hydrogel showed a similar behavior.

20.4.4 Cytotoxicity of Pilocarpine-loaded Hydrogels

The cytotoxicity of AVa hydrogels was evaluated using the NIH3T3 mouse fibroblasts cell line. Non-confluent adhered cells were incubated with each swollen hydrogel both before and after loading with pilocarpine. After 24 hours of incubation, no cytotoxic effect was observed.[36] In particular, the percentage of viable cells in contact with AVa-1, AVa-2, AVa-5 and pilocarpine-loaded AVa-5 was not statistically different from the negative control (high-density polyethylene, HDPE) (Figure 20.10). Tests carried out with pilocarpine-loaded AVa-1 and AVa-2 hydrogels revealed greater cell viability than when the cells

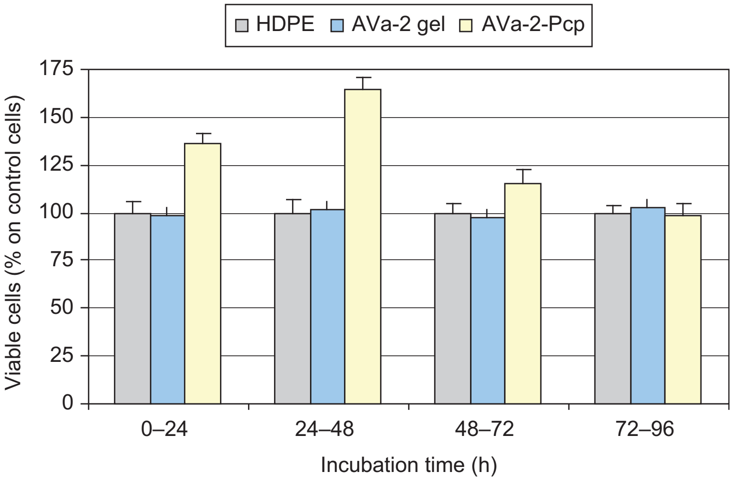

Figure 20.10 Effect of pilocarpine release from AVa-2 hydrogels on the NIH3T3 cells proliferation. The values obtained for AVa-2-Pcp after 24, 48 and 72 h of incubation were statistically different from those obtained for HDPE and AVa-2 hydrogel ($p < 0.05$).
Reproduced from Ref. 36 with permission of Elsevier.

were in contact with HDPE or pilocarpine; the number of viable cells ranked in the order pilocarpine-loaded AVa-2 > pilocarpine-loaded AVa-1 > pilocarpine-loaded AVa-5. This trend may be due to the different cross-linking degree of the hydrogels. In fact, the AVa-2, with an intermediate cross-linking degree, showed a structure that promotes an optimal drug release.

The effect of pilocarpine released from the AVa-2 gels (see Figure 20.9 for the *in vitro* profiles) on cell viability was evaluated for a total incubation time of 96 h (Figure 20.10). Every 24 h the gels were removed and placed on new cell layers in the presence of fresh medium. The results showed that the released pilocarpine led to an increase in the percentage of viable cells from 0 to 24 h, from 24 to 48 h and from 48 to 72 h.[36] The maximum cell viability was observed for the drug released from 24 to 48 h. The amount of drug released in the 72 to 96 h interval was not able to influence the cell viability significantly, which was the same as that observed for HDPE or the non-loaded AVa-2 hydrogel.

20.5 Outlook for the Future

The research for new stimuli-responsive hydrogels continues to move rapidly, offering novel platforms to be effective for disease prevention and treatment. In the particular case of the α-amino acid-based hydrogels, combined incorporation of temperature-responsive NIPAAm and PEG-based (of different molecular weights) cross-linkers may provide advanced features (Table 20.2). These hydrogels show multiple-stimuli responsiveness and the effect of pH and temperature on the swelling (Figure 20.11) is strongly related to the magnitude of the electrostatic potential created around the hydrated ionic groups.

It is worth noting that the pH that triggers the shrinking depends on the log K° of the carboxylic group belonging to the α-amino acid residues. As previously reported for linear polymer analogues,[30,41,42] the log K° of the PHE residues is always greater than that of the AVa moiety. Copolymerization with NIPAAm increases the polyelectrolyte behavior of the PHE compounds,[30] whereas it decreases that of the AVa ones.[41,42] This respectively reflects an increase and a decrease of log K as the degree of protonation increases. Thus, NIP-PHE-PEG-258 and NIP-AVa-PEG-258 collapsed at pH 4.2 and 3.5, respectively. Moreover, the longer segments of PEG-575 cross-linker led to a higher EDS and a smaller pH responsiveness. This is likely ascribed to a further low log K° of the ionized carboxylic groups that, being more distant from each other, created an environment with a lower electrostatic field. The hydrophilic character of the PEG segments may further enhance the swelling of the network.

The temperature effect on the swelling properties of the copolymer hydrogels at different pH media is close to that shown for the homopolymer networks, in spite of the fact that the presence of NIPAAm should improve the temperature-sensitiveness. The behavior of two similar hydrogels differing only in the PEG segment length, namely NIP-AVa-PEG-258 and NIP-AVa-PEG-575, is reported in Figure 20.11. In the 15–50 °C range, the EDS of both hydrogels linearly decreases as pH decreases, although the swelling was always greater for

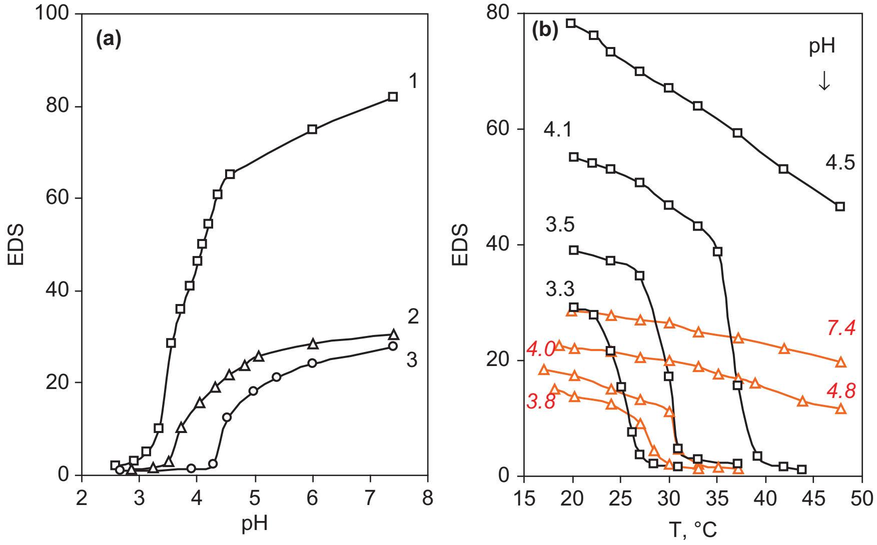

Figure 20.11 Dependence of EDS on (**a**) pH for the NIP-AVa-PEG-575 (1), NIP-AVa-PEG-258 (2) and NIP-PHE-PEG-258 (3) hydrogels at 25 °C; and (**b**) temperature for the NIP-AVa-PEG-575 (squares) and NIP-AVa-PEG-258 (red triangles) hydrogels in acetate and PBS buffers in 0.15 M NaCl.

the NIP-AVa-PEG-575 hydrogel. For a given pH, a sharp decrease in the EDS was observed when the temperature surpasses a value that makes the hydrophilicity provided by the charged groups outweighed by the hydrophobic influence of the isopropyl groups; this drives the collapse of the network in a narrow range of the critical temperature. This critical temperature regularly decreases with pH; about 13 °C for each pH unit in the temperature range tested. For these two hydrogels, the same critical temperature may lead to the shrinking at different pH or, conversely, at the same pH the collapse may occur at different temperature. For example, NIP-AVa-PEG-575 at pH 3.5 and NIP-AVa-PEG-258 at pH 4.0 collapse around 31°C, which is coincident with the LCST of poly(NIPAAm). For a given pH, the collapsing temperature is greater for the NIP-AVa-PEG-575 hydrogel. We envision the hydrogels as components of magnetic nanocomposites for remote-controlled pulsate drug release and as drug carriers for brain diseases. The magnetic nanocomposites are becoming promising for various applications in medical and pharmaceutical fields;[67–69] as reported, for example, for hydrogels based on NIPAAm that, under a high frequency alternating magnetic field, collapse due to the rise of the temperature, and release the drug. Further details on magnetic-responsive nanoparticles for drug delivery can be found in Chapter 14.

As regards brain diseases, the lithium ion is one of the standard pharmacological treatments for bipolar disorder.[70] Bipolar disorder is a psychiatric diagnosis that describes a category of mood disorders, involving one or more episodes of abnormally elevated energy levels, cognition and mood with or without one or more depressive episodes.[71] These events are usually separated by periods of "normal" mood; but, in some individuals, depression and mania may rapidly alternate, which is known as "rapid cycling". Severe manic episodes can sometimes lead to psychotic symptoms as delusions and hallucinations. Estimates of the lifetime prevalence of bipolar disorder vary from 0.4 to 1.6%.[71] Bipolar disorder is often treated with mood stabilizing medications and, sometimes, other psychiatric drugs. Clinically, lithium is a strong anti-suicidal drug and it is used together with other mood stabilizers (*i.e.* valproic acid and/or carbamazepine) to enhance or prolong both treatment response and remission.[72] Although lithium has a narrow therapeutic margin and well-known adverse effects, such as dry mouth, gastro-intestinal disturbances, weight gain, tremor or thyroid dysfunction, it is safe if the concentration is maintained in the therapeutic range (4.2 to 8.3 mg L^{-1}). For this purpose, controlled-release matrix tablets comprising polyelectrolyte hydrogels have been proposed.[73] Some preliminary data show that the amount of lithium released from α-amino acid-based hydrogels depends on both the α-amino acid residues and the cross-linking agent (Figure 20.12).

Unlike the release profile of the copolymeric hydrogels, which resembles the one shown by the available sustained-release tablets of commercially available

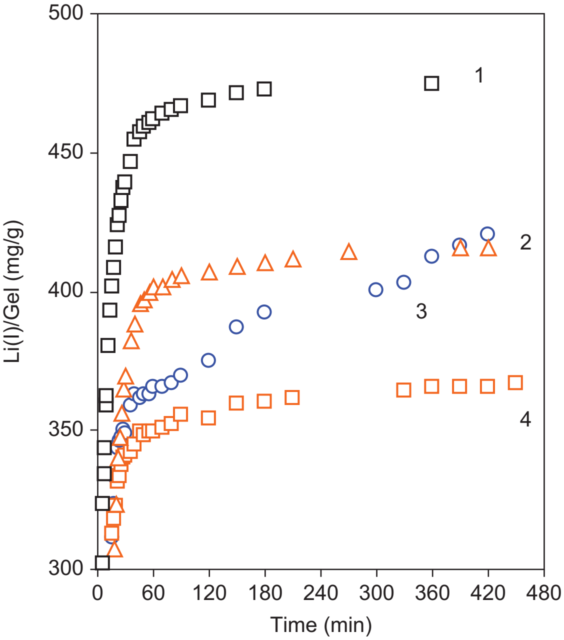

Figure 20.12 Release profile in deionized water at 25°C of lithium(I) ion from the NIP-PHE-PEG-258 (1), NIP-AVa-PEG-575 (2), AVa-5 (3) and NIP-AVa-PEG-258 (4) hydrogels.

Eskalith CR®, the presence of more negative charges on the AVa-5 hydrogel allowed the release to be sustained for a longer time. In clinical practice, lithium is often associated with valproic acid, which also presents a narrow therapeutic margin (40–100 mg L^{-1}) and causes severe side effects. To maintain constant blood levels of mood-stabilizing drugs in order to ensure adequate therapeutic efficacy, more than one dose is required daily, with a risk of reduced adherence to therapy by the patient. A controlled-release system for lithium, valproic acid and/or the two drugs associated would be desirable to improve treatment possibilities for such a highly debilitating disorder as bipolar disorder. The α-amino acid-based hydrogels may find here a good niche.

20.6 Conclusion

Purposely designed charged hydrogels, having multiple-stimuli-responsiveness, can be suitable vehicles for controlled release of actives under determined conditions.[16] Some research is focused on the development of hydrogel platforms based on α-amino acid residues to release the drug to the target site. The hydrogels containing carboxylic acid and amphoteric moieties represent an opportunity because of their ability to form complexes of different bonding strength with either ionic and/or metal-based drugs[24,26] to be implanted or injected.[61,74] For example, the α-amino acid-based hydrogels are suitable platforms for the release of liable Pt(II)-complexed species for the chemotherapy of solid tumors. The homopolymeric materials carrying COOH groups close to each other are able to form complex species with a well-defined 2:1 molar ratio stoichiometry between the ligand and the metal center.[26–28] This allows proper polymeric networks to be designed that can tune the release rate of the Pt(II)-species. Further, the zero-order release rate and the increase in release rate triggered by the temperature are advantageous features. The apoptotic cell death due to the released Pt(II)-species from the hydrogel is remarkable and close to that afforded by native cisplatin. Furthermore, the synergistic effect of temsirolimus remarkably increases the cytotoxic effect of cisplatin, compared to the native drugs action.[28]

Even when simple ionic species that are weaker electrostatically interact with the ionized hydrogels, these can still be suitable platforms for a sustained release. The hydrogels provide a sustained pilocarpine release and show resistance and good optical transmission in the swollen state.[36] These features together with the good cytocompatibility make the hydrogels promising prototypes of inserts for glaucoma therapy.[38] After an initial burst, sustained release may occur and the rate can be increased by the effect of temperature. Similar release patterns were noticed for the lithium ion, which is one of the standard pharmacological treatments for bipolar disorder. The hydrogels may be also utilized to control drug release rate when formulated as matrix tablets.[70,73] On the whole, the hydrogels carrying α-amino acid residues show a good biocompatibility that allows them to be promising candidates as soft materials.

References

1. Z. M. O. Rzaev, S. Dincer and E. Piskin, *Prog. Polym. Sci.*, 2007, **32**, 534.
2. I. Dimitrov, B. Trzebicka, A. H. E. Muller, A. Dworak and C. B. Tsvetanov, *Prog. Polym. Sci.*, 2007, **32**, 1275.
3. Y. H. Bae, T. Okano and S. W. Kim, *J. Polym. Sci. Polym. Phys.*, 1990, **28**, 923.
4. H. Feil, Y. H. Bae, J. Feijen and S. W. Kim, *Macromolecules*, 1993, **26**, 2496.
5. D. Schmaljohann, *Adv. Drug Deliver. Rev.*, 2006, **58**, 1655.
6. M. Heskins and J. E. Guillet, *J. Macromol. Sci. Chem.*, 1968, **A2**, 1441.
7. A. S. Hoffman, A. Afrassiabi and L. C. Dong, *J. Control. Release*, 1986, **4**, 213.
8. A. S. Hoffman, *J. Control. Release*, 1987, **6**, 297.
9. Y. H. Bae, T. Okano and S. W. Kim, *J. Control. Release*, 1989, **9**, 271.
10. S. Tacheuchi, I. Omodaka, K. Hasegawa, Y. Maeda and H. Kitano, *Makromol. Chem.*, 1993, **194**, 1991.
11. H. G. Schild and D. A. Tirrel, *J. Phys. Chem.*, 1990, **94**, 4352.
12. H. Iwata, H. Oodate, Y. Uyama, H. Amemiya and Y. Ikada, *J. Membr. Sci.*, 1991, **55**, 119.
13. Y. Ito, M. Casolaro, K. Kono and Y. Imanishi, *J. Control. Release*, 1989, **10**, 195.
14. Y. Osada, *Adv. Polym. Sci.*, 1987, **82**, 1.
15. C. C. Lin and A. T. Metters, *Adv. Drug Deliver. Rev.*, 2006, **58**, 1379.
16. T. R. Hoare and D. S. Kohane, *Polymer*, 2008, **49**, 1993.
17. K. Y. Lee and D. J. Mooney, *Chem. Rev.*, 2001, **101**, 1869.
18. H. J. van der Linden, S. Herber, W. Olthuis and P. Bergveld, *Analyst*, 2003, **128**, 325.
19. K. Wang, J. Burban and E. Cussler, *in Responsive Gels: Volume Transitions II*, ed. K. Dusek, Springer-Verlag, New York, 1993, p. 67.
20. S. L. Bennett, D. A. Melanson, D. F. Torchiana, D. M. Wiseman and A. S. Sawhney, *J. Card. Surg.*, 2003, **18**, 494.
21. B. Lippert (ed.), *Cisplatin*, Wiley-VCH, Weinheim, 1999.
22. R. Cini, S. Defazio, G. Tamasi, M. Casolaro, L. Messori, A. Casini, M. Morpurgo and M. Hursthouse, *Inorg. Chem.*, 2007, **46**, 79.
23. G. Tamasi, F. Serinelli, M. Consumi, A. Magnani, M. Casolaro and R. Cini, *J. Inorg. Biochem.*, 2008, **102**, 1862.
24. G. Tamasi, M. Casolaro, A. Magnani, A. Sega, L. Chiasserini, L. Messori, C. Gabbiani, S. M. Valiahdi, M. A. Jakupec and B. K. Keppler, *J. Inorg. Biochem.*, 2010, **104**, 799.
25. R. C. DeConti, B. R. Toftness, R. C. Lange and W. A. Creasey, *Cancer Res.*, 1973, **33**, 1310.
26. M. Casolaro, R. Cini, B. Del Bello, M. Ferrali and E. Maellaro, *Biomacromolecules*, 2009, **10**, 944.
27. X. Yan and R. A. Gemeinhart, *J. Control. Release*, 2005, **106**, 198.

28. M. Casolaro, B. Del Bello and E. Maellaro, *Colloid Surface B*, 2011, **88**, 389.
29. H. Park and J. R. Robinson, *Pharm. Res.*, 1987, **4**, 457.
30. M. Casolaro, E. Paccagnini, R. Mendichi and Y. Ito, *Macromolecules*, 2005, **38**, 2460.
31. M. Casolaro, S. Bottari, A. Cappelli, R. Mendichi and Y. Ito, *Biomacromolecules*, 2004, **5**, 1325.
32. M. Casolaro, S. Bottari and Y. Ito, *Biomacromolecules*, 2006, **7**, 1439.
33. M. Casolaro, Y. Ito, T. Ishii, S. Bottari, F. Samperi and R. Mendichi, *eXPRESS Polym. Lett.*, 2008, **2**, 165.
34. L. Ballou and R. Z. Lin, *J. Chem. Biol.*, 2008, **1**, 27.
35. S. Jhunjhunwala, G. Raimondi, A. W. Thomson and S. R. Little, *J. Control. Release*, 2009, **133**, 191.
36. M. Casolaro, I. Casolaro and S. Lamponi, *Eur. J. Pharm. Biopharm.*, 2012, **80**, 553.
37. J. D. Bartlett and S. D. Jaanus (eds.), *Clinical Ocular Pharmacology*, Butterworth-Heinemann, New York, 2007.
38. F. Lee, Y. T. Shen and M. Eberle, *Invest. Ophthalmol.*, 1975, **14**, 43.
39. S. K. Murthy and N. Ravi, *Curr. Eye Res.*, 2001, **22**, 384.
40. K. S. Rathore and R. K. Nema, *Int. J. Pharm. Tech. Res.*, 2009, **1**, 164.
41. M. Casolaro, *Macromolecules*, 1995, **28**, 2351.
42. M. Casolaro, *React. Polym.*, 1994, **23**, 71.
43. Y. Iwakura, F. Toda and H. Suzuki, *J. Org. Chem.*, 1967, **32**, 440.
44. M. Casolaro, *Polymer*, 1997, **38**, 4215.
45. M. Casolaro and R. Barbucci, *Polym. Adv. Techn.*, 1996, **7**, 831.
46. M. Casolaro, in *Frontiers in Biomedical Polymer Applications*, Vol. 1, ed. R. M. Ottenbrite, Technomic Publishing Co., Lancaster, Basel, 1998, p. 109.
47. M. Penco, F. Bignotti, L. Sartore, I. Peroni, M. Casolaro and A. D'Amore, *Macromol. Chem. Phys.*, 2001, **202**, 1150.
48. R. Barbucci, M. Casolaro and A. Magnani, *Coord. Chem. Rev.*, 1992, **120**, 29.
49. A. Katchalsky and P. Spitnik, *J. Polym. Sci.*, 1947, **2**, 432.
50. T. G. Park and A. S. Hoffman, *Macromolecules*, 1993, **26**, 5045.
51. S. E. Kudaibergenov (ed.), *Polyampholytes: Synthesis, Characterization and Applications*, Kluwer Academic Press, New York, 2002.
52. I. Bertini and A. Scozzafava, in *Metal Ions in Biological Systems,* Vol. 12, ed. H. Sigel, Marcel Dekker, New York, 1981, p. 31.
53. E. D. Golla and G. H. Ayres, *Talanta*, 1973, **20**, 199.
54. M. Ali, S. Horikawa, S. Venkatesh, J. Saha, J. W. Hong and M. E. Byrne, *J. Control. Release*, 2007, **124**, 154.
55. J. H. Kim, S. B. Lee, S. J. Kim and Y. M. Lee, *Polymer*, 2002, **43**, 7549.
56. C. S. Brazel and N. A. Peppas, *Eur. J. Pharm. Biopharm.*, 2000, **49**, 47.
57. S. J. Fisher, L. M . Benson, A. Fauq, S. Naylor and A. J. Windebank, *Neurotoxicology*, 2008, **29**, 444.

58. W. J. Sundquist, K. J. Ahmed, L. S. Hallis and S. I. Lippard, *Inorg. Chem.*, 1987, **26**, 1524.
59. C. Thallinger, W. Poeppl, B. Pratscher, M. Mayerhofer, P. Valent, G. Tappeiner and C. Joukhadar, *Pharmacology*, 2007, **79**, 207.
60. G. H. Hsiue, J. A. Guu and C. C. Cheng, *Biomaterials*, 2001, **22**, 1763.
61. L. Verestiuc, C. Ivanov, E. Barbu and J. Tsibouklis, *Int. J. Pharm.*, 2004, **269**, 185.
62. A. Ludwig, *Adv. Drug Deliver. Rev.*, 2005, **57**, 1595.
63. Th. F. Vandamme and L. Brobeck, *J. Control. Release*, 2005, **102**, 23.
64. S. S. Anumolu, Y. Singh, D. Gao, S. Stein and P. J Sinko, *J. Control. Release*, 2009, **137**, 152.
65. M. Meloun and P. Černohorský, *Talanta*, 2000, **52**, 931.
66. S. R. Sershen, S. L. Westcott, N. J. Halas and J. L. West, *J. Blomed. Mat. Res., Part A,* 2000, **51**, 293.
67. N. S. Satarkar and J. Z. Hilt, *J. Control. Release*, 2008, **130**, 246.
68. N. S. Satarkar and J. Z. Hilt, *Acta Biomater.*, 2008, **4**, 11.
69. R. Barbucci, D. Pasqui, G. Giani, M. De Cagna, M. Fini, R. Giardino and A. Atrei, *Soft Matter*, 2011, **7**, 5558.
70. C. T. Chiu and D. M. Chuang, *Pharmac. Therap*, 2010, **128**, 281.
71. American Psychiatric Association. *DSM-IV-TR Diagnostic and Statistical Manual of Mental Disorders*, American Psychiatric Press, Washington DC, 2000.
72. S. D. Friedman, S. R. Dager, A. Parow, F. Hirashima, C. Demopulos, A. L. Stoll, I. K. Lyoo, D. L. Dunner and P. F. Renshaw, *Biol. Psychiatry*, 2004, **56**, 340.
73. J. Emami, N. Tavakoli and A. Movahedian, *J. Pharm. Pharmaceut. Sci.*, 2004, **7**, 338.
74. A. Serres, M. Baudys and S. W. Kim, *Pharm. Res.*, 1996, **13**, 196.

CHAPTER 21

Molecularly Imprinted Hydrogels for Affinity-controlled and Stimuli-responsive Drug Delivery

C. ALVAREZ-LORENZO,* C. GONZÁLEZ-CHOMÓN
AND A. CONCHEIRO

Departamento de Farmacia y Tecnología Farmacéutica, Facultad de
Farmacia, Universidad de Santiago de Compostela, Spain
*Email: Carmen.alvarez.lorenzo@usc.es

21.1 Introduction

The general concept of smart or intelligent drug-delivery systems (DDSs) involves devices that sense and act in response to a stimulus in a predictable and repeatable way, performing a macroscopic function, namely regulation of drug release. In most cases, the sensor and actuator features are due to changes in the structure of a polymer, which affects its solubility, conformation or state of aggregation, as explained in detail in Chapter 1. Many nice examples of such performance are reported in this book, and typically the switching on-off of the release is due to changes in the permeability of the DDS components. Although still less explored, there are also cases in which the responsiveness involves a change in the affinity of the polymer chains for the drug itself. Differently from the cases in which the substance that acts as a stimulus causes rupture or erosion of the responsive network, affinity-controlled release involves either

---

RSC Smart Materials No. 3
Smart Materials for Drug Delivery: Volume 2
Edited by Carmen Alvarez-Lorenzo and Angel Concheiro
© The Royal Society of Chemistry 2013
Published by the Royal Society of Chemistry, www.rsc.org

i) competitive binding of a biomarker that displaces the drug or interacts with a critical moiety in the DDS (biomolecule-sensitive networks), or ii) reversible physical changes in the spatial arrangement of the chemical groups in a polymer network that cooperatively bind the drug (responsive imprinted networks). The first option requires the conjugation of the polymer with biological molecules that can recognize specific biomarkers, such as carbohydrates,[1] DNA,[2] enzymes,[3] antibodies[4,5] or proteins.[6] For example, coupling a polymer network with lectins enables an enhanced loading of glycosylated insulin, which is hosted inside the DDS through specific interactions with the lectins. In a medium without glucose, the DDS does not release insulin. By contrast, if glucose is present, the glucose molecules compete for the binding to lectins, triggering the release of insulin.[7] A combination of glycosylated polymers with lectin-conjugated polymers renders networks in which the interactions between glycosylated groups and lectins act as cross-linking points. In this case, the trapped insulin is only released when glucose breaks the cross-linking bridges.[8] The design and applications of biomolecule-sensitive hydrogels are reviewed in detail in Chapter 22.

The second option tries to go further in the mimicking of the recognition ability of natural molecules by designing the whole network with receptors able to recognize the drug when the polymer chains adopt a specific conformation, but that lose that ability if the conformation of the polymer is altered. Biological receptors, enzymes or antibodies possess a spatial conformation that is critical for the recognition. Such a conformation is given by the sequence of the structural unities, namely amino acids. Proteins find their desired conformation out of a nearly infinite number, thanks to the unique details of their native state. Similarly, a specific conformation can be memorized in synthetic polymers if the sequence of monomers is properly selected.[9] Differently from randomly made polymers that do not fold in just one way, the memorization of the conformation should allow the polymer always to revert back into the same conformation after being stretched and unfolded.[10–12] Such bioinspired principles can be materialized by adapting the classical molecular imprinting technology to the design of stimuli-responsive networks.[13–16] This chapter starts with a general overview of the molecular imprinting fundamentals, and then focuses on the efforts that are being carried out to adapt this technology to the synthesis of stimuli-responsive systems discussing illustrative examples of their applications in the drug-delivery field.

21.2 Molecular Imprinting Technology

This technology was born in the context of the analytical field searching for synthetic receptors specifically to bind/separate analytes of interest. It aims to create tailor-made cavities by synthesizing the polymer network in the presence of the target substance that should act as a template. It is expected that the template molecules alter the distribution of the monomers as a function of their ability to interact with them (Figure 21.1). Therefore, each target molecule should be surrounded by the monomers showing the highest affinity

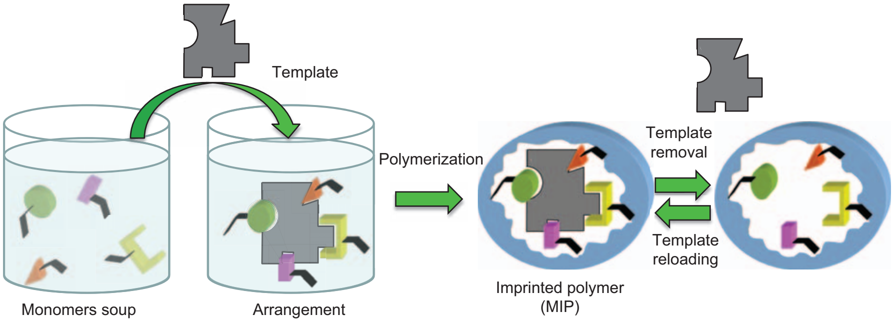

Figure 21.1 Diagram of the synthesis of an imprinted hydrogel. The template is added to the monomers soup in order to cause the arrangement of the monomers as a function of their affinity for the template molecules. The arrangement is made permanent by means of polymerization with a cross-linker. When the template molecules are removed from the network, cavities complementary in size and functional groups to those of the template molecules are created. Such cavities can rebind the template molecules showing high affinity and selectivity.

(thereinafter called functional monomers). When polymerization occurs in the presence of high cross-linker proportions such spatial distribution is made permanent. Then, the template is removed, leaving in the polymer network cavities or pockets that are complementary both sterically and chemically to the original template molecule. As a consequence, once the polymer network again comes into contact with the target molecules, these specifically interact with the empty cavities.[13,17]

In practice, there are two main ways to obtain molecularly imprinted polymers (MIPs) depending on the type of interactions between the target molecule and the functional monomers, namely:

a) Covalent bonds. In the *pre-organized* or *covalent approach*, introduced in the 1970s by Wulff and coworkers,[18] the template is covalently bound to the monomers prior to polymerization. After the synthesis of the networks, these bonds are broken to form the imprinted cavities.
b) Non-covalent interactions. In the *self-assembly* or *non-covalent approach*, proposed in the 1980s by Arshady, Mosbach and coworkers,[19,20] the template molecules and the functional monomers establish ionic, hydrogen bond, hydrophobic or charge transfer interactions, prior to polymerization, to form stable and soluble complexes of appropriate stoichiometry. Since the interactions are relatively weak, multiple-point links between each template molecule and various functional monomers are required to form strong complexes. In general, the non-covalent imprinting protocol allows more versatile combinations of templates and monomers, and provides faster bond association and dissociation kinetics than the covalent imprinting approach.[21]

Disregarding the procedure applied, the preparation of MIPs requires the co-polymerization of the functional monomer-template complexes with high proportions of cross-linking agents, and the subsequent removal of the template molecules in order to create vacant receptors available for rebinding the template and/or structurally related analogues. Thus, both the polymerization step and the removal procedure are critical for obtaining good performing imprinted pockets. The template should not bear polymerizable groups that could attach themselves irreversibly to the polymer network, it should not interfere in the polymerization process and it should be stable at the moderately elevated temperatures or upon exposure to UV radiation used to synthesize the polymer network.[22] It is also important to choose the functional monomers adequately, commonly acrylate-, styrene- and silane-based monomers, taking into account their suitability to reversibly interact with the template and to render networks that are not altered in the subsequent washing step. Acrylate monomers are the most frequently used, since they readily participate in free-radical polymerization and the template molecules minimally interfere in the reaction.[22,23] The nature and proportion of the monomers and solvents strongly determine the efficiency of the imprinting. Ideally all template molecules should be surrounded by the adequate functional monomers (all the same or different from each other) and fulfill their ability to form stable complexes. Thus, also ideally, all cavities will have the same composition and consequently the same binding affinity. However, that is not easy to attain in practice. In fact, literature on the traditional non-covalent approach reports the use of the functional monomers at 4 : 1 molar ratio with respect to the target molecule or in a greater excess. That leads to the concomitant existence of complexes of different stoichiometry: those with the optimal stoichiometry (specific for each pair template:functional monomer), those in which the monomer is in excess and those with not enough monomer.[24] The final result is the coexistence in the MIP of a small number of cavities with medium to high binding affinity (likely 0.5–1% of the theoretical binding sites) and a larger number of cavities with low binding affinity (Figure 21.2).[25,26] This heterogeneity, which is evidenced during the rebinding and the elution of the target molecules (Figure 21.2), complicates the performance of the MIP.

To optimize the quality of the imprinted cavities avoiding the tedious trial-and-error approach, the MIPs can be rationally designed by performing preliminary analysis of the interactions of the template molecules with the functional monomers, under the conditions at which the polymer synthesis will occur. Combinatorial and computational simulations enable a fast screening of the monomers with highest interaction energy from a large library.[27–31] Analytical techniques, such as Raman and NMR spectroscopy, UV spectrophotometry or microcalorimetry, can also provide information about the efficiency of the complexation process and its stoichiometry.[32–36] This information and the use of factorial designs or chemometric models for optimizing the synthesis procedure may notably shorten the time required to develop efficient MIPs.[16,37–39]

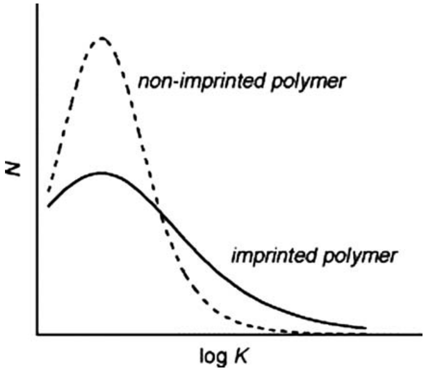

Figure 21.2 Affinity distributions showing the greater heterogeneity of imprinted (solid line) over non-imprinted (broken line) polymers. The affinity distribution, also called site–energy distribution, plots the number of sites N that have association constant K. The exponentially tailing portion of the MIP corresponds to the high-affinity binding sites. Such a high affinity region is particularly evidenced when the template reloading of the MIP is far from saturation.
Reproduced from Ref. 24 with permission of Elsevier.

The solvent and the cross-linker proportion used in the synthesis of the polymer are two other important factors with a strong influence on the conformation of the imprinted cavities. The solvent should not hinder the interactions between the target molecules and the functional monomers and has to prevent precipitation of the complexes.[40] This is particularly critical in the case of the non-covalent imprinting approach. Apolar solvents are preferred to increase the likelihood of formation of hydrogen-bonds, while water and other polar solvents facilitate the hydrophobic interactions.[41] However, since the formation of the receptor sites usually involves the combination of hydrogen-bonding, ion-pairing and hydrophobic interactions between the template and the functional monomer(s), the effect of the solvents on the efficiency of non-covalent imprinting is not easy to predict. The use of organic solvents is limited by compatibility problems with some templates such as peptides, oligonucleotides or sugars; therefore, molecular imprinting in water is gaining increasing attention in the synthesis of MIPs for pharmaceutical applications. Difficulties arise in materializing the methodology, because of the weakness of electrostatic and hydrogen-bonding interactions in this polar medium, which decrease the affinity and selectivity of MIPs for the ligands.[16] A combination of hydrophobic interactions (*e.g.* using cyclodextrins as functional monomers) and metal coordination can strengthen the association of the template with the functional monomers in water.[42–44] The proportion of solvent also determines the porosity and the size of the MIPs; low proportions lead to bulk monoliths, while large proportions may lead to porous micro-/nanoparticulate systems.[41] On the other hand, the cross-linker is usually the major component among the monomers (>50 mol.%) in order to ensure that the cavities have a structure stable enough to maintain the conformation in the absence of the template.

The reactivity of all comonomers (functional, non-functional and cross-linkers) should be similar to avoid an uneven distribution.[45] A rigid conformation (the imprinted receptor resembles an engraved hole in a stone) makes the MIP resistant to the mechanical stress and the chemical and enzymatic attacks that it may suffer during its subsequent use, and aims to ensure that the cavities still have the shape adequate to host the target molecules.[46] As a drawback, the high cross-linking density may hinder the washing out of the template molecules after synthesis, both physically as the mesh size impedes the diffusion of the template, and chemically as the receptor maintains too high affinity for the template.

The removal of the template molecules is another critical step in the preparation of MIPs, despite the lack of attention received so far. Few papers indicate the yield of template extraction after applying a certain procedure[47,48] and even fewer explain the basis behind the use of a given technique.[49,50] Such a lack of attention makes the template removal the least cost-effective step of the MIPs development. The efficiency of common discontinuous immersion (incubation) in organic solvents or salt solutions and continuous extraction in a Soxhlet apparatus is far from 100%. As a consequence, the number of cavities suitable for rebinding decreases, and the trapped template molecules could elute during the use of the MIP, interfering in its performance (Figure 21.3). Extraction assisted by ultrasounds, microwaves or heating under pressure and extraction with subcritical water or supercritical CO_2 have been shown to increase notably the template removal, while taking less time and using fewer solvents.[48] However, extreme conditions may alter the structure of the MIPs causing swelling of the networks during extraction and collapse during subsequent desiccation, distorting the binding points and the strength of the interactions (Figure 21.3).[50,51] Advances in operation in continuous mode, automation of the template removal process and on-line integration with instrumental techniques for real-time monitoring of the template extracted are expected to improve notably the efficiency of the removal step, while maintaining the conformation of the imprinted cavities upon synthesis as close as possible.[50]

The current state of the art of the molecular imprinting technology enables the preparation of materials of very diverse formats, physical and chemical properties, with a wide scope of applications in quite diverse fields. MIPs are used in the analytical field as components of stationary phases in chromatographic columns[52,53] and as fillers of solid phase extraction cartridges,[54] mainly for separation and quantification of a wide range of substances contained in relatively complex matrices. MIPs have been shown to be useful as replacements of biological antibodies in immunoassays,[55–57] as catalysts[58,59] and as efficient traps for bioremediation.[60] Imprinted materials that mimic biological receptors for the screening of new substances with potential pharmacological activity, that detect specific drugs in biological fluids in screening assays for drugs of abuse or that can serve as diagnostic sensors or chemical traps to remove undesirable substances from the body are receiving enormous attention in the pharmaceutical field.[31,61–69]

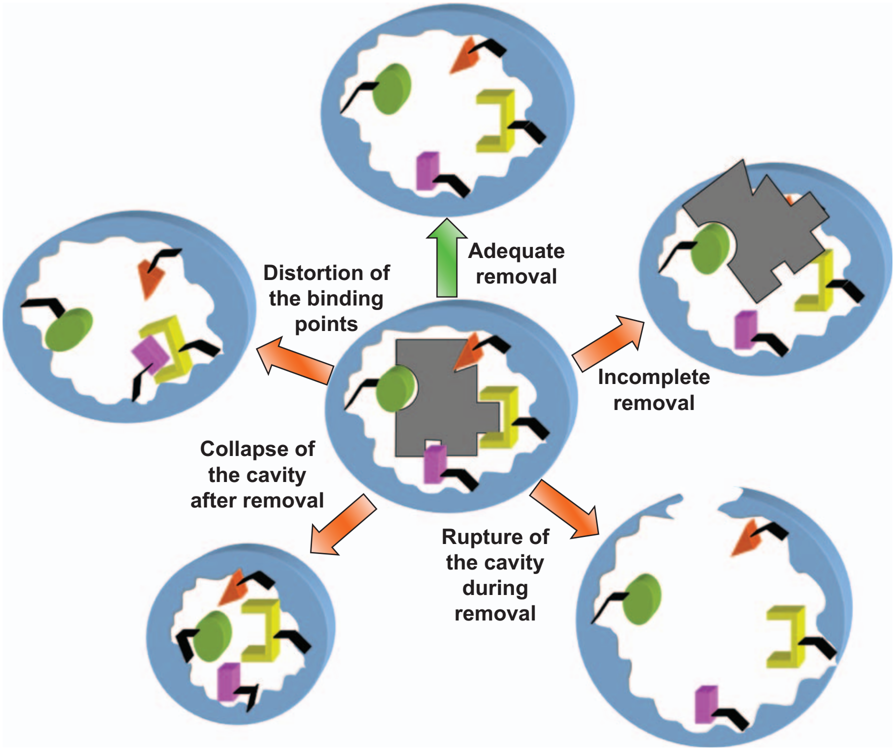
Adequate removal
Distortion of the binding points
Incomplete removal
Collapse of the cavity after removal
Rupture of the cavity during removal

Figure 21.3 Schematic view of the different effects that the template removal process can cause on the structure of the imprinted cavities.
Adapted from Ref. 50 © 2011 by the authors.

The molecular imprinting technology is being progressively incorporated in the design of DDSs, as reflected in the growing number of papers and patents.[15,69–72] The enhancement of the affinity for specific drugs and physiological substances has already been shown as an exciting and versatile way to improve drug loading and controlled release.[15,73–76] For these applications, an adequate balance between the performance of the materials as imprinted systems – that determines their efficiency as DDSs or biological sensors – and the safety for application/administration to the body should be reached. The design and functioning of the imprinted DDSs prepared applying the conventional molecular imprinting technology have been addressed in comprehensive reviews.[15,77,78] The high-affinity imprinted cavities are expected to provide enhanced drug loading and contribute to a more prolonged release through a "Tarzan-swing" mechanism; namely, the target drug moves from one imprinted site to another by means of successive decomplexation/complexation reaction steps. Nevertheless, high cross-linking level increases the hydrophobicity of the network and prevents the polymer from changing the conformation adopted during synthesis. In consequence, the affinity for the template is not dependent on external variables and it is not foreseen that the device will have regulatory or switching capabilities. A high cross-linker proportion also considerably increases the stiffness of the network making the adjustment of the shape to the administration site difficult and causing mechanical friction with the surrounding tissues (especially when administered by topical and ocular routes or as implant). In the last decade, the molecular imprinting technology has been adapted to create loosely cross-linked imprinted hydrogels and stimuli-responsive imprinted networks with tunable affinity and improved performance as drug carriers.[72,79–81] These two types of materials are covered in the next sections.

21.3 Imprinted Hydrogels

21.3.1 Affinity-controlled Release from Bioinspired Networks

A typical example of a loosely cross-linked hydrogel is that of soft contact lenses, which are made of thin, flexible and hydrophilic polymer sheets. Their monomer composition and shape are chosen to combine the ability to correct impaired vision with the biocompatibility with the ocular surface. Oppositely to the rigid imprinted networks described above, they have to be synthesized with a low cross-linking density, using small proportions of conventional cross-linkers or intermediate proportions of long-chain cross-linkers. Medicated contact lenses may be particularly useful for increasing ocular bioavailability of drugs applied on the cornea, while the systemic absorption and side effects result diminished.[71,82–85] The feasibility of using drug-loaded soft contact lenses depends on whether the drug and the hydrogel material can be matched, so that the lens takes up a sufficient quantity of drug and releases it in a controlled fashion. In general, drug-loading capacity of conventional soft contact lenses is insufficient and, therefore, they have rarely been employed for ophthalmic drug delivery.[83,86,87] The creation of high-affinity receptors for the drug molecules could overcome this drawback. However, application of molecular imprinting technology has to face up to relevant restrictions: i) due to the requirements of optical clarity, flexibility and oxygen permeability, the main composition of soft contact lenses is restricted to some approved monomers that differ in water affinity and hydrogen-bonding capacity;[88] thus, the list of feasible functional monomers is quite short; and ii) the proportions of functional monomer and cross-linking agent have to be relatively low and, in consequence, the physical stability of the binding sites is a main concern. Therefore, the interactions between the template and the functional monomers have to be maximized in order to compensate the minor physical stability of the receptor cavities. The drug-imprinted lenses are in the anhydrous state upon polymerization, then they are washed to extract the template and finally reloaded using an aqueous solution of drug. The process causes the swelling of the network and thus the distortion of the imprinted cavities. Only the cavities with high affinity are able to recover the original conformation when the contact lens is again immersed in the template molecules solution. Thus, the reconstruction of the imprinted cavities is due to an "induced fit".[72] Such a phenomenon has been also reported for stimuli-responsive hydrogels.[89] However, differently from the stimuli-responsive imprinted networks in which the volume phase transition leads to the switch on/off of the affinity for the template molecules (as described in Section 21.4), loosely cross-linked non-responsive networks aim to keep a certain affinity for the target drug even when swollen, which is the state in which the device has to remain during the time it is functional in the body. Only high-affinity cavities will be able to load the drug and, subsequently, to sustain the release process.

The feasibility of adapting the MIPs to the synthesis of soft contact lenses was first experimentally evidenced for timolol, a drug used in glaucoma therapy. Timolol is a suitable molecule for providing imprinted systems, since it offers multiple sites for the interaction with the functional monomers acrylic acid (AAc) and methacrylic acid (MAA). These monomers can interact through ionic and hydrogen bonds with timolol before polymerization with the backbone monomers 2-hydroxyethylmethacrylate (HEMA) or *N*,*N*-diethylacrylamide (DEAA).[90] HEMA and DEAA are liquid and enable the dissolution of the drug without adding any other solvent. Imprinted lenses synthesized with different proportions of MAA (1.28–5.12 mol.%) and ethylene glycol dimethacrylate (EGDMA, cross-linker, 0.32–8.34 mol.%) were able to take up more timolol than the corresponding non-imprinted ones (Figure 21.4). Some imprinted lenses loaded therapeutic amounts of timolol, prolonged the release in lachrymal fluid for more than 12 hours and reloaded another dose of timolol overnight, being ready for use the next day.[91,92] The suitability of the imprinting technology to endow the contact lenses with affinity for timolol was also demonstrated for networks prepared with a variety of backbone monomers.[90,93,94]

The suitability of the imprinted networks for the *in vivo* control of the release of timolol was demonstrated for ultrathin DEAA-based lenses (14 mm diameter and 80 µm center thickness). Imprinted (34 µg drug) and non-imprinted (21 µg drug) lenses were inserted on rabbit eyes and the level of

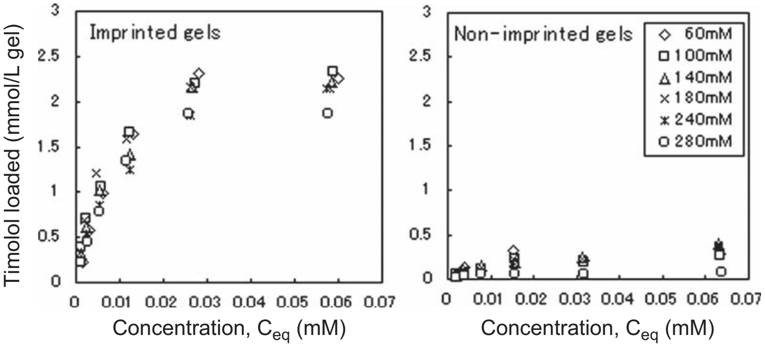

Figure 21.4 Timolol uptake from its aqueous solutions by imprinted and non-imprinted *N*,*N*-diethylacrylamide-based contact lenses made with methacrylic acid (100 mM) and different proportions of ethylene glycol dimethacrylate. Reproduced from Ref. 92 with permission of Elsevier Science.

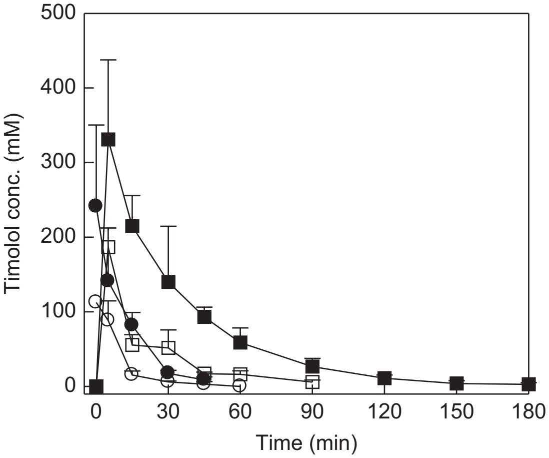

Figure 21.5 Timolol tear fluid concentration-time profiles, on rabbits' eyes, after application of timolol loaded imprinted and non-imprinted contact lenses (■ and □, respectively) and instillation of timolol eye drops (0.068% ○; 0.25% ●) on rabbits' eyes. The doses were 34 μg per imprinted contact lens, 21 μg per non-imprinted contact lens, 34 μg as 0.068% timolol eye drops and 125 μg as 0.25% timolol eye drops. Each point represents the mean ± SD ($n = 3$–5).
Reproduced from Ref. 95 with permission from Elsevier.

timolol in the lachrymal fluid was monitored for several hours and compared to that achieved after instillation of timolol eye-drop solutions of 0.068% (total dose 34 μg) and 0.25% (commercial solution, total dose 125 μg) (Figure 21.5).[95] Timolol applied as drops was rapidly eliminated from the eye surface. The imprinted lenses sustained the release for 180 min, compared to the 90 min of the non-imprinted ones. The lenses displayed the maximum ocular level at around 5 min, followed by a monoexponential decay. Imprinted contact lenses led to an area under the timolol concentration-time curve (AUC) 3.3-fold and 8.7-fold greater than non-imprinted lenses and eye drops, respectively. Therefore, imprinted contact lenses notably reduced the precorneal elimination of the drug and, in consequence, a much smaller amount of drug was needed to achieve the desired therapeutic levels, compared to the eye drops.

The benefits of the imprinting technology have also been demonstrated for antimicrobial agents (norfloxacin), antihistaminics (ketotifen), carbonic anhydrase inhibitors (acetazolamide and ethoxzolamide) and some comfort ingredients.[72] Hydrogels imprinted for norfloxacin were designed by first predicting the optimum template/functional monomer ratio before polymerization using isothermal titration calorimetry (ITC). Titration with AAc showed a strong exothermic interaction with an inflexion point at norfloxacin:AA 1:1 molar ratio, and binding saturation at 1:4 (Figure 21.6). This later molar ratio was confirmed to be the most convenient to create high-affinity receptors in the lens structure, in a comparative study with hydrogels synthesized using norfloxacin:AAc 1:2 to 1:16 molar ratios, at two fixed AAc

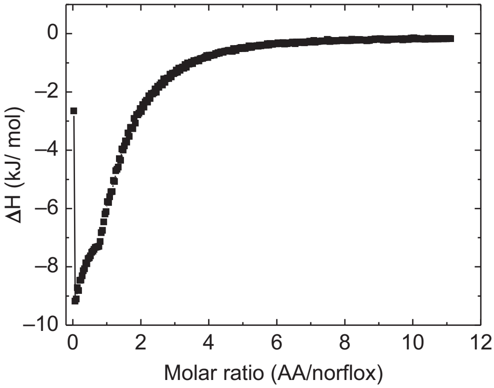

Figure 21.6 ITC titration at 298 K of norfloxacin 0.01 M with AA 0.50 M in HEMA solution.
Reproduced from Ref. 36 with permission of Elsevier.

total concentrations; with the cross-linker molar concentration being 1.6 times that of AAc. Hydrogels synthesized using norfloxacin : AAc 1 : 4 molar ratio were those that provided the most sustained release, with a rate 3.5 times lower than that of non-imprinted ones (Figure 21.7). Norfloxacin-imprinted hydrogels of various AAc contents and thicknesses exhibited similar loading/release behavior, proving the robustness of the imprinting approach.

In the case of ketotifen, the functional monomers were selected according to a configurational biomimesis approach, based on the chemical functionality of the natural receptors of the drug in the body.[16,96] Taking into account the composition in amino acids of the histamine H1-receptor, monomers that resemble the chemical functionalities of the amino acids at the active center were chosen and used individually or combined to synthesize imprinted networks of grading affinities for ketotifen. The hydrogels were prepared by photopolymerization starting from 92 mol% HEMA, 5 mol% cross-linker (polyethylene glycol 200 dimethacrylate, PEG200DMA) and 3 mol% functional monomers.[97] The most biomimetic formulation, poly(AA-co-AM-co-NVP-co-HEMA-co-PEG200DMA), demonstrated six times enhanced loading over the control network and three times enhanced loading over the networks containing one or two functional monomers. Drug partition coefficient was remarkably higher in the biomimetic network.[98] Sustained delivery of therapeutically relevant concentrations of drug was observed over 2–4 days in salt solutions.[99] *In vivo* experiments carried out with ketotifen-imprinted poly(AA-co-AM-co-NVP-co-HEMA-co-PEG200DMA) lenses (11.8 mm diameter and 100 μm center thickness) evidenced the presence of the drug in the lachrymal fluid for 26 hours, compared to 10 hours for the non-imprinted lenses.[71]

Also following a biomimetic approach, soft contact lenses with high affinity for carbonic anhydrase inhibitors, such as acetazolamide and ethoxzolamide, were synthesized by creating binding pockets that resemble the receptor of

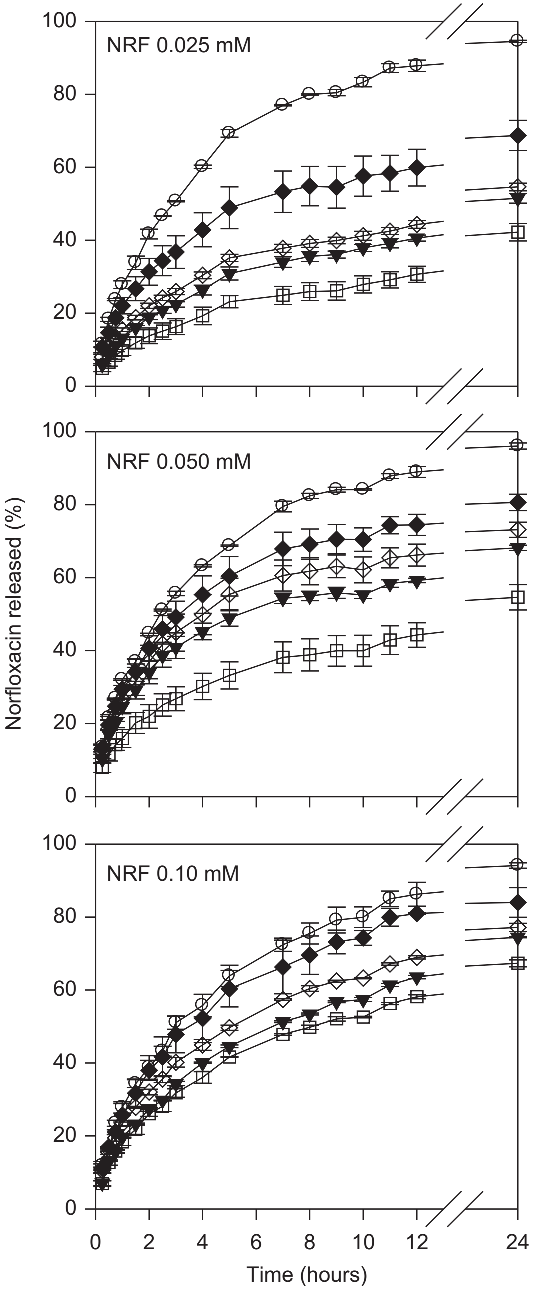

Figure 21.7 Norfloxacin release profiles in lachrymal fluid from PHEMA hydrogels synthesized with AA 200 mM and EGDMA 160 mM using different norfloxacin:AA molar ratios; zero, *i.e.* non-imprinted hydrogels (○), 1:16 (◆), 1:10 (◇), 1:6 (▼) and 1:4 (□). The hydrogels (thickness 0.4 mm) were previously loaded by immersion in 0.025 mM, 0.050 mM or 0.10 mM norfloxacin (NRF) solutions ($n = 3$).

Reproduced from Ref. 36 with permission of Elsevier.

carbonic anhydrase. This metallo-enzyme consists of an active site with a cone-shaped cavity that contains a Zn^{2+} ion coordinated to three histidine residues in a tetrahedral geometry with a solvent molecule as the fourth ligand (Figure 21.8).[100] Monomers bearing chemical groups similar to those of the amino acids involved in the active binding site were chosen to prepare biomimetic hydrogels: the zinc ions were introduced as methacrylate salt ($ZnMA_2$); the hydroxyl and amino groups can be supplied by 2-hydroxyethyl methacrylate (HEMA) and *N*-hydroxyethyl acrylamide (HEAA); and 4-vinylimidazole (4-VI) resembles histidine.[101] A set of hydrogels with a fixed content of $ZnMA_2$ and various comonomer combinations was prepared and characterized regarding their ability to load and to sustain the release of acetazolamide and ethoxzolamide. pHEMA-$ZnMA_2$ hydrogels bearing 4VI moieties exhibited the greatest ability to host acetazolamide or ethoxzolamide (2–3 times greater network/water partition coefficient) and to sustain the release of these antiglaucoma drugs, with 50% lower release rate than non-biomimetic networks. Application of this approach to *N*,*N*-dimethylacrylamide (DMA) and *N*-vinylpyrrolidone (NVP) hydrogels also resulted in biomimetic pockets with high affinity for the carbonic anhydrase inhibitors. Acetazolamide-imprinted networks achieved the highest loading and controlled the release for 9 hours in artificial lachrymal fluid. These light-transparent networks were also able to uptake ethoxzolamide and sustain its release for more than one week.[102]

21.3.2 Competitive Displacement Release

Imprinted hydrogels are also suitable candidates to attain activation-modulated delivery. This approach consists of having an imprinted hydrogel that releases the drug because of the competitive binding of another substance to the polymer. Let's consider that a non-imprint drug can be loaded in the imprinted cavities of the network. When the imprint molecule appears in the medium, it will compete for the binding to the imprinted cavity, causing the release of the drug. If a fall in the concentration of the free imprint molecule in the medium occurs, the release stops. For example, hydrocortisone-imprinted hydrogels have been shown able to release testosterone at a rate depending on the concentration of free hydrocortisone in the medium.[103] Competitive binding release in aqueous medium was also observed for particles imprinted for bupivacaine, when loaded with other local anesthetic drugs,[104] for particles imprinted for theophylline and loaded with caffeine or theobromine and for particles imprinted for 17-β-estradiol and loaded with other structurally related sterols (17-α-estradiol, 17-α-ethynylestradiol).[105]

Imprinted thin layers have been designed to change their permeability when the template is in the medium, mimicking the behavior of a cell membrane with receptors and channels. Theophylline-imprinted nanometric layers made of MAA and EGDMA and grafted onto an indium-tin oxide electrode[106] or cellulosic dialysis membrane[107] showed a faster release of creatinine in the presence of theophylline. Applying living radical polymerization, it has been shown that the "gate effect", which regulates the permeability of the network

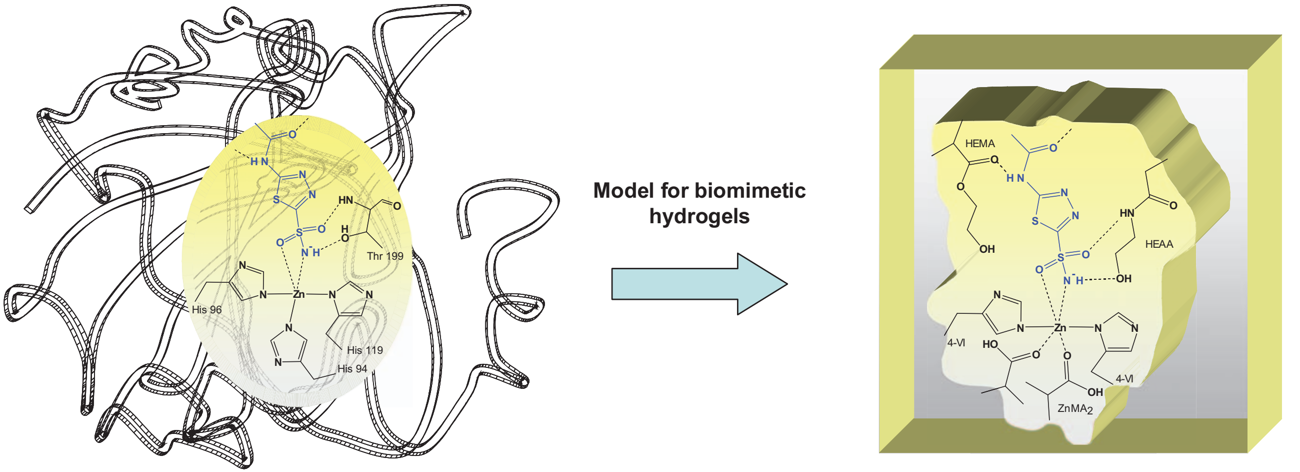
HN
O
N
S
H
Thr 199
His 96
Zn
His 119
His 94
Model for biomimetic hydrogels
HEMA
OH
HEAA
4-VI
HO
ZnMA$_2$

The active site of human carbonic anhydrase II, interacting with acetazolamide

Hydrogels with receptor-like binding sites uptake and control the release of carbonic anhydrase inhibitors

Figure 21.8 Schematic drawing of the active site of human carbonic anhydrase II after binding acetazolamide, and of the mimicking binding pockets expected to be created in the biomimetic imprinted hydrogels.
Reproduced from Ref. 101. Copyright (2011) the American Chemical Society.

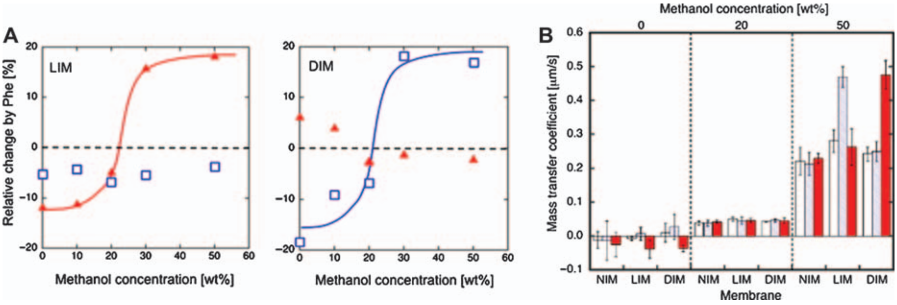

Figure 21.9 Template-induced swelling of L-phenylalanine (LIM) and D-phenylalanine (DIM) imprinted membranes when 5 mM L-phenylalanine (triangle) or 5 mM D-phenylalanine (square) was added to the water : methanol medium (A), and relationship between the overall mass transfer coefficient of creatinine across a non-imprinted (NIM) and an imprinted (LIM or DIM) membrane in batchwise dialysis in the presence of 0.5 mM L-phenylalanine (grey bars) or 0.5 mM D-phenylalanine (red bars), and in the absence of phenylalanine (white bars) (B). Adapted from Ref. 109, with permission of Elsevier.

automatically by responding to the presence of the template, can be optimized through the thickness of the imprinted layer applying repeated UV-polymerization cycles.[108] This gate effect is due to the shrinking or the swelling that the binding of the template causes in the polymer network. Such conformational change induces the opening of pores or gates in the network, which enable the passing of molecules with smaller size than that of the template. It has been shown recently that the template-induced volume change is strongly dependent on the nature of the solvent (Figure 21.9). For example, L-phenylalanine did not trigger the release of creatinine from L-phenylalanine-imprinted networks in water, but it occurred when the medium was replaced by 50% methanol.[109] These MIPs could be applied to develop DDSs with molecular recognition that exclusively release the drug when a specific substance appears in the medium.

21.3.3 Hydrolytically Induced Drug Release

MIPs can be designed to regulate drug release by means of hydrolysis of drug-network ester/amide bonds through covalent imprinting for the drug, but also through non-covalent imprinting for the group that will act as catalyzer of the rupture of the drug-network covalent bond. Hydrogels intended for the release of *p*-amino benzoic acid have been prepared dissolving HEMA, *N*-vinylimidazole (NVIm) and 2-methacryloylethyl *p*-aminobenzoate (PAP) in methanol, and then adding Co^{2+} ions to coordinate PAP with NVIm (nucleophilic catalyst) (Figure 21.10). After polymerization, the removal of the metal ions led to polymers having the labile bond and the imidazole group located in contiguous positions on the same chain. In ethanol/pH 8 phosphate buffer, the release of *p*-amino benzoic acid from the imprinted system

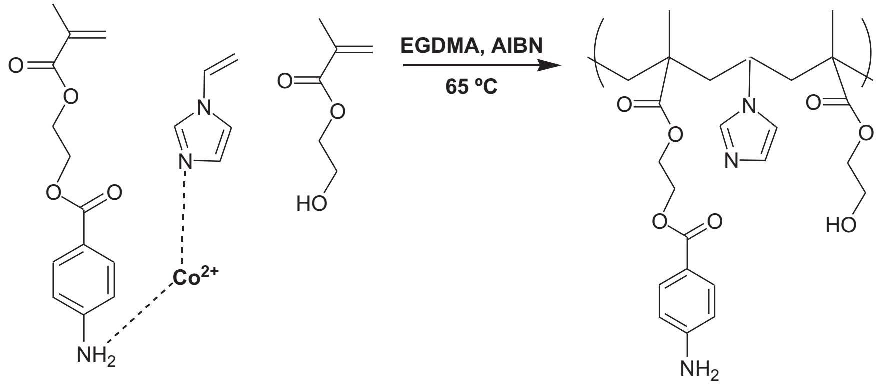

Figure 21.10 Route for creating imprinted cavities in which the imidazole catalytic group is positioned close to the drug-polymer bond. The monomeric drug interacts with the imidazole group through a metal bridge, and then the complex is polymerized in HEMA and EGDMA medium. Reproduced from Ref. 110 with permission of Elsevier.

(synthesized in the presence of Co^{2+} ions) was one order of magnitude faster than that recorded from the non-imprinted networks.[110] For template drugs that can directly interact with the imidazole group, the addition of ions during polymerization is not needed to get the imprinting effect.[111] It should be noticed that the hydrolysis rate could be altered by changes in pH or temperature that lead to modifications of the swelling degree of the network, and hence of the distance between the bond and the catalyzer.[112,113]

21.4 Stimuli-responsive Imprinted Networks

The lack of response through a change in polymer conformation, to the alterations of the physico-chemical properties of the medium or to the presence of a specific substance limits the potential application of classical imprinted networks as *activation-modulated* or *feedback-modulated* DDSs. The combination of stimuli-sensitivity and imprinting is revealed as an advantageous tool: the imprinting provides a high loading capacity of specific molecules, and the ability to respond to external stimuli modulates the affinity of the network for the target molecules, providing a regulatory or switching capability of the loading/release processes (Figure 21.11).

Adaptation of the molecular imprinting technology to the synthesis of stimuli-responsive hydrogels requires the polymer to be synthesized in the presence of the template in a conformation that corresponds to the global minimum energy. The "memorization" of the imprinted pockets after the swelling of the network and the washing of the template is only possible if the network folds back into the conformation adopted upon synthesis.[9] When the centers of molecular recognition are located in a stimuli-sensitive hydrogel, the conformation of the receptors can be deformed and re-constituted as a

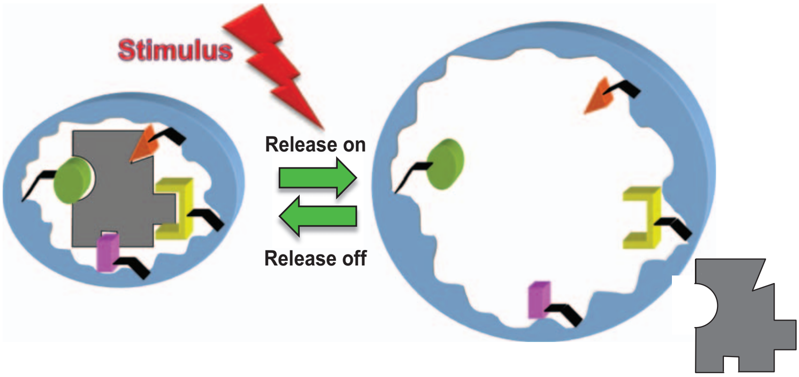

Figure 21.11 Schematic view of the effect of a stimulus on the conformation of the drug-imprinted cavities in a responsive hydrogel.

function of an external or a physiological signal. There is only one out of almost infinite conformations in which the network is able to reconstruct the original imprinted cavities and, thus, to exhibit larger affinity for the template than that shown by non-imprinted networks. Therefore, efficient memorization of such a conformation is critical to maintain the imprinting effect. Stimuli-responsive imprinted hydrogels are particularly suitable to develop advanced intelligent DDSs able to: i) selectively and effectively load a certain drug; ii) release the drug at a rate modulated by a stimulus; and iii) uptake again the released drug from the environment if the drug remains around the hydrogel when the stimulus stops or diminishes its intensity and the cavities are reformed (Figure 21.11).

Stimuli-sensitive imprinted hydrogels can be obtained combining responsive monomers with some functional monomers able to interact with the drug molecules. The synthesis is typically carried out under conditions that ensure that the network grows in the collapsed state. After polymerization, if the hydrogel swells due to a stimulus, the structure of the receptors is altered and the drug is released. If the stimulus disappears or its intensity decreases, the receptors can be reconstituted and as a consequence the release slows down or stops. The optimization of imprinted stimuli-responsive hydrogels is particularly challenging, since memorization of the cavities structure is required in order to maintain the recognition ability after several swelling/collapse cycles.[14,79]

The theoretical basis of the dependence of the affinity of an imprinted hydrogel for a certain template molecule on the functional monomer concentration, on the cross-linker proportion and on the ionic strength of the medium has been summarized in the Tanaka equation:[14]

$$\mathrm{Affinity} \approx \frac{[\mathrm{Ad}]^{p}}{p[\mathrm{Re}]^{p}} \exp(-p\beta\varepsilon)\exp\left(-(p-1)\,c\,\frac{[\mathrm{X1}]}{[\mathrm{Ad}]^{2/3}}\right) \tag{1}$$

where [Ad] represents the total concentration of functional monomers in the gel, [Re] is the concentration of replacement molecules, *e.g.* ions that are bound to the target molecule when it is not bound to the functional monomers (in the case that they have ionic or protonized groups), [Xl] is the concentration of cross-linker, p is the number of bonds that each template can establish with the functional monomers, β is the Boltzmann factor ($1/k_BT$), ε is the difference between the binding energy of an adsorbing monomer to the target molecule and that of a replacement molecule to the target molecule, and c is a constant that can be estimated from the persistence length and concentration of the main component of the gel chains (*e.g.* NIPAAm). The main assumption in 1 is that the adsorption of target molecules is dominated by one value of p at each state of the gel. The value of p changes from 1 in the swollen state to p_{max} in the collapsed state.[114]

The basic concept of stimuli-responsive imprinted hydrogels is that the imprinted cavities develop affinity for the template molecules when the functional monomers come into proximity (shrinking state), but when they are separated, the affinity diminishes (swollen state). The proximity is controlled by the reversible phase transition of the hydrogel, which in turn switches the affinity on and off and controls the adsorption/release of the template. The Tanaka equation allows one to predict the composition of hydrogels, which will drastically change affinity during the phase transition. Low affinity in the swollen state is obtained if each functional monomer has only a weak attraction to the target molecules and each target molecule can only interact with one functional moiety ($p = 1$). To have a high affinity in the collapsed phase, the adsorption should involve as many functional monomers as possible ($p = p_{max}$).[14]

21.4.1 Temperature-sensitive Imprinted Hydrogels

First experiments to create stimuli sensitive gels able to recognize and capture target molecules involved polymerization of *N*-isopropylacrylamide (NIPAAm) as temperature-sensitive component with small proportions of functional monomer MAA and cross-linker *N*,*N*-methylenbis(acrylamide), in the absence (non-imprinted) or in the presence of divalent cations (imprinted networks).[9,115] MAA can form complexes with divalent ions, such as calcium or lead. After removing the template and swelling in water at room temperature, the affinity for divalent ions notably decreased. When the hydrogels shrank due to an increase in temperature, the affinity was recovered. The imprinted gels showed a stronger affinity because the MAA moieties are ordered such that they already form imprinted sites with their unique partners (Figure 21.12). Hence, the functional monomers are ordered in groups of two to give the highest possible binding constant. Importantly, the affinity of the imprinted gels was not affected by the cross-linking density, while in the case of random gels, the affinity decreased as the cross-linker proportion increased due to frustrations of the MAAs to form pairs to bind the divalent ions (Figure 21.12). Therefore, the greater adsorption capacity of the imprinted hydrogels comes

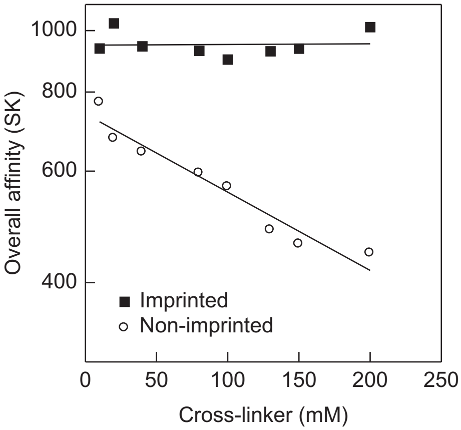

Figure 21.12 Influence of the cross-linker concentration on the overall affinity for calcium ions of the imprinted (full symbols) and non-imprinted (open symbols) NIPAAm (6 M) hydrogels in the shrunken state in water. The concentration of functional monomers (MAA) was fixed at 32 mM. Reproduced from Ref. 9. Copyright (2000) American Chemical Society.

from the successfully memorized MAA pairs.[116,117] Several other examples of temperature-dependent binding of bi- or multi-valent ions by imprinted hydrogels have been reported.[118–121] Even a monovalent ion, such as potassium, could be used as template if it acts as a ligand of two or more functional monomers, as occurs for 15-crown-5 crown ethers.[122]

To avoid a shift in the critical temperature of the NIPAAm networks when copolymerized with ionic functional monomers, preparation of interpenetrating networks (IPNs) has been proposed.[123,124] IPNs have been imprinted with metal ions as follows: a) polymerization of AAc monomers to have a loosely cross-linked (1 mol.%) polyAAc network; b) immersion of polyAAc in copper solution to enable the ions to act as junction points between different chains; c) transfer of polyAAc-copper ion complexes to a NIPAAm solution containing a cross-linker (9.1 or 16.7 mol.%); and d) synthesis of the NIPAAm network in the collapsed state (Figure 21.13). The non-imprinted IPNs (*i.e.* prepared in the absence of copper ions) showed a similar affinity for Cu^{2+} and Zn^{2+}. By contrast, the imprinted IPNs in the collapsed state could discriminate between the square planar structure of Cu^{2+} and the tetrahedral structure of Zn^{2+}.[125]

Temperature-responsive imprinted hydrogels have also been prepared using organic molecules, particularly drugs, as templates.[126,127] 4-Aminopyridine and l-pyroglutamic-imprinted PNIPAAm hydrogels exhibited significantly larger saturation and affinity constants than the non-imprinted ones, and were also highly selective (Figure 21.14). Furthermore, the ability to sorb and release the drug was repeatable after several shrunken-swollen cycles. Similar behavior was observed for other temperature-responsive l-pyroglutamic-imprinted

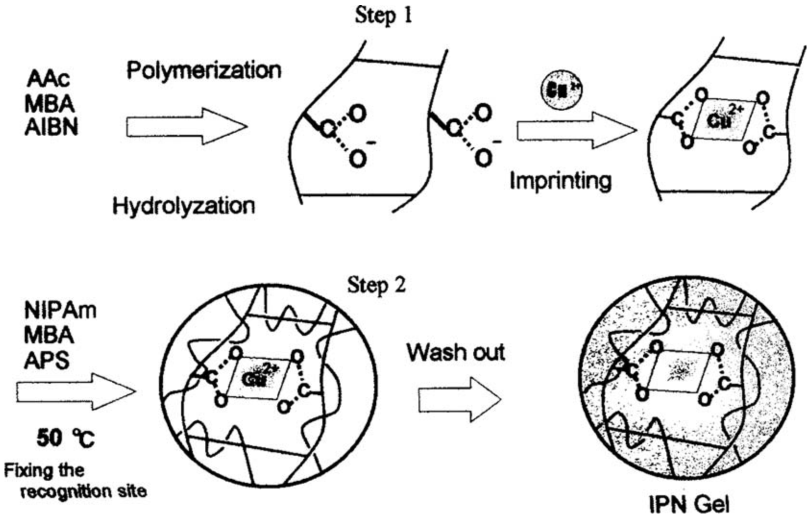
Step 1
AAc
MBA
AIBN
Polymerization
Hydrolyzation
Imprinting
Step 2
NIPAm
MBA
APS
50 ℃
Fixing the recognition site
Wash out
IPN Gel

Figure 21.13 Two-step procedure to obtain an interpenetrated system comprising a Cu^{2+} imprinted poly(acrylic acid) hydrogel and a poly(*N*-isopropyl acrylamide) temperature-sensitive hydrogel.
Reproduced from Ref. 125 with permission from the Society of Polymer Science of Japan.

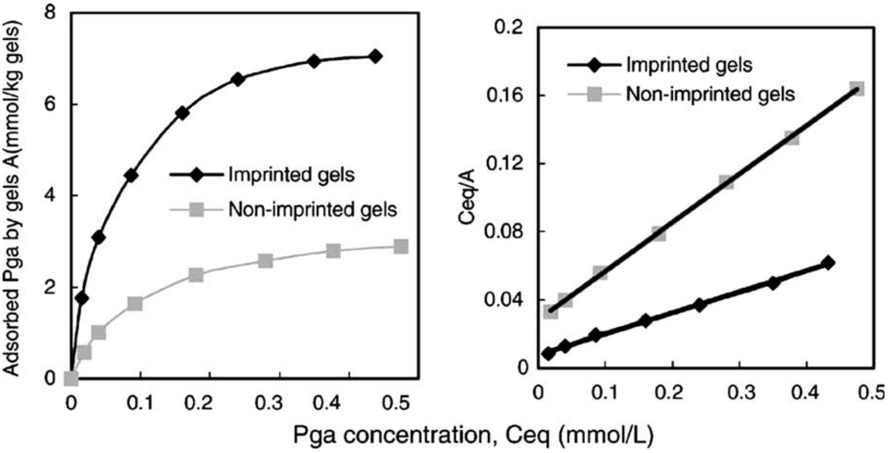

Figure 21.14 Adsorption of l-pyroglutamic acid (Pga) by imprinted and non-imprinted hydrogels in the shrunken state at 55 °C. MIPs were prepared with *N*-isopropylacrylamide (40 mmol), methacrylic acid (2 mmol), ethylene glycoldimethacrylate (6 mmol) and Pga (0.5 mmol).
Reproduced from Ref. 127 with permission from Wiley Interscience.

networks.[128] The reversibility of drug release and re-uptake as a function of temperature may be useful for the treatment of some pathological events that are accompanied by local changes in temperature, or to stop the delivery by means of externally applied local hyperthermia.

Natural polymers, such as chitosan, have also been evaluated as a basis for temperature-sensitive hydrogels.[129] Chitosan is an aminopolysaccharide obtained from chitin, which can be chemically cross-linked through the Schiff base reaction between its amine groups and the aldehyde ends of some molecules, such as glutaraldehyde.[130] If the cross-linking is carried out in the presence of template molecules such as dibenzothiophenes (DBT), imprinted networks with a remarkably greater adsorption capability than non-imprinted ones can be obtained. This effect was particularly important when the rebinding was carried out in the same solvent (acetonitrile) and at the same temperature (50 °C) as those set for the cross-linking; namely with the hydrogel in the collapsed state.[129] Additionally, the DBT-imprinted hydrogels showed a high selectivity for the target molecules compared to other structurally related compounds.

Double coating of MIP beads with PNIPAAm layers has been explored as a way to improve the temperature-responsiveness of protein-imprinted networks. The MIPs were prepared with an internal layer of lysozyme-imprinted PNIPAAm network with AAm and MAA as functional monomers, and an external PNIPAAm layer. The coated MIP beads showed better selectivity to lysozyme and superior temperature stimulus-responsive behavior than the MIP beads without the external PNIPAAm layer. Lysozyme was loaded in the internal imprinted layer; the affinity being maximum at 38 °C. Proteins larger than lysozyme did not fit into the internal layer, and thus remained adhered to the external one, particularly at temperature close to 43 °C (Figure 21.15). Each layer of PNIPAAm acted as a gate during the release; *i.e.* the internal layer behaved as a selective gate, while the external one performed as a non-selective gate. The double-coated MIP beads could release a non-imprint protein and the

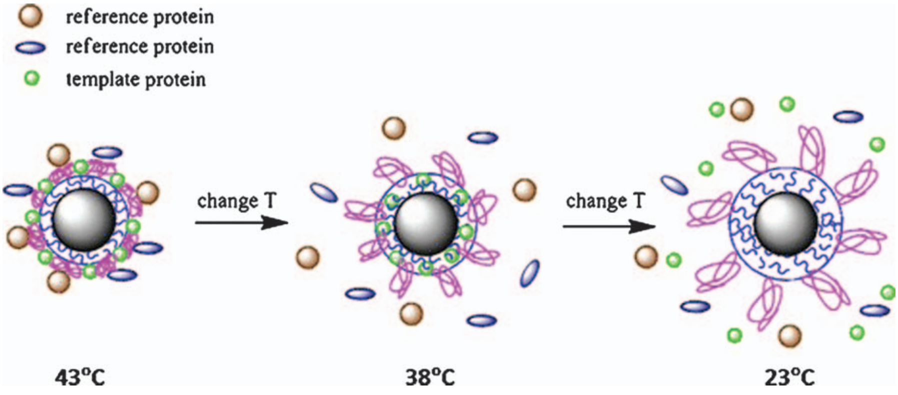

Figure 21.15 Thermo-sensitive swelling/collapse phase transitions for selective adsorption/release of proteins in protein-imprinted beads with double thermo-responsive gates, prepared by surface-initiated living radical polymerization.
Reproduced from Ref. 131 with kind permission from Springer Science and Business Media.

template lysozyme separately at 38 °C and at 23 °C, respectively (Figure 21.15). The corresponding non-imprinted beads did not have such double thermo-sensitive "gates" with specific selectivity for a particular protein.[131]

Poly(*N*-tertbutylacrylamide-co-acrylamide/maleic acid) hydrogels synthesized in the presence of serum albumin (BSA) exhibited both pH- and temperature-switchable affinity for this protein.[132] The hydrogels were synthesized at the swollen state (22.8 °C); at low temperature the interaction between BSA and the hydrogel through hydrogen bonds was maximum. Thus, the rebinding was also the highest when the hydrogel was swollen. In contrast, when the hydrogel collapsed, the protein found the diffusion into the network difficult. Furthermore, the imprinted cavities were distorted and the nature of the interactions was altered, since as the temperature rose, hydrogen bonds became weaker while hydrophobic interactions became predominant. A similar behavior has been observed with ibuprofen-imprinted thermo-responsive cryogels synthesized in a frozen aqueous medium, which showed drug binding constants of 119 and 5 M^{-1} in the collapsed and the swollen states, respectively.[133] These results clearly highlight the relevance of the memorization of the conformation achieved during polymerization to provide the gel with the ability to recognize a given template. An abrupt change in affinity during the gel volume phase transition allows drug release to be switched on and off.

21.4.2 pH-sensitive Imprinted Gels

One of the first strategies of preparing pH-sensitive imprinted hydrogels consisted in combining the ability of amylose chains to form inclusion complexes and the capability of AAc monomers to endow the networks with pH-responsiveness.[134,135] Amylose chains were modified with acryloyl groups (acryloylamylose), and then formed in aqueous medium helical inclusion-complexes with bisphenol-A molecules acting as templates. The complexes were copolymerized with AAc in the presence of a cross-linker (Figure 21.16). Similarly, other MIPs were prepared with acrylamide instead of AAc. In all cases, the polymers were directly obtained as particles. The rebinding ability of MIPs prepared with AAc strongly depended on the pH. At alkaline pH, the MIP lost the affinity for bisphenol-A, because of the conformational changes in the amylose chains caused by the electrostatic repulsions among the ionized groups of AAc and the subsequent disruption of the imprinted cavities. A decrease in pH restored the cavities and the binding affinity.

Imprinted particles prepared *via* precipitation polymerization also have a great potential in the controlled drug-delivery field. Homogeneous spherical microparticles imprinted for sulfasalazine, a prodrug used in colon diseases management, and prepared with MAA as functional monomer showed a pH-dependent release (Figure 21.17).[136] At pH 1.0, the MAA groups are not ionized and can strongly interact with sulfasalazine in the imprinted cavities. When the pH of the medium rises to 6.8 mimicking intestinal conditions, the carboxylic acid groups become ionized and the drug is released. Disregarding the pH, the imprinted particles sustain the release of sulfasalazine more

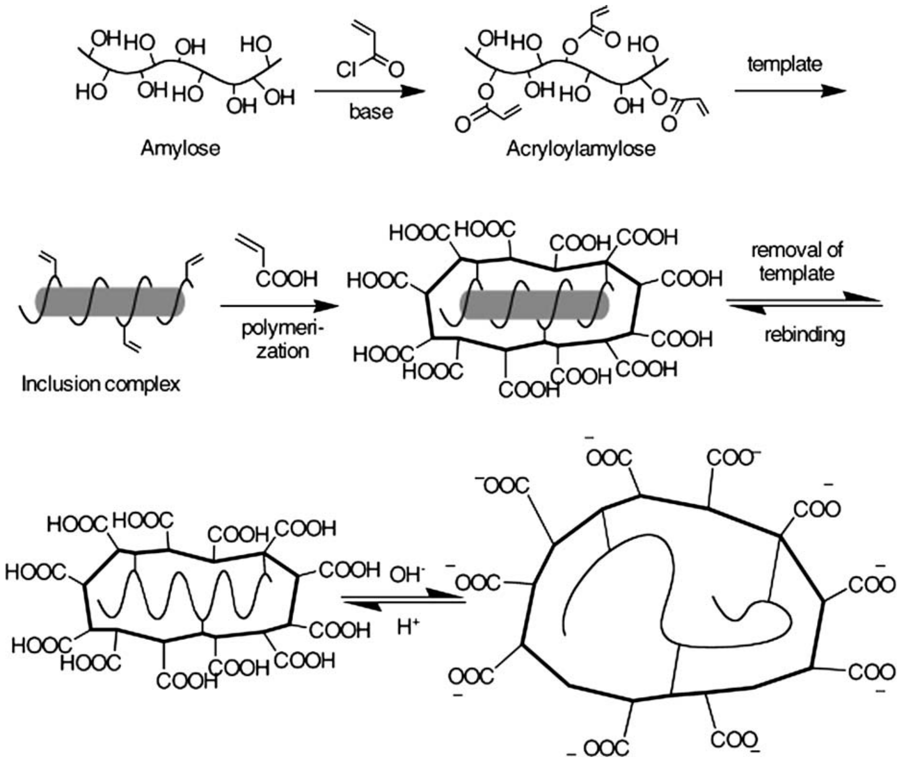
Amylose
Cl
O
base
Acryloylamylose
template
Inclusion complex
COOH
polymerization
removal of template
rebinding
OH⁻
H⁺
HOOC
COOH
⁻OOC
COO⁻

Figure 21.16 Steps of the synthesis of an amylose-based imprinted polymer, and schematic view of its pH-induced structural changes.
Reproduced from Ref. 134 with permission of the Royal Society of Chemistry.

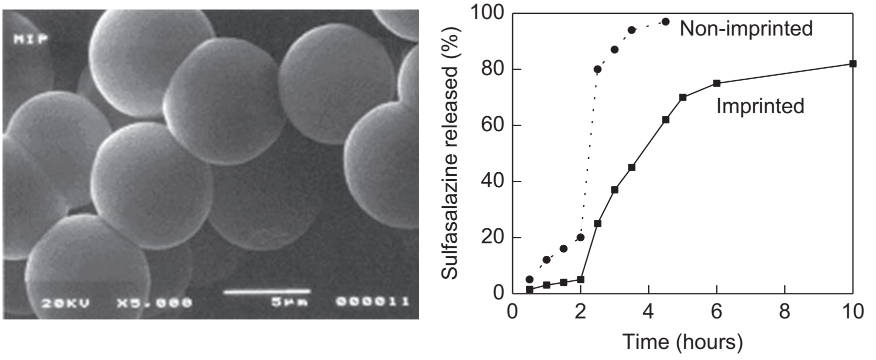

Figure 21.17 Release profile of sulfasalazine at pH 1 (0–2 h) and at pH 6.8 (2–20 h) from non-imprinted and imprinted (0.23 mmol of template) particles (in the micrograph) obtained by precipitation polymerization using methacrylic acid (12 mmol) and ethylene glycol dimethacrylate (16 mmol).
Adapted from Ref. 136 with permission from Wiley Interscience.

efficiently than the corresponding non-imprinted ones at both pH 1 and 6.8, which clearly proves the greater affinity of the imprinted cavities for the drug. Theophylline-imprinted systems with modulated loading capacity and release rate were obtained using different proportions of MAA and methylmethacrylate (MMA) functional monomers.[137] Enantioselective release of *S*-omeprazole from imprinted nanoparticles-on-microspheres prepared using methacryloyl quinine and methacryloyl quinidine as functional monomers and ethylene glycol dimethacrylate as a cross-linker has recently been shown also to be pH dependent.[138]

21.4.3 Light-responsive Imprinted Networks

Imprinted networks responsive to UV-Vis light have been designed taking benefit of the conformational changes that the light can induce in certain chemical groups of the functional monomers, which do not necessarily cause a light-induced phase transition of the network.[139,140] That is the case of functional monomers bearing azobenzene groups, which simultaneously act as binding agents and responsive species. Azobenzene undergoes *trans*-to-*cis* isomerization when light wavelength shifts from visible to UV range. The planar *trans* form is more hydrophobic than the non-planar *cis* form. The wavelength that triggers the isomerization depends on the nature of the substituent groups and, thus, can be readily tuned.[141,142] The *cis* form is unstable at body temperature, so that in darkness or if exposed to a higher wavelength radiation, it reverts to the *trans* form. The features of this and other light-responsive species are covered in detail in Chapter 12.

One of the first attempts to prepare MIPs bearing azo-containing functional groups involved the use of *p*-phenylazoacrylanilide (polymerizable derivative of azobenzene) as the functional monomer, dansylamide as template and mixtures of tetraethylene glycol diacrylate and ethylene glycol dimethacrylate as cross-linkers. The recognition of the MIP for the template molecules was reversibly altered by irradiation with UV or visible light. Nevertheless, the selectivity was limited, since the functional monomers did not form strong hydrogen bonds with the template.[143,144] A MIP for methotrexate has been prepared using a di(ureidoethylene methacrylate)azobenzene derivative as the functional monomer. The polymerization was carried out with the functional monomer in the thermodynamically less stable *cis*-form. The MIP released methotrexate when irradiated at 440 nm, and rebound the molecular template from solution after irradiation at 365 nm (Figure 21.18).[145]

The subtle changes induced by light in the conformation of the imprinted cavities have also been exploited to regulate paracetamol uptake and release.[146] Hydrogels were prepared with acrylamide, 4-[(4-methacryloyloxy)phenylazo]benzenesulfonic acid and *N*,*N*′-hexylenebismethacrylamide in the presence of the drug. The azobenzene chromophores in the hydrogel undergo reversible photo-isomerization under alternating irradiation at 353 and 440 nm, changing their binding affinity for paracetamol (Figure 21.19). In the dark (*trans* conformation), the hydrogels rebound paracetamol from aqueous media.

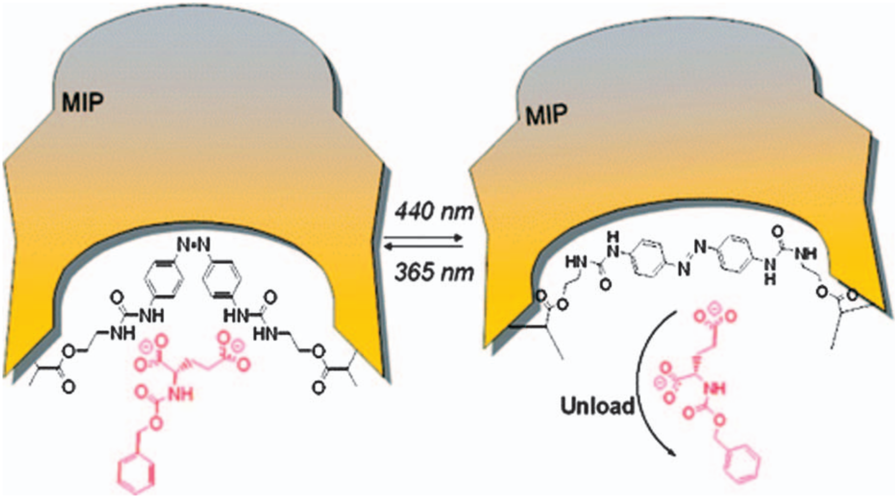

Figure 21.18 Photoresponsive molecularly imprinted polymer prepared from a di(ureidoethylene methacrylate)azobenzene monomer, using a methotrexate analogue as template. Photo-isomerization of the 3D cross-linked polymer matrix allowed switching the substrate affinity, by altering the geometry and spatial arrangement of the receptor binding sites. As a consequence, controlled release and uptake of the template (or an analogous ligand) can be obtained.
Reproduced from Ref. 145. Copyright (2007) American Chemical Society.

Irradiation at 353 nm triggered the isomerization to the *cis* form and, in turn, drug release, which was almost completed after 120 min. Subsequent irradiation at 440 nm caused the imprinted receptors to recover their initial *trans* conformation, being able to capture the paracetamol that had been previously released. After several light cycles, a progressive decrease in the amount of paracetamol that the hydrogels can rebind was observed, probably because of a gradual deformation of the imprinted receptors. Paracetamol-imprinted hydrogels exhibited a notable selectivity for the template drug when compared to other structural analogs.[146]

Light-responsive imprinted microparticles have been prepared using a methacrylate azo functional monomer, and applying precipitation polymerization under dark conditions. The template 2,4-dichlorophenoxyacetic acid only interacts with the functional monomer in the *trans* conformation (Figure 21.20). Thus, the affinity and the number of specific binding points notably decrease upon UV light irradiation, whereas they can be recovered after thermal or visible light-induced back-isomerization.[147] The uptake/release of the target molecules was shown to be highly repeatable under UV light on/off cycles. For a similar purpose, a hybrid MIP was synthesized with a photoresponsive functional monomer bearing a siloxane polymerizable group

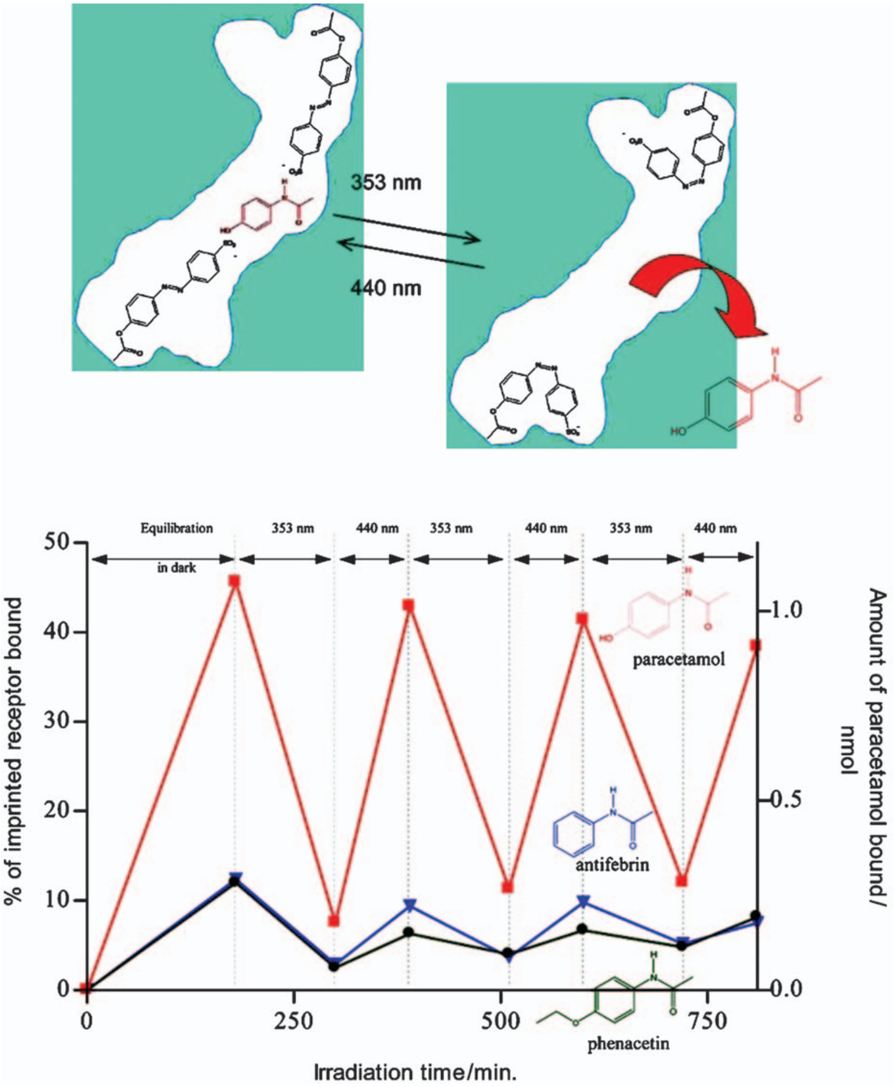

Figure 21.19 Photoregulated release and uptake of paracetamol, antifebrin or phenacetin by paracetamol-imprinted 4-[(4-methacryloyloxy)phenylazo] benzenesulfonic acid-containing polyacrylamide hydrogel in HEPES buffer pH 7.16. The shown binding data are values corrected by subtracting the non-specific binding of the substrate to non-imprinted control hydrogels. Reproduced from Ref. 146. Copyright (2008) American Chemical Society.

and azobenzene moieties. The organic cavities in the inorganic frame showed switchable binding affinity; being able to release and selectively rebind to 2,4-dichlorophenoxyacetic acid upon successive cycles of 360/440 nm irradiation.[148]

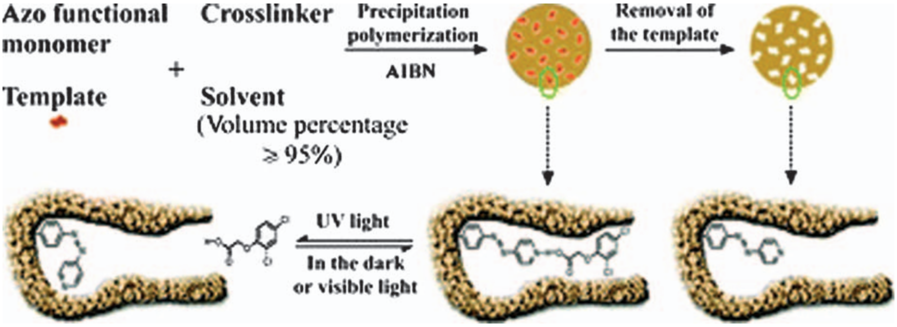

Figure 21.20 Scheme of the preparation of photoresponsive MIP microspheres containing a methacrylate azo functional monomer. The affinity for the template decreased upon UV light irradiation, and was recovered during the subsequent thermal (or visible light-induced) back-isomerization.
Reproduced from Ref. 147 with permission of The Royal Society of Chemistry.

21.5 Conclusions and Future Aspects

Loosely cross-linked imprinted hydrogels can regulate drug release i) through an affinity-mediated mechanism, as occurs with drug-imprinted contact lenses that sustain the release for a prolonged time in the precorneal area, ii) through a competitive displacement of a non-imprint drug by an imprinted molecule, which can be a biomarker, and iii) through a hydrolytically induced mechanism such as that of the rupture of the links of the drug to the network due to the presence of a catalyzer. Combination of the stimuli-responsiveness with the molecular imprinting technology provides novel performances in the drug-delivery field. There are already relevant examples of the suitability of temperature-, pH- and light-responsive imprinted hydrogels for site-specific controlled release. As a unique feature, the enhanced affinity for a specific drug leads responsive imprinted hydrogels to exhibit improved drug loading, double regulation of drug release (the effect of the stimulus plus the affinity of the imprinted cavities) and ability to recapture the released drug if it is not absorbed from the surroundings of the delivery site. Such promising gathering of advantages is expected to be the seeds for the growth of this family of novel advanced biomaterials.

Acknowledgements

Work supported by MICINN (SAF2011-22771), Xunta de Galicia (10CSA203013PR) and FEDER. C.G.C. acknowledges an FPU grant of MEC, Spain.

References

1. D. S. W. Benoit, S. D. Collins and K. S. Anseth, *Adv. Funct. Mater.*, 2007, **17**, 2085.
2. Z. Li, Y. Zhang, P. Fullhart and C. A. Mirkin, *Nano Lett.*, 2004, **4**, 1055.
3. R. V. Ulijn, *J. Mater. Chem.*, 2006, **16**, 2217.
4. T. Miyata, T. Uragami and K. Nakamae, *Adv. Drug Deliver. Rev.*, 2002, **54**, 79.
5. T. Miyata, T. Hayashi, Y. Kuriu and T. Uragami, *J. Mol. Recognit.*, 2012, **25**, 336.
6. A. S. Hoffman, *Clin. Chem.*, 2000, **46**, 1478.
7. K. Makino, E. J. Mack, T. Okano and S. W. Kim, *J. Control. Release*, 1990, **12**, 235.
8. T. Miyata, A. Jikihara, K. Nakamae and A. S. Hoffman, *J. Biomat. Sci. Polym. E.*, 2004, **15**, 1085.
9. C. Alvarez-Lorenzo, O. Guney, T. Oya, Y. Sakai, M. Kobayashi, T. Enoki, Y. Takeoka, T. Ishibashi, K. Kuroda, K. Tanaka, G. Q. Wang, A. Y. Grosberg, S. Masamune and T. Tanaka, *Macromolecules*, 2000, **33**, 8693.
10. T. Tanaka and M. Annaka, *J. Intel. Mat. Syst. Str.*, 1993, **4**, 548.
11. V. S. Pande, A. Y. Grosberg and T. Tanaka, *Biophys. J.*, 1997, **73**, 3192.
12. V. S. Pande, A. Y. Grosberg and T. Tanaka, *P. Natl. Acad. Sci. USA*, 1994, **91**, 12972.
13. G. Wulff, *Angew. Chem. Int. Ed.*, 1995, **34**, 1812.
14. K. Ito, J. Chuang, C. Alvarez-Lorenzo, T. Watanabe, N. Ando and A. Y. Grosberg, *Prog. Polym. Sci.*, 2003, **28**, 1489.
15. C. Alvarez-Lorenzo and A. Concheiro, *J. Chromatogr. B*, 2004, **804**, 231.
16. D. R. Kryscio and N. A. Peppas, *Acta Biomater.*, 2012, **8**, 461.
17. M. Maeda and R. A. Bartsch, in *Molecular and Ionic Recognition with Imprinted Polymers: A Brief Overview*, ed. R. A. Barstch and M. Maeda, American Chemical Society, Washington DC, 1998, p. 1.
18. G. Wulff and A. Biffis, in *Molecularly Imprinted Polymers*, ed. B. Sellergren, Elsevier, Amsterdam, 2001, p. 71.
19. R. Arshady and K. Mosbach, *Makromol. Chem.*, 1981, **182**, 687.
20. B. Sellergren, in *Molecularly Imprinted Polymers*, ed. B. Sellergren, Elsevier, Amsterdam, 2001, p. 113.
21. C. J. Allender, K. R. Brain and C. M. Heard, in *Progress in Medicinal Chemistry*, Vol. 36, ed. F. D. King and A. W. Oxford, Elsevier, Amsterdam, 1999, p. 235.
22. E. Oral and N. A. Peppas, *Polymer*, 2004, **45**, 6163.
23. O. Ramström and R. J. Ansell, *Chirality*, 1998, **10**, 195.
24. R. J. Umpleby II, S. C. Baxter, A. M. Rampey, G. T. Rushton, Y. Chen and K. D. Shimizu, *J. Chromatogr. B*, 2004, **804**, 141.

25. H. S. Andersson, J. G. Karlsson, S. A. Piletsky, A. C. Koch-Schmidt, K. Mosbach and I. Nicholls, *J. Chromatogr. A*, 1999, **848**, 39.
26. A. M. Rampey, R. J. Umpleby II, G. T. Rushton, J. C. Iseman, R. N. Shah and K. D. Shimizu, *Anal. Chem.*, 2004, **76**, 1123.
27. D. Batra and K. J. Shea, *Curr. Opin. Chem. Biol.*, 2003, **7**, 434.
28. W. G. Dong, M. Yan, M. L. Zhang, Z. Liu and Y. M. Li, *Anal. Chim. Acta*, 2005, **542**, 186.
29. D. Pavel and J. Lagowski, *Polymer*, 2005, **46**, 7528.
30. E. V. Piletska, N. W. Turner, A. P. F. Turner and S. A. Piletsky, *J. Control. Release*, 2005, **108**, 132.
31. F. Yañez, I. Chianella, S. A. Piletsky, A. Concheiro and C. Alvarez-Lorenzo, *Anal. Chim. Acta*, 2010, **659**, 178.
32. A. Molinelli, J. O'Mahony, K. Nolan, M. R. Smyth, M. Jakusch and B. Mizaikoff, *Anal. Chem.*, 2005, **77**, 5196.
33. D. McStay, A. H. Al-Obaidi, R. Hoskins and P. J. Quinn, *J. Opt. A Pure Appl. Opt.*, 2005, **7**, 340.
34. W. P. Fish, J. Ferreira, R. D. Sheardy, N. H. Snow and T. P. O'Brien, *J. Liq. Chromatogr. Relat. Technol.*, 2005, **28**, 1.
35. J. O'Mahony, A. Molinelli, K. Nolan, M. R. Smyth and B. Mizaikoff, *Biosens. Bioelectron.*, 2005, **20**, 1884.
36. C. Alvarez-Lorenzo, F. Yañez, R. Barreiro-Iglesias and A. Concheiro, *J. Control. Release*, 2006, **113**, 236.
37. M. P. Davies, V. D. Biasi and D. Perrett, *Anal. Chim. Acta*, 2004, **504**, 7.
38. A. M. Rosengren, J. G. Karlsson, P. O. Andersson and I. A. Nicholls, *Anal. Chem.*, 2005, **77**, 5700.
39. M. J. Whitcombe, I. Chianella, L. Larcombe, S. A. Piletsky, J. Noble, R. Porter and A. Horgan, *Chem. Soc. Rev.*, 2011, **40**, 1547.
40. R. H. Schmidt, A. S. Belmont and K. Haupt, *Anal. Chim. Acta*, 2005, **542**, 118.
41. P. A. G. Cormack and A. Z. Elorza, *J. Chromatogr. B*, 2004, **804**, 173.
42. M. Komiyama, T. Takeuchi, T. Mukawa and H. Asanuma, in *Molecular Imprinting*, Wiley-VCH, Weinheim, 2003.
43. S. A. Piletsky, H. S. Andersson and I. A. Nicholls, *Macromolecules*, 1999, **32**, 633.
44. T. Kubo, K. Hosoya, M. Nomachi, N. Tanaka and K. Kaya, *Anal. Bioanal. Chem.*, 2005, **382**, 1698.
45. R. Z. Greenley, in *Polymer Handbook* 3rd edn, ed. J. Brandrup and E. H. Immergut, John Wiley & Sons, New York, 1989, p. II153.
46. J. Svenson and I. A. Nicholls, *Anal. Chim. Acta*, 2001, **435**, 19.
47. P. Luliński, D. Maciejewska, M. Bamburowicz-Klimkowska and M. Szutowski, *Molecules*, 2007, **12**, 2434.
48. B. M. Batlokwa, J. Mokgadi, T. Nyokong and N. Torto, *Chromatographia*, 2011, **73**, 589.
49. A. Ellwanger, C. Berggren, S. Bayoudh, C. Crecenzi, L. Karlsson, P. K. Owens, K. Ensing, P. Cormack, D. Sherrington and B. Sellergren, *Analyst*, 2001, **126**, 784.

50. R. A. Lorenzo, A. M. Carro, C. Alvarez-Lorenzo and A. Concheiro, *Int. J. Mol. Sci.*, 2011, **12**, 4327.
51. I. Yungerman and S. Srebnik, *Chem. Mater.*, 2006, **18**, 657.
52. N. Denderz, J. Lehotay, J. Cizmarik, Z. Cibulkova and P. Simon, *J. Chromatogr. A*, 2012, **1235**, 77.
53. C. Zheng, Y. P. Huang and Z. S. Liu, *J. Sep. Sci.*, 2011, **34**, 1988.
54. B. Buszewski and M. Szultka, *Crit. Rev. Anal. Chem.*, 2012, **42**, 198.
55. R. J. Ansell, *J. Chromatogr. B*, 2004, **804**, 151.
56. L. Ye and K. Mosbach, *Chem. Mater.*, 2008, **20**, 859.
57. Z. X. Xu, H. J. Gao, L. M. Zhang, X. Q. Chen and X. G. Qiao, *J. Food Sci.*, 2011, **76**, 69.
58. M. Resmini, *Anal. Bioanal. Chem.*, 2012, **402**, 3021.
59. G. Diaz-Diaz, D. Antuna-Jimenez, M. C. Blanco-Lopez, M. J. Lobo-Castanon, A. J. Miranda-Ordieres and P. Tunon-Blanco, *Trac-Trend. Anal. Chem.*, 2012, **33**, 68.
60. X. T. Shen, L. H. Zhu, N. Wang, L. Ye and H. Q. Tang, *Chem. Commun.*, 2012, **48**, 788.
61. C. Chassing, J. Stokes, R. F. Venn, F. Lanza, B. Sellergren, A. Holmberg and C. Berggren, *J. Chromatogr. B*, 2004, **804**, 71.
62. E. V. Piletska, M. Romero-Guerra, I. Chianella, K. Karim, A. P. F. Turner and S. A. Piletsky, *Anal. Chim. Acta*, 2005, **542**, 111.
63. N. Nakamura, M. Ono, T. Nakajima, Y. Ito, T. Aketo and J. Haginaka, *J. Pharm. Biomed. Anal.*, 2005, **37**, 231.
64. P. S. Sharma, F. D'Souza and W. Kutner, *Trac-Trend. Anal. Chem.*, 2012, **34**, 59.
65. L. Fuguang, L. Huaijiangi, S. Min, F. Lulu, Q. Huamin, L. Xiangjun and L. Chuannan, *Anal. Chim. Acta*, 2012, **718**, 84.
66. K. Yano and I. Karube, *Trac-Trend. Anal. Chem.*, 1999, **18**, 199.
67. X. Xu, L. Zhu and L. Chen, *J. Chromatogr. B*, 2004, **804**, 61.
68. B. Sellergren, J. Wieschemeyer, K. S. Boos and D. Seidel, *Chem. Mater.*, 1998, **10**, 4037.
69. J. Z. Hilt and M. E. Byrne, *Adv. Drug Deliver. Rev.*, 2004, **56**, 1599.
70. D. R. Kryscio and N. A. Peppas, *Aiche J.*, 2009, **55**, 1311.
71. A. Tieppo, C. J. White, A. C. Paine, M. L. Voyles, M. K. McBride and M. E. Byrne, *J. Control. Release*, 2012, **157**, 391.
72. C. Alvarez-Lorenzo, F. Yañez and A. Concheiro, *J. Drug Deliv. Sci. Tec.*, 2010, **20**, 237.
73. B. Sellergren and C. J. Allender, *Adv. Drug Deliver. Rev.*, 2005, **57**, 1733.
74. C. Alvarez-Lorenzo and A. Concheiro, in *Smart Nano- and Microparticles*, eds. R. Arshady and K. Kono, Kentus Books, London, 2006, p. 279.
75. F. Puoci, G. Cirillo, M. Curcio, O. I. Parisi, F. Iemma and N. Picci, *Expert Opin. Drug Del.*, 2011, **8**, 1379.
76. X. Kan, Z. Geng, Y. Zhao, Z. Wang and J. J. Zhu, *Nanotechnology*, 2009, **20**, 165601.

77. M. E. Byrne, K. Park and N. A. Peppas, *Adv. Drug Deliver. Rev.*, 2002, **54**, 149.
78. D. Cunliffe, A. Kirby and C. Alexander, *Adv. Drug Deliver. Rev.*, 2005, **57**, 1836.
79. C. Alvarez-Lorenzo and A. Concheiro, in *Biotechnology Annual Review Vol. 12*, ed. M. R. El-Gewely, Elsevier, Amsterdam, 2006, p. 225.
80. B. Singh, N. Chauhan and V. Sharma, *Ind. Eng. Chem. Res.*, 2011, **50**, 13742.
81. M. E. Byrne and V. Salian, *Int. J. Pharmaceut.*, 2008, **364**, 188.
82. G. Wajs and J. C. Meslard, *Crit. Rev. Ther. Drug*, 1986, **2**, 275.
83. C. C. Peng, A. Ben-Shlomo, E. O. Mackay, C. E. Plummer and A. Chauhan, *Curr. Eye Res.*, 2012, **37**, 204.
84. C. C. Li and A. Chauhan, *Ind. Eng. Chem. Res.*, 2006, **45**, 3718.
85. H. Hiratani, A. Fujiwara, Y. Tamiya, Y. Mizutani and C. Alvarez-Lorenzo, *Biomaterials*, 2005, **26**, 1293.
86. C. C. S. Karlgard, N. S. Wong, L. W. Jones and C. Moresoli, *Int. J. Pharmaceut.*, 2003, **257**, 141.
87. T. Sato, R. Uchida, H. Tanigawa, K. Uno and A. Murakami, *J. Appl. Polym. Sci.*, 2005, **98**, 731.
88. P. C. Nicolson and J. Vogt, *Biomaterials*, 2001, **22**, 3273.
89. Z. Chen, Z. Hua, L. Xu, Y. Huang, M. Zhao and Y. Li, *J. Mol. Recognit.*, 2008, **21**, 71.
90. F. Yañez, A. Chauhan, A. Concheiro and C. Alvarez-Lorenzo, *J. Appl. Polym. Sci.*, 2011, **122**, 1333.
91. C. Alvarez-Lorenzo, H. Hiratani, J. L. Gómez-Amoza, R. Martínez-Pacheco, C. Souto and A. Concheiro, *J. Pharm. Sci.*, 2002, **91**, 2182.
92. H. Hiratani and C. Alvarez-Lorenzo, *J. Control. Release*, 2002, **83**, 223.
93. H. Hiratani and C. Alvarez-Lorenzo, *Biomaterials*, 2003, **25**, 1105.
94. H. Hiratani, Y. Mizutani and C. Alvarez-Lorenzo, *Macromol. Biosci.*, 2005, **5**, 728.
95. H. Hiratani, A. Fujiwara, Y. Tamiya, Y. Mizutani and C. Alvarez-Lorenzo, *Biomaterials*, 2005, **26**, 1293.
96. S. Venkatesh, S. P. Sizemore and M. E. Byrne, *Biomaterials*, 2007, **28**, 717.
97. S. Venkatesh, S. P. Sizemore and M. E. Byrne, *Mater. Res. Soc. Symp. Proc.*, 2006, 897E.
98. S. Venkatesh, J. Saha, S. Pass and M. E. Byrne, *Eur. J. Pharm. Biopharm.*, 2008, **69**, 852.
99. M. Ali, S. Horikawa, S. Venkatesh, J. Saha, S. Pass, J. W. Hong and M. E. Byrne, *J. Control. Release*, 2007, **124**, 154.
100. F. Abbate, A. Casini, A. Scozzafava and C. T. Supuran, *Bioorgan. Med. Chem.*, 2004, **14**, 2357.
101. A. Ribeiro, F. Veiga, D. Santos, J. J. Torres-Labandeira, A. Concheiro and C. Alvarez-Lorenzo, *Biomacromolecules*, 2011, **12**, 701.
102. A. Ribeiro, F. Veiga, D. Santos, J. J. Torres-Labandeira, A. Concheiro and C. Alvarez-Lorenzo, *J. Membrane Sci.*, 2011, **383**, 60.

103. K. Sreenivasan, *J. Appl. Polym. Sci.*, 1999, **71**, 1819.
104. J. G. Karlsson, L. I. Andersson and I. A. Nicholls, *Anal. Chim. Acta*, 2001, **435**, 57.
105. L. Ye, P. A. G. Cormack and K. Mosbach, *Anal. Chim. Acta*, 2001, **435**, 187.
106. Y. Yoshimi, R. Ohdaira, C. Iiyama and K. Sakai, *Sensor Actuat. B- Chem.*, 2001, **73**, 49.
107. K. Hattori, Y. Yoshimi and K. Sakai, *J. Chem. Eng. Jpn*, 2001, **34**, 1466.
108. K. Hattori, M. Hiwatari, C. Iiyama, Y. Yoshimi, F. Kohori, K. Sakai and S. A. Piletsky, *J. Membrane Sci.*, 2004, **233**, 169.
109. Y. Yoshimi, R. Arai and S. Nakayama, *Anal. Chim. Acta*, 2010, **682**, 110.
110. R. N. Karmalkar, M. G. Kulkarni and R. A. Mashelkar, *J. Control. Release*, 1997, **43**, 235.
111. A. Leonhardt and K. Mosbach, *React. Polym.*, 1987, **6**, 285.
112. R. A. Mashelkar, M. G. Kulkarni and R. N. Karmalkar, *US Pat.* 5,851,546, Dec. 22, 1998.
113. G. Wang, K. Kuroda, T. Enoki, A. Grosberg, S. Masamune, T. Oya, Y. Takeoka and T. Tanaka, *P. Natl. Acad. Sci. USA*, 2000, **97**, 9861.
114. C. Alvarez-Lorenzo, A. Concheiro, J. Chuang and A. Y. Grosberg, in *Smart Polymers: Production, Study and Application in Biotechnology and Biomedicine*, eds. I. Galaev and B. Mattiasson, CRC Press, Boca Raton, FL, USA, 2008, p. 211.
115. C. Alvarez-Lorenzo, O. Guney, T. Oya, Y. Sakai, M. Kobayashi, T. Enoki, Y. Takeoka, T. Ishibashi, K. Kuroda, K. Tanaka, G. Wang, A. Y. Grosberg, S. Masamune and T. Tanaka, *J. Chem. Phys.*, 2001, **114**, 2812.
116. K. A. Stancil, M. S. Feld and M. Kardar, *J. Phys. Chem. B*, 2005, **109**, 6636.
117. H. Hiratani, C. Alvarez-Lorenzo, J. Chuang, O. Guney, A. Y. Grosberg and T. Tanaka, *Langmuir*, 2001, **17**, 4431.
118. O. Güney, Y. Yilmaz and O. Pekcan, *Sensor Actuat. B- Chem.*, 2002, **85**, 86.
119. O. Güney, *J. Mol. Recognit.*, 2003, **16**, 67.
120. R. Kanazawa, T. Yoshida, T. Gotoh and S. Sakohara, *J. Chem. Eng. Jpn*, 2004, **37**, 59.
121. R. Kanazawa, K. Mori, H. Tokuyama and S. Sakohara, *J. Chem. Eng. Jpn.*, 2004, **37**, 804.
122. H. G. Wu, X. J. Ju, R. Xie, Y. M. Liu, J. G. Deng, C. H. Niu and L. Y. Chu, *Polym. Adv. Technol.*, 2011, **22**, 1389.
123. C. Alvarez-Lorenzo, A. Concheiro, A. S. Dubovik, N. V. Grinberg, T. V. Burova and V. Y. Grinberg, *J. Control. Release*, 2005, **102**, 629.
124. K. Yamashita, T. Nishimura and M. Nango, *Polym. Adv. Technol.*, 2003, **14**, 189.
125. K. Yamashita, T. Nishimura, K. Ohashi, H. Ohkouchi and M. Nango, *Polym. J.*, 2003, **35**, 545.

126. X. Y. Liu, X. B. Ding, Y. Guan, Y. X. Peng, X. P. Long, X. C. Wang, K. Chang and Y. Zhang, *Macromol. Biosci.*, 2004, **4**, 412.
127. X. Y. Liu, Y. Guan, X. B. Ding, Y. X. Peng, X. P. Long, X. C. Wang and K. Chang, *Macromol. Biosci.*, 2004, **4**, 680.
128. X. Liu, T. Zhou, Z. Du, Z. Wei and J. Zhang, *Soft Matter*, 2011, **7**, 1986.
129. J. Aburto and S. Le Borgne, *Macromolecules*, 2004, **37**, 2938.
130. J. Berger, M. Reist, J. M. Mayer, O. Felt, N. A. Peppas and R. Gurny, *Eur. J. Pharm. Biopharm.*, 2004, **57**, 19.
131. L. Qin, X. W. He, X. Yuan, W. Y. Li and Y. K. Zhang, *Anal. Bioanal. Chem.*, 2011, **399**, 3375.
132. G. Demirel, G. Ozcetin, E. Turan and T. Caykara, *Macromol. Biosci.*, 2005, **5**, 1032.
133. T. V. Burova, N. V. Grinberg, E. V. Kalinina, R. V. Ivanov, V. I. Lozinsky, C. Alvarez-Lorenzo and V. Y. Grinberg, *Macromol. Chem. Phys.*, 2011, **212**, 72.
134. Y. Kanekiyo, R. Naganawa and H. Tao, *Chem. Commun.*, 2002, 2698.
135. Y. Kanekiyo, R. Naganawa and H. Tao, *Angew. Chem. Int. Ed.*, 2003, **42**, 3014.
136. F. Puoci, F. Iemma, R. Muzzalupo, U. G. Spizzirri, S. Trombino, R. Cassano and N. Picci, *Macromol. Biosci.*, 2004, **4**, 22.
137. G. Ciardelli, B. Cioni, C. Cristallini, N. Barbani, D. Silvestri and P. Giusti, *Biosens. Bioelectron.*, 2004, **20**, 1083.
138. R. Suedee, C. Jantarat, W. Lindner, H. Viernstein, S. Songkro and T. Srichana, *J. Control. Release*, 2010, **142**, 122.
139. S. Marx-Tibbon and I. Willner, *Chem. Commun.*, 1994, **10**, 1261.
140. C. Alvarez-Lorenzo, L. Bromberg and A. Concheiro, *Photochem. Photobiol.*, 2009, **85**, 848.
141. R. H. El Halabieh, O. Mermut and C. J. Barrett, *Pure Appl. Chem.*, 2004, **76**, 1445.
142. F. P. Nicoletta, D. Cupelli, P. Formoso, G. De Filpo, V. Colella and A. Gugliuzza, *Membranes*, 2012, **2**, 134.
143. N. Minoura, K. Idei, A. Rachkov, H. Uzawa and K. Matsuda, *Chem. Mater.*, 2003, **15**, 4703.
144. N. Minoura, K. Idei, A. Rachkov, Y. Choi, M. Ogiso and K. Matsuda, *Macromolecules*, 2004, **37**, 9571.
145. C. Gomy and A. R. Schmitzer, *Org. Lett.*, 2007, **9**, 3865.
146. C. Gong, K. L. Wong and M. H. W. Lan, *Chem. Mater.*, 2008, **20**, 1353.
147. L. Fang, S. Chen, Y. Zhang and H. Zhang, *J. Mater. Chem.*, 2011, **21**, 2320.
148. G. S. Jiang, S. A. Zhomg, L. Chen, I. Blakey and A. Whitaker, *Radiat. Phys. Chem.*, 2011, **80**, 130.

CHAPTER 22
Biomolecule-sensitive Hydrogels

TAKASHI MIYATA

Department of Chemistry and Materials Engineering, Kansai University,
Suita, Osaka 564-8680, Japan
Email: tmiyata@kansai-u.ac.jp

22.1 Introduction

Hydrogels are composed of physically or chemically cross-linked polymer networks and a large amount of aqueous solutions. They have already been utilized as foods, absorbents, chromatography columns and various industrial materials because of their fascinating properties such as swelling, mechanical, permeation, separation, surface and optical features.[1–3] Since hydrogels are soft and wet materials with many useful properties, they are important as biomaterials for drug delivery, diagnosis and tissue engineering. In addition, hydrogels have been focused on as smart biomaterials that respond to environmental changes since volume phase transition phenomena were discovered by Tanaka in 1978. A variety of hydrogels that undergo abrupt changes in volume in response to alterations in environmental conditions, such as pH and temperature, have been developed as stimuli-sensitive or smart hydrogels.[4–7] Stimuli-sensitive hydrogels are fascinating soft materials that sense a stimulus as a signal and that undergo volume changes. The unique features of stimuli-sensitive hydrogels can provide useful tools for constructing innovative devices such as self-regulated drug-delivery systems (DDSs), sensors, actuators, cell supports and tissue engineering scaffolds.

Temperature and pH are important signals for monitoring physiological changes. Therefore, a variety of stimuli-sensitive hydrogels that exhibit swelling/shrinking changes in response to pH and temperature have been

---

RSC Smart Materials No. 3
Smart Materials for Drug Delivery: Volume 2
Edited by Carmen Alvarez-Lorenzo and Angel Concheiro
© The Royal Society of Chemistry 2013
Published by the Royal Society of Chemistry, www.rsc.org

prepared by using polymer chains with carboxyl or amino groups as pH-sensitive moieties and poly(*N*-alkylacrylamide) or poly(ethylene oxide)-poly(propylene oxide)-poly(ethyelene oxide) as temperature-sensitive moieties.[8–18] Biological molecules like proteins and saccharides give important signals for monitoring living biological systems. For example, glucose is a signal molecule to treat diabetes, because insulin that controls the glucose metabolism must be administered with monitoring the blood glucose concentration. Therefore, stimuli-sensitive hydrogels that undergo changes in volume in response to the concentration of a target biomolecule like glucose (biomolecule-sensitive hydrogels) are very useful devices for developing molecular diagnostics and self-regulated DDSs.[19–21] There have been few studies on biomolecule-sensitive hydrogels with biomolecule recognition abilities, in spite of their many potential applications in biomedical fields. This is attributed to no convenient strategy for combining biomolecule recognition abilities with responsive functions within a hydrogel.

For preparing biomolecule-sensitive hydrogels, both biomolecule recognition abilities and responsive functions, which enable a target biomolecule to be perceived and structural changes to be induced, must be strategically introduced into hydrogel networks. Studies on biomolecule-sensitive hydrogels not only contribute significantly to the progress in fundamental biomaterials science, but also lead to innovative science and technology in biomedical applications. For example, self-regulated administration of a drug in response to a concentration of a target biomolecule such as a tumor marker or an antibody can be achieved using biomolecule-sensitive hydrogels. This chapter provides an overview of innovative researches regarding biomolecule-sensitive hydrogels as smart biomaterials applicable to self-regulated DDSs and so on.

22.2 Strategies for Designing Biomolecule-sensitive Hydrogels

In designing biomolecule-sensitive hydrogels, biomolecular recognition ability of the ligands must be combined with responsive functions of the networks. Standard strategy for preparing traditional biomolecule-sensitive hydrogels, such as glucose-sensitive ones, uses both the catalytic reaction of enzymes for recognizing a target biomolecule, and the pH-sensitivity for inducing structural changes of the network. For example, in the case of glucose-sensitive hydrogels, the chemicals produced by enzymatic reaction of glucose oxidase induce pH changes, followed by pH-sensitive swelling/shrinking of, networks with amine groups. Thus, enzymes play important roles both as sensors for recognizing a target biomolecule and as transducers for converting it into a change in pH. Combination of enzymes and pH-sensitive polymers enables the development of biomolecule-sensitive systems.

Another standard strategy for preparing biomolecule-sensitive hydrogels utilizes temperature-sensitive polymers such as poly(*N*-isopropylacrylamide) (PNIPAAm). PNIPAAm is soluble in water below the lower critical solution temperature (LCST) but becomes insoluble above the LCST. Therefore, hydrogels consisting of PNIPAAm undergo a drastic change in volume by rising temperature. The LCST is directly influenced by introducing hydrophilic and hydrophobic moieties into the temperature-sensitive networks. Therefore, biomolecule-sensitive hydrogels can be prepared by introduction of molecular recognition sites into temperature-sensitive polymer networks consisting of PNIPAAm. For example, when target biomolecules are bound to temperature-sensitive networks with molecular recognition sites, the LCST of the networks is shifted due to a change in hydrophilicity of the polymer chains. As shown in Figure 22.1, when a temperature-sensitive hydrogel with molecular recognition sites shows LCST1 and LCST2 (or LCST3) in the absence and presence of a target biomolecule, respectively, they undergo a drastic change in volume in response to the target biomolecule at a temperature in between LCST1 and LCST2 (or LCST3). Thus, utilizing temperature-sensitive polymers enables preparing biomolecule-sensitive hydrogels in which the molecular recognition ability of ligands is combined with the responsive function of networks.

A novel strategy for designing biomolecule-sensitive hydrogels uses biomolecular complexes as dynamic cross-links. Swelling ratio of hydrogels depends on the affinity of polymer chains for water, the states of charged groups and the cross-linked structures. Responsive volume changes of general stimuli-sensitive hydrogels (such as pH- and temperature-sensitive ones) are mainly caused by changes in the affinity of polymer chains for water and/or in the states of charged groups. The standard strategies for preparing biomolecule-sensitive hydrogels described above also use the changes in the affinity of polymer chains and/or the state of charged groups. Recently, dynamic cross-linking has been proposed as a novel strategy for designing biomolecule-sensitive hydrogels, focusing on the effect of cross-linked

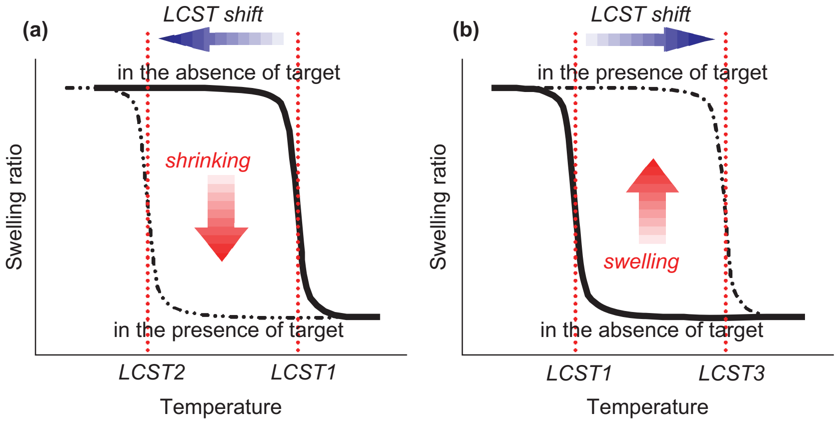

Figure 22.1 Responsive shrinking (a) and swelling (b) of a temperature-sensitive hydrogel with molecular recognition sites that shift the LCST in the presence of the target molecule.

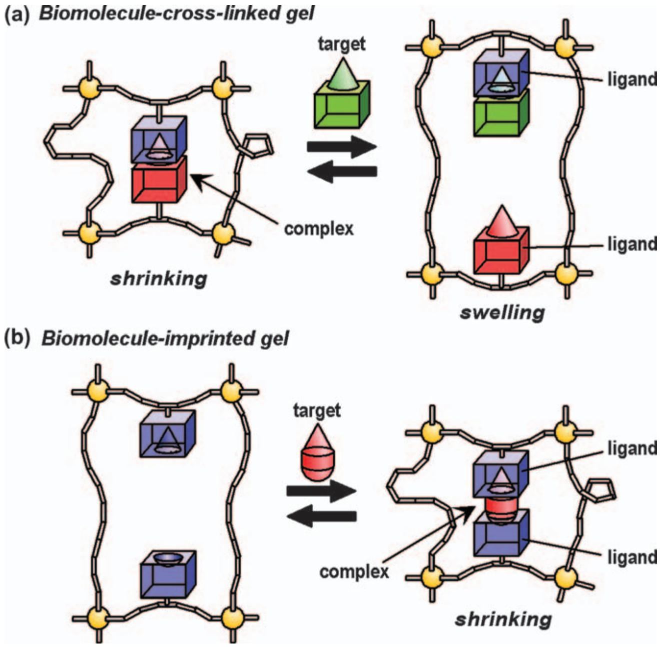

Figure 22.2 Schematic of the swelling/shrinking behavior of biomolecule-sensitive hydrogels: biomolecule-cross-linked hydrogel (a) and biomolecule-imprinted hydrogel (b).

structures on the swelling ratio.[22] For example, bioconjugated hydrogels with biomolecular complexes as dynamic cross-links undergo changes in volume in response to a target biomolecule, because their cross-linking density changes by formation or dissociation of the biomolecular complexes. Biomolecule-sensitive hydrogels designed using biomolecular complexes as dynamic cross-links are classified into two types: biomolecule-cross-linked and biomolecule-imprinted hydrogels (Figure 22.2). In the presence of a target biomolecule, the biomolecule-cross-linked hydrogels swell and the biomolecule-imprinted hydrogels shrink, because their cross-linking density decreases and increases by the dissociation and formation of biomolecular complexes as dynamic cross-links of their networks, respectively. This chapter describes a variety of biomolecule-sensitive hydrogels designed on the basis of standard and novel strategies.

22.3 Glucose-sensitive Hydrogels

22.3.1 Glucose-sensitive Hydrogels Using Enzymatic Reaction

To treat diabetes, a specific amount of insulin must be administered with monitoring the blood glucose concentration, and they have been developed exploiting a few standard strategies. A typical approach for designing glucose-sensitive hydrogels is the combination of an enzymatic reaction of glucose oxidase (GOD) and the pH-sensitive behavior of polymers with amine groups. For example, GOD was loaded within pH-sensitive hydrogels with amine groups. As GOD converts glucose to gluconic acid, the pH within the hydrogel is lowered in the presence of glucose. Then, the pH-sensitive polymers expand as the amine groups become positively charged and the osmotic pressure increases.

A representative glucose-sensitive insulin release system was developed by loading GOD within a pH-sensitive copolymer of *N*,*N*-diethylaminoethyl methacrylate (DEA) and 2-hydroxypropyl methacrylate (HPMA).[23] Insulin permeability through a GOD-loaded DEA-HPMA copolymer membrane was enhanced by increasing glucose concentration (Figure 22.3). When the DEA-HPMA copolymer hydrogel was immersed in an aqueous solution containing glucose, the glucose diffused into the hydrogel and was oxidized to gluconic acid by enzymatic reaction of GOD. Because the pH-sensitive hydrogel was swollen by lowering pH, insulin permeability through the hydrogel was enhanced in response to the glucose concentration. On the other hand, glucose-sensitive polymer capsules that regulated insulin release in response to the glucose concentration were prepared by a conventional interfacial precipitation method.[24] Similarly, glucose-sensitive behavior of DEA-hydroxyethyl methacrylate copolymer hydrogel with entrapped GOD was investigated from theoretical and experimental points of view.[25–27] The complex formation between methacrylic acid (MAAc) and ethylene glycol (EG) was also utilized to form pH-sensitive networks for designing glucose-sensitive hydrogels.[28,29] The complex of the copolymer hydrogels consisting of MAAc and EG dissociates or associates in response to pH changes. Therefore, pH-responsive behavior of the complexes can be combined with the enzymatic reaction of GOD for developing glucose-sensitive hydrogels.

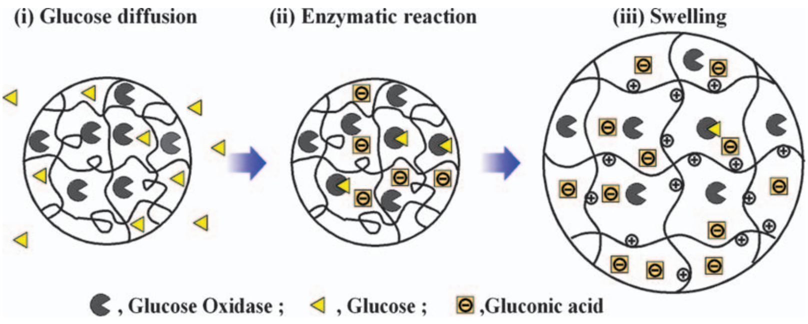

Figure 22.3 Schematic representation of a glucose-sensitive hydrogel consisting of pH-sensitive networks and glucose-oxidase.

22.3.2 Glucose-sensitive Hydrogels Using Phenylboronic Acid

Phenylboronic acid and its derivatives form complexes with polyol compounds such as saccharides and poly(vinyl alcohol) (PVA). Glucose-sensitive hydrogels can be prepared by using phenylboronic acid as a ligand for target glucose. For example, a copolymer with phenylboronic acid moieties was synthesized by copolymerization of *N*-vinyl-2-pyrrolidone (NVP) and 3-(acrylamide)phenylboronic acid (PBA). The complexes between the NVP-PBA copolymer and PVA enable us to construct glucose-sensitive insulin release systems because the complexes dissociated in response to the glucose concentration.[30,31]

Based on a strategy of combining the temperature-sensitivity of PNIPAAm with the glucose-recognition ability of phenylboronic acid, glucose-sensitive hydrogels were prepared by copolymerization of PBA with NIPAAm.[32,33] Uncharged and charged forms of phenylboronic acid in the hydrogel were in equilibrium, as shown in Figure 22.4. Complex formation between phenylboronic acid and glucose resulted in a shift in the equilibrium from the uncharged to the charged form. Therefore, the LCST of the NIPAAm-PBA copolymer hydrogels rose in the presence of free glucose, because the proportion of charged phenylboronic acid increased by complex formation between phenylboronic acid and glucose (Figure 22.4). The shift in LCST of the hydrogels resulted in a drastic increase in the volume in response to glucose. Repeated on-off release of insulin on changing the concentration of external glucose was also achieved by using the glucose-sensitive hydrogels (Figure 22.5). However, the NIPAAm-PBA copolymer hydrogels did not exhibit glucose-sensitive swelling behavior at the physiological aqueous condition. To design glucose-sensitive hydrogels undergoing drastic changes in volume at the physiological aqueous condition, a PBA derivative with a low pK_a and an acrylamide derivative with a higher LCST than that of PNIPAAm were utilized.[34,35]

Recently, a biosensor for detecting glucose concentration was developed by forming a glucose-sensitive hydrogel layer on a field-effect transistor (FET) gate.[36] Electrical signal changes in response to glucose concentration were detected with FET, because glucose-sensitive swelling of the hydrogel layer induced an abrupt permittivity change at the hydrogel layer/gate interface. Thus, glucose-sensitive hydrogels may contribute significantly to developing glucose sensors as well as self-regulated DDSs for treating diabetes.

22.3.3 Glucose-sensitive Hydrogels Using Lectin

Lectins are carbohydrate-binding proteins that recognize carbohydrate chains of glycoproteins and glycolipids on a cell surface. In constructing sensor systems for monitoring saccharides, lectins are useful tools because of their unique property of saccharides recognition ability. Therefore, smart devices from which insulin is released in response to glucose concentration were prepared taking benefit of reversible complex formation between lectin and glucose. For example, glucose-sensitive insulin release systems that can regulate

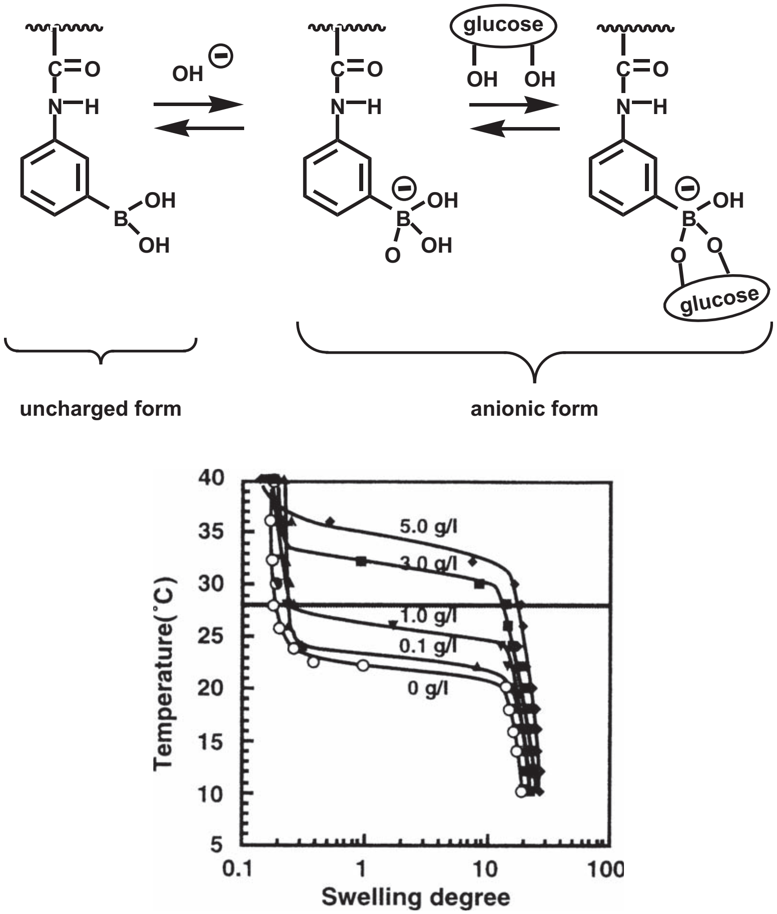

Figure 22.4 Temperature dependence of swelling curves for PNIPAAm copolymer hydrogel with phenylboronic acid moieties at different glucose concentrations. Reprinted, with permission, from Ref. 32. Copyright 1998 American Chemical Society.

insulin release in response to the glucose concentration were proposed, based on competitive complex formation of lectin with glycosylated insulin and free glucose.[37–40] The carbohydrate-binding property of lectin, which was combined with temperature-sensitivity of PNIPAAm, was also utilized in preparing saccharide-sensitive hydrogels that underwent a change in volume in response to a target saccharide with charged groups.[41] The saccharide-sensitive systems were prepared by loading lectin within PNIPAAm hydrogels. The saccharide-sensitive swelling of lectin-loaded PNIPAAm hydrogels was based on a shift in LCST of PNIPAAm, caused by complex formation between lectin and ionic saccharide dextran sulfate.

Glucose-sensitive hydrogels were also designed by utilizing lectin-glycopolymer complexes as dynamic cross-links. A polymer with pendant

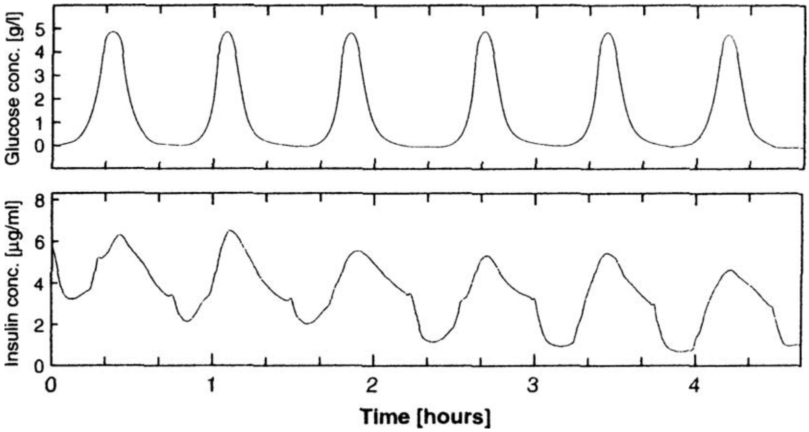

Figure 22.5 Repeated on-off release of FITC-insulin from a glucose-sensitive hydrogel at 28 °C and pH 9.0, in response to the external glucose concentration. Reprinted, with permission, from Ref. 32. Copyright 1998 American Chemical Society.

glucose (poly(2-glucosyloxyethyl methacrylate), PGEMA) formed a complex with lectin (concanavalin A, ConA).[42,43] The complex between PGEMA and ConA dissociated in the presence of free glucose and mannose, but did not dissociate in the presence of free galactose, because ConA is a lectin that recognizes glucose and mannose, but does not recognize galactose. Therefore, the dissociation of the PGEMA-ConA complex is attributed to complex exchange of PGEMA with glucose and mannose. This means that the PGEMA-ConA complexes can be used as smart cross-links responsive to glucose or mannose as a target monosaccharide. To design bioconjugated hydrogels with PGEMA-ConA complexes as dynamic cross-links, GEMA was copolymerized with a cross-linker after its complex formation with ConA.[44] The resulting PGEMA-ConA hydrogels swelled gradually in a buffer solution with glucose and mannose, but exhibited no change in volume in a buffer solution with galactose (Figure 22.6). Measurements of compressive modulus of the hydrogels revealed that the cross-linking density decreased with an increase in glucose concentration of a buffer solution. Therefore, the glucose- and mannose-sensitive volume changes of the PGEMA-ConA hydrogels were attributed to a decrease in the cross-linking density by competitive complex exchange of PGEMA with free glucose or mannose (Figure 22.7).

Reversible glucose-sensitive hydrogels were strategically synthesized by copolymerization of GEMA, cross-linkers and a polymerizable ConA derivative.[45] The resulting hydrogels in which ConA was covalently conjugated with PGEMA networks (ConA-copolymerized PGEMA hydrogels) swelled gradually in the presence of a free glucose, but shrank in its absence. On the other hand, PGEMA hydrogels in which ConA was entrapped also swelled in the presence of a free glucose, but did not change their volume at all in its

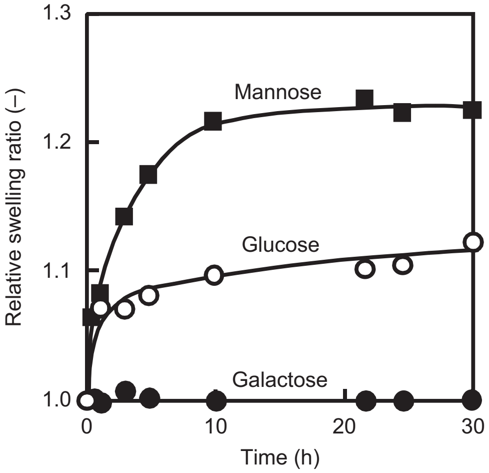

Figure 22.6 Swelling ratio changes underwent by PGEMA-ConA hydrogel as a function of time, when the hydrogel was immersed in a buffer solution containing 1 wt.% of glucose (○), mannose (■) or galactose (●). Reprinted, with permission, from Ref. 44. Copyright 1996 Wiley-VCH.

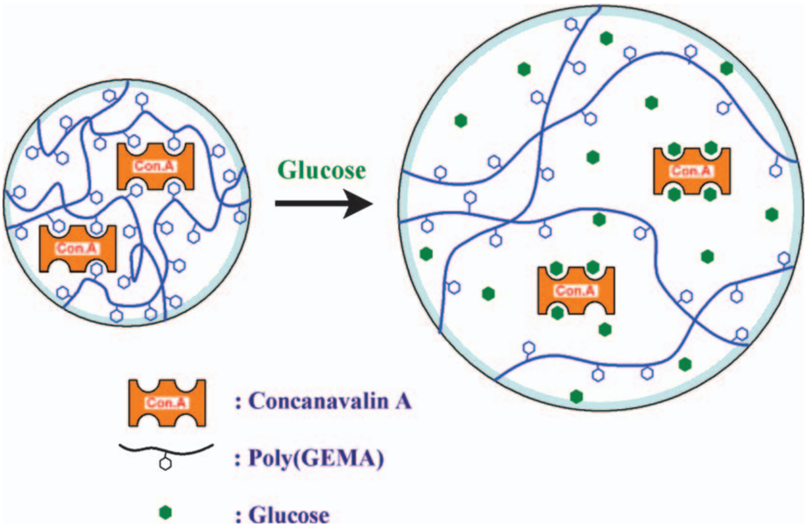

Figure 22.7 Schematic representation of the glucose-sensitive swelling changes underwent by PGEMA-ConA hydrogel. Reprinted, with permission, from Ref. 44. Copyright 1996 Wiley-VCH.

absence. Covalent conjugation of ConA with PGEMA networks enabled repeated formation and dissociation of the complex between ConA and pendant glucose on PGEMA in response to stepwise changes in glucose concentration. Thus, reversibly glucose-sensitive hydrogels that undergo reversible changes in volume in response to a certain glucose concentration were prepared, taking benefit from complex formation between a pendant glucose of PGEMA and lectin covalently conjugated with hydrogel networks.

By utilizing complex formation between a polymer with pendant glucose and ConA, sol-gel transitions in response to glucose concentration were also achieved.[46,47] For example, glycopolymers with pendant glucose, such as vinylpyrrolidinone-allylglucose and acrylamide-allylglucose copolymers, underwent gelation by adding ConA into their aqueous solutions. Complex formation between the glycopolymers with pendant glucose and ConA resulted in cross-linking of linear glycopolymers followed by formation of hydrogels. However, the hydrogels consisting of the glycopolymers and ConA changed to the sol state by the addition of free glucose. The glucose-sensitive sol-gel transitions enabled controlled release of lysozyme and insulin in response to changes in glucose concentration in a buffer solution.[48] The glucose-sensitive drug release behavior is explained by the fact that the diffusivity of lysozyme and insulin in the sol state was higher than that in the gel state. Thus, glucose-sensitive hydrogels and sol-gel transition are applicable to the development of self-regulated DDSs that release drugs in response to a blood glucose concentration.

22.4 Protein-sensitive Hydrogels

22.4.1 Enzyme-sensitive Hydrogels

Enzymes located in specific areas of the human body are promising signals for site-specific drug delivery. Some enzymes provide us with important information about physiological changes. Therefore, enzyme-sensitive hydrogels that undergo structural changes by selective catalysis of target enzymes are widely employed as smart biomaterials for constructing diagnostic sensors to monitor physiological changes or DDSs to regulate drug release in response to physiological changes in specific sites. Such enzyme-sensitive hydrogels can be prepared by using biodegradable polymers that are degraded by the catalytic activity of specific enzymes.[49] For example, a few researchers have focused on microbial enzymes located predominantly in the colon for constructing colon-specific drug-delivery systems. Since azoreductase, an enzyme produced by the microbial flora of the colon, degrades azoaromatic bonds, enzyme-sensitive hydrogels were prepared from pH-sensitive monomers and cross-linked with azoaromatic bonds.[50–55] When the pH-sensitive hydrogels with azoaromatic bonds as cross-links shrink at low pH, protein drugs loaded within the hydrogels are protected against digestion by proteolytic enzymes in the stomach. At higher pH, however, colonic azoreductases can degrade the azoaromatic cross-links because of swelling of the network, triggering drug release. Dextranases existing in the colon are also useful for colon-specific drug delivery. As dextranases are microbial enzymes that degrade dextran, enzyme-sensitive hydrogels were synthesized by cross-linking dextran with diisocyanate.[56] The resulting hydrogels were degraded *in vitro* and *in vivo* by the enzymatic activity of dextranases, being suitable for colon-specific DDSs.

α-Chymotrypsin, which is synthesized in the pancreas, is a proteolytic enzyme that facilitates the cleavage of peptide bonds by a hydrolysis reaction. Enzyme-sensitive hydrogels degradable by α-chymotrypsin were prepared using a tetrapeptide sequence, Cys-Tyr-Lys-Cys, as a cross-linker for the formation of poly(acrylamide) (PAAm) networks.[57] The resulting PAAm hydrogels cross-linked with tetrapeptide sequence underwent degradation in the presence of α-chymotrypsin that cleaved the tetrapeptide cross-linker. A novel disulfide-based temperature-sensitive triblock copolymer was also produced by atom transfer radical polymerization (ATRP) of NIPAAm and 2-(methacryloyloxy)ethyl phosphorylcholine (MPC) using a disulfide-based initiator.[58] The micellar gel formed from the triblock copolymer was disintegrated by cleavage of the disulfide bonds.

Simultaneous monitoring of two or more enzymes to sense physiological changes is attracting interest for clinical screening of several diseases at the same time. Therefore, dual enzyme-sensitive hydrogels that degrade in the presence of two enzymes were prepared by interpenetration of two enzyme degradable polymer networks. For example, interpenetrating polymer networks (IPNs) of oligopeptide-terminated poly(ethylene glycol) (PEG) and dextran can be degraded in the presence of both papain and dextranase that are enzymes for oligopeptides and dextran, respectively, but did not degrade in the presence of either enzyme alone.[59,60] Furthermore, lipid microspheres were released from gelatin/dextran IPN hydrogels in the presence of both α-chymotrypsin and dextranase that catalyze the degradation of gelatin and dextran, respectively, but were not released in the presence of either enzyme alone (Figure 22.8). Temperature-sensitive biodegradation of hydrogels that degrade in the presence of a target enzyme within a certain temperature range was achieved using IPNs composed of enzymatic degradable networks and temperature-sensitive PNIPAAm networks.[61,62]

Contrary to enzymatic degradable hydrogels described above, enzyme-sensitive hydrogel formation can also occur. That is the case of the networks that involved the cross-linking of PEG-peptide conjugates or glutaminamide-functionalized PEG with a lysine-containing polypeptide, by enzymatic activity of transglutaminase (TGase).[63,64] TGase catalyzes an acyl-transfer reaction between the γ-carboxamide group of protein bound glutaminyl residues and the ε-amino group of Lys residues, resulting in the formation of ε-(γ-glutamyl)lysine isopeptide side-chain bridges. For example, an aqueous solution containing two PEG-peptide conjugates formed a hydrogel by enzymatic activity of TGase within minutes under physiologic conditions. Such enzyme-sensitive hydrogel formation can provide the tools for controlling the migration, the growth and the organization of cells during tissue regeneration and for stabilization of encapsulated cells.

There is considerable demand for creating enzyme-sensitive hydrogels that undergo changes in volume triggered by a target enzyme, because they can be useful to regulate the release of entrapped molecules such as protein drugs.[65,66]

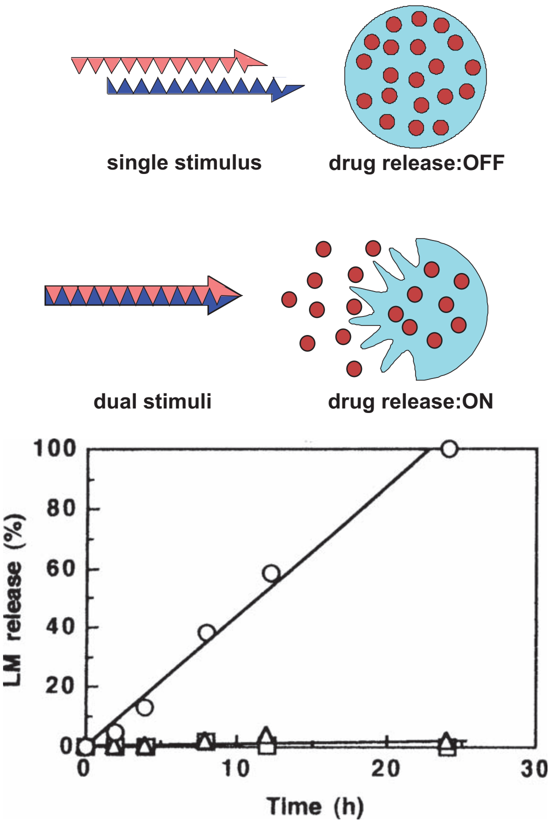

Figure 22.8 Lipid microspheres release from a gelatin/dextran IPN hydrogel in phosphate buffer at 37 °C, with 5 U mL^{-1} α-chymotrypsin + 0.5 U mL^{-1} dextranase (○), 5 U mL^{-1} α-chymotrypsin (△) or 0.5 U mL^{-1} dextranase (□). Reprinted, with permission, from Ref. 60. Copyright 1998 Elsevier Science BV.

For example, enzyme-sensitive PEG-based hydrogel particles were prepared using an enzyme-cleavable linker as the sensing part, and two oppositely changed amino acids that flank the linker on either side as the actuation part (Figure 22.9). When the zwitterionic peptide linker was cleaved by a specific enzyme, the originated doubly charged peptide fragments caused the hydrogel particles to swell. The release of dextran and proteins from the enzyme-sensitive hydrogels was switched on in response to a specific enzyme that caused the swelling as the peptide linker was cleaved.

22.4.2 Antigen-sensitive Hydrogels

Antibodies have been used for developing immunological assays to monitor physiological changes, due to their ability to bind to specific antigens.

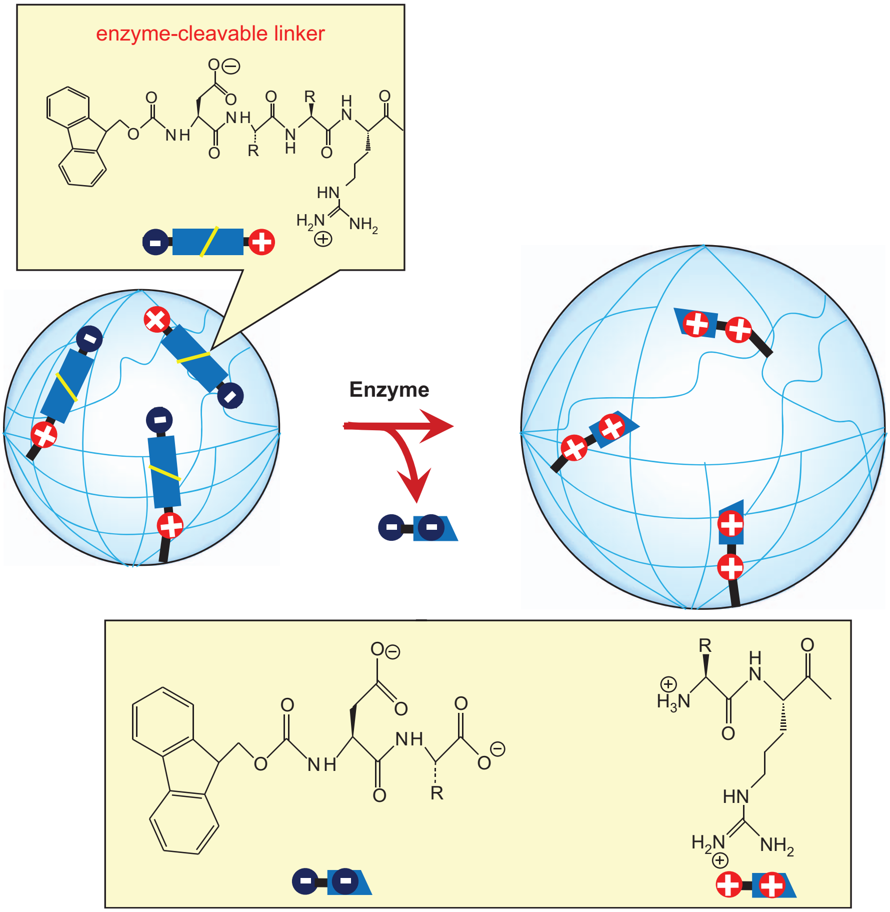

Figure 22.9 Schematic representation of the selective enzyme-triggered charge-induced swelling exhibited by an enzyme-sensitive hydrogel with zwitterionic peptide linkers that are hydrolyzed by a specific enzyme.

Antibodies are also useful tools for preparing antigen-sensitive hydrogels that undergo changes in volume in response to a target antigen. Antigen-sensitive hydrogels can be strategically prepared by utilizing antigen-antibody bindings as dynamic cross-links of the hydrogel networks.[67–71] For example, polymerizable groups were introduced in rabbit IgG antigen and copolymerized with acrylamide (AAm) and *N*,*N*′-methylenebisacrylamide (MBAA) in the presence of goat anti-rabbit IgG (GAR IgG) antibody. The antibody was entrapped within the resulting hydrogels by formation of antigen-antibody bindings that acted as dynamic cross-links. The swelling ratio of the antigen-antibody entrapment hydrogels increased gradually with an increase in the concentration of rabbit IgG as a free antigen in a buffer solution. An increase in rabbit IgG concentration induced dissociation of antigen-antibody bindings linked with PAAm networks, by competitive complex exchange. Therefore, the antigen-sensitive swelling behavior of the antigen-antibody entrapment hydrogels was attributed to a decrease in cross-linking density of their networks by dissociation of the antigen-antibody bindings acting as cross-links.

Reversibly antigen-sensitive hydrogels that exhibit reversible swelling/shrinking in response to changes in the antigen concentration of a buffer solution, were also synthesized by forming semi-interpenetrating polymer networks (semi-IPNs) consisting of PAAm networks with antigens and PAAm linear polymer with antibodies (Figure 22.10).[67,69] As described above, the antigen-antibody entrapment hydrogels in which antibodies were not covalently bound to PAAm chains swelled gradually in a buffer solution with a target antigen. However, these hydrogels did not shrink completely after their re-immersion in a buffer solution without free antigen. Since the antibodies that acted as cross-linkers were not covalently bound to PAAm networks, they easily leaked out of the swollen hydrogel in a buffer solution with a target antigen. By contrast, the antigen-antibody semi-IPN hydrogels underwent reversible swelling/shrinking changes when they were alternately immersed in a phosphate buffer solution with and without free antigen (Figure 22.11). Since the antibody acting as a cross-link was immobilized by the entanglement between PAAm linear polymers with antibodies and PAAm networks with antigens, it did not leak out of the hydrogel. These results indicate that the semi-IPN structure allows the hydrogel networks to swell and shrink reversibly in response to changes in the free antigen concentration. In addition, semi-IPN structures played an important role in enhancing the responsive behavior of the hydrogels.[70]

Reversible antigen-sensitive hydrogels are highly promising biomaterials for constructing self-regulated DDSs. Permeation of drugs with different molecular weight through antigen-sensitive hydrogels was investigated in both the absence and the presence of a target antigen.[67,71] Drug permeation was suppressed in the absence of a target antigen, but the permeation became enhanced in its presence (Figure 22.11). The permeation rate of a drug through the antigen-sensitive hydrogel increased gradually when the antigen concentration in the buffer solution rose. Thus the antigen-sensitive hydrogels can control drug permeation in response to the concentration of a target antigen and enable antigen-sensitive on-off regulation of drug permeation. The antigen-sensitive hydrogels are likely to become important biomaterials for constructing self-regulated DDSs in which drugs are administered in response to specific physiological changes.

Other antigen-sensitive hydrogels were prepared by combining the antigen-binding ability of an antibody with the temperature-sensitivity of PNIPAAm. The temperature-sensitive hydrogels with antibody Fab' fragments as antigen recognition sites were synthesized by copolymerization of functionalized antibody fragments with NIPAAm and MBAA.[72] The PNIPAAm hydrogels with Fab' fragments as fluorescein-binding sites underwent reversible volume changes in response to alternative immersion in a buffer solution with and without hydrophobic fluorescein and hydrophilic dendrimer-modified

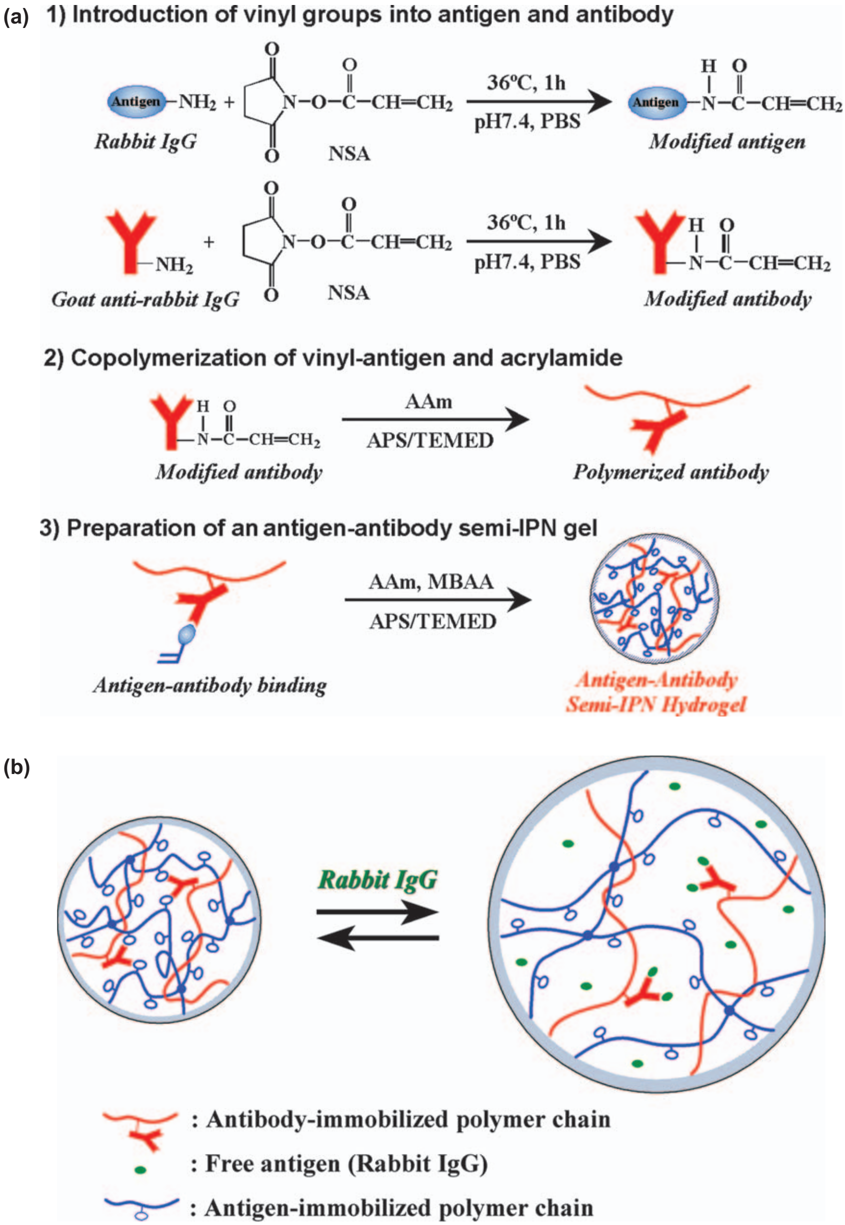
(a)
1) Introduction of vinyl groups into antigen and antibody
Antigen
Rabbit IgG
NSA
36°C, 1h
pH7.4, PBS
Modified antigen
Goat anti-rabbit IgG
Modified antibody
2) Copolymerization of vinyl-antigen and acrylamide
AAm
APS/TEMED
Modified antibody
Polymerized antibody
3) Preparation of an antigen-antibody semi-IPN gel
AAm, MBAA
APS/TEMED
Antigen-antibody binding
Antigen-Antibody Semi-IPN Hydrogel
(b)
Rabbit IgG
: Antibody-immobilized polymer chain
: Free antigen (Rabbit IgG)
: Antigen-immobilized polymer chain

Figure 22.10 Scheme of the preparation (a) and the responsive behavior (b) of an antigen-sensitive hydrogel with semi-IPN structure.

fluorescein as target antigens. The reversible volume changes in response to target antigens were caused by shifts in LCST of PNIPAAm networks due to the binding of Fab' fragment to hydrophobic fluorescein and hydrophilic dendrimer-modified fluorescein.

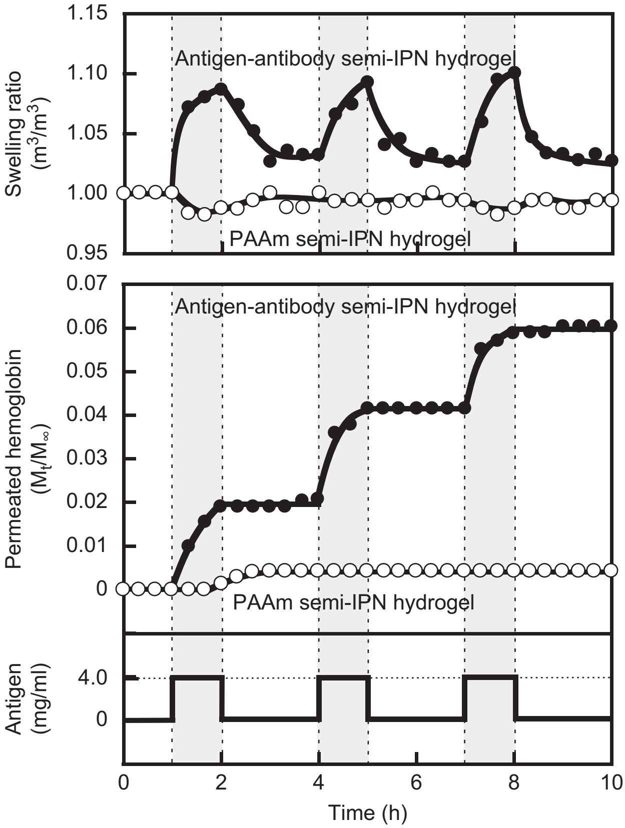

Figure 22.11 Reversible swelling and antigen-sensitive permeation profiles of hemoglobin through a PAAm semi-IPN (○) or an antigen-antibody semi-IPN (●) hydrogel in response to successive changes (between 0 and 4 mg mL^{-1}) in the antigen concentration.

22.5 Biomolecule-sensitive Hydrogels Prepared by Molecular Imprinting

Molecular imprinting is a useful technique for making synthetic hosts with cavities for molecular recognition.[73–80] In standard molecular imprinting, functional monomers with a ligand group are copolymerized with a large amount of cross-linker after the monomers are prearranged around a template molecule by non-covalent interactions. Molecularly imprinted polymers with molecular recognition ability are then obtained by removing the template molecules from the resulting polymer networks, to create complementary molecular cavities. The resulting molecularly imprinted polymers can recognize the target (template molecule) on the basis of a combination of its binding to complementarily arranged functional groups (ligands), and the shape complementarity of the cavity. Biomolecule-sensitive hydrogels with molecular recognition sites were also synthesized by molecular imprinting utilizing a minute amount of cross-linker, which is different from standard molecular imprinting.

Temperature-sensitive hydrogels with molecular recognition sites were prepared by copolymerization of NIPAAm and AAc in the presence of norephedrine as a template molecule.[81] The norephedrine-imprinted hydrogels underwent changes in volume in response to temperature changes, because of the temperature-sensitivity of PNIPAAm. The norephedrine-imprinted hydrogel swollen at a low temperature exhibited no volume change in the presence of norephedrine, but in the collapsed state at a high temperature swelled gradually with increasing norephedrine concentration (Figure 22.12). The binding of norephedrine to the complementary recognition sites created by molecular imprinting induced a shift in the LCST of the hydrogel networks, and the norephedrine-imprinted hydrogels changed from a shrunken state to a swollen state by the presence of norephedrine. Nevertheless, there are still few studies on combination of temperature-sensitivity of PNIPAAm hydrogels with memorization of a target molecule within hydrogel networks by molecular imprinting.[82,83]

A novel imprinting approach that utilizes biomolecules (such as proteins) as ligands has been proposed. The most important feature of biomolecular imprinting is that it utilizes a minute amount of cross-linker which enables the imprinted networks to undergo conformational changes by complex formation between ligand biomolecules and a target biomolecule. For example, tumor marker-imprinted hydrogels that shrink in response to a target tumor marker glycoprotein were designed by biomolecular imprinting using protein ligands. α-Fetoprotein (AFP) was chosen as a target tumor marker glycoprotein that is widely used for the serum diagnosis of primary hepatoma, because there is abnormal glycosylation patterns in primary hepatoma and cirrhosis. In preparing AFP-imprinted hydrogels by biomolecular imprinting, lectins (ConA) and antibodies (anti-AFP) were utilized as ligands for saccharide and peptide chains of AFP, respectively (Figure 22.13).[84]

With increasing AFP concentration in a buffer solution, the swelling ratio of AFP-imprinted hydrogel decreased gradually, but that of non-imprinted hydrogel prepared without a template AFP increased a little (Figure 22.14). In addition, both AFP-imprinted and non-imprinted hydrogels swelled a little in a buffer solution with ovalbumin, which has a saccharide chain similar to that of AFP but a different peptide chain. Thus, only AFP-imprinted hydrogels can dynamically recognize a target AFP by means of ConA and anti-AFP, and undergo volume changes in response to the AFP concentration of a buffer solution. The strong relationship between the AFP concentration and the swelling ratio of the AFP-imprinted hydrogels means that they are tumor marker-sensitive. The compressive modulus measurements revealed that the formation of ConA-AFP-anti-AFP complexes caused an increase in the cross-linking density of the AFP-imprinted hydrogels, followed by AFP-sensitive shrinking. Furthermore, to evaluate the effect of the molecular weight of the cross-linkers, hydrogels were prepared using low-molecular-weight and

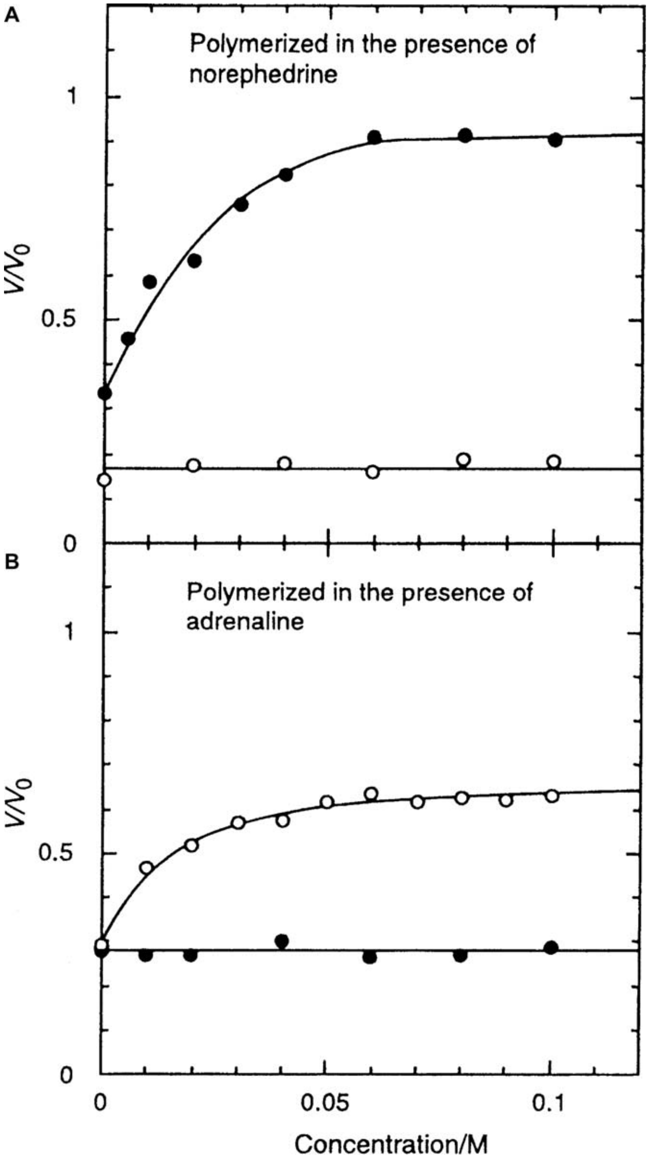

Figure 22.12 Equilibrium swelling ratio at 50 °C as a function of concentration of norphedrine (●) or adrenaline (○) in water for molecularly imprinted hydrogels prepared in the presence of norphedrine (A) or adrenaline (B). Reprinted, with permission, from Ref. 81. Copyright 1998 American Chemical Society.

high-molecular-weight cross-linkers.[85] The AFP-imprinted hydrogels with a high-molecular-weight cross-linker of an optimal chain length shrank more remarkably than those obtained using a low-molecular-weight cross-linker. However, when the high-molecular-weight cross-linker had a too long

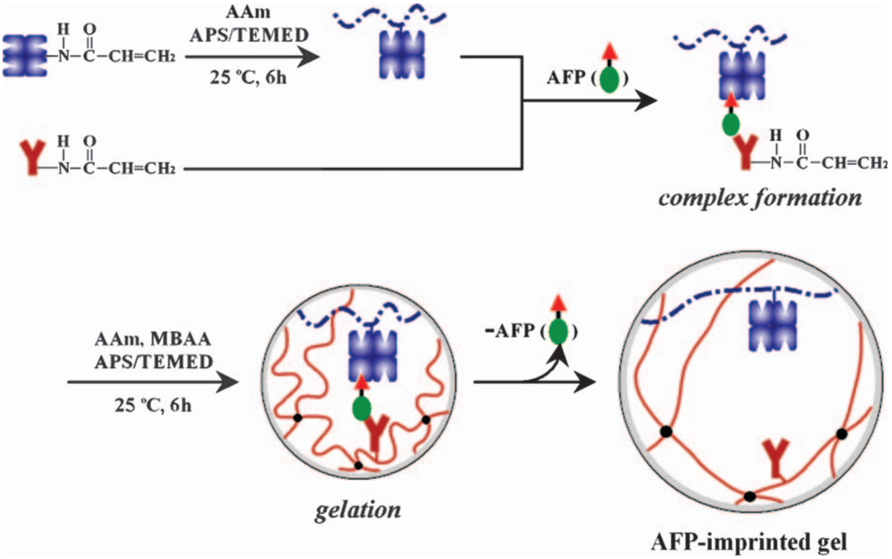

Figure 22.13 Synthesis of a tumor marker-sensitive hydrogel using lectins and antibodies as ligands for recognition of glycoprotein molecules (tumor-specific marker AFP) in biomolecular imprinting.

chain, no volume change in a buffer solution with AFP occurred. Therefore, the chain length of the cross-linker is an important factor for determining the dynamic glycoprotein recognition and the responsive behavior of AFP-imprinted hydrogels. Such responsiveness of AFP-imprinted hydrogels in response to glycoproteins enables the accurate detection and recognition of a target tumor marker glycoprotein with a double-lock function. Tumor marker glycoprotein-sensitive hydrogels have many future opportunities as smart biomaterials for constructing self-regulated DDSs and also in molecular diagnostics.

22.6 Biomolecule-sensitive Hydrogel Particles

Particles with nanoscale sizes are promising nanomaterials with a wide variety of uses because of their unique features such as large surface area, dispersiveness and size effect.[86,87] In particular, stimuli-sensitive hydrogel particles that undergo size changes in response to environmental changes like pH or temperature, are of significant interest as drug carriers for DDSs, columns for separation and devices for sensor systems. An important advantage of stimuli-sensitive hydrogel particles with nanoscale sizes is that they exhibit more rapidly responsive change in size than usual stimuli-sensitive hydrogels with macroscale sizes. Many researchers have focused on pH- and temperature-sensitive hydrogel particles from the viewpoint of fundamental interfacial science and of their applications in a wide variety of fields. In addition, there are a few publications on biomolecule-sensitive hydrogel particles that undergo

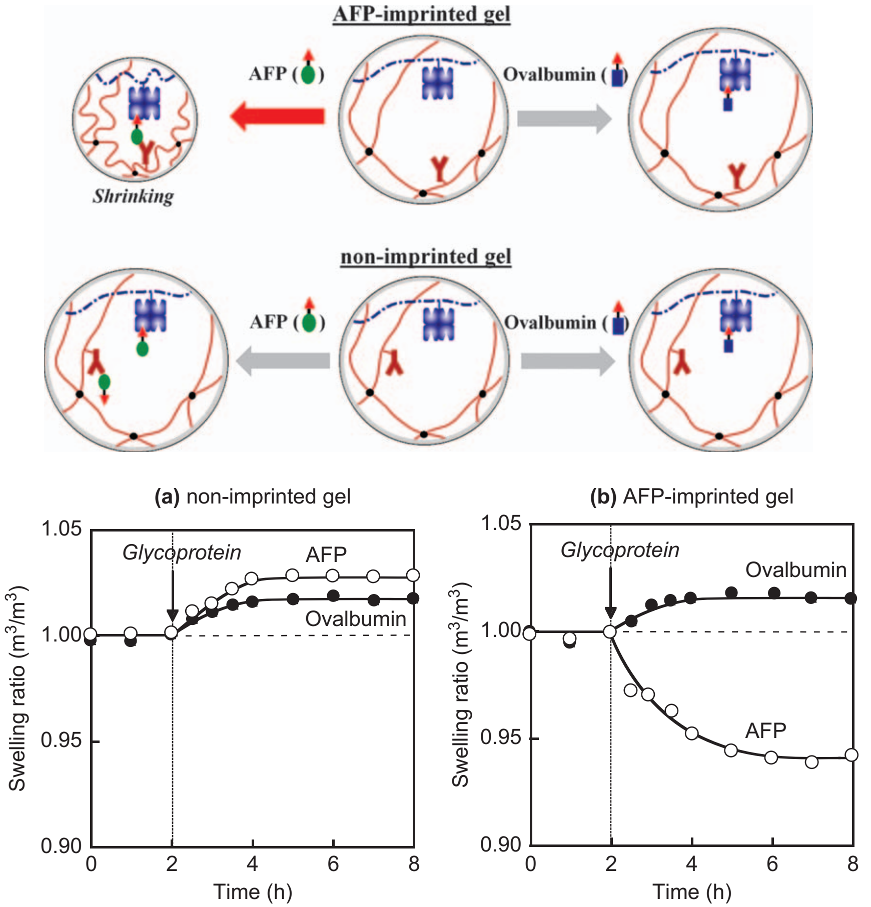

Figure 22.14 Swelling ratio changes underwent by non-imprinted (a) and AFP-imprinted (b) hydrogels following the addition of AFP (○) or ovalbumin (●) in a phosphate buffer medium at 25 °C.

changes in size in response to a target biomolecule, which can be useful as smart carriers for self-regulated DDS and imaging.

Based on the strategy for preparing glucose-sensitive hydrogels using PGEMA-ConA complexes as dynamic cross-links (described in Section 22.3.3), glucose-sensitive hydrogel particles were synthesized by surfactant-free emulsion polymerization of *N*,*N*-diethylaminoethyl methacrylate (DEAEMA), poly(ethylene glycol) dimethacrylate (PEGDMA), GEMA and ConA modified with polymerizable groups, after the formation of GEMA-ConA complexes.[88] The resultant hydrogel particles having GEMA-ConA complexes (GEMA-ConA hydrogel particles) were colloidally stable in a phosphate buffer solution and had a diameter of approximately 750 nm. Hydrophilic PEGDMA played important roles as both surfactant and cross-linker in preparing colloidally stable GEMA-ConA hydrogel particles by surfactant-free emulsion polymerization. The GEMA-ConA hydrogel particles had core-shell structures composed of a hydrophobic core of DEAEMA and a hydrophilic shell of PEGMA and GEMA containing ConA. The swelling ratio of the GEMA-ConA hydrogel particles augmented gradually with an increase in glucose concentration of a buffer solution (Figure 22.15), but did not change at all in the presence of galactose. The glucose-sensitive swelling was attributed to the dissociation of the GEMA-ConA complexes acting as cross-links by competitive complex exchange of GEMA with a free glucose. Such glucose-sensitive hydrogel particles behave as smart drug carriers for self-regulated DDSs in which insulin can be released in response to a blood glucose concentration.

Dynamically tunable microlens arrays were fabricated using stimuli-sensitive hydrogel particles with microscale sizes.[89–92] A label-free biosensing method for new protein-detection technology was developed by using biomolecule-sensitive hydrogel particles as tunable microlenses in a simple bright field optical microscopy technique. After microgels were synthesized by free-radical precipitation polymerization of NIPAAm and acrylic acid and functionalized with biotin, hydrogel microlenses were prepared by coulombic assembly of the biotinylated microgels onto a substrate. The bright field optical microscopy technique revealed that the optical properties of the biotinylated hydrogel microlenses changed as a function of the avidin and antibiotin concentrations. The avidin- and antibiotin-sensitive optical changes of the biotinylated hydrogel microlenses were caused by changes in the cross-linking density based on complex formation between avidin and biotin. Thus, unique optical properties of biomolecule-sensitive hydrogel microlenses provide useful tools to determine the presence of target biomolecules by monitoring their focal length.

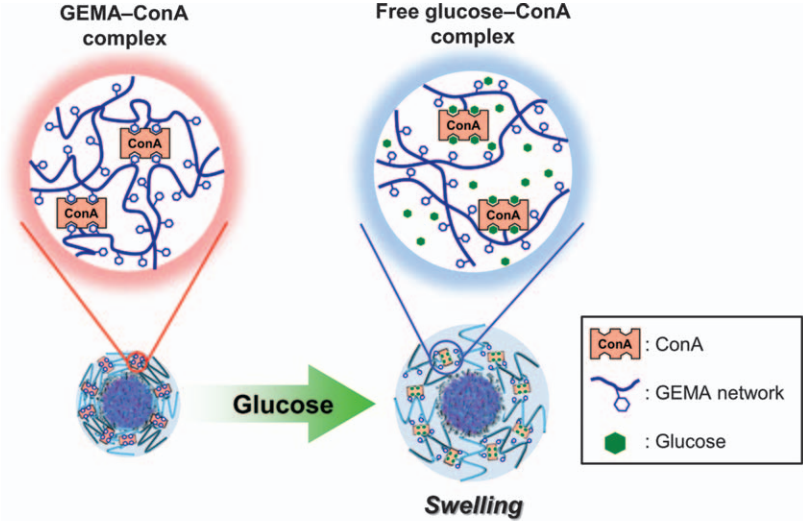

Figure 22.15 Glucose-sensitive behavior of GEMA–ConA hydrogel particles. Reprinted, with permission, from Ref. 88. Copyright 2012 Elsevier.

22.7 Other Biomolecule-sensitive Hydrogels

Based on the strategy that uses biomolecular complexes as dynamic cross-links of hydrogel networks (described in Section 22.2), a variety of biomolecule-sensitive hydrogels that undergo structural changes in response to a target biomolecule has been reported. For example, complementary molecular recognition abilities of DNAs provided useful tools for developing DNA-sensitive sol-gel transition systems.[93] Trapping and release of fluorescent semiconductor quantum dots (QDs) were achieved using DNA-sensitive hydrogels that underwent sol-gel transition in response to a target DNA.[94] Molecularly engineered target-sensitive hydrogels were formed by hybridization between a DNA aptamer as cross-linker, and linear PAAm chains with its complementary DNA (Figure 22.16).[95] The addition of adenosine, which was a target molecule of the DNA aptamer, induced the dissolution of the hydrogels, because the duplexes between the aptamer and the complementary DNA dissociated by competitive binding of the target to the aptamer. DNA aptamer-cross-linked hydrogel with entrapped gold nanoparticles was dissolved upon addition of the target adenosine and released the gold nanoparticles into a buffer solution. Furthermore, a DNA-sensitive sol-gel transition system combined with a specific thrombin-binding aptamer, which forms a double-stacked G quadruplex with high affinity to α-thrombin, enabled the capture and release of thrombin.[96] Differing from sol-gel transition, DNA-sensitive hydrogels that undergo change in volume in response to DNA were also prepared using a stem-loop structured DNA as a cross-linker.[97,98] As competitive formation of double strands of a probe DNA with a target DNA caused conformational change of cross-linker DNA, the hydrogels swelled in response to the target DNA. Thus DNA-sensitive sol-gel transition and hydrogels provide promising and potentially convenient tools for controlled drug release and biomolecular detection.

Cell-sensitive sol-gel transition systems were also developed using gelation of multi-armed PEG having an adhesion receptor-binding motif (an adhesion ligand based on the RGD peptide) by the addition of bis-cysteine peptide cross-linker (Figure 22.17).[99,100] The cross-linker peptide sequence was sensitive to

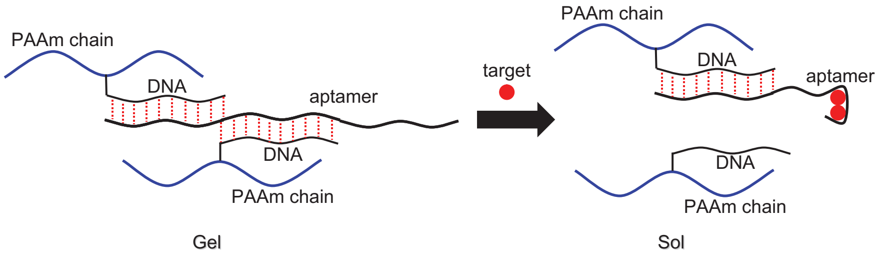

Figure 22.16 Scheme of the target molecule-sensitive sol-gel transition caused by hybridization of the DNA aptamer and DNA-PAAm conjugates.

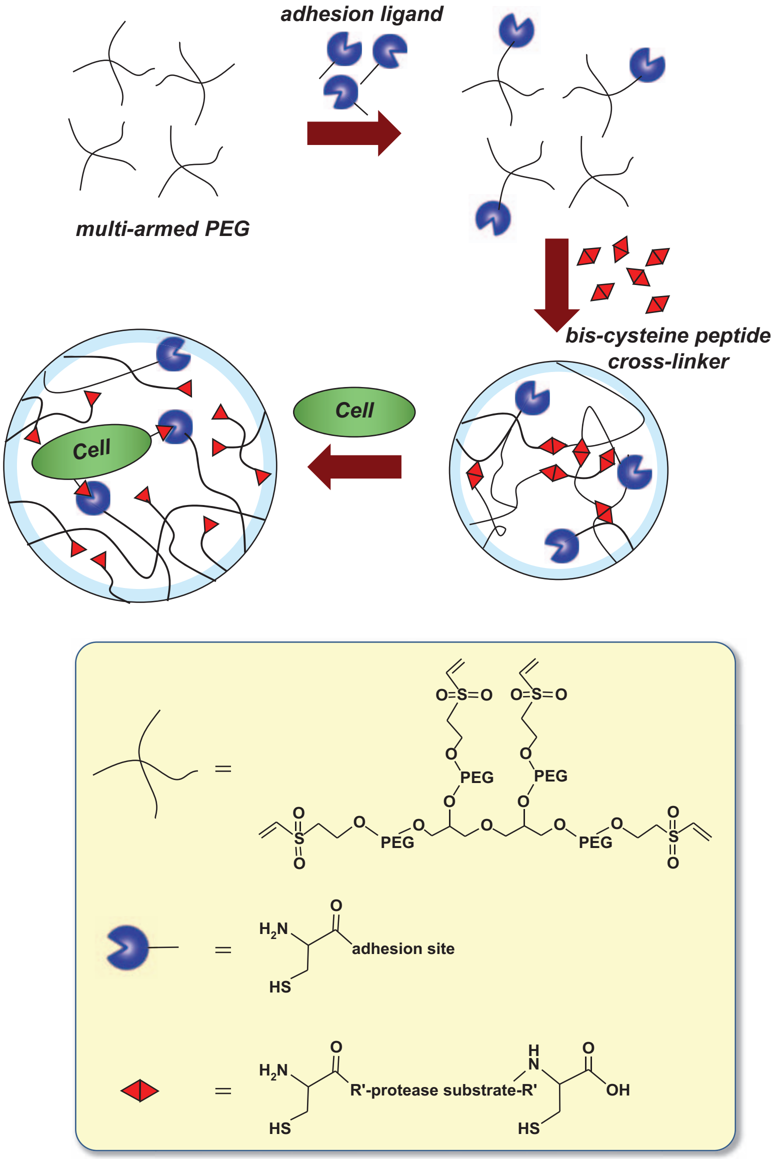
adhesion ligand
multi-armed PEG
bis-cysteine peptide cross-linker
Cell
Cell
=
O=S=O
O=S=O
PEG
PEG
PEG
PEG
=
H2N
adhesion site
HS
=
H2N
R'-protease substrate-R'
H
N
OH
HS
HS

Figure 22.17 Cell-sensitive sol-gel transition systems obtained by gelation of multi-armed PEG with an adhesion receptor-binding motif and cross-linking with a bis-cysteine peptide.

matrix metalloproteinases (MMPs), which belong to a family of proteases extensively involved in tissue development and remodeling. Vinyl sulfone-functionalized multi-armed PEGs formed hydrogels by the Michael-type addition reaction with mono-cysteine adhesion or bis-cysteine MMP substrate peptides. The resultant hydrogels, which are sensitive to local proteases such as MMP at the cell surface, were proteolytically invaded by primary human fibroblasts. The MMP-sensitive hydrogels are very useful in delivering recombinant human bone morphogenetic protein-2 to the site of critical defect in rat cranium, because bone regeneration depends on the proteolytic invasion into the hydrogels. Therefore, such cell-sensitive hydrogels have many potential applications in regenerative medicine and tissue engineering.

Non-covalently cross-linked hydrogels were obtained by complex formation between a low-molecular-weight heparin-modified polyethylene glycol star polymer (PEG-LMWH) and a dimeric heparin-binding growth factor (VEGF), which acted as dynamic cross-linkers (Figure 22.18).[101] The PEG-LMWH/VEGF hydrogels eroded in the presence of VEGF receptors because of the selective removal of VEGF acting as a cross-linker. The receptor-mediated erosion of the PEG-LMWH/VEGF hydrogels enabled the VEGF release in response to cell surface receptors. Thus, the PEG-LMWH/VEGF hydrogels are cell receptor-sensitive, and could be utilized as smart biomaterials for selective release of growth factors in vascular therapy.

To design stimuli-sensitive hydrogels showing programmable structural changes, some researchers have focused on conformational changes of proteins in response to a given stimulus. For example, well-defined folding motifs of proteins were bioconjugated with synthetic polymers, for preparing stimuli-sensitive hydrogels that undergo changes in volume or sol-gel transitions in response to pH and temperature.[102,103] Similarly, biomolecule-sensitive bioconjugated hydrogels were produced using a conformational change of genetically engineered proteins. Protein calmodulin (CaM), which is a calcium-binding protein that modifies its conformation from extended in the presence of Ca^{2+} to collapsed upon the binding of phenotiazine as a ligand, was used as cross-linker of hybrid hydrogels.[104] These hydrogels were composed of PAAm networks with non-covalent bonds between CaM and phenotiazine as cross-linking points. Since the binding between CaM and phenotiazine is strongly influenced by Ca^{2+}, the addition of Ca^{2+} chelator induced the swelling of the

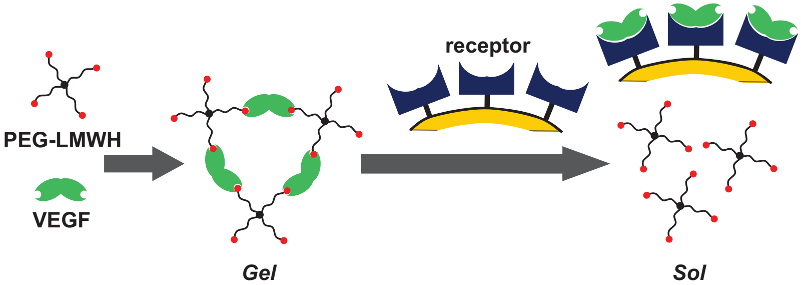

Figure 22.18 Scheme of hydrogel formation by cross-linking of a heparin-modified star polymer by means of heparin-binding growth factors dimeric complexes, followed by receptor-mediated erosion.

hydrogels because of the dissociation of the non-covalent bonds. The hybrid hydrogels regulated the transport of small molecules in response to Ca^{2+} and controlled the flow from a reservoir in micro fluidics. In addition, chemically tunable hydrogel lenses were prepared from PAAm hydrogel microlens arrays based on the non-covalent bonds between CaM and phenotiazine as dynamic cross-linkers.[105]

Finally, PAAm conjugated with genetically engineered bacterial gyrase subunit B (GyrB) was prepared for achieving trigger-inducible release of human vascular endothelial growth factor.[106] The GyrB-bioconjugated PAAm formed a hydrogel by its dimerization with the aminocoumarin antibiotic coumermycin, but the hydrogel dissociated by the addition of clinically validated novobiocin (albamycin), which triggered the release of human vascular endothelial growth factor (VEGF). Thus, a wide variety of biomolecule-sensitive hydrogels that undergo volume changes or sol-gel transitions in response to a target biomolecule can be prepared on the basis of a novel strategy using biomolecular complexes as dynamic cross-linkers of hydrogel networks.

22.8 Conclusion

This chapter focuses on biomolecule-sensitive hydrogels that undergo structural changes such as swelling/shrinking and sol-gel transitions in response to specific biomolecules. More than ten years ago, there were very few reports on biomolecule-sensitive hydrogels, most researchers focusing on pH- and temperature-sensitive networks and on only glucose-sensitive networks as biomolecule-sensitive hydrogels. However, the unique properties of biomolecule-sensitive systems can provide useful tools for designing smart biomaterials with various biomedical uses. Major advances in synthesizing biomolecule-sensitive hydrogels possessing both biomolecular recognition abilities and unique responsive functions have been made in the past ten years. Even though most biomolecule-sensitive hydrogels still require further research work for possible applications, they are likely to become quite important biomaterials in the future.

References

1. N. A. Peppas, *Hydrogels in Medicine and Pharmacy*, CRC Press, Boca Raton, 1987.
2. D. DeRossi, K. Kajiwara, Y. Osada and A. Yamauchi, *Polymer Gels, Fundamentals and Biomedical Applications*, Plenum, New York, 1991.
3. T. Miyata, in *Supramolecular Design for Biological Applications*, ed. N. Yui, CRC Press, Boca Raton, 2002, p. 95.
4. K. Dusek, *Responsive Gels: Volume Transitions I*, Springer, Berlin, 1993.
5. K. Dusek, *Responsive Gels: Volume Transitions II*, Springer, Berlin, 1993.
6. T. Okano, *Biorelated Polymers and Gels*, Academic Press, Boston, 1998.
7. T. Miyata, in *Supramolecular Design for Biological Applications*, ed. N. Yui, CRC Press, Boca Raton, 2002, p. 191.

8. R. A. Siegel, *Adv. Polym. Sci.*, 1993, **109**, 233.
9. L. Brannon-Peppas and N. A. Peppas, *J. Control. Release*, 1989, **8**, 267.
10. C. S. Brazel and N. A. Peppas, *Macromolecules*, 1995, **28**, 8016.
11. L. C. Dong and A. S. Hoffman, *J. Control. Release*, 1991, **15**, 141.
12. T. Miyata, K. Nakamae, A. S. Hoffman and Y. Kanzaki, *Macromol. Chem. Phys.*, 1994, **195**, 1111.
13. K. Nakamae, T. Nizuka, T. Miyata, M. Furukawa, T. Nishino, K. Kato, T. Inoue, A. S. Hoffman and Y. Kanzaki, *J. Biomater. Sci. Polym. Ed.*, 1997, **9**, 43.
14. A. S. Hoffman, *J. Control. Release*, 1987, **6**, 297.
15. T. Okano, *Adv. Polym. Sci.*, 1993, **110**, 179.
16. L. C. Dong and A. S. Hoffman, *J. Control. Release*, 1990, **13**, 21.
17. T. Okano, Y. H. Bae, H. Jacobs and S. W. Kim, *J. Control. Release*, 1990, **11**, 255.
18. H. Katono, A. Maruyama, K. Sanui, N. Ogata, T. Okano and Y. Sakurai, *J. Control. Release*, 1991, **16**, 215.
19. T. Miyata, T. Uragami and K. Nakamae, *Adv. Drug Deliver. Rev.*, 2002, **54**, 79.
20. T. Miyata and T. Uragami, in *Polymeric Biomaterials*, 2nd Ed., ed. S. Dumitriu, Marcel Dekker, New York, 2002, p. 959.
21. T. Miyata, in *Biomedical Applications of Hydrogels Handbook*, ed. R. M. Ottenbrite, K. Park and T. Okano, Springer, New York, 2010, p. 65.
22. T. Miyata, *Polym. J.*, 2010, **42**, 277.
23. K. Ishihara, M. Kobayashi, N. Ishimaru and I. Shinohara, *Polym. J.*, 1984, **16**, 625.
24. K. Ishihara and K. Matsui, *J. Polym. Sci. Polym. Lett. Ed*, 1986, **24**, 413.
25. G. Albin, T. A. Horbett and B. D. Ratner, *J. Control. Release*, 1985, **2**, 153.
26. G. W. Albin, T. A. Horbett, S. R. Miller and N. L. Ricker, *J. Control. Release*, 1987, **6**, 267.
27. S. Cartier, T. A. Horbett and B. D. Ratner, *J. Membr. Sci*, 1995, **106**, 17.
28. C. M. Hassan, F. J. Doyle III and N. A. Peppas, *Macromolecules*, 1997, **30**, 6166.
29. R. S. Parker, F. J. Doyle III and N. A. Peppas, *IEEE Trans. Biomed. Eng.*, 1999, **46**, 148.
30. K. Kataoka, H. Miyazaki, T. Okano and Y. Sakurai, *Macromolecules*, 1994, **27**, 1061.
31. D. Shiino, Y. Murata, A. Kubo, Y. J. Kim, K. Kataoka, Y. Koyama, A. Kikuchi, M. Yokoyama, Y. Sakurai and T. Okano, *J. Control. Release*, 1995, **37**, 269.
32. K. Kataoka, H. Miyazaki, M. Bunya, T. Okano and Y. Sakurai, *J. Am. Chem. Soc.*, 1998, **120**, 12694.
33. A. Matsumoto, T. Kurata, D. Shiino and K. Kataoka, *Macromolecules*, 2004, **37**, 1502.
34. A. Matsumoto, R. Yoshida and K. Kataoka, *Biomacromolecules*, 2004, **5**, 1038.

35. A. Matsumoto, K. Yamamoto, R. Yoshida, K. Kataoka, T. Aoyagi and Y. Miyahara, *Chem. Comm.*, 2010, **46**, 2203.
36. A. Matsumoto, N. Sato, T. Sakata, R. Yoshida, K. Kataoka and Y. Miyahara, *Adv. Mater.*, 2009, **43**, 4372.
37. M. Brownlee and A. Cerami, *Science*, 1979, **206**, 1190.
38. L. A. Seminoff, G. B. Olsen and S. W. Kim, *In. J. Pharm.*, 1989, **54**, 241.
39. S. W. Kim, C. M. Pai, K. Makino, L. A. Seminoff, D. L. Holmberg, J. M. Gleeson, D. E. Wilson and E. J. Mack, *J. Control. Release*, 1990, **11**, 193.
40. K. Makino, E. J. Mack, T. Okano and S. W. Kim, *J. Control. Release*, 1990, **12**, 235.
41. E. Kokufuta, Y. Q. Zhang and T. Tanaka, *Nature*, 1991, **351**, 302.
42. T. Miyata and K. Nakamae, *Trend. Polym. Sci.*, 1997, **5**, 198.
43. K. Nakamae, T. Miyata, A. Jikihara and A. S. Hoffman, *J. Biomater. Sci. Polym. Ed.*, 1994, **6**, 79.
44. T. Miyata, A. Jikihara, K. Nakamae and A. S. Hoffman, *Macromol. Chem. Phys.*, 1996, **197**, 1135.
45. T. Miyata, A. Jikihara, K. Nakamae and A. S. Hoffman, *J. Biomaterials Sci. Polym. Ed.*, 2004, **15**, 1085.
46. S. J. Lee and K. Park, *J. Mol. Recognit.*, 1996, **9**, 549.
47. A. A. Obaidat and K. Park, *Pharm. Res.*, 1996, **13**, 989.
48. A. A. Obaidat and K. Park, *Biomaterials*, 1997, **18**, 801.
49. R. V. Ulijn, *J. Mater. Chem.*, 2006, **16**, 2217.
50. M. Saffran, G. S. Kumar, C. Savariar, J. C. Burnham, F. Williams and D. C. Neckers, *Science*, 1986, **233**, 1081.
51. P. Y. Yeh, P. Kopeckova and J. Kopecek, *J. Polym. Sci. Pol. Chem.*, 1994, **32**, 1627.
52. P. Y. Yeh, P. Kopeckova and J. Kopecek, *Macromol. Chem. Phys.*, 1995, **196**, 2183.
53. H. Ghandehari, P. Kopeckova, P. Y. Yeh and J. Kopecek, *Macromol. Chem. Phys.*, 1996, **197**, 965.
54. H. Ghandehari, P. Kopeckova and J. Kopecek, *Biomaterials*, 1997, **18**, 861.
55. E. O. Akala, P. Kopeckova and J. Kopecek, *Biomaterials*, 1998, **19**, 1037.
56. L. Hovgaard and H. Brøndsted, *J. Control. Release*, 1995, **36**, 159.
57. K. N. Plunkett, K. L. Berkowski and J. S. Moore, *Biomacromolecules*, 2005, **6**, 632.
58. C. Li, J. Madsen, S. P. Armes and A. L. Lewis, *Angew. Chem. Int. Ed.*, 2006, **45**, 3510.
59. N. Yamamoto, M. Kurisawa and N. Yui, *Macromol. Rapid Commun.*, 1996, **17**, 313.
60. M. Kurisawa and N. Yui, *J. Control. Release*, 1998, **54**, 191.
61. M. Kurisawa, Y. Matsuo and N. Yui, *Macromol. Chem. Phys.*, 1998, **199**, 705.
62. K. M. Huh, J. Hashi, T. Ooya and N. Yui, *Macromol. Chem. Phys.*, 2000, **201**, 613.

63. J. J. Sperinde and L. G. Griffith, *Macromolecules*, 1997, **30**, 5255.
64. B. H. Hu and P. B. Messersmith, *J. Am. Chem. Soc.*, 2003, **125**, 14298.
65. P. D. Thornton, G. McConnell and R. V. Ulijn, *Chem. Commun.*, 2005, **47**, 5913.
66. P. D. Thornton, R. J. Mart and R. V. Ulijn, *Adv. Mater.*, 2007, **19**, 1252.
67. T. Miyata, N. Asami and T. Uragami, *Nature*, 1999, **399**, 766.
68. T. Miyata, N. Asami and T. Uragami, *Macromolecules*, 1999, **32**, 2082.
69. T. Miyata, N. Asami and T. Uragami, *J. Polym. Sci. Pol. Phys.*, 2009, **47**, 2144.
70. T. Miyata, N. Asami, K. Okawa and T. Uragami, *Polym. Adv. Tech.*, 2006, **17**, 794.
71. T. Miyata, N. Asami, Y. Okita and T. Uragami, *Polym. J.*, 2010, **42**, 834.
72. Z. R. Lu, P. Kopeckova and J. Kopecek, *Macromol. Biosci.*, 2003, **3**, 296.
73. G. Wulff, A. Sarhan and K. Zabrocki, *Tetrahedron Lett.*, 1973, **44**, 4329.
74. B. Sellergren, M. Lepisto and K. Mosbach, *J. Am. Chem. Soc.*, 1988, **110**, 5853.
75. K. Mosbach, *Trends Biochem. Sci.*, 1994, **19**, 9.
76. K. Shea, *Trends Polym. Sci.*, 1994, **2**, 166.
77. G. Wulff, *Angew. Chem. Int. Ed.*, 1995, **34**, 1812.
78. M. Byrne, K. Park and N. A. Peppas, *Adv. Drug Deliver. Rev.*, 2002, **54**, 149.
79. N. M. Bergmann and N. A. Peppas, *Prog. Polym. Sci.*, 2008, **33**, 271.
80. C. Alvarez-Lorenzo and A. Concheiro, in *Biotechnology Annual Review Vol. 12*, ed. M. R. El-Gewely, Elsevier, Amsterdam, 2006, p. 225.
81. M. Watanabe, T. Akahoshi, Y. Tabata and D. Nakayama, *J. Am. Chem. Soc.*, 1998, **120**, 5577.
82. G. Q. Wang, K. Kuroda, T. Enoki, A. Grosberg, S. Masamune, T. Oya, Y. Takeoka and T. Tanaka, *P. Natl. Acad. Sci. USA*, 2000, **97**, 9861.
83. T. Oya, T. Enoki, A. Y. Grosberg, S. Masamune, T. Sakiyama, Y. Takeoka, K. Tanaka, G. Q. Wang, Y. Yilmaz, M. S. Feld, R. Dasari and T. Tanaka, *Science*, 1999, **286**, 1543.
84. T. Miyata, M. Jige, T. Nakaminami and T. Uragami, *P. Natl. Acad. Sci. USA*, 2006, **103**, 1190.
85. T. Miyata, T. Hayashi, Y. Kuriu and T. Uragami, *J. Mol. Recognit.*, 2012, **25**, 336.
86. H. Kawaguchi, *Prog. Polym. Sci.*, 2000, **25**, 1171.
87. Y. Xia, B. Gates, Y. Yin and Y. Lu, *Adv. Mater.*, 2000, **12**, 693.
88. A. Kawamura, Y. Hata, T. Miyata and T. Uragami, *Colloid Surface B*, 2012, **99**, 74.
89. S. Nayak and L. A. Lyon, *Angew. Chem. Int. Ed.*, 2005, **44**, 7686.
90. J. Kim, S. Nayak and L. A. Lyon, *J. Am. Chem. Soc.*, 2005, **127**, 9588.
91. J. Kim, N. Singh and L. A. Lyon, *Angew. Chem. Int. Ed.*, 2006, **45**, 1446.
92. J. Kim, N. Singh and L. A. Lyon, *Chem. Mater.*, 2007, **19**, 2527.
93. D. C. Lin, B. Yurke and N. A. Langrana, *J. Biomech. Eng.*, 2004, **126**, 104.
94. T. Liedl, H. Dietz, B. Yurke and F. Simmel, *Small*, 2007, **3**, 1688.

95. H. Yang, H. Liu, H. Kang and W. Tan, *J. Am. Chem. Soc.*, 2008, **130**, 6320.
96. B. Wei, I. Cheng, K. Q. Luo and Y. Mi, *Angew. Chem. Int. Ed.*, 2008, **47**, 331.
97. Y. Murakami and M. Maeda, *Macromolecules*, 2005, **38**, 1535.
98. Y. Murakami and M. Maeda, *Biomacromolecules*, 2005, **6**, 2927.
99. M. P. Lutolf, G. P. Raeber, A. H. Zisch, N. Tirelli and J. A. Hubbell, *Adv. Mater.*, 2003, **15**, 888.
100. M. P. Lutolf, J. L. Lauer-Fields, H. G. Schmoekel, A. T. Metters, F. E. Weber, G. B. Fields and J. A. Hubbell, *P. Natl Acad. Sci. USA*, 2003, **100**, 5413.
101. N. Yamaguchi, L. Zhang, B. S. Chae, C. S. Palla, E. M. Furst and K. L. Kiick, *J. Am. Chem. Soc.*, 2007, **129**, 3040.
102. W. A. Petka, J. L. Harden, K. P. McGrath, D. Wirtz and D. A. Tirrell, *Science*, 1998, **281**, 389.
103. C. Wang, R. J. Stewart and J. Kopecek, *Nature*, 1999, **397**, 417.
104. J. D. Ehrick, S. K. Deo, T. W. Browning, L. G. Bachas, M. J. Madou and S. Daunert, *Nat. Mater.*, 2005, **4**, 298.
105. J. D. Ehrick, S. Stokes, S. Bachas-Daunert, E. A. Moschou, S. K. Deo, L. G. Bachas and S. Daunert, *Adv. Mater.*, 2007, **19**, 4024.
106. M. Ehrbar, R. Schoenmakers, E. H. Christen, M. Fussenegger and W. Weber, *Nat. Mater.*, 2008, **7**, 800.

CHAPTER 23

Intelligent Surfaces for Cell and Tissue Delivery

HIRONOBU TAKAHASHI AND TERUO OKANO*

Institute of Advanced Biomedical Engineering and Science, Tokyo Women's Medical University (TWIns), 8-1 Kawada-cho, Shinjuku-ku,
Tokyo 162-8666, Japan
*Email: tokano@abmes.twmu.ac.jp

23.1 Introduction

Cell/tissue-based therapies now promise to provide cures for a multitude of diseases and disorders. To obtain sufficient therapeutic effects, transplanted cell populations need to survive and function appropriately in the transplanted site. Although cells are conventionally delivered by direct injection of cells suspended in an appropriate medium into the target site in the body, this method has the drawback of poor cell retention and survival at the target site. One of the major challenges in cell/tissue-based therapy is, therefore, the development of a suitable system to deliver viable cells to the injured site. The number of cells that can communicate with the host cellular and extra-cellular matrix (ECM) components is critically dependent on the design of cell/tissue carriers and the method to deliver them to target sites. From this viewpoint, cell transplantation systems are traditionally designed using a variety of polymeric materials, in terms of providing appropriate physical (*e.g.* strength) and chemical (*e.g.* degradation rate) properties.[1] For example, polymeric membranes are used for encapsulating cells and can successfully prevent immune rejection in the body. As a result, the delivered cells show high therapeutic effects for a long term. In particular, microencapsulated

---

RSC Smart Materials No. 3
Smart Materials for Drug Delivery: Volume 2
Edited by Carmen Alvarez-Lorenzo and Angel Concheiro
© The Royal Society of Chemistry 2013
Published by the Royal Society of Chemistry, www.rsc.org

pancreatic islets are being widely evaluated for reducing diabetic complications.

The progress in tissue engineering is changing the role of polymeric materials in cell transplantation. Fabrication of scaffolds using biodegradable polymers is now a key technology for cell/tissue delivery systems. To date, various kinds of natural and synthetic polymeric materials have been shown to provide cells with an adequate environment for their adhesion, proliferation and differentiation into a specific cell phenotype.[2] Current technology enables the three-dimensional (3D) organization and arrangement of cells *in vitro* for preparing artificial 3D tissues, which can be delivered to target sites *in vivo*. Whereas a variety of naturally derived ECM molecules (*e.g.* type I collagen and fibrin) and biocompatible synthetic polymers (*e.g.* poly(lactic-co-glycolic acid), PLGA) are currently employed,[3] the thermo-responsive polymer poly(*N*-isopropylacrylamide) (PNIPAAm) is uniquely used for scaffold-free cell/tissue delivery. This intelligent polymer is grafted at a nanoscale thickness on cell culture surfaces, which allows cultured cells to be released without enzymatic treatments. Based on this thermally induced cell detachment, confluently cultured cells are harvested and delivered as a tissue-like cell monolayer ‘‘cell sheet’’ to damaged sites with intact associated ECM. This unique technology provides a scaffold-free cell/tissue delivery and opens up a new field in regenerative medicine.

23.2 Overview of Polymeric Materials for Cell/Tissue Delivery

23.2.1 Self-regulating Insulin Delivery System as a Substitute for Cell Transplantation

Organ supply suffers from a shortage of donations, and solid organ transplantation often requires life-long immunosuppression, which increases the risks of getting infections and cancer, and may lead to damage of other organs. To overcome these issues, chemically regulated drug release systems have been developed as organ substitutes. A number of biocompatible polymers have been investigated for drug delivery, particularly for diabetic treatment.[4,5] To avoid daily insulin injections, intelligent insulin release systems able to closely simulate the normal body response to blood glucose concentration have been devised. For example, glucose oxidase-immobilized hydrogels consisting of *N*,*N*-dimethylaminoethylmethacrylate (DMA) and hydroxyethylmethacrylate (HEMA) are able to release insulin through a pH-sensitive mechanism.[6,7] Glucose is converted to gluconic acid in the hydrogel, leading to a decrease in the pH and thereby causing the gel to swell. Kim *et al.*[8] have reported that insulin release can be regulated by competition between glucose and synthetic glycosylated insulin (G-insulin) for the binding to the concanavalin A (Con A) present in the polymeric membrane. As glucose concentration increases, the G-insulin bound to Con A in the membrane is released through an exchange mechanism as glucose permeates the membrane. To date, various kinds of system using HEMA, Nucleopore® poly(carbonate) membrane or Durapore® poly(vinylidene difluoride) (PVDF) membrane have been developed. However, these insulin-release systems have barely reached patients for treating their diabetes. Consequently, diabetic patients still need the multiple daily injections using insulin delivery devices (*e.g.* insulin pen). To improve patients' quality of life, insulin pumps that can deliver the hormone constantly have been developed.[9,10] Although these smart devices have many advantages for the clinical management of diabetes, some severe problems still remain (*e.g.* diabetic ketoacidosis caused by accidentally stopping insulin infusion).

23.2.2 Microencapsulation of Cells with Polymeric Membranes for Cell Delivery

Biocompatible membranes also allow cells themselves to be delivered into the body without host immune rejection, enabling the preparation of hybrid artificial organs containing xenogeneic cells. To deliver cells into the body without severe host responses, they are encapsulated with biocompatible polymers and isolated from the immune system.[11–13] At present, biohybrid artificial pancreas composed of living cells and synthetic and/or natural polymeric materials, is one of the most promising approaches to supply solid pancreas to the body. Sun's group and others have reported that the pancreas can provide normal blood glucose control and, thus, potentially prevent or reduce diabetic complications.[11,14–16] In particular, alginate-poly(L-lysine)-alginate membrane showed high capability of islet isolation and long-term insulin-secretion (Figure 23.1).[14,17] However, anions in the body often induce the destruction of alginate-based microcapsules after the transplantation and

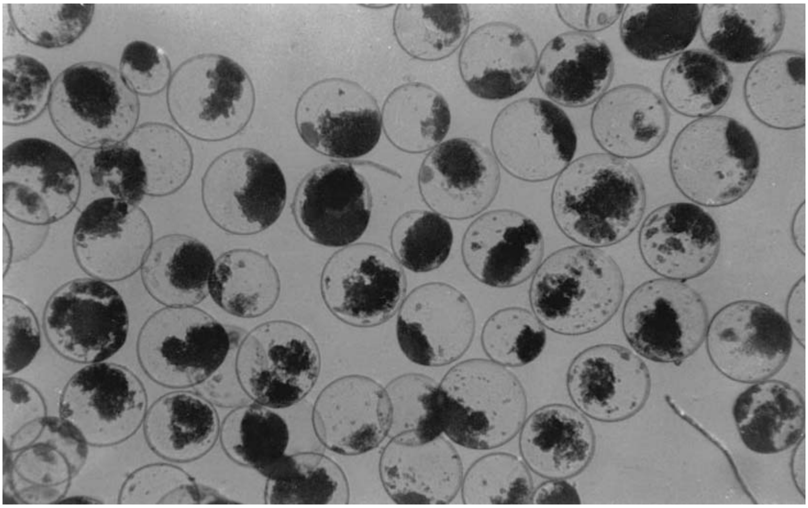

Figure 23.1 Microscopic photograph of porcine islets microencapsulated in alginate-poly(L-lysine)-alginate membranes.
Reprinted with permission from Ref. 16.

therefore coating with a cationic polymer such as poly(L-lysine) is usually mandatory. The immunoisolated insulin-secreting cells (*e.g.* INS-1) releasing insulin for one month in an *in-vitro* experiment are transplantable to diabetic mice, rats and monkeys for insulin treatment.[15,16]

Although the transplantation of rat pheochromocytoma cell line (PC12) has also shown a therapeutic potential in animal models of Parkinson's disease, the number of survival cells dramatically decreases by immunosuppression in the host. For example, PC12 cells encapsulated in hydroxyethyl methacrylate-methyl methacrylate (HEMA-MMA) copolymer successfully secrete dopamine in rodent models.[12,18] Tresco and coworkers have reported that polyacrylonitrile/polyvinyl chloride (PAN/PVC) can be used for encapsulating PC12 cells.[19,20] Recently, hepatocytes have been encapsulated in PEG-based hydrogels to prevent immune response in the body.[21] The artificial liver implanted in "humanized" mice exhibited liver-specific functions such as sustained albumin secretion and urea synthesis.

23.2.3 Scaffold-based Cell/Tissue Delivery in Tissue Engineering

Although clinically implantable biohybrid artificial organs, including pancreas and liver, have been developed, prevention of immune rejection by enclosure in the polymeric membrane barrier is still limited, due to the difficulty in the separation of insulin from antibodies because of the difference in the permeability of the polymeric membranes. Tissue engineering, first proposed in the 1980s by R. Langer and J. P. Vacanti, promises to overcome the problems in the field of artificial organs.[1,3,22,23] To deliver the cultured cells to patients, primary cells require supporting materials that provide specific environments for cell growth *in vitro* and allow them to be delivered while maintaining their structure. From this viewpoint, at present cells are often cultured together with a scaffold and a variety of substrates has been developed for scaffold-based cell delivery. For example, collagen, fibrin and alginate have been investigated as scaffolds to mimic the ECM of targeted tissue type.[24–26] However, the implantation of naturally derived polymers may trigger an immune rejection in the patients. Synthetic polymers, therefore, have been widely used for tissue construction.[3,27,28] Biodegradable polymers can be easily processed into many different structures for guiding the repair and restoration of functions of the damaged tissue. In particular, PLGA and its derivatives are commonly used for scaffold fabrication, because their physical properties and degradation kinetics can be designed on-demand.[29,30] The mechanical strength, 3D architecture and pore size are key factors to maintain cell activities, including cell proliferation and differentiation. To design various kinds of scaffolds according to each target site, several processing methods have been developed.[3,31] However, they still have limitations such as an insufficient cell migration into scaffold and an insufficient permeability to permit the ingress of cells and nutrients. In addition, inflammatory responses are often observed upon the biodegradation of the scaffolds. Furthermore, scaffolds need to occupy some space by themselves, though cell-dense tissue is necessary to be reconstructed depending on target tissues. The scaffold-free cell/tissue delivery systems, therefore, are pointed out as a new class of regenerative medicine approach that involves the use of intelligent thermo-responsive cell culture substrates.

23.3 The Intelligence of Thermo-responsive Polymers for Cell/Tissue Delivery

23.3.1 Thermo-responsive Poly(*N*-isopropylacrylamide)

In the fields of diagnostics, drug delivery and tissue engineering, stimuli-responsive polymers play important roles.[32–35] These materials exhibit changes in their physical properties, being triggered by a change in temperature or pH, light irradiation or exposure to an electric or magnetic field. Thermo-responsive PNIPAAm has been used as one of the most efficient components of thermally induced drug release systems,[36–38] thermally regulated separation systems and so on.[39–41] PNIPAAm exhibits thermo-responsiveness in aqueous media by changing its properties across its lower critical solution temperature (LCST) of 32 °C.[42–44] Specifically, it shows a hydrophilic character due to the hydration of polymer chain on surface below the LCST, while the polymer undergoes a phase transition and becomes hydrophobic, changing the chain conformation to be a compact globule, above the LCST. The concept of on-off switching system using this polymer[36,37] has been widely used, particularly for the design of controlled release systems for various kinds of drugs (*e.g.* hydrophobic small molecules, biopharmaceuticals).[45–48]

23.3.2 Thermo-responsive Encapsulation of Cells for Cell Delivery

Intelligent polymers enable the encapsulation of islets without triggering the host immune response. Polysaccharides, such as alginate and agarose, have often been employed as the ECM for the encapsulated cells, because they form gels under mild conditions. Although to achieve that, alginate and agarose require a previous chemical or high-temperature treatment, respectively. PNIPAAm can be used for islet encapsulation without any treatment for gel formation. Due to its LCST of 32 °C, islet/PNIPAAm mixed solution is injectable into the body at room temperature and it becomes a gel when it reaches body temperature.[49,50] In this biohybrid artificial pancreas, the polymer works as a simple physical barrier for preventing the contact among islets and, simultaneously, minimizes insulin diffusion. Specifically, islets isolated from Sprague-Dawley rat pancreas can be effectively entrapped in a poly(*N*-isopropylacrylamide-co-acrylic acid) (PNIPAAm-co-PAAc) copolymer matrix, which forms a gel at around 30–34 °C. The insulin secretion function of the entrapped islets was maintained for one month in an *in-vitro* experiment.[49,50] This thermo-responsive polymer is also used to encapsulate hepatocytes spheroids. As mentioned above, hepatocytes need ECM microenvironment to exhibit their specific activities in tissue-like 3D space. RGD-incorporated PNIPAAm-co-PAAc hydrogel effectively entraps hepatocytes as spheroids and prolongs *in-vitro* liver-specific functions.[51] The thermo-responsiveness of the polymer allows cells to be delivered and to maintain their functions *in vivo*.

23.4 Thermo-responsive Surface for Cell Sheet-based Tissue Delivery

23.4.1 Cell Sheet Engineering for Scaffold-free Cell/Tissue Delivery Systems

Over the past decade, a tissue-like cellular monolayer, called a "cell sheet", has been developed as the result of a new class of tissue reconstruction technology, designed as "cell sheet engineering".[52–55] In contrast to scaffold-based cell/tissue delivery, thermo-responsive surfaces allow us to produce cell-dense tissues and deliver them to desired sites in the body without the synthetic polymer. The objective of regenerative medicine is to provide cells with a local environment containing artificial ECM that promotes cells to proliferate efficiently. For this purpose, in scaffold-based tissue delivery, naturally derived materials are widely used because of their similarities to ECM. By contrast, the thermo-responsive surface is able to release a cell sheet with associated ECM only by reducing the temperature (Figure 23.2). In general, the cell-cell junction is damaged by enzymatic treatment when cultured cells are collected applying conventional techniques. As a unique feature, thermo-responsive surfaces enable cell sheets to be obtained without any complicated treatment, and the technique is now being applied for regenerative medicine.[56–58]

23.4.2 Thermo-responsive Polymer Grafting on Cell Culture Substrates

Nanoscale thin PNIPAAm grafted cell-culture substrates can fabricate cell sheets through thermo-responsive alternations of the surface properties across the LCST at 32 °C in an aqueous medium.[43,44,59] PNIPAAm can be grafted covalently to commercially available tissue culture polystyrene (TCPS) dishes

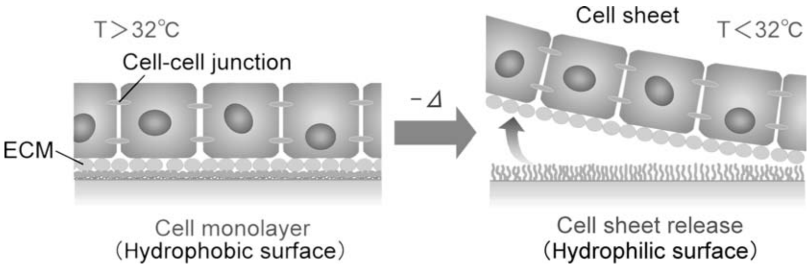

Figure 23.2 Schematic illustration of cell sheet release from a thermo-responsive polymer-grafted surface while maintaining the cell-cell junctions and the associated ECM, by reducing the temperature to below its LCST (32 °C).

by electron-beam (EB) irradiation of NIPAAm monomer solution in the dishes. The resultant thin PNIPAAm-gel coating provides hydrophilicity to the TCPS surface at below 32 °C, whereas the surface changes to more hydrophobic at above 32 °C as PNIPAAm dehydrates. Consequently, the surface allows cells to adhere and spread at normal cell culture temperature (37 °C), whereas it becomes more hydrophilic and exhibits a cell-repellent behavior when the temperature is decreased below PNIPAAm LCST (*e.g.* 20 °C). This responsiveness induces the spontaneous detachment of cells adhering on the PNIPAAm-grafted surface without any other treatment (*e.g.* enzymatic treatment).

To achieve effectively the thermally induced cell detachment, the grafted amount and thickness of PNIPAAm are key factors to obtain surfaces with the alternating behavior required for cell detachment.[59] Therefore, PNIPAAm grafting should be tuned to fit the individual cell type requirements. EB irradiation conditions have to be adjusted for obtaining an optimized polymer thickness. Recent studies demonstrate that surface-initiated living radical polymerization (LRP) can provide polymer-brush-type thermo-responsive surfaces.[60,61] Since LRP leads to molecular weight-controlled polymers even under mild conditions,[62–64] the thermo-responsive properties of surfaces covered with PNIPAAm brush are more precisely controllable. In addition, the resultant polymer brushes have received significant attention due to their unique physico-chemical properties (*e.g.* highly stretched and extended architectures, wetability and negligible protein adsorption).[41,60,64–66] Atom transfer radical polymerization (ATRP), which is widely used for densely polymer grafting, provides PNIPAAm brushes onto cell culture surfaces.[60] Reversible addition-fragmentation chain transfer (RAFT) polymerization has also been extensively studied for the last decade.[67–73] RAFT-mediated process involves a conventional free-radical polymerization of substituted monomers in the presence of a dithiobenzoate compound (so-called "RAFT agent") that acts as a chain transfer agent (CTA) (Figure 23.3). Since an equilibrium chain transfer reaction in a RAFT process gives well-defined polymers with a narrow polydispersity,[71] surface-initiated RAFT approaches achieve the fabrication of polymer brushes with a uniform chain length.[61] Adjusting both the chain length and the graft density of PNIPAAm, cell adhesion/detachment behavior is successfully controlled to harvest cell sheets according to cell types (Figure 23.4). At present, since graft architectures (*e.g.* cross-linked structure and polymer brush structure) greatly affect the thermo-responsive changes of hydrophilicity/hydrophobicity and expanded/globule conformation,[74] a variety of thermo-responsive surfaces can be developed and used effectively to obtain desired cell sheets according to circumstances.

23.4.3 Cell Sheet-based Tissue Delivery in Regenerative Medicine

Cell sheet-based tissue delivery systems have already been applied to humans in clinical studies for specific treatments, *e.g.* cornea reconstruction or esophageal recovery after ulceration caused by endoscopic submucosal dissection

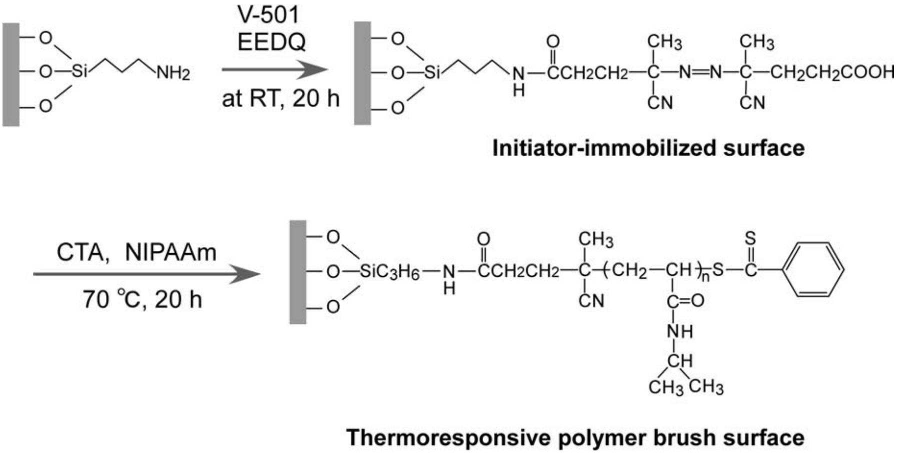
V-501
EEDQ
at RT, 20 h
Initiator-immobilized surface
CTA, NIPAAm
70 °C, 20 h
Thermoresponsive polymer brush surface

Figure 23.3 Schematic pathway of the grafting of a thermo-responsive polymer on a glass substrate *via* surface-initiated RAFT polymerization. First, an azo-initiator, V-501, is immobilized on the glass substrate using the condensing agent, EEDQ. *N*-isopropylacrylamide (NIPAAm) is then polymerized on the initiator-immobilized surface in the presence of a chain transfer agent (CTA).

(ESD).[56,57,75] Severe trauma or disease can cause the complete loss of corneal epithelial stem cells, resulting in corneal opacification and severe visual loss. Nishida *et al.*[56] have demonstrated that autologous mucosal epithelial cell sheets are transplantable simply by thermally induced release from a thermo-responsive surface and subsequent delivery by means of supporting PVDF membrane to patient corneal stroma, without the need of a scaffold. Since thermo-responsive surfaces allow cell sheets to be released with intact associated ECM, the transplanted cell sheets can adhere rapidly and stably onto the host corneal surface without suturing. Mucosal epithelial cell sheets are also transplanted successfully to ulcer wound bed after ESD (Figure 23.5).[57]

Skeletal myoblasts have been widely employed for clinical cell transplantation.[76–78] Sawa and coworkers have demonstrated that autologous skeletal myoblast sheets can be used as a new cell-delivery system for the treatment of dilated cardiomyopathy (DCM). Myoblasts transplantation has been investigated as a treatment measure for end-stage heart disease, because of its advantages including autologous origin, high obtainability, high proliferative potential *in vitro* and strong resistance to hypoxia followed by ischemia.[79,80] Direct injection methods have several limitations for efficient cell delivery in the treatment of DCM, due to cell loss caused by the leakage of injected cells from the myocardium. Myoblast cell sheets maintaining their inter-cellular communication junction can be transplanted to the damaged site, resulting in a significant decrease of the dilation of the left ventricle.[81–83] In addition to being a unique method to deliver to desired sites, the well-organized cellular microenvironment (*e.g.* cell-to-cell cross-talk) of the myoblast sheets potentially enhances the release of cytokines including stromal-derived factor-1

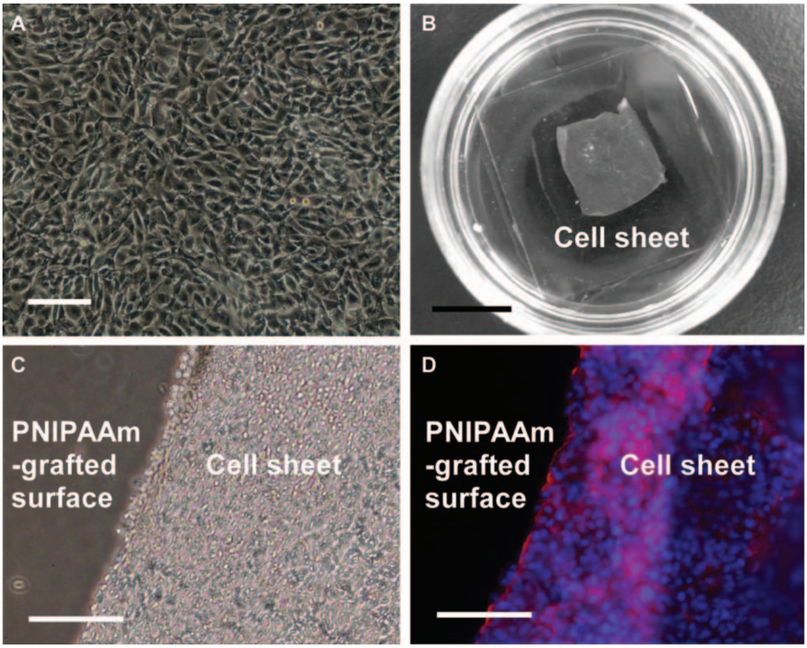

Figure 23.4 Thermally induced cell-sheet detachment from a thermo-responsive polymer-grafted surface. A confluent cell monolayer (A) is released from the surface solely by reducing culture temperature to 20 °C (B). The phase contrast (C) and fluorescence (D) microscopic photographs show that the associated ECM is also released with the cell sheet. Red and blue in (D) indicate fibronectin and cell nuclei, respectively. Scale bars: 100 μm in (A, C and D), 10 mm in (B).
Adapted with permission from Ref. 61. Copyright (2010) American Chemical Society.

(SDF-1), hepatocyte growth factor (HGF) and vascular endothelial growth factor (VEGF) from the transplanted cells (Figure 23.6).[84] Although conventional scaffold-based cell transplantation also enables cell delivery, it is unable to form the cell-dense microenvironment that is observed after the cell sheet transplantation, and its inflexible bulky properties are unable to follow the dynamic pulsation of cardiomyocytes. Recent studies demonstrate that the scaffold-free cell/tissue delivery systems are also suitable for delivering other cell types (*e.g.* cardiac stem cells, adipocytes) as sheets for the treatment of myocardial infarction in mice.[85–87] These strategies also have a potential to become a novel delivery system for myocardial treatment.

23.4.4 Local Drug Release Technique with Cell Sheet Transplantation

Based on the cell-sheet delivery technique, engineered cells and their secreting proteins are able to be delivered efficiently to target sites. Genetically

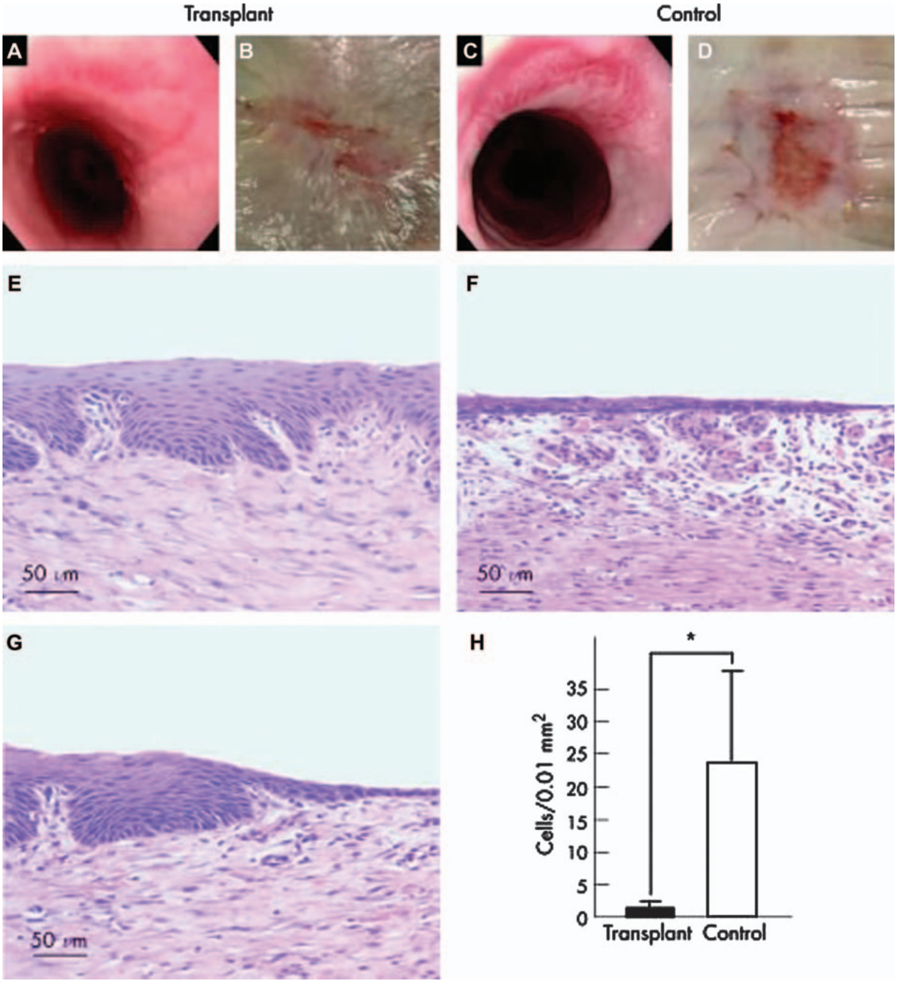

Figure 23.5 Transplantation of oral mucosal epithelial cell sheets, using a PVDF supporting membrane, to the surgical site of endoscopic submucosal dissection (ESD). Left and right photographs represent transplant and the control groups, respectively. Endoscopic (A, C) and macroscopic (B, D) photographs of the oesophageal sites 4 weeks after ESD. The hematoxylin and eosin (H&E) staining of the central portions of the surgical sites are depicted in E and F. H&E staining of the border region between the transplanted cell sheet and the outer portions of the ulcer site is shown in G. Comparison of the number of inflammatory cells appearing on the surgical sites between transplant and the control groups is depicted in H. $*p < 0.01$.

Reprinted from Ref. 57 with permission of the British Society of Gastroenterology (BSG) and the BMJ Group.

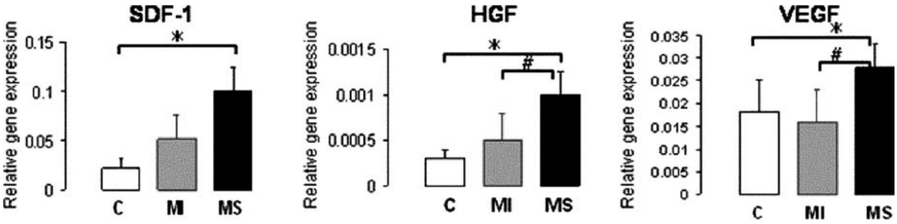

Figure 23.6 Relative levels of expression of stromal-derived factor 1 (SDF-1), hepatocyte growth factor (HGF) and vascular endothelial growth factor (VEGF) at the delivered site of myoblasts 1 week after myoblast implantation. The efficient delivery of myoblast in the form of sheets (MS group) that overlapped the scar area leads to a greater release of these cytokines, compared with that observed for control group (C) and myoblast injection (MI) group, and results suitable for repairing the infracted myocardial wall. $^{*}p<0.05$ *versus* the control group; $^{\#}p<0.05$ *versus* the MI group.

Reprinted from Ref. 84 with permission of The American Association for Thoracic Surgery and The Western Thoracic Surgical Association.

transfected cells can be transplanted as a cell sheet to a target site, and the therapeutic effects of specific proteins are successfully enhanced at the transplanted site.[88–91] This concept possibly becomes a novel gene therapy approach for the treatment of various kinds of diseases.[92,93] In general, compared with small-molecular weight pharmaceuticals, oligonucleotides (*e.g.* plasmid DNA (pDNA) and small-interfering RNA (siRNA)) and proteins still need well-organized strategies for their effective delivery to target sites. Cell sheet-based delivery systems enable efficient local release of growth factors secreted from transplanted cell sheets. As occurs with drug-eluting stents, the sustained release of pDNA or siRNA from implanted materials can dramatically increase transfection levels in target cells, resulting in efficient protein expression at the target sites.[94,95] Transplanted cell sheets that can maintain their proper cell functions on the target sites are also expected to produce and release locally therapeutic agents. For example, it has been shown that corneal epithelial cells can be transfected *ex vivo* using a retroviral vector, and then the genetically engineered cells are successfully transplanted as a cell sheet onto a target site.[88] As a result, specific biopharmaceuticals produced by the engineered cells can be delivered directly to the target site.

Skeletal myoblast sheet transplantation is now a promising strategy for treatment of myocardial infarction.[82,83] Although several studies have reported that the cell sheet-based therapy showed significant effects on the regenerating functions of damaged heart, myoblast sheets are still subject to the apoptosis-promoting environment of the infarct scar. For improving cell survival in transplanted cell sheet, anti-apoptotic gene is transduced into myoblasts *ex vivo*.[89,90] B-cell lymphoma 2 (Bcl-2), an apoptotic member of the Bcl-2 family of apoptosis-related proteins, regulates apoptosis, and their over-expression is expected to promote cell survival and inhibit cell death (Figure 23.7). Kitabayashi *et al.*[89] have reported that Bcl-2 expressing myoblast

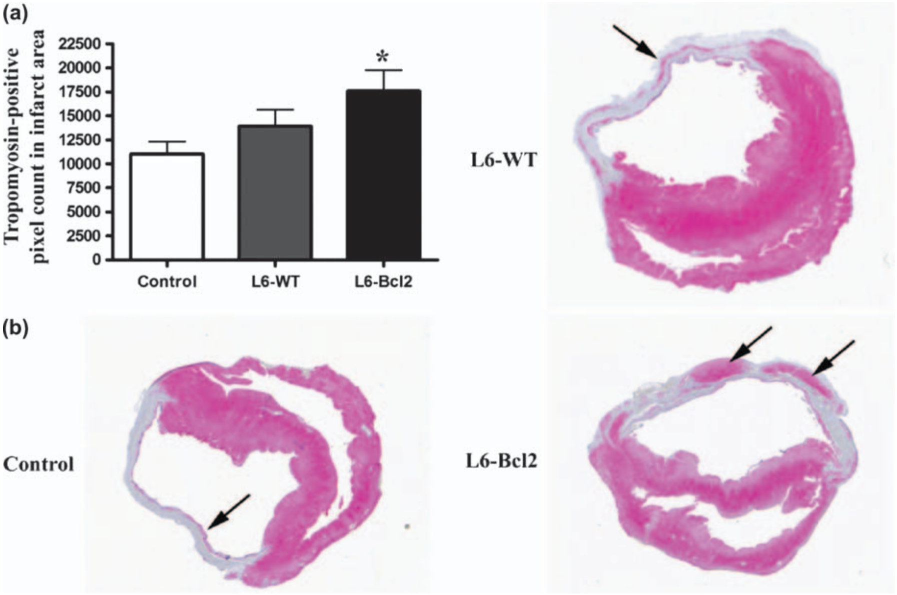

Figure 23.7 Local B-cell lymphoma 2 (Bcl-2) release from a myoblast sheet to improve the myocyte survival in an infarct area. The amounts of tropomyosin-positive cells within the infarct for the controls and animals treated with wild-type myoblast sheet (L6-WT) or transfected myoblast sheet with retroviral vector encoding Bcl-2 (L6-Bcl2) are depicted in (a); $*p < 0.05$ *versus* the control group. Images of infracted ventricular wall displaying tropomyosin-positive tissue (arrows) in the control, L6-WT and L6-Bcl2 groups are shown in (b). Sections are counterstained with hematoxylin.
Reprinted from Ref. 90 with permission of Mary Ann Liebert, Inc. Publishers.

sheets provide (i) protection against both nutrient deprivation and staurosporine-induced apoptosis, and (ii) enhanced production of pro-angiogenic mediators, vascular endothelial growth factor-A (VEGF-A) and placental growth factor (PlGF) at the target sites in a rat model of acute myocardial infarction. This *ex-vivo* transfection and the resultant local protein release enhance effectively myocardium regeneration through the cell sheet transplantation. In addition, HGF overexpression in genetically engineered myoblast sheets enhances their angiogenic potential and stimulates effectively angiogenesis in the infracted myocardium.[91]

23.4.5 Micro-fabricated Thermo-responsive Surfaces for Delivery of Tissue-mimicking Cell Sheets

23.4.5.1 Co-patterning for Creating Cellular Micro-environment

With the progress in cell sheet-based technology, various kinds of cell sheets have recently been applied to various damaged tissues and organs.[81,96–99]

Construction of large-scale complex tissues is challenging. Living tissues comprise multiple cell types wherein cell-to-cell interactions influence and maintain the development of characteristic physiological functions and activities. To mimic hepatocyte cellular interactions *in vitro*, various cell types are required to be organized harmonically. Bhatia *et al.*[100] fabricated a micropatterned surface for co-culturing different types of cells, and Tsuda *et al.*[101,102] have demonstrated that dually thermo-responsive polymers, PNIPAAm and poly(*n*-butyl methacrylate) (PBMA), can be patterned by EB-induced PBMA polymerization on PNIPAAm-grafted surfaces with photomasks (Figure 23.8). The patterned PBMA induces LCST of the thermo-responsive copolymer to decrease and gives cell-adhesive regions at 27 °C site-specifically on the surface, whereas the PNIPAAm homopolymer regions show cell-repellent ability at this temperature. The difference in the LCST causes the co-patterning of hepatocytes and endothelial cells on the thermo-responsive surface. The resultant co-patterns allow hepatocytes to maintain a favorable microenvironment; the synthesis of albumin and urea acting as the indicators of the hepatic function. Microcontact printing method is another technique to produce the co-patterns of hepatocyte and endothelial cells on thermo-responsive PNIPAAm surfaces.[103] Because these fabrication techniques are applied to thermo-responsive surfaces, the co-patterned cell sheets can be

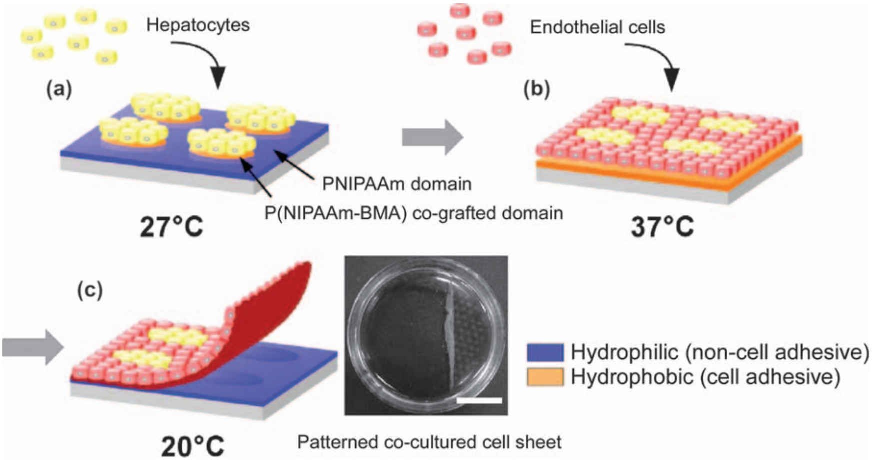
Hepatocytes
(a)
PNIPAAm domain
P(NIPAAm-BMA) co-grafted domain
27°C
Endothelial cells
(b)
37°C
(c)
20°C
Patterned co-cultured cell sheet
Hydrophilic (non-cell adhesive)
Hydrophobic (cell adhesive)

Figure 23.8 Schematic illustration of the co-patterning of hepatocytes and endothelial cells and the harvesting of the co-cultured cell sheet using a dually patterned thermo-responsive surface. Since the poly(*N*-butyl methacrylate) (PBMA) grafted site specifically decreases the LCST of poly(*N*-isopropylacrylamide-butyl methacrylate) copolymer P(NIPAAm-BMA), hepatocytes adhere only on the P(NIPAAm-BMA) co-grafted regions at 27 °C (a). At incubation at 37 °C, the second cell type, endothelial cells adhere on all regions, resulting in a co-patterned cell monolayer (b). The co-cultured cell sheet can be harvested by reducing temperature to 20 °C (c). Scale bar in the photograph: 1 cm. Reprinted from Ref. 102 with permission of Elsevier.

harvested only by reducing the temperature to 20 °C and allowed to become a highly functional tissue that is potentially deliverable to target sites.

23.4.5.2 Vascularization in Cell Sheets for Large-scale Tissue Construction

Cell sheets released from thermo-responsive surfaces are transplantable without any treatment such as suturing, because the associated ECM plays a role as glue on the transplanted site. This advantage also provides the possibility to construct 3D tissue.[53,104,105] For example, a gelatin-coated plunger is useful to manipulate cell sheets and layer them. After being incubated at 20 °C, a cell sheet can be transferred onto another cell sheet by a gelatin-gel plunger. The layered cell sheets stack each other, due to the presence of ECM glue. Importantly, this stacking process allows multiple cell sheets to contact each other physically and to communicate biologically.[105,106] For example, multi-layered cardiomyocyte sheets are found to communicate electrically, giving a synchronized constant beating in 3D myocardial tissue with millimeter-scale thickness. Whereas having a potential to construct large-scale tissues, multi-layered cell sheets need vascularization, which can supply oxygen sufficient for surviving in the 3D tissue long term.[107,108] The cell sheet manipulation technique produces not only multi-layered cell sheets but also vascular-like networks in multi-layered cell sheets. First, cell-repellent polyacrylamide (PAAm) is patterned photolithographically on PNIPAAm-grafted surface. Human umbilical vein endothelial cells (HUVECs) form stripe patterns on the micropatterned polymer surface, and then the patterned HUVECs are sandwiched between two normal human dermal fibroblast (NHDF) sheets, *via* cell sheet manipulation processes (Figure 23.9).[109] After five days' incubation, the patterned endothelial cells migrate on the fibroblast sheets and form self-organized vascular-like networks in the multi-layered fibroblast sheets, indicating that the networks potentially promote angiogenesis and connect with the host vasculature.

23.4.5.3 Control of Cell Orientation for Designing Anisotropy of Cell Sheets

Some parts of native tissues are observed to have well-organized cell/ECM orientations, rendering the tissue to be anisotropic, which has important functional consequences[110–119] (*e.g.* in skeletal muscle tissues and myocardial tissues). Therefore, the design of cell alignment is necessary to construct biomimetic tissues that have the natively organized orientation of cells and ECM proteins. Cell sheet-based tissue engineering has a potential to achieve 3D complex tissue reconstruction *via* the cell sheet layering technique. The use of cell sheets, therefore, allows one to design anisotropy three-dimensionally by controlling cell alignment in cell sheets.[120,121] Microgrooved polydimethylsiloxane (PDMS) substrates are widely used to control cell

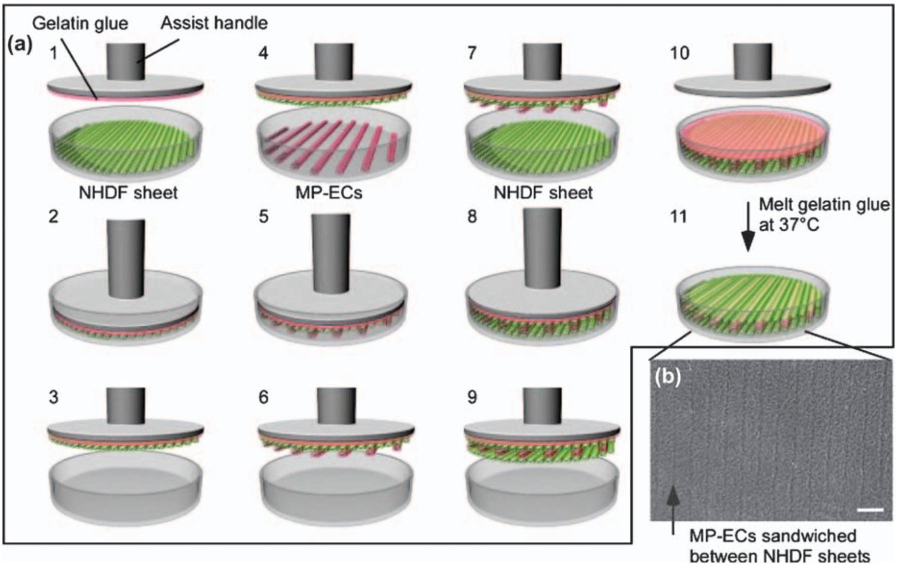

Figure 23.9 Scheme of the 3D manipulation of layered fibroblast cell sheets containing micro-patterned endothelial cells using a gelatin-coated stacking manipulator (a). Normal human dermal fibroblast (NHDF) sheet is taken by the manipulator from a non-patterned thermo-responsive surface after incubation for 20 min. at 20 °C (1–3), and then the cell sheet is transferred gently onto micro-patterned endothelial cells (MP-ECs) (4, 5). After incubating for 20 min. at 20 °C, the bilayer is placed onto another NHDF sheet in a similar manner (6–9). Multi-layered cell sheets adhere on a tissue culture polystyrene (TCPS), then the gelatin gel is melted and removed from the multi-layered cell sheets by incubating at 37 °C (10, 11). Phase contrast microscopic photograph of MP-ECs sandwiched between two NHDF sheets is shown in (b). Scale bar: 100 μm.
Reprinted from Ref. 109 with permission of Elsevier.

alignment,[122,123] and they are also applicable for preparing cell sheets with a well-controlled oriented structure.[124] On the other hand, RAFT-mediated polymerization is useful for grafting copolymer brushes on solid surfaces in order to fabricate physico-chemically patterned surfaces for designing cell alignment (Figure 23.10).[125] By being combined with the photolithography technique, hydrophilic poly(*N*-acryloylmorpholine) (PAcMo) was grafted site-specifically on PNIPAAm brush regions, resulting in block polymer, poly(*N*-isopropylacrylamide)-*b*-poly(*N*-acryloylmorpholine) (PNIPAAm-*b*-PAcMo) brush domains and PNIPAAm brush domains (50 μm/50 μm stripes). Due to the difference in cell-to-surface affinity on the micropatterned surfaces, NHDFs are automatically aligned in a parallel direction with the stripe patterns only by cell seeding. The aligned fibroblasts proliferate and reach confluency while maintaining the alignment (Figure 23.11). Whereas cell sheets are generally harvested by means of a two-dimensional shrinking and

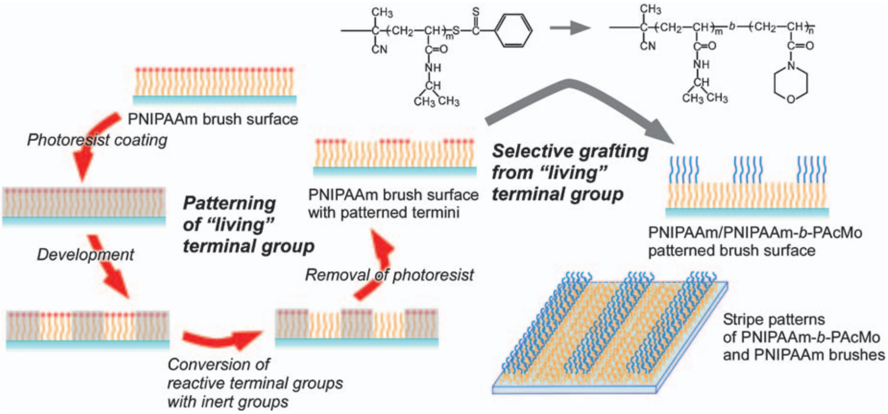
PNIPAAm brush surface
Photoresist coating
Development
Patterning of "living" terminal group
PNIPAAm brush surface with patterned termini
Removal of photoresist
Conversion of reactive terminal groups with inert groups
Selective grafting from "living" terminal group
PNIPAAm/PNIPAAm-b-PAcMo patterned brush surface
Stripe patterns of PNIPAAm-b-PAcMo and PNIPAAm brushes

Figure 23.10 Schematic representation of a photolithographically patterned thermo-responsive brush surface through the selective grafting of poly(*N*-acryloylmorpholine) (PAcMo) segments from poly(*N*-isopropylacrylamide) (PNIPAAm) blocks. The red termini indicate chain-transfer active groups. PAcMo segments, shown as the blue brushes, are grafted only on the red termini through a second-step RAFT polymerization.
Reprinted from Ref. 125. Copyright (2011) the American Chemical Society.

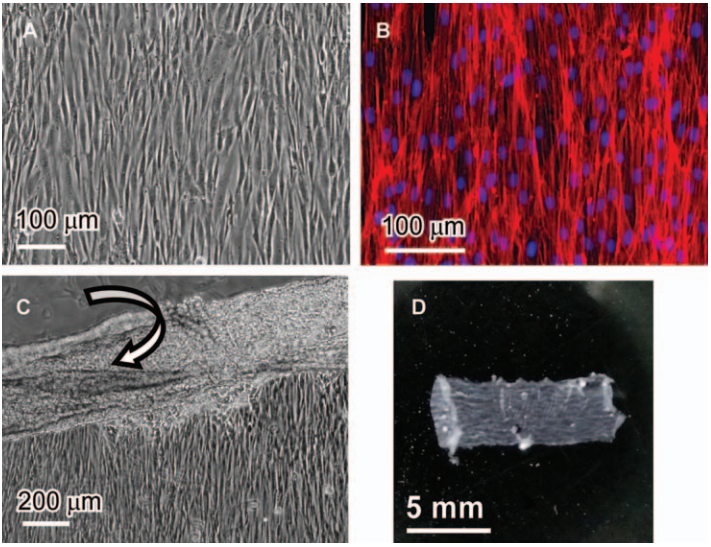
A
100 µm
B
100 µm
C
200 µm
D
5 mm

Figure 23.11 Microscopic photographs of aligned cells on a micro-patterned thermo-responsive surface (A,B) and photographs of the cell detachment from the surface by reducing temperature to 20 °C and the completely harvested cell sheet showing orientation (C,D). Actin (red) and nuclei (blue) in the aligned cells were stained with AlexaFluor568-phalloidin and Hoechst 33258, respectively (B).
Adapted with permission from Ref. 125. Copyright (2011) the American Chemical Society.

they keep the original aspect of the cell monolayer,[61] well-aligned actin fibers in the cell monolayer induced two distinctive shrinking rates in the vertical and parallel sides of the cell alignment, suggesting that the cell sheet may show unique mechanical properties.

In addition to the structural anisotropy, cell alignment influences cell sheets biologically. In the case of NHDF sheet, VEGF secretion is obviously increased by organizing the alignment of fibroblasts.[120] Increase in VEGF secretion potentially enhances vascularization in multi-layered cell sheets.[126–128] As described above, vascularization is one of the main issues to achieve the reconstruction of large-scale complex artificial tissues for supplying oxygen and nutrients to the tissue and maintaining its normal functions.[107] Therefore, the control of cell alignment may also enhance local VEGF delivery to the transplanted site of cell sheet.

Importantly, cell sheets can be manipulated and then stacked on each other with a gelatin-coated manipulator or a PVDF supporting membrane. Although various biomaterials including micropatterned surfaces have been fabricated for controlling cell alignment (*e.g.* skeletal muscle myoblasts) and creating mechanical functions similar to native tissue,[123,129–132] cell orientation is necessary to be designed three-dimensionally for reconstructing complex tissues. Complex tissues, as myocardium, systematically organize mechanical and electrical 3D anisotropy for producing a unique electrical propagation *in vivo*.[119,133,134] Based on the cell sheet technology, cell orientation in anisotropic cell sheets is successfully transferred to desired sites. For example, different cell orientation can be produced in layered cell sheets only by stacking cell sheets orthogonally (Figure 23.12).[120] The upper and lower fibroblast sheets

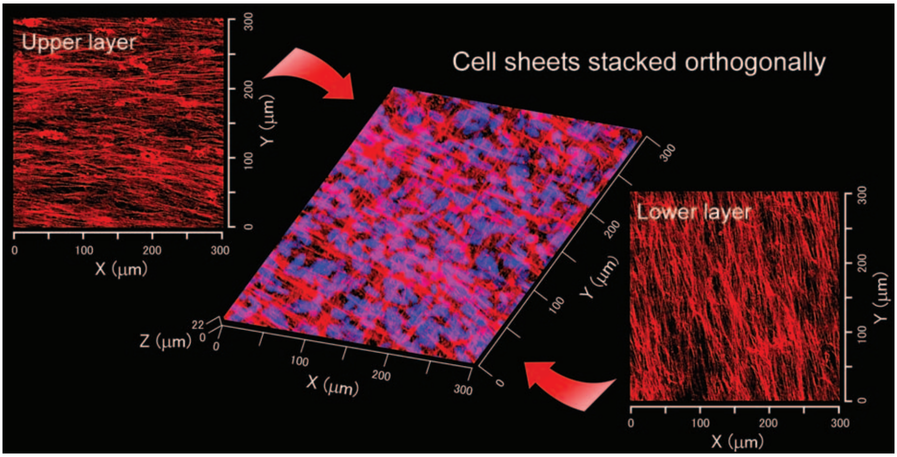

Figure 23.12 Three-dimensional confocal microscopic image of two cell sheets stacked orthogonally using an automatic cell sheet stacking device. The 2D images of the upper and lower cell sheets show individual cell orientations for at least seven days. Actin fibers and nuclei are stained with AlexaFluor568 (red) and Hoechst 33258 (blue), respectively. Reprinted from Ref. 120 with permission of Elsevier.

show individual cell alignments as designed for at least seven days after the stacking. The control of cell alignment will be a key factor in delivery of tissue-mimicking cell sheets to tissues having well-oriented structures.

23.5 Conclusions

A variety of polymeric biomaterials have contributed to the establishment of cell/tissue delivery technology. With progress in tissue engineering, cells can be cultured three-dimensionally on polymeric scaffolds, and then transplanted at desired sites for tissue regeneration. Simultaneously to the development of scaffold-based tissue delivery, cell sheet-based tissue delivery technique is expanding its uniqueness and advantages for regenerative medicine. The intelligent surfaces with a nanoscale thermo-responsive polymer coating have already been applied for the delivery of reconstructed tissues to damaged sites in human clinical studies. Moreover, microfabrication techniques provide thermo-responsive surfaces having various functions for creating 3D complex tissue. New cell sheet technologies including polymer grafting, cell patterning and 3D cell sheet layering, can be foreseen to push advances in delivery systems for tissue reconstruction and regenerative medicine.

References

1. R. Langer and J. P. Vacanti, *Science*, 1993, **260**, 920.
2. Y. Cao, J. P. Vacanti, K. T. Paige, J. Upton and C. A. Vacanti, *Plast. Reconstr. Surg.*, 1997, **100**, 297.
3. S. Yang, K. F. Leong, Z. Du and C. K. Chua, *Tissue Eng.*, 2001, **7**, 679.
4. V. Ravaine, C. Ancla and B. Catargi, *J. Control. Release*, 2008, **132**, 2.
5. J. Brange and L. Langkjaer, in *Protein Delivery: Physical Systems*, ed. L. Sanders and R. Hendren, Kluwer Academic Publishers, NY, 2002, p. 343.
6. T. A. Horbett, J. Kost and B. D. Ratner, *Abstracts of papers of the American Chemical Society*, 1983, **185**, 86-POLY.
7. J. Kost and R. Langer, *Adv. Drug Deliver. Rev.*, 2001, **46**, 125.
8. S. W. Kim, C. M. Pai, K. Makino, L. A. Seminoff, D. L. Holmberg, J. M. Gleeson, D. E. Wilson and E. J. Mack, *J. Control. Release*, 1990, **11**, 193.
9. E. A. Doyle, S. A. Weinzimer, A. T. Steffen, J. A. H. Ahern, M. Vincent and W. V. Tamborlane, *Diabetes Care*, 2004, **27**, 1554.
10. M. Peyrot and R. R. Rubin, *Diabetes Care*, 2005, **28**, 53.
11. F. Lin and A. M. Sun, *Science*, 1980, **210**, 908.
12. M. V. Sefton, L. Kharlip, V. Horvath and T. Roberts, *J. Control. Release*, 1992, **19**, 289.
13. P. Soon-Shiong and P. A. Sandford, *Surg. Tech. Int.*, 1995, **IV**, 93.
14. P. de Vos, M. M. Faas, B. Strand and R. Calafiore, *Biomaterials*, 2006, **27**, 5603.

15. D. Zhou, E. Kintsourashvili, S. Mamujee, I. Vacek and A. M. Sun, *Ann. NY Acad. Sci.*, 1999, **875**, 208.
16. Y. Sun, X. Ma, D. Zhou, I. Vacek and A. M. Sun, *J. Clin. Invest.*, 1996, **98**, 1417.
17. U. Siebers, A. Horcher, R. G. Bretzel, K. Federlin and T. Zekorn, *Ann. NY Acad. Sci.*, 1997, **831**, 304.
18. T. Roberts, U. De Boni and M. V. Sefton, *Biomaterials*, 1996, **17**, 267.
19. P. A. Tresco, S. R. Winn and P. Aebischer, *Asaio J.*, 1992, **38**, 17.
20. P. A. Tresco, S. R. Winn, S. Tan, C. B. Jaeger, L. A. Greene and P. Aebischer, *Cell Transplant.*, 1992, **1**, 255.
21. A. A. Chen, D. K. Thomas, L. L. Ong, R. E. Schwartz, T. R. Golub and S. N. Bhatia, *P. Natl. Acad. Sci. USA*, 2011, **108**, 11842.
22. J. P. Vacanti and R. Langer, *Lancet*, 1999, **354**, SI32.
23. L. G. Griffith, *Ann. NY Acad. Sci.*, 2002, **961**, 83.
24. X. Shao and C. J. Hunter, *J. Biomed. Mater. Res.*, 2007, **82**, 701.
25. Y. Wang, F. Z. Cui, K. Hu, X. D. Zhu and D. D. Fan, *J. Biomed. Mater. Res. B*, 2008, **86**, 29.
26. Y. Liu, S. Bharadwaj, S. J. Lee, A. Atala and Y. Zhang, *Biomaterials*, 2009, **30**, 3865.
27. C. H. Lee, A. Singla and Y. Lee, *Int. J. Pharm.*, 2001, **221**, 1.
28. L. Guan and J. E. Davies, *J. Biomed. Mater. Res.*, 2004, **71**, 480.
29. S. K. Sahoo, A. K. Panda and V. Labhasetwar, *Biomacromolecules*, 2005, **6**, 1132.
30. E. Saito, E. E. Liao, W. W. Hu, P. H. Krebsbach and S. J. Hollister, *J. Tissue Eng. Regen. Med.*, 2012.
31. D. W. Hutmacher, *J. Biomater. Sci.*, 2001, **12**, 107.
32. A. S. Hoffman, *Adv. Drug Deliver. Rev.*, 2002, **54**, 3.
33. E. Smela, *Adv. Mater.*, 2003, **15**, 481.
34. M. A. Cole, N. H. Voelcker, H. Thissen and H. J. Griesser, *Biomaterials*, 2009, **30**, 1827.
35. A. Kikuchi and T. Okano, *Adv. Drug Deliver. Rev.*, 2002, **54**, 53.
36. Y. H. Bae, T. Okano, R. Hsu and S. W. Kim, *Makromol. Chem. Rapid Comm.*, 1987, **8**, 481.
37. T. Okano, Y. H. Bae, H. Jacobs and S. W. Kim, *J. Control. Release*, 1990, **11**, 255.
38. M. Kurisawa, M. Yokoyama and T. Okano, *J. Control. Release*, 2000, **69**, 127.
39. H. Kanazawa, K. Yamamoto, Y. Matsushima, N. Takai, A. Kikuchi, Y. Sakurai and T. Okano, *Anal. Chem.*, 1996, **68**, 100.
40. A. Kikuchi and T. Okano, *Macromol. Symp.*, 2004, **207**, 217.
41. K. Nagase, J. Kobayashi, A. I. Kikuchi, Y. Akiyama, H. Kanazawa and T. Okano, *Langmuir*, 2008, **24**, 511.
42. M. Heskins and J. E. Guillet, *J. Macromol. Sci. A*, 1968, **2**, 1441.
43. N. Yamada, T. Okano, H. Sakai, F. Karikusa, Y. Sawasaki and Y. Sakurai, *Makromol. Chem. Rapid Comm.*, 1990, **11**, 571.

44. T. Okano, N. Yamada, M. Okuhara, H. Sakai and Y. Sakurai, *Biomaterials*, 1995, **16**, 297.
45. F. Eeckman, A. J. Moes and K. Amighi, *Int. J. Pharm.*, 2002, **241**, 113.
46. C. A. Kavanagh, Y. A. Rochev, W. M. Gallagher, K. A. Dawson and A. K. Keenan, *Pharmacol. Therapeut.*, 2004, **102**, 1.
47. C. Cheng, H. Wei, B. X. Shi, H. Cheng, C. Li, Z. W. Gu, S. X. Cheng, X. Z. Zhang and R. X. Zhuo, *Biomaterials*, 2008, **29**, 497.
48. M. Talelli and W. E. Hennink, *Nanomedicine UK*, 2011, **6**, 1245.
49. Y. H. Bae, B. Vernon, C. K. Han and S. W. Kim, *J. Control. Release*, 1998, **53**, 249.
50. B. Vernon, S. W. Kim and Y. H. Bae, *J. Biomater. Sci. Polym. Ed.*, 1999, **10**, 183.
51. K. H. Park and Y. H. Bae, *Biosci. Biotechnol. Biochem.*, 2002, **66**, 1473.
52. M. Yamato and T. Okano, *Mater. Today*, 2004, **7**, 42.
53. J. Yang, M. Yamato, C. Kohno, A. Nishimoto, H. Sekine, F. Fukai and T. Okano, *Biomaterials*, 2005, **26**, 6415.
54. A. Kikuchi and T. Okano, *J. Control. Release*, 2005, **101**, 69.
55. N. Matsuda, T. Shimizu, M. Yamato and T. Okano, *Adv. Mater.*, 2007, **19**, 3089.
56. K. Nishida, M. Yamato, Y. Hayashida, K. Watanabe, K. Yamamoto, E. Adachi, S. Nagai, A. Kikuchi, N. Maeda, H. Watanabe, T. Okano and Y. Tano, *N. Engl. J. Med.*, 2004, **351**, 1187.
57. T. Ohki, M. Yamato, D. Murakami, R. Takagi, J. Yang, H. Namiki, T. Okano and K. Takasaki, *Gut*, 2006, **55**, 1704.
58. I. Ishikawa, T. Iwata, K. Washio, T. Okano, T. Nagasawa, K. Iwasaki and T. Ando, *Periodontol. 2000*, 2009, **51**, 220.
59. Y. Akiyama, A. Kikuchi, M. Yamato and T. Okano, *Langmuir*, 2004, **20**, 5506.
60. A. Mizutani, A. Kikuchi, M. Yamato, H. Kanazawa and T. Okano, *Biomaterials*, 2008, **29**, 2073.
61. H. Takahashi, M. Nakayama, M. Yamato and T. Okano, *Biomacromolecules*, 2010, **11**, 1991.
62. S. Yamamoto, M. Ejaz, Y. Tsujii, M. Matsumoto and T. Fukuda, *Macromolecules*, 2000, **33**, 5602.
63. S. Yamamoto, M. Ejaz, Y. Tsujii and T. Fukuda, *Macromolecules*, 2000, **33**, 5608.
64. R. Barbey, L. Lavanant, D. Paripovic, N. Schuwer, C. Sugnaux, S. Tugulu and H. A. Klok, *Chem. Rev.*, 2009, **109**, 5437.
65. D. M. Jones, J. R. Smith, W. T. S. Huck and C. Alexander, *Adv. Mater.*, 2002, **14**, 1130.
66. N. Idota, A. Kikuchi, J. Kobayashi, Y. Akiyama and T. Okano, *Langmuir*, 2006, **22**, 425.
67. M. Baum and W. J. Brittain, *Macromolecules*, 2002, **35**, 610.
68. Y. S. Jo, A. J. van der Vlies, J. Gantz, S. Antonijevic, D. Demurtas, D. Velluto and J. A. Hubbell, *Macromolecules*, 2008, **41**, 1140.

69. K. Kiani, D. J. T. Hill, F. Rasoul, M. Whittaker and L. Rintoul, *J. Polym. Sci. Pol. Chem.*, 2007, **45**, 1074.
70. F. Ganachaud, M. J. Monteiro, R. G. Gilbert, M. A. Dourges, S. H. Thang and E. Rizzardo, *Macromolecules*, 2000, **33**, 6738.
71. G. Moad, E. Rizzardo and S. H. Thang, *Aust. J. Chem.*, 2005, **58**, 379.
72. M. Nakayama and T. Okano, *Biomacromolecules*, 2005, **6**, 2320.
73. M. H. Stenzel, *Chem. Commun.*, 2008, 3486.
74. T. Yakushiji, K. Sakai, A. Kikuchi, T. Aoyagi, Y. Sakurai and T. Okano, *Langmuir*, 1998, **14**, 4657.
75. J. Yang, M. Yamato, T. Shimizu, H. Sekine, K. Ohashi, M. Kanzaki, T. Ohki, K. Nishida and T. Okano, *Biomaterials*, 2007, **28**, 5033.
76. V. Mouly, A. Aamiri, S. Perie, K. Mamchaoui, A. Barani, A. Bigot, B. Bouazza, V. Francois, D. Furling, V. Jacquemin, E. Negroni, I. Riederer, A. Vignaud, J. L. Guily and G. S. Butler-Browne, *Acta Myol.*, 2005, **24**, 128.
77. J. T. Vilquin, *Acta Myol.*, 2005, **24**, 119.
78. D. A. Taylor, B. Z. Atkins, P. Hungspreugs, T. R. Jones, M. C. Reedy, K. A. Hutcheson, D. D. Glower and W. E. Kraus, *Nat. Med.*, 1998, **4**, 929.
79. F. D. Pagani, H. DerSimonian, A. Zawadzka, K. Wetzel, A. S. B. Edge, D. B. Jacoby, J. H. Dinsmore, S. Wright, T. H. Aretz, H. J. Eisen and K. D. Aaronson, *J. Am. Coll. Cardiol.*, 2003, **41**, 879.
80. P. Menasche, *J. Mol. Cell. Cardiol.*, 2008, **45**, 545.
81. T. Shimizu, M. Yamato, A. Kikuchi and T. Okano, *Biomaterials*, 2003, **24**, 2309.
82. H. Kondoh, Y. Sawa, S. Miyagawa, S. Sakakida-Kitagawa, I. A. Memon, N. Kawaguchi, N. Matsuura, T. Shimizu, T. Okano and H. Matsuda, *Cardiovas. Res.*, 2006, **69**, 466.
83. H. Hata, G. Matsumiya, S. Miyagawa, H. Kondoh, N. Kawaguchi, N. Matsuura, T. Shimizu, T. Okano, H. Matsuda and Y. Sawa, *J. Thorac. Cardiovasc. Surg.*, 2006, **132**, 918.
84. I. A. Memon, Y. Sawa, N. Fukushima, G. Matsumiya, S. Miyagawa, S. Taketani, S. K. Sakakida, H. Kondoh, A. N. Aleshin, T. Shimizu, T. Okano and H. Matsuda, *J. Thorac. Cardiovasc. Surg.*, 2005, **130**, 1333.
85. K. Matsuura, A. Honda, T. Nagai, N. Fukushima, K. Iwanaga, M. Tokunaga, T. Shimizu, T. Okano, H. Kasanuki, N. Hagiwara and I. Komuro, *J. Clin. Invest.*, 2009, **119**, 2204.
86. Y. Imanishi, S. Miyagawa, N. Maeda, S. Fukushima, S. Kitagawa-Sakakida, T. Daimon, A. Hirata, T. Shimizu, T. Okano, I. Shimomura and Y. Sawa, *Circulation*, 2011, **124**, S10.
87. Y. Miyahara, N. Nagaya, M. Kataoka, B. Yanagawa, K. Tanaka, H. Hao, K. Ishino, H. Ishida, T. Shimizu, K. Kangawa, S. Sano, T. Okano, S. Kitamura and H. Mori, *Nat. Med.*, 2006, **12**, 459.
88. K. Watanabe, M. Yamato, Y. Hayashida, J. Yang, A. Kikuchi, T. Okano, Y. Tano and K. Nishida, *Biomaterials*, 2007, **28**, 745.
89. K. Kitabayashi, A. Siltanen, T. Patila, M. A. Mahar, I. Tikkanen, J. Koponen, M. Ono, Y. Sawa, E. Kankuri and A. Harjula, *Cell Transplant.*, 2010, **19**, 573.

90. A. Siltanen, K. Kitabayashi, T. Patila, M. Ono, I. Tikkanen, Y. Sawa, E. Kankuri and A. Harjula, *Tissue Eng*., 2011, **17**, 115.
91. A. Siltanen, K. Kitabayashi, P. Lakkisto, J. Makela, T. Patila, M. Ono, I. Tikkanen, Y. Sawa, E. Kankuri and A. Harjula, *PLoS One*, 2011, **6**, e19161.
92. D. Jolly, *Cancer Gene Ther*., 1994, **1**, 51.
93. R. I. Mahato, L. C. Smith and A. Rolland, *Adv. Genet*., 1999, **41**, 95.
94. P. Wu and D. W. Grainger, *Biomaterials*, 2006, **27**, 2450.
95. H. Takahashi, D. Letourneur and D. W. Grainger, *Biomacromolecules*, 2007, **8**, 3281.
96. T. Iwata, M. Yamato, H. Tsuchioka, R. Takagi, S. Mukobata, K. Washio, T. Okano and I. Ishikawa, *Biomaterials*, 2009, **30**, 2716.
97. K. Ohashi, T. Yokoyama, M. Yamato, H. Kuge, H. Kanehiro, M. Tsutsumi, T. Amanuma, H. Iwata, J. Yang, T. Okano and Y. Nakajima, *Nat. Med*., 2007, **13**, 880.
98. H. Shimizu, K. Ohashi, R. Utoh, K. Ise, M. Gotoh, M. Yamato and T. Okano, *Biomaterials*, 2009, **30**, 5943.
99. M. Kanzaki, M. Yamato, J. Yang, H. Sekine, C. Kohno, R. Takagi, H. Hatakeyama, T. Isaka, T. Okano and T. Onuki, *Biomaterials*, 2007, **28**, 4294.
100. S. N. Bhatia, U. J. Balis, M. L. Yarmush and M. Toner, *FASEB J*., 1999, **13**, 1883.
101. Y. Tsuda, A. Kikuchi, M. Yamato, A. Nakao, Y. Sakurai, M. Umezu and T. Okano, *Biomaterials*, 2005, **26**, 1885.
102. Y. Tsuda, A. Kikuchi, M. Yamato, G. Chen and T. Okano, *Biochem. Biophys. Res. Commun*., 2006, **348**, 937.
103. I. Elloumi Hannachi, K. Itoga, Y. Kumashiro, J. Kobayashi, M. Yamato and T. Okano, *Biomaterials*, 2009, **30**, 5427.
104. T. Shimizu, M. Yamato, A. Kikuchi and T. Okano, *Tissue Eng*., 2001, **7**, 141.
105. Y. Haraguchi, T. Shimizu, M. Yamato, A. Kikuchi and T. Okano, *Biomaterials*, 2006, **27**, 4765.
106. Y. Haraguchi, T. Shimizu, M. Yamato and T. Okano, *J. Tissue Eng. Regen. Med*., 2010, **4**, 291.
107. R. K. Jain, P. Au, J. Tam, D. G. Duda and D. Fukumura, *Nat. Biotechnol*., 2005, **23**, 821.
108. R. Ogawa, K. Oki and H. Hyakusoku, *Regen. Med*., 2007, **2**, 831.
109. Y. Tsuda, T. Shimizu, M. Yarnato, A. Kikuchi, T. Sasagawa, S. Sekiya, J. Kobayashi, G. Chen and T. Okano, *Biomaterials*, 2007, **28**, 4939.
110. S. J. Jones, A. Boyde and J. B. Pawley, *Cell Tissue Res*., 1975, **159**, 73.
111. K. D. Costa, E. J. Lee and J. W. Holmes, *Tissue Eng*., 2003, **9**, 567.
112. E. C. Goldsmith, A. Hoffman, M. O. Morales, J. D. Potts, R. L. Price, A. McFadden, M. Rice and T. K. Borg, *Dev. Dyn*., 2004, **230**, 787.
113. P. Camelliti, T. K. Borg and P. Kohl, *Cardiovasc. Res*., 2005, **65**, 40.
114. C. Boote, S. Hayes, M. Abahussin and K. M. Meek, *Invest. Ophthalmol. Visual Sci*., 2006, **47**, 901.

115. J. Foolen, C. van Donkelaar, N. Nowlan, P. Murphy, R. Huiskes and K. Ito, *J. Orthop. Res.*, 2008, **26**, 1263.
116. C. J. Connon and K. M. Meek, *Wound Repair Regen.*, 2003, **11**, 71.
117. M. H. Ross, G. I. Kaye and W. Pawlina, *Histology: A Text and Atlas*, Lippincott Williams & Wilkins, Philadelphia PA, USA, 2003.
118. P. M. Wigmore and D. J. Evans, *Int. Rev. Cytol.*, 2002, **216**, 175.
119. G. Vunjak-Novakovic, N. Tandon, A. Godier, R. Maidhof, A. Marsano, T. P. Martens and M. Radisic, *Tissue Eng. B*, 2010, **16**, 169.
120. H. Takahashi, M. Nakayama, T. Shimizu, M. Yamato and T. Okano, *Biomaterials*, 2011, **32**, 8830.
121. C. Williams, A. W. Xie, M. Yamato, T. Okano and J. Y. Wong, *Biomaterials*, 2011, **32**, 5625.
122. L. C. McSpadden, R. D. Kirkton and N. Bursac, *Am. J. Physiol. Cell Physiol.*, 2009, **297**, C339.
123. N. F. Huang, R. J. Lee and S. Li, *Am. J. Transl. Res.*, 2010, **2**, 43.
124. B. C. Isenberg, Y. Tsuda, C. Williams, T. Shimizu, M. Yamato, T. Okano and J. Y. Wong, *Biomaterials*, 2008, **29**, 2565.
125. H. Takahashi, M. Nakayama, K. Itoga, M. Yamato and T. Okano, *Biomacromolecules*, 2011, **12**, 1414.
126. J. Folkman and M. Klagsbrun, *Science*, 1987, **235**, 442.
127. S. Liekens, E. De Clercq and J. Neyts, *Biochem. Pharmacol.*, 2001, **61**, 253.
128. G. Ferrari, G. Pintucci, G. Seghezzi, K. Hyman, A. C. Galloway and P. Mignatti, *P. Natl. Acad. Sci. USA*, 2006, **103**, 17260.
129. J. S. Choi, S. J. Lee, G. J. Christ, A. Atala and J. J. Yoo, *Biomaterials*, 2008, **29**, 2899.
130. Y. Zhao, H. Zeng, J. Nam and S. Agarwal, *Biotechnol. Bioeng.*, 2009, **102**, 624.
131. W. W. Ahmed, T. Wolfram, A. M. Goldyn, K. Bruellhoff, B. A. S. Rioja, M. Moller, J. P. Spatz, T. A. Saif, J. G. Groll and R. Kemkemer, *Biomaterials*, 2010, **31**, 250.
132. W. Bian, B. Liau, N. Badie and N. Bursac, *Nat. Protoc.*, 2009, **4**, 1522.
133. A. J. Pope, G. B. Sands, B. H. Smaill and I. J. LeGrice, *Am. J. Physiol-Heart C.*, 2008, **295**, H1243.
134. D. A. Hooks, M. L. Trew, B. J. Caldwell, G. B. Sands, I. J. LeGrice and B. H. Smaill, *Circ. Res.*, 2007, **101**, e103.

CHAPTER 24

Drug/Medical Device Combination Products with Stimuli-responsive Eluting Surface

C. ALVAREZ-LORENZO AND A. CONCHEIRO*

Departamento de Farmacia y Tecnología Farmacéutica, Facultad de
Farmacia, Universidad de Santiago de Compostela, 15782-Santiago de
Compostela, Spain, Email: Carmen.alvarez.lorenzo@usc.es
*Email: angel.concheiro@usc.es

24.1 Combination Products

Drugs and medical devices have typically followed different development criteria because they are intended to pursue dissimilar aims. Drugs are expected to exert their therapeutic effect at a local or systemic level through certain biological/biochemical pathways. By contrast, medical devices to be inserted/implanted in the body are sought to play a physical role in the diagnosis or the therapy (in some cases just to facilitate the application of a probe or the administration of a drug) and in the replacement of a tissue, organ or function of the body.[1] Thus, drugs and medical devices have separately evolved until a few decades ago, when combined use was realized to offer synergic therapeutic outcomes.[2,3]

Systems that join together the catheter/prosthesis role and the drug-delivery performance belong to the large heterogeneous family known as ‘‘combination products’’. Although some combination products have been in the market for a number of decades,[4] over the last years a large body of regulations has been

---

RSC Smart Materials No. 3
Smart Materials for Drug Delivery: Volume 2
Edited by Carmen Alvarez-Lorenzo and Angel Concheiro
© The Royal Society of Chemistry 2013
Published by the Royal Society of Chemistry, www.rsc.org

implemented into the USA and also, although with some differences, in Europe and Asia.[5] In particular, the US FDA has had a specific Office of Combination Products since 2002 and the first drug-eluting stents were approved in 2003. According to the current FDA criteria, the term combination product includes:[6]

(1) *A product comprised of two or more regulated components, i.e. drug/device, biologic/device, drug/biologic or drug/device/biologic, that are physically, chemically or otherwise combined or mixed and produced as a single entity;*
(2) *Two or more separate products packaged together in a single package or as a unit and comprised of drug and device products, device and biological products or biological and drug products;*
(3) *A drug, device or biological product packaged separately that according to its investigational plan or proposed labeling is intended for use only with an approved individually specified drug, device or biological product where both are required to achieve the intended use, indication or effect and where upon approval of the proposed product the labeling of the approved product would need to be changed, e.g. to reflect a change in intended use, dosage form, strength, route of administration or significant change in dose; or*
(4) *Any investigational drug, device or biological product packaged separately that according to its proposed labeling is for use only with another individually specified investigational drug, device or biological product where both are required to achieve the intended use, indication or effect.*

Therefore, any binary or ternary combination of drug, biological product and device is considered a combination product.[7] Since two or more regulated products form a single integral product or are placed together in a single package to be used jointly, there may also be two or more means by which the intended therapeutic effect is achieved. The mode of action that makes the greatest contribution to the overall intended therapeutic effects is called the primary mode of action (PMOA). According to the PMOA, combination products can be divided into three categories:

a) Drug PMOA, also designed as a device-based drug-delivery system, *e.g.* a transdermal patch or a pulmonary inhaler, were the pioneers in the field (the first metered-dose inhalers were commercialized 50 years ago) and the role of the device is limited to improving drug delivery. Namely, the device acts as a platform for optimized drug administration/delivery, but without the drug it has no other application.[4]
b) Biologic PMOA, *e.g.* a scaffold seeded with autologous cells for organ replacement, a device impregnated with genetically modified bacteria to produce antimicrobial factors that will control opportunistic pathogens or a device including cellular or tissue components, which can be used as factories to produce an array of therapeutic factors over the lifetime of the cells;[8]

c) Device PMOA, also called a drug-enhanced device product, *e.g.* a drug-eluting stent or a vertebroplasty implant with an extended-release analgesic.[9–12]

Once the PMOA is identified, one of the following FDA centers will have the primary responsibility for the studies, evaluation and approval: the Center for Drug Evaluation and Research (CDER), the Center for Biologics Evaluation and Research (CBER) or the Center for Devices and Radiological Health (CDRH). Sometimes it is not easy to assign a combination product to just one specific category and in those cases the pioneer in the development of the product may play a relevant role in the selection of the FDA center to proceed with the regulatory evaluation (Figure 24.1).[4]

Better patient compliance and improved local curative efficiency and long-term biocompatibility could be among the first motives that prompted the preparation of increasingly sophisticated combination products.[13] The current state-of-the-art of the biomaterials and a better knowledge of tissue and cellular physiology under healthy and illness conditions have driven the design of high-value combination products with performances unforeseeable a few years ago. The market of combination products is rapidly increasing, not only due to their therapeutic advantages regarding maximization of the effects but also because most drugs involved in combination products have already been approved, which simplifies and shortens the regulatory approval.[14] Thus, the development of combination products has had a greater success rate than drug development in terms of the number of products effectively launched (1/6 *vs.* 1/10,000), time spent (4–8 years *vs.* 13–15 years) and costs ($250 million *vs.* $500–2,000 million).[14,15] Importantly, drugs facing patent expiration could find new openings if combined with a device. Since the first sirolimus-eluting stents were approved in 2003, a variety of drug-eluting stents and catheters have now become

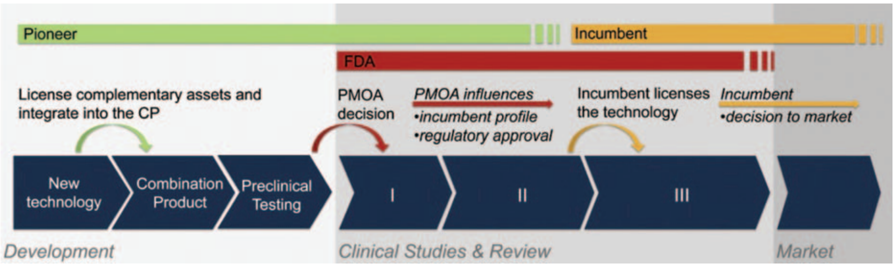
Pioneer
Incumbent
FDA
License complementary assets and integrate into the CP
PMOA decision
PMOA influences
•incumbent profile
•regulatory approval
Incumbent licenses the technology
Incumbent
•decision to market
New technology
Combination Product
Preclinical Testing
I
II
III
Development
Clinical Studies & Review
Market

Figure 24.1 Steps that a drug-device combination product follows from the development to the launch in the market. A pioneer sets the path by introducing a new technology into the combination product space. The FDA decides the primary mode of action (PMOA), which strongly determines the profile of the company, *i.e.* the incumbent (pharmaceutical, biopharmaceutical or medical device), that takes the product through regulatory approval into the market.
Reproduced from Ref. 4 with permission from Elsevier.

commercially available. Comprehensive texts on drug-device combination products, including an updated analysis of the combination products that are commercialized or undergoing clinical trials, have been published elsewhere.[1,5,16]

This chapter is mainly focused on the medical devices that have functionality by themselves and the techniques available to endow them with the ability to host drugs/biological products and to regulate their release. The approaches for surface modification with stimuli-responsive polymers or networks are analyzed in detail and the performance of the modified materials as drug-delivery systems discussed.

24.2 Benefits of Combining Medical Devices and Drugs/Biological Products

Medical devices, such as implants, catheters, vascular grafts and sutures, have become an essential part of modern medical care, playing an important role in common diagnostic and therapeutic procedures and in the management of critically ill patients.[17] Nevertheless, their use has an inherent risk of causing adverse foreign-body reactions (inflammatory response that may result in encapsulation by fibrosis) or other side effects derived from the adherence of host proteins and cells or of the proliferation of microorganisms.[18,19] For example, restenosis associated to endovascular stents[20] or posterior capsule opacification after intra-ocular lens implantation[21] are two clinically relevant examples of the deleterious effects of host cells growth and proliferation. The adhesion of macrophages and foreign body giant cells reduces the bactericidal capability, favoring the formation of microbial colonies (biofilm) and the persistence of infections.[22] Implantable devices are indeed considered as a haven for opportunistic bacteria and are responsible for almost 50% of all nosocomial infections, which are associated with considerable morbidity and mortality.[23] Although the risk of infection is slowly decreasing due to implementation of extreme hygienic and prophylactic conditions, the increasing population of patients with orthopedic implants makes considering infections very relevant due to the serious consequences on health and costs.[24] Furthermore, the deleterious effects of adherent inflammatory cells constitute a potential risk for the degradation of the biomaterial and the clinical failure of the medical device.[25] These host and microbial reactions may decrease the lifespan of the device. On the other hand, some therapeutic applications require the administration of medicines, namely drug/biologic products that are orally/parentally delivered, concomitantly to the insertion/implantation of the medical device.[26] Drug-eluting medical devices seek to find synergisms in the performance of the medical device and the drug/biologic product in a single entity and, in particular, to improve the device function with the local drug release.[1,27,28] The incorporation of the drug serves to tune the host/microbial responses to the medical device, while the medical device can enable the delivery of the drug for a prolonged time just at the site where it is needed.

Consequently, the efficacy and the safety of the treatment, as well as its cost-effectiveness, are improved. Furthermore, device-related complications that are refractory to conventional systemic drug administration can be successfully overcome through the local release.

Most of the current drug-eluting devices passively control the release, *i.e.* the rate is governed by dissolution or diffusion through inert or erodible depots. Nevertheless, active control of both loading and release kinetics is attracting growing attention. Smart systems that can work on demand may open up the possibility of delivering the drug only when certain relevant changes in the surroundings of the medical device happen, *i.e.* physico-chemical or physiological alterations or bacterial adhesion.[16,29] In future, it could even be possible to design devices that allow the drug release process to be monitored in real time and to communicate the progress of the treatment for a feed-back regulation by wireless.[16]

24.3 Materials for Medical Devices

Medical devices can be made of almost any material: metals and alloys, based on metallic bonds; ceramics, based on ionic bonds (*e.g.* glass, glass-ceramics and carbons); polymers, based on covalent bonds (*e.g.* thermosets, thermoplastics, elastomers and textiles); or organic-inorganic hybrids.[30] To be implantable in the body, they should behave as biomaterials, namely they have to be adequate to deal with the living body for the intended application during the planned time period.[31] Some features of the materials used for the medical devices are summarized below.

- Metals. They have been largely used for applications that require strength and ductility, such as bearing of heavy load without large deformation and permanent size changes; *e.g.* fracture fixation, prosthetic joints, dental implants, cranial plates or stents. Alloys lead to inert products in the saline environment.
- Ceramics. They are stiff and brittle, but highly biocompatible and chemically inert. Bioglasses are made of silica, calcium and sodium oxides and can be reabsorbable by living tissues, favoring bone regeneration. Ceramics are also used as surgical fillers or binders.
- Polymers. Natural but mainly synthetic polymers are widely used to prepare medical devices, owing to the versatile composition, structural arrangement and physical properties.[32] They can be processed to obtain a variety of shapes (wire, film, tube) and, depending on the monomeric composition, they can be absorbable.[33] Silk, polyesters (PLA, PLGA), polyethylene (PE), polypropylene (PP), poly(styrene), poly(tetrafluoroethylene) (PTFE) and poly(ethylene terephthalate) (PET) are present in prostheses, meshes, sutures and catheters. For these applications, the polymers usually require a surface treatment in order to improve the biocompatibility features.[34]
- Organic-inorganic hybrids. Combinations of polymers with ceramics or metals may overcome the limitations of the individual components and

provide improved or even novel properties. For example, hydroxyapatite and polymers are commonly combined to prepare materials with mechanical properties similar to those of the bones.[35]

24.4 Procedures to Incorporate Drugs

The direct soaking of the medical devices inside drug solutions usually does not result in efficient loading/controlled release.[12,36] Thus, specific approaches are required to incorporate drugs and other bioactive substances. Since the distinctive advantage of a combination product is to work in tandem as prosthetic functional or structural replacement of host tissue and as a drug-delivery system, the implementation of the drug-eluting feature should not cause any detriment in its function as a medical device.[1] On the other hand, to work competently as a delivery system, the drug release profiles have to match with the particular clinical context, taking into account the anatomy and physiology of the implantation site, the disease or the pathogen to be addressed, the local toxicity and the clearance mechanisms of the drug. Subtherapeutic levels may lead to failure and, in the case of antimicrobial drugs, even cause adverse events such as microbial resistance. The large number of formulation parameters that can affect the success of the delivery and the high doses required to enable long-term (months/years) release makes the design of most drug-eluting medical devices more complex than that of a conventional medicine.[1] Nevertheless, the experience gained in the last years and the better knowledge about the local therapeutic/toxic effects at the tissue site should serve to improve the still suboptimal performance of current drug-eluting medical devices and to pave the way for the design of new device-PMOA combination products.

The approaches for preparing drug-eluting medical devices can be categorized into two large groups: i) those that enable the incorporation of the drug in the bulk of the material that constitutes the medical device, during its fabrication (compounding) or in a later step (presoaking); and ii) those that incorporate the drug in the outer layers of the device by means of coating procedures, covalent binding or weak chemical interactions (Figure 24.2).

24.4.1 Compounding

The drug/active substance can be incorporated, mixed together with the components of the medical device during the synthesis/molding.[37] Combinations of several drugs, such as antibiotics (minocycline/rifampicin) and antiseptics (chlorhexidine/silver sulfadiazine), are also feasible.[38,39] Excipients able to modulate drug release rate can also be co-formulated. Since compounding may compromise certain mechanical properties, particularly the flexibility, of the device matrix if the amount of drug and coadjuvants is high,[39] this approach is mainly reserved for hard antibiotic-containing bone cements.[16,40,41] In recent times it has also been applied to prepare wound dressings by means of co-electrospinning.[42,43]

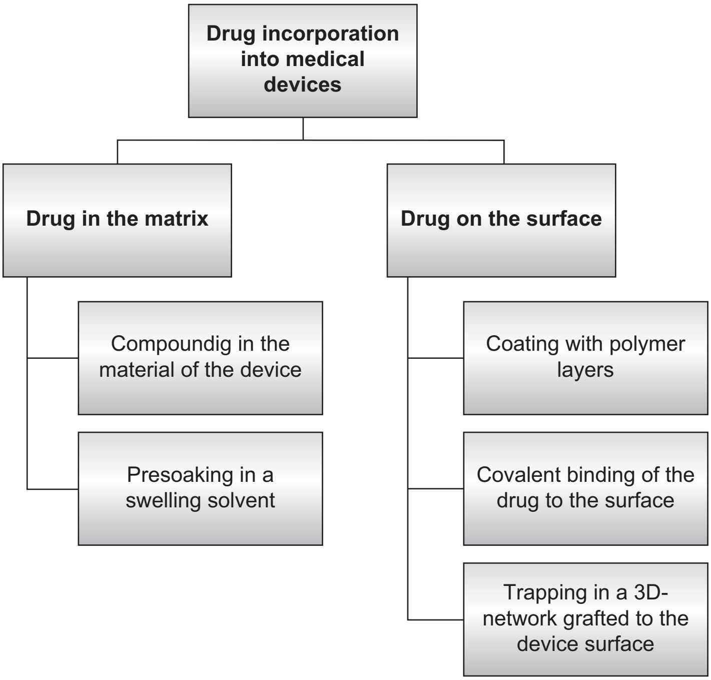
Drug incorporation into medical devices
Drug in the matrix
Drug on the surface
Compoundig in the material of the device
Presoaking in a swelling solvent
Coating with polymer layers
Covalent binding of the drug to the surface
Trapping in a 3D-network grafted to the device surface

Figure 24.2 General approaches for preparing drug-eluting medical devices by incorporation of drugs in the bulk or on the surface.

24.4.2 Impregnation Using a Swelling Solvent

Most polymer-based medical devices can be swollen in organic solvents of polarity that matches that of the polymer. The plasticizing effect caused by the solvent and the subsequent expansion of the network facilitate the penetration of dissolved molecules into the device structure. Common techniques involve the use of quite toxic solvents that have to be completely and controllably removed at the end of the process. For example, applying this approach rifampicin solely and combined with miconazole have been incorporated into polydimethylsiloxane and polyurethane catheters in order to prevent bacterial colonization, with successful clinical results.[44,45] Lately, the impregnation applying supercritical fluid-based technologies is being tested.[46,47] Supercritical CO_2 ($scCO_2$) is a non-toxic good solvent for most drugs and also a very efficient plasticizer of hydrophobic polymer networks. As a consequence, drug impregnation yield is higher than that achieved with conventional presoaking and the procedure can be adapted to a commercially suitable scale.[27] In general, the success of the impregnation becomes greater when ionic or hydrophobic interactions can be established between the drug molecules and the device components, although the impregnation conditions may also play a relevant role in the yield.[48,49]

24.4.3 Coating

The first attempts at preparing drug-eluting stents and catheters were focused on coating with non-degradable polymers (*e.g.* polyisobutylene or polymethacrylate) in order to regulate drug release through partitioning and diffusion mechanisms.[50] Degradable polymeric coatings (*e.g.* polylactic acid) are becoming more frequent, since they allow an extended release for a more prolonged time as they slowly erode. Antiseptics, antibiotics, anti-inflammatory or antiproliferative drugs can be dissolved or physically dispersed in the coating solution, which is then applied on the surface of the device. As the solvent evaporates, a layer of polymer containing the drug is adsorbed through physical or weak chemical interactions (hydrophobic or ionic bonds) on the device. The coating can also be applied by a layer-by-layer technique, incorporating different drugs and/or doses into each layer.[51,52] The basis of this latter approach of incipient application in the medical devices field is described in Chapter 17. Responsive biodegradable coatings have not yet been tested *in vivo*. Another modality of coating involves the wetting of the device surface with a cyclodextrin solution also containing a chemical cross-linker. After cross-linking, a layer of cyclodextrin network is formed wrapping the device. Cyclodextrins can form inclusion complexes with a variety of drugs and regulate the release rate through an affinity-based mechanism.[53–56]

Although the clinical success of the drug-containing physical coating is unquestionable,[1] it has been pointed out that polymeric coatings present some limitations due to premature delamination in the wet biological environment, which can lead to poor control of drug-release kinetics and local inflammatory reactions.[18,57–59] Inorganic and inorganic-polymer composite (“biomimetic”) coatings could overcome some of these limitations, enabling a tunable surface nanostructure that can regulate cell adhesion and proliferation and, if mimicking the bone matrix, it may even induce biomimeralization for a better integration of the prosthesis.[60,61]

24.4.4 Drug Chemically Bonded to the Surface

Alternatives to compounding and physical coating require previous functionalization of the medical device. Chemical activation of the substrate surface may enable functional groups to be created in a suitable amount for the covalent binding of the bioactive substance to be incorporated. The bonds can be reversible allowing the release of the drug as the bonds are broken in the physiological environment at a rate that is constant or that is feed-back regulated by the concentration of a given substance. An alternative is the conjugation through permanent links, and the drug is expected to exert its function while attached to the surface. The state-of-the-art of covalent conjugation of bioactive compounds to modified surfaces has been addressed in detail in recent reviews.[29,62]

24.4.5 Polymer Grafting to the Device Surface

Quite diverse techniques have been applied to functionalize the surface of medical devices with functional polymers forming dense brushes or hydrogel-type layers, where the drug molecules can be effectively hosted and retained and from where they are released in a controlled way once in contact with the biological fluids (Table 24.1).[62,63] Surfaces modified with covalently grafted polymers bearing functional groups capable of interacting with the target drug molecules are being intensively explored for this purpose. The grafted polymers can partially cover the surface, adopting a certain patterning, or provide an entirely new interface. Two grafting methods are usually distinguished: i) ‘‘grafting-from’’, which consists of starting the polymerization of the monomers from the substrate surface, resulting in polymer chains that grow toward the surrounding environment; and ii) ‘‘grafting-to’’, in which reactive preformed polymers are chemically linked to the substrate. The first approach is the most used in the biomedical field.[64] Depending on the chemical structure of the substrate and of the monomers/polymers that are going to be grafted, different performances can be achieved.[65,66]

Free radicals and reactive points can be created on the substrate by means of chemical, irradiation or plasma methods (Figure 24.3). Then, the polymerization of the grafted monomers commonly occurs by conventional free-radical polymerization mechanism. In this way stimuli-responsive interfaces have been successfully created. However, the control of the morphology and the chemical functionality of the resulting grafted polymer is quite limited. Compared to conventional free-radical graft polymerization, controlled/‘‘living’’ polymerization enables command of the molecular weight and the structure of the resulting grafted polymer and makes the design of block, star or dendritic forms possible.[65] As in the conventional polymerization, generated free radicals propagate and terminate, but under appropriate conditions the termination can be minimized and the reactive groups at the end of the polymer grafts remain as ‘‘dormant’’ entities that can be activated again if more monomer (equal to or different from the first one) is added. The IUPAC name for this technique is ‘‘reversible-deactivation radical polymerization’’, which graphically depicts this fact.[67] Additionally, the conversion of dormant forms in active ones is more rapid than the propagation and, consequently, all polymer chains grow at the same rate (different from what happens in conventional polymerization) and their lengths remain very similar.[68] Controlled free radical polymerization can be achieved *via* atom transfer (ATRP) or nitroxide-mediated (NMRP) radical polymerization, reversible addition fragmentation transfer (RAFT) polymerization and iniferter techniques.[69] The main difficulty of applying the controlled/living graft polymerization remains in the generation of suitable initiating sites on the substrate. Two pathways can be followed: i) transformation of original functional groups of the substrate into the dormant initiators, and ii) immobilization of suitable dormant initiators on the substrate. The first approach usually involves two or more sequential chemical reactions, while the second one can occur by chemical

Table 24.1 Relevant techniques used for modifying polymer surfaces with chemical groups that reversibly interact with drug molecules or that serve as precursors for the conjugation of drug molecules. Adapted from Ref. 63 with permission of Informa Ltd.

Technique	*Procedure*	*Advantages*	*Disadvantages*
Wet chemical	The material is immersed in solutions of reagents that generate reactive functional groups (mainly oxygen-containing moieties) on the surface.	No specialized equipment is required. Better penetration into pores than plasma and other techniques.	Non-specific. A range of oxygen-containing functional groups is generated. Extended treatment in concentrated corrosive solution. Hazardous waste.
Silane monolayers	Treatment of surfaces with oxygen plasma, followed by chemical vapor deposition of the silane. Different end functionalities can be obtained.	Enables the coupling of an organic polymer to inorganic substrates or to hydroxylated polymer surfaces.	The siloxane linkage can be hydrolyzed at high temperatures or alkaline pH.
Plasma	A gas is partially ionized into charged particles and electrons. Provide modification of the top nanometer of the surface, generating hydroxyl, carboxyl or amine groups. Coating with "plasma polymers" is possible.	No solvents. No chemical waste. Less degradation and roughening of the material. Versatile plasma polymerization.	Many parameters (time, temperature, power, gas composition/flow/pressure, distance to plasma source) affect the yield. High inter-lab variability.
Corona discharge / flame treatment	A stream of ionized air bombards the polymer surface and generates oxidation products.	Low cost. Continuous process.	Unstable surface polar groups.
UV irradiation	Reactive sites generated by radiation can become functional groups upon exposure to gas or can initiate graft polymerization.	The depth of the functionalization can be tuned by varying wavelength.	Risk of modifying the optical properties of the polymer.
γ-ray irradiation	Direct irradiation of the polymer in contact with a monomer or pre-irradiation in an inert atmosphere or in the presence of oxygen, followed by immersion in a monomer solution.	Versatile grafted structure. No high temperature. Useful in large-scale processes.	Homopolymerization.

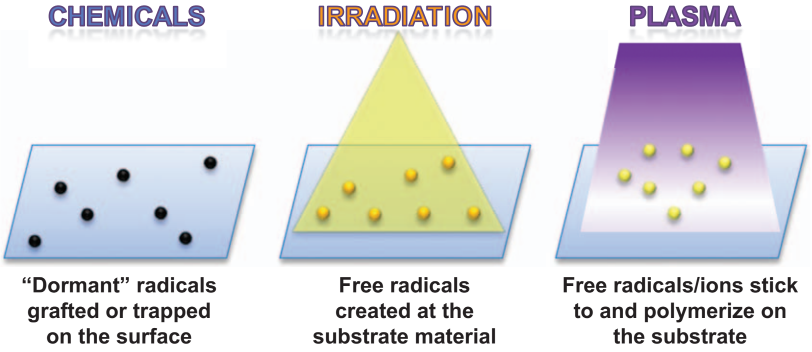
CHEMICALS
IRRADIATION
PLASMA
"Dormant" radicals grafted or trapped on the surface
Free radicals created at the substrate material
Free radicals/ions stick to and polymerize on the substrate

Figure 24.3 Main approaches to create free radical and reactive points on the surface of materials that may lead to surface-functionalized medical devices.

or high-energy activation of the surface to fix the initiator directly or to fix a spacer to which the initiator can be bound.[70] In either case, the result should be the formation of bromoester, bromoamide, chloromethylphenyl, sulfonylchloride or related chemical groups able to act as initiating sites. ATRP and NMRP have been shown to be useful at growing polymer brushes on almost any material for a variety of applications.[65] As an example, the surfaces of poly(ethylene terephthalate) and poly(ethylene naphthalate) films have been grafted with poly(*N*-isopropylacrylamide) (PNIPAAm) *via* ATRP, through previous oxidation of the surface that enabled the immobilization of monolayers of trichlorosilane initiator.[71] In some cases the initiators for grafting can be created on the substrate by applying an irradiation technique, and then the copolymerization of the monomers can be controlled by adding a suitable "living" monomer, such as 2,2,6,6-tetramethylpiperidinyl-1-oxy (TEMPO).[72] Despite the clear advantages of the reversible-deactivation free-radical polymerization, the technical difficulties of activating the surfaces with dormant initiators explain why few papers have reported the use of controlled polymerization to create responsive surfaces for drug loading on medical devices.[65]

The most versatile methods for the functionalization of preformed materials are currently based on initiator-free irradiation using an adequate source of energy, such as gamma ray, UV or electron beams.[73,74] Polymer grafting applying irradiation, which does not require chemical initiators or catalysts, can start from a variety of monomers or prepolymers with different functionalities to fulfill specific requirements, covering a large surface in a short time, and enables a fine control of the polymerization and degree of crosslinking.[75] Furthermore, it is possible greatly to modify the surface with minor changes in the bulk features of the substrate.[76–81] Grafting by applying γ-rays enables the formation of active sites on the polymer substrate according to three different approaches:[74,82]

i) Direct method, which consists in irradiation of the polymer substrate once in contact with the monomer(s). The irradiation generates radicals in the polymer, which initiate both the grafting of the monomer and the growth of the new polymer chains. Homopolymer formation in the reaction medium should be kept as low as possible, so as not to decrease too much the yield of grafting.

ii) Pre-irradiation, which involves the irradiation of the polymer substrate *in vacuo* or under an inert atmosphere and, in a second step, the pre-irradiated substrate is placed in contact with the monomer(s) to be grafted. Although homopolymerization is prevented, higher irradiation doses than for the direct method are needed, which may damage the substrate.

iii) Pre-irradiation oxidative, in which the irradiation of the substrate is carried out in the presence of air or oxygen to generate peroxides or hydroperoxides. Immersion of the pre-irradiated substrate into the monomer solution followed by heating causes the peroxides and hydroperoxides to decompose as macroradicals that act as active sites for graft polymerization.

Plasma techniques have the advantage over irradiation approaches of causing changes only at the very top nanometers of the polymer surface, minimizing the repercussion on the bulk features of the material. Plasma surface treatments are based on radio- or microwave-frequency power sources to break molecules at gas state into charge-bearing subparticles, namely electrons and ions, generating a plasma state. Such subparticles, when they collide with a solid substrate, can cause three differentiated effects: i) removal of surface material, namely etching or ablation; ii) deposition as a solid film in a process known as plasma-enhanced chemical vapor deposition (particularly if the plasma leads to a film of polymeric material, the technique is called plasma polymerization); and iii) chemical and/or physical modification of the surface without significant addition/removal of material during exposure to particles and radiation from the plasma (Figure 24.4).[83] This latter approach is of great interest for introducing new reactive chemical groups on the substrate, which can subsequently be used to covalently graft drugs or polymer chains.[29] Such a direct grafting of polymers is suitable for further chemical immobilization of drug molecules or proteins at the end of the polymer chains, which can stimulate the desired cellular responses at the surface of the medical device.[84–86]

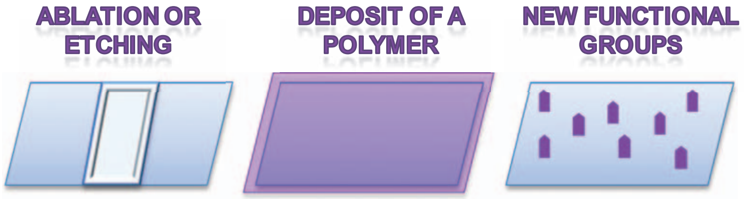

Figure 24.4 Effects of different plasma treatments on the surface of a material: removal of a portion of surface (ablation or etching), deposition of a solid polymer film (plasma polymerization) and modification of chemical groups.

However, the distance between the chains and the thinness of the coverage do not provide a good control of the release of drugs just weakly interacting.[29] An alternative is the generation of a plasma in a mixed vapor of monomers and inert gases to create plasma polymers by various mechanisms.[87–90] The polymers obtained by plasma polymerization show an excellent adhesion to a variety of substrates/devices, rendering thin pinhole-free layers that do not alter the mechanical properties of the device, *e.g*. flexibility in the case of catheters, but with a network structure hard to define.[90] Relevant advantages of plasma polymers are the uniform distribution of chemical groups, the possibility to regulate the out-diffusion rate of entrapped molecules, either *via* their cross-linking density or *via* a plasma polymer overlayer, and durability.[29]

Although still few, the number of publications referring to the grafting of stimuli-responsive polymers on diverse substrates applying any of the techniques described above has rapidly increased in the last years. The main objective is to regulate the hydrophilicity of the surface and the adhesion of cells and proteins to polymeric materials as a function of environmental variables, but also to attain self-healing coatings and sensors.[91–94] The success of responsive brushes for cell delivery is highlighted in Chapter 23. The next section focuses on recent achievements related to the non-covalent incorporation of bioactive molecules, mainly drugs, on the surface of stimuli-responsive polymer-grafted medical devices.

24.5 Responsive Surfaces for Drug Loading/Controlled Release

The preparation and the applications of stimuli-responsive hydrogels of sizes ranging from macro- to nanometric scale are currently well established,[95–100] as covered in Chapters 18, 19 and 20. Grafting to solid substrates of those responsive hydrogels has received much less attention in spite of the inherent advantages that it can offer in terms of mechanical strength for handling, enduring harsh application conditions, recovering after being used and reconditioning for reusability, not only for topical or mucosal drug delivery but also in the fields of biochemical sensors, biotechnology and environmental remediation.[66,91,94] Surface functionalization of medical devices with stimuli-responsive brushes and networks adequate for drug delivery during the time the device is inserted/implanted in the body is still incipient, but the research groups devoted to implement suitable synthesis routes are steeply rising.

24.5.1 Polymers Grafted by Means of Chemical Initiators

Surface-initiated living polymerization has recently been applied to graft temperature-, light-, pH- or saccharide-responsive brushes on diverse substrates.[65,101] For example, an ATRP technique was implemented to graft PNIPAAm brushes on the surface pores of silica, being able to load up to 58 wt. % ibuprofen at a temperature below the LCST and to rapidly release the

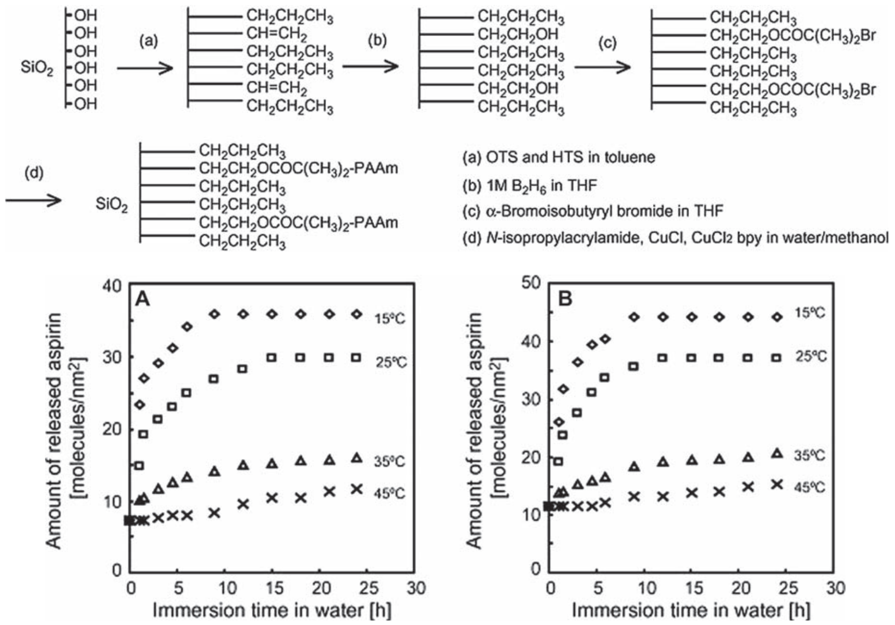

Figure 24.5 Steps to graft PNIPAAm brushes on silicon surfaces and aspirin release profiles from the modified surfaces with pNIPAAm brushes (A: 0.85 chain nm^{-2}; B: 0.65 chain nm^{-2}) at various temperatures. Reproduced from Ref. 103 with permission from Elsevier.

drug above LCST.[102] Similarly, PNIPAAm has been grafted onto silicon to regulate the uptake/release of aspirin (Figure 24.5), the density of PNIPAAm brushes having a strong influence on the temperature-responsiveness and on the release kinetics.[103]

More recently, 3-aminopropyl triethoxy silane (APTES) has been immobilized onto silicon wafers or quartz glass and, then, reacted with 2-bromo-2-methylpropionyl bromide to render Br-functionalized initiator surfaces that were used to graft polystyrene (PS) or poly(*N*,*N*-dimethylacrylamyde) (PDMA).[104] Temperature-responsive brushes were obtained by subsequent polymerization of NIPAAm on the PS- or PDMA-modified substrates, leading to 187 and 167 nm thick PS-b-PNIPAAm and PDMA-b-PNIPAAm brushes, respectively. To prepare photosensitive brushes, the PS-grafted substrate was treated with 4,5-dimethoxy-2-nitrobenzyl methacrylate (NBA). PolyNBA is hydrophobic but converts into hydrophilic poly(methacrylic acid) (PMAc) upon exposure to UV light, inducing, thereby, the transition from the collapsed to the extended state of the top region of the brushes. This photochemical reaction is not reversible, but the resultant PS-b-PMAc shows pH-sensitive swelling. The effect of temperature-, light- and pH-induced transitions of the brushes on the release of two probes, Nile red and 1,3,6,8-pyrenetetrasulfonic acid tetrasodium salt, was investigated in detail.[104] The general idea of this

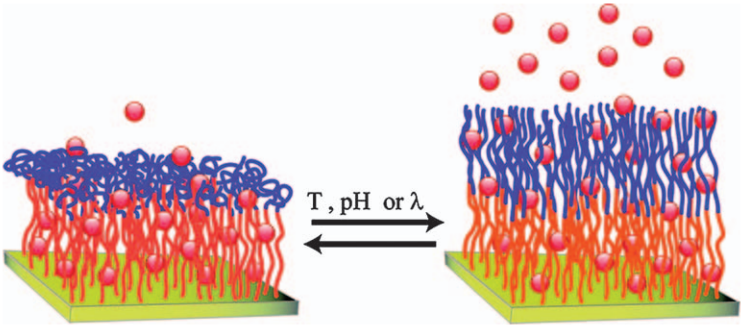

Figure 24.6 Surface-grafted diblock copolymer brushes with a top layer able to switch between collapsed and extended chains in response to temperature, pH or light.
Reprinted with permission from Ref. 104. Copyright 2011 American Chemical Society.

work was to graft a first polymer to form an inner layer that acts as a reservoir for guest molecules and, then, a stimuli-responsive polymer that can close or open the brush layer in response to a change in temperature, pH or light wavelength. Such stimuli-induced switching has been shown to be able to regulate the release rate of entrapped guest molecules (Figure 24.6). Nevertheless, since some drug leakage was observed even when the top brush had completely collapsed, studies regarding the influence of the relative length of the blocks on the changes in drug permeability between the extended and the collapsed states are ongoing.

Saccharide-sensitive brushes may also be interesting for responsive drug elution. Silicon surfaces with such responsiveness were obtained by treatment with aminopropyl trimethoxysilane (ATMS) to create a layer suitable for immobilization of the initiator bromoisobutyryl bromide, followed by controlled grafted polymerization of 3-(acryloylthioureido) phenylboronic acid (ATPBA) and NIPAAm.[101] The ATPBA-co-NIPAAm brushes provide a superhydrophobic coating to the silicon, due to strong hydrogen-bond interactions between thiourea and phenylboronic acid of ATPBA and imine groups of NIPAAm, which renders a collapsed configuration. By contrast, in the presence of glucose, the inter-molecular interactions are broken as the phenylboronic-sugar-thiourea complexes are formed and, as a consequence, the surface becomes superhydrophilic (Figure 24.7). When the sugar solution becomes diluted with water, the complex is broken and the inter-molecular hydrogen-bonds are reformed, the surface recovering the starting, collapsed state and the superhydrophobic features. Cycling experiments proved the reversibility and reproducibility of the changes. Furthermore, a linear dependence of the contact angle on the logarithm of the glucose concentration was found. All these finds make a saccharide-sensitive surface very attractive as platforms for drug loading/release with kinetics dependent on the concentration of glucose or other biorelevant sugars.

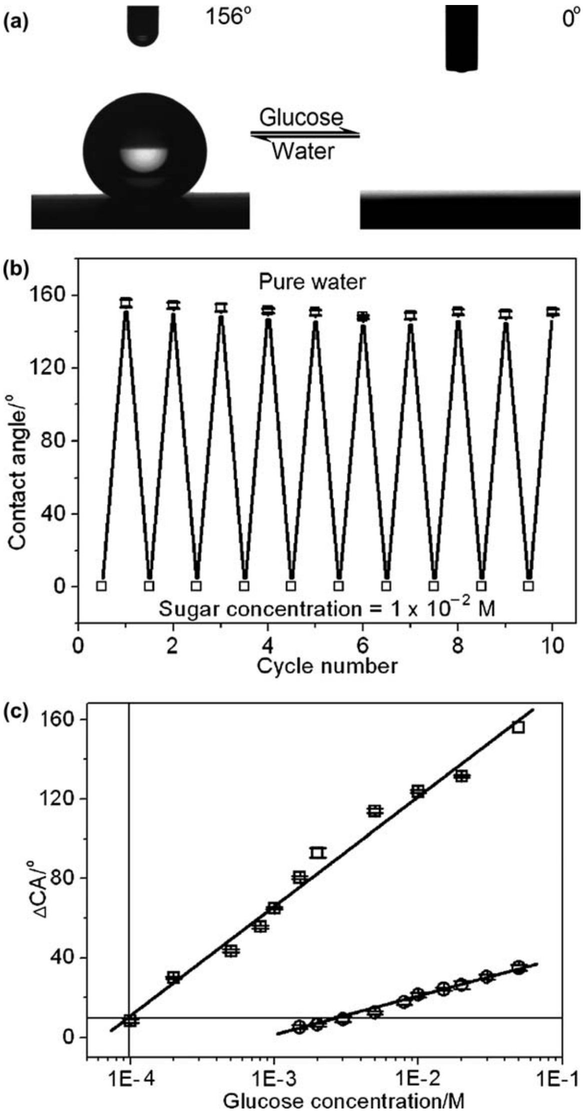

Figure 24.7 Changes in the water contact angle of a PATPBA-co-PNIPAAm film as a function of sugar concentration. (a) Glucose-induced wettability switching from superhydrophobicity (in the absence of glucose) to superhydrophilicity (after treatment with 5×10^{-2} M glucose solution for 15 min.). (b) Cycling changes in contact angle values induced by immersion of the film in sugar solution for 15 min. and transfer to pure water for 5 min.; the films were dried before each measurement. (c) Dependence of the contact angle values of the PATPBA-co-PNIPAAm film (squares) and the silicon substrate (circles) on the concentration of glucose.
Reproduced from Ref. 101 with permission from The Royal Society of Chemistry.

24.5.2 Polymers and Networks Grafted Applying Radiation

Gamma radiation has been shown to be particularly useful for functionalizing surfaces with mono-, dually or even multi-responsive polymers, in order to tailor the hydrophilicity and the capability to adsorb therapeutic substances and to control the release. Depending on the monomers and the grafting conditions (absorbed dose, reaction time and temperature), three different types of structures can be formed at the surface: i) relatively long chains of polymers, each one behaving as independent bristles of a brush; ii) cross-linked polymer chains that create a hydrogel-like network; or iii) cross-linked polymer chains that form a first network, which is, in a second step, inter-penetrated by a network of the same or other nature, resulting in inter-penetrating networks (IPNs)-like structures (Figure 24.8).[79,105,106]

Silk sutures and twisted yarns have been modified, applying γ-ray irradiation, with grafted brushes of methacrylic acid (MAc) to facilitate the loading of the antimicrobial agent 8-hydroxy quinoline hydrochloride.[107] Similarly, graft polymerization of 1-vinylimidazole and acrylonitrile onto PP monofilament resulted in sutures that load and sustain the release of ciprofloxacin and tetracycline for several days.[108–112] Tests in animal models clearly evidenced the performance of these drug-eluting sutures to inhibit bacterial growth, without compromising the biocompatibility.[113] Antimicrobial surfaces have also been prepared by immobilization of silver ions on polypropylene fabrics previously grafted with acrylic acid (AAc).[114] Although the monomers involved may lead to stimuli-responsive surfaces, this feature was not tested.

Surface grafting of temperature- and pH-responsive polymers to polypropylene (PP) and polyethylene (PE) has recently been shown suitable for preparing vancomycin-eluting devices.[77] Vancomycin is one of the most frequently chosen antibiotics for the treatment of methicillin-resistant *S. aureus* (MRSA) infections associated with the use of catheters.[115] This large glycopeptide antibiotic bears a variety of functional groups, such as amine, amide, carboxylic acid or hydroxyl, and in aqueous solution it is positively charged at

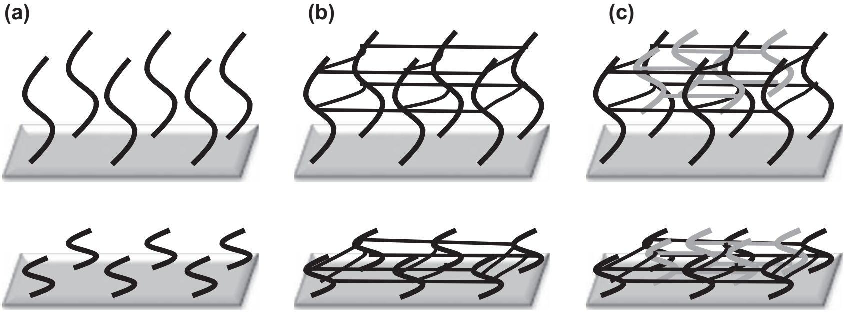

Figure 24.8 Structures that can adopt γ-ray grafted polymers at the surface of a polymeric substrate: (a) independent brushes, (b) cross-linked network and (c) inter-penetrating polymer networks.

the primary and secondary amine groups. The aim was to functionalize the surface of PP and PE with a hydrogel layer containing chemical groups with affinity for those of the drug and to take advantage of the responsiveness to the stimuli to modulate drug diffusion in (loading) and out of (release) the hydrogel. For a rational selection of the monomers, their ability to interact with the drug was screened applying isothermal titration calorimetry (ITC). Acrylic acid sodium salt resulted to be the one with the highest affinity. Three sets of surface-functionalized PP films were prepared: a) one having grafted and cross-linked poly(acrylic acid) (PP-g-PAAc) in order to achieve specific binding; b) another with grafted and cross-linked poly(*N*-isopropyl acrylamide) (PP-g-PNIPAAm), to test the effect of the volume phase transition on the drug loading and release processes; and c) the third set having inter-penetrating networks (IPNs) of PNIPAAm and PAAc, designed as *net*-PP-g-PNIPAAm-*inter*-*net*-PAAc, for combining the affinity- and swelling-controlled mechanisms of action (Figure 24.9).

The IPNs were synthesized by pre-irradiation of PP with a ^{60}Co γ-source, followed by immersion in a NIPAAm solution to induce the grafting and cross-linking of PNIPAAm onto PP, and then the second inter-penetrating network was formed by redox polymerization and cross-linking of AAc.

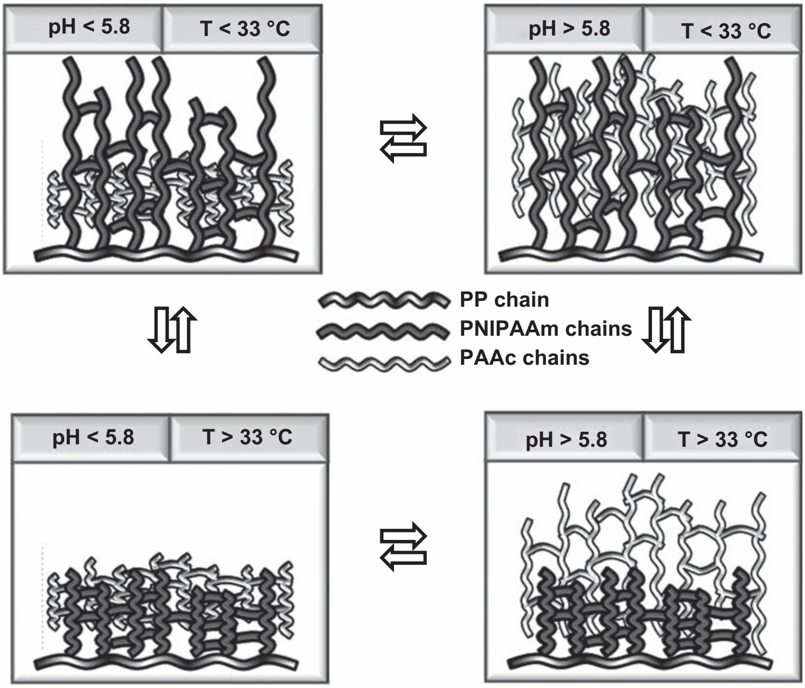

Figure 24.9 Dually temperature- and pH-responsive PNIPAAm and PAAc inter-penetrating networks grafted on polypropylene surface (namely, *net*-PP-g-PNIPAAm-*inter*-*net*-PAAc).
Reproduced from Ref. 116 with permission from Elsevier.

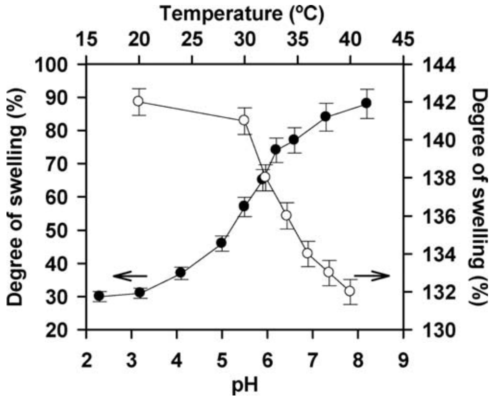

Figure 24.10 Dependence of the degree of swelling of *net*-PP-g-PNIPAAm-*inter*-*net*-PAAc on the temperature (water, open symbols) and on the pH (buffer at 37 °C, full symbols).
Reproduced from Ref. 77 with permission from Elsevier.

The *net*-PP-g-PNIPAAm-*inter*-*net*-PAAc films were both pH- and temperature-responsive with critical values in the range of 5.2–6.3 and 30–34 °C (Figure 24.10). Such a design enabled the loading of vancomycin when the IPN was swollen, *i.e.* at temperature below LCST and/or at neutral pH.[77]

Immersion of the surface-functionalized PP films in 0.4 mg mL^{-1} vancomycin aqueous solutions revealed that the grafted PNIPAAm hydrogel layer can only host 1–2 mg of vancomycin per gram, mainly in the aqueous phase of the network. PP grafted with PAAc was able to load up to 75 mg/g when previously swollen in pH 7.4 phosphate buffer to ionize the AAc groups and optimally interact with vancomycin. PP-g-PAAc films could take up almost all the drug present in the loading solution, avoiding any waste of non-sorbed drug. The *net*-PP-g-PNIPAAm-*inter*-*net*-PAAc exhibited a synergistic performance. At 20 °C the PNIPAAm hydrogel was completely swollen and made the PAAc network expand. This facilitated the contact of the drug with the acrylic acid groups and also enhanced the volume of aqueous phase entrapped into the IPN. At 37 °C the grafted IPN was capable of controlling drug release rate by the concomitance of the affinity of PAAc network and the hindering of the diffusion through the collapsed PNIPAAm mesh (Figure 24.11). Vancomycin release was sustained for 8 hours in pH 7.4 phosphate buffer owing to the strength of the drug-PAAc interactions, which are at maximum when the acrylic acid groups are ionized. Importantly from the point of view of reusability, the *net*-PP-g-PNIPAAm-*inter*-*net*-PAAc maintained its ability to uptake and to sustain the release after at least four cycles of drug loading/release. The "instantaneous" release rate of drug per surface area unit (ARR) recorded *in vitro* can be used as an index of the ability of a drug-eluting device to kill bacteria attempting to adhere to the surface.[117] For example, the minimum required flux of vancomycin that must be delivered to kill *Staphylococcus spp.* (N_{kill}) is 3.5×10^{-3} μg cm^{-2} s^{-1}. The films that combined a high

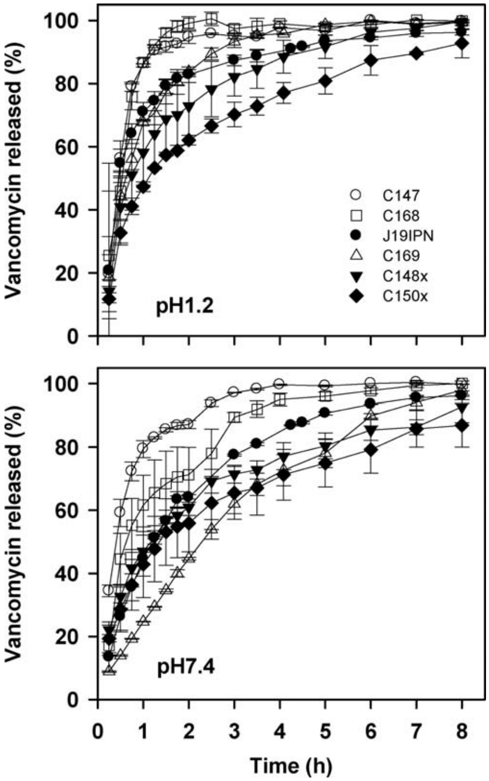

Figure 24.11 Vancomycin release profiles from PP-g-PAAc (C147, C168 and C169 with 7.12, 9.15 and 12.30 mg PAAc/cm^2, respectively), net-PP-g-PAAc (C148x cross-linked using *N*,*N*-methylenbisacrylamide and radiation and C150x cross-linked applying radiation, with 9.57 and 9.58 mg PAAc/cm^2, respectively) and *net*-PP-g-PNIPAAm-*inter*-*net*-PAAc (J19 IPN PAAc/PNIPAAm 45/55 molar ratio, 16.14 mg cm^{-2}) in HCl 0.1 M (pH 1.2) and in pH 7.4 phosphate buffer.
Reproduced from Ref. 77 with permission from Elsevier.

loading with sufficient ability to sustain the release at pH 7.4 provided ARR values above the N_{kill} for at least 6 h.[77] Fast release in the first hours following implantation has been shown to be critical in preventing the development of biofilm on catheters and implants.[118,119]

Microbiological experiments demonstrated that the vancomycin-loaded PP films have a small likelihood of biofilm formation by methicillin-resistant *Staphylococcus aureus* (MRSA). The experiments were carried out using the Modified Robbins Device (MRD) system, in which disks of PP are first subjected to the adhesion of microorganisms for 1 h and then to biofilm formation for 24 h under a continuous flow of fresh growth medium.[120] This not only creates ideal conditions for microbial growth (as nutrients are constantly provided to the bacteria and waste products are removed), but also prevents accumulation of vancomycin in the reactor since the drug released from the disks is immediately washed away. This set-up effectively reduces the contact time between the sessile bacteria and the vancomycin. Even under these extreme working conditions, the vancomycin-loaded PP disks showed a much reduced likelihood of biofilm formation by MRSA.[77]

Subsequent studies were devoted to optimizing the preparation of *net*-PP-g-PNIPAAm-*inter*-*net*-PAAc by applying γ-ray irradiation in every step of the synthesis: i) graft copolymerization of PNIPAAm onto PP films using the pre-irradiation oxidative method, ii) cross-linking of PP-g-PNIPAAm by irradiation in water to form the first network, with or without *N*,*N′*-methylenebis(acrylamide), and iii) formation of the second network through the polymerization and cross-linking of AAc inside cross-linked PP-g-PNIPAAm using a low radiation dose of 2.5 kGy.[116] These *net*-PP-g-PNIPAAm-*inter*-*net*-PAAc films loaded vancomycin up to 94 mg g^{-1} of IPN or 480 mg g^{-1} PAAc, values 2–3-fold greater than those previously obtained for the *net*-PP-g-PNIPAAm-*inter*-*net*-PAAc, in which the PAAc network was synthesized by redox polymerization (described above). It was also shown that the radiation doses applied to graft and to cross-link PNIPAAm notably determines the amount of drug loaded. The higher the PNIPAAm grafted on PP and the lower the cross-linking radiation dose, the more the PAAc that can be inter-penetrated in the IPN and, consequently, the higher the amount of vancomycin loaded through specific interactions and the more sustained the release (Figure 24.12). These effects can be explained as follows: i) the loading mainly takes place through ionic interactions between vancomycin and PAAc, and ii) the mesh creates an environment suitable for interaction with PAAc, but also with the PNIPAAm mesh through unspecific hydrophobic interactions. This explains why the amount of vancomycin loaded per gram of PAAc grafted is not constant, but increases as the content in PNIPAAm rises. Nevertheless, if the PNIPAAm network is too dense, the amount of PAAc that can be grafted decreases and the drug diffusion into the IPN is also sterically hindered. At pH 7.4 drug-loaded films sustained the delivery for several hours and provided ARR values adequate in reducing the likelihood of infection.[121] Overall these results suggest that grafting of pH- and temperature-responsive IPNs has great potential to endow PP surfaces with the ability to elute vancomycin and thus to prevent infections associated to the use of PP-based medical devices.

Simultaneous grafting of PNIPAAm and *N*-(3-aminopropyl) methacrylamide (APMA) on PP has also been investigated for obtaining interfaces that are stimuli-responsive under physiological conditions. To do that, a pre-irradiation method was implemented tuning the radiation dose, reaction time, temperature and monomers concentrations.[122] APMA combines pH-responsiveness with affinity for anionic drugs, such as the antimicrobial agent nalidixic acid. However, APMA is positively charged and cannot be grafted alone. Thus, it requires copolymerization with neutral comonomers, such as NIPAAm, to grow from the PP surface. PP-g-(1NIPAAm-r-0.5APMA), which was prepared by the immersion of pre-irradiated PP in 1 M NIPAAm/0.5 M APMA aqueous solution, exhibited an LCST (36 °C) close to that of pure PNIPAAm (34 °C). Higher APMA/NIPAAm ratios rendered too hydrophilic

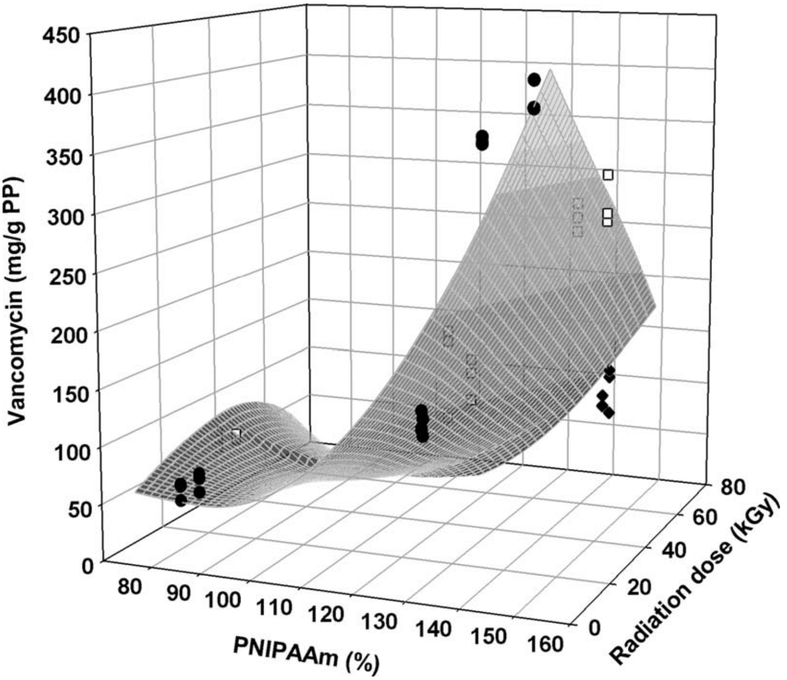

Figure 24.12 Dependence of the amount of vancomycin loaded (referred to gram of PP substrate) by *net*-PP-g-PNIPAAm-*inter*-*net*-PAAc on the amount of PNIPAAm grafted to PP (percentage referred to the weight of PP substrate) and the cross-linking dose (● 10 kGy, □ 40 kGy and ◆ 70 kGy). The response surface represents predicted values ($R^2 = 0.866$; $F_{5,36} = 59.66$; $\alpha < 0.01$).
Reproduced from Ref. 121 with permission from Elsevier.

hydrogel layers that did not shrink even when heated at 60 °C. Maintaining an APMA/NIPAAm ratio adequate to achieve temperature-responsiveness of around 37 °C, it was possible to regulate the total amount of copolymer grafted to PP varying the time of permanence of the pre-irradiated PP slabs in the monomers solution from 4 to 16 h.[123] The grafted PP slabs (initially of 1.7 mm thickness) were covered each side by 0.17–0.45 mm of copolymer layer. The surface-functionalized PP showed good hemocompatibility when tested using human blood; the improvement with respect to the pristine PP confirmed the role of APMA in the creation of biocompatible surfaces.[124] Pristine PP films did not adsorb nalidixic acid when immersed in a drug solution. The capability of PP-g-NIPAAm to load the antimicrobial agent was also minor; just 0.4 μg cm^{-2}. By contrast, the copolymerization of NIPAAm with APMA increased the ability of the grafted PP to host nalidixic acid by two orders of magnitude, attaining values of 0.036 mg cm^{-2}. The greater the content in APMA on the PP surface, the slower the release rate in phosphate buffer pH 7.4 was, due to the concomitance of two mechanisms: affinity-controlled release by

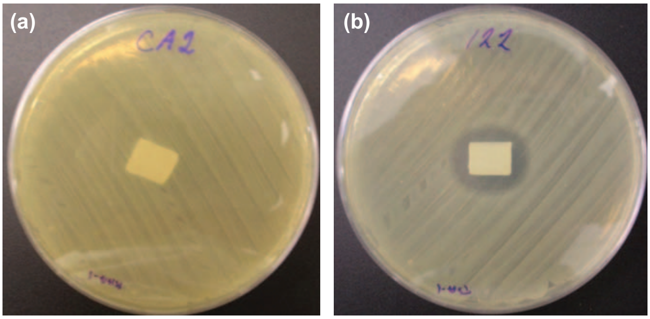

Figure 24.13 Results of the microbiological tests against *E. coli* on Müller–Hinton agar plates carried out with (a) unloaded and (b) nalidixic acid-loaded PP-g-(1NIPAAm-r-0.5APMA) slabs at 24 hours.
Reproduced from Ref. 123 with permission from Elsevier.

APMA and temperature-dependent shrinking of the mesh by NIPAAm. The antibacterial efficiency of the nalidixic acid-loaded films was evaluated *in vitro* against an *Escherichia coli* strain, which is a relevant pathogen involved in urinary catheter-related infections. Diffusion tests in Müller-Hinton agar plates revealed inhibition zones of up to 25 mm in diameter after 24 h, which were maintained for at least 6 days (Figure 24.13).

A further step on surface modification for improving hemocompatibility together with the ability to elute antimicrobial agents was the sequential grafting of *N*,*N*′-dimethylacrylamide (DMAAm) and NIPAAm on PP films applying γ-ray irradiation. The (PP-g-DMAAm)-g-NIPAAm films exhibited significantly lower hemolytic and thrombogenic activity than pristine PP. Furthermore they adsorbed serum albumin but did not uptake fibrinogen, which are considered as proteins that impede and promote, respectively, the adherence of microorganisms. Norfloxacin is a broad-spectrum antibiotic, active against Gram-positive and Gram-negative bacteria,[125] but its hydrophobicity hinders the uptake into hydrogel networks that do not posses specific groups with affinity for the drug.[126] Both DMAAm and NIPAAm could interact with norfloxacin through hydrophobic and hydrogen bonds, but more relevantly the carbonyl groups of the monomers can recognize the norfloxacin C-F bond, an interaction mechanism that occurs in many biological events.[127] DMAAm promoted the loading of norfloxacin when the hydrogel layer was swollen, reaching values of up to 13.3 mg cm^{-2}. At 37 °C, the shrinking of NIPAAm enabled the delivery to be sustained for 6 hours.[128]

A challenge in this field is to create antifouling surfaces by grafting polymers that are bactericidal by themselves, namely without adding conventional antimicrobial agents.[129–132] Even if the delivery of an antimicrobial agent is required for prophylaxis or treatment of infections, the self-microbicide surfaces have the notable advantage that, once the drug is completely eluted, the surface may still avoid adhesion or proliferation of the microorganisms. Stimuli-responsive drug-eluting self-microbicide surfaces were obtained by direct grafting of 2-(dimethylaminoethyl) methacrylate (DMAEMA) to low density polyethylene (LDPE) and silicone rubber (SR).[133] DMAEMA hydrogels exhibit temperature-responsiveness in the 30–40 °C range; the lower-critical solubility temperature (LCST) being tunable by the pH of the medium.[134,135] Furthermore, the ability of DMAEMA to interact with anionic compounds makes it a useful component of drug-delivery systems and non-viral gene carriers.[136–138] It is known that the quaternization of the amine groups of pDMAEMA increases the antimicrobial activity and reduces biofilm formation on substrates coated with this polymer.[130,139] Since long alkyl chains facilitate the insertion of the polymer into the erythrocyte membrane causing hemolysis, quaternization was carried out with short chains (namely, methyl) in order to minimize toxic effects on mammalian cells.[140] The degree of quaternization (DQ) of the grafted pDMAEMA after treatment with methyl iodide was estimated to be above 90%, using the equation

$$DQ(\%) = 100 \cdot \left(\frac{(W_3 - W_2)}{[(W_2 - W_1)(157.22/141.94)]} \right) \tag{2}$$

in which W_1, W_2 and W_3 represent the weight of pristine, grafted and quaternized films, respectively, and 157.22 and 141.94 are the molecular weights of DMAEMA and methyl iodide, respectively.

The grafting of DMAEMA occurred only at the surface of LDPE, but both at the surface and in the bulk of SR as revealed by Raman spectra. Consequently, the grafted chains caused changes in surface-related features (water contact angle and viscoelastic behavior at dry state) of LDPE and in the bulk-related properties (swelling and viscoelasticity at swollen state) of SR. Quaternization of the amine group of DMAEMA diminished water contact angles on surfaces of both LDPE and SR from 101° and 106° to 56° and 73°, respectively.[133]

Cytocompatibility tests were carried out in order to have an overall view of the potential of PE-g-DMAEMA and SR-g-DMAEMA as components of medical devices. The grafted films maintained the good cytocompatibility of the pristine material, but after quaternization fibroblast cell viability decreased although to a small extent (cell survival >70%). Microbiological tests confirmed that LDPE and SR are easily colonized by *Candida albicans* and *Staphylococcus aureus*. By contrast, surfaces grafted with DMAEMA were able to reduce *C. albicans* biofilm formation (almost no biofilm was observed on SR) and, after quaternization, inhibited *C. albicans* and *S. aureus* biofilm with more than 99% compared to pristine materials. The DMAEMA-grafted LDPE and SR films were also tested regarding the ability to host nalidixic acid at 4 °C and to sustain its release at 37 °C. Pristine LDPE adsorbed an irrelevant amount (0.0007 mg cm^{-2}) of this anionic antimicrobial drug, while pristine SR was able to load 0.004 mg per cm^2 due to swelling in the drug solution. The affinity of the drug for the films progressively increased with the grafting percentage of DMAEMA, which was swollen at 4 °C (Figure 24.14). Quaternization remarkably enhanced drug loading (up to 0.037 mg cm^{-2}) due to the interactions between the cationic groups of quaternized amine and the carboxylate anionic moieties of nalidixic acid. At 37 °C, the release of the nalidixic acid from the grafted films was sustained for 8 h, grafted LDPE slabs showing an important burst effect (20–36% in 30 min.) compared to grafted SR slabs (10–18%). In general, the release rate was slower from SR-g-DMAEMA, because the grafting to SR occurred at both the surface and the bulk (Figure 24.14) and thus nalidixic acid could diffuse during loading to inner parts that serve as reservoirs that slowly supply the drug to the surface. The drug concentrations achieved in the *in vitro* release tests were above the MIC required to inhibit the growth of *E. coli* and other frequently encountered microorganisms in urinary tract infections under the quasi-static conditions of the environment of medical implants when used *in vivo*. Then, surface functionalization with stimuli-responsive polymers that can host drugs and are microbicide by themselves may hold great promise for developing long-term antibiofouling materials.[133]

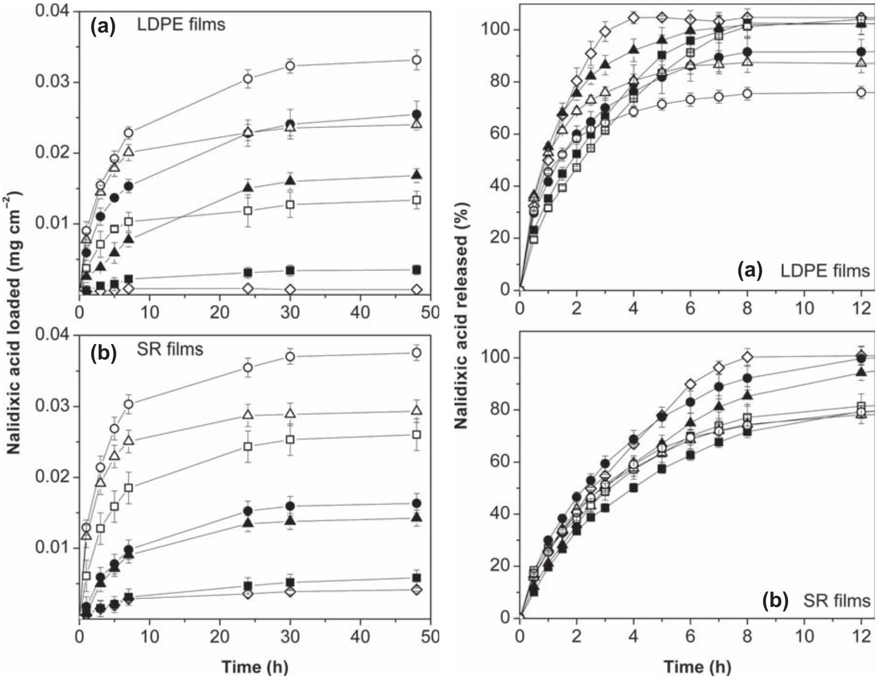

Figure 24.14 Nalidixic acid loading and release profiles from LDPE films (a): pristine LDPE (rhombus), LDPE-g-DMAEMA$_N$ films with 10% (squares), 16% (triangles) and 33% (circles) of grafting; and SR films (b): pristine SR (rhombus), SR-g-DMAEMA$_N$ films with 14% (squares), 30% (triangles) and 42% (circles) of grafting. The full and open symbols correspond, respectively, to non-ionic and quaternized DMAEMA for both graphics.
Reproduced from Ref. 133 with permission from Taylor & Francis Ltd.

In addition to γ-ray grafting techniques, electron-beam lithography has been applied to prepare precisely nanopatterned, surface-attached hydrogels whose swelling degree can be controlled by different stimuli.[141] For example, PAAc conjugated with bacteriorhodopsin was deposited on solid surfaces by spin-coating and then cross-linked applying e-beam radiation. Bacteriorhodopsin is a light-driven proton pump, found in the purple membrane of *Halobacterium Halobium*, that causes a local decrease of the pH when exposed to light.[142] In the dark the hydrogels are swollen, while when irradiated with green light, the network collapses, the system showing a reproducible response during various dark/light cycles (Figure 24.15).[143] Although the drug-eluting capability has not yet been tested, the possibilities of development in genetically engineered variants of bacteriorhodopsin responsive to different wavelengths of light may open up a range of applications for light-regulated drug-delivery systems.

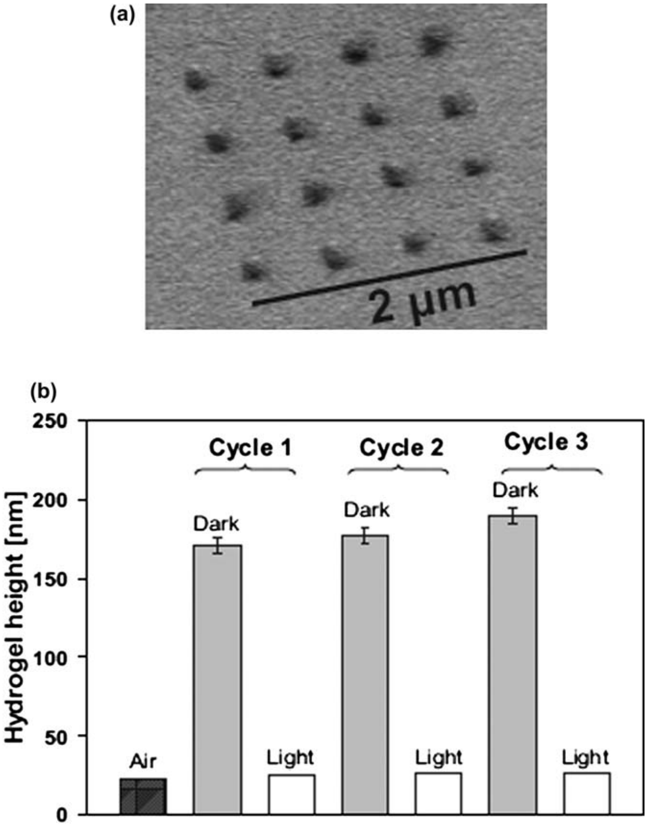

Figure 24.15 Grafted PAAc conjugated with bacteriorhodopsin: (a) SEM images and (b) dependence of the hydrogel height on the illumination conditions. Reproduced from Ref. 142 with permission from John Wiley & Sons.

24.5.3 Surface Modification Applying Plasma Techniques

Functionalization of materials by means of plasma techniques is receiving growing attention as suitable commercial equipments that work at lab scale are becoming available and novel applications are being found.[144] The techniques are easy to implement, reproducible, non-pollutant and can be performed in clean rooms.[145] Two approaches have been tested for preparing surfaces able to regulate drug loading and release: i) plasma-induced formation of reactive groups at the surface, which are used in a subsequent step to graft the polymer; and ii) plasma polymerization in one step. For example, the first approach was followed to graft poly(acrylic acid) (PAAc) on PP. To do that, PP monofilaments were exposed to oxygen plasma using an RF reactor operating at 13.6 MHz for 180 s and then transferred to ampoules containing a solution of the monomer at a controlled temperature. The treated samples were washed to remove the homopolymer adhered to the surface. The grafted amount of PAAc ranged between 24 and 290 mg cm^{-2} and did not alter the crystalline structure of the filaments. The modified PP monofilaments showed ability to uptake silver ions.[146] Similarly, metallic stents activated with silane and covered with PAAc *via* plasma polymerization have been shown to be useful for covalent immobilization of estradiol, which can be released at a constant rate as the ester linkages hydrolyze.[147] Atmospheric plasma has been used to treat PP and polyamide 6.6 fabrics in order to oxidize the surface (incorporating hydroxyl, carboxylic acid, epoxy, esters or hydroperoxide groups) and to improve the uptake of an anti-inflammatory drug.[148]

Self-regulation of insulin release as a function of the glucose concentration has been achieved by grafting poly(vinylidene fluoride) membranes (0.22 μm pore size) with PAAc, applying a plasma-graft pore-filling polymerization technique, and then conjugating glucose oxidase to the PAAc chains.[149] At neutral pH, the carboxylic acid groups of PAAc are ionized and the polymer chains are extended and entangled in the pore, acting as gates that close the pores and notably diminish the permeability of the membrane. When glucose is present in the medium, glucose oxidase hydrolyzes it and the generated glucuronic acid causes a decrease in the pH. Such acidification prompts the shrinking of the PAAc chains, which facilitates the flux of insulin solution through the pores. A 10-fold increase in the protein diffusion coefficient was registered when glucose concentration rose to 0.2 mmol L^{-1} (Figure 24.16).[149] On the other hand, grafting of PNIPAAm onto nylon and polystyrene surfaces has been achieved by pretreatment of the substrates in a He atmospheric plasma followed by graft copolymerization in NIPAAm monomer solution. It was shown that the addition of $[Fe(NH_4)_2(SO_4)_2 \cdot 6H_2O]$ suppresses the homopolymerization and enhances graft copolymerization, rendering surfaces that show temperature-responsive hydrophobicity and swelling.[150] However, the performance of these materials for drug loading/elution has not yet been tested.

Plasma polymerization enables the simultaneous deposition of the growing polymer chains and microbicide metallic nanoparticles by concurrent sputtering off the metal target. By contrast, drug molecules usually cannot stand

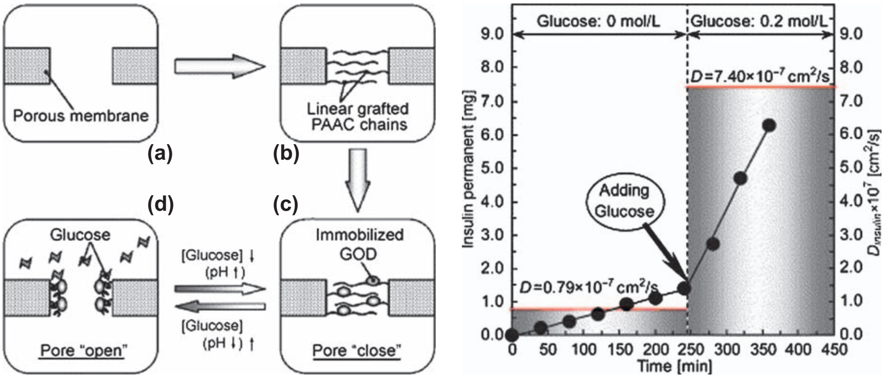

Figure 24.16 Glucose-responsive control of insulin permeation through poly(vinylidene fluoride) membranes grafted with pH-responsive poly(acrylic acid) (PAAC) brushes conjugated to glucose oxidase (GOD). At neutral pH in the absence of glucose, the carboxyl groups of the grafted PAAC chains are dissociated and extended, closing the pores. When glucose concentration increases, GOD catalyzes its oxidation into glucuronic acid, the pH becomes lower and the grafted PAAC chains shrink. The effect of the glucose concentration on the insulin diffusion coefficient through the PAAc-grafted membranes is depicted in the plot on the right.
Reprinted from Ref. 149 with permission from Elsevier.

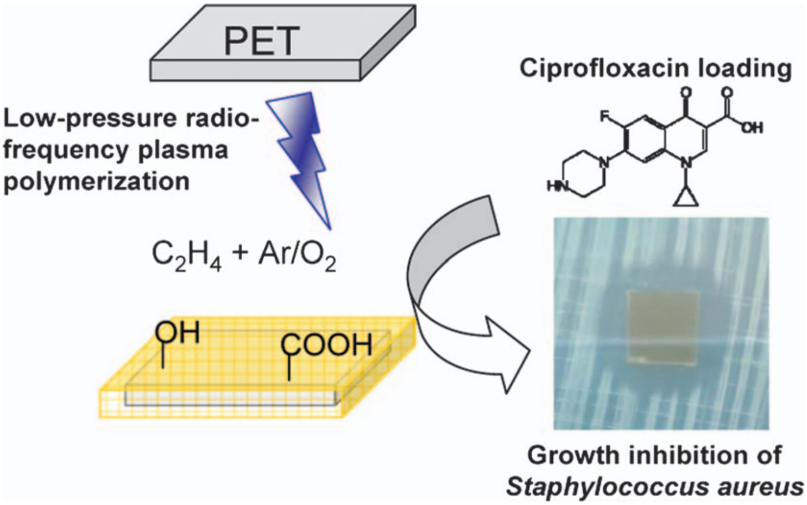
PET
Low-pressure radio-frequency plasma polymerization
$C_2H_4 + Ar/O_2$
OH
COOH
Ciprofloxacin loading
F
O
O
OH
N
N
HN
Growth inhibition of *Staphylococcus aureus*

Figure 24.17 Plasma polymerization of C_2H_4 in the presence of O_2 at various flow ratios leads to poly(ethylene terephthalate) films coated with L-PPE:O of varying thickness and oxygen content. The micrometer-thick coatings are able to load sufficient amount of ciprofloxacin and to elute it at an adequate rate to prevent the growth of bacteria responsible of biofilm formation on medical devices.
Reproduced from Ref. 151 with permission from Springer.

plasma conditions and are loaded into the plasma polymer layer after deposition, by soaking the coated device in a drug solution. If the molecular size of the compound is large, usually much bigger than that of metal ions, diffusion into the plasma polymer network might be too slow. A good example of this behavior has been shown for low-pressure plasma-polymerized ethylene film coatings rich in bonded oxygen groups (L-PPE:O) deposited on poly(ethylene terephthalate) in order to act as hosts for antimicrobial drugs.[151] L-PPE:O coatings were able to uptake ciprofloxacin but not vancomycin, a much larger antimicrobial agent. Ciprofloxacin-loaded L-PPE:O coatings sustained drug release for at least 6 hours and efficiently inhibited *in vitro* the growth of *Staphylococcus aureus* (Figure 24.17).

A suitable approach for poorly soluble drugs that find loading difficult by the presoaking of the plasma-polymer-coated device might be the spreading of drug nanocrystals on the device surface followed by the application of plasma polymerization.[29] The polymer layers ensure that the nanocrystals remain close to the device surface and, once the physiological fluids permeate in the coating, regulate the release by acting as a diffusion barrier. This approach has been successful for the entrapment of acetylsalicylic acid with allyl alcohol-based polymer.[152]

24.6 Conclusions and Future Aspects

Currently a wide range of techniques are available for the surface modification and polymer grafting from almost any substrate material. This opens up enormous potential for the development of medical devices endowed with surface functionalities for hosting drugs and eluting them at a controlled release rate. It is possible to create tailor-made outer layers, with minimal perturbation of the bulk properties, which are specifically adapted to the requirements of therapeutic treatments with specific drugs. As a result, the primary function as a medical device can be efficiently combined with the role as a drug-delivery system, rendering device-PMOA combination products. Although the number of studies is still limited, the efficiency of the drug-eluting medical devices could be notably improved if the grafted brushes/networks are able to respond to physiological or pathological stimuli. For certain applications one can envision that an optimum scenario will be the case of combination products that do not release the drug if it is not needed, but that can rapidly elute it when there is a demand. More ideally, the release should occur at a rate that fits the required therapeutic levels (neither sub- nor over-dosage) and should be switchable on/off as a function of the progression of the event (*e.g.* healing, body integration, biofouling or biofilm formation). To pave the way towards this idyllic scenario, further knowledge in the four-bands medical device-surface grafted polymer/network-drug-local site of insertion/implantation interaction is required (Figure 24.18). Namely, it is essential to know how the device composition determines the possibilities of polymer grafting, to what extent the grafting alters the bulk features of the device substrate and may offer hosting for the drug and sensitiveness to the stimulus of interest, how the drug may affect the responsiveness and also the body response to the foreign device and

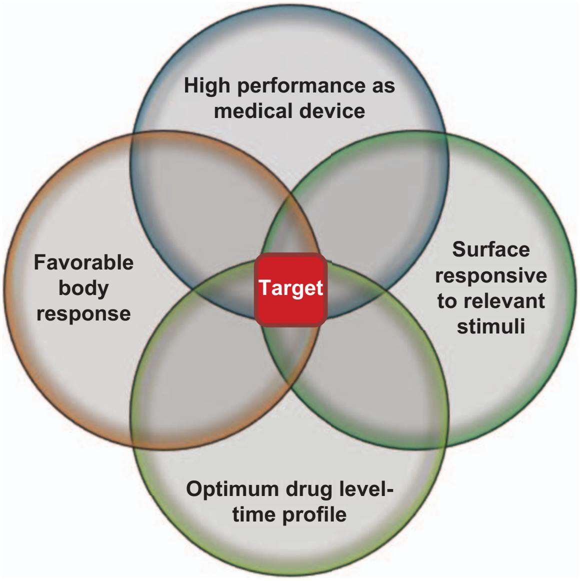
High performance as medical device
Favorable body response
Surface responsive to relevant stimuli
Target
Optimum drug level-time profile

Figure 24.18 Schematic view of the four aspects that have to be taken into account when a stimuli-responsive drug-eluting medical device is designed.

how the body response may alter the performance as a medical device and as a drug-delivery system. This knowledge should facilitate the jump from *in vitro* to *in vivo* studies and the production scale-up, and thus the commercialization of advanced device-PMOA combination products not too far in the future.

Acknowledgements

Work supported by MICINN (SAF2011-22771), Xunta de Galicia (10CSA203013PR) and FEDER.

References

1. P. Wu and D. W. Grainger, *Biomaterials*, 2006, **27**, 2450.
2. M. Zilberman and J. J. Elsner, *J. Control. Release*, 2008, **130**, 202.
3. C. Alvarez-Lorenzo, H. Hiratani and A. Concheiro, *Am. J. Drug Del.*, 2006, **4**, 131.
4. D. S. Couto, L. Perez-Breva, P. Saraiva and C. L. Cooney, *Adv. Drug Deliver. Rev.*, 2012, **64**, 69.
5. M. Donowa, *Medical Device Technol.*, 2008, **19**(6) (October), 32; 2008, **19**(7) (November/December), 26.
6. http://www.fda.gov/CombinationProducts/AboutCombinationProducts/ucm118332.htm, accessed January 2012.
7. http://www.fda.gov/CombinationProducts/AboutCombinationProducts/ucm101464.htm, accessed January 2012.

8. D. G. Amodei, M. G. Bangera, X. R. Bao, A. Bershteyn, B. Bethke, P. A. Eckhoff, K. M. Esvelt, K. B. Gustafson, E. K. Y. Jung, W. M. Kaminsky, J. T. Kare, L. Y. Kim, E. C. Leuthardt, E. Lieberman, A. Moitra, C. Somogyi, C. T. Tegreene, L. L. Wood and J. J. Zartman, *US Pat.* US 20110028945, 2011.
9. K. J. Lauritsen and T. Nguyen, *Clinical Pharm. Ther.*, 2009, **85**, 468.
10. FDA, Definition of Primary Mode of Action of a Combination Product. 21 CFR Part 3, Federal Register 2005, 70, No. 164, 49848.
11. Y. Wang and D. J. Burgess, in *Drug-Device Combination Products*, ed. A. Lewis, Woodhead Publishing Limited and CRC Press LLC, Oxford, 2010, p. 3.
12. C. Alvarez-Lorenzo, F. Yañez and A. Concheiro, *J. Drug Del. Sci. Tech.*, 2010, **20**, 237.
13. H. F. Hildebrand, N. Blanchemain, G. Mayer, F. Chai, M. Lefebvre and F. Boschin, *Surf. Coatings Technol.*, 2006, **200**, 6318.
14. M. A. Z. Hupcey and S. Ekins, *Drug Discov. Today*, 2007, **12**, 844.
15. U. A. K. Betz, *Drug Discov. Today*, 2011, **16**, 609.
16. M. Arruebo, N. Vilaboa and J. Santamaria, *Expert Opin. Drug Deliv.*, 2010, **75**, 1.
17. C. von Eiff, B. Jansen, W. Kohnene and K. Becker, *Drugs*, 2005, **65**, 179.
18. Y. Ikada, *Biomaterials*, 1994, **15**, 725.
19. J. M. Anderson, *Annu. Rev. Mater. Res.*, 2001, **31**, 81.
20. C. Indolfi, A. Mongiardo, A. Curcio and D. Torella, *Trends Cardiovasc. Med.*, 2003, **13**, 142.
21. L. Werner, *Curr. Opin. Ophthalmol.*, 2008, **19**, 41.
22. D. Pavithra and M. Doble, *Biomed. Mater.*, 2008, **3**, 034003.
23. J. M. Schierholz and J. Beuth, *J. Hosp. Infect.*, 2001, **49**, 87.
24. D. Campoccia, L. Montanaro and C. R. Arciola, *Biomaterials*, 2006, **27**, 2331.
25. J. M. Anderson, A. Rodriguez and D. T. Chang, *Semin. Immunol.*, 2008, **20**, 86.
26. D. R. Holmes, M. Savage, J. M. LaBlanche, L. Grip, P. W. Serruys, P. Fitzgerald, D. Fischman, S. Goldberg, J. A. Brinker, A. M. Zeiher, L. M. Shapiro, J. Willerson, B. R. Davis, J. J. Ferguson, J. Popma, S. B. King III, A. M. Lincoff, J. E. Tcheng, R. Chan, J. R. Granett and M. Poland, *Circulation*, 2002, **106**, 1243.
27. C. González-Chomón, A. Concheiro and C. Alvarez-Lorenzo, *Materials*, 2011, **4**, 1927.
28. J. C. Wenke and S. A. Guelcher, *Expert Opin. Drug Deliv.*, 2011, **8**, 1555.
29. K. Vasilev, S. S. Griesser and H. J. Griesser, *Plasma Process. Polym.*, 2011, **8**, 1010.
30. D. F. Williams, *Biomaterials*, 2009, **30**, 5897.
31. C. C. Perry, in *Encyclopedia of Physical Science and Technology*, ed. R. A. Meyers, Academic Press, New York, 3rd edn, 2003, p. 173.
32. S. Venkatraman, F. Boey and L. L. Lao, *Prog. Polym. Sci.*, 2008, **33**, 853.

33. J. C. Middleton and A. J. Tipton, *Biomaterials*, 2000, **21**, 2335.
34. A. L. Hook, N. H. Voelcker and H. Thissen, *Acta Biomater.*, 2009, **5**, 2350.
35. M. Vallet-Regí, M. Colilla and B. González, *Chem. Soc. Rev.*, 2011, **40**, 596.
36. L. Cormio, P. La Forgia, D. La Forgia, A. Siitonen and M. Ruutu, *Eur. Urol.*, 2001, **40**, 354.
37. X. Zhang, in *Antimicrobial/anti-infective Materials: Principles, Applications and Devices*, ed. S. P. Sawan and L. G. Manivannan, Technomic Publishing Co., Lancaster, PA, 2000, p. 149.
38. P. E. Marik, G. Abraham, P. Careau, J. Varon and R. E. Fromm Jr, *Crit. Care Med.*, 1999, **27**, 1128.
39. N. Yuecel, R. Lefering, M. Maegele, M. Max, R. Rossaint, A. Koch, R. Schwarz, M. Korenkov, J. Beuth, A. Bach, J. Schierholz, G. Pulverer and E. A. Neugebauer, *J. Antimicrob. Chemother.*, 2004, **54**, 1109.
40. D. Stengel, K. Bauwens, J. Sehouli, A. Ekkernkamp and F. Porzsolt, *Lancet Infect. Dis.*, 2001, **1**, 175.
41. H. Alvarez, C. Castro, L. Moujir, A. Perera, A. Delgado, I. Soriano, C. Evora and E. Sanchez, *J. Biomed. Mater. Res. B Appl. Biomater.*, 2008, **85B**, 93.
42. H. S. Yoo, T. G. Kim and T. G. Park, *Adv. Drug Deliver. Rev.*, 2009, **61**, 1033.
43. M. Jannesari, J. Varshosaz, M. Morshed and M. Zamani, *Int. J. Nanomed.*, 2011, **6**, 993.
44. J. Schierholz, B. Tansen, L. Taenicke and G. Pulverer, *Biomaterials*, 1994, **15**, 996.
45. J. M. Schierholz, K. Nagelschmidt, M. Nagelschmidt, R. Lefering, N. Yucel and J. Beuth, *Anticancer Res.*, 2010, **30**, 1353.
46. F. Yañez, L. Martikainen, M. E. M. Braga, C. Alvarez-Lorenzo, A. Concheiro, C. M. M. Duarte, M. H. Gil and H. C. de Sousa, *Acta Biomater.*, 2011, **7**, 1019.
47. V. P. Costa, M. E. M. Braga, J. P. Guerra, A. R. C. Duarte, C. M. M. Duarte, E. O. B. Leite, M. H. Gil and H. C. de Sousa, *J. Supercrit. Fluids*, 2010, **52**, 306.
48. A. Piozzi, I. Francolini, L. Occhiaperti, M. Venditti and W. Marconi, *Int. J. Pharm.*, 2004, **280**, 173.
49. Y. Masmoudi, L. Ben Azzouk, O. Forzano, J.-M. Andre and E. Badens, *J. Supercrit. Fluids*, 2011, **60**, 98.
50. C. W. Hwang, D. Wu and R. E. Elazer, *Int. J. Cardiovasc. Interven.*, 2003, **5**, 7.
51. T. G. Kim, H. Lee, Y. Jang and T. G. Park, *Biomacromolecules*, 2009, **10**, 1532.
52. A. Raval, J. Parikh and C. Engineer, *Ind. Engin. Chem. Res.*, 2011, **50**, 9539.
53. T. R. Thatiparti, A. J. Shoffstall and H. A. von Recum, *Biomaterials*, 2010, **31**, 2335.
54. N. Blanchemain, S. Haulon, B. Martel, M. Traisnel, M. Morcellet and H. Hildebrand, *Eur. J. Vasc. Endovasc.*, 2005, **29**, 628.

55. Y. El Ghoul, N. Blanchemain, T. Laurent, C. Campagne, A. El Achari, S. Roudesli, M. Morcellet, B. Martel and H. F. Hildebrand, *Acta Biomater.*, 2008, **4**, 1392.
56. N. Blanchemain, Y. Karrout, N. Tabary, C. Neut, M. Bria, J. Siepmann, H. F. Hildebrand and B. Martel, *Acta Biomater.*, 2011, **7**, 304.
57. H. Hao, H. Ishibashi-Ueda, M. Tsujimoto, Y. Ueda, J. Shite, G. Gabbiani, K. Fujii and S. Hirota, *Circ. J.*, 2011, **75**, 1548.
58. L. Yue, B. Ravinay and K. Levon, *J. Molecular Med. JMM*, 2011, **89**, 545.
59. L. Lei, G. Sheng-Rong, C. Wei-Luan and F. Lu, *Expert Opin. Drug Deliv.*, 2011, **8**, 813.
60. H. F. Hildebrand, N. Blanchemain, G. Mayer, F. Chai, M. Lefebvre and F. Boschin, *Surf. Coatings Technol.*, 2006, **200**, 6318.
61. A. Simchi, E. Tamjid, F. Pishbin and A. R. Boccaccini, *Nanomedicine NBM*, 2011, **7**, 22.
62. J. M. Goddard and J. H. Hotchkiss, *Prog. Polym. Sci.*, 2007, **32**, 698.
63. C. Alvarez-Lorenzo, E. Bucio, G. Burillo and A. Concheiro, *Expert Opin. Drug Deliv.*, 2010, **7**, 173.
64. S. Minko, in *Polymer Surfaces and Interfaces*, ed. M. Stamm, Springer, Berlin, 2008, p. 215.
65. J. Fristrup, K. Jankova and S. Hvilsted, *Soft Matter*, 2009, **5**, 4623.
66. K. G. Neoh and E. T. Kang, *MRS Bulletin*, 2010, **35**, 673.
67. A. D. Jenkins, R. G. Jones and G. Moad, *Pure Appl. Chem.*, 2010, **82**, 483.
68. W. A. Braunecker and K. Matyjaszewski, *Prog. Polym. Sci.*, 2007, **32**, 93.
69. P. Liu, *e-Polymers*, 2007, no. 062.
70. B. R. Coad, Y. Lu and L. Meagher, *Acta Biomater.*, 2012, **8**, 608.
71. T. Farhan and W. T. S. Huck, *Eur. Polym. J.*, 2004, **40**, 1599.
72. Y. Sugino, K. Yamamoto, Y. Miwa, M. Sakaguchi and S. Shimada, *e-Polymers*, 2003, no. 007.
73. P. Sadurni, A. Alagon, R. Aliev, G. Burillo and A. S. Hoffman, *J. Biomat. Sci. Polym. Ed.*, 2005, **16** , 181.
74. E. Bucio, A. Contreras-García, H. I. Meléndez-Ortiz, F. D. Muñoz-Muñoz, C. Alvarez-Lorenzo and A. Concheiro, in *Smart Polymeric Materials for Biomedical Applications*, ed. S. Li, A. Tiwari, M. Prabaharan and S. Aryal, Novapublishers, New York, 2010, p. 277.
75. A. Bhattacharya, *Prog. Polym. Sci.*, 2000, **25**, 371.
76. C. A. B. Nava-Ortiz, G. Burillo, E. Bucio and C. Alvarez-Lorenzo, *Radiat. Phys. Chem*, 2009, **78**, 19.
77. J. C. Ruiz, C. Alvarez-Lorenzo, P. Taboada, G. Burillo, E. Bucio, K. De Prijck, H. S. Nelis, T. Coenye and A. Concheiro, *Eur. J. Pharm. Biopharm.*, 2008, **70**, 467.
78. F. Meléndez-Ortiz and E. Bucio, *Polymer Bull*, 2008, **61**, 619.
79. A. Contreras-García, G. Burillo, R. Aliev and E. Bucio, *Radiat. Phys. Chem*, 2008, **77**, 936.
80. E. Adem, M. Avalos-Borja, E. Bucio, G. Burillo, F. F. Castillon and L. Cota, *Nucl. Instrum. Meth. B*, 2005, **234**, 471.

81. J. M. Rosiak, P. Ulanski, L. A. Pajewski, F. Yoshii and K. Makuuchi, *Radiat. Phys. Chem*, 1995, **46**, 161.
82. A. Chapiro, *Radiation Chemistry of Polymeric Systems*, Interscience, New York, 1962.
83. R. d'Agostino, P. Favia, C. Oehr and M. R. Wertheimer, *Plasma Process. Polym.*, 2005, **2**, 7.
84. L. Francesch, E. Garreta, M. Balcells, E. R. Edelman and S. Borrós, *Plasma Process. Polym.*, 2005, **2**, 605.
85. K. S. Siow, L. Britcher, S. Kumar and H. J. Griesser, *Plasma Process. Polym.*, 2006, **3**, 392.
86. Y. Yin, K. Fisher, N. J. Nosworthy, D. Bax, S. Rubanov, B. Gong, A. S. Weiss, D. R. McKenzie and M. M. M. Bilek, *Plasma Process. Polym.*, 2009, **6**, 658.
87. C. Oehr, M. Müller, B. Elkin, D. Hegemann and U. Vohrer, *Surf. Coat. Technol*, 1999, **116**, 25.
88. M. Haupt, J. Barz and C. Oehr, *Plasma Process. Polym.*, 2008, **5**, 33.
89. M. Hori and T. Goto, *Appl. Surf. Sci.*, 2007, **253**, 6657.
90. J. Friedrich, *Plasma Process. Polym.*, 2011, **8**, 783.
91. M. A. Cole, N. H. Voelcker, H. Thissen and H. J. Griesser, *Biomaterials*, 2009, **30**, 1827.
92. A. Galperin, T. J. Longand and B. D. Ratner, *US Pat.* US 20110256628, 2011.
93. M. A. C. Stuart, W. T. S. Huck, J. Genzer, M. Müller, C. Ober, M. Stamm, G. B. Sukhorukov, I. Szleifer, V. V. Tsukruk, M. Urban, F. Winnik, S. Zauscher, I. Luzinov and S. Minko, *Nat. Mater.*, 2010, **9**, 101.
94. T. Sun and G. Qing, *Adv. Mater.*, 2011, **23**, H57.
95. C. Alvarez-Lorenzo and A. Concheiro, *Mini-Rev. Med. Chem.*, 2008, **8**, 1065.
96. S. Chaterji, I. K. Kwon and K. Park, *Prog. Polym. Sci.*, 2007, **32**, 1083.
97. B. Jeong and A. Gutowska, *Trends Biotechnol.*, 2002, **20**, 305.
98. A. Lendlein and S. Kelch, *Mater. Sci. Forum*, 2005, **492**, 219.
99. M. Yoshida, R. Langer, A. Lendlein and J. Lahann, *Polym. Rev.*, 2006, **46**, 347.
100. J. Kost and R. Langer, *Adv. Drug Deliver. Rev.*, 2001, **46**, 125.
101. G. Qing, X. Wang, L. Jiang, H. Fuchs and T. Sun, *Soft Matter*, 2009, **5**, 2759.
102. Z. Zhou, S. Zhu and Z. Di, *J. Mater. Chem.*, 2007, **17**, 2428.
103. T. Tsukagoshi, Y. Kondo and N. Yoshino, *Colloids Surf. B*, 2007, **57**, 219.
104. S. Kumar, Y. L. Dory, M. Lepage and Y. Zhao, *Macromolecules*, 2011, **44**, 7385.
105. G. Burillo, E. Bucio, E. Arenas and G. P. Lopez, *Macromol. Mater. Eng.*, 2007, **292**, 214.
106. J. C. Ruiz, G. Burillo and E. Bucio, *Macromol. Mater. Eng.*, 2007, **292**, 1176.
107. H. Singh and P. K. Tyagi, *Angew. Makromol. Chem.*, 1989, **172**, 87.

108. N. Anjum, S. K. H. Gulrez, H. Singh and B. Gupta, *J. Appl. Polym. Sci.*, 2006, **101**, 3895.
109. B. Gupta, N. Anjum, S. K. H. Gulrez and H. Singh, *J. Appl. Polym. Sci.*, 2007, **103**, 3534.
110. B. Gupta, R. Jain, N. Anjum and H. Singh, *Radiat. Phys. Chem*, 2006, **75**, 161.
111. R. Jain, B. Gupta, N. Anjum, N. Revagade and H. Singh, *J. Appl. Polym. Sci.*, 2004, **93**, 1224.
112. B. Gupta, R. Jain, N. Anjum and H. Singh, *J. Appl. Polym. Sci.*, 2004, **94**, 2509.
113. B. Gupta, R. Jain and H. Singh, *Polym. Adv. Technol*, 2008, **19**, 1698.
114. J. S. Park, J. H. Kim, Y. C. Nho and O. H. Kwon, *J. Appl. Polym. Sci.*, 1998, **69**, 2213.
115. I. Raad, H. Hanna and D. Maki, *Lancet Infect. Dis.*, 2007, **7**, 645.
116. F. Muñoz-Muñoz, J. C. Ruiz, C. Alvarez-Lorenzo, A. Concheiro and E. Bucio, *Eur. Polym. J.*, 2009, **45**, 1859.
117. C. S. Kwok, C. X. Wan, S. Hendricks, J. D. Bryers, T. A. Horbett and B. D. Ratner, *J. Control. Release*, 1999, **62**, 289.
118. L. Montanaro, D. Campoccia and C. R. Arciola, *Biomaterials*, 2007, **28**, 5155.
119. C. S. Kwok, T. A. Horbett and B. D. Ratner, *J. Control. Release*, 1999, **62**, 301.
120. K. Honraet and H. J. Nelis, *J. Microbiol. Methods*, 2006, **64**, 217.
121. F. D. Muñoz-Muñoz, J. C. Ruiz, C. Alvarez-Lorenzo, A. Concheiro and E. Bucio, *Rad. Phys. Chem.*, 2012, **81**, 531.
122. A. Contreras-García, C. Alvarez-Lorenzo, A. Concheiro and E. Bucio, *Radiat. Phys. Chem*, 2010, **79**, 615.
123. A. Contreras-García, E. Bucio, A. Concheiro and C. Alvarez-Lorenzo, *React. Funct. Polym.*, 2010, **70**, 836.
124. C. H. Bamford and K. G. Al-Lamee, *Polymer*, 1996, **37**, 4885.
125. N. Rahman, Y. Ahmad and S. N. H. Azmi, *Eur. J. Pharm. Biopharm.*, 2004, **57**, 359.
126. C. Alvarez-Lorenzo, F. Yañez, R. Barreiro-Iglesias and A. Concheiro, *J. Control. Release*, 2006, **113**, 236.
127. W. K. Hagmann, *J. Med. Chem.*, 2008, **51**, 4359.
128. A. Contreras-García, E. Bucio, A. Concheiro and C. Alvarez-Lorenzo, *J. Bioact. Compat. Polym.*, 2011, **26**, 405.
129. D. Campoccia, L. Montanaro and C. R. Arciola, *Biomaterials*, 2006, **27**, 2331.
130. K. De Prijck, N. De Smet, T. Coenye, E. Schacht and H. J. Nelis, *Mycopathologia*, 2010, **170**, 213.
131. M. Sakuragi, S. Tsuzuki, S. Obuse, A. Wada, K. Matoba, I. Kubo and Y. Ito, *Mat. Sci. Eng. C Mater*, 2010, **30**, 316.
132. A. Muñoz-Bonilla and M. Fernandez-García, *Prog. Polym. Sci.*, 2012, **37**, 281.

133. A. Contreras-García, E. Bucio, G. Brackman, T. Coenye, A. Concheiro and C. Alvarez-Lorenzo, *Biofouling*, 2011, **27**, 123.
134. C. Yanfeng and Y. Min, *Radiat. Phys. Chem*, 2001, **61**, 65.
135. G. Liu, D. Wu, C. Ma, G. Zhang, H. Wang and S. Yang, *Chem. Phys. Chem*, 2007, **8**, 2254.
136. J. Guan, C. Gao, L. Feng and J. Shen, *Eur. Polym. J.*, 2001, **36**, 2707.
137. L. Bromberg, S. Deshmukh, M. Temchenko, L. Iourtchenko, V. Alakhov, C. Alvarez-Lorenzo, R. Barreiro-Iglesias, A. Concheiro and T. A. Hatton, *Bioconjugate Chem.*, 2005, **16**, 626.
138. S. Keely, S. M. Ryan, D. M. Haddleton, A. Limer, G. Mantovani, E. P. Murphy, S. P. Colgan and D. J. Brayden, *J. Control. Release*, 2009, **135**, 35.
139. L. B. Rawlinson, S. M. Ryan, G. Mantovani, J. A. Syrett, D. M. Haddleton and D. J. Brayden, *Biomacromolecules*, 2010, **11**, 443.
140. S. Venkataraman, Y. Zhang, L. Liu and Y. Y. Yang, *Biomaterials*, 2010, **31**, 1751.
141. E. Bucio, G. Burillo, E. Adem and X. Coqueret, *Macromol. Mater. Eng.*, 2005, **290**, 745.
142. D. Ho, B. Chu, H. Lee, E. K. Brooks, K. Kuo and C. D. Montemagno, *Nanotechnology*, 2005, **16**, 3120.
143. I. Saaem and J. Tian, *Adv. Mater.*, 2007, **19**, 4268.
144. G. Ozaydin-Ince, A. M. Coclite and K. K. Gleason, *Rep. Prog. Phys*, 2012, **75**, 016501.
145. C. Canal, F. Gaboriau, S. Villeger, U. Cvelbar and A. Ricard, *Int. J. Pharm.*, 2009, **367**, 155.
146. S. Saxena, A. R. Ray, J. Mindemart, J. Hilborn and B. Gupta, *Plasma Process. Polym.*, 2010, **7**, 610.
147. Y. K. Joung, H. I. Kimb, S. S. Kim, K. H. Chung, Y. S. Jang and K. D. Park, *J. Control. Release*, 2003, **92**, 83.
148. C. Labay, C. Canal and M. J. García-Celma, *Plasma Chem. Plasma Process*, 2010, **30**, 885.
149. L. Y. Chu, Y. Li, J. H. Zhu, H. D. Wang and Y. J. Liang, *J. Control. Release*, 2004, **97**, 43.
150. X. Wang and M. G. McCord, *J. Appl. Polym. Sci.*, 2007, **104**, 3614.
151. M. J. Garcia-Fernandez, L. Martinez-Calvo, J. C. Ruiz, M. R. Wertheimer, A. Concheiro and C. Alvarez-Lorenzo, *Plasma Process Polym.*, 2012, **9**, 540.
152. C. Susut and R. B. Timmons, *Int. J. Pharm.*, 2005, **288**, 253.

Subject Index

Abbreviation DDS = drug delivery systems
Page numbers in **bold** refer to figures/tables
Page numbers prefixed by 1. refer to Volume One
Page numbers prefixed by 2. refer to Volume Two

AAc. *see* polyacrylic acid
AAm (acrylamide). *see* polyacrylamide
AB/ABA-type block copolymers 1.157
ABC. *see* accelerated blood clearance phenomenon
ABCs (ATPase ATP-binding cassette superfamily) 1.116
Abelson cytoplasmic tyrosine (ABL) kinase inhibitors 1.234
ABLATE study, colorectal liver metastases 1.69, 1.70, **1.70**
accelerated blood clearance (ABC) phenomenon 1.132, 1.84, 1.86, 1.9
acetazolamide 2.238–40, **2.241**
acetylcholine 2.100
acetylcysteine 1.105
acoustic pressure, ultrasound 1.154
acoustic streaming, ultrasound 1.155, 1.167–8
acquired immune deficiency syndrome. *see* HIV/AIDS
acrylamide (AAm). *see* polyacrylamide
acrylic acid (AAc). *see* polyacrylic acid
acryloylthioureido phenylboronic acid (ATPBA) 2.327, **2.328**
activation-modulated DDS 1.2, **1.3**, 2.243, **2.244**
active excipients 1.3
active pharmaceutical ingredients, evolution 1.1
active targeting
  polymersomes 1.191, 1.198, 1.199
  reduction-sensitive nanosystems 1.210, 1.227
  ultrasound-responsive DDSs 1.160–1
actuating devices, intrinsically conducting polymers 1.292–6, **1.293**, **1.295**
acute toxicity, definitions 2.104
adamantyl capped pores 1.249, 2.79
adeno-associated virus (AAV) delivery systems 2.190
AESH (aminoethanthiol) **2.172**
ATP (adenosine-triphosphate) 1.243, 1.247–8, 1.257
ATPase ATP-binding cassette superfamily (ABCs) 1.116
administration routes
  enzyme-responsive materials 1.236–7
  hydrogels 1.238
  polymeric micelles 1.122
adrenalin **2.278**
adriamycin (ADR) 1.96
adsorption, isolated polymer phase transitions 1.12

advanced excipients 1.4–9, **1.5**, **1.7**, **1.8**
aerosol/spray-drying 2.65, 2.72
α. *see* alpha
affinity-controlled release, hydrogels. *see* imprinted hydrogels
AFM (atomic force microscopy) 1.186, **1.187**, 1.287, **1.314**
AFP (α-fetoprotein) 2.277–9, **2.279**, **2.280**
age factors, patients 1.9
age-related macular degeneration 1.100
aggregation properties
  anionic nanoparticles 1.194
  polymeric micelles 1.123, 1.126
AIBN (azobisisobutyronitrile) **2.172**, 2.203
AIDS. *see* HIV/AIDS
albumin 1.189, 1.240
alginates
  cell/tissue delivery systems **2.292**, 2.292–3
  dual responsive hydrogels 2.172
  layer-by-layer assemblies 2.125
  pH responsive microgels 2.158
  tissue engineering 2.293
alkyl acrylamide homopolymers/copolymers 2.199
alkylhalides 2.95
all-*trans* retinoic acid (ATRA) 1.102
α-amino acid based hydrogels 2.199–203, **2.201–3**, 2.224
  cisplatin 2.211–17, **2.212**, **2.213**, **2.215**, **2.216**
  future perspectives 2.221–4, **2.222–3**
  pH/ion-responsive 2.204–9, **2.207–10**, 2.210, 2.213, 2.214, 2.222
  pilocarpine 2.217–21, **2.218**, **2.219**, **2.220**
  swelling properties 2.204, **2.207**, 2.209, 2.211, 2.214, 2.217, **2.218**, 2.219, 2.221–2, **2.222**
  syntheses **2.203**, 2.203–4, **2.205**
  temperature responsive 2.209–11, 2.213, 2.221
α,β-poly(hydroxyethyl aspartamide-g-maleic anhydride) (PHEA-g-MA) 2.157–8
α-chymotrypsin 2.271, **2.272**
α-fetoprotein (AFP) 2.277–9, **2.279**, **2.280**
α-folate receptors (FR) 2.67
alternating magnetic fields (AMFs) 2.72, 2.75
aluminum phthalocyanine 1.101
Alzheimer's disease 1.20, 1.194, **1.233**, 2.100
American National Standards Institute (ANSI) 1.306–7
amino acid biomimetics 2.181, 2.182. *see also* α-amino acid based hydrogels; elastin-like recombiners
aminoethanthiol (AESH) **2.172**
aminopropyl methacrylamide (APMA) 2.333–5
aminopropyl triethoxy silane (APTES) 2.326
aminopropyl trimethoxysilane (ATMS) 2.74–5, 2.327
aminoquinoline (AQ) 1.241
aminosalicylic acid 1.239
ammonium persulfate (APS) 2.203
amphiphiles 1.179–80, **1.181**, 1.182
amphiphilic block copolymers. *see* block copolymers
amphiphilic hyperbranched polyphosphates (HPHDP) 1.214, **1.215**
amphiphilic micelles 1.308–17, **1.309**, **1.315–16**, **1.319**, 1.320–7, 2.41–4, **2.42**, **2.43**
amphiphilic oligopeptides 1.220
amphoteric hydrogels 2.208–9, 2.211, **2.212**
amphotericin B 1.80, 1.134–5, 2.99–100
amplitude mapping, polymersomes **1.187**
AND logic gates 2.80
angiogenesis, tumors 1.198. *see also* vascularisation

animal models
  biochemical-responsive DDS 1.21
  carbon nanotubes 2.107
  enzyme-responsive DDS 1.19
  low temperature sensitive liposomes 1.38, 1.60–2, 1.64
  magnetic nanoparticles 2.57, **2.58**
  polyplexes 1.258–9
  ultrasound triggered 1.165–6
anion driven actuation, polypyrrole 1.289
anionic hydrogels 2.204–8, **2.207**
anionic nanoparticles 1.193, 1.194
anisotropy, cell sheet engineering 2.303, 2.306
ANNs (artificial neural networks) 1.164
ANSI (American National Standards Institute) 1.306–7
anthracyclines 2.97. *see also* doxorubicin
anti-apoptotic gene delivery 2.300
antibiotics 2.189. *see also specific drugs by name*
antibodies
  biochemical-responsive DDS 1.21
  biomolecule-sensitive hydrogels 2.262
  enzyme prodrug therapy 1.235
anticancer drugs. *see* chemotherapeutic agents
antiepileptic drugs 2.57, **2.58**
antifungal agents 2.99–100. *see also specific drugs by name*
antigens 1.9, 1.21
  biomolecule-sensitive hydrogels 2.272–6, **2.275**, **2.276**
  mesoporous silica nanoparticles 2.79
anti-inflammatory drugs. *see also specific drugs by name*
  carbon nanotubes 2.100
  pH triggered drug release 2.129, 2.161
antimicrobial therapy 2.189. *see also specific drugs by name*
antisense oligonucleotides 1.84, 2.6
APMA (aminopropyl methacrylamide) 2.333–5
apolar solvents 2.232
apolipoproteins 1.189
approved excipients, FDA 1.122
APS (ammonium persulfate) 2.203
APTES (aminopropyl triethoxy silane) 2.326
AQ (aminoquinoline) 1.241
area under the curve (AUC)
  pH sensitive liposomes 1.89
  timolol 2.237
  ultrasound-responsive DDSs 1.156
arginineglycine-aspartic acid (RGD) peptides 1.262, 2.96
arthritis 1.240
artificial neural networks (ANNs) 1.164
asbestos 2.107–8
ascorbic acid 2.156–7
aspartic acid 1.159
aspirin 1.332, **2.326**
ATMS (aminopropyl trimethoxysilane) 2.74–5, 2.327
atom transfer radical polymerization (ATRP) 1.226, 2.271, 2.296, 2.321, 2.323, 2.325–6
atomic force microscopy (AFM) 1.186, **1.187**, 1.287, **1.314**
ATP (adenosine-triphosphate) 1.243, 1.247–8, 1.257
ATPase ATP-binding cassette superfamily (ABCs) 1.116
ATPBA (acryloylthioureido phenylboronic acid) 2.327, **2.328**
ATRA (all-*trans* retinoic acid) 1.102
ATRP (atom transfer radical polymerization) 1.226, 2.271, 2.296, 2.321, 2.323, 2.325–6
AUC. *see* area under the curve
Au NPs. *see* gold nanoparticles
autoimmune diseases 2.98. *see also* immune responses
avidin 1.108, 1.240, 1.251, 2.79

azobenzene 1.307, 1.310, 1.313–14, 1.330–2, 1.334, **1.337**
  layer-by-layer assemblies 2.138
  light responsive hydrogels 2.251, **2.252**, 2.253
  light-sensitive polymeric micelles 1.317–18, **1.318**
  light-sensitive polymeric vesicles 1.322–3
azobisisobutyronitrile (AIBN) **2.172**, 2.203
AzoMI-VPy (poly(4-phenylazomaleinanil-co-4-vinylpyridine) 1.313

bacterial infections. *see* infected tissues
bacteriorhodopsin, polymer grafting 2.338, **2.338**
BADS (bis(2-acryloyloxyethyl) disulfide) **1.226**, 1.227
basic fibroblast growth factor (bFGF) 1.264
BBB (blood–brain barrier) 1.125, 1.153
B-cell lymphoma 2 (Bcl-2) 2.300, **2.301**
BCMs. *see* block copolymer micelles
BCPs. *see* block copolymers
BCRP (breast cancer resistant protein) pump 1.125
BCS (Biopharmaceutic Classification System) 1.115
bilayers, lipid 1.34–5, **1.35**, 1.36, 1.42–3
binding agents 1.20–21
Bingel cyclopropanation 2.95
biochemical-responsive DDSs **1.17**, 1.19–21, 2.229. *see also* biomolecule-sensitive hydrogels
biocompatibility
  carrier systems 2.63
  cell/tissue delivery systems **2.292**, 2.292–3
  liposomes 2.121
  mesoporous silica nanoparticles 2.80–1
  polymer grafting 2.336
  polypyrrole 1.287–8
biodegradability, hydrogels 2.171–2
biofilms 2.316, 2.341
biofouling, combination products 2.341
bioinformatics 1.115
bioinspired networks 2.235–40, **2.236**, **2.237**, **2.238**, **2.239**
bilayers, lipid. *see* lipid bilayers
biologic primary modes of action 2.314
biological barriers 1.188, 1.197–8
biological interfaces, layer-by-layer assemblies 2.142–4
biological models, carbon nanotubes 2.106–7
biological stimuli. *see* internal stimuli
biomacromolecules 1.6
biomarkers, disease states 1.191, 2.262, 2.277–9, **2.279**
biomaterials
  definitions 1.4
  evolution 1.4, 1.5, **1.5**, 1.5–6
  first generation 1.4
  second generation 1.5
  third generation 1.6–7, **1.8**
biomedical implants. *see* implants
biomimetics 2.180–1, 2.320
biomolecular imprinting 2.277–9, **2.278**, **2.279**
biomolecule-sensitive hydrogels 2.229, 2.261–2, **2.282**, 2.282–5, **2.283**, **2.284**
  design strategies 2.262–4, **2.263**, **2.264**
  DNA sensitive **2.282**, 2.282
  glucose-sensitive 2.264–70, **2.265**, **2.267–9**
  imprinted 2.276–9, **2.278**, **2.279**
  nanoparticles 2.279–81
  protein-sensitive 2.270–6, **2.272–3**, **2.275–6**

biopersistence, carbon nanotubes 2.105, 2.108
Biopharmaceutic Classification System (BCS) 1.115
biosensing, intrinsically conducting polymers 1.286
biotin 1.108, 1.130, 1.134, 1.186, 1.251
bipolar disorder 2.222–4, **2.223**
bis (2-acryloyloxyethyl) disulfide (BADS) **1.226**, 1.227
block copolymer micelles (BCMs) 2.120, 2.127, 2.128, 2.131, 2.136, **2.136–7**
block copolymers (BCPs) 1.14, 1.194, 2.44, 2.96
  light-sensitive polymeric micelles 1.308–17, **1.309**, **1.315–16**, **1.319**, 1.320–7
  light-sensitive polymeric vesicles **1.321**, **1.324–6**
  magnetic nanoparticles 2.50–1, **2.51**
  phototriggered micelles/ nanoparticles 1.327–31, **1.332**
  surface modification **2.39**, 2.39–40
block junctions, light-sensitive micelles **1.317**, 1.317–18
blood circulation half-life, liposomes **1.46**
blood vessel fenestrations. *see* enhanced permeability and retention effect
blood–brain barrier (BBB) 1.125, 1.153
BMA (butyl methacrylate) 2.164
Boltzmann factor 2.245
bone morphogenetic proteins (BMPs) 2.192
bottom up approaches, DDSs 2.40
bovine serum albumin (BSA) 2.157, 2.249
breast cancer
  carbon nanotubes 2.96, 2.98–9
  doxorubicin **1.68**, 1.68–9
  pH responsive nanogels 2.159
  pH sensitive liposomes **1.87**, 1.88, 1.90
  ultrasound triggered 1.158, 1.164, 1.165, 1.166
breast cancer resistant protein (BCRP) pump 1.125
bright field optical microscopy 2.281
Brownian relaxation 2.35–6
brushes, polymer 2.296, **2.297**, 2.304, **2.305**, 2.320, **2.322**, 2.323, 2.325–38, **2.327**
brush-like nanosystems 1.315
butyl methacrylate (BMA) 2.164
butoxyl-capped pores 1.108

calcein 1.249–50
calmodulin (CaM) 2.284–5
camptothecin (CPT) 1.100, 1.212
  carbon nanotubes 2.99
  dendrimers, smart 1.106
  magnetic nanoparticles **2.53**, 2.53–4
  mesoporous silica nanoparticles 2.67, 2.75, 2.81
  pH responsive nanogels 2.160
cancer cells. *see* chemotherapy drugs; tumor cells
Candida spp. 2.100, 2.336
canine model of cancer 1.64
capped pores. *see also* corking
  adamantyl 1.249, 2.79
  dendrimers, smart 1.108
  layer-by-layer assemblies 2.125, **2.126**
  mesoporous silica nanoparticles 2.65, 2.66, 2.74–80
  silica nanocontainers 1.248–9
capsules, polymeric. *see also* hollow capsules; nanocapsules
  layer-by-layer assemblies 2.118, 2.120, **2.122**, 2.122, **2.123**, 2.132, **2.133**, **2.139**
  phototriggered 1.327–31, **1.328–30**

carbon nanotubes (CNTs) 2.90–3, **2.91**, **2.93**, 2.110
  encapsulation properties 2.100–3, **2.102**
  external attachment of drugs 2.96–100
  functionalization 2.91–7, **2.91**, 2.102–3, **2.103**, 2.106
  toxicity/environmental impacts 2.104–10, **2.106**
carbonic anhydrase inhibitors 2.238–40
carboplatin 1.71, 2.97–8, 2.102
carboxyfluoroscene (CF) 1.53–4, **1.54**
carboxylic acid 2.204–8, **2.207**, 2.211, **2.212**, 2.262
carboxymethyl-chitosan (CMCS) 1.89–90
cardiomyopathy 1.50
catalase 1.238
catalysts, toxicity 2.105–6, 2.108
catheters, combination products 2.319, 2.320, 2.325, 2.329
cation driven actuation 1.289
cationic nanoparticles, cytotoxicity 1.193–4
cavitation, ultrasound. *see* gas bubble cavitation
CBER (Center for Biologics Evaluation and Research) 2.315
CDs. *see* cyclodextrins
CDER (Center for Drug Evaluation and Research) 2.315
CDRH (Center for Devices and Radiological Health) 2.315
cefazolin 2.130, 2.189
cell delivery systems 2.290–1, 2.307
  cell sheet engineering 2.295–307, **2.295**, **2.297–302**, **2.304–6**
  polymeric materials used 2.291–4, **2.292**
  thermo-responsive polymers 2.294–5
cell lines, table of abbreviations **1.276**
cell membranes
  permeability 1.9
  poration damage 1.193
  stress and strain parameters 1.43
  ultrasound effects 1.165, 1.167, 1.168
cell orientation, sheet engineering 2.303–7, **2.305**, **2.306**
cell-penetrating peptides (CPP) 1.87
cell sheet engineering 2.295–307, **2.295**, **2.297–302**, **2.304–6**
cell sorting 2.33
cells, as biomaterials 1.6
cellular uptake
  carbon nanotubes 2.92
  nanoparticles 1.191–2, 2.78–9
  polymersomes **1.190**, 1.191–2, 1.194, **1.195**
cellulose derivatives 2.173
Center for Biologics Evaluation and Research (CBER) 2.315
Center for Devices and Radiological Health (CDRH) 2.315
Center for Drug Evaluation and Research (CDER) 2.315
ceramic combination products 2.317
CF (carboxyfluorescein) 1.53–4, **1.54**
chain transfer agents (CTA) 2.296, **2.297**
charge-shifting polymers 2.128, **2.128**
chemical bonding, combination products 2.320
chemical hydrogels 1.238–44, **1.239**, **1.242**
chemical initiation, polymer grafting 2.325–8
chemical polymer hydrogels
  cross-linkage 2.185–8, **2.186**
  elastin-like recombinamers **2.184**, 2.184–5
chemotherapy drugs 1.4. *see also specific drugs by name*
  α-amino acid based hydrogels 2.200, 2.211–17
  carbon nanotubes 2.99
  delivery from micelles 1.167–9
  elastin-like recombinamers 2.188–9, **2.189**, 2.193
  gold nanoparticles 2.3

  low temperature sensitive liposome 1.34
  magnetic nanoparticles 2.46–8, **2.48**
  mesoporous silica nanoparticles 2.72
  pH sensitive liposomes 1.87–9
  polymersomes 1.198
  risk-benefit ratios 2.63
  synergistic effects **2.20**
  ultrasonography synergistic effect 1.165–6
  zero premature release 2.64, 2.65
CHEMS (cholesteryl hemisuccinate) 1.81
chitosan (CHIT)
  cysteamine-conjugated 1.225–6
  dual responsive hydrogels 2.172, 2.173
  imprinted hydrogels 2.248
  layer-by-layer assemblies 2.121, 2.125, 2.129, 2.132, 2.141–2
  nanoparticles 1.193, 1.225–6
  pH responsive microgels 2.158, **2.159**
chloroquine 2.103
chloroquinone 1.264
cholesterol 1.46, 1.81
cholesteryl hemisuccinate (CHEMS) 1.81
chromatography, polymersomes 1.187
chromophores
  amphiphilic block copolymers 1.309–17
  phototriggered micelles/nanoparticles 1.328
chronic toxicity, definition 2.104
cinnamic acid 1.319
ciprofloxacin 2.341
cis-aconityl pH-responsive dendrimers **1.103**, 1.104–5
cisplatin
  α-amino acid based hydrogels 2.200, 2.202, 2.211–17, **2.212**–**13**, **2.215**–**16**
  carbon nanotubes 2.97–8, 2.101–2
  low temperature sensitive liposomes 1.71
  pH sensitive liposomes **1.85**, 1.89
  polymeric micelles **1.136**
cis–trans isomerization
  light-sensitive polymeric micelles 1.310, 1.313, 1.317, **1.318**
  light-sensitive polymeric vesicles 1.323
clathrates 1.180
clay nanoplatelets 2.119
CLDPD (CMCS-cationic liposome-coated DNA/protamine/DNA complexes) 1.90
clearance, filomicelles 1.193. *see also* accelerated blood clearance (ABC) phenomenon
cleavable linkers, carbon nanotubes 2.98
click chemistry 1.214, 1.224, **1.225**, 1.226
  elastin-like recombinamers 2.185
  layer-by-layer assemblies 2.125, 2.142
  light-sensitive polymeric micelles 1.315
  mesoporous silica nanoparticles 2.79
  silica nanocontainers 1.249
clinical trials
  changed criteria for 1.115
  doxorubicin 1.64–9, **1.66**, **1.68**, 1.70, **1.70**
  new excipients 1.7, 1.8
cloud point. *see* lower critical temperature of dissolution
CMC. *see* critical micellar concentration
CMCS (carboxymethyl-chitosan) 1.89–90
CMSC (critical micelle salt concentration) 1.123
CNTs. *see* carbon nanotubes
coacervates 2.181

coating, combination products 2.320
cochlear implants 1.297, **1.298**, 1.300
collagen
  mimics 1.99
  phase transitions 1.11
  tissue engineering 2.293
collapse cavitation, ultrasound 1.151–5, **1.152**, 1.168, 1.170
collapse transition, phase transitions 1.12–13
colloid templates
  layer-by-layer assemblies **2.119**
  magnetic nanoparticles 2.50, **2.51**
colorectal cancer
  α-amino acid based hydrogels 2.200
  animal models 1.166
  hollow capsules 1.224
  layer-by-layer assemblies 2.144
  oxaliplatin 2.98
combination products 2.313–17, **2.315**
  design strategies **2.342**
  drug-incorporation 2.318–25, **2.319**, **2.322**, **2.323**, **2.324**
  future perspectives 2.341–2
  materials used 2.317–18
  responsive surfaces 2.325–41, **2.326–32**, **2.334–5**, **2.337–8**
combination therapy 2.92
competitive displacement 2.229
  biochemical-responsive DDS 1.20–21
  imprinted hydrogels 2.240–2
composite drug-delivery membranes 2.56–9, **2.57–9**
composition-structure-property relationships 1.34, 1.35, 1.36, 1.40–51, **1.40**, **1.41**, **1.44–6**, **1.48**, **1.49**
compounding 2.318, **2.319**
concanavalin A 1.20
conductivity. *see* intrinsically conducting polymers
configurational biomimesis approach 2.238
conformational imprinting. *see* molecularly imprinted polymers
conjugate released gentamicins 1.19
conjugation properties, dendrimers 1.96
contact lenses, soft 2.235–40, **2.236**, **2.237**, **2.239**
continuous wave (CW) lasers 1.306
contrast agents
  carbon nanotubes 2.101
  magnetic resonance
    imaging 2.73–4
controlled drug release
  chemical hydrogels 1.238
  intrinsically conducting
    polymers 1.288–9
co-patterning, tissue-mimicking cell sheets 2.301–3, **2.302**
copolymer poloxamines 1.193
copper-oxicam complexes 2.200
coprecipitation, magnetic nanoparticles 2.37–8
core–corona nanostructures 2.191
core cross-linking
  polymeric micelles 1.119–20
  reduction-sensitive
    nanosystems 1.214–19, **1.215**, **1.217**
core-shell nanoparticles 2.171
corking 2.101–2, **2.102**. *see also* capped pores
cornea reconstruction 2.296–7
corneal epithelial cells 2.300
corona cross-linking 1.119–20
corona discharge **2.322**
co-solvent methods 1.128
cost-effectiveness, DDSs 1.25
Coulomb interactions 1.12
coumarin 1.249, 1.314, 1.315, 1.319, 1.326
coupled phase transitions 1.14
covalent bonds, molecularly imprinted polymers 2.230

covalent functionalization, carbon nanotubes 2.91, 2.93–5
CPPs (cell-penetrating peptides) 1.87
CPT. *see* camptothecin
creatinine 2.240, 2.242
critical micellar concentration (CMC) 1.156–8, 1.180
  light-sensitive polymeric micelles 1.308, 1.310
  polymeric micelles 1.116–19, 1.122–3, 1.126, 1.167
  reduction-sensitive nanosystems 1.219
critical micellar temperature (CMT), polymeric micelles 1.120–1, 1.122, 1.123, 1.126
critical micelle salt concentration (CMSC) 1.123
critical solubility temperature (CST), polymers 1.21–2. *see also* lower critical temperature of dissolution; upper critical solution temperature
cross-linkage. *see also* PEGylation
  α-amino acid based hydrogels 2.200, 2.204, **2.205**, 2.206, **2.209**, 2.209, 2.220, 2.221
  biomolecule-sensitive hydrogels 2.263–4, **2.264**, 2.271, 2.274, **2.284**
  chemical hydrogels 1.238, 1.238–44, **1.239**, **1.242**
  combination products, drug/medical devices 2.320
  dual-responsive hydrogels 2.170
  elastin-like recombinamers 2.185–8, **2.186**
  glucose-sensitive hydrogels 2.267–8
  hydrogels 2.235, 2.236
  imprinted hydrogels 2.238, 2.245, **2.246**, 2.248
  light-sensitive polymeric micelles 1.318–20, **1.319**
  micelles 1.163, 1.218, 1.319–20
  molecularly imprinted polymers 2.231, 2.232, 2.234–5
  polymer grafting 2.330
  polymeric capsules 1.307, 1.328–9, **1.329**
  polymeric micelles 1.119–20, 1.130, 1.135, 1.157
  poly(*N*-acryloxysuccinimide) 2.78
  reduction-sensitive nanosystems 1.214–19, **1.215**, **1.217**
cross-talk, cellular 2.297
cryogenic electron microscopy (CryoEM) 1.185, **1.187**
Cryptococcus neoformans 2.100
crystallization, phase transitions 1.13
CTA (chain transfer agents) 2.296, **2.29**
CTAB (hexadecyltrimethylammonium bromide) 2.6
curcumin 1.241
CW (continuous wave) lasers 1.306
cyclic voltametry (CV) 1.287, **1.288**
cyclo-addition reactions, carbon nanotubes 2.95
cyclodextrins (CDs) 1.116, 1.249
  combination products 2.320
  layer-by-layer assemblies **2.127**, 2.127
  mesoporous silica nanoparticles 2.75–6, 2.80
cylindrical nanoparticles 1.192
cystamine 2.78
cystaminebisacrylamide 1.265–6
cysteamine-conjugated chitosan-based nanoparticles 1.225–6
cysteine 1.105, 1.223, **1.263**, 1.264
cytokines 2.297
cytosine arabinoside 1.165
cytosine-phosphate-guanosine (CpG)-gold nanoparticles 2.6
cytosol
  pH 1.16
  reduction-sensitive nanosystems **1.211**, 1.211
cytotoxicity. *see* toxicology

daidzein 1.97
dapsone 2.100
dasatinib 1.234
daunorubicin (DNR) 2.125
DBS (dodecylbenzenesulfonate) 1.294
DBT (dibenzothiophenes) 2.248
DCC (dicyclohexylcarbodiimide) 1.158
DCM (dilated cardiomyopathy) 2.297
DDSs. *see* drug delivery systems
DEAA (diethylacrylamide) 2.236
DEAMA (diethylaminoethyl methacrylate) 2.265, 2.280, 2.281, 2.291
Debye theory 2.34, 2.36
defect group functionalization 2.93, 2.94
defences, bodily 1.37. *see also* immune responses
definitions
  biomaterials 1.4
  combination products 2.314
  enzyme-responsive materials 1.235
  gene therapy 1.200
  intelligent DDS 1.15–16
  nanogels/microgels 2.154
  new excipients 1.7
  pharmaceutical excipients 1.4
  prodrugs 1.234
  toxicity 2.104
  ultrasound 1.149
degradable hydrogels, enzyme-responsive 1.238–40, **1.239**
delayed-release 1.2
dendrimer-phthalocyanine (DPc) 1.100
dendrimers, smart 1.94–6, 1.109
  cytotoxicity 1.193
  enzyme-responsive 1.105–8, **1.106**, **1.107**
  layer-by-layer assemblies 2.129
  photoresponsive 1.100–2, **1.101**
  pH-responsive 1.102–5, **1.103**
  polyamidoamine **1.95**
  redox-responsive 1.105
  temperature-responsive 1.96–9, **1.97**
  theragnostic 1.108–9
deoxyribonucleic acid. *see* DNA
dephosphorylation/phosphorylation 1.242
dermal contact, carbon nanotubes 2.105, 2.108
device primary mode of action 2.315
dexamethasone 2.100, 2.192
dextran
  hydrogels **1.239**
  layer-by-layer assemblies 2.121, 2.129, 2.131, 2.132
  pH responsive nanogels 2.160
  temperature-responsive hydrogels 2.165
dextran-lipoic acid derivatives (Dex-LAs) 1.221–3, **1.222**
dextranases 1.239
DHLA (dihydrolipoic acid) 1.223
diabetic treatment. *see* glucose-sensitive hydrogels
diagnosis. *see* theranostics
diazonaphthoquinone (DNQ) 1.310, 1.315–16
diazoresin 2.125
dibenzothiophenes (DBT) 2.248
dichloromethane 2.102
diclofenac 1.24
dicyclohexylcarbodiimide (DCC) 1.158
diethylacrylamide (DEAA) 2.236
diethylaminoethyl methacrylate (DEAMA) 2.265, 2.280, 2.281, 2.291
diffusion-controlled drug release 2.124–5
DIGNITY breast cancer study **1.68**, 1.68–9, **1.70**, 1.70
dihydrolipoic acid (DHLA) 1.223
dilated cardiomyopathy (DCM) 2.297
diltiazem hydrochloride (DIL-HCl) 2.157

DIM (D-phenylalanine) **2.242**
dimethylacrylamide (DMAAm) 2.240
  dual responsive hydrogels 2.171
  polymer grafting 2.335
  temperature-responsive hydrogels 2.164
dimethylaminoethyl methacrylate (DMAEMA) 2.336, 2.337, **2.337**
dimethyl-1,3-dioxan-2-yloxy) ethyl acrylate (DMDEA) **1.226**, 1.227
dimethylformamide (DMF) 2.215, **2.216**
dimethyl sulfoxide (DMSO) 2.211, **2.212**, 2.215
dimyristoyl phosphatidic acid (DMPA) 2.131
dimyristoylphosphatidylcholine (DMPC) 1.45
dioleoylphosphatidylcholine (DOPC) 1.81
dioleoylphosphatidyl-ethanolamine (DOPE) 1.81, 1.262
dioleoyl-3-trimethylammonium-propane (DOTAP) 1.264
dipalmitoyl phosphatidyl choline (DPPC) 1.43, 1.71
  composition–structure–property relationships 1.45, 1.47
  lipid membrane components **1.41**, 1.41–2
  low temperature-sensitive liposome **1.54**, 1.54
  permeability **1.48**, 1.49
  in vitro performance-in-service 1.54–6, **1.55**, 1.57, 1.58
dipalmitoyl-*sn*-glycero-3-phosphoglyceroglycerol (DPPGOG) 1.71
direct sidewall functionalization, carbon nanotubes 2.93, 2.94–5
disease-responsive DDS 1.15–25, **1.17**, **1.22**, 2.161
disregulation, enzyme activity 1.232, **1.233**
disruptive enzyme-responsive micelles 1.244–6, **1.245**
distearoyl phosphatidyl choline, (DSPC) 1.44, 1.47
distearoyl phosphatidyl ethanolamine
  lipid membrane components **1.41**, 1.41–2, 1.50–1
  low temperature-sensitive liposomes 1.54, **1.54**
  in vitro performance-in-service **1.57**, 1.57, 1.57–8, 1.59
disulfonated aluminum phthalocyanine 1.101
dithionite assay, low temperature-sensitive liposome 1.54–6, **1.55**
dithiothreitol (DTT) 1.212, 1.214, 1.216, 1.218, 1.219, 1.221–3, **1.222**, 1.225, 2.78
DLS. *see* dynamic light scattering
DMAEMA (dimethylaminoethyl) methacrylate) 2.336, 2.337, **2.337**
DMDEA (dimethyl-1,3-dioxan-2-yloxy) ethyl acrylate) **1.226**, 1.227
DMF (dimethylformamide) 2.215, **2.216**
DMAAm. *see* dimethylacrylamide
DMPA (dimyristoyl phosphatidic acid) 2.131
DMPC (dimyristoylphosphatidylcholine) 1.45
DMSO (dimethyl sulfoxide) 2.211, **2.212**, 2.215
DNA damage, ultrasound triggered 1.168–9
DNA delivery systems. *see* gene delivery
DNA sensitive sol–gel transition systems 2.282, **2.282**
DNQ (diazonaphthoquinone) 1.310, 1.315–16
DNR (daunorubicin) 2.125
docetaxel 1.129
dodecylbenzenesulfonate (DBS) 1.294
dopamine 2.293

DOPC (dioleoylphosphatidylcholine) 1.81
DOPE (dioleoylphosphatidylethanolamine) 1.81, 1.262
dosage forms, evolution/development 1.1–4, **1.3**
DOTAP (dioleoyl-3-trimethylammonium-propane) 1.264
DPPC. *see* dipalmitoyl phosphatidyl choline
DPPGOG (dipalmitoyl-sn-glycero-3-phosphoglyceroglycerol) 1.71
double-walled carbon nanotubes (DWCNTs) 2.92, 2.103, **2.103**, 2.104, 2.110
doxorubicin 1.80
  carbon nanotubes 2.96–7
  dendrimers, smart 1.96, 1.100, 1.101, 1.103–4, 1.106
  enzyme-responsive DDS 1.235, 1.243, **1.245**, 1.246
  gold nanoparticles 2.3, 2.10, 2.20
  layer-by-layer assemblies 2.142
  magnetic responsive DDS 2.42, **2.42**, 2.46, 2.139–40, **2.140**
  mesoporous silica nanoparticles 2.68, 2.71, 2.72, 2.74, 2.81
  pH responsive DDS **1.85**, **1.87**, 1.88, 2.160
  polymeric micelles 1.130, 1.133, **1.136**, 1.157–8, 1.160
  polymersomes 1.198–9, 1.199–200, 1.201
  production 1.51–2, **1.52**
  reduction-sensitive DDS 1.213–14, 1.216, 1.216–18, 1.224, 1.226–7
  shell-sheddable micelles 1.210–11, **1.211**, 1.212
  temperature-responsive DDS 1.34, 1.39, **1.49**, 1.49–50, 2.167
  ultrasound triggered 1.159, 1.162–9
  in vitro performance-in-service 1.56–60, **1.56**, **1.57**, **1.59**
  in vivo performance-in-service 1.60–9, **1.62**, **1.63**, **1.66**, **1.68**
DPc (dendrimer-phthalocyanine) 1.100
D-phenylalanine (DIM) **2.242**
DPPC (dipalmitoyl phosphatidyl choline) 1.71
drug delivery systems (DDSs), general information
  advanced 1.4–9, **1.7**, **1.8**
  carrier systems **2.64**
  evolution 1.1–4, **1.3**
  future perspectives 1.25
  intelligent 1.15–25, **1.17**, **1.22**
  main approaches **1.3**
  stimuli responsive
    networks 1.9–15, **1.10**, **1.15**. *see also specific stimuli by name*
drug dissolution test 1.2
drug efflux pumps 1.9, 1.82, 1.125, 2.71–2
drug-eluting devices. *see* combination products
drug excipients. *see* excipients
drug-loaded soft contact lenses 2.235–40, **2.236**, **2.237**, **2.239**
drug partition coefficients, imprinted hydrogels 2.238
drug–polymer conjugates 1.158–9, 1.235
drug primary mode of action 2.314
drug release rates. *see* release rate
drug resistance. *see* multi-drug resistance
drug trapping liposomes 1.51
DSPC (distearoyl phosphatidyl choline) 1.44, 1.47
DTT (dithiothreitol) 1.212, 1.214, 1.216, 1.218–19, 1.221–3, **1.222**, 1.225, 2.78
dual-responsive DDS. *see also* synergistic effects
  hydrogels 2.154, 2.170–3
  mesoporous silica
    nanoparticles 2.71, 2.79–80
  polyelectrolyte complexes 1.274–5
Durapores poly(vinylidene difluoride) membranes 2.292, 2.297, **2.299**, 2.307

dynamic light scattering (DLS)
  elastin-like recombinamers 2.192
  polymersomes **1.187**
dysopsonins 2.41, 2.131

EB (electron-beam) irradiation 2.296
EBA (ethylene-bisacrylamide) 2.200, 2.204, **2.205**
ECM (extra-cellular matrix) 2.290–1, 2.294, **2.295**, 2.297, **2.298**, 2.303
EDC (ethyl- 3-(3-dimethyl-aminopropyl) carbodimide hydrochloride) 1.290–1
EDS, *see* equilibrium degree of swelling
efavirenz (EFV) 1.119, 1.124–5, **1.125**, 1.126, **1.136**
efflux pumps 1.9, 1.82, 1.125, 2.71–2
EGF. *see* epidermal growth factor
Ehrlich, Paul 1.232
Ehrlich tumors 1.89
elastic modulus liposomes 1.46, **1.46**
elastin, biomimetics 2.181
elastin-like recombinamers (ELRs) 2.181–3, **2.182**, **2.183**, 2.195–6
  hydrogels **2.184**, 2.184–90, **2.186**, **2.189**
  nanoparticles 2.190–5, **2.191**, **2.194**, **2.195**
electric field responsive DDS **1.22**, 1.24–5, 2.100
electroactive molecularly imprinted polymers (EMIP) 1.296
electrochemical responsive drug release 2.134–5, **2.135**
electro-conductive hydrogels 1.294–6. *see also* intrinsically conducting polymers
electrodes, implantable 1.297, **1.298**, 1.300
electron microscopy 1.185, **1.187**, 2.94, 2.101
electron-beam irradiation 2.296
electron-beam lithography 2.338
electron microscopy. *see* transmission electron microscopy
electronic properties, carbon nanotubes 2.92
electrophilic addition, carbon nanotubes 2.95
electrophoretic deposition (EPD) 2.56
electrospraying 2.193
electrostatic forces, intrinsically conducting polymers 1.288–9
elimination assessments, new excipients 1.7
elimination mechanisms, carbon nanotubes 2.108–9
ELRs. *see* elastin-like recombinamers
EMA (European Medicines Agency) 1.122
EMIP (electroactive molecularly imprinted polymers) 1.296
emulsion polymerization techniques 1.299
encapsulating membranes, lipid bilayers 1.43–7, **1.44**
encapsulation properties
  carbon nanotubes 2.100–3, **2.102**
  dendrimers, smart 1.96
  polymeric micelles 1.117–18, 1.123
encephalitis 1.125
endocytosis 1.86, 1.167, 1.168, 1.191, 1.192, 2.105
endoscopic submucosal dissection (ESD) 2.296–7, **2.299**
endosome, pH 1.16, 1.257
endovascular stents 2.316
engineering 1.4, **1.5**
  cell/tissue delivery systems 2.293–4
  low temperature sensitive liposomes 1.36–51, **1.38–41**, **1.44–6**, **1.48–9**
enhanced permeability and retention (EPR) effect 1.3, 1.9, 1.81, **1.82**, 1.167
  carbon nanotubes 2.99
  dendrimers, smart 1.96
  elastin-like recombinamers 2.188, **2.189**
  gold nanoparticles 2.2

enhanced permeability and retention (EPR) effect (*continued*)
  low temperature-sensitive liposome 1.37–8, **1.38**, 1.62, 1.73
  mesoporous silica nanoparticles 2.67
  new excipients 1.9
  and particle size 1.236
  pH-sensitive liposomes 1.81, **1.82**, 1.87
  polymeric micelles 1.116
  polymersomes 1.198–9
  ultrasound-responsive DDSs 1.23, 1.159–60
entangled membranes, polymersomes 1.188
Enterococcus faecalis 1.123–4
entropy-driven micellization mechanisms 1.122
entropy-driven polymersomes 1.180
environmental impacts/interactions
  carbon nanotubes **2.106**, 2.109–10
  dual responsive hydrogels 2.171
enzymatic degradation, gastrointestinal tract 1.2
enzyme cross-linkage, elastin-like recombiners 2.187
enzyme delivery, polymersomes 1.201
enzyme inhibitors 1.234
enzyme-responsive materials (ERMs) **1.17**, 1.18–19, 1.232–6, 1.251–2
  advantages/drawbacks **1.236**
  biomolecule-sensitive hydrogels 2.270–2, **2.272**
  dendrimers, smart 1.105–8, **1.106**, **1.107**
  drug design 1.236–7, **1.237**
  enzyme disregulation **1.233**
  glucose-sensitive hydrogels 2.264–5, **2.265**
  gold nanoparticles 2.20–1
  hydrogels 1.237–44, **1.239**, **1.242**
  layer-by-layer assemblies 2.141–2, **2.143**
  mesoporous silica nanoparticles 2.71, 2.79
  micelles 1.244–8, **1.245**
  silica nanocontainers **1.248**, 1.248–51, **1.249**
EPD (electrophoretic deposition) 2.56
epidermal growth factor (EGF)
  carbon nanotubes 2.98
  pH sensitive liposomes 1.89
  receptor active targeting 1.191
epilepsy 2.57, **2.58**
epirubicin 2.99
EPR effect. *see* enhanced permeability and retention effect
equilibrium degree of swelling (EDS), α-amino acid based hydrogels 2.204, 2.206–11, **2.207**, **2.208**, **2.210**, 2.214, 2.217, **2.218**, 2.219, 2.221–2, **2.222**
equilibrium polymerization, phase transitions 1.12
ERMs. *see* enzyme-responsive materials
erythrocytes, stress and strain parameters 1.43
erythromycin 2.160
Escherichia coli 2.335, 2.337
ESD (endoscopic submucosal dissection) 2.296–7, **2.299**
estrogen anchored pH-sensitive liposomes 1.86, **1.87**
ethosuximide 2.57, **2.58**
ethoxzolamide 2.238–40
ethyl- 3-(3-dimethyl-aminopropyl) carbodiimide hydrochloride (EDC) 1.290–1
ethylene-bisacrylamide (EBA) 2.200, 2.204, **2.205**
ERMs. *see* enzyme-responsive materials
ethylene glycol (EG) 2.236, **2.236**, 2.265
ethylenediamine 1.122, 1.133–4
European Medicines Agency (EMA) 1.122

excipients. *see also* drug delivery systems
  active/passive 1.3
  advanced 1.4–9, **1.5**, **1.7**, **1.8**
  evolution 1.1, 1.2
excretion. *see* elimination
explodable systems, layer-by-layer assemblies 2.122, 2.129, 2.138
extended-release DDS 1.2, 2.122, 2.125, **2.126**
external attachment of drugs, carbon nanotubes 2.91, 2.96–100, 2.101
external stimuli-responsive DDSs 1.96, 1.305, 2.2, **2.76**, 2.154. *see also* light-responsive DDS; temperature-responsive DDS
extra-cellular matrix (ECM) 2.290–1, 2.294, **2.295**, 2.297, **2.298**, 2.303
extrusion procedures, liposomes 1.51

FA. *see* folate/folic acid
FDA. *see* Food and Drug Administration
feedback-modulated DDSs 1.2, **1.3**, 2.243, **2.244**
fenestrations, tumor. *see* enhanced permeability and retention effect
fiber paradigm, pulmonary toxicology 2.107
fibrillation 1.194
fibrin 2.293
fibrinogen 1.189
field-effect transistor (FET) gates 2.266
filomicelles, clearance 1.193
first generation
  biomaterials 1.4
  excipients 1.2
first order phase transitions 1.11–12
5-fluorouracil (5-FU) 1.96, 1.166
5-fluorouracilhexyl-carbamoyl fluorouracil (HCFU) 2.166
flame treatment, polymer grafting **2.322**
flow dynamics, carbon nanotubes (CNTs) 2.92
flower-like micelles 1.127, 1.130–1
fluorescein 2.75
fluorescein isothiocyanate (FITC) 2.74
fluorescent resonance energy transfer (FRET) mechanism 2.21
fluorination, carbon nanotubes 2.95
Fmoc-Phe-*p*Tyr 1.243
folate/folic acid (FA) 1.160
  binding protein 1.160
  carbon nanotubes 2.96–7, 2.98
  gold nanoparticles 2.3
  mesoporous silica
    nanoparticles 2.67–8
  polyplexes 1.262
  tumor cell receptors 1.191
Food and Drug Administration (FDA) 1.197, 1.234
  approved excipients 1.122
  Office of Combination
    Products 2.314–15, **2.315**
force mapping, Atomic Force Microscopy **1.187**
fouling. *see* opsonisation
FR (α-folate receptors) 2.67
free-radical graft polymerization 2.321, **2.323**, 2.323–4
free radicals, ultrasound-triggered 1.152, 1.153
freeze-drying
  pH-sensitive liposomes 1.89
  polymeric micelles 1.120
FRET (fluorescent resonance energy transfer) 2.21
frustrated endocytosis 1.192, 2.105
fullerenes 2.101–2, **2.102**, 2.102
functional monomers 2.230, 2.231, 2.238
  biomolecule-sensitive 2.276
  drug-loaded soft contact
    lenses 2.235, 2.236
  pH-responsive 2.251
  stimuli-responsive imprinted
    networks 2.245
  temperature-responsive 2.245–6

functionalization
  carbon nanotubes 2.91–7, **2.91**, 2.102–3, **2.103**, 2.106
  combination products 2.325–38, **2.326–32**, **2.334–5**, **2.337–8**
  plasma polymerization 2.339–41
fusogenic liposomes 1.82–3, 1.86
future perspectives
  α-amino acid based hydrogels 2.221–4, **2.222–3**
  combination products 2.341–2
  imprinted hydrogels 2.254
  mesoporous silica nanoparticles 2.81–2
  ultrasound-responsive DDSs 1.169–70

gadolinium 1.196, 1.197, 2.73, 2.101
galactose 2.144
gamma ray polymer grafting **2.322**, 2.323–4, **2.329**, 2.329–38
gammainterferon-inducible lysosomal thiol reductase (GILT) **1.209**, 1.210
gas bubble cavitation 1.150–5, **1.152**, 1.163, 1.168, 1.170. *see also* microbubbles
gastrointestinal tract
  doxorubicin toxicity 1.50
  drug release in 1.239
  enzyme-responsive materials 1.236–7
  pH responsive DDS 1.16, 1.102, 2.129, 2.154, 2.155
gate effects, imprinted hydrogels 2.240, 2.242, **2.248**, 2.248–9. *see also* capped pores
gel phases. *see* phase transitions
gene delivery (for gene therapy) 1.4. *see also* RNA
  cell/tissue delivery systems 2.300
  elastin-like recombinamers 2.190, 2.192
  gold nanoparticles 2.6, **2.8**, 2.16–17, **2.18**
  layer-by-layer assemblies 2.124, 2.126, 2.135
  magnetic nanoparticles 2.48–50, **2.50**
  mesoporous silica nanoparticles 2.71–2
  pH-sensitive liposomes **1.85**, 1.89–90
  phase transitions 1.11–12
  polymeric micelles 1.135
  polymersomes 1.200
  polyplexes 1.256–8, 1.261–7, **1.263**, 1.269–70, **1.273**, 1.273–4
  ultrasound-sensitive systems 1.154
gene silencing effect 2.13
genotoxicity. *see also* toxicology
  carbon nanotubes 2.109, 2.110
  definitions 2.104
  new excipients 1.9
gentamicin 2.130
GFP (green fluorescent protein) 1.201
giant unilamellar vesicles (GUVs) 1.35, 1.43, 1.44, **1.45**. *see also* low temperature sensitive liposomes
GILT (gammainterferon- inducible lysosomal thiol reductase) **1.209**, 1.210
G-insulin (synthetic glycosylated insulin) 2.291
glass transitions 1.13
glaucoma 2.203, 2.211, 2.236. *see also* pilocarpine
glucose oxidase (GOD) 1.238
  combination products **2.340**
  glucose-sensitive hydrogels **2.265**, 2.265
  insulin cell/tissue delivery systems 2.291
glucose-responsive DDS. *see also* insulin
  biomolecule-sensitive hydrogels 2.262, 2.264–70, **2.265**, **2.267–9**
  combination products 2.339–40, **2.340**
  layer-by-layer assemblies 2.141
  nanocarriers 1.20

glutathione tripeptide (g-glutamyl-cysteinyl-glycine) 1.209, **1.209**. *see also* redox-responsive drug release
glycerylphosphorylcholine 1.34–5, **1.35**, 1.43, 1.46, 1.47
glycine-proline-(hydroxy)proline (Gly-Pro-Pro (Hyp)) 1.99
glycolphosphatidylethanolamine conjugates 1.161
glycosidases 1.19
GOD. *see* glucose oxidase
gold nanoparticles 2.1–7, **2.3**, **2.4**, **2.5**, 2.7, **2.8**, 2.23
  carbon nanotubes 2.101–2
  cytotoxicity 1.193
  dendrimers, smart 1.108
  enzyme-responsive 2.20–1
  glutathione-responsive 2.10, **2.12**
  layer-by-layer assemblies 2.119–20, **2.120**, 2.137–8
  light-responsive DDSs 1.23
  mesoporous silica nanoparticles 2.77
  pH-responsive DDS **2.9**, 2.9–10, **2.11**
  photo-active/photodynamic 2.10–14, **2.13**, **2.15**
  photothermal therapy 1.100, 2.14–20, **2.16**, **2.17**, **2.18**, **2.19**
  surface modification 2.39
  synergistic effects **2.20**, 2.20
  temperature-responsive DDS 1.22
  theranostics 2.21–3, **2.22**, **2.23**
Golgi apparatus 1.16
graft copolymers 1.313, 1.323
grafting-from/to 2.321. *see also* polymer grafting
Graham, Thomas 1.237
green fluorescent protein (GFP) 1.201
griseofulvin 1.123
growth factors
  electric field responsive DDS 1.25
  hepatocyte 2.298, **2.300**
  layer-by-layer assemblies 2.142–3
guar gum 2.165
GUVs. *see* giant unilamellar vesicles
gyrase subunit B (GyrB) 2.285

Halobacterium halobium 2.338
HB (hypocrellin B) 2.138
Hc (hysteresis coercivity) 2.37
HCC (hepatocellular carcinoma) 1.65–8, **1.66**, 1.258–9
HCFU (5-fluorouracilhexyl-carbamoyl fluorouracil) 2.166
HDF. *see* human dermal fibroblast
HDPE (high-density polyethylene) 2.220–1
HEAA (hydroxyethyl acrylamide) 2.240
HEAT study, HepatoCellular Carcinoma 1.67–8, **1.70**, 1.70
heating, ultrasound 1.150. *see also* temperature-responsive DDS
helix-to-random coil transitions 1.11–12
HEMA. *see* hydroxyethylmethacrylate
hemoglobin **2.276**
Henderson–Hasselbalch equation 2.206
heparin 2.125, 2.284, **2.284**
hepatitis C virus (HCV) 1.116
hepatocarcinoma 1.104
hepatocellular carcinoma (HCC) 1.65–8, **1.66**, 1.258–9
hepatocyte growth factor (HGF) 2.298, **2.300**
hepatocytes
  cell/tissue delivery systems 2.293
  tissue-mimicking cell sheets **2.302**, 2.302
HER2 complex (human epidermal growth factor receptor) 1.160
hexadecyltrimethylammonium bromide (CTAB) 2.6
hexamethylamine 2.102
hierarchical delivery systems, layer-by-layer assemblies 2.122–3, **2.123**

high-affinity binding sites **2.232**, 2.234, 2.235, 2.236. *see also* imprinted hydrogels
high-density polyethylene (HDPE) 2.220–1
high-energy radiation 2.187
high frequency ultrasound (HIFU) 1.70, **1.70**, 1.149–50
high-frequency magnetic field (HFMF) 2.35, **2.43**, **2.55**, **2.56**, **2.57**. *see also* magnetic nanoparticles
high-performance liquid chromatography (HPLC) **1.258**
high-resolution transmission electron microscopy (HRTEM) 2.54, **2.55**
histamine H1-receptor 2.238
histidine monomers **2.205**, 2.208–9, **2.209**, 2.218, 2.219, **2.219**, 2.220
histidine-rich peptides 1.257, 1.262
HIV-1 encephalitis (HIVE-1) 1.125
HIV/AIDS 1.124–5, 1.234
HLB. *see* hydrophilic-lipophilic balance
HNE (human neutrophil elastase) 1.240
hollow capsules
  reduction-sensitive
    nanosystems 1.223–6, **1.225**
  layer-by-layer assemblies 2.118
hollow vesicles 2.194–5, **2.195**
homeostasis, and DDSs 1.3
hormones, bodily release 2.153–4
horse spleen ferritin (HSF) 1.325
horseradish peroxidase (HRP) 1.201
HPC (hydroxypropylcellulose) 2.173
HPHDP (hyperbranched polyphosphates) 1.214, **1.215**
HPLC (high-performance liquid chromatography) **1.258**
HPMA (hydroxypropyl methacrylamide) 1.158, 2.265
HRP (horseradish peroxidase) 1.201
HRTEM (high-resolution transmission electron microscopy) 2.54, **2.55**
HSBA (hydrazinosulfonyl benzoic acid) **1.103**, 1.104
HSF (horse spleen ferritin) 1.325
human dermal fibroblast (HDF) 1.200, 2.303, 2.304, **2.304**, 2.306
human epidermal growth factor receptor II (HER2) complex 1.160
human immunodeficiency virus. *see* HIV/AIDS
human neutrophil elastase (HNE) 1.240
human serum albumin (HSA) 2.41, 2.131
human umbilical vein endothelial cells (HUVECs) 2.303
hydrazone **1.103**, 1.104–5
hydrazinosulfonyl benzoic acid (HSBA) **1.103**, 1.104
hydrogel collapse transition 1.12
hydrogel-conducting polymer composites 1.294–6
hydrogels 2.154, 2.173–4. *see also* α-amino acid based hydrogels; biomolecule-sensitive hydrogels; microgels; nanogels
  affinity-controlled
    release 2.235–43, **2.236–9**, **2.241–3**
  chemical 1.238–44, **1.239**, **1.242**
  conformational
    imprinting 1.14–15
  dual responsive 2.154, 2.170–3
  elastin-like recombinamers **2.184**, 2.184–90, **2.186**
  enzyme-responsive
    materials 1.237–44, **1.239**, **1.242**
  pH-responsive 1.18, 2.154, **2.155**, 2.155–61, **2.156**, **2.159**, 2.173–4
  physical 1.238, **2.184**, 2.184, 2.188
  properties 2.200
  temperature-responsive 2.154, **2.161**, 2.161–9, **2.162**, **2.163**, **2.166**, **2.169**, 2.173–4
hydrogen bonds 1.12, 1.19
hydrolases 1.19

hydrolysis
  imprinted hydrogels 2.242–3
  layer-by-layer assemblies 2.125–9, **2.127**, **2.128**
  phase transitions 1.14
hydrophilic building blocks 1.132–3
hydrophilic particles 1.189
hydrophilic poly(*N*-acryloylmorpholine) (PAcMo) 2.304
hydrophilic/hydrophobic balance
  α-amino acid based hydrogels 2.210
  light-sensitive micelles 1.309–20, **1.311**, **1.314**, **1.315**, **1.317**
  switching 2.154
  temperature-responsive hydrogels 2.162, **2.163**
hydrophilic-lipophilic balance (HLB), polymeric micelles 1.118, 1.122, 1.127
hydrophobic colloids 1.189
hydrophobic effect 1.35, 1.180, 1.183
hydrophobic interactions 1.12
hydrophobic poly(*N*-butyl acrylate)-co-polystyrene 1.246
hydroxyethyl acrylamide (HEAA) 2.240
hydroxyethylmethacrylate (HEMA) 2.236, 2.238, 2.240, 2.242-3, 2.291–3
hydroxyl radicals 2.187
hydroxypropylcellulose (HPC) 2.173
hydroxypropyl methacrylamide (HMPA) 1.158, 2.265
hyperbranched polyphosphates 1.214, **1.215**
hyperthermia 2.174. *see also* temperature-responsive DDS
  dendrimers, smart 1.96
  elastin-like recombinamers 2.193–4
  imprinted hydrogels 2.247
  mesoporous silica nanoparticles 2.73
  temperature-responsive nanogels 2.166
  theory 2.33, 2.34–7, **2.35**, **2.36**
  ultrasound triggered 1.165
hypocrellin B (HB) 2.138
hypo-/hyperexpression, enzymes 1.232, **1.233**
hypoxia, tumor cells 1.210
hysteresis coercivity (Hc) 2.37

IBAM (isobutylamide) group 1.98
ibuprofen
  layer-by-layer assemblies 2.132
  magnetic nanoparticles 2.42
  upper critical solution temperature 2.169
ICAM-1 (intra-cellular cell adhesion molecule 1) 1.191
ICPs. *see* intrinsically conducting polymers
IM (imprint molecules) 1.296
imaging compounds **2.41**
imatinib mesylate 1.234
imidazole 2.242–3, **2.243**
immune responses 1.9
  autoimmune diseases 2.98
  elastin-like recombinamers 2.190, 2.195
  low temperature-sensitive liposomes 1.37
  to medical devices 2.316
  opsonins 1.189
immunoglobulins 1.189, 2.272–3
immunomicelles 1.161
implantable electrodes 1.297, **1.298**, 1.299, 1.300
implants, biomedical
  biomaterials 1.5
  intrinsically conducting polymers 1.297, **1.298**, 1.299, 1.300
  layer-by-layer assemblies 2.142
  opportunistic bacteria 2.316
imprint molecules (IM) 1.296

imprinted hydrogels 2.228–9, 2.235–43, **2.236–9**, **2.241–3**
  biomolecule-sensitive 1.21, 2.229, 2.276–9, **2.278**, **2.279**
  light-responsive 2.251–4, **2.252**, **2.253**, **2.254**, 2.254
  molecular imprinting 2.229–35, **2.230**, **2.232**, **2.234**
  pH-responsive 2.249–51, **2.250**
  stimuli-responsive networks 2.243–5, **2.244**
  temperature-responsive 2.245–9, **2.246–8**
  see also molecularly imprinted polymers
in vitro performance-in-service, mesoporous silica nanoparticles 2.73
in vivo performance-in-service, polymeric micelles 1.131–2, **1.132**
indium tin oxide (ITO) 1.290, 2.134
indomethacin 1.126, 1.294
induced fit, molecularly imprinted polymers 2.235
induced metastasis, ultrasound-triggered 1.155
industrial revolution 1.2
inertial cavitation, ultrasound 1.152
infected tissues
  gold nanoparticles 2.3
  and implantable devices 2.316
  layer-by-layer assemblies 2.130, **2.131**
  pH changes 1.83, 1.134
  temperature-responsive DDS 2.154
inflamed tissues
  carbon nanotubes 2.98
  enzyme-responsive DDS 1.19
  pH changes 1.16, 1.83, 1.134
  responses to medical devices 2.316
infrared (IR) spectroscopy 1.286
infrared radiation 1.23
inhalation, carbon nanotubes 2.105, 2.107–8
inorganic mesoporous silica. *see* mesoporous silica nanoparticles
inorganic shells **2.39**, 2.40
insulin 1.238. *see also* glucose-responsive DDS
  cell/tissue delivery systems 2.290–3, **2.292**
  combination products 2.339–40, **2.340**
  competitive binding 2.229
  electric field responsive DDS 1.24
  layer-by-layer assemblies 2.141
  pH responsive microgels 2.156
  synthetic glycosylated 2.291
integrins 1.191
intelligent DDS. *see* stimuli-responsive DDSs
interdisciplinary research
  biomaterials 1.6
  excipients 1.4
internal stimuli-responsive DDSs. *see* self-regulated DDS
interpenetrating polymer networks (IPNs) 1.157, 2.330
  biomolecule-sensitive hydrogels 2.271, **2.272**, 2.274, **2.275**, **2.276**
  dual-responsive hydrogels 2.173
  imprinted hydrogels 2.246
  polymer grafting 2.331, 2.333
  temperature-responsive hydrogels 2.165
intra-cellular cell adhesion molecule 1 (ICAM-1) 1.191
intra-ocular lens implantation 2.316
intravascular release
  doxorubicin **1.62**, 1.62–4, **1.63**
  hypothesis 1.72–3
intrinsically conducting polymers (ICPs) 1.283–5, **1.290**, 1.290–9, 1.300. *see also* polypyrrole
  biocompatibility 1.287–8
  biological applications 1.299–300
  characterization 1.286–7, **1.288**
  conducting polymer nanotubes 1.297–9
  controlled drug release mechanisms 1.288–9

DDS **1.290**, 1.290–9, **1.291**, **1.293**, **1.295**, **1.298**
electric field-responsive DDS 1.25
properties 1.285–6
inverse temperature transition (ITT) 2.182
inverted hexagonal phase, pH sensitive liposomes 1.86
inverted micelles 1.36
ionic interactions, cross-linkage 2.188
ion-responsive DDSs 1.16–18, **1.17**
α-amino acid-based hydrogels 2.202, 2.204–9, **2.207**, **2.208**, **2.209**, 2.210
IPNs. *see* interpenetrating polymer networks
iron oxide nanoparticles (IONP) 1.108. *see also* magnetic nanoparticles
iron-free apoferritin (HSAF) **1.325**, 1.325
irradiation, polymer grafting **2.322**, 2.323, 2.324, 2.329–38, **2.338**
ischemia, pH changes 1.134
isobutylamide (IBAM) group 1.98
isoprene 1.157
isothermal titration calorimetry (ITC) 2.330
isotherms, Langmuir type 1.168
isotropic (random) phase liquid crystals 1.13
ITT (inverse temperature transition) 2.182

jellyfish aggregate, polymersomes **1.181**, 1.184
Jurkat cells 2.98

KALA polyplexes 1.268
ketoprofen 2.100
ketotifen 2.238
kinases/kinase inhibitors 1.19, 1.234, 1.243, 1.247
knob elastin-like recombinamers 2.193
Kupffer cells 1.37

L-phenylalanine (LIM) 2.208, **2.242**, 2.242
L-pyroglutamic acid (Pga) 2.247
L-valine. *see* valine
laser light irradiation 1.306–7
layer-by-layer (LbL) assemblies 2.117
biological interfaces 2.142–4
biological stimuli 2.141–2, **2.143**
constituents/architectures 2.119–23, **2.120–3**
diffusion-controlled DDS 2.124–5
drug incorporation strategies 2.123–4
electrochemical/redox-responsive DDS 2.134–5, **2.135**
hydrolytic degradation 2.125–9, **2.127**, **2.128**
light-triggered DDS 2.137–9, **2.139**
magnetic field triggered DDS 2.139–40, **2.140**
pH-triggered DDS 2.129–32, **2.130**, **2.131**, **2.132**
salt-triggered DDS 2.132, **2.132**, **2.133**, 2.133–4
substrates/templates 2.117–18, **2.119**
temperature-responsive DDS 2.136–7, **2.136–7**
ultrasound-responsive DDSs 2.140–1
LCST. *see* lower critical temperature of dissolution
LDPE (low density polyethylene) 2.336, **2.337**, 2.337
leakiness, tumor cell blood vessels 1.37–8, **1.38**. *see also* enhanced permeability and retention effect
lectins
biochemical-responsive DDS 1.20
competitive binding 2.229
concanavalin A 2.268–70, **2.269**, 2.277, **2.280**, **2.281**
glucose-sensitive hydrogels 2.266–70

leukocytes, stress and strain parameters 1.43
ligand-anchored pH-sensitive liposomes 1.86, **1.87**
ligand-driven active targeting 1.3
ligand exchange method 2.39, **2.39**
light-responsive DDS **1.22**, 1.23–4. *see also* near-infrared; photodynamic therapy; ultraviolet light-responsive DDS
  dendrimers, smart 1.100–2, **1.101**
  gold nanoparticles 2.10–14, **2.13**
  imprinted hydrogels 2.251–4, **2.252**, **2.253**, **2.254**
  layer-by-layer assemblies 2.137–9, **2.139**
  mesoporous silica nanoparticles 2.70, 2.77–8
  polymer grafting 2.338
  polymeric micelles 1.304–5, 1.308–20, **1.309**, **1.311**, **1.312**, **1.314–19**
  polymeric nano-/microparticles 1.327–37, **1.328–30**, **1.332**, **1.333**, **1.335–7**, 1.338
  polymeric vesicles 1.320–7, **1.321**, **1.324–6**
  polyplexes **1.273**, 1.273–4
  release mechanisms 1.307–8
LIM (L-phenylalanine) 2.208, **2.242**, 2.242
lipases, enzyme-responsive DDS 1.19
lipid bilayers
  encapsulating membrane 1.43–7, **1.44**
  light-sensitive polymeric vesicles 1.322
  low temperature-sensitive liposome **1.41**
lipids as smart materials 1.33–6, **1.35**
  nanoparticles 1.188. *see also* liposomes; micelles
lipofectamine 1.200, 1.201
liposomes. *see also* low temperature sensitive liposomes
  comparison with polymersomes 1.190
  cytotoxicity 1.193
  elastic modulus 1.46, **1.46**
  elastin-like recombinamers 2.194
  enzyme-responsive DDS 1.19
  layer-by-layer assemblies 2.119, 2.120–1
  self-assembly 1.94
  thermo-sensitive 2.46, **2.47**
liquid crystals, phase transitions 1.13
liquid electron microscopy 1.186
liquid–liquid phase transitions 1.13
lithium α-amino acid based hydrogels 2.222–4, **2.223**
living radical polymerization (LRP) 2.296
local drug release systems, cell sheet engineering 2.298–301. *see also* targeted drug delivery
localized surface plasmon resonance (LSPR) 2.20
logic gates, AND 2.80
low density polyethylene (LDPE) 2.336, **2.337**, 2.337
low temperature-sensitive liposomes (LTSL) 1.33–6, **1.35**, 1.72–4
  future perspectives 1.69–74
  production 1.51–2, **1.52**
  reverse engineering 1.36–51, **1.38–41**, **1.44–6**, **1.48**, **1.49**
  in vitro performance-in-service 1.53–60, **1.54**
  in vivo performance-in-service 1.60–9, **1.62–3**, **1.66**, **1.68**
lower critical temperature of dissolution (LCST)
  α-amino acid based hydrogels 2.199, 2.204, 2.210
  biomolecule-sensitive hydrogels 2.262–3, **2.263**, 2.275, 2.277
  combination products 2.325–6
  core-cross-linked micelles 1.216
  dendrimers, smart 1.96–7, 1.98, 1.99
  dual-responsive hydrogels 2.173

  elastin-like recombinamers 2.181, 2.187
  glucose-sensitive hydrogels 2.266, 2.267
  gold nanoparticles 2.17
  layer-by-layer assemblies 2.137
  light-sensitive polymeric micelles 1.313, 1.320
  light-sensitive polymeric vesicles **1.321**
  magnetic nanoparticles 2.44, 2.45, 2.46
  mesoporous silica nanoparticles 2.69, 2.70
  micro-patterned surfaces 2.302
  phototriggered micelles/nanoparticles 1.338
  PNIPAAm/PMAA films 2.136
  polymer grafting 2.331, 2.336
  polymeric micelles 1.121, 1.126, 1.129
  polyplexes 1.269, 1.270, 1.271
  reduction-sensitive nanosystems 1.219, **1.220**
  switchable micelles 1.247
  temperature-responsive hydrogels 2.161, **2.161–3**, 2.162–7
  temperature-sensitive polymers 1.21–2
low-frequency ultrasound 1.149–50
low-permeability barrier layers 2.125
L-phenylalanine (LIM) 2.208, **2.242**, 2.242
L-pyroglutamic acid (Pga) **2.172**, 2.247
LRP (living radical polymerization) 2.296
LSPR (localized surface plasmon resonance) 2.20
LTSL. *see* low temperature-sensitive liposomes
luciferase 1.259, 1.261, 1.265, 1.267–8, 1.271
lung cancer 1.158
lung toxicology, fiber paradigm 2.107
L-valine. *see* valine
lysine residues 1.135, 1.262, 1.264
lysosomes 1.16, 2.100
lysosomotropic micelles 1.18

MAA. *see* methacrylic acid
macroradicals 2.187
macular degeneration 1.100
Mag-Dye@MSNs 2.74
magnetic nanoparticles (MNPs) 2.32–4, **2.33**, **2.48**, 2.59–60
  amphiphilic/organic 2.41–4, **2.42**, **2.43**
  composite membranes 2.56–9, **2.57**, **2.58**, **2.59**
  hyperthermia theory 2.33, 2.34–7, **2.35**, **2.36**
  mesoporous silica 2.51–4, **2.52**, **2.53**, 2.72–5
  nanoshells 2.50–6, **2.51**, **2.52**, **2.53**, **2.55**, **2.56**
  surface modification **2.38**, 2.38–40, **2.39**
  synthesis 2.37–8
  temperature-responsive DDS **2.44**, 2.44–50, **2.45–7**
magnetic resonance imaging (MRI) 2.33
  carbon nanotubes 2.101
  dendrimers 1.108
  imaging compounds 1.196
  mesoporous silica nanoparticles 2.66, 2.73–4
  pH-sensitive liposomes 1.90
  polymersome imaging compounds **1.196**, 1.197
  rat fibrosarcoma model 1.60–1
magnetic-responsive DDSs **1.22**, 1.24
  α-amino acid based hydrogels 2.222
  layer-by-layer assemblies 2.139–40, **2.140**
  polymersomes 1.200
main chain degradation, light-sensitive micelles 1.318

malaria **1.233**
maleic acid residues 1.135
manganese prophyrins 1.71
materials matrix, low temperature sensitive liposome **1.40**
materials science 1.4, **1.5**
  combination products 2.317
matrix metalloproteinases (MMPs) 1.239, 1.241, 2.21
  biomolecule-sensitive hydrogels 2.283–4
  dendrimers, smart 1.108
matrix type intrinsically conducting polymers 1.296–7
maximum permissible exposures (MPE) to laser light irradiation 1.306–7
MBA (methylene-bisacrylamide) 2.200, 2.204, **2.205**
MBAA biomolecule-sensitive hydrogels 2.274, **2.275**
MCM-41 mesoporous silica 2.48, **2.49**
MDR. *see* multi-drug resistance
ME (mercaptoethanol) 2.78
mechanical cavitation, ultrasound 1.150–5, **1.152**, 1.163, 1.168, 1.170. *see also* microbubbles
mechanical index (MI), ultrasound 1.153, 1.155
medicated contact lenses, soft 2.235–40, **2.236**, **2.237**, **2.239**
melanoma 1.158, 2.214, **2.215**, 2.216, **2.216**
melphalan dendrimers, smart 1.106
membrane elastic modulus liposomes 1.46, **1.46**
membranes
  bilayers. *see* lipid bilayers
  biocompatible **2.292**, 2.292–3
  composite drug-delivery 2.56–9, **2.57–9**
  phase transitions 1.14
memorization
  imprinted hydrogels 2.243–4
  responsive polymers 1.14–15
MEMS (microelectromechanical systems) 1.299
mercaptoethanol (ME) 2.78
mesoporous silica nanoparticles (MSNPs) 1.223, 1.290, 2.63–6
  biocompatibility 2.80–1
  future perspectives 2.81–2
  layer-by-layer assemblies 2.119
  magnetic 2.42, **2.43**, 2.46–8, **2.48**, **2.49**, 2.51–4, **2.52**, **2.53**, 2.72–5
  multifunctionality 2.66, **2.67**, 2.74
  polymeric coatings 2.68–72
  stimuli-responsive DDSs 2.75–80, **2.76**
  targeting agents 2.66–8
mesothelioma 2.108
metal-based drugs 2.200. *see also* carboplatin; cisplatin; oxaliplatin
metal combination products 2.317
metal-enhanced fluorescence (MEF) **2.132**
metallic stents 1.296–7
metastases
  α-amino acid based hydrogels 2.200
  enzyme-responsive DDS 1.240
  ultrasound-triggered 1.155
methacrylic acid (MAA) 2.157
  α-amino acid-based hydrogels **2.208**, 2.208
  drug-loaded soft contact lenses 2.236
  glucose-sensitive hydrogels 2.265
  imprinted hydrogels **2.236**, 2.240, 2.248
  monomers 2.203
  pH-responsive hydrogels **2.250**, 2.251
  pH-responsive microgels 2.156, 2.158
  pH-responsive nanogels 2.159–60
  polymer grafting 2.329
  temperature-responsive hydrogels 2.165, 2.245–6, **2.246**
methacryloylethyl *p*-aminobenzoate 2.242–3

methacryloyloxy ethyl phosphorylcholine (MPC) 2.271
methicillin 1.123–4
methicillin-resistant *Staphylococcus aureus*. *see* MRSA
methotrexate (MTX) 1.218
  carbon nanotubes 2.98
  dendrimers, smart 1.96, 1.102, **1.107**
  gold nanoparticles 2.3, **2.4**
  light responsive hydrogels **2.252**
  mesoporous silica nanoparticles 2.68
  polymeric micelles 1.135
methoxy poly(ethylene glycol) (MPEG) 1.160, 1.247–8
methyl methacrylate 1.319, 1.320
methyl tetrazolium test (MTT) 2.160
methylene-bisacrylamide 2.200, 2.204, **2.205**
methylmethacrylate (MMA) 2.251–4
metoprolol tartarate 2.156
MI (mechanical index), ultrasound 1.153, 1.155
micelles 1.181
  amphilic 1.308–17, **1.309**, **1.315–16**, **1.319**, 1.320–7, 2.41–4, **2.42**, **2.43**
  biochemical-responsive DDS 1.20
  comparison with liposomes 1.169–70
  delivery mechanisms 1.167–9
  dendrimers, smart 1.107, **1.107**
  elastin-like recombinamers 2.193, 2.194–5
  enzyme-responsive DDS 1.19, 1.244–8, **1.245**
  formation 1.183
  gene delivery 1.18
  layer-by-layer assemblies 2.120
  low temperature sensitive liposomes 1.36
  phase transitions 1.14
  polymeric. *see* polymeric micelles
  self-assembly 1.94, **1.181**
  temperature-responsive DDS 1.22
  ultrasound-responsive DDSs 1.155–9
Michael-type addition reaction 2.283
miconazole 2.319
micro jets 1.154
microbial colonies (biofilms) 2.316, 2.341
microbubbles. *see also* gas bubble cavitation
  layer-by-layer assemblies 2.118
  polymersome imaging compounds 1.197
microcapsules. *see* capsules
microchips
  intrinsically conducting polymers 1.292
  magnetic nanoparticles 2.57, **2.58**
microcontact printing 2.302
microelectromechanical systems (MEMS) 1.299
microencapsulation, cell/tissue delivery systems 2.290–1, **2.292**, 2.292–3
micro-fabricated thermo-responsive surfaces 2.301–7, **2.302**, **2.304**, **2.305**, **2.306**
microgels
  definitions 2.154
  pH-responsive 2.156–8
  temperature-responsive 2.163–5
microgrooved polydimethylsiloxane (PDMS) 2.303
microneedles **1.293**, 1.293–4
microorganism-triggered DDS
  enzyme-responsive 1.19
  pH responsive 1.16
microparticles, polymer. *see* polymer nano-/microparticles
micro-patterned surfaces, cell sheet engineering 2.302, **2.302**, **2.304**, **2.305**
micropipet manipulation 1.43, 1.44, 1.47
micropumps 1.292–3
MIPs. *see* molecularly imprinted polymers
mitochondria 2.100
mitomycin C 2.99

MMA (methylmethacrylate) 2.251–4
MMPs. *see* metalloproteinases
MNPs. *see* magnetic nanoparticles
model predictive control (MPC), ultrasound-responsive DDSs 1.164
models, carbon nanotubes 2.106–7
Modified Robbins Device (MRD) 2.332
modified Stõber method 2.65
molar solubilization ratio (MSR) 1.117
molecular weight, elastin-like recombinamers 2.187
molecularly imprinted polymers (MIPs) 2.229–35, **2.230**, **2.232**, **2.234**
  biochemical-responsive 1.21, 2.229, 2.276–9, **2.278**, **2.279**
  covalent bonds 2.230
  responsive polymers 1.14–15
  see also imprinted hydrogels
monoclonal antibodies 1.88, 1.161, 2.97
mononuclear phagocyte system (MPS) 1.156, 1.189
monooleoylphosphatidylcholine (MOPC) 1.48
monostearoylphosphatidylcholine (MSPC) **1.41**, 1.41–2, 1.54–6
  low temperature-sensitive liposome 1.53, **1.54**, **1.55**
  in vitro performance-in-service 1.57, **1.57**, 1.58, 1.59
mortars, evolution 1.2
MPC. *see* model predictive control
MPC (methacryloyloxy ethyl phosphorylcholine) 2.271
MPE. *see* maximum permissible exposures
MPEG (methoxy poly(ethylene glycol)) 1.160, 1.247–8
MPS (mononuclear phagocyte system) 1.156, 1.189
MRI. *see* magnetic resonance imaging
MSNPs. *see* mesoporous silica nanoparticles
MRSA (methicillin-resistant *Staphylococcus aureus*)
  combination products, drug/medical devices 2.329
  polymer grafting 2.331–2
MSPC. *see* monostearoylphosphatidylcholine
MSR (molar solubilization ratio) 1.117
MTT (methyl tetrazolium test) 2.160
MTX. *see* methotrexate
mucosal epithelial cell sheets 2.297, **2.299**
multi-drug release system, supramolecular hydrogels 1.241
multi-drug resistance (MDR) 1.82, 1.89, 2.1
  carbon nanotubes 2.97
  dendrimers, smart 1.101
  drug–polymer conjugates 1.159
  mesoporous silica nanoparticles 2.72
  polymeric micelles 1.116
  polymersomes 1.199
  reduction-sensitive nanosystems 1.212, 1.227
  tumours 1.9
multifunctionality
  carbon nanotubes 2.91, **2.91**, **2.93**, 2.94, 2.99, 2.101
  mesoporous silica nanoparticles 2.66, **2.67**, 2.74
multilayered cardiomyocyte sheets 2.303
multiple stimuli responsive polymer-based hydrogels. *see* α-amino acid based hydrogels
multi-walled carbon nanotubes (MWCNTs) 2.90, 2.92
  encapsulation properties 2.101
  environmental impacts 2.104, 2.110
  external attachment of drugs 2.96–7, 2.99–100
  toxicity 2.104, 2.106, 2.107, 2.108
myoblast sheets 2.297, **2.300**, 2.300, **2.301**

myocardial infarction 2.298, 2.300, 2.303
Myocet 1.34

NADPH (nicotinamide adenine dinucleotide phosphate) 1.201, 1.210, 1.239
NaAlg (sodium alginate) 2.158. *see also* alginates
nalidixic acid 2.333–7, **2.335**, **2.337**
N-alkyl acrylamide homopolymers 2.199
nanocaps/gates 2.74–5, 2.77, 2.79–80. *see also* capped pores
nanocapsules 1.34, 2.41, 2.118
nanocarriers, glucose-responsive 1.20
nanocontainers
  carbon 2.100–3, **2.102**
  silica **1.248**, 1.248–51, **1.249**. *see also* mesoporous silica nanoparticles
nanogels
  definitions 2.154
  magnetic nanoparticles 2.58, 2.59, **2.59**
  pH-responsive 2.158–61
  phototriggered 1.331–4, **1.332**, **1.333**
  reduction-sensitive **1.226**, 1.226–7
  temperature-responsive DDS 1.22, 2.166–7
  tumor-targeted delivery 1.18
nanoparticles 1.188. *see also* dendrimers; gold nanoparticles; liposomes; mesoporous silica nanoparticles; micelles; polymer nanoparticles; polymersomes
  biomolecule-sensitive hydrogels 2.279–81
  cellular internalisation mechanism 1.191–2
  elastin-like recombinamers 2.190–5, **2.191**, **2.194**, **2.195**
  low temperature sensitive liposomes 1.62
  organic 2.41–4, **2.42**, **2.43**
  reduction-sensitive nanosystems 1.221–3, **1.222**
nanopores 1.59–60
nanoreactors 1.201
nanoshells, magnetic nanoparticles 2.50–6, **2.51**, **2.52**, **2.53**, **2.55**, **2.56**
nano-straws, carbon nanotubes 2.101
nanostructured conducting polymers 1.297–9
nanotechnology 1.3, 1.188, 1.195
nanothermometers 2.101
nanowire arrays 1.299
naproxen 1.126
nature-designed materials 1.5
$NaYF_4$ **1.316**, 1.316–17
NBA (nitrobenzyl methacrylate) 2.326
Néel relaxation 2.36
near infrared fluorophores (NIRF) 1.196–7
near-infrared radiation (NIR) 1.23, 1.305–7
  carbon nanotubes 2.92
  gold nanoparticles 2.14
  layer-by-layer assemblies 2.138
  micelles/nanoparticles 1.338
  nanogels 1.331
  polymeric micelles 1.315, 1.316
  solid polymeric nanoparticles 1.335
nematic (parallel alignment) phase, liquid crystals 1.13
neural growth factor (NGF) 1.290, **1.290**
neurotrophins 1.25, 1.297
new excipients 1.7–8, **1.8**
nicotinamide adenine dinucleotide phosphate (NADPH) 1.201, 1.210, 1.239
N-hydroxysuccinimide (NHS) 1.290–1
NIR. *see* near-infrared radiation
NIRF (near infrared fluorophores) 1.196–7

N-isopropylacrylamide (NIPAAm) 1.216
  α-amino acid based hydrogels 2.204, **2.205**, 2.206, 2.220, 2.221, 2.222
  biomolecule-sensitive hydrogels 2.271, 2.274, 2.277, 2.281
  cell sheet engineering 2.296, **2.297**
  dendrimers, smart 1.97, 1.98
  dual-responsive hydrogels 2.170, 2.172
  glucose-sensitive hydrogels 2.266
  plasma polymerization 2.339
  polymer grafting 2.327, **2.330**, 2.334, 2.335
  temperature-responsive hydrogels 2.163–5, **2.166**, 2.245–6, **2.246**
  temperature-responsive nanogels 2.167
N-isopropylmethacrylamide (NIPMAM) 2.58
nitrobenzyl methacrylate (NBA) 2.326
nitroxide-mediated (NMRP) radical polymerization 2.321, 2.323
N-methylated poloxamines 1.124, **1.125**
Nobel Prize in Chemistry (2000) 1.283
non-covalent functionalization
  carbon nanotubes 2.91, 2.95–6
  molecularly imprinted polymers 2.230, 2.232
noradrenalin **2.278**
norfloxacin
  imprinted hydrogels 2.237–8, **2.238**, **2.239**
  polymer grafting 2.335
nosocomial infections 2.316
NNDEA (poly(*N,N*-diethylacrylamide) 1.157
N-succinyl-DOPE 1.81
nucleic acids (NAs). *see* gene delivery
nucleophilic addition, carbon nanotubes 2.95
nucleopores poly(carbonate) membrane 2.292
N-vinylcaprolactam 2.167
N-vinylimidazole (NVIm) 2.242–3, **2.243**
N-vinylpyrrolidone (NVP) 2.240, 2.266

octopus structures, polymersomes 1.184
oil-in-water emulsions 2.118
oligodeoxynucleotides (ODNs) 1.258, 1.258
oligo(ethylene glycol) (OEG) **1.226**, 1.246, 1.98, 1.99, 1.107
oligonucleotides 1.84, 1.220, 1.296, 2.6
1D crystallization phase transitions 1.12
o-nitrobenzyl (ONB) 1.310, 1.315, 1.317, 1.318, 1.320, 1.325, 1.332
ophthalmic drug delivery 2.235–40, **2.236**, **2.237**, **2.239**
opportunistic bacteria 2.316. *see also* infected tissues
opsonisation 1.37, 1.189, 2.109
optical imaging, polymersome compounds **1.196**, 1.196–7
Optison 1.197
OR logic triggers 1.107
oral administration
  enzyme-responsive materials 1.236–7
  pH-responsive hydrogels 2.155
oral mucosal epithelial cell sheets 2.297, **2.299**
organelles, artificial 1.201
organic nanoparticles 2.41–4, **2.42**, **2.43**
organic polymers, phase transitions 1.14
organic solvents 1.218, 2.171
  anticancer drugs 1.198
  elastin-like recombinamers 2.188
  layer-by-layer assemblies 2.121–2
organic-inorganic hybrids, combination products 2.317–18

orientation, cell sheet
  engineering 2.303–7, **2.305**, **2.306**
osteolysis, enzyme-responsive
  DDS 1.240
osteoporosis **1.233**
ovalbumin (OVA) protein 1.224
ovarian cancer
  carbon nanotubes 2.98–9
  reduction-sensitive
    nanosystems 1.216, **1.217**
  ultrasound triggered DDS 1.164,
    1.158–9, 1.160
oxaliplatin
  carbon nanotubes 2.97–8, 2.99
  dual responsive hydrogels 2.173
  polymeric micelles **1.136**
oxidation/oxidative stress. *see also*
  reactive oxygen species
  biochemical-responsive DDS 1.20
  carbon nanotubes 2.94, 2.108
  phase transitions 1.14
  photosensitization-induced
    oxidation 1.307
  polypyrrole **1.284**, 1.284–5
oxidative photodynamic
  therapy 1.100
oxidoreductases 1.20

PAA. *see* polyacrylic acid
PAAm. *see* polyacrylamide
packing factor theory 1.180, **1.181**,
  1.184
paclitaxel (taxol) 2.98–9
  dendrimers, smart 1.96, 1.105
  electric field responsive DDS 1.25
  layer-by-layer assemblies 2.118
  pH responsive nanogels 2.160
  polymeric micelles 1.128 drug,
    1.135, **1.136**
  polymersomes 1.198–9, 1.200
  reduction-sensitive
    nanosystems 1.216
  supramolecular hydrogels 1.242
PAcMo (poly(*N*-
  acryloylmorpholine) **2.305**
PAGs (photo-acid generators) 1.330
PAH (poly(alylamine hydrochloride)
  2.120, 2.138, 2.141–2
palmitoyloleoylphosphatidylcholine
  (POPC) **1.55**, 1.55–6
PAMAM (polyamidoamine)
  dendrimers 1.94, **1.95**, 1.98, 1.101,
  1.102, 1.103–4, 1.257
p-aminobenzoate (PAP) 2.242–3
pancreatic cancer 2.67
pancreatic islets, microencapsulated
  2.290–1, **2.292**, 2.292–3
pancreatin 1.250
PANI (polyanaline) 1.25, 1.294
paracetamol 2.251, 2.252, **2.254**
parenteral drug applications 1.6,
  1.117, 1.122
Parkinson's disease 2.293
PARP (poly(ADP-ribose)
  polymerase) **2.216**, 2.217
particle size. *see* size factors
Passerini condensation 2.186
passive excipients 1.3
passive targeting. *see* enhanced
  permeability and retention effect
patterning, tissue-mimicking cell
  sheets 2.301–3, **2.302**,
  2.304, **2.305**
PAZO (poly(1-4[4-3(3carboxy-4-
  hydroxyphenyl-azo)benzene-
  sulfonamido]- 1,2-ethanediyl)
  1.329–30
PBA (phenylboronic acid) 2.266,
  2.267, **2.268**
PBD (poly-butadiene) 1.184, 1.200
PBH (peptide-based hydrogels)
  1.242–3
PBLG-HYA (poly(g-benzyl
  l-glutamate)-hyaluronan)
  1.199–200
PBMA (poly(n-butyl
  methacrylate) 2.302, **2.302**
PBO (poly(butylene oxide) 1.126–7
PCI (photochemical
  internalization) 1.100–1, **1.101**
PCL (poly(caprolactone) 1.120,
  1.160, 1.212, 1.128, **1.318**, 2.6

PCL-SS-PEEP (poly(ethyl ethylene phosphate) 1.212
PDADMAC (poly(diallyldimethylammonium chloride) 2.124
PDEAEMA (poly(2-(diethylamino)-ethyl methacrylate) **1.225**, 2.70, **2.155**, 2.155, 2.195
PDMA (poly(*N,N*-dimethylacrylamyde) 2.326
PDMAEMA (poly(dimethyl amino ethyl methacrylate) 1.257, 1.320, **2.155**, 2.155, **2.156**, 1.257, 1.320
PDMS (polydimethylsiloxane) 2.303, 2.319
PDT. *see* photodynamic therapy
PE (phosphatidylethanolamine) 1.83, 1.84, 1.86
PEDOT (poly(3,4-ethylenedioxythiophene) 1.25, 1.284, 1.299
PEGylation (polyethylene glycol) 1.3, 1.9
  accelerated blood clearance phenomenon 1.9, 1.84
  α-amino acid based hydrogels 2.200, 2.221
  biochemical-responsive DDS 1.20
  biomolecule-sensitive hydrogels 2.262, 2.271–2, **2.283**, 2.280, 2.281, 2.283–4
  dendrimers 1.97
  elastin-like recombinamers 2.187
  enzyme-responsive materials 1.235
  gold nanoparticles **2.4**, 2.4
  hydrogels **1.239**, 1.240
  hydrophilic particles 1.189
  imprinted hydrogels 2.238
  layer-by-layer assemblies 2.128
  light-sensitive polymeric micelles 1.313, **1.314**
  light-sensitive polymeric vesicles 1.325
  low temperature-sensitive liposomes 1.62
  magnetic nanoparticles 2.41, 2.44–5, **2.45**, 2.56, 2.57
  mesoporous silica nanoparticles 2.68, 2.81
  micelles 1.134–5, 1.158
  multi-walled carbon nanotubules 2.97
  pH-responsive microgels 2.156, 2.157
  pH-sensitive liposomes 1.183, 1.184, 1.185
  polyelectrolyte complexes 1.258, 1.267
  polyester block copolymers 1.127–8
  polymeric micelles 1.118, **1.121**, 1.121–7, **1.125**, **1.129**
  polymersomes 1.189–90, 1.193, 1.197, 1.198
  poloxamines 1.119
  reduction-sensitive nanosystems 1.210, 1.212, 1.214, 1.216, 1.219–20, **1.220**
  switchable micelles 1.247
  temperature-responsive nanogels 2.166
  ultrasound-triggered release 1.156, 1.157, 1.159
  see also stealth properties
PEI (poly(ethylene imine) 1.257, 1.261, 1.265, **1.266**, 2.70, 2.71, 2.75–6, 2.118
PEMs. *see* polyelectrolyte multilayers
pendant glucose (poly(2-glucosyloxyethyl methacrylate), (PGEMA) 2.268–70, **2.269**, 2.280, 2.281, **2.281**
PEO (poly(ethylene oxide). *see* PEGylation
peptide-based hydrogels (PBH) 1.242–3
peptides, therapeutic
  elastin-like recombinamers 2.189–90
  pH-sensitive liposome delivery **1.85**, 1.90

perfluoropentane 1.170
peristaltic pumps 1.292–3
permeability changes, DDSs 1.40, 1.47–9, **1.48**, 2.228
PET (polyethylene terephthalate) 2.56, 2.57
PGA (poly(l-glutamic acid) **2.172**, 2.247
P-glycoprotein 1.9, 1.199, 2.71–2
PGMA-PHPMA (poly(glycerol monomethacrylate)–poly(2-hydroxypropyl methacrylate) 1.184
PGO (poly(phenyl glycidyl ether) 1.126–7
pH-responsive DDS 1.2, 1.16–18, **1.17**
  α-amino acid based hydrogels 2.202, 2.204–9, **2.207–10**, 2.210, 2.213, 2.214, 2.222
  biomolecule-sensitive hydrogels 2.261–2, 2.263, 2.270
  carbon nanotubes 2.103
  dendrimers, smart 1.102–5, **1.103**
  dual-responsive hydrogels 2.170–3
  elastin-like recombinamers 2.193, **2.194**
  electric field-responsive DDS 1.24
  glucose-sensitive hydrogels **2.265**, 2.265
  gold nanoparticles **2.9**, 2.9–10, **2.11**
  hydrogels 2.154, **2.155**, 2.155–61, **2.156**, **2.159**
  hydrolytically-induced drug release 2.243
  imprinted hydrogels 2.249–51, **2.250**
  insulin cell/tissue delivery systems 2.291
  layer-by-layer assemblies 2.129–32, **2.130**, **2.131**, **2.132**
  low temperature-sensitive liposomes 1.38
  mesoporous silica nanoparticles 2.70, 2.75–7
  micelles, polymeric 1.122, 1.133–5
  poly(butadiene)–poly(methacrylic acid) 1.184
  polymer grafting **2.331**
  polymersomes 1.200
  polyplexes 1.257, **1.258–60**, 1.258–61, 1.274, **1.275**
  ultrasound triggered 1.164
pH-sensitive liposomes 1.80–6, 1.90–1
  cancer therapy applications **1.83**
  passive accumulation in tumor cells **1.82**
  therapeutic applications 1.87–90
  uptake/intra-cellular delivery **1.84**, 1.86–7, **1.87**
phagocytosis 1.191, 1.192
pharmaceutical companies 1.115
phase transitions. *see also* lower critical temperature of dissolution; upper critical temperature of dissolution
  α-amino acid based hydrogels 2.204, 2.206–11, **2.207**, **2.208**, **2.210**, 2.214, 2.217–19, **2.218**, 2.221–2, **2.222** 209
  biomolecule-sensitive hydrogels 2.262–4, **2.263**, **2.264**, 2.274, **2.276**, **2.278**
  dendrimers, smart 1.96–7
  dual-responsive hydrogels 2.171
  enzyme-responsive hydrogels 1.240–1
  glucose-sensitive hydrogels **2.269**
  imprinted hydrogels 2.233, 2.235, 2.236, 2.242–7, **2.247**, **2.248**
  interpenetrating networks 2.173
  polymeric micelles 1.121
  polymersomes 1.183
  stimuli-responsive networks 1.11–14, **1.15**, 2.245
  temperature-responsive hydrogels 2.161, 2.181

PHEA-g-MA (α,β-poly(hydroxyethyl aspartamide-g-maleic anhydride) 2.157–8
PHEMA (poly(AA-co-AM-co-NVP-co-HEMA-co-PEG200DMA) 2.238, **2.239**, 2.240
phenylalanine 2.208, **2.242**, 2.242
phenylboronic acid (PBA) 2.266, **2.267**, **2.268**
PHMA (poly(hydroxyethyl methacrylate) 1.190, 1.238
phosphatases 1.19, 1.243, 1.246–8
phosphatidylethanolamine (PE) 1.83, 1.84, 1.86
phosphorylation 1.242
photo-acid generators (PAGs) 1.330
photo-active gold nanoparticles 2.10–14, **2.13**. *see also* light-responsive DDS
photochemical internalization (PCI) 1.100–1, **1.101**
photocross-linking, polymeric capsules 1.307, 1.328–9, **1.329**
photodegradable moieties 1.101–2
photodynamic therapy (PDT)
  dendrimers, smart 1.100, 1.101
  gold nanoparticles **2.13**, 2.14, **2.15**
  oxidative 1.100. *see also* reactive oxygen species
  polymeric micelles 1.135
photo-excitation 1.307–8
photo-isomerization 1.307, 1.310, **1.312**
photolithography technique 2.304, **2.305**
photoluminescence 2.92
photo responsive DDS. *see* light responsive DDS
photosensitization 1.100–2, 1.307, 2.14
photothermal therapy (PTT) 1.100
  carbon nanotubes 2.92
  gold nanoparticles 2.14–20, **2.16**, **2.17**, **2.18**, **2.19**
  layer-by-layer assemblies 2.138
pHPMA (2-hydroxypropylacrylamide) 1.133, 1.264, 2.173
physical hydrogels 1.238, **2.184**, 2.184, 2.188
physically cross-linked elastin-like recombinamers 2.188
physics of ultrasound 1.149–5, **1.152**
PIC (polyion complex) micelles **1.258**, 1.267, **1.268**
pilocarpine 2.203, 2.211, 2.217–21, **2.218**, **2.219**, **2.220**
pinocytosis 1.167, 1.191
PLA (poly(lactic acid) 1.127, 1.128, 1.158, 1.245, 2.128
placental growth factor (PlGF) 2.301
plasma polymerization 2.325
  polymer grafting **2.322**, **2.324**, 2.324–5
  surface modification 2.339–41
Plasmodium falciparum 1.264
plastic crystals, phase transitions 1.13
platinum 1.241
platinum-based anticancer drugs 2.97–8, 2.100–2. *see also* carboplatin; cisplatin; oxaliplatin
PLGA (poly(lactide-co-glycolide) 1.299, 2.160, 2.291, 2.293
PLL (poly(L-lysine) 2.121, **2.121**, 2.130, 2.134–5, **2.135**, 1.259, **1.259**
PLLA (poly(L-lactide) 1.299
Pluronic F-127 2.6, 2.96
pluronic polymers 1.157, 1.160, 1.161–3, **1.162**, 1.164, 1.167, 1.169
PMAA. *see* poly(methacrylic acid)
PMOA. *see* primary mode of action (PMOA)
PMOXA (poly(2-methyl-2-oxazoline) 1.190
PMPC (poly(2-methacryloyloxyethyl phosphorylcholine) 1.190, 1.194, 1.200
PNH (poly(*N*-isopropylacrylamide-co-2-hydroxyethyl methacrylate) **2.172**
PNIPAAm. *see* poly(isopropylacrylamide)
PNVCL (poly(*N*-vinylcaprolactam) **2.162**, 2.166–7

POs (polyoxazolines) 1.133
poloxamers/poloxamine **1.121**, 1.121–6, **1.125**
poly(AA-co-AM-co-NVP-co-HEMA-co-PEG200DMA) (PHEMA) 2.238, **2.239**, 2.240
polyacrylamide (PAAm) 2.158, 2.164, 2.170, 2.199, 2.248
  biomolecule-sensitive hydrogels 2.271, 2.274
  cell sheet engineering 2.303
  dual responsive hydrogels 2.173
  enzyme-responsive materials 1.235
  layer-by-layer assemblies 2.141
  upper critical solution temperature 2.168–9
polyacrylic acid (PAA) 1.133, **1.239**, 2.339, **2.340**
  α-amino acid based hydrogels **2.208**, 2.208
  biomolecule-sensitive hydrogels 2.277, 2.281
  cell/tissue delivery systems 2.293
  drug-loaded soft contact lenses 2.236
  functional monomers 2.203, 2.231
  imprinted hydrogels 2.237, **2.247**
  layer-by-layer assemblies 2.118
  light responsive hydrogels 2.251
  light-sensitive polymeric micelles **1.318**
  mesoporous silica nanoparticles 2.70
  pH responsive hydrogels **2.155**, 2.155, **2.156**, 2.249
  polymer grafting 2.329–30, **2.330**, **2.331**, 2.333, **2.338**, 2.338
poly(acryloylmorpholine) (PAcMo) **2.305**
poly(acryloxysuccinimide) 2.78
poly(ADP-ribose) polymerase (PARP) **2.216**, 2.217
poly(allylamine hydrochloride) (PAH) 2.120, 2.138, 2.141–2
polyamidoamine (PAMAM) dendrimers 1.94, **1.95**, 1.98, 1.101, 1.102, 1.103–4, 1.257
poly(aminoethyl)methacrylamide) 1.216
polyaminoacids 1.134, 1.235
poly(ampholyte) hydrogels 2.208–9, 2.211, **2.212**
polyanaline (PANI) 1.25, 1.294
poly(β-amino esters) 2.125–6
poly(g-benzyl l-glutamate)-hyaluronan (PBLG-HYA) 1.199–200
polybutadiene 1.313
poly-butadiene (PBD) 1.184, 1.200
poly(butyl methacrylate) (PBMA) 2.302, **2.302**
poly(butylene oxide) (PBO) 1.126–7
poly(caprolactone (PCL) 1.120, 1.160, 1.212, 1.128, **1.318**, 2.6
poly(carboxylic acids) 2.129
poly(carboxymethyl-β-cyclodextrin) **2.127**
polycarboxy-4-hydroxyphenyl-azobenzenesulfonamidoethanedyil (PAZO) 1.329–30
poly(diallyldimethylammonium chloride) (PDADMAC) 2.124
poly(2-(diethylamino)ethyl methacrylate) (PDEAEMA) **1.225**, 2.70, **2.155**, 2.155, 2.195
poly(dimethylacrylamyde) (PDMA) 2.326
poly(*N,N*-dimethyl aminoethyl methacrylate) (PDMAEMA) 1.257, 1.320, **2.155**, 2.155, **2.156**
polydimethylsiloxane (PDMS) 2.303, 2.319
polyelectrolyte complexes (polyplexes) 1.256–8, 1.275
  charge-conversion ternary **1.260**
  dual-responsive 1.274–5
  light-responsive **1.273**, 1.273–4
  pH-responsive **1.258**, 1.258–61, **1.259**, **1.260**, 1.274, **1.275**
  reducible 1.261–9, **1.263**, **1.264**, **1.266**, **1.268**, 1.274
  temperature-responsive **1.269**, 1.269–73, **1.272**

polyelectrolyte multilayers (PEMs) 2.118–29, **2.120**, **2.121**, 2.133–5, 2.137–41, 2.143–4
poly(ethyl ethylene phosphate) (PCL-SS-PEEP) 1.212
poly(3,4-ethylenedioxythiophene) (PEDOT) 1.25, 1.284, 1.299
polyethylene glycol. *see* PEGylation
poly(ethylene imine) (PEI) 1.257, 1.261, 1.265, **1.266**, 2.70, 2.71, 2.75–6, 2.118
poly(ethylene oxide). *see* PEGylation
polyethylene terephthalate (PET) 2.56, 2.57
poly(l-glutamic acid) (PGA)) **2.172**, 2.247
poly(L-glutamic acid) (PG)-paclitaxel 1.158, 2.130
poly(glycerol monomethacrylate)–poly(2-hydroxypropyl methacrylate) (PGMA-PHPMA) 1.184
poly(hydroxyethyl methacrylate) (PHMA) 1.190, 1.238
poly(hydroxyethylaspartamide) 1.134
poly(hydroxypropyl methacrylate) (PHPMA) 1.133, 1.264, 2.173
polyion complex (PIC) micelles **1.258**, 1.267, **1.268**
poly(isopropylacrylamide) (PNIPAAm) 1.200, **1.269**, 1.269, 2.171, **2.171**. *see also* temperature-responsive DDS
  α-amino acid based hydrogels 2.199
  biomolecule-sensitive hydrogels 2.262–3, 2.275, 2.277
  cell/tissue delivery systems 2.291
  cell sheet engineering **2.295**, 2.295–6, 2.303, 2.304, **2.305**
  cell/tissue delivery systems 2.294–5
  combination products 2.323
  dendrimers, smart 1.96–7, 1.98
  dual-responsive hydrogels **2.172**, 2.172, 2.173
  glucose-sensitive hydrogels 2.266, 2.267, **2.267**
  imprinted hydrogels 2.246, 2.248
  layer-by-layer assemblies 2.120, 2.129–30, **2.130**, 2.136, 2.137
  magnetic nanoparticles **2.45**, 2.58, **2.59**
  mesoporous silica nanoparticles 2.69, 2.70
  plasma polymerization 2.339
  polymer grafting 2.325–6, **2.326**, **2.330**, 2.330, **2.331**, **2.332**, 2.333, **2.334**
  polymeric micelles 1.128–32, **1.130**, **1.132**
  shell-sheddable micelles 1.213
  temperature-responsive hydrogels 2.163–5
  temperature-responsive nanogels 2.166, 2.167
  tissue-mimicking cell sheets **2.302**, 2.302
poly(lactic acid) (PLA) 1.127, 1.128, 1.158, 1.245, 2.128
poly(L-lactide) (PLLA) 1.299
poly(L-lactide)-co-NIPAAm 1.98
poly(lactide-co-glycolide) (PLGA) 1.299, 2.160, 2.291, 2.293
poly(lactone)-PEG-poly(lactone) block copolymers 1.127
poly(L-lysine (PLL) 2.121, **2.121**, 2.130, 2.134–5, **2.135**, 1.259, **1.259**
polymer backbone photodegradation 1.307
polymer blends 1.13
polymer brushes 2.296, **2.297**, 2.304, **2.305**, 2.320, **2.322**, 2.323, 2.325–38, **2.327**
polymer capsules. *see* capsules
polymer coatings
  combination products, drug/medical devices 2.320
  mesoporous silica nanoparticles 2.68–72
polymer combination products 2.317

polymer grafting
  cell sheet engineering **2.295**, 2.295–6, **2.297**
  combination products 2.320–5, **2.322**, **2.323**, **2.324**
  responsive surfaces 2.325–38, **2.326–32**, **2.334–5**, **2.337–8**
polymer membranes 2.290. *see also* cell/tissue delivery systems
polymer micelles 1.115–20
  clinical applications 1.135, **1.136**
  comparison with polymersomes 1.198
  light-sensitive 1.308–20, **1.309**, **1.311**, **1.312**, **1.314–19**
  pH-responsive 1.122, 1.133–5
  preparation methodology 1.118–19
  reduction-sensitive 1.210–19, **1.211**, **1.213**, **1.215**, **1.217**
  temperature-responsive 1.120–33, **1.121**, **1.125**, **1.129**, **1.130**, **1.132**
  ultrasound-responsive 1.157–8
polymer nano-/microparticles 1.188, 1.327–37, **1.328–30**, **1.332–3**, **1.335–7**. *see also* dendrimers; micelles; polymersomes
polymer threading, membrane phase transitions 1.11
polymer vesicles. *see* polymersomes
polymerisation process **1.284**, 1.284–5
polymer–polymer interactions 1.12
polymers, general information 1.2, 1.94
  as drug delivery systems **1.7**, 1.15–25, **1.17**, **1.22**
  evolution 1.6
  phase transitions 1.11–14
  temperature-responsive DDS 1.72
  therapeutic functionality 1.9
  thermosensitive **1.97**, 1.97–8
polymer–solvent interactions 1.12
polymersomes 1.117
  cellular uptake **1.190**, 1.191–2, 1.194, **1.195**
  characterization 1.185–7, **1.187**, 1.188
  comparison with liposomes 1.190
  comparison with polymer micelles 1.198
  as delivery vectors 1.188–96, **1.195**
  formation 1.179–85, **1.181**, **1.182**
  light-sensitive 1.320–7, **1.321**, **1.324–6**
  medical applications **1.196**, 1.196–201
  reduction-sensitive nanosystems 1.219–21, **1.220**
polymethacrylate bearing spiropyran moieties (PSPMA) 1.313, **1.314**
poly(methacrylic acid) (PMAA) 1.224, 2.130, **2.131**
  light-sensitive polymeric micelles 1.314
  pH responsive hydrogels **2.155**, 2.155–7, 2.159
  polymer grafting 2.326
poly(methacryloyloxyethyl phosphorylcholine) (PMPC) 1.190, 1.194, 1.200
poly(methyl-2-oxazoline) (PMOXA) 1.190
polymorphic liposomes 1.82–3
poly(*N,N*-diethylacrylamide) (NNDEA) 1.157
poly(*N*-isopropylacrylamide). *see* poly(isopropylacrylamide
poly(*N*-isopropylacrylamide- co-2-hydroxyethyl methacrylate) (PNH) **2.172**
poly(2-nitrobenzylmethyl methacrylate) (PNBMA) 1.314, **1.315**
poly(*N*-tertbutylacrylamide-co-acrylamide/maleic acid) 2.249
poly(*N*-vinyl pyrrolidone) (PVP) 1.190
poly(*N*-vinylcaprolactam) (PNVCL) **2.162**, 2.166–7
poly(*N*-vinylisobutyramide) 1.98
poloxamines 1.193
polyoxazolines (POs) 1.133

polypeptides, phase transitions 1.11
poly(phenyl glycidyl ether) (PGO) 1.126–7
poly(4-phenylazomaleinanil-co-4-vinylpyridine) (AzoMI-VPy) 1.313
polyplexes. *see* polyelectrolyte complexes
polypropylene (PP)
  plasma polymerization 2.339
  polymer grafting 2.317, 2.329–33, **2.330**, **2.331–2**, **2.334–5**, 2.335
poly(propylene glycol) 1.120
poly(propylene oxide) (PPO) 1.157–8
polypropyleneimine (PPI) dendrimer 1.97, 1.198, 1.102
polypyrrole (PPy) 1.283. *see also* intrinsically conducting polymers
  actuating devices **1.293**, 1.293–4, 1.294, **1.295**
  cyclic voltammetry 1.287, **1.288**
  electro-conductive hydrogels 1.296
  electrostatic forces 1.288–9
  implantable electrodes 1.297
  microchips 1.292
  nanostructured conducting polymers 1.297–9
  polymerization **1.284**, 1.284–5
  reservoir systems 1.290–2, **1.290**, **1.291**
  solubility 1.286
  stability 1.285–6
  volume changes 1.289
poly(1-pyrenylmethyl methacrylate) (PPyMA) 1.314
polysaccharide-based nanogels 2.160
polysaccharides 2.41
polystyrene (PS) 2.326
polystyrene beads 2.195
poly(styrene oxide) (PSO) 1.126–7
polystyrene sulfonate (PSS) 2.120, 2.124, 2.125, **2.126**
polystyrene-poly(acrylic acid) (PS-PAA) 1.183
poly(sulfonamide) (PSD) 1.260
poly(trimethylene carbonate)- b-poly(L-glutamic acid) (PTMC-PGA) polymersomes 1.201
polyurethane catheters 2.319
poly(vinyl alcohol) (PVA) 2.141, 2.173, 2.266
poly(vinyl) sulfonate 1.329–30
poly(vinylidene difluoride) (PVDF) 2.292, 2.297, **2.299**, 2.307
poly(4-vinylpyridine) 1.133, 2.70
poly(vinylpyrrolidone) (PVPON) 1.224
poly(VPGVG) (poly(Val-Pro-Gly-Val-Gly) 2.181, 2.191, 2.192. *see also* elastin-like recombinamers
POPC (palmitoyloleoylphosphatidylcholine) **1.55**, 1.55–6
pores, capped. *see* capped pores
posterior capsule opacification 2.316
PP. *see* polypropylene
PPI (polypropyleneimine) 1.97, 1.198, 1.102
PPO (poly(propylene oxide) 1.157–8
PPy. *see* polypyrrole
PPyMA (poly(1-pyrenylmethyl methacrylate) 1.314
precipitation, magnetic nanoparticles 2.37–8
prednisone 2.100
presoaking, combination products 2.318, 2.319, **2.319**
pressure waves, ultrasound 1.149, 1.154
primary mode of action (PMOA), combination products 2.314–15, **2.315**, 2.318, 2.341
principle of precaution, carbon nanotubes 2.105, 2.110
processing–structure–function relationships **1.8**
processing–structure–property relationships 1.4, 1.5–6
prodrugs 1.234–5
promyelocytic leukemia, ultrasound triggered 1.164
proof-of-principle experiments 2.102
property-composition-structure relationships 1.34, 1.35, 1.36, 1.40–51, **1.40–1**, **1.44–6**, **1.48–9**
propyl 1.134
prostate cancer 1.64–5, **1.233**

protease inhibitors 1.234
proteases 1.19
protein-based materials, biomimetics 2.181. *see also* elastin-like recombinamers
proteins
  folding, biomolecule-sensitive hydrogels 2.284
  nanoparticle interactions 1.194
  reduction-sensitive nanosystems 1.219
  therapeutic 1.256, 2.189
protein-sensitive hydrogels 2.270–6, **2.272**, **2.273**, **2.275–6**
proteoglycans 1.193
proton gradients, layer-by-layer assemblies 2.134
proton-sponge effect 1.257, 2.81
PS. *see* polystyrene
PSD (poly(sulfonamide)) 1.260
PSO (poly(styrene oxide)) 1.126–7
PSPMA (polymethacrylate bearing spiropyran moieties) 1.313, **1.314**
PSS (polystyrene sulfonate) 2.120, 2.124, 2.125, **2.126**
PTMC-PGA (poly(trimethylene carbonate)-*b*-poly(L-glutamic acid) polymersomes 1.201
PTT. *see* photothermal therapy
pulmonary toxicology, fiber paradigm 2.107
PVA (poly(vinyl alcohol) 2.141, 2.173, 2.266
PVP (poly(*N*-vinyl pyrrolidone) 1.190
PVDF (poly(vinylidene difluoride)) 2.292, 2.297, **2.299** , 2.307
PVPON (poly(vinylpyrrolidone) 1.224
PVS (poly(vinyl) sulfonate) 1.329–30
pyrene 1.108, 2.130–1
pyroglutamic acid (Pga) 2.247

quantum dots (QDs) **2.38**

radical polymerization 2.185
radio frequency ablation (RFA) 1.65–8, **1.66**, 1.96
radioactive substances **1.85**
RAFT. *see* reversible addition fragmentation transfer
Raman spectroscopy 1.286, 2.92
rapamycin 2.215
rate-programmed drug release. *see* release rate
reactive oxygen species (ROS). *see also* oxidation
  carbon nanotubes 2.106, 2.109
  photodynamic therapy 2.14
  photothermal therapy 1.100
receptor-mediated endocytosis 1.167
receptor specific ligands 1.82
recognition, responsive polymers 1.14–15
redox cycling, intrinsically conducting polymers **1.290**
redox-responsive drug release **1.17**, 1.21, 1.210, 1.223, 1.288
  dendrimers, smart 1.105
  gold nanoparticles 2.10, **2.12**
  intrinsically conducting polymers 1.283, 1.291, 1.295
  layer-by-layer assemblies 2.134–5
  mesoporous silica nanoparticles 2.78–9
  nanovehicles **1.209**, 1.210, 1.214
reducible cleavable polycation (RPC vectors) **1.264**, 1.265
reducible polyelectrolyte complexes (polyplexes) 1.261–9, **1.263**, **1.264**, **1.266**, **1.268**, 1.274
reducing agents, layer-by-layer assemblies 2.135
reduction-sensitive nanosystems 1.208–10, **1.209**, 1.227
  hollow capsules 1.223–6, **1.225**
  nanogels **1.226**, 1.226–7
  nanoparticles 1.221–3, **1.222**
  polymeric micelles 1.210–19, **1.211**, **1.213**, **1.215**, **1.217**
  polymersomes 1.219–21, **1.220**
regenerative medicine 2.295, 2.296–8. *see also* cell/tissue delivery systems
relative exposure index (REI), polymeric micelles 1.125

release rate, drug 1.2
  enzyme-responsive DDS 1.240
  evolution **1.3**
  layer-by-layer assemblies 2.122, 2.125, **2.126**
  supramolecular hydrogels 1.242
renal clearance, drug delivery systems 1.188–9
renal thresholds, particle size 1.236
reservoir systems, intrinsically conducting polymers **1.290**, 1.290–2, **1.291**
residual catalysts, toxicity 2.105–6, 2.108
resistance. *see* multi-drug resistance
responsive imprinted networks 2.229. *see also* molecular imprinting
restenosis 2.316
reticulo-endothelial (RES) system 1.81, 2.41
  gold nanoparticles 2.3–4
  mesoporous silica nanoparticles 2.68
  opsonin recognition 1.189
reverse engineering, low temperature sensitive liposomes 1.36–51, **1.38–41**, **1.44–6**, **1.48–9**
reversible addition fragmentation transfer (RAFT)
  cell sheet engineering 2.296, **2.297**, 2.304
  polymerization 1.216, 2.321
reversible cross-linking, light-sensitive polymeric micelles 1.318–20, **1.319**
reversible-deactivation radical polymerization 2.321
reversible photoswitching **1.314**, **1.315**. *see also* switching
  polymeric micelles **1.312**, 1.313, 1.317, **1.318**
  polymeric vesicles **1.321**, 1.322
RFA (radio frequency ablation) 1.65–8, **1.66**, 1.96
RGD (arginine–glycine–aspartic acid) peptides 1.262, 2.96
rhodamine 6G 1.99, **1.107**, 1.107
rhodamine B 1.102, 1.161, 1.223, 1.249, 1.332, 2.48
rifampicin
  combination products 2.319
  enzyme-responsive DDS 1.246
  polymeric micelles 1.128
ring opening polymerization (ROP) reactions 1.127
risk–benefit ratios, chemotherapy drugs 2.63
RNA. *see also* gene delivery
  cell/tissue delivery systems 2.300
  gene delivery 1.265
  gold nanoparticles 2.6
  mesoporous silica nanoparticles 2.71–2
  polyplexes 1.268
rod-shaped
  nanoparticles 1.192
  polymersomes 1.193
ROP (ring opening polymerization) reactions 1.127
ROS. *see* reactive oxygen species
RPC (reducible cleavable polycation) vectors **1.264**, 1.265
ruboxyl 1.162–3
ruthenium 2.200

saccharide-sensitive polymer brushes 2.327, **2.328**
safety assessments, drug delivery systems 1.25
  molecularly imprinted polymers 2.234
  new excipients 1.7, 1.8
  phototriggered micelles/nanoparticles 1.338
  ultrasound 1.155
safranin 1.296
salt-triggered release, layer-by-layer assemblies **2.132**, 2.132, **2.133**, 2.133–4
saporin-conjugated dendrimers 1.100

SAXS (small angle X-Ray scattering) 1.183
scaffold-based cell/tissue delivery systems 2.293–4
scanning electron microscopy (SEM) 1.44, **1.44**, **1.291**, 1.291
scattering techniques 1.186–7
scCO$_2$ (supercritical CO$_2$) 2.319
SCID (severe combined immunodeficiency) mice 1.258–9
SCL (shell cross-linked) micelles 1.218
SCRM (shell-cross-linked reverse micelles) 1.319–20
SDF-1. *see* stromal-derived factor-1
second generation
  biomaterials 1.5
  excipients 1.2
second order phase transitions 1.11–12
self-assembly
  elastin-like recombinamers 2.188, 2.191, 2.192, 2.194, 2.195, 2.199–200
  hydrogels 1.238
  light-sensitive polymeric vesicles 1.322–3
  lipids 1.33, 1.34
  liposomes/micelles 1.94
  magnetic nanoparticles 2.40, **2.43**
  micelles 1.169
  molecularly imprinted polymers 2.230, 2.232
  polymeric micelles 1.116
  polymersomes 1.179–85, **1.182**
  polysaccharide-based nanogels 2.160
  shell cross-linked micelles 1.218
  solid polymeric nanoparticles 1.334
  supramolecular hydrogels 1.242, 1.243
self-regulated DDS 1.96, 1.305, 2.154
  layer-by-layer assemblies 2.141–2
  mesoporous silica nanoparticles **2.76**
SEM (scanning electron microscopy) 1.44, **1.44**, **1.291**, 1.291
sequestering agents, polymers 1.9
sequestration, micelles 1.169–70
severe combined immunodeficiency (SCID) mice 1.258–9
SGNs (spiral ganglionic neurons) 1.297, 1.300
shape
  carbon nanotubes 2.92, 2.110
  nanoparticles 1.192–3
  polymersomes 1.193
shear-stress induced release, micelles 1.170
shell cross-linked (SCL) micelles 1.218
shell-cross-linked reverse micelles (SCRM) 1.319–20
shell-sheddable micelles, reduction-sensitive 1.210–13, **1.211**, **1.213**
signal amplification, enzyme-responsive materials 1.232
signal-to-noise ratio, polymersome imaging compounds 1.196
silane coupling chemistry 2.69
silane monolayers **2.322**
silica nanocontainers (SN) **1.248**, 1.248–51, **1.249**. *see also* mesoporous silica nanoparticles
silicon brushes, polymer 2.327
simvastatin 1.124
single-crystal shell drug nanocarriers 2.54–6, **2.55**, **2.56**
single-walled carbon nanotubes (SWCNTs) 2.90, 2.92, 2.100
  encapsulation properties 2.101
  environmental impacts 2.110
  external attachment of drugs 2.96–7
  layer-by-layer assemblies 2.119
  toxicity/environmental impacts 2.104, 2.106, 2.107, 2.108
size factors
  carbon nanotubes 2.105
  enzyme-responsive materials 1.236–7

size factors (*continued*)
  mesoporous silica
    nanoparticles 2.65
  nanoparticles 1.191–2
  proteins, therapeutic 1.256
  switching 2.154
skeletal myoblast sheets 2.297, **2.300**, **2.301**
skin contact, carbon nanotubes 2.105, 2.108
small angle X-Ray scattering (SAXS) 1.183
small interfering ribonucleic acid (siRNA) 1.257
small unilamellar vesicles (SUVs) 1.34
smart membranes, intrinsically conducting polymers 1.294, **1.295**. *see also* stimuli responsive DDS
snap-top systems 2.78
sodium alginate (NaAlg) 2.158. *see also* alginates
soft contact lenses 2.235–40, **2.236**, **2.237**, **2.239**
soft coronal cross-linking 1.327
sol–gel phase transitions 1.13
sol–gel technology 1.130
solid polymeric nanoparticles 1.334–7, **1.335**, **1.336**, **1.337**
solid tumor targeting 1.198
solubility, drugs 1.115
solvents. *see also* organic solvents
  combination products 2.319
  dimethylformamide 2.215, **2.216**
  imprinted hydrogels **2.242**, 2.242, 2.248
  molecularly imprinted
    polymers 2.232
  polymer–solvent interactions 1.12
sonoporation 1.153, 1.165, 1.167, 1.168. *see also* ultrasound
SOPC (stearoyl-2-oleoyl-*sn*-glycero-3-phosphocholine) 1.34–5, **1.35**, 1.43, 1.46, 1.47
spatial conformation, polymer chains 2.229
spherical
  nanoparticles 1.192
  polymersomes 1.193
spike-wave discharges (SWD) 2.57, **2.58**
spiral ganglionic neurons (SGNs) 1.297, 1.300
spiropyran 1.307, 1.310, **1.311**, 1.313, 1.314, 1.324, 1.333–4, 1.338
spongy phases, polymersomes 1.183
SPR (surface plasmon resonance) effects 2.14
spray-drying 2.65, 2.72
stability, intrinsically conducting polymers 1.285–6
stacking devices, cell sheet engineering **2.306**
Staphylococcus aureus. *see also* MRSA
  combination products **2.340**, 2.341
  layer-by-layer assemblies 2.130
  polymer grafting 2.336
  polymeric micelles 1.123–4
  wounds 1.19
star-shaped micelles 1.131
Staundinger, Hermann 1.6
stealth systems 1.38, 1.50. *see also* PEGylation; PHMA; PMOXA; PMPC; PVP
  lipid membrane components 1.42
  mesoporous silica
    nanoparticles 2.68–9
  pH-sensitive liposomes 1.84, **1.85**, 1.90
  polymersomes 1.197
  switchable micelles 1.247
stents 1.296–7, 2.316
stearoyl-2-oleoyl-*sn*-glycero-3-phosphocholine (SOPC) 1.34–5, **1.35**, 1.43, 1.46, 1.47
stimulated emission depletion (STED) microscopy 1.185
stimuli responsive DDS 2.229. *see also specific DDS*
  combination products 2.321
  general information 1.9–25, **1.10**, **1.17**, **1.22**

stress and strain parameters, cell membranes 1.43
stromal-derived factor-1 (SDF-1)
  cytokines 2.297–8
  regenerative medicine **2.300**
structure-property-composition relationships 1.34–6, 1.40–51, **1.40**, **1.41**, **1.44–6**, **1.48**, **1.49**
substrates, layer-by-layer assemblies 2.117–18, **2.119**
sugar-induced release. *see* glucose-responsive DDS
supercritical CO_2 ($scCO_2$) 2.319
superparamagnetism 2.34
supramolecular hydrogels 1.241–4, **1.242**
surface area-to-volume ratios
  mesoporous silica
    nanoparticles 2.65
  nanoparticles 1.193
surface chemistry, carbon nanotubes 2.106, 2.109
surface functionalization. *see* functionalization
surface modification
  magnetic nanoparticles **2.38**, 2.38–40, **2.39**
  plasma polymerization 2.339–41
surface plasmon resonance (SPR) effects 2.14
surface topologies, polymersomes 1.194, **1.195**
surfactant micelles 1.156–7
surfactants 2.171
SUVs (small unilamellar vesicles) 1.34
SWCNTs. *see* single-walled carbon nanotubes
SWD (spike-wave discharges) 2.57, **2.58**
swelling–collapse phenomenon 1.12. *see also* equilibrium degree of swelling; phase transitions
swelling solvents, combination products 2.319, **2.319**
switching. *see also* magnetic nanoparticles; reversible photoswitching
  α-amino acid based
    hydrogels 2.200
  enzyme-responsive DDS 1.243
  hydrophilic/hydrophobic
    state 2.154
  imprinted hydrogels 2.245
  mesoporous silica
    nanoparticles 2.75, 2.79, 2.79–80
  micelles 1.246–8
  size/shape 2.154
  solid polymeric
    nanoparticles 1.335
  temperature-responsive
    DDS 2.136
synergistic effects. *see also* dual-responsive DDS
  chemotherapy drugs/
    ultrasound 1.165–6
  cisplatin/temsirolimus **2.216**, 2.216–17
  combination products 2.316
  gold nanoparticles **2.20**, 2.20
  magnetic nanoparticles 2.42
  mesoporous silica
    nanoparticles 2.71, 2.72, 2.73
  pH/redox-stimulated DDS 1.213
synthetic glycosylated insulin (G-insulin) 2.291
synthetic metals, electric field responsive DDS 1.25

tamoxifen 2.118, 2.159
Tanaka equation 2.244–5
targeted drug delivery 2.1. *see also* active targeting; *specific DDS*
  cancer chemotherapeutics 2.3
  cell sheet engineering 2.298–301
  mesoporous silica
    nanoparticles 2.66–8
  nanogels 1.18
  ultrasound-responsive
    DDSs 1.159–61

Tarzan-swing mechanism 2.234
TAT (transactivator of transcription) 1.88, 1.265
taxol. *see* paclitaxel
TCEP (tri(2-carboxyethyl)phosphine hydrochloride) 1.218
TCPS (tissue culture polystyrene) dishes 2.295–6
TEM. *see* transmission electron microscopy
temperature-responsive DDS **1.17**, 1.21–4, **1.22**. *see also* hyperthermia; low temperature-sensitive liposomes; photothermal therapy; poly(isopropylacrylamide)
  α-amino acid based hydrogels 2.202, 2.209–11, 2.213, 2.214, 2.221
  biomolecule-sensitive hydrogels 2.261–2, 2.277
  cell/tissue delivery systems 2.294–5, **2.295**, **2.297–302**, **2.304–6**
  dendrimers, smart 1.96–9, **1.97**
  dual responsive hydrogels 2.170–3
  elastin-like recombinamers 2.193–4
  glucose-sensitive hydrogels **2.267**
  hydrogels 2.154, **2.161**, 2.161–9, **2.162–3**, **2.166**, **2.169**
  hydrolytically induced drug release 2.243
  imprinted hydrogels 2.245–9, **2.246–8**
  layer-by-layer assemblies **2.136–7**, 2.136–7
  liposomes 2.46, **2.47**
  magnetic nanoparticles **2.44**, 2.44–50, **2.45–7**
  mesoporous silica nanoparticles 2.69, 2.70
  micelles, polymeric 1.120–33, **1.121**, **1.125**, **1.129**, **1.130**, **1.132**
  moieties 1.98–9
  polyelectrolyte complexes **1.269**, 1.269–73, **1.272**
  polymer grafting **2.331**, 2.334
  polymersomes 1.200
  upper critical solution temperature 2.168–9, **2.169**
template extraction, molecularly imprinted polymers 2.233, **2.234**
templates, layer-by-layer assemblies 2.117–18, **2.119**
temsirolimus 2.202, 2.203, 2.215, 2.216, **2.216**, 2.217, 2.224
tetrahydropyran (THP)-protected 2-hydroxyethyl methacrylate) 1.213
tetramethylpiperidinyl-1-oxy (TEMPO) 2.323
TGF-β1 (transforming growth factor beta 1) 2.125
theophylline 2.100, 2.240, 2.251
theranostics
  carbon nanotubes 2.91
  dendrimers, smart 1.108–9
  enzymes in 1.232
  gold nanoparticles 2.21–3, **2.22**, **2.23**
  magnetic nanoparticles **2.41**
  pH-sensitive liposomes 1.90
  polymeric micelles 1.128
  polymersomes 1.196
therapeutic index, drug 1.120
therapeutic neutrophins 1.297
therapeutic proteins 1.256, 2.189
thermal decomposition, magnetic nanoparticles **2.38**, 2.38
thermal index (TI) 1.150, 1.155
thermal responsiveness. *see* temperature-responsive DDS
ThermoDox. *see* doxorubicin
thermodynamic characterization, ultrasound-responsive DDSs 1.163–4
thermodynamic phase transitions 1.14
thermoseeds 2.73
thiolated poly(methacrylic acid) (PMASH) 1.224
thiolates 2.5

thiol-disulfide exchange
  reactions 1.209
thiophene fluorophore 2.160
thioundecyl-tetraethyleneglycoestero-nitrobenzylethyldimethylammonium bromide (TUNA) 2.77–8
thioundecyltetraethyleneglycolcarboxylate (TUEC) 2.77–8
third generation
  biomaterials 1.6–7, **1.8**
  excipients 1.2
THP (tetrahydropyran-protected 2-hydroxyethyl methacrylate) 1.213
three dimensional networks
  α-amino acid based
    hydrogels 2.200
  layer-by-layer assemblies 2.143–4
three dimensional (3D) tissues 2.291, 2.293, 2.303, **2.304**. *see also* cell/tissue delivery systems
thrombin-sensitive peptide
  linkers 1.19
time-controlled release. *see* release rate
time-dependent tumor cell
  death 2.167
timolol 2.236, **2.237**, 2.237
TIRF (total internal reflectance fluorescence) 1.185
tissue culture polystyrene (TCPS) dishes 2.295–6
tissue engineering 2.293–4. *see also* cell/tissue delivery systems
tissue-mimicking cell sheets. *see* cell sheet engineering
TNF (tumor necrosis factor)
  1.199, **2.5**
topoisomerase inhibitors 1.169. *see also* doxorubicin
total internal reflectance fluorescence (TIRF) 1.185
toxicology 2.1
  capsules, polymeric 1.328
  carbon nanotubes 2.92, 2.97–8, 2.104–10
  cisplatin hydrogels 2.214–17, 2.200
  cross-linked micelles 1.216
  enzyme inhibitors 1.234
  fiber paradigm 2.107
  layer-by-layer assemblies 2.140
  light-sensitive polymeric
    micelles 1.310
  lipofectamine 1.200
  nanoparticles 1.193–4
  new excipients 1.9
  pH-responsive nanogels 2.160
  pilocarpine 2.220–1
  polyelectrolyte complexes 1.270
  reduction-sensitive
    nanosystems 1.218
  switchable micelles 1.247
  see also toxicology
transactivator of transcription (TAT) 1.88, 1.265
trans–cis isomerization
  light-responsive hydrogels 2.251, 2.252
  light-sensitive polymeric
    micelles 1.310, 1.313, 1.314, 1.317, **1.318**
  light-sensitive polymeric
    vesicles 1.323
  phototriggered micelles/
    nanoparticles 1.332
transdermal drug delivery, layer-by-layer assemblies 2.144
transferrin receptors, tumor
  cells 1.191
transforming growth factor beta 1 (TGF-β1) 2.125
transglutaminase 2.271, 2.187
transition temperature,
  liposomes 1.47
translocation, carbon nanotubes 2.108
transmission electron microscopy (TEM)
  elastin-like recombinamers 2.192
  lipid bilayers **1.44**, 1.44
  polymersomes **1.182**, 1.184, 1.185, **1.187**, **1.190**
trans-to-*cis* photoisomerization
  light-sensitive polymeric
    vesicles 1.322

tri(2-carboxyethyl)phosphine hydrochloride (TCEP) 1.218
triclocarban 1.118, 1.124
triclosan 1.118, 1.123
trimethyloylpropane ethoxylate triacrylate 1.194
tumor cells
  biochemical-responsive DDS 1.20, 1.21
  enzyme-responsive DDS 1.19
  enzyme disregulation **1.233**
  low temperature-sensitive liposomes 1.34, 1.37, **1.38**, 1.39
  magnetic-responsive DDSs 1.24
  nanogels 1.18
  passive accumulation 1.81, **1.82**
  pH 1.16, 1.83, 1.134, 2.70, 2.129, 2.155, 2.158–61
  reduction-sensitive nanosystems 1.210
  stress and strain parameters 1.43
  temperature-responsive nanogels 2.166
  ultrasound-responsive DDSs 1.23, 1.159–61
  vascularisation 1.37, **1.38**, 1.61, 1.63–4, 1.198
tumor diagnosis. *see* theranostics
tumor markers 2.262, 2.277–9, **2.279**
tumor necrosis factor (TNF) 1.199, **2.5**
TUEC (thioundecyltetraethyleneglycolcarboxylate) 2.77–8
TUNA (thioundecyltetraethyleneglycoestero-nitrobenzylethyldimethylammonium bromide) 2.77–8
TUNEL assay, gold nanoparticles **2.8**
two photon near-IR absorption 1.316
two-step model 1.183

UCST. *see* upper critical solution temperature
Ugi condensation 2.186
ultra-small superparamagnetic iron oxide (USPIO) 1.201
ultrasonication 2.95
ultrasound imaging compounds **1.196**, 1.196, 1.197
ultrasound-responsive DDSs **1.22**, 1.23, 1.148–9
  future perspectives 1.169–70
  layer-by-layer assemblies 2.140–1
  micelles 1.155–9
  physics of ultrasound 1.149–5, **1.152**
  polymeric micelles 1.123, 1.157–8
  targeting tumor cells 1.159–61
  triggered release from micelles 1.161–9, **1.162**
ultraviolet light-responsive DDSs 1.23, 1.305–7
  gold nanoparticles 2.14
  imprinted hydrogels 2.251, 2.252
  layer-by-layer assemblies 2.139
  mesoporous silica nanoparticles 2.70, 2.77–8
  micelles/nanoparticles 1.330, 1.338
  nanogels 1.331
  polymer grafting **2.322**, 2.323
  polymeric micelles 1.313, 1.314, 1.315
  polymeric vesicles 1.322, 1.323–4
  solid polymeric nanoparticles 1.334, **1.336**
United States Pharmacopoeia (USP), 21-National Formulary 1.2
upper critical solution temperature (UCST)
  dual responsive hydrogels 2.173
  magnetic nanoparticles 2.44
  polymeric micelles 1.121
  temperature-responsive hydrogels **2.161**, 2.161, 2.168–9, **2.169**
  temperature-sensitive polymers 1.21–2
Urry's model 2.181
USPIO (ultra-small superparamagnetic iron oxide) 1.201

vaginal pH 1.18
valine residues 2.200–1, 2.203, **2.205**, 2.206, **2.207**, **2.210**, 2.211, 2.213, **2.213**, 2.214, 2.219–21, **2.219**, **2.220**
Val-Pro-Gly-Xaa-Gly (VPGXG) 2.181, 2.182. *see also* elastin-like recombinamers
valproic acid 2.224
van der Waals interactions 1.12
  carbon nanotubes 2.95
  enzyme-responsive DDS 1.19
  lipid bilayers 1.43
vancomycin
  elastin-like recombinamers 2.189
  polymer grafting 2.329–33, **2.331**, **2.332**, **2.334**
  polymeric micelles 1.123–4
vascular cell adhesion molecule 1 (VCAM-1) 1.191
vascular diseases, enzyme disregulation **1.233**
vascular endothelial growth factor (VEGF)
  biomolecule-sensitive hydrogels 2.284, 2.285
  cell sheet engineering 2.306
  polyelectrolyte complexes 1.268
  regenerative medicine 2.298, **2.300**, 2.301
vascularization
  tissue-mimicking cell sheets 2.303, 2.306
  tumor cells 1.37, **1.38**, 1.61, 1.63–4, 1.198
VCAM-1 (vascular cell adhesion molecule) 1.191
VEGF. *see* vascular endothelial growth factor
vesicle area dilation experiment **1.45**
vesicles
  elastin-like recombinamers 2.194, **2.195**
  fenestrations. *see* enhanced permeability and retention effect
  hollow 2.194–5, **2.195**
  light-sensitive polymeric 1.320–7, **1.321**, **1.324–6**
  lipid bilayers 1.43
  phase transitions 1.14
vesicle-to-micelle transitions 1.184
vinyl hydrogels 2.200–3, **2.201–2**
viscoelasticity, biomaterials 1.6
VPGXG (Val-Pro-Gly-Xaa-Gly) 2.181, 2.182. *see also* elastin-like recombinamers
volume changes, intrinsically conducting polymers 1.289. *see also* swelling–collapse phenomenon

water solubility, drugs 1.115
wave nature, ultrasound 1.149–50
wet chemical polymer grafting **2.322**
wet-chemical synthesis, mesoporous silica nanoparticles 2.65
wild-type myoblast sheets **2.301**
window chambers, optical imaging 1.196
Wolf rearrangement reaction 1.315–16
Wolman disease **1.233**
worm-like micelles 1.193
wounds
  enzyme-responsive DDS 1.19
  pH 1.16–18, 2.155

X-ray contrast agents. *see* contrast agents

zero premature release, chemotherapy drugs 2.64, 2.65
zinc porphyrin 1.135
zwitterionic ligands 2.10
zwitterionic peptide linkers 2.272, **2.273**

RSC Smart Materials

The intelligent way to find your materials solution

The progress of new functional materials plays a vital role in solving many of today's global challenges, from energy and sustainability to medicine and healthcare. With a wealth of information available it's hard to find a resource providing a complete overview of the different types of smart materials available. Each book in the RSC Smart Materials series covers the fundamentals and applications of different material system from renowned international experts. Stay in the know with the RSC Smart Materials series.

Series Editors:

Hans-Jörg Schneider, Saarland University, Germany

Mohsen Shahinpoor, University of Maine, USA

Key Features

- Listed in ISI Books Citation Index^{SM} and SciVerse Scopus
- All books in the Series can be viewed via Google Book Search and the Amazon Search Inside service
- Included in the RSC eBook Collection

Materials Design Inspired by Nature
Magnetorheology
Smart Materials for Drug Delivery
RSC Publishing
RSC Publishing
RSC Publishing

Journals of interest

- Journal of Materials Chemistry A/B/C
- Soft Matter
- Polymer Chemistry
- Biomaterials Science

www.rsc.org/publishing

Series ISSN: 2046-0066

RSC Publishing

http://rsc.li/smart-materials

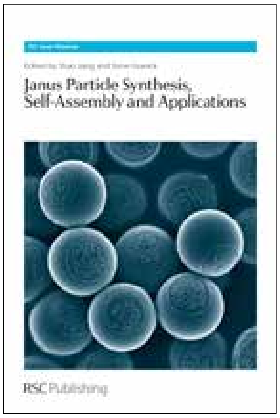

Janus Particle Synthesis, Self-Assembly and Applications

Edited by **Shan Jiang,** Massachusetts Institute of Technology, USA | **Steve Granick,** Univeristy of Illinois at Urbana-Champaign, USA

Named after the two-faced roman god, Janus particles have gained much attention due to their potential in a variety of applications, including drug delivery. This is the first book devoted to Janus particles and covers their methods of synthesis, how these particles self-assemble, and their possible uses. It goes beyond a simple summary and offers a logical way of selecting the proper synthetic route for Janus particles for certain applications. Written by pioneering experts in the field, the book introduces the Janus concept to those new to the topic and highlights the most recent research progress on the topic for those active in the field.

Hardback | 312 pages | ISBN 9781849734233 | 2012 | £153.99

Magnetorheology
Advances and Applications
RSC Publishing

Magnetorheology

Advances and Applications

Edited by **Norman Wereley,** University of Maryland, USA

Magnetorheological fluids, smart fluids which change viscosity in the presence of a magnetic field, are of great commercial interest for many engineering applications such as shock absorbers and dampers in aerospace. Magnetorheology: Advances and Applications provides an update on the key developments in the physics, chemistry and uses of magnetorheological fluids. Edited by a leading expert and with contributions from distinguished scientists in the field this timely book is suitable for chemists, physicists and engineers wanting to gain a comprehensive overview of these smart materials.

Hardback | 400 pages | ISBN 9781849736671 | 2013 | £159.99

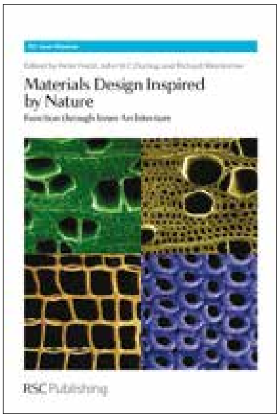
Materials Design Inspired by Nature
Function through Inner Architecture
RSC Publishing

Materials Design Inspired by Nature

Function through Inner Architecture

Edited by **Peter Fratzl, John W C Dunlop, Richard Weinkamer,** Max Planck Institute of Colloids and Interfaces, Germany

The inner architecture of a material can have an astonishing effect on its overall properties and is vital to understand when designing new materials. Nature is a master at designing hierarchical structures and so researchers are looking at biological examples for inspiration to create man-made materials. Materials Design Inspired by Nature is the first book to address the relationship between the inner architecture of natural materials and their physical properties for materials design. The book explores examples from plants, the marine world, arthropods and bacteria, where the inner architecture is exploited to obtain specific mechanical, optical or magnetic properties along with how these design principles are used in man-made products. Experimental methods used to investigate hierarchical structures are also covered. Written by leading experts in bio-inspired materials research, this is essential reading for anyone developing new materials.

Hardback | 400 pages | ISBN 9781849735537 | 2013 | £159.99

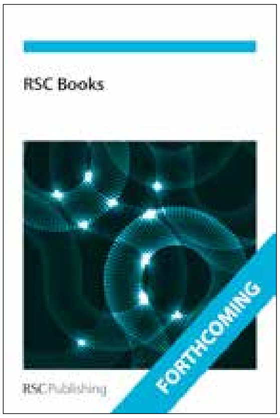

Responsive Photonic Nanostructures

Smart Nanoscale Optical Materials

Edited by **Yadong Yin,** University of California, Riverside, USA

Photonic crystal nanostructures, whose photonic properties can be tuned in response to external stimuli, are desired for a wide range of applications in colour displays, biological and chemical sensors, and inks and paints. Until now there is no single resource which gives a complete overview of these exciting smart materials. This book details the fabrication of photonic crystal structures through self-assembly approaches, general strategies and approaches for creating responsive photonic structures for different responsive systems such as chemical, optical, electrical and magnetic as well as their applications. With contributions from leading experts in the field, this comprehensive summary on responsive photonic nanostructures is suitable for postgraduates and researchers in academia and industry interested in smart materials and their potential applications.

Hardback | 300 pages | ISBN 9781849736534 | 2013 | £149.99

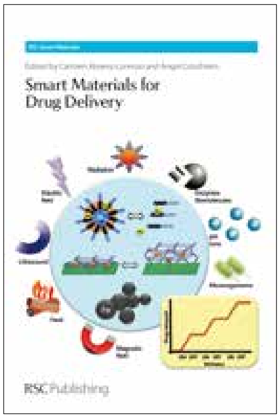
Smart Materials for Drug Delivery

RSC Publishing

Smart Materials for Drug Delivery
Complete Set

Edited by **Carmen Alvarez-Lorenzo, Angel Concheiro,** Universidad de Santiago de Compostela, Spain

Novel smart materials are needed for the design of intelligent drug delivery systems to enable the controlled release of active molecules. With so many papers available on smart and stimuli-responsive materials for drug delivery applications it's hard to know where to start reading about this exciting topic. This set pulls together the recent findings in the area and provides a critical analysis of the information available and how it can be applied to advanced drug delivery. Written by leading experts in the field, including a foreword from distinguished scientist Nicholas Peppas, The University of Texas at Austin, USA, the book will provide both an introduction to the key areas for graduate students and new researchers in the stimuli-responsive field as well as serving as a reference for those already working on fundamental materials research or their applications.

Volume 1 | ISBN 9781849738774 | £159.99 Volume 2 | ISBN 9781849738781 | £159.99

Hardback | 800 pages | ISBN 9781849735520 | 2013 | £230.00

Forthcoming titles

Biointerfaces
Where Material Meets Biology

Dietmar Hutmacher, Queensland University of Technology, Australia | **Wojciech Chrzanowski,** University of Sydney, Australia

Hardback | 240 pages | ISBN 9781849738767 | 2014 | £145.00

Bio-Synthetic Hybrid Materials and Bionanoparticles
A Biological Chemical Approach Towards Material Science

Alexander Böker, Patrick van Rijn, RWTH Aachen University, Germany

Hardback | 400 pages | ISBN 9781849738224 | 2014 | £165.00

Cell Surface Engineering

Rawil Fakhrullin, Kazan Federal University, Russian | **Choi Insung,** KAIST, South Korea | **Lvov Yuri,** Louisiana Tech University, USA

Hardback | 400 pages | ISBN 9781849738224 | 2014 | £165.00

Functional Nanometer-Sized Clusters of Transition Metals
Synthesis, Properties and Applications

Wei Chen, Chinese Academy of Sciences, China | **Shaowei Chen,** University of California, USA

Hardback | 450 pages | ISBN 9781849738248 | 2014 | £175.00

Mechanochromic Fluorescent Materials
Phenomena, Materials and Application

Jiarui Xu, Zhenguo Chi, Sun Yat-sen University, China

Hardback | 250 pages | ISBN 9781849738217 | 2014 | £145.00

Semiconductor Nanowires
From next-generation electronics to sustainable energy

Wei Lu, University of Michigan, USA | **Jie Xiang,** University of California, San Diego, USA

Hardback | 500 pages | ISBN 9781849738156 | 2014 | £175.00

Supramolecular Materials for Opto-Electronics

Norbert Koch, Humboldt University of Berlin, Germany

Hardback | 350 pages | ISBN 9781849738262 | 2014 | £165.00

Other titles of interest

Functional Molecular Gels

Beatriu Escuder, Juan Miravet, Universitat Jaume I, Spain

Hardback | 280 pages | ISBN 9781849736657 | 2013 | £149.99

Functional Polymers for Nanomedicine

Youqing Shen, Zhejiang University, China

Hardback | 350 pages | ISBN 9781849736206 | 2013 | £159.99

Healable Polymer Systems

Wayne Hayes, Barnaby W Greenland, University of Reading, UK

Hardback | 200 pages | ISBN 9781849736268 | 2013 | £99.99

Hierarchical Nanostructures for Energy Devices

Seung H Ko, KAIST, South Korea | **Costas P Grigoropoulos,** University of California, Berkeley, USA

Hardback | 300 pages | ISBN 9781849736282 | 2014 | £149.99

Materials for a Sustainable Future

Trevor M Letcher, University of KwaZulu-Natal, South Africa | **Janet L Scott,** University of Bath, UK

Hardback | 828 pages | ISBN 9781849734073 | 2012 | £74.99

Molecular Design and Applications of Photofunctional Polymers and Materials

Wai-Yeung Wong, Hong Kong Baptist University, Hong Kong | **Alaa S Abd-El-Aziz,** University of Prince Edward Island, Canada

Hardback | 300 pages | ISBN 9781849735759 | 2012 | £153.99

Also of interest

Intelligent Materials

Edited by Mohsen Shahinpoor, University of Maine, USA | **Hans-Jörg Schneider,** Saarland University, Germany

In this exceptional text the expertise of specialists across the globe is drawn upon to present a truly interdisciplinary outline of the topic. The influence of current research in this field on future technology is undisputed and potential applications of intelligent materials span nanoscience, nanotechnology, medicine, engineering, biotechnology, pharmaceutical and many other industries. This is an authoritative introduction to the most recent developments in the area, which will provide the reader with a better understanding of the almost unlimited opportunities in the progress and design of new intelligent materials. An indispensable reference for anyone contemplating working in the field.

"This will be the starting point for all researchers looking for industrial solutions involving smart materials. Congratulations to the Editors for providing such a vast and interdisciplinary book." P.-G de Gennes, France Prix Nobel de Physic 1991

Hardback | 552 pages | ISBN 978084043354 | 2007 | £139.99

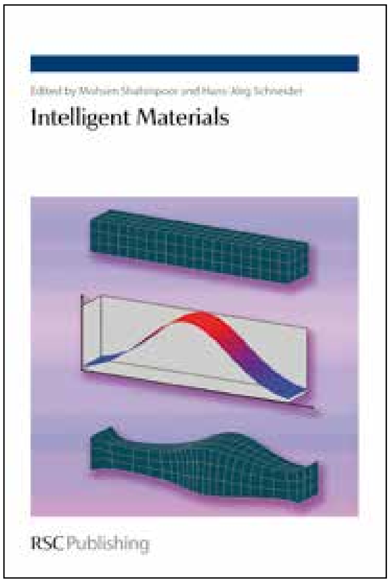

Edited by Mohsen Shahinpoor and Hans-Jörg Schneider

Intelligent Materials

RSC Publishing

For your next book

The RSC is committed to the advancement of the chemical sciences through our publications. We are always keen to see proposals for new books and would be delighted to consider your ideas.

Why publish with us?

- Fast publication times
  (manuscript submission to publication average 24 weeks)
- Friendly, efficient, experienced editorial service
- High visabilty through Indexing and the RSC eBook Collection
- Discount on RSC books
- Competitive royalties
- Effective marketing and promotion
- International sales support

Take the first step

If you would like to discuss a proposal with one of our Books Commissioning Editors please get in touch
Email: books@rsc.org
Tel: +44(0)1223 420066

"My sincere gratitude also goes out to the editorial and production staff at RSC Publishing who all have worked efficiently and diligently under tight deadlines to ensure that the high standards of the RSC have been maintained in the book."

Lew P. Christopher, South Dakota School of Mines and Technology, USA
(Editor of Integrated Forest Biorefineries)

To order

Royal Society of Chemistry
Marston Book Services Ltd
160 Milton Park
Abingdon
Oxfordshire
OX14 4SB, UK
Tel: +44 (0) 1235 465522
Fax: +44 (0) 1235 465555
Email: **enquiries@marston.co.uk**
www.marston.co.uk

USA and Canada
Please contact:
Ingram Publisher Services
Customer Service, Box 631
14 Ingram Blvd
La Vergne, TN 37086, USA
Tel: +1 (866) 400 5351
Fax: +1 (800) 838 1149
Email: **ips@ingramcontent.com**

RSC Publishing

http://rsc.li/smart-materials

Registered charity number 207890